

**Ongoing Face Recognition  
Vendor Test (FRVT)**  
**Part 1: Verification**

Patrick Grother  
Mei Ngan  
Kayee Hanaoka  
*Information Access Division  
Information Technology Laboratory*

This publication is available free of charge from:  
<https://www.nist.gov/programs-projects/face-recognition-vendor-test-frvt-ongoing>

2019/10/16

## ACKNOWLEDGMENTS

The authors are grateful to Wayne Salamon and Greg Fiumara at NIST for robust software infrastructure, particularly that which leverages [Berkeley DB Btrees](#) for storage of images and templates, and [Open MPI](#) for parallel execution of algorithms across our computers. Thanks also to Brian Cochran at NIST for providing highly available computers and network-attached storage.

## DISCLAIMER

Specific hardware and software products identified in this report were used in order to perform the evaluations described in this document. In no case does identification of any commercial product, trade name, or vendor, imply recommendation or endorsement by the National Institute of Standards and Technology, nor does it imply that the products and equipment identified are necessarily the best available for the purpose.

## FRVT STATUS

**This report** is a draft NIST Interagency Report, and is open for comment. It is the sixteenth edition of the report since the first was published in June 2017. Prior editions of this report are maintained on the FRVT website, and may contain useful information about older algorithms and datasets no longer used in FRVT.

**FRVT remains open:** All [four tracks](#) of the FRVT remain open to new algorithm submissions indefinitely. This report will be updated as new algorithms are evaluated, as new datasets are added, and as new analyses are included. Comments and suggestions should be directed to [frvt@nist.gov](mailto:frvt@nist.gov).

### Changes since September 11, 2019:

- ▷ The report adds results for five new participants: Awidit Systems (Awiros), Momenmtum Digital (Sertis), Trueface AI, Shanghai Jiao Tong University, and X-Laboratory.
- ▷ The reports adds results for five new algorithms from returning developers: Cyberlink, Hengrui AI Technology, Idemia, Panasonic R+D Singapore, and Tevian. This causes three algorithm, to be de-listed from the report per policy to list results for two algorithms per developer.

### Changes since July 31 2019:

- ▷ The HTML table on the [FRVT 1:1 homepage](#) has been updated to include a column for cross-domain Visa-Border verification. Results for this new dataset appeared in the July 29 report under the name "CrossEV" - these are now renamed "Visa-Border".
- ▷ The [FRVT 1:1 homepage](#) lists algorithms according to lowest mean rank accuracy:
 
$$\begin{aligned} &\text{Rank(FNMR}_{\text{VISA}} \text{ at FMR = 0.000001}) + \\ &\text{Rank(FNMR}_{\text{VISA-BORDER}} \text{ at FMR = 0.000001}) + \\ &\text{Rank(FNMR}_{\text{MUGSHOT}} \text{ at FMR = 0.00001 after 14 years}) + \\ &\text{Rank(FNMR}_{\text{WILD}} \text{ at FMR = 0.00001}) \end{aligned}$$
 This ordering rewards high accuracy across all datasets.
- ▷ The main results in Table 8 is now in landscape format to accomodate extra columns for the Visa-Border set, and mugshot comparisons after at least 12 years.
- ▷ The report adds results for nine new participants: Alpha SSTG, Intel Research, ULSee, Chungwa Telecon, iSAP Solution, Rokid, Shenzhen EI Networks, CSA Intellicloud, Shenzhen Intellifusion Technologies.
- ▷ The reports adds results for six new algorithms from returning developers: Innovatrics, Dahua Technology, Tech5 SA, Intellivision, Nodeflux and Imperial College, London. One algorithm, from Imperial has been retired, per policy to list results for two algorithms per developer.
- ▷ The cross-country false match rate heatmaps starting from Figure 295 have been replotted to reveal more structure by listing countries by region instead of alphabetically.
- ▷ The next version of this report will be posted around October 18, 2019.

### Changes since July 3 2019:

- ▷ The HTML table on the [FRVT 1:1 homepage](#) has been updated to list the 20 most accurate developers rather than algorithms, choosing the most accurate algorithm from each developer based on visa and mugshot results. Also, the algorithms are ordered in terms of lowest mean rank across mugshot, visa and wild datasets, rewarding broad accuracy over a good result on one particular dataset.
- ▷ This report includes results for a new dataset - see the column labelled "crossEV" in Table 5. It compares a new set of high quality visa portraits with a set webcam photos that exhibit moderately poor pose variations and background illumination. The two new sets are described in sections 2.3 and 2.5. The

comparisons are “cross-domain” in that the algorithm must compare “visa” and “wild” images. Results for other algorithms will be added in future reports as they become available.

- ▷ This report adds results for algorithms from 9 developers submitted in early July 2019. These are from 3DiVi, Camvi, EverAI-Paravision, Facesoft, Farbar (F8), Institute of Information Technologies, Shanghai U. Film Academy, Via Technologies, and Ulucu Electronics Tech. Six of these are new participants.
- ▷ Several other algorithms have been submitted and are being evaluated. Results will be released in the next report, scheduled for September 5. That report will include results for new datasets.
- ▷ Older algorithms from Everai, Camvi and 3DiVi, have been retired, per the policy to list only two algorithms per developer.

#### **Changes since June 2019:**

- ▷ This report adds results for algorithms from 18 developers submitted in early June 2019. These are from CTBC Bank, Deep Glint, Thales Cogent, Ever AI Paravision, Gorilla Technology, Imagus, Incode, Kneron, N-Tech Lab, Neurotechnology, Notiontag Technologies, Star Hybrid, Videonetics, Vigilant Solutions, Winsense, Anke Investments, CEIEC, and DSK. Nine of these are new participants.
- ▷ Several other algorithms have been submitted and are being evaluated. Results will be released in the next report, scheduled for August 1.
- ▷ Older algorithms from Everai, Thales Cogent, Gorilla Technology, Incode, Neurotechnology, N-Tech Lab and Vigilant Solutions have been retired, per the policy to list only two algorithms per developer.

#### **Changes since April 2019:**

- ▷ This report adds results for nine algorithms from nine developers submitted in early June 2019. These are from Tencent Deepsea, Hengrui, Kedacom, Moontime, Guangzhou Pixel, Rank One Computing, Synesis, Sensetime and Vocord.
- ▷ Another 23 algorithms have been submitted and are being evaluated. Results will be released in the next report, scheduled for July 3.
- ▷ Older algorithms for Rank One, Synesis, and Vocord have been retired, per the policy to list only two algorithms per developer.

#### **Changes since February 2019:**

- ▷ This report adds results for 49 algorithms from 42 developers submitted in early March 2019.
- ▷ This report omits results for algorithms that we retired. We retired for three reasons: 1. The developer submitted a new algorithm, and we only list two. 2. The algorithm needs a GPU, and we no longer allow GPU-based algorithms. 3. Inoperable algorithms.
- ▷ Previous results for retired algorithms are available in older editions of this report linked [here](#).
- ▷ The mugshot database used from February 2017 to January 2019 has been replaced with an extract of the mugshot database documented in NIST Interagency Report 8238, November 2018. The new mugshot set is described in section [2.4](#) and is adopted because:
  - ▷▷ It has much better identity label integrity, so that false non-match rates are substantially lower than those reported in FRVT 1:1 reports to date - see Figure [34](#).
  - ▷▷ It includes images collected over a 17 year period such that ageing can be much better characterized - - see Figure [126](#).
- ▷ Using the new mugshot database, Figure [126](#) shows accuracy for four demographic groups identified in the biographic metadata that accompanies the data: black females, black males, white females and white males.

- ▷ The report adds Figure 10 with results for the twenty human-difficult pairs used in the May 2018 paper *Face recognition accuracy of forensic examiners, superrecognizers, and face recognition algorithms* by Phillips et al. [1].
- ▷ The report uses an update to the wild image database that corrects some ground truth labels.
- ▷ Some results for the child exploitation database are not complete. They are typically updated less frequently than for other image sets.

## Contents

<b>ACKNOWLEDGMENTS</b>	<b>1</b>
<b>DISCLAIMER</b>	<b>1</b>
<b>1 METRICS</b>	<b>27</b>
1.1 CORE ACCURACY . . . . .	27
<b>2 DATASETS</b>	<b>28</b>
2.1 CHILD EXPLOITATION IMAGES . . . . .	28
2.2 VISA IMAGES . . . . .	28
2.3 VISA IMAGES II . . . . .	28
2.4 MUGSHOT IMAGES . . . . .	29
2.5 WEBCAM IMAGES . . . . .	29
2.6 WILD IMAGES . . . . .	30
<b>3 RESULTS</b>	<b>30</b>
3.1 TEST GOALS . . . . .	30
3.2 TEST DESIGN . . . . .	30
3.3 FAILURE TO ENROLL . . . . .	33
3.4 RECOGNITION ACCURACY . . . . .	37
3.5 GENUINE DISTRIBUTION STABILITY . . . . .	138
3.5.1 EFFECT OF BIRTH PLACE ON THE GENUINE DISTRIBUTION . . . . .	138
3.5.2 EFFECT OF AGEING . . . . .	152
3.5.3 EFFECT OF AGE ON GENUINE SUBJECTS . . . . .	163
3.6 IMPOSTOR DISTRIBUTION STABILITY . . . . .	178
3.6.1 EFFECT OF BIRTH PLACE ON THE IMPOSTOR DISTRIBUTION . . . . .	178
3.6.2 EFFECT OF AGE ON IMPOSTORS . . . . .	485

## List of Tables

1 ALGORITHM SUMMARY . . . . .	17
2 ALGORITHM SUMMARY . . . . .	18
3 ALGORITHM SUMMARY . . . . .	19
4 ALGORITHM SUMMARY . . . . .	20
5 FALSE NON-MATCH RATE . . . . .	21
6 FALSE NON-MATCH RATE . . . . .	22
7 FALSE NON-MATCH RATE . . . . .	23
8 FALSE NON-MATCH RATE . . . . .	24
9 FAILURE TO ENROL RATES . . . . .	34
10 FAILURE TO ENROL RATES . . . . .	35
11 FAILURE TO ENROL RATES . . . . .	36

## List of Figures

1 PERFORMANCE SUMMARY: FNMR VS. TEMPLATE SIZE TRADEOFF . . . . .	25
2 PERFORMANCE SUMMARY: FNMR VS. TEMPLATE TIME TRADEOFF . . . . .	26
3 EXAMPLE IMAGES . . . . .	30
(A) VISA . . . . .	30
(B) MUGSHOT . . . . .	30
(C) WILD . . . . .	30

4	PERFORMANCE ON 20 HUMAN-DIFFICULT PAIRS . . . . .	38
5	PERFORMANCE ON 20 HUMAN-DIFFICULT PAIRS . . . . .	39
6	PERFORMANCE ON 20 HUMAN-DIFFICULT PAIRS . . . . .	40
7	PERFORMANCE ON 20 HUMAN-DIFFICULT PAIRS . . . . .	41
8	PERFORMANCE ON 20 HUMAN-DIFFICULT PAIRS . . . . .	42
9	PERFORMANCE ON 20 HUMAN-DIFFICULT PAIRS . . . . .	43
10	PERFORMANCE ON 20 HUMAN-DIFFICULT PAIRS . . . . .	44
11	ERROR TRADEOFF CHARACTERISTIC: VISA IMAGES . . . . .	45
12	ERROR TRADEOFF CHARACTERISTIC: VISA IMAGES . . . . .	46
13	ERROR TRADEOFF CHARACTERISTIC: VISA IMAGES . . . . .	47
14	ERROR TRADEOFF CHARACTERISTIC: VISA IMAGES . . . . .	48
15	ERROR TRADEOFF CHARACTERISTIC: VISA IMAGES . . . . .	49
16	ERROR TRADEOFF CHARACTERISTIC: VISA IMAGES . . . . .	50
17	ERROR TRADEOFF CHARACTERISTIC: VISA IMAGES . . . . .	51
18	ERROR TRADEOFF CHARACTERISTIC: VISA IMAGES . . . . .	52
19	ERROR TRADEOFF CHARACTERISTIC: VISA IMAGES . . . . .	53
20	ERROR TRADEOFF CHARACTERISTIC: VISA IMAGES . . . . .	54
21	ERROR TRADEOFF CHARACTERISTIC: VISA IMAGES . . . . .	55
22	ERROR TRADEOFF CHARACTERISTIC: VISA IMAGES . . . . .	56
23	ERROR TRADEOFF CHARACTERISTIC: VISA IMAGES . . . . .	57
24	ERROR TRADEOFF CHARACTERISTIC: VISA IMAGES . . . . .	58
25	ERROR TRADEOFF CHARACTERISTIC: VISA IMAGES . . . . .	59
26	ERROR TRADEOFF CHARACTERISTIC: VISA IMAGES . . . . .	60
27	ERROR TRADEOFF CHARACTERISTIC: MUGSHOT IMAGES . . . . .	61
28	ERROR TRADEOFF CHARACTERISTIC: MUGSHOT IMAGES . . . . .	62
29	ERROR TRADEOFF CHARACTERISTIC: MUGSHOT IMAGES . . . . .	63
30	ERROR TRADEOFF CHARACTERISTIC: MUGSHOT IMAGES . . . . .	64
31	ERROR TRADEOFF CHARACTERISTIC: MUGSHOT IMAGES . . . . .	65
32	ERROR TRADEOFF CHARACTERISTIC: MUGSHOT IMAGES . . . . .	66
33	ERROR TRADEOFF CHARACTERISTIC: MUGSHOT IMAGES . . . . .	67
34	ERROR TRADEOFF CHARACTERISTIC: MUGSHOT IMAGES . . . . .	68
35	ERROR TRADEOFF CHARACTERISTIC: WILD IMAGES . . . . .	69
36	ERROR TRADEOFF CHARACTERISTIC: WILD IMAGES . . . . .	70
37	ERROR TRADEOFF CHARACTERISTIC: WILD IMAGES . . . . .	71
38	ERROR TRADEOFF CHARACTERISTIC: WILD IMAGES . . . . .	72
39	ERROR TRADEOFF CHARACTERISTIC: WILD IMAGES . . . . .	73
40	ERROR TRADEOFF CHARACTERISTIC: WILD IMAGES . . . . .	74
41	ERROR TRADEOFF CHARACTERISTIC: WILD IMAGES . . . . .	75
42	ERROR TRADEOFF CHARACTERISTICS: CHILD EXPLOITATION IMAGES . . . . .	76
43	ERROR TRADEOFF CHARACTERISTICS: CHILD EXPLOITATION IMAGES . . . . .	77
44	ERROR TRADEOFF CHARACTERISTICS: CHILD EXPLOITATION IMAGES . . . . .	78
45	ERROR TRADEOFF CHARACTERISTICS: CHILD EXPLOITATION IMAGES . . . . .	79
46	CMC CHARACTERISTICS: CHILD EXPLOITATION IMAGES . . . . .	80
47	CMC CHARACTERISTICS: CHILD EXPLOITATION IMAGES . . . . .	81
48	CMC CHARACTERISTICS: CHILD EXPLOITATION IMAGES . . . . .	82
49	CMC CHARACTERISTICS: CHILD EXPLOITATION IMAGES . . . . .	83
50	FALSE MATCH RATES WITHIN AND ACROSS DEMOGRAPHIC GROUPS . . . . .	84
51	FALSE MATCH RATES WITHIN AND ACROSS DEMOGRAPHIC GROUPS . . . . .	85
52	FALSE MATCH RATES WITHIN AND ACROSS DEMOGRAPHIC GROUPS . . . . .	86
53	FALSE MATCH RATES WITHIN AND ACROSS DEMOGRAPHIC GROUPS . . . . .	87
54	FALSE MATCH RATES WITHIN AND ACROSS DEMOGRAPHIC GROUPS . . . . .	88
55	FALSE MATCH RATES WITHIN AND ACROSS DEMOGRAPHIC GROUPS . . . . .	89
56	FALSE MATCH RATES WITHIN AND ACROSS DEMOGRAPHIC GROUPS . . . . .	90
57	FALSE MATCH RATES WITHIN AND ACROSS DEMOGRAPHIC GROUPS . . . . .	91
58	SEX AND RACE EFFECTS: MUGSHOT IMAGES . . . . .	92
59	SEX AND RACE EFFECTS: MUGSHOT IMAGES . . . . .	93
60	SEX AND RACE EFFECTS: MUGSHOT IMAGES . . . . .	94

61	SEX AND RACE EFFECTS: MUGSHOT IMAGES . . . . .	95
62	SEX AND RACE EFFECTS: MUGSHOT IMAGES . . . . .	96
63	SEX AND RACE EFFECTS: MUGSHOT IMAGES . . . . .	97
64	SEX AND RACE EFFECTS: MUGSHOT IMAGES . . . . .	98
65	SEX AND RACE EFFECTS: MUGSHOT IMAGES . . . . .	99
66	SEX EFFECTS: VISA IMAGES . . . . .	100
67	SEX EFFECTS: VISA IMAGES . . . . .	101
68	SEX EFFECTS: VISA IMAGES . . . . .	102
69	SEX EFFECTS: VISA IMAGES . . . . .	103
70	SEX EFFECTS: VISA IMAGES . . . . .	104
71	SEX EFFECTS: VISA IMAGES . . . . .	105
72	SEX EFFECTS: VISA IMAGES . . . . .	106
73	SEX EFFECTS: VISA IMAGES . . . . .	107
74	SEX EFFECTS: VISA IMAGES . . . . .	108
75	SEX EFFECTS: VISA IMAGES . . . . .	109
76	SEX EFFECTS: VISA IMAGES . . . . .	110
77	SEX EFFECTS: VISA IMAGES . . . . .	111
78	SEX EFFECTS: VISA IMAGES . . . . .	112
79	FALSE MATCH RATE CALIBRATION: MUGSHOT IMAGES . . . . .	113
80	FALSE MATCH RATE CALIBRATION: MUGSHOT IMAGES . . . . .	114
81	FALSE MATCH RATE CALIBRATION: MUGSHOT IMAGES . . . . .	115
82	FALSE MATCH RATE CALIBRATION: MUGSHOT IMAGES . . . . .	116
83	FALSE MATCH RATE CALIBRATION: MUGSHOT IMAGES . . . . .	117
84	FALSE MATCH RATE CALIBRATION: MUGSHOT IMAGES . . . . .	118
85	FALSE MATCH RATE CALIBRATION: MUGSHOT IMAGES . . . . .	119
86	FALSE MATCH RATE CALIBRATION: MUGSHOT IMAGES . . . . .	120
87	FALSE MATCH RATE CALIBRATION: VISA IMAGES . . . . .	121
88	FALSE MATCH RATE CALIBRATION: VISA IMAGES . . . . .	122
89	FALSE MATCH RATE CALIBRATION: VISA IMAGES . . . . .	123
90	FALSE MATCH RATE CALIBRATION: VISA IMAGES . . . . .	124
91	FALSE MATCH RATE CALIBRATION: VISA IMAGES . . . . .	125
92	FALSE MATCH RATE CALIBRATION: VISA IMAGES . . . . .	126
93	FALSE MATCH RATE CALIBRATION: VISA IMAGES . . . . .	127
94	FALSE MATCH RATE CALIBRATION: VISA IMAGES . . . . .	128
95	FALSE MATCH RATE CALIBRATION: VISA IMAGES . . . . .	129
96	FALSE MATCH RATE CALIBRATION: VISA IMAGES . . . . .	130
97	FALSE MATCH RATE CALIBRATION: VISA IMAGES . . . . .	131
98	FALSE MATCH RATE CALIBRATION: VISA IMAGES . . . . .	132
99	FALSE MATCH RATE CALIBRATION: VISA IMAGES . . . . .	133
100	FALSE MATCH RATE CALIBRATION: VISA IMAGES . . . . .	134
101	FALSE MATCH RATE CALIBRATION: VISA IMAGES . . . . .	135
102	FALSE MATCH RATE CALIBRATION: VISA IMAGES . . . . .	136
103	FALSE MATCH RATE CONCENTRATION: VISA IMAGES . . . . .	137
104	EFFECT OF COUNTRY OF BIRTH ON FNMR . . . . .	139
105	EFFECT OF COUNTRY OF BIRTH ON FNMR . . . . .	140
106	EFFECT OF COUNTRY OF BIRTH ON FNMR . . . . .	141
107	EFFECT OF COUNTRY OF BIRTH ON FNMR . . . . .	142
108	EFFECT OF COUNTRY OF BIRTH ON FNMR . . . . .	143
109	EFFECT OF COUNTRY OF BIRTH ON FNMR . . . . .	144
110	EFFECT OF COUNTRY OF BIRTH ON FNMR . . . . .	145
111	EFFECT OF COUNTRY OF BIRTH ON FNMR . . . . .	146
112	EFFECT OF COUNTRY OF BIRTH ON FNMR . . . . .	147
113	EFFECT OF COUNTRY OF BIRTH ON FNMR . . . . .	148
114	EFFECT OF COUNTRY OF BIRTH ON FNMR . . . . .	149
115	EFFECT OF COUNTRY OF BIRTH ON FNMR . . . . .	150
116	EFFECT OF COUNTRY OF BIRTH ON FNMR . . . . .	151
117	ERROR TRADEOFF CHARACTERISTIC: MUGSHOT IMAGES . . . . .	153

118	ERROR TRADEOFF CHARACTERISTIC: MUGSHOT IMAGES	154
119	ERROR TRADEOFF CHARACTERISTIC: MUGSHOT IMAGES	155
120	ERROR TRADEOFF CHARACTERISTIC: MUGSHOT IMAGES	156
121	ERROR TRADEOFF CHARACTERISTIC: MUGSHOT IMAGES	157
122	ERROR TRADEOFF CHARACTERISTIC: MUGSHOT IMAGES	158
123	ERROR TRADEOFF CHARACTERISTIC: MUGSHOT IMAGES	159
124	ERROR TRADEOFF CHARACTERISTIC: MUGSHOT IMAGES	160
125	ERROR TRADEOFF CHARACTERISTIC: MUGSHOT IMAGES	161
126	ERROR TRADEOFF CHARACTERISTIC: MUGSHOT IMAGES	162
127	EFFECT OF SUBJECT AGE ON FNMR	164
128	EFFECT OF SUBJECT AGE ON FNMR	165
129	EFFECT OF SUBJECT AGE ON FNMR	166
130	EFFECT OF SUBJECT AGE ON FNMR	167
131	EFFECT OF SUBJECT AGE ON FNMR	168
132	EFFECT OF SUBJECT AGE ON FNMR	169
133	EFFECT OF SUBJECT AGE ON FNMR	170
134	EFFECT OF SUBJECT AGE ON FNMR	171
135	EFFECT OF SUBJECT AGE ON FNMR	172
136	EFFECT OF SUBJECT AGE ON FNMR	173
137	EFFECT OF SUBJECT AGE ON FNMR	174
138	EFFECT OF SUBJECT AGE ON FNMR	175
139	EFFECT OF SUBJECT AGE ON FNMR	176
140	WORST CASE REGIONAL EFFECT FNMR	179
141	IMPOSTOR DISTRIBUTION SHIFTS FOR SELECT COUNTRY PAIRS	181
142	ALGORITHM 3DIVI-003 CROSS REGION FMR	182
143	ALGORITHM 3DIVI-004 CROSS REGION FMR	183
144	ALGORITHM ADERA-001 CROSS REGION FMR	184
145	ALGORITHM ALCHERA-000 CROSS REGION FMR	185
146	ALGORITHM ALCHERA-001 CROSS REGION FMR	186
147	ALGORITHM ALLGOVISION-000 CROSS REGION FMR	187
148	ALGORITHM ALPHAFACE-001 CROSS REGION FMR	188
149	ALGORITHM AMPLIFIEDGROUP-001 CROSS REGION FMR	189
150	ALGORITHM ANKE-003 CROSS REGION FMR	190
151	ALGORITHM ANKE-004 CROSS REGION FMR	191
152	ALGORITHM ANYVISION-002 CROSS REGION FMR	192
153	ALGORITHM ANYVISION-004 CROSS REGION FMR	193
154	ALGORITHM AWARE-003 CROSS REGION FMR	194
155	ALGORITHM AWARE-004 CROSS REGION FMR	195
156	ALGORITHM AWIROS-001 CROSS REGION FMR	196
157	ALGORITHM AYONIX-000 CROSS REGION FMR	197
158	ALGORITHM BM-001 CROSS REGION FMR	198
159	ALGORITHM CAMVI-002 CROSS REGION FMR	199
160	ALGORITHM CAMVI-004 CROSS REGION FMR	200
161	ALGORITHM CEIEC-001 CROSS REGION FMR	201
162	ALGORITHM CEIEC-002 CROSS REGION FMR	202
163	ALGORITHM CHTFACE-001 CROSS REGION FMR	203
164	ALGORITHM COGENT-003 CROSS REGION FMR	204
165	ALGORITHM COGENT-004 CROSS REGION FMR	205
166	ALGORITHM COGNITEC-000 CROSS REGION FMR	206
167	ALGORITHM COGNITEC-001 CROSS REGION FMR	207
168	ALGORITHM CTBCBANK-000 CROSS REGION FMR	208
169	ALGORITHM CYBEREXTRUDER-001 CROSS REGION FMR	209
170	ALGORITHM CYBEREXTRUDER-002 CROSS REGION FMR	210
171	ALGORITHM CYBERLINK-002 CROSS REGION FMR	211
172	ALGORITHM CYBERLINK-003 CROSS REGION FMR	212

173 ALGORITHM DAHUA-002 CROSS REGION FMR . . . . .	213
174 ALGORITHM DAHUA-003 CROSS REGION FMR . . . . .	214
175 ALGORITHM DEEPLINT-001 CROSS REGION FMR . . . . .	215
176 ALGORITHM DEEPSEA-001 CROSS REGION FMR . . . . .	216
177 ALGORITHM DERMALOG-005 CROSS REGION FMR . . . . .	217
178 ALGORITHM DERMALOG-006 CROSS REGION FMR . . . . .	218
179 ALGORITHM DIGITALBARRIERS-002 CROSS REGION FMR . . . . .	219
180 ALGORITHM DSK-000 CROSS REGION FMR . . . . .	220
181 ALGORITHM EINetworks-000 CROSS REGION FMR . . . . .	221
182 ALGORITHM EVERAI-002 CROSS REGION FMR . . . . .	222
183 ALGORITHM F8-001 CROSS REGION FMR . . . . .	223
184 ALGORITHM FACESOFT-000 CROSS REGION FMR . . . . .	224
185 ALGORITHM GLORY-000 CROSS REGION FMR . . . . .	225
186 ALGORITHM GLORY-001 CROSS REGION FMR . . . . .	226
187 ALGORITHM GORILLA-002 CROSS REGION FMR . . . . .	227
188 ALGORITHM GORILLA-003 CROSS REGION FMR . . . . .	228
189 ALGORITHM HIK-001 CROSS REGION FMR . . . . .	229
190 ALGORITHM HR-001 CROSS REGION FMR . . . . .	230
191 ALGORITHM HR-002 CROSS REGION FMR . . . . .	231
192 ALGORITHM ID3-003 CROSS REGION FMR . . . . .	232
193 ALGORITHM ID3-004 CROSS REGION FMR . . . . .	233
194 ALGORITHM IDEMIA-004 CROSS REGION FMR . . . . .	234
195 ALGORITHM IDEMIA-005 CROSS REGION FMR . . . . .	235
196 ALGORITHM IIT-000 CROSS REGION FMR . . . . .	236
197 ALGORITHM IIT-001 CROSS REGION FMR . . . . .	237
198 ALGORITHM IMAGUS-000 CROSS REGION FMR . . . . .	238
199 ALGORITHM IMPERIAL-000 CROSS REGION FMR . . . . .	239
200 ALGORITHM IMPERIAL-002 CROSS REGION FMR . . . . .	240
201 ALGORITHM INCODE-003 CROSS REGION FMR . . . . .	241
202 ALGORITHM INCODE-004 CROSS REGION FMR . . . . .	242
203 ALGORITHM INNOVATRICS-004 CROSS REGION FMR . . . . .	243
204 ALGORITHM INNOVATRICS-006 CROSS REGION FMR . . . . .	244
205 ALGORITHM INTELLICLOUDAI-001 CROSS REGION FMR . . . . .	245
206 ALGORITHM INTELLIFUSION-001 CROSS REGION FMR . . . . .	246
207 ALGORITHM INTELLIVISION-001 CROSS REGION FMR . . . . .	247
208 ALGORITHM INTELLIVISION-002 CROSS REGION FMR . . . . .	248
209 ALGORITHM INTELRESEARCH-000 CROSS REGION FMR . . . . .	249
210 ALGORITHM INTSYSMSU-000 CROSS REGION FMR . . . . .	250
211 ALGORITHM IQFACE-000 CROSS REGION FMR . . . . .	251
212 ALGORITHM ISAP-001 CROSS REGION FMR . . . . .	252
213 ALGORITHM ISITYOU-000 CROSS REGION FMR . . . . .	253
214 ALGORITHM ISYSTEMS-001 CROSS REGION FMR . . . . .	254
215 ALGORITHM ISYSTEMS-002 CROSS REGION FMR . . . . .	255
216 ALGORITHM ITMO-005 CROSS REGION FMR . . . . .	256
217 ALGORITHM ITMO-006 CROSS REGION FMR . . . . .	257
218 ALGORITHM KAKAO-001 CROSS REGION FMR . . . . .	258
219 ALGORITHM KAKAO-002 CROSS REGION FMR . . . . .	259
220 ALGORITHM KEDACOM-000 CROSS REGION FMR . . . . .	260
221 ALGORITHM KNERON-003 CROSS REGION FMR . . . . .	261
222 ALGORITHM LOOKMAN-002 CROSS REGION FMR . . . . .	262
223 ALGORITHM LOOKMAN-004 CROSS REGION FMR . . . . .	263
224 ALGORITHM MEGVII-001 CROSS REGION FMR . . . . .	264
225 ALGORITHM MEGVII-002 CROSS REGION FMR . . . . .	265
226 ALGORITHM MEIYA-001 CROSS REGION FMR . . . . .	266
227 ALGORITHM MICROFOCUS-001 CROSS REGION FMR . . . . .	267
228 ALGORITHM MICROFOCUS-002 CROSS REGION FMR . . . . .	268
229 ALGORITHM MT-000 CROSS REGION FMR . . . . .	269

230 ALGORITHM NEUROTECHNOLOGY-005 CROSS REGION FMR . . . . .	270
231 ALGORITHM NEUROTECHNOLOGY-006 CROSS REGION FMR . . . . .	271
232 ALGORITHM NODEFLUX-001 CROSS REGION FMR . . . . .	272
233 ALGORITHM NODEFLUX-002 CROSS REGION FMR . . . . .	273
234 ALGORITHM NOTIONTAG-000 CROSS REGION FMR . . . . .	274
235 ALGORITHM NTECHLAB-006 CROSS REGION FMR . . . . .	275
236 ALGORITHM NTECHLAB-007 CROSS REGION FMR . . . . .	276
237 ALGORITHM PIXELALL-002 CROSS REGION FMR . . . . .	277
238 ALGORITHM PSL-002 CROSS REGION FMR . . . . .	278
239 ALGORITHM PSL-003 CROSS REGION FMR . . . . .	279
240 ALGORITHM RANKONE-006 CROSS REGION FMR . . . . .	280
241 ALGORITHM RANKONE-007 CROSS REGION FMR . . . . .	281
242 ALGORITHM REALNETWORKS-002 CROSS REGION FMR . . . . .	282
243 ALGORITHM REALNETWORKS-003 CROSS REGION FMR . . . . .	283
244 ALGORITHM REMARKAI-000 CROSS REGION FMR . . . . .	284
245 ALGORITHM REMARKAI-001 CROSS REGION FMR . . . . .	285
246 ALGORITHM ROKID-000 CROSS REGION FMR . . . . .	286
247 ALGORITHM SAFFE-001 CROSS REGION FMR . . . . .	287
248 ALGORITHM SAFFE-002 CROSS REGION FMR . . . . .	288
249 ALGORITHM SENSETIME-001 CROSS REGION FMR . . . . .	289
250 ALGORITHM SENSETIME-002 CROSS REGION FMR . . . . .	290
251 ALGORITHM SERTIS-000 CROSS REGION FMR . . . . .	291
252 ALGORITHM SHAMAN-000 CROSS REGION FMR . . . . .	292
253 ALGORITHM SHAMAN-001 CROSS REGION FMR . . . . .	293
254 ALGORITHM SHU-001 CROSS REGION FMR . . . . .	294
255 ALGORITHM SIAT-002 CROSS REGION FMR . . . . .	295
256 ALGORITHM SIAT-004 CROSS REGION FMR . . . . .	296
257 ALGORITHM SJTU-001 CROSS REGION FMR . . . . .	297
258 ALGORITHM SMILART-002 CROSS REGION FMR . . . . .	298
259 ALGORITHM SMILART-003 CROSS REGION FMR . . . . .	299
260 ALGORITHM STARHYBRID-001 CROSS REGION FMR . . . . .	300
261 ALGORITHM SYNESIS-004 CROSS REGION FMR . . . . .	301
262 ALGORITHM SYNESIS-005 CROSS REGION FMR . . . . .	302
263 ALGORITHM TECH5-002 CROSS REGION FMR . . . . .	303
264 ALGORITHM TECH5-003 CROSS REGION FMR . . . . .	304
265 ALGORITHM TEVIAN-004 CROSS REGION FMR . . . . .	305
266 ALGORITHM TEVIAN-005 CROSS REGION FMR . . . . .	306
267 ALGORITHM TIGER-002 CROSS REGION FMR . . . . .	307
268 ALGORITHM TIGER-003 CROSS REGION FMR . . . . .	308
269 ALGORITHM TONGYI-005 CROSS REGION FMR . . . . .	309
270 ALGORITHM TOSHIBA-002 CROSS REGION FMR . . . . .	310
271 ALGORITHM TOSHIBA-003 CROSS REGION FMR . . . . .	311
272 ALGORITHM TRUEFACE-000 CROSS REGION FMR . . . . .	312
273 ALGORITHM ULSEE-001 CROSS REGION FMR . . . . .	313
274 ALGORITHM ULUFACE-002 CROSS REGION FMR . . . . .	314
275 ALGORITHM UPC-001 CROSS REGION FMR . . . . .	315
276 ALGORITHM VCOG-002 CROSS REGION FMR . . . . .	316
277 ALGORITHM VD-001 CROSS REGION FMR . . . . .	317
278 ALGORITHM VERIDAS-001 CROSS REGION FMR . . . . .	318
279 ALGORITHM VERIDAS-002 CROSS REGION FMR . . . . .	319
280 ALGORITHM VIA-000 CROSS REGION FMR . . . . .	320
281 ALGORITHM VIDEONETICS-001 CROSS REGION FMR . . . . .	321
282 ALGORITHM VIGILANTSOLUTIONS-006 CROSS REGION FMR . . . . .	322
283 ALGORITHM VIGILANTSOLUTIONS-007 CROSS REGION FMR . . . . .	323
284 ALGORITHM VION-000 CROSS REGION FMR . . . . .	324
285 ALGORITHM VISIONBOX-000 CROSS REGION FMR . . . . .	325
286 ALGORITHM VISIONBOX-001 CROSS REGION FMR . . . . .	326

287 ALGORITHM VISIONLABS-006 CROSS REGION FMR . . . . .	327
288 ALGORITHM VISIONLABS-007 CROSS REGION FMR . . . . .	328
289 ALGORITHM VOCORD-006 CROSS REGION FMR . . . . .	329
290 ALGORITHM VOCORD-007 CROSS REGION FMR . . . . .	330
291 ALGORITHM WINSENSE-000 CROSS REGION FMR . . . . .	331
292 ALGORITHM X-LABORATORY-000 CROSS REGION FMR . . . . .	332
293 ALGORITHM YISHENG-004 CROSS REGION FMR . . . . .	333
294 ALGORITHM YITU-003 CROSS REGION FMR . . . . .	334
295 ALGORITHM 3DIVI-003 CROSS COUNTRY FMR . . . . .	335
296 ALGORITHM 3DIVI-004 CROSS COUNTRY FMR . . . . .	336
297 ALGORITHM ADERA-001 CROSS COUNTRY FMR . . . . .	337
298 ALGORITHM ALCHERA-000 CROSS COUNTRY FMR . . . . .	338
299 ALGORITHM ALCHERA-001 CROSS COUNTRY FMR . . . . .	339
300 ALGORITHM ALLGOVISION-000 CROSS COUNTRY FMR . . . . .	340
301 ALGORITHM ALPHAFACE-001 CROSS COUNTRY FMR . . . . .	341
302 ALGORITHM AMPLIFIEDGROUP-001 CROSS COUNTRY FMR . . . . .	342
303 ALGORITHM ANKE-003 CROSS COUNTRY FMR . . . . .	343
304 ALGORITHM ANKE-004 CROSS COUNTRY FMR . . . . .	344
305 ALGORITHM ANYVISION-002 CROSS COUNTRY FMR . . . . .	345
306 ALGORITHM ANYVISION-004 CROSS COUNTRY FMR . . . . .	346
307 ALGORITHM AWARE-003 CROSS COUNTRY FMR . . . . .	347
308 ALGORITHM AWARE-004 CROSS COUNTRY FMR . . . . .	348
309 ALGORITHM AWIROS-001 CROSS COUNTRY FMR . . . . .	349
310 ALGORITHM AYONIX-000 CROSS COUNTRY FMR . . . . .	350
311 ALGORITHM BM-001 CROSS COUNTRY FMR . . . . .	351
312 ALGORITHM CAMVI-002 CROSS COUNTRY FMR . . . . .	352
313 ALGORITHM CAMVI-004 CROSS COUNTRY FMR . . . . .	353
314 ALGORITHM CEIEC-001 CROSS COUNTRY FMR . . . . .	354
315 ALGORITHM CEIEC-002 CROSS COUNTRY FMR . . . . .	355
316 ALGORITHM CHTFACE-001 CROSS COUNTRY FMR . . . . .	356
317 ALGORITHM COGENT-003 CROSS COUNTRY FMR . . . . .	357
318 ALGORITHM COGENT-004 CROSS COUNTRY FMR . . . . .	358
319 ALGORITHM COGNITEC-000 CROSS COUNTRY FMR . . . . .	359
320 ALGORITHM COGNITEC-001 CROSS COUNTRY FMR . . . . .	360
321 ALGORITHM CTBCBANK-000 CROSS COUNTRY FMR . . . . .	361
322 ALGORITHM CYBEREXTRUDER-001 CROSS COUNTRY FMR . . . . .	362
323 ALGORITHM CYBEREXTRUDER-002 CROSS COUNTRY FMR . . . . .	363
324 ALGORITHM CYBERLINK-002 CROSS COUNTRY FMR . . . . .	364
325 ALGORITHM DAHUA-002 CROSS COUNTRY FMR . . . . .	365
326 ALGORITHM DAHUA-003 CROSS COUNTRY FMR . . . . .	366
327 ALGORITHM DEEPLINT-001 CROSS COUNTRY FMR . . . . .	367
328 ALGORITHM DEEPSEA-001 CROSS COUNTRY FMR . . . . .	368
329 ALGORITHM DERMALOG-005 CROSS COUNTRY FMR . . . . .	369
330 ALGORITHM DERMALOG-006 CROSS COUNTRY FMR . . . . .	370
331 ALGORITHM DIGITALBARRIERS-002 CROSS COUNTRY FMR . . . . .	371
332 ALGORITHM DSK-000 CROSS COUNTRY FMR . . . . .	372
333 ALGORITHM EINETWORKS-000 CROSS COUNTRY FMR . . . . .	373
334 ALGORITHM EVERAI-002 CROSS COUNTRY FMR . . . . .	374
335 ALGORITHM F8-001 CROSS COUNTRY FMR . . . . .	375
336 ALGORITHM FACESOFT-000 CROSS COUNTRY FMR . . . . .	376
337 ALGORITHM GLORY-000 CROSS COUNTRY FMR . . . . .	377
338 ALGORITHM GLORY-001 CROSS COUNTRY FMR . . . . .	378
339 ALGORITHM GORILLA-002 CROSS COUNTRY FMR . . . . .	379
340 ALGORITHM GORILLA-003 CROSS COUNTRY FMR . . . . .	380
341 ALGORITHM HIK-001 CROSS COUNTRY FMR . . . . .	381
342 ALGORITHM HR-001 CROSS COUNTRY FMR . . . . .	382
343 ALGORITHM HR-002 CROSS COUNTRY FMR . . . . .	383

344 ALGORITHM ID3-003 CROSS COUNTRY FMR . . . . .	384
345 ALGORITHM ID3-004 CROSS COUNTRY FMR . . . . .	385
346 ALGORITHM IDEMIA-004 CROSS COUNTRY FMR . . . . .	386
347 ALGORITHM IDEMIA-005 CROSS COUNTRY FMR . . . . .	387
348 ALGORITHM IIT-000 CROSS COUNTRY FMR . . . . .	388
349 ALGORITHM IIT-001 CROSS COUNTRY FMR . . . . .	389
350 ALGORITHM IMAGUS-000 CROSS COUNTRY FMR . . . . .	390
351 ALGORITHM IMPERIAL-000 CROSS COUNTRY FMR . . . . .	391
352 ALGORITHM IMPERIAL-002 CROSS COUNTRY FMR . . . . .	392
353 ALGORITHM INCODE-003 CROSS COUNTRY FMR . . . . .	393
354 ALGORITHM INCODE-004 CROSS COUNTRY FMR . . . . .	394
355 ALGORITHM INNOVATRICS-004 CROSS COUNTRY FMR . . . . .	395
356 ALGORITHM INNOVATRICS-006 CROSS COUNTRY FMR . . . . .	396
357 ALGORITHM INTELLICLOUDAI-001 CROSS COUNTRY FMR . . . . .	397
358 ALGORITHM INTELLIFUSION-001 CROSS COUNTRY FMR . . . . .	398
359 ALGORITHM INTELLIVISION-001 CROSS COUNTRY FMR . . . . .	399
360 ALGORITHM INTELLIVISION-002 CROSS COUNTRY FMR . . . . .	400
361 ALGORITHM INTELRESEARCH-000 CROSS COUNTRY FMR . . . . .	401
362 ALGORITHM INTSYSMSU-000 CROSS COUNTRY FMR . . . . .	402
363 ALGORITHM IQFACE-000 CROSS COUNTRY FMR . . . . .	403
364 ALGORITHM ISAP-001 CROSS COUNTRY FMR . . . . .	404
365 ALGORITHM ISITYOU-000 CROSS COUNTRY FMR . . . . .	405
366 ALGORITHM ISYSTEMS-001 CROSS COUNTRY FMR . . . . .	406
367 ALGORITHM ISYSTEMS-002 CROSS COUNTRY FMR . . . . .	407
368 ALGORITHM ITMO-005 CROSS COUNTRY FMR . . . . .	408
369 ALGORITHM ITMO-006 CROSS COUNTRY FMR . . . . .	409
370 ALGORITHM KAKAO-001 CROSS COUNTRY FMR . . . . .	410
371 ALGORITHM KAKAO-002 CROSS COUNTRY FMR . . . . .	411
372 ALGORITHM KEDACOM-000 CROSS COUNTRY FMR . . . . .	412
373 ALGORITHM KNERON-003 CROSS COUNTRY FMR . . . . .	413
374 ALGORITHM LOOKMAN-002 CROSS COUNTRY FMR . . . . .	414
375 ALGORITHM LOOKMAN-004 CROSS COUNTRY FMR . . . . .	415
376 ALGORITHM MEGVII-001 CROSS COUNTRY FMR . . . . .	416
377 ALGORITHM MEGVII-002 CROSS COUNTRY FMR . . . . .	417
378 ALGORITHM MEIYA-001 CROSS COUNTRY FMR . . . . .	418
379 ALGORITHM MICROFOCUS-001 CROSS COUNTRY FMR . . . . .	419
380 ALGORITHM MICROFOCUS-002 CROSS COUNTRY FMR . . . . .	420
381 ALGORITHM MT-000 CROSS COUNTRY FMR . . . . .	421
382 ALGORITHM NEUROTECHNOLOGY-005 CROSS COUNTRY FMR . . . . .	422
383 ALGORITHM NEUROTECHNOLOGY-006 CROSS COUNTRY FMR . . . . .	423
384 ALGORITHM NODEFLUX-001 CROSS COUNTRY FMR . . . . .	424
385 ALGORITHM NODEFLUX-002 CROSS COUNTRY FMR . . . . .	425
386 ALGORITHM NOTIONTAG-000 CROSS COUNTRY FMR . . . . .	426
387 ALGORITHM NTECHLAB-006 CROSS COUNTRY FMR . . . . .	427
388 ALGORITHM NTECHLAB-007 CROSS COUNTRY FMR . . . . .	428
389 ALGORITHM PIXELALL-002 CROSS COUNTRY FMR . . . . .	429
390 ALGORITHM PSL-002 CROSS COUNTRY FMR . . . . .	430
391 ALGORITHM RANKONE-006 CROSS COUNTRY FMR . . . . .	431
392 ALGORITHM RANKONE-007 CROSS COUNTRY FMR . . . . .	432
393 ALGORITHM REALNETWORKS-002 CROSS COUNTRY FMR . . . . .	433
394 ALGORITHM REALNETWORKS-003 CROSS COUNTRY FMR . . . . .	434
395 ALGORITHM REMARKAI-000 CROSS COUNTRY FMR . . . . .	435
396 ALGORITHM REMARKAI-001 CROSS COUNTRY FMR . . . . .	436
397 ALGORITHM ROKID-000 CROSS COUNTRY FMR . . . . .	437
398 ALGORITHM SAFFE-001 CROSS COUNTRY FMR . . . . .	438
399 ALGORITHM SAFFE-002 CROSS COUNTRY FMR . . . . .	439

400 ALGORITHM SENSETIME-001 CROSS COUNTRY FMR . . . . .	440
401 ALGORITHM SENSETIME-002 CROSS COUNTRY FMR . . . . .	441
402 ALGORITHM SHAMAN-000 CROSS COUNTRY FMR . . . . .	442
403 ALGORITHM SHAMAN-001 CROSS COUNTRY FMR . . . . .	443
404 ALGORITHM SHU-001 CROSS COUNTRY FMR . . . . .	444
405 ALGORITHM SIAT-002 CROSS COUNTRY FMR . . . . .	445
406 ALGORITHM SIAT-004 CROSS COUNTRY FMR . . . . .	446
407 ALGORITHM SJTU-001 CROSS COUNTRY FMR . . . . .	447
408 ALGORITHM SMILART-002 CROSS COUNTRY FMR . . . . .	448
409 ALGORITHM SMILART-003 CROSS COUNTRY FMR . . . . .	449
410 ALGORITHM STARHYBRID-001 CROSS COUNTRY FMR . . . . .	450
411 ALGORITHM SYNESIS-004 CROSS COUNTRY FMR . . . . .	451
412 ALGORITHM SYNESIS-005 CROSS COUNTRY FMR . . . . .	452
413 ALGORITHM TECH5-002 CROSS COUNTRY FMR . . . . .	453
414 ALGORITHM TECH5-003 CROSS COUNTRY FMR . . . . .	454
415 ALGORITHM TEVIAN-004 CROSS COUNTRY FMR . . . . .	455
416 ALGORITHM TIGER-002 CROSS COUNTRY FMR . . . . .	456
417 ALGORITHM TIGER-003 CROSS COUNTRY FMR . . . . .	457
418 ALGORITHM TONGYI-005 CROSS COUNTRY FMR . . . . .	458
419 ALGORITHM TOSHIBA-002 CROSS COUNTRY FMR . . . . .	459
420 ALGORITHM TOSHIBA-003 CROSS COUNTRY FMR . . . . .	460
421 ALGORITHM TRUEFACE-000 CROSS COUNTRY FMR . . . . .	461
422 ALGORITHM ULSEE-001 CROSS COUNTRY FMR . . . . .	462
423 ALGORITHM ULUFACE-002 CROSS COUNTRY FMR . . . . .	463
424 ALGORITHM UPC-001 CROSS COUNTRY FMR . . . . .	464
425 ALGORITHM VCOG-002 CROSS COUNTRY FMR . . . . .	465
426 ALGORITHM VD-001 CROSS COUNTRY FMR . . . . .	466
427 ALGORITHM VERIDAS-001 CROSS COUNTRY FMR . . . . .	467
428 ALGORITHM VERIDAS-002 CROSS COUNTRY FMR . . . . .	468
429 ALGORITHM VIA-000 CROSS COUNTRY FMR . . . . .	469
430 ALGORITHM VIDEONETICS-001 CROSS COUNTRY FMR . . . . .	470
431 ALGORITHM VIGILANTSOLUTIONS-006 CROSS COUNTRY FMR . . . . .	471
432 ALGORITHM VIGILANTSOLUTIONS-007 CROSS COUNTRY FMR . . . . .	472
433 ALGORITHM VION-000 CROSS COUNTRY FMR . . . . .	473
434 ALGORITHM VISIONBOX-000 CROSS COUNTRY FMR . . . . .	474
435 ALGORITHM VISIONBOX-001 CROSS COUNTRY FMR . . . . .	475
436 ALGORITHM VISIONLABS-006 CROSS COUNTRY FMR . . . . .	476
437 ALGORITHM VISIONLABS-007 CROSS COUNTRY FMR . . . . .	477
438 ALGORITHM VOCORD-006 CROSS COUNTRY FMR . . . . .	478
439 ALGORITHM VOCORD-007 CROSS COUNTRY FMR . . . . .	479
440 ALGORITHM WINSENSE-000 CROSS COUNTRY FMR . . . . .	480
441 ALGORITHM X-LABORATORY-000 CROSS COUNTRY FMR . . . . .	481
442 ALGORITHM YISHENG-004 CROSS COUNTRY FMR . . . . .	482
443 ALGORITHM YITU-003 CROSS COUNTRY FMR . . . . .	483
444 IMPOSTOR COUNTS FOR CROSS COUNTRY FMR CALCULATIONS . . . . .	484
445 ALGORITHM 3DIVI-003 CROSS AGE FMR . . . . .	486
446 ALGORITHM 3DIVI-004 CROSS AGE FMR . . . . .	487
447 ALGORITHM ADERA-001 CROSS AGE FMR . . . . .	488
448 ALGORITHM ALCHERA-000 CROSS AGE FMR . . . . .	489
449 ALGORITHM ALCHERA-001 CROSS AGE FMR . . . . .	490
450 ALGORITHM ALLGOVISION-000 CROSS AGE FMR . . . . .	491
451 ALGORITHM ALPHAFACE-001 CROSS AGE FMR . . . . .	492
452 ALGORITHM AMPLIFIEDGROUP-001 CROSS AGE FMR . . . . .	493
453 ALGORITHM ANKE-003 CROSS AGE FMR . . . . .	494
454 ALGORITHM ANKE-004 CROSS AGE FMR . . . . .	495
455 ALGORITHM ANYVISION-002 CROSS AGE FMR . . . . .	496

456 ALGORITHM ANYVISION-004 CROSS AGE FMR . . . . .	497
457 ALGORITHM AWARE-003 CROSS AGE FMR . . . . .	498
458 ALGORITHM AWARE-004 CROSS AGE FMR . . . . .	499
459 ALGORITHM AWIROS-001 CROSS AGE FMR . . . . .	500
460 ALGORITHM AYONIX-000 CROSS AGE FMR . . . . .	501
461 ALGORITHM BM-001 CROSS AGE FMR . . . . .	502
462 ALGORITHM CAMVI-002 CROSS AGE FMR . . . . .	503
463 ALGORITHM CAMVI-004 CROSS AGE FMR . . . . .	504
464 ALGORITHM CEIEC-001 CROSS AGE FMR . . . . .	505
465 ALGORITHM CEIEC-002 CROSS AGE FMR . . . . .	506
466 ALGORITHM CHTFACE-001 CROSS AGE FMR . . . . .	507
467 ALGORITHM COGENT-003 CROSS AGE FMR . . . . .	508
468 ALGORITHM COGENT-004 CROSS AGE FMR . . . . .	509
469 ALGORITHM COGNITEC-000 CROSS AGE FMR . . . . .	510
470 ALGORITHM COGNITEC-001 CROSS AGE FMR . . . . .	511
471 ALGORITHM CTBCBANK-000 CROSS AGE FMR . . . . .	512
472 ALGORITHM CYBEREXTRUDER-001 CROSS AGE FMR . . . . .	513
473 ALGORITHM CYBEREXTRUDER-002 CROSS AGE FMR . . . . .	514
474 ALGORITHM CYBERLINK-002 CROSS AGE FMR . . . . .	515
475 ALGORITHM CYBERLINK-003 CROSS AGE FMR . . . . .	516
476 ALGORITHM DAHUA-002 CROSS AGE FMR . . . . .	517
477 ALGORITHM DAHUA-003 CROSS AGE FMR . . . . .	518
478 ALGORITHM DEEPLINT-001 CROSS AGE FMR . . . . .	519
479 ALGORITHM DEEPSEA-001 CROSS AGE FMR . . . . .	520
480 ALGORITHM DERMALOG-005 CROSS AGE FMR . . . . .	521
481 ALGORITHM DERMALOG-006 CROSS AGE FMR . . . . .	522
482 ALGORITHM DIGITALBARRIERS-002 CROSS AGE FMR . . . . .	523
483 ALGORITHM DSK-000 CROSS AGE FMR . . . . .	524
484 ALGORITHM EINETWORKS-000 CROSS AGE FMR . . . . .	525
485 ALGORITHM EVERAI-002 CROSS AGE FMR . . . . .	526
486 ALGORITHM F8-001 CROSS AGE FMR . . . . .	527
487 ALGORITHM FACESOFT-000 CROSS AGE FMR . . . . .	528
488 ALGORITHM GLORY-000 CROSS AGE FMR . . . . .	529
489 ALGORITHM GLORY-001 CROSS AGE FMR . . . . .	530
490 ALGORITHM GORILLA-002 CROSS AGE FMR . . . . .	531
491 ALGORITHM GORILLA-003 CROSS AGE FMR . . . . .	532
492 ALGORITHM HIK-001 CROSS AGE FMR . . . . .	533
493 ALGORITHM HR-001 CROSS AGE FMR . . . . .	534
494 ALGORITHM HR-002 CROSS AGE FMR . . . . .	535
495 ALGORITHM ID3-003 CROSS AGE FMR . . . . .	536
496 ALGORITHM ID3-004 CROSS AGE FMR . . . . .	537
497 ALGORITHM IDEMIA-004 CROSS AGE FMR . . . . .	538
498 ALGORITHM IDEMIA-005 CROSS AGE FMR . . . . .	539
499 ALGORITHM IIT-000 CROSS AGE FMR . . . . .	540
500 ALGORITHM IIT-001 CROSS AGE FMR . . . . .	541
501 ALGORITHM IMAGUS-000 CROSS AGE FMR . . . . .	542
502 ALGORITHM IMPERIAL-000 CROSS AGE FMR . . . . .	543
503 ALGORITHM IMPERIAL-002 CROSS AGE FMR . . . . .	544
504 ALGORITHM INCODE-003 CROSS AGE FMR . . . . .	545
505 ALGORITHM INCODE-004 CROSS AGE FMR . . . . .	546
506 ALGORITHM INNOVATRICS-004 CROSS AGE FMR . . . . .	547
507 ALGORITHM INNOVATRICS-006 CROSS AGE FMR . . . . .	548
508 ALGORITHM INTELLICLOUDAI-001 CROSS AGE FMR . . . . .	549
509 ALGORITHM INTELLIFUSION-001 CROSS AGE FMR . . . . .	550
510 ALGORITHM INTELLIVISION-001 CROSS AGE FMR . . . . .	551
511 ALGORITHM INTELLIVISION-002 CROSS AGE FMR . . . . .	552
512 ALGORITHM INTELRESEARCH-000 CROSS AGE FMR . . . . .	553

513 ALGORITHM INTSYSMSU-000 CROSS AGE FMR . . . . .	554
514 ALGORITHM IQFACE-000 CROSS AGE FMR . . . . .	555
515 ALGORITHM ISAP-001 CROSS AGE FMR . . . . .	556
516 ALGORITHM ISITYOU-000 CROSS AGE FMR . . . . .	557
517 ALGORITHM ISYSTEMS-001 CROSS AGE FMR . . . . .	558
518 ALGORITHM ISYSTEMS-002 CROSS AGE FMR . . . . .	559
519 ALGORITHM ITMO-005 CROSS AGE FMR . . . . .	560
520 ALGORITHM ITMO-006 CROSS AGE FMR . . . . .	561
521 ALGORITHM KAKAO-001 CROSS AGE FMR . . . . .	562
522 ALGORITHM KAKAO-002 CROSS AGE FMR . . . . .	563
523 ALGORITHM KEDACOM-000 CROSS AGE FMR . . . . .	564
524 ALGORITHM KNERON-003 CROSS AGE FMR . . . . .	565
525 ALGORITHM LOOKMAN-002 CROSS AGE FMR . . . . .	566
526 ALGORITHM LOOKMAN-004 CROSS AGE FMR . . . . .	567
527 ALGORITHM MEGVII-001 CROSS AGE FMR . . . . .	568
528 ALGORITHM MEGVII-002 CROSS AGE FMR . . . . .	569
529 ALGORITHM MEIYA-001 CROSS AGE FMR . . . . .	570
530 ALGORITHM MICROFOCUS-001 CROSS AGE FMR . . . . .	571
531 ALGORITHM MICROFOCUS-002 CROSS AGE FMR . . . . .	572
532 ALGORITHM MT-000 CROSS AGE FMR . . . . .	573
533 ALGORITHM NEUROTECHNOLOGY-005 CROSS AGE FMR . . . . .	574
534 ALGORITHM NEUROTECHNOLOGY-006 CROSS AGE FMR . . . . .	575
535 ALGORITHM NODEFLUX-001 CROSS AGE FMR . . . . .	576
536 ALGORITHM NODEFLUX-002 CROSS AGE FMR . . . . .	577
537 ALGORITHM NOTIONTAG-000 CROSS AGE FMR . . . . .	578
538 ALGORITHM NTECHLAB-006 CROSS AGE FMR . . . . .	579
539 ALGORITHM NTECHLAB-007 CROSS AGE FMR . . . . .	580
540 ALGORITHM PIXELALL-002 CROSS AGE FMR . . . . .	581
541 ALGORITHM PSL-002 CROSS AGE FMR . . . . .	582
542 ALGORITHM PSL-003 CROSS AGE FMR . . . . .	583
543 ALGORITHM RANKONE-006 CROSS AGE FMR . . . . .	584
544 ALGORITHM RANKONE-007 CROSS AGE FMR . . . . .	585
545 ALGORITHM REALNETWORKS-002 CROSS AGE FMR . . . . .	586
546 ALGORITHM REALNETWORKS-003 CROSS AGE FMR . . . . .	587
547 ALGORITHM REMARKAI-000 CROSS AGE FMR . . . . .	588
548 ALGORITHM REMARKAI-001 CROSS AGE FMR . . . . .	589
549 ALGORITHM ROKID-000 CROSS AGE FMR . . . . .	590
550 ALGORITHM SAFFE-001 CROSS AGE FMR . . . . .	591
551 ALGORITHM SAFFE-002 CROSS AGE FMR . . . . .	592
552 ALGORITHM SENSETIME-001 CROSS AGE FMR . . . . .	593
553 ALGORITHM SENSETIME-002 CROSS AGE FMR . . . . .	594
554 ALGORITHM SERTIS-000 CROSS AGE FMR . . . . .	595
555 ALGORITHM SHAMAN-000 CROSS AGE FMR . . . . .	596
556 ALGORITHM SHAMAN-001 CROSS AGE FMR . . . . .	597
557 ALGORITHM SHU-001 CROSS AGE FMR . . . . .	598
558 ALGORITHM SIAT-002 CROSS AGE FMR . . . . .	599
559 ALGORITHM SIAT-004 CROSS AGE FMR . . . . .	600
560 ALGORITHM SJTU-001 CROSS AGE FMR . . . . .	601
561 ALGORITHM SMILART-002 CROSS AGE FMR . . . . .	602
562 ALGORITHM SMILART-003 CROSS AGE FMR . . . . .	603
563 ALGORITHM STARHYBRID-001 CROSS AGE FMR . . . . .	604
564 ALGORITHM SYNESIS-004 CROSS AGE FMR . . . . .	605
565 ALGORITHM SYNESIS-005 CROSS AGE FMR . . . . .	606
566 ALGORITHM TECH5-002 CROSS AGE FMR . . . . .	607
567 ALGORITHM TECH5-003 CROSS AGE FMR . . . . .	608
568 ALGORITHM TEVIAN-004 CROSS AGE FMR . . . . .	609
569 ALGORITHM TEVIAN-005 CROSS AGE FMR . . . . .	610

570 ALGORITHM TIGER-002 CROSS AGE FMR . . . . .	611
571 ALGORITHM TIGER-003 CROSS AGE FMR . . . . .	612
572 ALGORITHM TONGYI-005 CROSS AGE FMR . . . . .	613
573 ALGORITHM TOSHIBA-002 CROSS AGE FMR . . . . .	614
574 ALGORITHM TOSHIBA-003 CROSS AGE FMR . . . . .	615
575 ALGORITHM TRUEFACE-000 CROSS AGE FMR . . . . .	616
576 ALGORITHM ULSEE-001 CROSS AGE FMR . . . . .	617
577 ALGORITHM ULUFACE-002 CROSS AGE FMR . . . . .	618
578 ALGORITHM UPC-001 CROSS AGE FMR . . . . .	619
579 ALGORITHM VCOG-002 CROSS AGE FMR . . . . .	620
580 ALGORITHM VD-001 CROSS AGE FMR . . . . .	621
581 ALGORITHM VERIDAS-001 CROSS AGE FMR . . . . .	622
582 ALGORITHM VERIDAS-002 CROSS AGE FMR . . . . .	623
583 ALGORITHM VIA-000 CROSS AGE FMR . . . . .	624
584 ALGORITHM VIDEONETICS-001 CROSS AGE FMR . . . . .	625
585 ALGORITHM VIGILANTSOLUTIONS-006 CROSS AGE FMR . . . . .	626
586 ALGORITHM VIGILANTSOLUTIONS-007 CROSS AGE FMR . . . . .	627
587 ALGORITHM VION-000 CROSS AGE FMR . . . . .	628
588 ALGORITHM VISIONBOX-000 CROSS AGE FMR . . . . .	629
589 ALGORITHM VISIONBOX-001 CROSS AGE FMR . . . . .	630
590 ALGORITHM VISIONLABS-006 CROSS AGE FMR . . . . .	631
591 ALGORITHM VISIONLABS-007 CROSS AGE FMR . . . . .	632
592 ALGORITHM VOCORD-006 CROSS AGE FMR . . . . .	633
593 ALGORITHM VOCORD-007 CROSS AGE FMR . . . . .	634
594 ALGORITHM WINSENSE-000 CROSS AGE FMR . . . . .	635
595 ALGORITHM X-LABORATORY-000 CROSS AGE FMR . . . . .	636
596 ALGORITHM YISHENG-004 CROSS AGE FMR . . . . .	637
597 ALGORITHM YITU-003 CROSS AGE FMR . . . . .	638

	Developer	Short	Seq.	Validation	Config <sup>1</sup>	Template		GPU	Comparison Time (ns) <sup>3</sup>
	Name	Name	Num.	Date	Data (KB)	Size (B)	Time (ms) <sup>2</sup>	Genuine	Impostor
1	3DiVi	3divi	003	2018-10-09	191636	146 4096 ± 0	97 650 ± 90	No	20 627 ± 11    24 623 ± 32
2	3DiVi	3divi	004	2019-07-22	263670	80 2048 ± 0	154 984 ± 131	No	33 794 ± 35    35 801 ± 40
3	Adera Global PTE Ltd	aderा	001	2019-06-17	0	135 2560 ± 0	497 ± 0	No	68 1604 ± 71    69 1649 ± 56
4	Alchera	alchera	000	2019-03-01	258450	72 2048 ± 0	85 587 ± 13	No	98 3189 ± 32    96 3031 ± 142
5	Alchera	alchera	000	2019-03-01	174013	70 2048 ± 0	91 627 ± 11	No	100 3342 ± 81    99 3243 ± 47
6	AllGoVision	allgovision	000	2019-03-01	172509	92 2048 ± 0	54 384 ± 8	No	145 29903 ± 406    146 29735 ± 194
7	AlphaSSTG	alphaface	001	2019-09-03	259849	76 2048 ± 0	88 613 ± 3	No	102 3482 ± 41    101 3279 ± 91
8	Amplified Group	amplifiedgroup	001	2019-03-01	0	29 866 ± 2	393 ± 0	No	149 57803 ± 4210    149 56365 ± 1196
9	Anke Investments	anke	003	2019-02-27	340160	121 2056 ± 0	131 811 ± 23	No	6 425 ± 28    8 437 ± 32
10	Anke Investments	anke	004	2019-06-27	349388	119 2056 ± 0	90 625 ± 1	No	21 633 ± 22    26 632 ± 34
11	AnyVision	anyvision	002	2018-01-31	662659	38 1024 ± 0	24 248 ± 0	No	150 74069 ± 188    150 74019 ± 198
12	AnyVision	anyvision	004	2018-06-15	401001	34 1024 ± 0	47 355 ± 1	No	76 1891 ± 51    73 1829 ± 85
13	Aware	aware	003	2018-10-19	377729	138 3108 ± 0	128 783 ± 10	No	60 1392 ± 42    62 1334 ± 80
14	Aware	aware	004	2019-03-01	427829	131 2084 ± 0	147 900 ± 10	No	56 1279 ± 50    61 1287 ± 100
15	Awudit Systems	awiros	001	2019-09-23	15499	16 512 ± 0	599 ± 8	No	74 1868 ± 100    89 2467 ± 78
16	Ayonix	ayonix	000	2017-06-22	58505	39 1036 ± 0	18 8 ± 2	No	19 621 ± 23    23 620 ± 26
17	Bitmain	bitmain	001	2018-10-17	287734	1 64 ± 0	61 444 ± 88	No	75 1887 ± 31    75 1877 ± 26
18	Camvi Technologies	camvitech	002	2018-10-19	236278	36 1024 ± 0	110 677 ± 7	No	18 612 ± 26    19 603 ± 20
19	Camvi Technologies	camvitech	004	2019-07-12	280733	86 2048 ± 0	124 759 ± 10	No	39 948 ± 40    41 963 ± 31
20	China Electronics Import-Export Corp	ceiec	001	2019-03-01	159618	37 1024 ± 0	40 314 ± 3	No	142 22831 ± 108    142 22813 ± 120
21	China Electronics Import-Export Corp	ceiec	002	2019-06-12	269063	69 2048 ± 0	87 612 ± 17	No	84 2188 ± 57    83 2301 ± 56
22	Chunghwa Telecom Co. Ltd	chtface	001	2019-08-06	94088	88 2048 ± 0	20 218 ± 12	No	81 2089 ± 45    80 2087 ± 23
23	Gemalto Cogent	cogent	003	2019-03-01	698290	30 973 ± 0	152 952 ± 0	No	131 12496 ± 75    130 11822 ± 163
24	Gemalto Cogent	cogent	004	2019-06-14	722919	57 1983 ± 0	151 941 ± 28	No	134 14448 ± 56    136 15882 ± 81
25	Cognitec Systems GmbH	cognitec	000	2018-10-19	474759	109 2052 ± 0	21 224 ± 1	No	108 3835 ± 108    106 3782 ± 83
26	Cognitec Systems GmbH	cognitec	001	2019-03-01	476809	115 2052 ± 0	36 297 ± 17	No	112 4253 ± 59    111 4102 ± 167
27	CTBC Bank Co. Ltd	ctbcbank	000	2019-06-28	257208	73 2048 ± 0	82 568 ± 43	No	104 3551 ± 87    114 4805 ± 209
28	Cyberextruder	cyberex	001	2017-08-02	121211	9 256 ± 0	146 893 ± 25	No	46 1083 ± 16    49 1079 ± 19
29	Cyberextruder	cyberex	002	2018-01-30	168909	60 2048 ± 0	71 532 ± 6	No	73 1803 ± 14    72 1779 ± 22
30	Cyberlink Corp	cyberlink	002	2019-06-12	222311	111 2052 ± 0	102 656 ± 22	No	86 2264 ± 71    93 2649 ± 195
31	Cyberlink Corp	cyberlink	002	2019-10-07	470949	108 2052 ± 0	59 424 ± 1	No	115 4857 ± 53    116 5168 ± 69
32	Dahua Technology Co. Ltd	dahua	002	2019-03-01	526452	71 2048 ± 0	92 628 ± 7	No	84 461 ± 23    10 454 ± 20
33	Dahua Technology Co. Ltd	dahua	003	2019-08-14	605337	87 2048 ± 0	73 537 ± 4	No	24 653 ± 28    20 606 ± 38
34	Deepglint	deepglint	001	2019-06-21	569802	143 4096 ± 0	115 721 ± 4	No	105 3680 ± 35    103 3517 ± 182
35	Tencent Deepsea Lab	deepsea	001	2019-06-03	147497	31 1024 ± 0	93 630 ± 7	No	62 1401 ± 37    65 1467 ± 50
36	Dermalog	dermalog	005	2018-02-02	0	2 128 ± 0	7 130 ± 11	No	11 499 ± 22    13 500 ± 22
37	Dermalog	dermalog	006	2018-10-18	0	3 128 ± 0	70 532 ± 12	No	12 506 ± 23    11 459 ± 23
38	Digital Barriers	barriers	002	2019-03-01	83002	122 2056 ± 0	17 209 ± 11	No	133 13409 ± 228    133 13267 ± 206
39	DSK	dsk	000	2019-06-28	11967	18 512 ± 0	38 304 ± 47	No	125 7152 ± 115    124 7134 ± 111
40	Shenzhen EI Networks Limited	einetworks	000	2019-08-13	372608	126 2056 ± 0	96 645 ± 3	No	116 4876 ± 66    115 5156 ± 77
41	Ever AI	everai	002	2019-03-01	561727	148 4096 ± 0	122 758 ± 0	No	23 644 ± 14    25 624 ± 35
42	Ever AI Paravision	everai paravision	003	2019-07-01	539802	142 4096 ± 0	108 674 ± 4	No	29 699 ± 20    30 713 ± 47
43	FarBar Inc.	f8	001	2019-07-11	272977	68 2048 ± 0	133 822 ± 39	No	135 15262 ± 139    135 15277 ± 212
44	FaceSoft Ltd.	facesoft	000	2019-07-10	370120	103 2048 ± 0	109 675 ± 18	No	85 2239 ± 28    82 2277 ± 96

## Notes

- 1 The configuration size does not capture static data included in libraries. We do not count these because some algorithms include common ancillary libraries for image processing (e.g. openCV) or numerical computation (e.g. blas).
- 2 The median template creation times are measured on Intel® Xeon® CPU E5-2630 v4 @ 2.20GHz processors or, for GPU-enabled implementations, NVidia Tesla K40.
- 3 The comparison durations, in nanoseconds, are estimated using std::chrono::high\_resolution\_clock which on the machine in (2) counts 1ns clock ticks. Precision is somewhat worse than that however. The ± value is the median absolute deviation times 1.48 for Normal consistency.

Table 1: Summary of algorithms and properties included in this report. The red superscripts give ranking for the quantity in that column.

	Developer	Short	Seq.	Validation	Config <sup>1</sup>	Template		GPU	Comparison Time (ns) <sup>3</sup>				
						Name	Num.		Date	Data (KB)	Size (B)	Time (ms) <sup>2</sup>	Genuine
45	Glory Ltd	glory	000	2018-06-06	0	14	418 ± 0	9165 ± 2	No	124	7003 ± 84	122	6978 ± 71
46	Glory Ltd	glory	001	2018-06-08	0	54	1726 ± 0	56393 ± 2	No	129	9607 ± 128	128	9539 ± 182
47	Gorilla Technology	gorilla	002	2018-10-17	93869	43	1132 ± 0	43322 ± 14	No	93	2715 ± 68	92	2585 ± 84
48	Gorilla Technology	gorilla	003	2019-06-19	94409	42	1132 ± 0	45334 ± 25	No	94	2840 ± 42	94	2865 ± 87
49	Hikvision	hik	001	2019-03-01	667866	47	1408 ± 0	98651 ± 0	No	10	488 ± 19	12	477 ± 22
50	Hengrui AI Technology Ltd	hr	001	2019-06-04	346156	128	2057 ± 0	103665 ± 3	No	137	17816 ± 260	137	17878 ± 464
51	Hengrui AI Technology Ltd	hr	001	2019-10-08	390059	129	2057 ± 0	149904 ± 4	No	143	24112 ± 766	143	23859 ± 739
52	ID3 Technology	id3	003	2018-10-05	265951	11	264 ± 0	41316 ± 19	No	59	1330 ± 25	63	1354 ± 28
53	ID3 Technology	id3	004	2019-03-01	171526	10	264 ± 0	77541 ± 11	No	47	1135 ± 23	54	1156 ± 32
54	Idemia	Idemia	004	2019-03-01	406924	13	352 ± 0	30366 ± 5	No	119	5592 ± 518	119	5533 ± 426
55	Idemia	Idemia	005	2019-10-11	509824	27	588 ± 0	69524 ± 20	No	126	7543 ± 370	129	10415 ± 174
56	Institute of Information Technologies	iitvision	000	2019-03-01	237317	35	1024 ± 0	16197 ± 8	No	65	1537 ± 81	60	1282 ± 20
57	Institute of Information Technologies	iitvision	001	2019-07-05	269176	82	2048 ± 0	112699 ± 4	No	44	1060 ± 48	47	1074 ± 54
58	Imagus Technology Pty Ltd	imagus	000	2019-06-19	183453	96	2048 ± 0	60425 ± 24	No	48	1145 ± 25	71	1718 ± 63
59	Imperial College London	imperial	000	2019-03-01	370120	79	2048 ± 0	105669 ± 1	No	82	2130 ± 32	79	2052 ± 100
60	Imperial College London	imperial	002	2019-08-28	472327	62	2048 ± 0	83570 ± 2	No	114	4827 ± 69	112	4557 ± 160
61	Incode Technologies Inc	incode	003	2019-03-01	170632	145	4096 ± 0	53384 ± 11	No	78	1928 ± 44	74	1876 ± 81
62	Incode Technologies Inc	incode	004	2019-06-12	260224	67	2048 ± 0	63479 ± 23	No	77	1913 ± 60	87	2443 ± 114
63	Innovatrics	innovatrics	004	2018-10-19	0	41	1076 ± 0	55391 ± 0	No	128	8573 ± 274	126	7929 ± 244
64	Innovatrics	innovatrics	006	2019-08-13	0	23	538 ± 0	136824 ± 10	No	121	5763 ± 217	120	5631 ± 824
65	CSA IntelliCloud Technology	intellicloudai	001	2019-08-13	220831	101	2048 ± 0	64479 ± 18	No	42	1010 ± 16	44	1024 ± 31
66	Shenzhen Intellifusion Technologies Co. Ltd	intellifusion	001	2019-08-22	271872	66	2048 ± 0	125778 ± 61	No	107	3756 ± 59	110	3953 ± 126
67	Intellivision	intellivision	001	2017-10-10	43692	124	2056 ± 0	262 ± 2	No	89	2573 ± 91	91	2544 ± 38
68	Intellivision	intellivision	002	2019-08-23	43692	120	2056 ± 0	46342 ± 30	No	136	16049 ± 195	134	15136 ± 389
69	Intel Research Group	intelresearch	000	2019-07-08	388229	63	2048 ± 0	148902 ± 6	No	113	4800 ± 152	113	4561 ± 97
70	Lomonosov Moscow State University	intsy whole	000	2019-06-18	650193	65	2048 ± 0	72535 ± 20	No	16	610 ± 22	22	613 ± 31
71	iQIYI Inc	iqface	000	2019-06-04	268819	152	4750 ± 32	74538 ± 26	No	153	636433 ± 38446	153	632654 ± 85615
72	iSAP Solution Corporation	isap	001	2019-08-07	99049	147	4096 ± 0	10171 ± 12	No	130	12413 ± 154	131	12251 ± 382
73	Is It You	isityou	000	2017-06-26	48010	153	19200 ± 0	6113 ± 5	No	151	237517 ± 1318	151	237374 ± 1279
74	Innovation Systems	isystems	001	2018-06-12	274621	58	2048 ± 0	34291 ± 9	No	14	557 ± 16	16	564 ± 22
75	Innovation Systems	isystems	002	2018-10-18	358984	85	2048 ± 0	134822 ± 8	No	31	749 ± 31	27	632 ± 28
76	ITMO University	itmo	005	2018-10-19	482155	151	4173 ± 0	123759 ± 1	No	132	13214 ± 164	132	12576 ± 257
77	ITMO University	itmo	006	2019-03-01	599187	134	2121 ± 0	132814 ± 1	No	144	26154 ± 148	144	26217 ± 260
78	Kakao Corp	kakao	001	2019-03-01	107616	33	1024 ± 0	52379 ± 1	No	37	930 ± 22	40	948 ± 38
79	Kakao Corp	kakao	002	2019-06-19	479406	104	2048 ± 0	119747 ± 6	No	71	1720 ± 62	70	1715 ± 83
80	Kedacom International Pte	kedacom	000	2019-06-03	245292	12	292 ± 0	67506 ± 3	No	25	684 ± 14	28	682 ± 16
81	Kneron Inc	kenron	003	2019-07-01	58366	77	2048 ± 0	32281 ± 3	No	118	5237 ± 63	118	5274 ± 99
82	Lookman Electroplast Industries	lookman	002	2018-06-13	138200	25	548 ± 0	11173 ± 1	No	17	610 ± 19	21	612 ± 22
83	Lookman Electroplast Industries	lookman	004	2019-06-03	244775	24	548 ± 0	68507 ± 5	No	35	871 ± 29	39	878 ± 29
84	Megvii/Face++	megvii	001	2018-06-15	1361523	100	2048 ± 0	78543 ± 0	No	117	5228 ± 32	117	5252 ± 60
85	Megvii/Face++	megvii	002	2018-10-19	1809564	150	4100 ± 0	95644 ± 0	No	148	50630 ± 183	148	47591 ± 716
86	Xiamen Meiya Pico Information Co. Ltd	meiya	001	2019-03-01	280055	106	2049 ± 0	80622 ± 12	No	127	8356 ± 615	127	8134 ± 97
87	MicroFocus	microfocus	001	2018-06-13	104524	8	256 ± 0	28264 ± 18	No	121	215 ± 8	121	21 ± 10
88	MicroFocus	microfocus	002	2018-10-17	96288	6	256 ± 0	26259 ± 18	No	337	337 ± 34	230	230 ± 25

Notes	
1	The configuration size does not capture static data included in libraries. We do not count these because some algorithms include common ancillary libraries for image processing (e.g. openCV) or numerical computation (e.g. blas).
2	The median template creation times are measured on Intel® Xeon® CPU E5-2630 v4 @ 2.20GHz processors or, for GPU-enabled implementations, NVidia Tesla K40.
3	The comparison durations, in nanoseconds, are estimated using std::chrono::high_resolution_clock which on the machine in (2) counts 1ns clock ticks. Precision is somewhat worse than that however. The ± value is the median absolute deviation times 1.48 for Normal consistency.

Table 2: Summary of algorithms and properties included in this report. The red superscripts give ranking for the quantity in that column.

Developer		Short	Seq.	Validation	Config <sup>1</sup>	Template		GPU	Comparison Time (ns) <sup>3</sup>	
Name		Name	Num.	Date	Data (KB)	Size (B)	Time (ms) <sup>2</sup>		Genuine	Impostor
89	Moontime Smart Technology	mt	000	2019-06-03	372169	105 2049 ± 0	116 724 ± 12	No	70 1678 ± 47	68 1614 ± 85
90	Neurotechnology	neurotech	005	2019-03-01	270450	7 256 ± 0	58 399 ± 0	No	2 238 ± 10	3 237 ± 7
91	Neurotechnology	neurotech	006	2019-06-26	525541	19 512 ± 0	111 678 ± 56	No	13 513 ± 14	15 535 ± 26
92	Nodeflux	nodeflux	001	2019-03-01	262553	84 2048 ± 0	23 247 ± 1	No	99 3242 ± 81	100 3255 ± 93
93	Nodeflux	nodeflux	002	2019-08-13	774668	102 2048 ± 0	114 717 ± 16	No	122 5922 ± 170	125 7911 ± 367
94	NotionTag Technologies Private Limited	notiontag	000	2019-06-12	92753	26 584 ± 0	80 548 ± 64	No	147 44672 ± 269	147 44593 ± 358
95	N-Tech Lab	ntech	006	2019-03-01	7901590	137 2600 ± 0	120 749 ± 1	No	43 1055 ± 93	38 844 ± 48
96	N-Tech Lab	ntech	007	2019-06-25	2509686	139 3348 ± 0	129 792 ± 3	No	51 1209 ± 59	58 1267 ± 65
97	Guangzhou Pixel Solutions Co. Ltd	pixelall	002	2019-06-06	0	136 2560 ± 0	15 191 ± 1	No	52 1223 ± 56	56 1230 ± 47
98	Panasonic R+D Center Singapore	psl	002	2019-02-28	804934	112 2052 ± 0	145 888 ± 9	No	67 1590 ± 48	50 1133 ± 78
99	Panasonic R+D Center Singapore	psl	003	2019-10-01	1159643	133 2120 ± 0	142 867 ± 7	No	110 3915 ± 50	109 3899 ± 226
100	Rank One Computing	rankone	006	2019-02-27	0	5 165 ± 0	18 210 ± 1	No	7 443 ± 26	6 395 ± 22
101	Rank One Computing	rankone	007	2019-06-03	0	4 165 ± 0	22 245 ± 5	No	26 688 ± 20	18 601 ± 16
102	Realnetworks Inc	realnetworks	002	2019-02-28	95328	56 1848 ± 0	25 250 ± 2	No	57 1285 ± 17	57 1247 ± 42
103	Realnetworks Inc	realnetworks	003	2019-06-12	95334	55 1848 ± 0	13 177 ± 10	No	64 1516 ± 29	66 1522 ± 60
104	KanKan Ai	remarkai	000	2019-03-01	240152	59 2048 ± 0	137 829 ± 7	No	36 873 ± 4	37 835 ± 35
105	KanKan Ai	remarkai	001	2019-03-01	241857	114 2052 ± 0	138 831 ± 6	No	53 1229 ± 20	36 805 ± 56
106	Rokid Corporation Ltd	rokid	000	2019-08-01	258612	125 2056 ± 0	79 547 ± 2	No	106 3711 ± 88	105 3746 ± 209
107	Saffe Ltd	saffe	001	2018-10-19	85973	45 1280 ± 0	31 281 ± 1	No	55 1274 ± 19	59 1277 ± 26
108	Saffe Ltd	saffe	002	2019-03-01	260622	94 2048 ± 0	13 817 ± 11	No	30 717 ± 7	31 714 ± 29
109	Sensetime Group Ltd	sensetime	002	2018-10-19	531783	107 2052 ± 0	117 725 ± 3	No	88 2546 ± 102	85 2371 ± 45
110	Sensetime Group Ltd	sensetime	002	2018-10-19	531783	116 2052 ± 0	130 797 ± 3	No	92 2713 ± 90	84 2301 ± 25
111	Momentum Digital Co. Ltd	sertis	000	2019-10-07	265572	64 2048 ± 0	121 755 ± 0	No	109 3883 ± 44	108 3884 ± 66
112	Shaman Software	shaman	000	2017-12-05	0	144 4096 ± 0	100 653 ± 16	No	4380 ± 25	5 379 ± 31
113	Shaman Software	shaman	001	2018-01-13	0	141 4096 ± 0	35 294 ± 2	No	22 635 ± 19	9 441 ± 25
114	Shanghai Universiy - Shanghai Film Academy	shu	001	2019-06-17	329513	99 2048 ± 0	86 612 ± 5	No	91 2619 ± 19	95 2987 ± 143
115	Shenzhen Inst. Adv. Integrated Tech. CAS	SIAT	002	2018-06-13	486842	117 2052 ± 0	84 579 ± 0	No	32 769 ± 13	33 750 ± 13
116	Shenzhen Inst. Adv. Integrated Tech. CAS	SIAT	004	2019-03-01	940063	149 4100 ± 0	106 670 ± 0	No	111 4013 ± 45	107 3782 ± 173
117	Shanghai Jiao Tong University	sjtu	001	2019-09-27	347115	61 2048 ± 0	99 651 ± 4	No	154 2674654 ± 64798	154 2376946 ± 202419
118	Smilart	smilart	002	2018-02-06	111826	32 1024 ± 0	12 176 ± 16	No	139 18784 ± 136	140 18795 ± 151
119	Smilart	smilart	003	2018-06-18	67339	17 512 ± 0	14 180 ± 12	No	61 1395 ± 74	45 1027 ± 66
120	Star Hybrid Limited	starhybrid	001	2019-06-19	100509	74 2048 ± 0	49 358 ± 82	No	45 1075 ± 51	48 1078 ± 53
121	Synesis	synesis	004	2019-03-01	270628	98 2048 ± 0	118 735 ± 15	No	5 424 ± 14	7 430 ± 22
122	Synesis	synesis	005	2019-06-06	146509	83 2048 ± 0	19 211 ± 9	No	15 599 ± 23	17 581 ± 32
123	Tech5 SA	tech5	002	2019-03-01	1150887	46 1280 ± 0	126 780 ± 10	No	63 1406 ± 120	46 1048 ± 57
124	Tech5 SA	tech5	003	2019-08-19	1427464	48 1536 ± 0	150 937 ± 39	No	58 1313 ± 35	64 1360 ± 41
125	Tevian	tevian	004	2019-03-01	863474	75 2048 ± 0	66 506 ± 30	No	9 474 ± 31	4 326 ± 20
126	Tevian	tevian	005	2019-09-21	921043	91 2048 ± 0	94 642 ± 32	No	96 3097 ± 31	104 3700 ± 278
127	TigerIT Americas LLC	tiger	002	2018-06-13	341638	123 2056 ± 0	57 393 ± 20	No	83 2135 ± 29	81 2137 ± 38
128	TigerIT Americas LLC	tiger	003	2018-10-16	426164	118 2056 ± 0	62 458 ± 21	No	80 2031 ± 35	78 2029 ± 38
129	TongYi Transportation Technology	tongyi	005	2019-06-12	1140701	132 2089 ± 0	8 165 ± 1	No	140 18924 ± 65	141 20158 ± 103
130	Toshiba	toshiba	002	2018-10-19	813606	51 1560 ± 0	76 541 ± 0	No	103 3521 ± 369	88 2449 ± 124
131	Toshiba	toshiba	003	2019-03-01	984125	52 1560 ± 0	75 540 ± 0	No	87 2390 ± 41	86 2407 ± 81
132	Trueface.ai	trueface	000	2019-10-08	255123	95 2048 ± 0	50 368 ± 11	No	95 3040 ± 26	97 3144 ± 51

## Notes

- 1 The configuration size does not capture static data included in libraries. We do not count these because some algorithms include common ancillary libraries for image processing (e.g. openCV) or numerical computation (e.g. blas).
- 2 The median template creation times are measured on Intel®Xeon®CPU E5-2630 v4 @ 2.20GHz processors or, for GPU-enabled implementations, NVidia Tesla K40.
- 3 The comparison durations, in nanoseconds, are estimated using std::chrono::high\_resolution\_clock which on the machine in (2) counts 1ns clock ticks. Precision is somewhat worse than that however. The ± value is the median absolute deviation times 1.48 for Normal consistency.

Table 3: Summary of algorithms and properties included in this report. The red superscripts give ranking for the quantity in that column.

	Developer	Short	Seq.	Validation	Config <sup>1</sup>	Template		GPU	Comparison Time (ns) <sup>3</sup>	
						Name	Date		Time (ms) <sup>2</sup>	Genuine
133	ULSee Inc	ulsee	001	2019-07-31	370519	<sup>93</sup> 2048 ± 0	<sup>101</sup> 654 ± 2	No	<sup>123</sup> 6065 ± 94	<sup>121</sup> 6228 ± 77
134	Shanghai Ulucu Electronics Technology Co. Ltd	uluface	002	2019-07-10	0	<sup>81</sup> 2048 ± 0	<sup>143</sup> 873 ± 42	No	<sup>141</sup> 19207 ± 1114	<sup>139</sup> 18501 ± 274
135	China University of Petroleum	upc	001	2019-06-05	0	<sup>40</sup> 1052 ± 0	<sup>81</sup> 551 ± 15	No	<sup>97</sup> 3114 ± 44	<sup>98</sup> 3165 ± 97
136	VCognition	vcog	002	2017-06-12	3229434	<sup>154</sup> 61504 ± 5	<sup>48</sup> 357 ± 25	No	<sup>152</sup> 296154 ± 3077	<sup>152</sup> 296436 ± 4183
137	Visidon	visidon	001	2019-02-26	170262	<sup>110</sup> 2052 ± 0	<sup>42</sup> 316 ± 6	No	<sup>54</sup> 1258 ± 38	<sup>52</sup> 1148 ± 109
138	Veridas Digital Authentication Solutions S.L.	veridas	001	2019-03-01	196540	<sup>78</sup> 2048 ± 0	<sup>107</sup> 671 ± 21	No	<sup>120</sup> 5748 ± 20	<sup>123</sup> 7111 ± 148
139	Veridas Digital Authentication Solutions S.L.	veridas	000	2019-03-01	193466	<sup>22</sup> 512 ± 0	<sup>104</sup> 669 ± 20	No	<sup>72</sup> 1733 ± 81	<sup>76</sup> 1934 ± 44
140	Via Technologies Inc.	via	000	2019-07-08	124422	<sup>89</sup> 2048 ± 0	<sup>113</sup> 707 ± 8	No	<sup>41</sup> 966 ± 28	<sup>43</sup> 1021 ± 44
141	Videonetech Technology Pvt Ltd	videonetech	001	2019-06-19	30875	<sup>15</sup> 512 ± 0	<sup>27</sup> 262 ± 3	No	<sup>49</sup> 11153 ± 38	<sup>51</sup> 1142 ± 65
142	Vigilant Solutions	vigilant	006	2019-03-01	343048	<sup>50</sup> 1548 ± 0	<sup>140</sup> 841 ± 8	No	<sup>38</sup> 939 ± 32	<sup>29</sup> 711 ± 37
143	Vigilant Solutions	vigilant	007	2019-06-27	255600	<sup>49</sup> 1548 ± 0	<sup>65</sup> 493 ± 6	No	<sup>34</sup> 803 ± 35	<sup>34</sup> 800 ± 40
144	Beijing Vion Technology Inc	vion	000	2018-10-19	228219	<sup>113</sup> 2052 ± 0	<sup>44</sup> 333 ± 1	No	<sup>146</sup> 39839 ± 3561	<sup>145</sup> 26830 ± 2241
145	Vision-Box	visionbox	000	2019-02-26	176501	<sup>97</sup> 2048 ± 0	<sup>37</sup> 304 ± 7	No	<sup>69</sup> 1648 ± 57	<sup>55</sup> 1192 ± 42
146	Vision-Box	visionbox	001	2019-03-01	256869	<sup>90</sup> 2048 ± 0	<sup>153</sup> 983 ± 7	No	<sup>50</sup> 11161 ± 22	<sup>53</sup> 1154 ± 20
147	VisionLabs	visionlabs	006	2019-03-01	353044	<sup>21</sup> 512 ± 0	<sup>29</sup> 270 ± 0	No	<sup>28</sup> 698 ± 19	<sup>32</sup> 734 ± 28
148	VisionLabs	visionlabs	007	2019-06-12	357204	<sup>20</sup> 512 ± 0	<sup>30</sup> 272 ± 0	No	<sup>40</sup> 965 ± 41	<sup>42</sup> 972 ± 31
149	Vocord	vocord	006	2019-03-01	559457	<sup>28</sup> 768 ± 0	<sup>144</sup> 886 ± 1	No	<sup>79</sup> 2020 ± 72	<sup>77</sup> 1969 ± 62
150	Vocord	vocord	007	2019-06-06	587489	<sup>53</sup> 1664 ± 0	<sup>127</sup> 780 ± 2	No	<sup>90</sup> 2593 ± 83	<sup>90</sup> 2526 ± 59
151	Winsense Co. Ltd	winsense	000	2019-06-17	270819	<sup>44</sup> 1280 ± 0	<sup>33</sup> 283 ± 1	No	<sup>66</sup> 1551 ± 31	<sup>67</sup> 1532 ± 42
152	X-Laboratory	x-laboratory	000	2019-09-03	520020	<sup>127</sup> 2056 ± 0	<sup>139</sup> 832 ± 38	No	<sup>101</sup> 3380 ± 91	<sup>102</sup> 3314 ± 253
153	Zhuhai Yisheng Electronics Technology	yisheng	004	2018-06-12	486351	<sup>140</sup> 3704 ± 0	<sup>51</sup> 378 ± 12	No	<sup>27</sup> 693 ± 137	<sup>14</sup> 526 ± 34
154	Shanghai Yitu Technology	yitu	003	2019-03-01	1525719	<sup>130</sup> 2082 ± 0	<sup>141</sup> 860 ± 0	No	<sup>138</sup> 18305 ± 71	<sup>138</sup> 18286 ± 62

## Notes

- |   |   |
|---|---|
| 1 | The configuration size does not capture static data included in libraries. We do not count these because some algorithms include common ancillary libraries for image processing (e.g. openCV) or numerical computation (e.g. blas).  |
| 2 | The median template creation times are measured on Intel®Xeon®CPU E5-2630 v4 @ 2.20GHz processors or, for GPU-enabled implementations, NVidia Tesla K40.  |
| 3 | The comparison durations, in nanoseconds, are estimated using std::chrono::high_resolution_clock which on the machine in (2) counts 1ns clock ticks. Precision is somewhat worse than that however. The ± value is the median absolute deviation times 1.48 for Normal consistency. |

Table 4: Summary of algorithms and properties included in this report. The red superscripts give ranking for the quantity in that column.

	Algorithm	FALSE NON-MATCH RATE (FNMR)											
		CONSTRAINED, COOPERATIVE						LESS CONSTRAINED, NON-COOP.					
		Name	VISAMC	VISA	VISA	MUGSHOT	MUGSHOT12+YRS	VISABORDER	WILD	CHILDEXP			
	FMR	0.0001	1E-06	0.0001	1E-05	0.0001	1E-05	0.0001	1E-06	0.0001	0.01		
1	3divi-003	0.0318	109	0.0588	109	0.0097	101	0.0389	108	0.0639	105	0.0619	98
2	3divi-004	0.0095	39	0.0153	42	0.0049	58	0.0097	38	0.0145	36	0.0175	46
3	adera-001	0.1021	124	0.1757	122	0.0368	123	0.1823	130	0.2967	128	0.1714	112
4	alchera-000	0.0165	80	0.0243	70	0.0086	95	0.0125	68	0.0186	63	0.0204	52
5	alchera-001	0.0183	85	0.0299	83	0.0078	91	0.0142	74	0.0234	77	0.0239	60
6	allgovision-000	0.0346	111	0.0527	105	0.0210	114	0.0232	95	0.0339	84	-	0.0607
7	alphaface-001	0.0065	21	0.0097	20	0.0025	21	0.0039	3	0.0063	6	0.0083	8
8	amplifiedgroup-001	0.5034	144	0.5848	144	0.2999	146	0.6973	144	0.8316	141	0.7807	125
9	anke-003	0.0131	61	0.0213	60	0.0056	64	0.0094	35	0.0175	56	0.0134	29
10	anke-004	0.0080	32	0.0154	43	0.0031	29	0.0073	19	0.0112	21	0.0102	16
11	anyvision-002	0.0660	118	0.0898	115	0.0387	124	0.0928	123	0.1512	119	-	0.2227
12	anyvision-004	0.0267	103	0.0385	98	0.0081	93	0.0258	97	0.0487	100	-	0.0470
13	aware-003	0.0793	120	0.1161	119	0.0288	121	0.1028	124	0.1708	122	0.1698	111
14	aware-004	0.0690	119	0.0949	117	0.0257	117	0.0837	121	0.1436	117	0.1171	109
15	awiros-001	0.4044	139	0.4622	138	0.2880	145	0.5530	139	0.6518	136	0.2008	113
16	ayonix-000	0.4351	141	0.4872	139	0.2299	141	0.6150	141	0.7510	138	0.6557	123
17	bm-001	0.7431	150	0.9494	151	0.6188	151	0.9586	148	0.9843	145	0.9049	129
18	camvi-002	0.0125	58	0.0221	65	0.0049	59	0.0089	32	0.0145	38	0.0142	30
19	camvi-004	0.0171	83	0.0316	87	0.0049	57	0.0042	5	0.0049	2	0.0097	15
20	ceitec-001	0.0328	110	0.0475	102	0.0163	109	0.0295	103	0.0478	99	0.0621	99
21	ceitec-002	0.0161	78	0.0193	55	0.0124	107	0.0122	65	0.0164	52	0.0270	65
22	chtface-001	0.9993	153	0.9994	153	0.9993	153	0.9999	150	-	1.0000	131	0.9980
23	cogent-003	0.0091	35	0.0188	53	0.0032	30	0.0098	40	0.0132	30	0.0187	48
24	cogent-004	0.0064	20	0.0116	30	0.0024	20	0.0096	36	0.0134	31	0.0157	34
25	cognitec-000	0.0116	51	0.0177	47	0.0036	35	0.0118	60	0.0167	53	0.0285	69
26	cognitec-001	0.0126	59	0.0185	52	0.0047	53	0.0120	63	0.0168	54	0.0270	64
27	ctcbcbank-000	0.0168	81	0.0250	76	0.0064	71	0.0146	77	0.0224	72	0.0211	53
28	cyberextruder-001	0.1972	132	0.2547	130	0.0755	133	0.4686	138	0.6387	135	-	0.1747
29	cyberextruder-002	0.0811	121	0.1336	121	0.0265	118	0.1465	128	0.2266	126	-	0.1000
30	cyberlink-002	0.0114	50	0.0195	56	0.0044	45	0.0101	44	0.0163	49	0.0160	35
31	cyberlink-003	0.0118	53	0.0192	54	0.0042	43	0.0098	41	0.0161	47	0.0153	33
32	dahua-002	0.0129	60	0.0157	44	0.0090	98	0.0116	59	0.0153	41	0.0134	28
33	dahua-003	0.0052	12	0.0068	10	0.0023	19	0.0056	10	0.0062	5	0.0113	22
34	deepglint-001	0.0040	6	0.0062	7	0.0014	8	0.0047	6	0.0067	7	0.0069	4
35	deepsea-001	0.0136	65	0.0215	62	0.0071	87	0.0142	75	0.0214	68	0.0163	39
36	dermalog-005	0.1526	130	0.1823	125	0.0658	131	0.2580	133	0.4018	130	-	0.0855
37	dermalog-006	0.0253	100	0.0369	96	0.0172	112	0.0171	83	0.0283	81	-	0.0623
38	digitalbarriers-002	0.3360	137	0.3690	135	0.0968	136	0.0877	122	0.1557	120	0.0971	108
39	dsk-000	0.1526	129	0.2169	127	0.0765	134	0.3787	137	0.5426	134	0.3115	118
40	einetworks-000	0.0099	42	0.0180	49	0.0047	52	0.0088	30	0.0140	34	0.0130	26
41	everai-002	0.0104	47	0.0159	45	0.0041	42	0.0063	15	0.0112	22	0.0182	47
42	everai-paravision-003	0.0034	2	0.0050	3	0.0011	3	0.0036	2	0.0052	3	0.0092	12
43	f8-001	0.0249	99	0.0336	88	0.0182	113	0.0178	85	0.0232	76	0.0303	76
44	facesoft-000	0.0085	34	0.0112	29	0.0032	31	0.0064	16	0.0107	18	0.0091	11

Table 5: FNMR is the proportion of mated comparisons below a threshold set to achieve the FMR given in the header on the fourth row. FMR is the proportion of impostor comparisons at or above that threshold. The light grey values give rank over all algorithms in that column. The pink column uses only same-sex impostors; others are selected regardless of demographics. The exception, in the green column, uses “matched-covariates” i.e. impostors of the same sex, age group, and country of birth. The pink column includes effects of extended ageing. Missing entries for border, visa, mugshot and wild images generally mean the algorithm did not run to completion. For child exploitation, missing entries arise because NIST executes those runs only infrequently.

Algorithm	FALSE NON-MATCH RATE (FNMR)									
	CONSTRAINED, COOPERATIVE						LESS CONSTRAINED, NON-COOP.			
	Name	VISAMC	VISA	VISA	MUGSHOT	MUGSHOT12+YRS	VISABORDER	WILD	CHILDEXP	
FMR	0.0001	1E-06	0.0001	1E-05	1E-05	1E-05	1E-06	0.0001	0.01	
45	glory-000	0.1094	125	0.1286	120	0.0514	128	0.2179	131	0.2656
46	glory-001	0.0902	122	0.1082	118	0.0410	125	0.1642	129	0.2065
47	gorilla-002	0.0256	101	0.0413	99	0.0076	90	0.0478	113	0.0912
48	gorilla-003	0.0165	79	0.0291	81	0.0053	61	0.0205	91	0.0437
49	hik-001	0.0096	40	0.0125	32	0.0036	37	0.0093	34	0.0164
50	hr-001	0.0044	9	0.0072	12	0.0019	13	0.0073	21	0.0108
51	hr-002	0.0043	7	0.0059	5	0.0017	10	0.0054	7	0.0076
52	id3-003	0.0361	112	0.0757	112	0.0104	105	0.0292	101	0.0476
53	id3-004	0.0198	90	0.0344	91	0.0084	94	0.0238	96	0.0423
54	idemia-004	0.0160	77	0.0244	72	0.0065	73	0.0199	90	0.0354
55	idemia-005	0.0132	62	0.0216	63	0.0057	66	0.0121	64	0.0218
56	iit-000	0.1516	128	0.1981	126	0.0620	130	0.0828	120	0.1442
57	iit-001	0.0104	45	0.0179	48	0.0048	56	0.0099	43	0.0142
58	imagus-000	0.0642	116	0.0882	113	0.0330	122	0.0497	114	0.0905
59	imperial-000	0.0067	24	0.0108	27	0.0022	18	0.0080	26	0.0134
60	imperial-002	0.0058	16	0.0081	15	0.0027	22	0.0055	9	0.0085
61	incode-003	0.0142	68	0.0249	75	0.0054	62	0.0448	111	0.0869
62	incode-004	0.0077	30	0.0132	34	0.0034	33	0.0096	37	0.0160
63	innovatrics-004	0.0194	88	0.0292	82	0.0068	79	0.0344	105	0.0617
64	innovatrics-006	0.0058	17	0.0089	17	0.0021	16	0.0061	14	0.0096
65	intellicloudai-001	0.0142	69	0.0234	69	0.0064	72	0.0092	33	0.0145
66	intellifusion-001	0.0072	27	0.0094	19	0.0028	26	0.0056	11	0.0085
67	intellifusion-001	0.1335	127	0.2205	128	0.0417	126	0.1090	126	0.1670
68	intellivision-002	0.1000	123	0.1775	123	0.0265	119	0.0610	117	0.1009
69	intelresearch-000	0.0307	106	0.0578	108	0.0093	99	0.0385	107	0.0751
70	intsysmsu-000	0.0135	64	0.0204	57	0.0069	81	0.0112	54	0.0161
71	iqface-000	0.0091	36	0.0143	38	0.0043	44	0.0075	24	0.0110
72	isap-001	0.5092	145	0.6588	146	0.2338	143	0.6899	143	0.7978
73	isityou-000	0.5682	147	0.7033	147	0.4145	149	1.0000	151	-
74	isystems-001	0.0149	73	0.0245	73	0.0067	77	0.0138	73	0.0210
75	isystems-002	0.0118	52	0.0182	51	0.0066	74	0.0111	51	0.0162
76	itmo-005	0.0182	84	0.0345	92	0.0067	78	0.0181	86	0.0348
77	itmo-006	0.0125	57	0.0220	64	0.0046	48	0.0149	78	0.0266
78	kakao-001	0.4553	143	0.5532	143	0.2034	140	0.6580	142	0.8150
79	kakao-002	0.0625	115	0.1779	124	0.0168	111	0.0791	119	0.1381
80	kedacom-000	0.0055	14	0.0081	16	0.0027	23	0.0111	53	0.0120
81	kneron-003	0.0542	114	0.0902	116	0.0218	115	0.0346	106	0.0562
82	lookman-002	0.0297	105	0.0547	107	0.0102	104	0.0339	104	0.0562
83	lookman-004	0.0074	29	0.0099	22	0.0037	38	0.0124	67	0.0149
84	megvii-001	0.0157	75	0.0244	71	0.0045	47	0.0392	109	0.0671
85	megvii-002	0.0104	46	0.0145	40	0.0036	36	0.0225	93	0.0345
86	meiya-001	0.0171	82	0.0275	80	0.0066	76	0.0159	82	0.0261
87	microfocus-001	0.4482	142	0.5524	142	0.2309	142	0.7256	145	0.8416
88	microfocus-002	0.3605	138	0.5057	140	0.1566	139	0.5783	140	0.7223

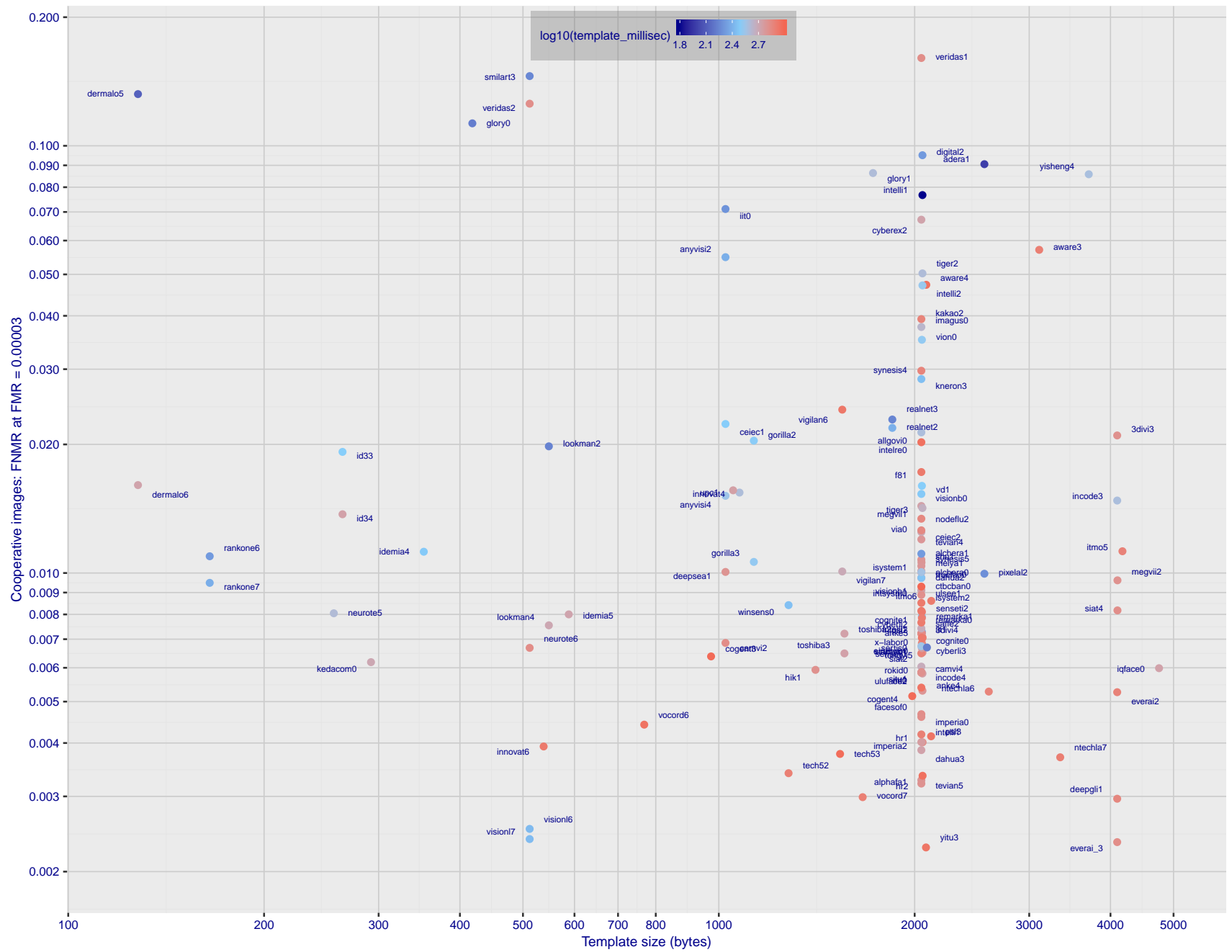
Table 6: FNMR is the proportion of mated comparisons below a threshold set to achieve the FMR given in the header on the fourth row. FMR is the proportion of impostor comparisons at or above that threshold. The light grey values give rank over all algorithms in that column. The pink column uses only same-sex impostors; others are selected regardless of demographics. The exception, in the green column, uses “matched-covariates” i.e. impostors of the same sex, age group, and country of birth. The pink column includes effects of extended ageing. Missing entries for border, visa, mugshot and wild images generally mean the algorithm did not run to completion. For child exploitation, missing entries arise because NIST executes those runs only infrequently.

	Algorithm	FALSE NON-MATCH RATE (FNMR)									
		CONSTRAINED, COOPERATIVE						LESS CONSTRAINED, NON-COOP.			
		Name	VISAMC	VISA	VISA	MUGSHOT	MUGSHOT12+YRS	VISABORDER	WILD	CHILDEXP	
	FMR	0.0001	1E-06	0.0001	1E-05	1E-05	1E-05	1E-06	0.0001	0.01	
89	mt-000	0.0100	43	0.0170	46	0.0047	51	0.0074	23	0.0118	24
90	neurotechnology-005	0.0141	67	0.0300	84	0.0051	60	0.0108	49	0.0163	50
91	neurotechnology-006	0.0098	41	0.0136	35	0.0040	41	0.0105	47	0.0182	60
92	nodeflux-001	1.0000	154	1.0000	154	1.0000	154	-	-	0.5169	122
93	nodeflux-002	0.0186	86	0.0340	89	0.0070	84	0.0261	98	0.0451	95
94	notiontag-000	0.6669	148	0.7885	148	0.3222	148	0.3715	136	0.4978	133
95	ntechlab-006	0.0078	31	0.0111	28	0.0021	17	0.0112	55	0.0227	75
96	ntechlab-007	0.0056	15	0.0076	13	0.0018	11	0.0073	22	0.0128	28
97	pixelall-002	0.0193	87	0.0340	90	0.0066	75	0.0127	70	0.0209	66
98	psl-002	0.0107	48	0.0180	50	0.0048	55	0.0089	31	0.0120	26
99	psl-003	0.0065	22	0.0099	23	0.0028	24	0.0055	8	0.0075	8
100	rankone-006	0.0242	95	0.0460	101	0.0070	83	0.0119	61	0.0188	64
101	rankone-007	0.0197	89	0.0366	95	0.0057	67	0.0113	57	0.0177	58
102	realnetworks-002	0.0248	97	0.0358	93	0.0099	102	0.0153	115	0.1127	113
103	realnetworks-003	0.0259	102	0.0372	97	0.0100	103	0.0541	116	0.1208	115
104	remarkai-000	0.0147	72	0.0257	78	0.0062	70	0.0102	45	0.0158	43
105	remarkai-001	0.0144	70	0.0256	77	0.0061	69	0.0102	46	0.0159	44
106	rokid-000	0.0093	38	0.0145	39	0.0038	39	0.0073	20	0.0102	17
107	saffe-001	0.4339	140	0.5261	141	0.2340	144	0.7539	147	0.8736	144
108	saffe-002	0.0119	55	0.0206	58	0.0054	63	0.0107	48	0.0177	57
109	sensetime-001	0.0063	19	0.0092	18	0.0030	27	0.0130	71	-	0.0252
110	sensetime-002	0.0068	25	0.0098	21	0.0035	34	0.0143	76	-	0.0278
111	sertis-000	0.0118	54	0.0208	59	0.0047	49	0.0080	25	0.0127	27
112	shaman-000	0.9297	152	0.9774	152	0.9128	152	0.9990	149	-	0.9999
113	shaman-001	0.3346	136	0.4616	137	0.1360	138	0.2368	132	0.3723	129
114	shu-001	0.0103	44	0.0140	37	0.0044	46	0.0293	102	0.0688	107
115	siat-002	0.0091	37	0.0126	33	0.0039	40	0.0109	50	0.0190	65
116	siat-004	0.0067	23	0.0099	24	0.0028	25	0.0152	80	-	0.0275
117	sjtu-001	0.0051	11	0.0080	14	0.0019	12	0.0211	92	0.0446	94
118	smilart-002	0.2440	135	0.3532	134	0.0821	135	-	-	0.3785	120
119	smilart-003	0.6944	149	0.8836	149	0.1088	137	0.0695	118	0.1193	114
120	starhybrid-001	0.0108	49	0.0138	36	0.0058	68	0.0081	27	0.0113	23
121	synesis-004	0.0310	107	0.0480	103	0.0166	110	0.0476	112	0.0443	93
122	synesis-005	0.0147	71	0.0226	67	0.0073	89	0.0153	81	0.0226	73
123	tech5-002	0.0046	10	0.0063	8	0.0009	2	0.0113	58	0.0216	70
124	tech5-003	0.0053	13	0.0070	11	0.0014	7	0.0099	42	0.0185	61
125	tevian-004	0.0228	93	0.0304	85	0.0069	80	0.0226	94	0.0478	97
126	tevian-005	0.0043	8	0.0062	6	0.0020	15	0.0057	12	0.0085	13
127	tiger-002	0.0658	117	0.0889	114	0.0227	116	0.1083	125	0.1766	123
128	tiger-003	0.0313	108	0.0602	111	0.0087	96	0.0188	88	0.0359	88
129	tongyi-005	0.0073	28	0.0146	41	0.0019	14	0.0187	87	0.0421	90
130	toshiba-002	0.0134	63	0.0222	66	0.0048	54	0.0097	39	0.0154	42
131	toshiba-003	0.0125	56	0.0214	61	0.0047	50	0.0085	29	0.0131	29
132	trueface-000	0.0249	98	0.4321	136	0.0069	82	0.0119	62	0.0180	59

Table 7: FNMR is the proportion of mated comparisons below a threshold set to achieve the FMR given in the header on the fourth row. FMR is the proportion of impostor comparisons at or above that threshold. The light grey values give rank over all algorithms in that column. The pink column uses only same-sex impostors; others are selected regardless of demographics. The exception, in the green column, uses “matched-covariates” i.e. impostors of the same sex, age group, and country of birth. The pink column includes effects of extended ageing. Missing entries for border, visa, mugshot and wild images generally mean the algorithm did not run to completion. For child exploitation, missing entries arise because NIST executes those runs only infrequently.

Algorithm	FALSE NON-MATCH RATE (FNMR)										
	CONSTRAINED, COOPERATIVE						LESS CONSTRAINED, NON-COOP.				
	Name	VISAMC	VISA	VISA	MUGSHOT	MUGSHOT12+YRS	VISABORDER	WILD	CHILDEXP		
FMR	0.0001	1E-06	0.0001	1E-05	1E-05	1E-06	0.0001	0.0001	0.01		
133 ulsee-001	0.0151	74	0.0246	74	0.0080	92	0.0113	56	0.0185	62	0.0187
134 uluface-002	0.0081	33	0.0123	31	0.0033	32	0.0071	18	0.0095	15	0.0107
135 upc-001	0.0234	94	0.0519	104	0.0071	86	0.0291	100	0.0490	101	0.0294
136 vcog-002	0.7522	151	0.9033	150	0.5040	150	-	-	-	-	0.7523
137 vd-001	0.0243	96	0.0452	100	0.0093	100	0.0271	99	0.0402	89	0.0424
138 veridas-001	0.1998	134	0.2724	131	0.0742	132	0.2987	135	0.4587	132	0.2599
139 veridas-002	0.1733	131	0.2257	129	0.0528	129	0.2617	134	0.4147	131	0.2073
140 via-000	0.0216	92	0.0365	94	0.0088	97	0.0177	84	0.0287	82	0.0296
141 videonetics-001	0.5483	146	0.6446	145	0.3063	147	0.7517	146	0.8607	143	0.8664
142 vigilantsolutions-006	0.1264	126	0.3221	132	0.0136	108	0.0150	79	0.0254	78	0.0493
143 vigilantsolutions-007	0.0202	91	0.0307	86	0.0070	85	0.0136	72	0.0227	74	0.0356
144 vion-000	0.0419	113	0.0590	110	0.0288	120	0.0422	110	0.0478	98	0.0581
145 visionbox-000	0.0293	104	0.0541	106	0.0110	106	0.0197	89	0.0339	83	0.0349
146 visionbox-001	0.0159	76	0.0270	79	0.0072	88	0.0111	52	0.0173	55	0.0190
147 visionlabs-006	0.0037	3	0.0066	9	0.0012	4	0.0041	4	0.0060	4	0.0061
148 visionlabs-007	0.0038	4	0.0048	2	0.0012	6	0.0036	1	0.0048	1	0.0057
149 vocord-006	0.0062	18	0.0102	25	0.0016	9	0.0082	28	0.0151	40	0.0475
150 vocord-007	0.0039	5	0.0053	4	0.0012	5	0.0061	13	0.0094	14	0.0520
151 winsense-000	0.0140	66	0.0228	68	0.0056	65	0.0125	69	0.0215	69	0.0226
152 x-laboratory-000	0.0071	26	0.0106	26	0.0030	28	0.0123	66	0.0138	33	0.0419
153 yisheng-004	0.1988	133	0.3329	133	0.0475	127	0.1147	127	0.1849	124	0.2044
154 yitu-003	0.0015	1	0.0026	1	0.0003	1	0.0066	17	0.0085	10	0.0064

Table 8: FNMR is the proportion of mated comparisons below a threshold set to achieve the FMR given in the header on the fourth row. FMR is the proportion of impostor comparisons at or above that threshold. The light grey values give rank over all algorithms in that column. The pink column uses only same-sex impostors; others are selected regardless of demographics. The exception, in the green column, uses “matched-covariates” i.e. impostors of the same sex, age group, and country of birth. The pink column includes effects of extended ageing. Missing entries for border, visa, mugshot and wild images generally mean the algorithm did not run to completion. For child exploitation, missing entries arise because NIST executes those runs only infrequently.



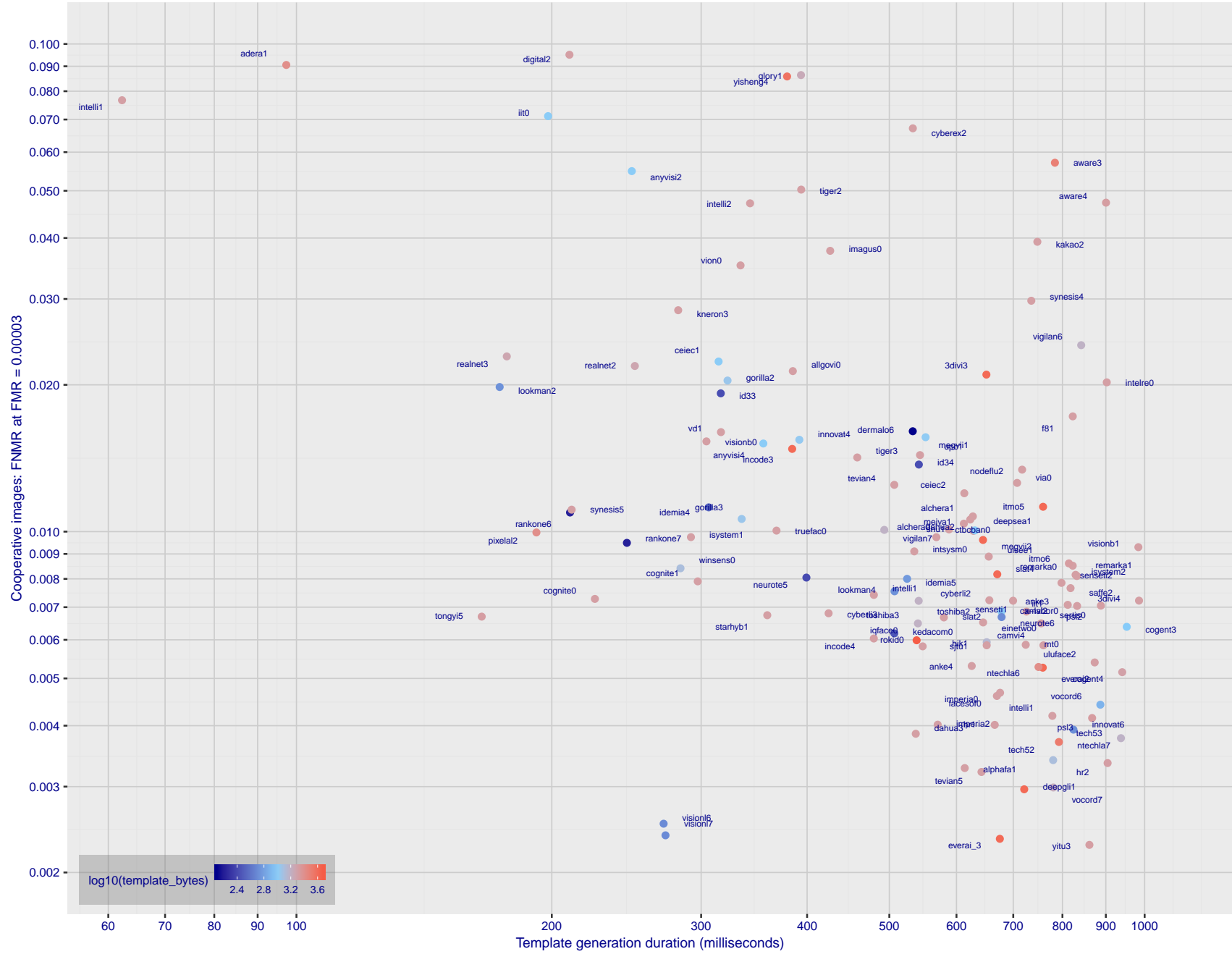


Figure 2: The points show false non-match rates (FNMR) versus the duration of the template generation operation. FNMR is the geometric mean of FNMR values for visa and mugshot images (from Figs. 26 and 34) at a false match rate (FMR) of 0.0001. Template generation time is a median estimated over 640 x 480 pixel portraits. It is measured on a single core of a c. 2016 Intel Xeon CPU E5-2630 v4 running at 2.20GHz. The color of the points encodes template size - which span two orders of magnitude. Algorithms with poor FNMR are omitted.

# 1 Metrics

## 1.1 Core accuracy

Given a vector of N genuine scores,  $u$ , the false non-match rate (FNMR) is computed as the proportion below some threshold, T:

$$\text{FNMR}(T) = 1 - \frac{1}{N} \sum_{i=1}^N H(u_i - T) \quad (1)$$

where  $H(x)$  is the unit step function, and  $H(0)$  taken to be 1.

Similarly, given a vector of N impostor scores,  $v$ , the false match rate (FMR) is computed as the proportion above T:

$$\text{FMR}(T) = \frac{1}{N} \sum_{i=1}^N H(v_i - T) \quad (2)$$

The threshold, T, can take on any value. We typically generate a set of thresholds from quantiles of the observed impostor scores,  $v$ , as follows. Given some interesting false match rate range,  $[\text{FMR}_L, \text{FMR}_U]$ , we form a vector of K thresholds corresponding to FMR measurements evenly spaced on a logarithmic scale

$$T_k = Q_v(1 - \text{FMR}_k) \quad (3)$$

where  $Q$  is the quantile function, and  $\text{FMR}_k$  comes from

$$\log_{10} \text{FMR}_k = \log_{10} \text{FMR}_L + \frac{k}{K} [\log_{10} \text{FMR}_U - \log_{10} \text{FMR}_L] \quad (4)$$

Error tradeoff characteristics are plots of FNMR(T) vs. FMR(T). These are plotted with  $\text{FMR}_U \rightarrow 1$  and  $\text{FMR}_L$  as low as is sustained by the number of impostor comparisons, N. This is somewhat higher than the “rule of three” limit  $3/N$  because samples are not independent, due to re-use of images.

## 2 Datasets

### 2.1 Child exploitation images

- ▷ The number of images is on the order of  $10^4$ .
- ▷ The number of subjects is on the order of  $10^3$ .
- ▷ The number of subjects with two images on the order of  $10^3$ .
- ▷ The images are operational. They are taken from ongoing investigations of child exploitation crimes. The images are arbitrarily unconstrained. Pose varies considerably around all three axes, including subject lying down. Resolution varies very widely. Faces can be occluded by other objects, including hair and hands. Lighting varies, although the images are intended for human viewing. Mis-focus is rare. Images are given to the algorithm without any cropping; faces may occupy widely varying areas.
- ▷ The images are usually large from contemporary cameras. The mean interocular distance (IOD) is 70 pixels.
- ▷ The images are of subjects from several countries, due to the global production of this imagery.
- ▷ The images are of children, from infancy to late adolescence.
- ▷ All of the images are live capture, none are scanned. Many have been cropped.
- ▷ When these images are input to the algorithm, they are labelled as being of type "EXPLOITATION" - see Table 4 of the FRVT API.

### 2.2 Visa images

- ▷ The number of images is on the order of  $10^5$ .
- ▷ The number of subjects is on the order of  $10^5$ .
- ▷ The number of subjects with two images on the order of  $10^4$ .
- ▷ The images have geometry in reasonable conformance with the ISO/IEC 19794-5 Full Frontal image type. Pose is generally excellent.
- ▷ The images are of size 252x300 pixels. The mean interocular distance (IOD) is 69 pixels.
- ▷ The images are of subjects from greater than 100 countries, with significant imbalance due to visa issuance patterns.
- ▷ The images are of subjects of all ages, including children, again with imbalance due to visa issuance demand.
- ▷ Many of the images are live capture. A substantial number of the images are photographs of paper photographs.
- ▷ When these images are input to the algorithm, they are labelled as being of type "ISO" - see Table 4 of the FRVT API.

### 2.3 Visa images II

- ▷ The number of images is on the order of  $10^6$ .
- ▷ The number of subjects is on the order of  $10^6$ .
- ▷ The number of subjects with two images on the order of  $10^6$ .

- ▷ The images have geometry in good conformance with the ISO/IEC 19794-5 Full Frontal image type. Pose is generally excellent.
- ▷ The images are of size 300x300 pixels. The mean interocular distance (IOD) is 61 pixels.
- ▷ The images are of subjects from greater than 100 countries, with significant imbalance due to population and immigration patterns.
- ▷ The images are of subjects of all ages, including children, again with imbalance due to population and immigration patterns and demand.
- ▷ All of the images are live capture.
- ▷ When these images are input to the algorithm, they are labelled as being of type "ISO" - see Table 4 of the FRVT API.

## 2.4 Mugshot images

- ▷ The number of images is on the order of  $10^6$ .
- ▷ The number of subjects is on the order of  $10^6$ .
- ▷ The number of subjects with two images on the order of  $10^6$ .
- ▷ The images have geometry in reasonable conformance with the ISO/IEC 19794-5 Full Frontal image type.
- ▷ The images are of variable sizes. The median IOD is 105 pixels. The mean IOD is 113 pixels. The 1-st, 5-th, 10-th, 25-th, 75-th, 90-th and 99-th percentiles are 34, 58, 70, 87, 121, 161 and 297 pixels.
- ▷ The images are of subjects from the United States.
- ▷ The images are of adults.
- ▷ The images are all live capture.
- ▷ When these images are input to the algorithm, they are labelled as being of type "mugshot" - see Table 4 of the FRVT API.

## 2.5 Webcam images

- ▷ The number of images is on the order of  $10^6$ .
- ▷ The number of subjects is on the order of  $10^6$ .
- ▷ All subjects have a webcam image, and a portrait image.
- ▷ The portrait images are in poor conformance with the ISO/IEC 19794-5 Full Frontal image type.
- ▷ The webcam images are taken with a camera oriented by an attendant toward a cooperating subject. This is done under time constraints so there are roll, pitch and yaw angle variation. Also background illumination is sometimes strong, so the face is under exposed. There is sometimes perspective distortion due to close range images.
- ▷ The images have mean IOD of 38 pixels.
- ▷ The images are all live capture.
- ▷ When these images are input to the algorithm, they are labelled as being of type "WILD" - see Table 4 of the FRVT API.



*Figure 3: The figure gives simulated samples of image types used in this report.*

## 2.6 Wild images

- ▷ The number of images is on the order of  $10^5$ .
- ▷ The number of subjects is on the order of  $10^3$ .
- ▷ The number of subjects with two images on the order of  $10^3$ .
- ▷ The images include many photojournalism-style images. Images are given to the algorithm using a variable but generally tight crop of the head. Resolution varies very widely. The images are very unconstrained, with wide yaw and pitch pose variation. Faces can be occluded, including hair and hands.
- ▷ The images are of adults.
- ▷ All of the images are live capture, none are scanned.
- ▷ When these images are input to the algorithm, they are labelled as being of type "WILD" - see Table 4 of the FRVT API.

## 3 Results

### 3.1 Test goals

- ▷ To state overall accuracy.
- ▷ To compare algorithms.

### 3.2 Test design

**Method:** For visa images:

- ▷ The comparisons are of visa photos against visa photos.
- ▷ The number of genuine comparisons is on the order of  $10^4$ .
- ▷ The number of impostor comparisons is on the order of  $10^{10}$ .
- ▷ The comparisons are fully zero-effort, meaning impostors are paired without attention to sex, age or other covariates. However, later analysis is conducted on subsets.

- ▷ The number of persons is on the order of  $10^5$ .
- ▷ The number of images used to make 1 template is 1.
- ▷ The number of templates used to make each comparison score is two corresponding to simple one-to-one verification.

For mugshot images:

- ▷ The comparisons are of mugshot photos against mugshot photos.
- ▷ The number of genuine comparisons is on the order of  $10^6$ .
- ▷ The number of impostor comparisons is on the order of  $10^8$ .
- ▷ The impostors are paired by sex, but not by age or other covariates.
- ▷ The number of persons is on the order of  $10^6$ .
- ▷ The number of images used to make 1 template is 1.
- ▷ The number of templates used to make each comparison score is two corresponding to simple one-to-one verification.

**Method:** For wild images:

- ▷ The comparisons are of wild photos against wild photos.
- ▷ The number of genuine comparisons is on the order of  $10^6$ .
- ▷ The number of impostor comparisons is on the order of  $10^7$ .
- ▷ The comparisons are fully zero-effort, meaning impostors are paired without attention to sex, age or other covariates.
- ▷ The number of persons is on the order of  $10^4$ .
- ▷ The number of images used to make 1 template is 1.
- ▷ The number of templates used to make each comparison score is two corresponding to simple one-to-one verification.

For child exploitation images:

- ▷ The comparisons are of unconstrained child exploitation photos against others of the same type.
- ▷ The number of genuine comparisons is on the order of  $10^4$ .
- ▷ The number of impostor comparisons is on the order of  $10^7$ .
- ▷ The comparisons are fully zero-effort, meaning impostors are paired without attention to sex, age or other covariates.
- ▷ The number of persons is on the order of  $10^3$ .
- ▷ The number of images used to make 1 template is 1.
- ▷ The number of templates used to make each comparison score is two corresponding to simple one-to-one verification.

▷ We produce two performance statements. First, is a DET as used for visa and mugshot images. The second is a cumulative match characteristic (CMC) summarizing a simulated one-to-many search process. This is done as follows.

- We regard  $M$  enrollment templates as items in a gallery.
- These  $M$  templates come from  $M > N$  individuals, because multiple images of a subject are present in the gallery under separate identifiers.
- We regard the verification templates as search templates.
- For each search we compute the rank of the highest scoring mate.
- This process should properly be conducted with a 1:N algorithm, such as those tested in NIST IR 8009. We use the 1:1 algorithms in a simulated 1:N mode here to a) better reflect what a child exploitation analyst does, and b) to show algorithm efficacy is better than that revealed in the verification DETs.

### 3.3 Failure to enroll

	Algorithm Name	Failure to Enrol Rate <sup>1</sup>					
		CHILD-EXPLOIT	MUGSHOT	VISA	WILD		
1	3divi-003	0.1806	58	0.0007	111	0.0006	105
2	3divi-004	-	154	0.0008	114	0.0006	107
3	adera-001	0.1928	61	0.0003	83	0.0005	101
4	alchera-000	-	154	0.0004	98	0.0014	133
5	alchera-001	-	154	0.0004	97	0.0014	132
6	allgovision-000	-	154	0.0026	139	0.0052	151
7	alphaface-001	-	154	0.0000	48	0.0004	80
8	amplifiedgroup-001	-	154	0.0189	154	0.0279	156
9	anke-003	-	154	0.0001	61	0.0004	71
10	anke-004	0.0944	43	0.0001	62	0.0004	81
11	anyvision-002	0.4866	81	0.0070	150	0.0090	153
12	anyvision-004	0.1660	55	0.0001	69	0.0004	77
13	aware-003	0.3314	75	0.0016	134	0.0013	129
14	aware-004	-	154	0.0002	73	0.0005	89
15	awiros-001	-	154	0.0386	155	0.0872	157
16	ayonix-000	0.0000	3	0.0113	151	0.0137	155
17	bm-001	0.0000	18	0.0000	36	0.0000	14
18	camvi-002	0.0000	4	0.0000	21	0.0000	22
19	camvi-004	-	154	0.0000	25	0.0000	26
20	ceiec-001	-	154	0.0029	142	0.0023	140
21	ceiec-002	0.2482	69	0.0036	144	0.0031	146
22	chtface-001	-	154	0.0000	28	0.0000	29
23	cogent-003	-	154	0.0001	58	0.0004	74
24	cogent-004	0.0000	6	0.0000	4	0.0000	4
25	cognitec-000	0.6342	85	0.0007	112	0.0007	113
26	cognitec-001	-	154	0.0008	118	0.0010	115
27	ctcbcbank-000	0.3285	74	0.0011	125	0.0019	137
28	cyberextruder-001	0.5338	83	0.0024	137	0.0029	144
29	cyberextruder-002	0.2672	72	0.0027	140	0.0028	143
30	cyberlink-002	0.1463	54	0.0004	91	0.0004	87
31	cyberlink-003	-	154	0.0001	51	0.0004	62
32	dahua-002	-	154	0.0024	138	0.0022	139
33	dahua-003	-	154	0.0002	78	0.0003	43
34	deepglint-001	0.0000	19	0.0000	14	0.0000	15
35	deepsea-001	0.0000	8	0.0000	7	0.0000	7
36	dermalog-005	0.1796	56	0.0013	130	0.0041	148
37	dermalog-006	0.1797	57	0.0013	129	0.0041	149
38	digitalbarriers-002	-	154	0.0028	141	0.0027	142
39	dsk-000	0.0000	14	0.0000	11	0.0000	11
40	einetworks-000	-	154	0.0002	76	0.0005	99
41	everai-002	-	154	0.0002	79	0.0004	56
42	everai-paravision-003	0.0705	39	0.0002	72	0.0004	63
43	f8-001	0.2026	63	0.0035	143	0.0030	145
44	facesoft-000	0.0000	23	0.0000	35	0.0000	36
45	glory-000	0.0000	16	0.0053	148	0.0013	130
46	glory-001	0.0000	11	0.0051	147	0.0010	116
47	gorilla-002	0.1347	50	0.0003	90	0.0004	88
48	gorilla-003	0.1347	49	0.0003	89	0.0004	86
49	hik-001	-	154	0.0000	29	0.0000	28
50	hr-001	0.1198	48	0.0001	50	0.0004	65
51	hr-002	-	154	0.0002	75	0.0004	82
52	id3-003	0.3032	73	0.0016	135	0.0011	126
53	id3-004	-	154	0.0015	133	0.0011	125
54	idemia-004	-	154	0.0000	41	0.0004	59
55	idemia-005	-	154	0.0000	38	0.0003	48
56	iit-000	-	154	0.0007	110	0.0011	120
57	iit-001	0.0843	42	0.0001	71	0.0004	78
58	imagus-000	0.1107	46	0.0010	124	0.0012	128
59	imperial-000	-	154	0.0000	16	0.0000	17
60	imperial-002	-	154	0.0000	6	0.0000	6

Table 9: FTE is the proportion of failed template generation attempts. Failures can occur because the software throws an exception, or because the software electively refuses to process the input image. This would typically occur if a face is not detected. FTE is measured as the number of function calls that give EITHER a non-zero error code OR that give a “small” template. This is defined as one whose size is less than 0.3 times the median template size for that algorithm. This second rule is needed because some algorithms incorrectly fail to return a non-zero error code when template generation fails.

<sup>1</sup>The effects of FTE are included in the accuracy results of this report by regarding any template comparison involving a failed template to produce a low similarity score. Thus higher FTE results in higher FNMR and lower FMR.

	Algorithm Name	Failure to Enrol Rate <sup>1</sup>					
		CHILD-EXPLOIT	MUGSHOT	VISA	WILD		
61	incode-003	- 154	0.0004 102	0.0007 110	0.0014 83		
62	incode-004	0.2202 64	0.0004 101	0.0007 109	0.0014 82		
63	innovatrics-004	0.1170 47	0.0000 47	0.0004 79	0.0041 95		
64	innovatrics-006	- 154	0.0000 43	0.0004 55	0.0003 51		
65	intellicloudai-001	- 154	0.0000 34	0.0000 35	0.0001 38		
66	intellifusion-001	- 154	0.0001 55	0.0003 51	0.0005 63		
67	intellivision-001	0.5495 84	0.0048 146	0.0042 150	0.1358 146		
68	intellivision-002	- 154	0.0012 127	0.0005 103	0.0146 116		
69	intelresearch-000	- 154	0.0000 45	0.0003 50	0.0001 39		
70	intsy whole-000	- 154	0.0004 96	0.0012 127	0.0031 92		
71	iqface-000	0.0000 9	0.0000 26	0.0000 27	0.0000 23		
72	isap-001	- 154	0.0000 24	0.0000 25	0.0000 21		
73	isityou-000	0.4714 79	0.0023 136	0.0010 118	0.0663 140		
74	isystems-001	0.1421 52	0.0010 122	0.0007 111	0.0128 113		
75	isystems-002	0.1421 53	0.0010 123	0.0007 112	0.0128 114		
76	itmo-005	0.1353 51	0.0005 104	0.0002 38	0.0075 103		
77	itmo-006	- 154	0.0004 100	0.0004 76	0.0006 67		
78	kakao-001	- 154	0.0002 80	0.0005 92	0.0310 126		
79	kakao-002	0.2494 70	0.0002 81	0.0005 96	0.0310 127		
80	kedacom-000	0.0000 17	0.0000 13	0.0000 13	0.0000 10		
81	kneron-003	0.4883 82	0.0044 145	0.0016 136	0.1823 151		
82	lookman-002	- 154	0.0000 23	0.0000 24	0.0000 20		
83	lookman-004	0.0000 1	0.0000 20	0.0000 21	0.0000 17		
84	megvii-001	0.0274 28	0.0007 113	0.0004 61	0.0152 117		
85	megvii-002	0.0274 27	0.0054 149	0.0004 60	0.0126 112		
86	meiya-001	- 154	0.0004 103	0.0010 119	0.0025 89		
87	microfocus-001	0.0791 41	0.0008 117	0.0016 135	0.0220 123		
88	microfocus-002	0.0791 40	0.0008 116	0.0016 134	0.0220 122		
89	mt-000	0.1043 44	0.0002 77	0.0004 83	0.0004 54		
90	neurotechnology-005	- 154	0.0004 94	0.0004 67	0.0018 85		
91	neurotechnology-006	0.1068 45	0.0004 95	0.0004 68	0.0018 86		
92	nodeflux-001	- 154	0.0001 63	0.0002 40	0.0003 44		
93	nodeflux-002	- 154	0.0008 115	0.0005 98	0.0008 75		
94	notiontag-000	0.0000 21	0.0000 17	0.0000 18	0.0000 15		
95	ntechlab-006	- 154	0.0000 37	0.0004 53	0.0003 43		
96	ntechlab-007	0.0682 38	0.0001 52	0.0004 57	0.0005 62		
97	pixelall-002	0.0001 24	0.0000 10	0.0000 10	0.0001 35		
98	psl-002	- 154	0.0000 12	0.0000 12	0.0000 9		
99	psl-003	- 154	0.0000 46	0.0004 75	0.0003 48		
100	rankone-006	- 154	0.0000 32	0.0000 33	0.0000 27		
101	rankone-007	0.3518 77	0.0003 85	0.0004 84	0.0043 97		
102	realnetworks-002	- 154	0.0004 93	0.0003 45	0.0004 56		
103	realnetworks-003	0.0076 25	0.0004 92	0.0003 44	0.0004 58		
104	remarkai-000	- 154	0.0000 2	0.0000 2	0.0000 33		
105	remarkai-001	- 154	0.0000 19	0.0000 20	0.0000 34		
106	rokid-000	- 154	0.0001 60	0.0005 97	0.0354 132		
107	saffe-001	0.0000 20	0.0000 15	0.0000 16	0.0000 13		
108	saffe-002	- 154	0.0000 31	0.0000 32	0.0000 26		
109	sensetime-001	0.0631 37	0.0000 40	0.0004 70	0.0003 46		
110	sensetime-002	0.3345 76	0.0011 126	0.0005 102	0.0218 121		
111	sertis-000	- 154	0.0000 49	0.0004 64	0.0004 55		
112	shaman-000	0.0000 5	0.0000 22	0.0000 23	0.0000 19		
113	shaman-001	0.0000 2	0.0000 1	0.0000 1	0.0000 31		
114	shu-001	0.1822 59	0.0010 121	0.0006 104	0.0499 135		
115	siat-002	0.0616 34	0.0000 44	0.0004 73	0.0048 99		
116	siat-004	- 154	0.0000 42	0.0004 72	0.0003 47		
117	sjtu-001	- 154	0.0005 105	0.0004 85	0.0008 73		
118	smilart-002	0.2422 67	0.0003 88	0.0011 122	0.0575 138		
119	smilart-003	- 154	0.0014 131	0.0013 131	0.0555 137		
120	starhybrid-001	0.2340 66	0.0009 120	0.0023 141	0.0044 98		

Table 10: FTE is the proportion of failed template generation attempts. Failures can occur because the software throws an exception, or because the software electively refuses to process the input image. This would typically occur if a face is not detected. FTE is measured as the number of function calls that give EITHER a non-zero error code OR that give a “small” template. This is defined as one whose size is less than 0.3 times the median template size for that algorithm. This second rule is needed because some algorithms incorrectly fail to return a non-zero error code when template generation fails.

<sup>1</sup>The effects of FTE are included in the accuracy results of this report by regarding any template comparison involving a failed template to produce a low similarity score. Thus higher FTE results in higher FNMR and lower FMR.

	Algorithm	Failure to Enrol Rate <sup>1</sup>					
		CHILD-EXPLOIT	MUGSHOT	VISA	WILD		
121	synesis-004	- 154	0.0164 153	0.0035 147	0.0485 134		
122	synesis-005	0.1862 60	0.0001 59	0.0005 90	0.0021 87		
123	tech5-002	- 154	0.0001 57	0.0003 41	0.0000 32		
124	tech5-003	- 154	0.0001 56	0.0003 42	0.0002 40		
125	tevian-004	- 154	0.0002 74	0.0005 100	0.0057 100		
126	tevian-005	- 154	0.0006 109	0.0006 108	0.0012 81		
127	tiger-002	0.0619 35	0.0001 66	0.0004 69	0.0082 107		
128	tiger-003	0.0619 36	0.0001 64	0.0004 66	0.0082 106		
129	tongyi-005	0.0000 7	0.0000 5	0.0000 5	0.0000 3		
130	toshiba-002	0.0000 13	0.0000 9	0.0000 9	0.0000 7		
131	toshiba-003	- 154	0.0001 67	0.0001 37	0.0002 42		
132	trueface-000	- 154	0.0000 33	0.0000 34	0.0000 28		
133	ulsee-001	- 154	0.0000 30	0.0000 31	0.0001 36		
134	uluface-002	0.0000 22	0.0000 18	0.0000 19	0.0000 16		
135	upc-001	0.0450 29	0.0003 82	0.0003 49	0.0011 80		
136	vd-001	- 154	0.0004 99	0.0009 114	0.0024 88		
137	veridas-001	- 154	0.0001 65	0.0005 93	0.0006 65		
138	veridas-002	- 154	0.0001 68	0.0005 95	0.0006 66		
139	via-000	0.0000 10	0.0000 27	0.0000 30	0.0001 37		
140	videonetics-001	0.4799 80	0.0015 132	0.0010 117	0.0112 110		
141	vigilantsolutions-006	- 154	0.0001 54	0.0004 58	0.0005 61		
142	vigilantsolutions-007	0.2538 71	0.0001 53	0.0004 54	0.0005 60		
143	vion-000	0.6388 86	0.0130 152	0.0078 152	0.1389 147		
144	visionbox-000	- 154	0.0005 108	0.0011 124	0.0028 91		
145	visionbox-001	- 154	0.0005 107	0.0011 123	0.0028 90		
146	visionlabs-006	- 154	0.0003 87	0.0005 94	0.0009 78		
147	visionlabs-007	0.1939 62	0.0003 86	0.0005 91	0.0008 74		
148	vocord-006	- 154	0.0003 84	0.0003 47	0.0008 72		
149	vocord-007	0.0000 15	0.0001 70	0.0004 52	0.0009 77		
150	winsense-000	0.0000 12	0.0000 8	0.0000 8	0.0000 6		
151	x-laboratory-000	- 154	0.0005 106	0.0002 39	0.0000 29		
152	yisheng-004	0.4279 78	0.0013 128	0.0006 106	0.0321 129		
153	yitu-003	- 154	0.0009 119	0.0000 3	0.0000 1		

Table 11: FTE is the proportion of failed template generation attempts. Failures can occur because the software throws an exception, or because the software electively refuses to process the input image. This would typically occur if a face is not detected. FTE is measured as the number of function calls that give EITHER a non-zero error code OR that give a “small” template. This is defined as one whose size is less than 0.3 times the median template size for that algorithm. This second rule is needed because some algorithms incorrectly fail to return a non-zero error code when template generation fails.

<sup>1</sup> The effects of FTE are included in the accuracy results of this report by regarding any template comparison involving a failed template to produce a low similarity score. Thus higher FTE results in higher FNMR and lower FMR.

### 3.4 Recognition accuracy

Core algorithm accuracy is stated via:

▷ **Cooperative subjects**

- The summary table of Figure 8;
- The visa image DETs of Figure 26;
- The mugshot DETs of Figure 34;
- The mugshot ageing profiles of Figure 126;
- The human-difficult pairs of Figure 10

▷ **Non-cooperative subjects**

- The photojournalism DET of Figure 41
- The child-exploitation DET of Figure 45;
- The child-exploitation CMC of Figure 48.

Figure 102 shows dependence of false match rate on algorithm score threshold. This allows a deployer to set a threshold to target a particular false match rate appropriate to the security objectives of the application.

Figure 86 likewise shows FMR( $T$ ) but for mugshots, and specially four subsets of the population.

Note that in both the mugshot and visa sets false match rates vary with the ethnicity, age, and sex, of the enrollee and impostor - see section 3.6. For example figure 57 summarizes FMR for impostors paired from four groups black females, black males, white females, white males.

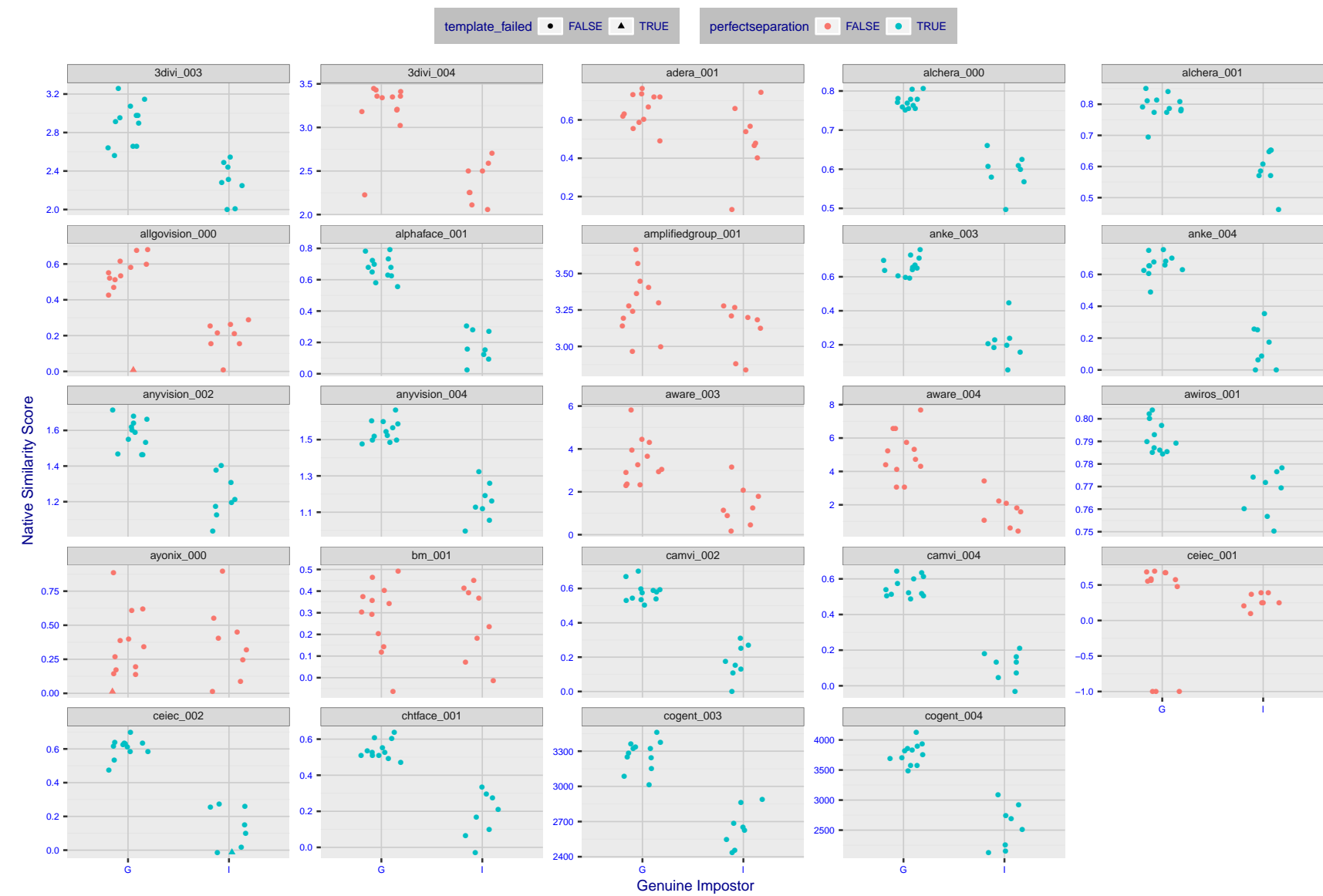


Figure 4: The Figure shows, in blue, algorithms that correctly separate the 12 genuine and 8 impostor pairs used in the May 2018 paper [Face recognition accuracy of forensic examiners, superrecognizers, and face recognition algorithms](#) (Phillips et al. [1]). In red are algorithms that are imperfect. Some algorithms fail only because they failed to make a template e.g. due to face detection failure (shown as a triangle). Others fail because the pairs were selected for that study because they had been difficult for three leading algorithms used in FRVT 2006. Caution: Given the small sample size ( $n=20$ ) the figure may change substantially if larger or different sets were used. The images can be downloaded from the [Supplemental Information](#) page provided with that publication.

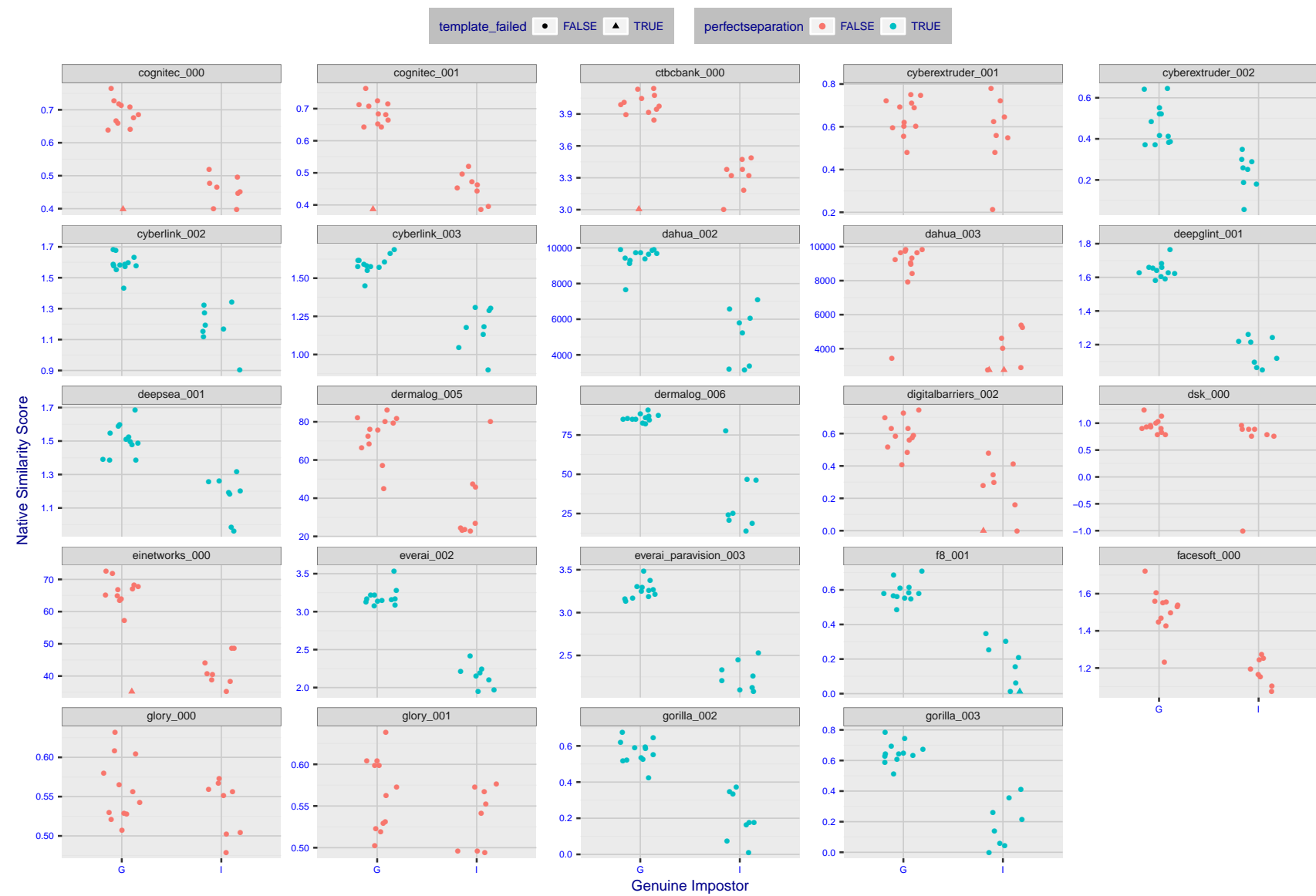


Figure 5: The Figure shows, in blue, algorithms that correctly separate the 12 genuine and 8 impostor pairs used in the May 2018 paper [Face recognition accuracy of forensic examiners, superrecognizers, and face recognition algorithms](#) (Phillips et al. [1]). In red are algorithms that are imperfect. Some algorithms fail only because they failed to make a template e.g. due to face detection failure (shown as a triangle). Others fail because the pairs were selected for that study because they had been difficult for three leading algorithms used in FRVT 2006. Caution: Given the small sample size ( $n=20$ ) the figure may change substantially if larger or different sets were used. The images can be downloaded from the [Supplemental Information](#) page provided with that publication.



Figure 6: The Figure shows, in blue, algorithms that correctly separate the 12 genuine and 8 impostor pairs used in the May 2018 paper [Face recognition accuracy of forensic examiners, superrecognizers, and face recognition algorithms](#) (Phillips et al. [1]). In red are algorithms that imperfect. Some algorithms fail only because they failed to make a template e.g. due to face detection failure (shown as a triangle). Others fail because the pairs were selected for that study because they had been difficult for three leading algorithms used in FRVT 2006. Caution: Given the small sample size ( $n=20$ ) the figure may change substantially if larger or different sets were used. The images can be downloaded from the [Supplemental Information](#) page provided with that publication.

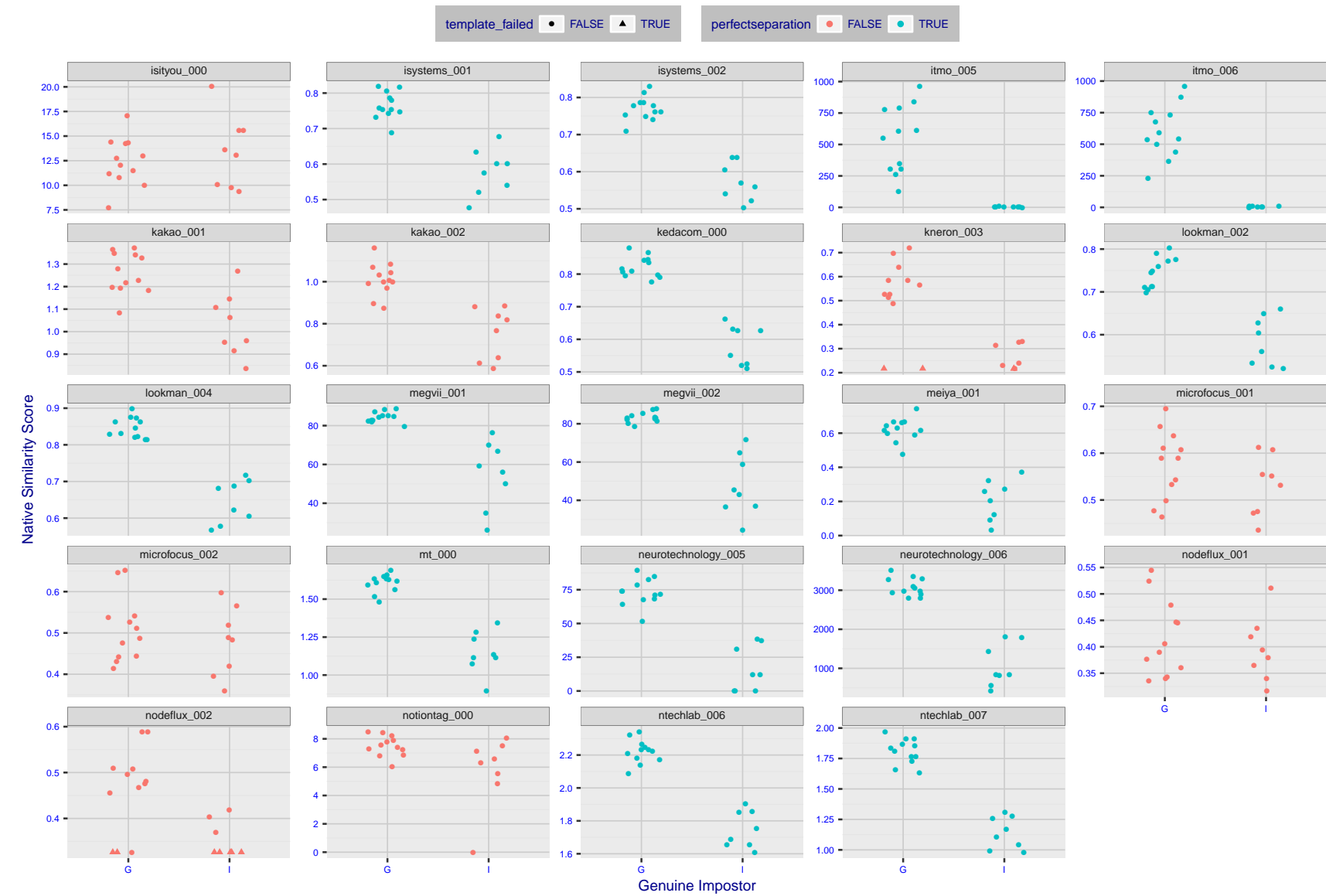


Figure 7: The Figure shows, in blue, algorithms that correctly separate the 12 genuine and 8 impostor pairs used in the May 2018 paper [Face recognition accuracy of forensic examiners, superrecognizers, and face recognition algorithms](#) (Phillips et al. [1]). In red are algorithms that imperfect. Some algorithms fail only because they failed to make a template e.g. due to face detection failure (shown as a triangle). Others fail because the pairs were selected for that study because they had been difficult for three leading algorithms used in FRVT 2006. Caution: Given the small sample size ( $n=20$ ) the figure may change substantially if larger or different sets were used. The images can be downloaded from the [Supplemental Information](#) page provided with that publication.

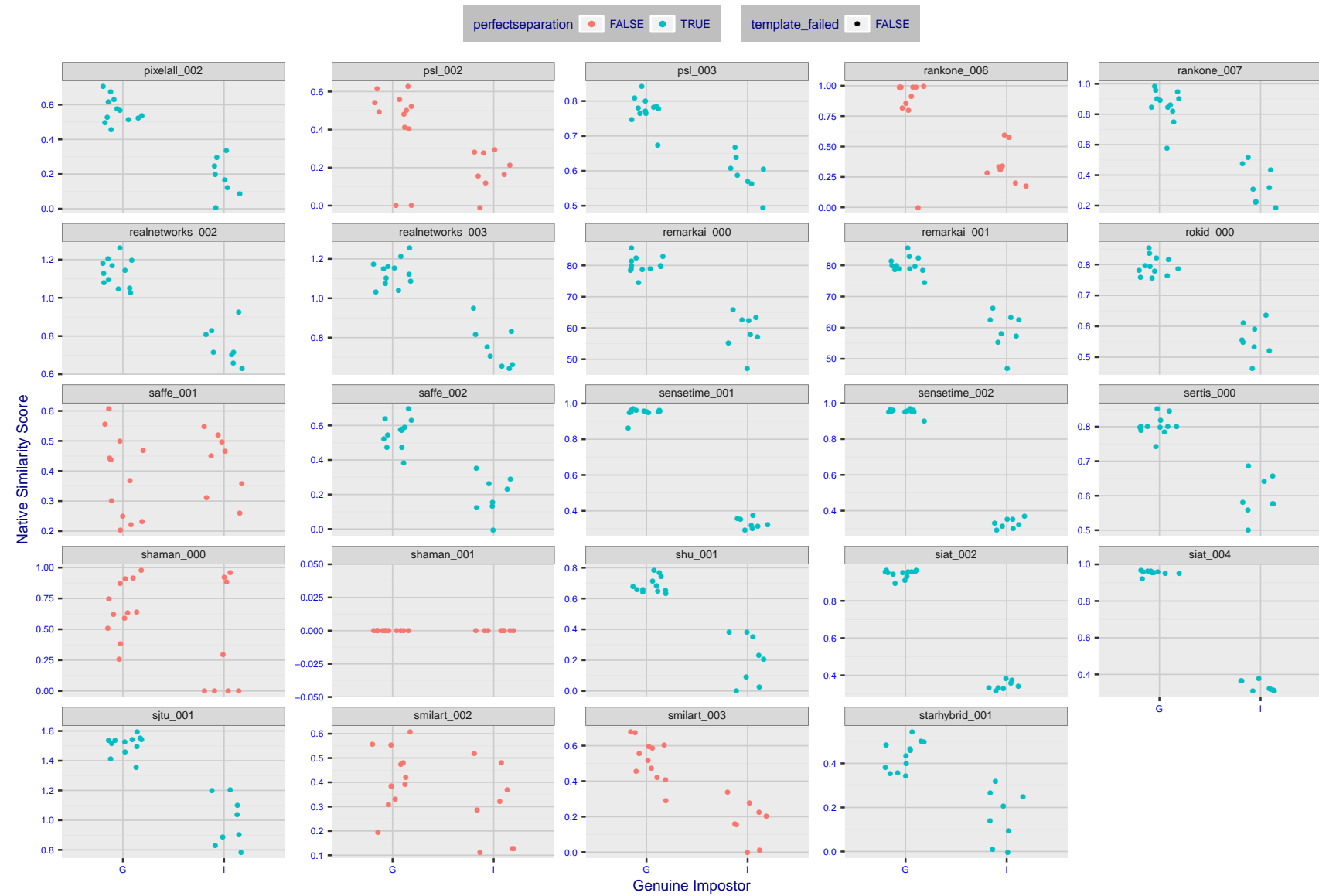


Figure 8: The Figure shows, in blue, algorithms that correctly separate the 12 genuine and 8 impostor pairs used in the May 2018 paper [Face recognition accuracy of forensic examiners, superrecognizers, and face recognition algorithms](#) (Phillips et al. [1]). In red are algorithms that are imperfect. Some algorithms fail only because they failed to make a template e.g. due to face detection failure (shown as a triangle). Others fail because the pairs were selected for that study because they had been difficult for three leading algorithms used in FRVT 2006. Caution: Given the small sample size ( $n=20$ ) the figure may change substantially if larger or different sets were used. The images can be downloaded from the [Supplemental Information](#) page provided with that publication.

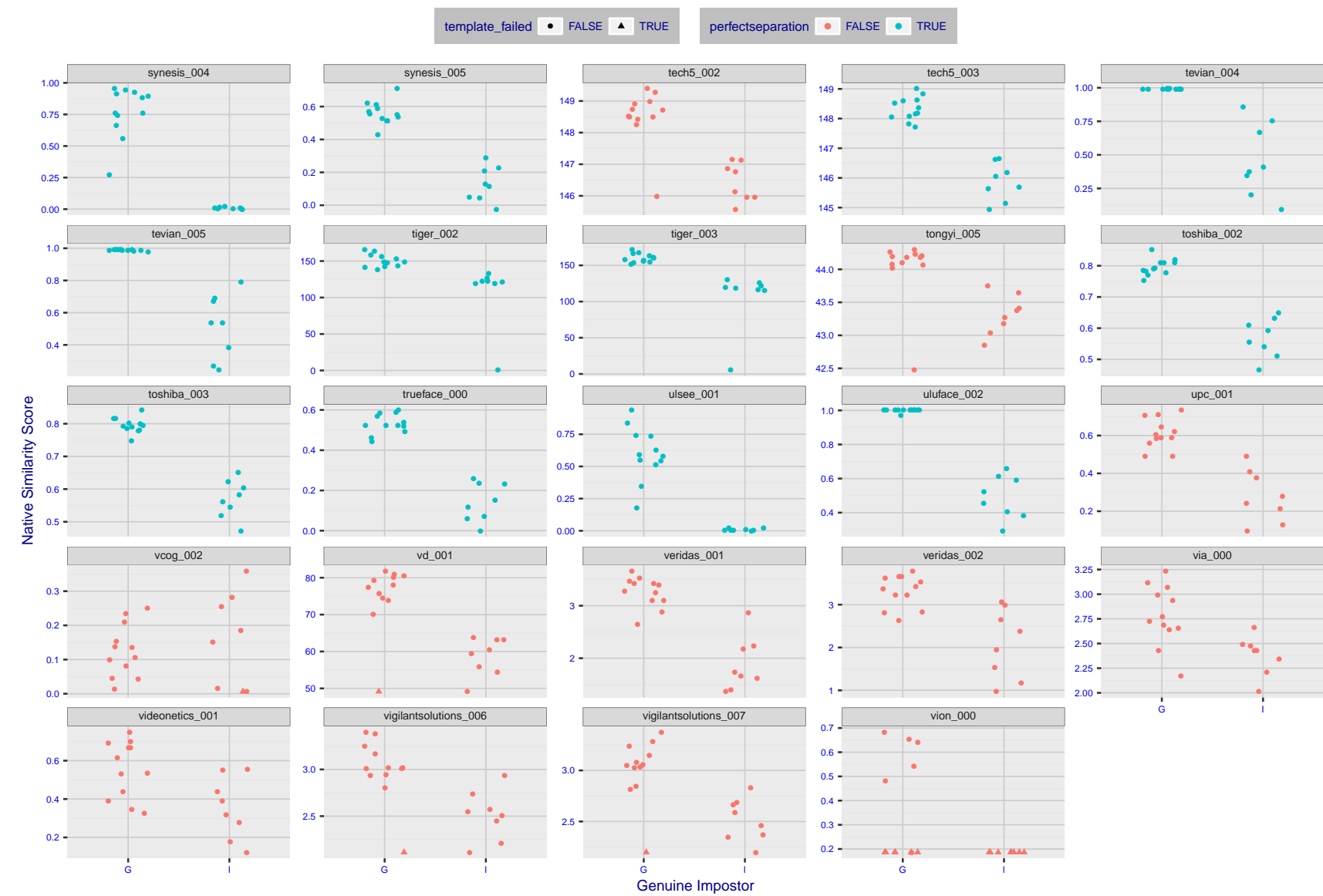


Figure 9: The Figure shows, in blue, algorithms that correctly separate the 12 genuine and 8 impostor pairs used in the May 2018 paper [Face recognition accuracy of forensic examiners, superrecognizers, and face recognition algorithms](#) (Phillips et al. [1]). In red are algorithms that are imperfect. Some algorithms fail only because they failed to make a template e.g. due to face detection failure (shown as a triangle). Others fail because the pairs were selected for that study because they had been difficult for three leading algorithms used in FRVT 2006. Caution: Given the small sample size ( $n=20$ ) the figure may change substantially if larger or different sets were used. The images can be downloaded from the [Supplemental Information](#) page provided with that publication.

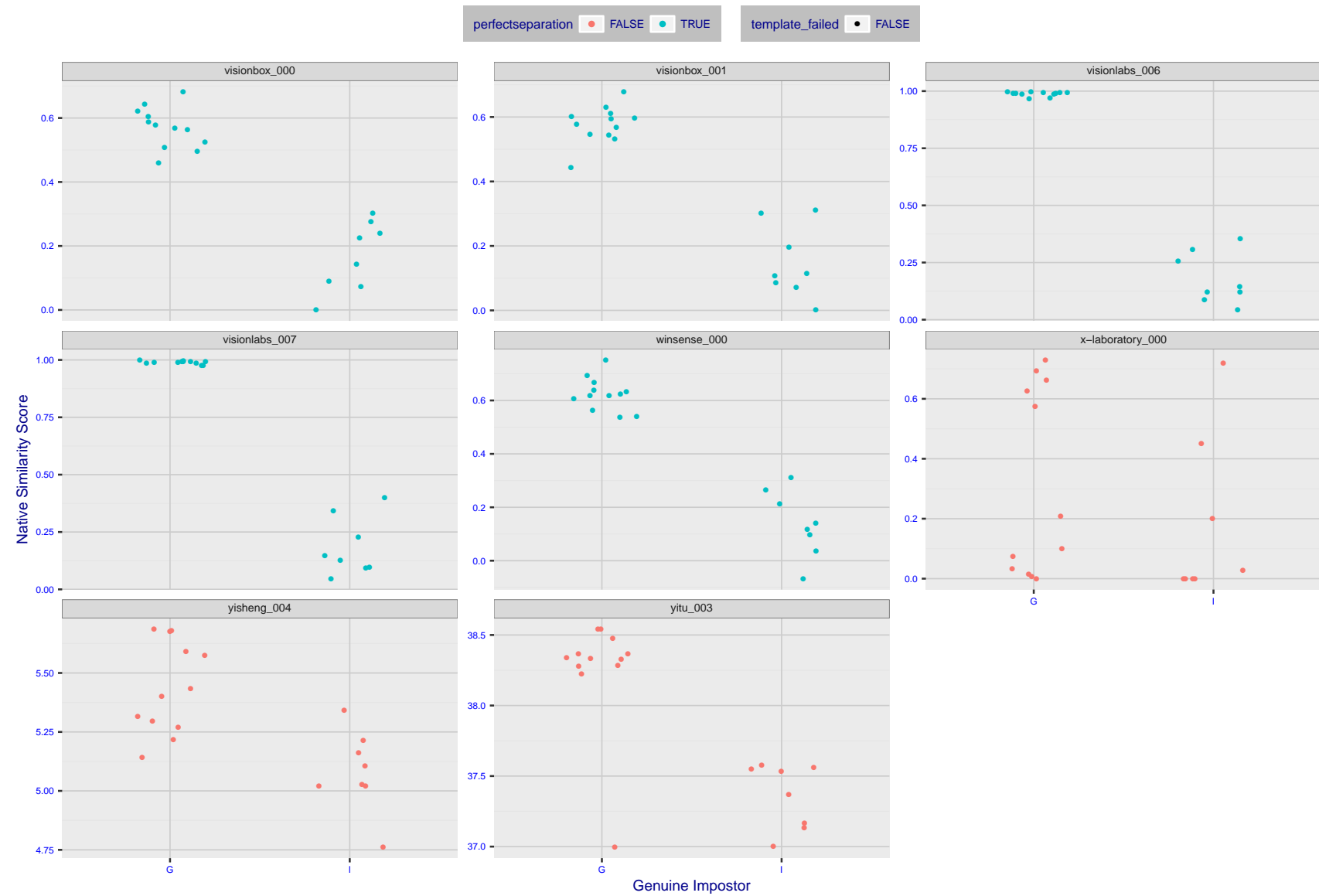


Figure 10: The Figure shows, in blue, algorithms that correctly separate the 12 genuine and 8 impostor pairs used in the May 2018 paper [Face recognition accuracy of forensic examiners, superrecognizers, and face recognition algorithms](#) (Phillips et al. [1]). In red are algorithms that are imperfect. Some algorithms fail only because they failed to make a template e.g. due to face detection failure (shown as a triangle). Others fail because the pairs were selected for that study because they had been difficult for three leading algorithms used in FRVT 2006. Caution: Given the small sample size ( $n=20$ ) the figure may change substantially if larger or different sets were used. The images can be downloaded from the [Supplemental Information](#) page provided with that publication.

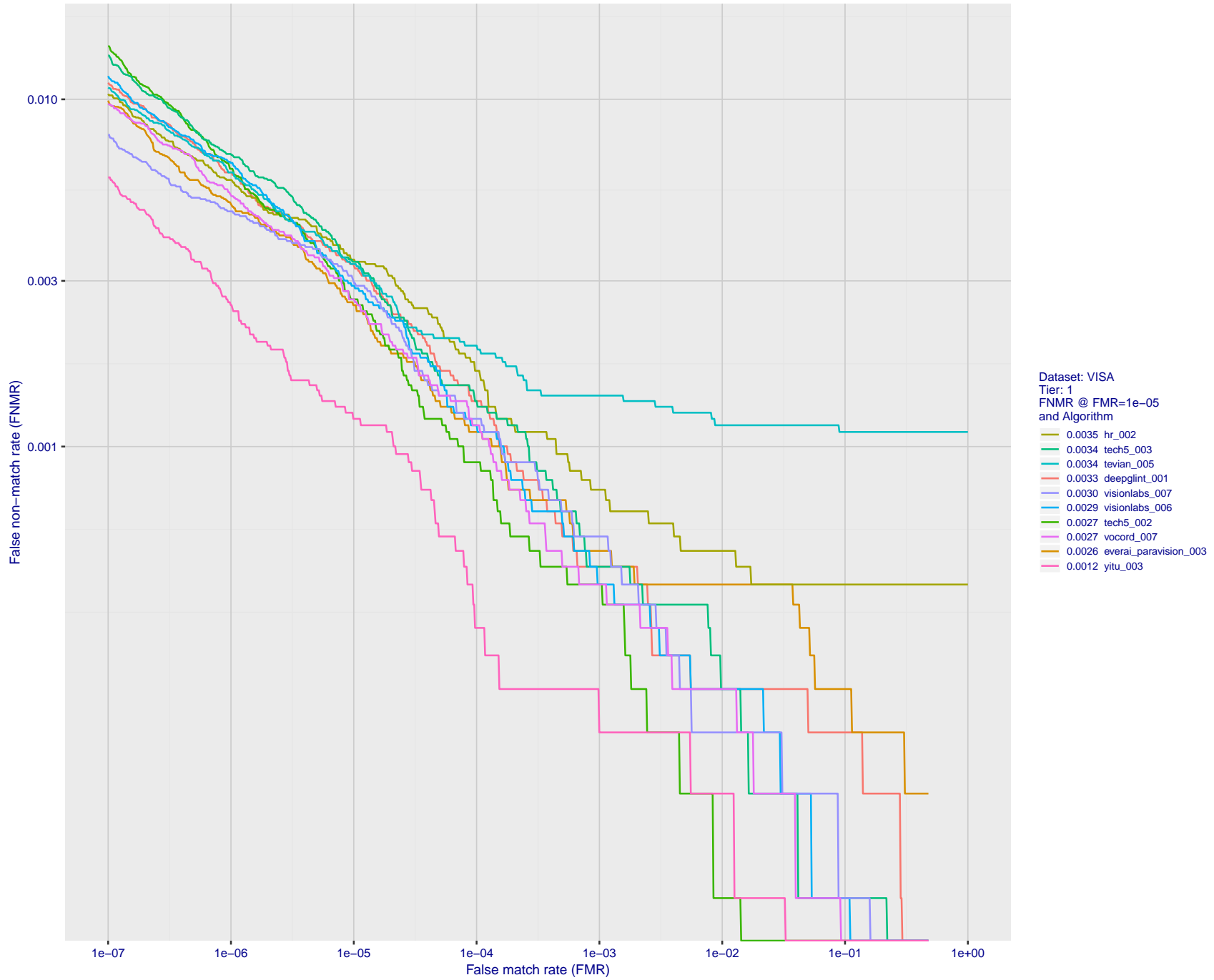


Figure 11: For the visa images, detection error tradeoff (DET) characteristics showing false non-match rate vs. false match rate plotted parametrically on threshold,  $T$ . The scales are logarithmic in order to show many decades of FMR.

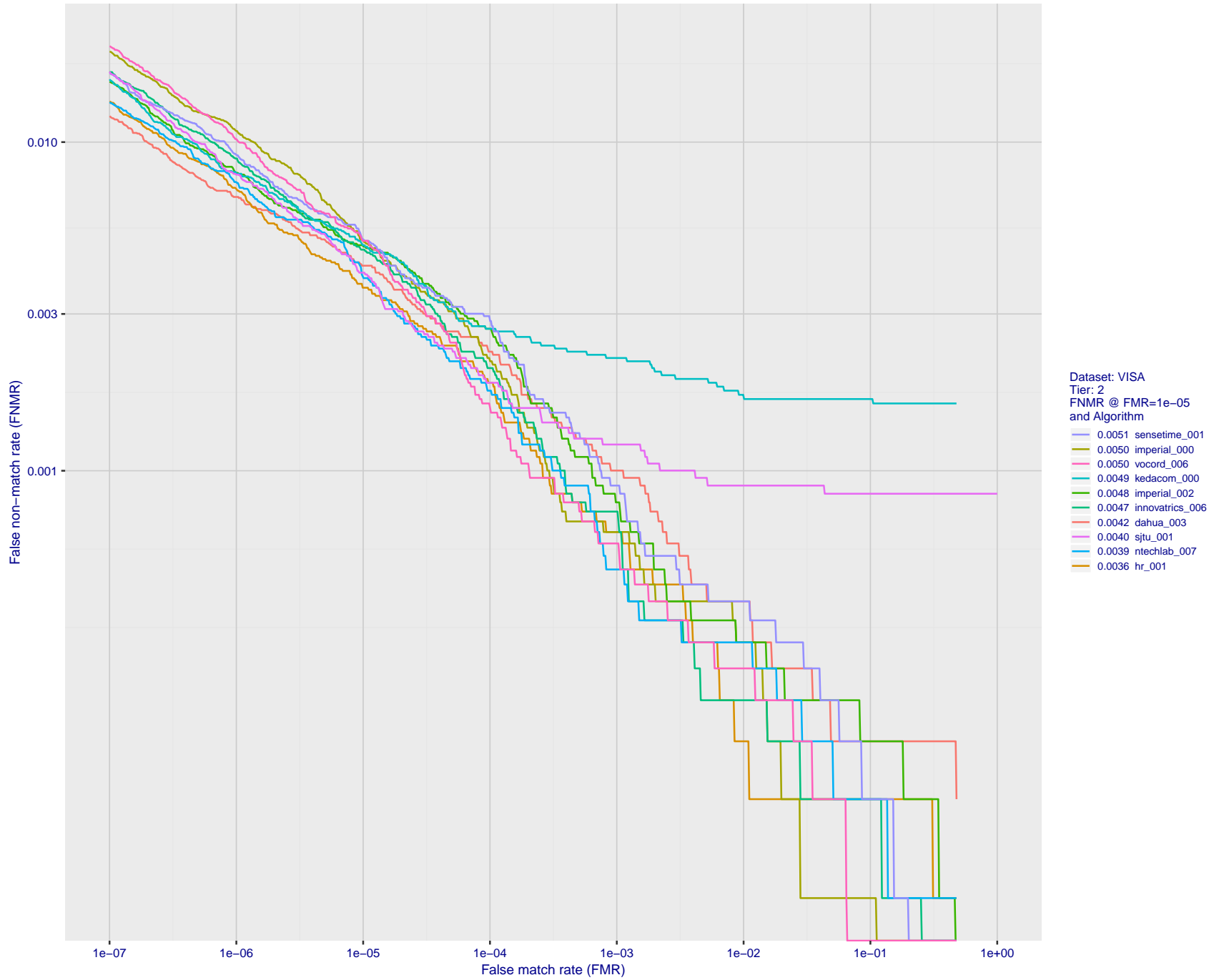


Figure 12: For the visa images, detection error tradeoff (DET) characteristics showing false non-match rate vs. false match rate plotted parametrically on threshold,  $T$ . The scales are logarithmic in order to show many decades of FMR.

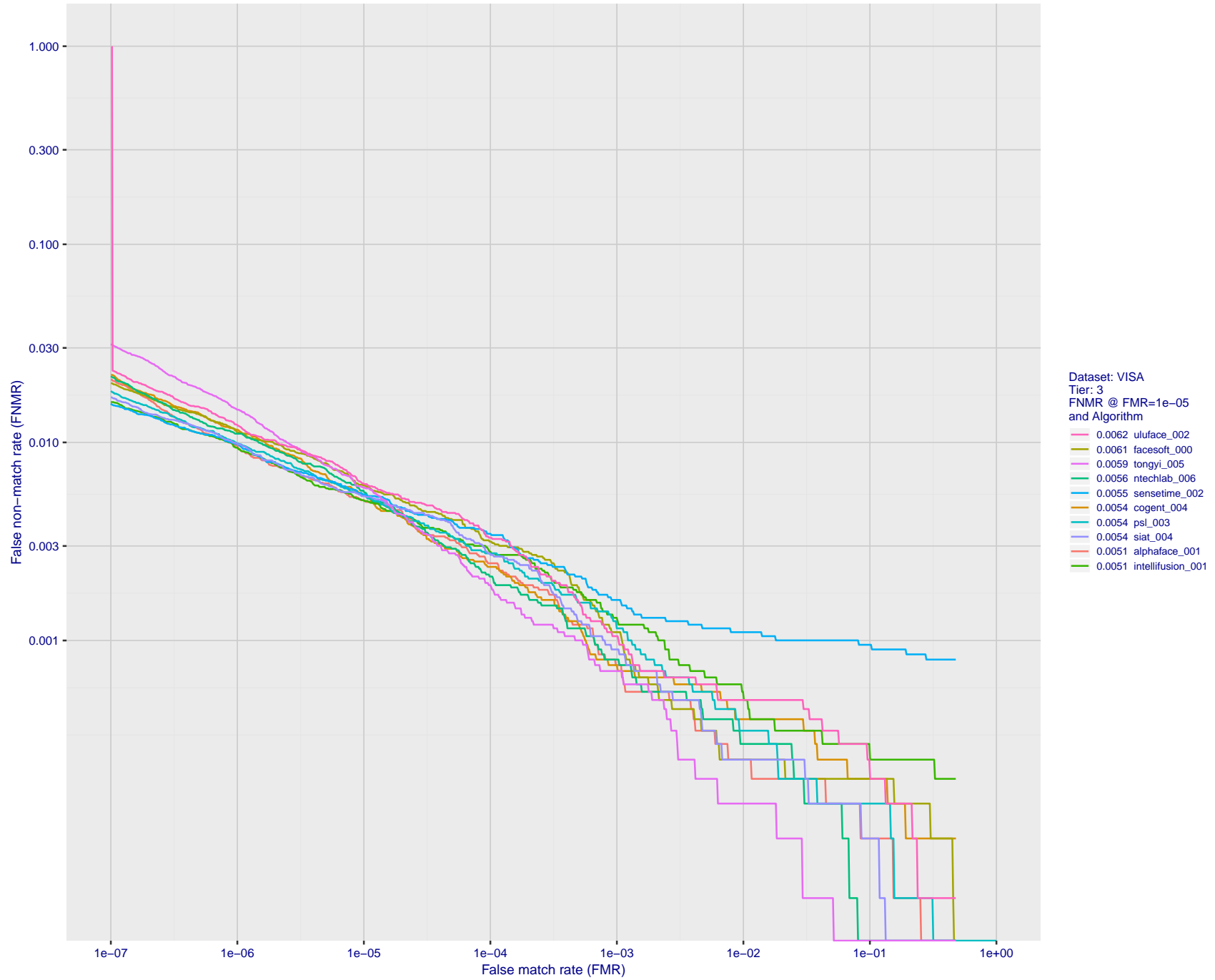


Figure 13: For the visa images, detection error tradeoff (DET) characteristics showing false non-match rate vs. false match rate plotted parametrically on threshold,  $T$ . The scales are logarithmic in order to show many decades of FMR.

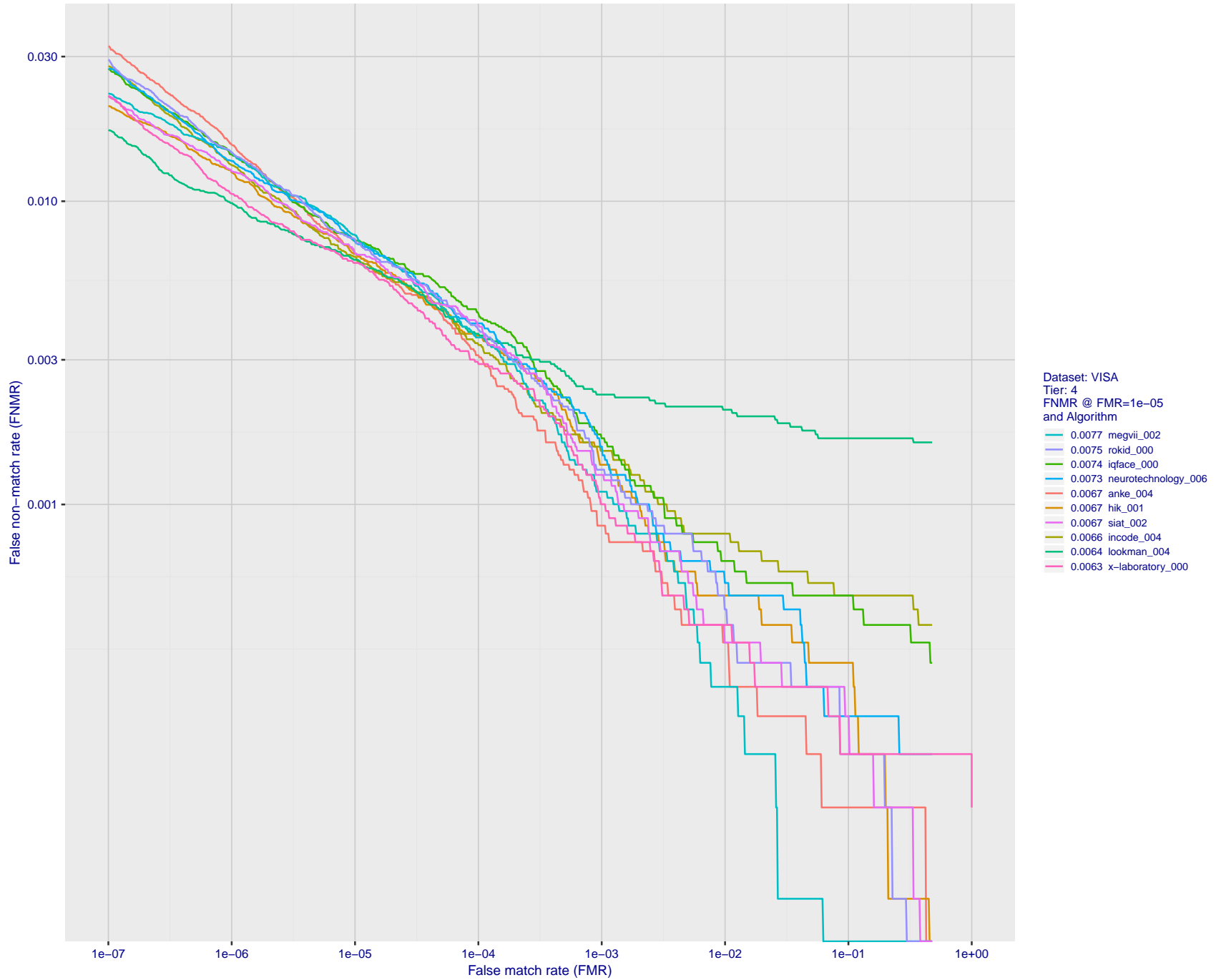


Figure 14: For the visa images, detection error tradeoff (DET) characteristics showing false non-match rate vs. false match rate plotted parametrically on threshold,  $T$ . The scales are logarithmic in order to show many decades of FMR.

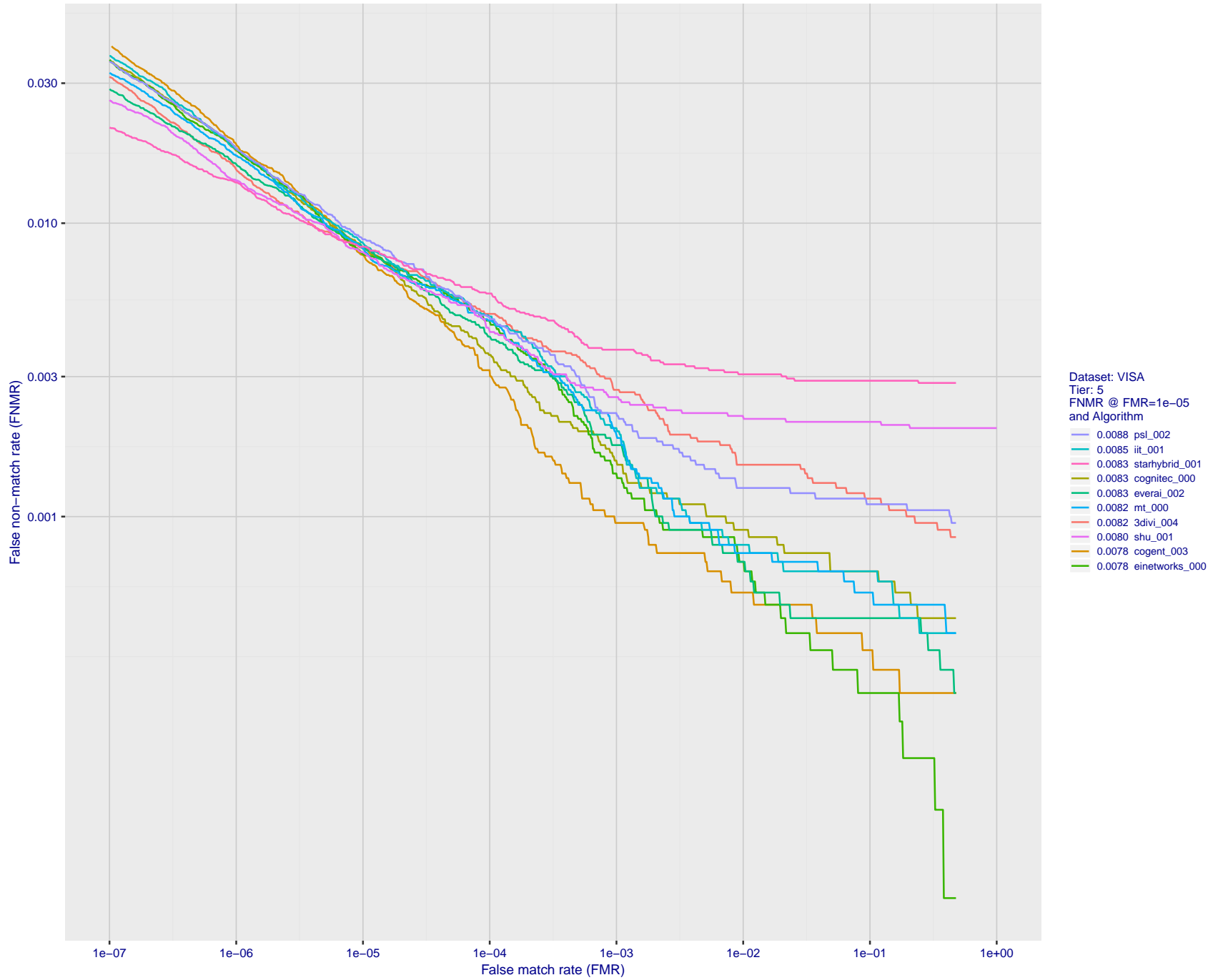


Figure 15: For the visa images, detection error tradeoff (DET) characteristics showing false non-match rate vs. false match rate plotted parametrically on threshold,  $T$ . The scales are logarithmic in order to show many decades of FMR.

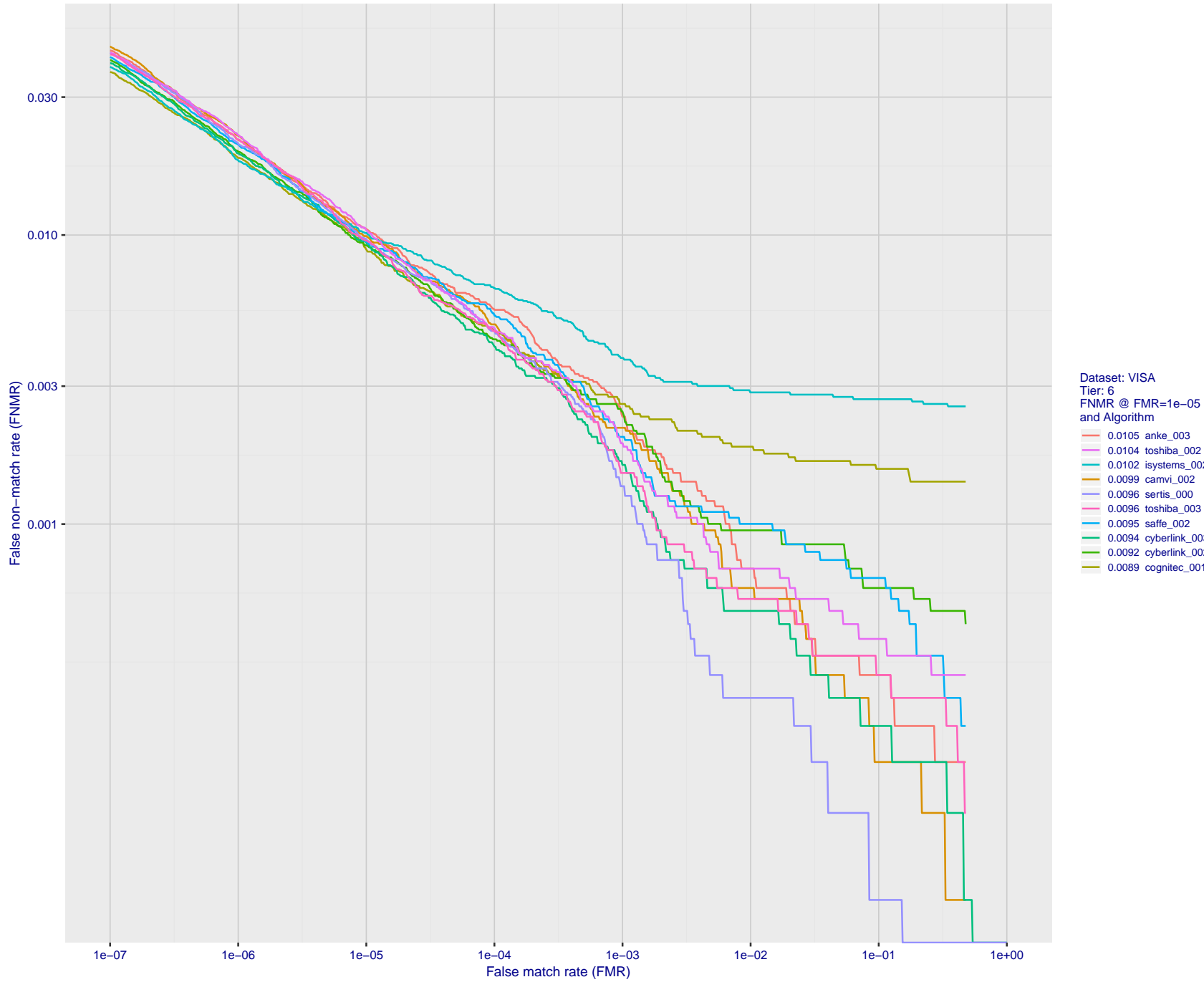


Figure 16: For the visa images, detection error tradeoff (DET) characteristics showing false non-match rate vs. false match rate plotted parametrically on threshold,  $T$ . The scales are logarithmic in order to show many decades of FMR.

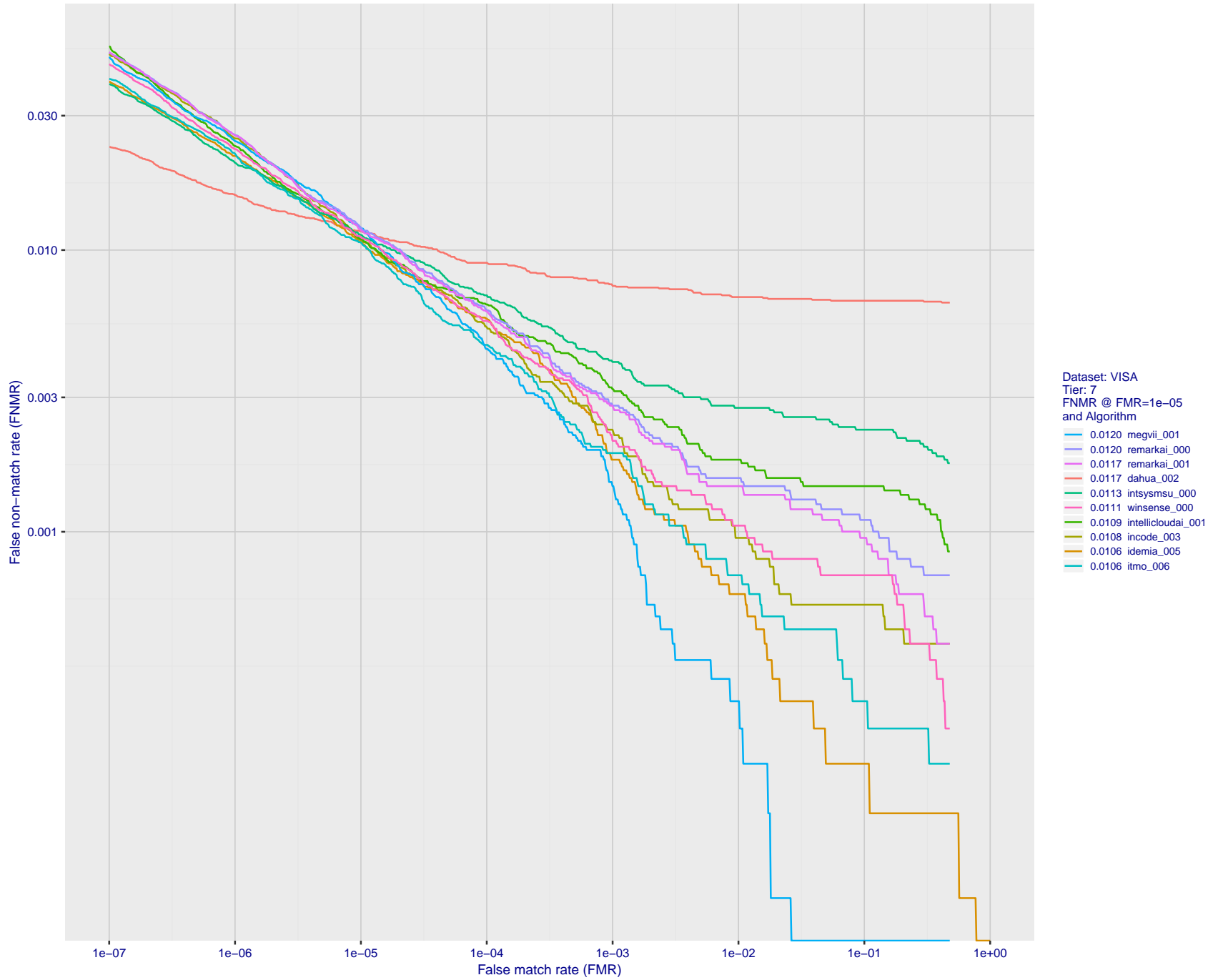


Figure 17: For the visa images, detection error tradeoff (DET) characteristics showing false non-match rate vs. false match rate plotted parametrically on threshold,  $T$ . The scales are logarithmic in order to show many decades of FMR.

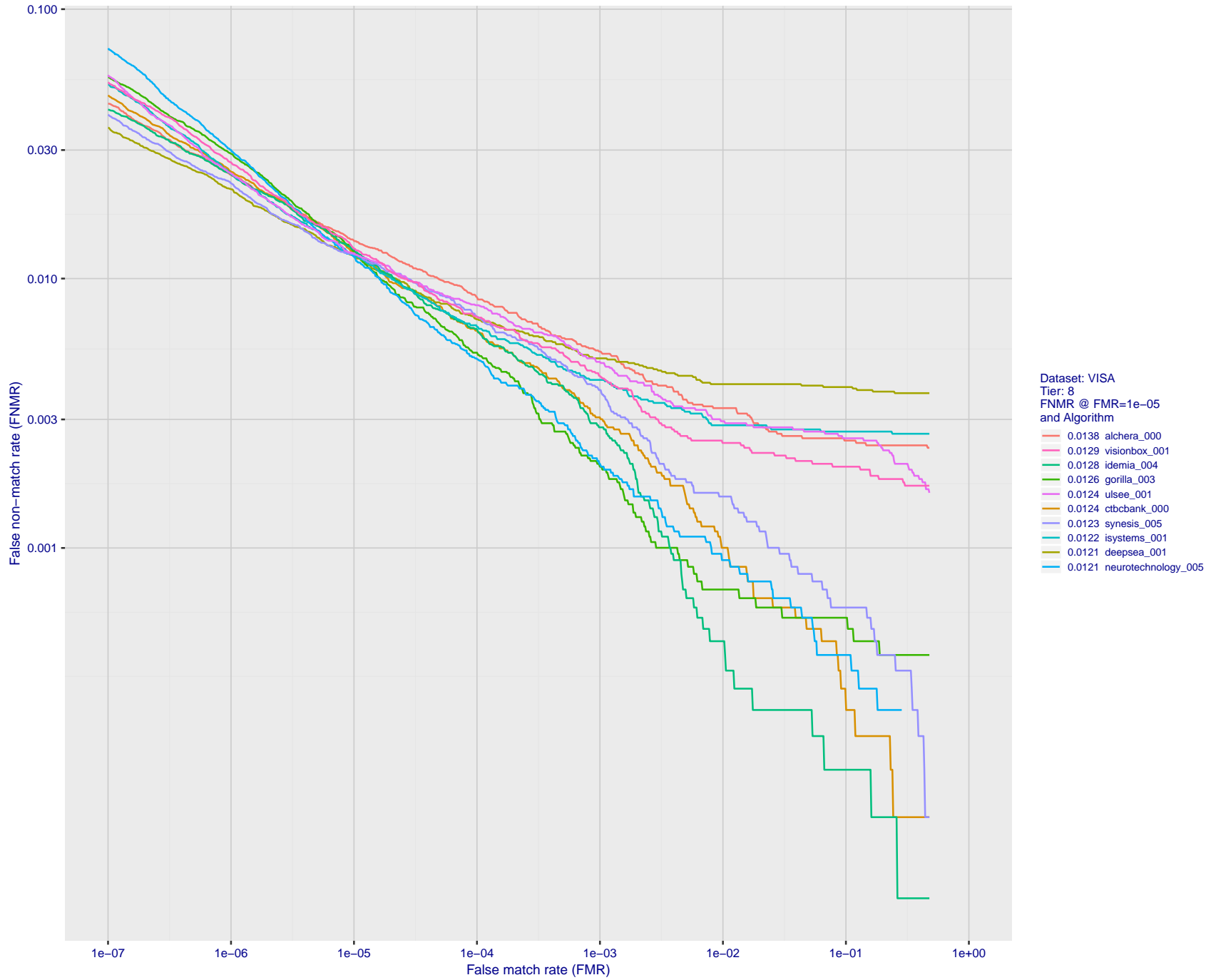


Figure 18: For the visa images, detection error tradeoff (DET) characteristics showing false non-match rate vs. false match rate plotted parametrically on threshold,  $T$ . The scales are logarithmic in order to show many decades of FMR.

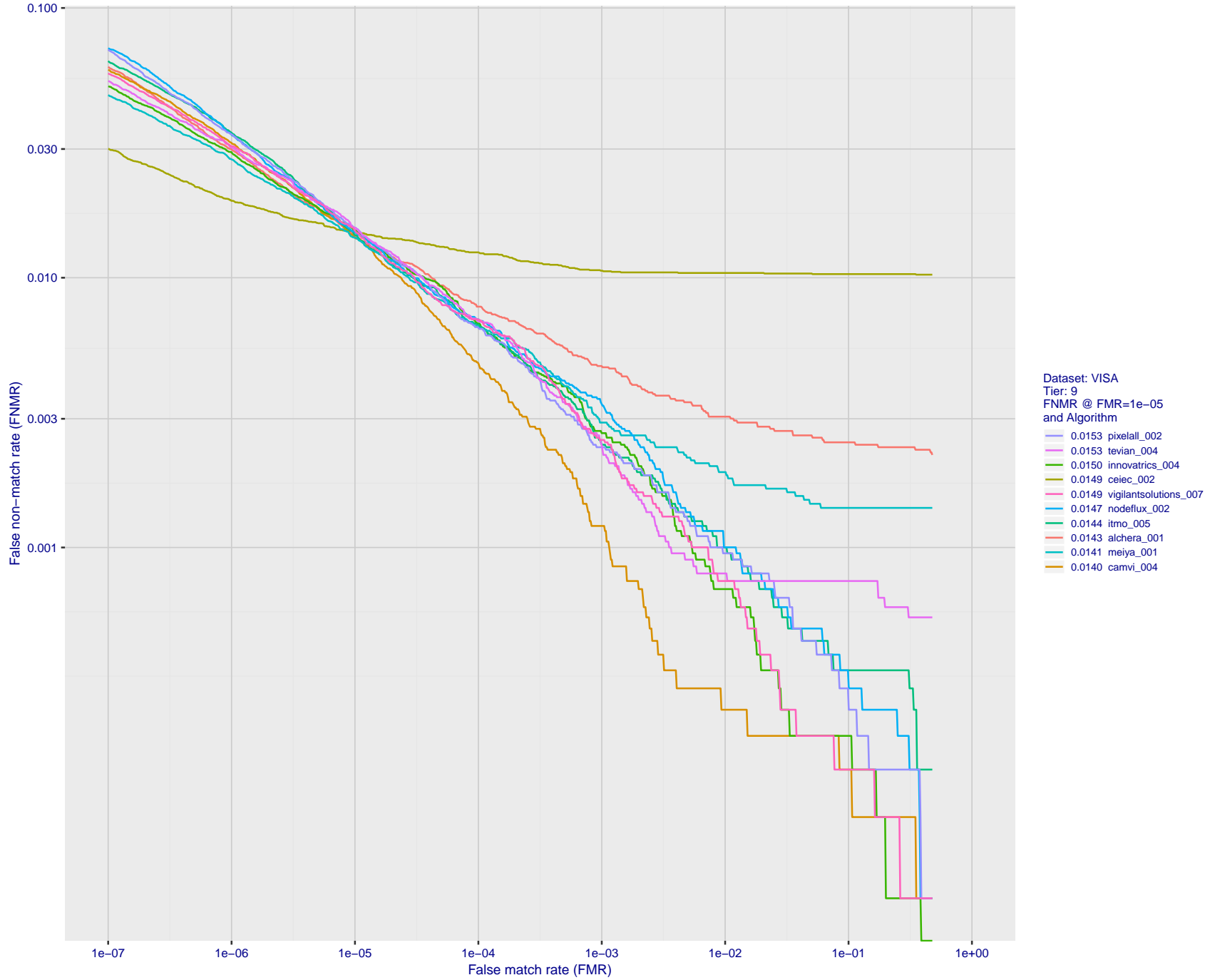


Figure 19: For the visa images, detection error tradeoff (DET) characteristics showing false non-match rate vs. false match rate plotted parametrically on threshold,  $T$ . The scales are logarithmic in order to show many decades of FMR.

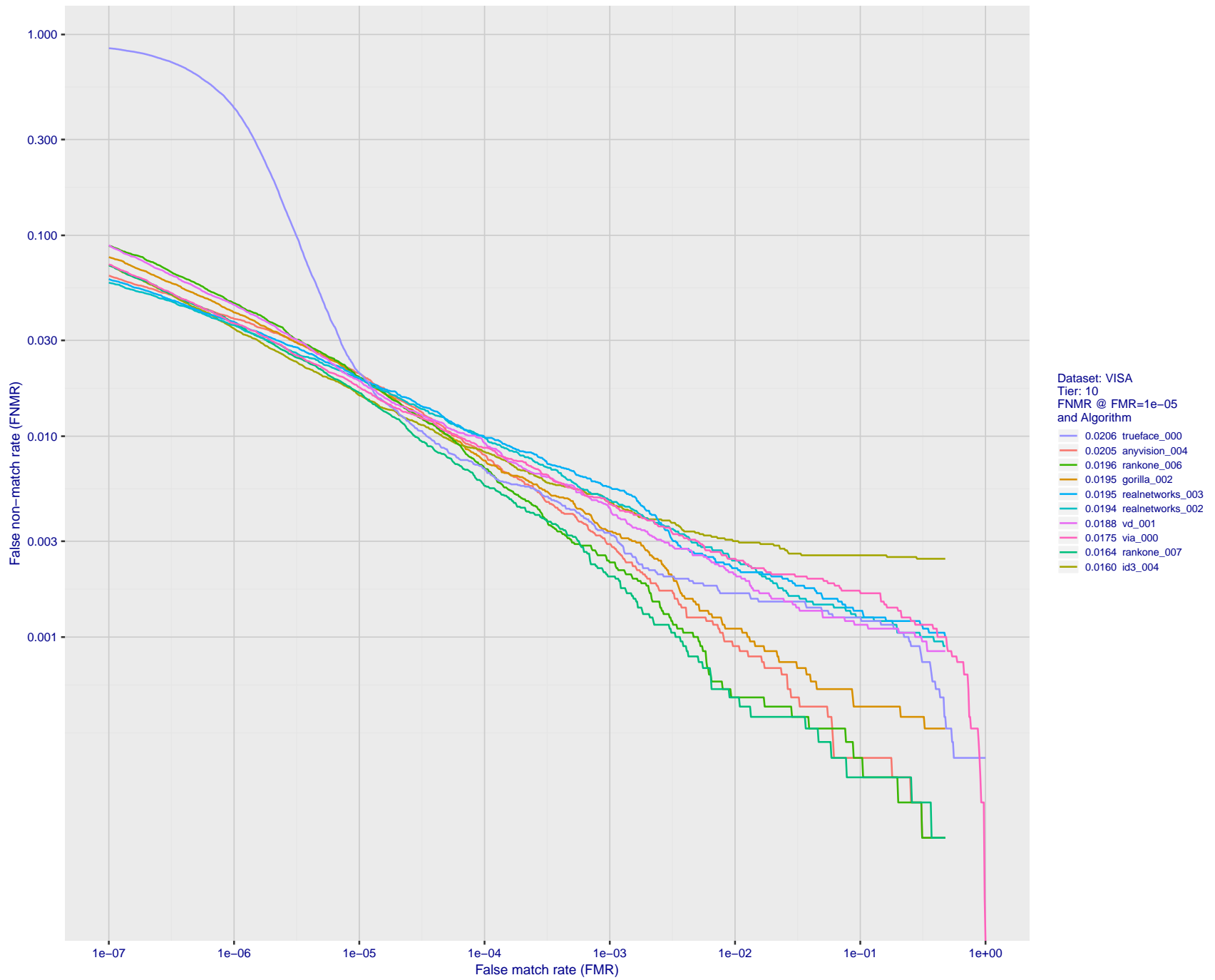


Figure 20: For the visa images, detection error tradeoff (DET) characteristics showing false non-match rate vs. false match rate plotted parametrically on threshold,  $T$ . The scales are logarithmic in order to show many decades of FMR.

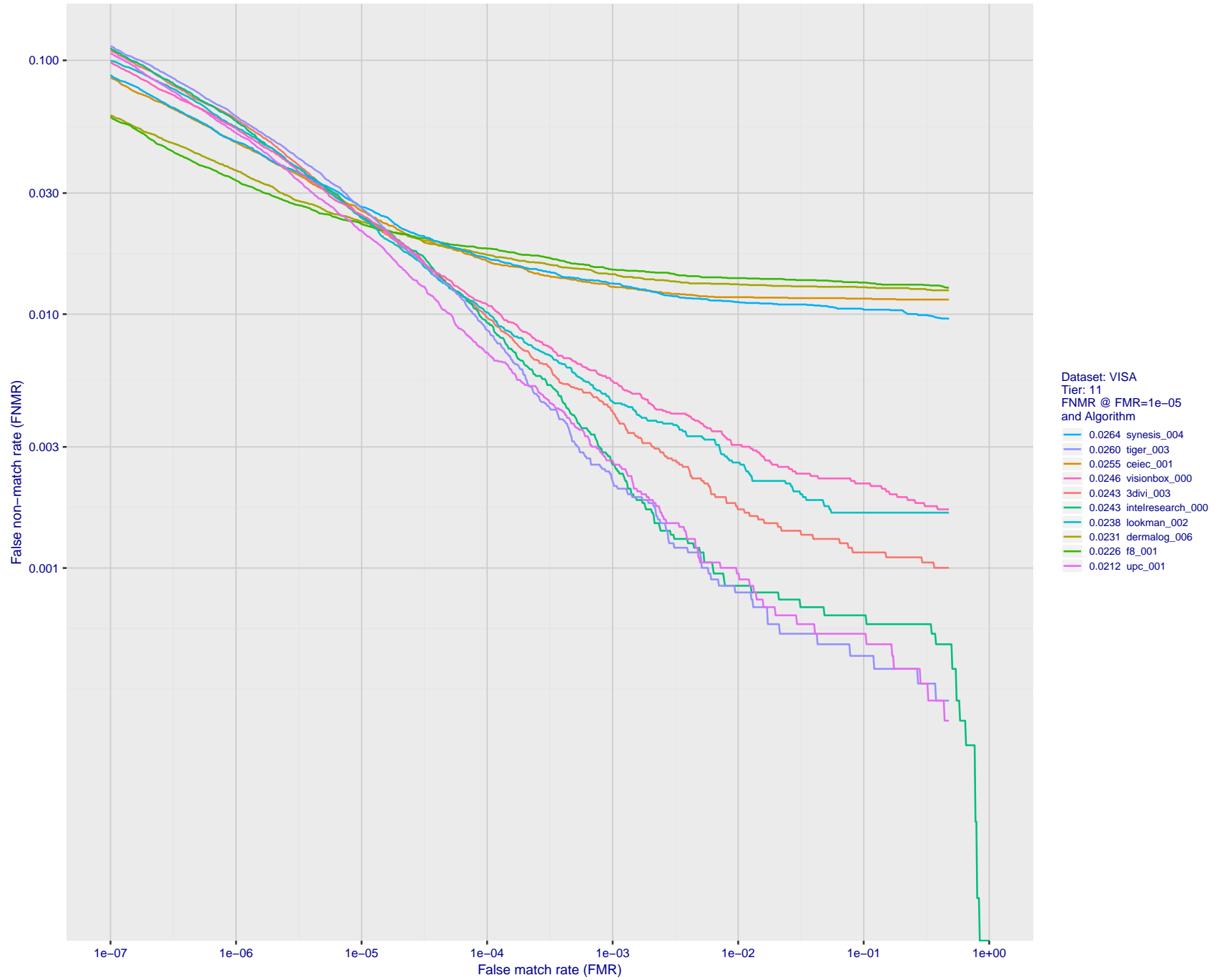


Figure 21: For the visa images, detection error tradeoff (DET) characteristics showing false non-match rate vs. false match rate plotted parametrically on threshold,  $T$ . The scales are logarithmic in order to show many decades of FMR.

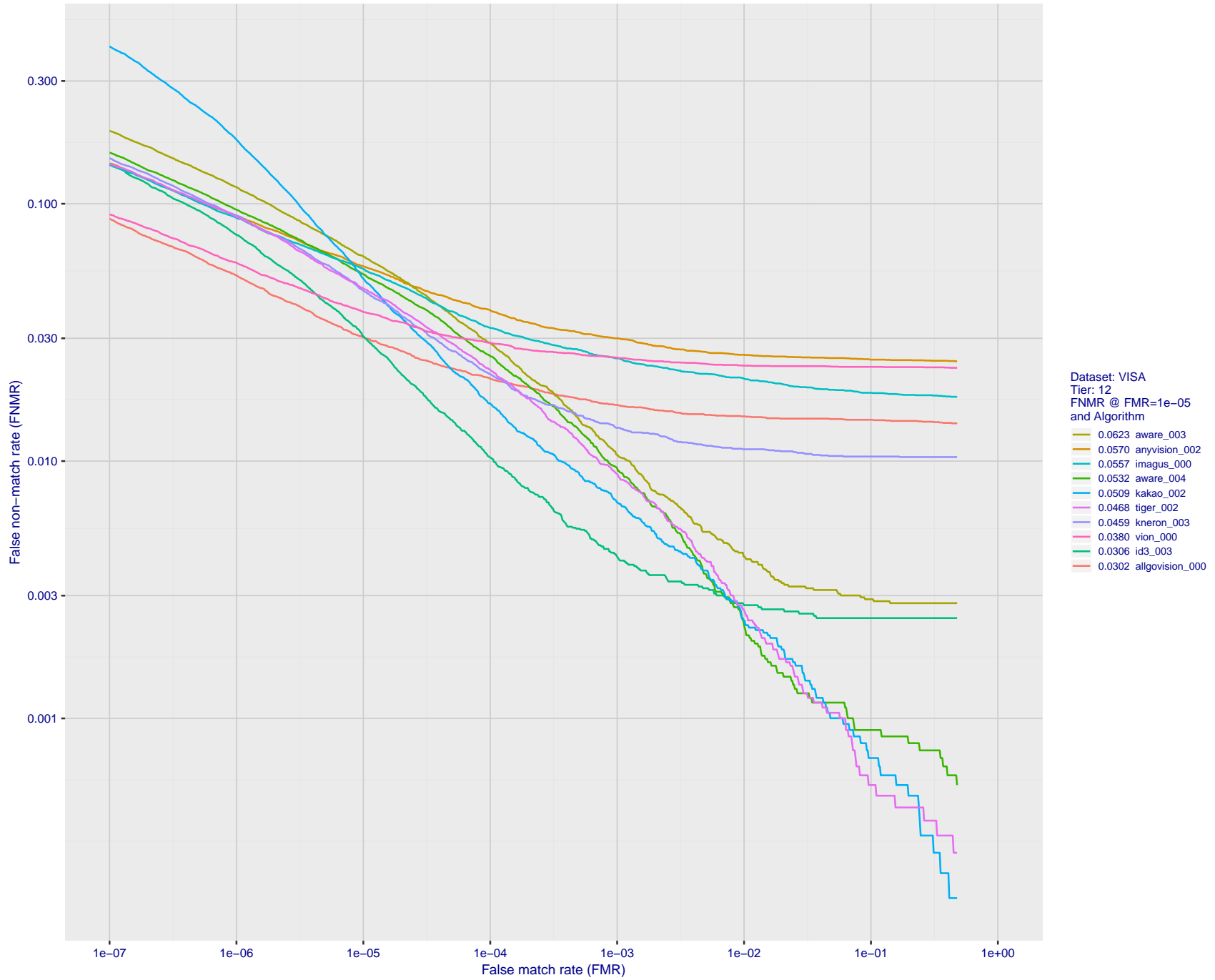


Figure 22: For the visa images, detection error tradeoff (DET) characteristics showing false non-match rate vs. false match rate plotted parametrically on threshold,  $T$ . The scales are logarithmic in order to show many decades of FMR.

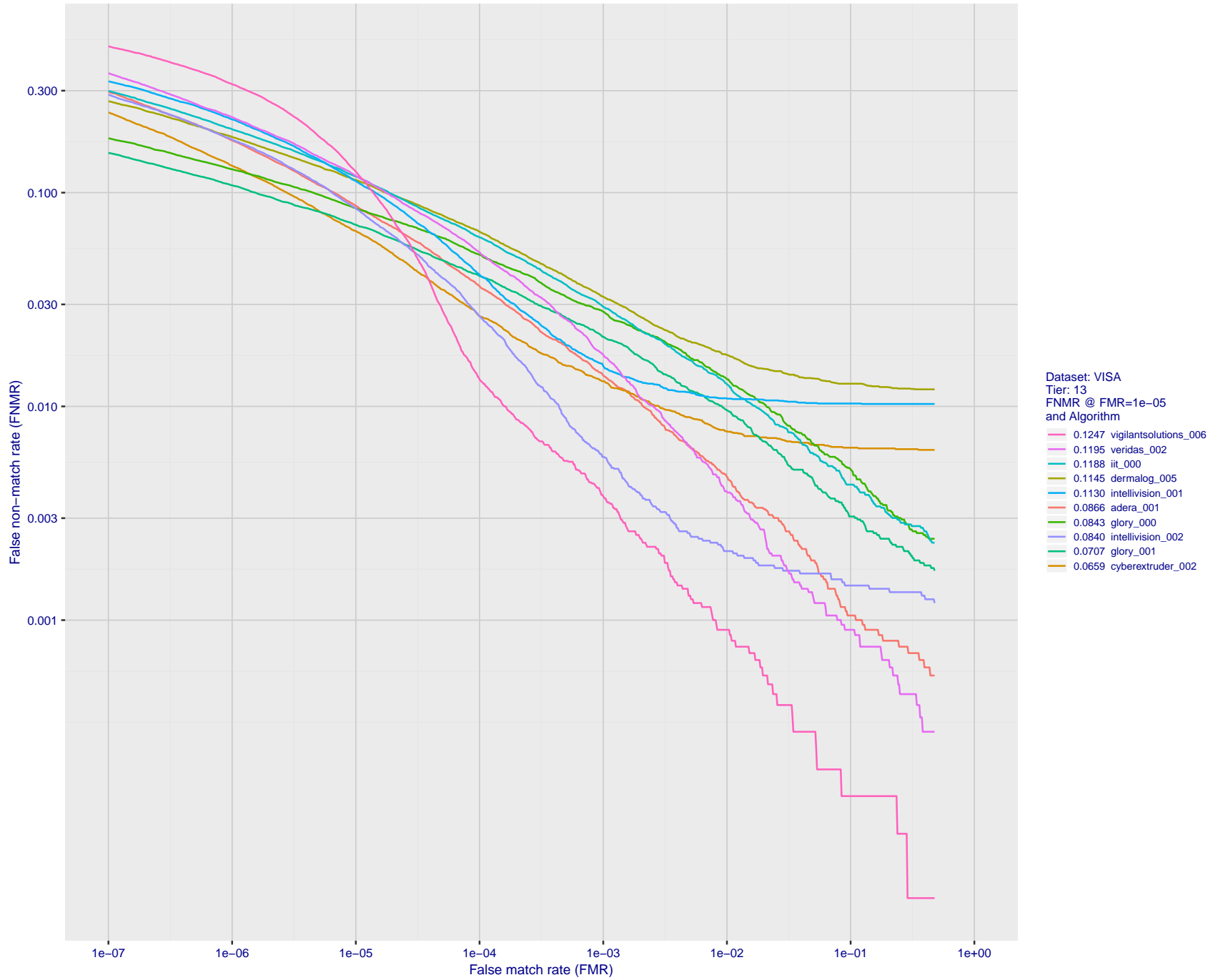


Figure 23: For the visa images, detection error tradeoff (DET) characteristics showing false non-match rate vs. false match rate plotted parametrically on threshold,  $T$ . The scales are logarithmic in order to show many decades of FMR.

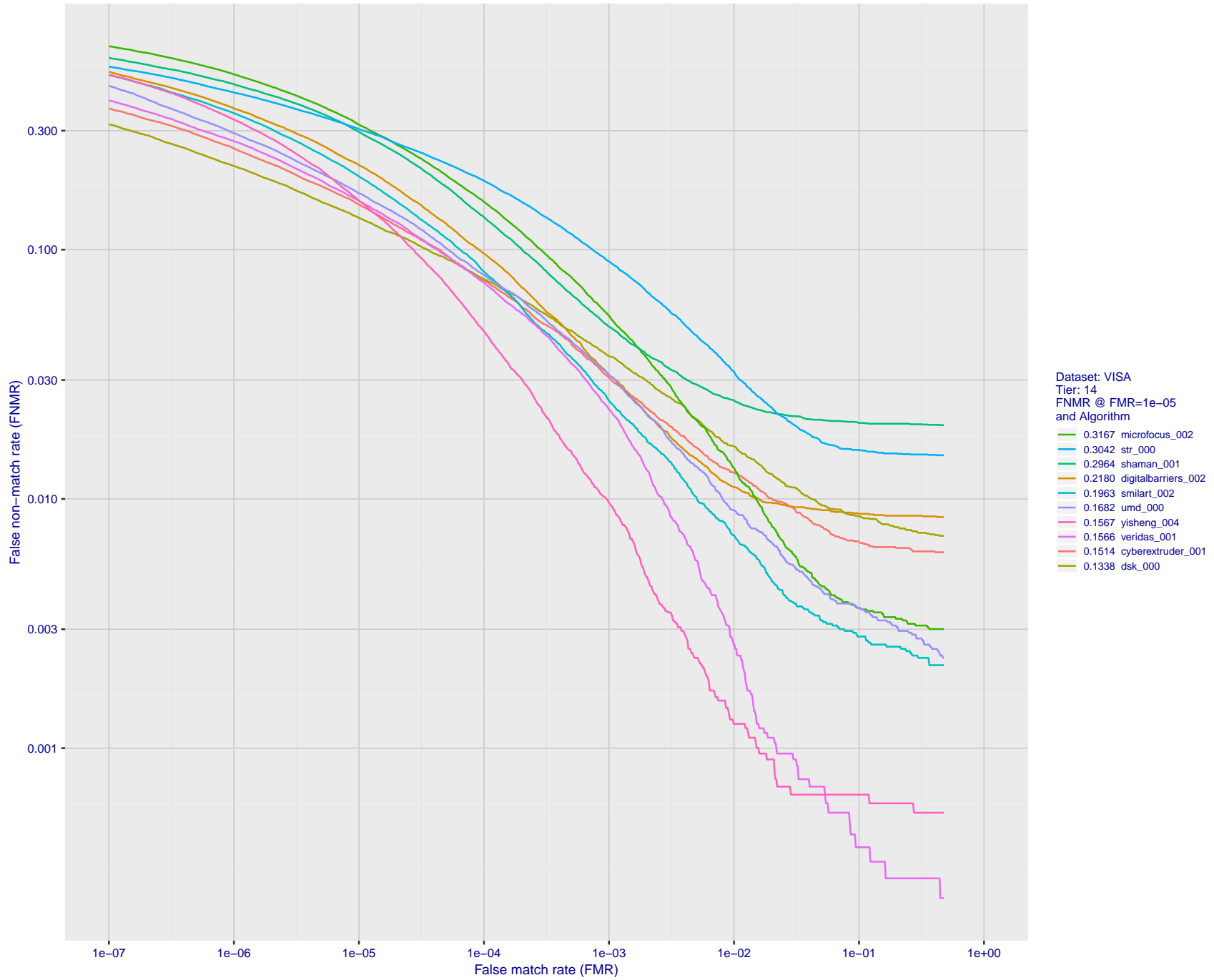


Figure 24: For the visa images, detection error tradeoff (DET) characteristics showing false non-match rate vs. false match rate plotted parametrically on threshold,  $T$ . The scales are logarithmic in order to show many decades of FMR.

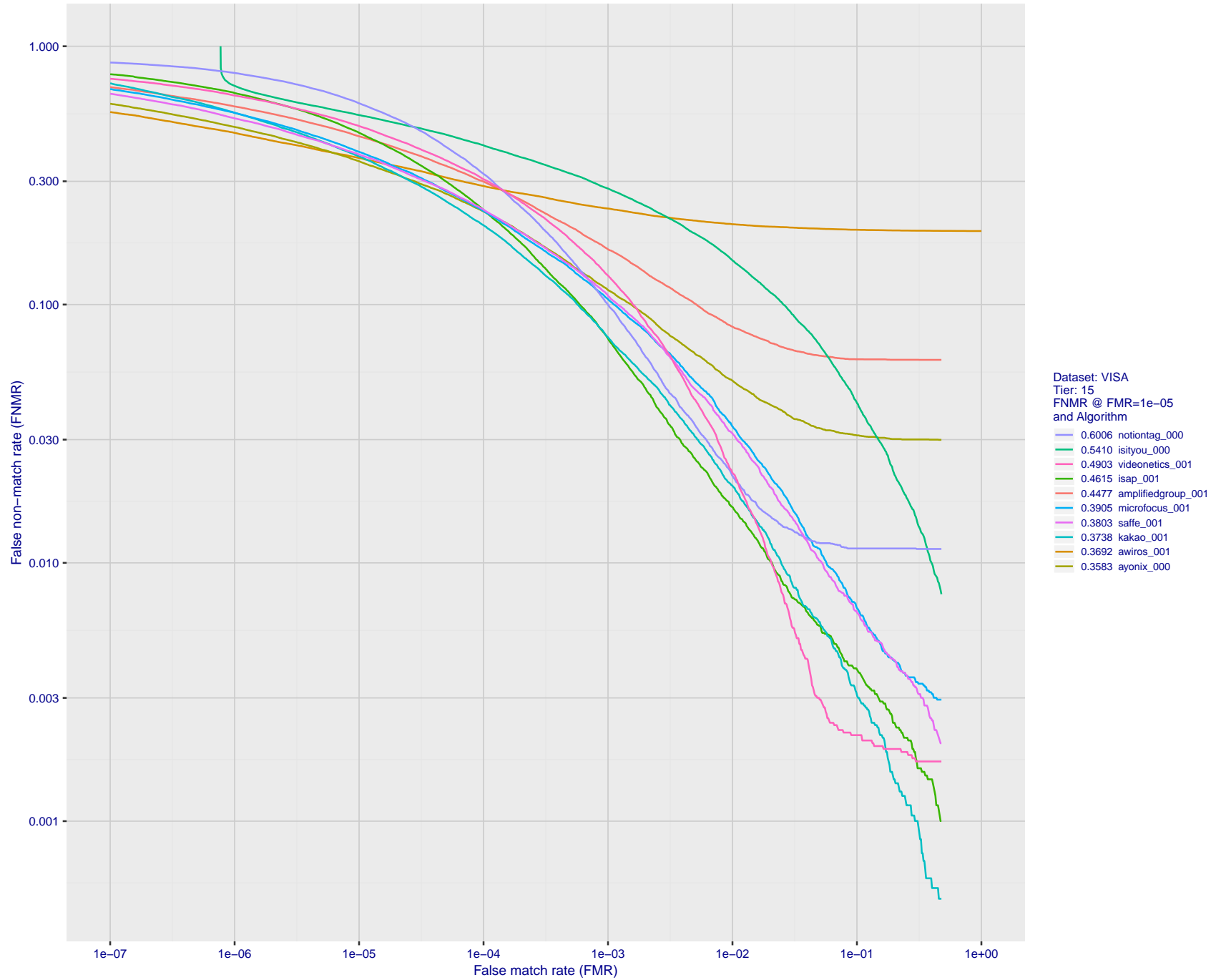


Figure 25: For the visa images, detection error tradeoff (DET) characteristics showing false non-match rate vs. false match rate plotted parametrically on threshold,  $T$ . The scales are logarithmic in order to show many decades of FMR.

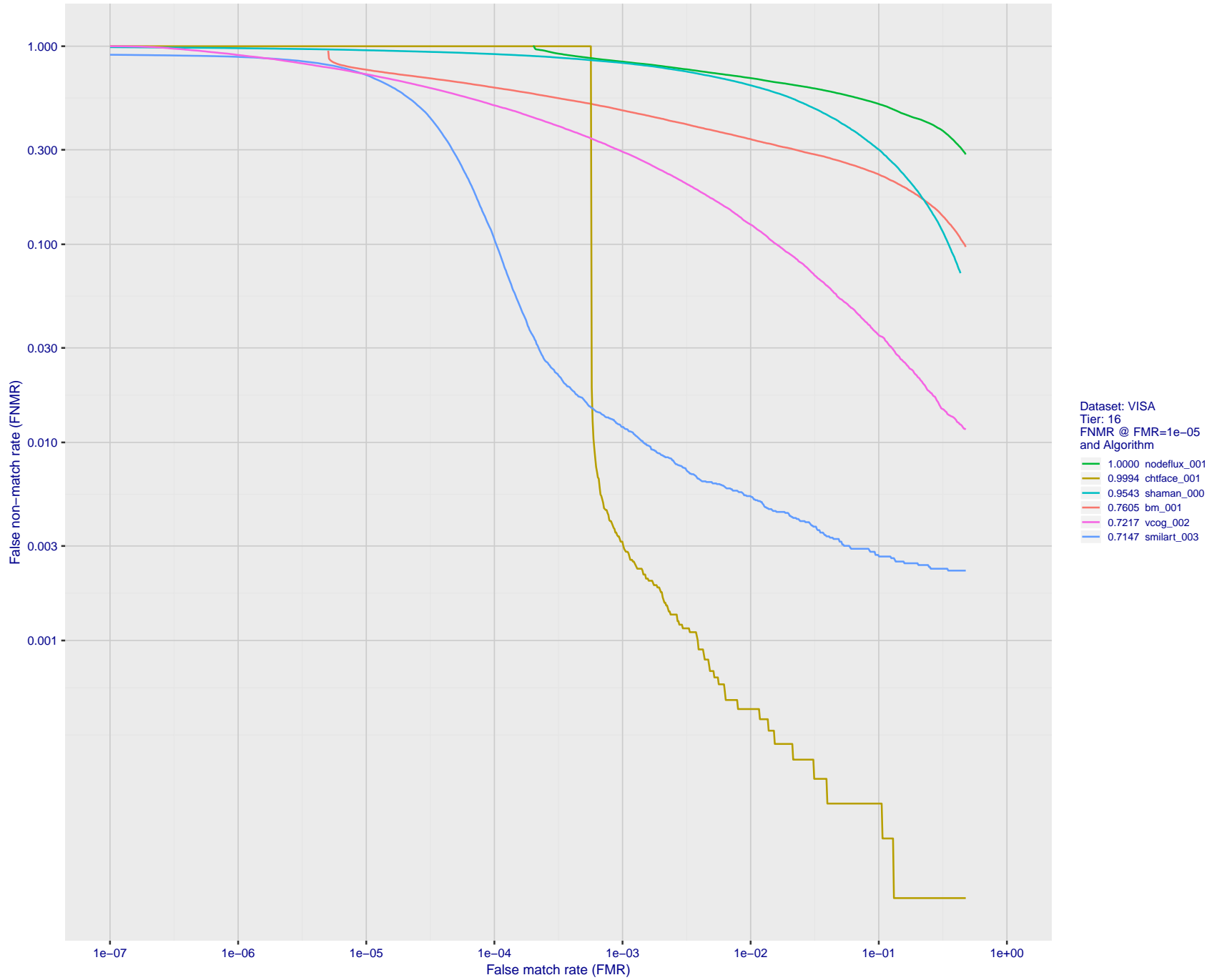


Figure 26: For the visa images, detection error tradeoff (DET) characteristics showing false non-match rate vs. false match rate plotted parametrically on threshold,  $T$ . The scales are logarithmic in order to show many decades of FMR.

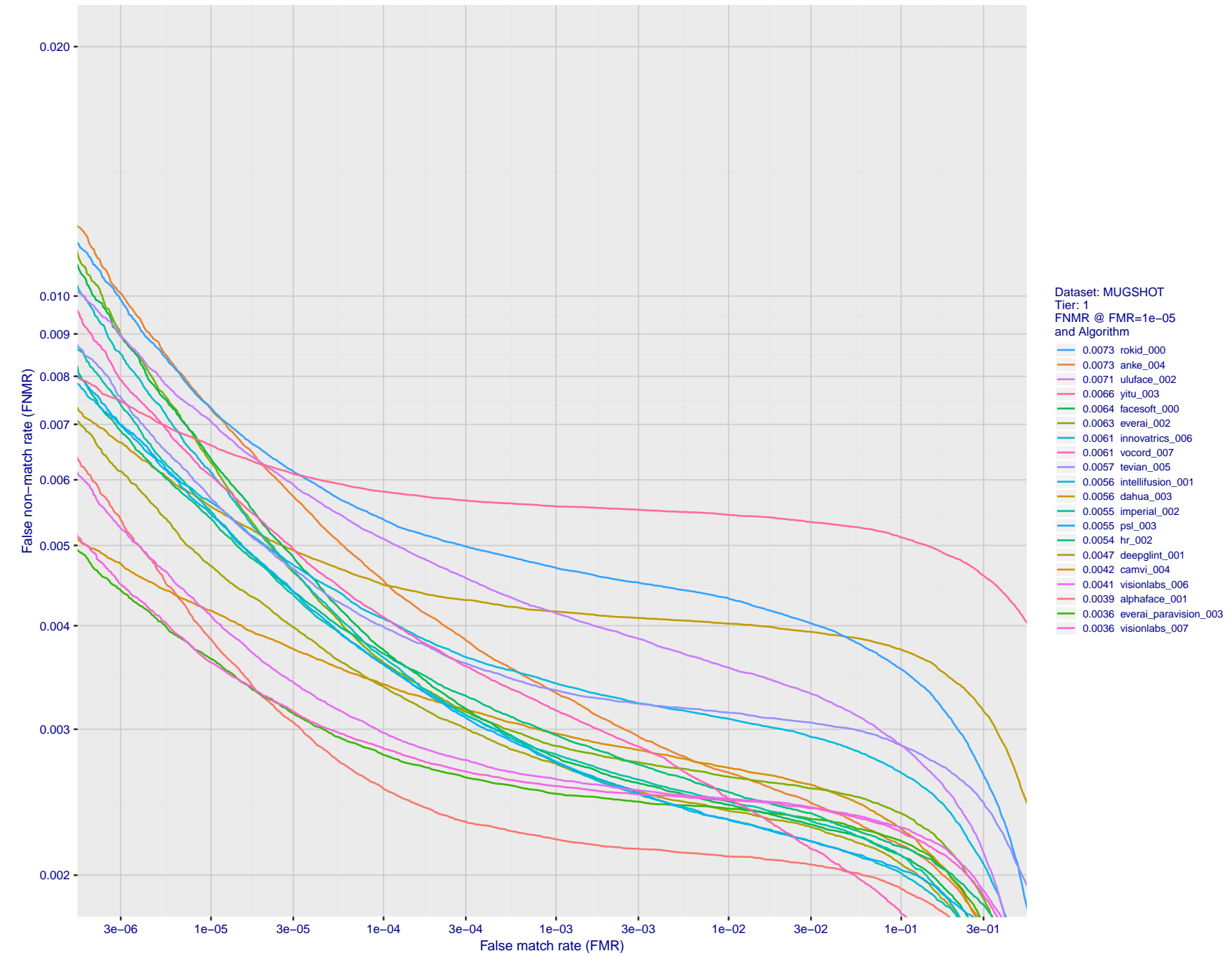


Figure 27: For the mugshot images, detection error tradeoff (DET) characteristics showing false non-match rate vs. false match rate plotted parametrically on threshold,  $T$ . The scales are logarithmic in order to show decades of FMR.

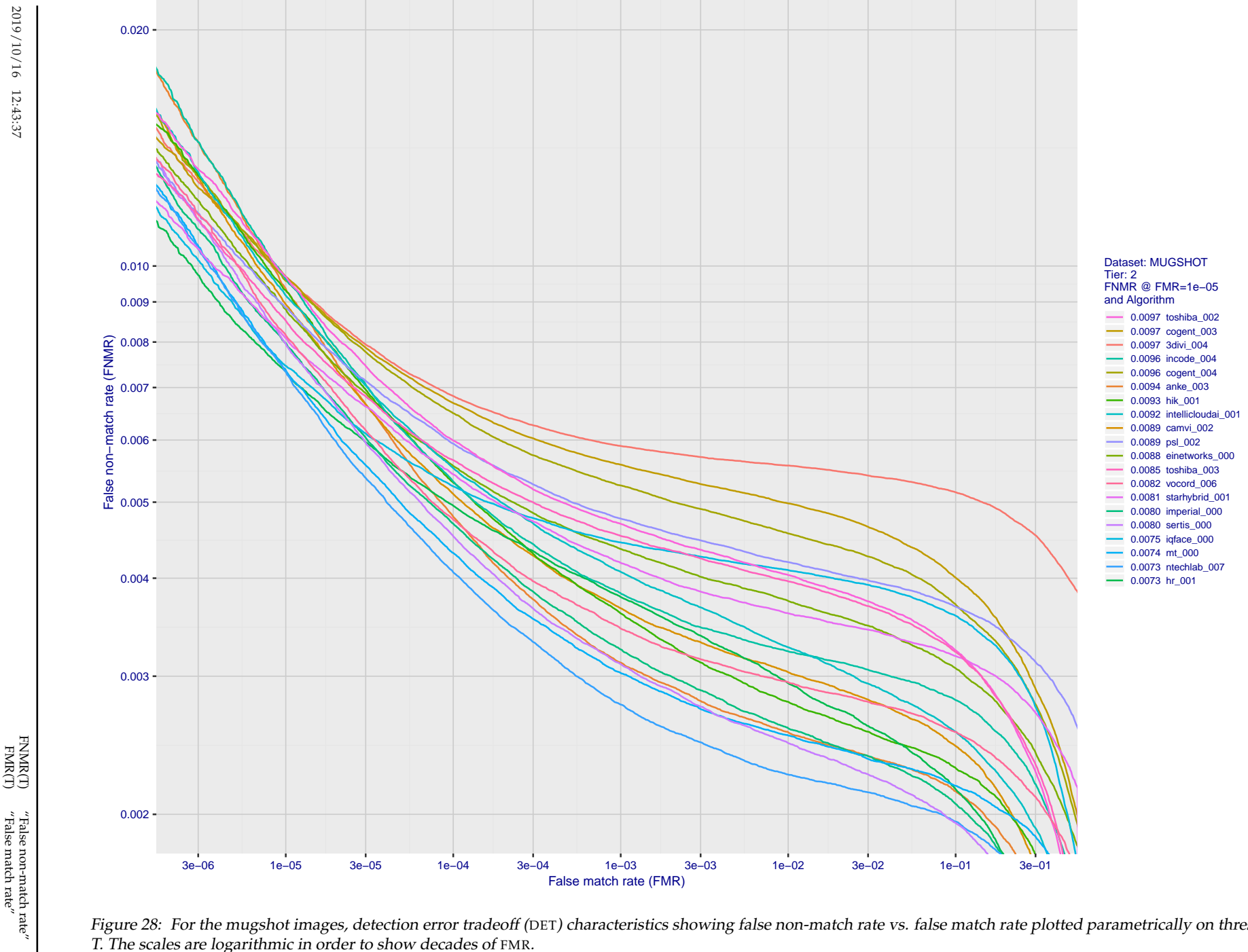


Figure 28: For the mugshot images, detection error tradeoff (DET) characteristics showing false non-match rate vs. false match rate plotted parametrically on threshold,  $T$ . The scales are logarithmic in order to show decades of FMR.

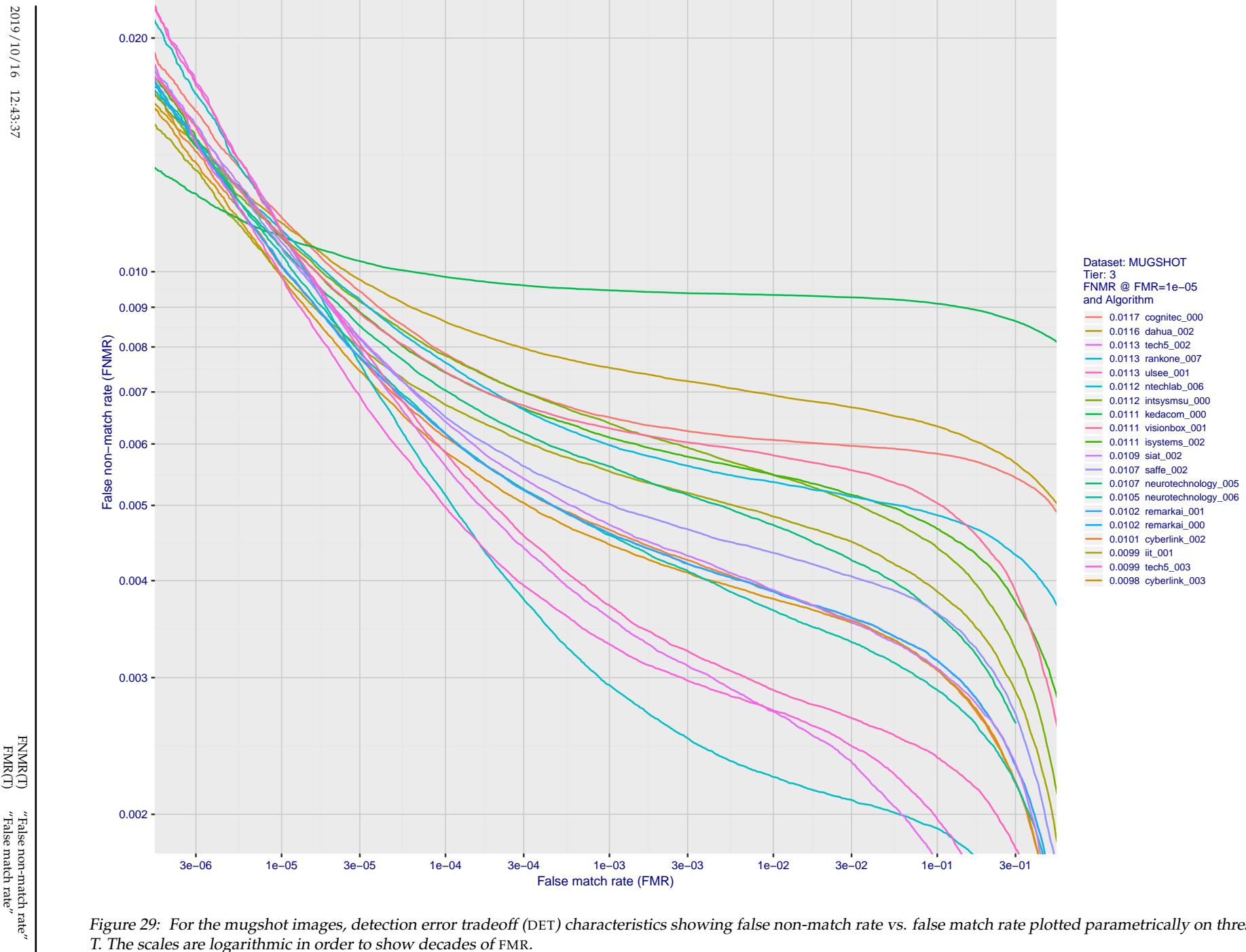


Figure 29: For the mugshot images, detection error tradeoff (DET) characteristics showing false non-match rate vs. false match rate plotted parametrically on threshold,  $T$ . The scales are logarithmic in order to show decades of FMR.

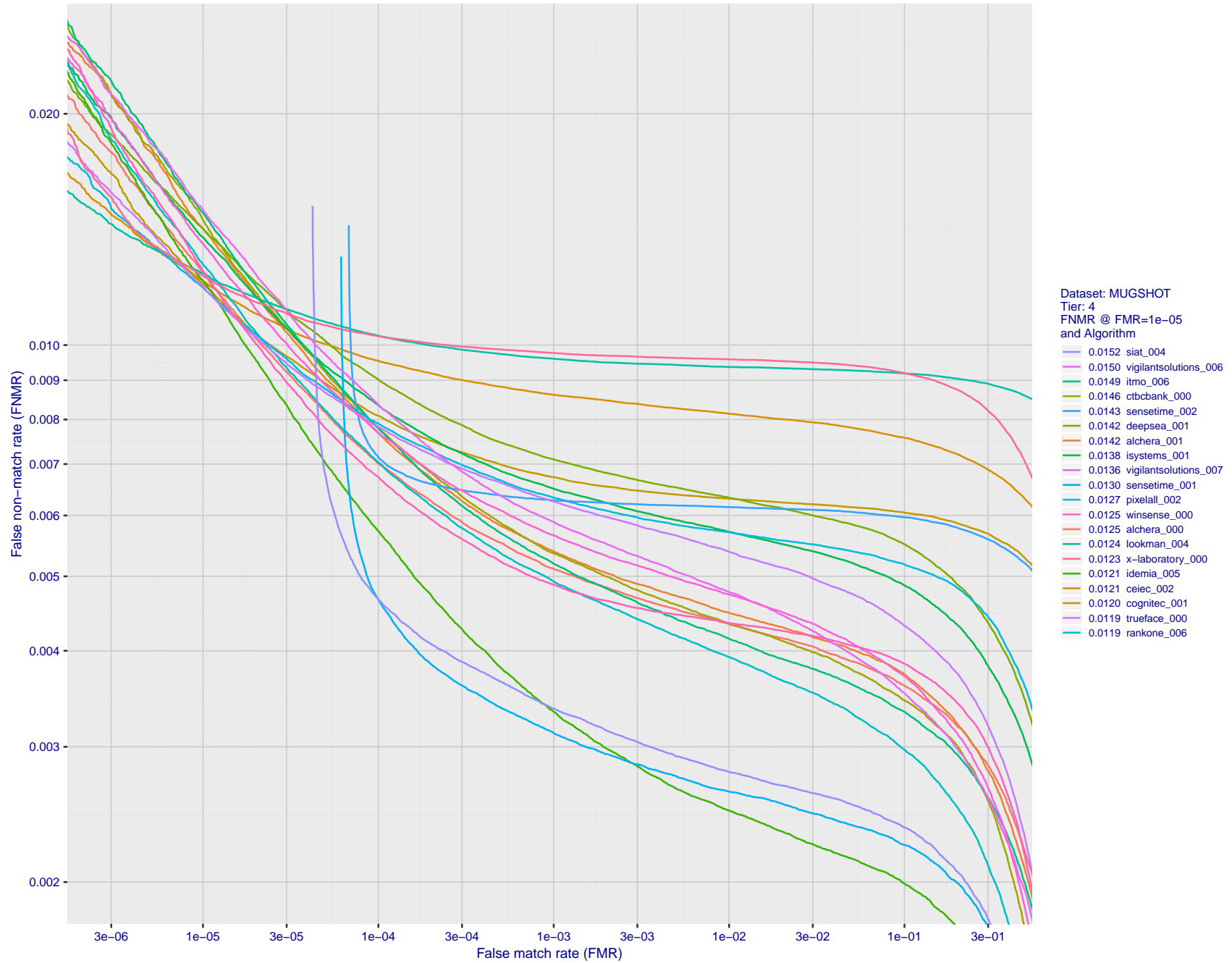


Figure 30: For the mugshot images, detection error tradeoff (DET) characteristics showing false non-match rate vs. false match rate plotted parametrically on threshold,  $T$ . The scales are logarithmic in order to show decades of FMR.

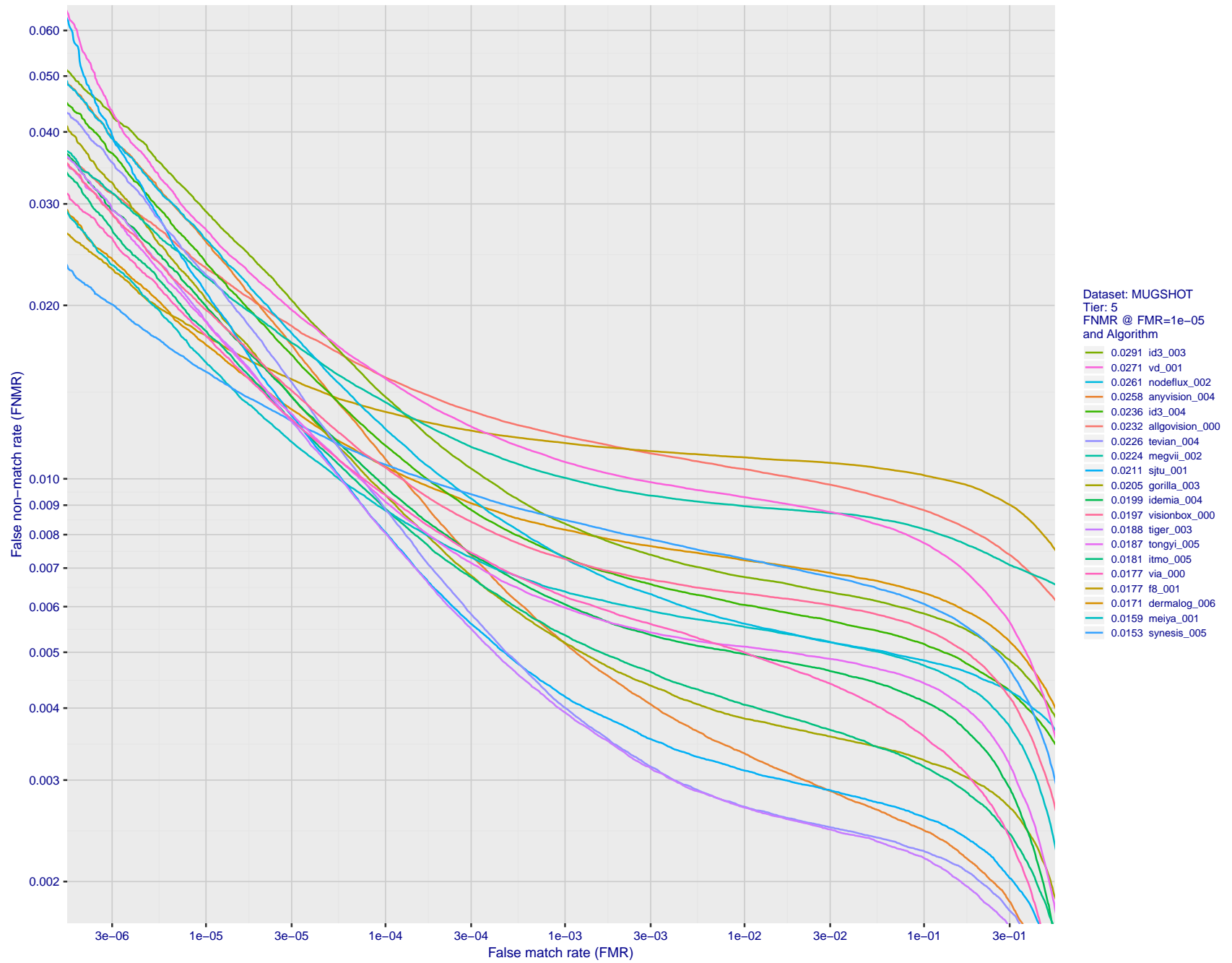


Figure 31: For the mugshot images, detection error tradeoff (DET) characteristics showing false non-match rate vs. false match rate plotted parametrically on threshold,  $T$ . The scales are logarithmic in order to show decades of FMR.

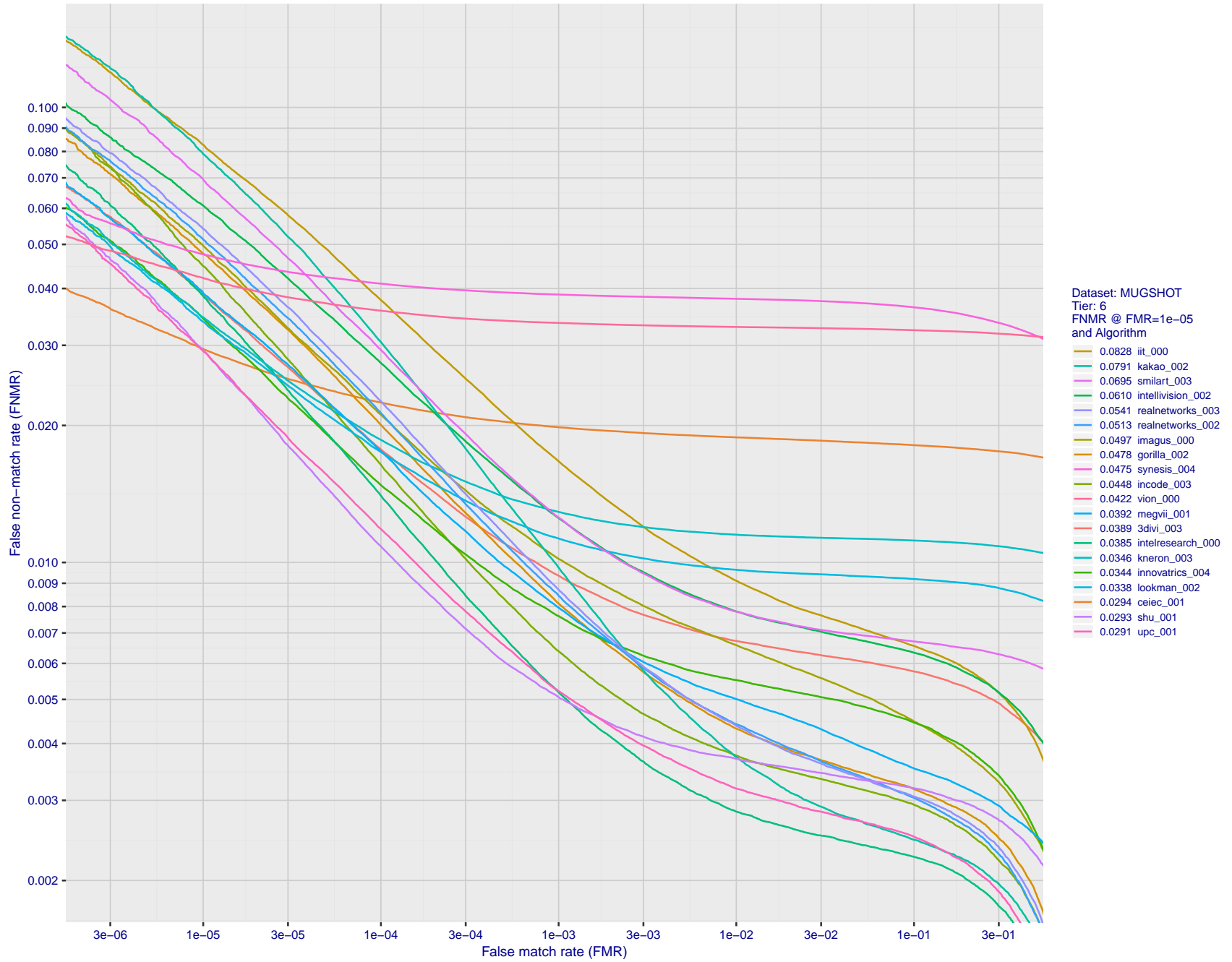


Figure 32: For the mugshot images, detection error tradeoff (DET) characteristics showing false non-match rate vs. false match rate plotted parametrically on threshold,  $T$ . The scales are logarithmic in order to show decades of FMR.

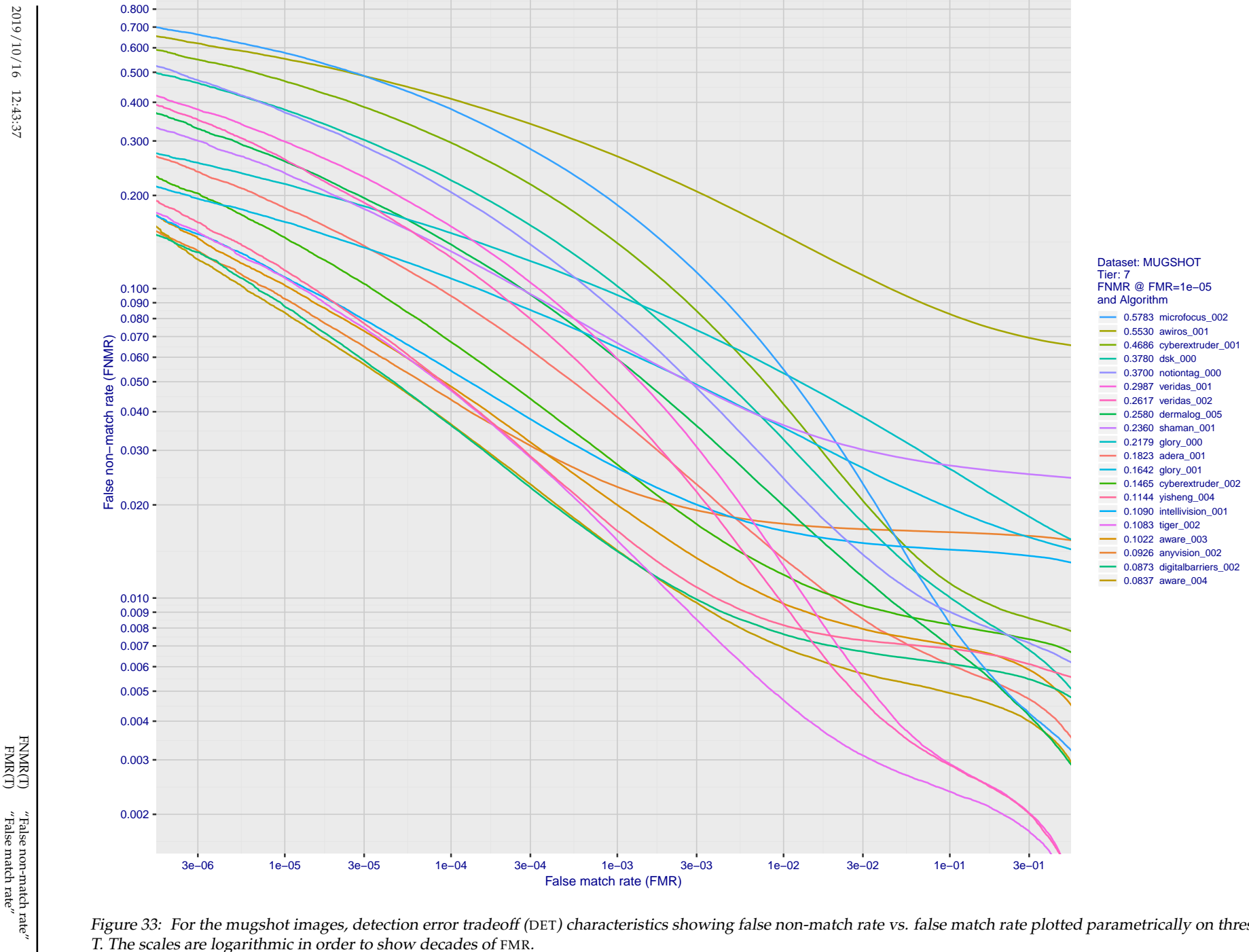


Figure 33: For the mugshot images, detection error tradeoff (DET) characteristics showing false non-match rate vs. false match rate plotted parametrically on threshold,  $T$ . The scales are logarithmic in order to show decades of FMR.

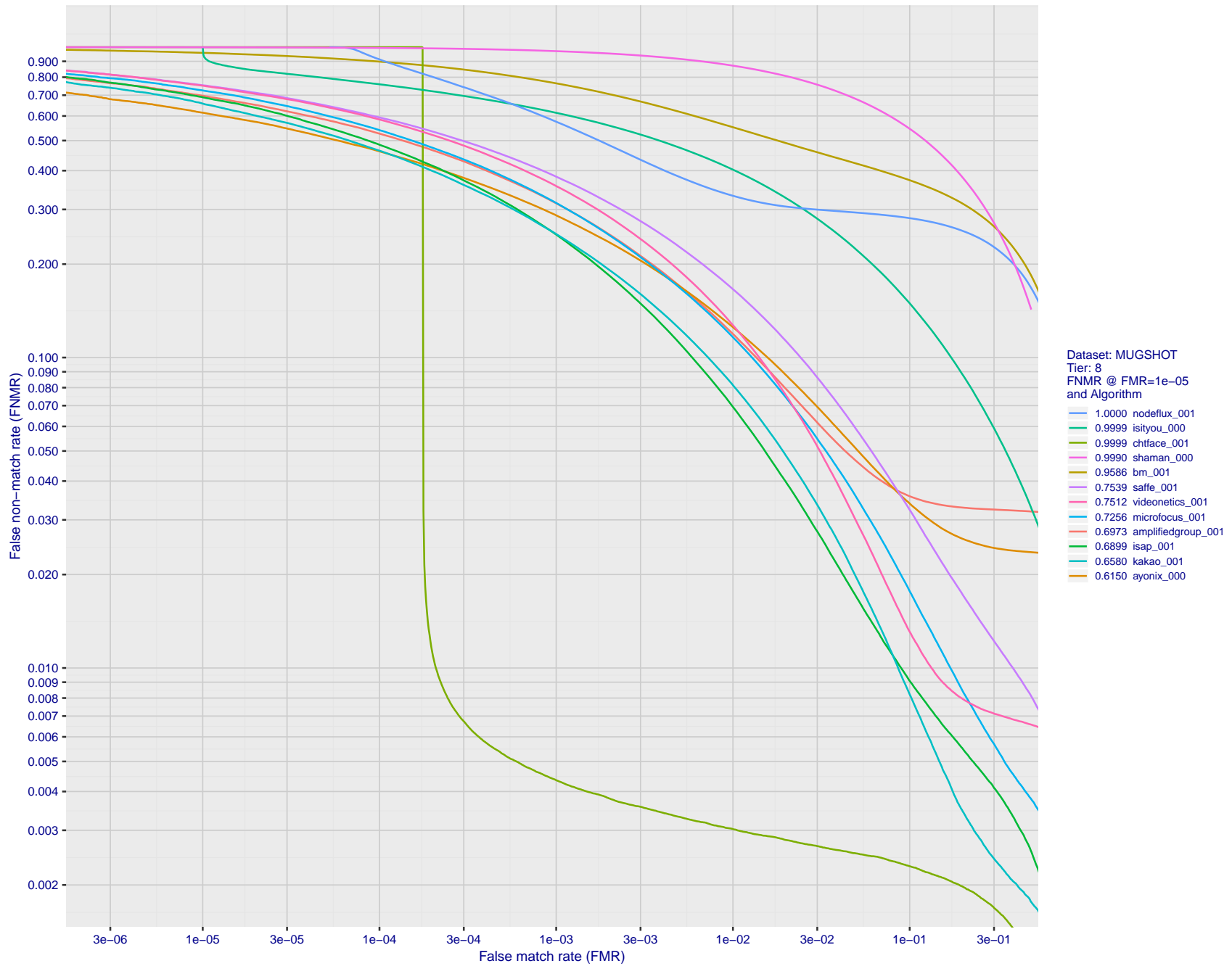


Figure 34: For the mugshot images, detection error tradeoff (DET) characteristics showing false non-match rate vs. false match rate plotted parametrically on threshold,  $T$ . The scales are logarithmic in order to show decades of FMR.

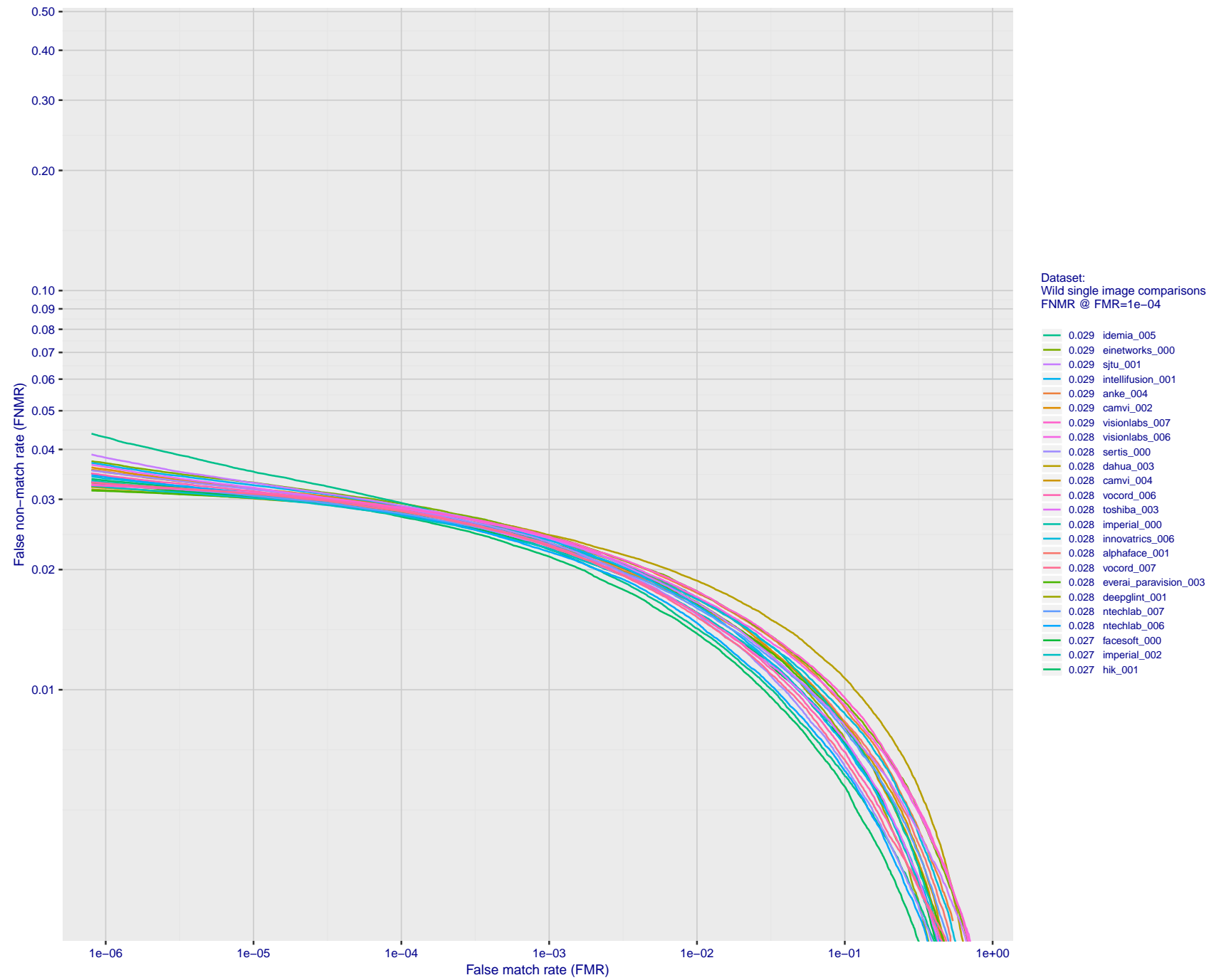


Figure 35: For the 2018 wild image comparisons, detection error tradeoff (DET) characteristics showing false non-match rate vs. false match rate plotted parametrically on threshold,  $T$ . The scales are logarithmic in order to show several decades of FMR.

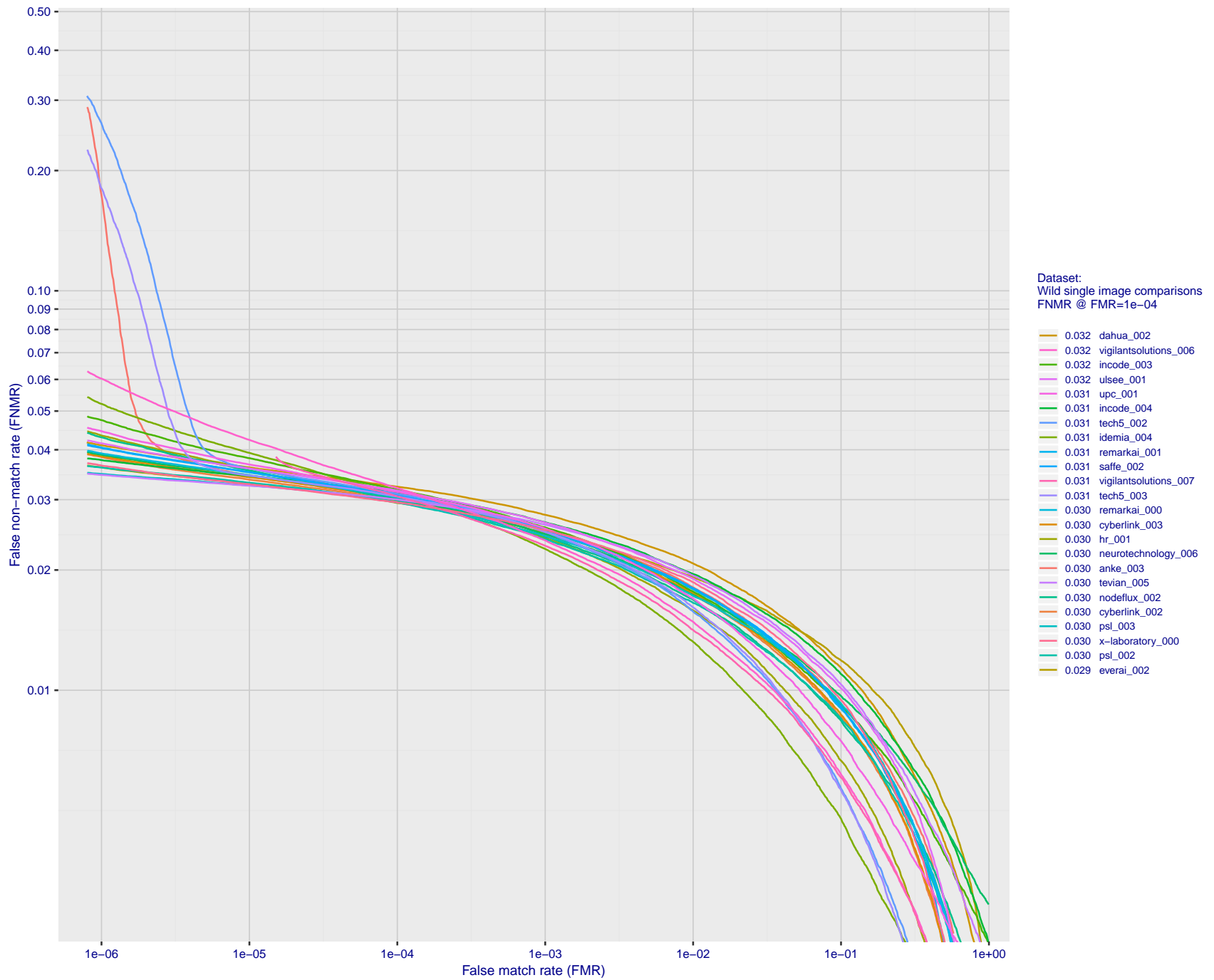


Figure 36: For the 2018 wild image comparisons, detection error tradeoff (DET) characteristics showing false non-match rate vs. false match rate plotted parametrically on threshold, T. The scales are logarithmic in order to show several decades of FMR.

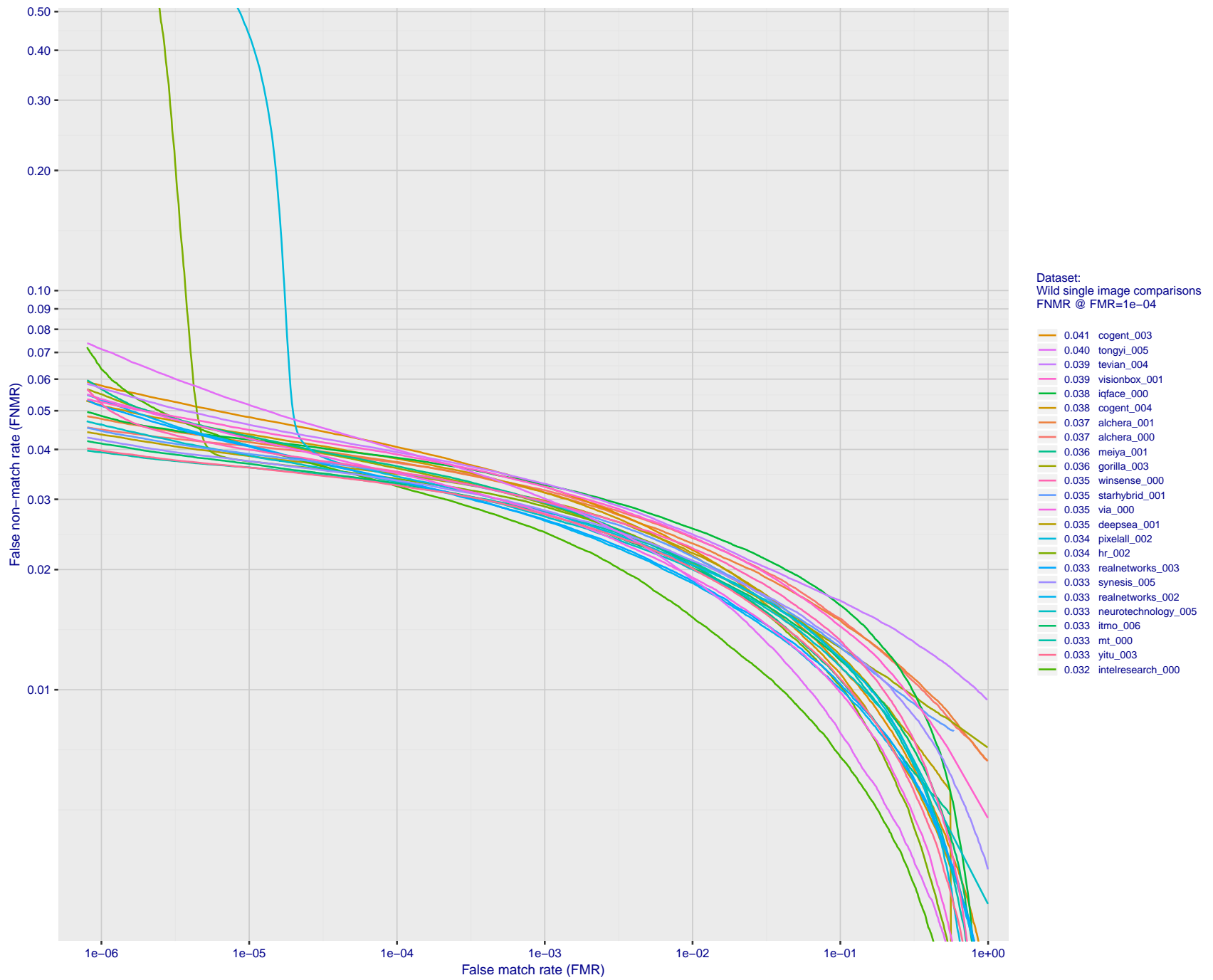


Figure 37: For the 2018 wild image comparisons, detection error tradeoff (DET) characteristics showing false non-match rate vs. false match rate plotted parametrically on threshold, T. The scales are logarithmic in order to show several decades of FMR.

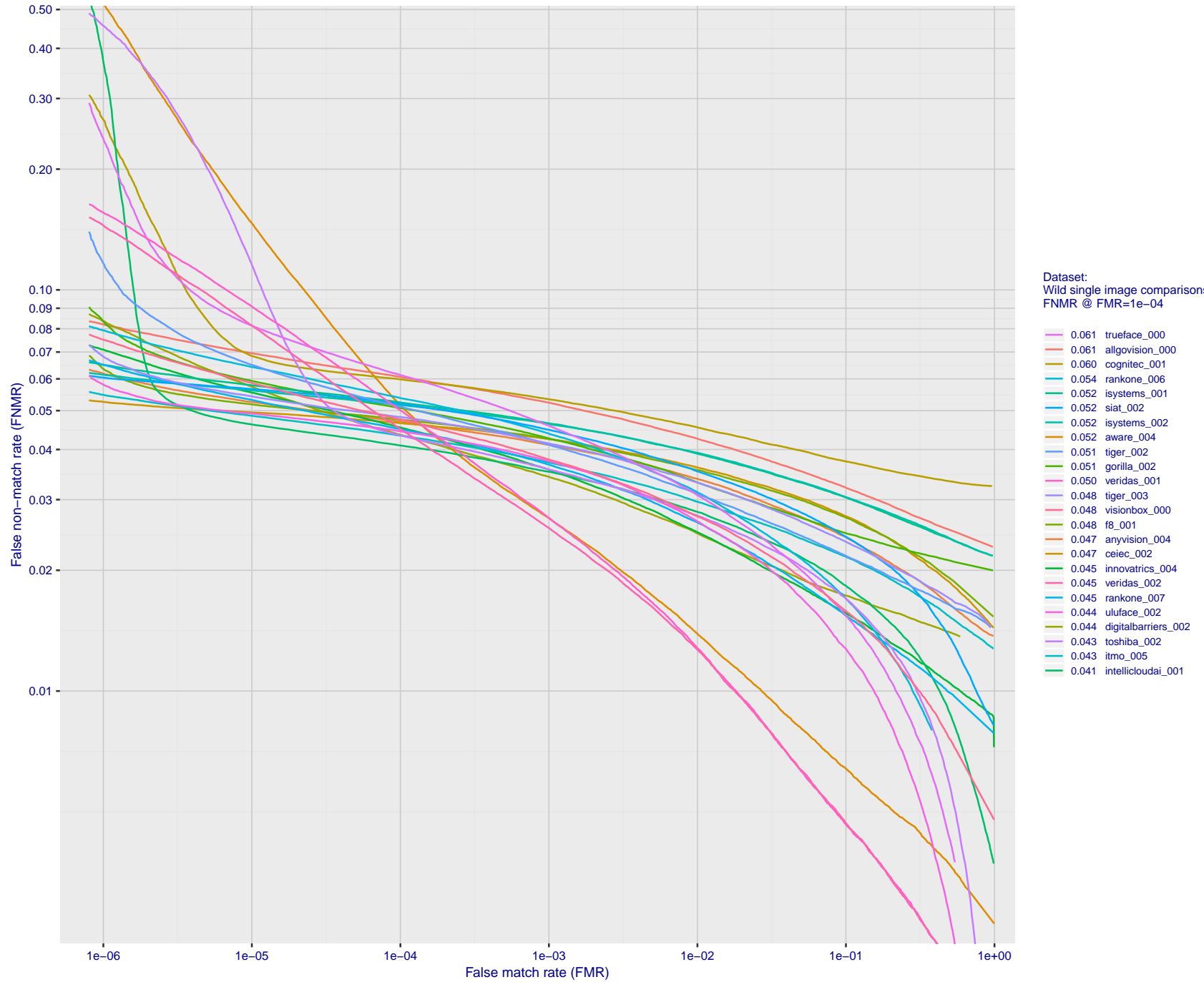


Figure 38: For the 2018 wild image comparisons, detection error tradeoff (DET) characteristics showing false non-match rate vs. false match rate plotted parametrically on threshold, T. The scales are logarithmic in order to show several decades of FMR.

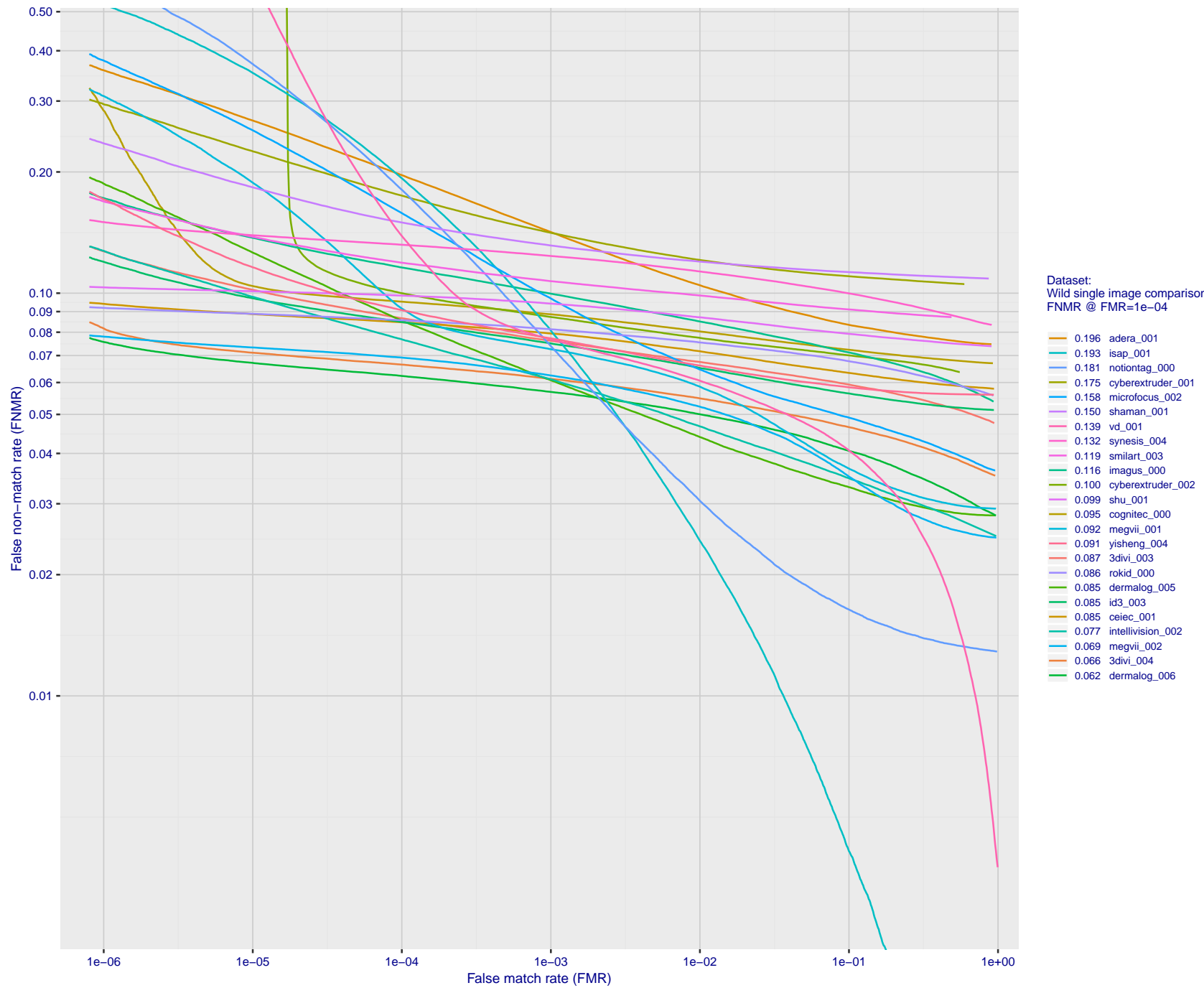


Figure 39: For the 2018 wild image comparisons, detection error tradeoff (DET) characteristics showing false non-match rate vs. false match rate plotted parametrically on threshold,  $T$ . The scales are logarithmic in order to show several decades of FMR.

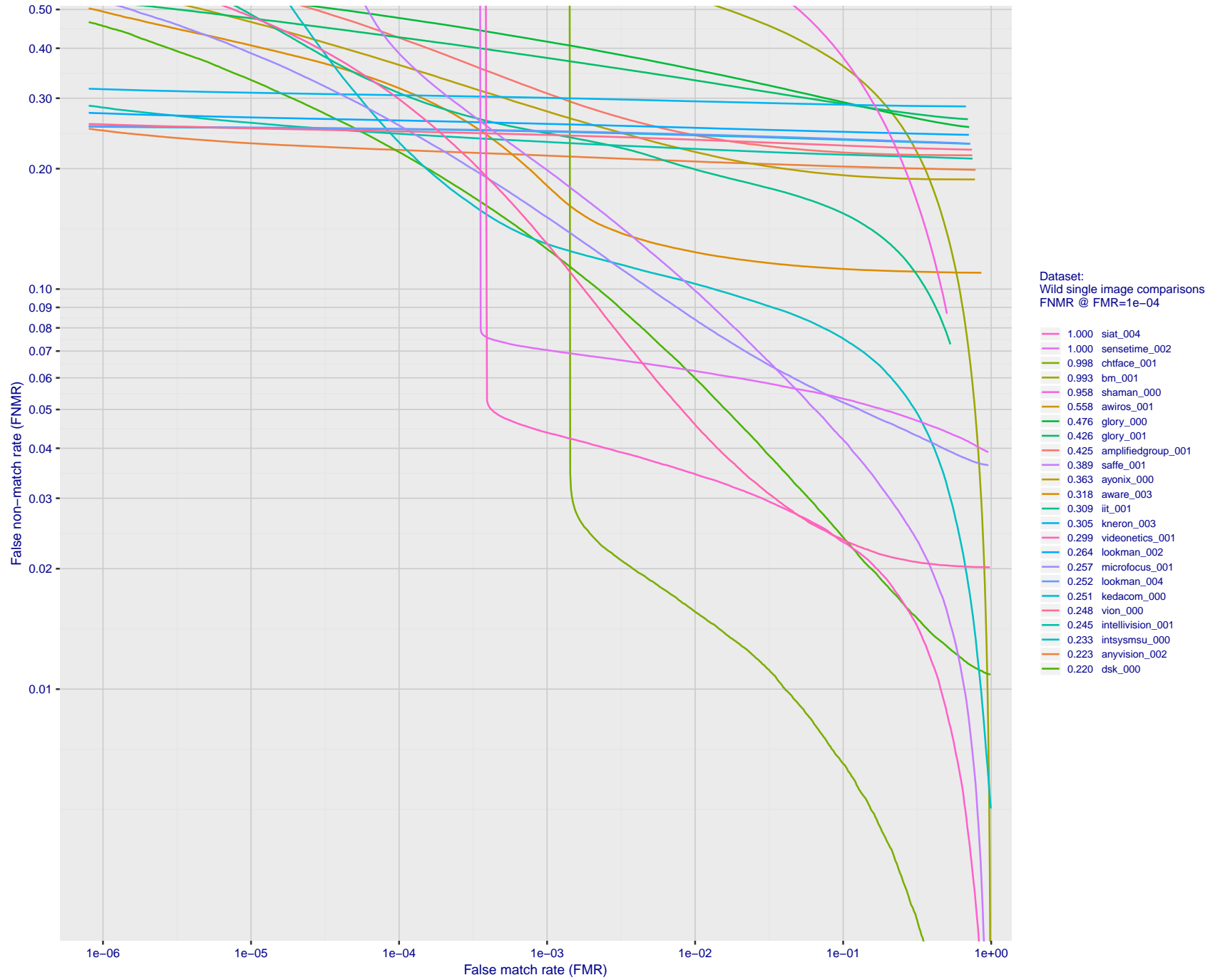


Figure 40: For the 2018 wild image comparisons, detection error tradeoff (DET) characteristics showing false non-match rate vs. false match rate plotted parametrically on threshold,  $T$ . The scales are logarithmic in order to show several decades of FMR.

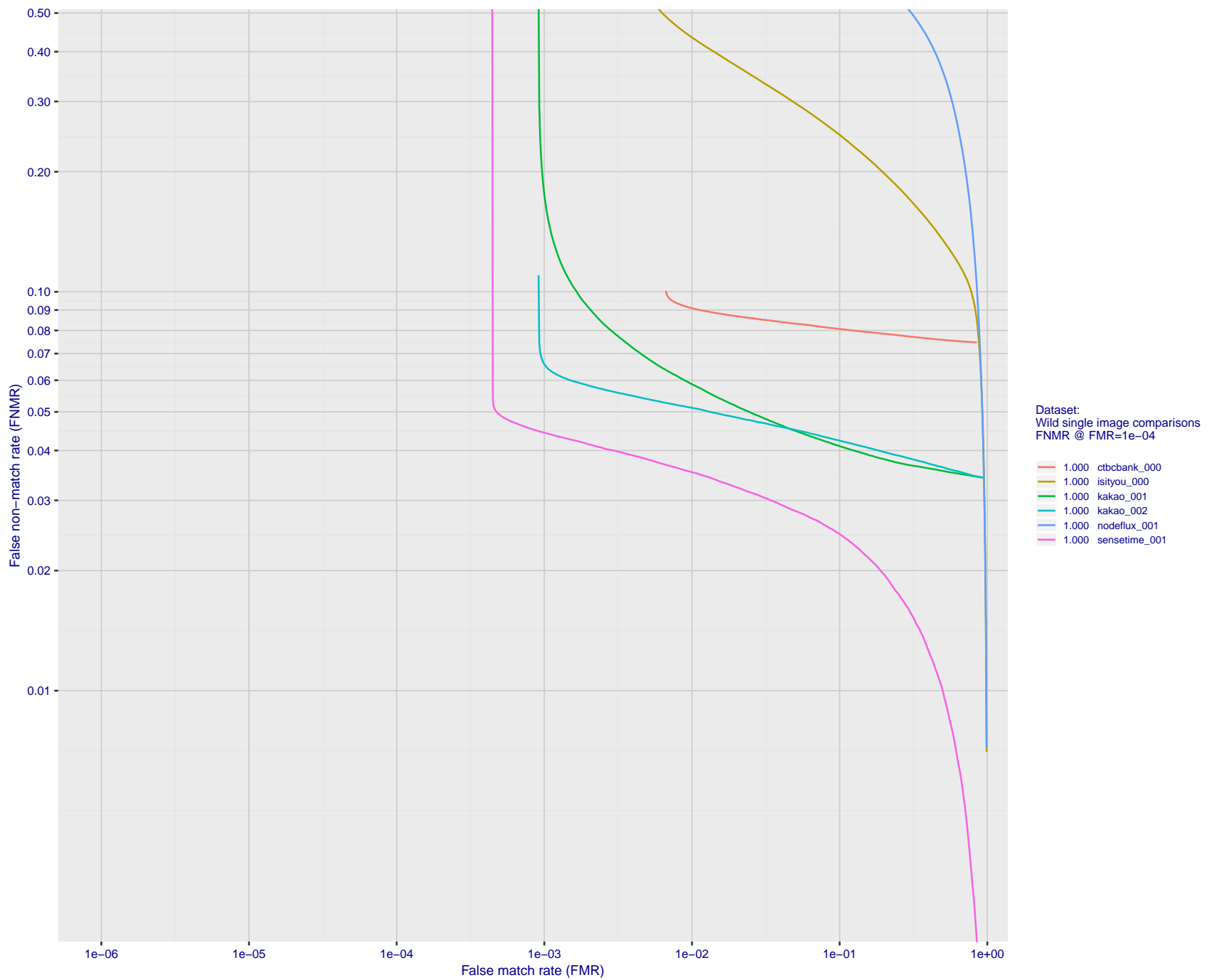


Figure 41: For the 2018 wild image comparisons, detection error tradeoff (DET) characteristics showing false non-match rate vs. false match rate plotted parametrically on threshold,  $T$ . The scales are logarithmic in order to show several decades of FMR.

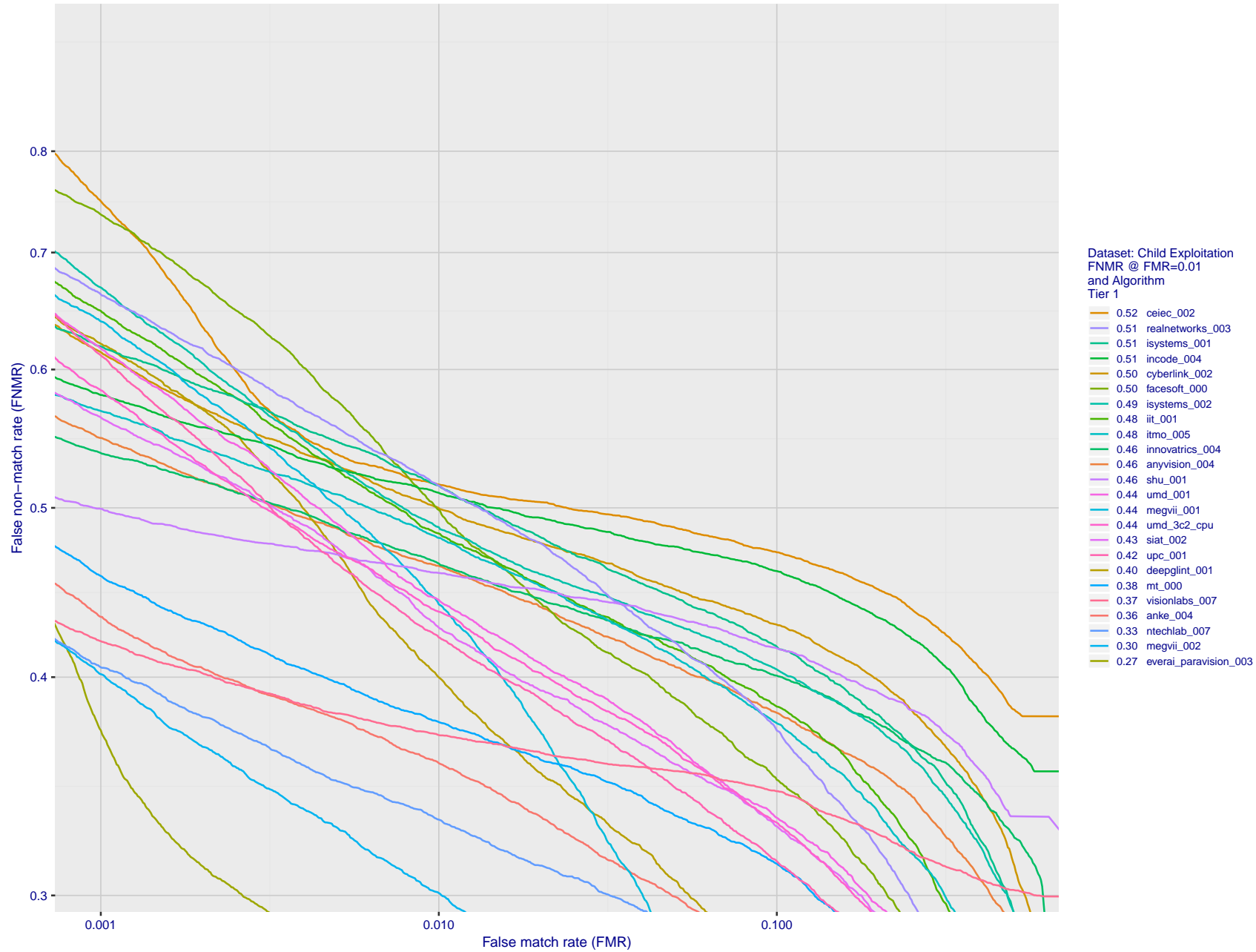


Figure 42: For child exploitation images, detection error tradeoff (DET) characteristics showing false non-match rate vs. false match rate plotted parametrically on threshold, T. The scales are logarithmic in order to show many decades of FMR. Accuracy is poor because many images have adverse quality characteristics, and because detection and enrollment fails.

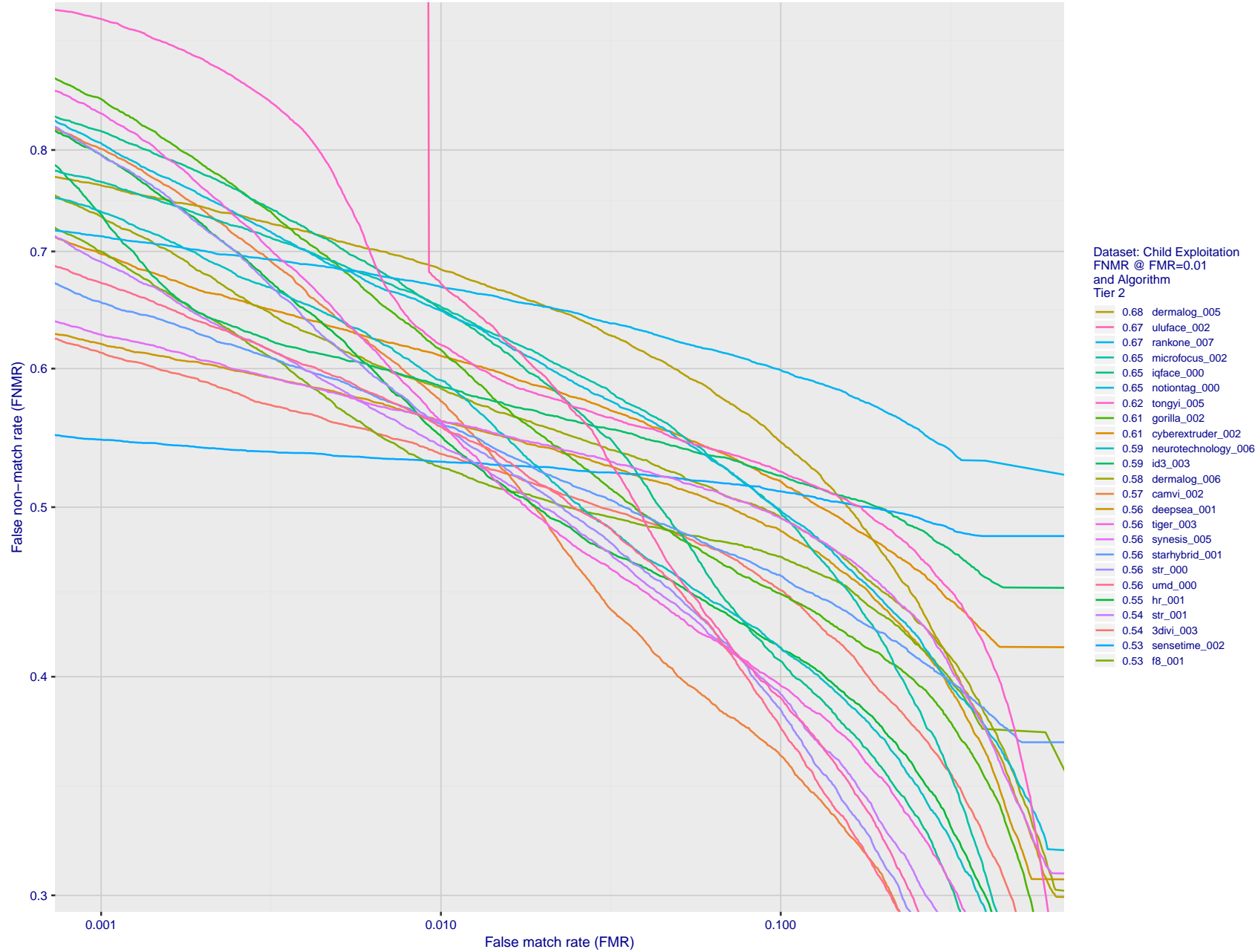


Figure 43: For child exploitation images, detection error tradeoff (DET) characteristics showing false non-match rate vs. false match rate plotted parametrically on threshold,  $T$ . The scales are logarithmic in order to show many decades of FMR. Accuracy is poor because many images have adverse quality characteristics, and because detection and enrollment fails.

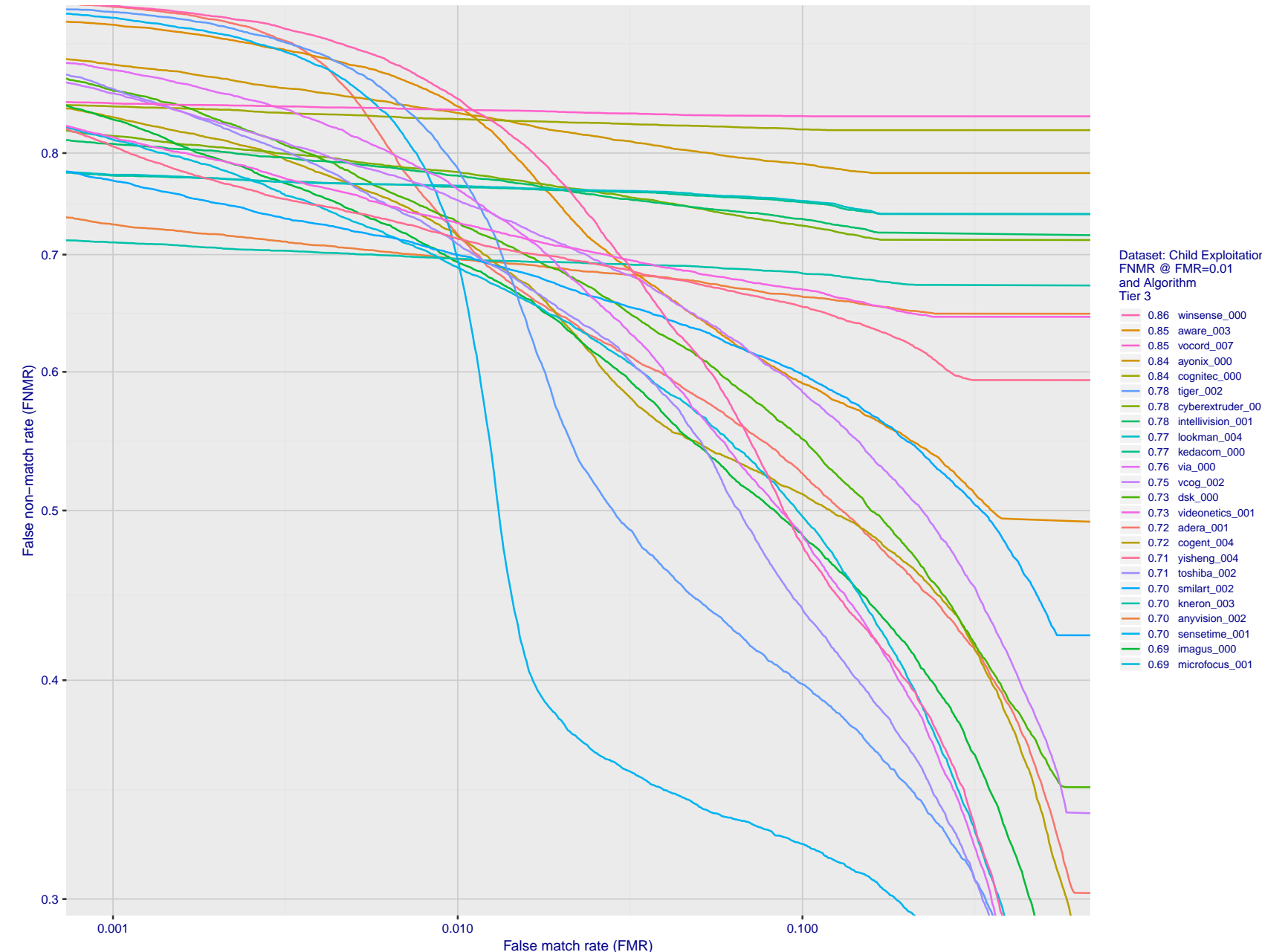


Figure 44: For child exploitation images, detection error tradeoff (DET) characteristics showing false non-match rate vs. false match rate plotted parametrically on threshold,  $T$ . The scales are logarithmic in order to show many decades of FMR. Accuracy is poor because many images have adverse quality characteristics, and because detection and enrollment fails.

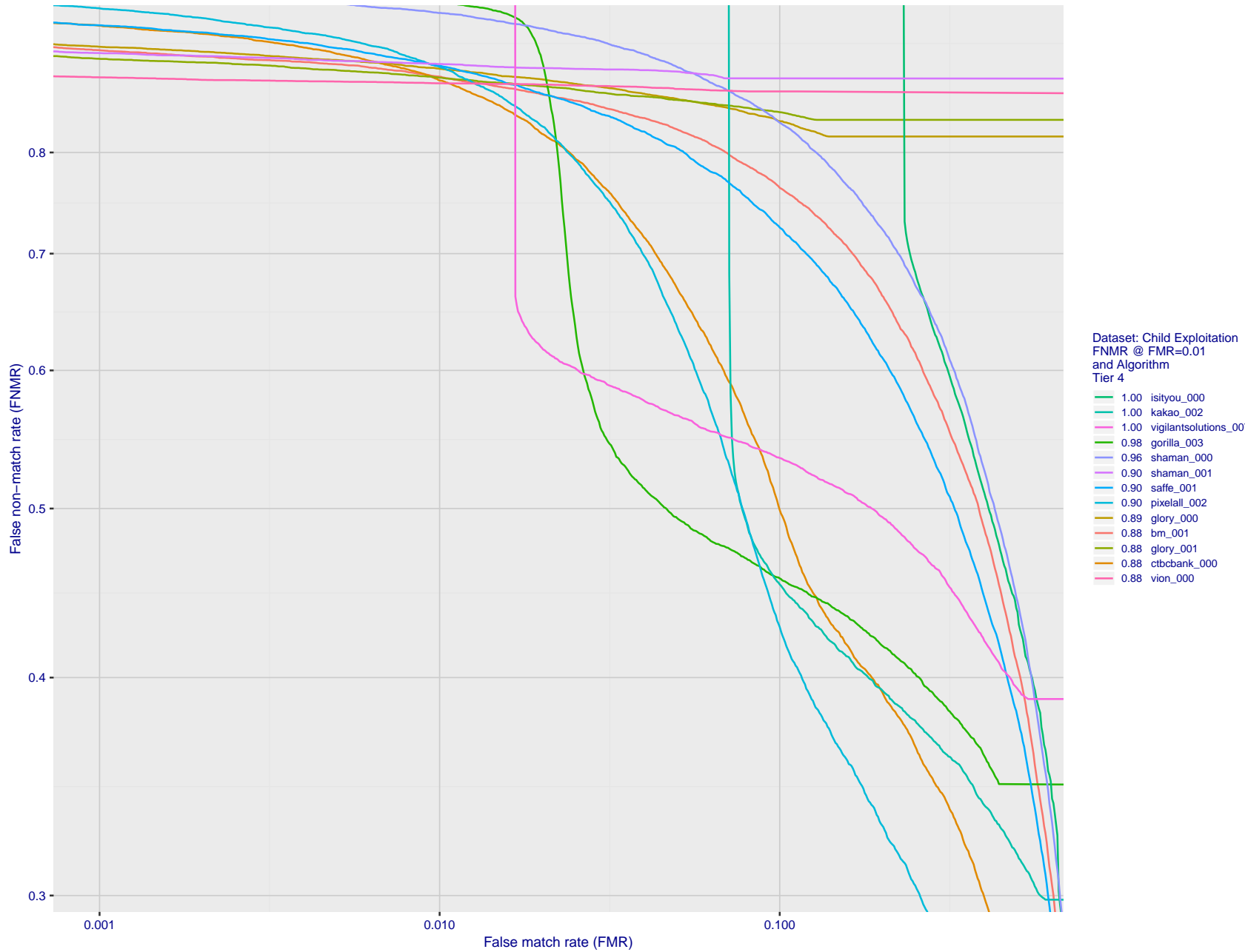


Figure 45: For child exploitation images, detection error tradeoff (DET) characteristics showing false non-match rate vs. false match rate plotted parametrically on threshold,  $T$ . The scales are logarithmic in order to show many decades of FMR. Accuracy is poor because many images have adverse quality characteristics, and because detection and enrollment fails.

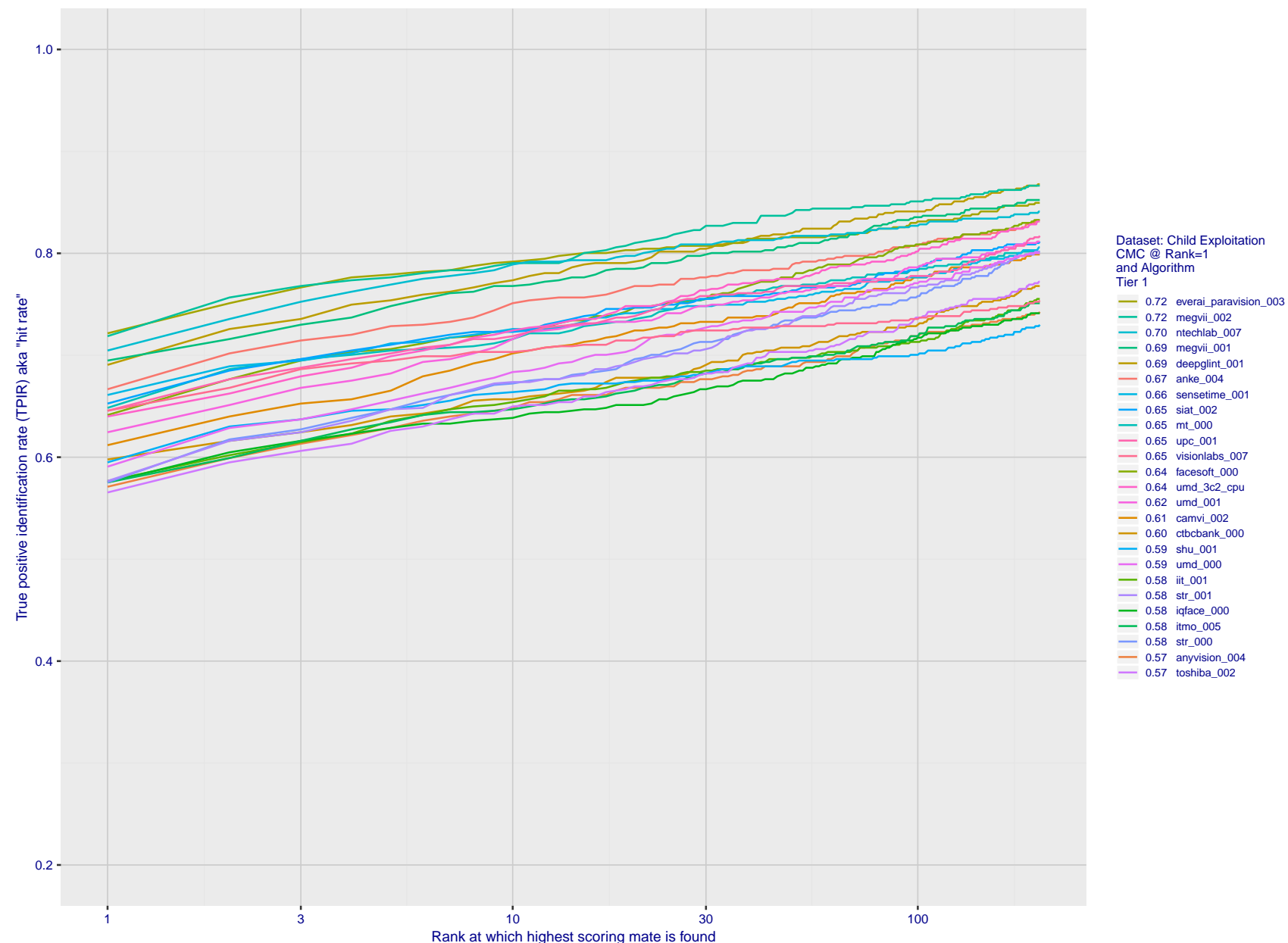


Figure 46: For child exploitation images, cumulative match characteristics (CMC) showing true positive identification rate vs. rank. This is simulation of a one-to-many search experiment - see discussion in section 3.2. The scales are logarithmic in order to show the effect of long candidate lists. Accuracy is poor but much improved relative to the 1:1 DETs of Fig. 45 because a search can succeed if any of a subject's several enrolled images matches the search image with a high score.

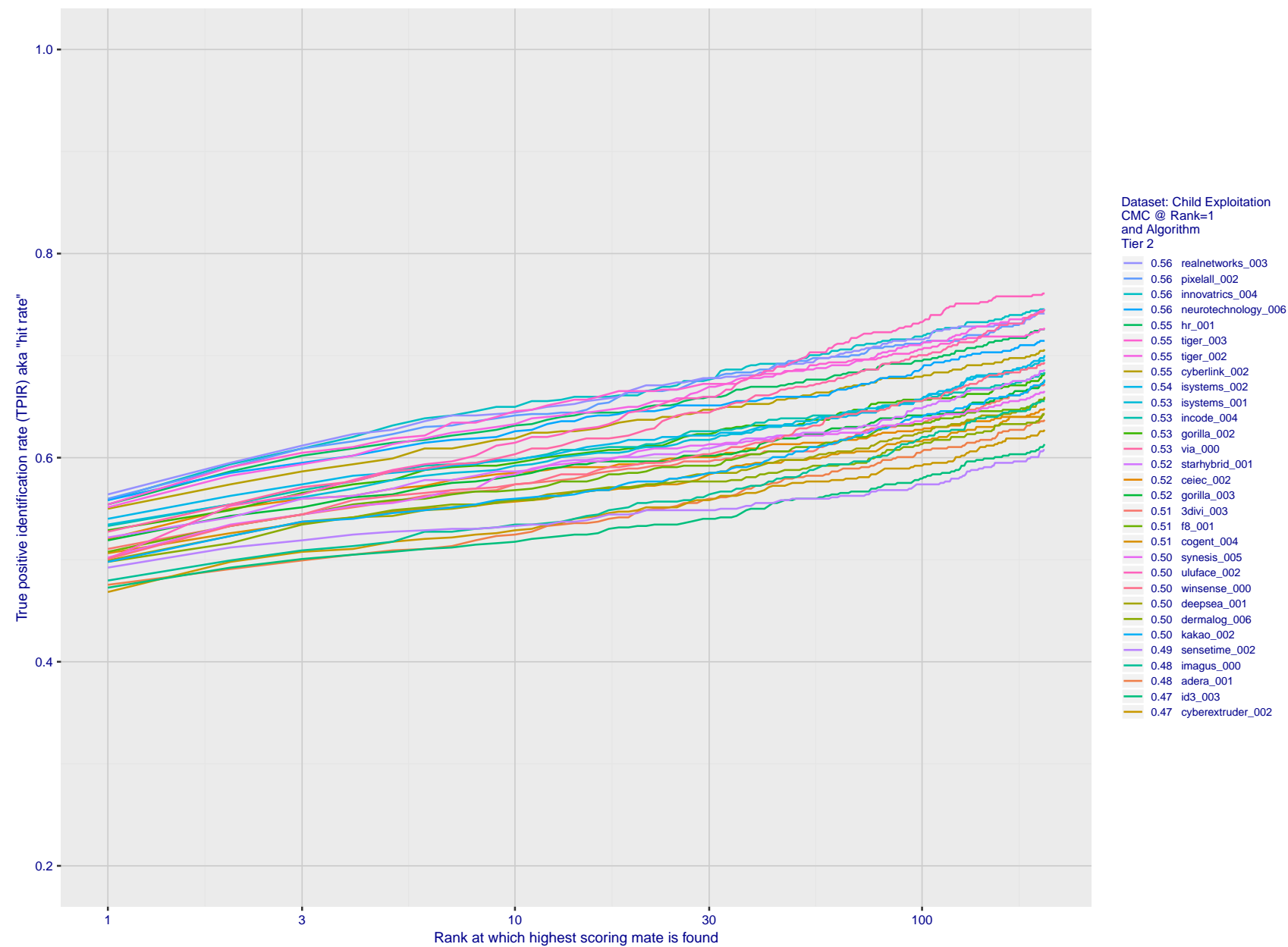


Figure 47: For child exploitation images, cumulative match characteristics (CMC) showing true positive identification rate vs. rank. This is simulation of a one-to-many search experiment - see discussion in section 3.2. The scales are logarithmic in order to show the effect of long candidate lists. Accuracy is poor but much improved relative to the 1:1 DETs of Fig. 45 because a search can succeed if any of a subject's several enrolled images matches the search image with a high score.

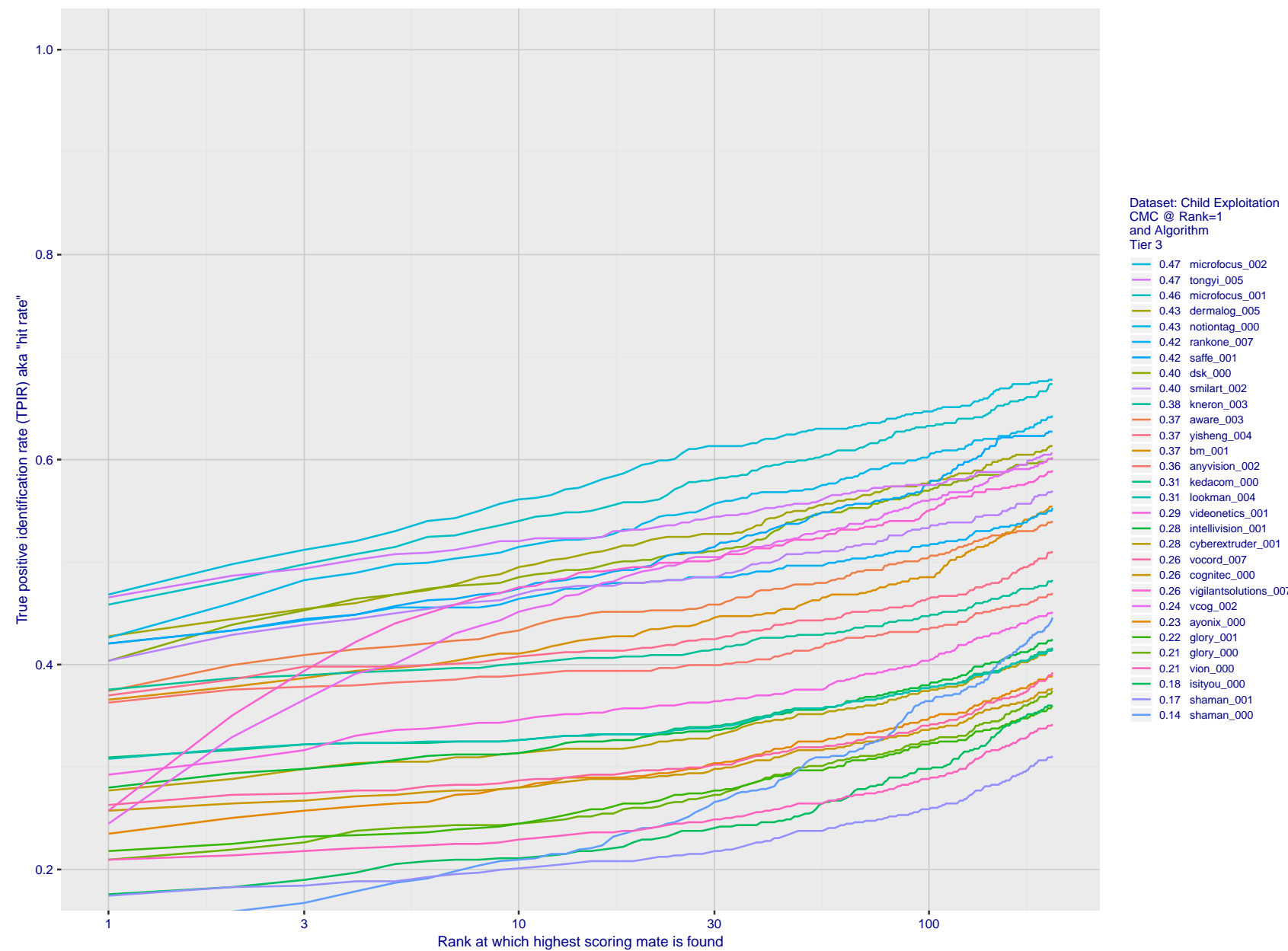


Figure 48: For child exploitation images, cumulative match characteristics (CMC) showing true positive identification rate vs. rank. This is simulation of a one-to-many search experiment - see discussion in section 3.2. The scales are logarithmic in order to show the effect of long candidate lists. Accuracy is poor but much improved relative to the 1:1 DETs of Fig. 45 because a search can succeed if any of a subject's several enrolled images matches the search image with a high score.



Figure 49: For child exploitation images, cumulative match characteristics (CMC) showing true positive identification rate vs. rank for two cases: 1. Whole image provided to the algorithm; 2. Human annotated rectangular region, cropped and provided to the algorithm. The difference between the traces is associated with detection of difficult faces, and fine localization.

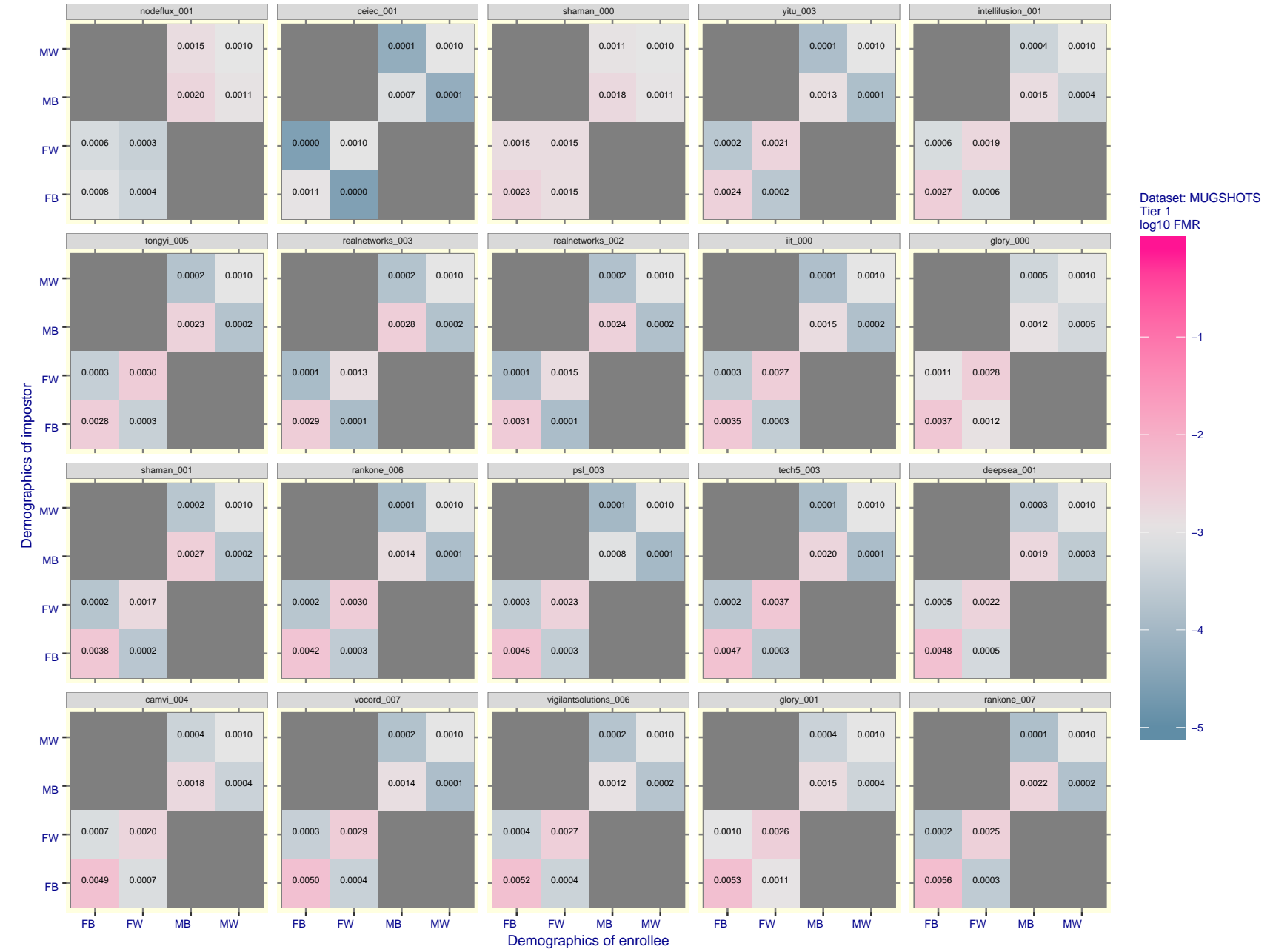


Figure 50: For the mugshot images, FMR for same-sex impostor pairs of images annotated with codes for black female, black male, white female, white male. The threshold is set for each algorithm to give  $FMR = 0.001$  for white males which is the demographic that usually gives the lowest FMR. This means the top right box is the same color in all panels. The panels are sorted over multiple pages in order of FMR on black females, which is the demographic that usually gives the highest FMR.

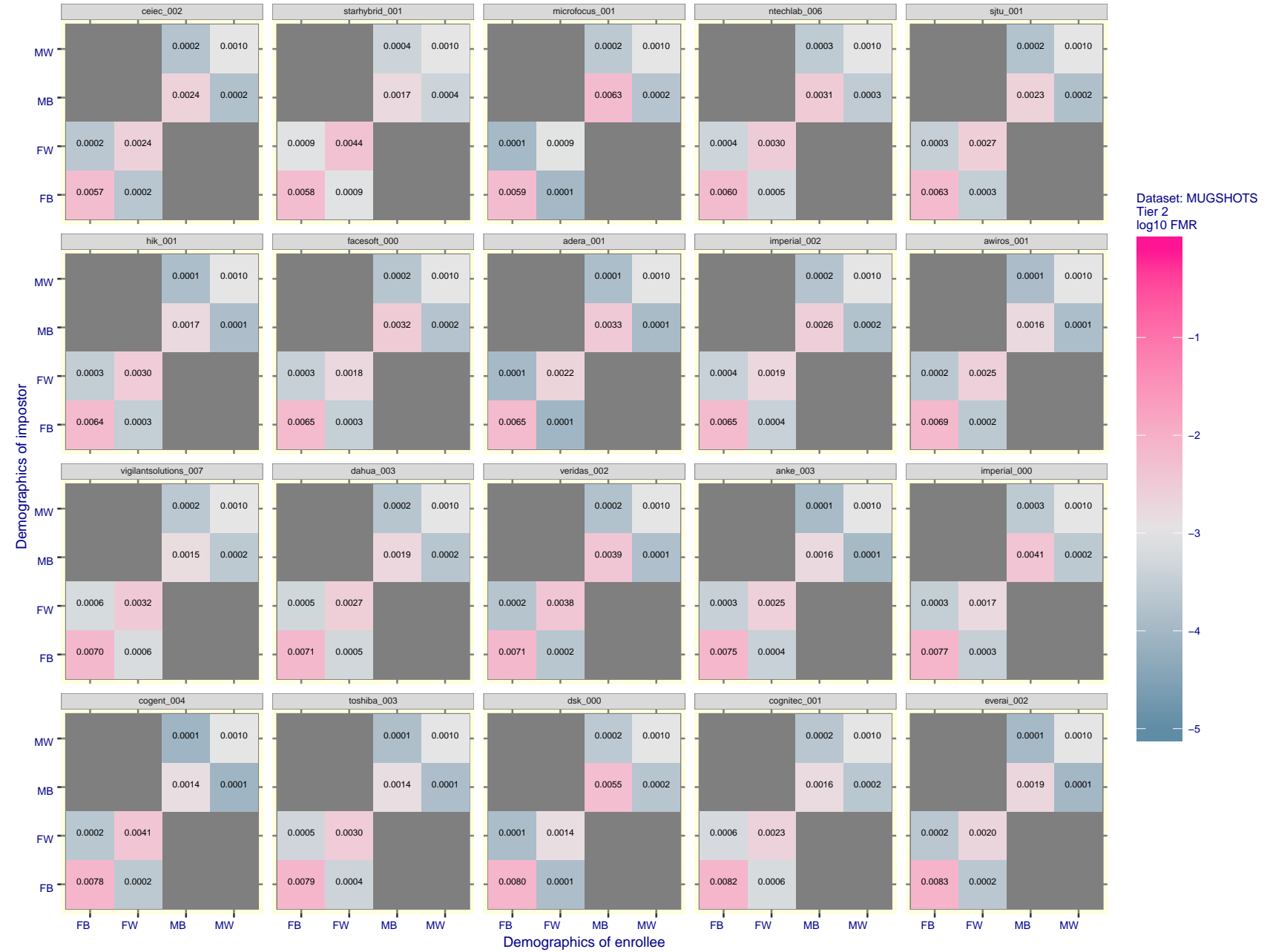


Figure 51: For the mugshot images, FMR for same-sex impostor pairs of images annotated with codes for black female, black male, white female, white male. The threshold is set for each algorithm to give FMR = 0.001 for white males which is the demographic that usually gives the lowest FMR. This means the top right box is the same color in all panels. The panels are sorted over multiple pages in order of FMR on black females, which is the demographic that usually gives the highest FMR.

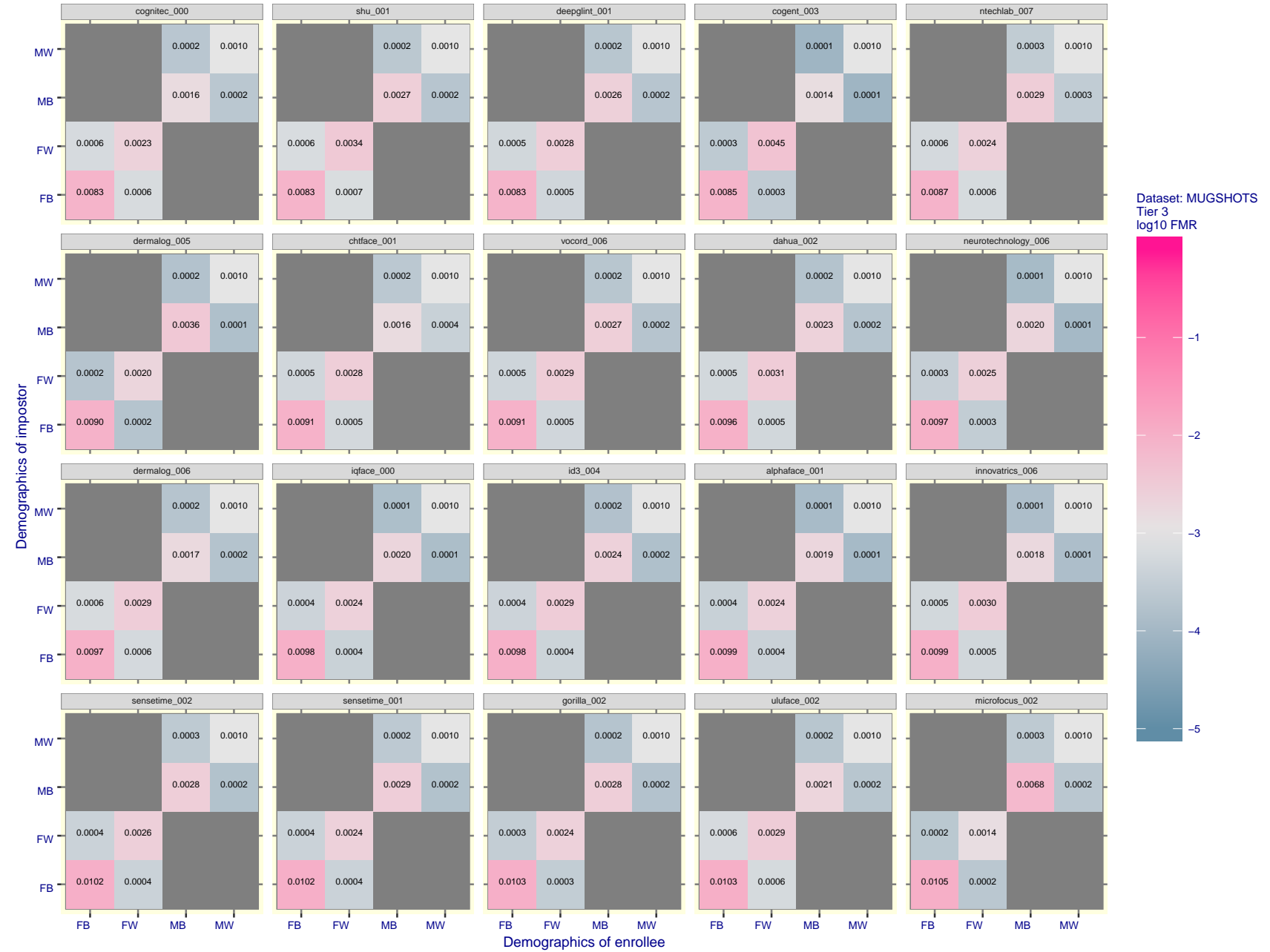


Figure 52: For the mugshot images, FMR for same-sex impostor pairs of images annotated with codes for black female, black male, white female, white male. The threshold is set for each algorithm to give FMR = 0.001 for white males which is the demographic that usually gives the lowest FMR. This means the top right box is the same color in all panels. The panels are sorted over multiple pages in order of FMR on black females, which is the demographic that usually gives the highest FMR.

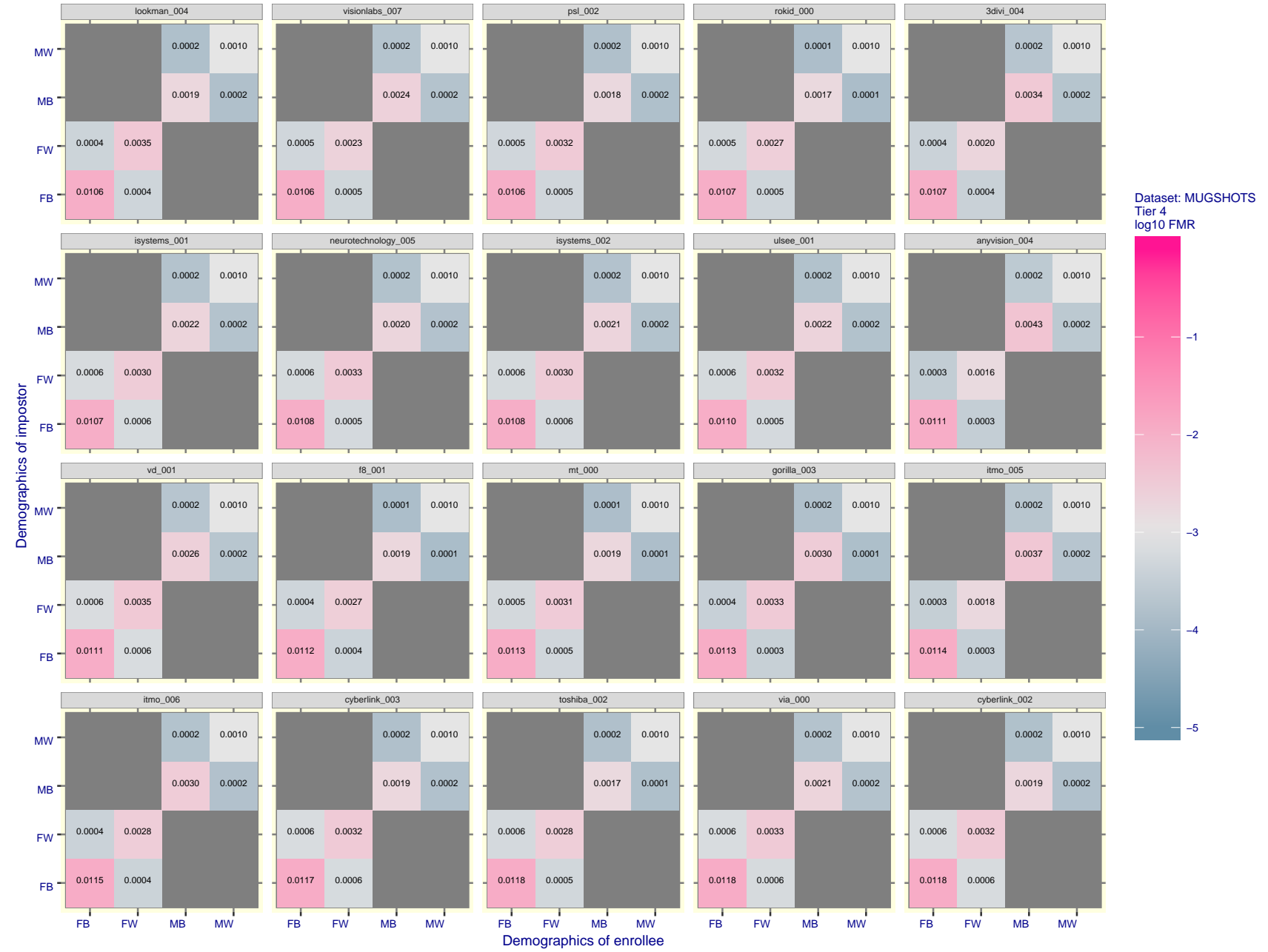


Figure 53: For the mugshot images, FMR for same-sex impostor pairs of images annotated with codes for black female, black male, white female, white male. The threshold is set for each algorithm to give  $FMR = 0.001$  for white males which is the demographic that usually gives the lowest FMR. This means the top right box is the same color in all panels. The panels are sorted over multiple pages in order of FMR on black females, which is the demographic that usually gives the highest FMR.

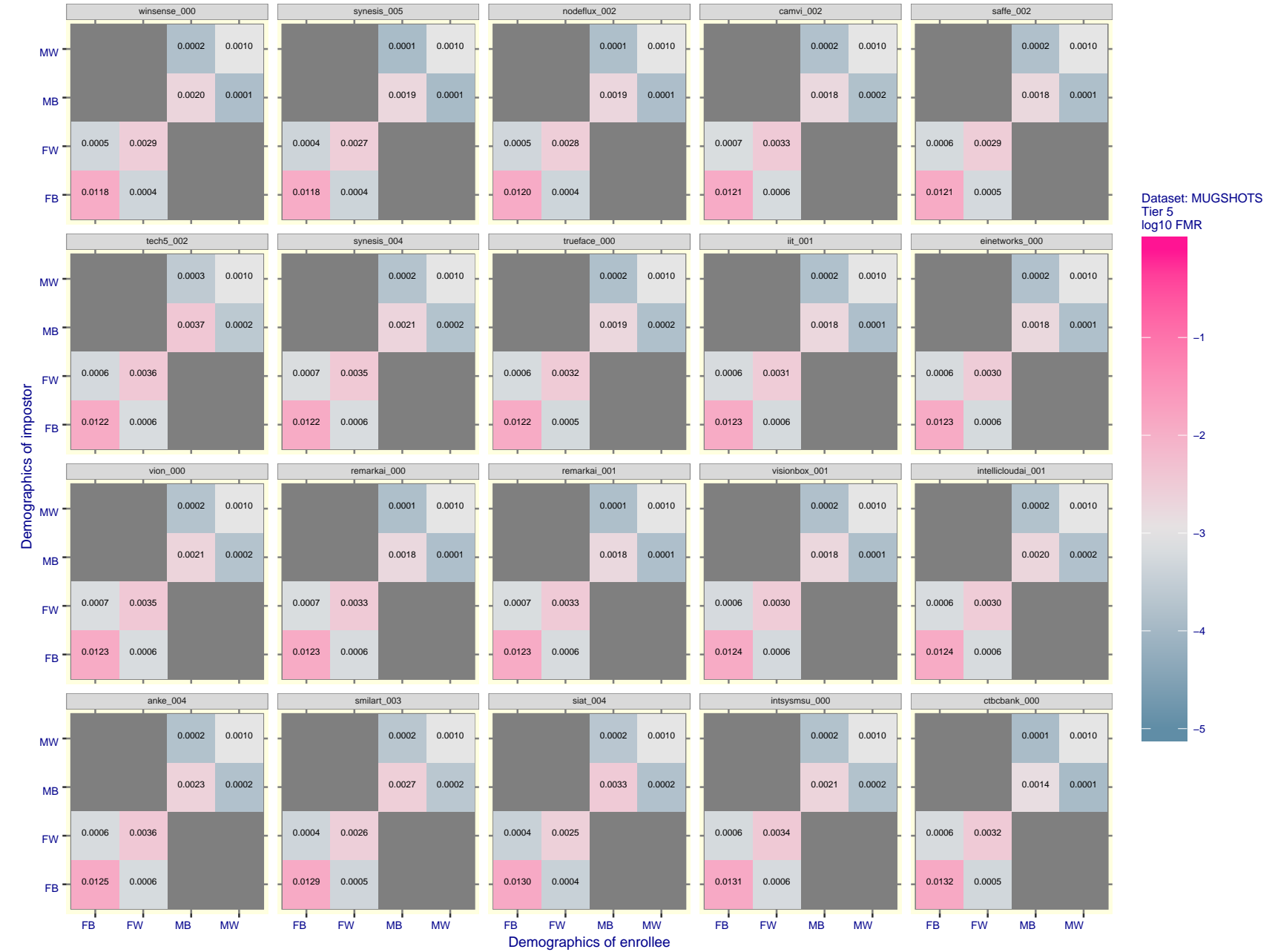


Figure 54: For the mugshot images, FMR for same-sex impostor pairs of images annotated with codes for black female, black male, white female, white male. The threshold is set for each algorithm to give FMR = 0.001 for white males which is the demographic that usually gives the lowest FMR. This means the top right box is the same color in all panels. The panels are sorted over multiple pages in order of FMR on black females, which is the demographic that usually gives the highest FMR.

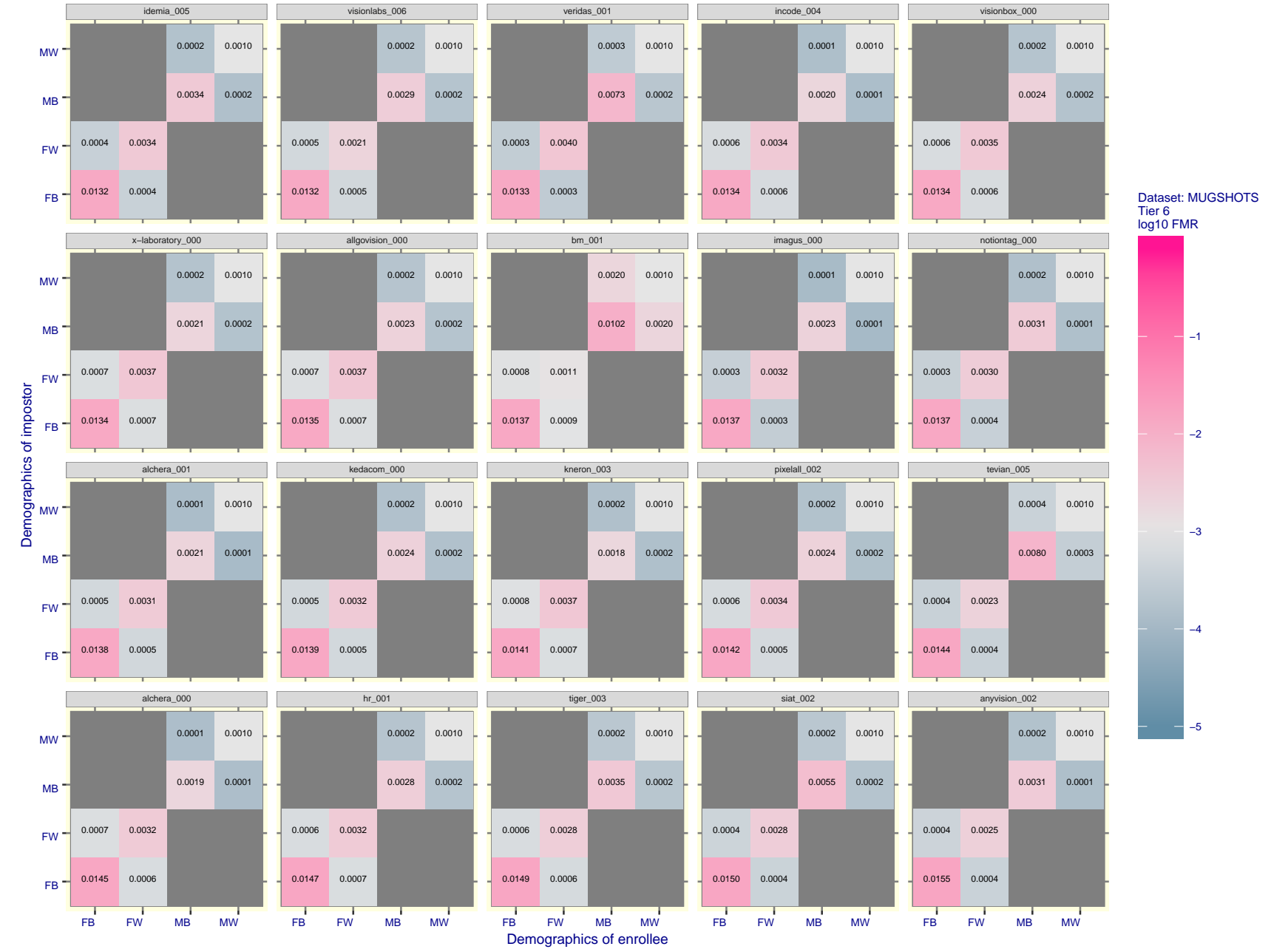


Figure 55: For the mugshot images, FMR for same-sex impostor pairs of images annotated with codes for black female, black male, white female, white male. The threshold is set for each algorithm to give FMR = 0.001 for white males which is the demographic that usually gives the lowest FMR. This means the top right box is the same color in all panels. The panels are sorted over multiple pages in order of FMR on black females, which is the demographic that usually gives the highest FMR.

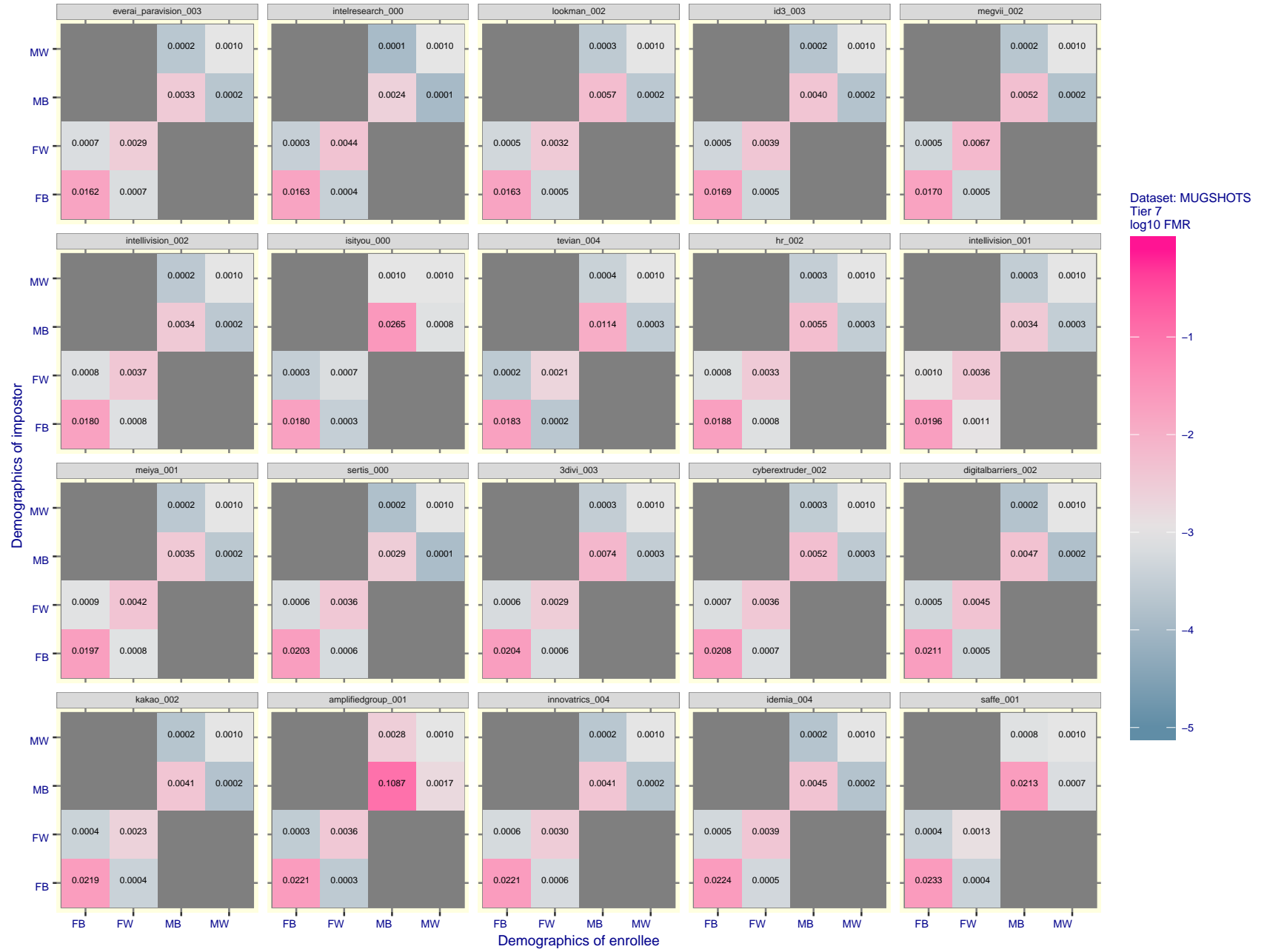


Figure 56: For the mugshot images, FMR for same-sex impostor pairs of images annotated with codes for black female, black male, white female, white male. The threshold is set for each algorithm to give FMR = 0.001 for white males which is the demographic that usually gives the lowest FMR. This means the top right box is the same color in all panels. The panels are sorted over multiple pages in order of FMR on black females, which is the demographic that usually gives the highest FMR.

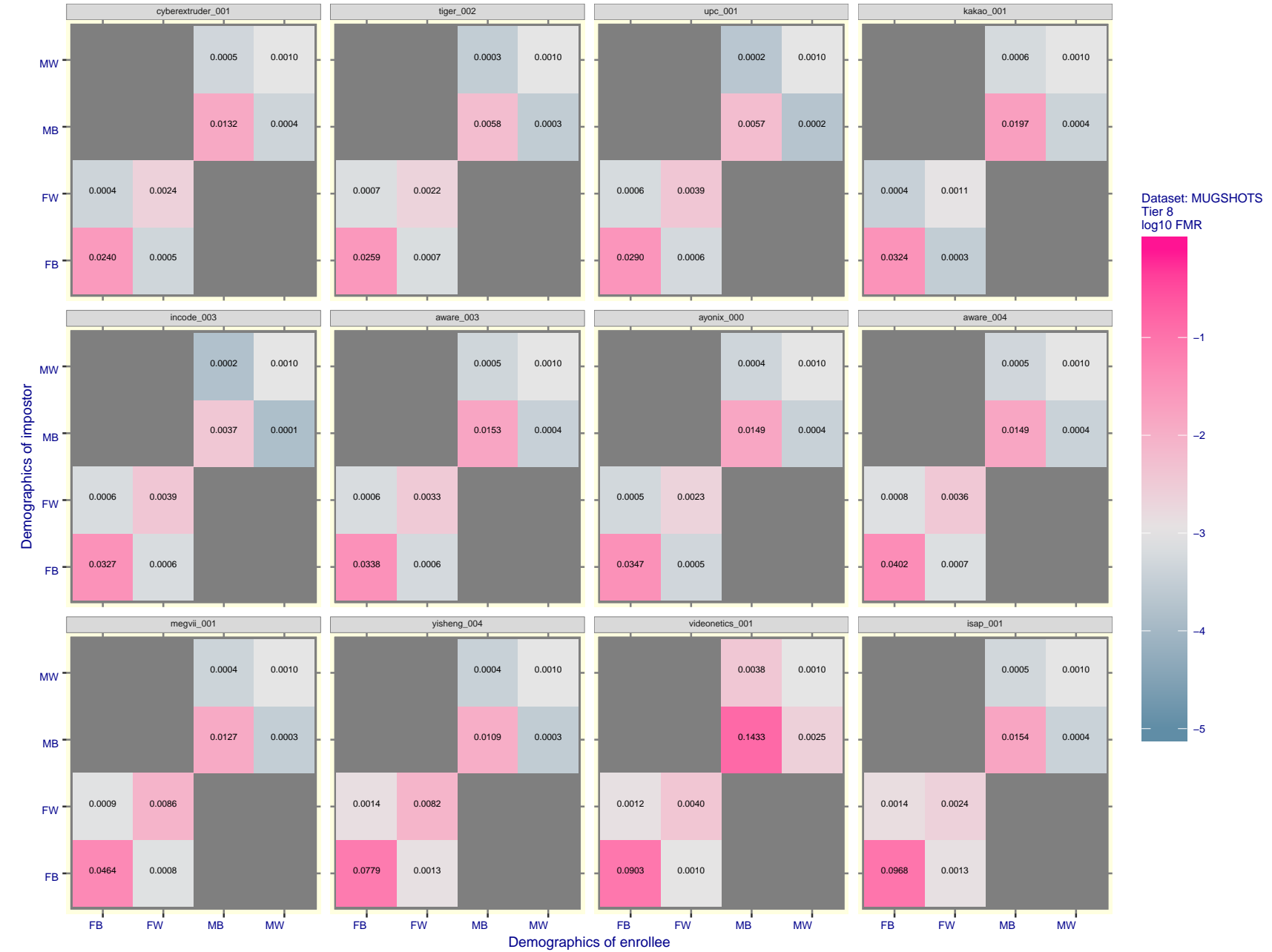


Figure 57: For the mugshot images, FMR for same-sex impostor pairs of images annotated with codes for black female, black male, white female, white male. The threshold is set for each algorithm to give  $\text{FMR} = 0.001$  for white males which is the demographic that usually gives the lowest FMR. This means the top right box is the same color in all panels. The panels are sorted over multiple pages in order of FMR on black females, which is the demographic that usually gives the highest FMR.

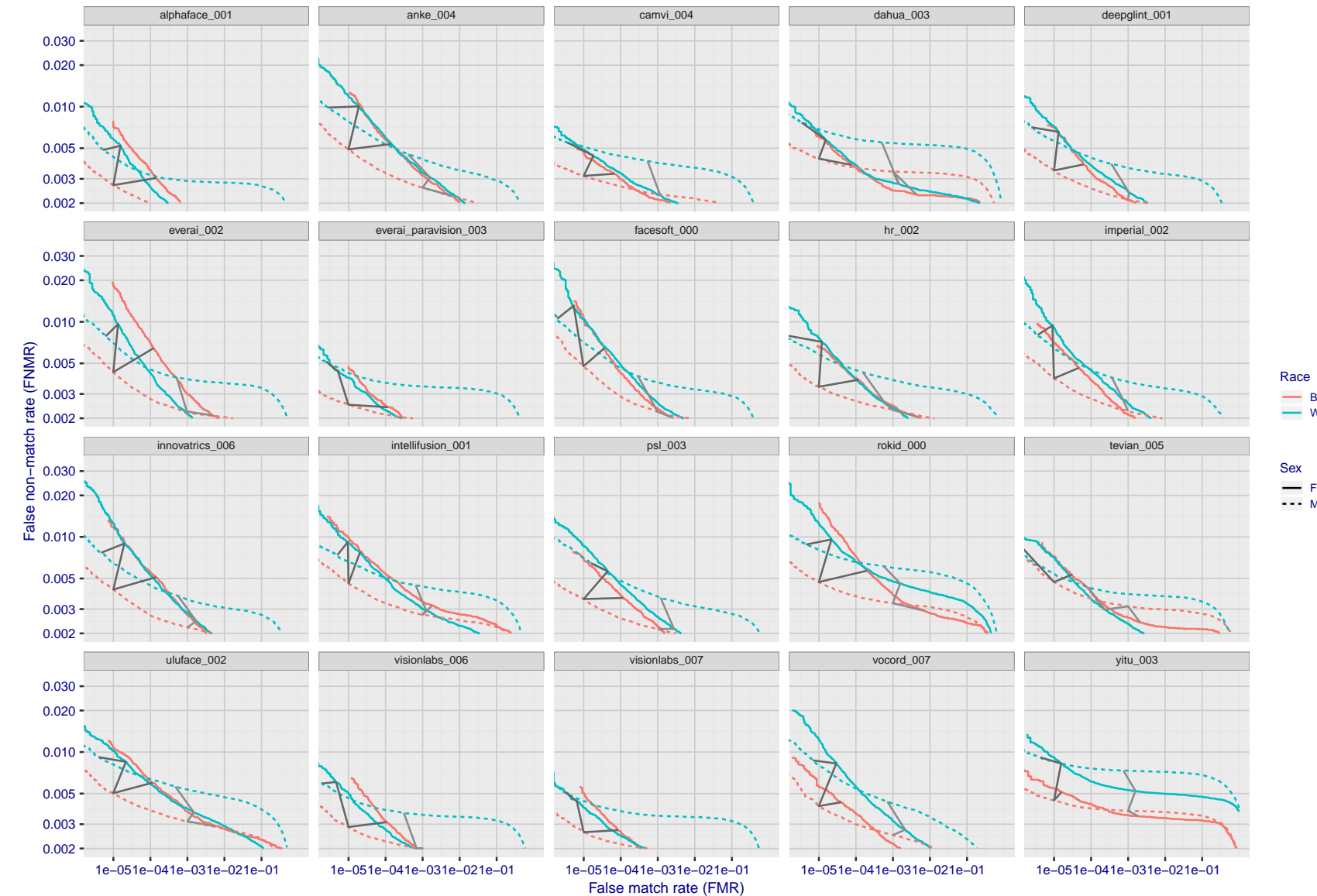


Figure 58: For the mugshot images, error tradeoff characteristics for white females, black females, black males and white males. The Z-shaped grey lines correspond to fixed thresholds, showing both FNMR and FMR vary at one T value. Note: Many of the plots will naively be read as saying women gives worse error rates than men because the solid traces lie above the dotted ones. However, this is misleading and incomplete: The grey lines show the traces reveal horizontal shifts. Thus for the cogent-003 algorithm FNMR for men is higher than for women at a fixed threshold but, at the same time, FMR is higher for women - see Figure 86. As access control systems almost always operate at a fixed threshold, the naive interpretation is incorrect.

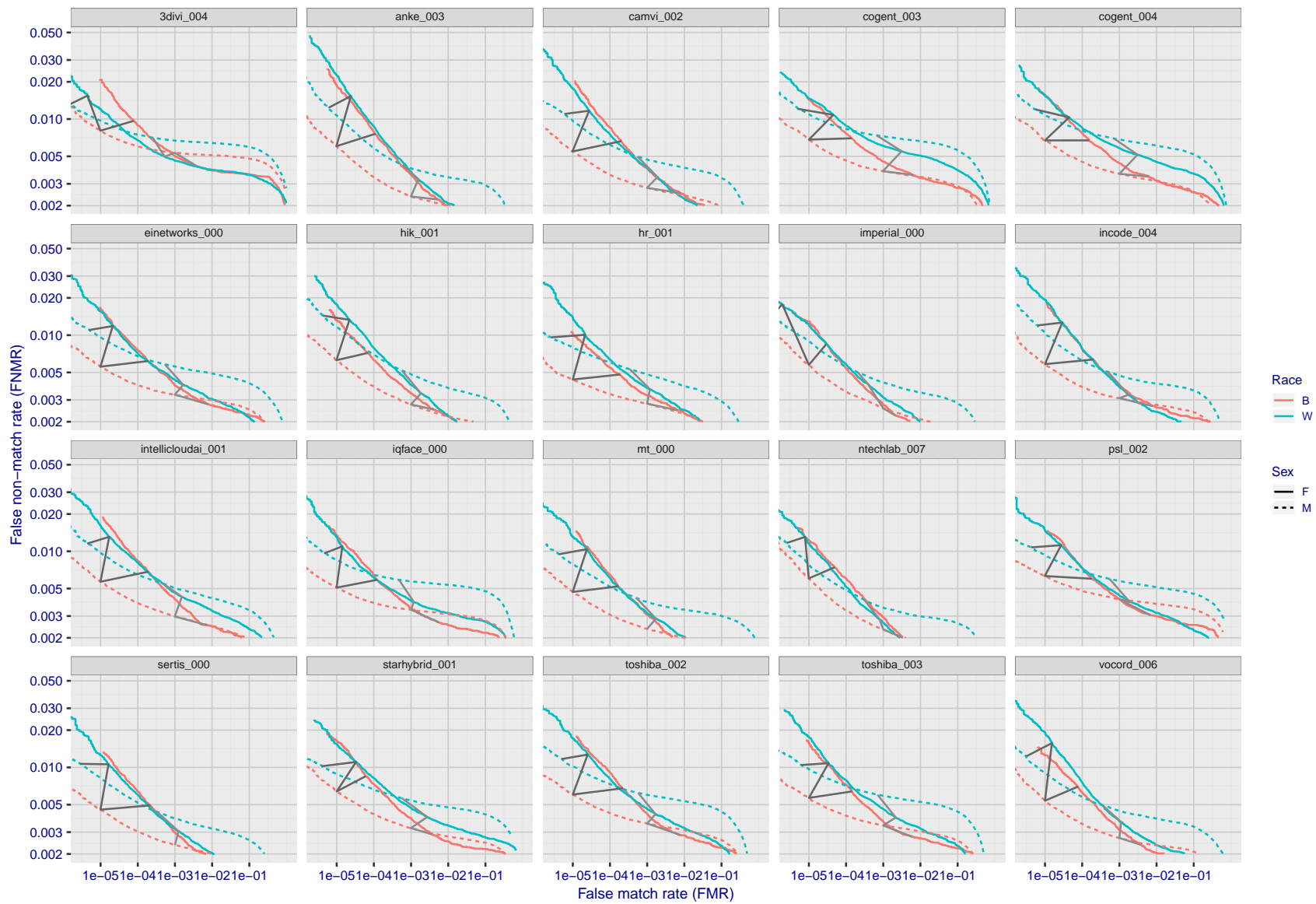


Figure 59: For the mugshot images, error tradeoff characteristics for white females, black females, black males and white males. The Z-shaped grey lines correspond to fixed thresholds, showing both FNMR and FMR vary at one T value. Note: Many of the plots will naively be read as saying women gives worse error rates than men because the solid traces lie above the dotted ones. However, this is misleading and incomplete: The grey lines show the traces reveal horizontal shifts. Thus for the cogent-003 algorithm FNMR for men is higher than for women at a fixed threshold but, at the same time, FMR is higher for women - see Figure 86. As access control systems almost always operate at a fixed threshold, the naive interpretation is incorrect.

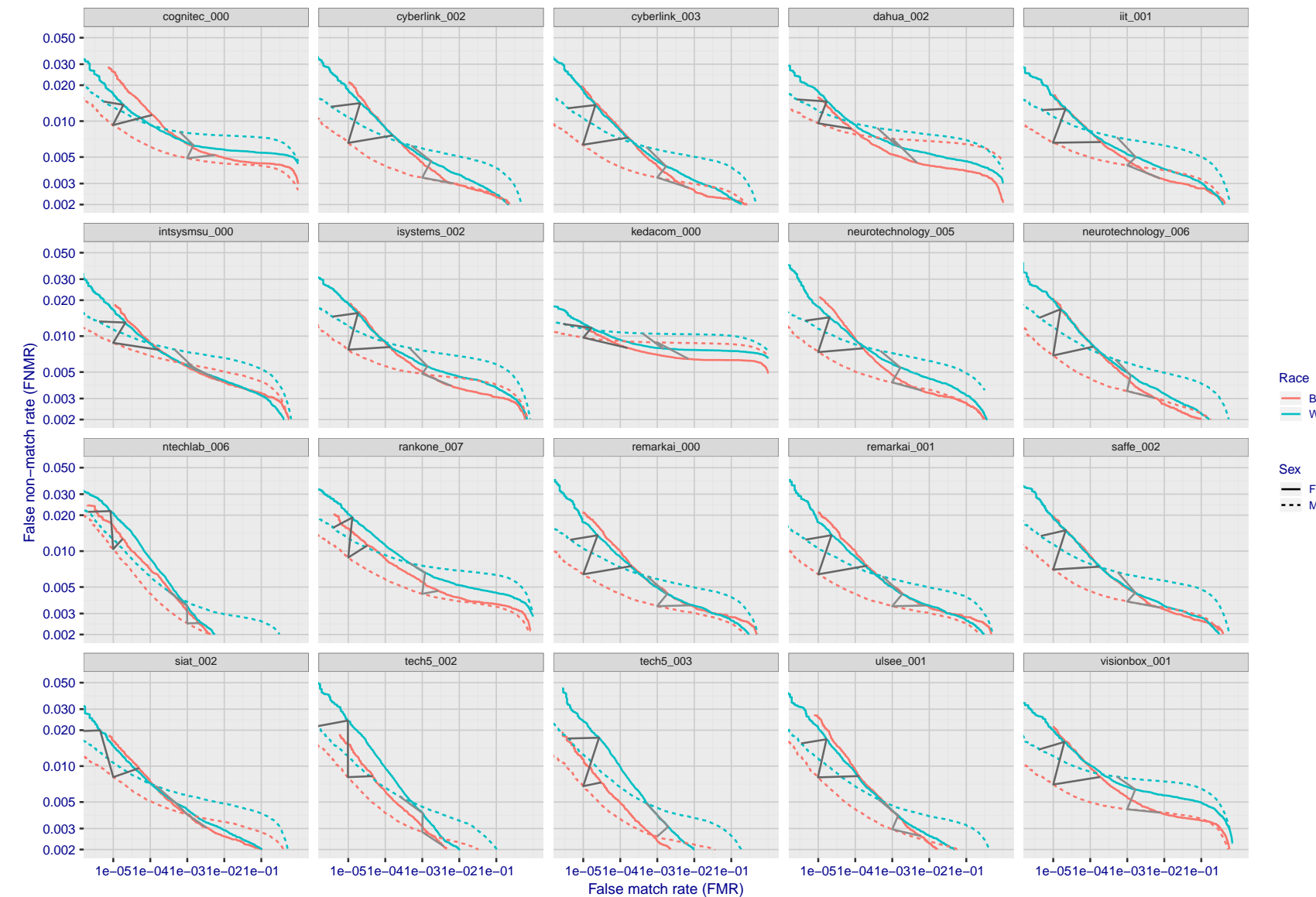


Figure 60: For the mugshot images, error tradeoff characteristics for white females, black females, black males and white males. The Z-shaped grey lines correspond to fixed thresholds, showing both FNMR and FMR vary at one T value. Note: Many of the plots will naively be read as saying women gives worse error rates than men because the solid traces lie above the dotted ones. However, this is misleading and incomplete: The grey lines show the traces reveal horizontal shifts. Thus for the cogent-003 algorithm FNMR for men is higher than for women at a fixed threshold but, at the same time, FMR is higher for women - see Figure 86. As access control systems almost always operate at a fixed threshold, the naive interpretation is incorrect.

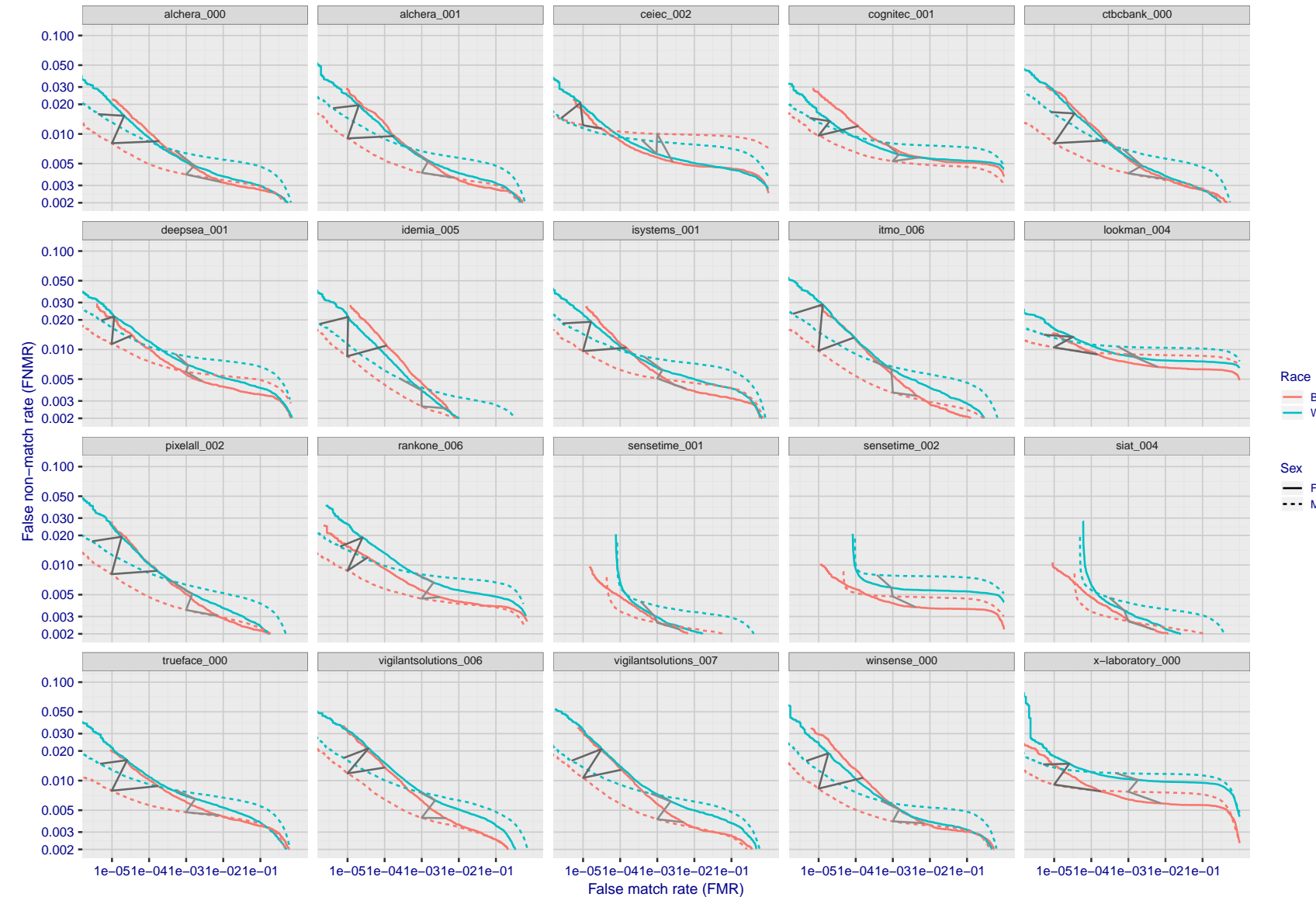


Figure 61: For the mugshot images, error tradeoff characteristics for white females, black females, black males and white males. The Z-shaped grey lines correspond to fixed thresholds, showing both FNMR and FMR vary at one T value. Note: Many of the plots will naively be read as saying women gives worse error rates than men because the solid traces lie above the dotted ones. However, this is misleading and incomplete: The grey lines show the traces reveal horizontal shifts. Thus for the cogent-003 algorithm FNMR for men is higher than for women at a fixed threshold but, at the same time, FMR is higher for women - see Figure 86. As access control systems almost always operate at a fixed threshold, the naive interpretation is incorrect.

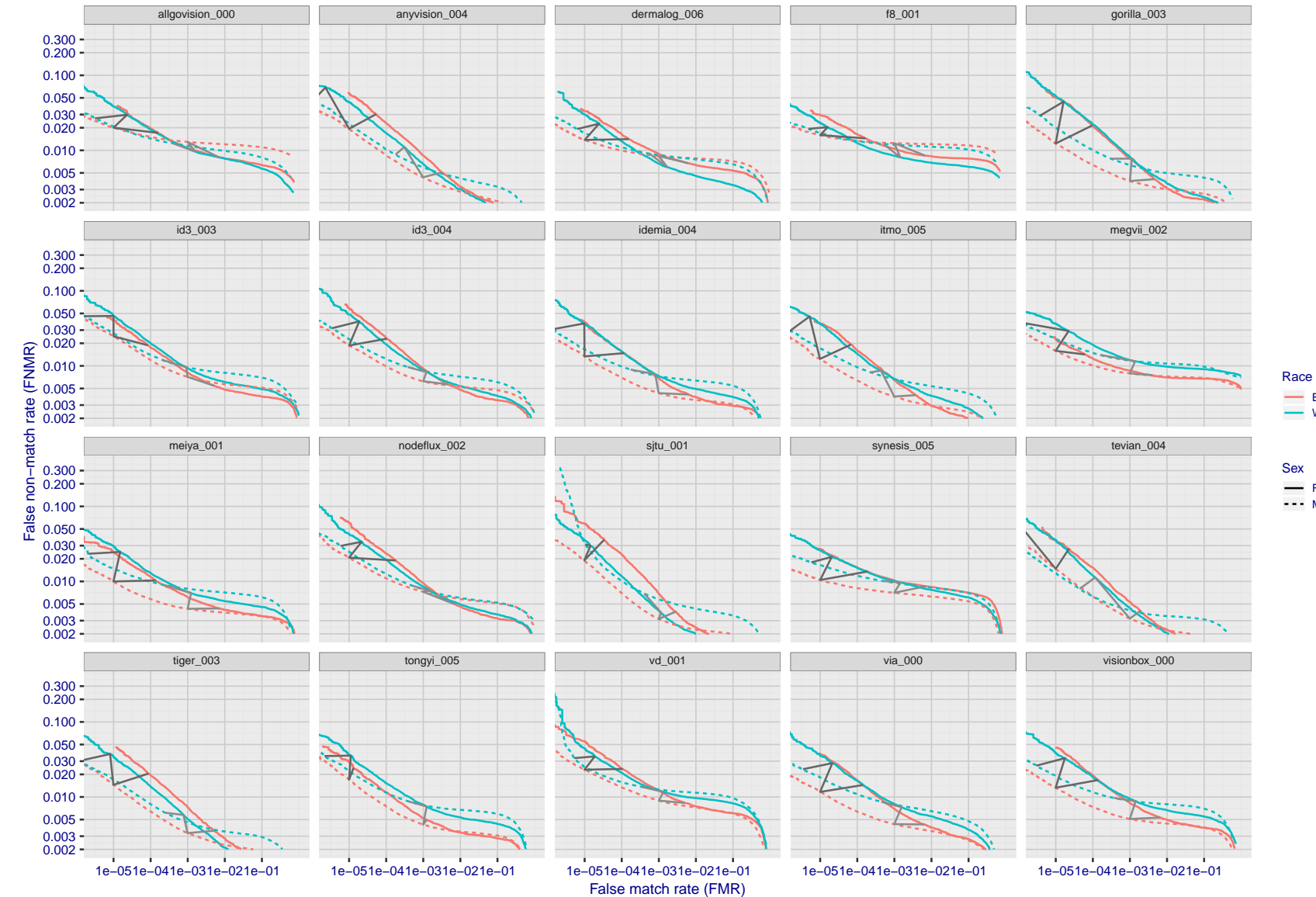


Figure 62: For the mugshot images, error tradeoff characteristics for white females, black females, black males and white males. The Z-shaped grey lines correspond to fixed thresholds, showing both FNMR and FMR vary at one T value. Note: Many of the plots will naively be read as saying women gives worse error rates than men because the solid traces lie above the dotted ones. However, this is misleading and incomplete: The grey lines show the traces reveal horizontal shifts. Thus for the cogent-003 algorithm FNMR for men is higher than for women at a fixed threshold but, at the same time, FMR is higher for women - see Figure 86. As access control systems almost always operate at a fixed threshold, the naive interpretation is incorrect.

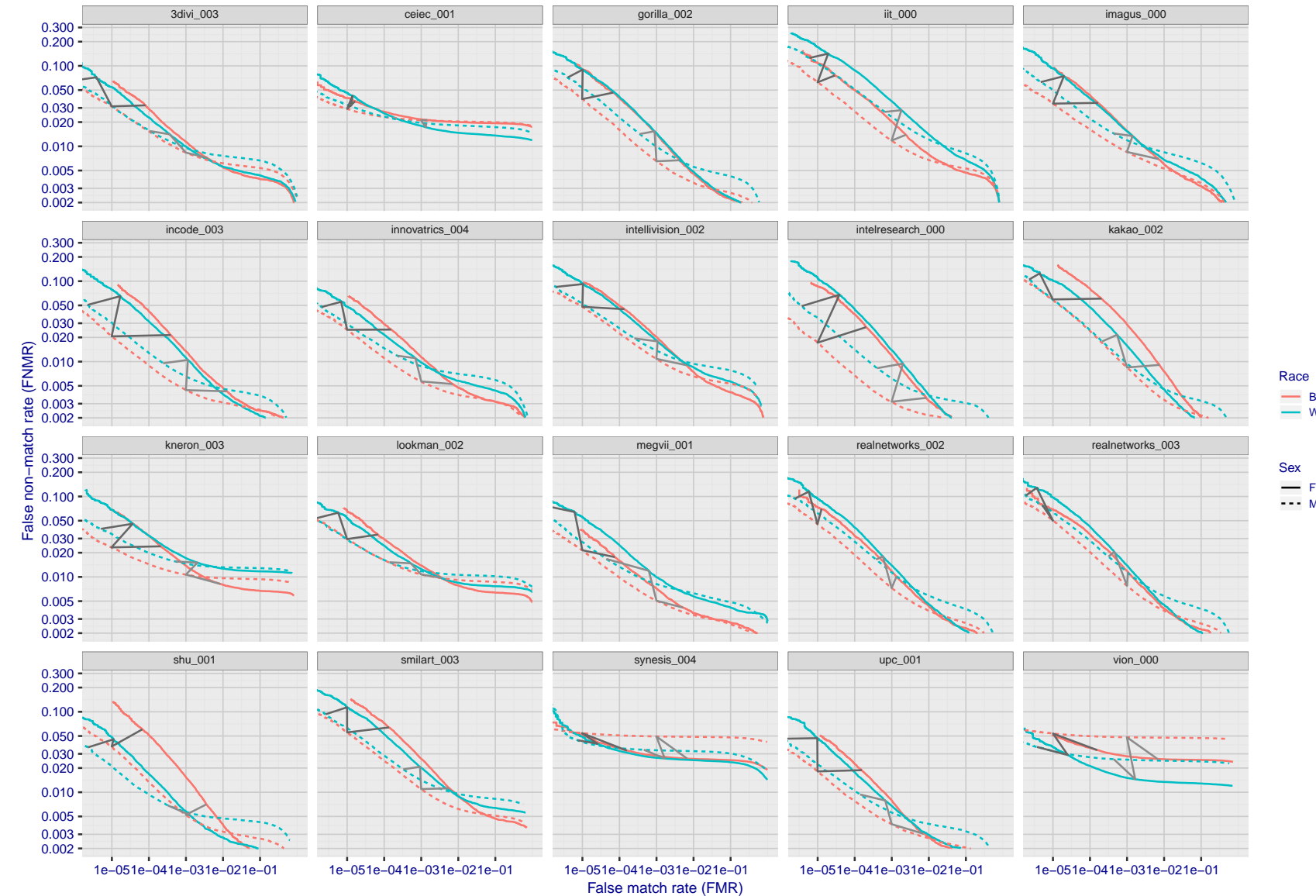


Figure 63: For the mugshot images, error tradeoff characteristics for white females, black females, black males and white males. The Z-shaped grey lines correspond to fixed thresholds, showing both FNMR and FMR vary at one T value. Note: Many of the plots will naively be read as saying women gives worse error rates than men because the solid traces lie above the dotted ones. However, this is misleading and incomplete: The grey lines show the traces reveal horizontal shifts. Thus for the cogent-003 algorithm FNMR for men is higher than for women at a fixed threshold but, at the same time, FMR is higher for women - see Figure 86. As access control systems almost always operate at a fixed threshold, the naive interpretation is incorrect.

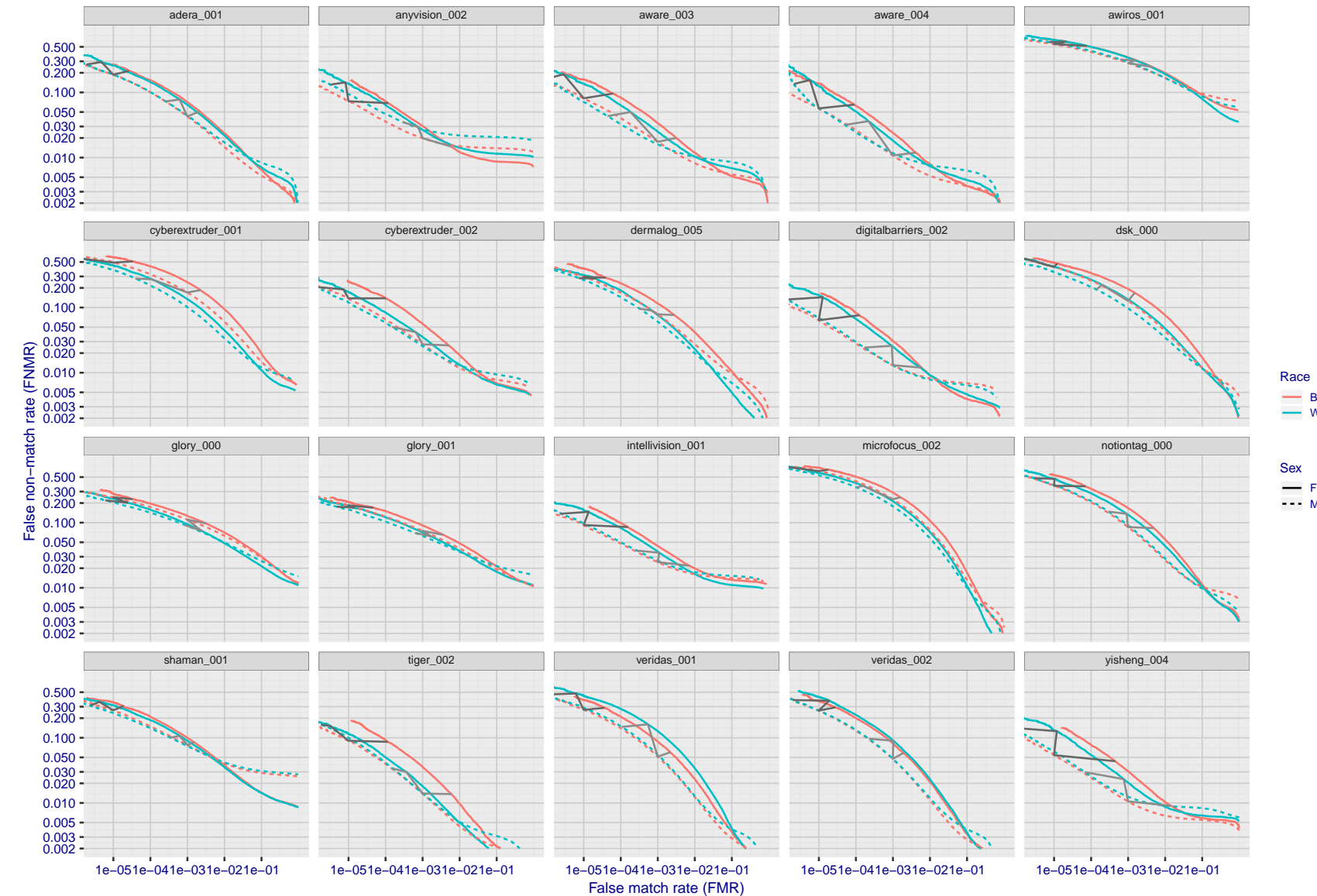


Figure 64: For the mugshot images, error tradeoff characteristics for white females, black females, black males and white males. The Z-shaped grey lines correspond to fixed thresholds, showing both FNMR and FMR vary at one T value. Note: Many of the plots will naively be read as saying women gives worse error rates than men because the solid traces lie above the dotted ones. However, this is misleading and incomplete: The grey lines show the traces reveal horizontal shifts. Thus for the cogent-003 algorithm FNMR for men is higher than for women at a fixed threshold but, at the same time, FMR is higher for women - see Figure 86. As access control systems almost always operate at a fixed threshold, the naive interpretation is incorrect.

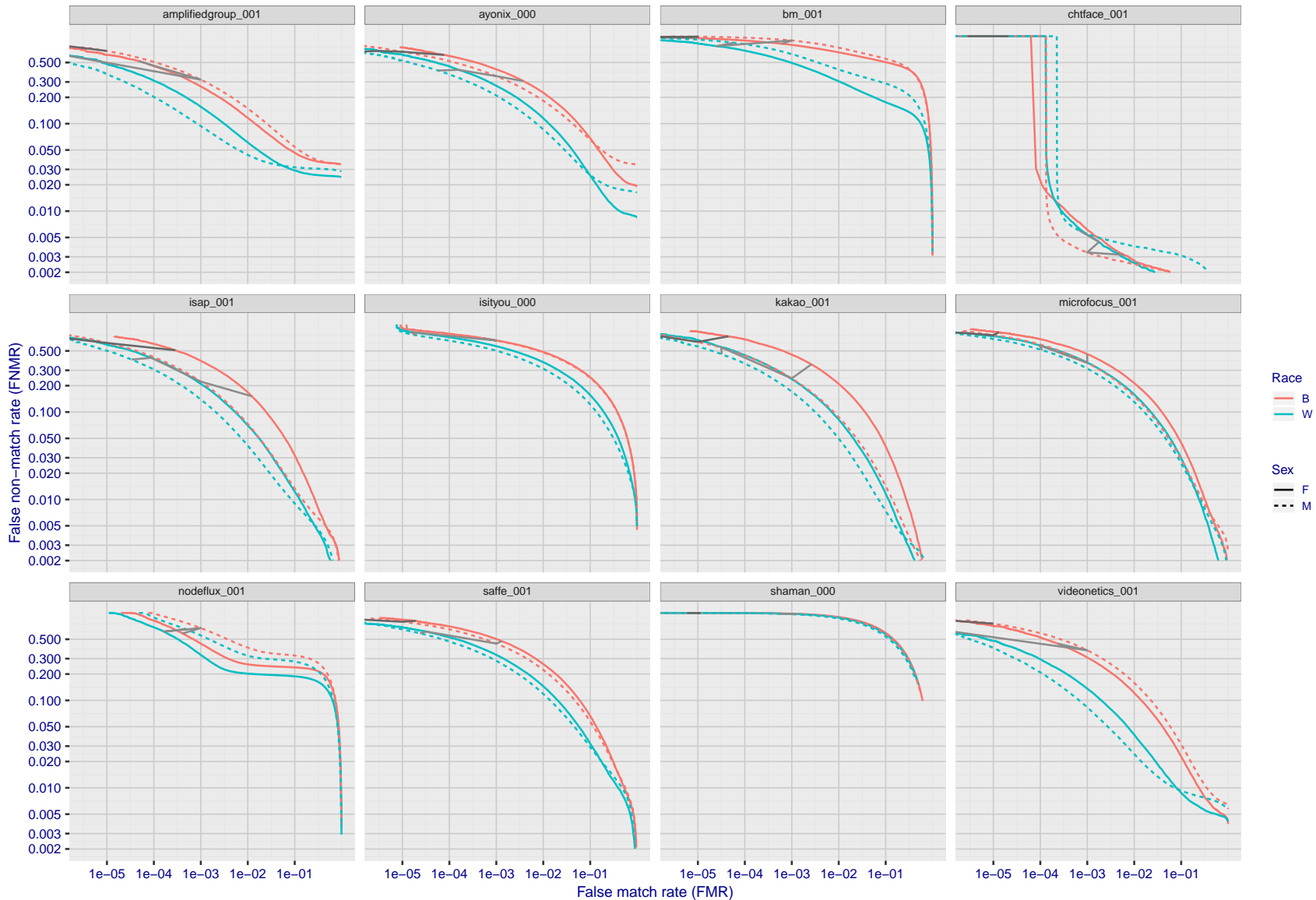


Figure 65: For the mugshot images, error tradeoff characteristics for white females, black females, black males and white males. The Z-shaped grey lines correspond to fixed thresholds, showing both FNMR and FMR vary at one T value. Note: Many of the plots will naively be read as saying women gives worse error rates than men because the solid traces lie above the dotted ones. However, this is misleading and incomplete: The grey lines show the traces reveal horizontal shifts. Thus for the cogent-003 algorithm FNMR for men is higher than for women at a fixed threshold but, at the same time, FMR is higher for women - see Figure 86. As access control systems almost always operate at a fixed threshold, the naive interpretation is incorrect.

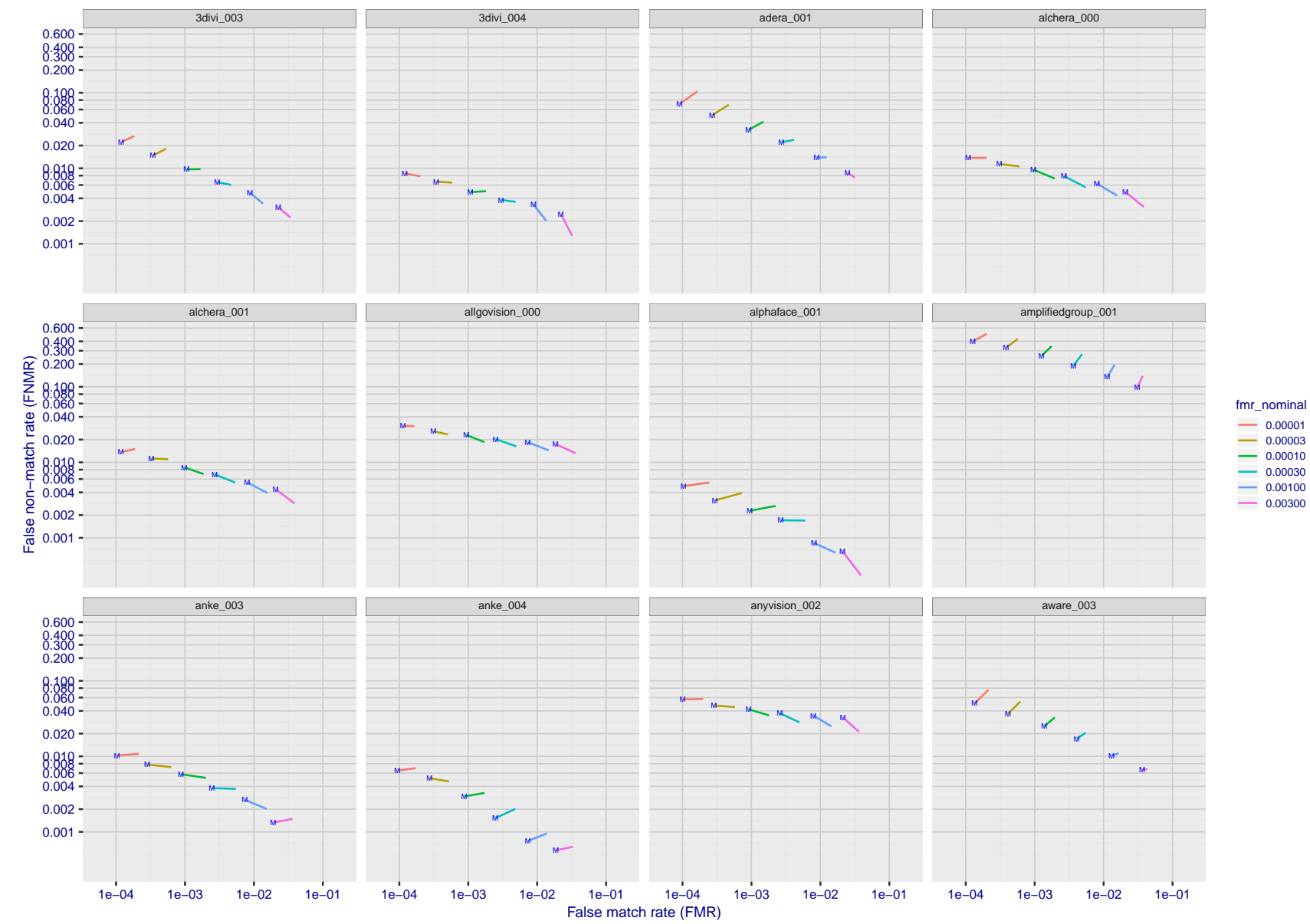


Figure 66: For the visa images, FNMR and FMR at six operating points along the DET characteristic. At each point a line is drawn between  $(FMR, FNMR)_{MALE}$  and  $(FMR, FNMR)_{FEMALE}$  showing how which sex has lower FMR and/or FNMR. The "M" label denotes male, the other end of the line corresponds to female. The six operating thresholds are selected to give the nominal false match rates given in the legend, and are computed over all impostor pairs regardless of age, sex, and place of birth. The plotted FMR values are broadly an order of magnitude larger than the nominal rates because FMR is computed over demographically-matched impostor pairs i.e individuals of the same sex, from the same geographic region (see section 3.6.1), and the same age group (see section 3.6.2).

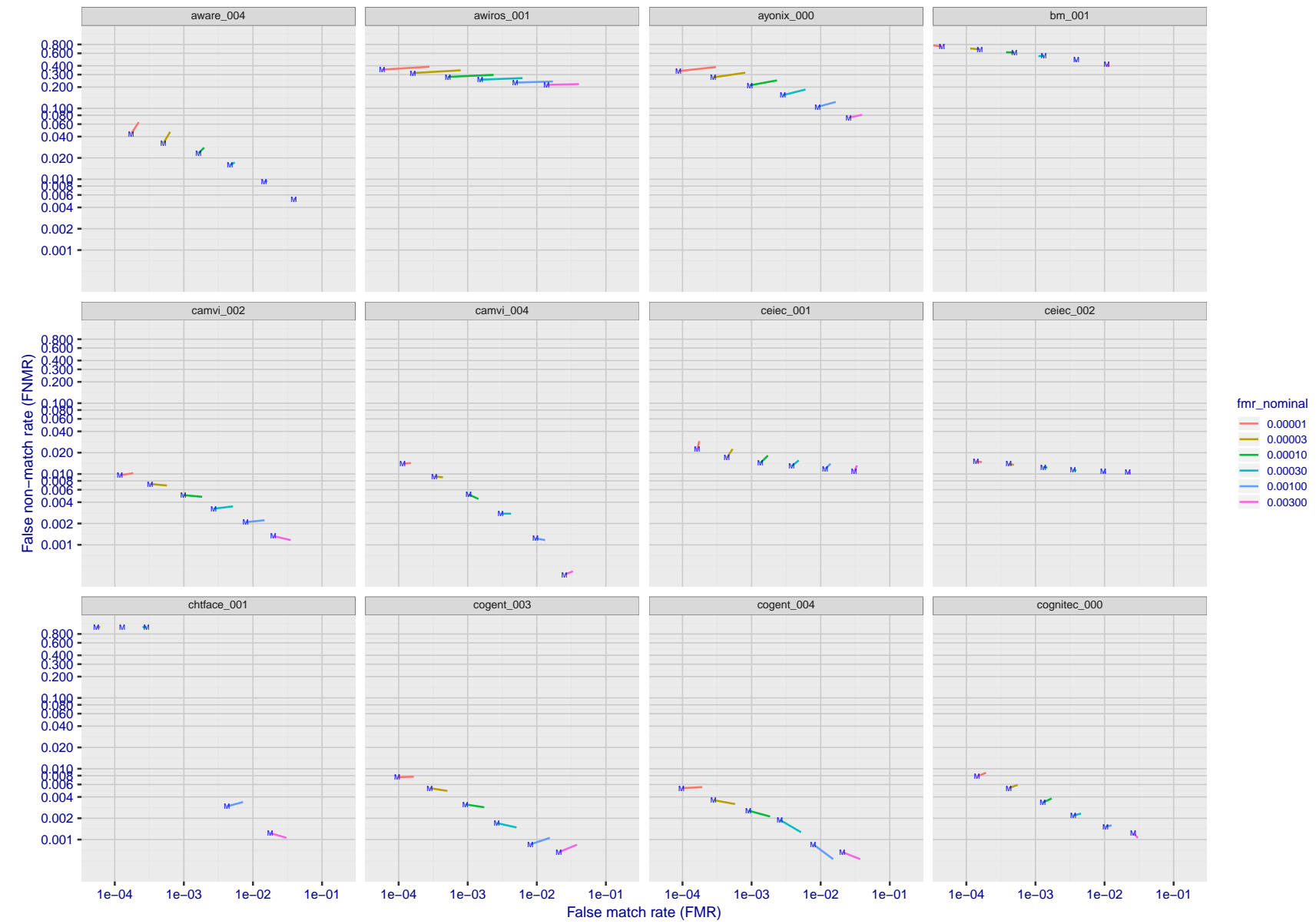


Figure 67: For the visa images, FNMR and FMR at six operating points along the DET characteristic. At each point a line is drawn between  $(FMR, FNMR)_{MALE}$  and  $(FMR, FNMR)_{FEMALE}$  showing how which sex has lower FMR and/or FNMR. The "M" label denotes male, the other end of the line corresponds to female. The six operating thresholds are selected to give the nominal false match rates given in the legend, and are computed over all impostor pairs regardless of age, sex, and place of birth. The plotted FMR values are broadly an order of magnitude larger than the nominal rates because FMR is computed over demographically-matched impostor pairs i.e individuals of the same sex, from the same geographic region (see section 3.6.1), and the same age group (see section 3.6.2).

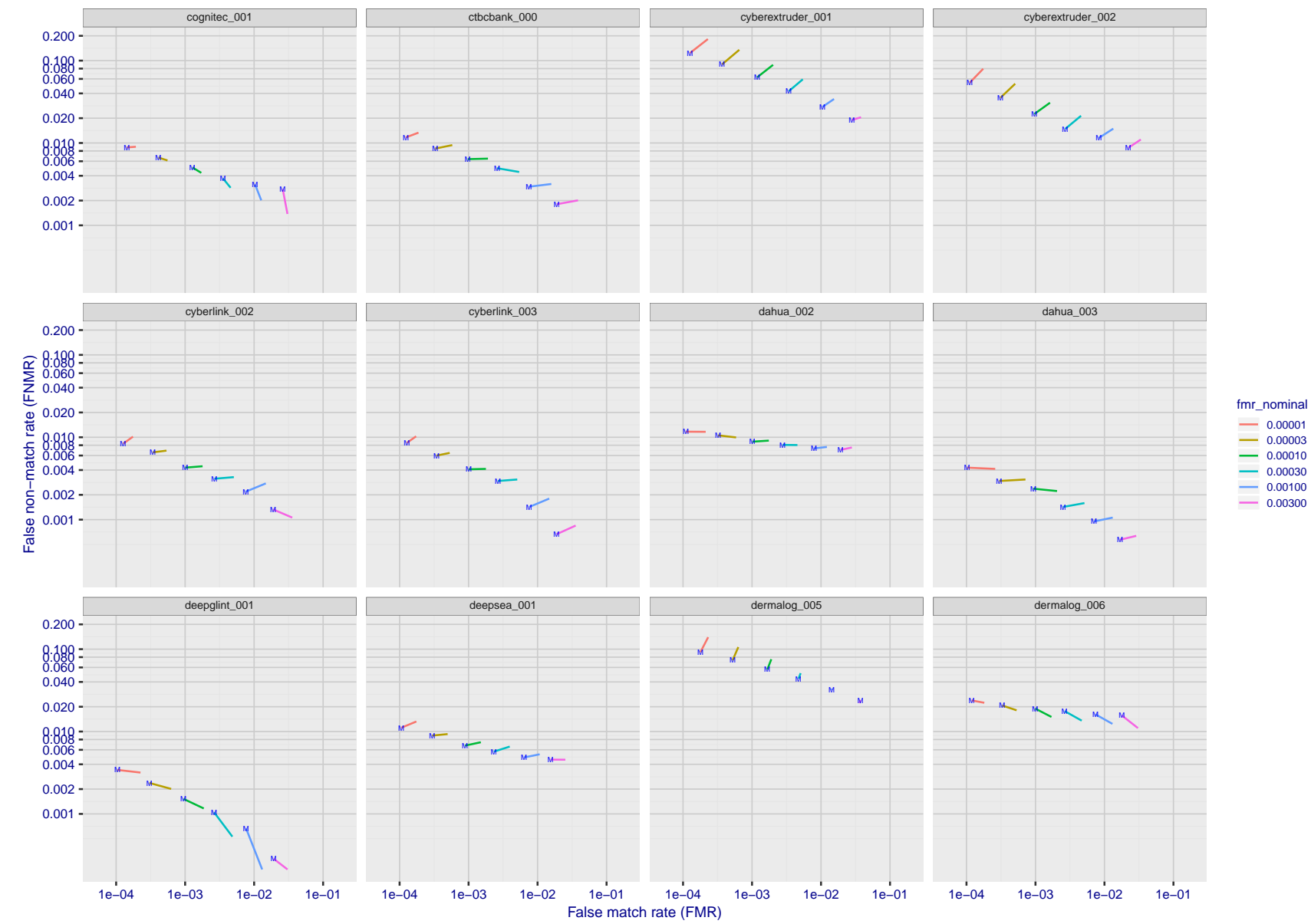


Figure 68: For the visa images, FNMR and FMR at six operating points along the DET characteristic. At each point a line is drawn between  $(FMR, FNMR)_{MALE}$  and  $(FMR, FNMR)_{FEMALE}$  showing how which sex has lower FMR and/or FNMR. The "M" label denotes male, the other end of the line corresponds to female. The six operating thresholds are selected to give the nominal false match rates given in the legend, and are computed over all impostor pairs regardless of age, sex, and place of birth. The plotted FMR values are broadly an order of magnitude larger than the nominal rates because FMR is computed over demographically-matched impostor pairs i.e individuals of the same sex, from the same geographic region (see section 3.6.1), and the same age group (see section 3.6.2).

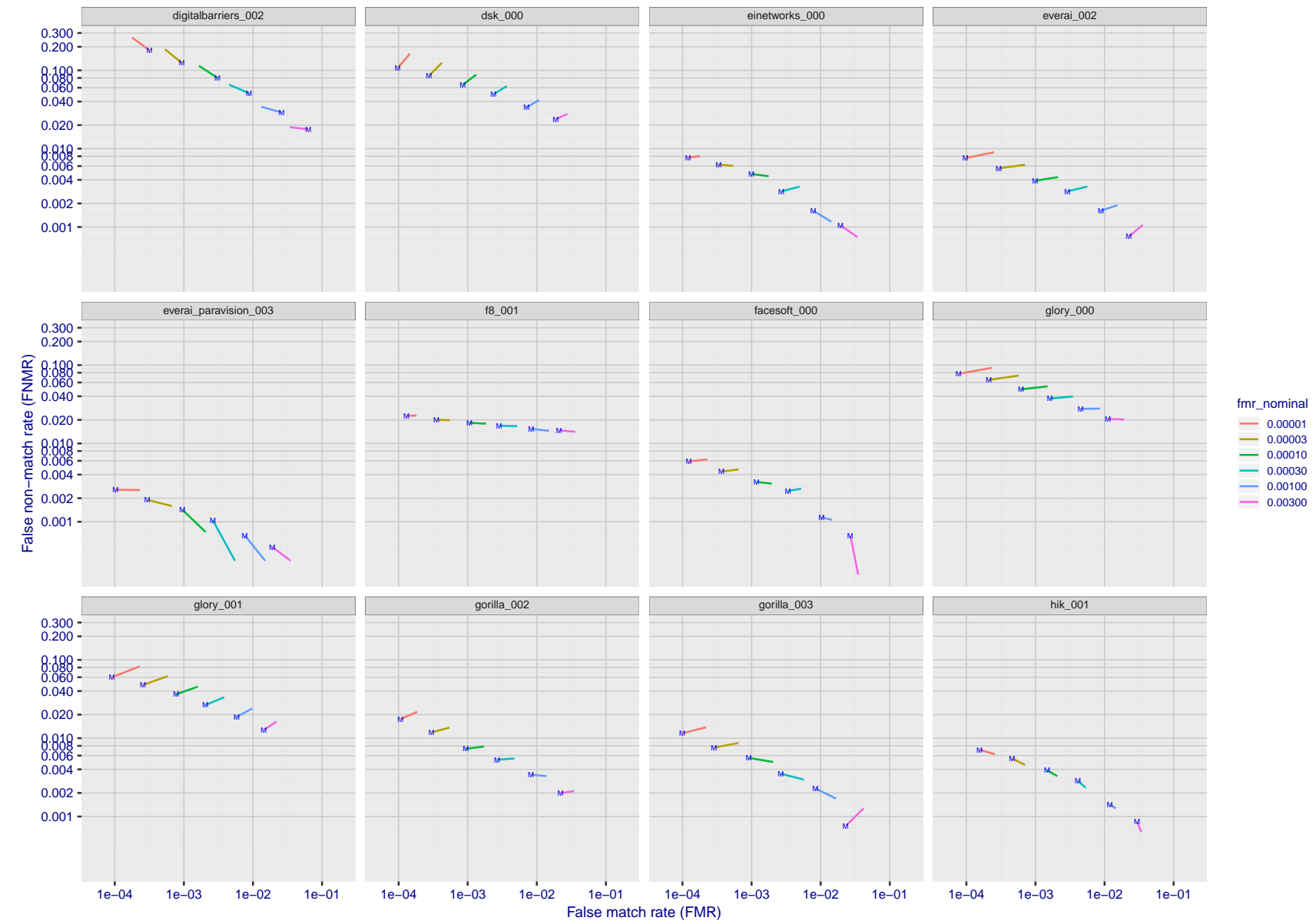


Figure 69: For the visa images, FNMR and FMR at six operating points along the DET characteristic. At each point a line is drawn between  $(FMR, FNMR)_{MALE}$  and  $(FMR, FNMR)_{FEMALE}$  showing how which sex has lower FMR and/or FNMR. The "M" label denotes male, the other end of the line corresponds to female. The six operating thresholds are selected to give the nominal false match rates given in the legend, and are computed over all impostor pairs regardless of age, sex, and place of birth. The plotted FMR values are broadly an order of magnitude larger than the nominal rates because FMR is computed over demographically-matched impostor pairs i.e individuals of the same sex, from the same geographic region (see section 3.6.1), and the same age group (see section 3.6.2).

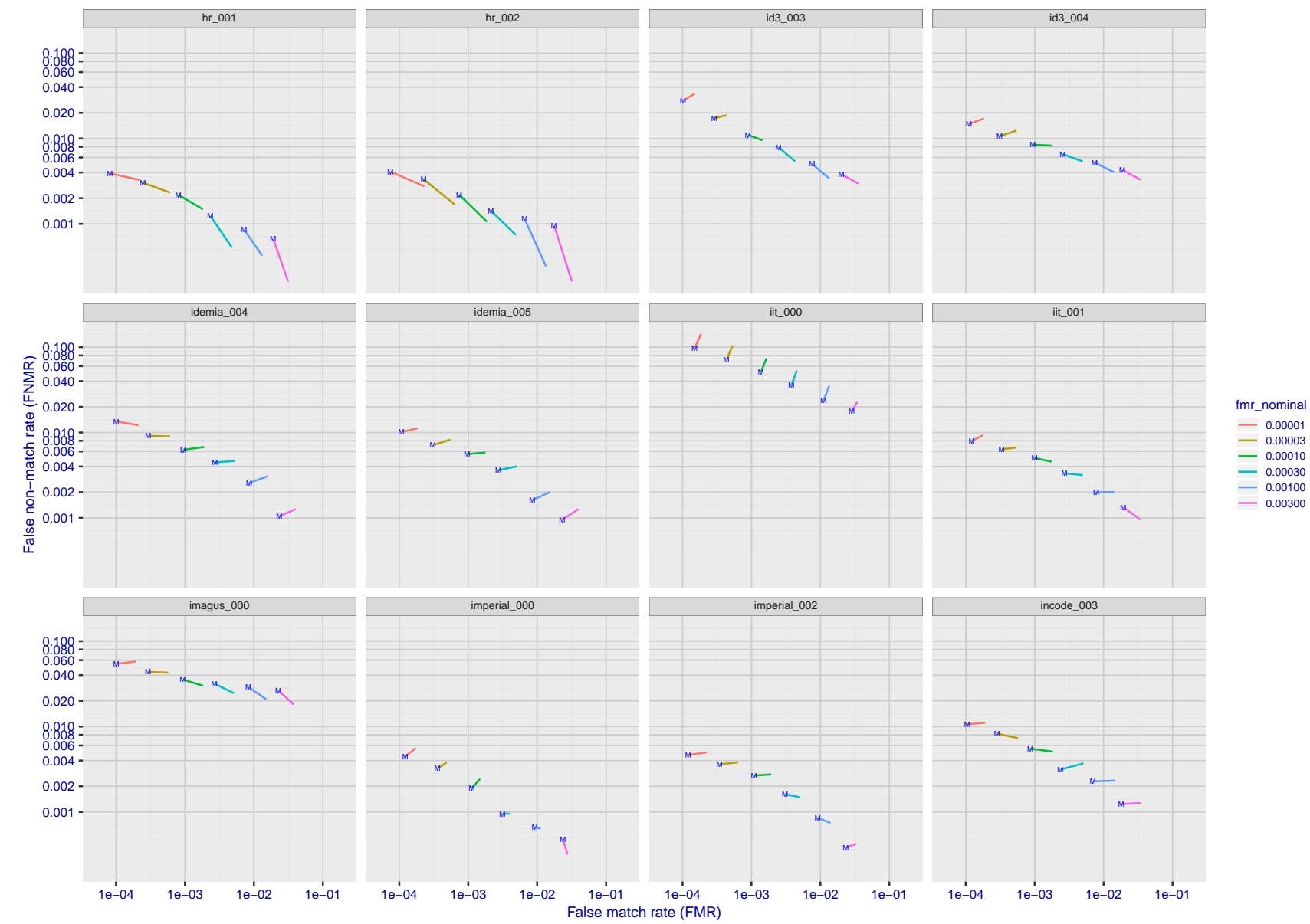


Figure 70: For the visa images, FNMR and FMR at six operating points along the DET characteristic. At each point a line is drawn between  $(FMR, FNMR)_{MALE}$  and  $(FMR, FNMR)_{FEMALE}$  showing how which sex has lower FMR and/or FNMR. The "M" label denotes male, the other end of the line corresponds to female. The six operating thresholds are selected to give the nominal false match rates given in the legend, and are computed over all impostor pairs regardless of age, sex, and place of birth. The plotted FMR values are broadly an order of magnitude larger than the nominal rates because FMR is computed over demographically-matched impostor pairs i.e individuals of the same sex, from the same geographic region (see section 3.6.1), and the same age group (see section 3.6.2).

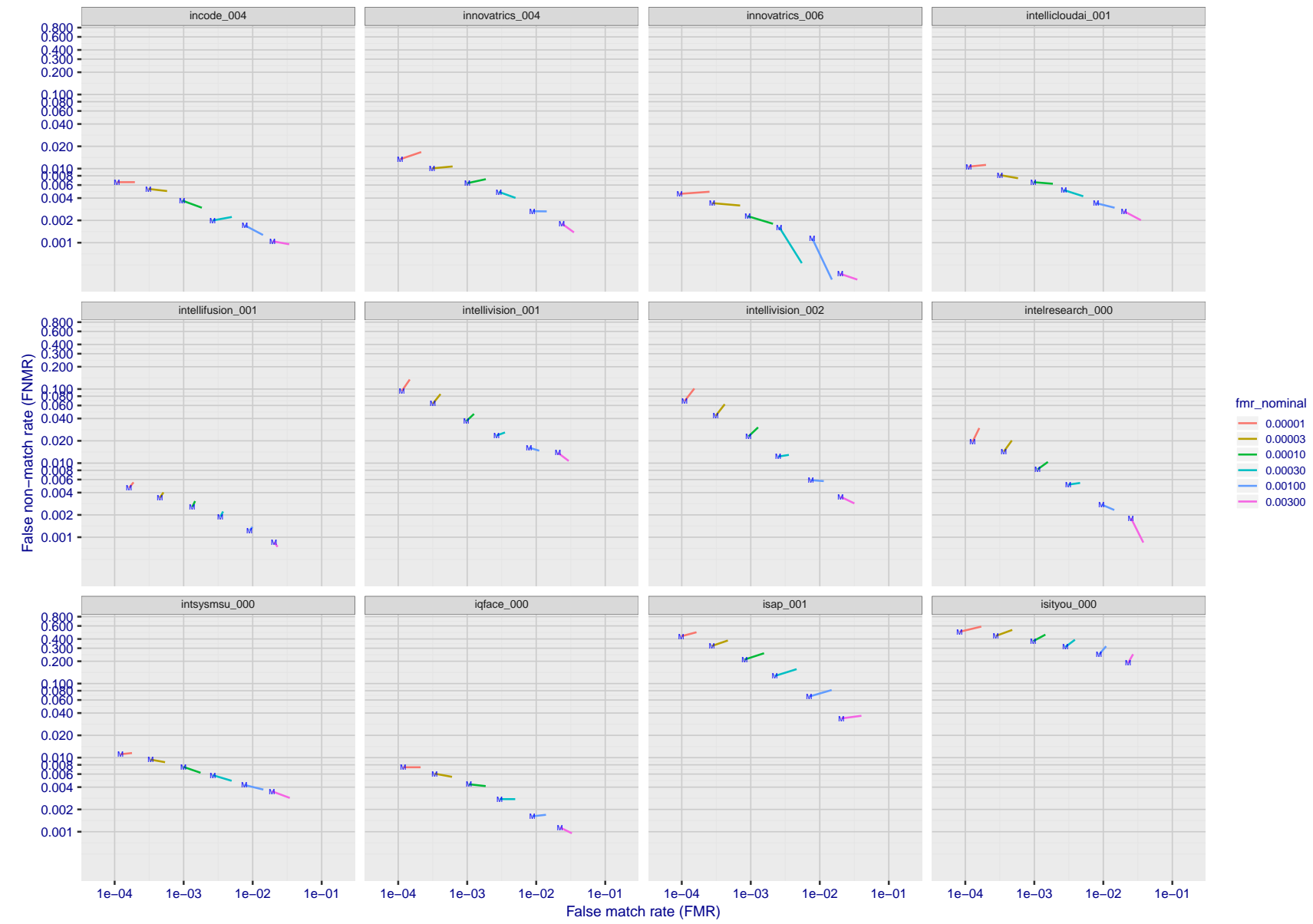


Figure 71: For the visa images, FNMR and FMR at six operating points along the DET characteristic. At each point a line is drawn between  $(FMR, FNMR)_{MALE}$  and  $(FMR, FNMR)_{FEMALE}$  showing how which sex has lower FMR and/or FNMR. The "M" label denotes male, the other end of the line corresponds to female. The six operating thresholds are selected to give the nominal false match rates given in the legend, and are computed over all impostor pairs regardless of age, sex, and place of birth. The plotted FMR values are broadly an order of magnitude larger than the nominal rates because FMR is computed over demographically-matched impostor pairs i.e individuals of the same sex, from the same geographic region (see section 3.6.1), and the same age group (see section 3.6.2).

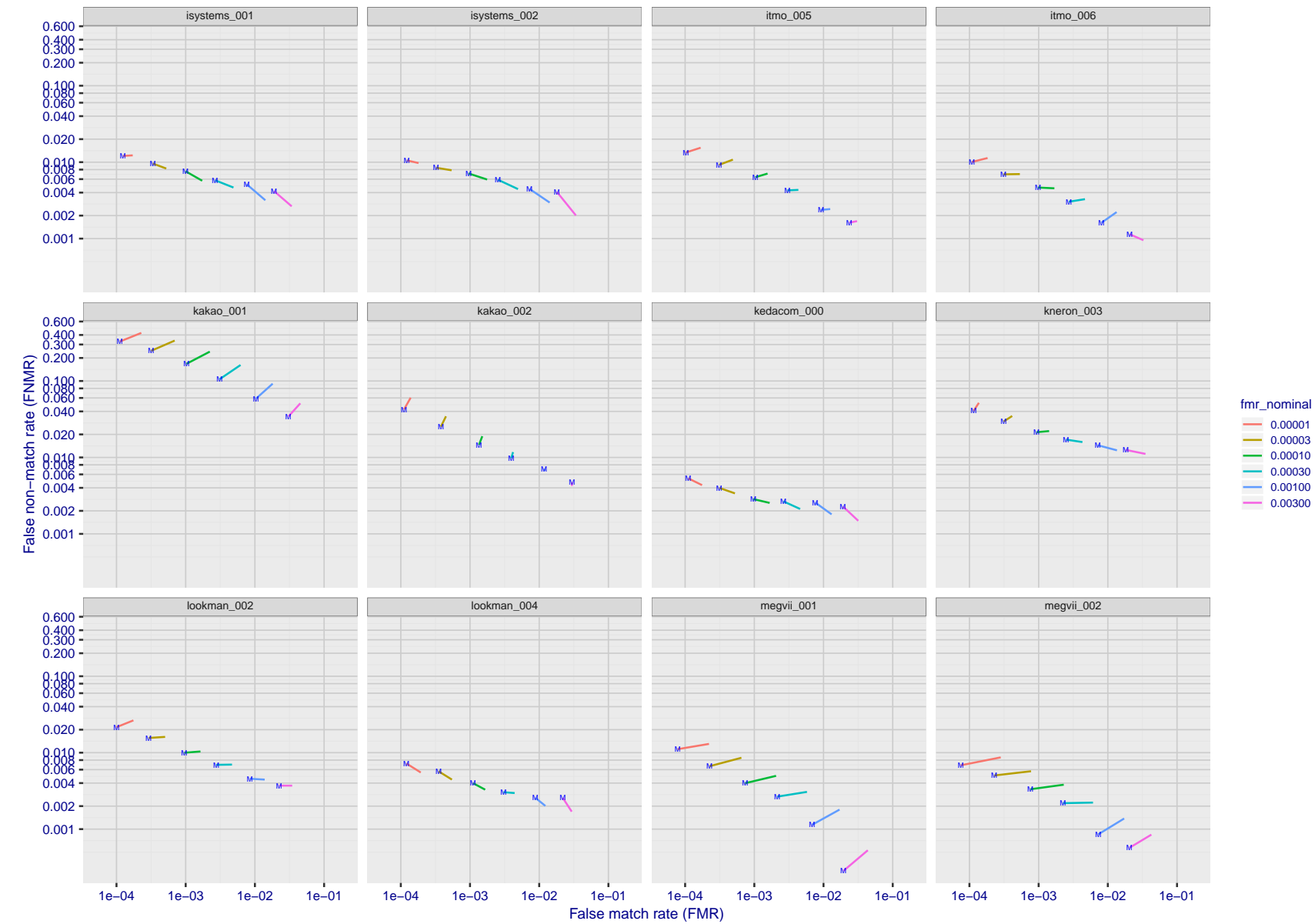


Figure 72: For the visa images, FNMR and FMR at six operating points along the DET characteristic. At each point a line is drawn between  $(FMR, FNMR)_{MALE}$  and  $(FMR, FNMR)_{FEMALE}$  showing how which sex has lower FMR and/or FNMR. The "M" label denotes male, the other end of the line corresponds to female. The six operating thresholds are selected to give the nominal false match rates given in the legend, and are computed over all impostor pairs regardless of age, sex, and place of birth. The plotted FMR values are broadly an order of magnitude larger than the nominal rates because FMR is computed over demographically-matched impostor pairs i.e individuals of the same sex, from the same geographic region (see section 3.6.1), and the same age group (see section 3.6.2).

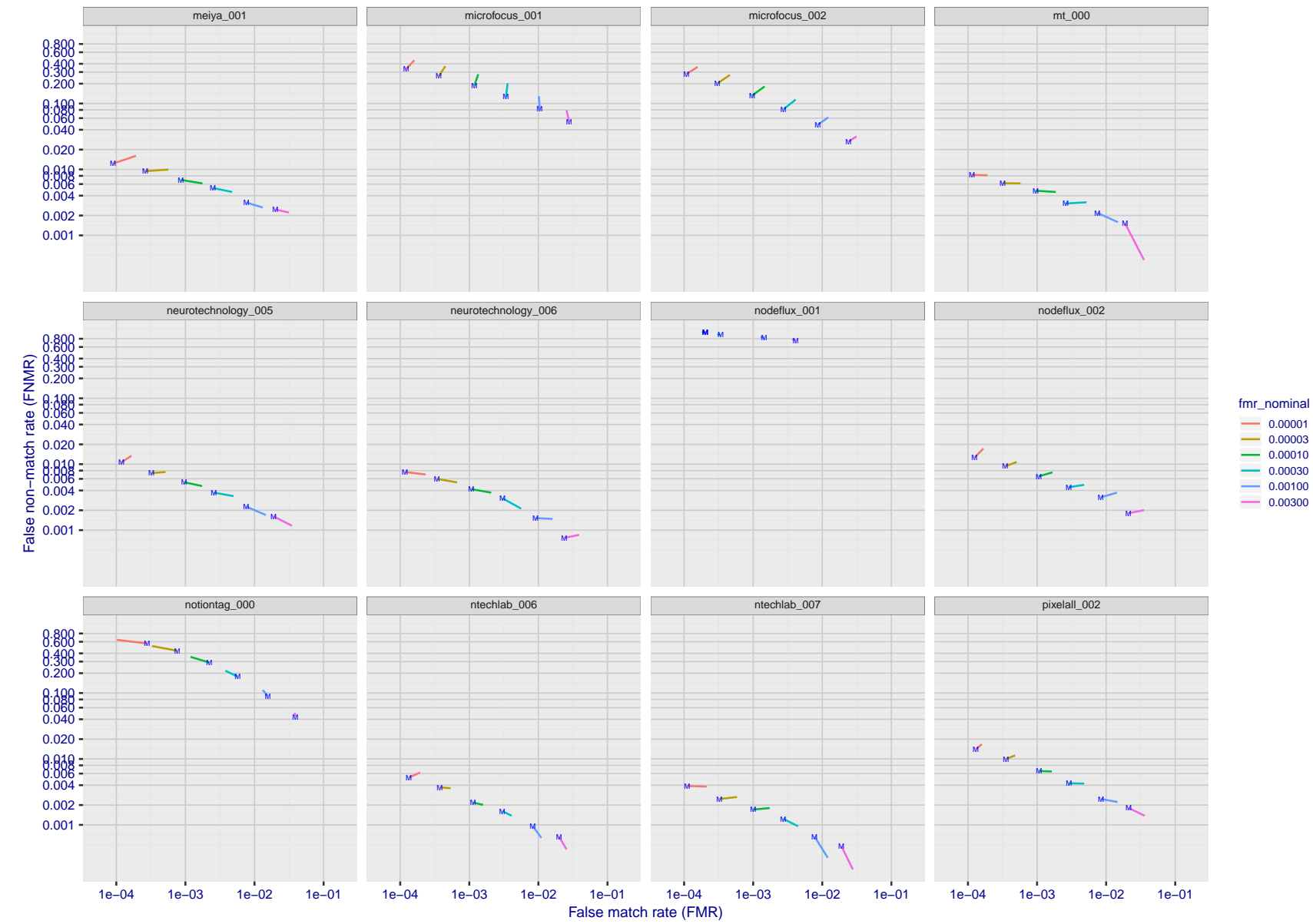


Figure 73: For the visa images, FNMR and FMR at six operating points along the DET characteristic. At each point a line is drawn between  $(FMR, FNMR)_{MALE}$  and  $(FMR, FNMR)_{FEMALE}$  showing how which sex has lower FMR and/or FNMR. The "M" label denotes male, the other end of the line corresponds to female. The six operating thresholds are selected to give the nominal false match rates given in the legend, and are computed over all impostor pairs regardless of age, sex, and place of birth. The plotted FMR values are broadly an order of magnitude larger than the nominal rates because FMR is computed over demographically-matched impostor pairs i.e individuals of the same sex, from the same geographic region (see section 3.6.1), and the same age group (see section 3.6.2).

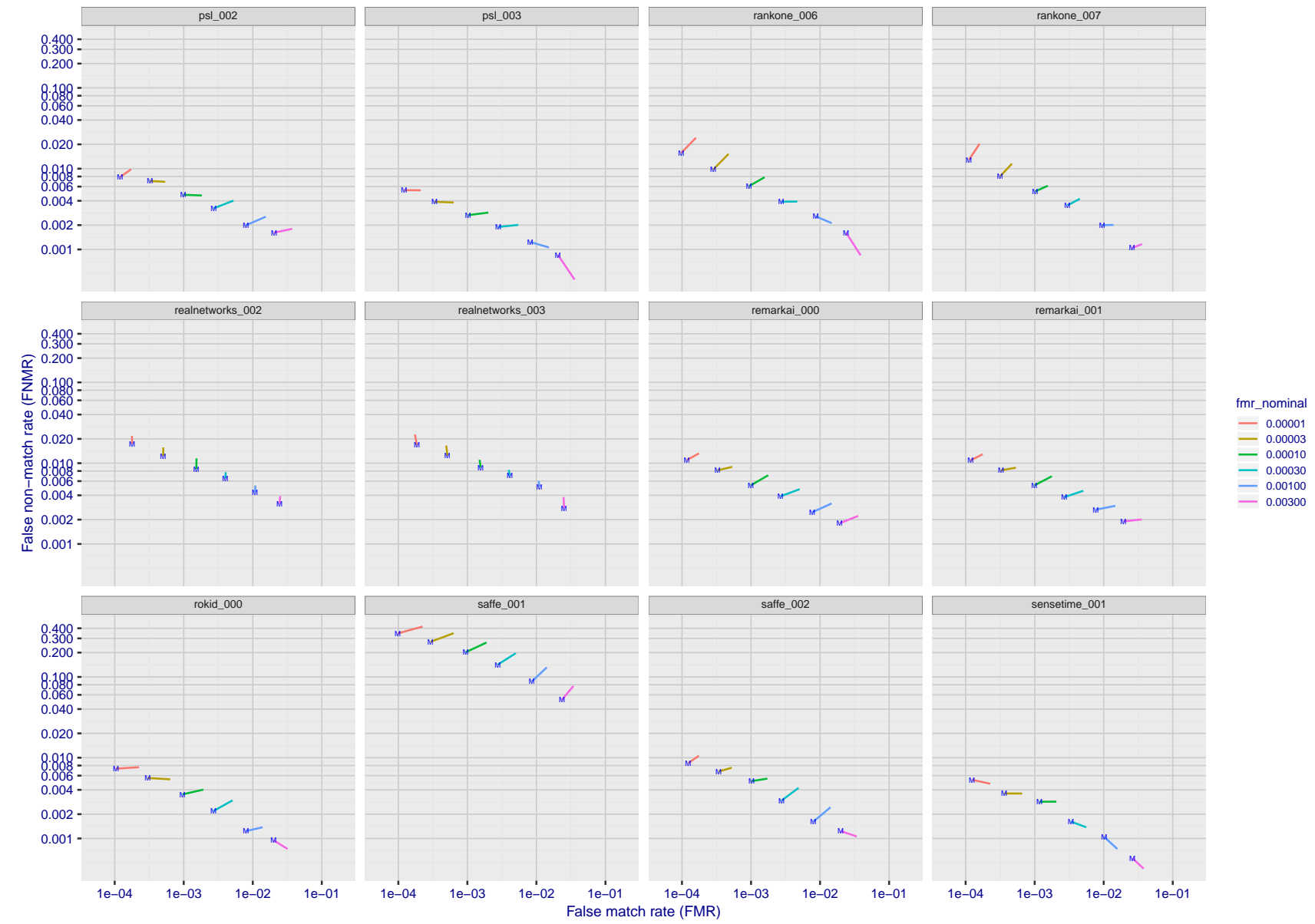


Figure 74: For the visa images, FNMR and FMR at six operating points along the DET characteristic. At each point a line is drawn between  $(FMR, FNMR)_{MALE}$  and  $(FMR, FNMR)_{FEMALE}$  showing how which sex has lower FMR and/or FNMR. The "M" label denotes male, the other end of the line corresponds to female. The six operating thresholds are selected to give the nominal false match rates given in the legend, and are computed over all impostor pairs regardless of age, sex, and place of birth. The plotted FMR values are broadly an order of magnitude larger than the nominal rates because FMR is computed over demographically-matched impostor pairs i.e individuals of the same sex, from the same geographic region (see section 3.6.1), and the same age group (see section 3.6.2).

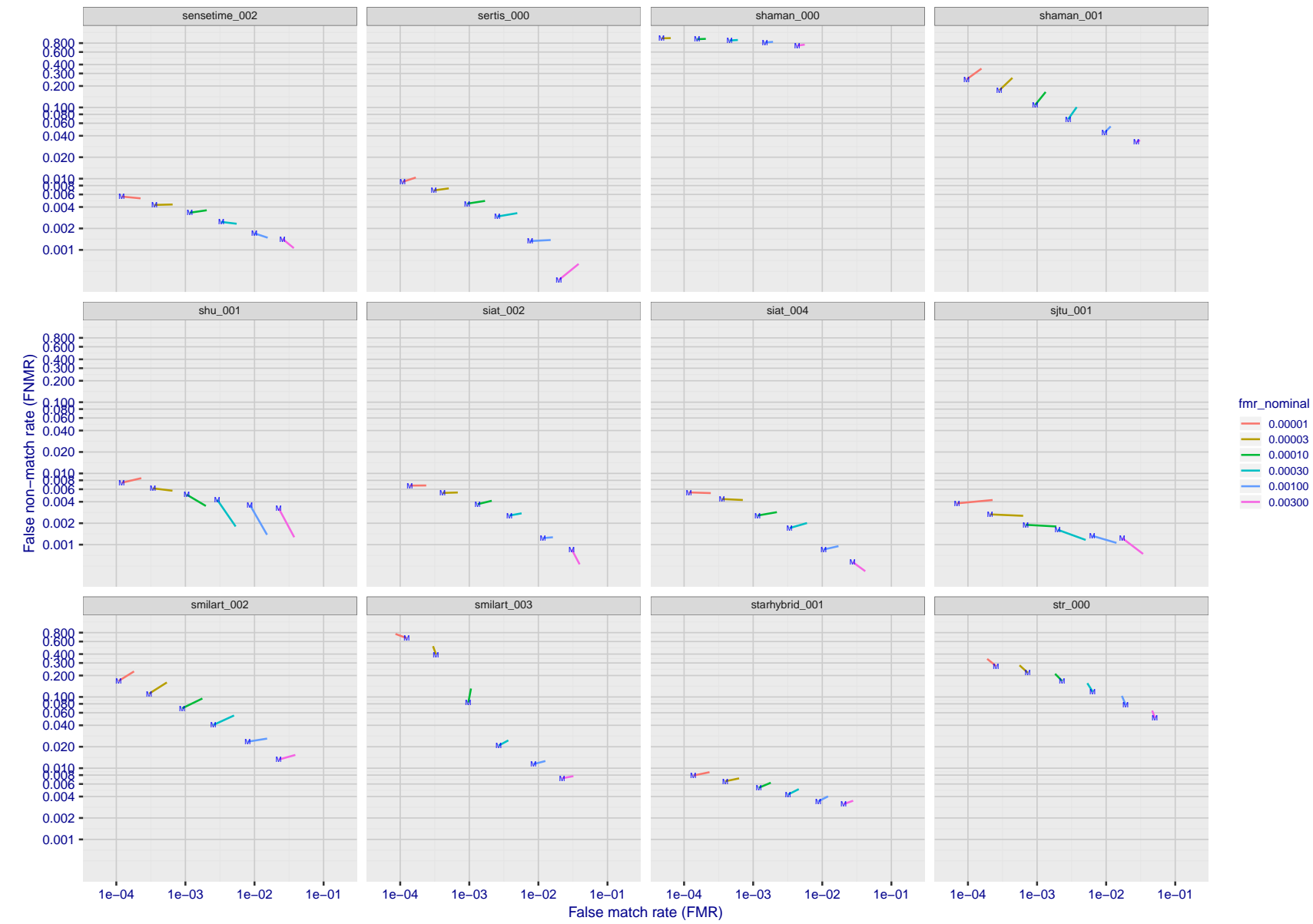


Figure 75: For the visa images, FNMR and FMR at six operating points along the DET characteristic. At each point a line is drawn between  $(FMR, FNMR)_{MALE}$  and  $(FMR, FNMR)_{FEMALE}$  showing how which sex has lower FMR and/or FNMR. The "M" label denotes male, the other end of the line corresponds to female. The six operating thresholds are selected to give the nominal false match rates given in the legend, and are computed over all impostor pairs regardless of age, sex, and place of birth. The plotted FMR values are broadly an order of magnitude larger than the nominal rates because FMR is computed over demographically-matched impostor pairs i.e individuals of the same sex, from the same geographic region (see section 3.6.1), and the same age group (see section 3.6.2).

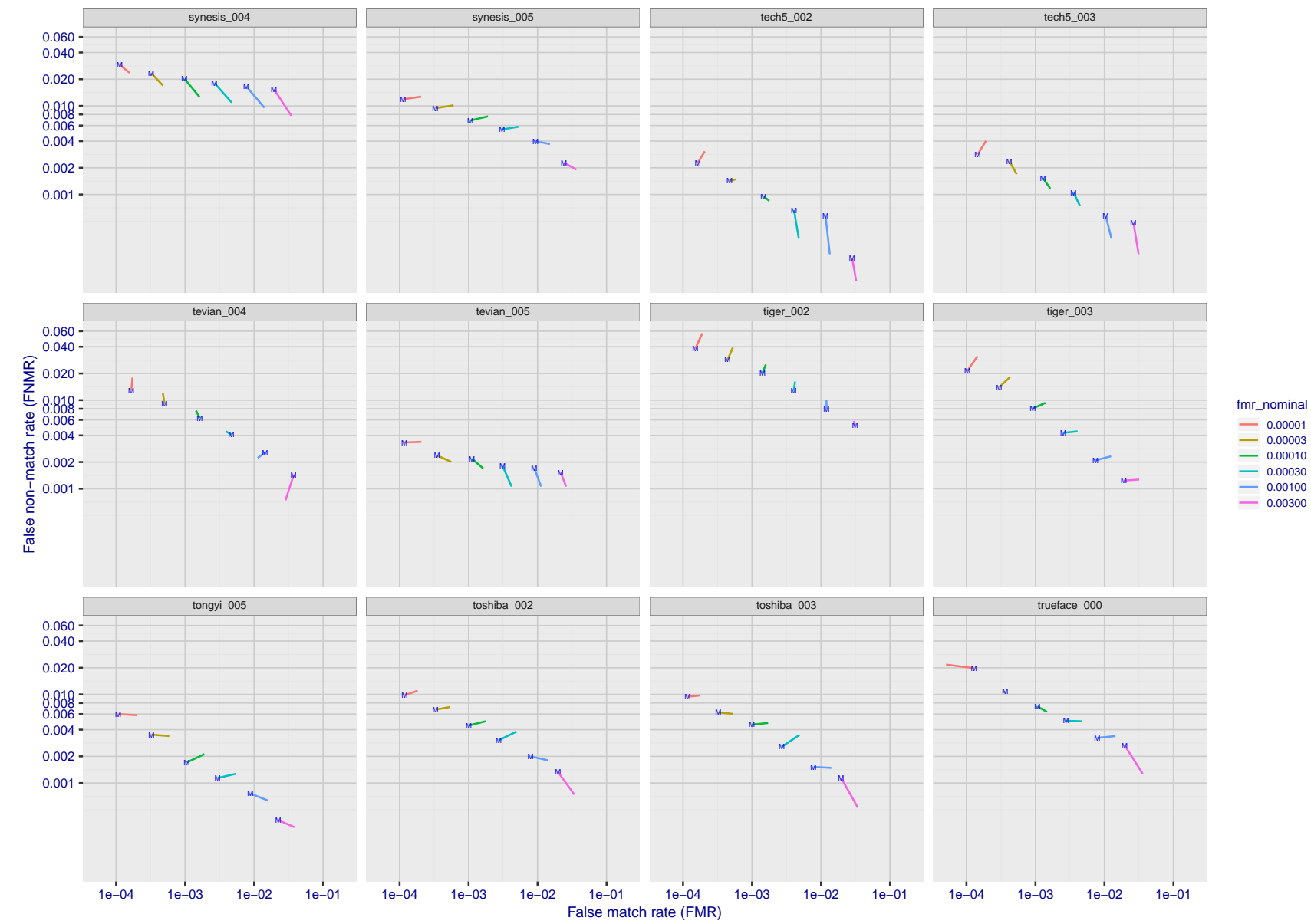


Figure 76: For the visa images, FNMR and FMR at six operating points along the DET characteristic. At each point a line is drawn between  $(FMR, FNMR)_{MALE}$  and  $(FMR, FNMR)_{FEMALE}$  showing how which sex has lower FMR and/or FNMR. The "M" label denotes male, the other end of the line corresponds to female. The six operating thresholds are selected to give the nominal false match rates given in the legend, and are computed over all impostor pairs regardless of age, sex, and place of birth. The plotted FMR values are broadly an order of magnitude larger than the nominal rates because FMR is computed over demographically-matched impostor pairs i.e individuals of the same sex, from the same geographic region (see section 3.6.1), and the same age group (see section 3.6.2).

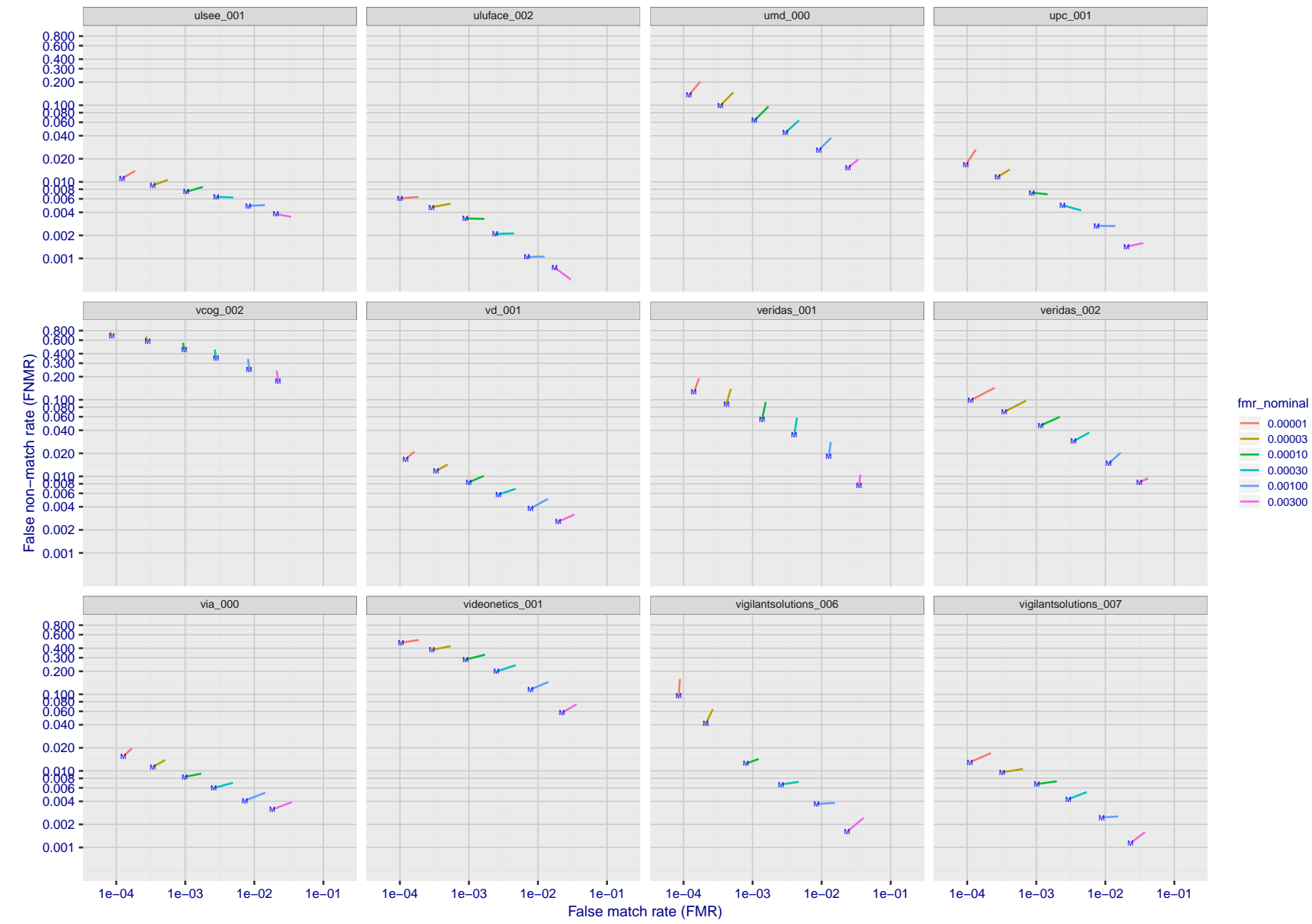


Figure 77: For the visa images, FNMR and FMR at six operating points along the DET characteristic. At each point a line is drawn between  $(FMR, FNMR)_{MALE}$  and  $(FMR, FNMR)_{FEMALE}$  showing how which sex has lower FMR and/or FNMR. The "M" label denotes male, the other end of the line corresponds to female. The six operating thresholds are selected to give the nominal false match rates given in the legend, and are computed over all impostor pairs regardless of age, sex, and place of birth. The plotted FMR values are broadly an order of magnitude larger than the nominal rates because FMR is computed over demographically-matched impostor pairs i.e individuals of the same sex, from the same geographic region (see section 3.6.1), and the same age group (see section 3.6.2).

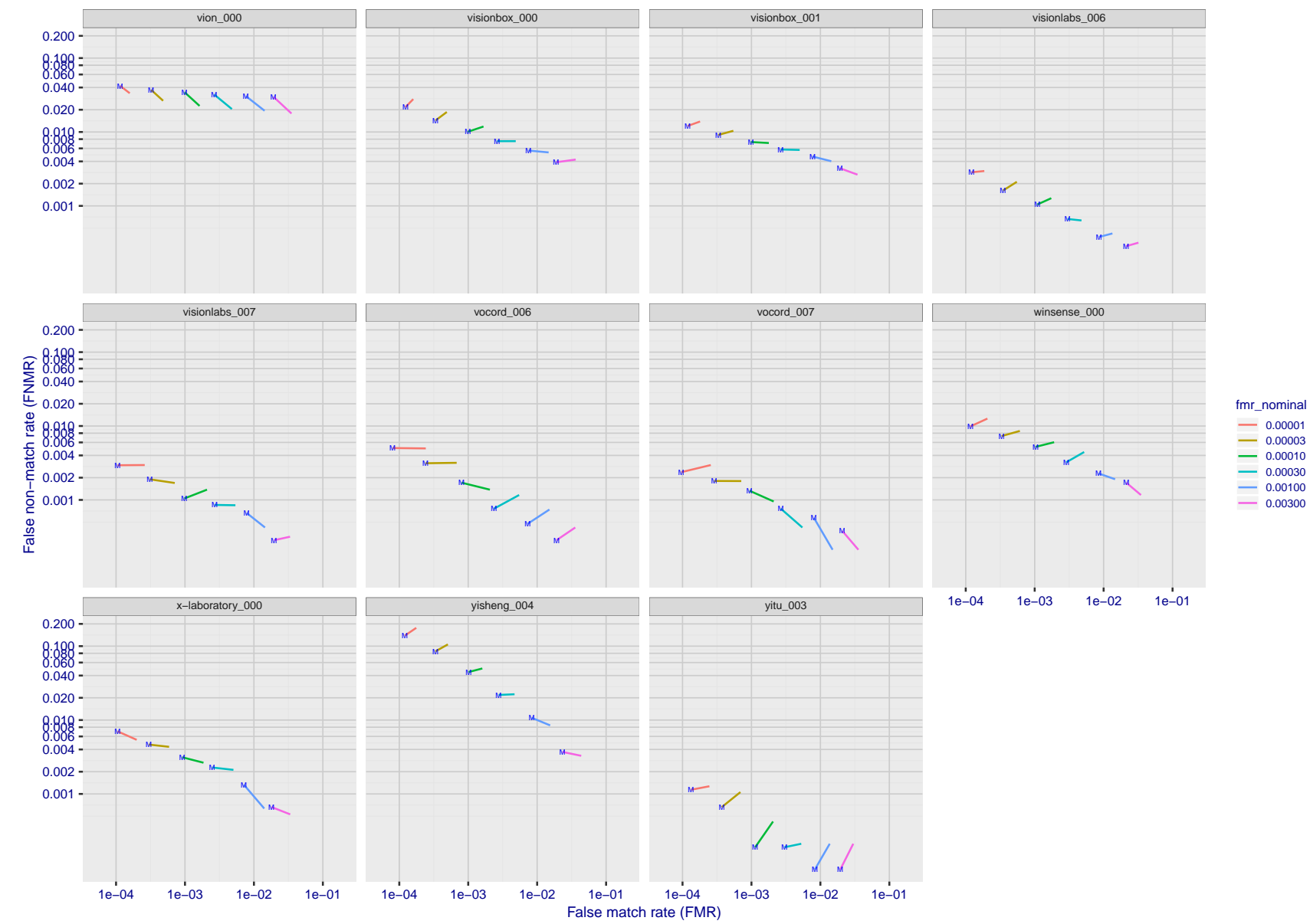


Figure 78: For the visa images, FNMR and FMR at six operating points along the DET characteristic. At each point a line is drawn between  $(FMR, FNMR)_{MALE}$  and  $(FMR, FNMR)_{FEMALE}$  showing how which sex has lower FMR and/or FNMR. The "M" label denotes male, the other end of the line corresponds to female. The six operating thresholds are selected to give the nominal false match rates given in the legend, and are computed over all impostor pairs regardless of age, sex, and place of birth. The plotted FMR values are broadly an order of magnitude larger than the nominal rates because FMR is computed over demographically-matched impostor pairs i.e individuals of the same sex, from the same geographic region (see section 3.6.1), and the same age group (see section 3.6.2).

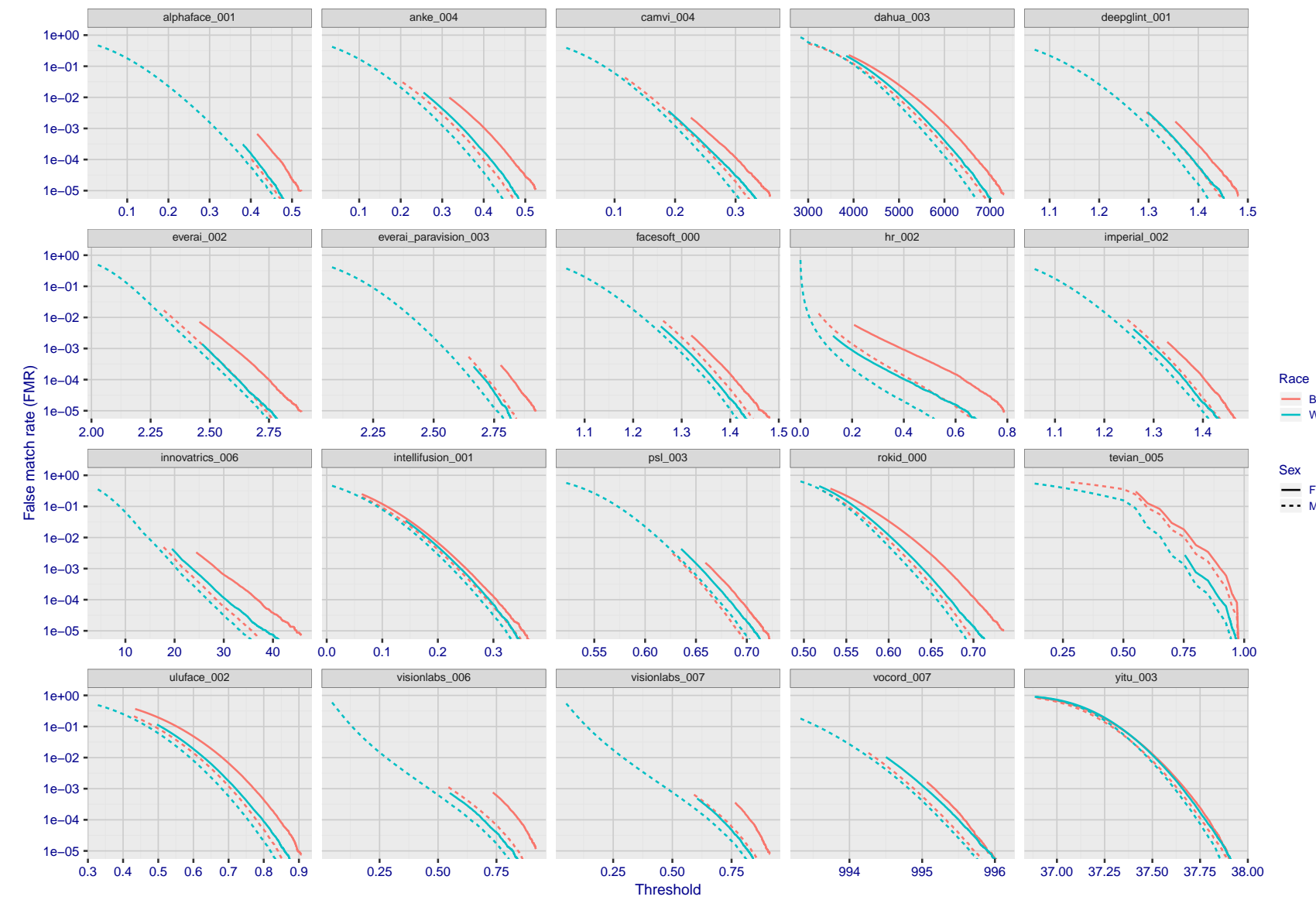


Figure 79: For the mugshot images, the false match calibration curves show false match rate vs. threshold. Separate curves appear for white females, black females, black males and white males.

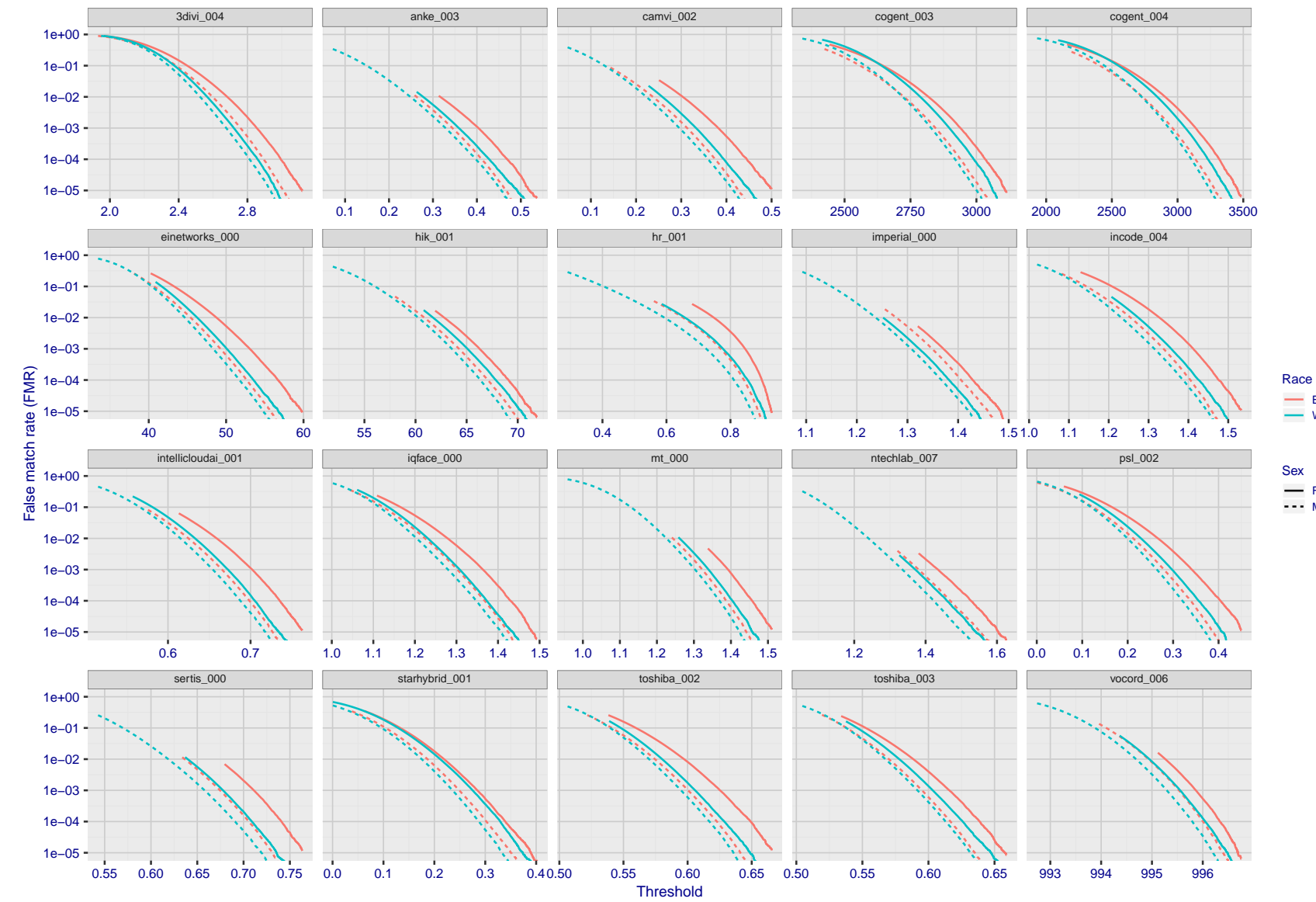


Figure 80: For the mugshot images, the false match calibration curves show false match rate vs. threshold. Separate curves appear for white females, black females, black males and white males.

2019/10/16 12:43:37

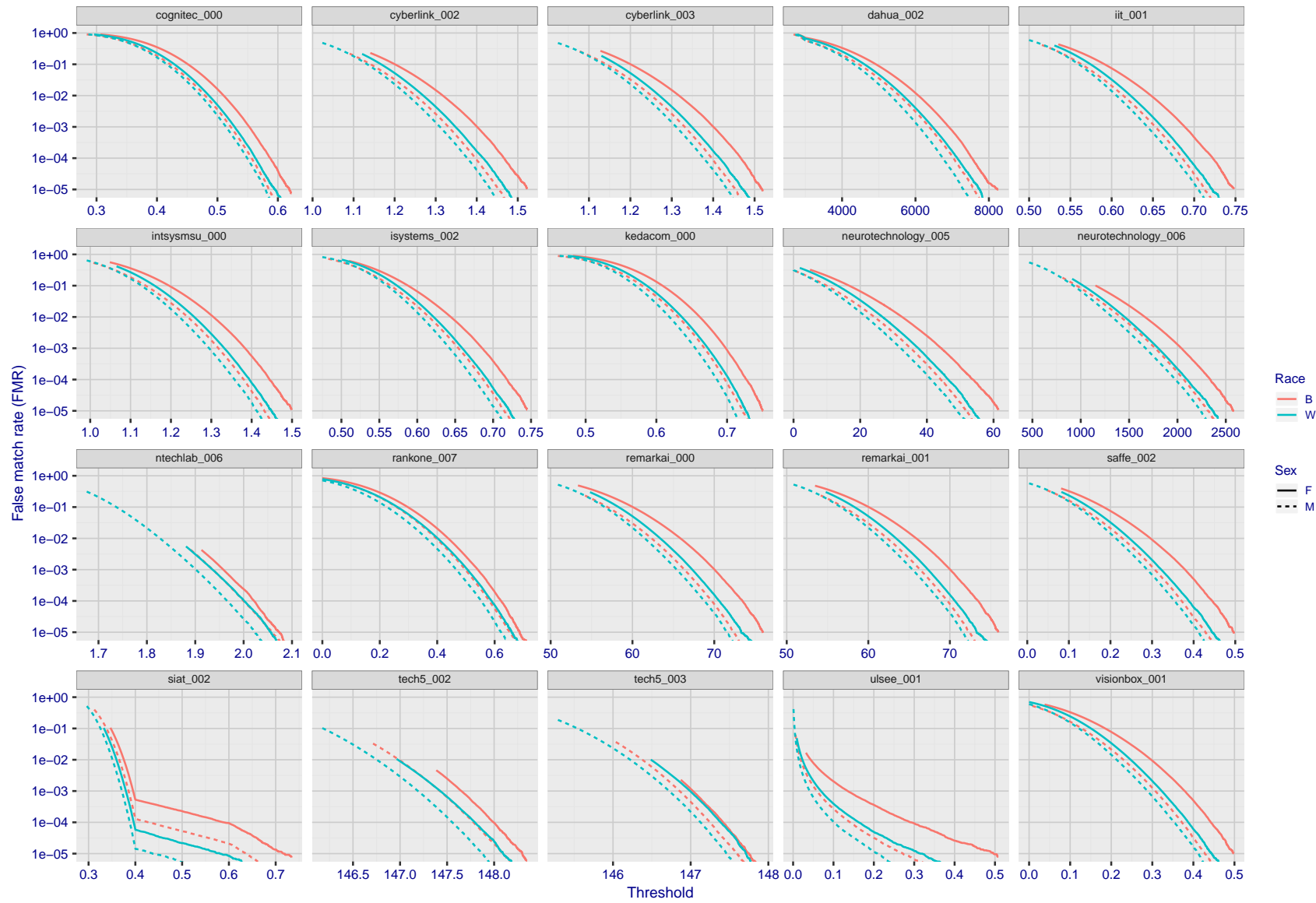


Figure 81: For the mugshot images, the false match calibration curves show false match rate vs. threshold. Separate curves appear for white females, black females, black males and white males.

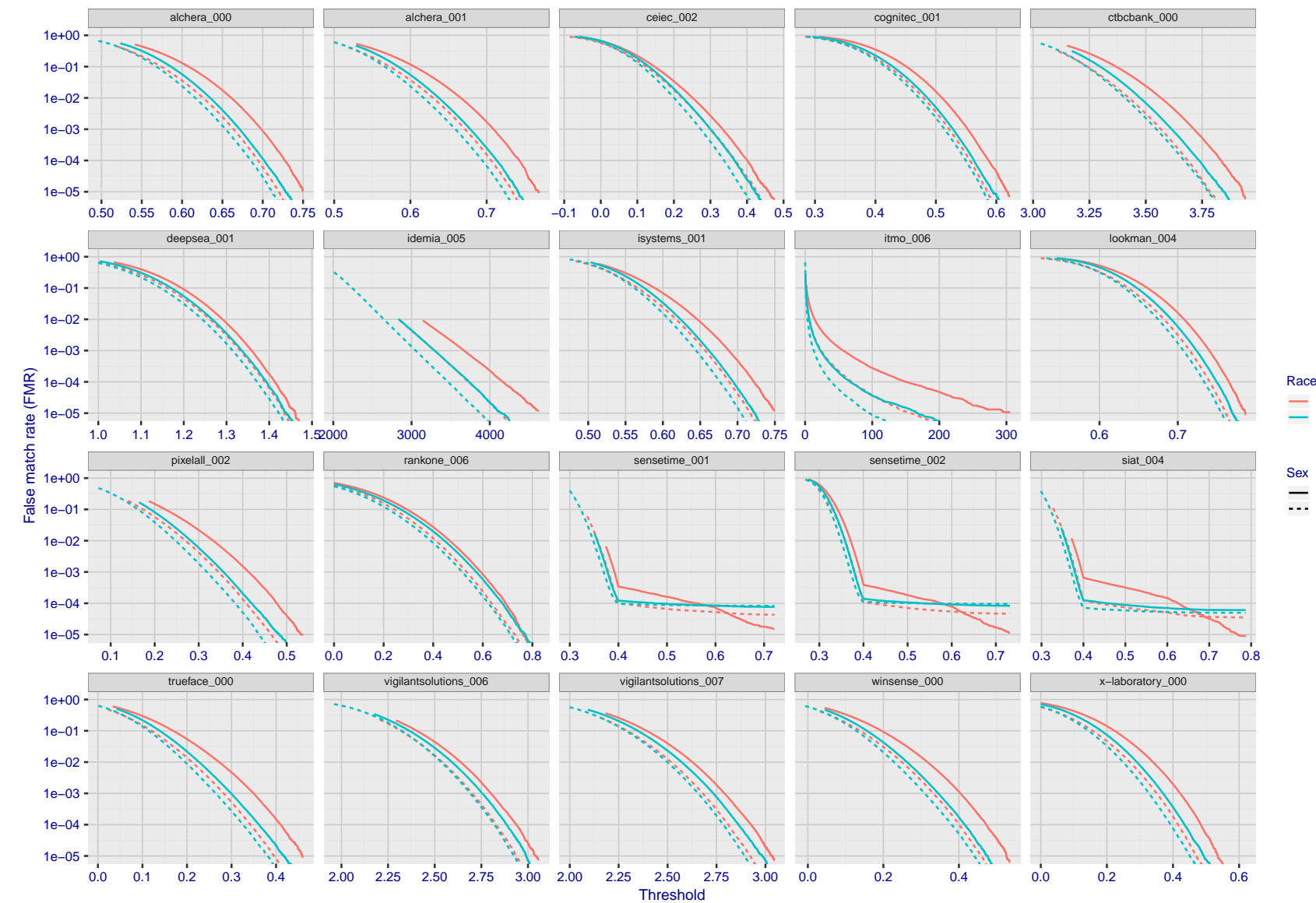


Figure 82: For the mugshot images, the false match calibration curves show false match rate vs. threshold. Separate curves appear for white females, black females, black males and white males.

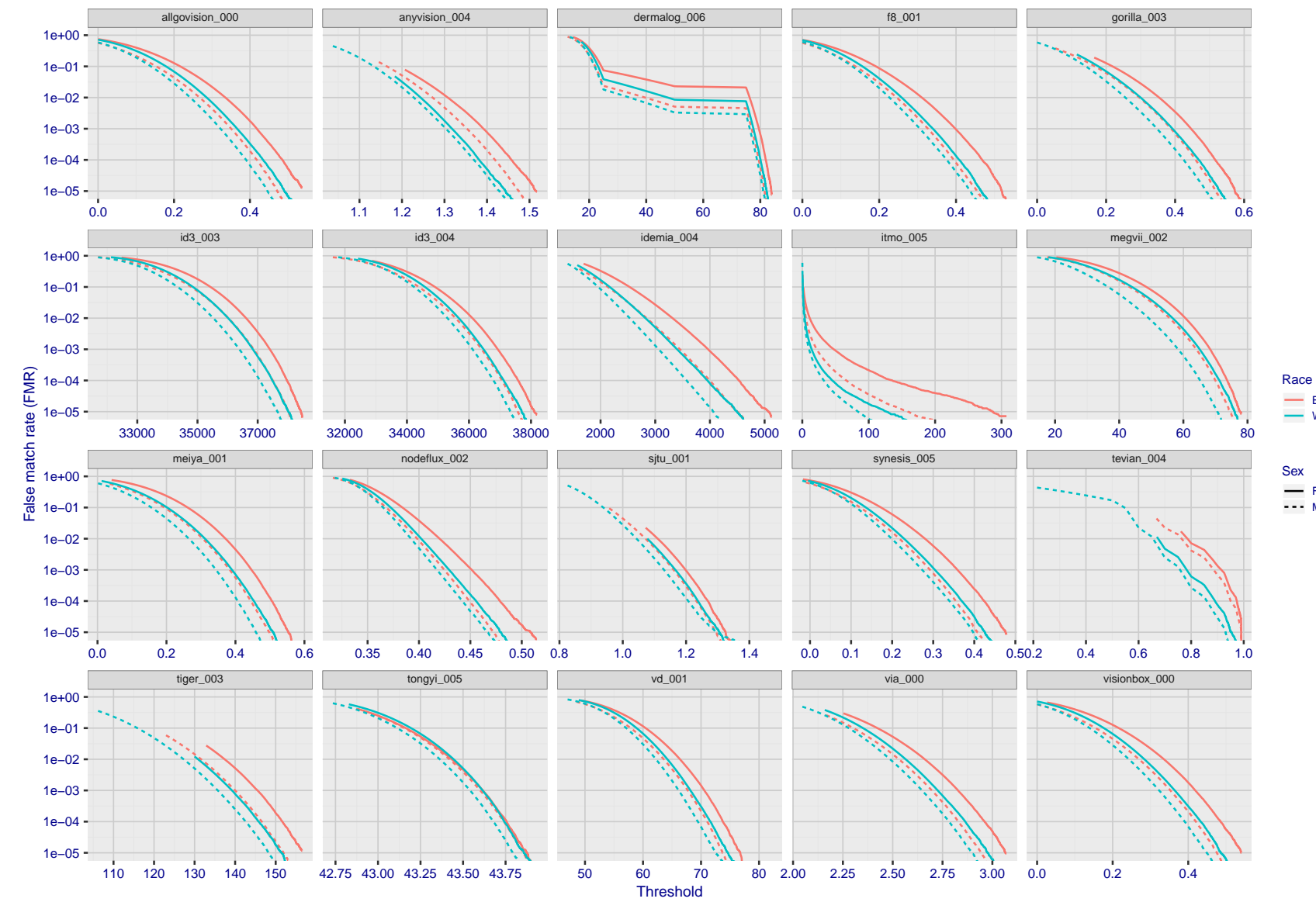


Figure 83: For the mugshot images, the false match calibration curves show false match rate vs. threshold. Separate curves appear for white females, black females, black males and white males.

2019/10/16 12:43:37

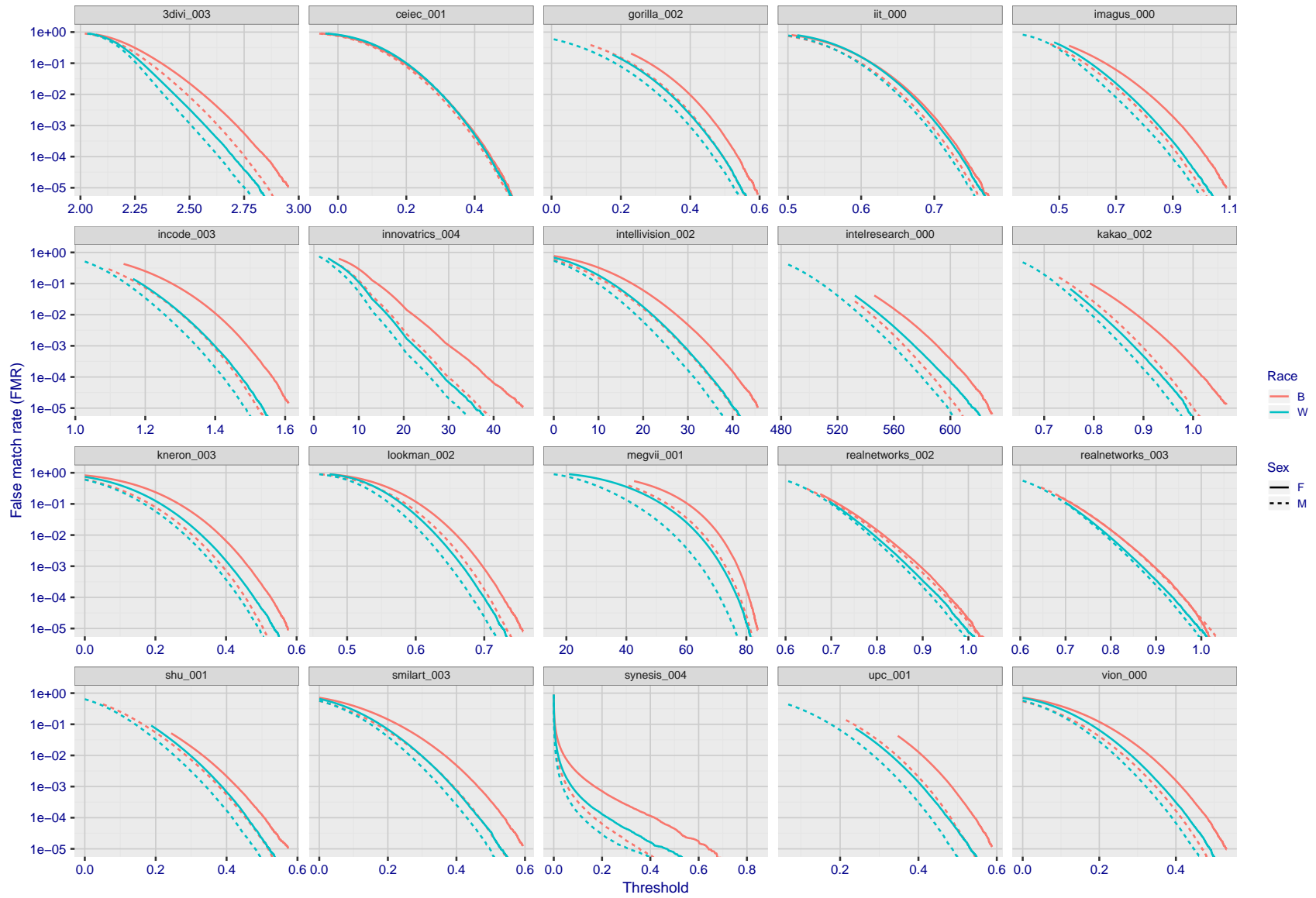


Figure 84: For the mugshot images, the false match calibration curves show false match rate vs. threshold. Separate curves appear for white females, black females, black males and white males.

FNMR(T)

"False non-match rate"

"False match rate"

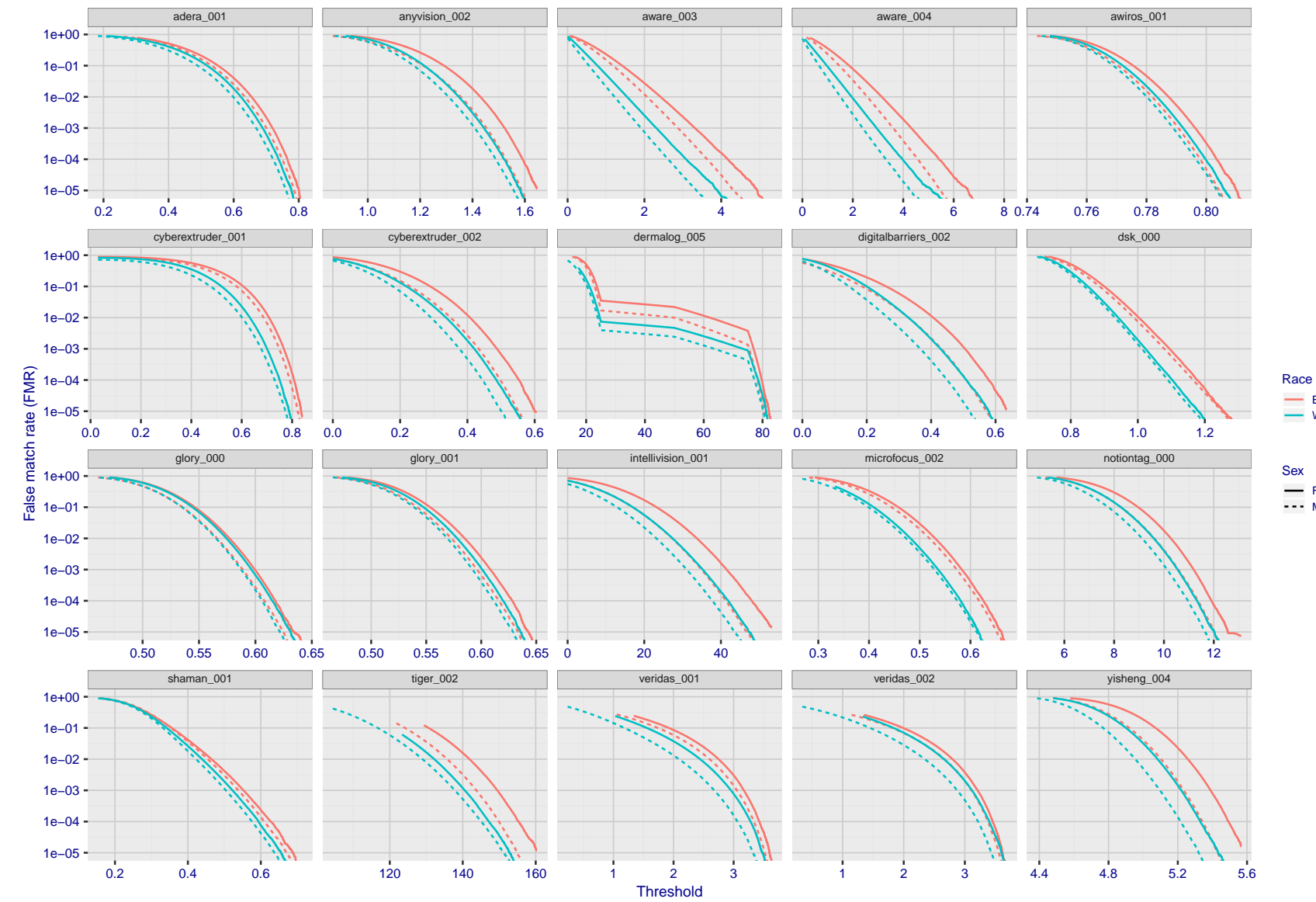


Figure 85: For the mugshot images, the false match calibration curves show false match rate vs. threshold. Separate curves appear for white females, black females, black males and white males.

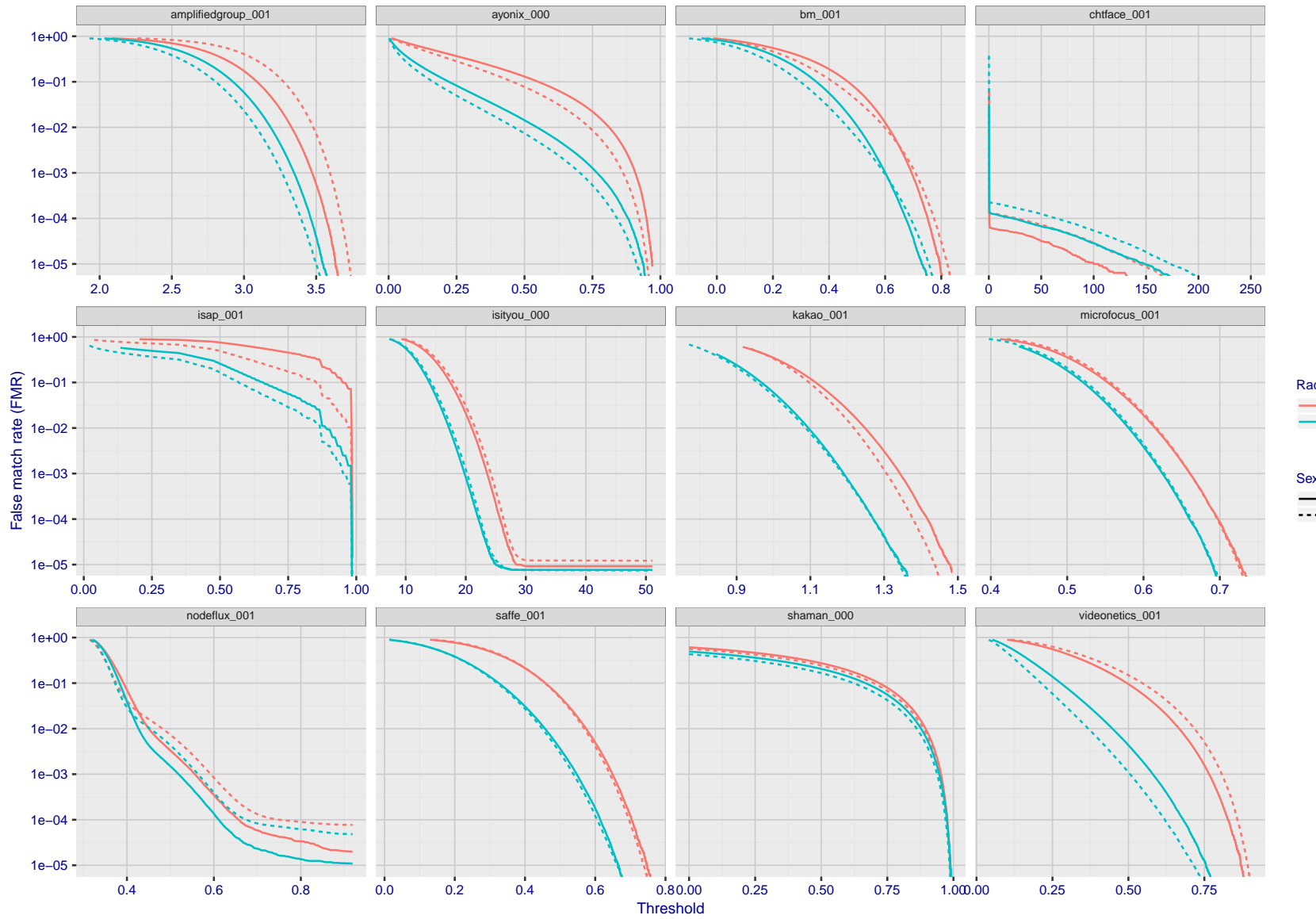


Figure 86: For the mugshot images, the false match calibration curves show false match rate vs. threshold. Separate curves appear for white females, black females, black males and white males.

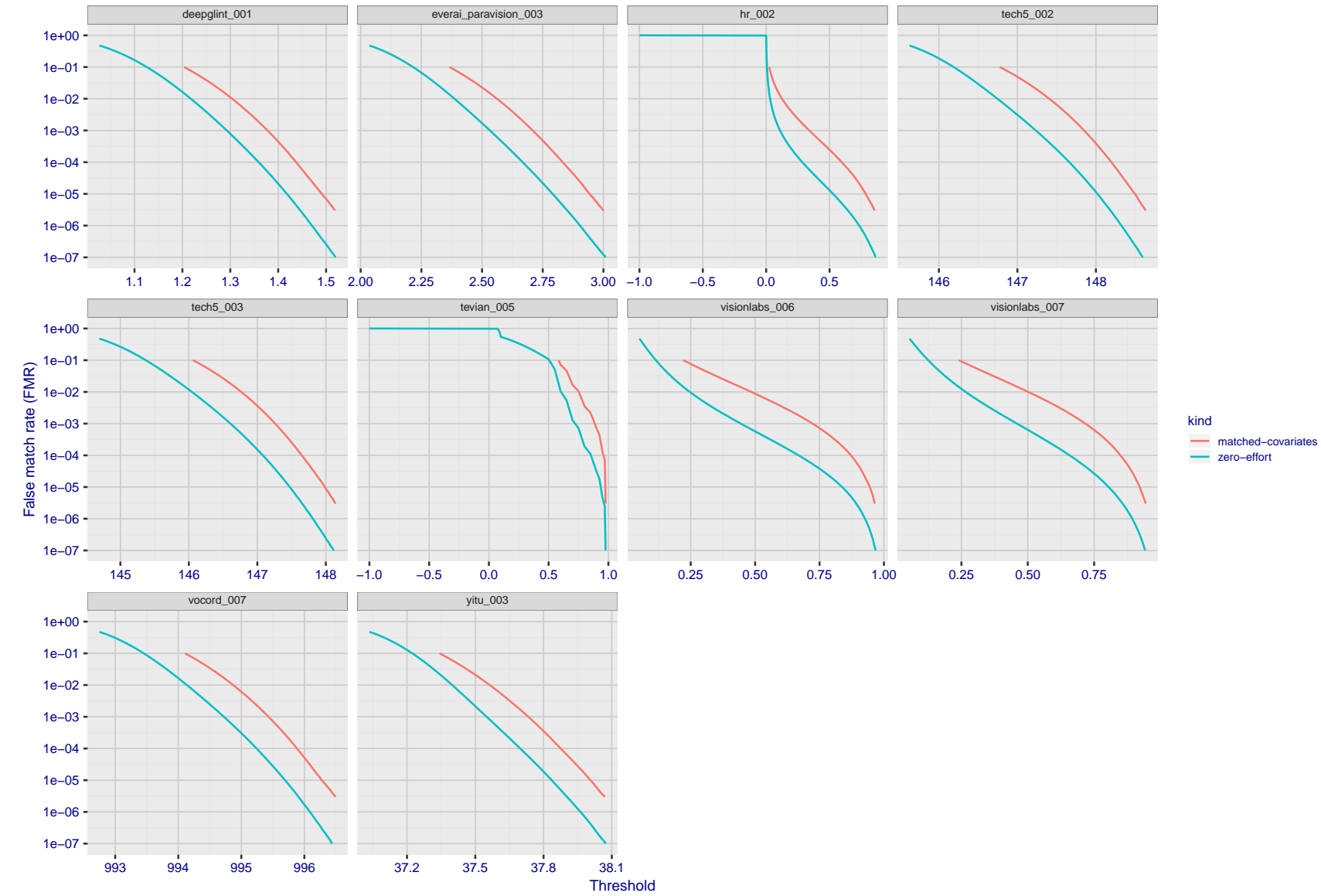


Figure 87: For the visa images, the false match calibration curves show FMR vs. threshold,  $T$ . The blue (lower) curves are for zero-effort impostors (i.e. comparing all images against all). The red (upper) curves are for persons of the same-sex, same-age, and same national-origin. This shows that FMR is underestimated (by a factor of 10 or more) by using a zero-effort impostor calculation to calibrate  $T$ . As shown later (sec. 3.6), FMR is higher for demographic-matched impostors.

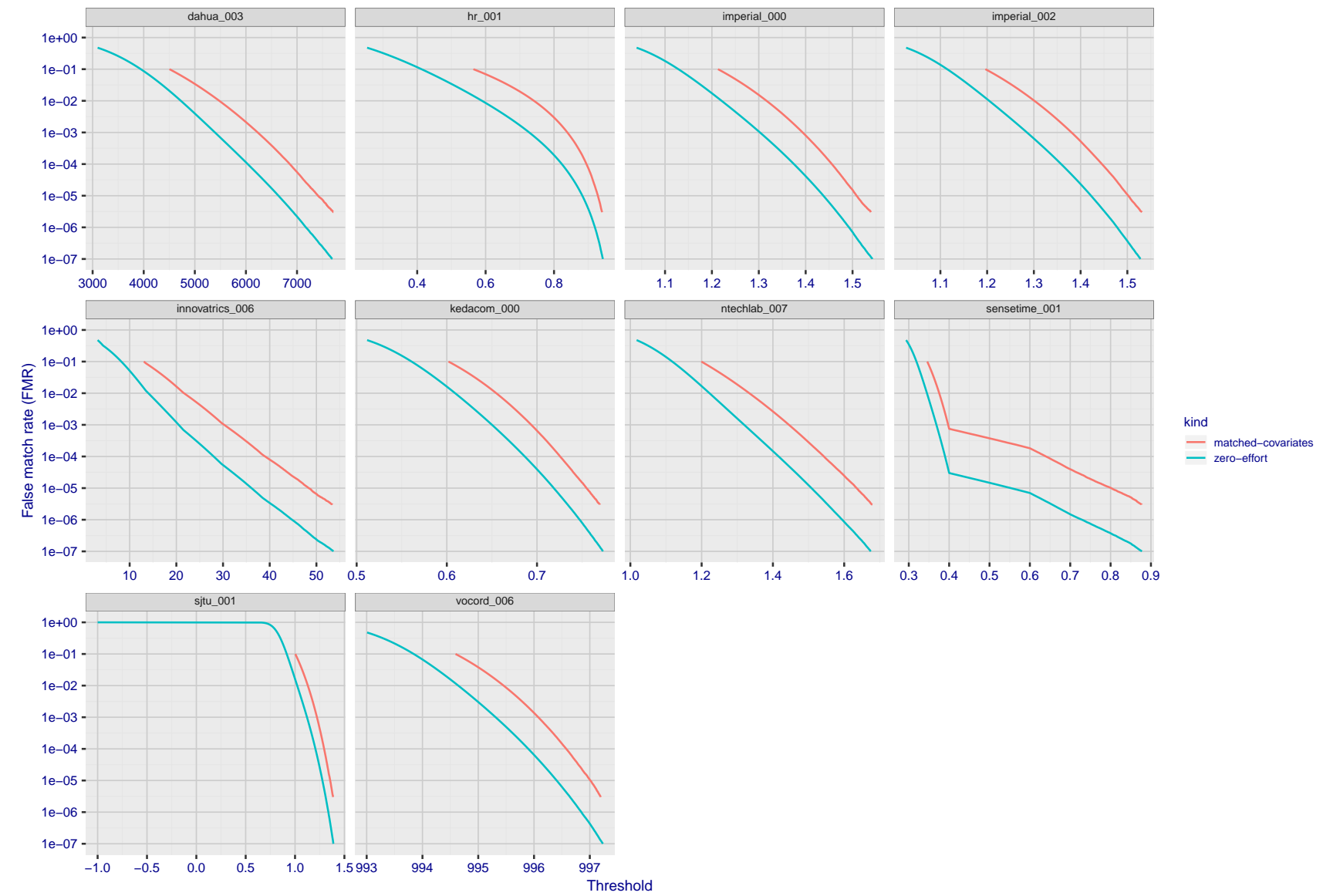


Figure 88: For the visa images, the false match calibration curves show FMR vs. threshold,  $T$ . The blue (lower) curves are for zero-effort impostors (i.e. comparing all images against all). The red (upper) curves are for persons of the same-sex, same-age, and same national-origin. This shows that FMR is underestimated (by a factor of 10 or more) by using a zero-effort impostor calculation to calibrate  $T$ . As shown later (sec. 3.6), FMR is higher for demographic-matched impostors.

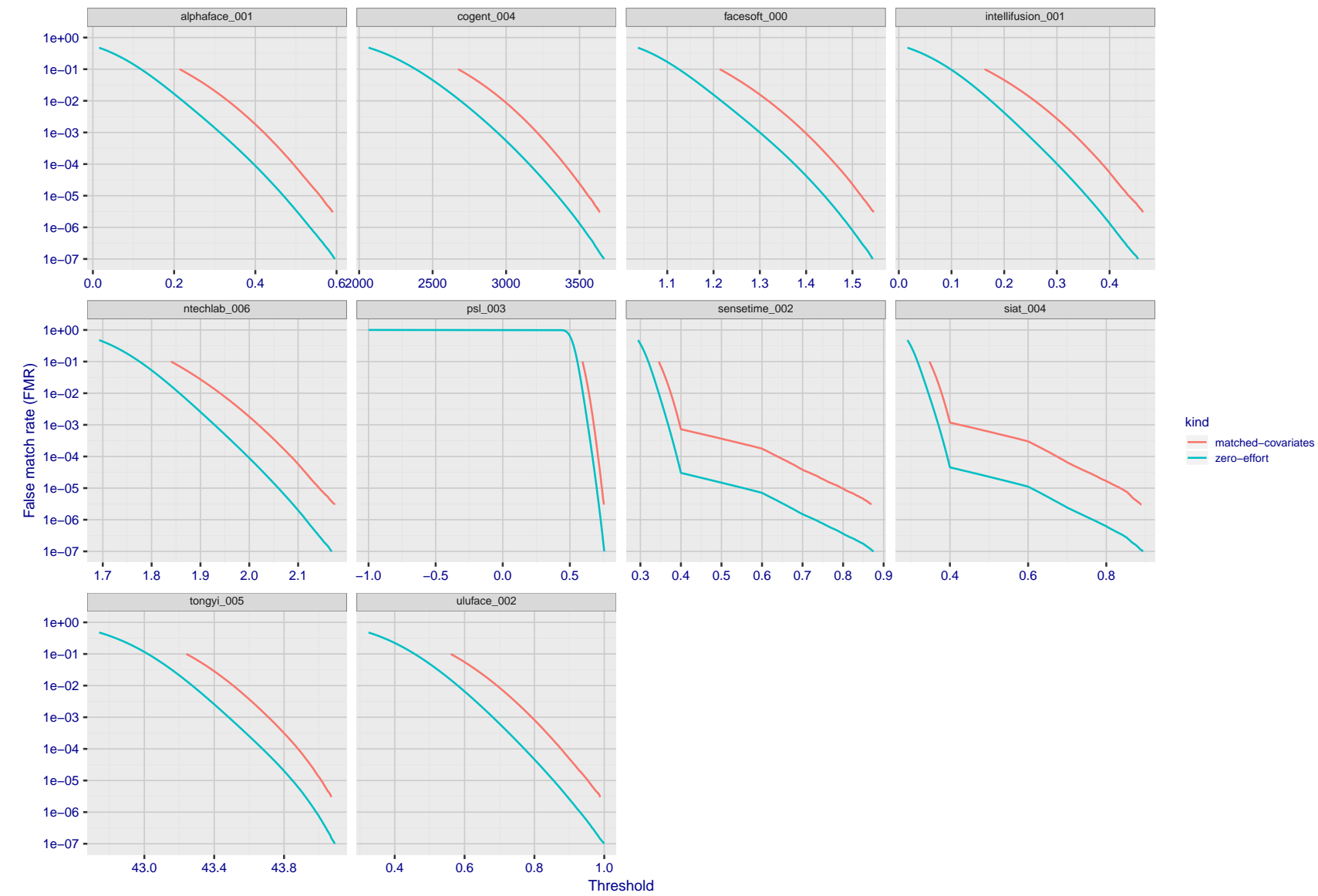


Figure 89: For the visa images, the false match calibration curves show FMR vs. threshold,  $T$ . The blue (lower) curves are for zero-effort impostors (i.e. comparing all images against all). The red (upper) curves are for persons of the same-sex, same-age, and same national-origin. This shows that FMR is underestimated (by a factor of 10 or more) by using a zero-effort impostor calculation to calibrate  $T$ . As shown later (sec. 3.6), FMR is higher for demographic-matched impostors.

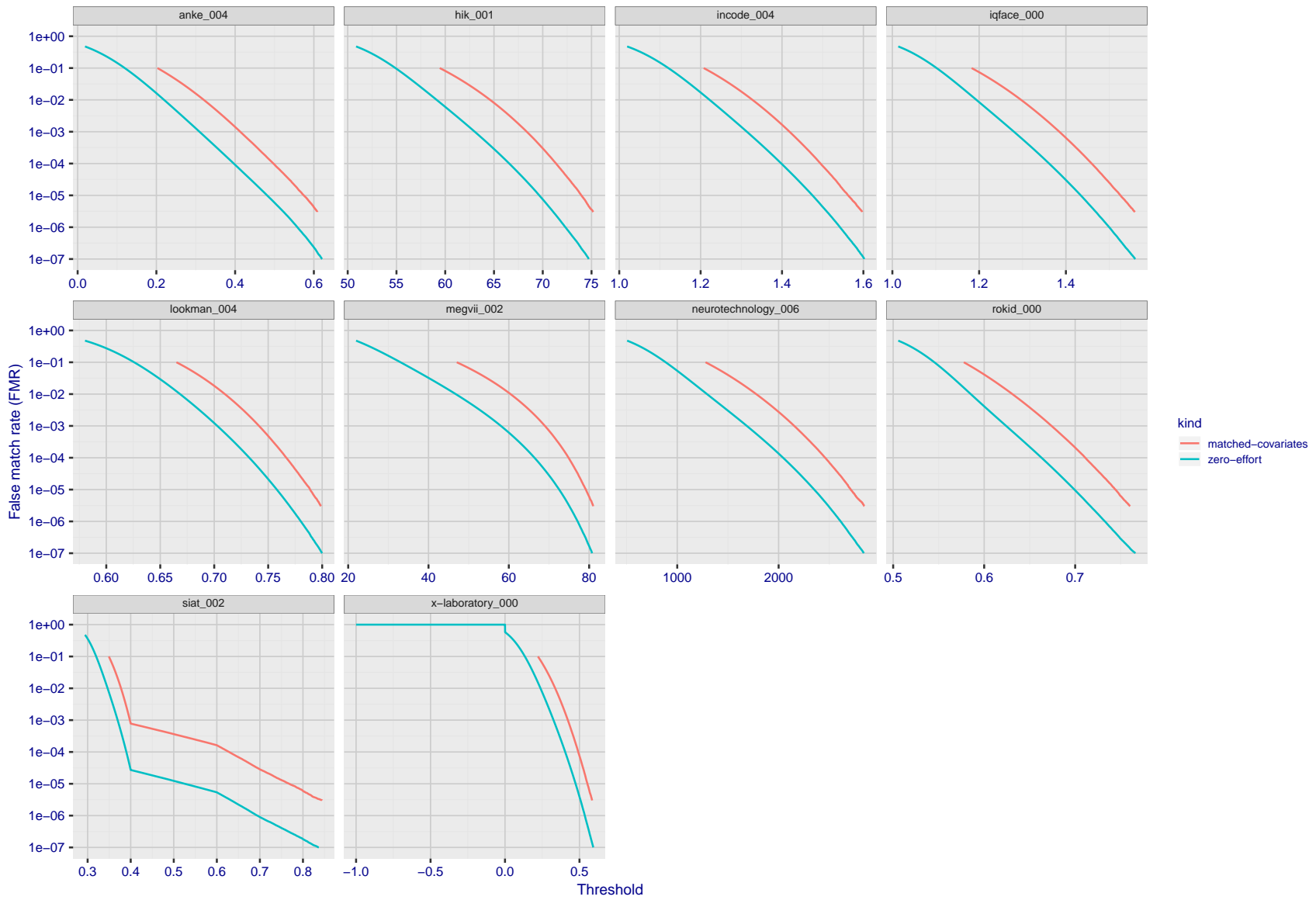


Figure 90: For the visa images, the false match calibration curves show FMR vs. threshold,  $T$ . The blue (lower) curves are for zero-effort impostors (i.e. comparing all images against all). The red (upper) curves are for persons of the same-sex, same-age, and same national-origin. This shows that FMR is underestimated (by a factor of 10 or more) by using a zero-effort impostor calculation to calibrate  $T$ . As shown later (sec. 3.6), FMR is higher for demographic-matched impostors.

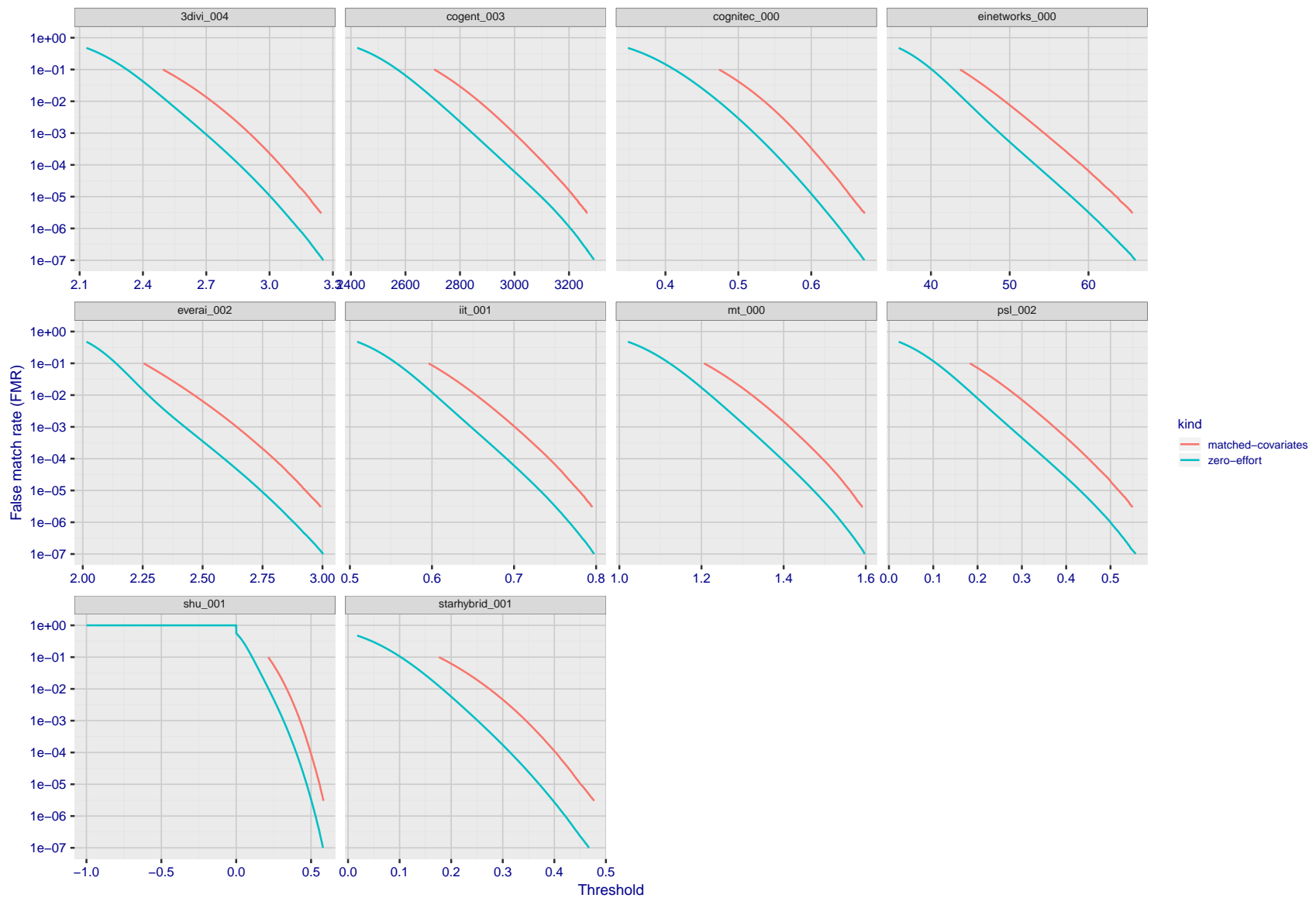


Figure 91: For the visa images, the false match calibration curves show FMR vs. threshold,  $T$ . The blue (lower) curves are for zero-effort impostors (i.e. comparing all images against all). The red (upper) curves are for persons of the same-sex, same-age, and same national-origin. This shows that FMR is underestimated (by a factor of 10 or more) by using a zero-effort impostor calculation to calibrate  $T$ . As shown later (sec. 3.6), FMR is higher for demographic-matched impostors.

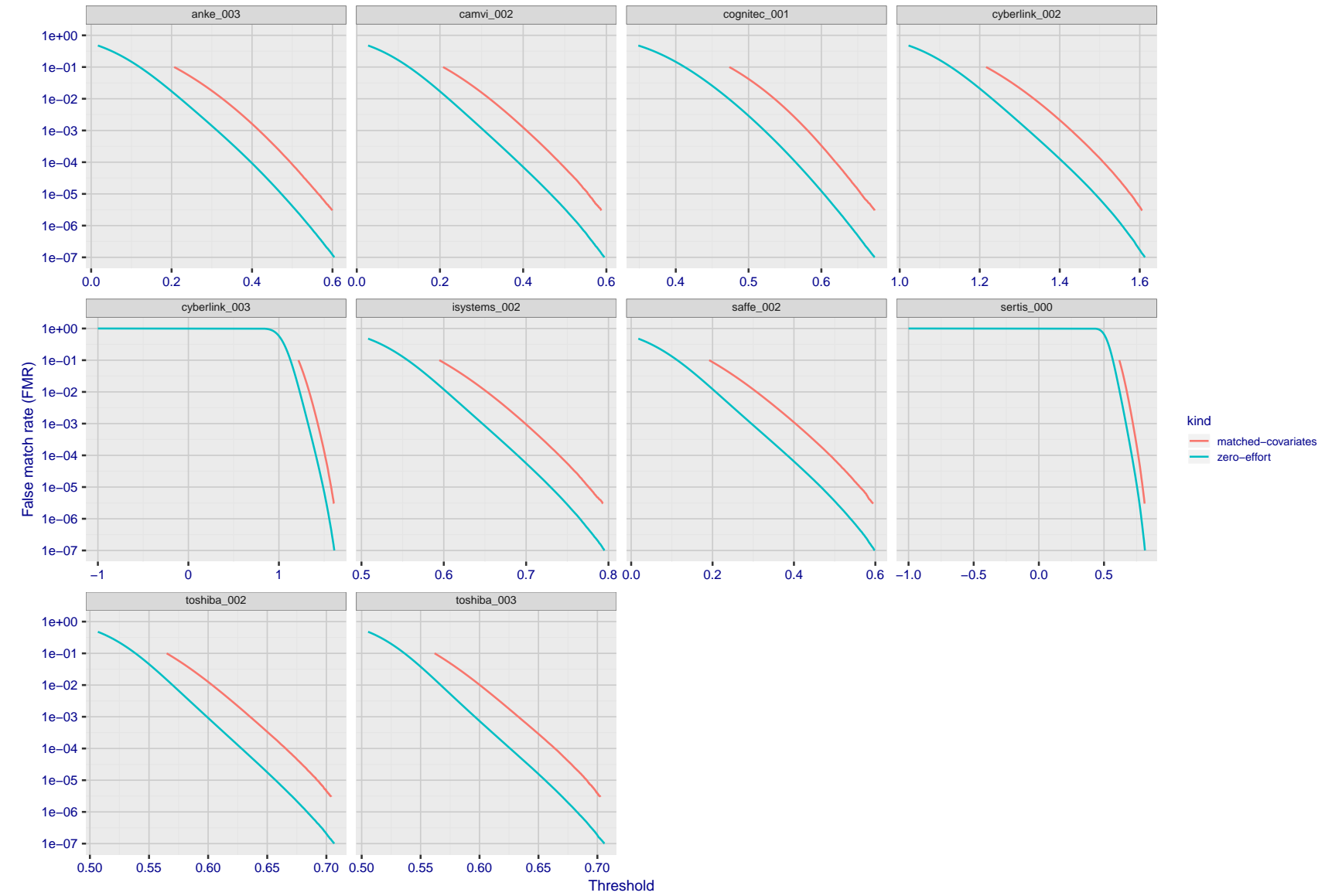


Figure 92: For the visa images, the false match calibration curves show FMR vs. threshold,  $T$ . The blue (lower) curves are for zero-effort impostors (i.e. comparing all images against all). The red (upper) curves are for persons of the same-sex, same-age, and same national-origin. This shows that FMR is underestimated (by a factor of 10 or more) by using a zero-effort impostor calculation to calibrate  $T$ . As shown later (sec. 3.6), FMR is higher for demographic-matched impostors.

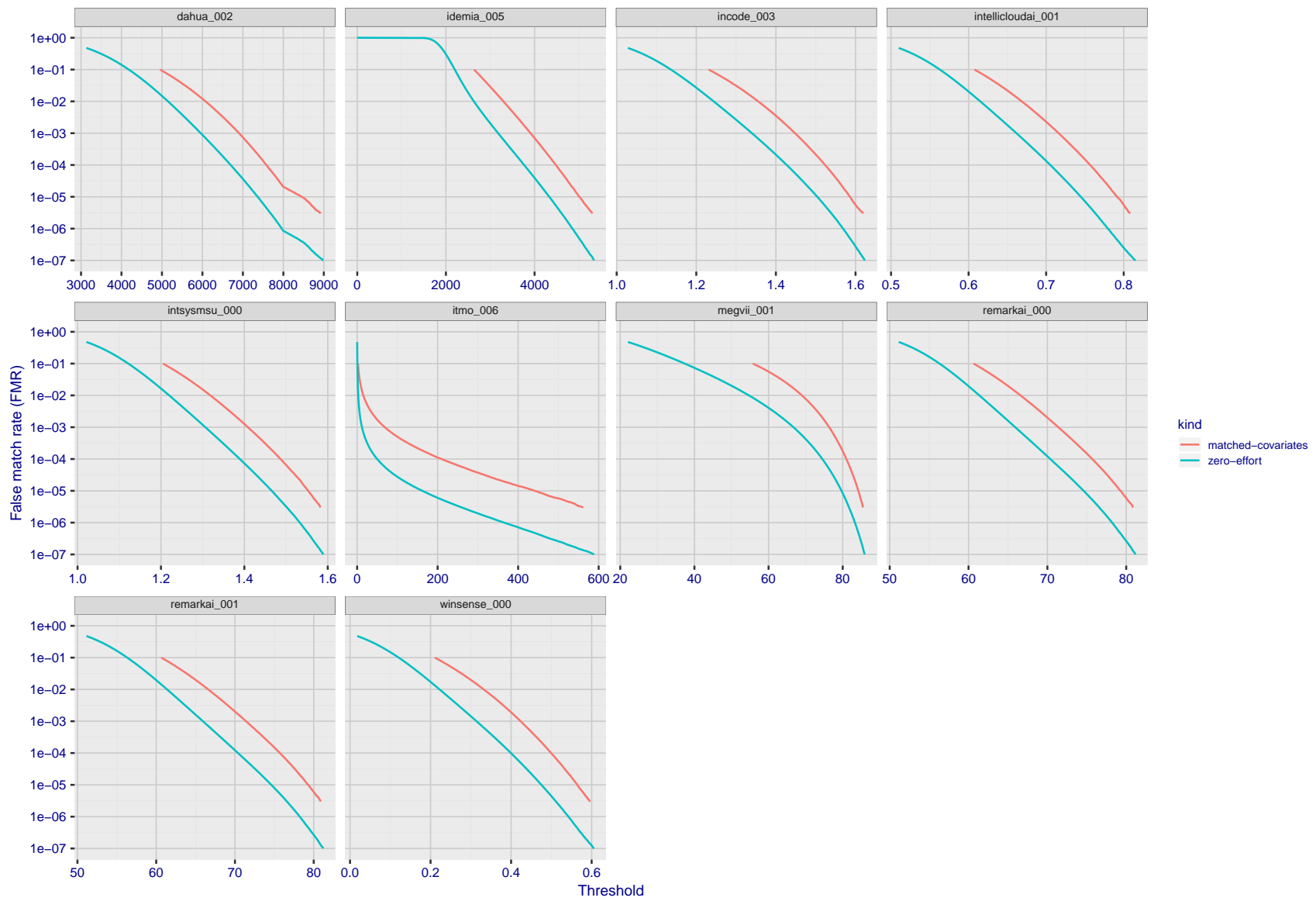


Figure 93: For the visa images, the false match calibration curves show FMR vs. threshold,  $T$ . The blue (lower) curves are for zero-effort impostors (i.e. comparing all images against all). The red (upper) curves are for persons of the same-sex, same-age, and same national-origin. This shows that FMR is underestimated (by a factor of 10 or more) by using a zero-effort impostor calculation to calibrate  $T$ . As shown later (sec. 3.6), FMR is higher for demographic-matched impostors.

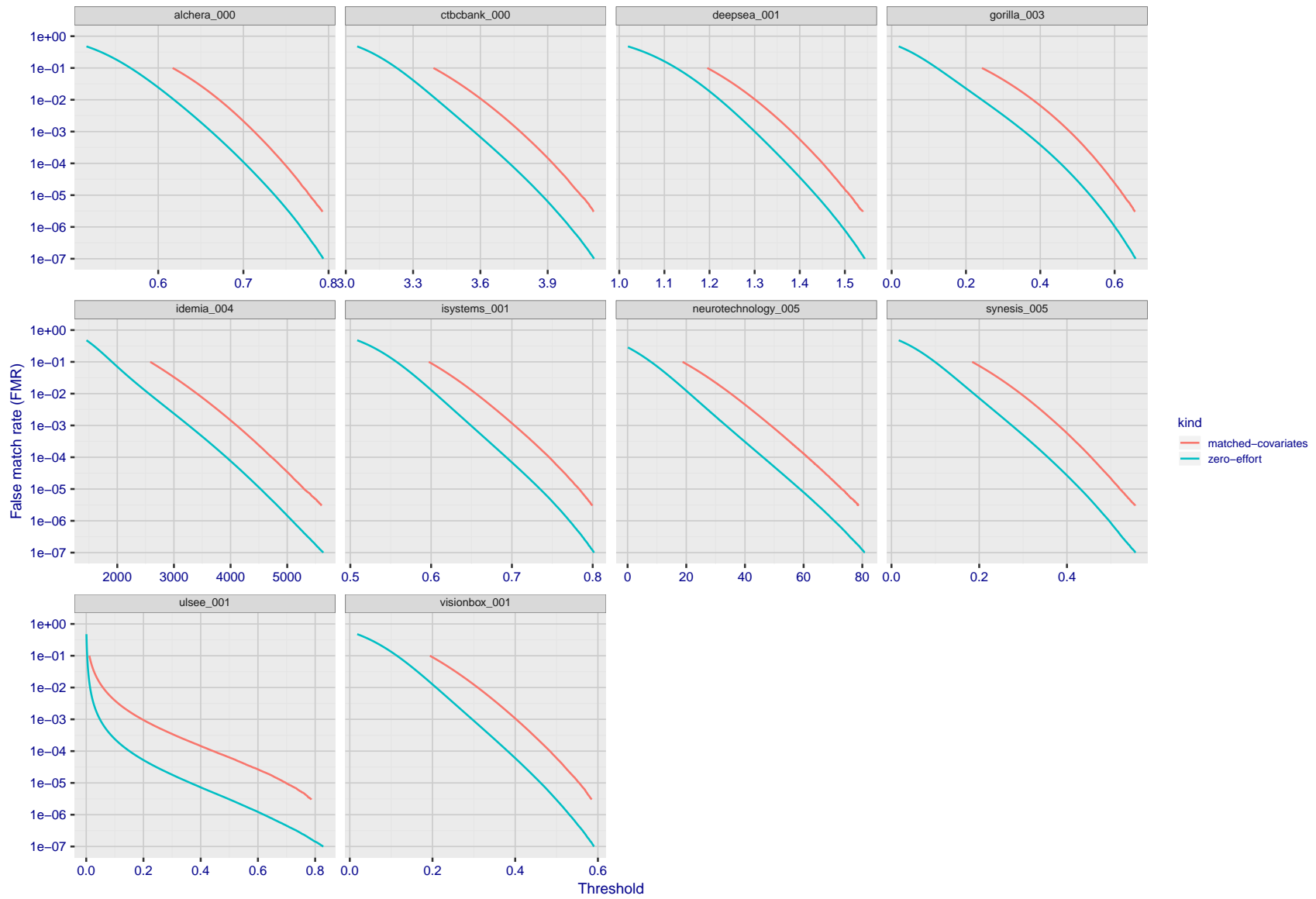


Figure 94: For the visa images, the false match calibration curves show FMR vs. threshold,  $T$ . The blue (lower) curves are for zero-effort impostors (i.e. comparing all images against all). The red (upper) curves are for persons of the same-sex, same-age, and same national-origin. This shows that FMR is underestimated (by a factor of 10 or more) by using a zero-effort impostor calculation to calibrate  $T$ . As shown later (sec. 3.6), FMR is higher for demographic-matched impostors.

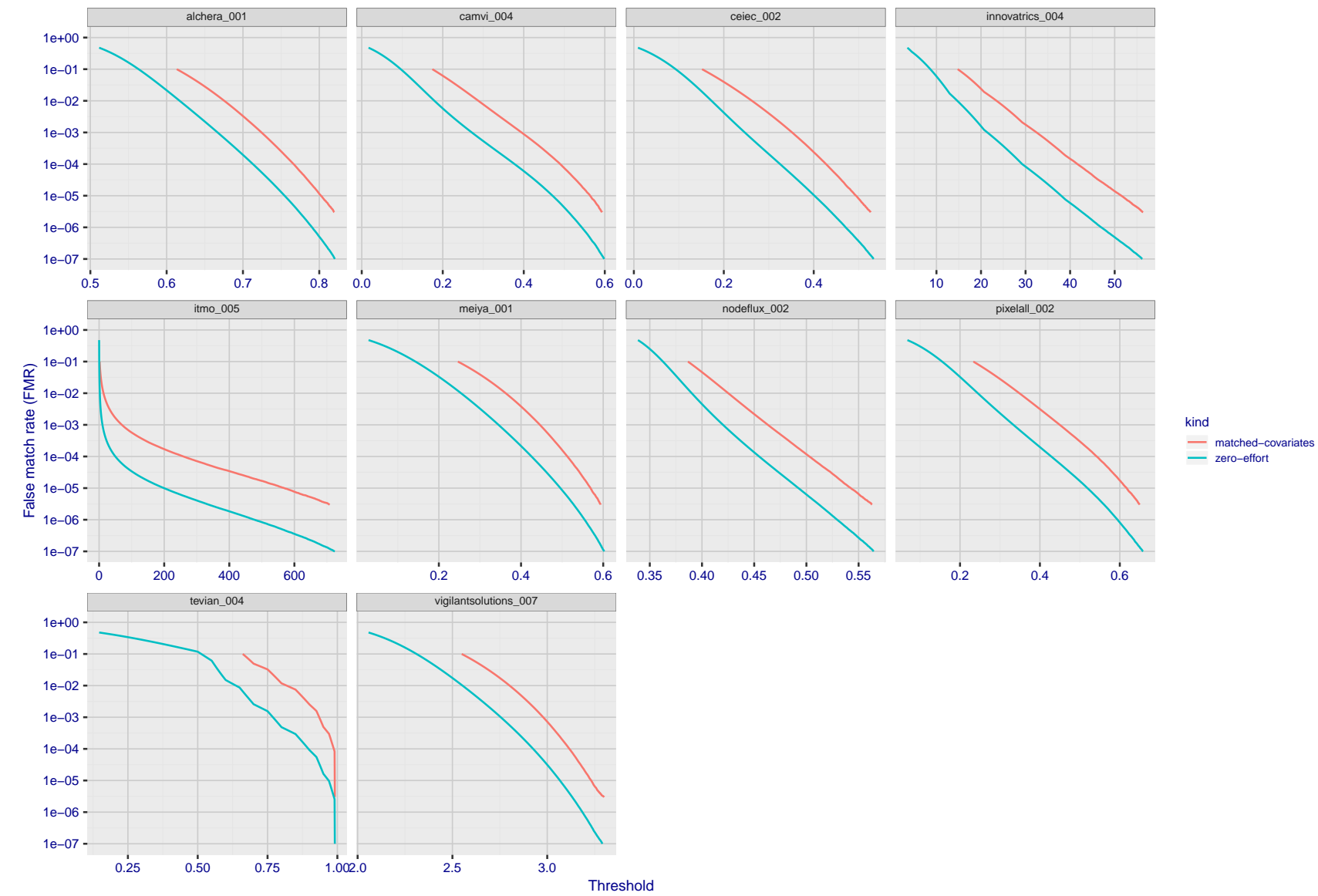


Figure 95: For the visa images, the false match calibration curves show FMR vs. threshold,  $T$ . The blue (lower) curves are for zero-effort impostors (i.e. comparing all images against all). The red (upper) curves are for persons of the same-sex, same-age, and same national-origin. This shows that FMR is underestimated (by a factor of 10 or more) by using a zero-effort impostor calculation to calibrate  $T$ . As shown later (sec. 3.6), FMR is higher for demographic-matched impostors.

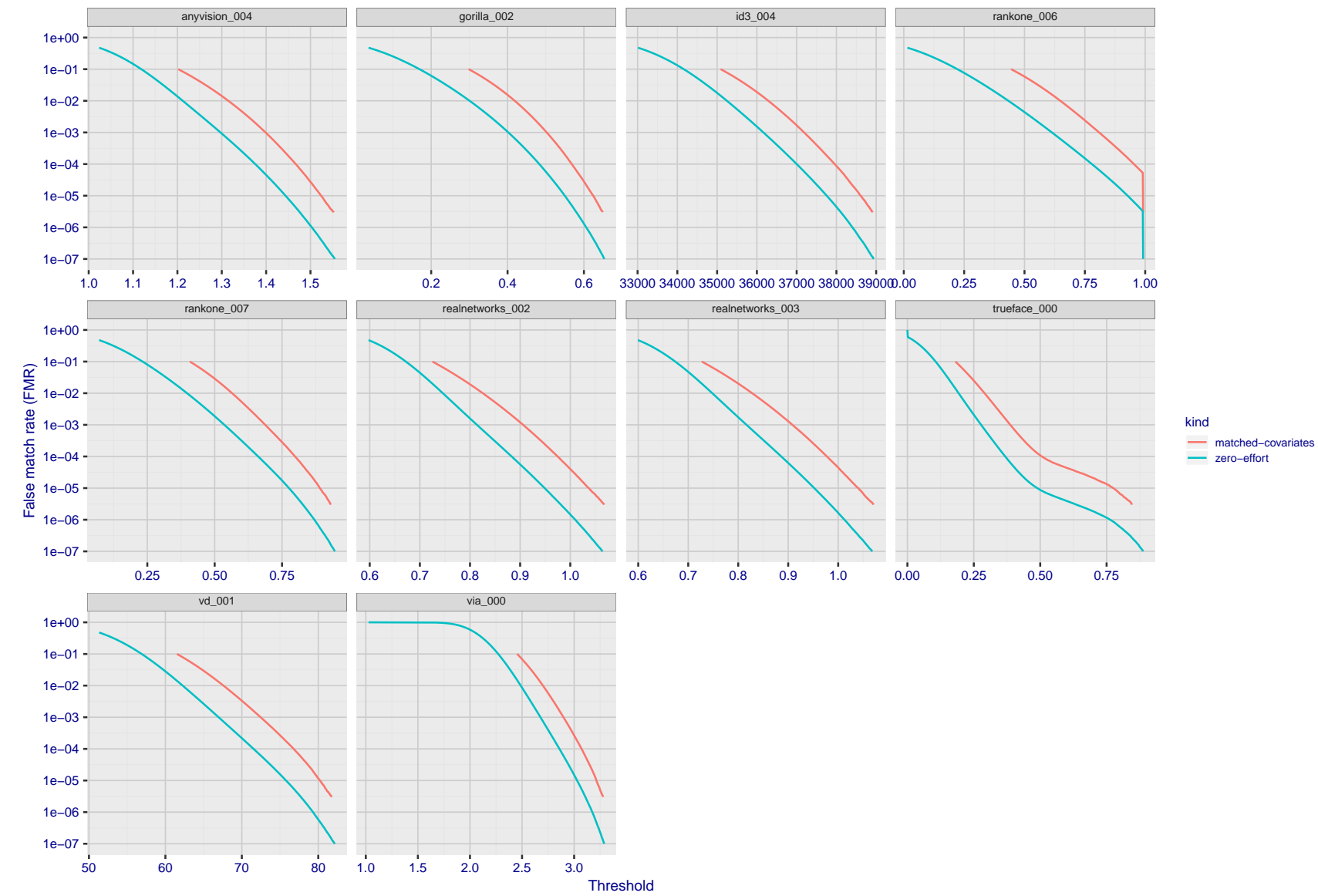


Figure 96: For the visa images, the false match calibration curves show FMR vs. threshold,  $T$ . The blue (lower) curves are for zero-effort impostors (i.e. comparing all images against all). The red (upper) curves are for persons of the same-sex, same-age, and same national-origin. This shows that FMR is underestimated (by a factor of 10 or more) by using a zero-effort impostor calculation to calibrate  $T$ . As shown later (sec. 3.6), FMR is higher for demographic-matched impostors.

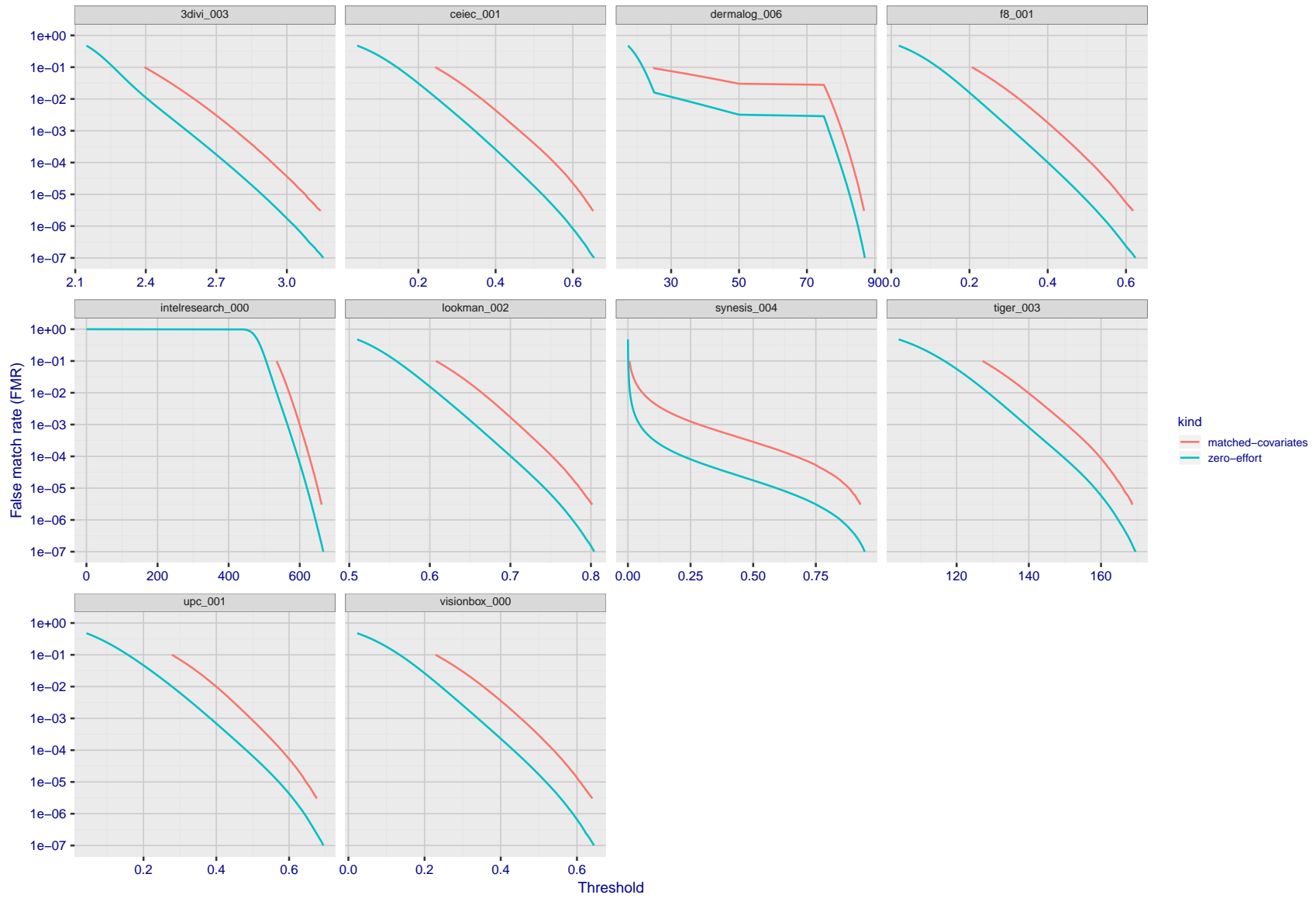


Figure 97: For the visa images, the false match calibration curves show FMR vs. threshold,  $T$ . The blue (lower) curves are for zero-effort impostors (i.e. comparing all images against all). The red (upper) curves are for persons of the same-sex, same-age, and same national-origin. This shows that FMR is underestimated (by a factor of 10 or more) by using a zero-effort impostor calculation to calibrate  $T$ . As shown later (sec. 3.6), FMR is higher for demographic-matched impostors.

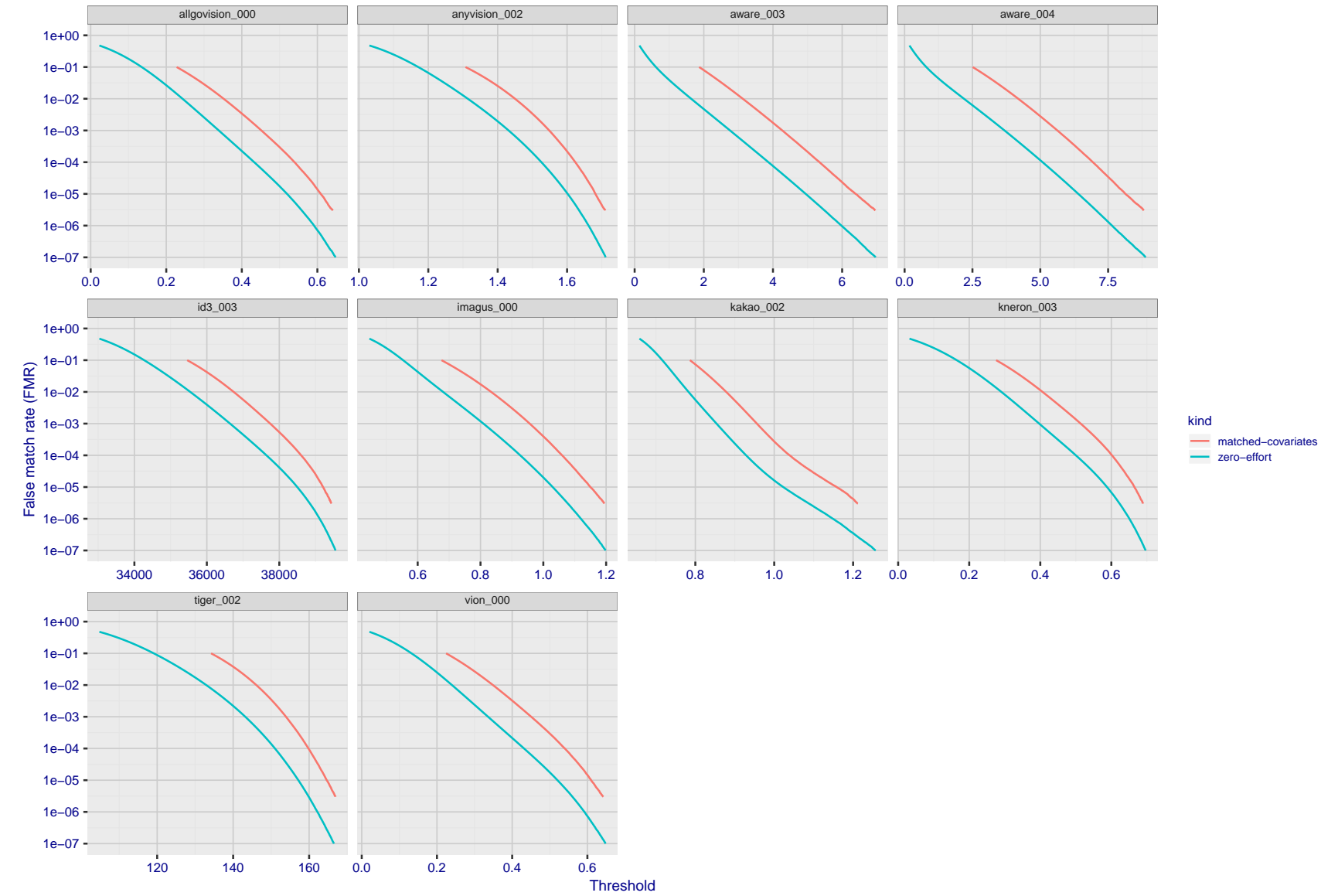


Figure 98: For the visa images, the false match calibration curves show FMR vs. threshold,  $T$ . The blue (lower) curves are for zero-effort impostors (i.e. comparing all images against all). The red (upper) curves are for persons of the same-sex, same-age, and same national-origin. This shows that FMR is underestimated (by a factor of 10 or more) by using a zero-effort impostor calculation to calibrate  $T$ . As shown later (sec. 3.6), FMR is higher for demographic-matched impostors.

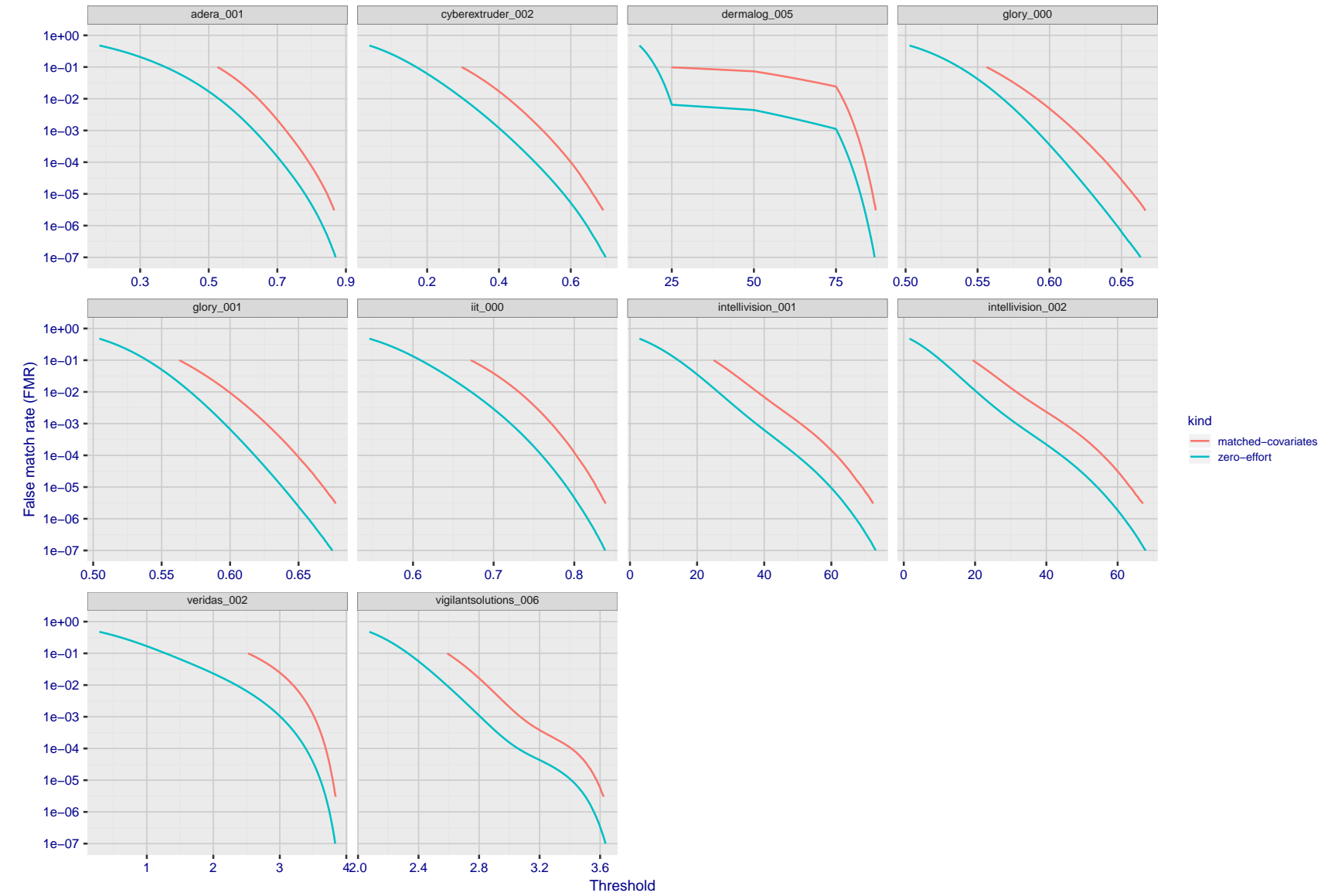


Figure 99: For the visa images, the false match calibration curves show FMR vs. threshold,  $T$ . The blue (lower) curves are for zero-effort impostors (i.e. comparing all images against all). The red (upper) curves are for persons of the same-sex, same-age, and same national-origin. This shows that FMR is underestimated (by a factor of 10 or more) by using a zero-effort impostor calculation to calibrate  $T$ . As shown later (sec. 3.6), FMR is higher for demographic-matched impostors.

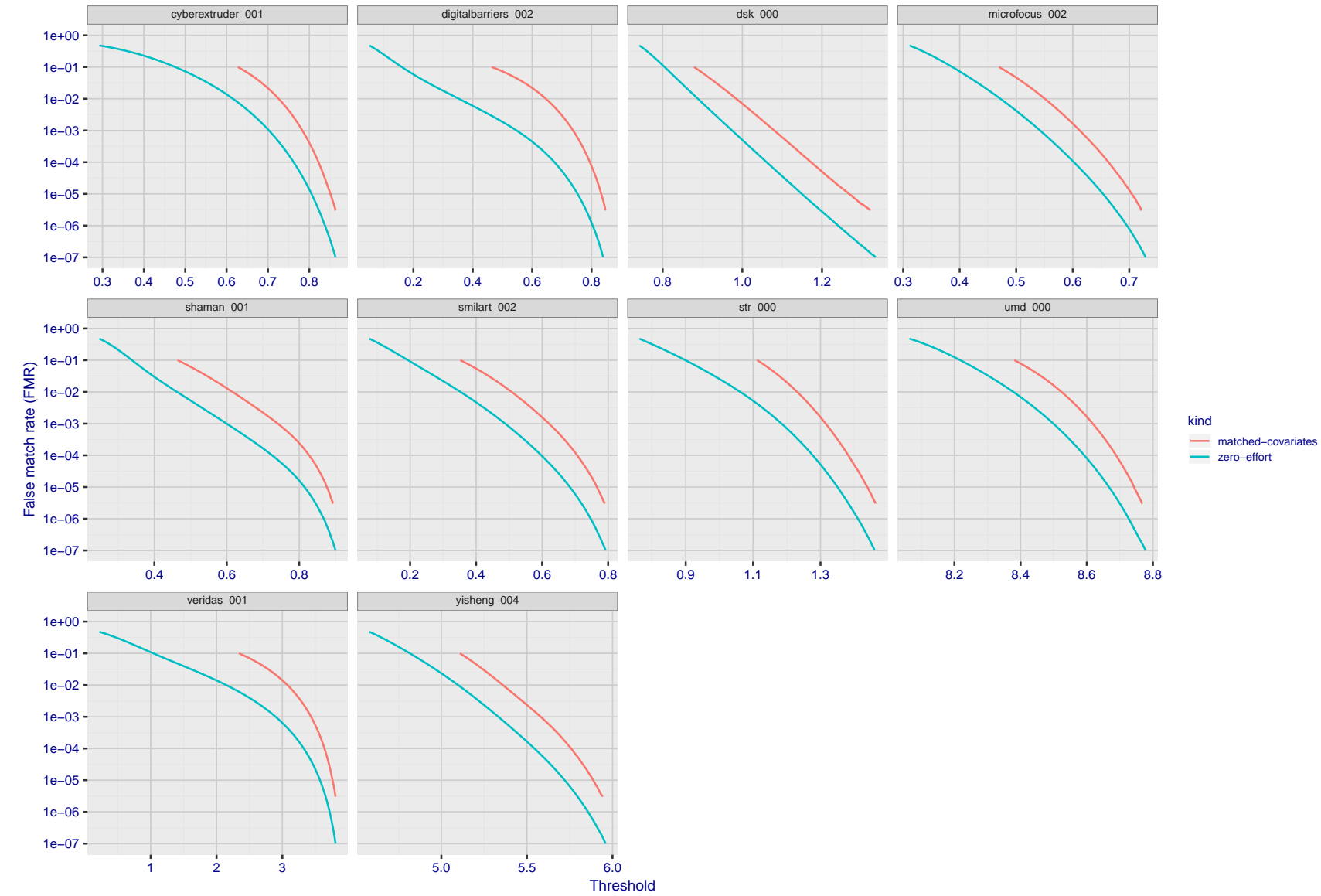


Figure 100: For the visa images, the false match calibration curves show FMR vs. threshold,  $T$ . The blue (lower) curves are for zero-effort impostors (i.e. comparing all images against all). The red (upper) curves are for persons of the same-sex, same-age, and same national-origin. This shows that FMR is underestimated (by a factor of 10 or more) by using a zero-effort impostor calculation to calibrate  $T$ . As shown later (sec. 3.6), FMR is higher for demographic-matched impostors.

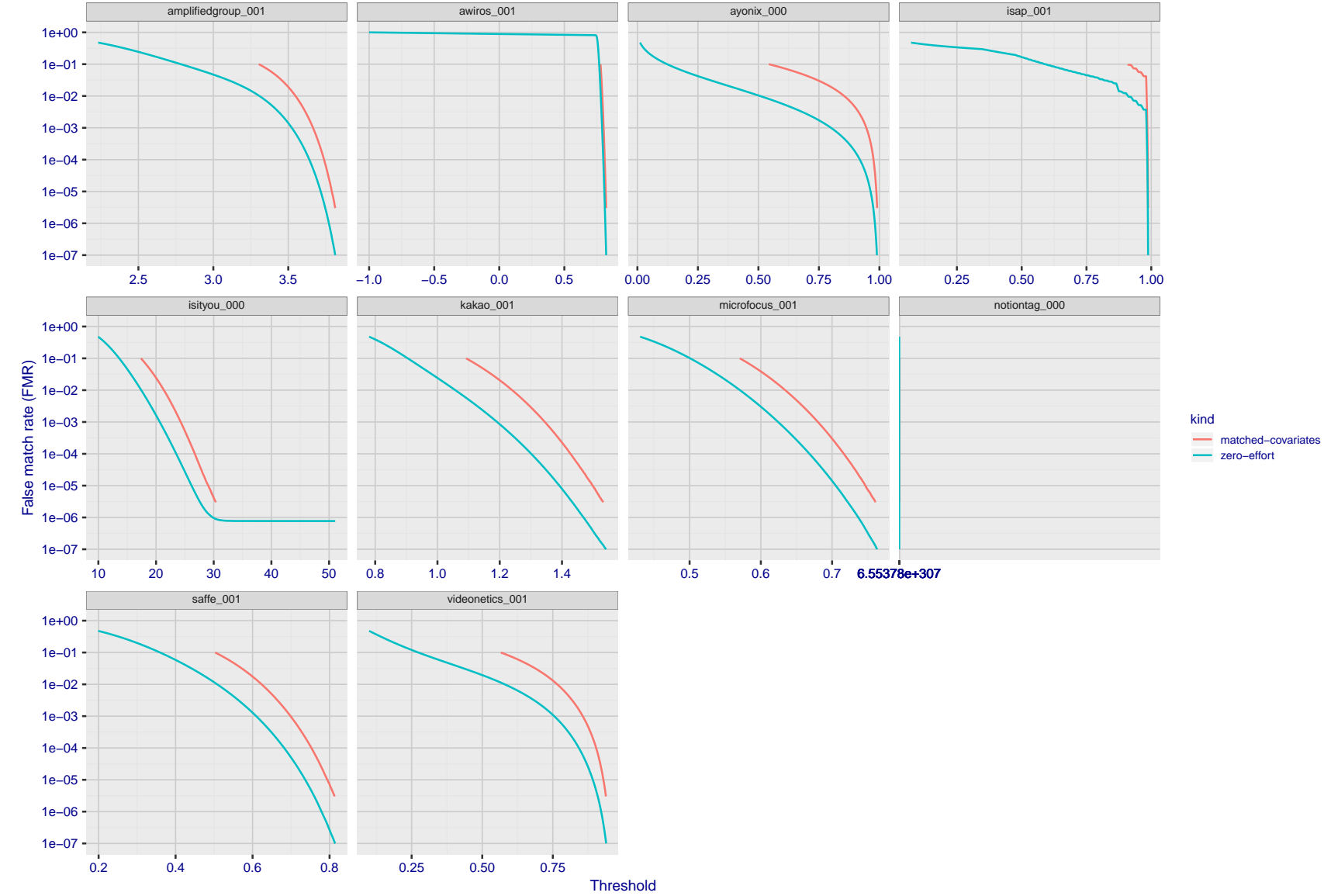


Figure 101: For the visa images, the false match calibration curves show FMR vs. threshold,  $T$ . The blue (lower) curves are for zero-effort impostors (i.e. comparing all images against all). The red (upper) curves are for persons of the same-sex, same-age, and same national-origin. This shows that FMR is underestimated (by a factor of 10 or more) by using a zero-effort impostor calculation to calibrate  $T$ . As shown later (sec. 3.6), FMR is higher for demographic-matched impostors.

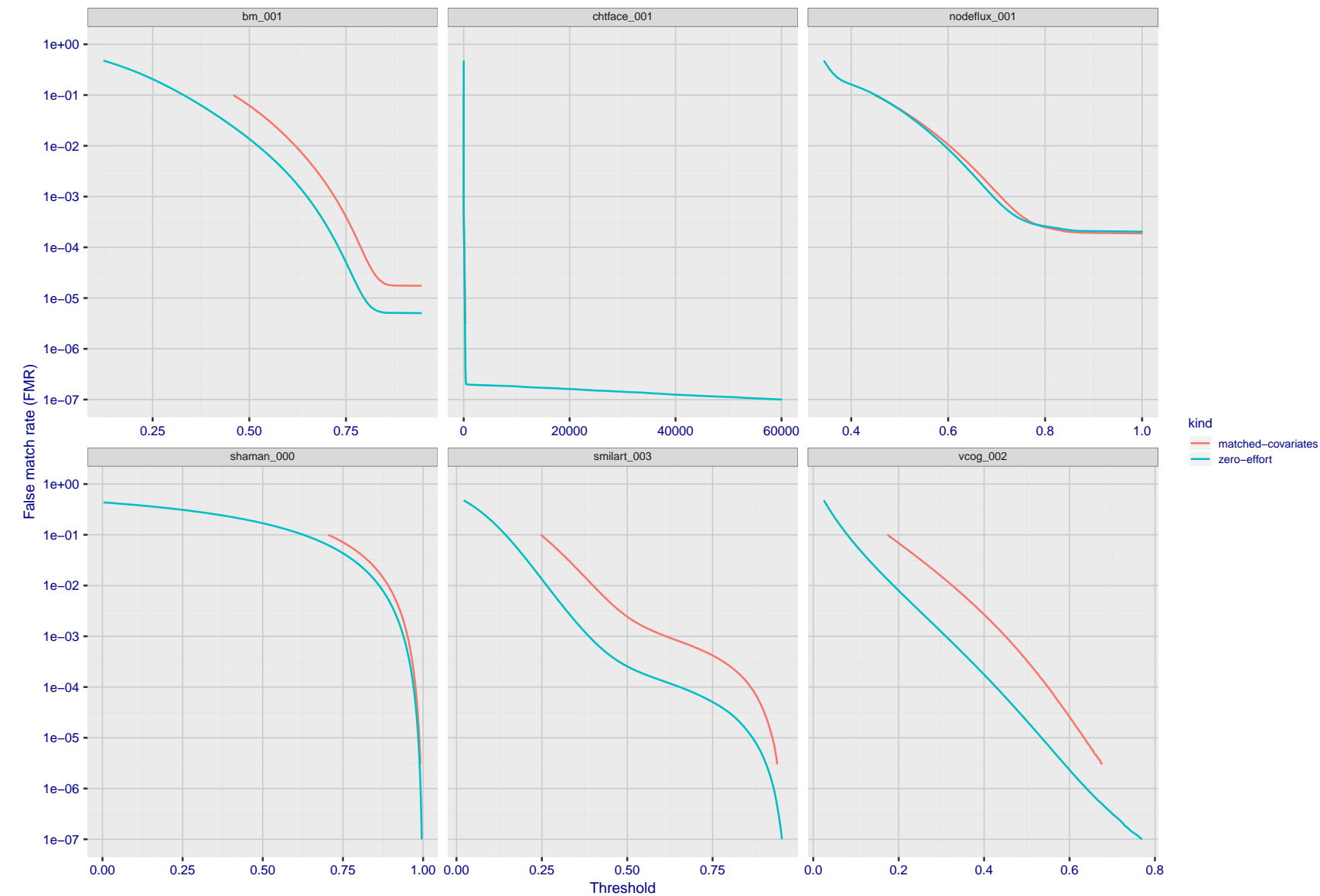


Figure 102: For the visa images, the false match calibration curves show FMR vs. threshold,  $T$ . The blue (lower) curves are for zero-effort impostors (i.e. comparing all images against all). The red (upper) curves are for persons of the same-sex, same-age, and same national-origin. This shows that FMR is underestimated (by a factor of 10 or more) by using a zero-effort impostor calculation to calibrate  $T$ . As shown later (sec. 3.6), FMR is higher for demographic-matched impostors.

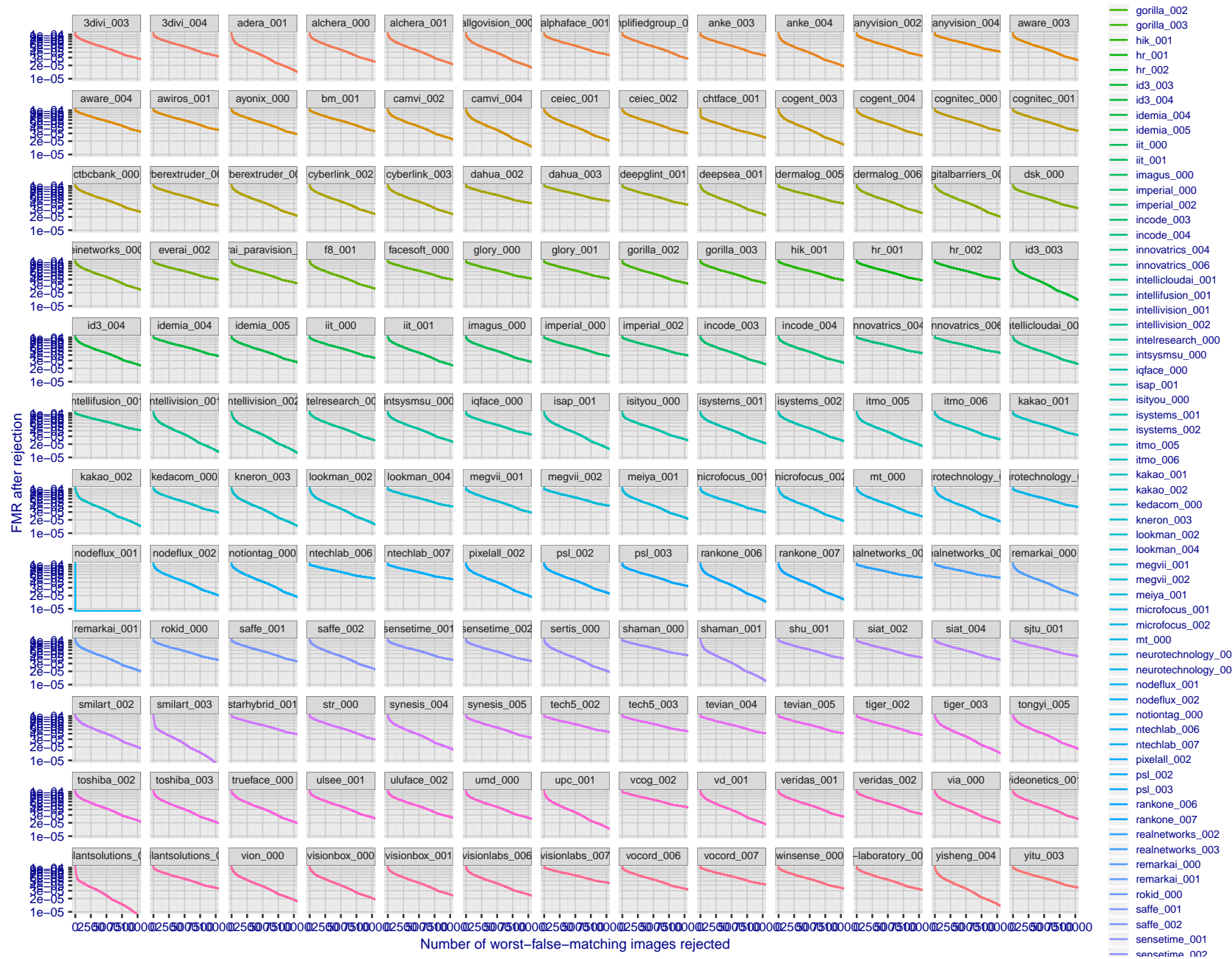


Figure 103: For the visa images, the curves show how false matches are concentrated in certain images. Specifically each line plots  $FMR(k)$  with  $k$  the number of images rejected in decreasing order of how many false matches that image was involved in.  $FMR(0) = 10^{-4}$ . In terms of the biometric zoo, the most “wolf-ish” images are rejected first i.e. those enrollment or verification images most often involved in false matches. A flatter response is considered superior. A steeply descending response indicates that certain kinds of images false match against others, e.g. if hypothetically images of men with particular mustaches would falsely match others.

## 3.5 Genuine distribution stability

### 3.5.1 Effect of birth place on the genuine distribution

**Background:** Both skin tone and bone structure vary geographically. Prior studies have reported variations in FNMR and FMR.

**Goal:** To measure false non-match rate (FNMR) variation with country of birth.

**Methods:** Thresholds are determined that give  $FMR = \{0.001, 0.0001\}$  over the entire impostor set. Then FNMR is measured over 1000 bootstrap replications of the genuine scores. Only those countries with at least 140 individuals are included in the analysis.

**Results:** Figure 116 shows FNMR by country of birth for the two thresholds.

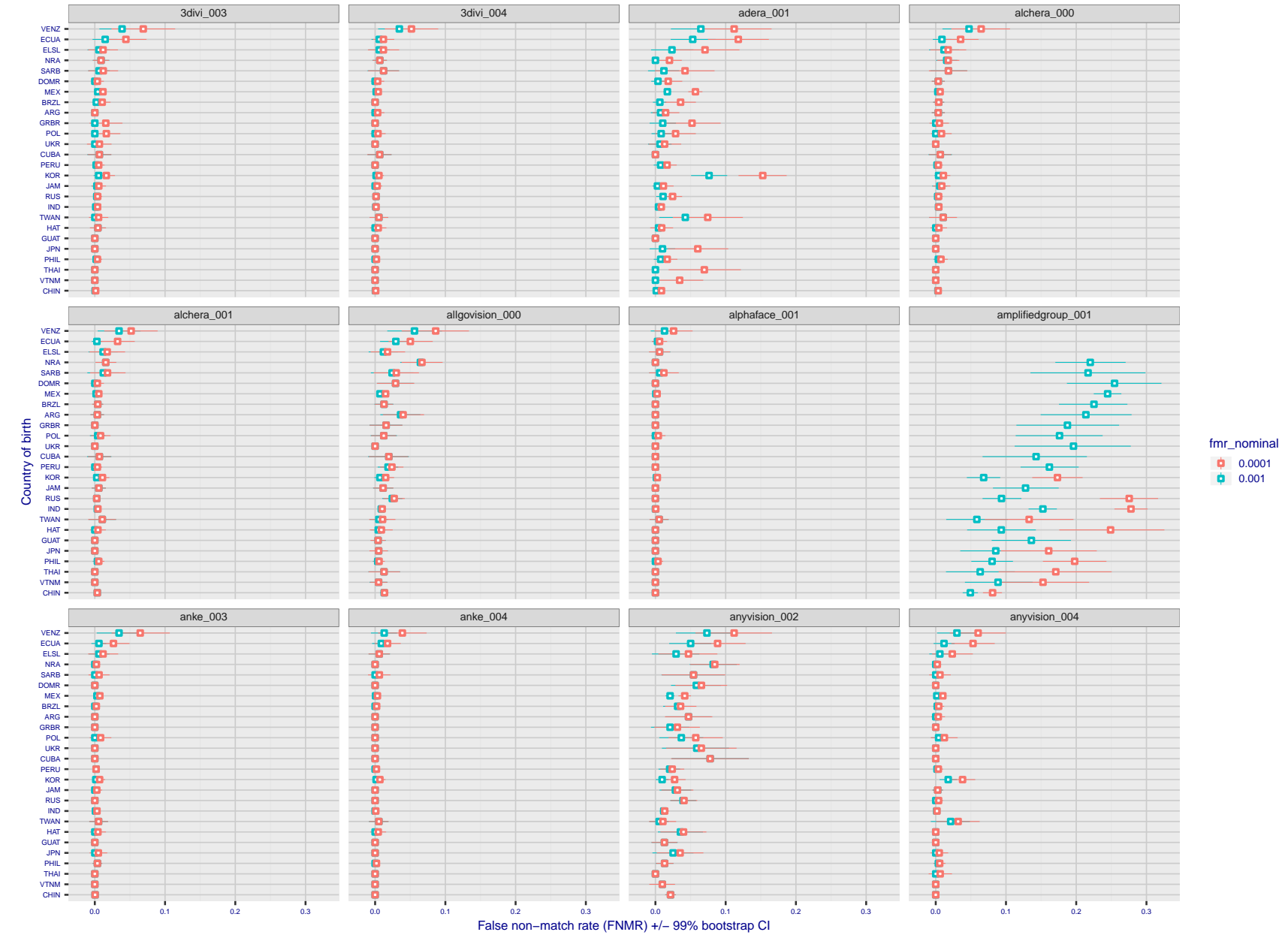


Figure 104: For the visa images, the dots show FNMR by country of birth for two globally set operating thresholds corresponding to  $FMR = \{0.001, 0.0001\}$  computed over all on the order of  $10^{10}$  impostor scores. The FMR in each bin will vary also - see subsequent impostor heatmaps in sec. 3.6.1. The figures shows an order of magnitude variation in FNMR across country of birth; these effects are likely due quality variations, then demographics like age and race. The error rates in some cases are zero, and in others the DET is flat so the error rates at the two thresholds are identical. The lines span 1% and 99% of bootstrap replicated FNMR estimates.

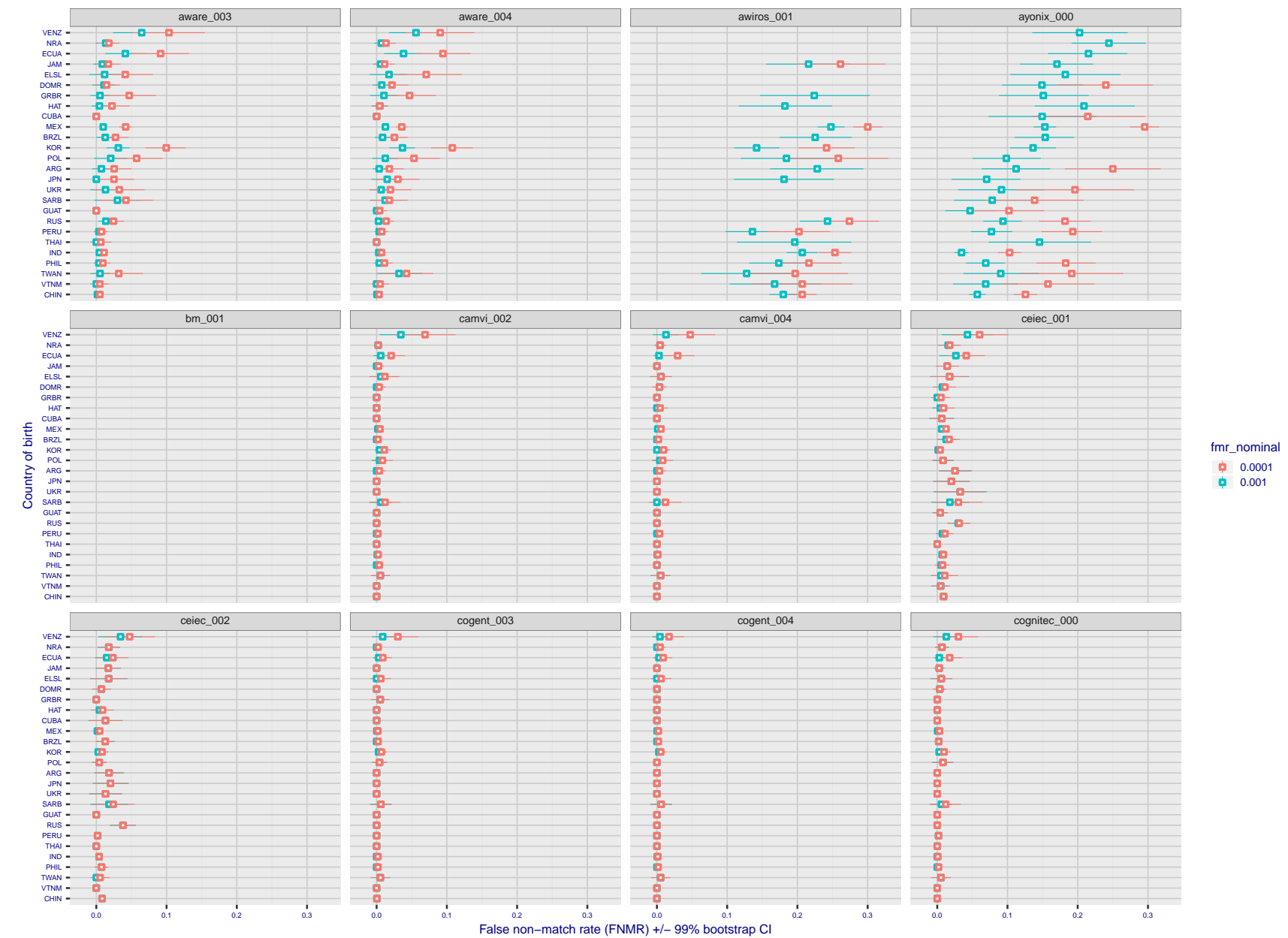


Figure 105: For the visa images, the dots show FNMR by country of birth for two globally set operating thresholds corresponding to  $FMR = \{0.001, 0.0001\}$  computed over all on the order of  $10^{10}$  impostor scores. The FMR in each bin will vary also - see subsequent impostor heatmaps in sec. 3.6.1. The figures shows an order of magnitude variation in FNMR across country of birth; these effects are likely due quality variations, then demographics like age and race. The error rates in some cases are zero, and in others the DET is flat so the error rates at the two thresholds are identical. The lines span 1% and 99% of bootstrap replicated FNMR estimates.

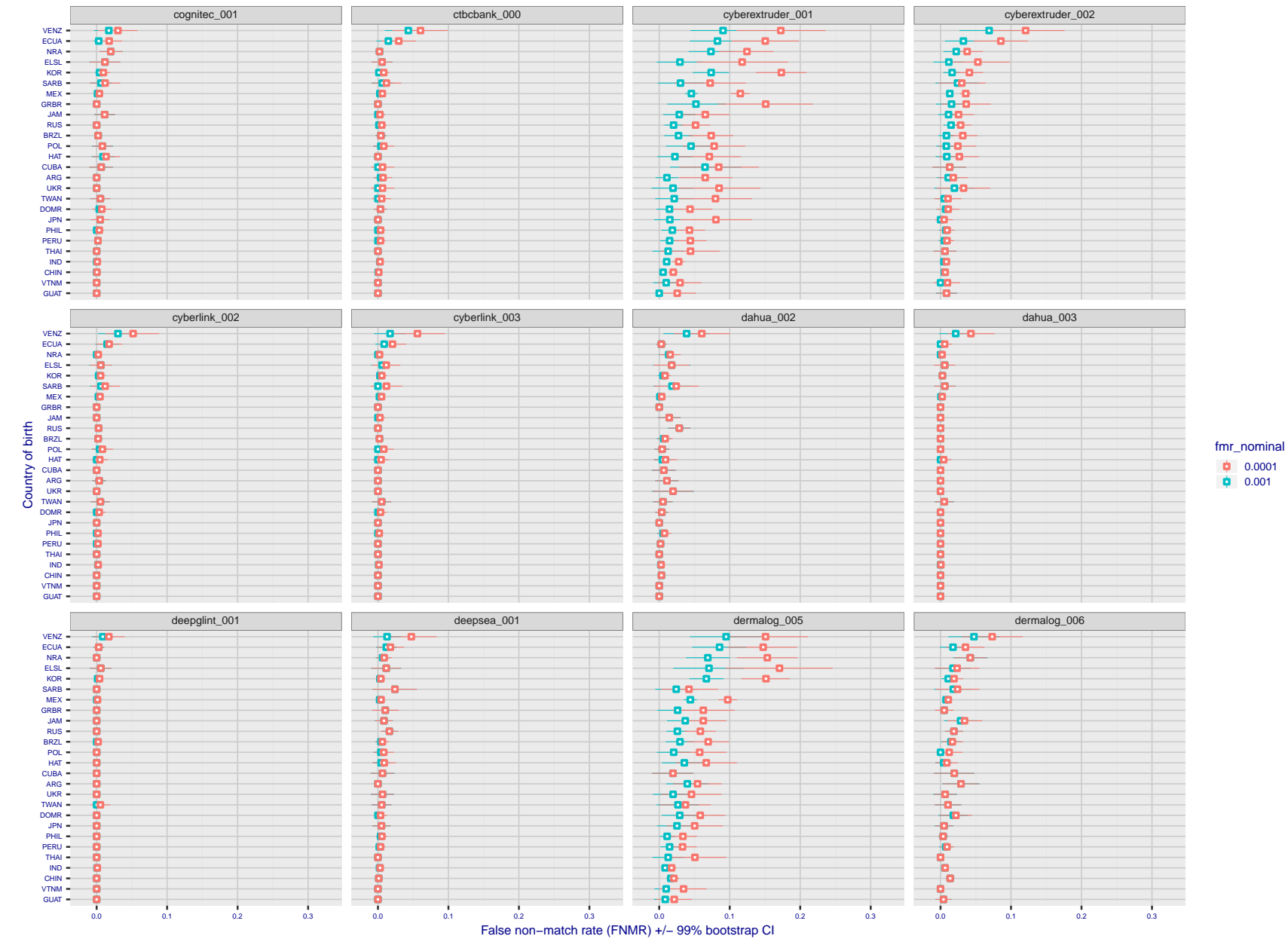


Figure 106: For the visa images, the dots show FNMR by country of birth for two globally set operating thresholds corresponding to  $FMR = \{0.001, 0.0001\}$  computed over all on the order of  $10^{10}$  impostor scores. The FMR in each bin will vary also - see subsequent impostor heatmaps in sec. 3.6.1. The figures shows an order of magnitude variation in FNMR across country of birth; these effects are likely due quality variations, then demographics like age and race. The error rates in some cases are zero, and in others the DET is flat so the error rates at the two thresholds are identical. The lines span 1% and 99% of bootstrap replicated FNMR estimates.

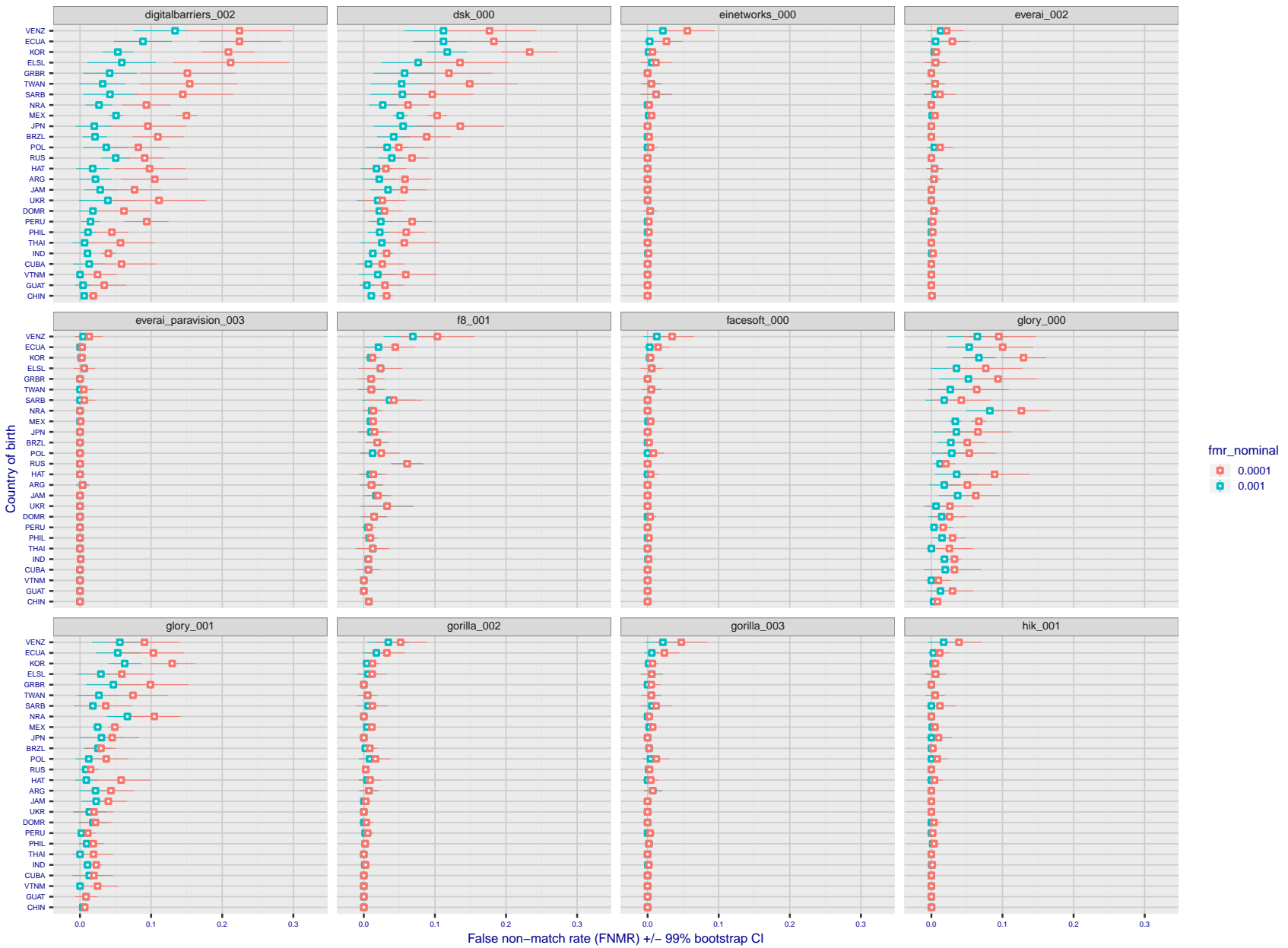


Figure 107: For the visa images, the dots show FNMR by country of birth for two globally set operating thresholds corresponding to  $FMR = \{0.001, 0.0001\}$  computed over all on the order of  $10^{10}$  impostor scores. The FMR in each bin will vary also - see subsequent impostor heatmaps in sec. 3.6.1. The figures shows an order of magnitude variation in FNMR across country of birth; these effects are likely due quality variations, then demographics like age and race. The error rates in some cases are zero, and in others the DET is flat so the error rates at the two thresholds are identical. The lines span 1% and 99% of bootstrap replicated FNMR estimates.

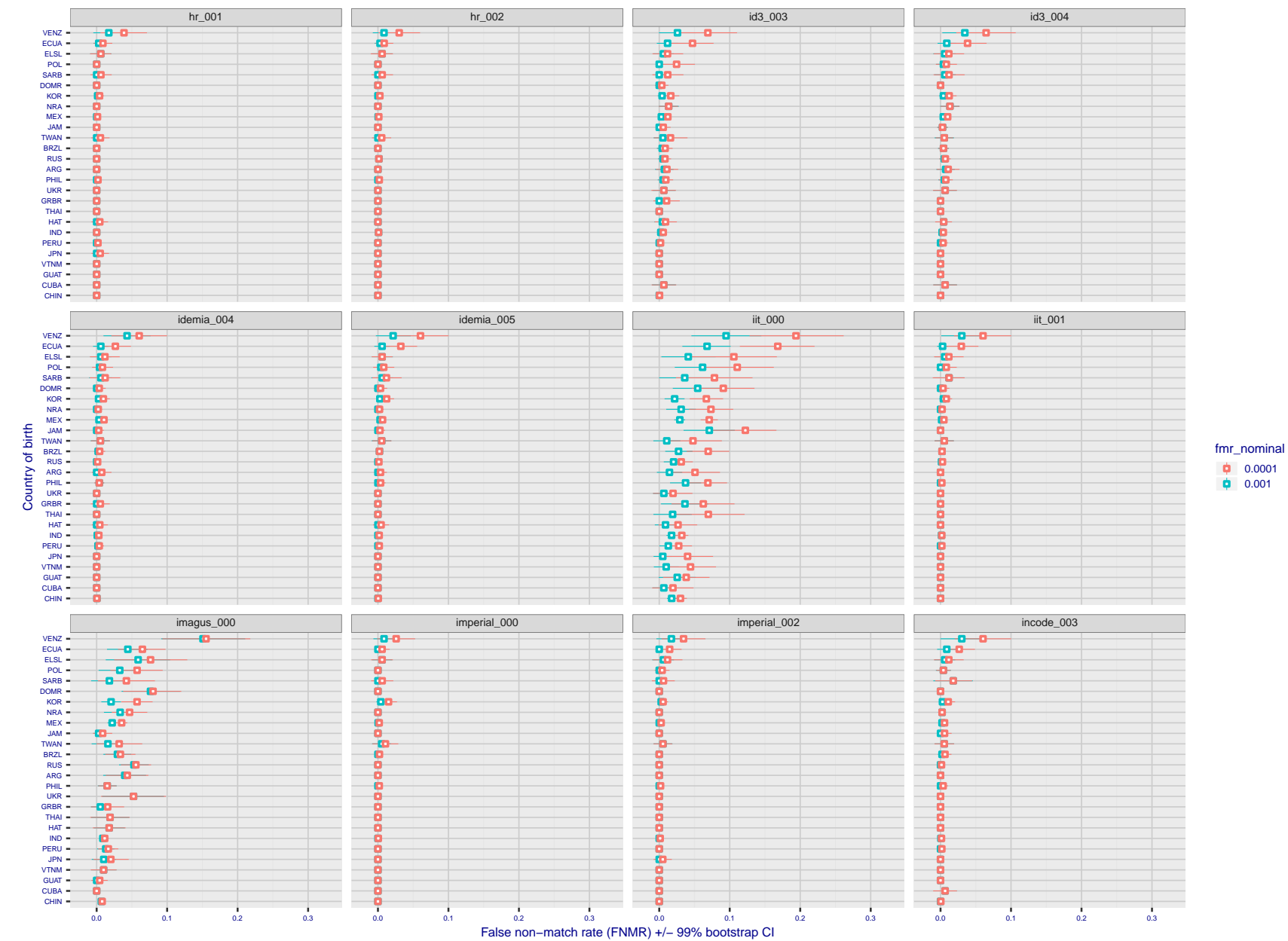


Figure 108: For the visa images, the dots show FNMR by country of birth for two globally set operating thresholds corresponding to  $FMR = \{0.001, 0.0001\}$  computed over all on the order of  $10^{10}$  impostor scores. The FMR in each bin will vary also - see subsequent impostor heatmaps in sec. 3.6.1. The figures shows an order of magnitude variation in FNMR across country of birth; these effects are likely due quality variations, then demographics like age and race. The error rates in some cases are zero, and in others the DET is flat so the error rates at the two thresholds are identical. The lines span 1% and 99% of bootstrap replicated FNMR estimates.

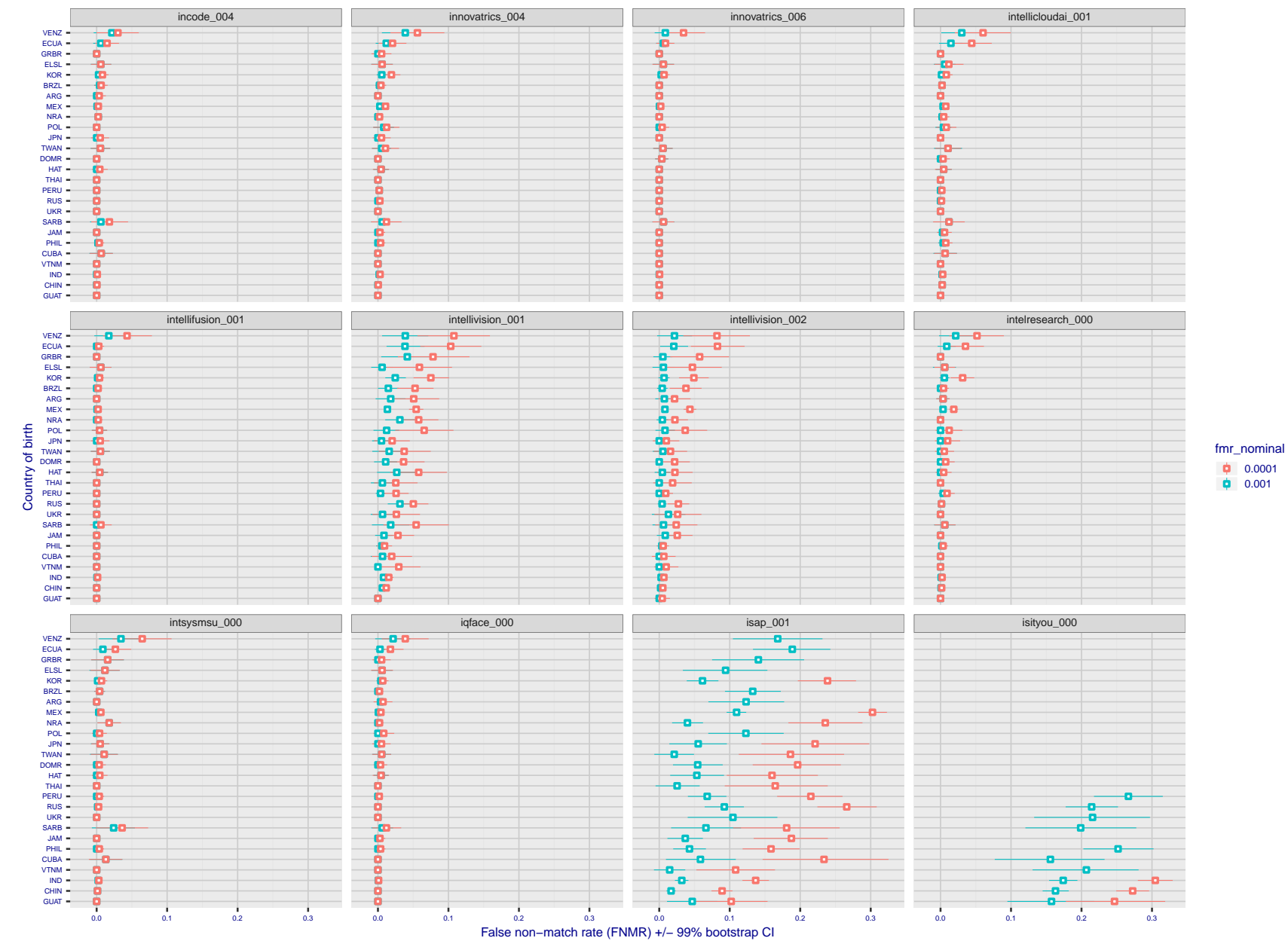


Figure 109: For the visa images, the dots show FNMR by country of birth for two globally set operating thresholds corresponding to  $FMR = \{0.001, 0.0001\}$  computed over all on the order of  $10^{10}$  impostor scores. The FMR in each bin will vary also - see subsequent impostor heatmaps in sec. 3.6.1. The figures shows an order of magnitude variation in FNMR across country of birth; these effects are likely due quality variations, then demographics like age and race. The error rates in some cases are zero, and in others the DET is flat so the error rates at the two thresholds are identical. The lines span 1% and 99% of bootstrap replicated FNMR estimates.

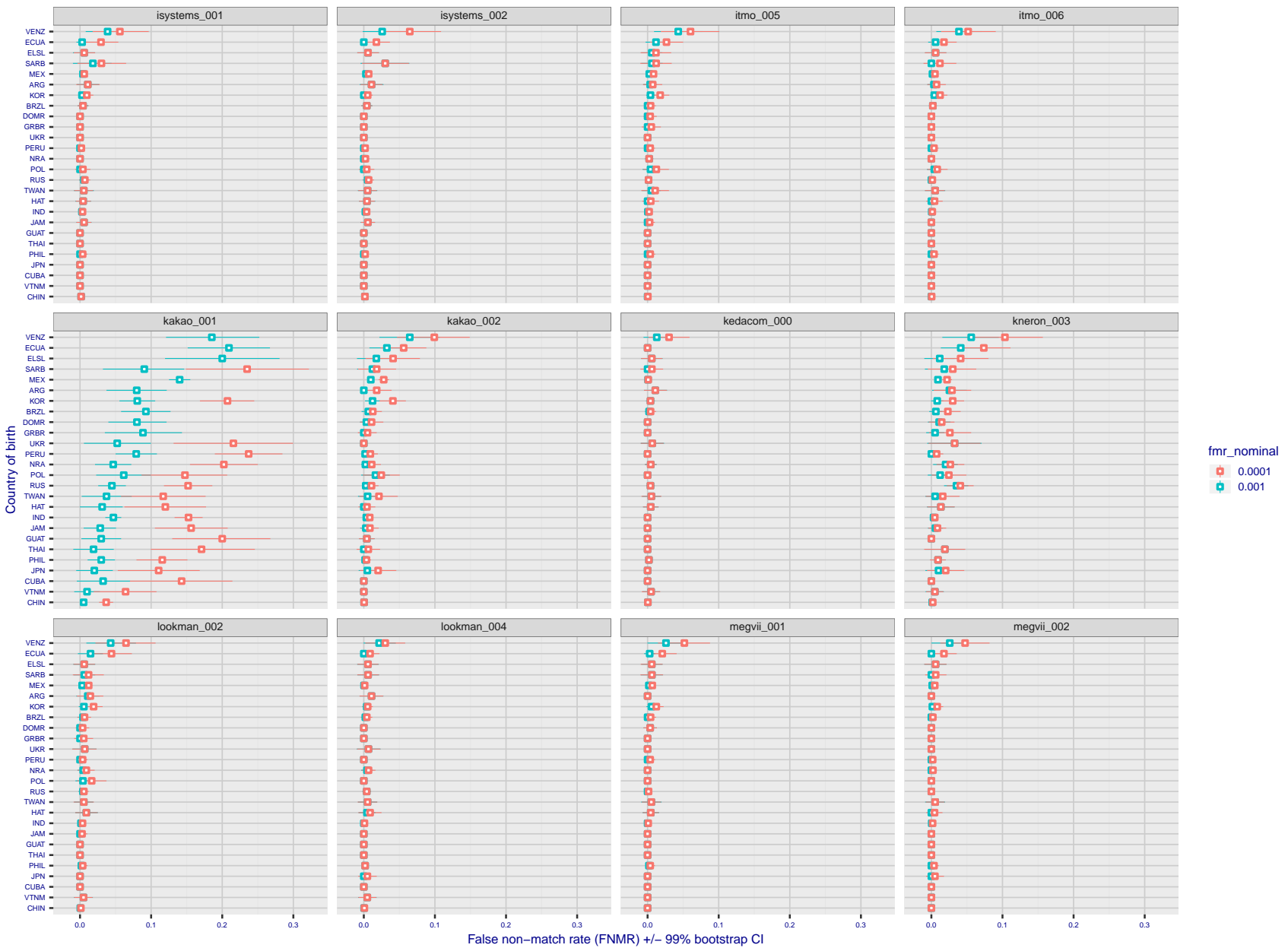


Figure 110: For the visa images, the dots show FNMR by country of birth for two globally set operating thresholds corresponding to  $FMR = \{0.001, 0.0001\}$  computed over all on the order of  $10^{10}$  impostor scores. The FMR in each bin will vary also - see subsequent impostor heatmaps in sec. 3.6.1. The figures shows an order of magnitude variation in FNMR across country of birth; these effects are likely due quality variations, then demographics like age and race. The error rates in some cases are zero, and in others the DET is flat so the error rates at the two thresholds are identical. The lines span 1% and 99% of bootstrap replicated FNMR estimates.

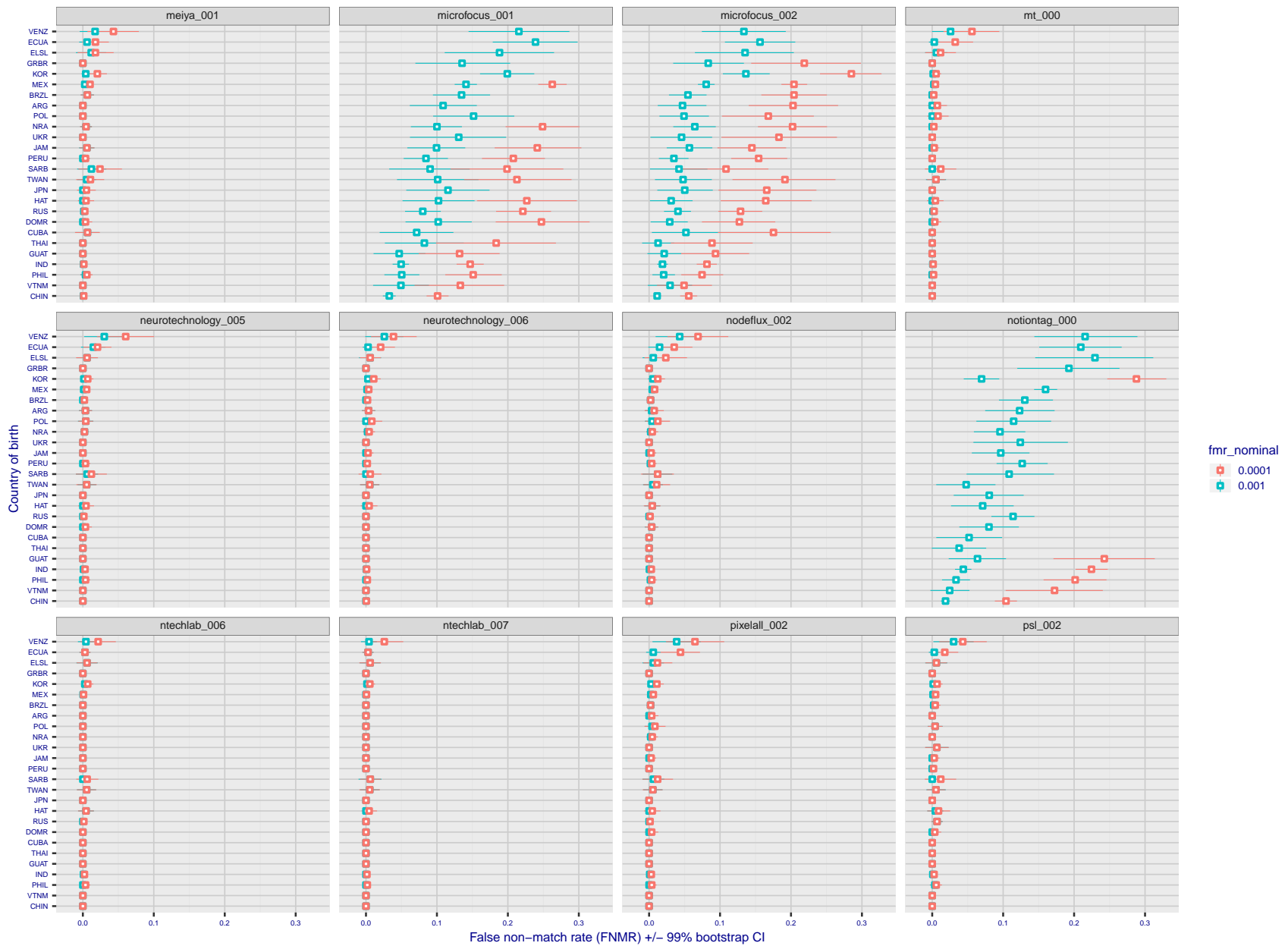


Figure 111: For the visa images, the dots show FNMR by country of birth for two globally set operating thresholds corresponding to  $FMR = \{0.001, 0.0001\}$  computed over all on the order of  $10^{10}$  impostor scores. The FMR in each bin will vary also - see subsequent impostor heatmaps in sec. 3.6.1. The figures shows an order of magnitude variation in FNMR across country of birth; these effects are likely due quality variations, then demographics like age and race. The error rates in some cases are zero, and in others the DET is flat so the error rates at the two thresholds are identical. The lines span 1% and 99% of bootstrap replicated FNMR estimates.

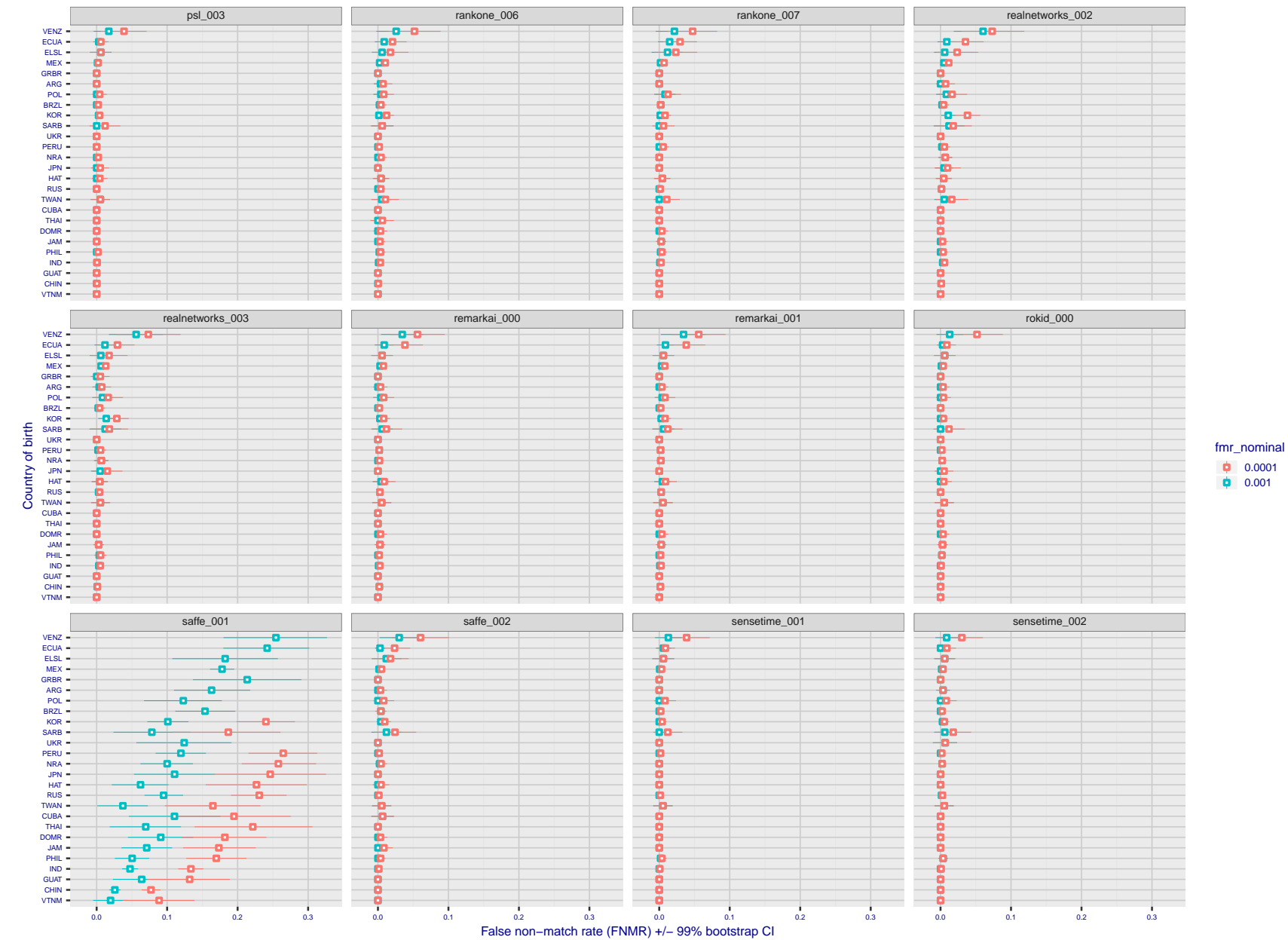


Figure 112: For the visa images, the dots show FNMR by country of birth for two globally set operating thresholds corresponding to  $FMR = \{0.001, 0.0001\}$  computed over all on the order of  $10^{10}$  impostor scores. The FMR in each bin will vary also - see subsequent impostor heatmaps in sec. 3.6.1. The figures shows an order of magnitude variation in FNMR across country of birth; these effects are likely due quality variations, then demographics like age and race. The error rates in some cases are zero, and in others the DET is flat so the error rates at the two thresholds are identical. The lines span 1% and 99% of bootstrap replicated FNMR estimates.

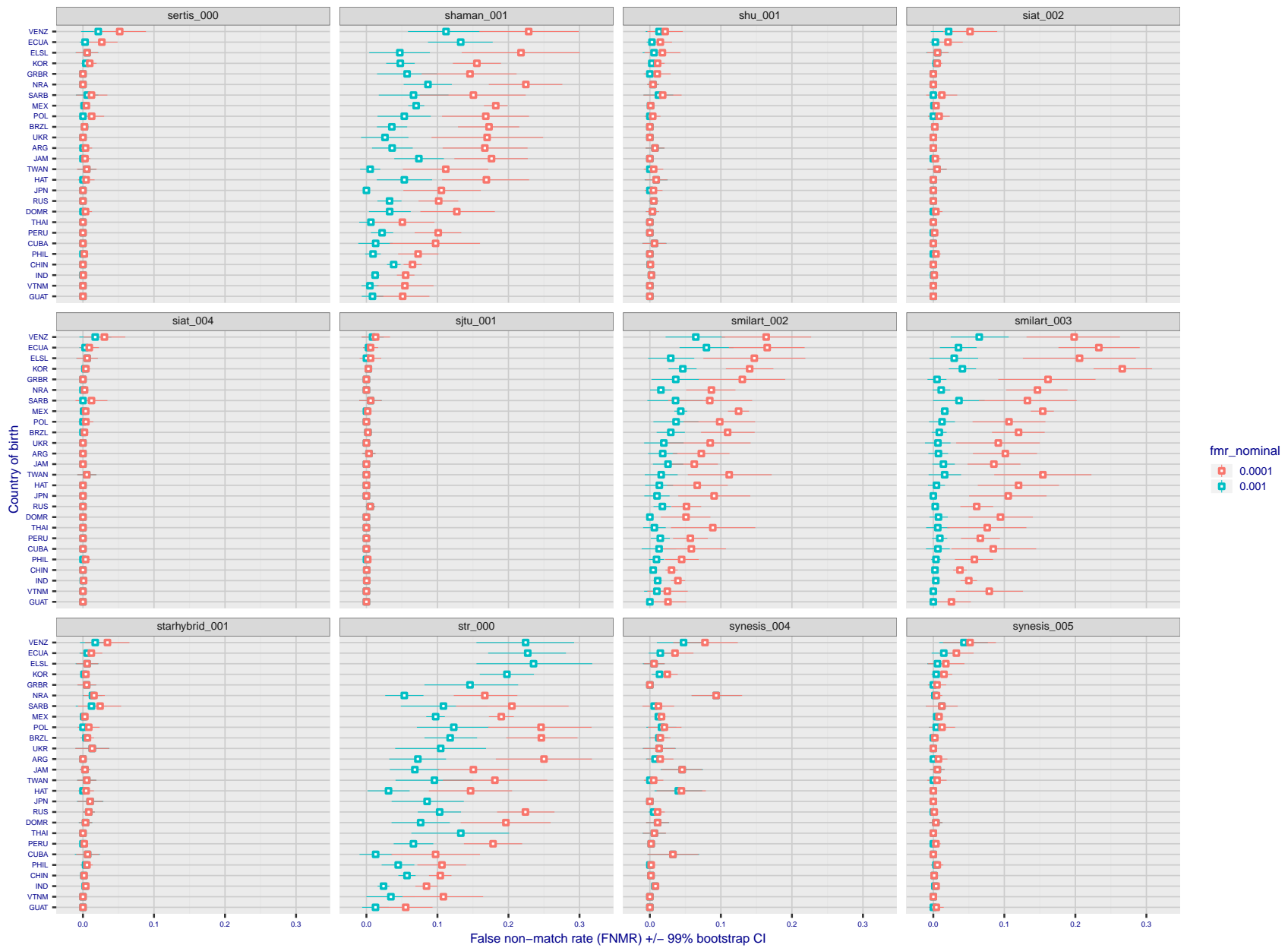


Figure 113: For the visa images, the dots show FNMR by country of birth for two globally set operating thresholds corresponding to  $FMR = \{0.001, 0.0001\}$  computed over all on the order of  $10^{10}$  impostor scores. The FMR in each bin will vary also - see subsequent impostor heatmaps in sec. 3.6.1. The figures shows an order of magnitude variation in FNMR across country of birth; these effects are likely due quality variations, then demographics like age and race. The error rates in some cases are zero, and in others the DET is flat so the error rates at the two thresholds are identical. The lines span 1% and 99% of bootstrap replicated FNMR estimates.

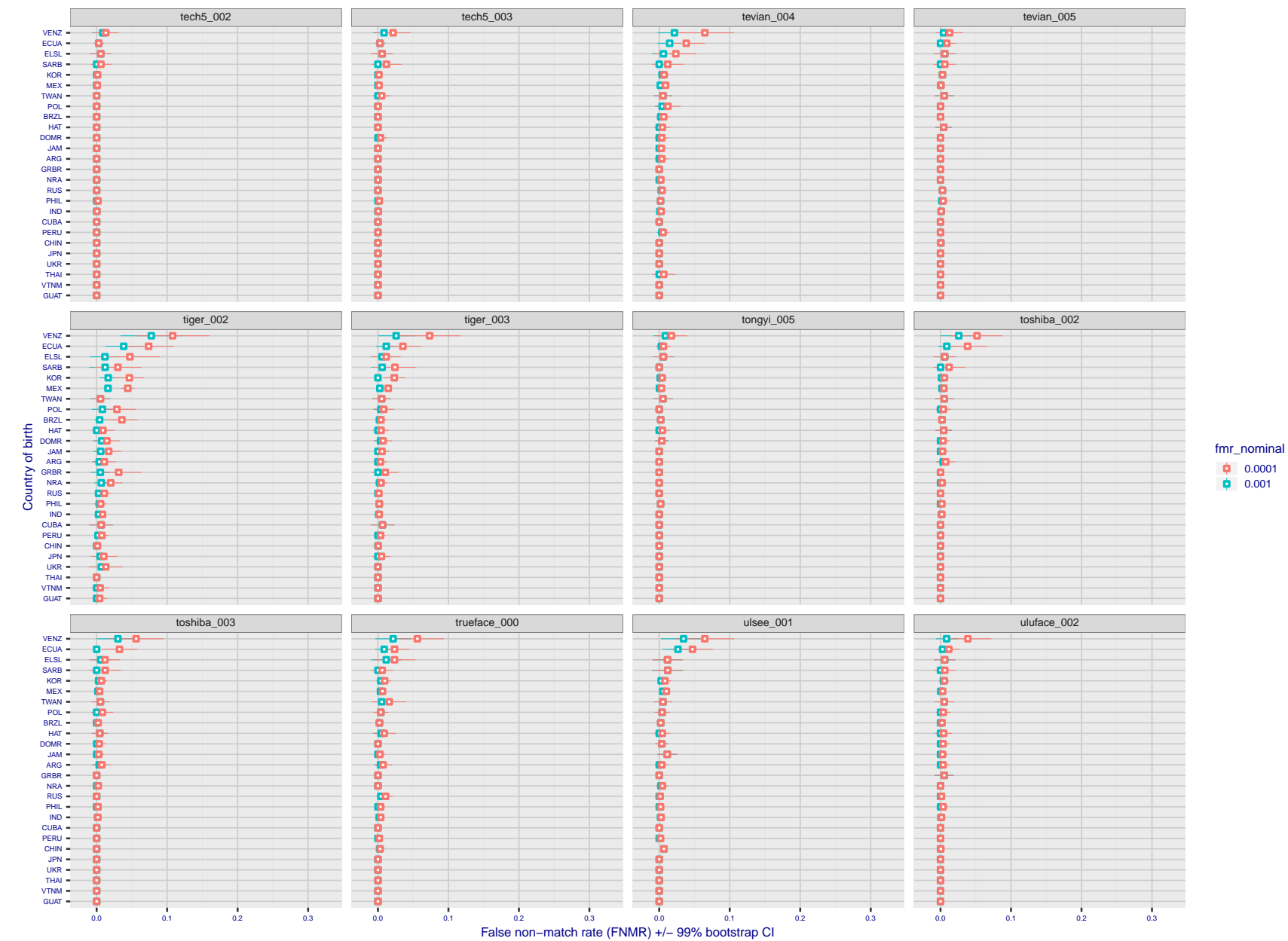


Figure 114: For the visa images, the dots show FNMR by country of birth for two globally set operating thresholds corresponding to  $FMR = \{0.001, 0.0001\}$  computed over all on the order of  $10^{10}$  impostor scores. The FMR in each bin will vary also - see subsequent impostor heatmaps in sec. 3.6.1. The figures shows an order of magnitude variation in FNMR across country of birth; these effects are likely due quality variations, then demographics like age and race. The error rates in some cases are zero, and in others the DET is flat so the error rates at the two thresholds are identical. The lines span 1% and 99% of bootstrap replicated FNMR estimates.

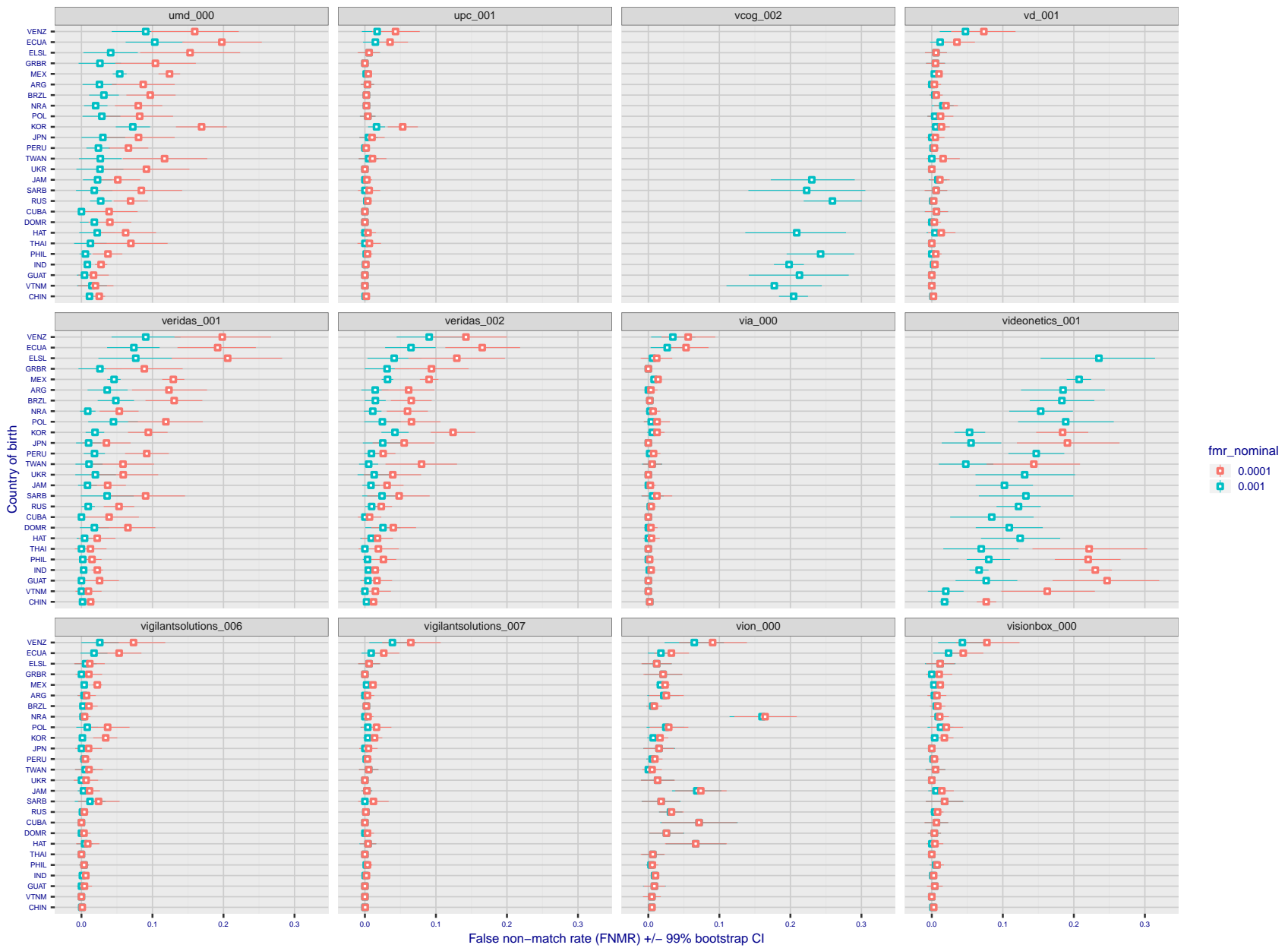


Figure 115: For the visa images, the dots show FNMR by country of birth for two globally set operating thresholds corresponding to  $FMR = \{0.001, 0.0001\}$  computed over all on the order of  $10^{10}$  impostor scores. The FMR in each bin will vary also - see subsequent impostor heatmaps in sec. 3.6.1. The figures shows an order of magnitude variation in FNMR across country of birth; these effects are likely due quality variations, then demographics like age and race. The error rates in some cases are zero, and in others the DET is flat so the error rates at the two thresholds are identical. The lines span 1% and 99% of bootstrap replicated FNMR estimates.

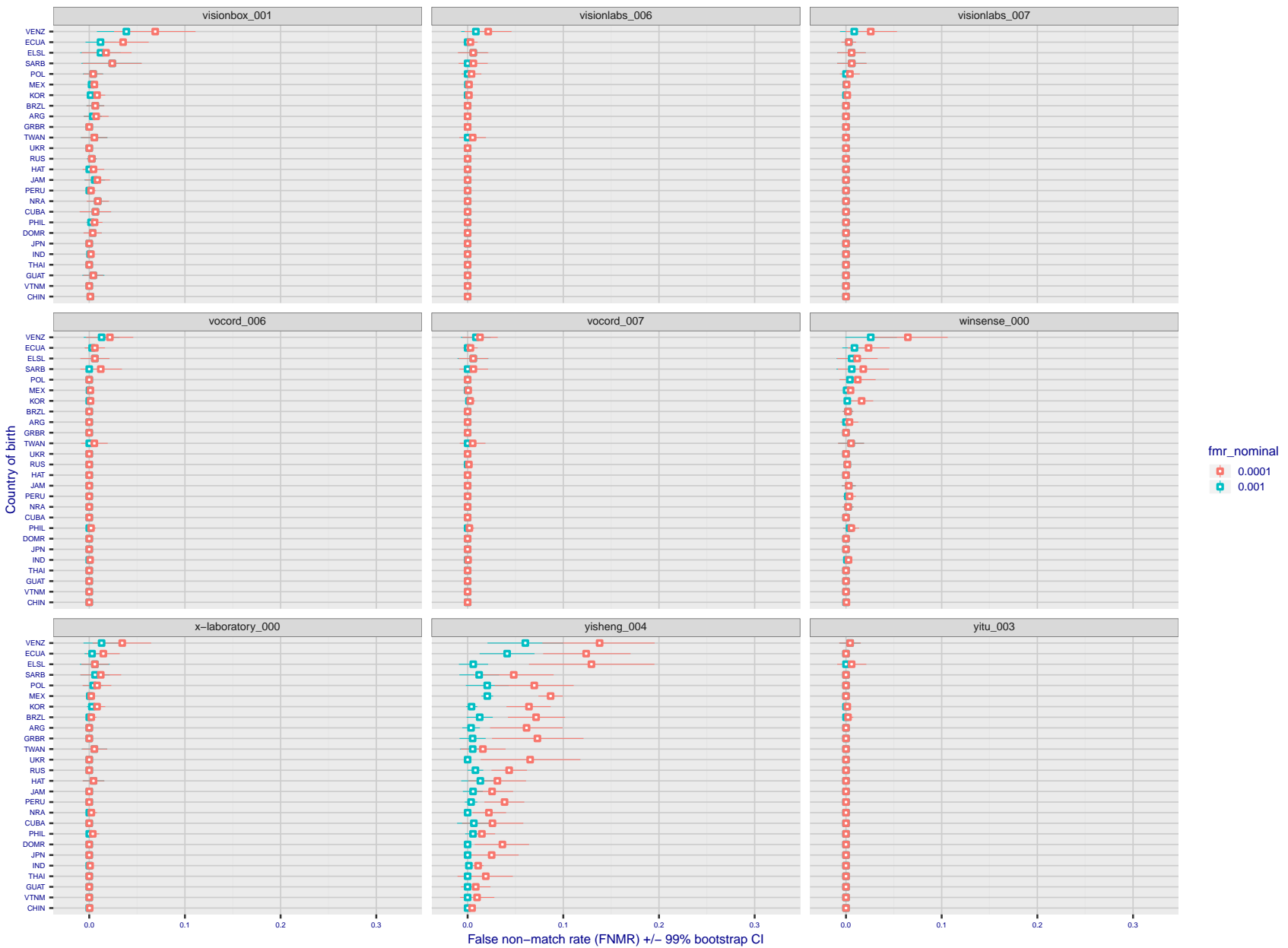


Figure 116: For the visa images, the dots show FNMR by country of birth for two globally set operating thresholds corresponding to  $FMR = \{0.001, 0.0001\}$  computed over all on the order of  $10^{10}$  impostor scores. The FMR in each bin will vary also - see subsequent impostor heatmaps in sec. 3.6.1. The figures shows an order of magnitude variation in FNMR across country of birth; these effects are likely due quality variations, then demographics like age and race. The error rates in some cases are zero, and in others the DET is flat so the error rates at the two thresholds are identical. The lines span 1% and 99% of bootstrap replicated FNMR estimates.

**Caveats:** The results may not relate to subject-specific properties. Instead they could reflect image-specific quality differences, which could occur due to collection protocol or software processing variations.

### 3.5.2 Effect of ageing

**Background:** Faces change appearance throughout life. This change gradually reduces similarity of a new image to an earlier image. Face recognition algorithms give reduced similarity scores and more frequent false rejections.

**Goal:** To quantify false non-match rates (FNMR) as a function of elapsed time in an adult population.

**Methods:** Using the mugshot images, a threshold is set to give FMR = 0.00001 over the entire impostor set. Then FNMR is measured over 1000 bootstrap replications of the genuine scores.

**Results:** For the visa images, Figure 126 shows how false non-match rates for genuine users, as a function of age group.

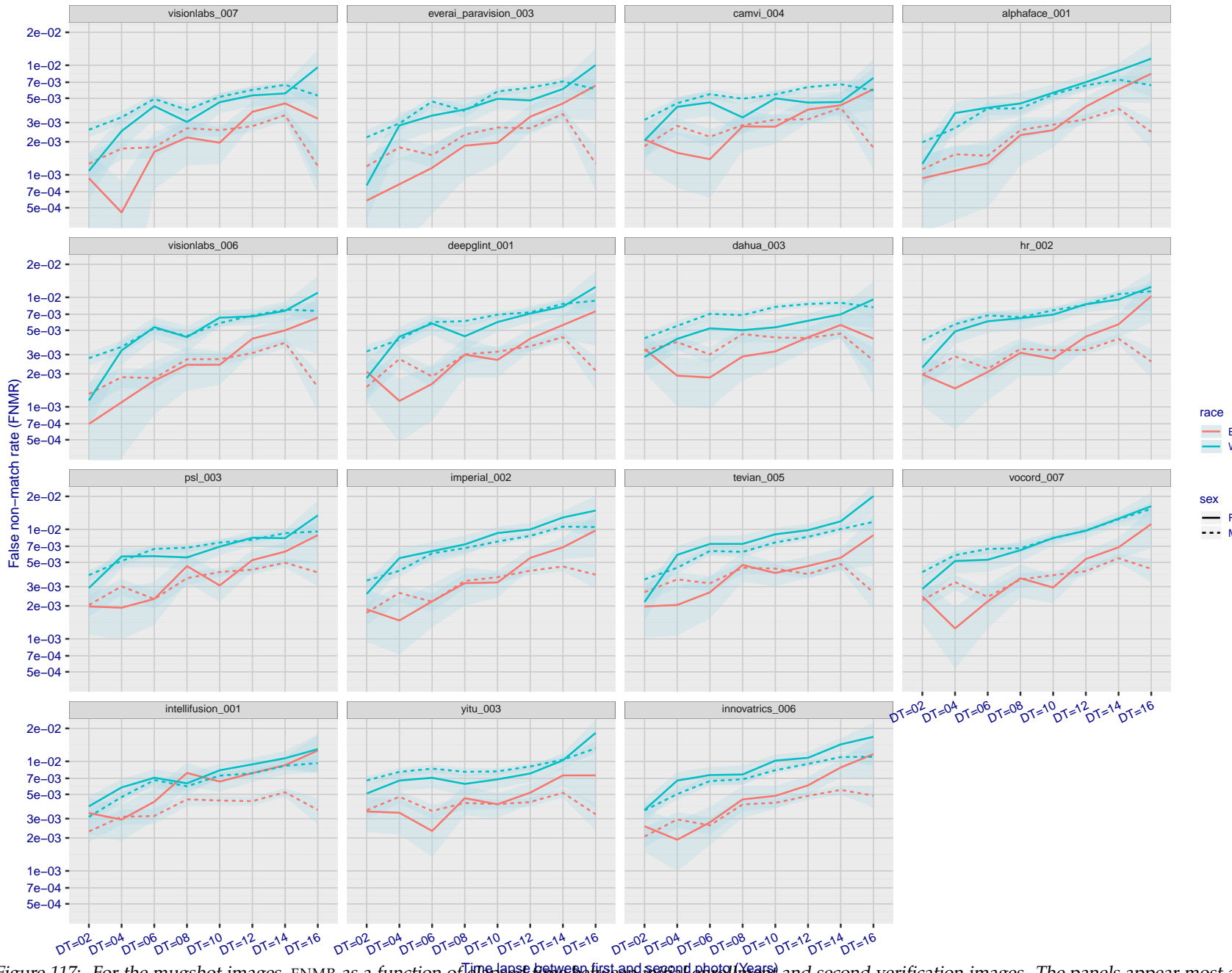


Figure 117: For the mugshot images, FNMR as a function of elapsed time between initial enrollment and second verification images. The panels appear most accurate first, and vertical scale changes on each page. The four traces correspond to images annotated with codes for black female, black male, white female, white male. The threshold is fixed for each algorithm to give FMR = 0.00001 over all ( $10^8$ ) impostor comparisons. For short time-lapses, the most accurate algorithms give very few errors (FNMR < 0.001) so that the uncertainty estimates are high.

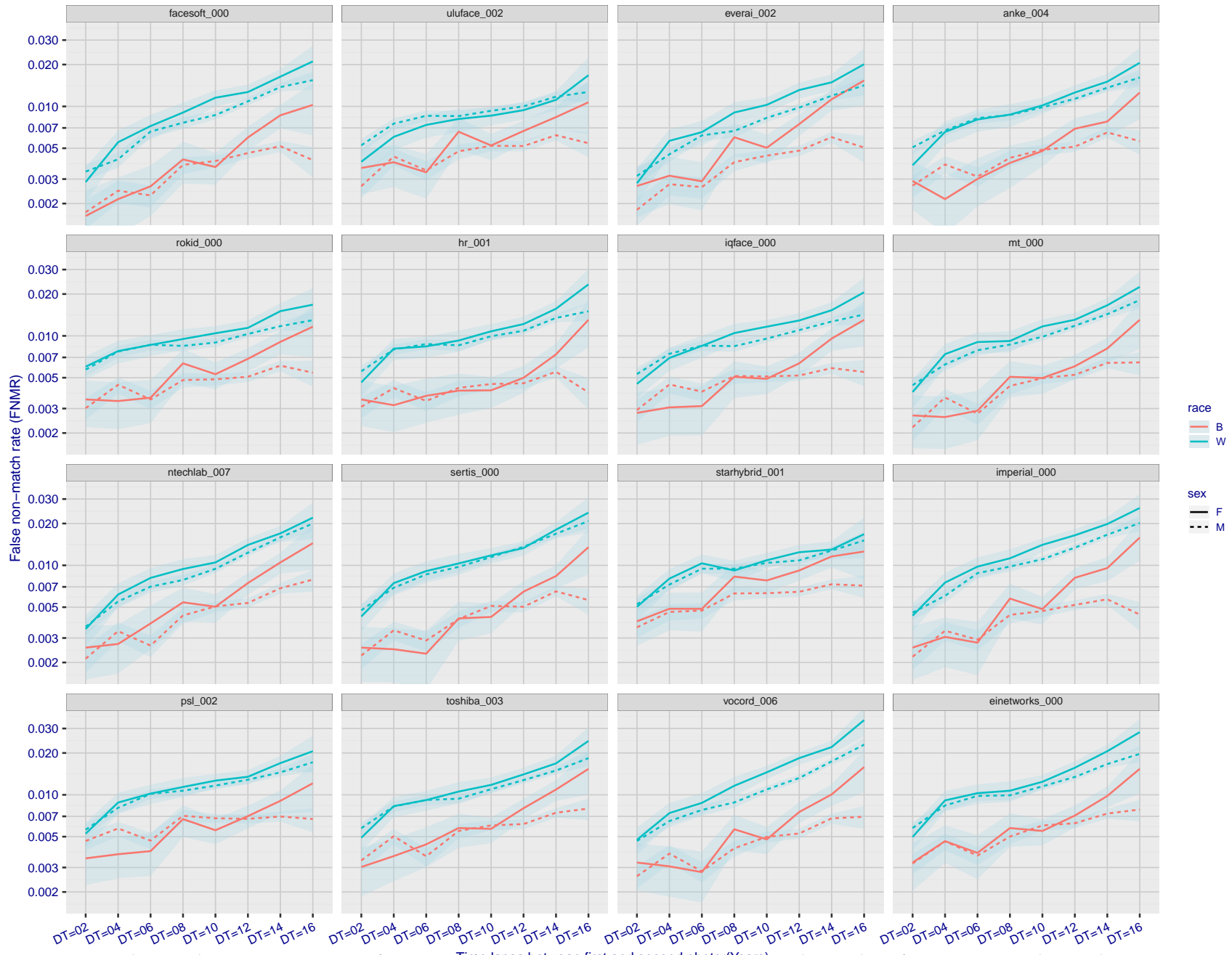


Figure 118: For the mugshot images, FNMR as a function of elapsed time between initial enrollment and second verification images. The panels appear most accurate first, and vertical scale changes on each page. The four traces correspond to images annotated with codes for black female, black male, white female, white male. The threshold is fixed for each algorithm to give FMR = 0.00001 over all ( $10^8$ ) impostor comparisons. For short time-lapses, the most accurate algorithms give very few errors (FNMR < 0.001) so that the uncertainty estimates are high.

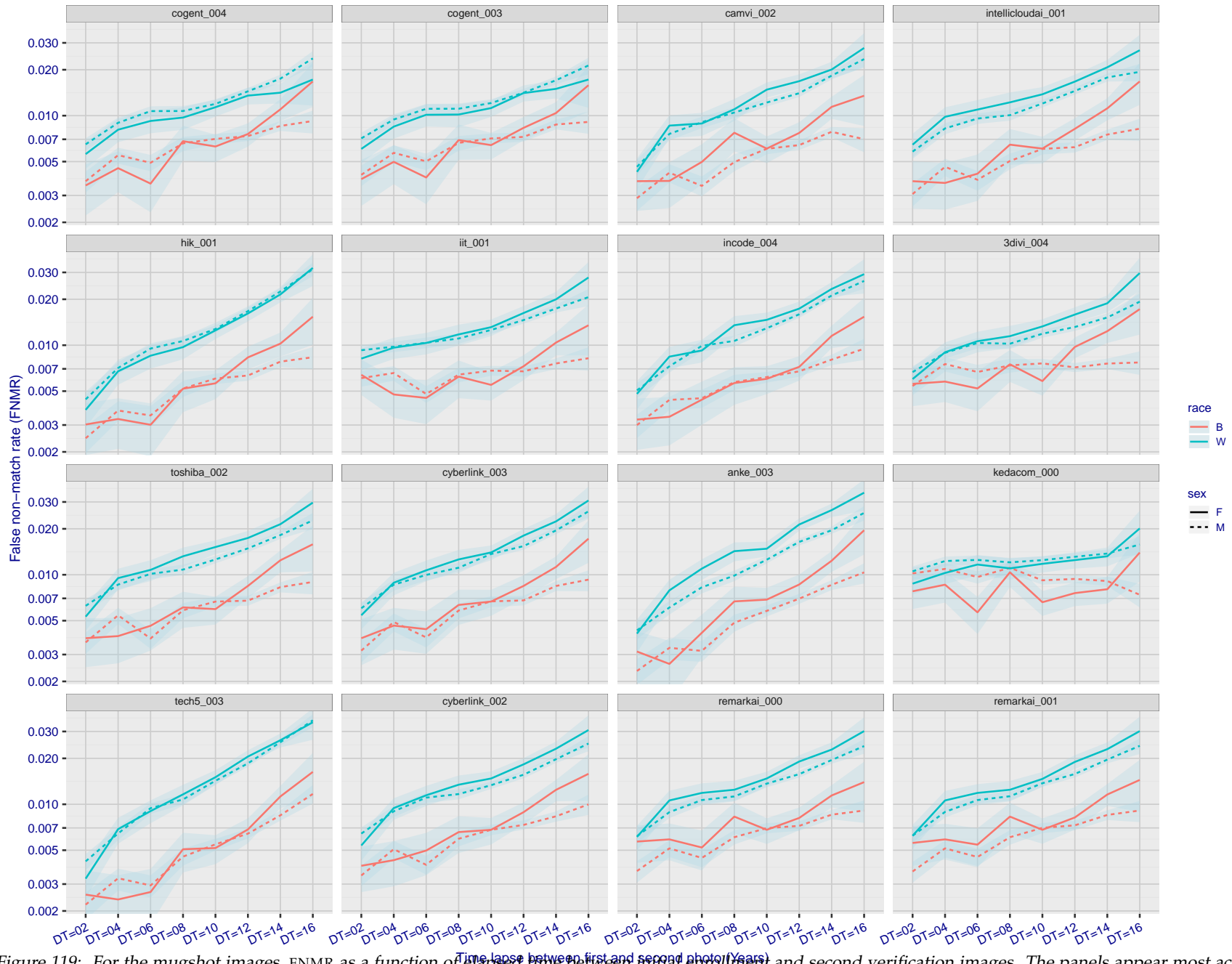


Figure 119: For the mugshot images, FNMR as a function of elapsed time between initial enrollment and second verification images. The panels appear most accurate first, and vertical scale changes on each page. The four traces correspond to images annotated with codes for black female, black male, white female, white male. The threshold is fixed for each algorithm to give  $FMR = 0.00001$  over all ( $10^8$ ) impostor comparisons. For short time-lapses, the most accurate algorithms give very few errors ( $FNMR < 0.001$ ) so that the uncertainty estimates are high.

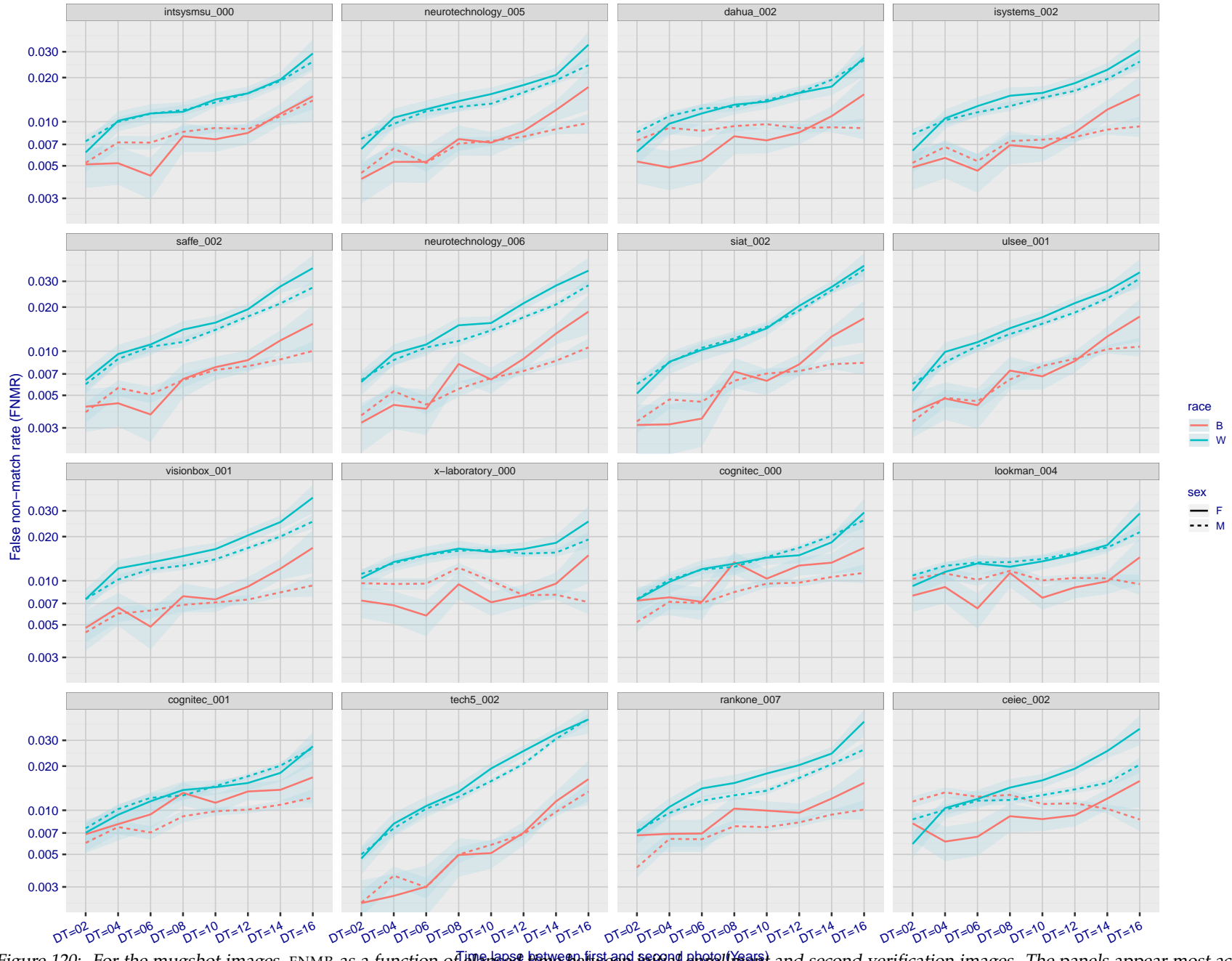


Figure 120: For the mugshot images, FNMR as a function of elapsed time between initial enrollment and second verification images. The panels appear most accurate first, and vertical scale changes on each page. The four traces correspond to images annotated with codes for black female, black male, white female, white male. The threshold is fixed for each algorithm to give FMR = 0.00001 over all ( $10^8$ ) impostor comparisons. For short time-lapses, the most accurate algorithms give very few errors (FNMR < 0.001) so that the uncertainty estimates are high.

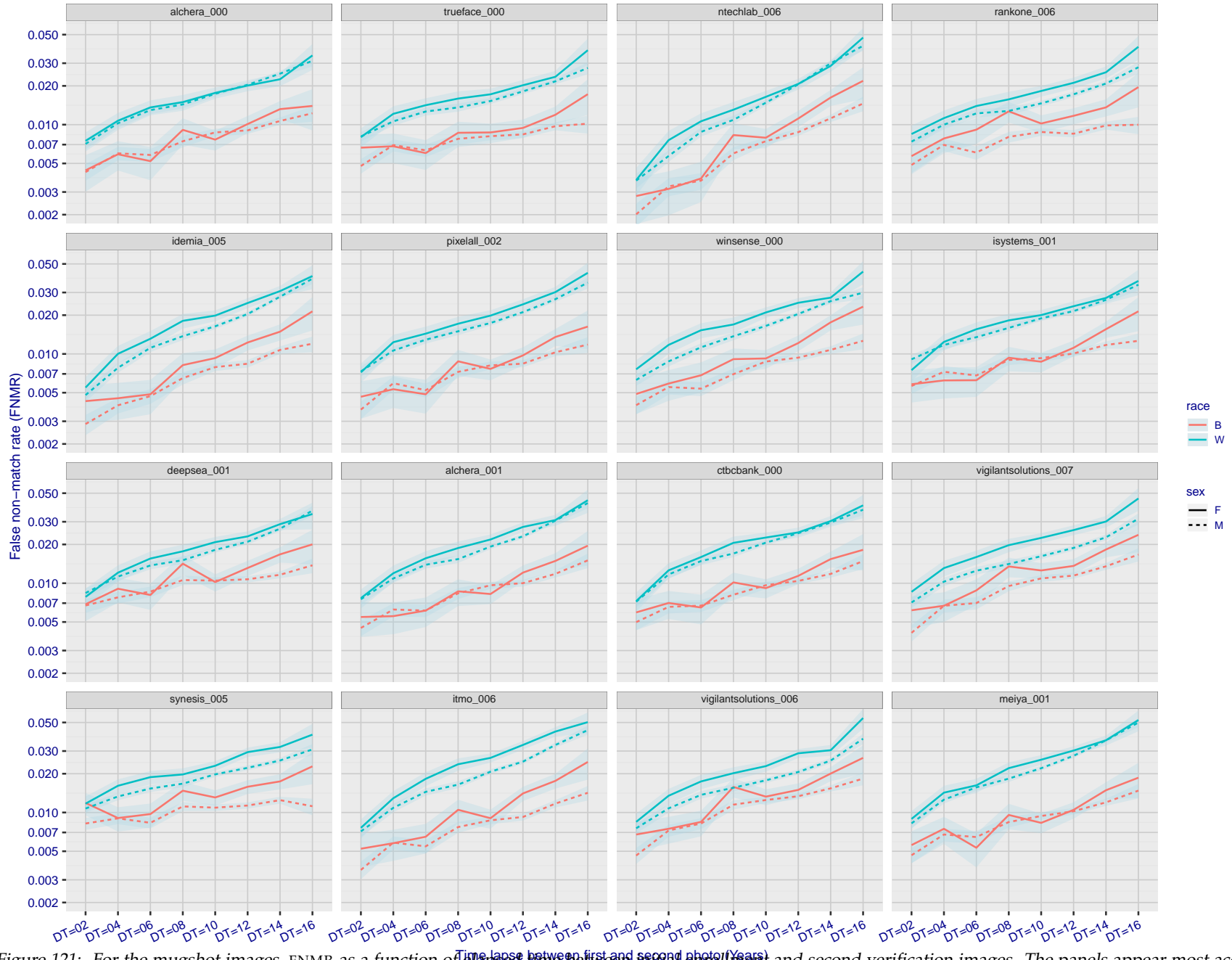


Figure 121: For the mugshot images, FNMR as a function of elapsed time between initial enrollment and second verification images. The panels appear most accurate first, and vertical scale changes on each page. The four traces correspond to images annotated with codes for black female, black male, white female, white male. The threshold is fixed for each algorithm to give FMR = 0.00001 over all ( $10^8$ ) impostor comparisons. For short time-lapses, the most accurate algorithms give very few errors (FNMR < 0.001) so that the uncertainty estimates are high.

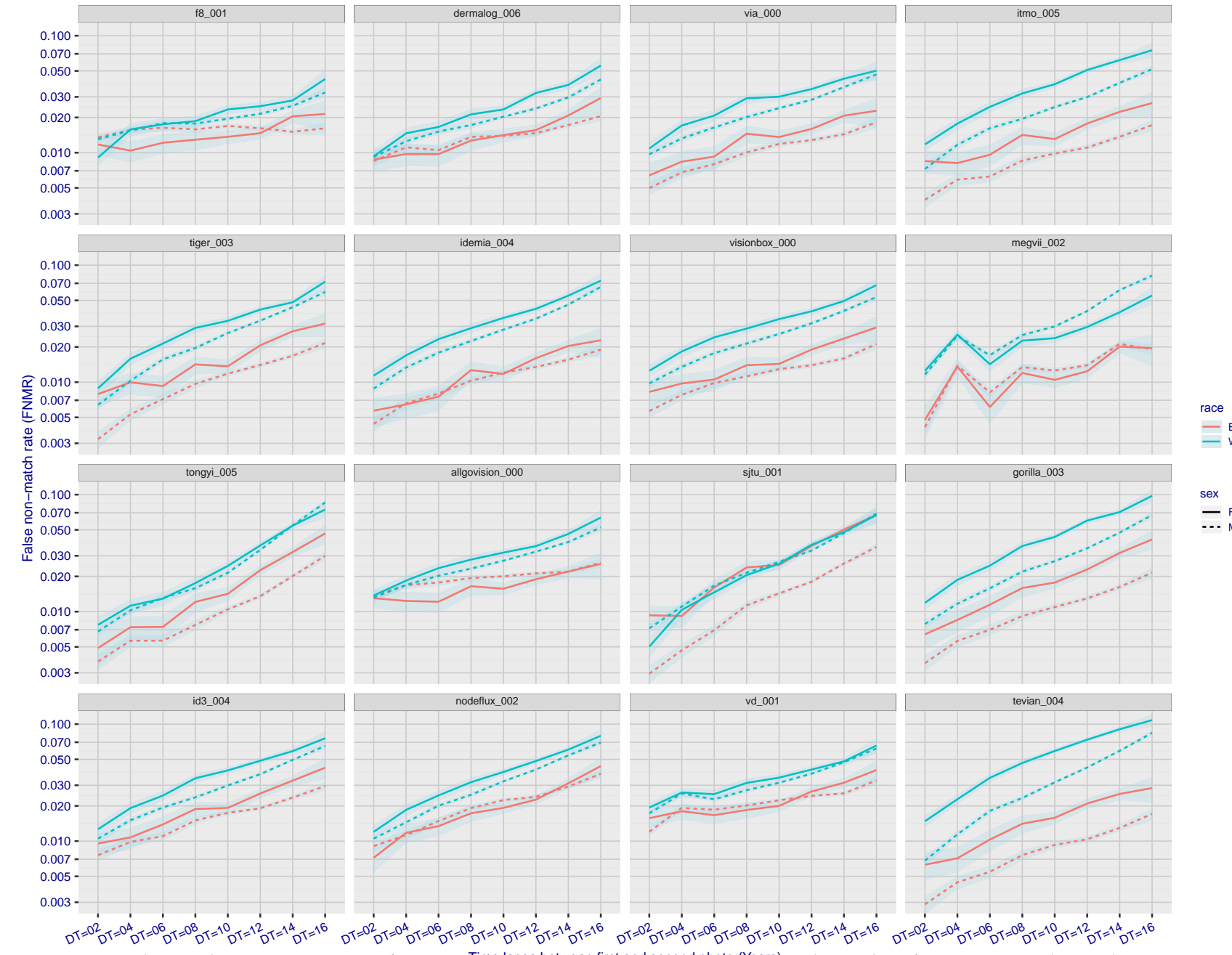


Figure 122: For the mugshot images, FNMR as a function of elapsed time between initial enrollment and second verification images. The panels appear most accurate first, and vertical scale changes on each page. The four traces correspond to images annotated with codes for black female, black male, white female, white male. The threshold is fixed for each algorithm to give FMR = 0.00001 over all ( $10^8$ ) impostor comparisons. For short time-lapses, the most accurate algorithms give very few errors (FNMR < 0.001) so that the uncertainty estimates are high.

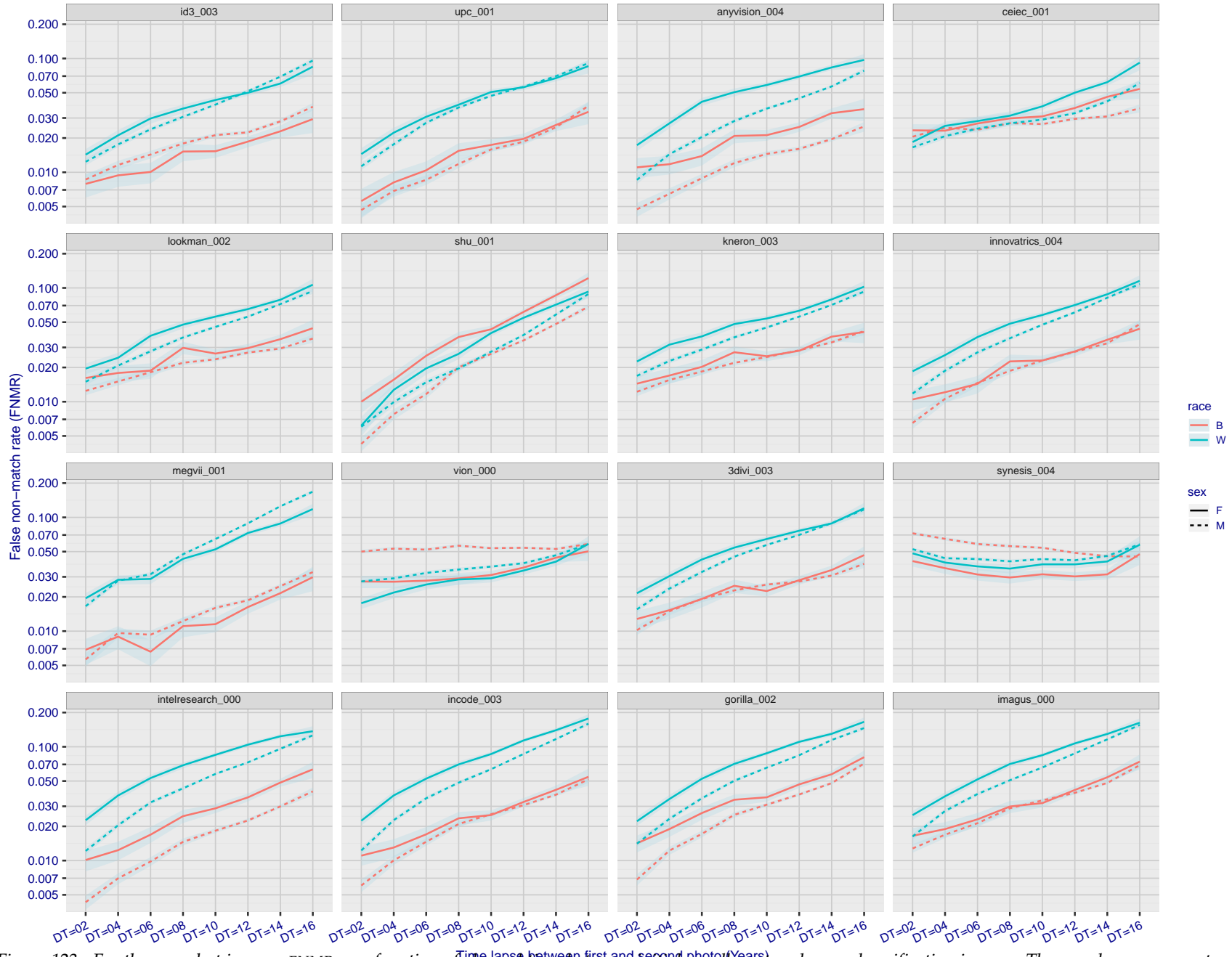


Figure 123: For the mugshot images, FNMR as a function of elapsed time between initial enrollment and second verification images. The panels appear most accurate first, and vertical scale changes on each page. The four traces correspond to images annotated with codes for black female, black male, white female, white male. The threshold is fixed for each algorithm to give FMR = 0.00001 over all ( $10^8$ ) impostor comparisons. For short time-lapses, the most accurate algorithms give very few errors (FNMR < 0.001) so that the uncertainty estimates are high.

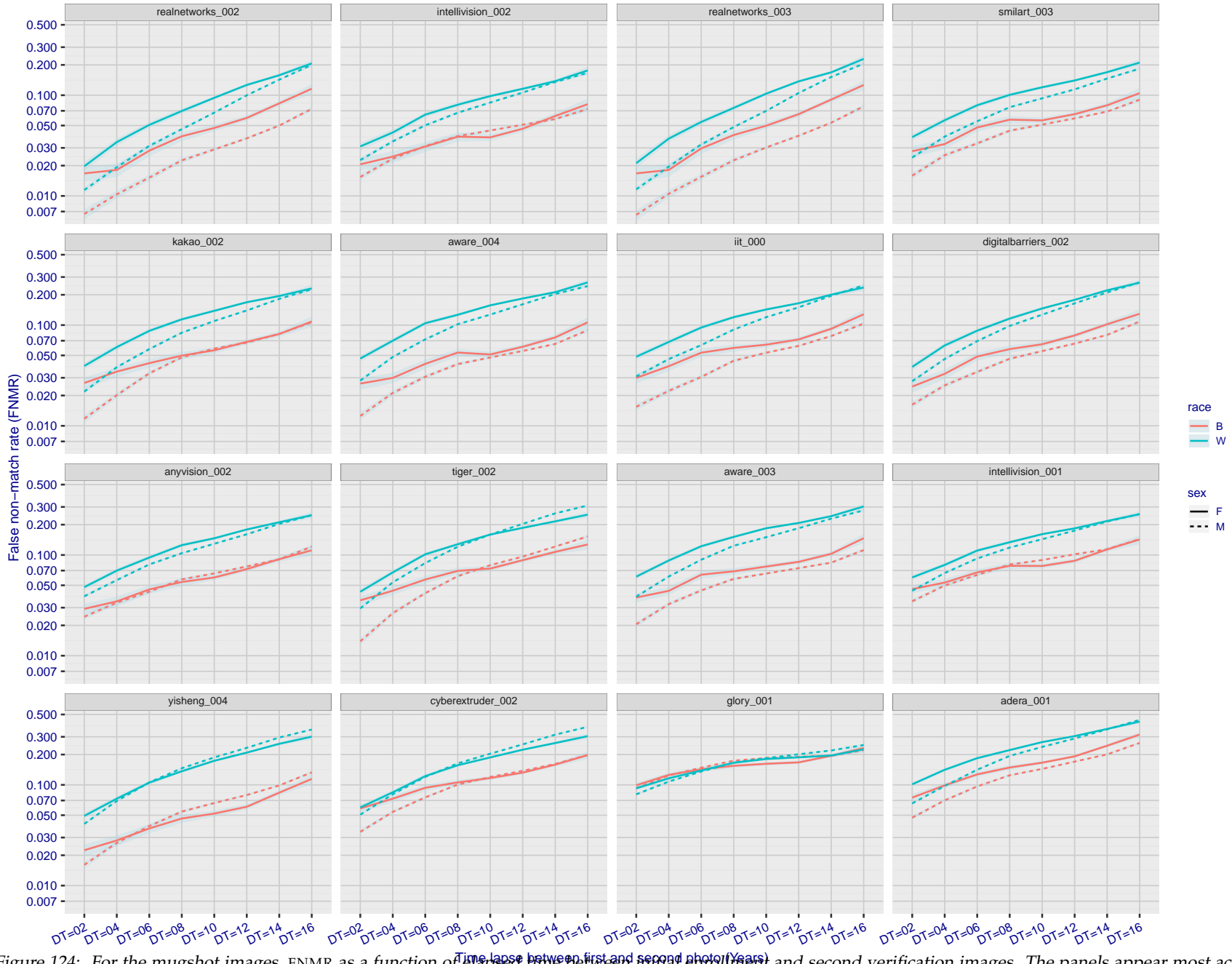


Figure 124: For the mugshot images, FNMR as a function of elapsed time between initial enrollment and second verification images. The panels appear most accurate first, and vertical scale changes on each page. The four traces correspond to images annotated with codes for black female, black male, white female, white male. The threshold is fixed for each algorithm to give FMR = 0.00001 over all ( $10^8$ ) impostor comparisons. For short time-lapses, the most accurate algorithms give very few errors (FNMR < 0.001) so that the uncertainty estimates are high.

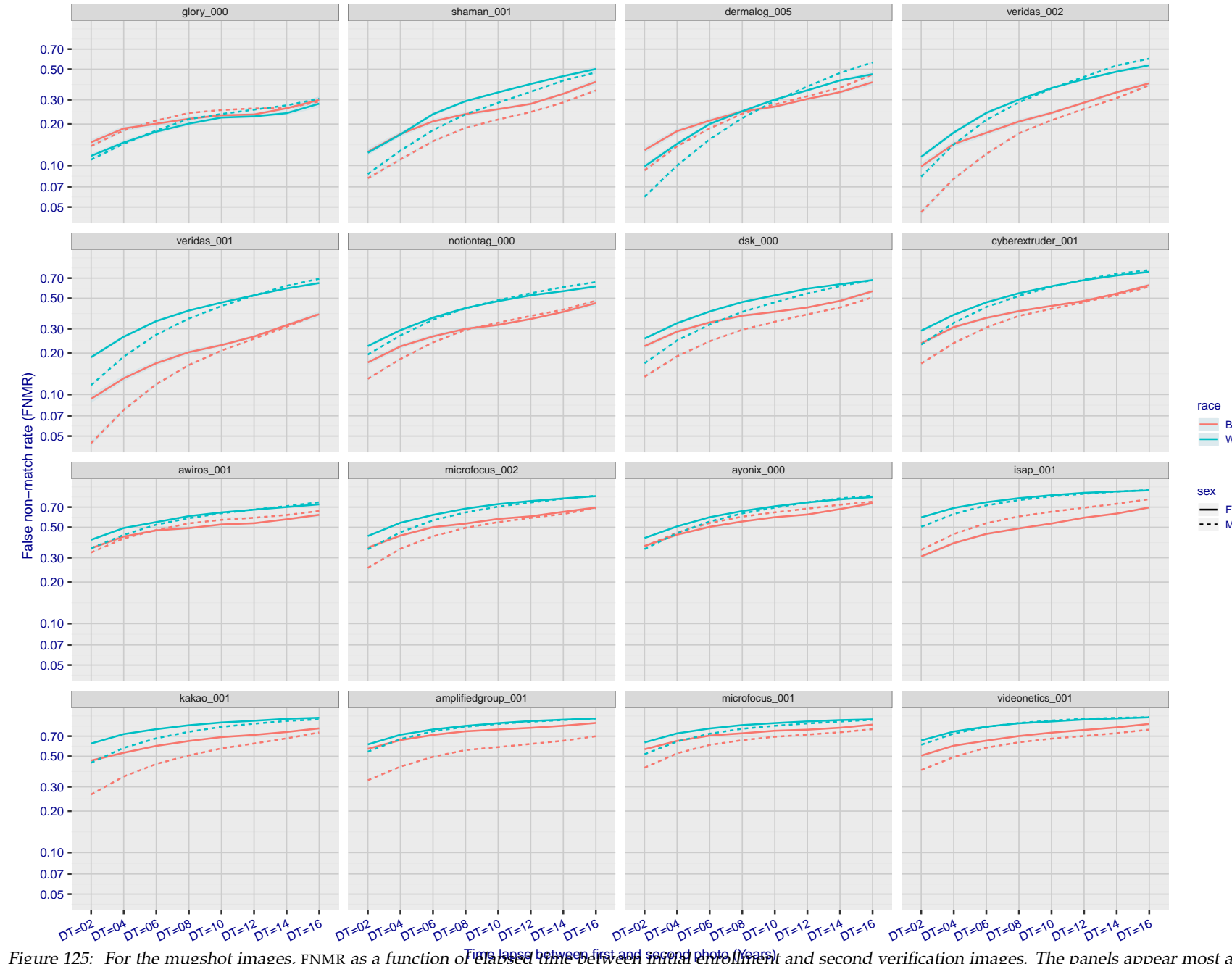


Figure 125: For the mugshot images, FNMR as a function of elapsed time between initial enrollment and second verification images. The panels appear most accurate first, and vertical scale changes on each page. The four traces correspond to images annotated with codes for black female, black male, white female, white male. The threshold is fixed for each algorithm to give  $FMR = 0.00001$  over all ( $10^8$ ) impostor comparisons. For short time-lapses, the most accurate algorithms give very few errors ( $FNMR < 0.001$ ) so that the uncertainty estimates are high.

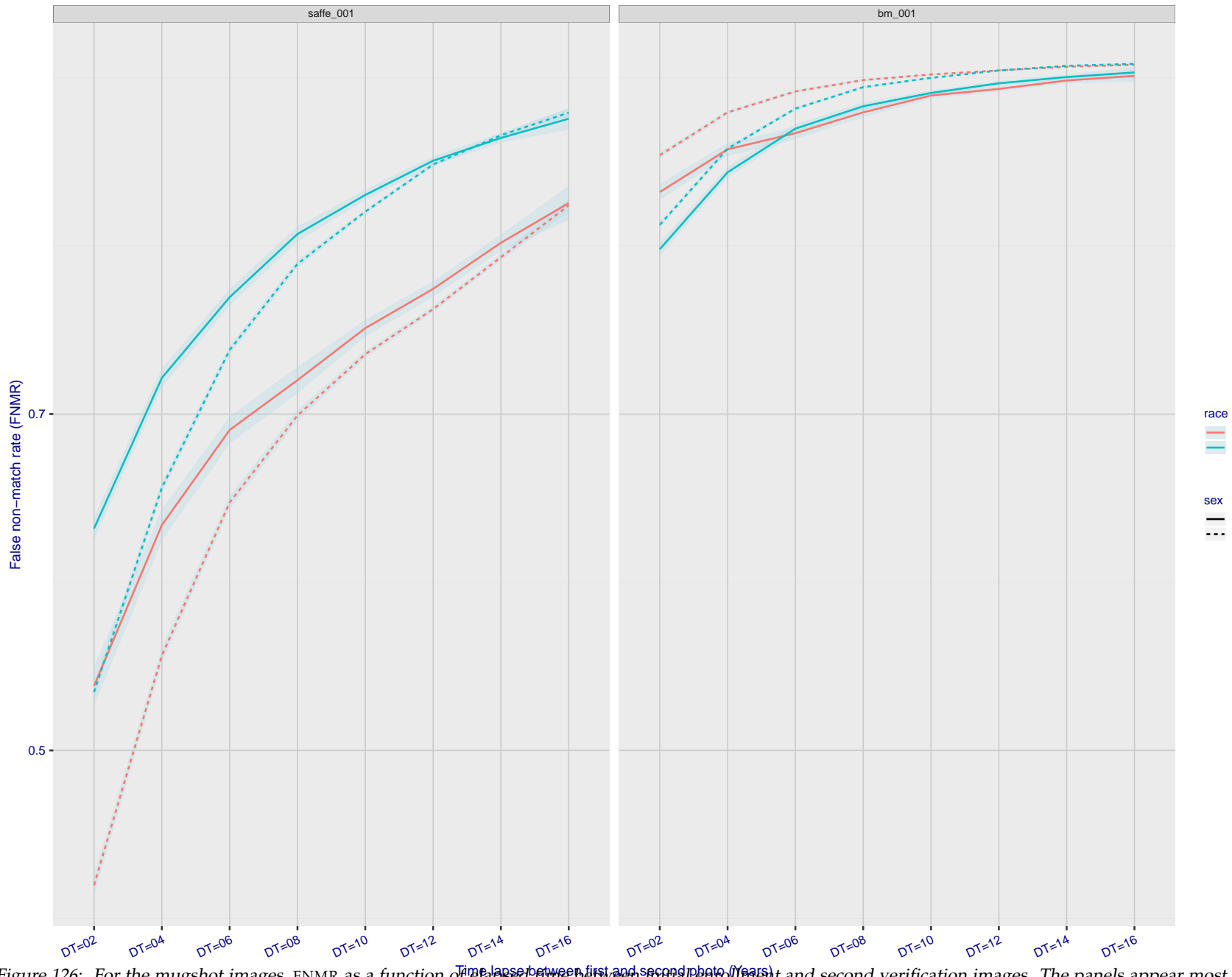


Figure 126: For the mugshot images, FNMR as a function of elapsed time between initial enrollment and second verification images. The panels appear most accurate first, and vertical scale changes on each page. The four traces correspond to images annotated with codes for black female, black male, white female, white male. The threshold is fixed for each algorithm to give FMR = 0.00001 over all ( $10^8$ ) impostor comparisons. For short time-lapses, the most accurate algorithms give very few errors (FNMR < 0.001) so that the uncertainty estimates are high.

### 3.5.3 Effect of age on genuine subjects

**Background:** Faces change appearance throughout life. Face recognition algorithms have previously been reported to give better accuracy on older individuals (See NIST IR 8009).

**Goal:** To quantify false non-match rates (FNMR) as a function of age, without an ageing component.

**Methods:** Using the visa images, which span fewer than five years, thresholds are determined that give FMR = 0.001 and 0.0001 over the entire impostor set. Then FNMR is measured over 1000 bootstrap replications of the genuine scores.

**Results:** For the visa images, Figure 139 shows how false non-match rates for genuine users, as a function of age group.

The notable aspects are:

- ▷ Younger subjects give considerably higher FNMR. This is likely due to rapid growth and change in facial appearance.
- ▷ FNMR trends down throughout life. The last bin, AGE > 72, contains fewer than 140 mated pairs, and may be affected by small sample size.

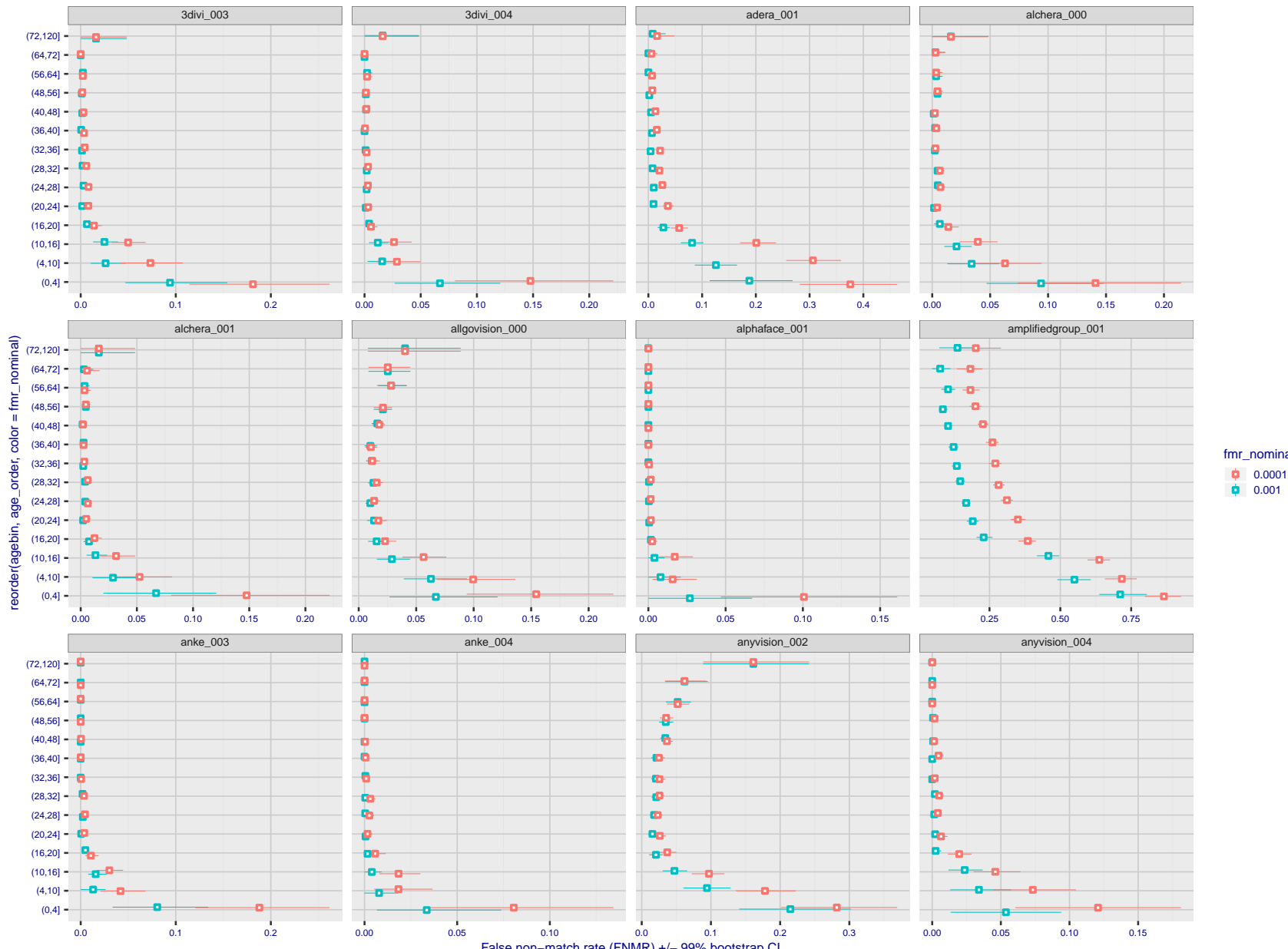


Figure 127: For the visa images, the dots show FNMR by age group for two operating thresholds corresponding to  $FMR = \{0.001, 0.0001\}$  computed over all on the order of  $10^{10}$  impostor scores. The FMR in each bin will vary also - see subsequent impostor heatmaps in sec. 3.6.2. Given a pair of face images taken at different times, we assign the comparison to the bin that is the arithmetic average of the subject's ages. This plot shows only the effect of age, not ageing. The number of comparisons in each bin is generally in the thousands, however the first and last bins are computed over 149 and 124 respectively. The error rates in some (adult) cases are zero, and in others the DET is flat so the error rates at the two thresholds are identical. The lines span 1% and 99% of bootstrap replicated FNMR estimates.

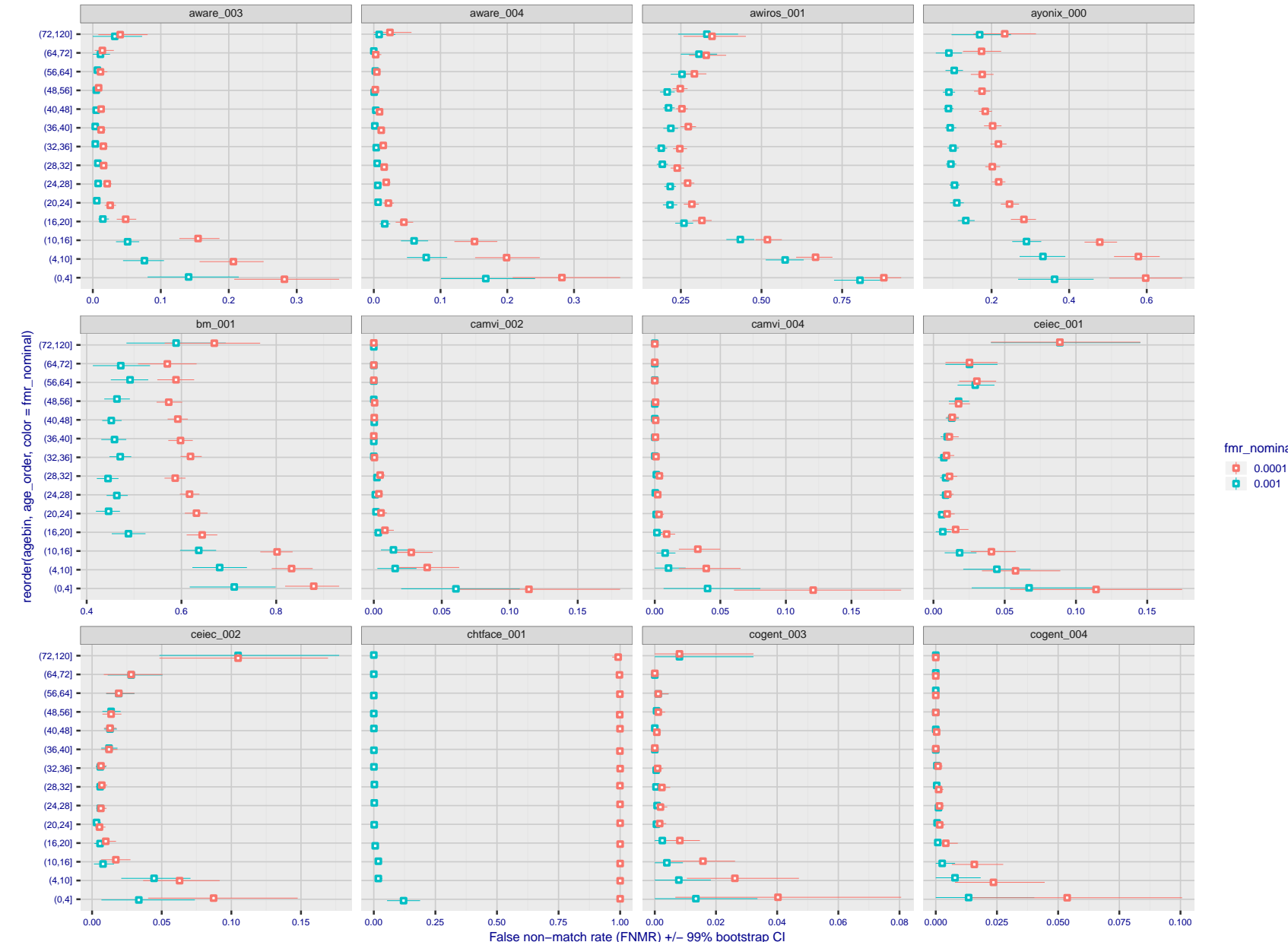


Figure 128: For the visa images, the dots show FNMR by age group for two operating thresholds corresponding to  $FMR = \{0.001, 0.0001\}$  computed over all on the order of  $10^{10}$  impostor scores. The FMR in each bin will vary also - see subsequent impostor heatmaps in sec. 3.6.2. Given a pair of face images taken at different times, we assign the comparison to the bin that is the arithmetic average of the subject's ages. This plot shows only the effect of age, not ageing. The number of comparisons in each bin is generally in the thousands, however the first and last bins are computed over 149 and 124 respectively. The error rates in some (adult) cases are zero, and in others the DET is flat so the error rates at the two thresholds are identical. The lines span 1% and 99% of bootstrap replicated FNMR estimates.

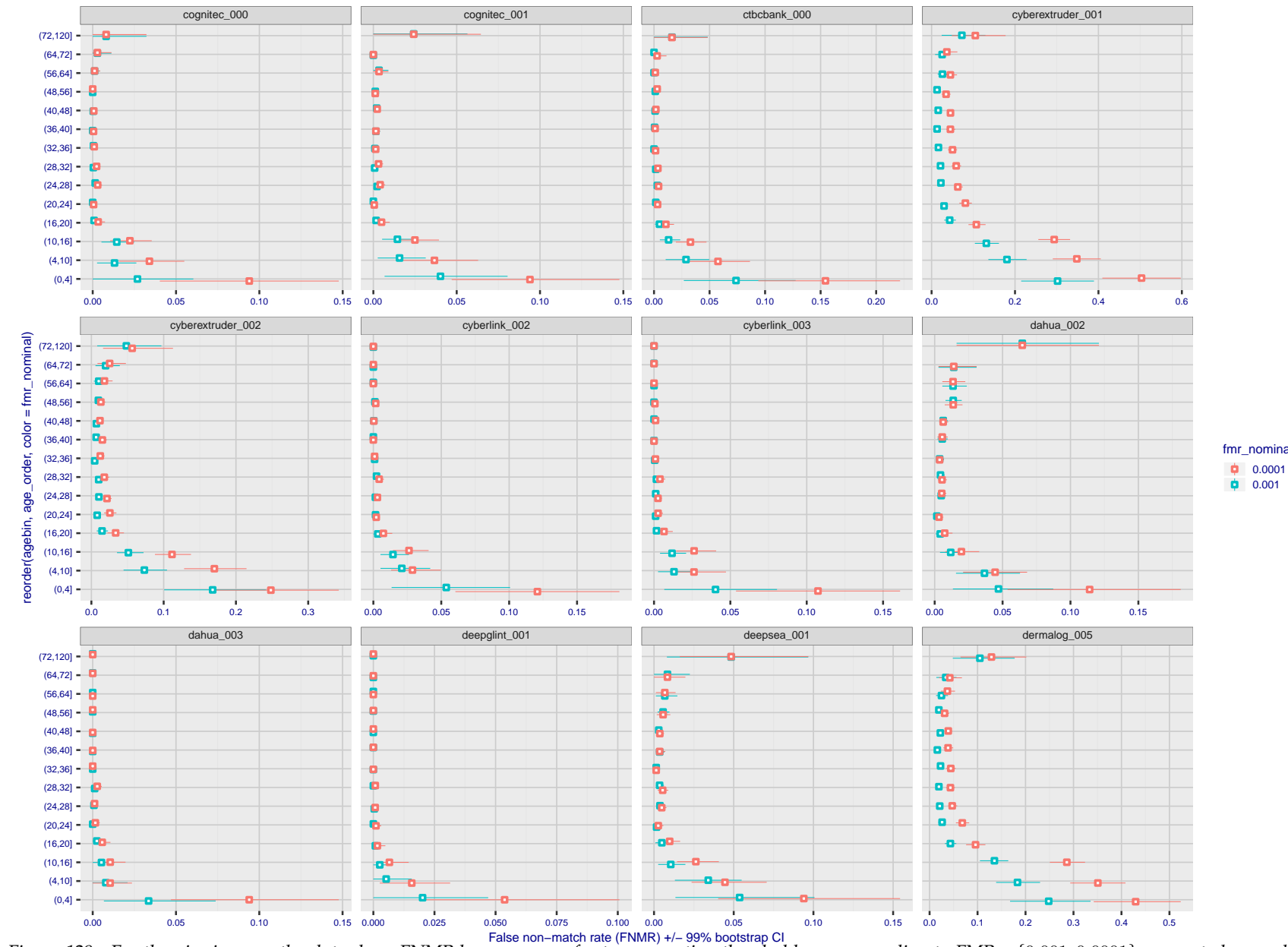


Figure 129: For the visa images, the dots show FNMR by age group for two operating thresholds corresponding to  $FMR = \{0.001, 0.0001\}$  computed over all on the order of  $10^{10}$  impostor scores. The FMR in each bin will vary also - see subsequent impostor heatmaps in sec. 3.6.2. Given a pair of face images taken at different times, we assign the comparison to the bin that is the arithmetic average of the subject's ages. This plot shows only the effect of age, not ageing. The number of comparisons in each bin is generally in the thousands, however the first and last bins are computed over 149 and 124 respectively. The error rates in some (adult) cases are zero, and in others the DET is flat so the error rates at the two thresholds are identical. The lines span 1% and 99% of bootstrap replicated FNMR estimates.

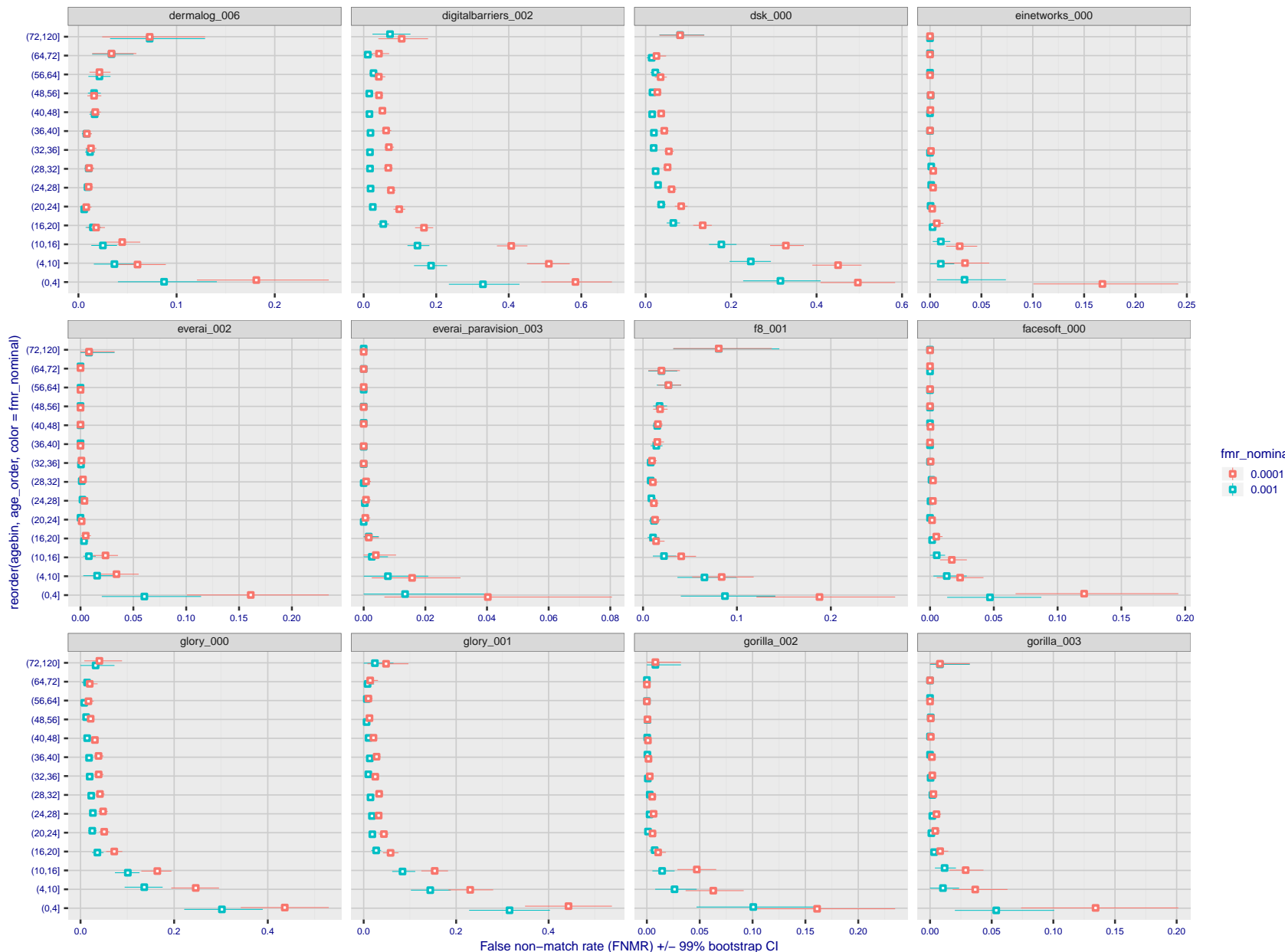


Figure 130: For the visa images, the dots show FNMR by age group for two operating thresholds corresponding to  $FMR = \{0.001, 0.0001\}$  computed over all on the order of  $10^{10}$  impostor scores. The FMR in each bin will vary also - see subsequent impostor heatmaps in sec. 3.6.2. Given a pair of face images taken at different times, we assign the comparison to the bin that is the arithmetic average of the subject's ages. This plot shows only the effect of age, not ageing. The number of comparisons in each bin is generally in the thousands, however the first and last bins are computed over 149 and 124 respectively. The error rates in some (adult) cases are zero, and in others the DET is flat so the error rates at the two thresholds are identical. The lines span 1% and 99% of bootstrap replicated FNMR estimates.



False non-match rate (FNMR) +/- 99% bootstrap CI

Figure 131: For the visa images, the dots show FNMR by age group for two operating thresholds corresponding to  $FMR = \{0.001, 0.0001\}$  computed over all on the order of  $10^{10}$  impostor scores. The FMR in each bin will vary also - see subsequent impostor heatmaps in sec. 3.6.2. Given a pair of face images taken at different times, we assign the comparison to the bin that is the arithmetic average of the subject's ages. This plot shows only the effect of age, not ageing. The number of comparisons in each bin is generally in the thousands, however the first and last bins are computed over 149 and 124 respectively. The error rates in some (adult) cases are zero, and in others the DET is flat so the error rates at the two thresholds are identical. The lines span 1% and 99% of bootstrap replicated FNMR estimates.

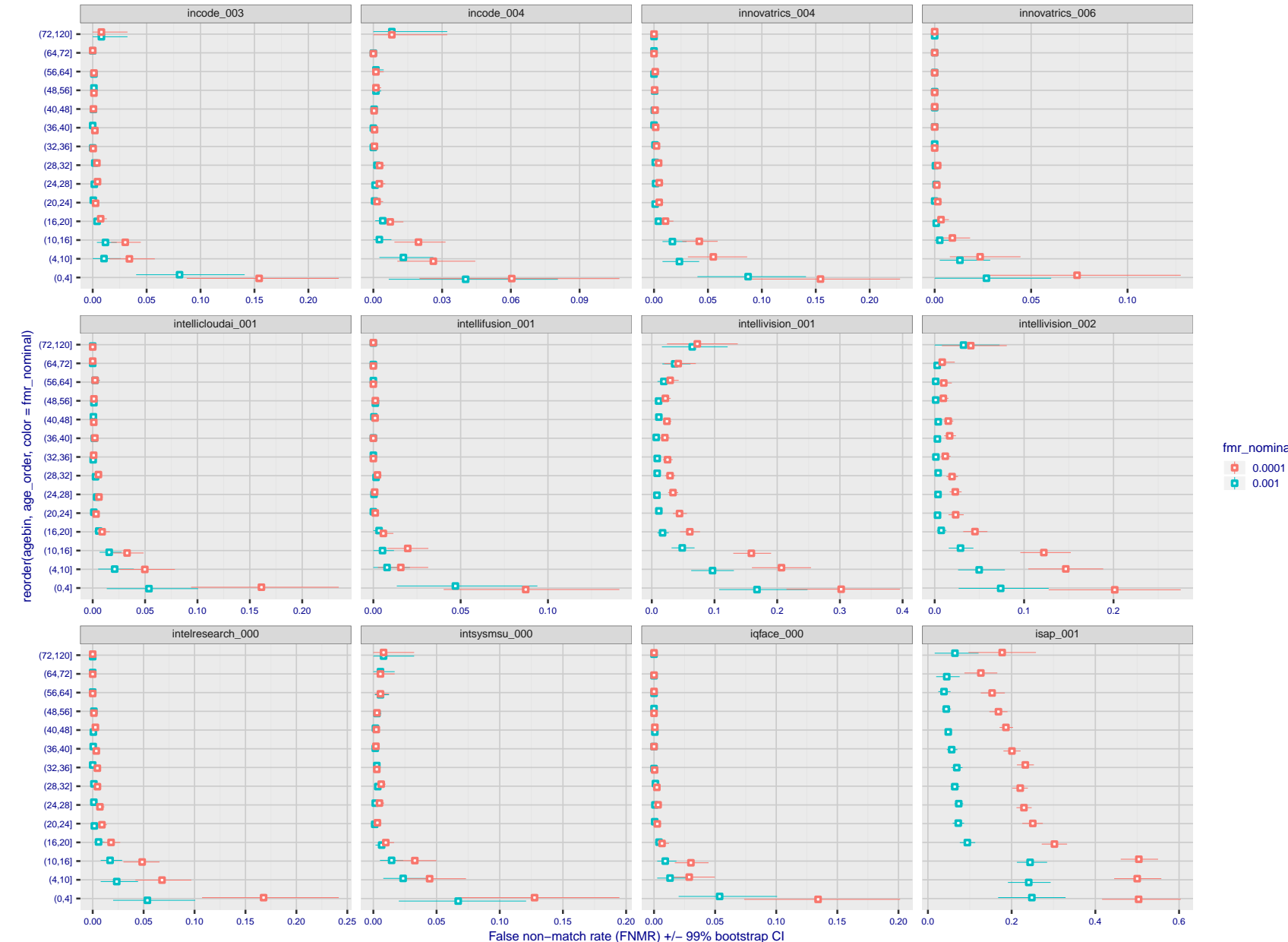


Figure 132: For the visa images, the dots show FNMR by age group for two operating thresholds corresponding to  $FMR = \{0.001, 0.0001\}$  computed over all on the order of  $10^{10}$  impostor scores. The FMR in each bin will vary also - see subsequent impostor heatmaps in sec. 3.6.2. Given a pair of face images taken at different times, we assign the comparison to the bin that is the arithmetic average of the subject's ages. This plot shows only the effect of age, not ageing. The number of comparisons in each bin is generally in the thousands, however the first and last bins are computed over 149 and 124 respectively. The error rates in some (adult) cases are zero, and in others the DET is flat so the error rates at the two thresholds are identical. The lines span 1% and 99% of bootstrap replicated FNMR estimates.

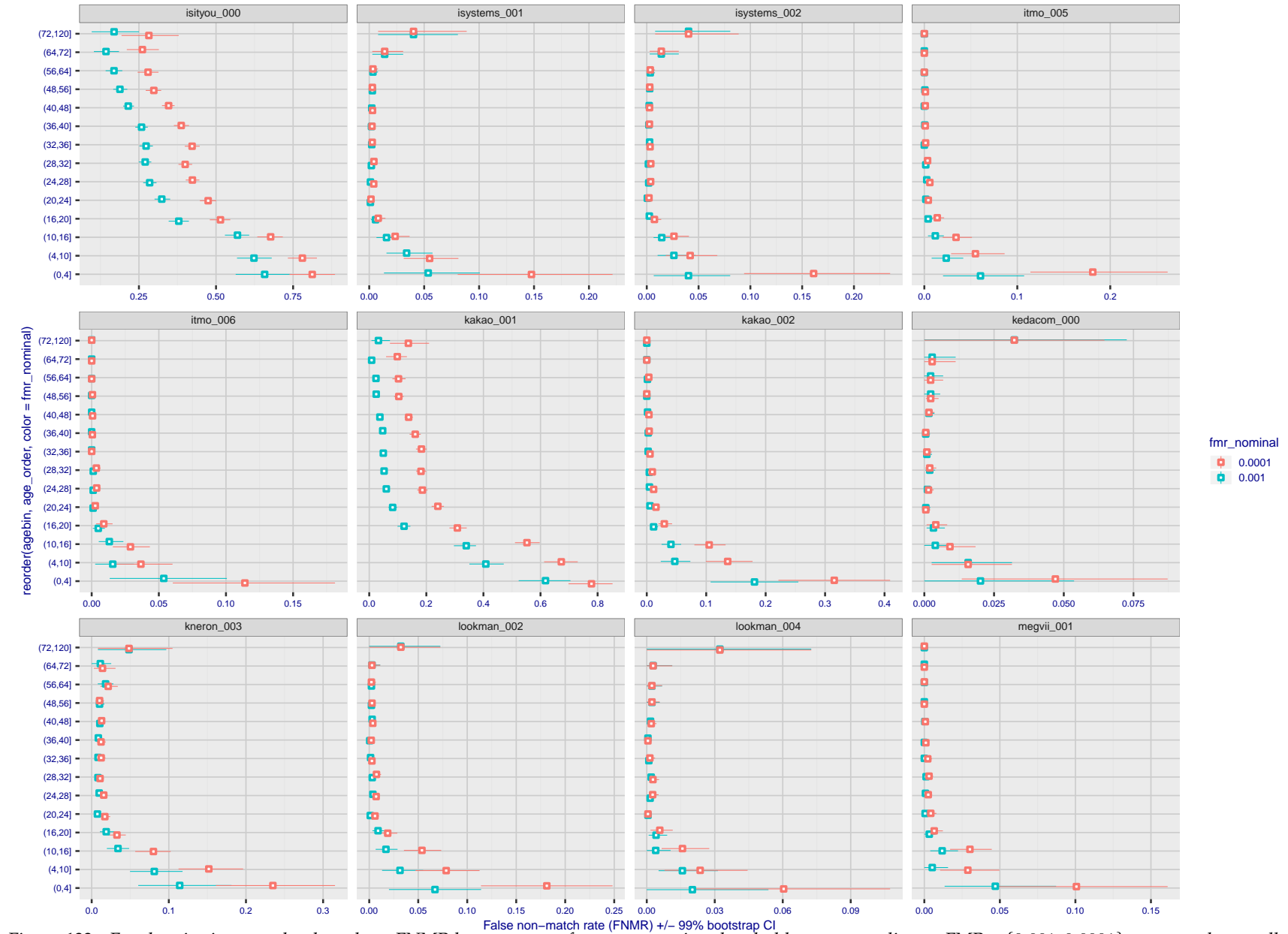


Figure 133: For the visa images, the dots show FNMR by age group for two operating thresholds corresponding to  $FMR = \{0.001, 0.0001\}$  computed over all on the order of  $10^{10}$  impostor scores. The FMR in each bin will vary also - see subsequent impostor heatmaps in sec. 3.6.2. Given a pair of face images taken at different times, we assign the comparison to the bin that is the arithmetic average of the subject's ages. This plot shows only the effect of age, not ageing. The number of comparisons in each bin is generally in the thousands, however the first and last bins are computed over 149 and 124 respectively. The error rates in some (adult) cases are zero, and in others the DET is flat so the error rates at the two thresholds are identical. The lines span 1% and 99% of bootstrap replicated FNMR estimates.

2019/10/16 12:43:37

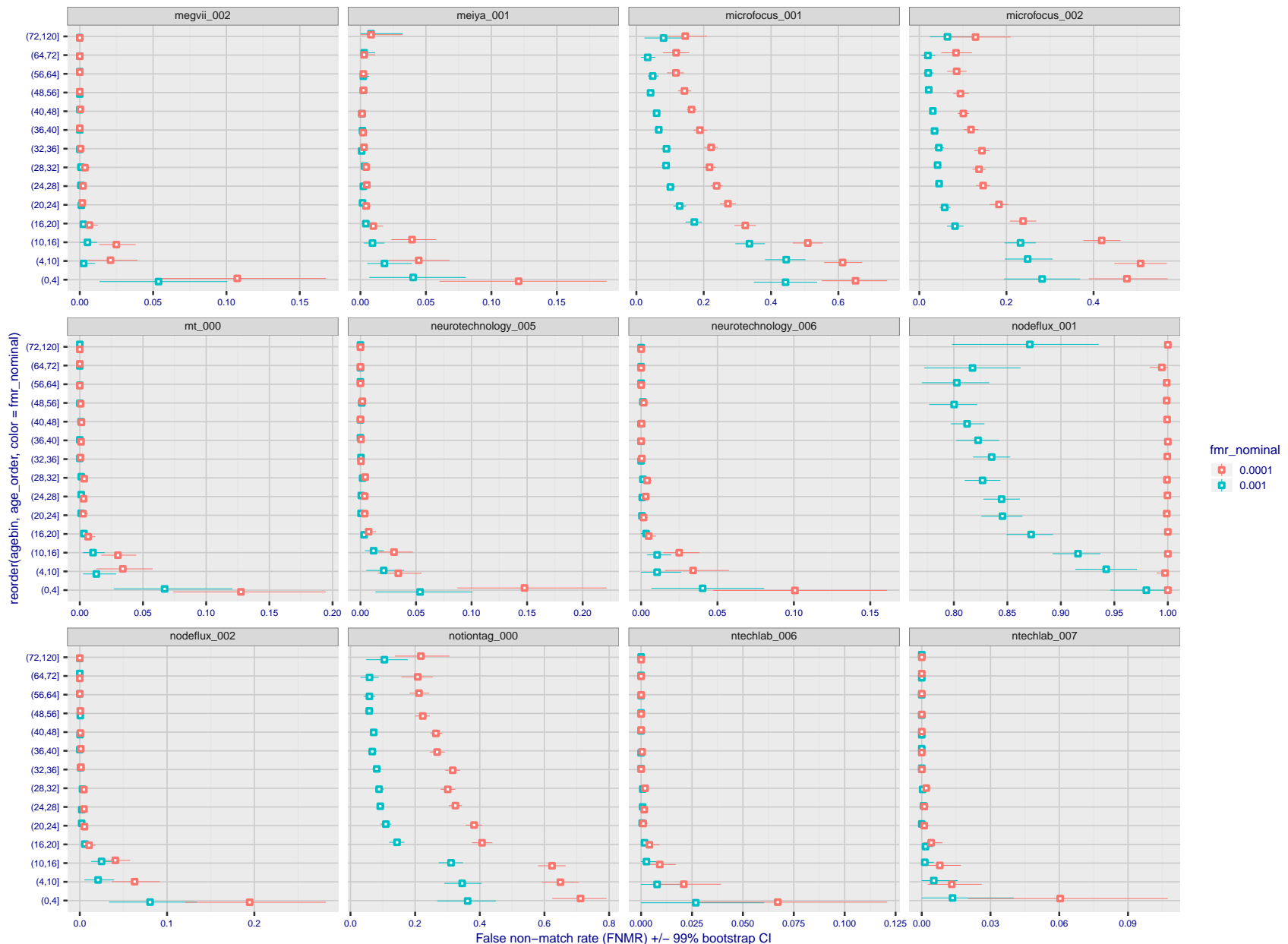


Figure 134: For the visa images, the dots show FNMR by age group for two operating thresholds corresponding to  $FMR = \{0.001, 0.0001\}$  computed over all on the order of  $10^{10}$  impostor scores. The FMR in each bin will vary also - see subsequent impostor heatmaps in sec. 3.6.2. Given a pair of face images taken at different times, we assign the comparison to the bin that is the arithmetic average of the subject's ages. This plot shows only the effect of age, not ageing. The number of comparisons in each bin is generally in the thousands, however the first and last bins are computed over 149 and 124 respectively. The error rates in some (adult) cases are zero, and in others the DET is flat so the error rates at the two thresholds are identical. The lines span 1% and 99% of bootstrap replicated FNMR estimates.

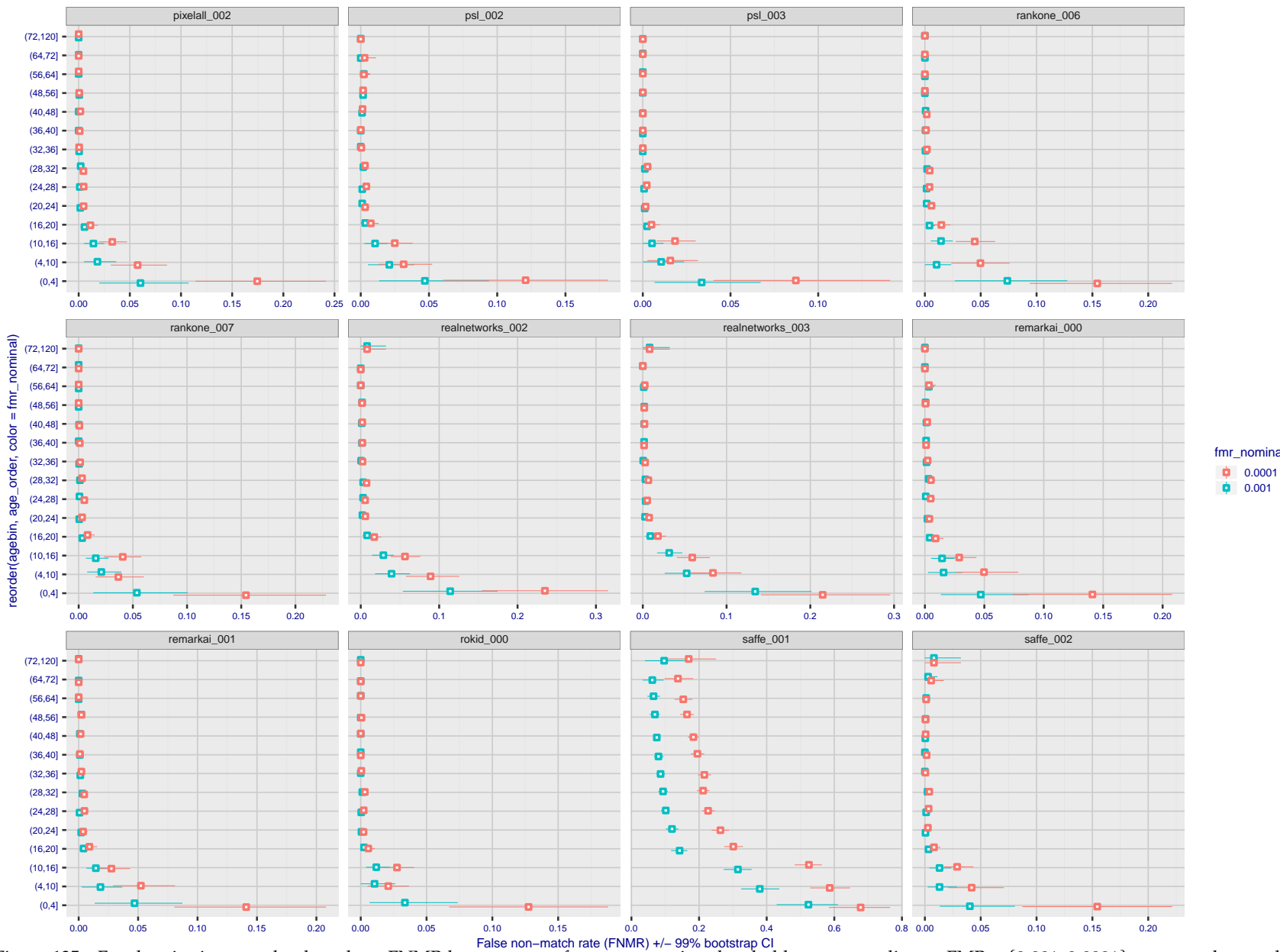


Figure 135: For the visa images, the dots show FNMR by age group for two operating thresholds corresponding to  $FMR = \{0.001, 0.0001\}$  computed over all on the order of  $10^{10}$  impostor scores. The FMR in each bin will vary also - see subsequent impostor heatmaps in sec. 3.6.2. Given a pair of face images taken at different times, we assign the comparison to the bin that is the arithmetic average of the subject's ages. This plot shows only the effect of age, not ageing. The number of comparisons in each bin is generally in the thousands, however the first and last bins are computed over 149 and 124 respectively. The error rates in some (adult) cases are zero, and in others the DET is flat so the error rates at the two thresholds are identical. The lines span 1% and 99% of bootstrap replicated FNMR estimates.

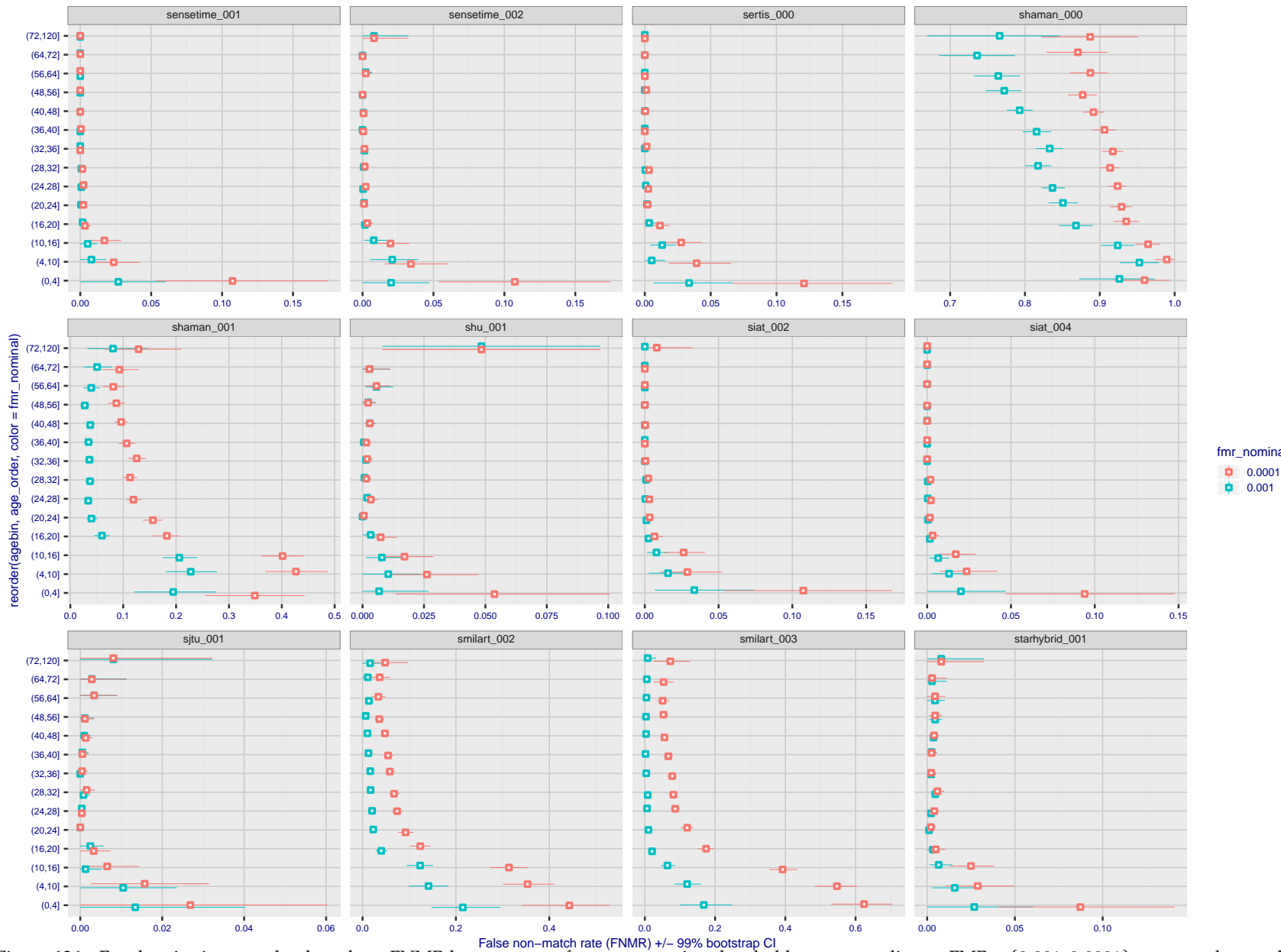


Figure 136: For the visa images, the dots show FNMR by age group for two operating thresholds corresponding to  $FMR = \{0.001, 0.0001\}$  computed over all on the order of  $10^{10}$  impostor scores. The FMR in each bin will vary also - see subsequent impostor heatmaps in sec. 3.6.2. Given a pair of face images taken at different times, we assign the comparison to the bin that is the arithmetic average of the subject's ages. This plot shows only the effect of age, not ageing. The number of comparisons in each bin is generally in the thousands, however the first and last bins are computed over 149 and 124 respectively. The error rates in some (adult) cases are zero, and in others the DET is flat so the error rates at the two thresholds are identical. The lines span 1% and 99% of bootstrap replicated FNMR estimates.



Figure 137: For the visa images, the dots show FNMR by age group for two operating thresholds corresponding to  $FMR = \{0.001, 0.0001\}$  computed over all on the order of  $10^{10}$  impostor scores. The FMR in each bin will vary also - see subsequent impostor heatmaps in sec. 3.6.2. Given a pair of face images taken at different times, we assign the comparison to the bin that is the arithmetic average of the subject's ages. This plot shows only the effect of age, not ageing. The number of comparisons in each bin is generally in the thousands, however the first and last bins are computed over 149 and 124 respectively. The error rates in some (adult) cases are zero, and in others the DET is flat so the error rates at the two thresholds are identical. The lines span 1% and 99% of bootstrap replicated FNMR estimates.

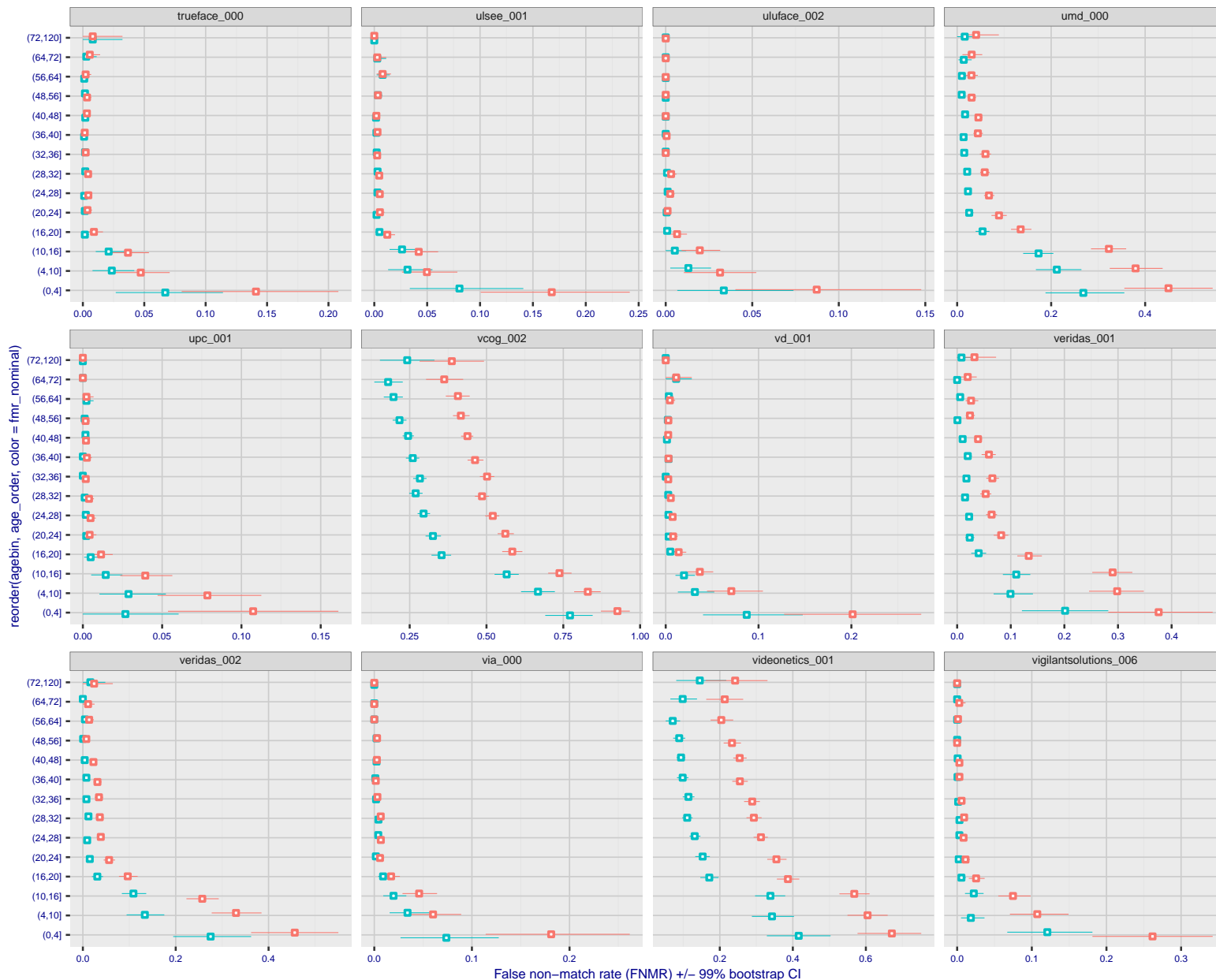


Figure 138: For the visa images, the dots show FNMR by age group for two operating thresholds corresponding to  $FMR = \{0.001, 0.0001\}$  computed over all on the order of  $10^{10}$  impostor scores. The FMR in each bin will vary also - see subsequent impostor heatmaps in sec. 3.6.2. Given a pair of face images taken at different times, we assign the comparison to the bin that is the arithmetic average of the subject's ages. This plot shows only the effect of age, not ageing. The number of comparisons in each bin is generally in the thousands, however the first and last bins are computed over 149 and 124 respectively. The error rates in some (adult) cases are zero, and in others the DET is flat so the error rates at the two thresholds are identical. The lines span 1% and 99% of bootstrap replicated FNMR estimates.

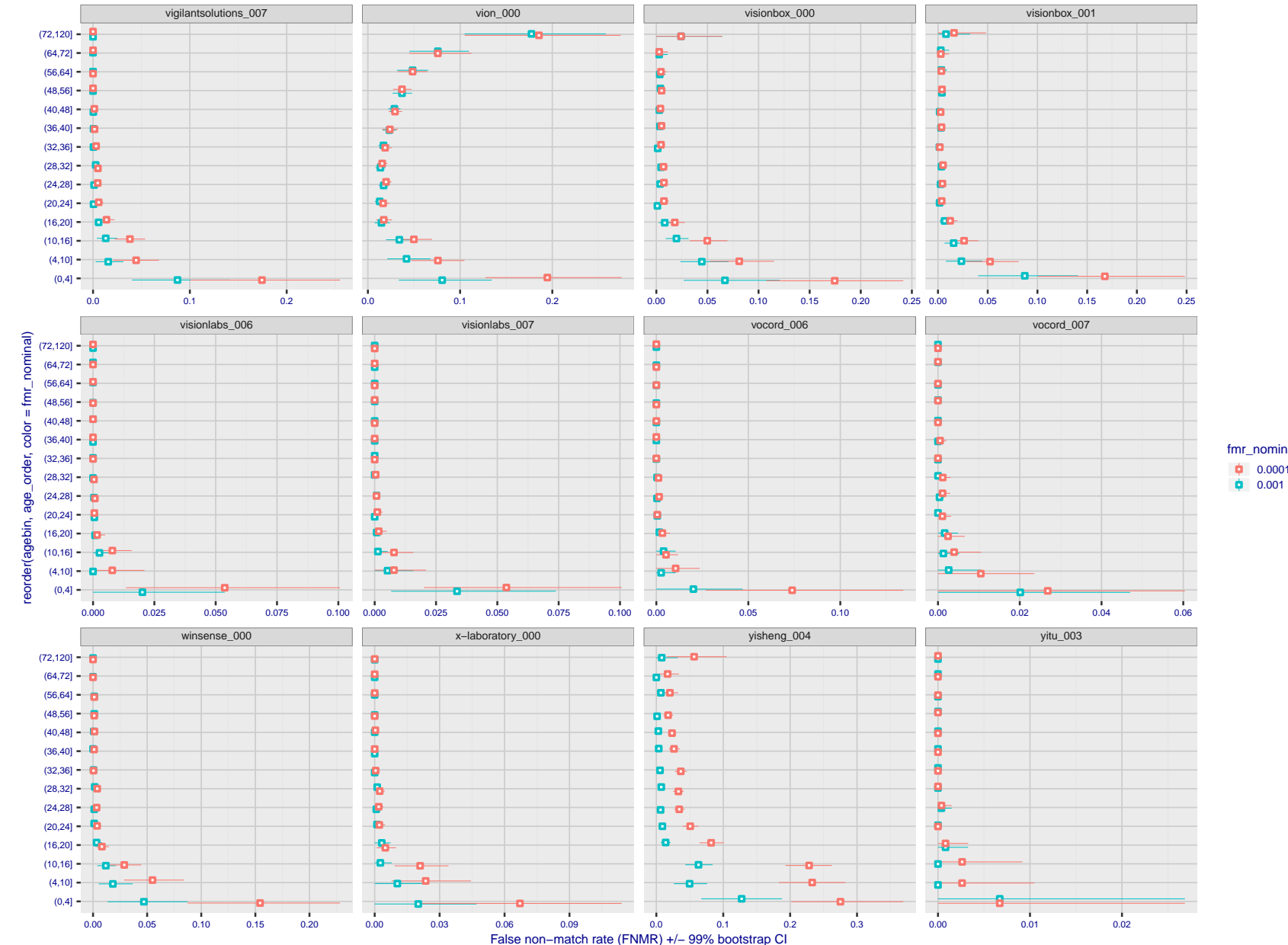


Figure 139: For the visa images, the dots show FNMR by age group for two operating thresholds corresponding to  $FMR = \{0.001, 0.0001\}$  computed over all on the order of  $10^{10}$  impostor scores. The FMR in each bin will vary also - see subsequent impostor heatmaps in sec. 3.6.2. Given a pair of face images taken at different times, we assign the comparison to the bin that is the arithmetic average of the subject's ages. This plot shows only the effect of age, not ageing. The number of comparisons in each bin is generally in the thousands, however the first and last bins are computed over 149 and 124 respectively. The error rates in some (adult) cases are zero, and in others the DET is flat so the error rates at the two thresholds are identical. The lines span 1% and 99% of bootstrap replicated FNMR estimates.

**Caveats:** None.

## 3.6 Impostor distribution stability

### 3.6.1 Effect of birth place on the impostor distribution

**Background:** Facial appearance varies geographically, both in terms of skin tone, cranio-facial structure and size. This section addresses whether false match rates vary intra- and inter-regionally.

**Goals:**

- ▷ To show the effect of birth region of the impostor and enrollee on false match rates.
- ▷ To determine whether some algorithms give better impostor distribution stability.

**Methods:**

- ▷ For the visa images, NIST defined 10 regions: Sub-Saharan Africa, South Asia, Polynesia, North Africa, Middle East, Europe, East Asia, Central and South America, Central Asia, and the Caribbean.
- ▷ For the visa images, NIST mapped each country of birth to a region. There is some arbitrariness to this. For example, Egypt could reasonably be assigned to the Middle East instead of North Africa. An alternative methodology could, for example, assign the Philippines to *both* Polynesia and East Asia.
- ▷ FMR is computed for cases where all face images of impostors born in region  $r_2$  are compared with enrolled face images of persons born in region  $r_1$ .

$$\text{FMR}(r_1, r_2, T) = \frac{\sum_{i=1}^{N_{r_1, r_2}} H(s_i - T)}{N_{r_1, r_2}} \quad (5)$$

where the same threshold,  $T$ , is used in all cells, and  $H$  is the unit step function. The threshold is set to give  $\text{FMR}(T) = 0.001$  over the entire set of visa image impostor comparisons.

- ▷ This analysis is then repeated by country-pair, but only for those country pairs where both have at least 1000 images available. The countries<sup>1</sup> appear in the axes of graphs that follow.
- ▷ The mean number of impostor scores in any cross-region bin is 33 million. The smallest number of impostor scores in any bin is 135000, for Central Asia - North Africa. While these counts are large enough to support reasonable significance, the number of individual faces is much smaller, on the order of  $N^{0.5}$ .
- ▷ The numbers of impostor scores in any cross-country bin is shown in Figure 444.

**Results:** Subsequent figures show heatmaps that use color to represent the base-10 logarithm of the false match rate. Red colors indicate high (bad) false match rates. Dark colors indicate benign false match rates. There are two series of graphs corresponding to aggregated geographical regions, and to countries. The notable observations are:

- ▷ The on-diagonal elements correspond to within-region impostors. FMR is generally above the nominal value of  $\text{FMR} = 0.001$ . Particularly there is usually higher FMR in, Sub-Saharan Africa, South Asia, and the Caribbean. Europe and Central Asia, on the other hand, usually give FMR closer to the nominal value.
- ▷ The off-diagonal elements correspond to across-region impostors. The highest FMR is produced between the Caribbean and Sub-Saharan Africa.
- ▷ Algorithms vary.

<sup>1</sup>These are Argentina, Australia, Brazil, Chile, China, Costa Rica, Cuba, Czech Republic, Dominican Republic, Ecuador, Egypt, El Salvador, Germany, Ghana, Great Britain, Greece, Guatemala, Haiti, Hong Kong, Honduras, Indonesia, India, Israel, Jamaica, Japan, Kenya, Korea, Lebanon, Mexico, Malaysia, Nepal, Nigeria, Peru, Philippines, Pakistan, Poland, Romania, Russia, South Africa, Saudi Arabia, Thailand, Trinidad, Turkey, Taiwan, Ukraine, Venezuela, and Vietnam.

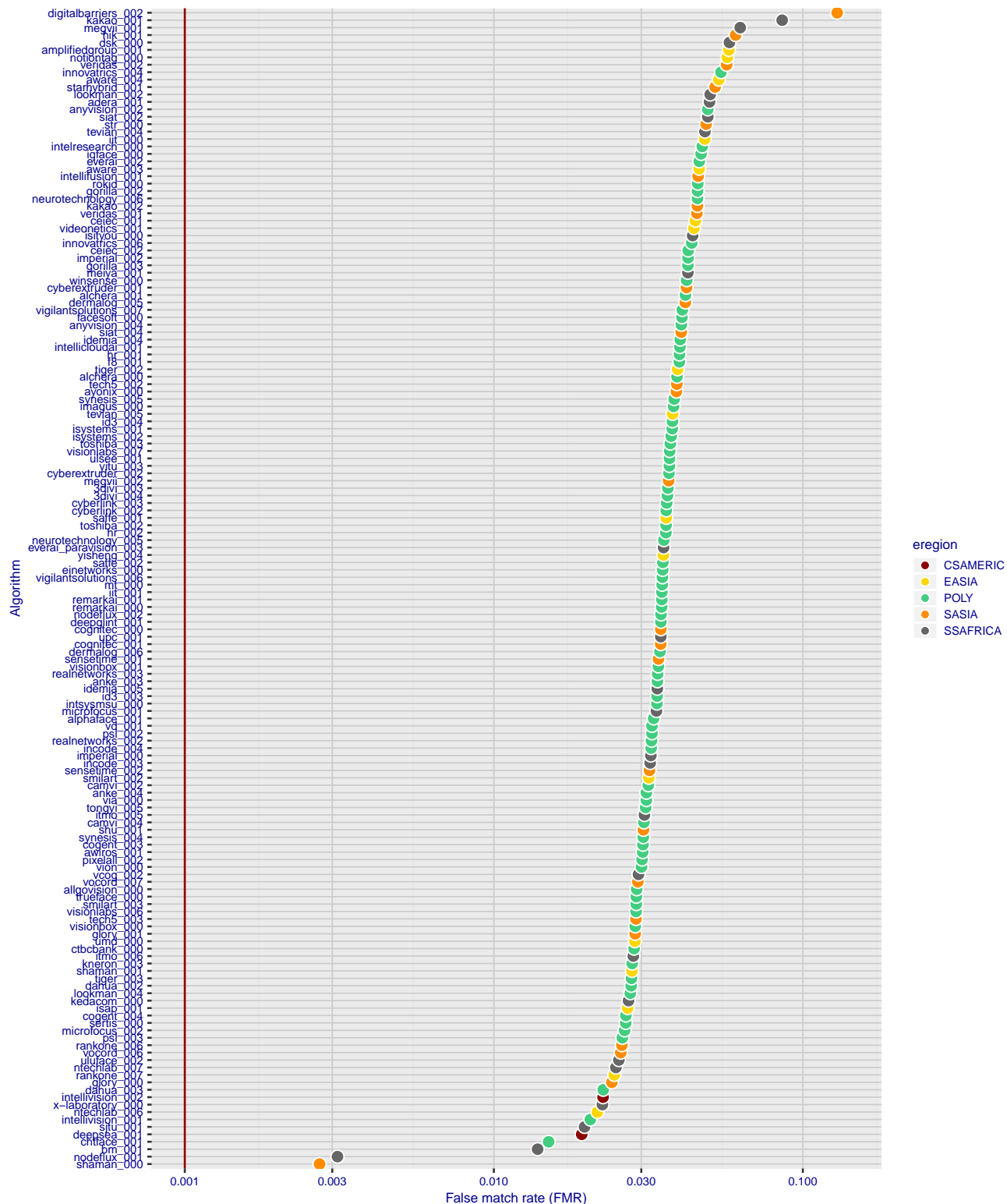


Figure 140: For the visa images, the dots show FMR for impostor comparisons of individuals of the same sex and same age group for the region of the world that gives the worst (highest) FMR when the threshold is set to give  $FMR = 0.001$  (red vertical line) over all on the order of  $10^{10}$  impostor scores i.e. zero-effort. The shift of the dots to right shows massive increases in FMR when impostors have the same sex, age, and region of birth. The color code indicates which region gives the worst case FMR. If the observed variation is due to the prevalence of one kind of images in the training imagery, then algorithms developed on one kind of data might be expected to give higher FMR on other kinds.

- ▷ We computed the same quantities for a global FMR = 0.0001. The effects are similar.

**Caveats:**

- ▷ The effects of variable impostor rates on one-to-many identification systems may well differ from what's implied by these one-to-one verification results. Two reasons for this are a) the enrollment galleries are usually imbalanced across countries of birth, age and sex; b) one-to-many identification algorithms often implement techniques aimed at stabilizing the impostor distribution. Further research is necessary.
- ▷ In principle, the effects seen in this subsection could be due to differences in the image capture process. We consider this unlikely since the effects are maintained across geography - e.g. Caribbean vs. Africa, or Japan vs. China.

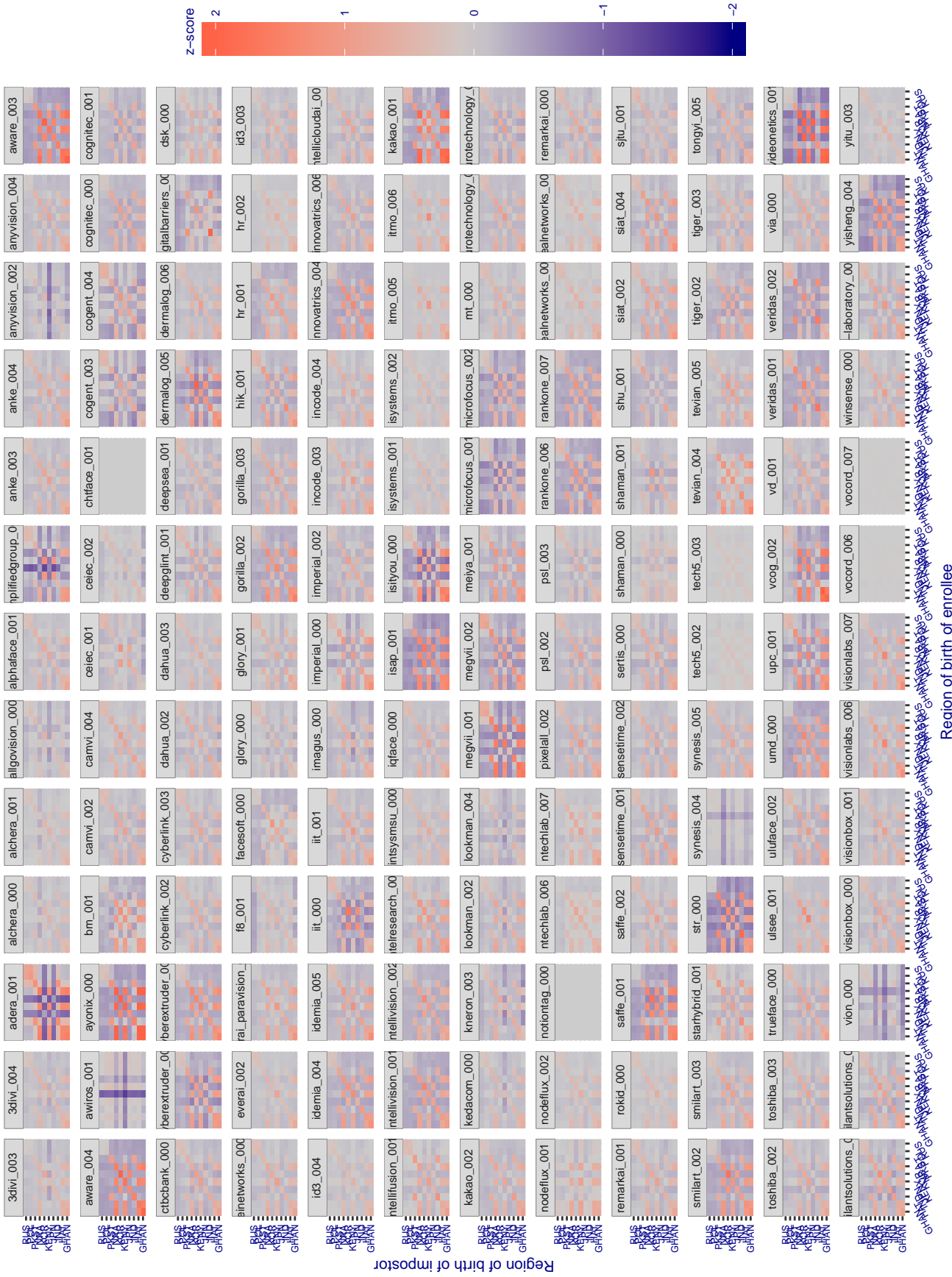


Figure 141: For visa images, the heatmap shows how the mean of the impostor distribution for the country pair (a,b) is shifted relative to the mean of the global impostor distribution, expressed as a number of standard deviations of the global impostor distribution. This statistic is designed to show shifts in the entire impostor distribution, not just tail effects that manifest as the anomalously high (or low) false match rates that appear in the subsequent figures. The countries are chosen to show that skin tone alone does not explain impostor distribution shifts. The reduced shift in Asian populations with the Yitu and Tong YiTrans algorithms, is accompanied by positive shifts in the European populations. This reversal relative to most other algorithms, may derive from use of nationally weighted training sets. The Visionlabs algorithm appears most insensitive to country effects. The figure is computed from same-sex and same-age impostor pairs.

### Cross region FMR at threshold T = 2.740 for algorithm 3divi\_003, giving FMR(T) = 0.0001 globally.

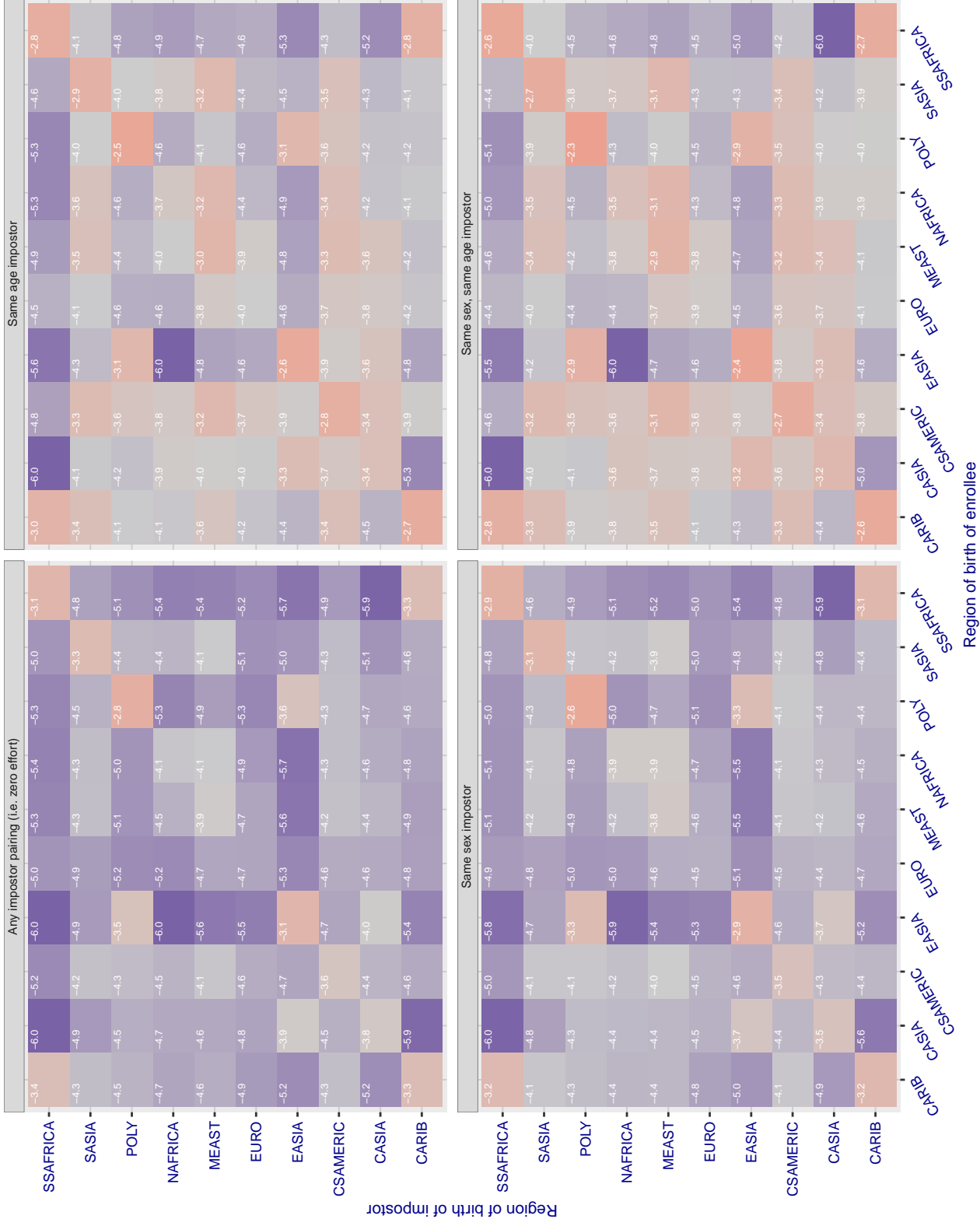


Figure 142: For algorithm 3divi-003 operating on visa images, the heatmap shows false match rates observed over impostor comparisons of faces from different individuals who were born in the given region pair. False matches are counted against a recognition threshold fixed globally to give the target FMR in the plot title, computed over all on the order of  $10^{10}$  impostor comparisons. If text appears in each box it give the same quantity as that coded by the color. Grey indicates FMR is at the intended FMR target level. Light red colors present a security vulnerability to, for example, a passport gate. Each +1 increase in  $\log_{10}$  FMR corresponds to a factor of 10 increase in FMR. The matrix is not quite symmetric because images in the enrollment and verification sets are different.

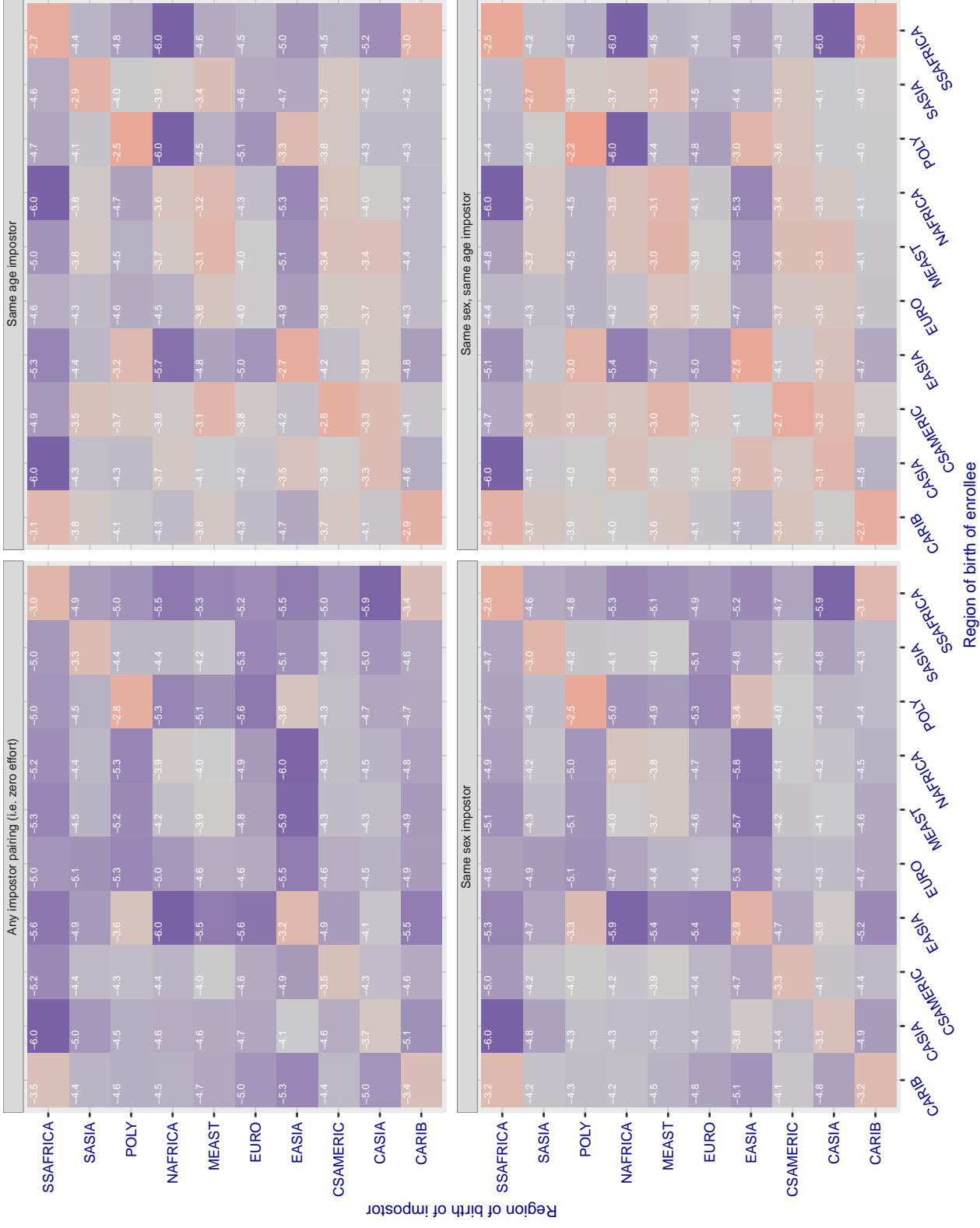
**Cross region FMR at threshold T = 2.857 for algorithm 3divi\_004, giving FMR(T) = 0.0001 globally.**

Figure 143: For algorithm 3divi\_004 operating on visa images, the heatmap shows false match rates observed over impostor comparisons of faces from different individuals who were born in the given region pair. False matches are counted against a recognition threshold fixed globally to give the target FMR in the plot title, computed over all on the order of  $10^{10}$  impostor comparisons. If text appears in each box it give the same quantity as that coded by the color. Grey indicates FMR is at the intended FMR target level. Light red colors present a security vulnerability to, for example, a passport gate. Each +1 increase in  $\log_{10}$  FMR corresponds to a factor of 10 increase in FMR. The matrix is not quite symmetric because images in the enrollment and verification sets are different.

### Cross region FMR at threshold T = 0.713 for algorithm adera\_001, giving $\text{FMR}(\text{T}) = 0.0001$ globally.

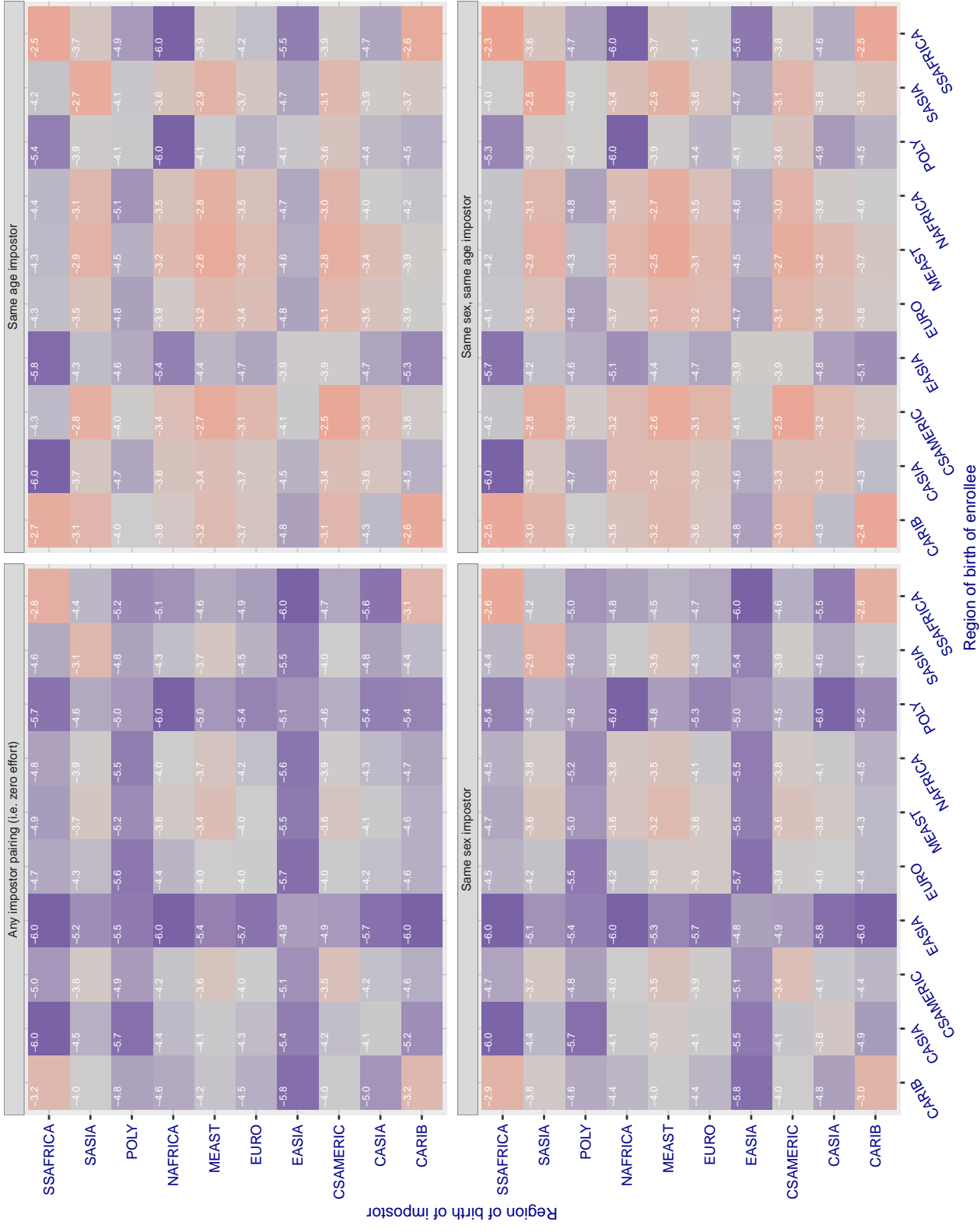


Figure 144: For algorithm adera-001 operating on visa images, the heatmap shows false match rates observed over impostor comparisons of faces from different individuals who were born in the given region pair. False matches are counted against a recognition threshold fixed globally to give the target FMR in the plot title, computed over all on the order of  $10^{10}$  impostor comparisons. If text appears in each box it give the same quantity as that coded by the color. Grey indicates FMR is at the intended FMR target level. Light red colors present a security vulnerability to, for example, a passport gate. Each +1 increase in  $\log_{10} \text{FMR}$  corresponds to a factor of 10 increase in FMR. The matrix is not quite symmetric because images in the enrollment and verification sets are different.

### Cross region FMR at threshold T = 0.702 for algorithm alchera\_000, giving FMR(T) = 0.0001 globally.

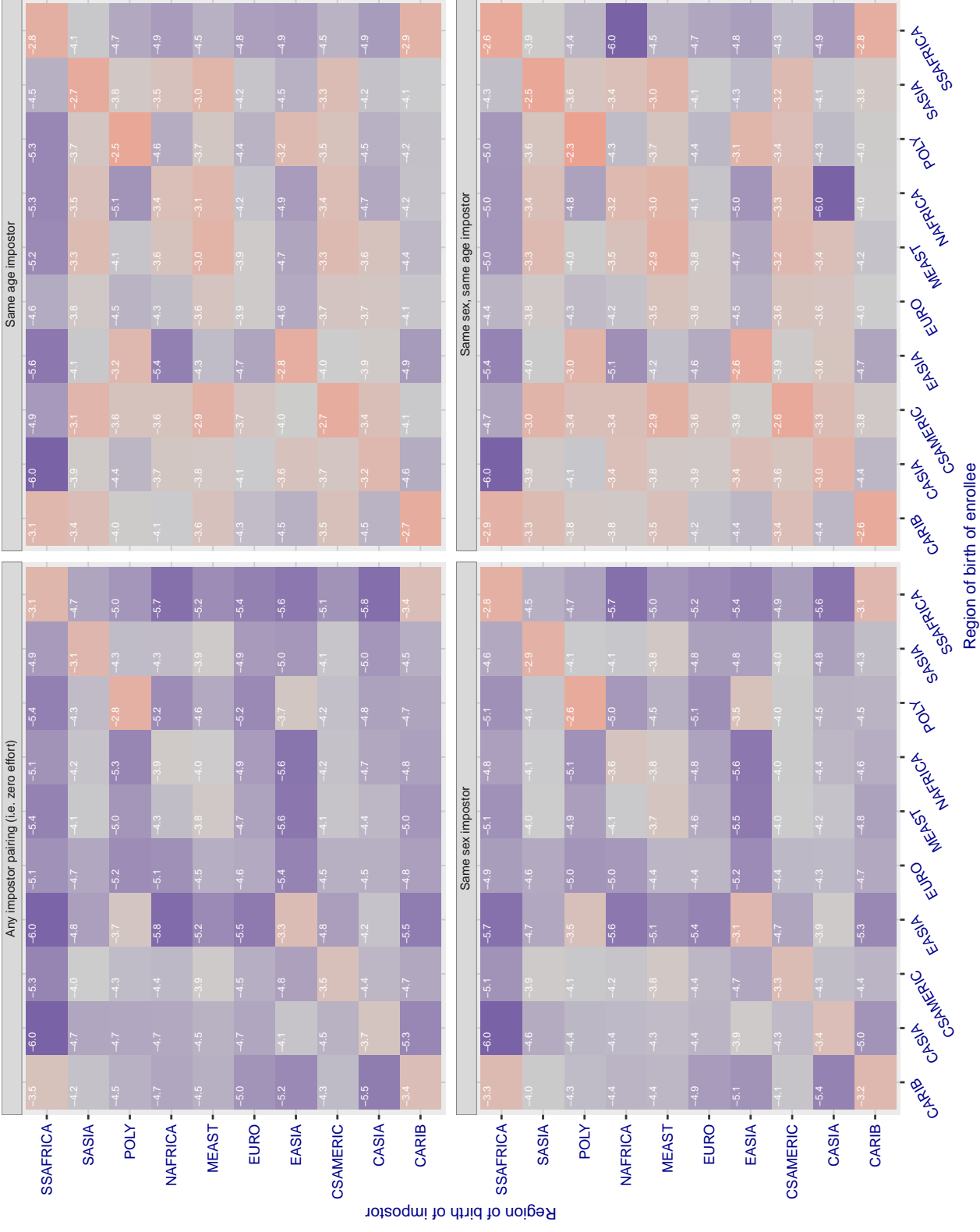


Figure 145: For algorithm alchera-000 operating on visa images, the heatmap shows false match rates observed over impostor comparisons of faces from different individuals who were born in the given region pair. False matches are counted against a recognition threshold fixed globally to give the target FMR in the plot title, computed over all on the order of  $10^{10}$  impostor comparisons. If text appears in each box it give the same quantity as that coded by the color. Grey indicates FMR is at the intended FMR target level. Light red colors present a security vulnerability to, for example, a passport gate. Each +1 increase in  $\log_{10} FMR$  corresponds to a factor of 10 increase in FMR. The matrix is not quite symmetric because images in the enrollment and verification sets are different.

### Cross region FMR at threshold T = 0.713 for algorithm alchera\_001, giving FMR(T) = 0.0001 globally.

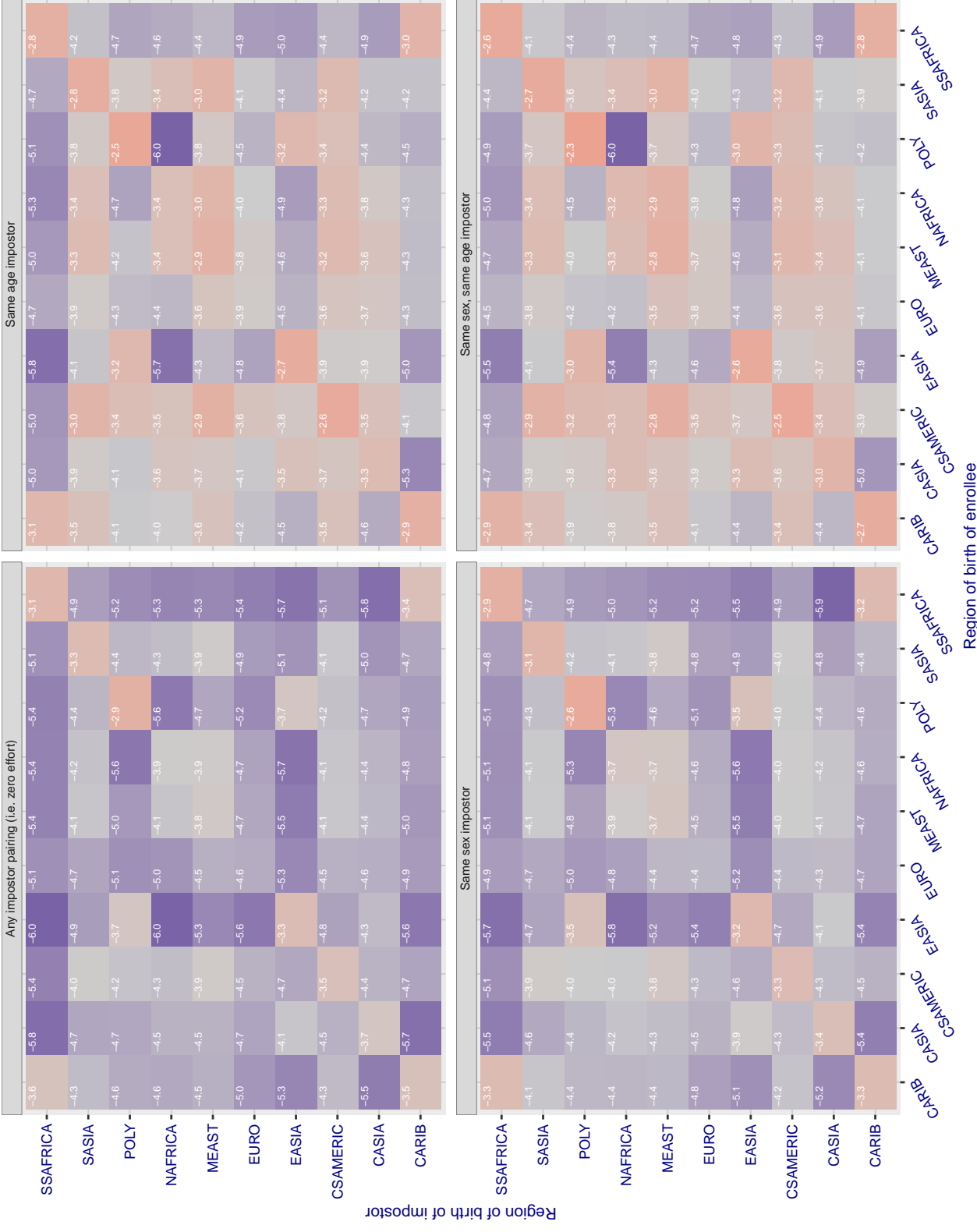


Figure 146: For algorithm alchera-001 operating on visa images, the heatmap shows false match rates observed over impostor comparisons of faces from different individuals who were born in the given region pair. False matches are counted against a recognition threshold fixed globally to give the target FMR in the plot title, computed over all on the order of  $10^{10}$  impostor comparisons. If text appears in each box it give the same quantity as that coded by the color. Grey indicates FMR is at the intended FMR target level. Light red colors present a security vulnerability to, for example, a passport gate. Each +1 increase in  $\log_{10} FMR$  corresponds to a factor of 10 increase in FMR. The matrix is not quite symmetric because images in the enrollment and verification sets are different.

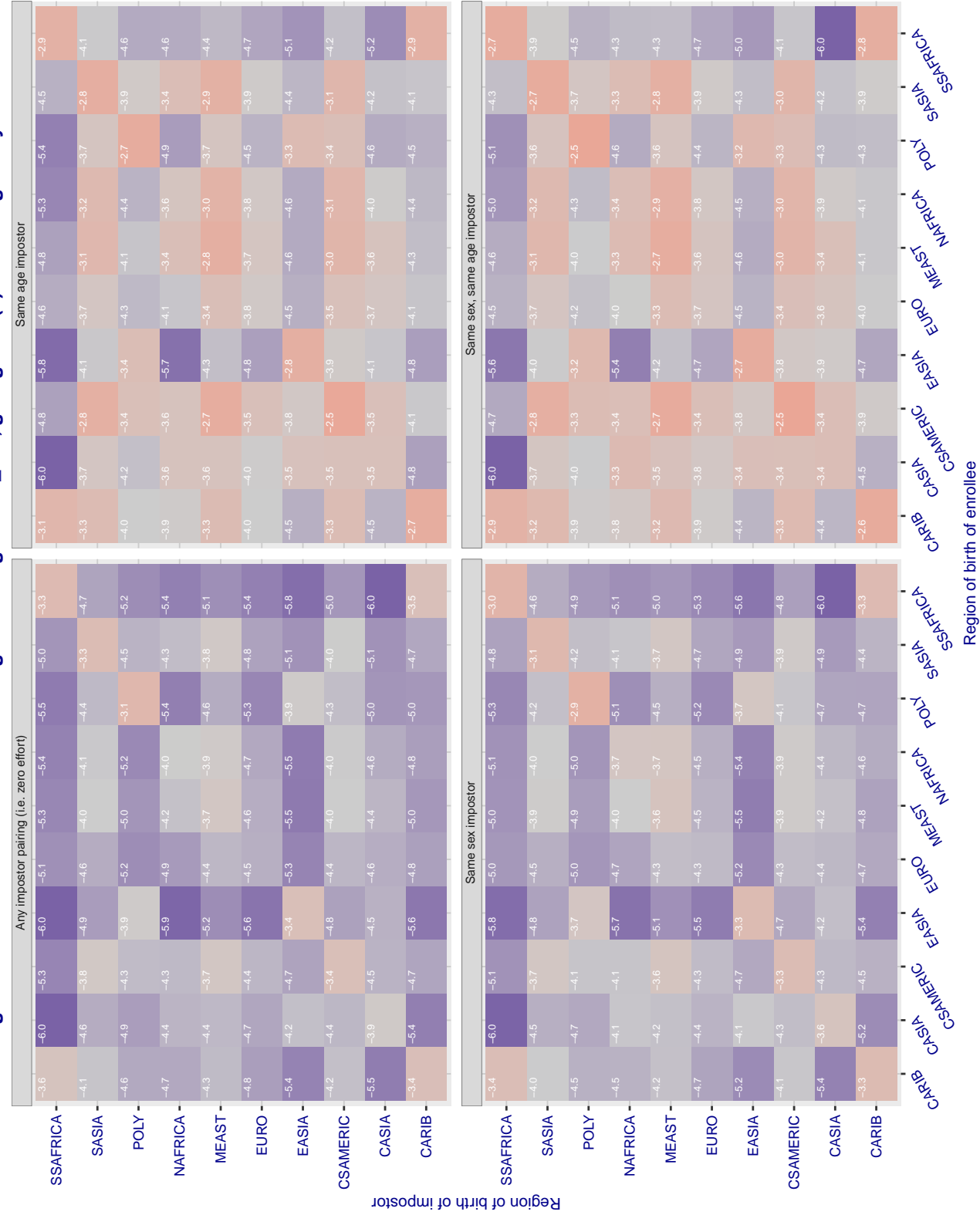


Figure 147: For algorithm allgovision-000 operating on visa images, the heatmap shows false match rates observed over impostor comparisons of faces from different individuals who were born in the given region pair. False matches are counted against a recognition threshold fixed globally to give the target FMR in the plot title, computed over all on the order of  $10^{10}$  impostor comparisons. If text appears in each box it give the same quantity as that coded by the color. Grey indicates FMR is at the intended FMR target level. Light red colors present a security vulnerability to, for example, a passport gate. Each +1 increase in  $\log_{10}$  FMR corresponds to a factor of 10 increase in FMR. The matrix is not quite symmetric because images in the enrollment and verification sets are different.

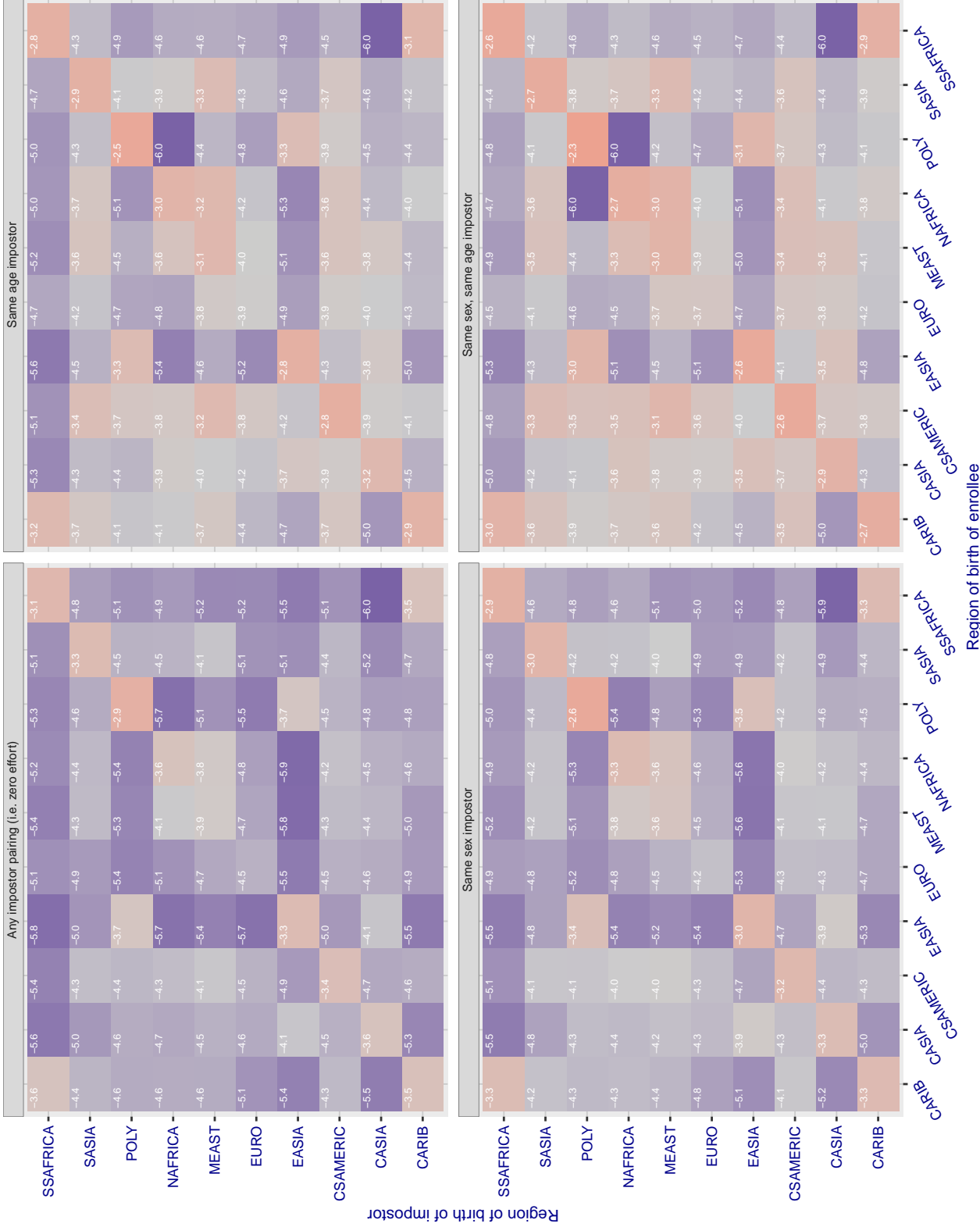
**Cross region FMR at threshold T = 0.396 for algorithm alphaface\_001, giving FMR(T) = 0.0001 globally.**

Figure 148: For algorithm alphaface-001 operating on visa images, the heatmap shows false match rates observed over impostor comparisons of faces from different individuals who were born in the given region pair. False matches are counted against a recognition threshold fixed globally to give the target FMR in the plot title, computed over all on the order of  $10^{10}$  impostor comparisons. If text appears in each box it give the same quantity as that coded by the color. Grey indicates FMR is at the intended FMR target level. Light red colors present a security vulnerability to, for example, a passport gate. Each +1 increase in  $\log_{10} FMR$  corresponds to a factor of 10 increase in FMR. The matrix is not quite symmetric because images in the enrollment and verification sets are different.

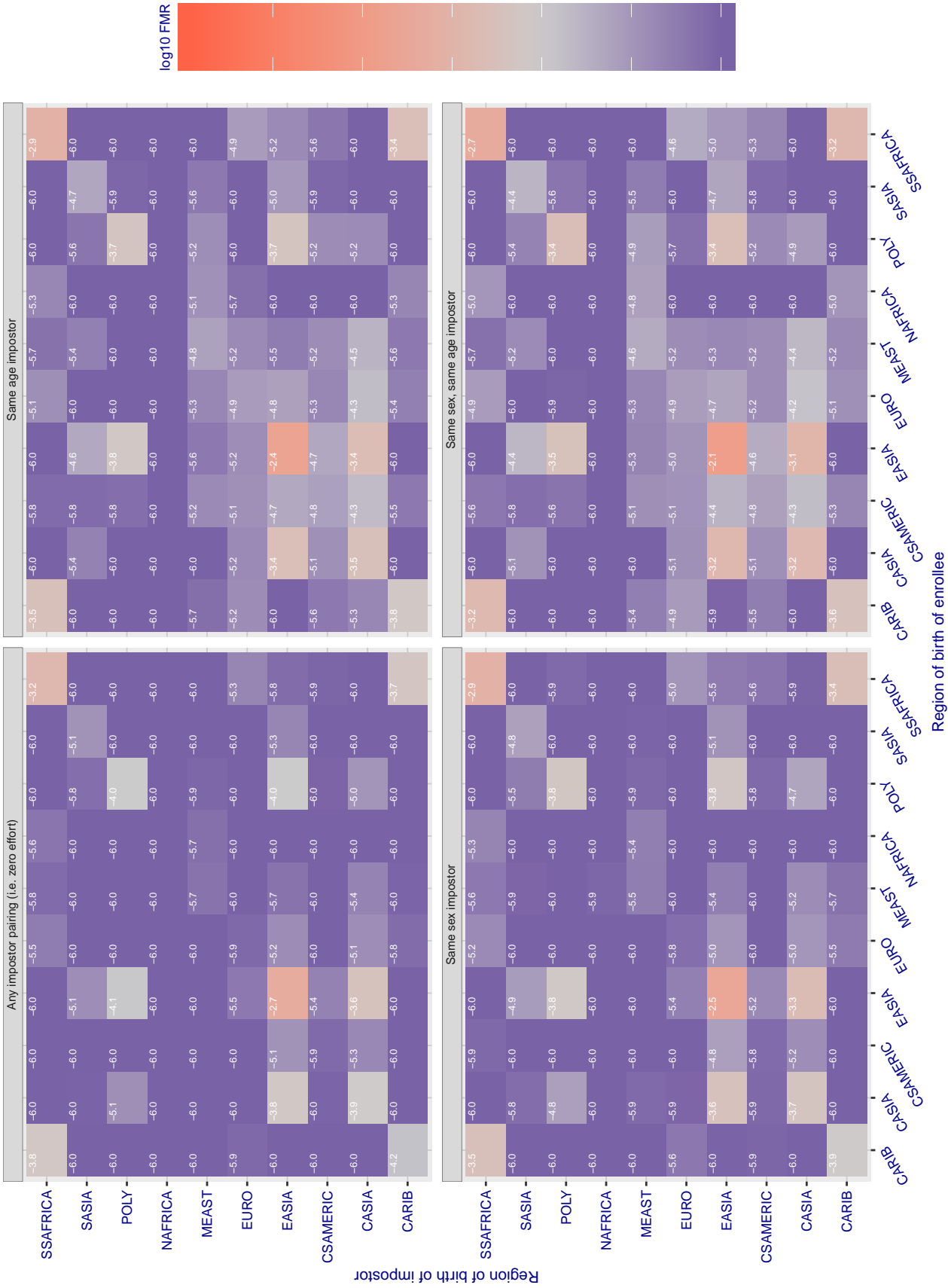
**Cross region FMR at threshold T = 3.640 for algorithm amplifiedgroup\_001, giving FMR(T) = 0.0001 globally.**

Figure 149: For algorithm amplifiedgroup-001 operating on visa images, the heatmap shows false match rates observed over impostor comparisons of faces from different individuals who were born in the given region pair. False matches are counted against a recognition threshold fixed globally to give the target FMR in the plot title, computed over all on the order of  $10^{10}$  impostor comparisons. If text appears in each box it give the same quantity as that coded by the color. Grey indicates FMR is at the intended FMR target level. Light red colors present a security vulnerability to, for example, a passport gate. Each +1 increase in  $\log_{10} FMR$  corresponds to a factor of 10 increase in FMR. The matrix is not quite symmetric because images in the enrollment and verification sets are different.

### Cross region FMR at threshold T = 0.397 for algorithm anke\_003, giving FMR(T) = 0.0001 globally.

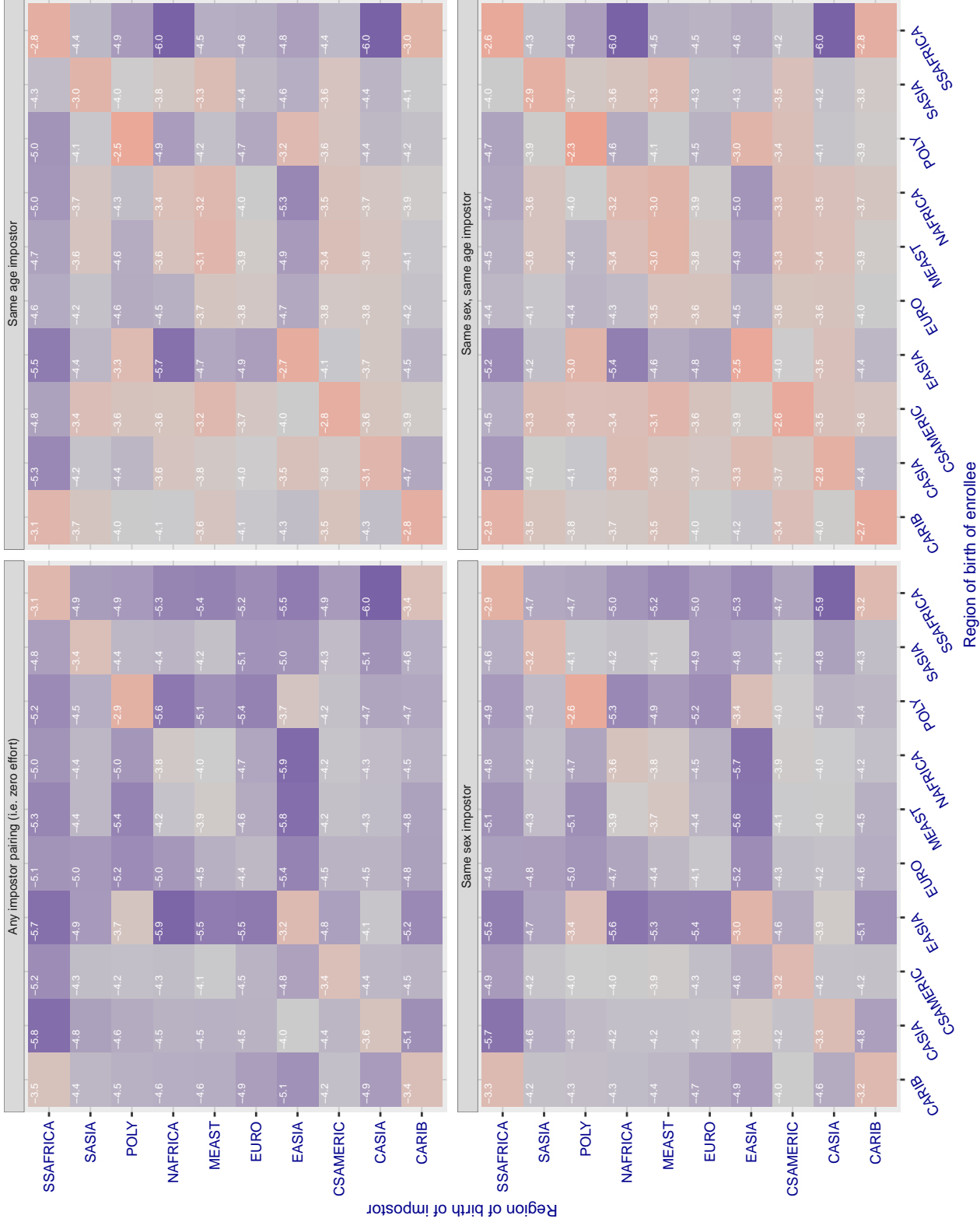


Figure 150: For algorithm anke-003 operating on visa images, the heatmap shows false match rates observed over impostor comparisons of faces from different individuals who were born in the given region pair. False matches are counted against a recognition threshold fixed globally to give the target FMR in the plot title, computed over all on the order of  $10^{10}$  impostor comparisons. If text appears in each box it give the same quantity as that coded by the color. Grey indicates FMR is at the intended FMR target level. Light red colors present a security vulnerability to, for example, a passport gate. Each +1 increase in  $\log_{10}$  FMR corresponds to a factor of 10 increase in FMR. The matrix is not quite symmetric because images in the enrollment and verification sets are different.

### Cross region FMR at threshold T = 0.397 for algorithm anke\_004, giving FMR(T) = 0.0001 globally.

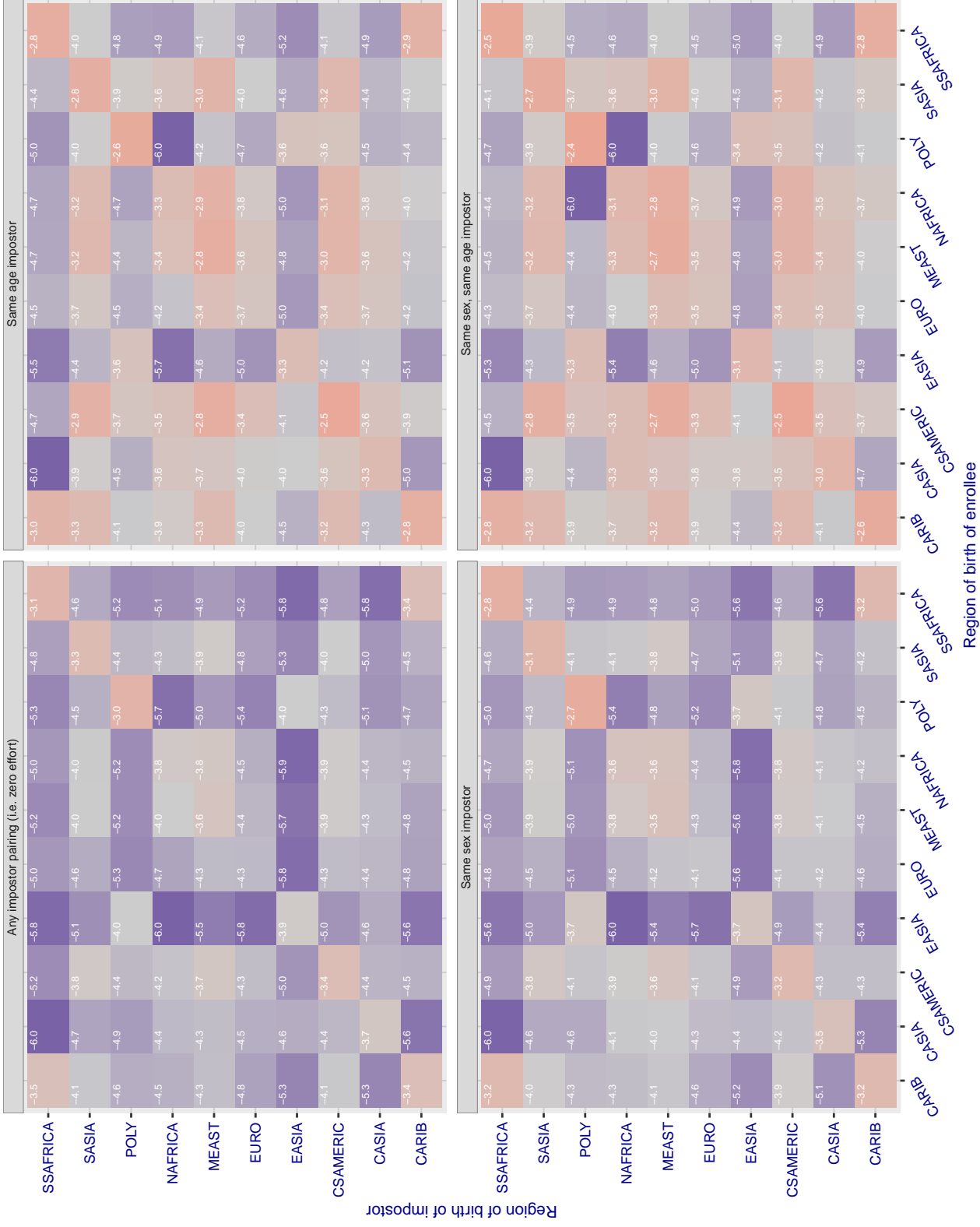


Figure 151: For algorithm anke-004 operating on visa images, the heatmap shows false match rates observed over impostor comparisons of faces from different individuals who were born in the given region pair. False matches are counted against a recognition threshold fixed globally to give the target FMR in the plot title, computed over all on the order of  $10^{10}$  impostor comparisons. If text appears in each box it give the same quantity as that coded by the color. Grey indicates FMR is at the intended FMR target level. Light red colors present a security vulnerability to, for example, a passport gate. Each +1 increase in  $\log 10$  FMR corresponds to a factor of 10 increase in FMR. The matrix is not quite symmetric because images in the enrollment and verification sets are different.

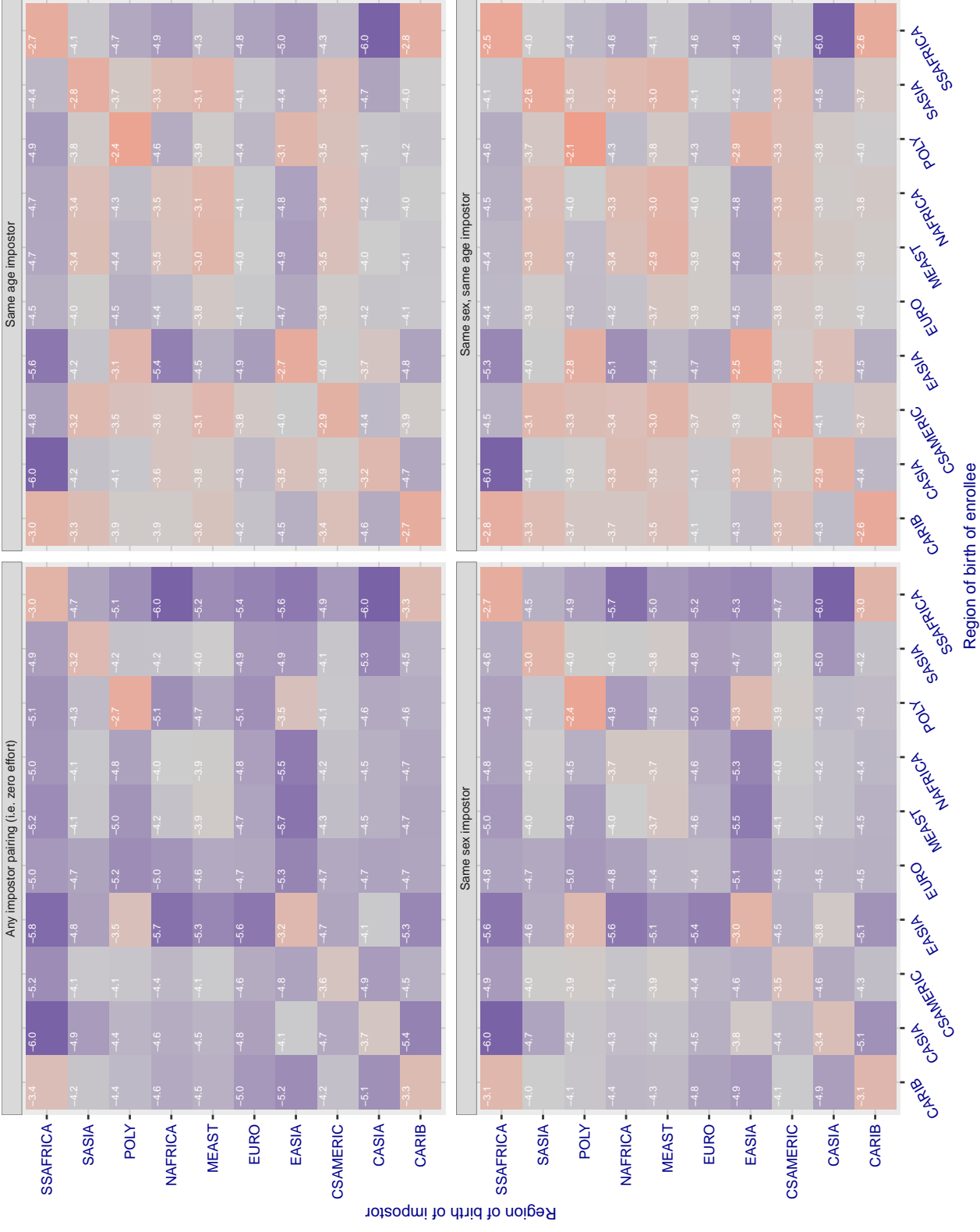
**Cross region FMR at threshold T = 1.526 for algorithm anyvision\_002, giving FMR(T) = 0.0001 globally.**

Figure 152: For algorithm anyvision-002 operating on visa images, the heatmap shows false match rates observed over impostor comparisons of faces from different individuals who were born in the given region pair. False matches are counted against a recognition threshold fixed globally to give the target FMR in the plot title, computed over all on the order of  $10^{10}$  impostor comparisons. If text appears in each box it give the same quantity as that coded by the color. Grey indicates FMR is at the intended FMR target level. Light red colors present a security vulnerability to, for example, a passport gate. Each +1 increase in  $\log_{10} FMR$  corresponds to a factor of 10 increase in FMR. The matrix is not quite symmetric because images in the enrollment and verification sets are different.

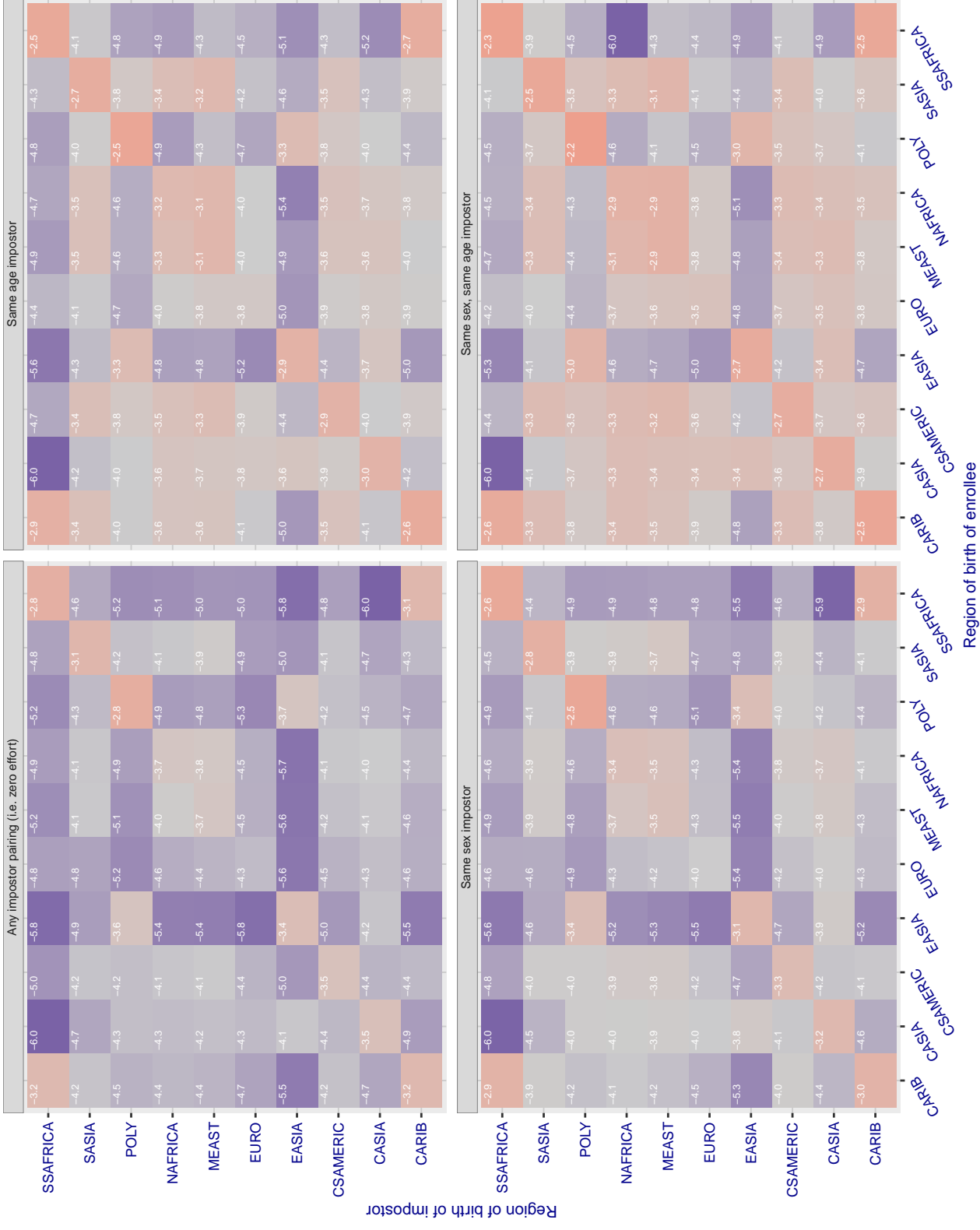
**Cross region FMR at threshold T = 1.375 for algorithm anyvision\_004, giving FMR(T) = 0.0001 globally.**

Figure 153: For algorithm anyvision-004 operating on visa images, the heatmap shows false match rates observed over impostor comparisons of faces from different individuals who were born in the given region pair. False matches are counted against a recognition threshold fixed globally to give the target FMR in the plot title, computed over all on the order of  $10^{10}$  impostor comparisons. If text appears in each box it give the same quantity as that coded by the color. Grey indicates FMR is at the intended FMR target level. Light red colors present a security vulnerability to, for example, a passport gate. Each +1 increase in  $\log_{10} FMR$  corresponds to a factor of 10 increase in FMR. The matrix is not quite symmetric because images in the enrollment and verification sets are different.

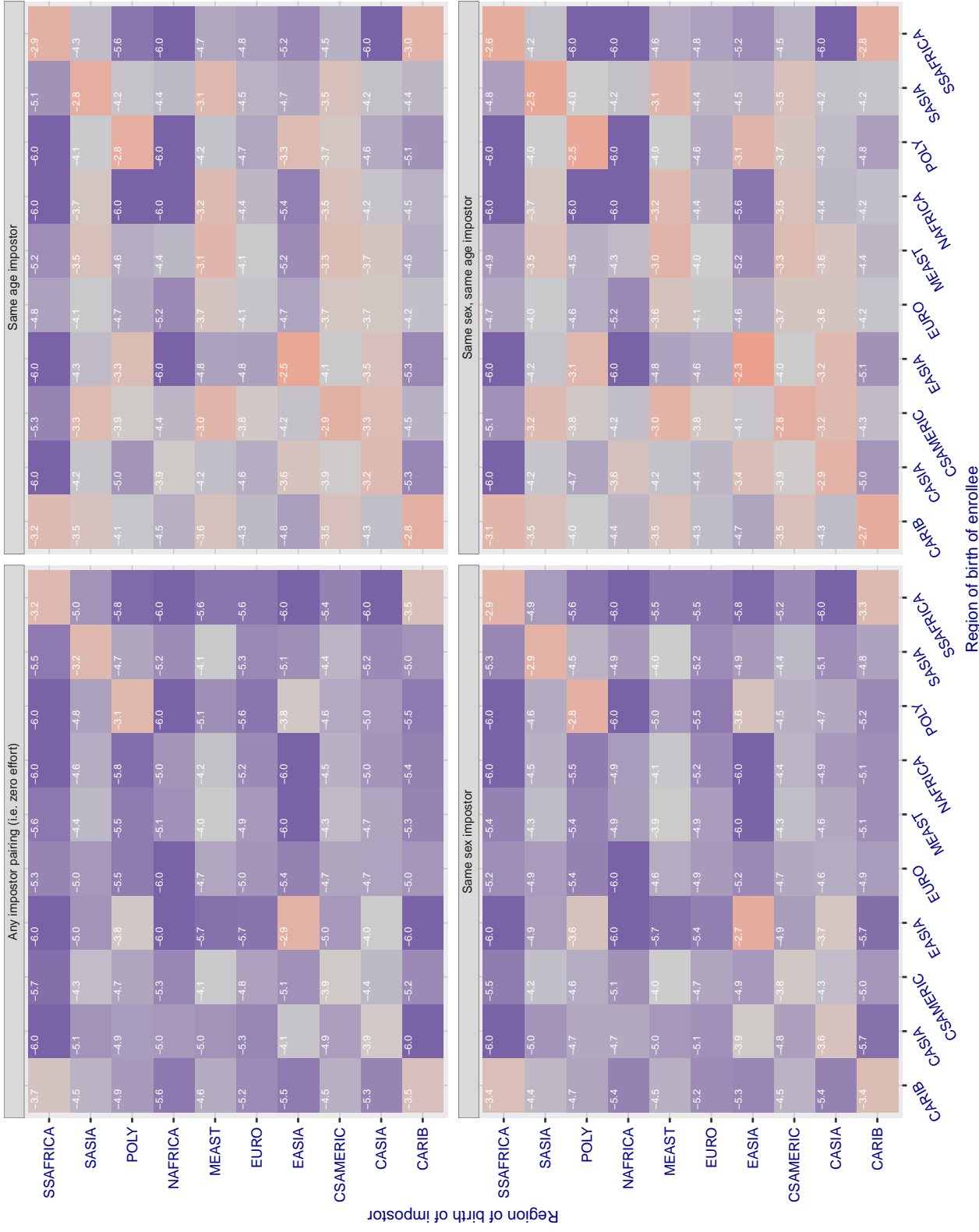
**Cross region FMR at threshold T = 3.868 for algorithm aware\_003, giving FMR(T) = 0.0001 globally.**

Figure 154: For algorithm aware-003 operating on visa images, the heatmap shows false match rates observed over impostor comparisons of faces from different individuals who were born in the given region pair. False matches are counted against a recognition threshold fixed globally to give the target FMR in the plot title, computed over all on the order of  $10^{10}$  impostor comparisons. If text appears in each box it give the same quantity as that coded by the color. Grey indicates FMR is at the intended FMR target level. Light red colors present a security vulnerability to, for example, a passport gate. Each +1 increase in  $\log_{10} FMR$  corresponds to a factor of 10 increase in FMR. The matrix is not quite symmetric because images in the enrollment and verification sets are different.

### Cross region FMR at threshold T = 5.084 for algorithm aware\_004, giving FMR(T) = 0.0001 globally.

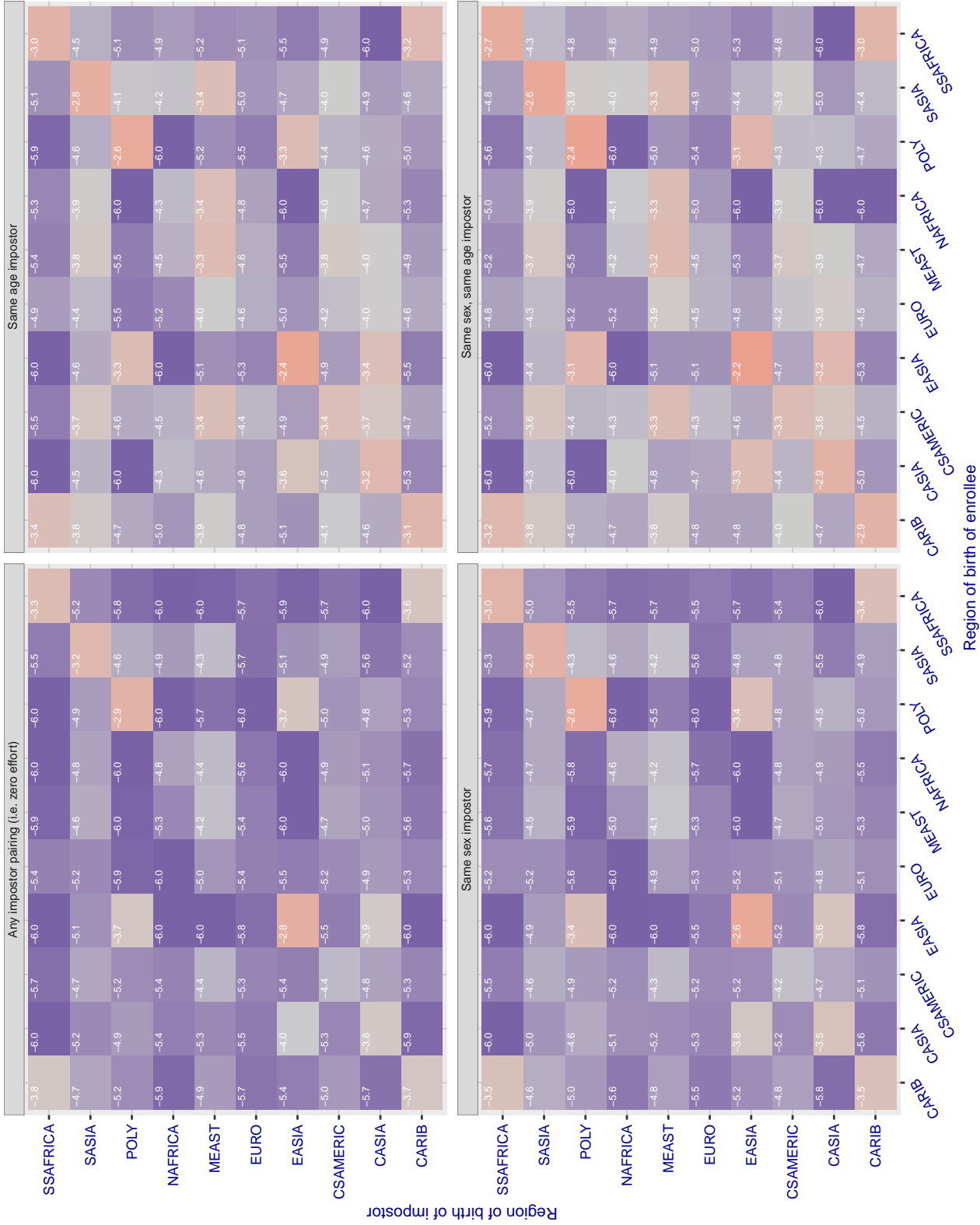


Figure 155: For algorithm aware-004 operating on visa images, the heatmap shows false match rates observed over impostor comparisons of faces from different individuals who were born in the given region pair. False matches are counted against a recognition threshold fixed globally to give the target FMR in the plot title, computed over all on the order of  $10^{10}$  impostor comparisons. If text appears in each box it give the same quantity as that coded by the color. Grey indicates FMR is at the intended FMR target level. Light red colors present a security vulnerability to, for example, a passport gate. Each +1 increase in  $\log_{10} FMR$  corresponds to a factor of 10 increase in FMR. The matrix is not quite symmetric because images in the enrollment and verification sets are different.

### Cross region FMR at threshold T = 0.799 for algorithm awiros\_001, giving FMR(T) = 0.0001 globally.

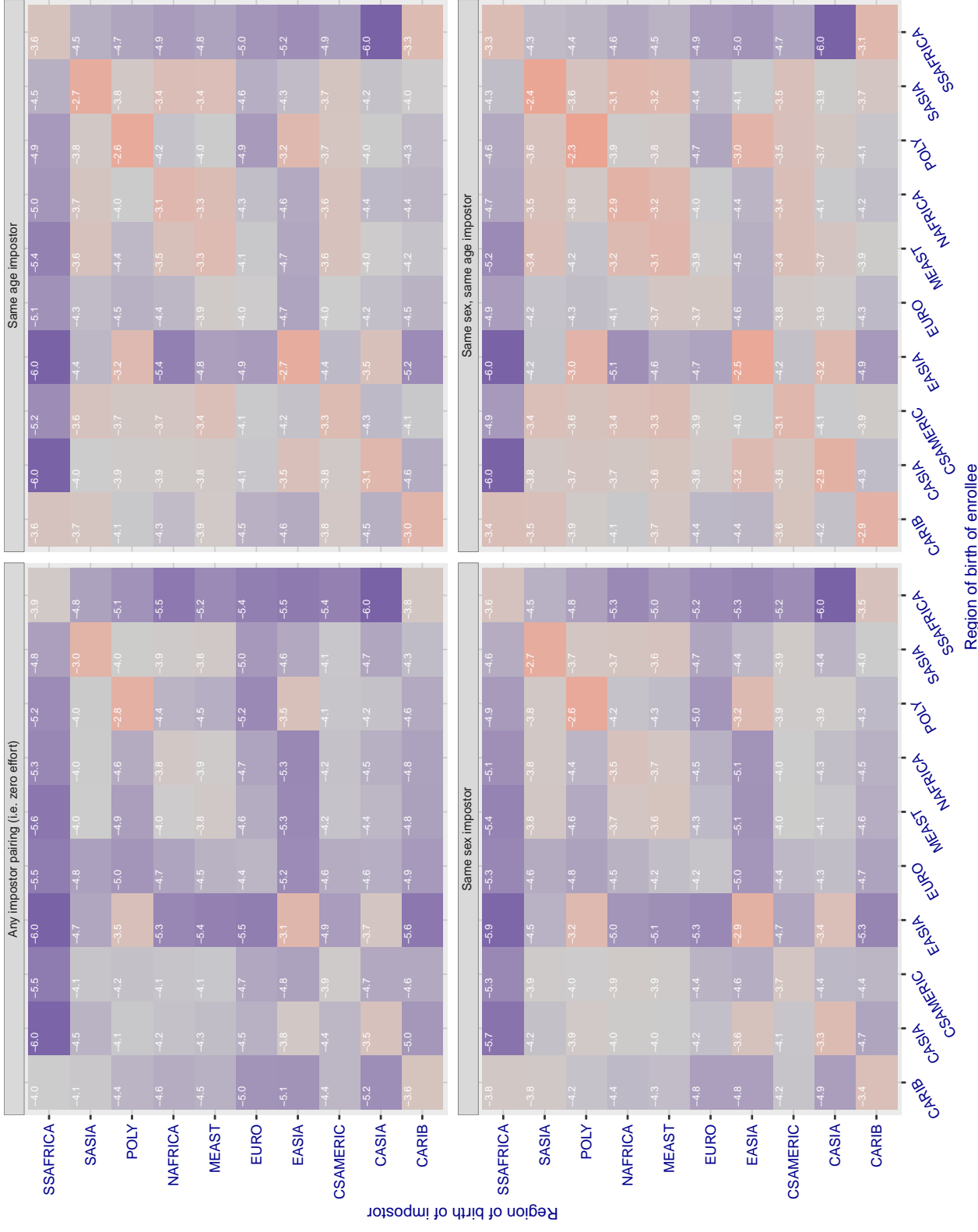


Figure 156: For algorithm awiros-001 operating on visa images, the heatmap shows false match rates observed over impostor comparisons of faces from different individuals who were born in the given region pair. False matches are counted against a recognition threshold fixed globally to give the target FMR in the plot title, computed over all on the order of  $10^{10}$  impostor comparisons. If text appears in each box it give the same quantity as that coded by the color. Grey indicates FMR is at the intended FMR target level. Light red colors present a security vulnerability to, for example, a passport gate. Each +1 increase in  $\log_{10} FMR$  corresponds to a factor of 10 increase in FMR. The matrix is not quite symmetric because images in the enrollment and verification sets are different.

### Cross region FMR at threshold T = 0.919 for algorithm ayonix\_000, giving FMR(T) = 0.0001 globally.

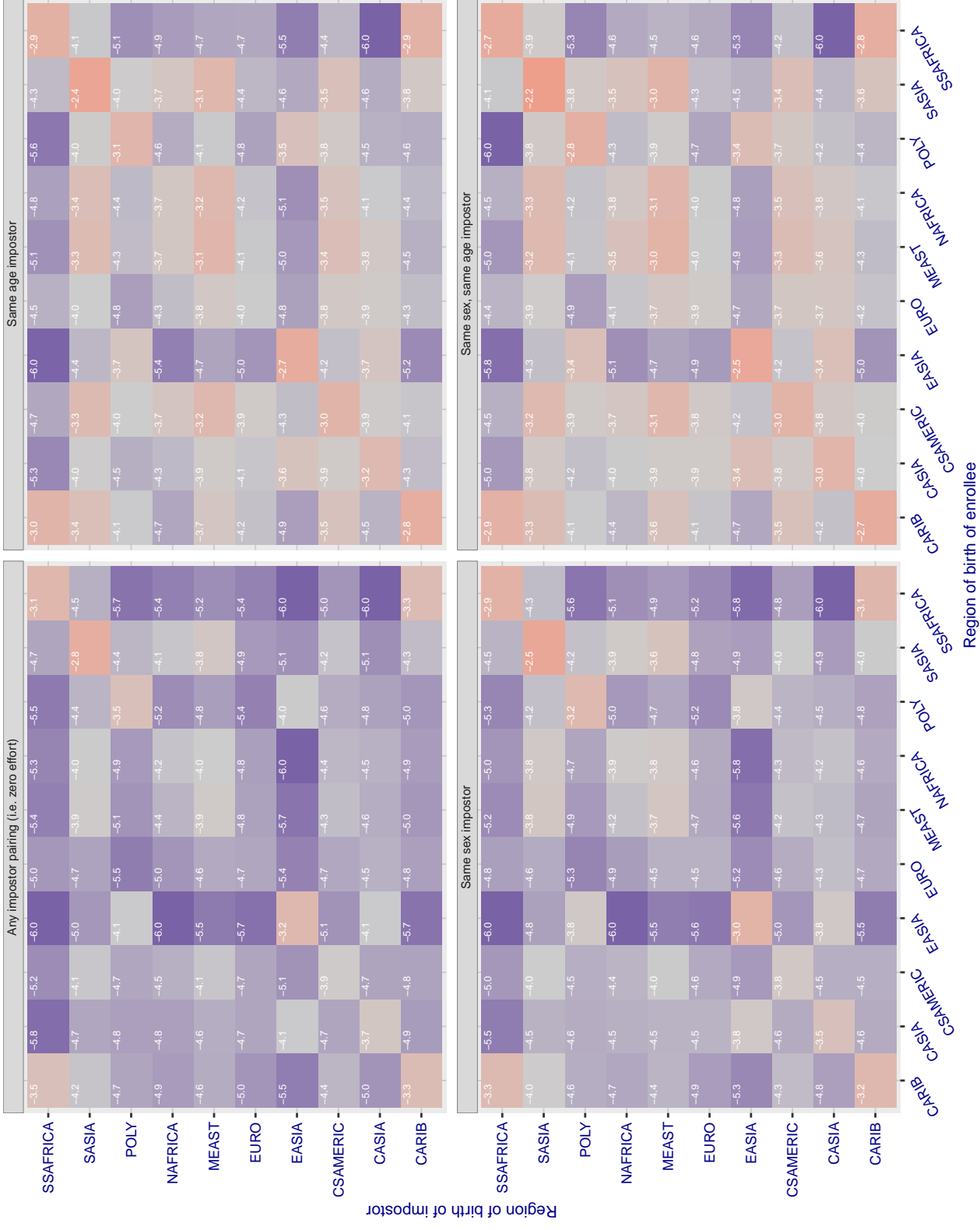


Figure 157: For algorithm ayonix-000 operating on visa images, the heatmap shows false match rates observed over impostor comparisons of faces from different individuals who were born in the given region pair. False matches are counted against a recognition threshold fixed globally to give the target FMR in the plot title, computed over all on the order of  $10^{10}$  impostor comparisons. If text appears in each box it give the same quantity as that coded by the color. Grey indicates FMR is at the intended FMR target level. Light red colors present a security vulnerability to, for example, a passport gate. Each +1 increase in  $\log_{10} FMR$  corresponds to a factor of 10 increase in FMR. The matrix is not quite symmetric because images in the enrollment and verification sets are different.

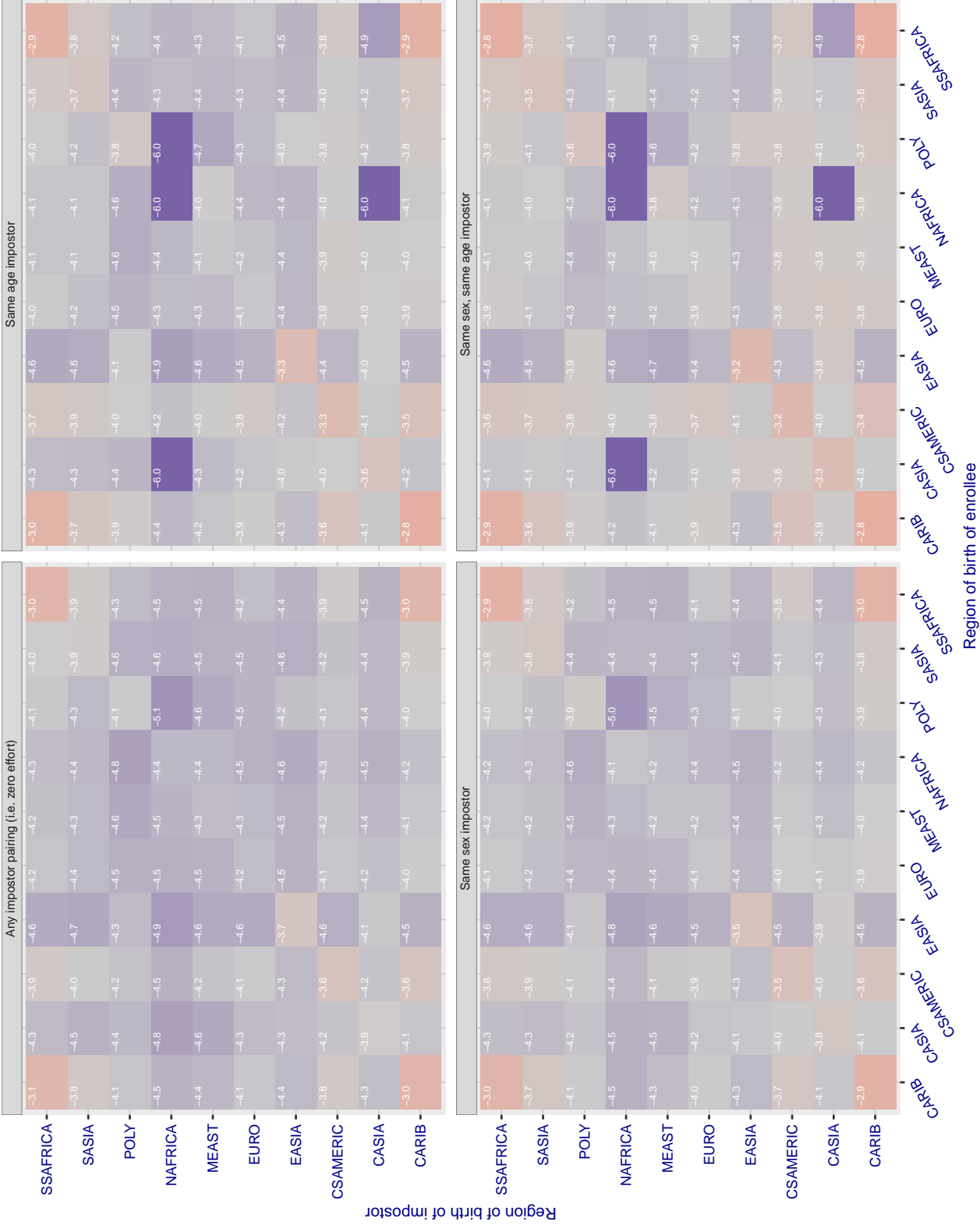
**Cross region FMR at threshold T = 0.731 for algorithm bm\_001, giving FMR(T) = 0.00001 globally.**

Figure 158: For algorithm bm-001 operating on visa images, the heatmap shows false match rates observed over impostor comparisons of faces from different individuals who were born in the given region pair. False matches are counted against a recognition threshold fixed globally to give the target FMR in the plot title, computed over all on the order of  $10^{10}$  impostor comparisons. If text appears in each box it give the same quantity as that coded by the color. Grey indicates FMR is at the intended FMR target level. Light red colors present a security vulnerability to, for example, a passport gate. Each +1 increase in  $\log_{10}$  FMR corresponds to a factor of 10 increase in FMR. The matrix is not quite symmetric because images in the enrollment and verification sets are different.

### Cross region FMR at threshold T = 0.388 for algorithm camvi\_002, giving $FMR(T) = 0.0001$ globally.

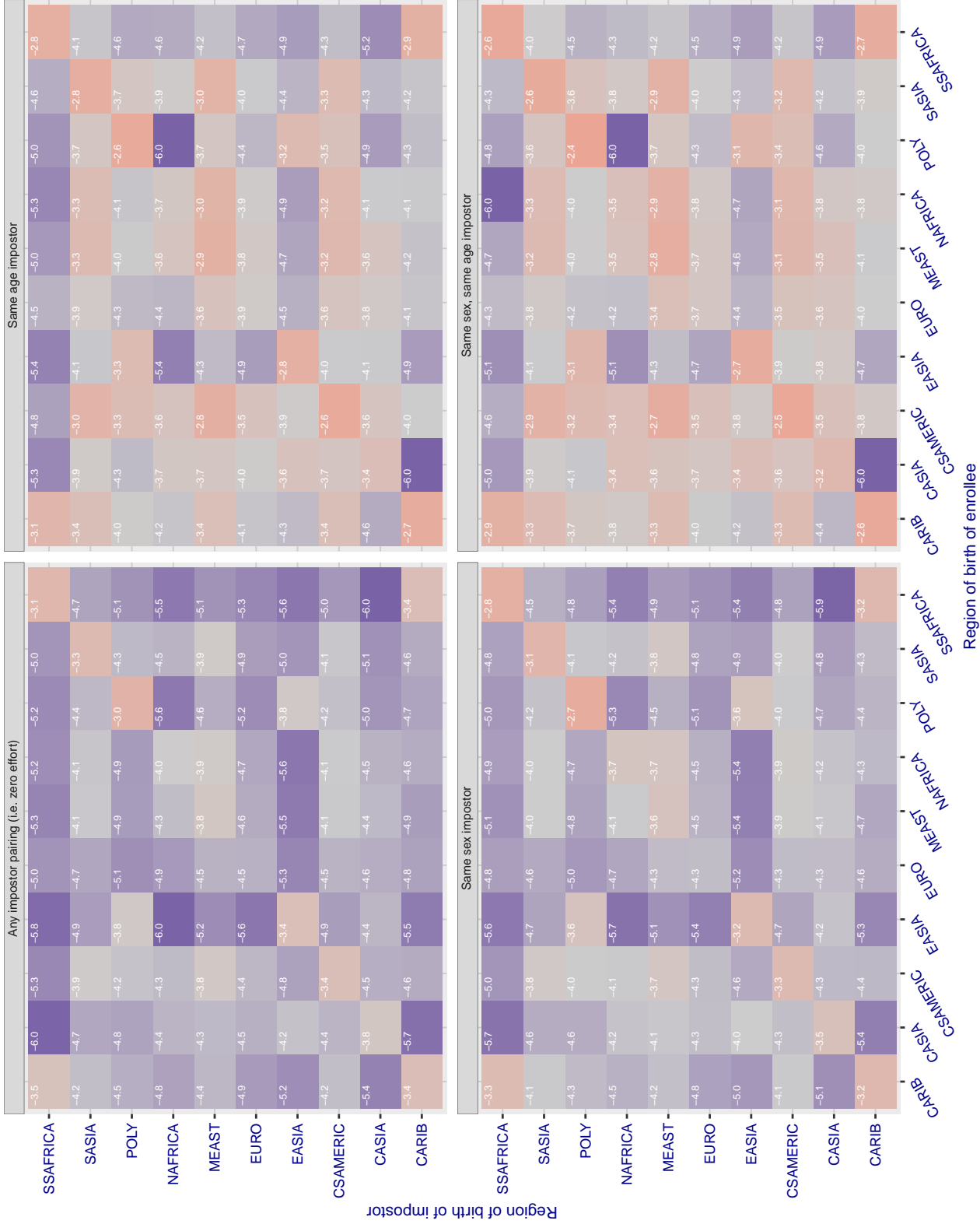


Figure 159: For algorithm camvi-002 operating on visa images, the heatmap shows false match rates observed over impostor comparisons of faces from different individuals who were born in the given region pair. False matches are counted against a recognition threshold fixed globally to give the target FMR in the plot title, computed over all on the order of  $10^{10}$  impostor comparisons. If text appears in each box it give the same quantity as that coded by the color. Grey indicates FMR is at the intended FMR target level. Light red colors present a security vulnerability to, for example, a passport gate. Each +1 increase in  $\log_{10} FMR$  corresponds to a factor of 10 increase in FMR. The matrix is not quite symmetric because images in the enrollment and verification sets are different.

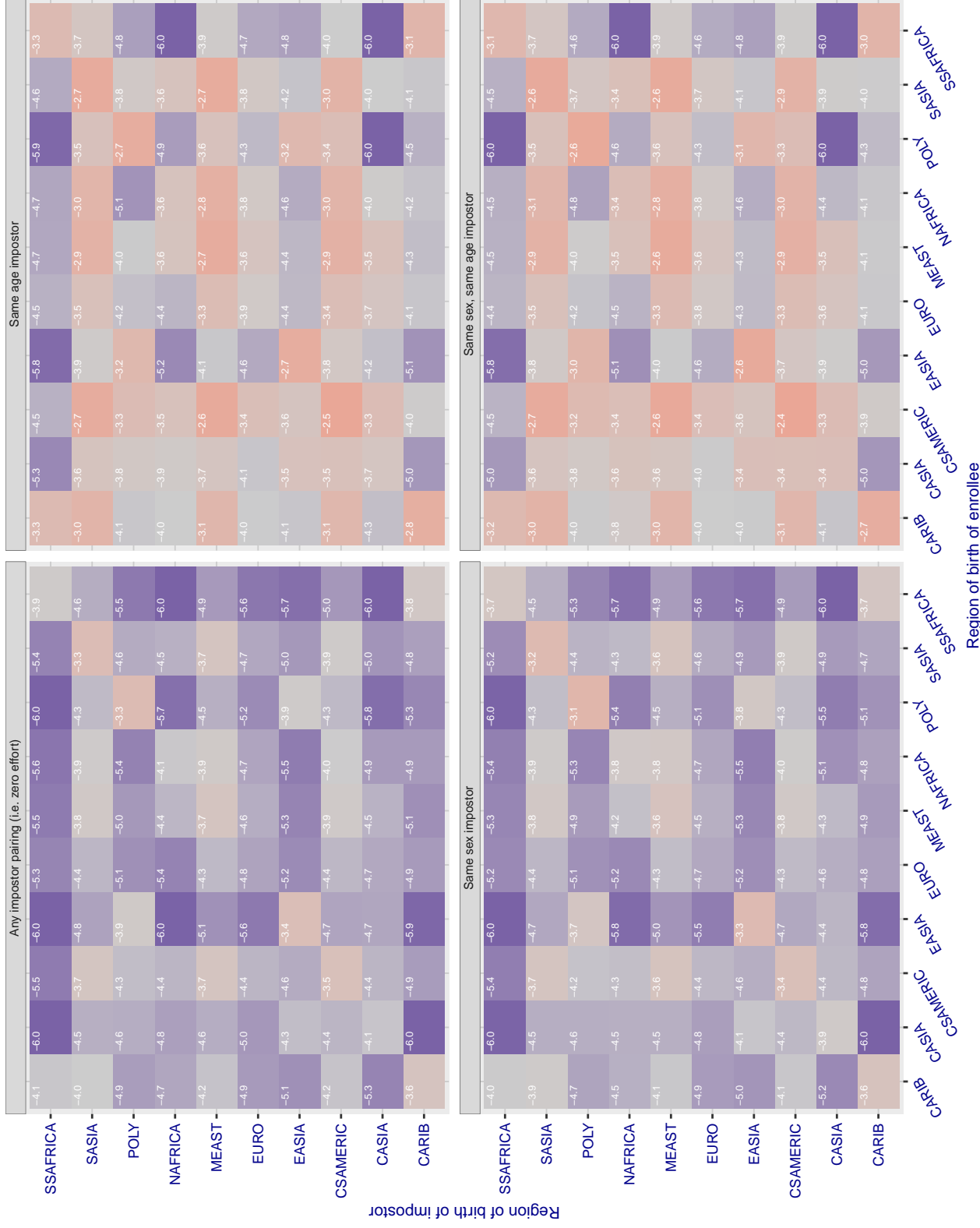
**Cross region FMR at threshold T = 0.377 for algorithm camvi\_004, giving  $FMR(T) = 0.0001$  globally.**

Figure 160: For algorithm camvi-004 operating on visa images, the heatmap shows false match rates observed over impostor comparisons of faces from different individuals who were born in the given region pair. False matches are counted against a recognition threshold fixed globally to give the target FMR in the plot title, computed over all on the order of  $10^{10}$  impostor comparisons. If text appears in each box it give the same quantity as that coded by the color. Grey indicates FMR is at the intended FMR target level. Light red colors present a security vulnerability to, for example, a passport gate. Each +1 increase in  $\log_{10} FMR$  corresponds to a factor of 10 increase in FMR. The matrix is not quite symmetric because images in the enrollment and verification sets are different.

### Cross region FMR at threshold T = 0.436 for algorithm ceiec\_001, giving FMR(T) = 0.0001 globally.

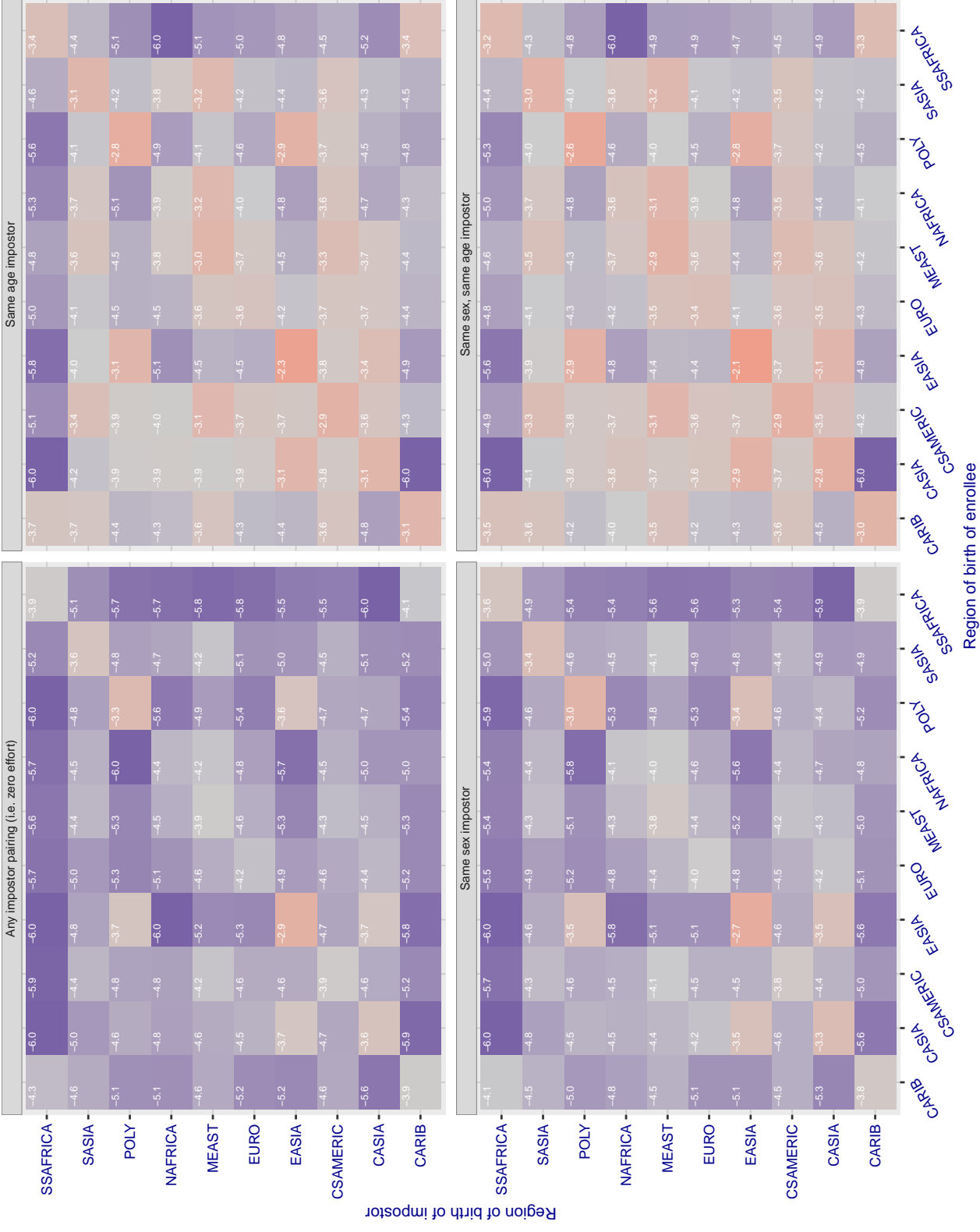


Figure 161: For algorithm ceiec-001 operating on visa images, the heatmap shows false match rates observed over impostor comparisons of faces from different individuals who were born in the given region pair. False matches are counted against a recognition threshold fixed globally to give the target FMR in the plot title, computed over all on the order of  $10^{10}$  impostor comparisons. If text appears in each box it give the same quantity as that coded by the color. Grey indicates FMR is at the intended FMR target level. Light red colors present a security vulnerability to, for example, a passport gate. Each +1 increase in  $\log_{10} \text{FMR}$  corresponds to a factor of 10 increase in FMR. The matrix is not quite symmetric because images in the enrollment and verification sets are different.

### Cross region FMR at threshold T = 0.325 for algorithm ceiec\_002, giving FMR(T) = 0.0001 globally.

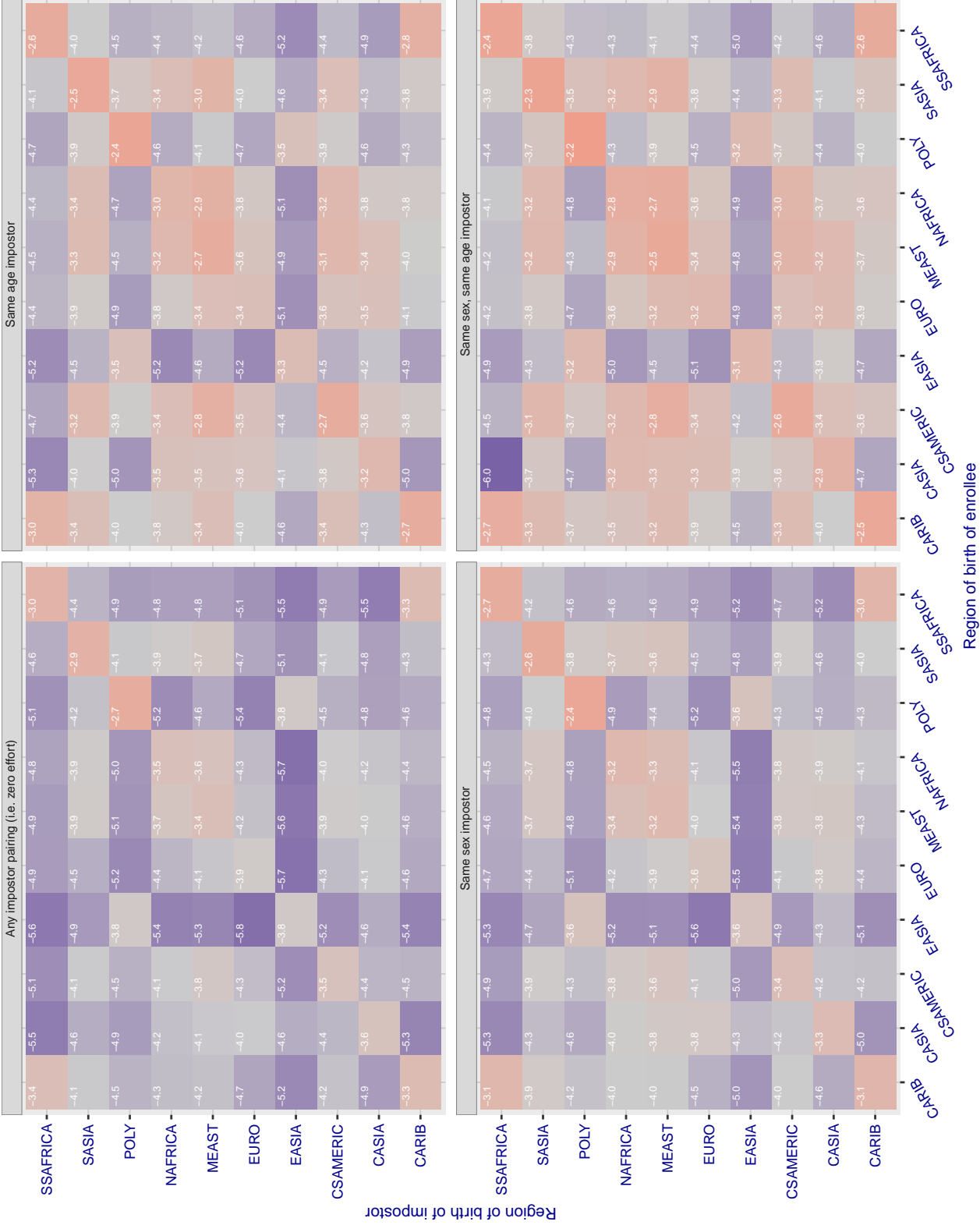


Figure 162: For algorithm ceiec-002 operating on visa images, the heatmap shows false match rates observed over impostor comparisons of faces from different individuals who were born in the given region pair. False matches are counted against a recognition threshold fixed globally to give the target FMR in the plot title, computed over all on the order of  $10^{10}$  impostor comparisons. If text appears in each box it give the same quantity as that coded by the color. Grey indicates FMR is at the intended FMR target level. Light red colors present a security vulnerability to, for example, a passport gate. Each +1 increase in  $\log_{10}$  FMR corresponds to a factor of 10 increase in FMR. The matrix is not quite symmetric because images in the enrollment and verification sets are different.

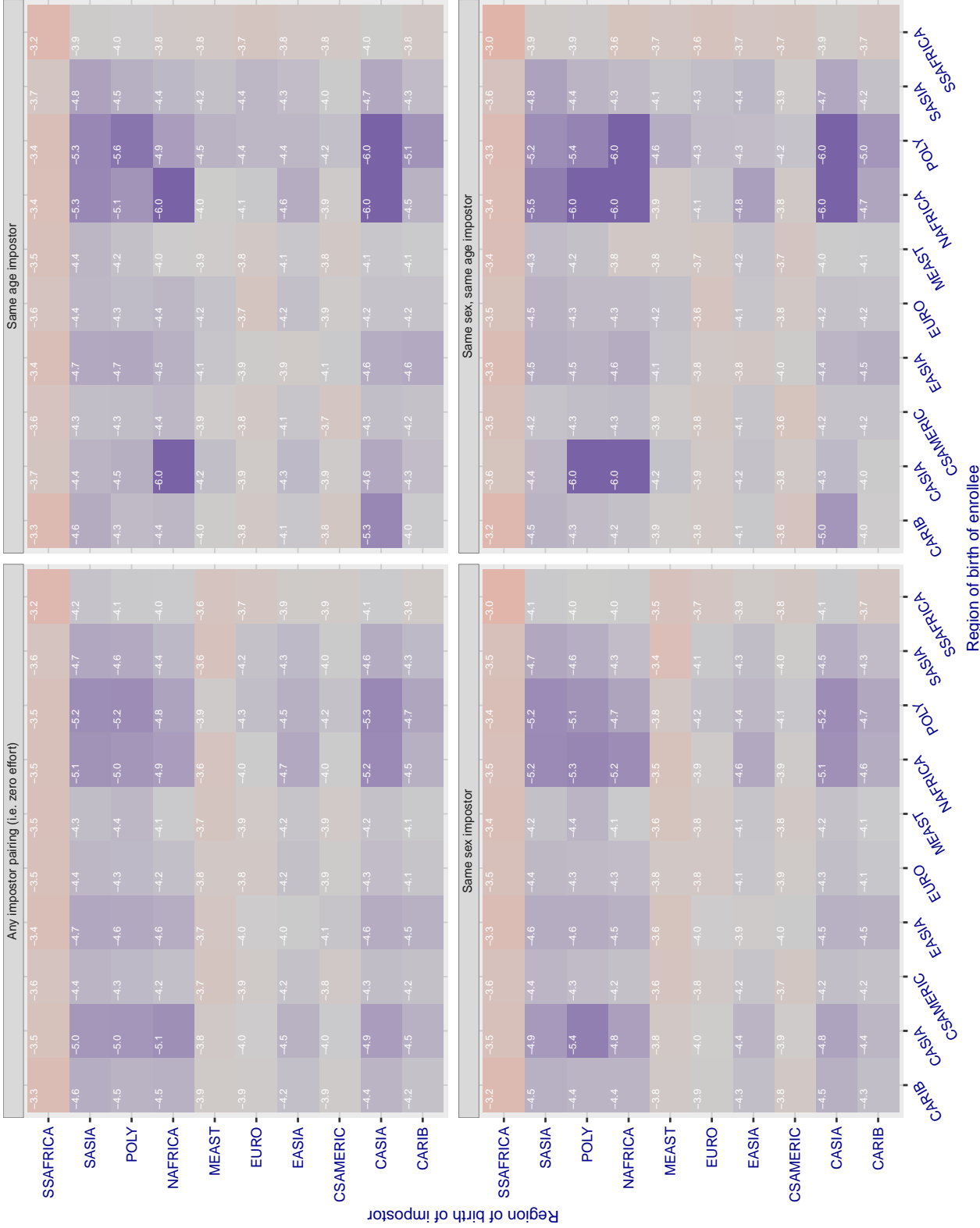
**Cross region FMR at threshold T = 106.748 for algorithm chtface\_001, giving FMR(T) = 0.00001 globally.**

Figure 163: For algorithm chtface-001 operating on visa images, the heatmap shows false match rates observed over impostor comparisons of faces from different individuals who were born in the given region pair. False matches are counted against a recognition threshold fixed globally to give the target FMR in the plot title, computed over all on the order of  $10^{10}$  impostor comparisons. If text appears in each box it give the same quantity as that coded by the color. Grey indicates FMR is at the intended FMR target level. Light red colors present a security vulnerability to, for example, a passport gate. Each +1 increase in  $\log_{10} FMR$  corresponds to a factor of 10 increase in FMR. The matrix is not quite symmetric because images in the enrollment and verification sets are different.

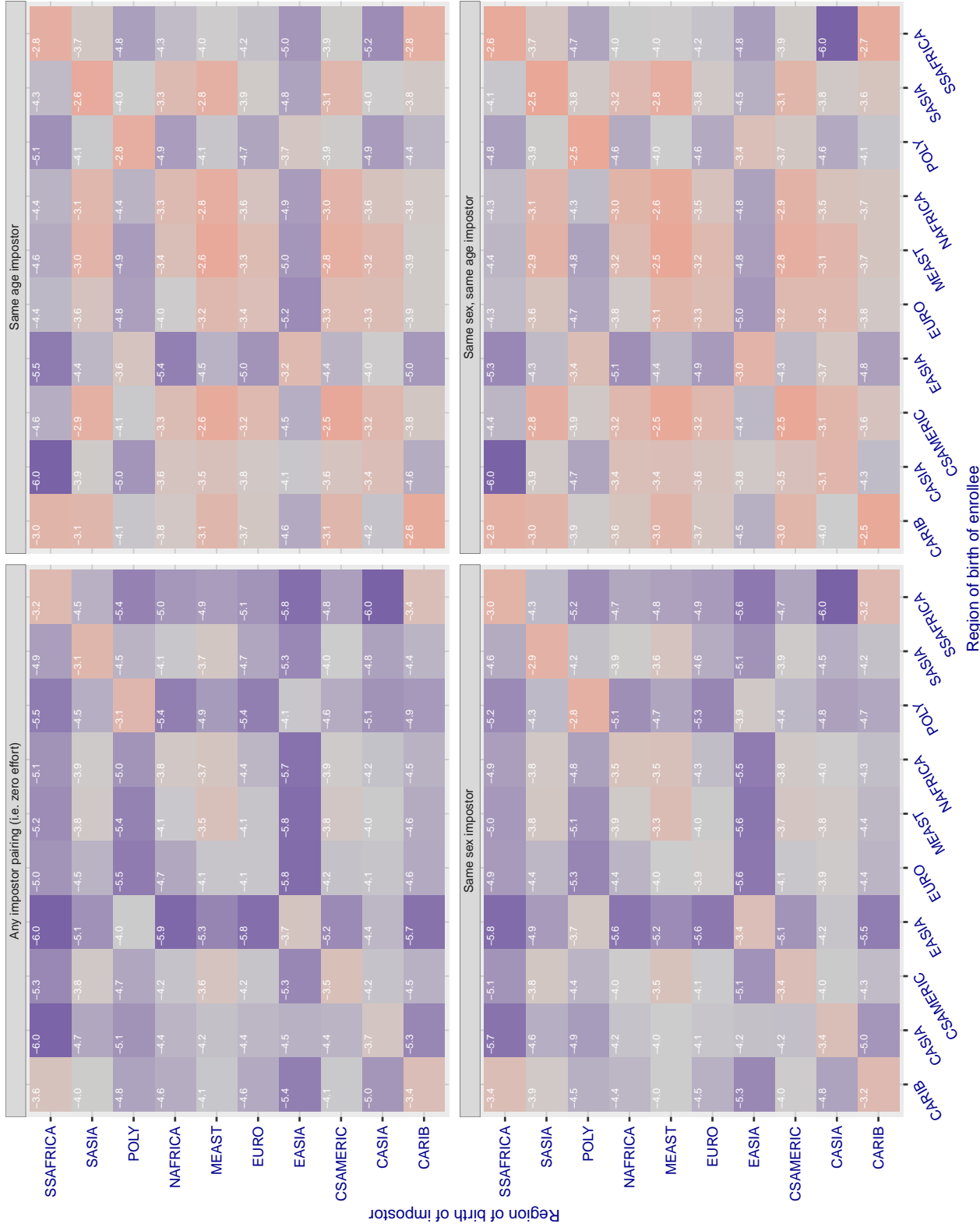
**Cross region FMR at threshold T = 2972.000 for algorithm cogent\_003, giving FMR(T) = 0.0001 globally.**

Figure 164: For algorithm cogent-003 operating on visa images, the heatmap shows false match rates observed over impostor comparisons of faces from different individuals who were born in the given region pair. False matches are counted against a recognition threshold fixed globally to give the target FMR in the plot title, computed over all on the order of  $10^{10}$  impostor comparisons. If text appears in each box it give the same quantity as that coded by the color. Grey indicates FMR is at the intended FMR target level. Light red colors present a security vulnerability to, for example, a passport gate. Each +1 increase in  $\log_{10} FMR$  corresponds to a factor of 10 increase in FMR. The matrix is not quite symmetric because images in the enrollment and verification sets are different.

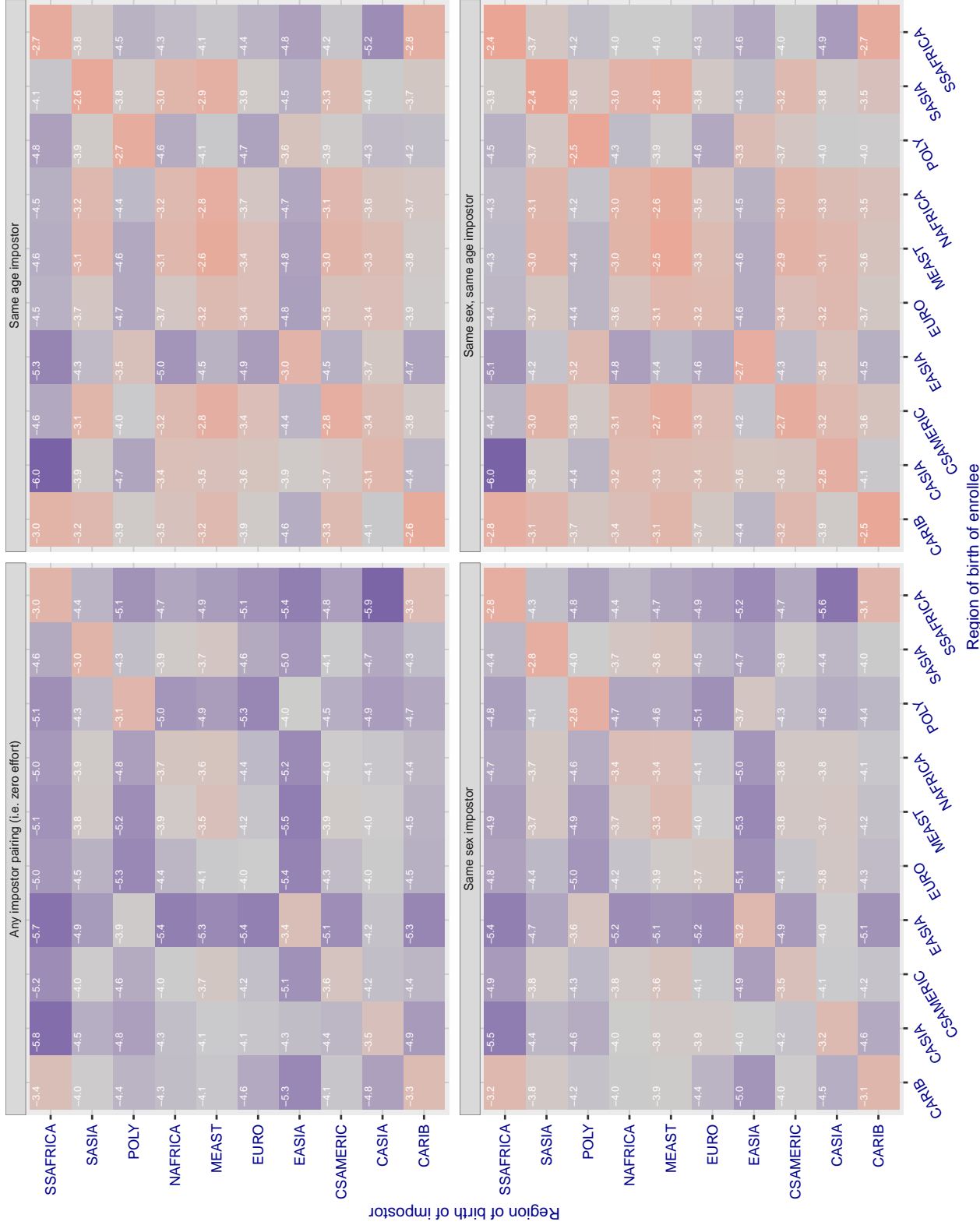
**Cross region FMR at threshold T = 3156.000 for algorithm cogent\_004, giving FMR(T) = 0.0001 globally.**

Figure 165: For algorithm cogent-004 operating on visa images, the heatmap shows false match rates observed over impostor comparisons of faces from different individuals who were born in the given region pair. False matches are counted against a recognition threshold fixed globally to give the target FMR in the plot title, computed over all on the order of  $10^{10}$  impostor comparisons. If text appears in each box it give the same quantity as that coded by the color. Grey indicates FMR is at the intended FMR target level. Light red colors present a security vulnerability to, for example, a passport gate. Each +1 increase in  $\log_{10} FMR$  corresponds to a factor of 10 increase in FMR. The matrix is not quite symmetric because images in the enrollment and verification sets are different.

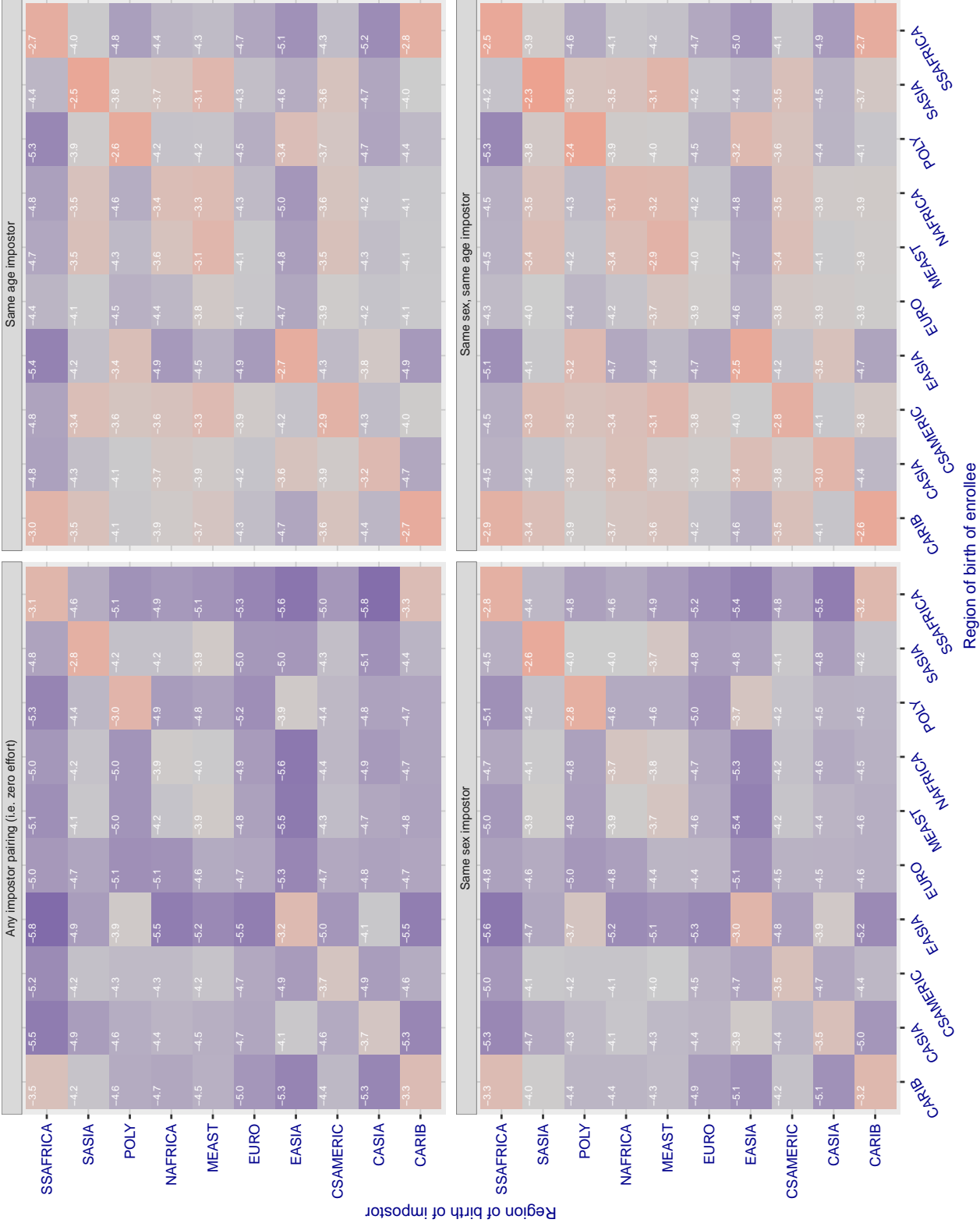
**Cross region FMR at threshold T = 0.565 for algorithm cognitec\_000, giving FMR(T) = 0.0001 globally.**

Figure 166: For algorithm cognitec-000 operating on visa images, the heatmap shows false match rates observed over impostor comparisons of faces from different individuals who were born in the given region pair. False matches are counted against a recognition threshold fixed globally to give the target FMR in the plot title, computed over all on the order of  $10^{10}$  impostor comparisons. If text appears in each box it give the same quantity as that coded by the color. Grey indicates FMR is at the intended FMR target level. Light red colors present a security vulnerability to, for example, a passport gate. Each +1 increase in  $\log_{10} FMR$  corresponds to a factor of 10 increase in FMR. The matrix is not quite symmetric because images in the enrollment and verification sets are different.

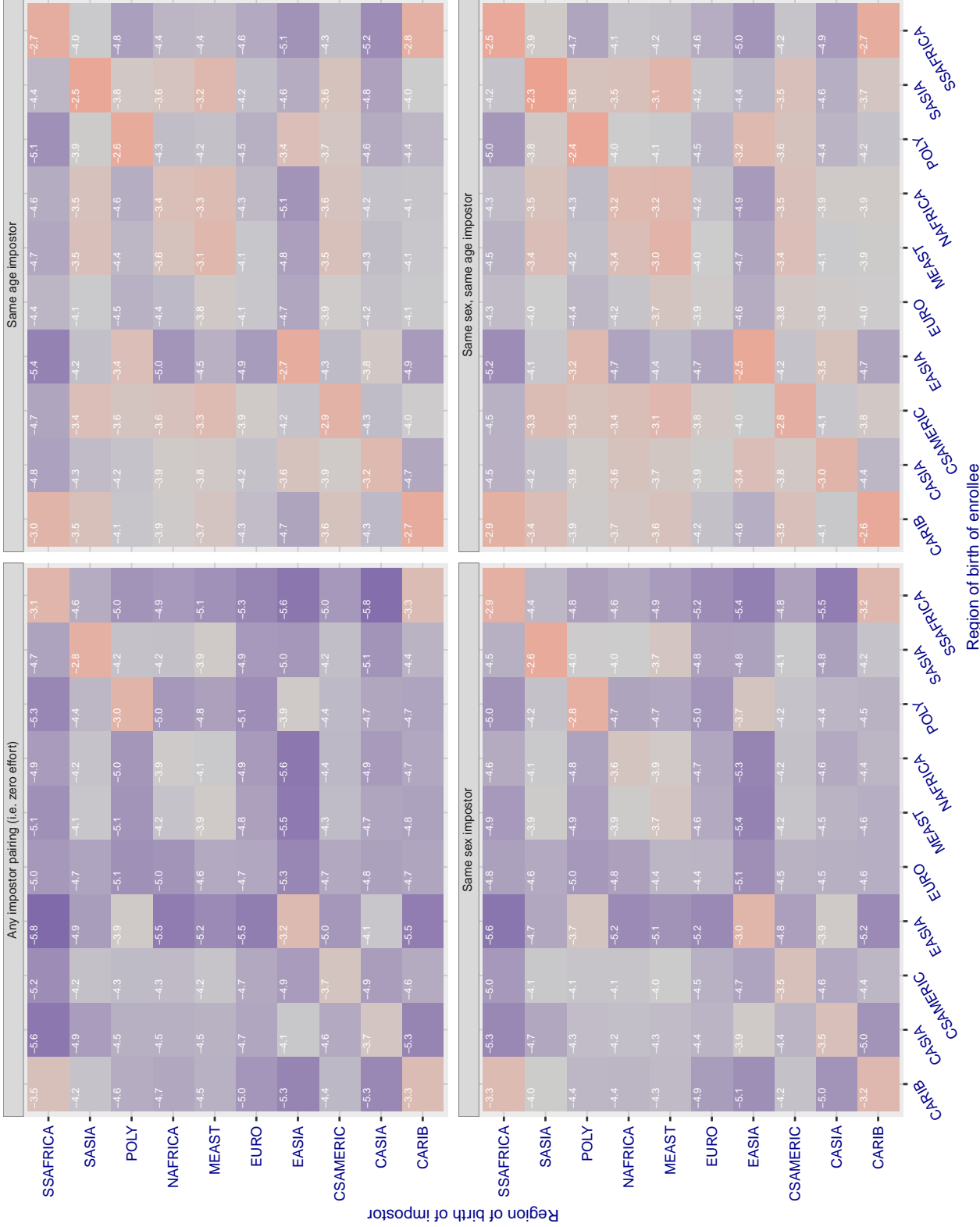
**Cross region FMR at threshold T = 0.565 for algorithm cognitec\_001, giving FMR(T) = 0.0001 globally.**

Figure 167: For algorithm cognitec-001 operating on visa images, the heatmap shows false match rates observed over impostor comparisons of faces from different individuals who were born in the given region pair. False matches are counted against a recognition threshold fixed globally to give the target FMR in the plot title, computed over all on the order of  $10^{10}$  impostor comparisons. If text appears in each box it give the same quantity as that coded by the color. Grey indicates FMR is at the intended FMR target level. Light red colors present a security vulnerability to, for example, a passport gate. Each +1 increase in  $\log_{10} FMR$  corresponds to a factor of 10 increase in FMR. The matrix is not quite symmetric because images in the enrollment and verification sets are different.

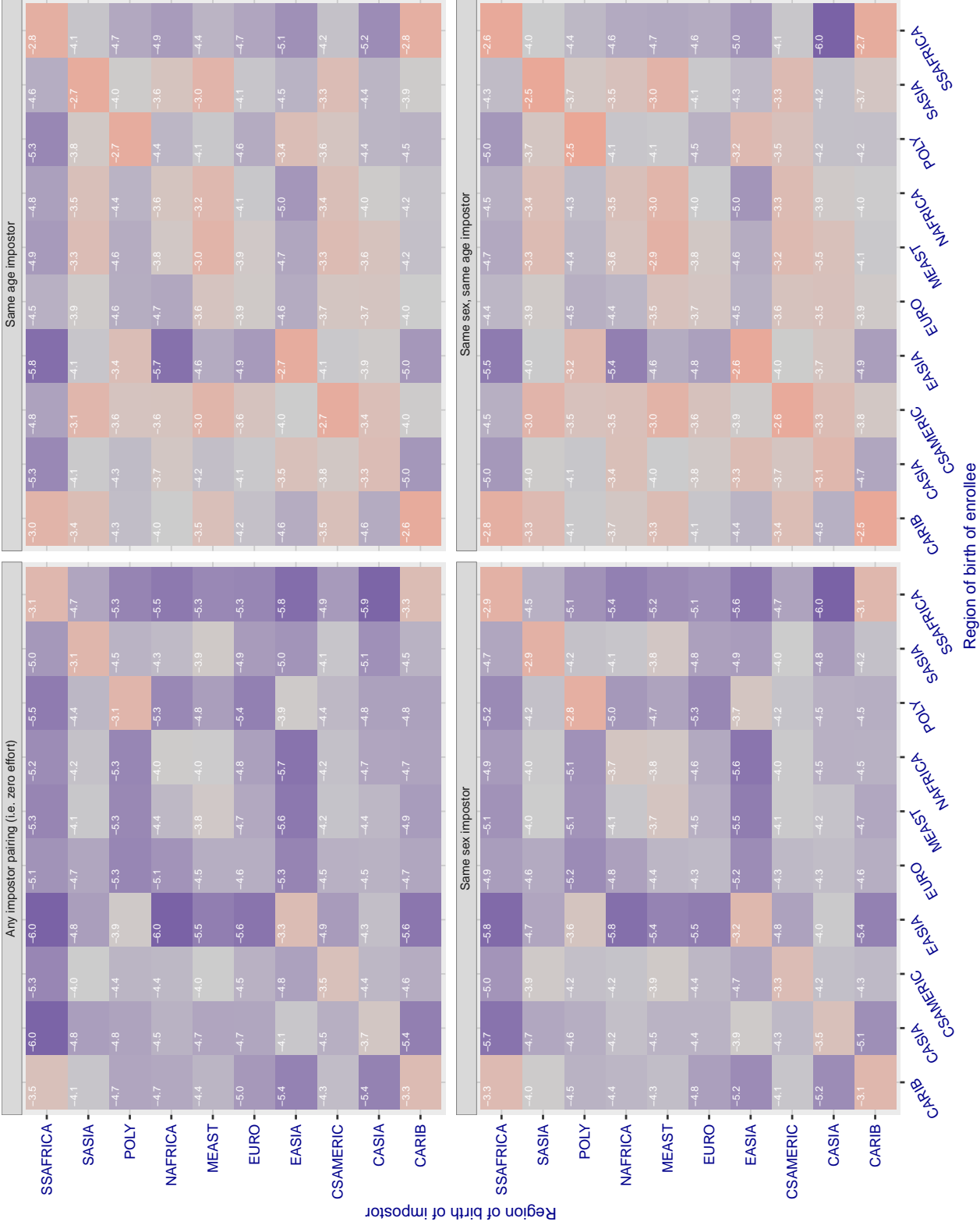
**Cross region FMR at threshold T = 3.730 for algorithm ct tcbcbank\_000, giving FMR(T) = 0.0001 globally.**

Figure 168: For algorithm ct tcbcbank-000 operating on visa images, the heatmap shows false match rates observed over impostor comparisons of faces from different individuals who were born in the given region pair. False matches are counted against a recognition threshold fixed globally to give the target FMR in the plot title, computed over all on the order of  $10^{10}$  impostor comparisons. If text appears in each box it give the same quantity as that coded by the color. Grey indicates FMR is at the intended FMR target level. Light red colors present a security vulnerability to, for example, a passport gate. Each +1 increase in  $\log_{10} FMR$  corresponds to a factor of 10 increase in FMR. The matrix is not quite symmetric because images in the enrollment and verification sets are different.

### Cross region FMR at threshold T = 0.762 for algorithm cyberextruder\_001, giving FMR(T) = 0.0001 globally.

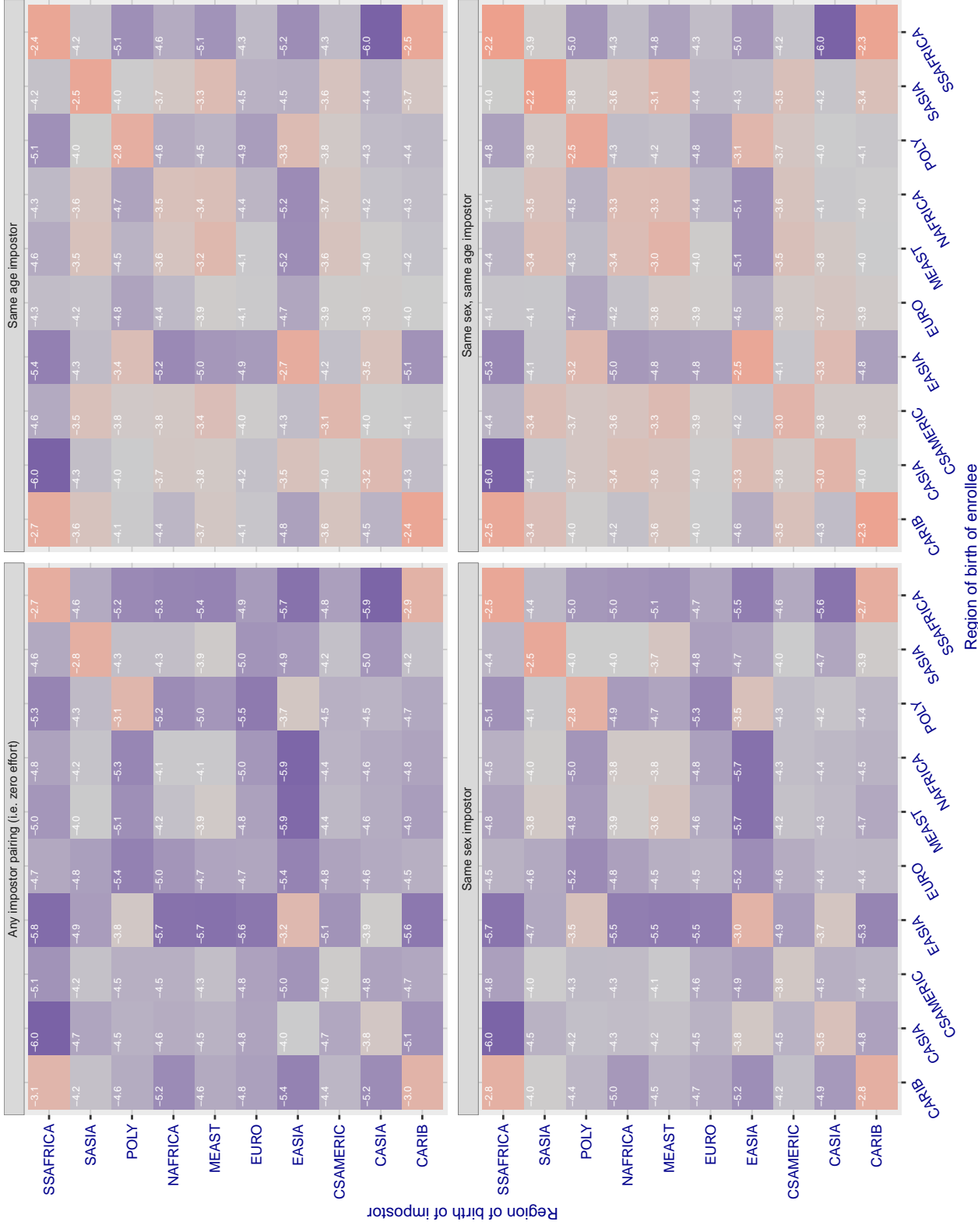


Figure 169: For algorithm cyberextruder-001 operating on visa images, the heatmap shows false match rates observed over impostor comparisons of faces from different individuals who were born in the given region pair. False matches are counted against a recognition threshold fixed globally to give the target FMR in the plot title, computed over all on the order of  $10^{10}$  impostor comparisons. If text appears in each box it give the same quantity as that coded by the color. Grey indicates FMR is at the intended FMR target level. Light red colors present a security vulnerability to, for example, a passport gate. Each +1 increase in  $\log_{10} FMR$  corresponds to a factor of 10 increase in FMR. The matrix is not quite symmetric because images in the enrollment and verification sets are different.

### Cross region FMR at threshold T = 0.500 for algorithm cyberextruder\_002, giving FMR(T) = 0.0001 globally.

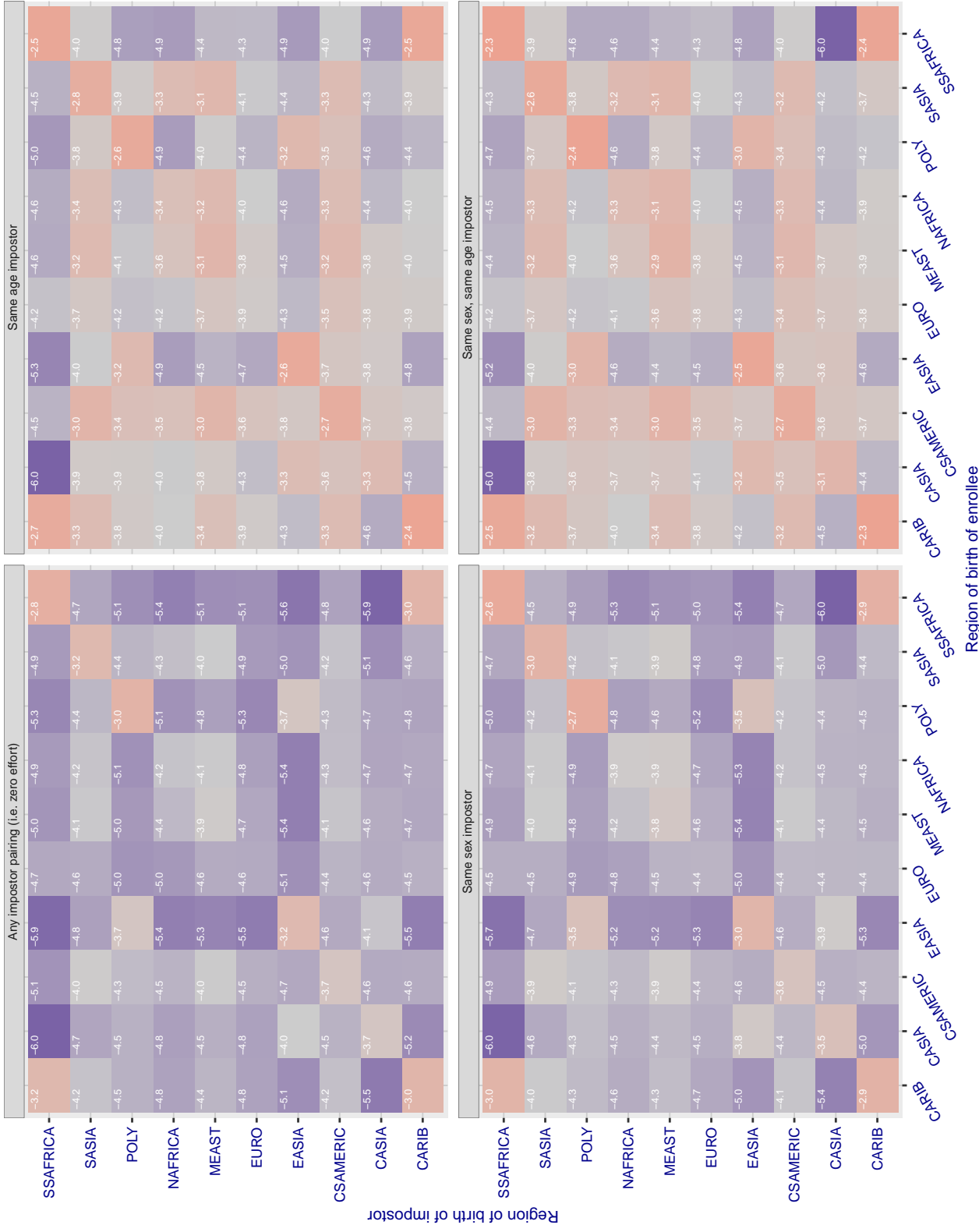


Figure 170: For algorithm cyberextruder-002 operating on visa images, the heatmap shows false match rates observed over impostor comparisons of faces from different individuals who were born in the given region pair. False matches are counted against a recognition threshold fixed globally to give the target FMR in the plot title, computed over all on the order of  $10^{10}$  impostor comparisons. If text appears in each box it give the same quantity as that coded by the color. Grey indicates FMR is at the intended FMR target level. Light red colors present a security vulnerability to, for example, a passport gate. Each +1 increase in  $\log_{10} FMR$  corresponds to a factor of 10 increase in FMR. The matrix is not quite symmetric because images in the enrollment and verification sets are different.

### Cross region FMR at threshold T = 1.409 for algorithm cyberlink\_002, giving $FMR(T) = 0.0001$ globally.

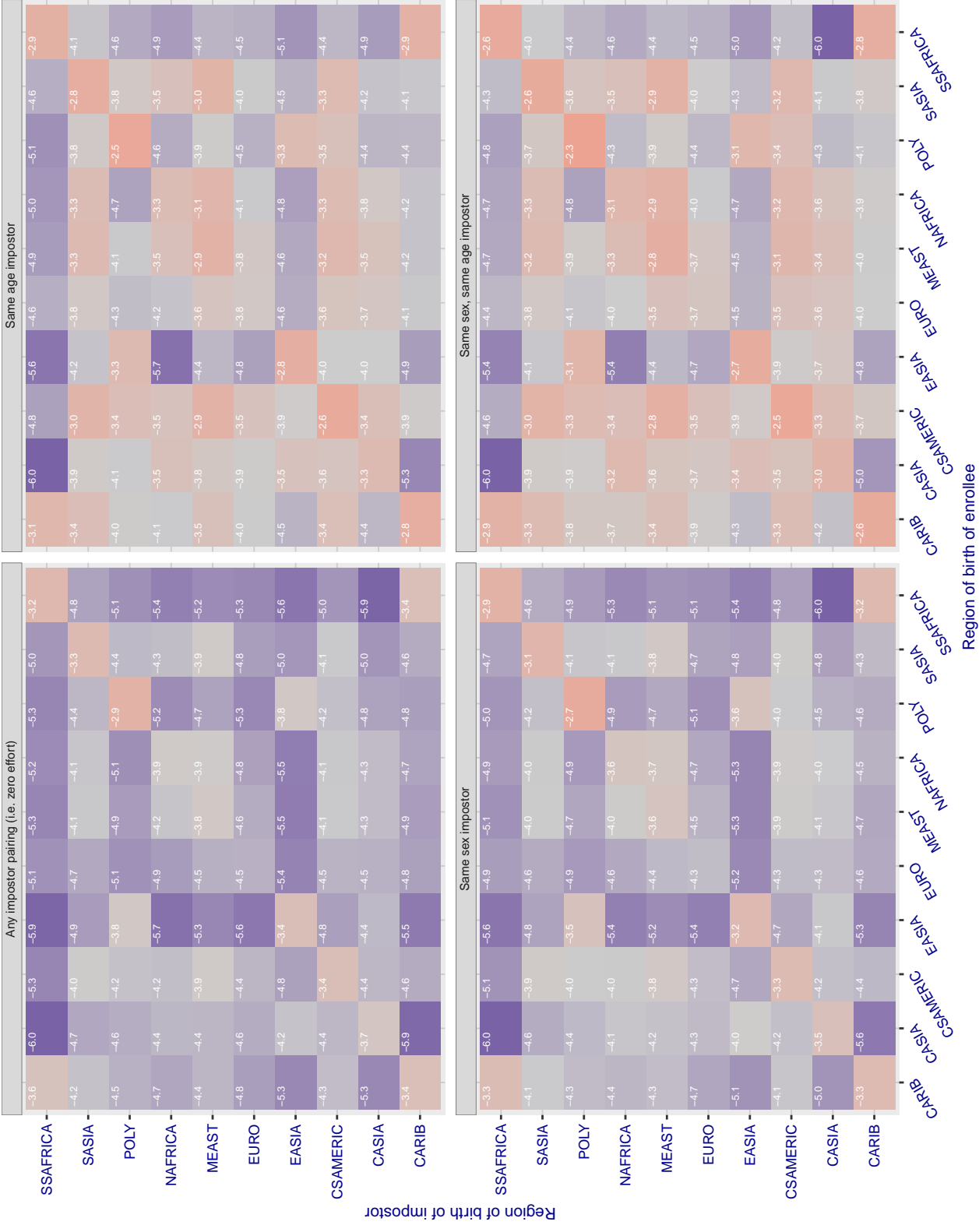


Figure 171: For algorithm cyberlink-002 operating on visa images, the heatmap shows false match rates observed over impostor comparisons of faces from different individuals who were born in the given region pair. False matches are counted against a recognition threshold fixed globally to give the target FMR in the plot title, computed over all on the order of  $10^{10}$  impostor comparisons. If text appears in each box it give the same quantity as that coded by the color. Grey indicates FMR is at the intended FMR target level. Light red colors present a security vulnerability to, for example, a passport gate. Each +1 increase in  $\log_{10} FMR$  corresponds to a factor of 10 increase in FMR. The matrix is not quite symmetric because images in the enrollment and verification sets are different.

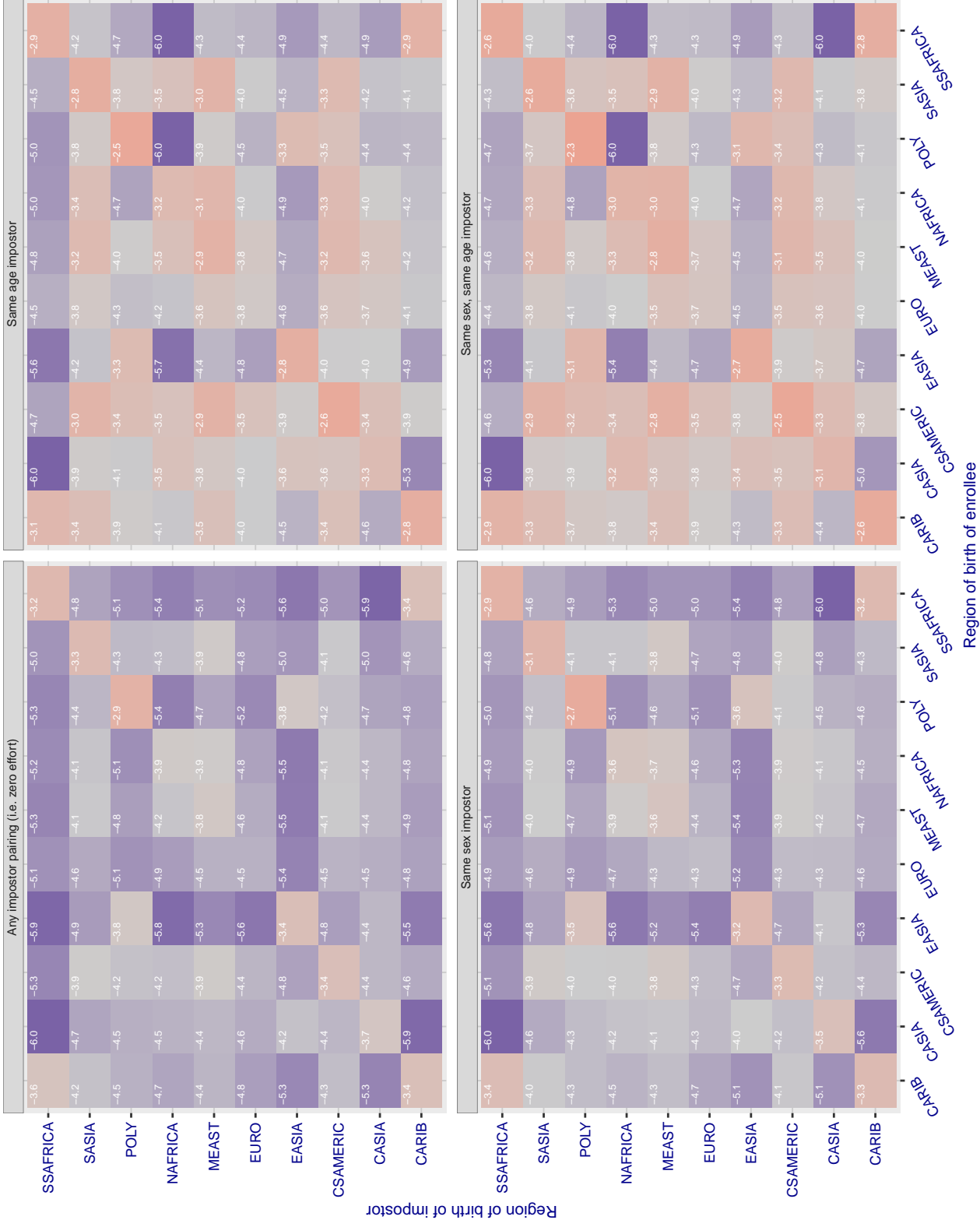
**Cross region FMR at threshold T = 1.409 for algorithm cyberlink\_003, giving  $FMR(T) = 0.0001$  globally.**

Figure 172: For algorithm cyberlink-003 operating on visa images, the heatmap shows false match rates observed over impostor comparisons of faces from different individuals who were born in the given region pair. False matches are counted against a recognition threshold fixed globally to give the target FMR in the plot title, computed over all on the order of  $10^{10}$  impostor comparisons. If text appears in each box it give the same quantity as that coded by the color. Grey indicates FMR is at the intended FMR target level. Light red colors present a security vulnerability to, for example, a passport gate. Each +1 increase in  $\log_{10} FMR$  corresponds to a factor of 10 increase in FMR. The matrix is not quite symmetric because images in the enrollment and verification sets are different.

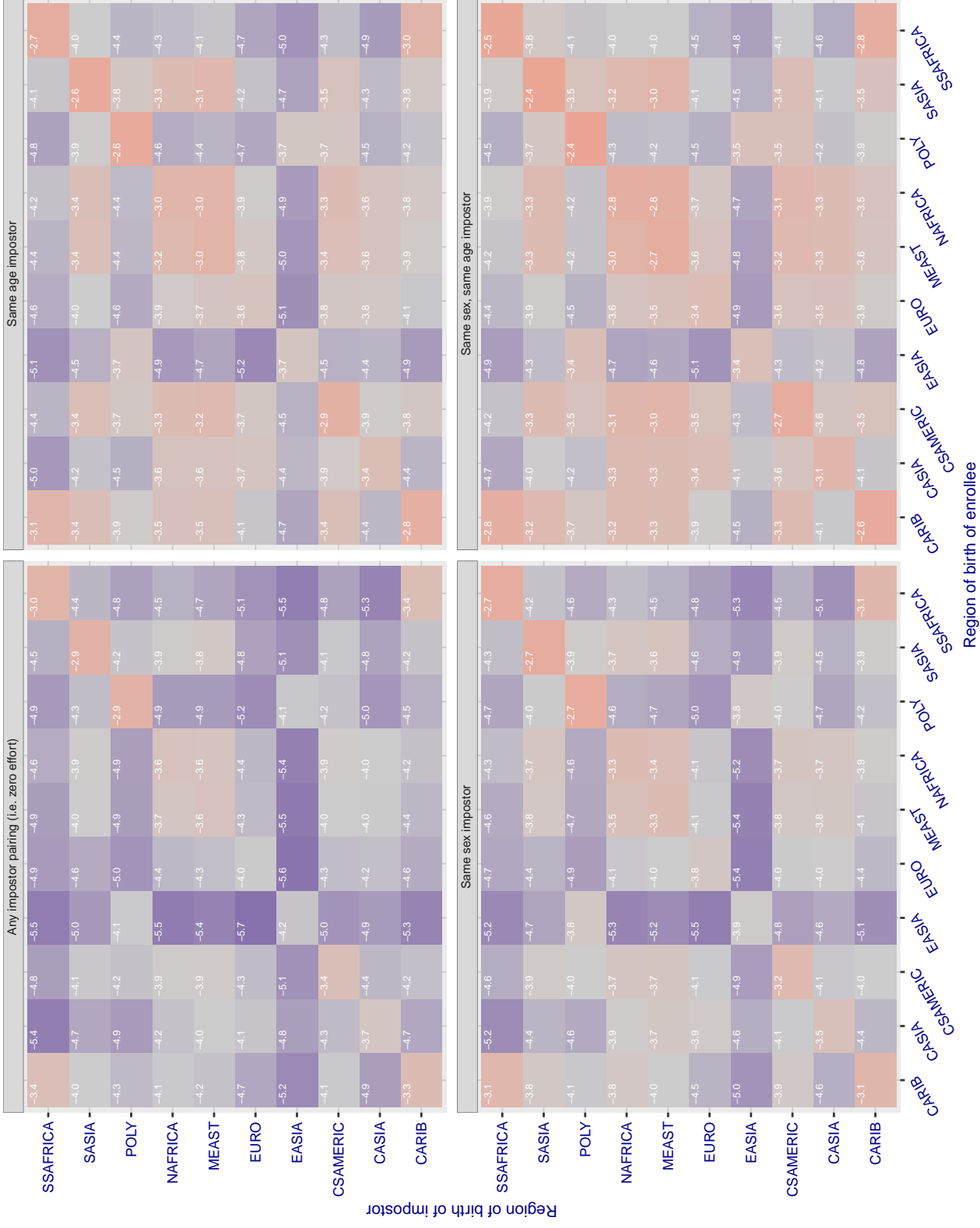
**Cross region FMR at threshold T = 6696.000 for algorithm dahua\_002, giving FMR(T) = 0.0001 globally.**

Figure 173: For algorithm dahua-002 operating on visa images, the heatmap shows false match rates observed over impostor comparisons of faces from different individuals who were born in the given region pair. False matches are counted against a recognition threshold fixed globally to give the target FMR in the plot title, computed over all on the order of  $10^{10}$  impostor comparisons. If text appears in each box it give the same quantity as that coded by the color. Grey indicates FMR is at the intended FMR target level. Light red colors present a security vulnerability to, for example, a passport gate. Each +1 increase in  $\log_{10} FMR$  corresponds to a factor of 10 increase in FMR. The matrix is not quite symmetric because images in the enrollment and verification sets are different.

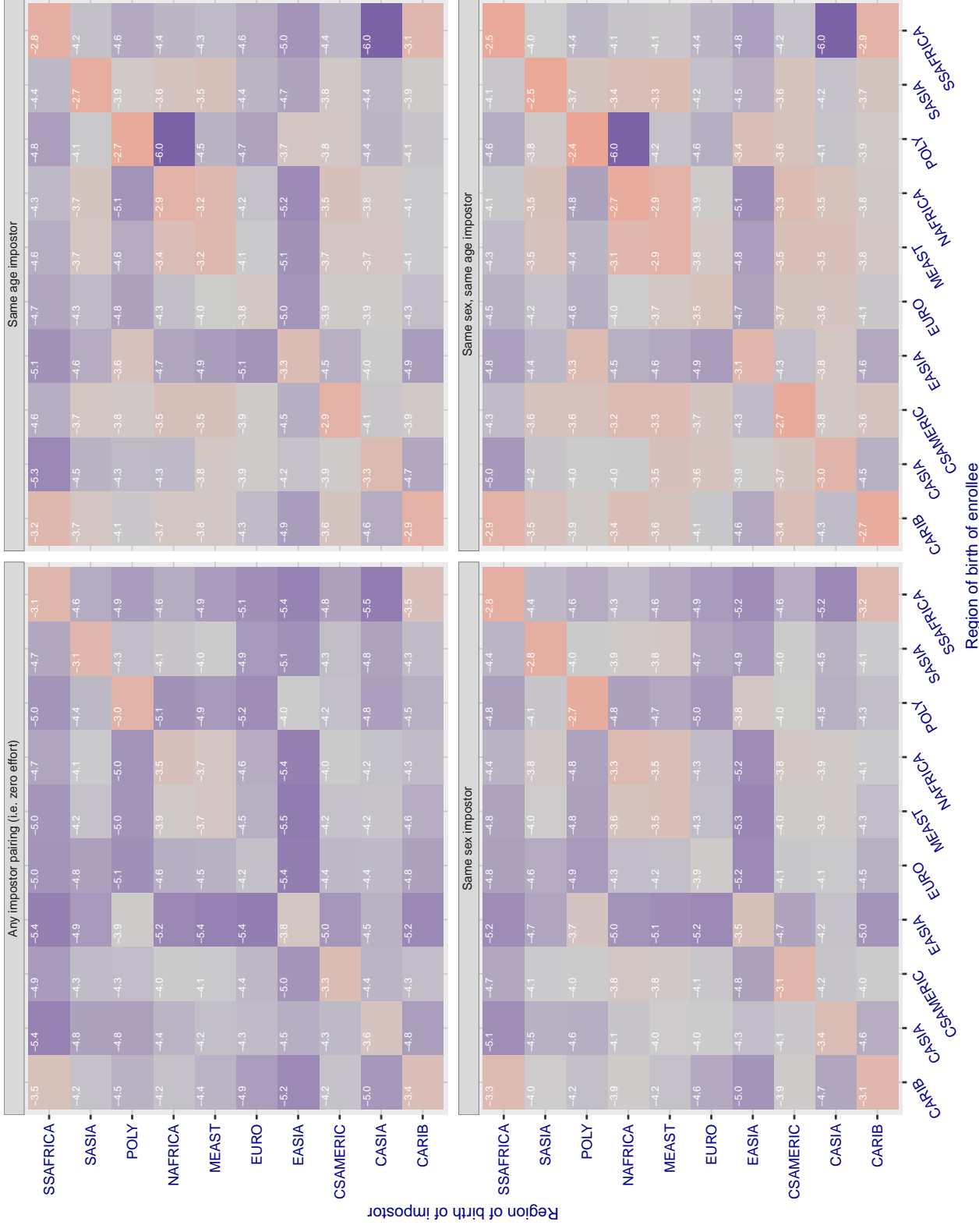
**Cross region FMR at threshold T = 6034.000 for algorithm dahua\_003, giving FMR(T) = 0.0001 globally.**

Figure 174: For algorithm dahua-003 operating on visa images, the heatmap shows false match rates observed over impostor comparisons of faces from different individuals who were born in the given region pair. False matches are counted against a recognition threshold fixed globally to give the target FMR in the plot title, computed over all on the order of  $10^{10}$  impostor comparisons. If text appears in each box it give the same quantity as that coded by the color. Grey indicates FMR is at the intended FMR target level. Light red colors present a security vulnerability to, for example, a passport gate. Each +1 increase in  $\log_{10} FMR$  corresponds to a factor of 10 increase in FMR. The matrix is not quite symmetric because images in the enrollment and verification sets are different.

### Cross region FMR at threshold T = 1.359 for algorithm deepglint\_001, giving $FMR(T) = 0.0001$ globally.

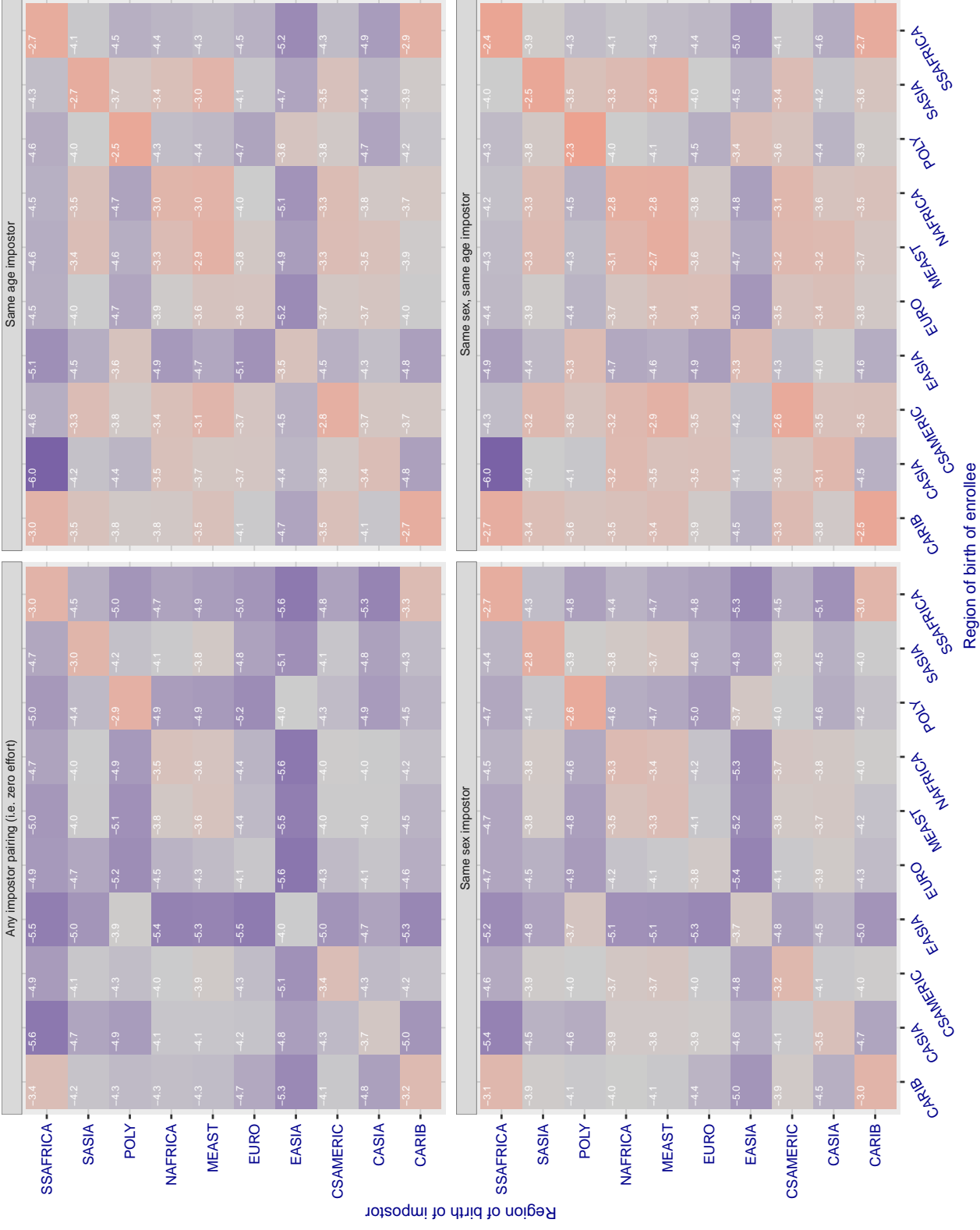


Figure 175: For algorithm deepglint-001 operating on visa images, the heatmap shows false match rates observed over impostor comparisons of faces from different individuals who were born in the given region pair. False matches are counted against a recognition threshold fixed globally to give the target FMR in the plot title, computed over all on the order of  $10^{10}$  impostor comparisons. If text appears in each box it give the same quantity as that coded by the color. Grey indicates FMR is at the intended FMR target level. Light red colors present a security vulnerability to, for example, a passport gate. Each +1 increase in  $\log_{10} FMR$  corresponds to a factor of 10 increase in FMR. The matrix is not quite symmetric because images in the enrollment and verification sets are different.

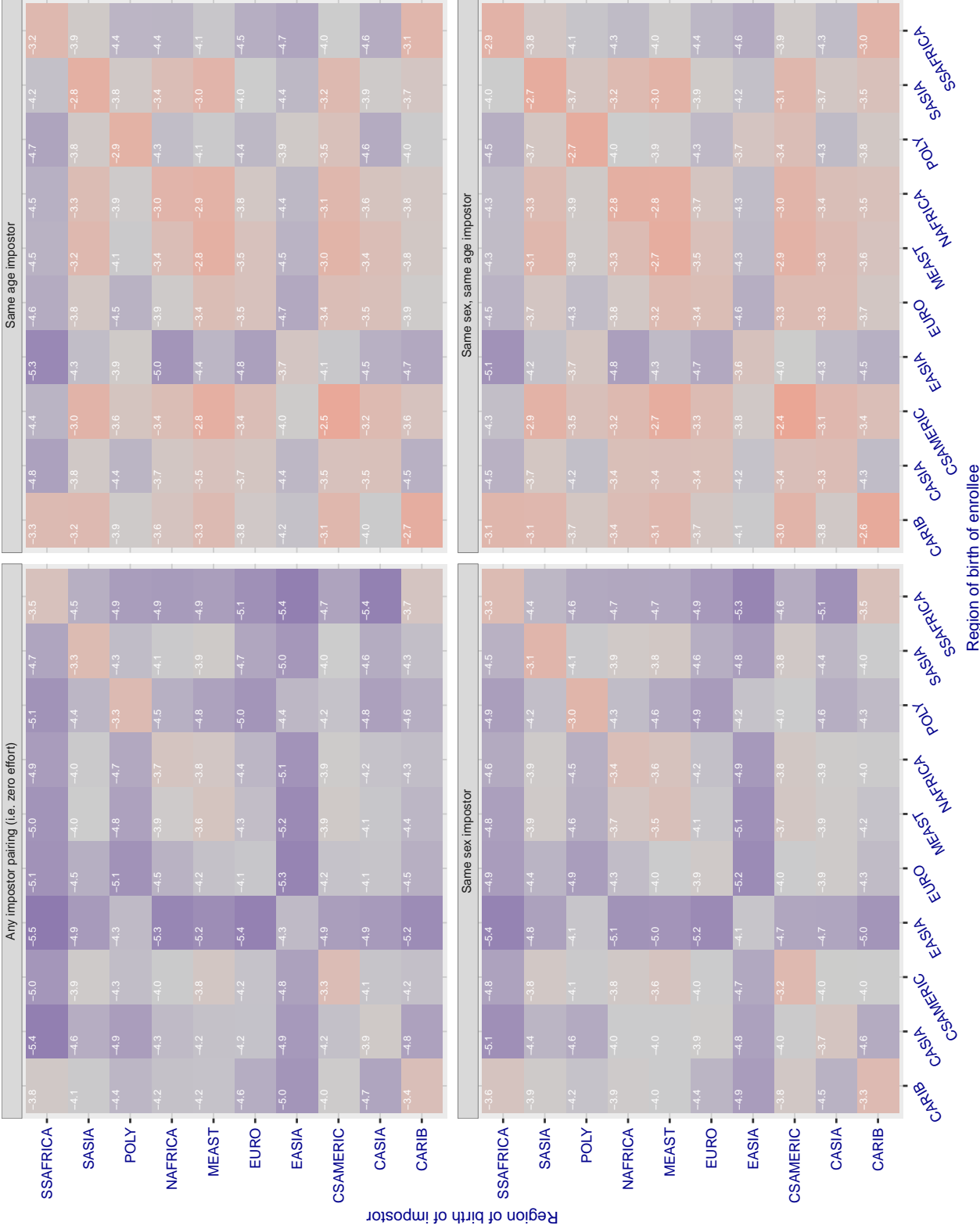
**Cross region FMR at threshold T = 1.371 for algorithm deepsea\_001, giving FMR(T) = 0.0001 globally.**

Figure 176: For algorithm deepsea-001 operating on visa images, the heatmap shows false match rates observed over impostor comparisons of faces from different individuals who were born in the given region pair. False matches are counted against a recognition threshold fixed globally to give the target FMR in the plot title, computed over all on the order of  $10^{10}$  impostor comparisons. If text appears in each box it give the same quantity as that coded by the color. Grey indicates FMR is at the intended FMR target level. Light red colors present a security vulnerability to, for example, a passport gate. Each +1 increase in  $\log_{10} FMR$  corresponds to a factor of 10 increase in FMR. The matrix is not quite symmetric because images in the enrollment and verification sets are different.

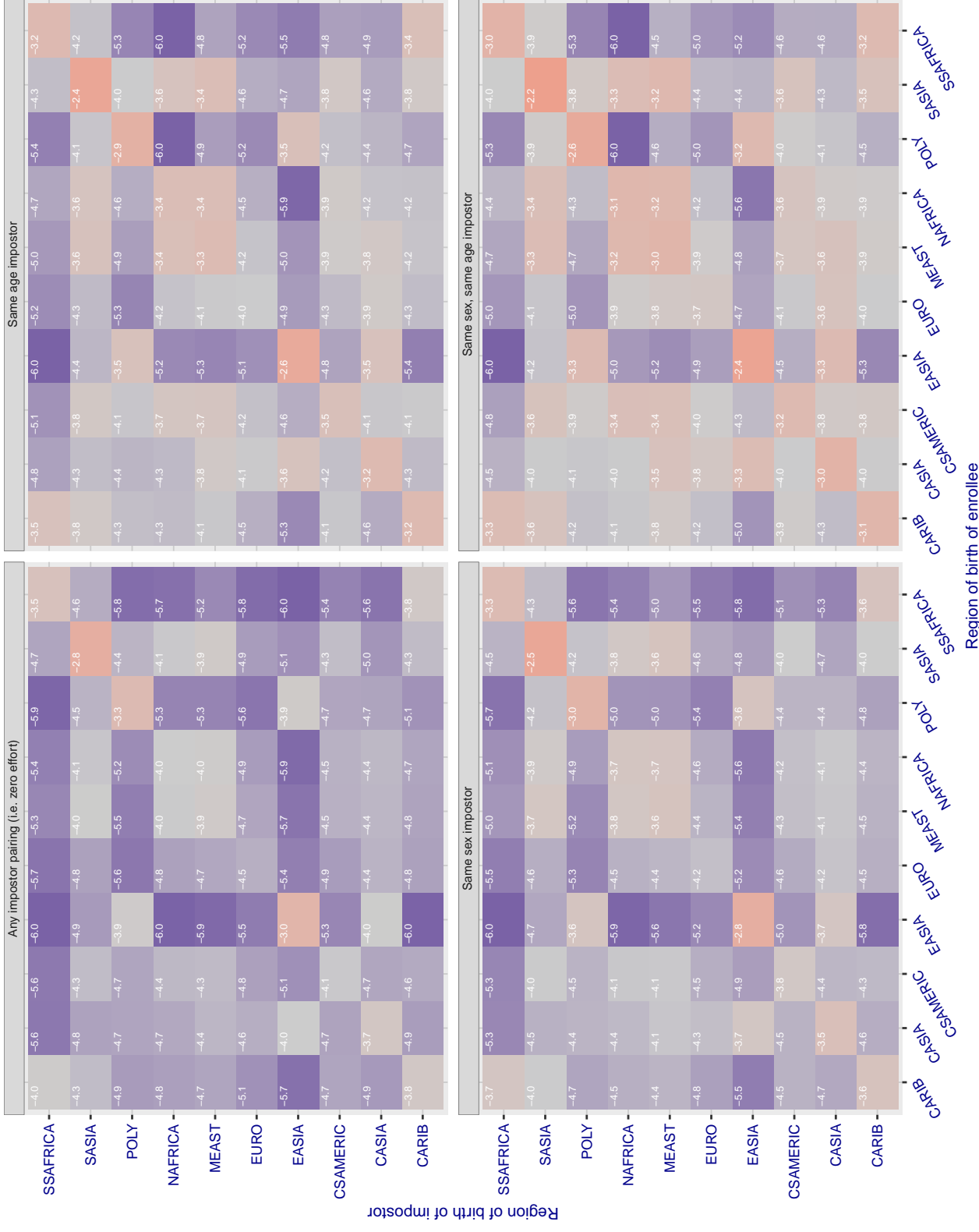
**Cross region FMR at threshold T = 79.344 for algorithm dermalog\_005, giving FMR(T) = 0.0001 globally.**

Figure 177: For algorithm dermalog-005 operating on visa images, the heatmap shows false match rates observed over impostor comparisons of faces from different individuals who were born in the given region pair. False matches are counted against a recognition threshold fixed globally to give the target FMR in the plot title, computed over all on the order of  $10^{10}$  impostor comparisons. If text appears in each box it give the same quantity as that coded by the color. Grey indicates FMR is at the intended FMR target level. Light red colors present a security vulnerability to, for example, a passport gate. Each +1 increase in  $\log_{10} FMR$  corresponds to a factor of 10 increase in FMR. The matrix is not quite symmetric because images in the enrollment and verification sets are different.

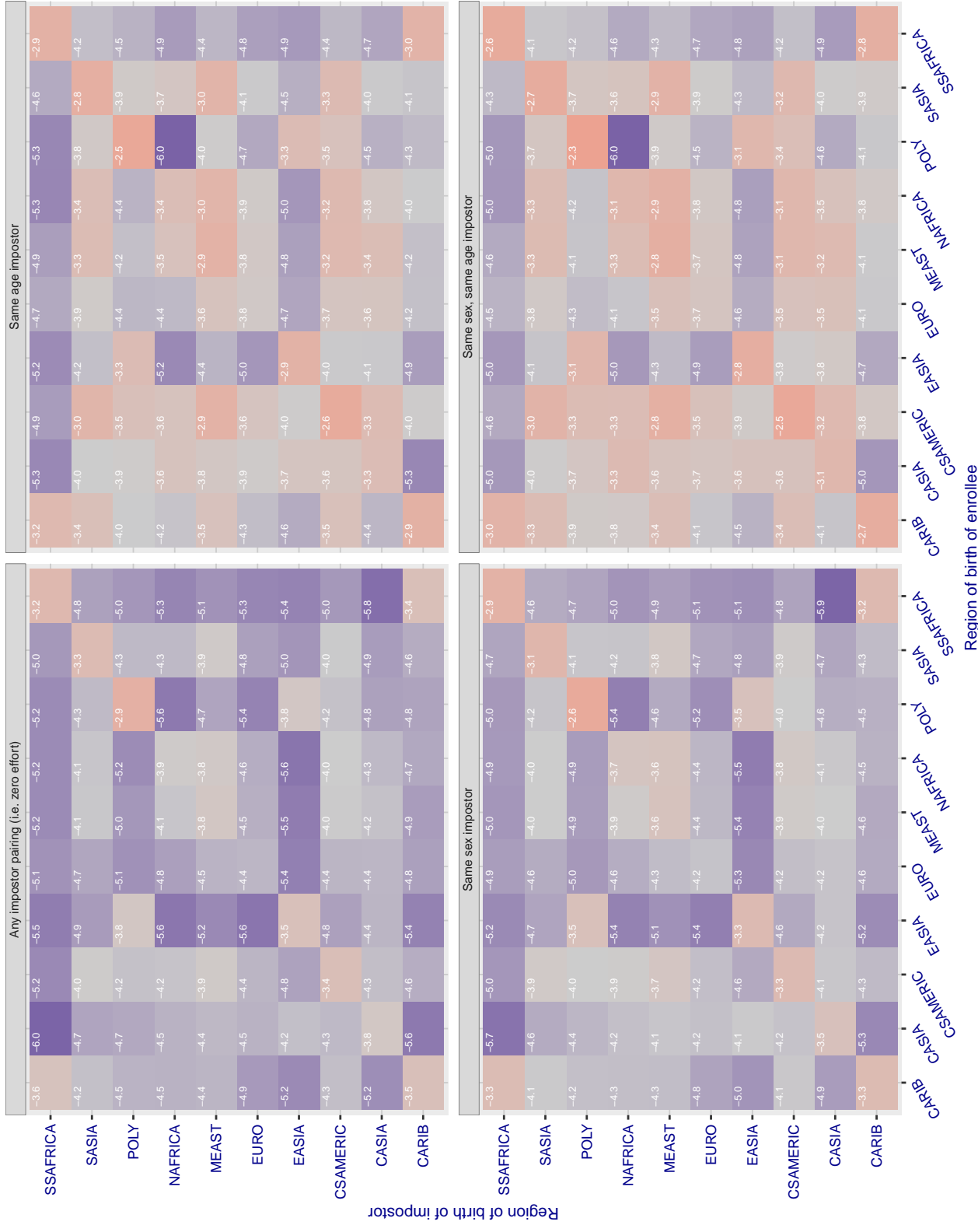
**Cross region FMR at threshold T = 79.670 for algorithm dermalog\_006, giving FMR(T) = 0.0001 globally.**

Figure 178: For algorithm dermalog-006 operating on visa images, the heatmap shows false match rates observed over impostor comparisons of faces from different individuals who were born in the given region pair. False matches are counted against a recognition threshold fixed globally to give the target FMR in the plot title, computed over all on the order of  $10^{10}$  impostor comparisons. If text appears in each box it give the same quantity as that coded by the color. Grey indicates FMR is at the intended FMR target level. Light red colors present a security vulnerability to, for example, a passport gate. Each +1 increase in  $\log_{10} FMR$  corresponds to a factor of 10 increase in FMR. The matrix is not quite symmetric because images in the enrollment and verification sets are different.

### Cross region FMR at threshold T = 0.675 for algorithm digitalbarriers\_002, giving FMR(T) = 0.0001 globally.

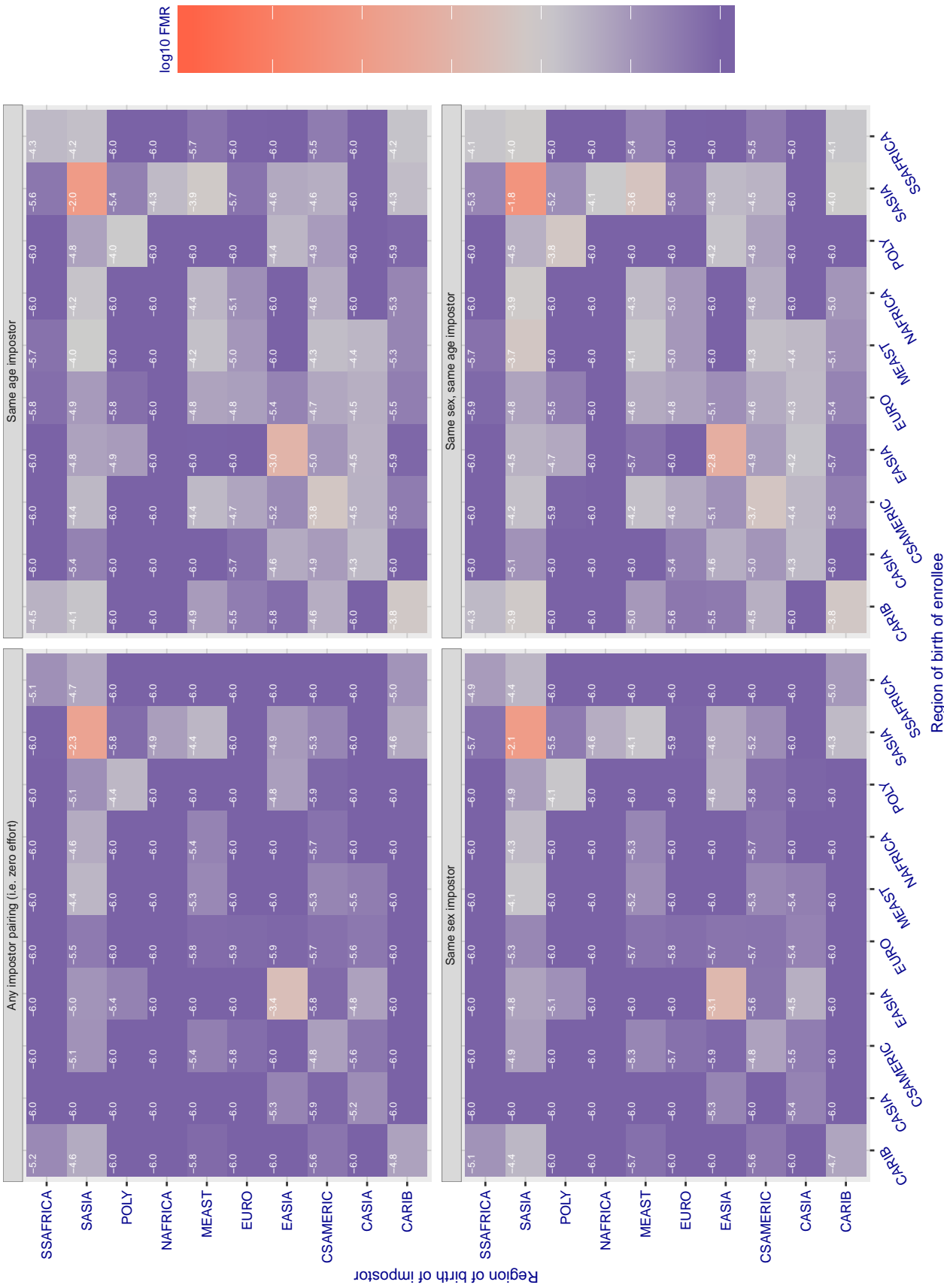


Figure 179: For algorithm digitalbarriers-002 operating on visa images, the heatmap shows false match rates observed over impostor comparisons of faces from different individuals who were born in the given region pair. False matches are counted against a recognition threshold fixed globally to give the target FMR in the plot title, computed over all on the order of  $10^{10}$  impostor comparisons. If text appears in each box it give the same quantity as that coded by the color. Grey indicates FMR is at the intended FMR target level. Light red colors present a security vulnerability to, for example, a passport gate. Each +1 increase in  $\log_{10} \text{FMR}$  corresponds to a factor of 10 increase in FMR. The matrix is not quite symmetric because images in the enrollment and verification sets are different.

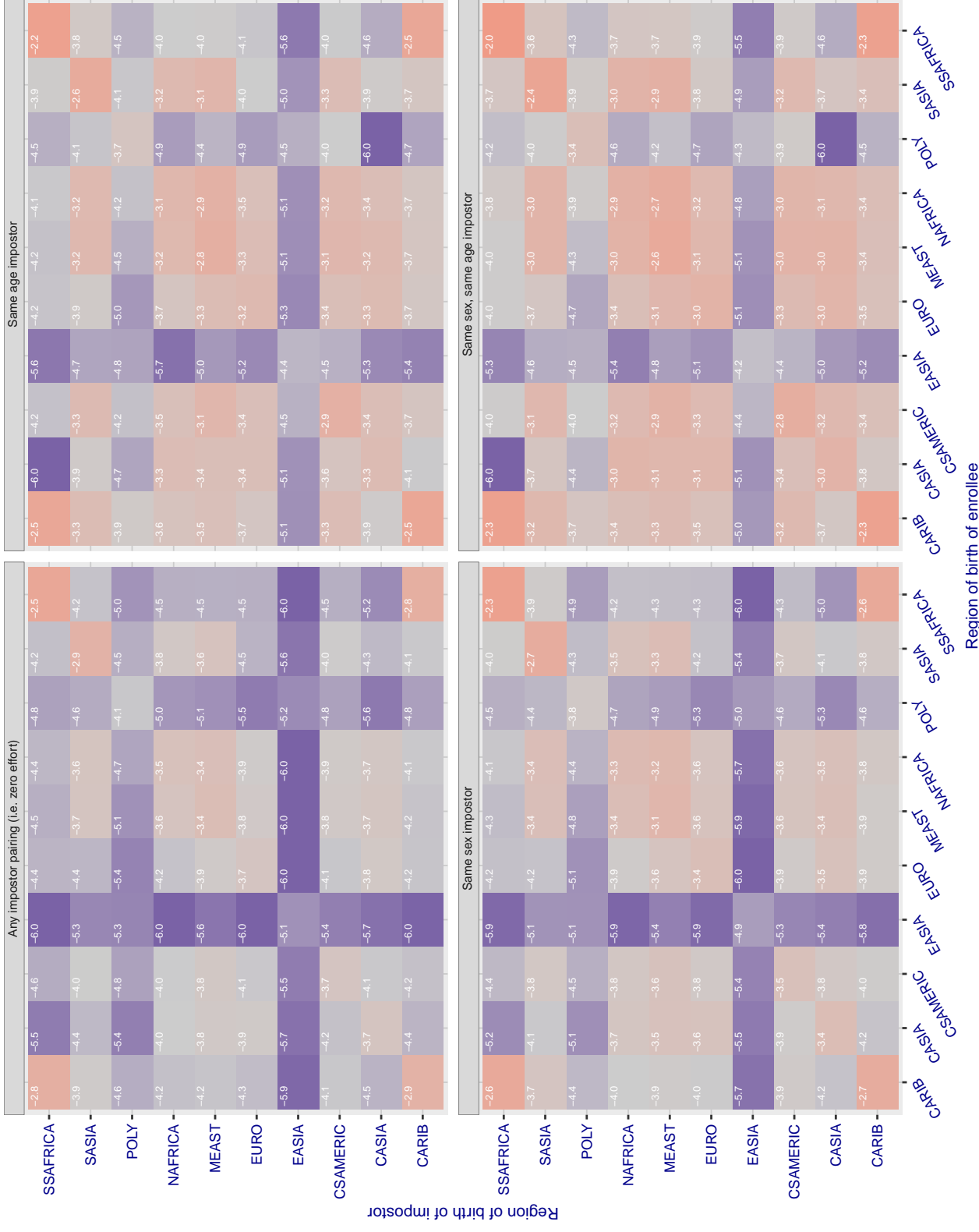
**Cross region FMR at threshold T = 1.061 for algorithm dsk\_000, giving FMR(T) = 0.0001 globally.**

Figure 180: For algorithm dsk\_000 operating on visa images, the heatmap shows false match rates observed over impostor comparisons of faces from different individuals who were born in the given region pair. False matches are counted against a recognition threshold fixed globally to give the target FMR in the plot title, computed over all on the order of  $10^{10}$  impostor comparisons. If text appears in each box it give the same quantity as that coded by the color. Grey indicates FMR is at the intended FMR target level. Light red colors present a security vulnerability to, for example, a passport gate. Each +1 increase in  $\log 10$  FMR corresponds to a factor of 10 increase in FMR. The matrix is not quite symmetric because images in the enrollment and verification sets are different.

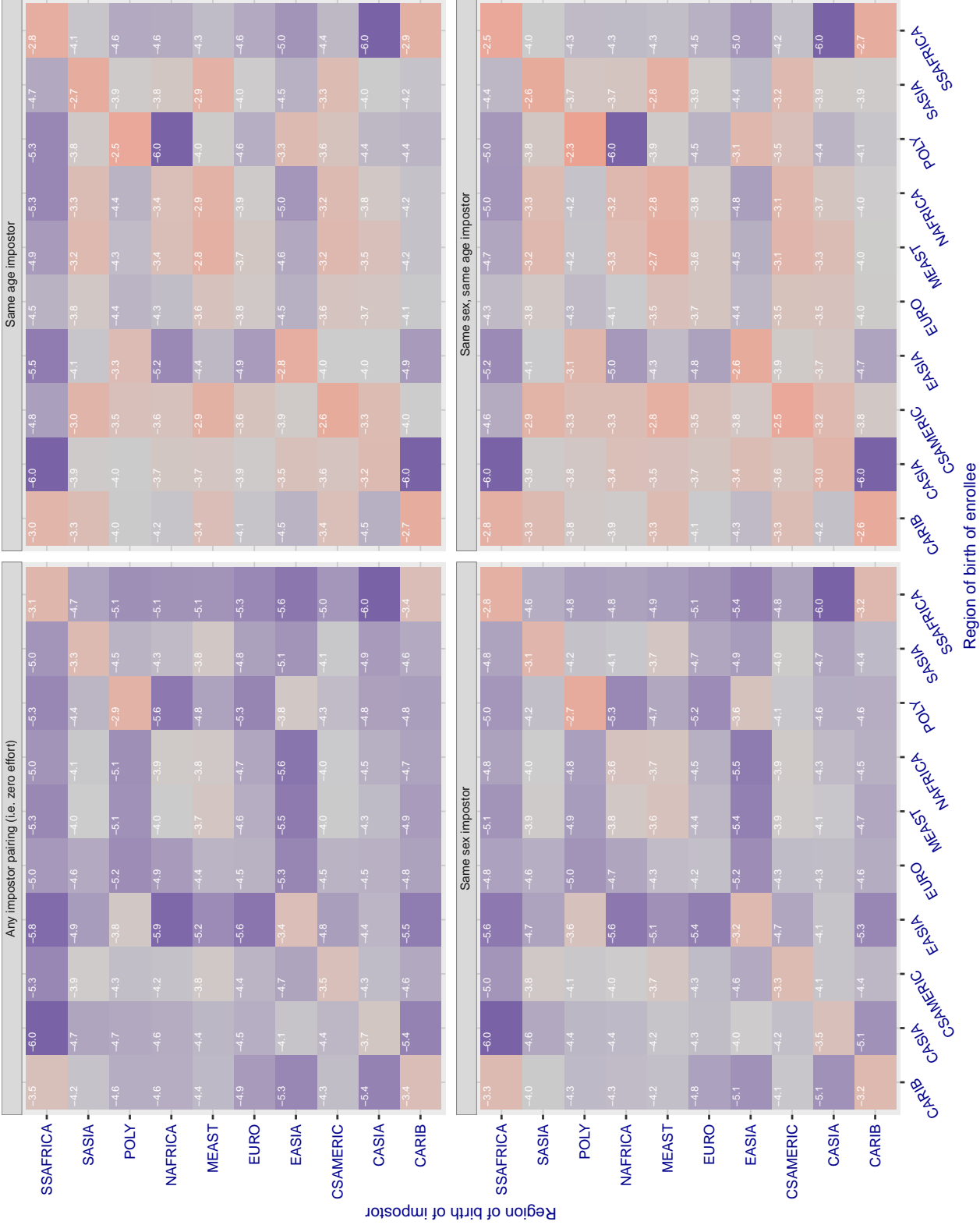
**Cross region FMR at threshold T = 53.280 for algorithm einetworks\_000, giving FMR(T) = 0.0001 globally.**

Figure 181: For algorithm einetworks-000 operating on visa images, the heatmap shows false match rates observed over impostor comparisons of faces from different individuals who were born in the given region pair. False matches are counted against a recognition threshold fixed globally to give the target FMR in the plot title, computed over all on the order of  $10^{10}$  impostor comparisons. If text appears in each box it give the same quantity as that coded by the color. Grey indicates FMR is at the intended FMR target level. Light red colors present a security vulnerability to, for example, a passport gate. Each +1 increase in  $\log_{10} FMR$  corresponds to a factor of 10 increase in FMR. The matrix is not quite symmetric because images in the enrollment and verification sets are different.

### Cross region FMR at threshold T = 2.589 for algorithm everai\_002, giving FMR(T) = 0.0001 globally.

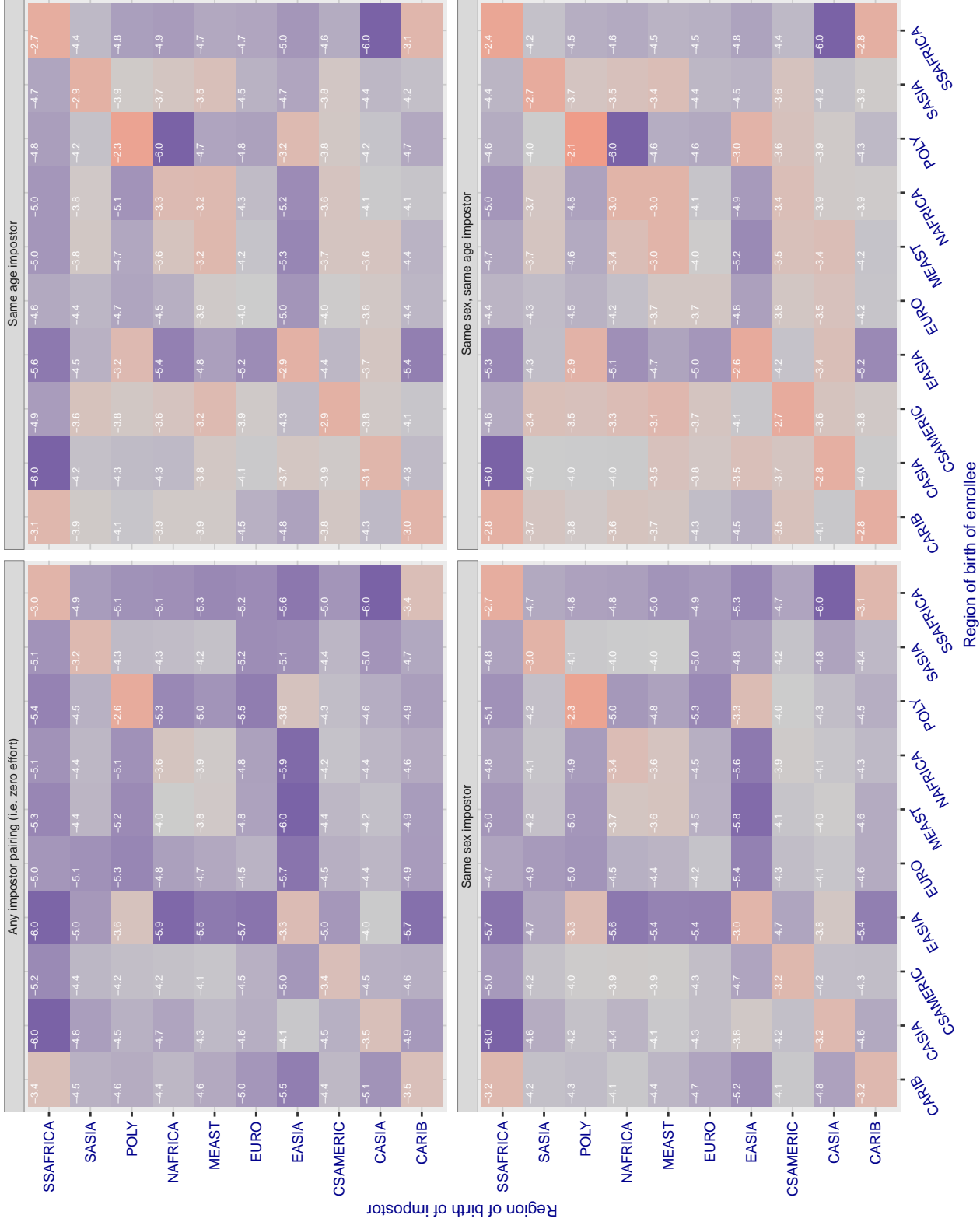


Figure 182: For algorithm everai-002 operating on visa images, the heatmap shows false match rates observed over impostor comparisons of faces from different individuals who were born in the given region pair. False matches are counted against a recognition threshold fixed globally to give the target FMR in the plot title, computed over all on the order of  $10^{10}$  impostor comparisons. If text appears in each box it give the same quantity as that coded by the color. Grey indicates FMR is at the intended FMR target level. Light red colors present a security vulnerability to, for example, a passport gate. Each +1 increase in  $\log_{10} \text{FMR}$  corresponds to a factor of 10 increase in FMR. The matrix is not quite symmetric because images in the enrollment and verification sets are different.

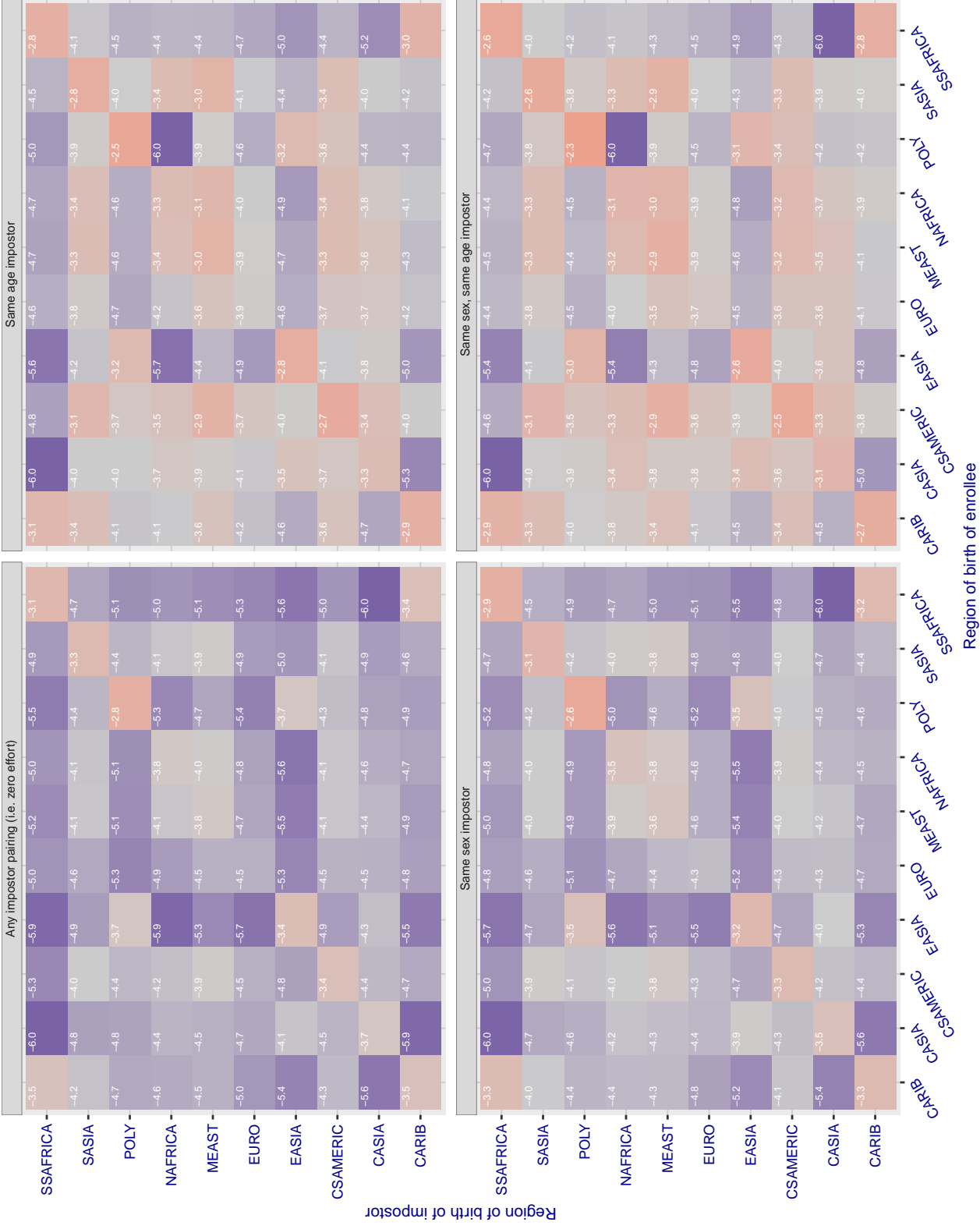
**Cross region FMR at threshold T = 0.400 for algorithm f8\_001, giving FMR(T) = 0.0001 globally.**

Figure 183: For algorithm f8-001 operating on visa images, the heatmap shows false match rates observed over impostor comparisons of faces from different individuals who were born in the given region pair. False matches are counted against a recognition threshold fixed globally to give the target FMR in the plot title, computed over all on the order of  $10^{10}$  impostor comparisons. If text appears in each box it give the same quantity as that coded by the color. Grey indicates FMR is at the intended FMR target level. Light red colors present a security vulnerability to, for example, a passport gate. Each +1 increase in  $\log 10$  FMR corresponds to a factor of 10 increase in FMR. The matrix is not quite symmetric because images in the enrollment and verification sets are different.

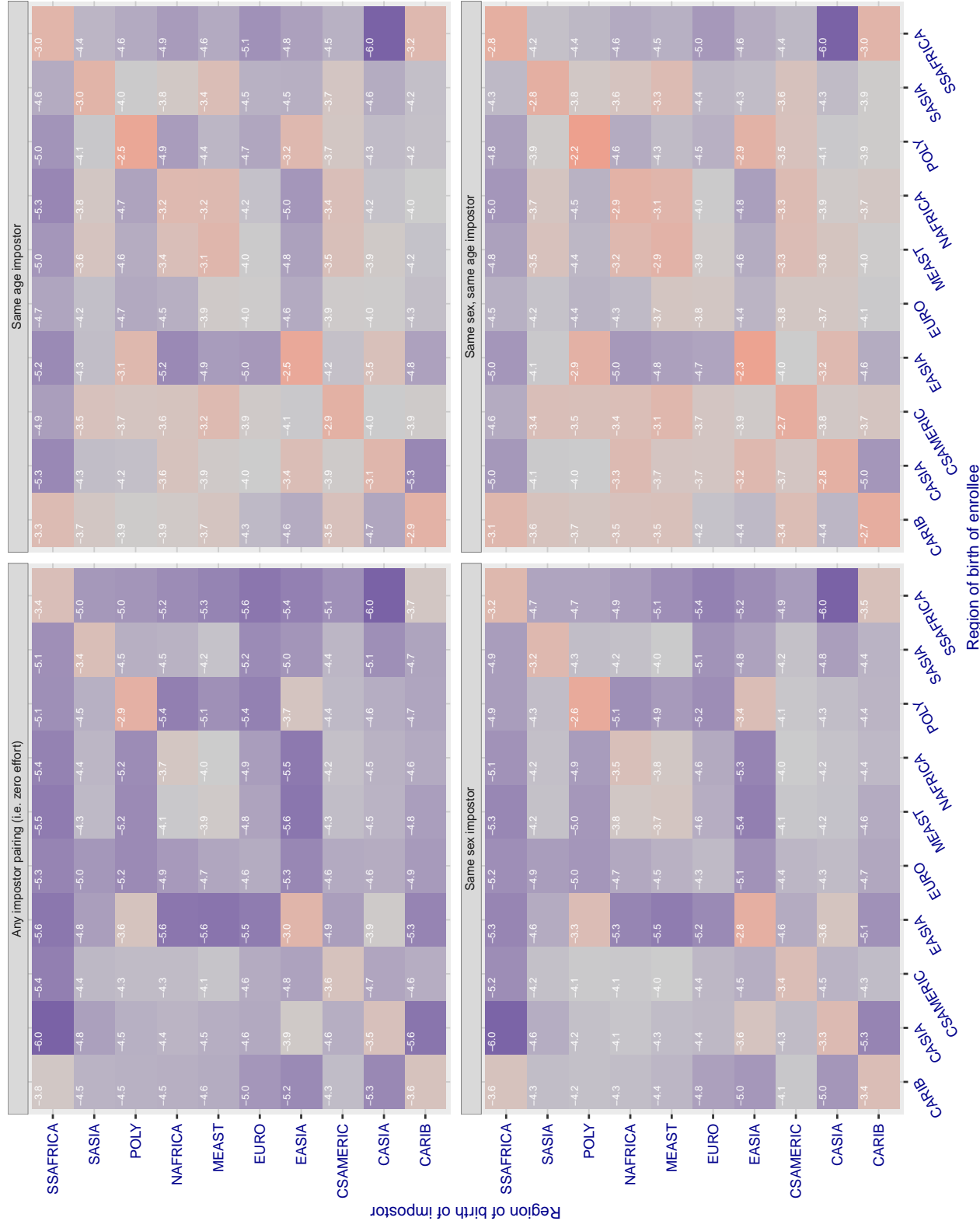


Figure 184: For algorithm facesoft-000 operating on visa images, the heatmap shows false match rates observed over impostor comparisons of faces from different individuals who were born in the given region pair. False matches are counted against a recognition threshold fixed globally to give the target  $FMR$  in the plot title, computed over all on the order of  $10^{10}$  impostor comparisons. If text appears in each box it give the same quantity as that coded by the color. Grey indicates  $FMR$  is at the intended  $FMR$  target level. Light red colors present a security vulnerability to, for example, a passport gate. Each +1 increase in  $\log_{10} FMR$  corresponds to a factor of 10 increase in  $FMR$ . The matrix is not quite symmetric because images in the enrollment and verification sets are different.

### Cross region FMR at threshold T = 0.611 for algorithm glory\_000, giving FMR(T) = 0.0001 globally.

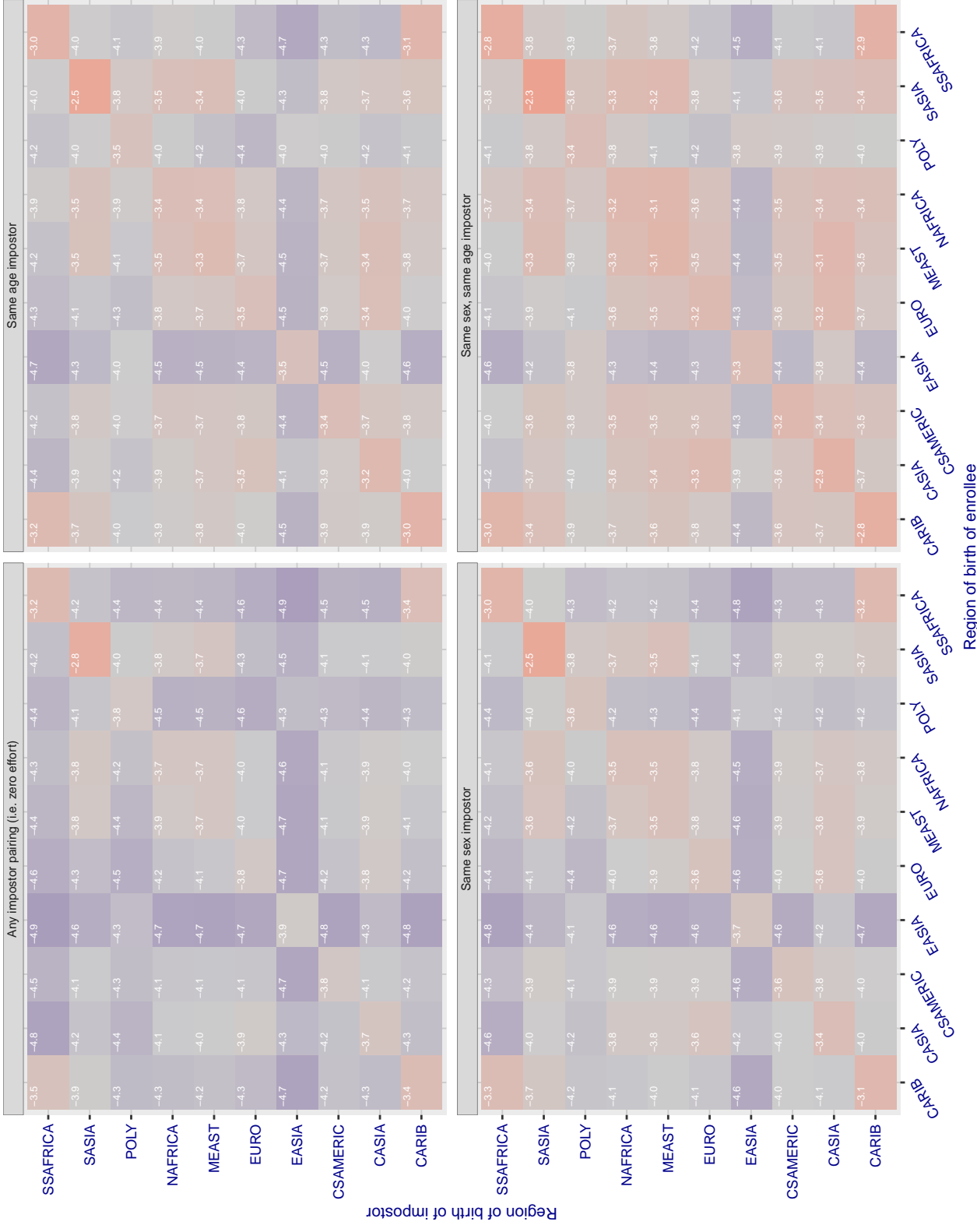


Figure 185: For algorithm glory-000 operating on visa images, the heatmap shows false match rates observed over impostor comparisons of faces from different individuals who were born in the given region pair. False matches are counted against a recognition threshold fixed globally to give the target FMR in the plot title, computed over all on the order of  $10^{10}$  impostor comparisons. If text appears in each box it give the same quantity as that coded by the color. Grey indicates FMR is at the intended FMR target level. Light red colors present a security vulnerability to, for example, a passport gate. Each +1 increase in  $\log_{10} FMR$  corresponds to a factor of 10 increase in FMR. The matrix is not quite symmetric because images in the enrollment and verification sets are different.

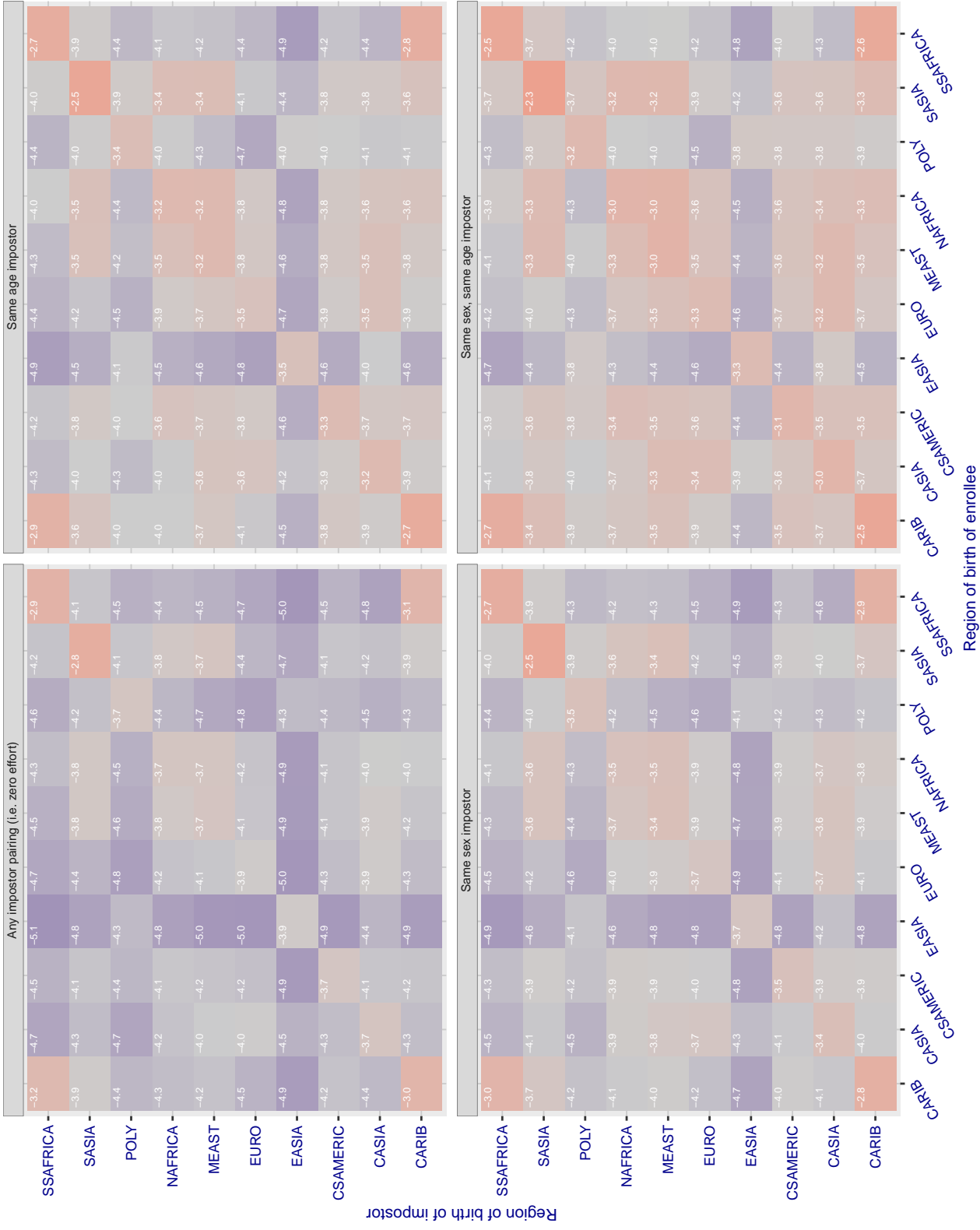
**Cross region FMR at threshold T = 0.618 for algorithm glory\_001, giving FMR(T) = 0.00001 globally.**

Figure 186: For algorithm glory-001 operating on visa images, the heatmap shows false match rates observed over impostor comparisons of faces from different individuals who were born in the given region pair. False matches are counted against a recognition threshold fixed globally to give the target FMR in the plot title, computed over all on the order of  $10^{10}$  impostor comparisons. If text appears in each box it give the same quantity as that coded by the color. Grey indicates FMR is at the intended FMR target level. Light red colors present a security vulnerability to, for example, a passport gate. Each +1 increase in  $\log_{10} \text{FMR}$  corresponds to a factor of 10 increase in FMR. The matrix is not quite symmetric because images in the enrollment and verification sets are different.

### Cross region FMR at threshold T = 0.483 for algorithm gorilla\_002, giving FMR(T) = 0.0001 globally.

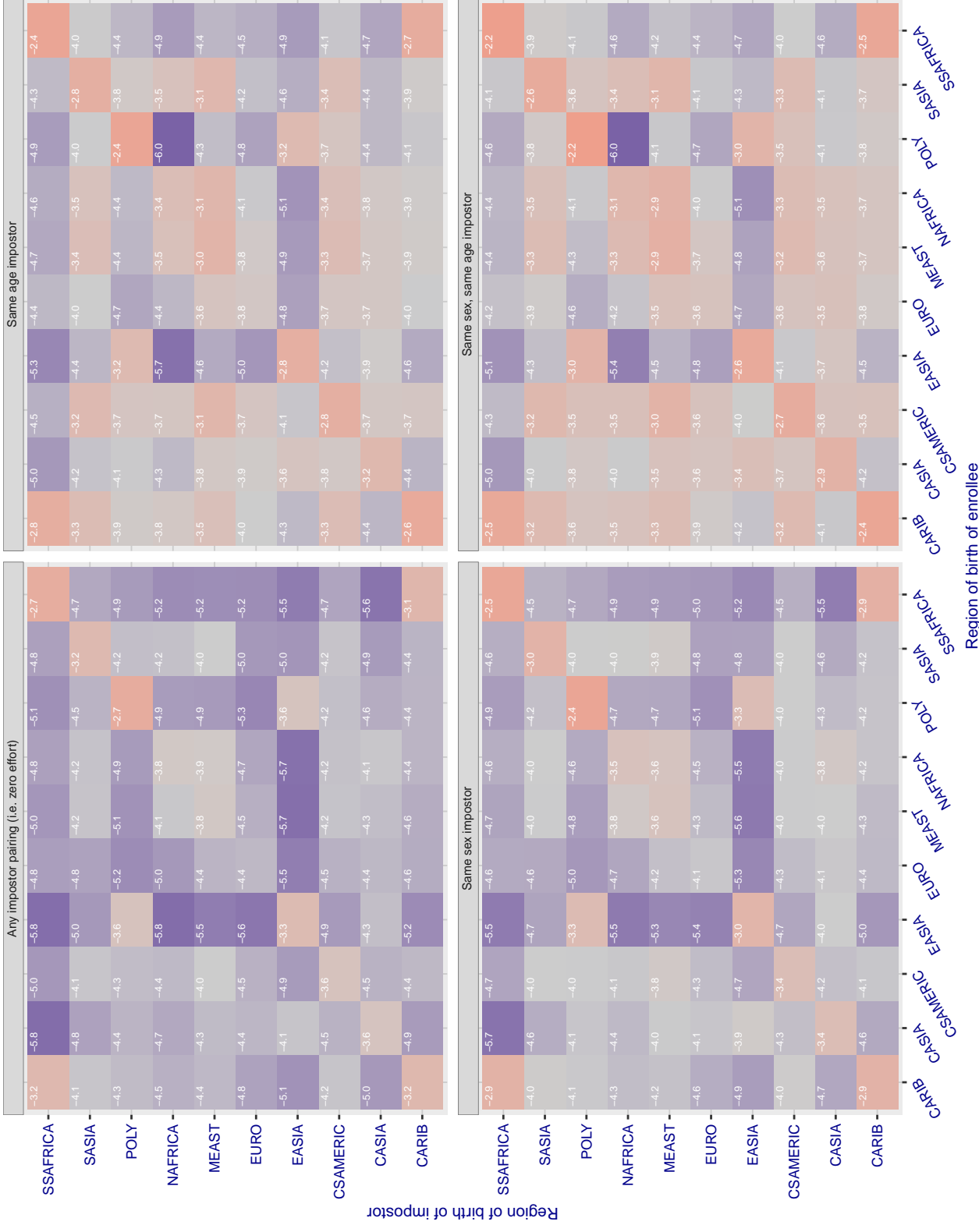


Figure 187: For algorithm gorilla-002 operating on visa images, the heatmap shows false match rates observed over impostor comparisons of faces from different individuals who were born in the given region pair. False matches are counted against a recognition threshold fixed globally to give the target FMR in the plot title, computed over all on the order of  $10^{10}$  impostor comparisons. If text appears in each box it give the same quantity as that coded by the color. Grey indicates FMR is at the intended FMR target level. Light red colors present a security vulnerability to, for example, a passport gate. Each +1 increase in  $\log_{10} FMR$  corresponds to a factor of 10 increase in FMR. The matrix is not quite symmetric because images in the enrollment and verification sets are different.

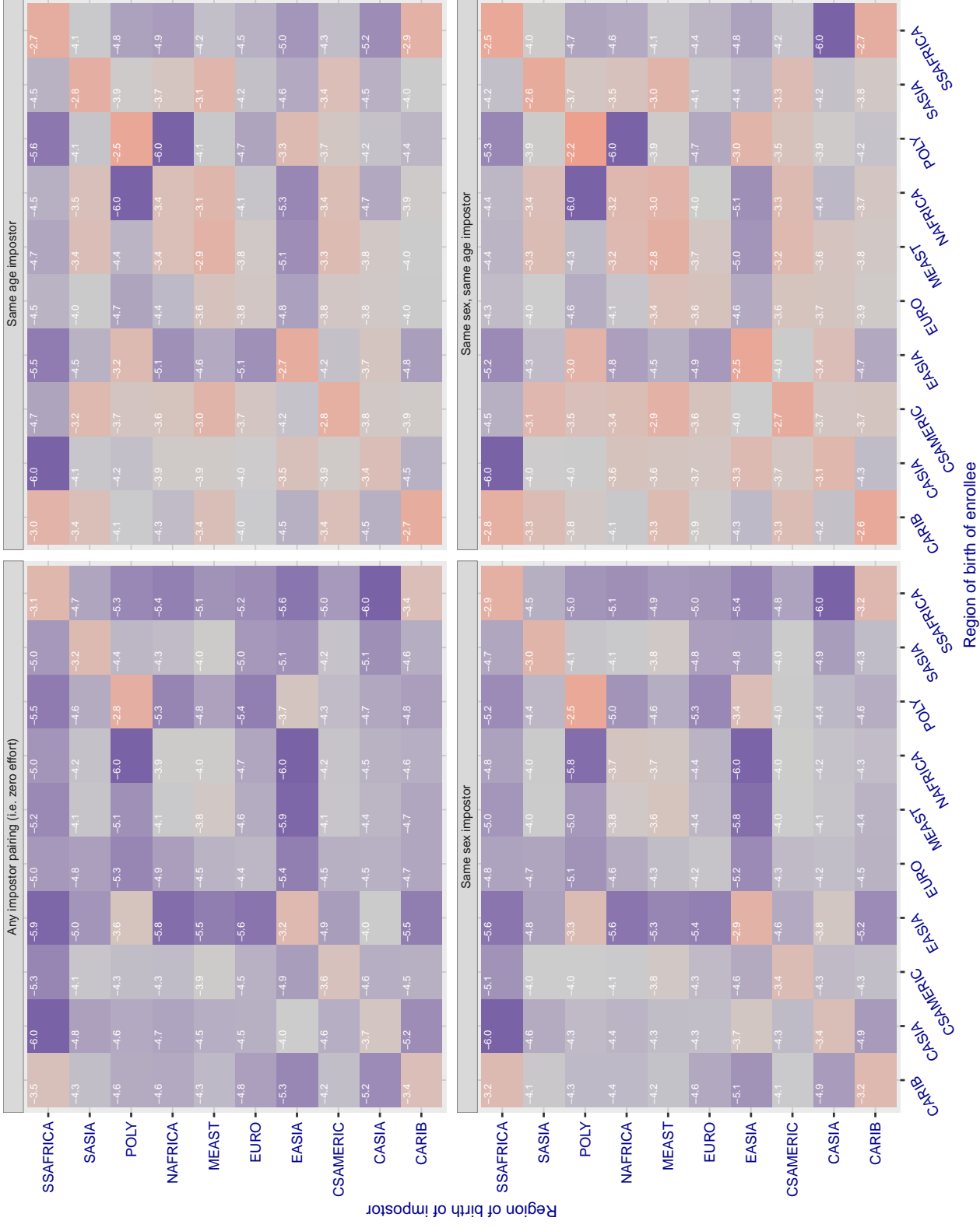
**Cross region FMR at threshold T = 0.454 for algorithm gorilla\_003, giving FMR(T) = 0.0001 globally.**

Figure 188: For algorithm gorilla-003 operating on visa images, the heatmap shows false match rates observed over impostor comparisons of faces from different individuals who were born in the given region pair. False matches are counted against a recognition threshold fixed globally to give the target FMR in the plot title, computed over all on the order of  $10^{10}$  impostor comparisons. If text appears in each box it give the same quantity as that coded by the color. Grey indicates FMR is at the intended FMR target level. Light red colors present a security vulnerability to, for example, a passport gate. Each +1 increase in  $\log_{10} \text{FMR}$  corresponds to a factor of 10 increase in FMR. The matrix is not quite symmetric because images in the enrollment and verification sets are different.

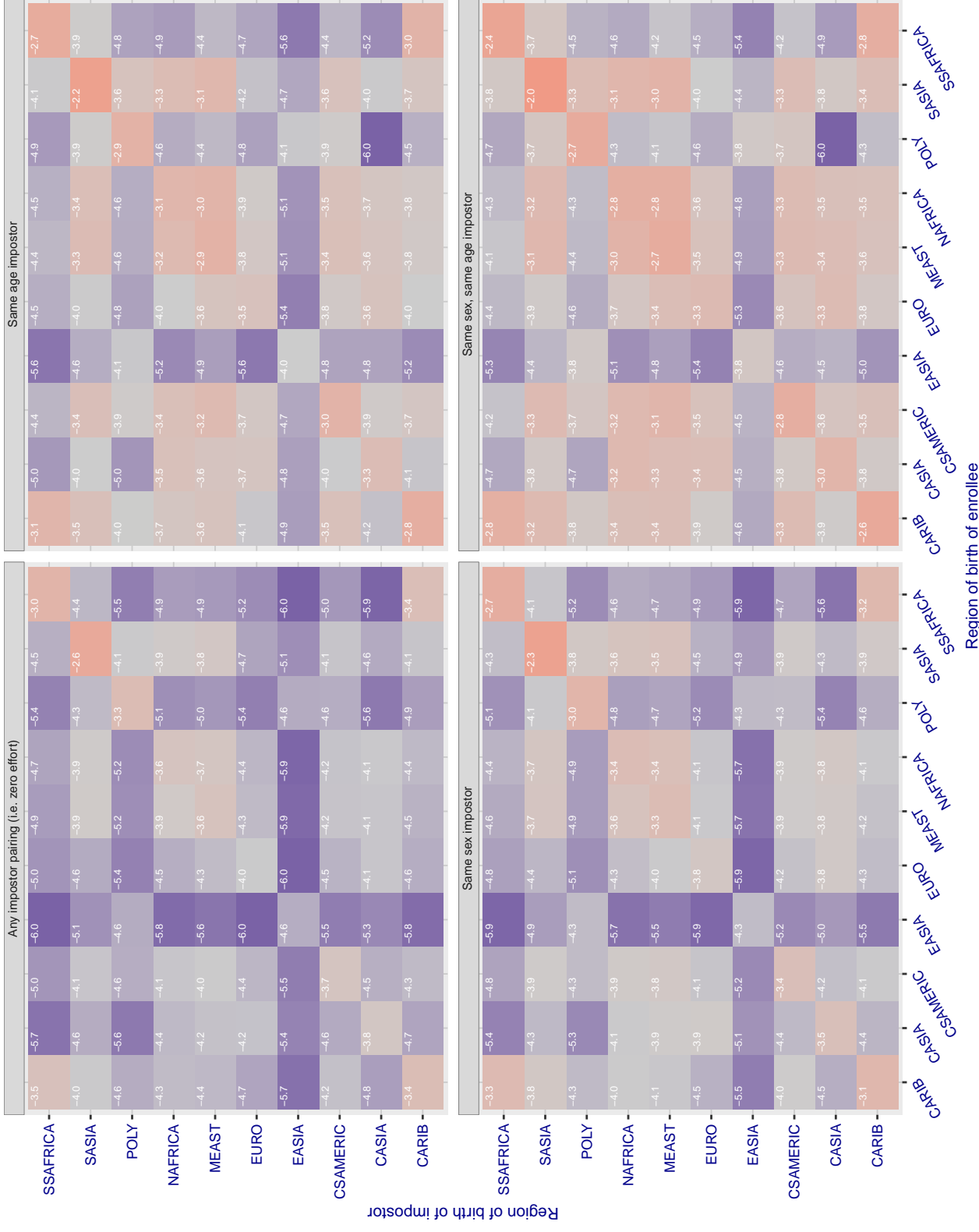
**Cross region FMR at threshold T = 66.565 for algorithm hik\_001, giving FMR(T) = 0.0001 globally.**

Figure 189: For algorithm hik-001 operating on visa images, the heatmap shows false match rates observed over impostor comparisons of faces from different individuals who were born in the given region pair. False matches are counted against a recognition threshold fixed globally to give the target FMR in the plot title, computed over all on the order of  $10^{10}$  impostor comparisons. If text appears in each box it give the same quantity as that coded by the color. Grey indicates FMR is at the intended FMR target level. Light red colors present a security vulnerability to, for example, a passport gate. Each +1 increase in  $\log 10$  FMR corresponds to a factor of 10 increase in FMR. The matrix is not quite symmetric because images in the enrollment and verification sets are different.

### Cross region FMR at threshold T = 0.823 for algorithm hr\_001, giving FMR(T) = 0.0001 globally.

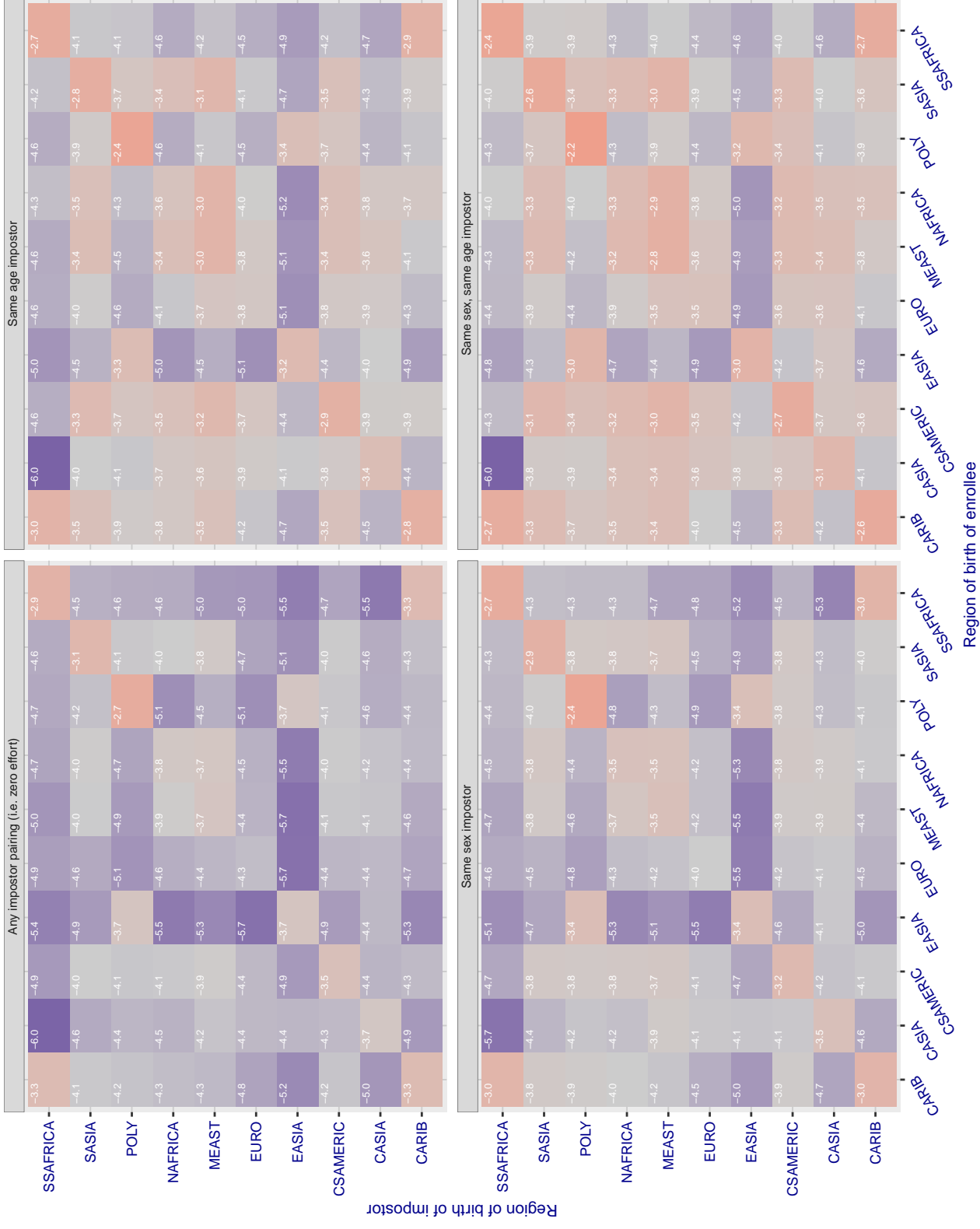


Figure 190: For algorithm hr-001 operating on visa images, the heatmap shows false match rates observed over impostor comparisons of faces from different individuals who were born in the given region pair. False matches are counted against a recognition threshold fixed globally to give the target FMR in the plot title, computed over all on the order of  $10^{10}$  impostor comparisons. If text appears in each box it give the same quantity as that coded by the color. Grey indicates FMR is at the intended FMR target level. Light red colors present a security vulnerability to, for example, a passport gate. Each +1 increase in  $\log_{10}$  FMR corresponds to a factor of 10 increase in FMR. The matrix is not quite symmetric because images in the enrollment and verification sets are different.

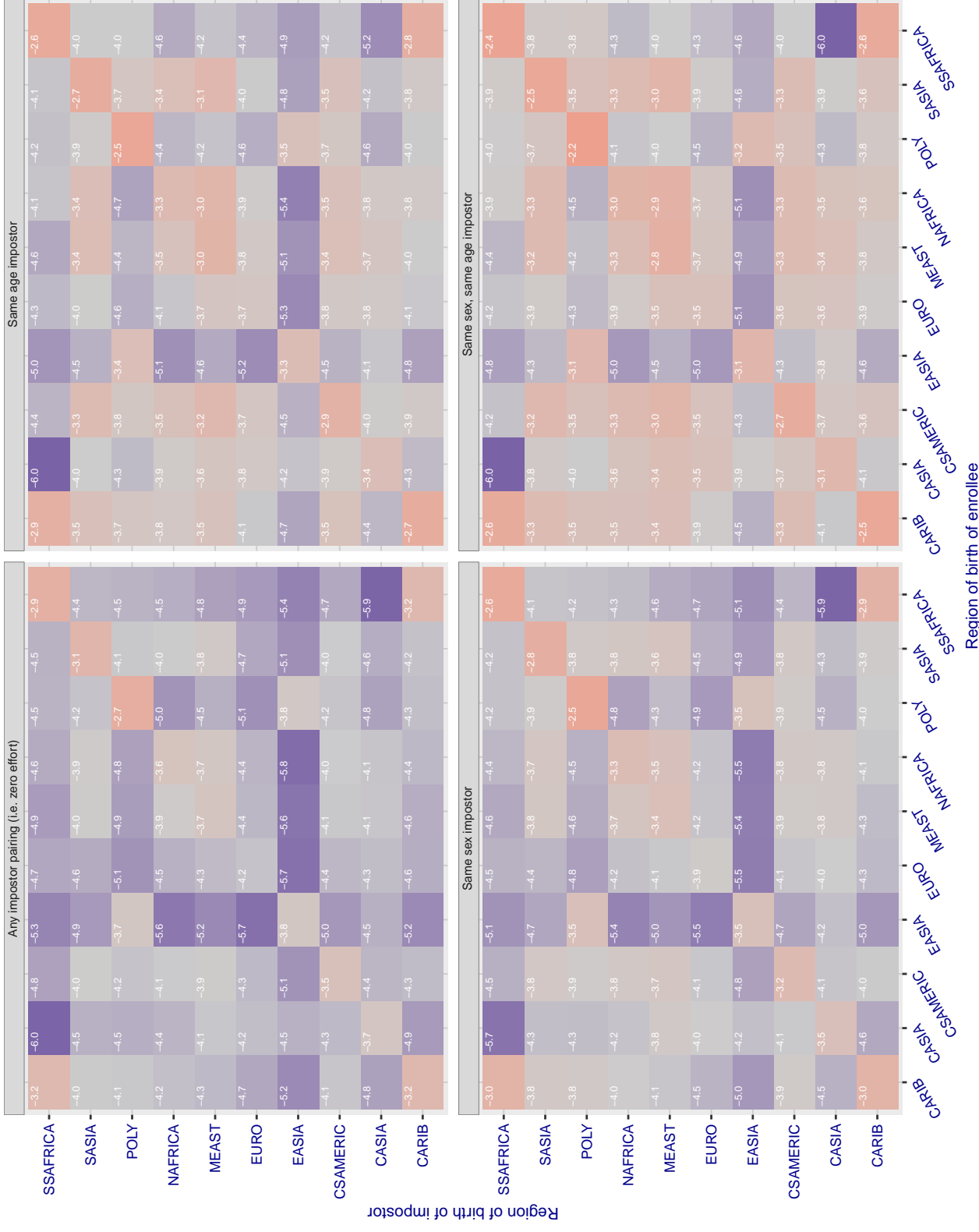
**Cross region FMR at threshold T = 0.285 for algorithm hr\_002, giving FMR(T) = 0.0001 globally.**

Figure 191: For algorithm hr-002 operating on visa images, the heatmap shows false match rates observed over impostor comparisons of faces from different individuals who were born in the given region pair. False matches are counted against a recognition threshold fixed globally to give the target FMR in the plot title, computed over all on the order of  $10^{10}$  impostor comparisons. If text appears in each box it give the same quantity as that coded by the color. Grey indicates FMR is at the intended FMR target level. Light red colors present a security vulnerability to, for example, a passport gate. Each +1 increase in  $\log_{10}$  FMR corresponds to a factor of 10 increase in FMR. The matrix is not quite symmetric because images in the enrollment and verification sets are different.

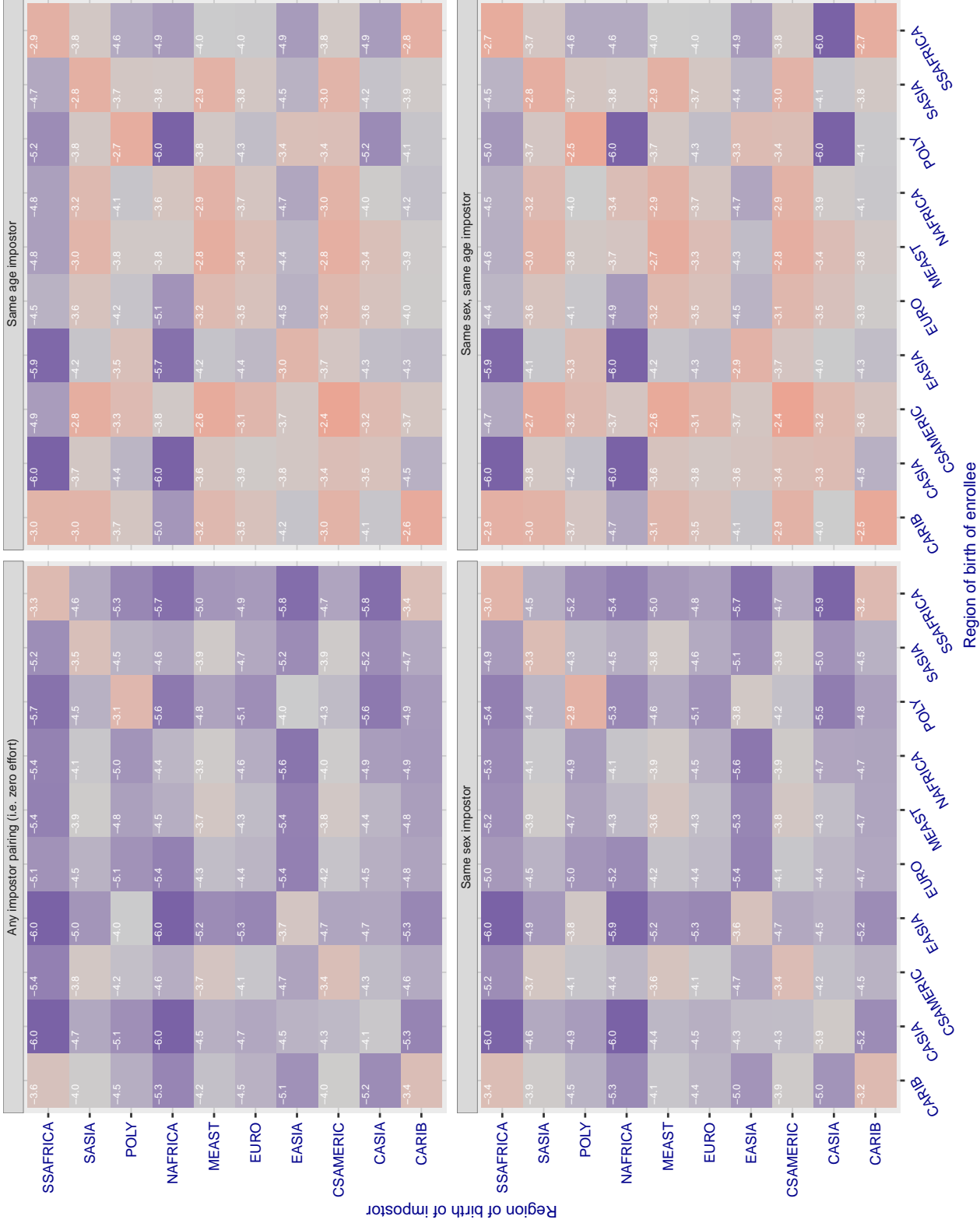
**Cross region FMR at threshold T = 37645.000 for algorithm id3\_003, giving FMR(T) = 0.0001 globally.**

Figure 192: For algorithm id3\_003 operating on visa images, the heatmap shows false match rates observed over impostor comparisons of faces from different individuals who were born in the given region pair. False matches are counted against a recognition threshold fixed globally to give the target FMR in the plot title, computed over all on the order of  $10^{10}$  impostor comparisons. If text appears in each box it give the same quantity as that coded by the color. Grey indicates FMR is at the intended FMR target level. Light red colors present a security vulnerability to, for example, a passport gate. Each +1 increase in  $\log_{10} \text{FMR}$  corresponds to a factor of 10 increase in FMR. The matrix is not quite symmetric because images in the enrollment and verification sets are different.

### Cross region FMR at threshold T = 37001.000 for algorithm id3\_004, giving FMR(T) = 0.0001 globally.

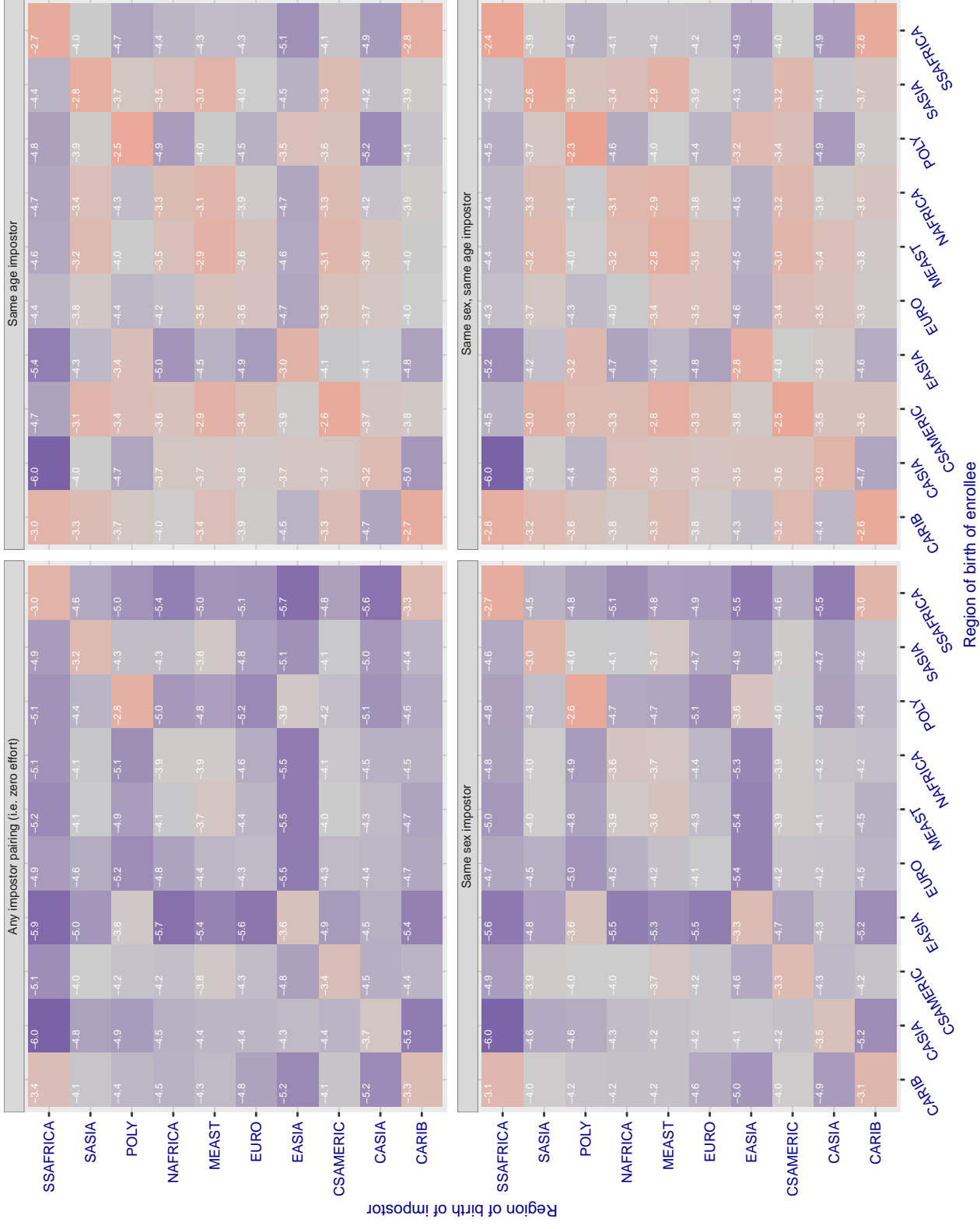


Figure 193: For algorithm id3\_004 operating on visa images, the heatmap shows false match rates observed over impostor comparisons of faces from different individuals who were born in the given region pair. False matches are counted against a recognition threshold fixed globally to give the target FMR in the plot title, computed over all on the order of  $10^{10}$  impostor comparisons. If text appears in each box it give the same quantity as that coded by the color. Grey indicates FMR is at the intended FMR target level. Light red colors present a security vulnerability to, for example, a passport gate. Each +1 increase in  $\log_{10}$  FMR corresponds to a factor of 10 increase in FMR. The matrix is not quite symmetric because images in the enrollment and verification sets are different.

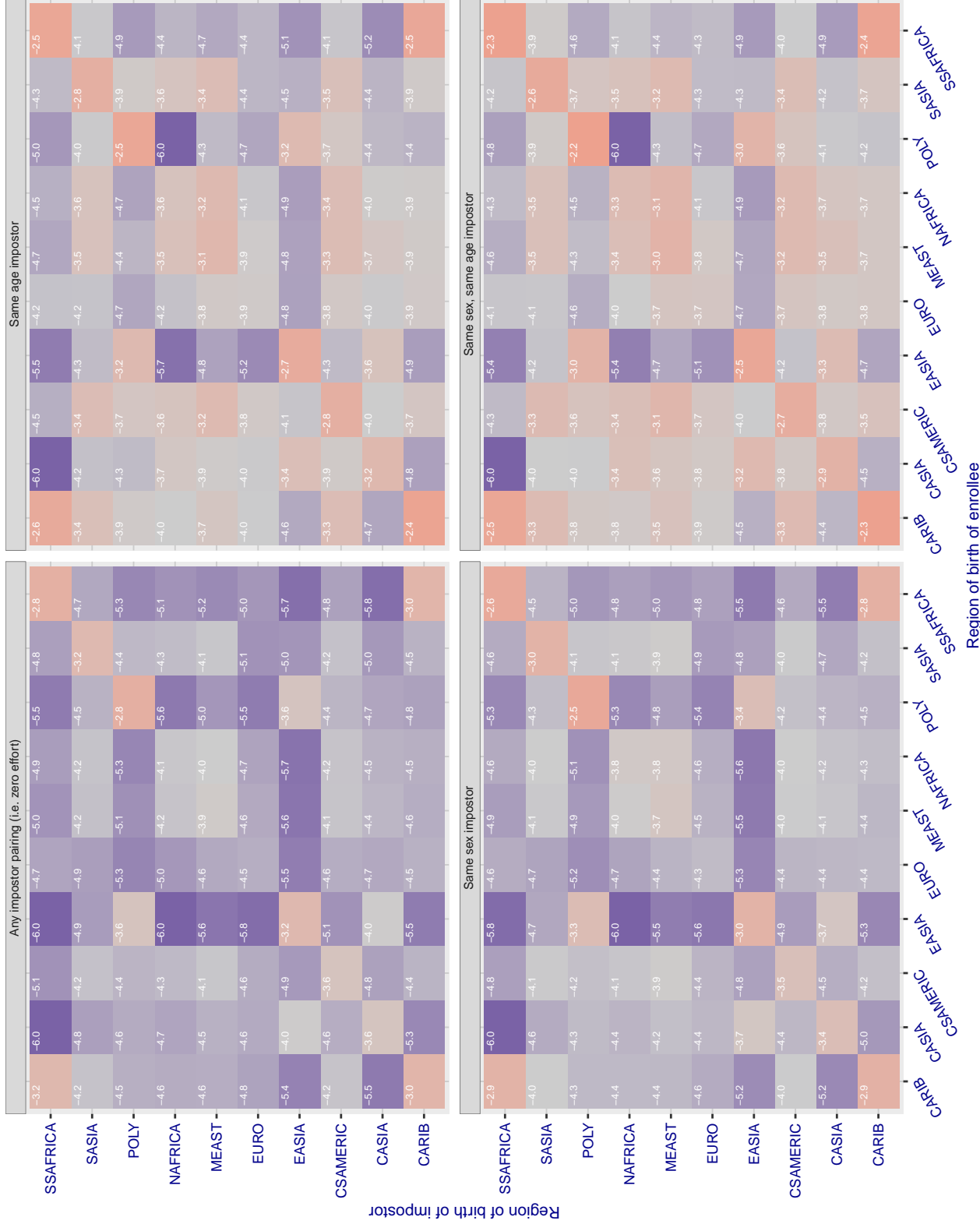
**Cross region FMR at threshold T = 3925.463 for algorithm idemia\_004, giving FMR(T) = 0.0001 globally.**

Figure 194: For algorithm idemia-004 operating on visa images, the heatmap shows false match rates observed over impostor comparisons of faces from different individuals who were born in the given region pair. False matches are counted against a recognition threshold fixed globally to give the target FMR in the plot title, computed over all on the order of  $10^{10}$  impostor comparisons. If text appears in each box it give the same quantity as that coded by the color. Grey indicates FMR is at the intended FMR target level. Light red colors present a security vulnerability to, for example, a passport gate. Each +1 increase in  $\log_{10} \text{FMR}$  corresponds to a factor of 10 increase in FMR. The matrix is not quite symmetric because images in the enrollment and verification sets are different.

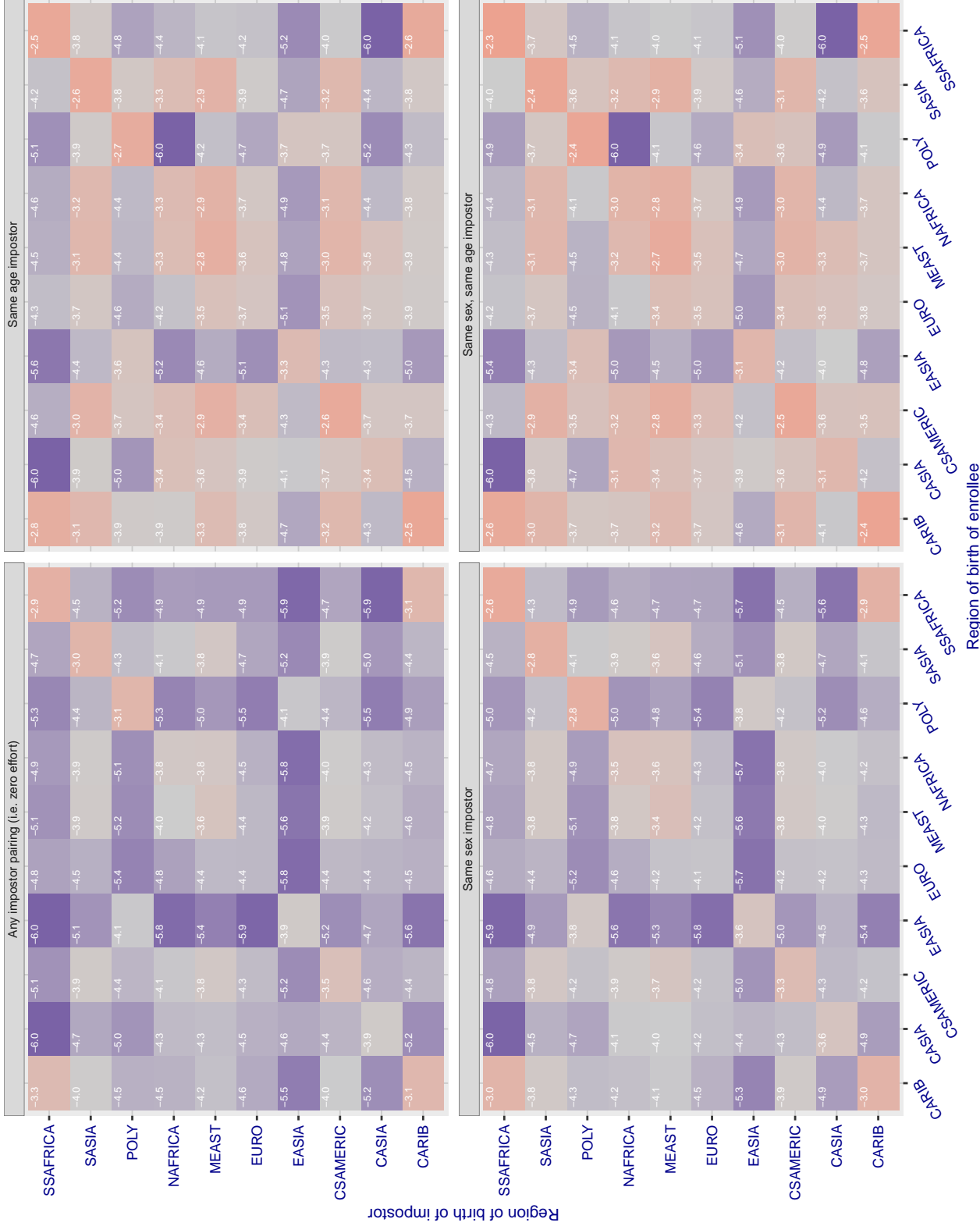
**Cross region FMR at threshold T = 3764.961 for algorithm idemia\_005, giving FMR(T) = 0.0001 globally.**

Figure 195: For algorithm idemia-005 operating on visa images, the heatmap shows false match rates observed over impostor comparisons of faces from different individuals who were born in the given region pair. False matches are counted against a recognition threshold fixed globally to give the target FMR in the plot title, computed over all on the order of  $10^{10}$  impostor comparisons. If text appears in each box it give the same quantity as that coded by the color. Grey indicates FMR is at the intended FMR target level. Light red colors present a security vulnerability to, for example, a passport gate. Each +1 increase in  $\log_{10} FMR$  corresponds to a factor of 10 increase in FMR. The matrix is not quite symmetric because images in the enrollment and verification sets are different.

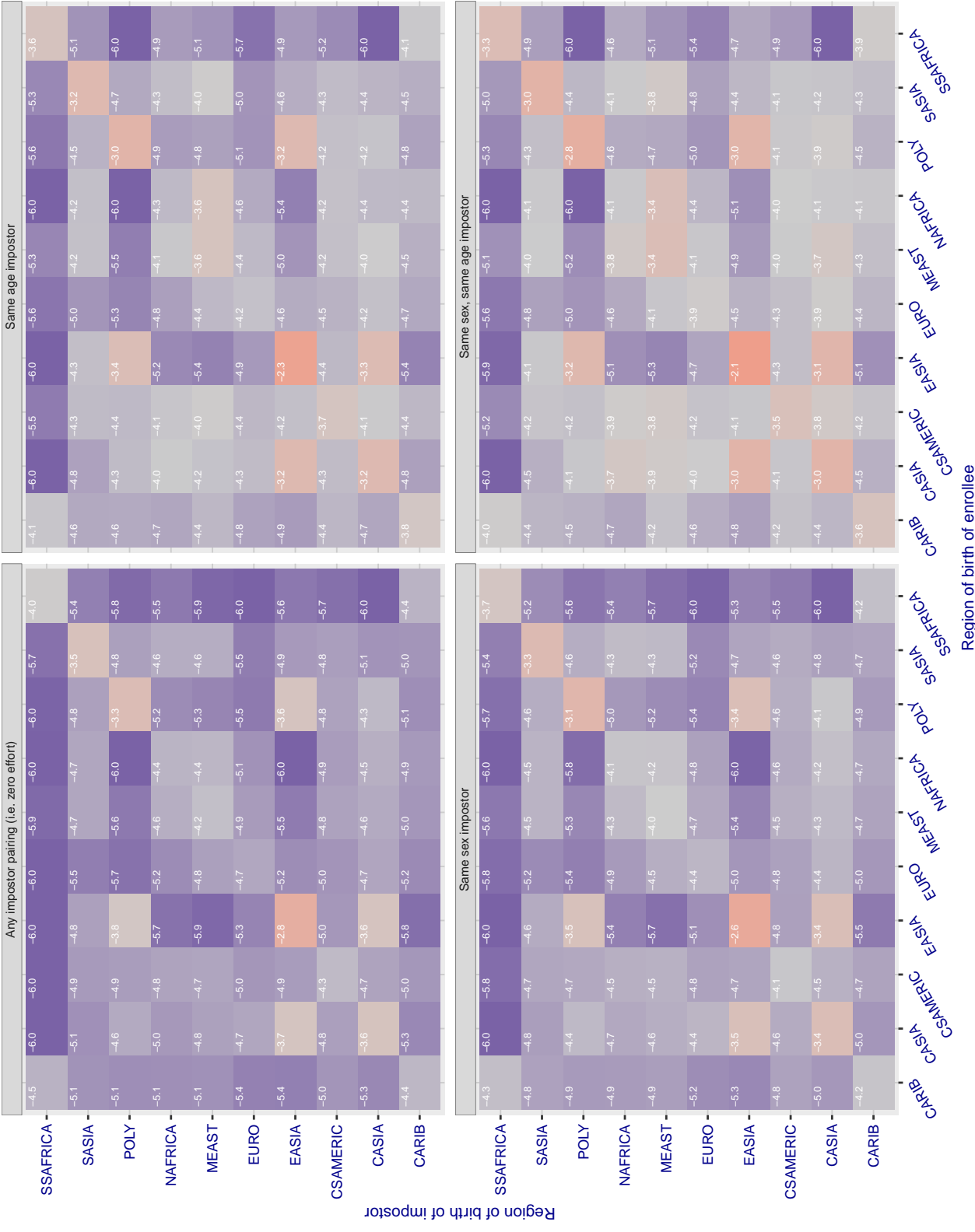
**Cross region FMR at threshold T = 0.760 for algorithm iit\_000, giving FMR(T) = 0.0001 globally.**

Figure 196: For algorithm iit-000 operating on visa images, the heatmap shows false match rates observed over impostor comparisons of faces from different individuals who were born in the given region pair. False matches are counted against a recognition threshold fixed globally to give the target FMR in the plot title, computed over all on the order of  $10^{10}$  impostor comparisons. If text appears in each box it give the same quantity as that coded by the color. Grey indicates FMR is at the intended FMR target level. Light red colors present a security vulnerability to, for example, a passport gate. Each +1 increase in  $\log_{10}$  FMR corresponds to a factor of 10 increase in FMR. The matrix is not quite symmetric because images in the enrollment and verification sets are different.

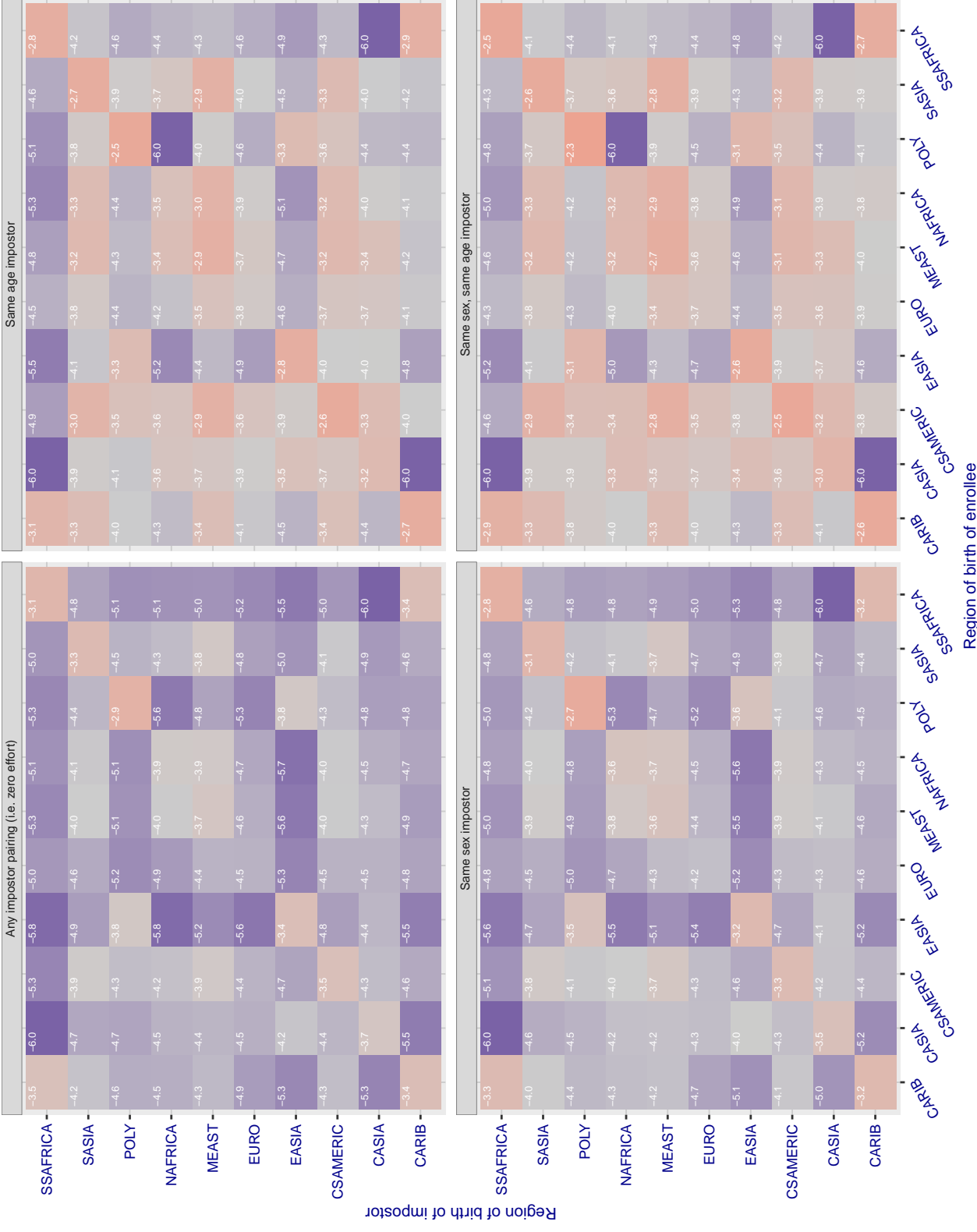
**Cross region FMR at threshold T = 0.691 for algorithm iit\_001, giving FMR(T) = 0.0001 globally.**

Figure 197: For algorithm iit-001 operating on visa images, the heatmap shows false match rates observed over impostor comparisons of faces from different individuals who were born in the given region pair. False matches are counted against a recognition threshold fixed globally to give the target FMR in the plot title, computed over all on the order of  $10^{10}$  impostor comparisons. If text appears in each box it give the same quantity as that coded by the color. Grey indicates FMR is at the intended FMR target level. Light red colors present a security vulnerability to, for example, a passport gate. Each +1 increase in  $\log 10 \text{ FMR}$  corresponds to a factor of 10 increase in FMR. The matrix is not quite symmetric because images in the enrollment and verification sets are different.

Cross region FMR at threshold  $T = 0.926$  for algorithm `imagus_000`, giving  $FMR(T) = 0.0001$  globally.

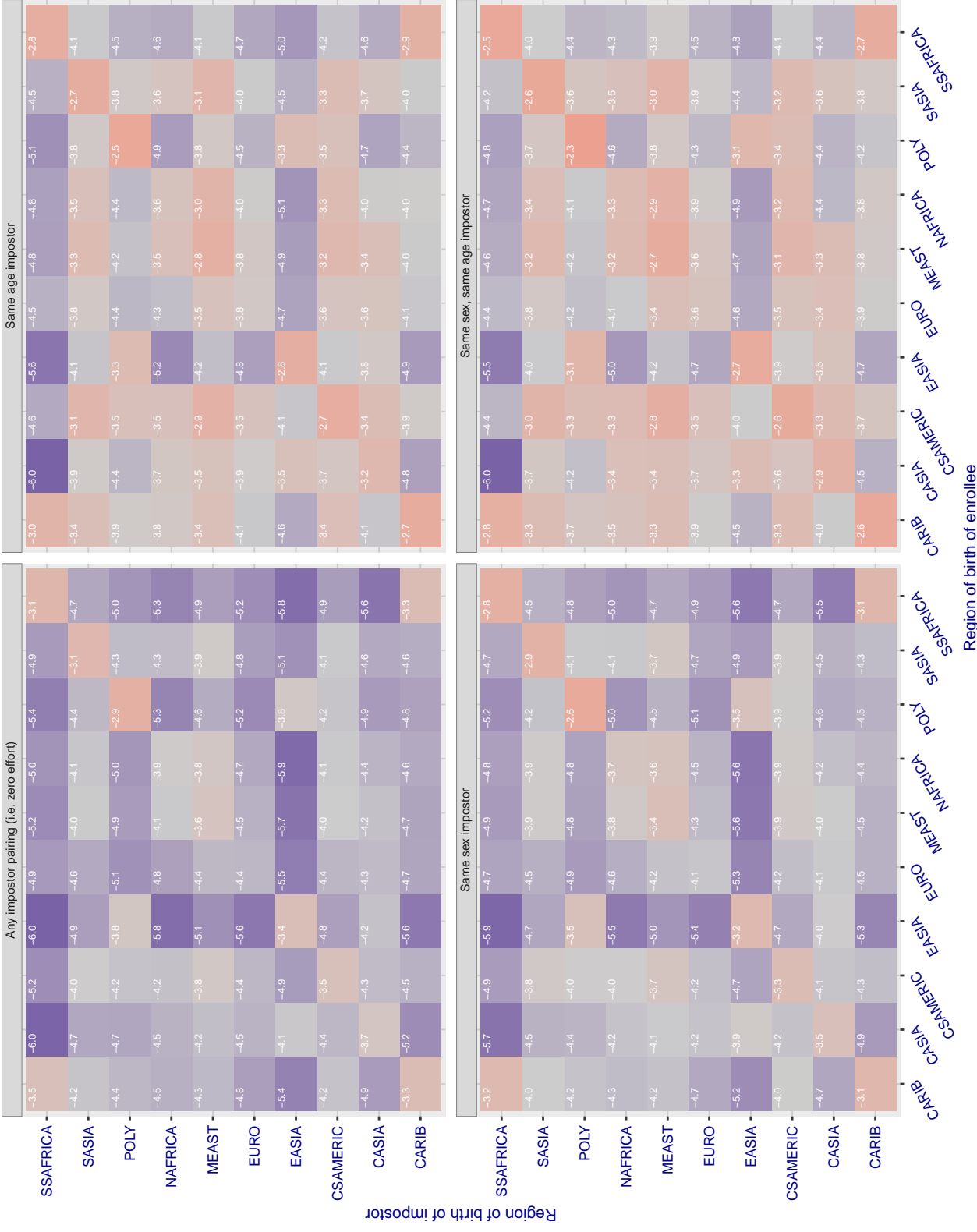


Figure 198: For algorithm *imagus-000* operating on visa images, the heatmap shows false match rates observed over impostor comparisons of faces from different individuals who were born in the given region pair. False matches are counted against a recognition threshold fixed globally to give the target *FMR* in the plot title, computed over all on the order of  $10^{10}$  impostor comparisons. If text appears in each box it give the same quantity as that coded by the color. Grey indicates *FMR* is at the intended *FMR* target level. Light red colors present a security vulnerability to, for example, a passport gate. Each +1 increase in  $\log_{10} \text{FMR}$  corresponds to a factor of 10 increase in *FMR*. The matrix is not quite symmetric because images in the enrollment and verification sets are different.

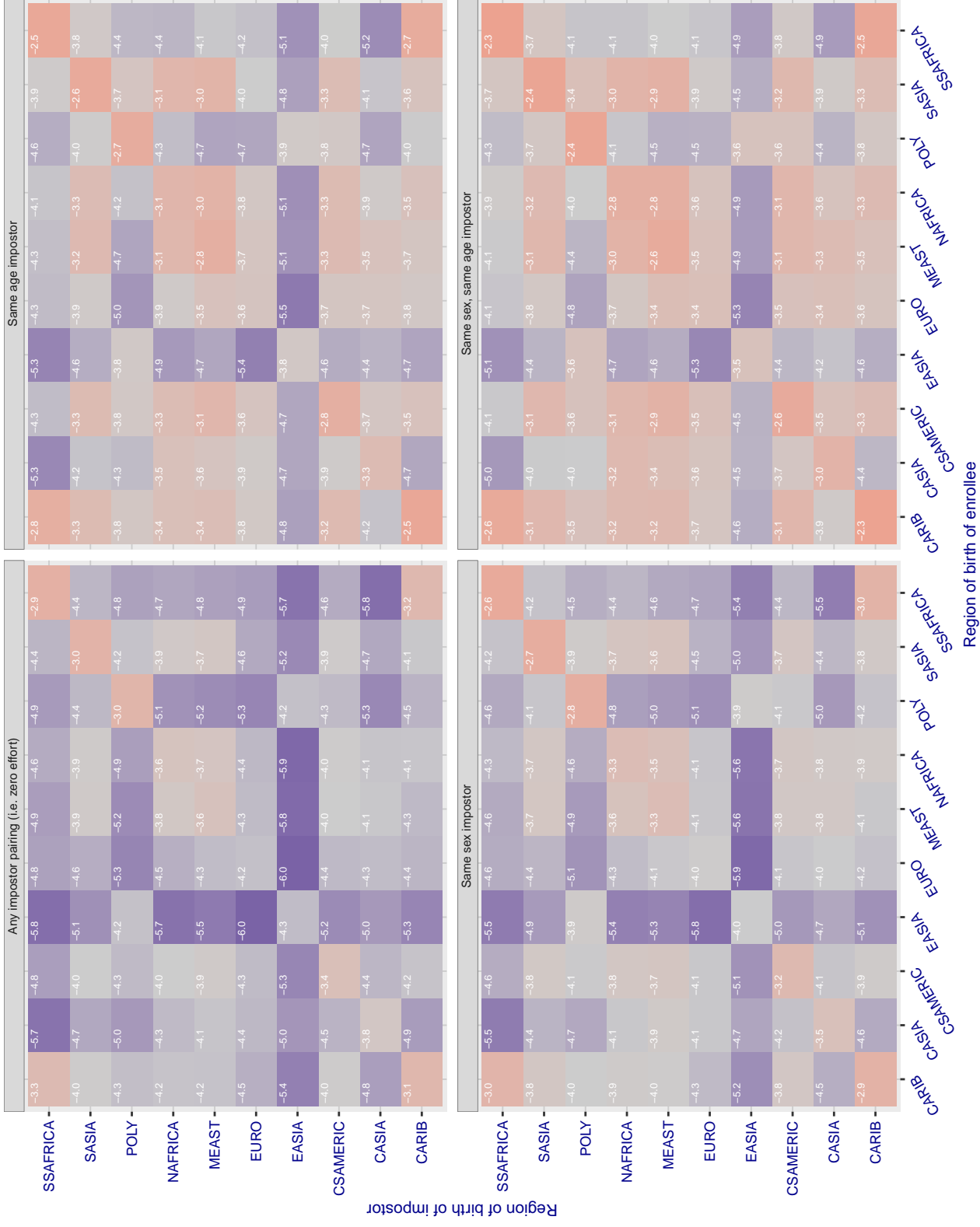
**Cross region FMR at threshold T = 1.375 for algorithm imperial\_000, giving FMR(T) = 0.0001 globally.**

Figure 199: For algorithm imperial-000 operating on visa images, the heatmap shows false match rates observed over impostor comparisons of faces from different individuals who were born in the given region pair. False matches are counted against a recognition threshold fixed globally to give the target FMR in the plot title, computed over all on the order of  $10^{10}$  impostor comparisons. If text appears in each box it give the same quantity as that coded by the color. Grey indicates FMR is at the intended FMR target level. Light red colors present a security vulnerability to, for example, a passport gate. Each +1 increase in  $\log_{10} FMR$  corresponds to a factor of 10 increase in FMR. The matrix is not quite symmetric because images in the enrollment and verification sets are different.

### Cross region FMR at threshold T = 1.358 for algorithm imperial\_002, giving FMR(T) = 0.0001 globally.

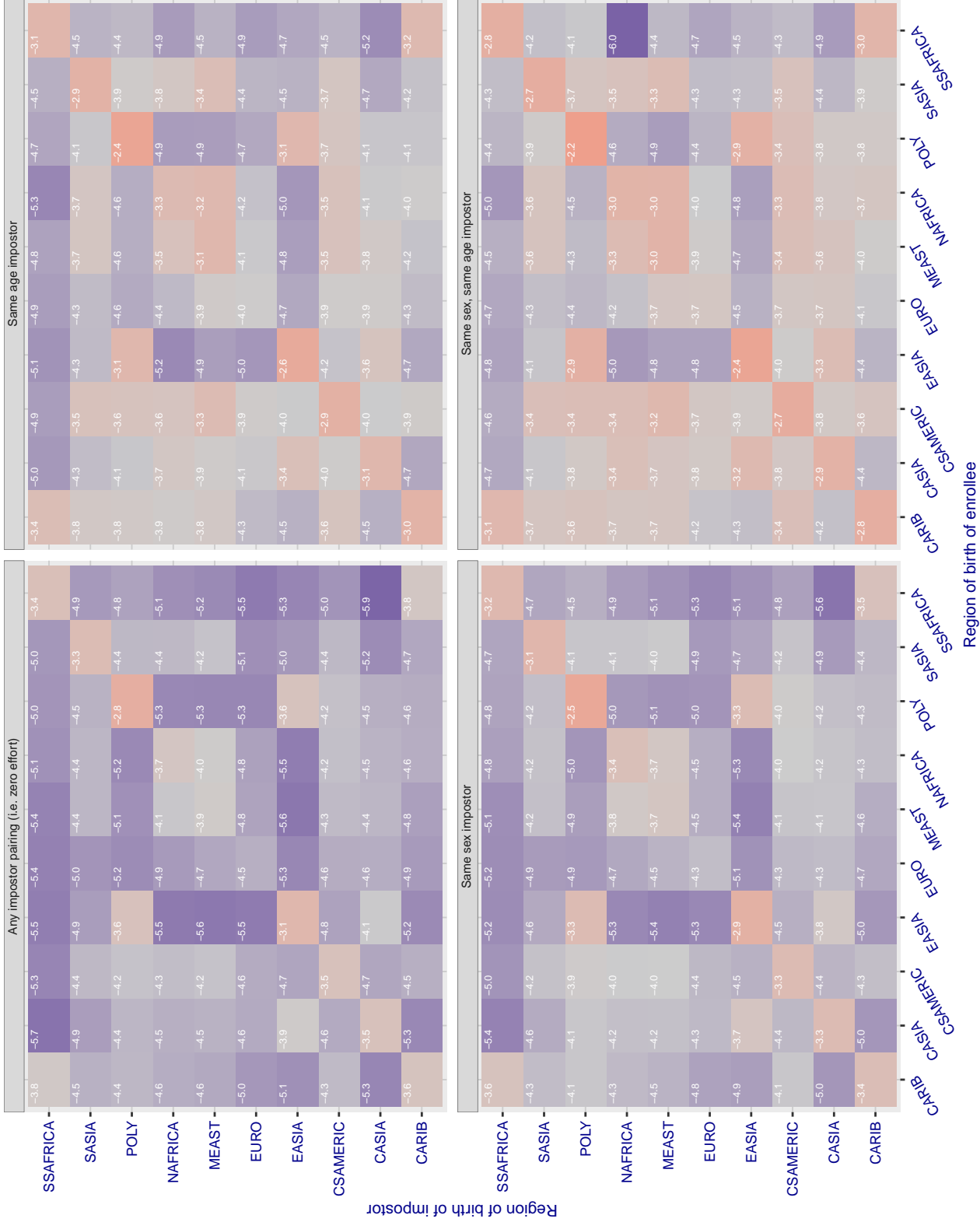


Figure 200: For algorithm imperial-002 operating on visa images, the heatmap shows false match rates observed over impostor comparisons of faces from different individuals who were born in the given region pair. False matches are counted against a recognition threshold fixed globally to give the target FMR in the plot title, computed over all on the order of  $10^{10}$  impostor comparisons. If text appears in each box it give the same quantity as that coded by the color. Grey indicates FMR is at the intended FMR target level. Light red colors present a security vulnerability to, for example, a passport gate. Each +1 increase in  $\log_{10} FMR$  corresponds to a factor of 10 increase in FMR. The matrix is not quite symmetric because images in the enrollment and verification sets are different.

### Cross region FMR at threshold T = 1.427 for algorithm incode\_003, giving FMR(T) = 0.0001 globally.

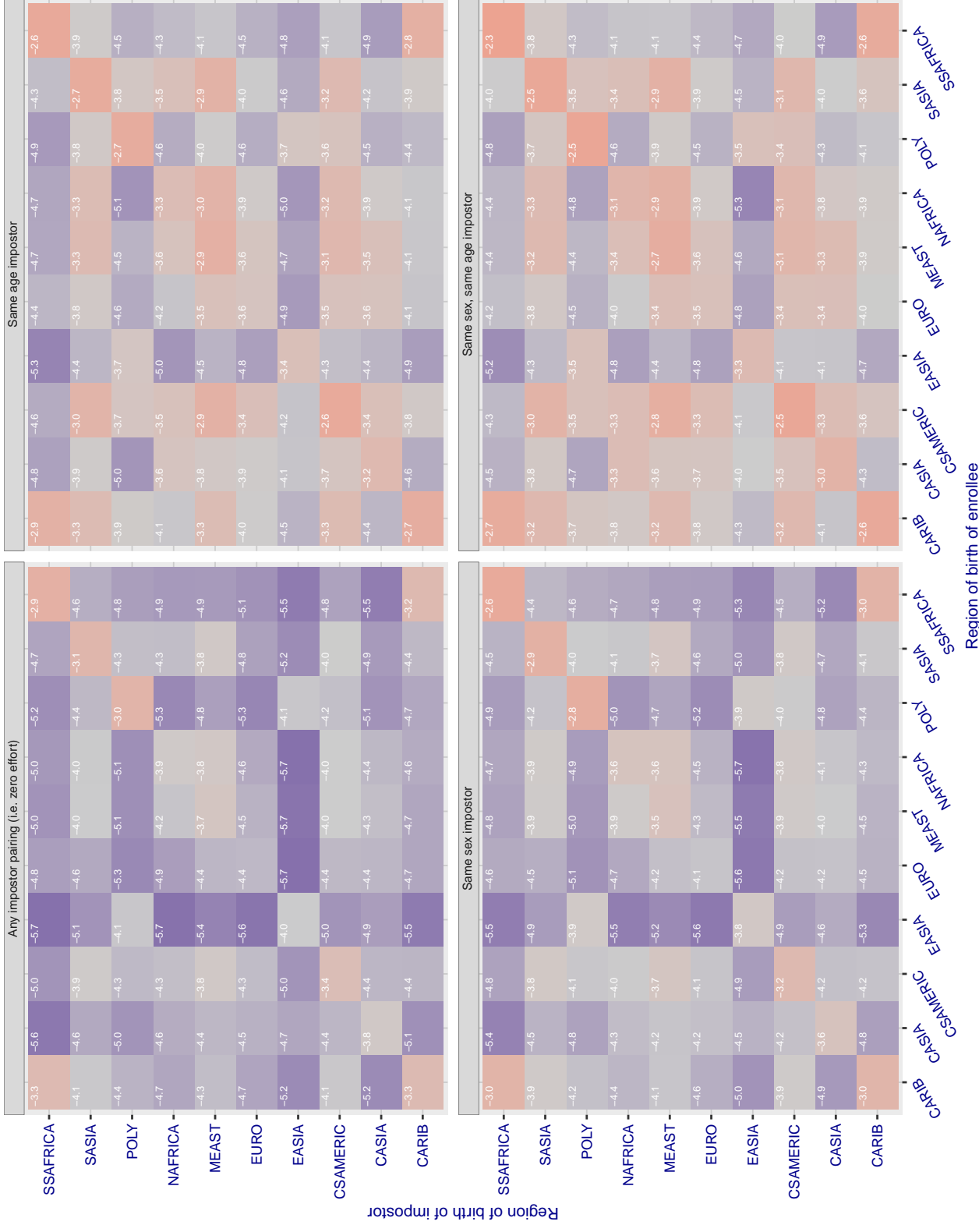


Figure 201: For algorithm incode-003 operating on visa images, the heatmap shows false match rates observed over impostor comparisons of faces from different individuals who were born in the given region pair. False matches are counted against a recognition threshold fixed globally to give the target FMR in the plot title, computed over all on the order of  $10^{10}$  impostor comparisons. If text appears in each box it give the same quantity as that coded by the color. Grey indicates FMR is at the intended FMR target level. Light red colors present a security vulnerability to, for example, a passport gate. Each +1 increase in  $\log_{10} FMR$  corresponds to a factor of 10 increase in FMR. The matrix is not quite symmetric because images in the enrollment and verification sets are different.

### Cross region FMR at threshold T = 1.398 for algorithm incode\_004, giving FMR(T) = 0.0001 globally.

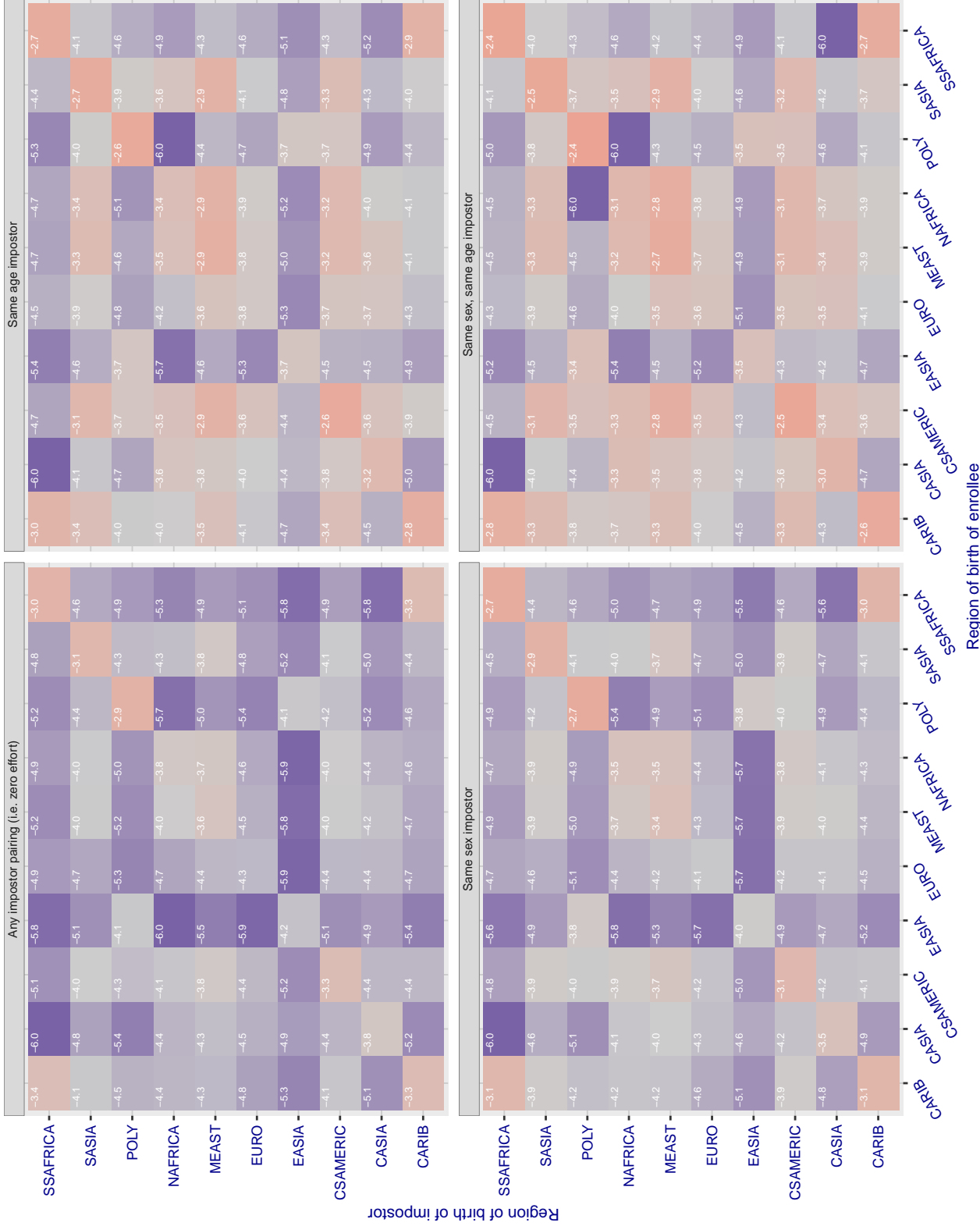


Figure 202: For algorithm incode-004 operating on visa images, the heatmap shows false match rates observed over impostor comparisons of faces from different individuals who were born in the given region pair. False matches are counted against a recognition threshold fixed globally to give the target FMR in the plot title, computed over all on the order of  $10^{10}$  impostor comparisons. If text appears in each box it give the same quantity as that coded by the color. Grey indicates FMR is at the intended FMR target level. Light red colors present a security vulnerability to, for example, a passport gate. Each +1 increase in  $\log_{10} \text{FMR}$  corresponds to a factor of 10 increase in FMR. The matrix is not quite symmetric because images in the enrollment and verification sets are different.

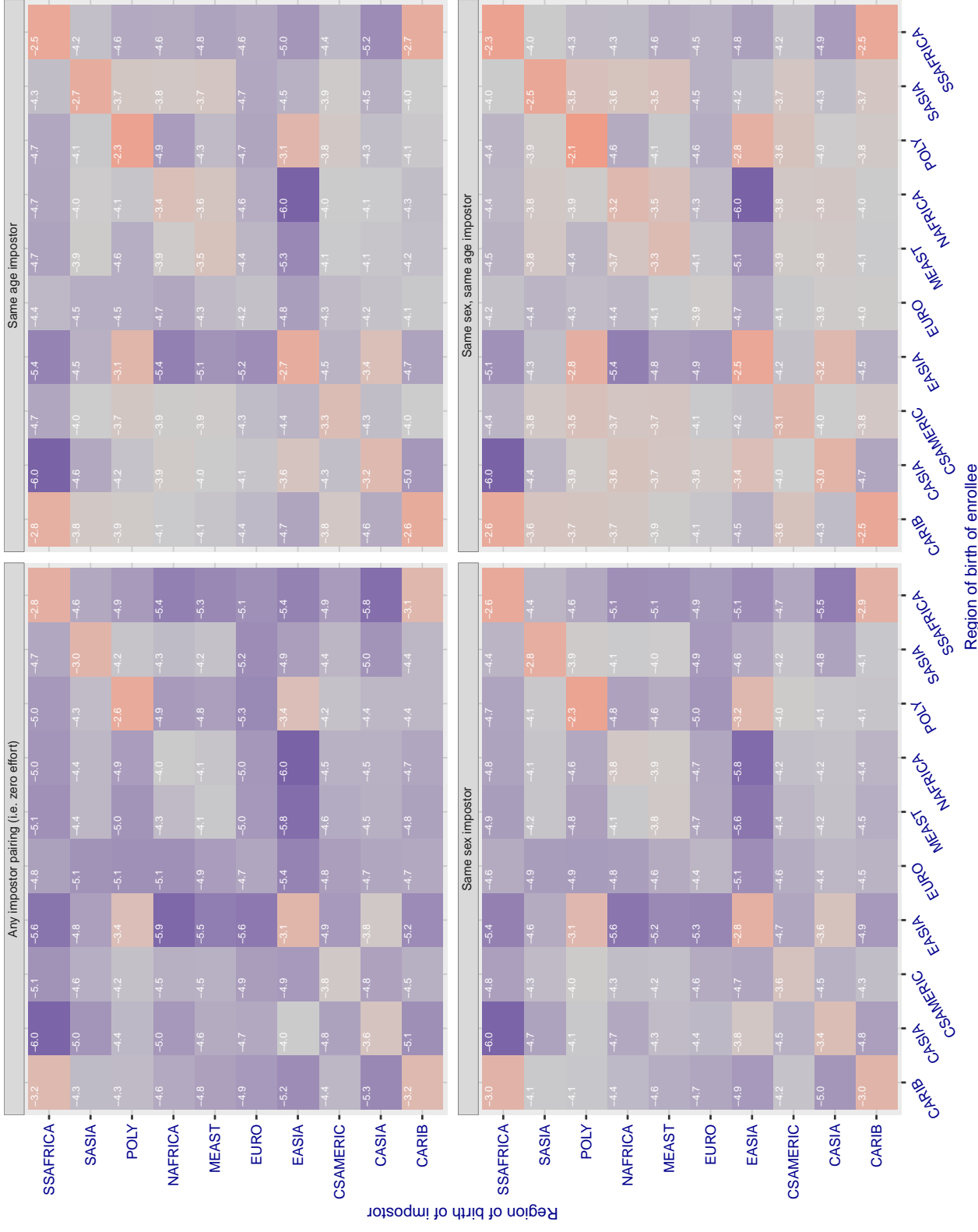
**Cross region FMR at threshold T = 29.232 for algorithm innovatrics\_004, giving FMR(T) = 0.0001 globally.**

Figure 203: For algorithm innovatrics-004 operating on visa images, the heatmap shows false match rates observed over impostor comparisons of faces from different individuals who were born in the given region pair. False matches are counted against a recognition threshold fixed globally to give the target FMR in the plot title, computed over all on the order of  $10^{10}$  impostor comparisons. If text appears in each box it give the same quantity as that coded by the color. Grey indicates FMR is at the intended FMR target level. Light red colors present a security vulnerability to, for example, a passport gate. Each +1 increase in  $\log_{10} FMR$  corresponds to a factor of 10 increase in FMR. The matrix is not quite symmetric because images in the enrollment and verification sets are different.

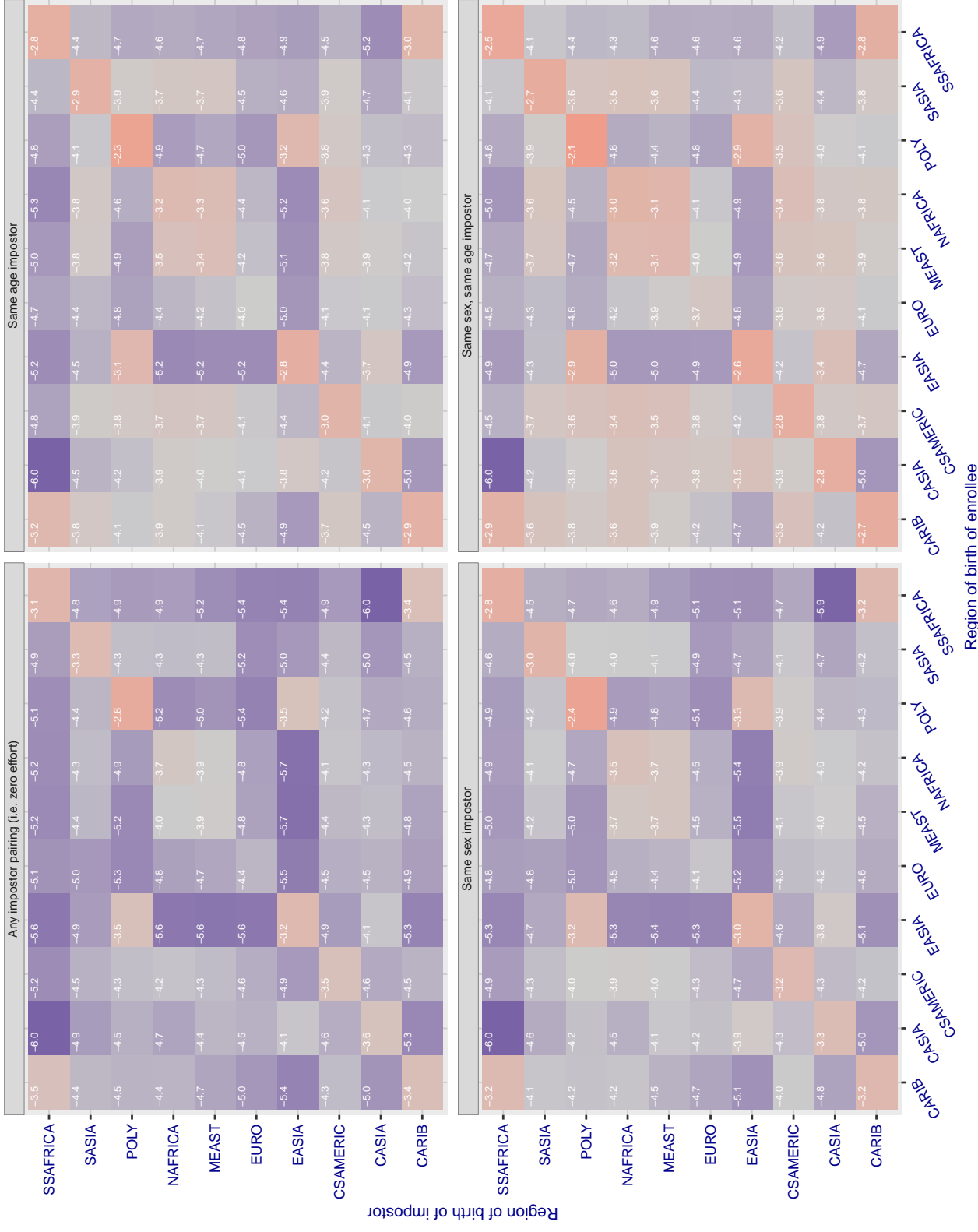
**Cross region FMR at threshold T = 27.987 for algorithm innovatrics\_006, giving FMR(T) = 0.0001 globally.**

Figure 204: For algorithm innovatrics-006 operating on visa images, the heatmap shows false match rates observed over impostor comparisons of faces from different individuals who were born in the given region pair. False matches are counted against a recognition threshold fixed globally to give the target FMR in the plot title, computed over all on the order of  $10^{10}$  impostor comparisons. If text appears in each box it give the same quantity as that coded by the color. Grey indicates FMR is at the intended FMR target level. Light red colors present a security vulnerability to, for example, a passport gate. Each +1 increase in  $\log_{10} FMR$  corresponds to a factor of 10 increase in FMR. The matrix is not quite symmetric because images in the enrollment and verification sets are different.

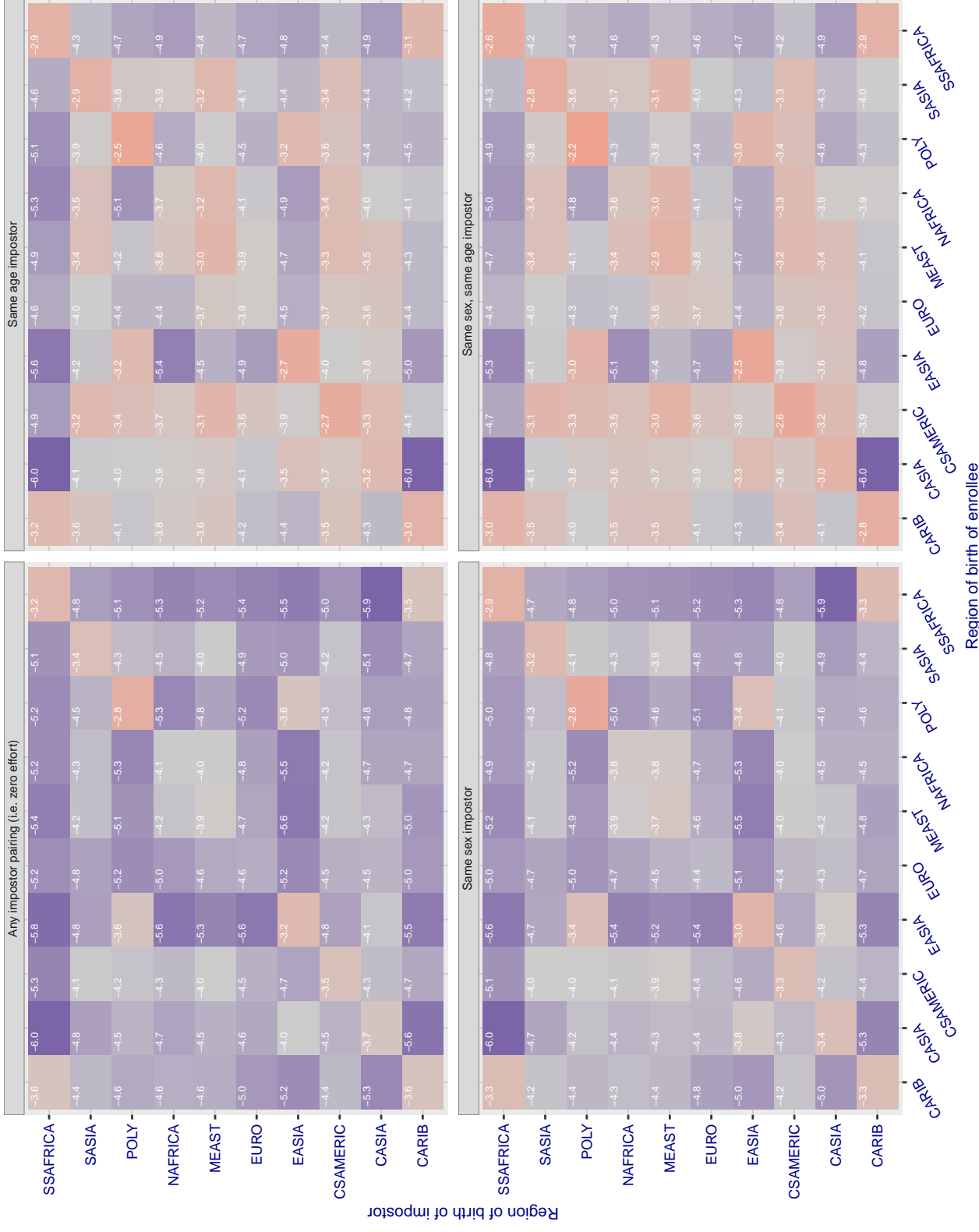
**Cross region FMR at threshold T = 0.705 for algorithm intellicloudai\_001, giving FMR(T) = 0.0001 globally.**

Figure 205: For algorithm intellicloudai-001 operating on visa images, the heatmap shows false match rates observed over impostor comparisons of faces from different individuals who were born in the given region pair. False matches are counted against a recognition threshold fixed globally to give the target FMR in the plot title, computed over all on the order of  $10^{10}$  impostor comparisons. If text appears in each box it give the same quantity as that coded by the color. Grey indicates FMR is at the intended FMR target level. Light red colors present a security vulnerability to, for example, a passport gate. Each +1 increase in  $\log_{10} FMR$  corresponds to a factor of 10 increase in FMR. The matrix is not quite symmetric because images in the enrollment and verification sets are different.

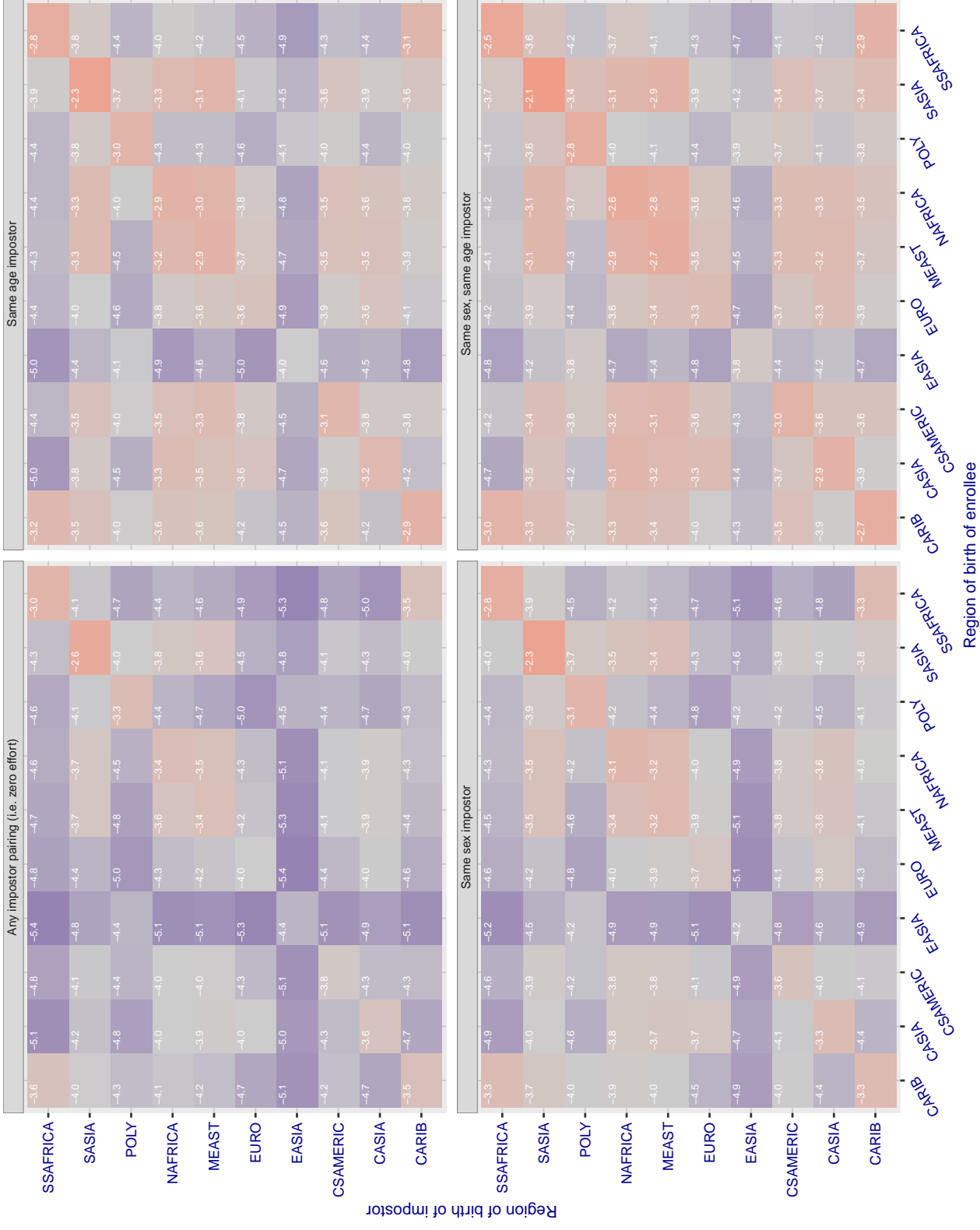
**Cross region FMR at threshold T = 0.300 for algorithm intellifusion\_001, giving FMR(T) = 0.0001 globally.**

Figure 206: For algorithm intellifusion-001 operating on visa images, the heatmap shows false match rates observed over impostor comparisons of faces from different individuals who were born in the given region pair. False matches are counted against a recognition threshold fixed globally to give the target FMR in the plot title, computed over all on the order of  $10^{10}$  impostor comparisons. If text appears in each box it give the same quantity as that coded by the color. Grey indicates FMR is at the intended FMR target level. Light red colors present a security vulnerability to, for example, a passport gate. Each +1 increase in  $\log_{10} FMR$  corresponds to a factor of 10 increase in FMR. The matrix is not quite symmetric because images in the enrollment and verification sets are different.

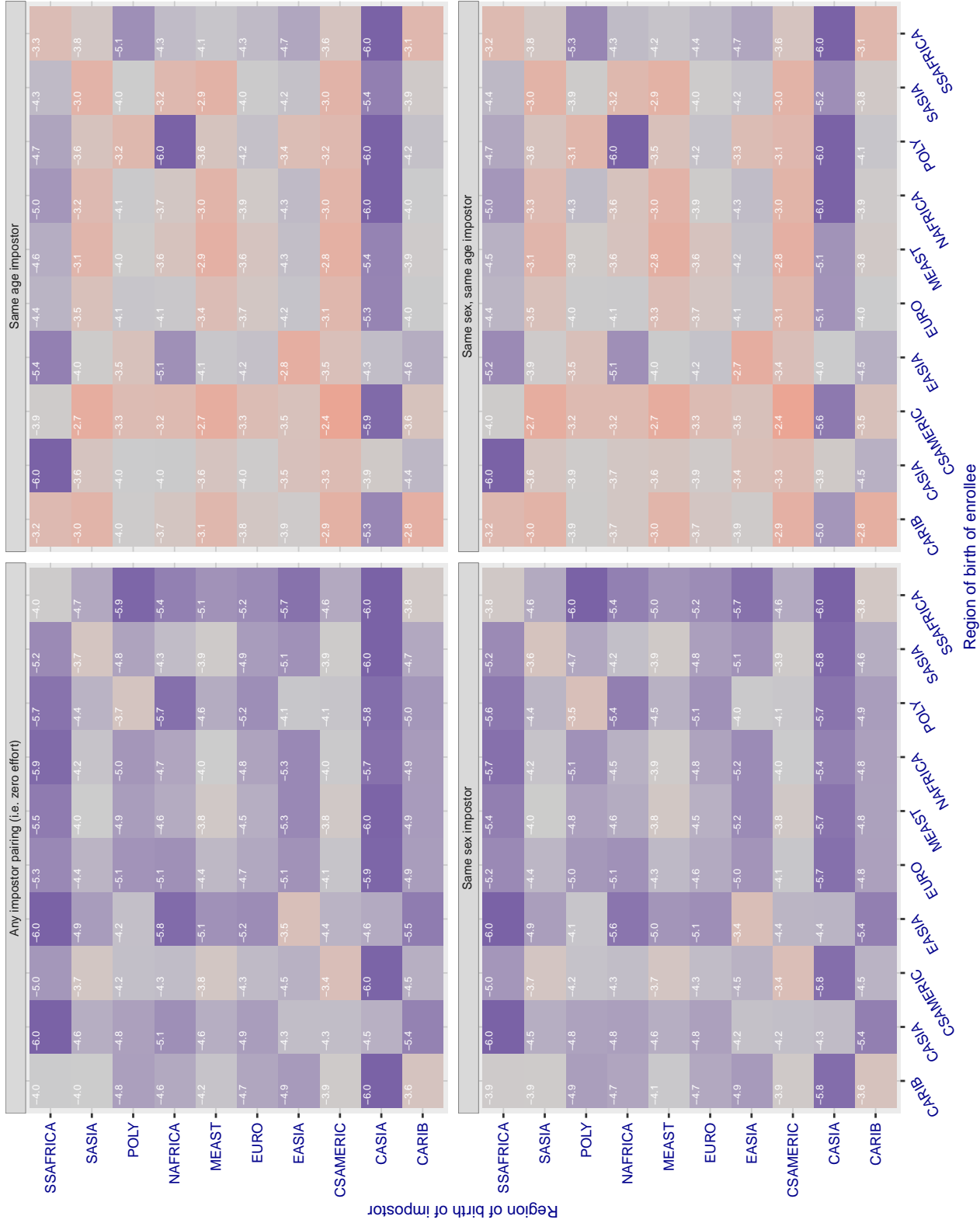
**Cross region FMR at threshold T = 49.664 for algorithm intellivision\_001, giving FMR(T) = 0.0001 globally.**

Figure 207: For algorithm intellivision-001 operating on visa images, the heatmap shows false match rates observed over impostor comparisons of faces from different individuals who were born in the given region pair. False matches are counted against a recognition threshold fixed globally to give the target FMR in the plot title, computed over all on the order of  $10^{10}$  impostor comparisons. If text appears in each box it give the same quantity as that coded by the color. Grey indicates FMR is at the intended FMR target level. Light red colors present a security vulnerability to, for example, a passport gate. Each +1 increase in  $\log_{10} FMR$  corresponds to a factor of 10 increase in FMR. The matrix is not quite symmetric because images in the enrollment and verification sets are different.

Cross region FMR at threshold  $T = 44.160$  for algorithm intellivision\_002, giving FMR( $T = 0.0001$ ) globally.

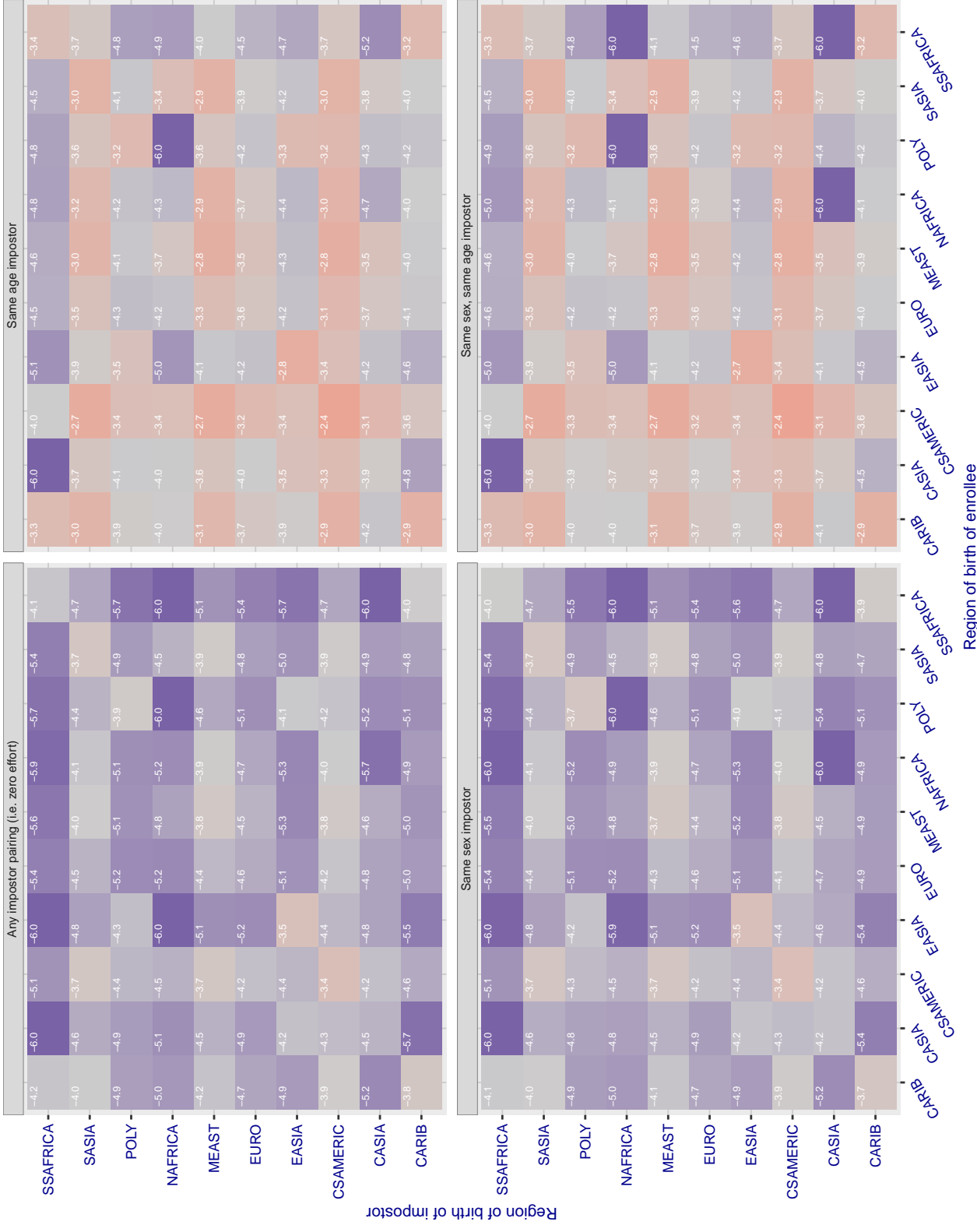


Figure 208: For algorithm intellivision-002 operating on visa images, the heatmap shows false match rates observed over impostor comparisons of faces from different individuals who were born in the given region pair. False matches are counted against a recognition threshold fixed globally to give the target FMR in the plot title, computed over all on the order of  $10^{10}$  impostor comparisons. If text appears in each box it give the same quantity as that coded by the color. Grey indicates FMR is at the intended FMR target level. Light red colors present a security vulnerability to, for example, a passport gate. Each +1 increase in  $\log_{10}$  FMR corresponds to a factor of 10 increase in FMR. The matrix is not quite symmetric because images in the enrollment and verification sets are different.

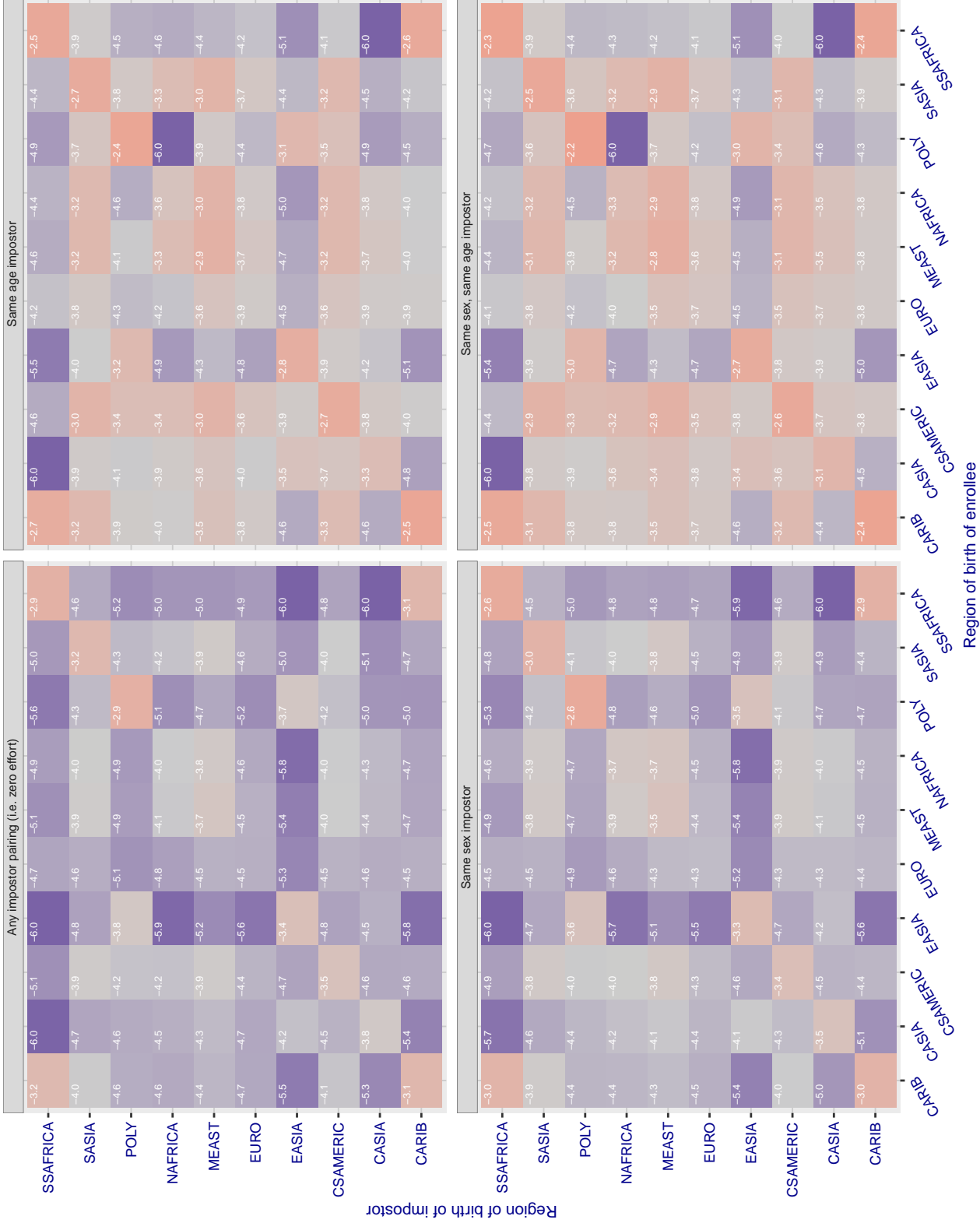
**Cross region FMR at threshold T = 594.014 for algorithm intelresearch\_000, giving FMR(T) = 0.0001 globally.**

Figure 209: For algorithm intelresearch-000 operating on visa images, the heatmap shows false match rates observed over impostor comparisons of faces from different individuals who were born in the given region pair. False matches are counted against a recognition threshold fixed globally to give the target FMR in the plot title, computed over all on the order of  $10^{10}$  impostor comparisons. If text appears in each box it give the same quantity as that coded by the color. Grey indicates FMR is at the intended FMR target level. Light red colors present a security vulnerability to, for example, a passport gate. Each +1 increase in  $\log_{10} \text{FMR}$  corresponds to a factor of 10 increase in FMR. The matrix is not quite symmetric because images in the enrollment and verification sets are different.

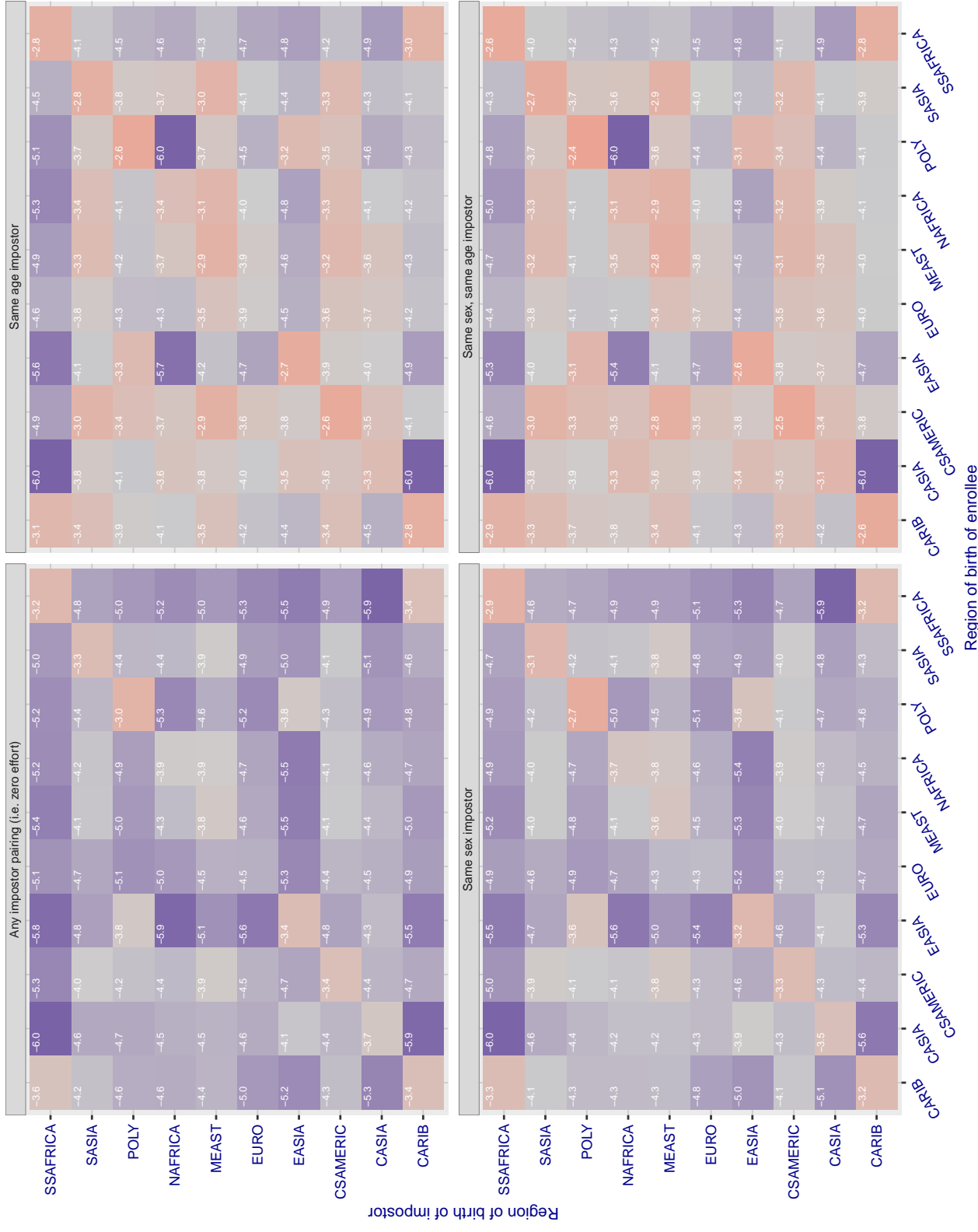
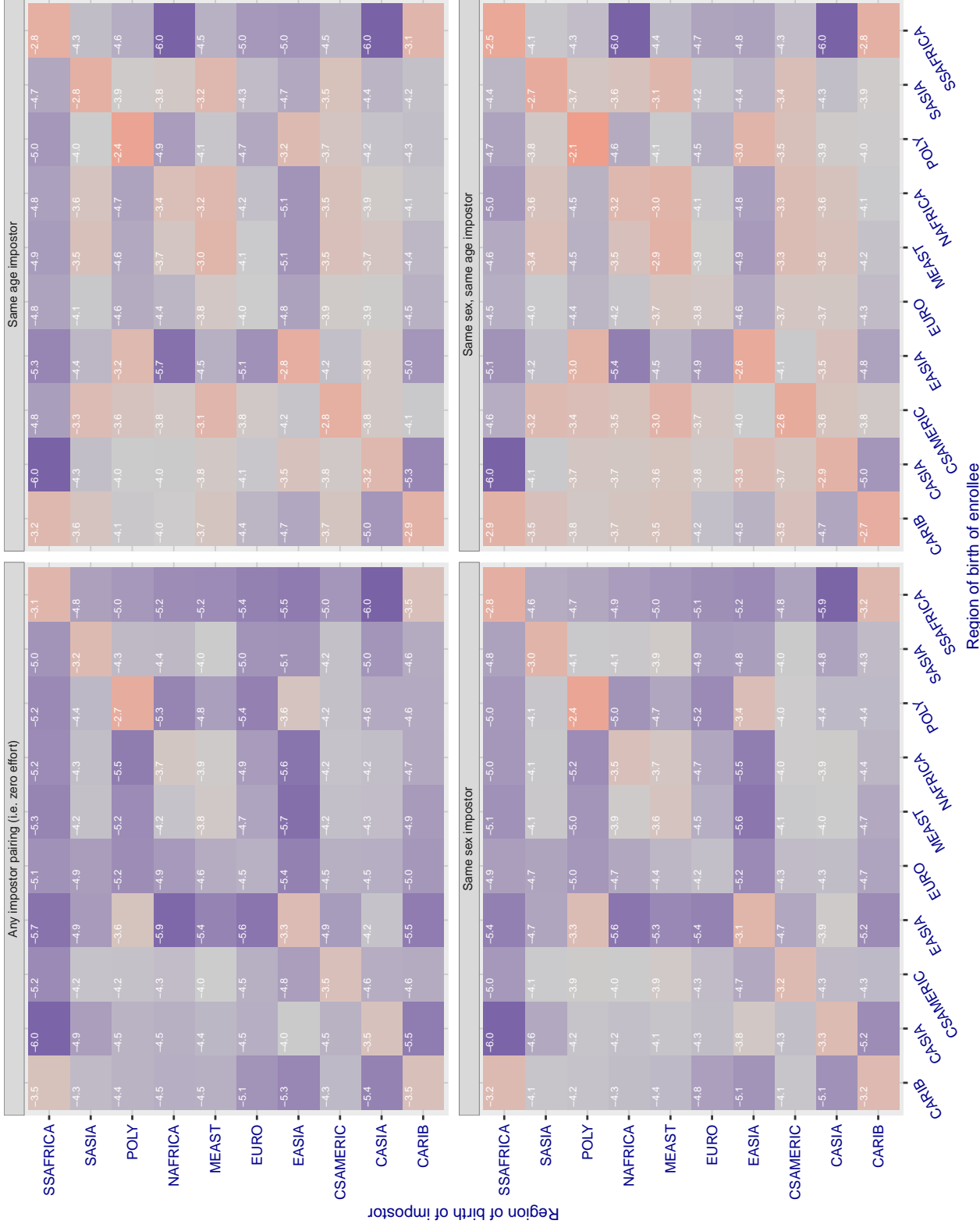
**Cross region FMR at threshold T = 1.389 for algorithm intsystemsu\_000, giving FMR(T) = 0.0001 globally.**

Figure 210: For algorithm intsystemsu-000 operating on visa images, the heatmap shows false match rates observed over impostor comparisons of faces from different individuals who were born in the given region pair. False matches are counted against a recognition threshold fixed globally to give the target FMR in the plot title, computed over all on the order of  $10^{10}$  impostor comparisons. If text appears in each box it give the same quantity as that coded by the color. Grey indicates FMR is at the intended FMR target level. Light red colors present a security vulnerability to, for example, a passport gate. Each +1 increase in  $\log_{10} \text{FMR}$  corresponds to a factor of 10 increase in FMR. The matrix is not quite symmetric because images in the enrollment and verification sets are different.

**Cross region FMR at threshold T = 1.361 for algorithm iiface\_000, giving FMR(T) = 0.0001 globally.**

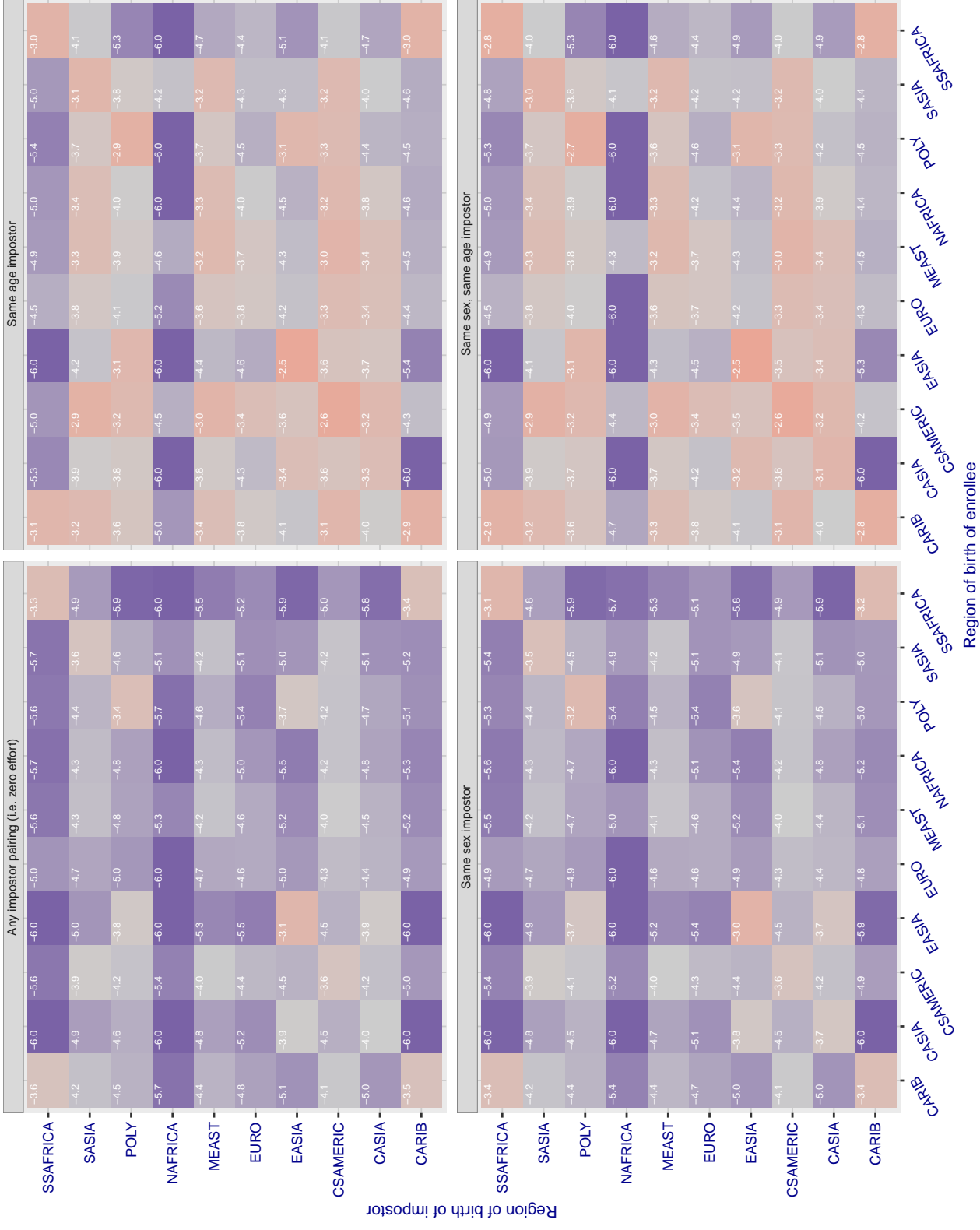
**Cross region FMR at threshold T = 0.985 for algorithm isap\_001, giving FMR(T) = 0.0001 globally.**

Figure 212: For algorithm isap-001 operating on visa images, the heatmap shows false match rates observed over impostor comparisons of faces from different individuals who were born in the given region pair. False matches are counted against a recognition threshold fixed globally to give the target FMR in the plot title, computed over all on the order of  $10^{10}$  impostor comparisons. If text appears in each box it give the same quantity as that coded by the color. Grey indicates FMR is at the intended FMR target level. Light red colors present a security vulnerability to, for example, a passport gate. Each +1 increase in  $\log_{10}$  FMR corresponds to a factor of 10 increase in FMR. The matrix is not quite symmetric because images in the enrollment and verification sets are different.

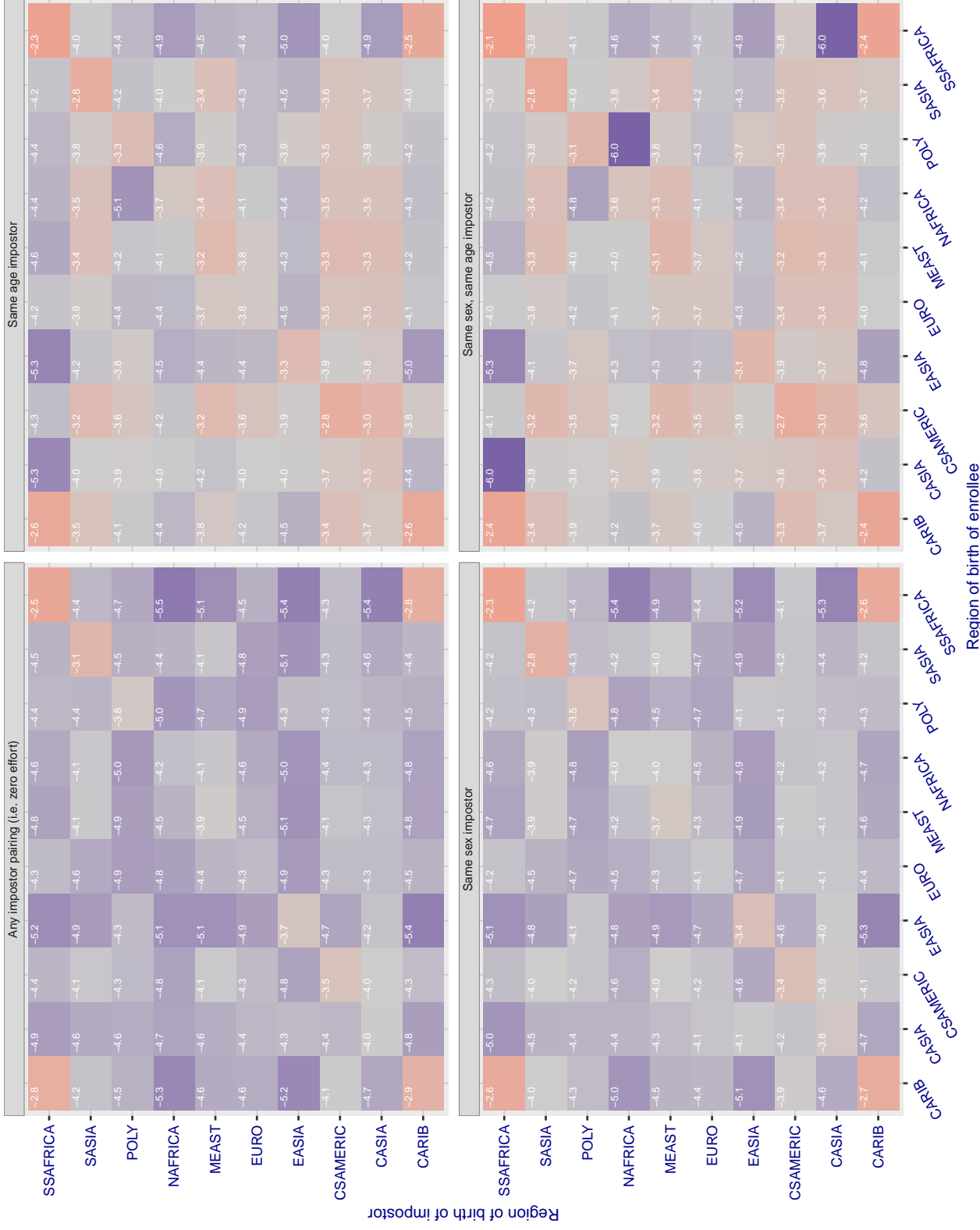
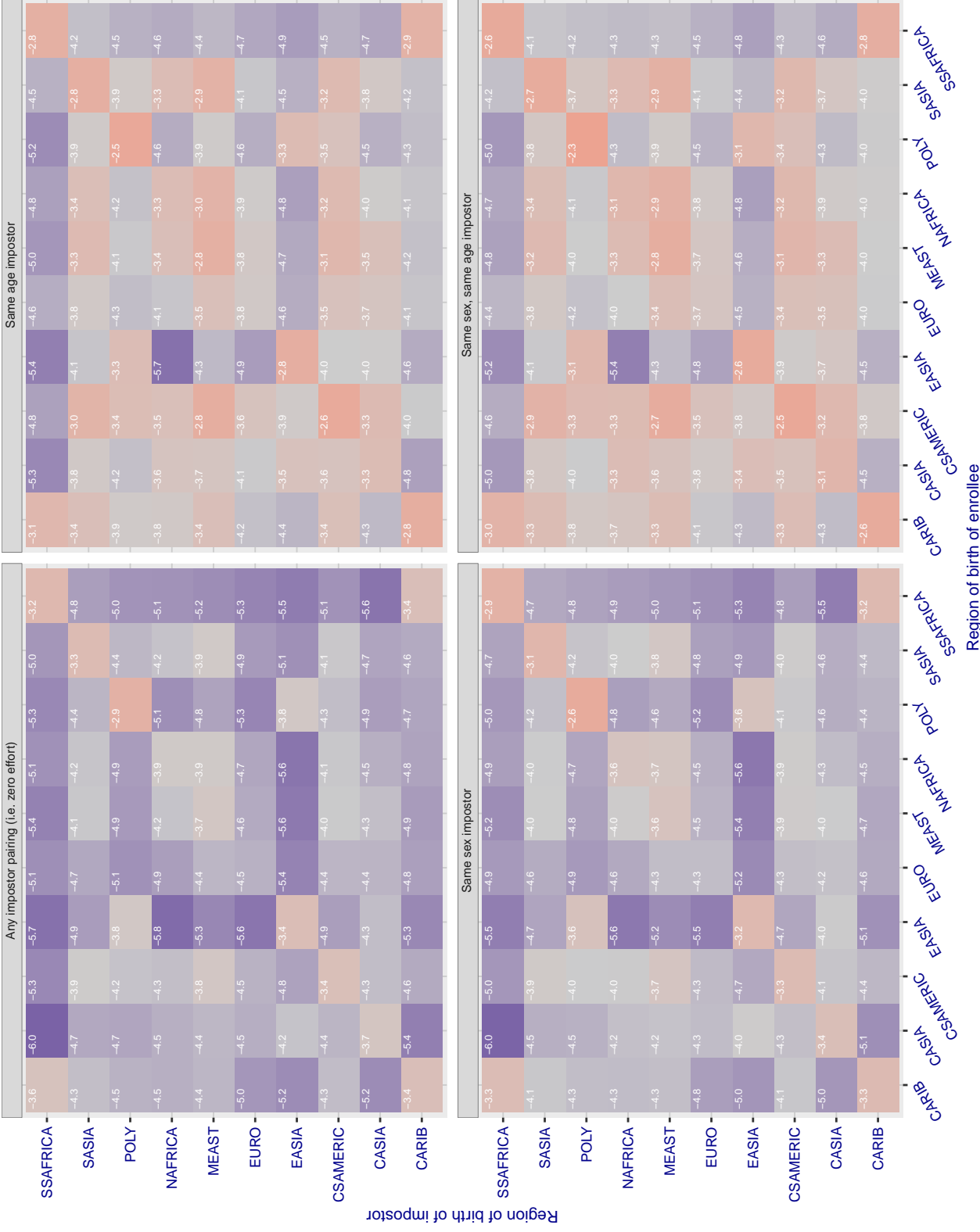
**Cross region FMR at threshold T = 23.498 for algorithm isityou\_000, giving FMR(T) = 0.0001 globally.**

Figure 213: For algorithm isityou-000 operating on visa images, the heatmap shows false match rates observed over impostor comparisons of faces from different individuals who were born in the given region pair. False matches are counted against a recognition threshold fixed globally to give the target FMR in the plot title, computed over all on the order of  $10^{10}$  impostor comparisons. If text appears in each box it give the same quantity as that coded by the color. Grey indicates FMR is at the intended FMR target level. Light red colors present a security vulnerability to, for example, a passport gate. Each +1 increase in  $\log_{10} FMR$  corresponds to a factor of 10 increase in FMR. The matrix is not quite symmetric because images in the enrollment and verification sets are different.

**Cross region FMR at threshold T = 0.693 for algorithm systems\_001, giving FMR(T) = 0.0001 globally.**

### Cross region FMR at threshold T = 0.690 for algorithm systems\_002, giving FMR(T) = 0.0001 globally.

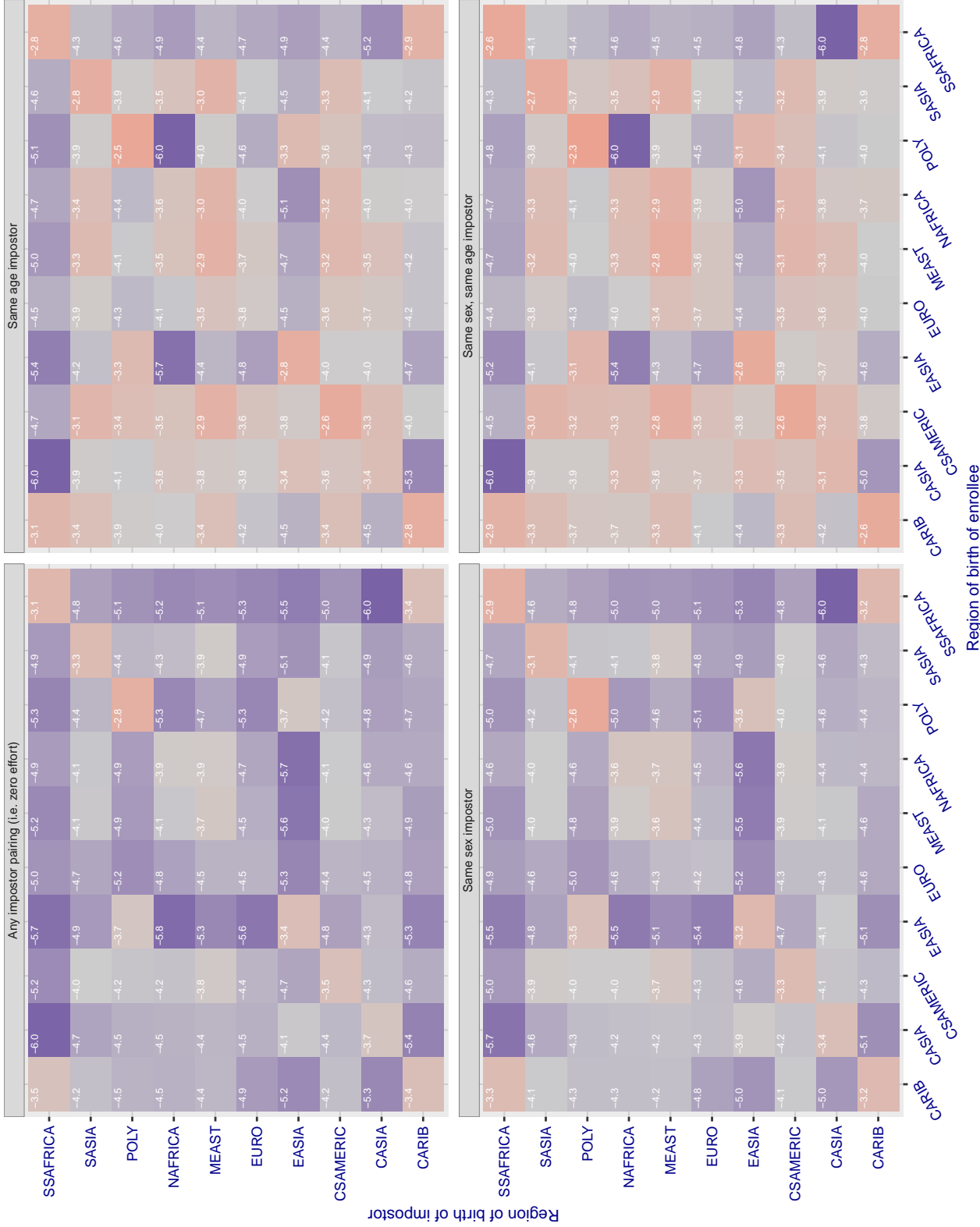


Figure 215: For algorithm systems-002 operating on visa images, the heatmap shows false match rates observed over impostor comparisons of faces from different individuals who were born in the given region pair. False matches are counted against a recognition threshold fixed globally to give the target FMR in the plot title, computed over all on the order of  $10^{10}$  impostor comparisons. If text appears in each box it give the same quantity as that coded by the color. Grey indicates FMR is at the intended FMR target level. Light red colors present a security vulnerability to, for example, a passport gate. Each +1 increase in  $\log_{10} FMR$  corresponds to a factor of 10 increase in FMR. The matrix is not quite symmetric because images in the enrollment and verification sets are different.

### Cross region FMR at threshold T = 49.879 for algorithm itmo\_005, giving $\text{FMR}(T) = 0.0001$ globally.

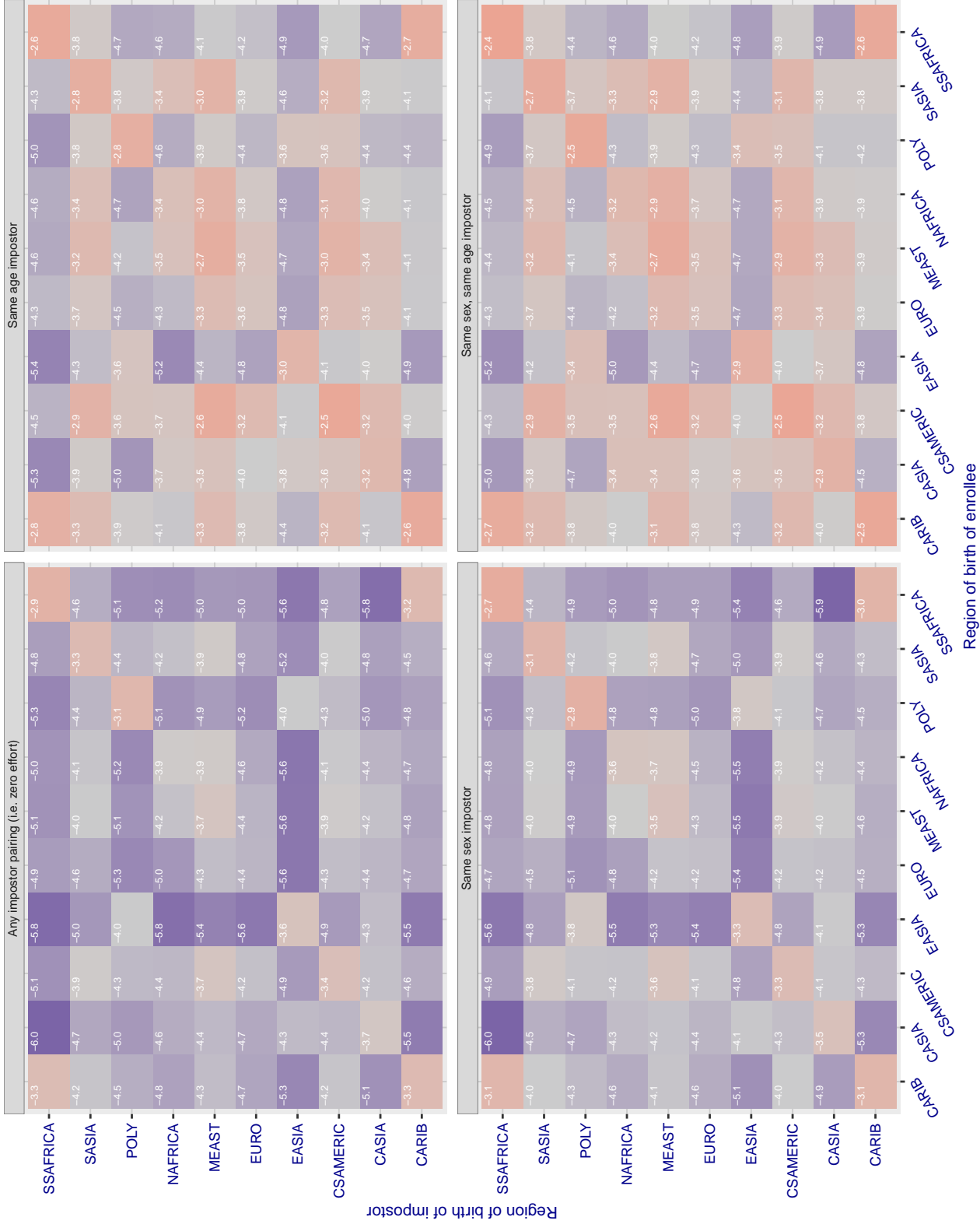


Figure 216: For algorithm itmo-005 operating on visa images, the heatmap shows false match rates observed over impostor comparisons of faces from different individuals who were born in the given region pair. False matches are counted against a recognition threshold fixed globally to give the target FMR in the plot title, computed over all on the order of  $10^{10}$  impostor comparisons. If text appears in each box it give the same quantity as that coded by the color. Grey indicates FMR is at the intended FMR target level. Light red colors present a security vulnerability to, for example, a passport gate. Each +1 increase in  $\log 10 \text{ FMR}$  corresponds to a factor of 10 increase in FMR. The matrix is not quite symmetric because images in the enrollment and verification sets are different.

### Cross region FMR at threshold T = 49.789 for algorithm itmo\_006, giving FMR(T) = 0.0001 globally.

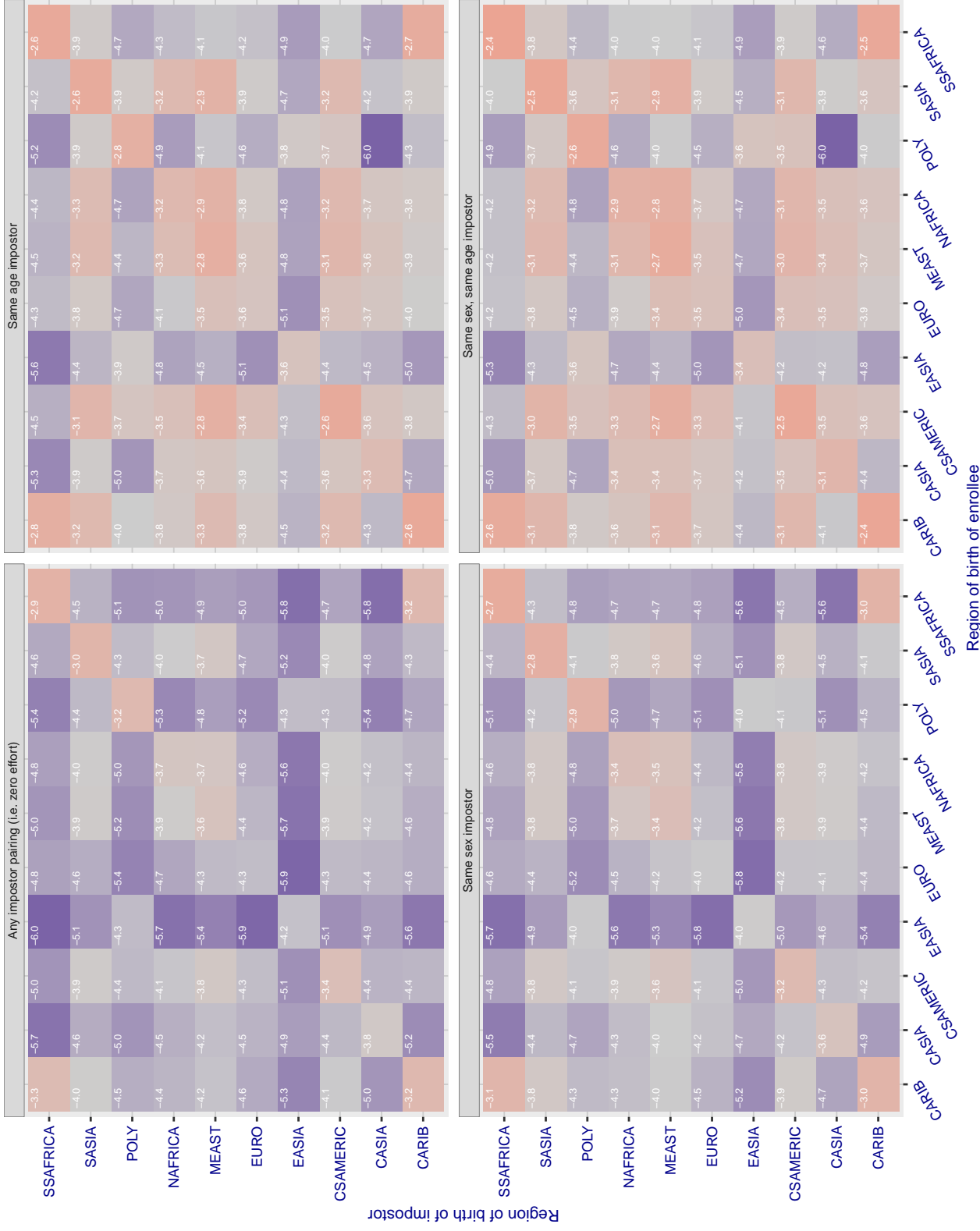


Figure 217: For algorithm itmo-006 operating on visa images, the heatmap shows false match rates observed over impostor comparisons of faces from different individuals who were born in the given region pair. False matches are counted against a recognition threshold fixed globally to give the target FMR in the plot title, computed over all on the order of  $10^{10}$  impostor comparisons. If text appears in each box it give the same quantity as that coded by the color. Grey indicates FMR is at the intended FMR target level. Light red colors present a security vulnerability to, for example, a passport gate. Each +1 increase in  $\log_{10}$  FMR corresponds to a factor of 10 increase in FMR. The matrix is not quite symmetric because images in the enrollment and verification sets are different.

### Cross region FMR at threshold T = 1.301 for algorithm kakao\_001, giving $FMR(T) = 0.0001$ globally.

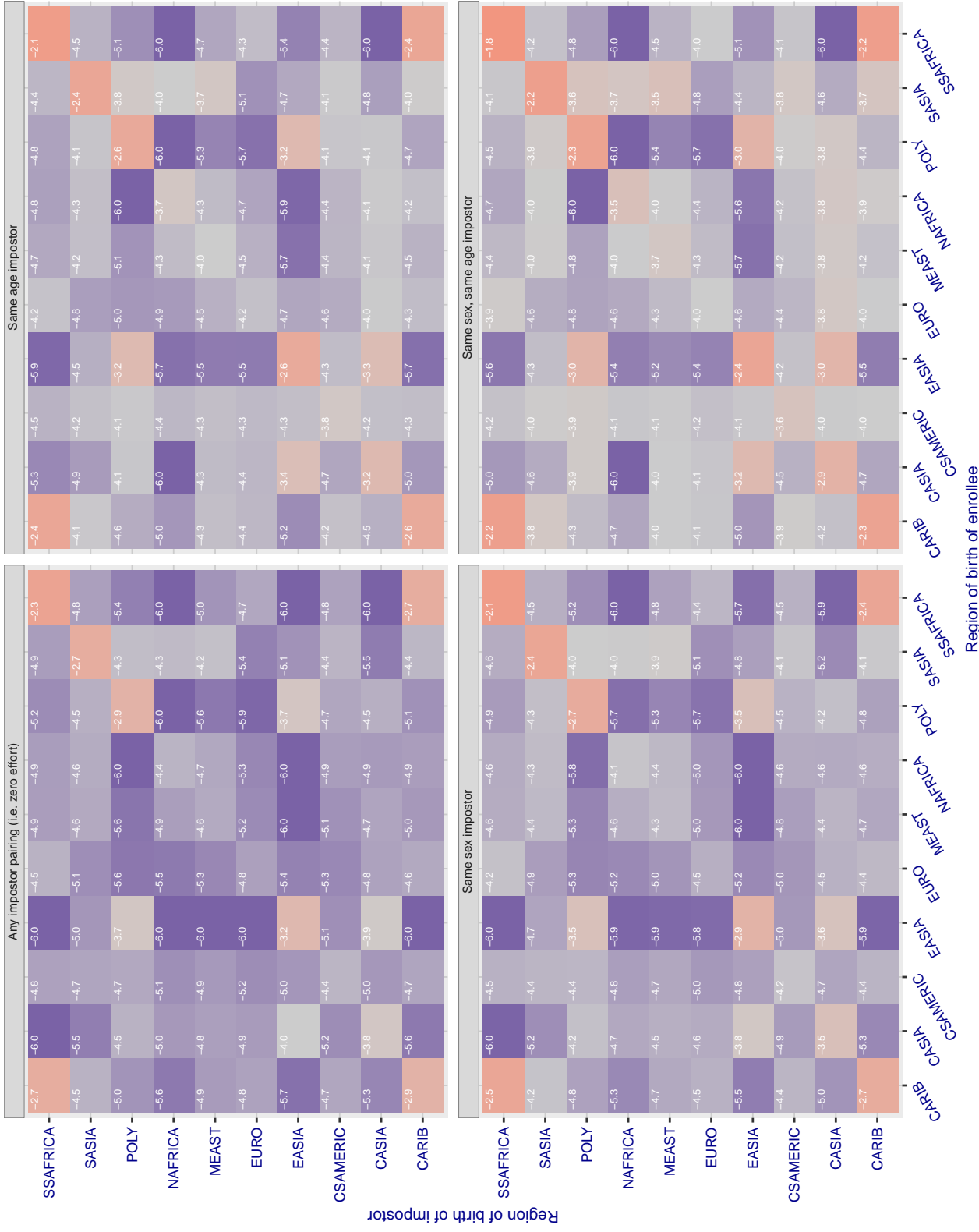


Figure 218: For algorithm kakao-001 operating on visa images, the heatmap shows false match rates observed over impostor comparisons of faces from different individuals who were born in the given region pair. False matches are counted against a recognition threshold fixed globally to give the target FMR in the plot title, computed over all on the order of  $10^{10}$  impostor comparisons. If text appears in each box it give the same quantity as that coded by the color. Grey indicates FMR is at the intended FMR target level. Light red colors present a security vulnerability to, for example, a passport gate. Each +1 increase in  $\log_{10} FMR$  corresponds to a factor of 10 increase in FMR. The matrix is not quite symmetric because images in the enrollment and verification sets are different.

### Cross region FMR at threshold T = 0.929 for algorithm kakao\_002, giving $FMR(T) = 0.0001$ globally.

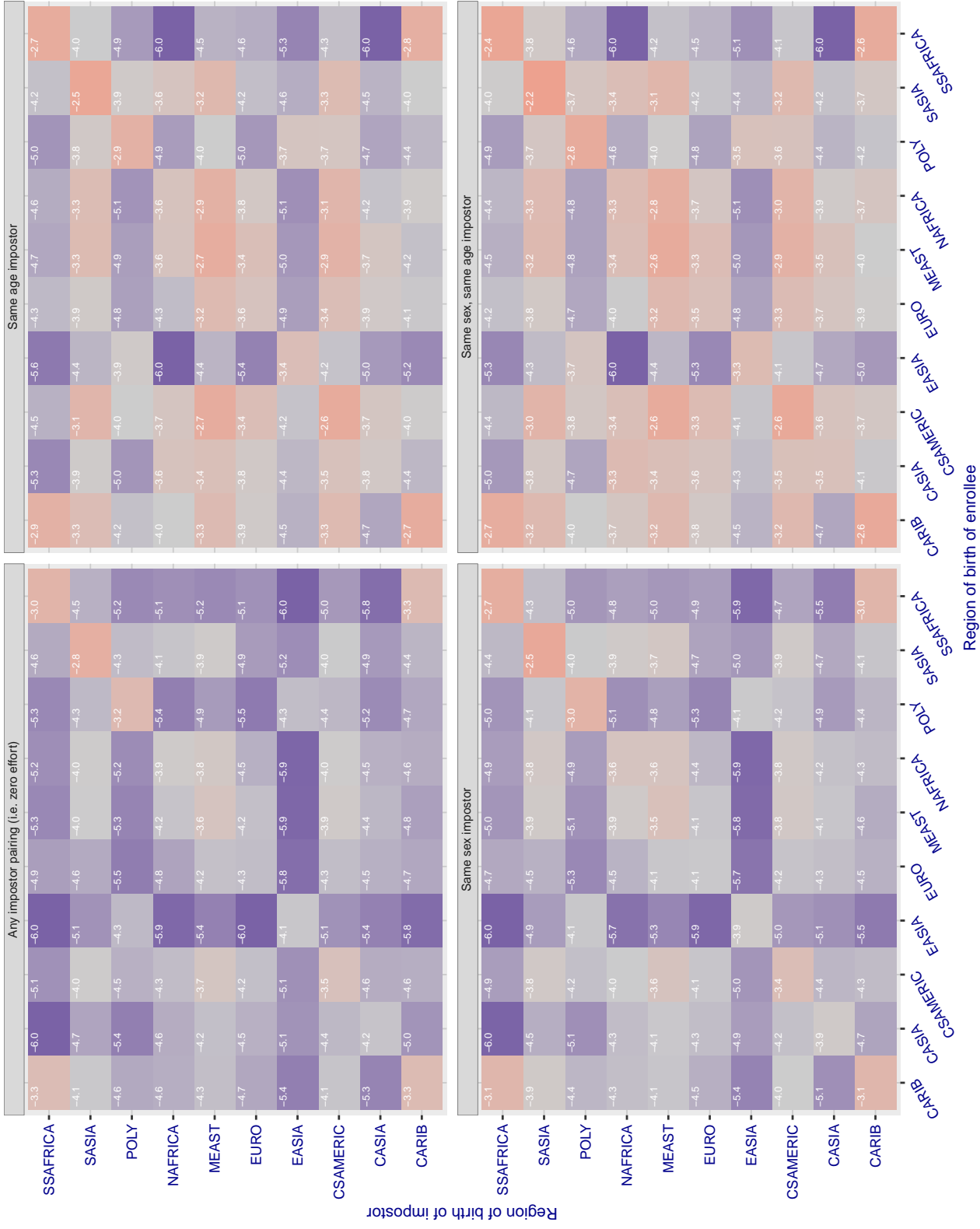


Figure 219: For algorithm kakao-002 operating on visa images, the heatmap shows false match rates observed over impostor comparisons of faces from different individuals who were born in the given region pair. False matches are counted against a recognition threshold fixed globally to give the target FMR in the plot title, computed over all on the order of  $10^{10}$  impostor comparisons. If text appears in each box it give the same quantity as that coded by the color. Grey indicates FMR is at the intended FMR target level. Light red colors present a security vulnerability to, for example, a passport gate. Each +1 increase in  $\log_{10} FMR$  corresponds to a factor of 10 increase in FMR. The matrix is not quite symmetric because images in the enrollment and verification sets are different.

### Cross region FMR at threshold T = 0.686 for algorithm kedacom\_000, giving $FMR(T) = 0.0001$ globally.

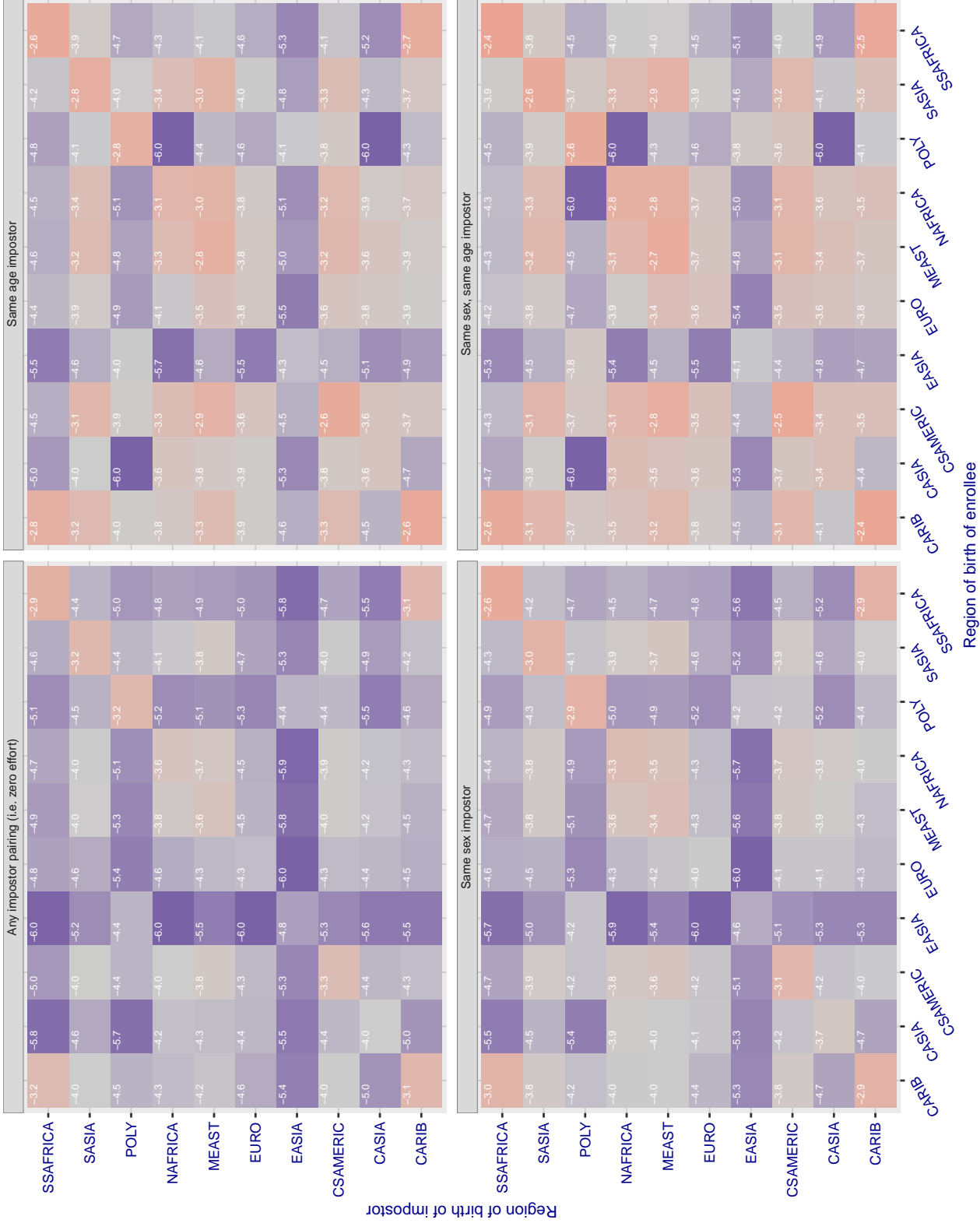


Figure 220: For algorithm kedacom-000 operating on visa images, the heatmap shows false match rates observed over impostor comparisons of faces from different individuals who were born in the given region pair. False matches are counted against a recognition threshold fixed globally to give the target FMR in the plot title, computed over all on the order of  $10^{10}$  impostor comparisons. If text appears in each box it give the same quantity as that coded by the color. Grey indicates FMR is at the intended FMR target level. Light red colors present a security vulnerability to, for example, a passport gate. Each +1 increase in  $\log_{10} FMR$  corresponds to a factor of 10 increase in FMR. The matrix is not quite symmetric because images in the enrollment and verification sets are different.

### Cross region FMR at threshold T = 0.500 for algorithm kneron\_003, giving FMR(T) = 0.0001 globally.

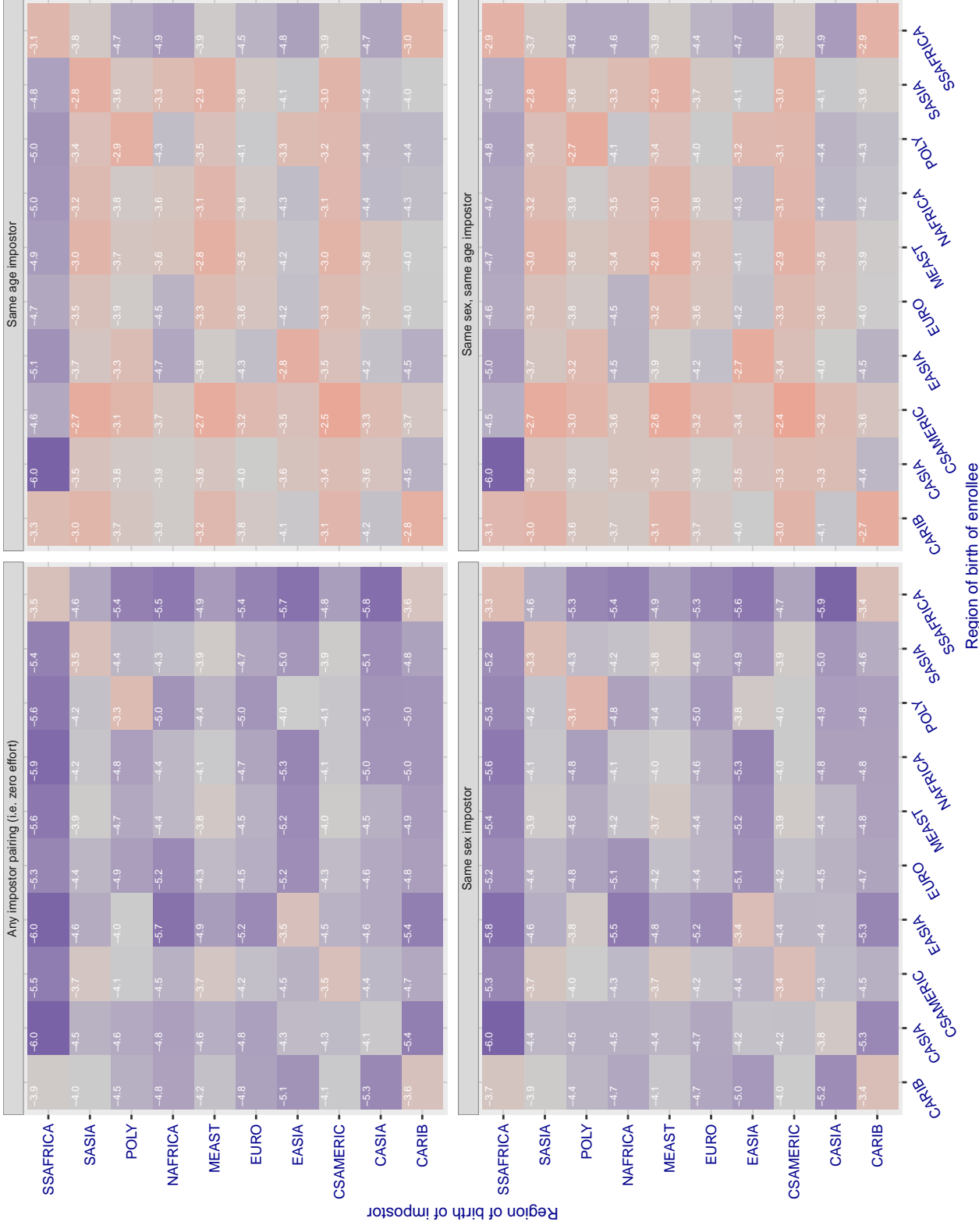


Figure 221: For algorithm kneron-003 operating on visa images, the heatmap shows false match rates observed over impostor comparisons of faces from different individuals who were born in the given region pair. False matches are counted against a recognition threshold fixed globally to give the target FMR in the plot title, computed over all on the order of  $10^{10}$  impostor comparisons. If text appears in each box it give the same quantity as that coded by the color. Grey indicates FMR is at the intended FMR target level. Light red colors present a security vulnerability to, for example, a passport gate. Each +1 increase in  $\log_{10} FMR$  corresponds to a factor of 10 increase in FMR. The matrix is not quite symmetric because images in the enrollment and verification sets are different.

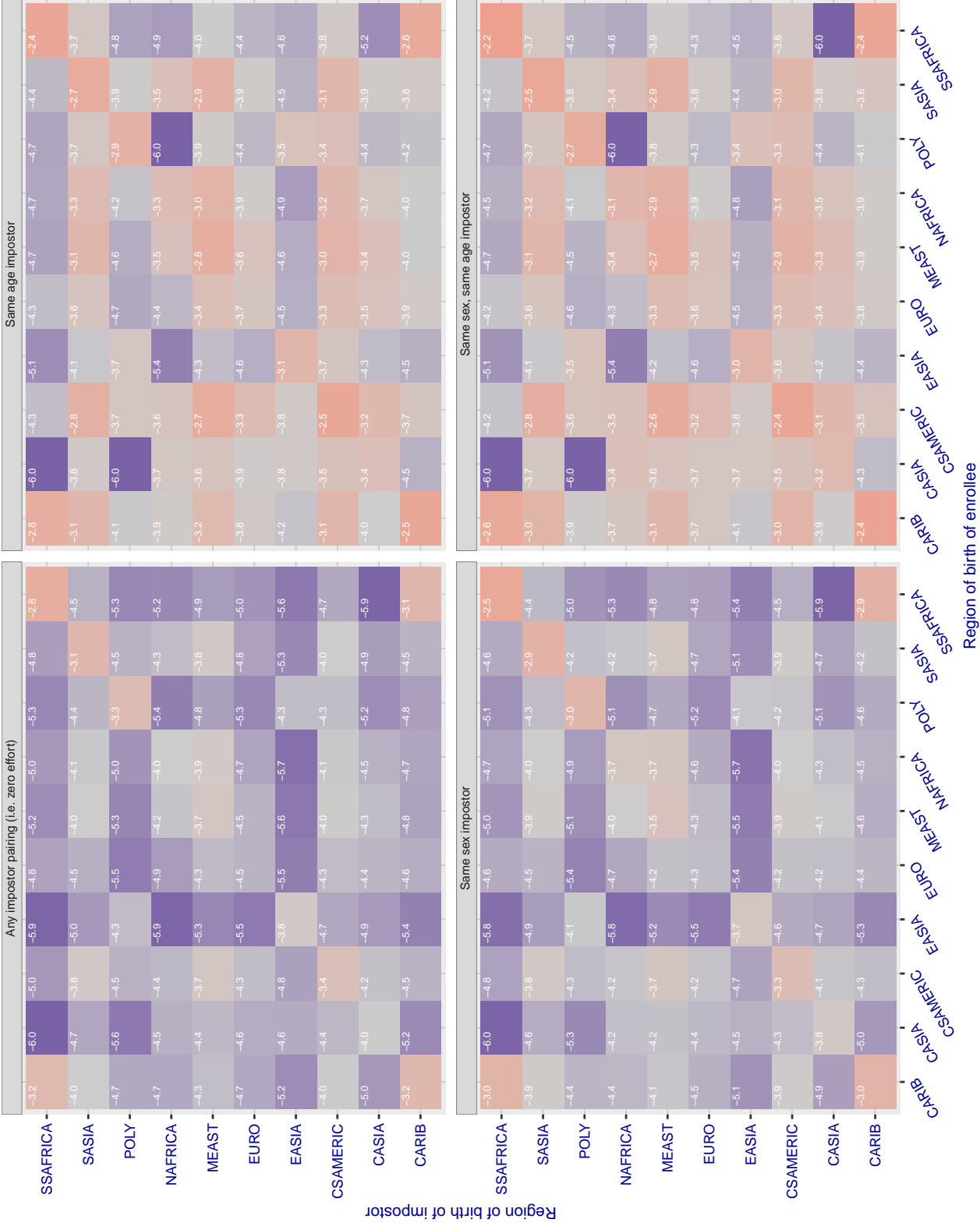
**Cross region FMR at threshold T = 0.701 for algorithm lookman\_002, giving FMR(T) = 0.0001 globally.**

Figure 222: For algorithm lookman-002 operating on visa images, the heatmap shows false match rates observed over impostor comparisons of faces from different individuals who were born in the given region pair. False matches are counted against a recognition threshold fixed globally to give the target FMR in the plot title, computed over all on the order of  $10^{10}$  impostor comparisons. If text appears in each box it give the same quantity as that coded by the color. Grey indicates FMR is at the intended FMR target level. Light red colors present a security vulnerability to, for example, a passport gate. Each +1 increase in  $\log_{10} FMR$  corresponds to a factor of 10 increase in FMR. The matrix is not quite symmetric because images in the enrollment and verification sets are different.

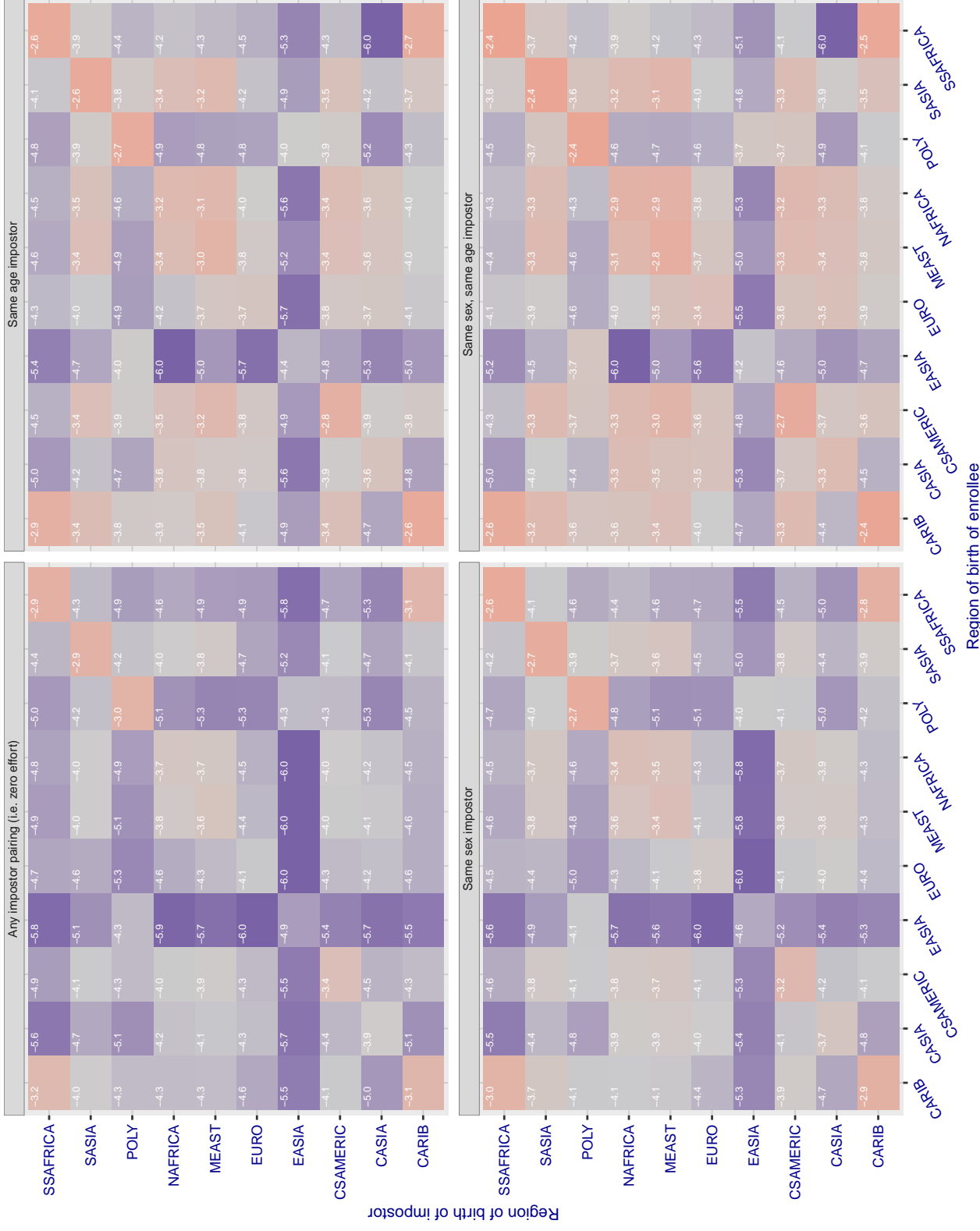
**Cross region FMR at threshold T = 0.733 for algorithm lookman\_004, giving FMR(T) = 0.0001 globally.**

Figure 223: For algorithm lookman-004 operating on visa images, the heatmap shows false match rates observed over impostor comparisons of faces from different individuals who were born in the given region pair. False matches are counted against a recognition threshold fixed globally to give the target FMR in the plot title, computed over all on the order of  $10^{10}$  impostor comparisons. If text appears in each box it give the same quantity as that coded by the color. Grey indicates FMR is at the intended FMR target level. Light red colors present a security vulnerability to, for example, a passport gate. Each +1 increase in  $\log_{10} FMR$  corresponds to a factor of 10 increase in FMR. The matrix is not quite symmetric because images in the enrollment and verification sets are different.

### Cross region FMR at threshold T = 74.511 for algorithm megvii\_001, giving FMR(T) = 0.0001 globally.

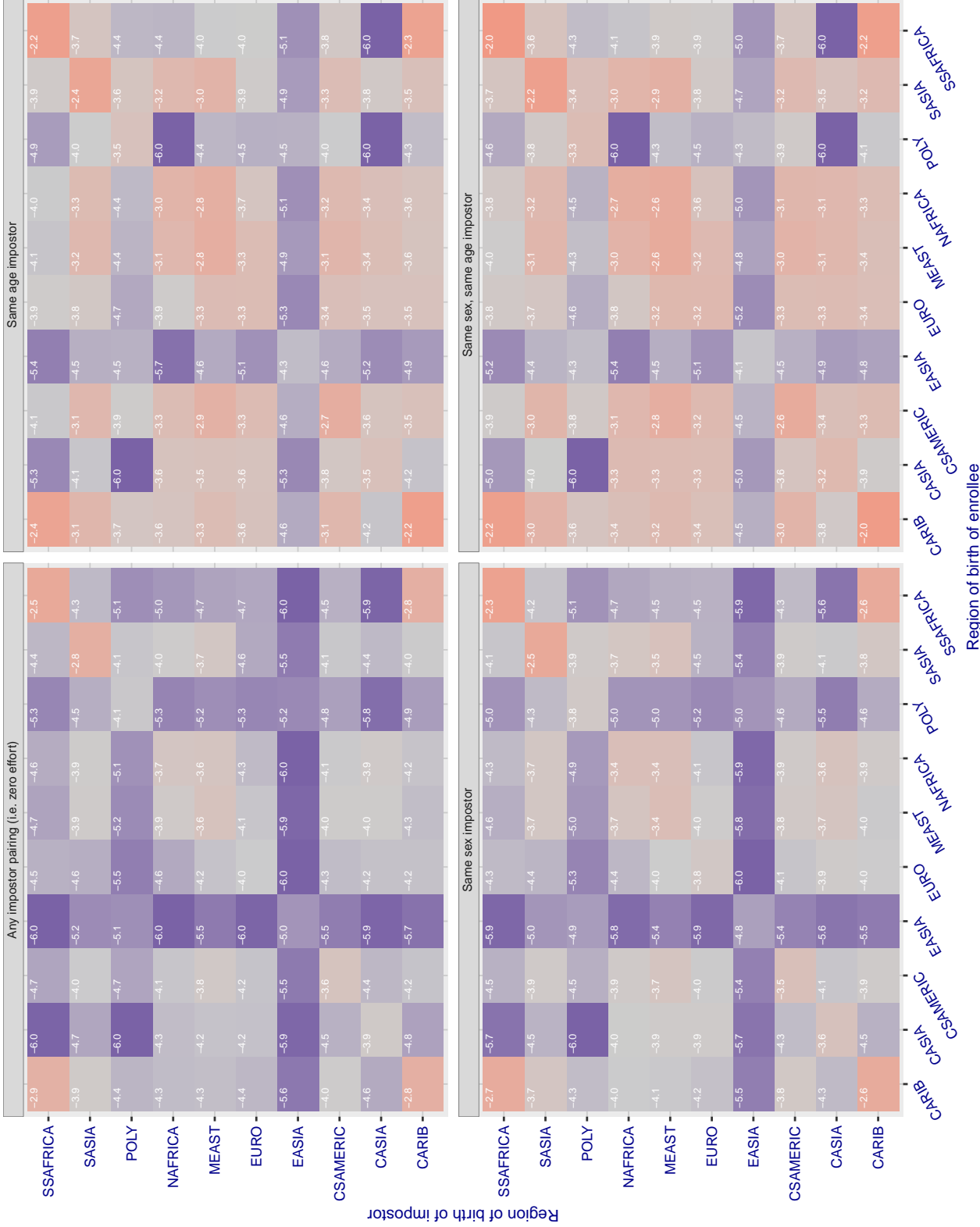


Figure 224: For algorithm megvii-001 operating on visa images, the heatmap shows false match rates observed over impostor comparisons of faces from different individuals who were born in the given region pair. False matches are counted against a recognition threshold fixed globally to give the target FMR in the plot title, computed over all on the order of  $10^{10}$  impostor comparisons. If text appears in each box it give the same quantity as that coded by the color. Grey indicates FMR is at the intended FMR target level. Light red colors present a security vulnerability to, for example, a passport gate. Each +1 increase in  $\log_{10} \text{FMR}$  corresponds to a factor of 10 increase in FMR. The matrix is not quite symmetric because images in the enrollment and verification sets are different.

### Cross region FMR at threshold T = 66.384 for algorithm megvii\_002, giving FMR(T) = 0.0001 globally.

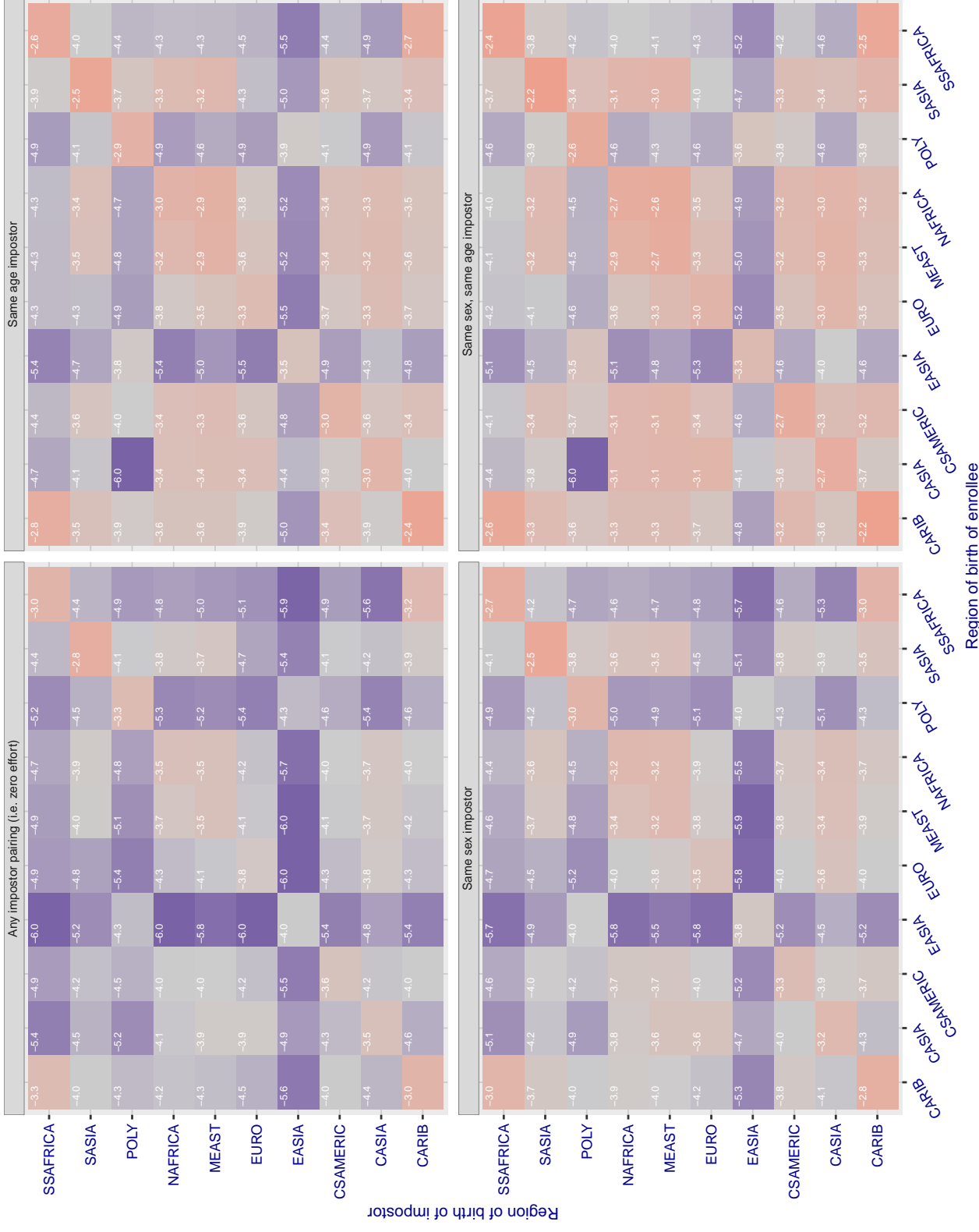


Figure 225: For algorithm megvii-002 operating on visa images, the heatmap shows false match rates observed over impostor comparisons of faces from different individuals who were born in the given region pair. False matches are counted against a recognition threshold fixed globally to give the target FMR in the plot title, computed over all on the order of  $10^{10}$  impostor comparisons. If text appears in each box it give the same quantity as that coded by the color. Grey indicates FMR is at the intended FMR target level. Light red colors present a security vulnerability to, for example, a passport gate. Each +1 increase in  $\log_{10} FMR$  corresponds to a factor of 10 increase in FMR. The matrix is not quite symmetric because images in the enrollment and verification sets are different.

### Cross region FMR at threshold T = 0.425 for algorithm meiya\_001, giving FMR(T) = 0.0001 globally.

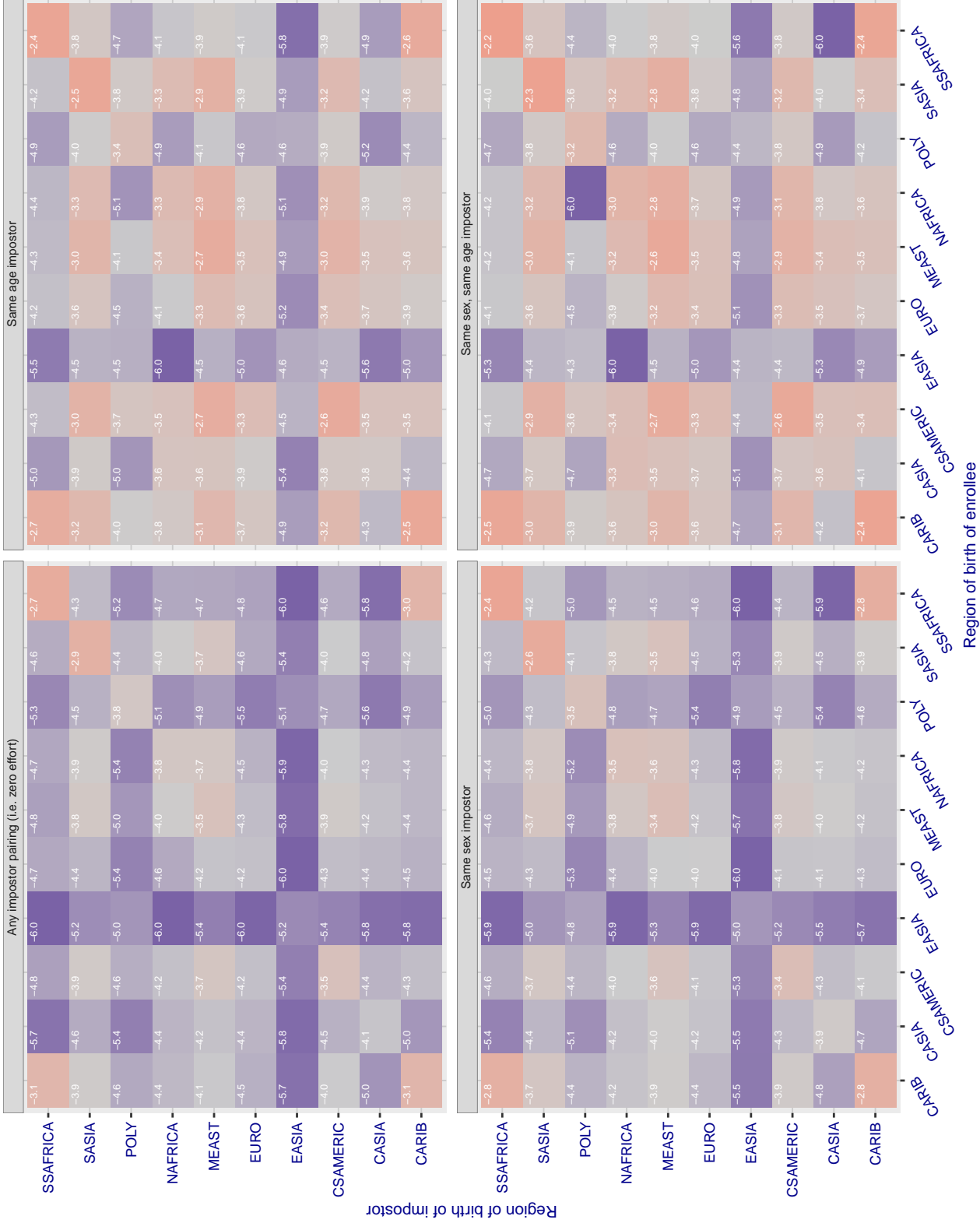


Figure 226: For algorithm meiya-001 operating on visa images, the heatmap shows false match rates observed over impostor comparisons of faces from different individuals who were born in the given region pair. False matches are counted against a recognition threshold fixed globally to give the target FMR in the plot title, computed over all on the order of  $10^{10}$  impostor comparisons. If text appears in each box it give the same quantity as that coded by the color. Grey indicates FMR is at the intended FMR target level. Light red colors present a security vulnerability to, for example, a passport gate. Each +1 increase in  $\log_{10} \text{FMR}$  corresponds to a factor of 10 increase in FMR. The matrix is not quite symmetric because images in the enrollment and verification sets are different.

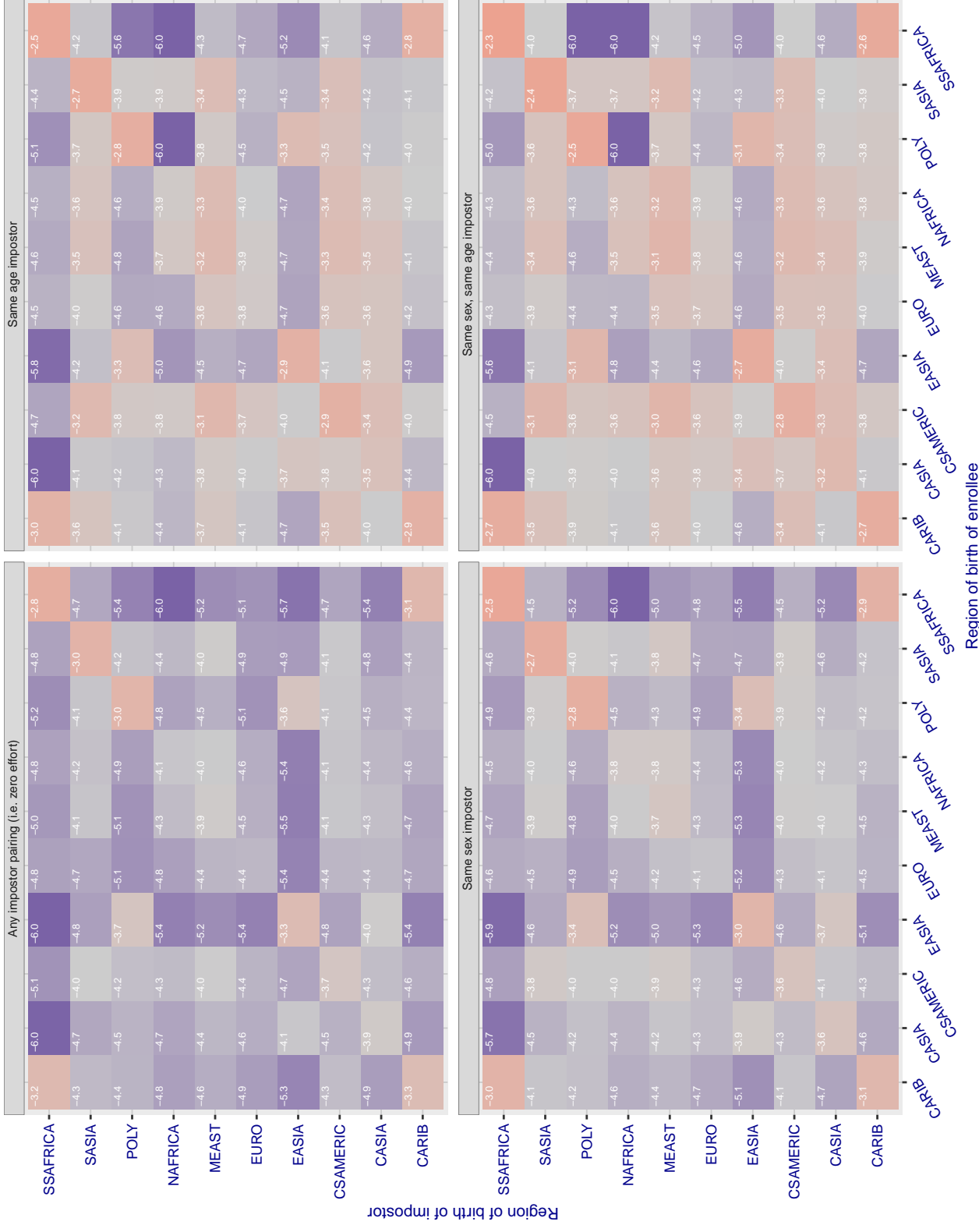
**Cross region FMR at threshold T = 0.668 for algorithm microfocus\_001, giving FMR(T) = 0.0001 globally.**

Figure 227: For algorithm microfocus-001 operating on visa images, the heatmap shows false match rates observed over impostor comparisons of faces from different individuals who were born in the given region pair. False matches are counted against a recognition threshold fixed globally to give the target FMR in the plot title, computed over all on the order of  $10^{10}$  impostor comparisons. If text appears in each box it give the same quantity as that coded by the color. Grey indicates FMR is at the intended FMR target level. Light red colors present a security vulnerability to, for example, a passport gate. Each +1 increase in  $\log_{10} FMR$  corresponds to a factor of 10 increase in FMR. The matrix is not quite symmetric because images in the enrollment and verification sets are different.

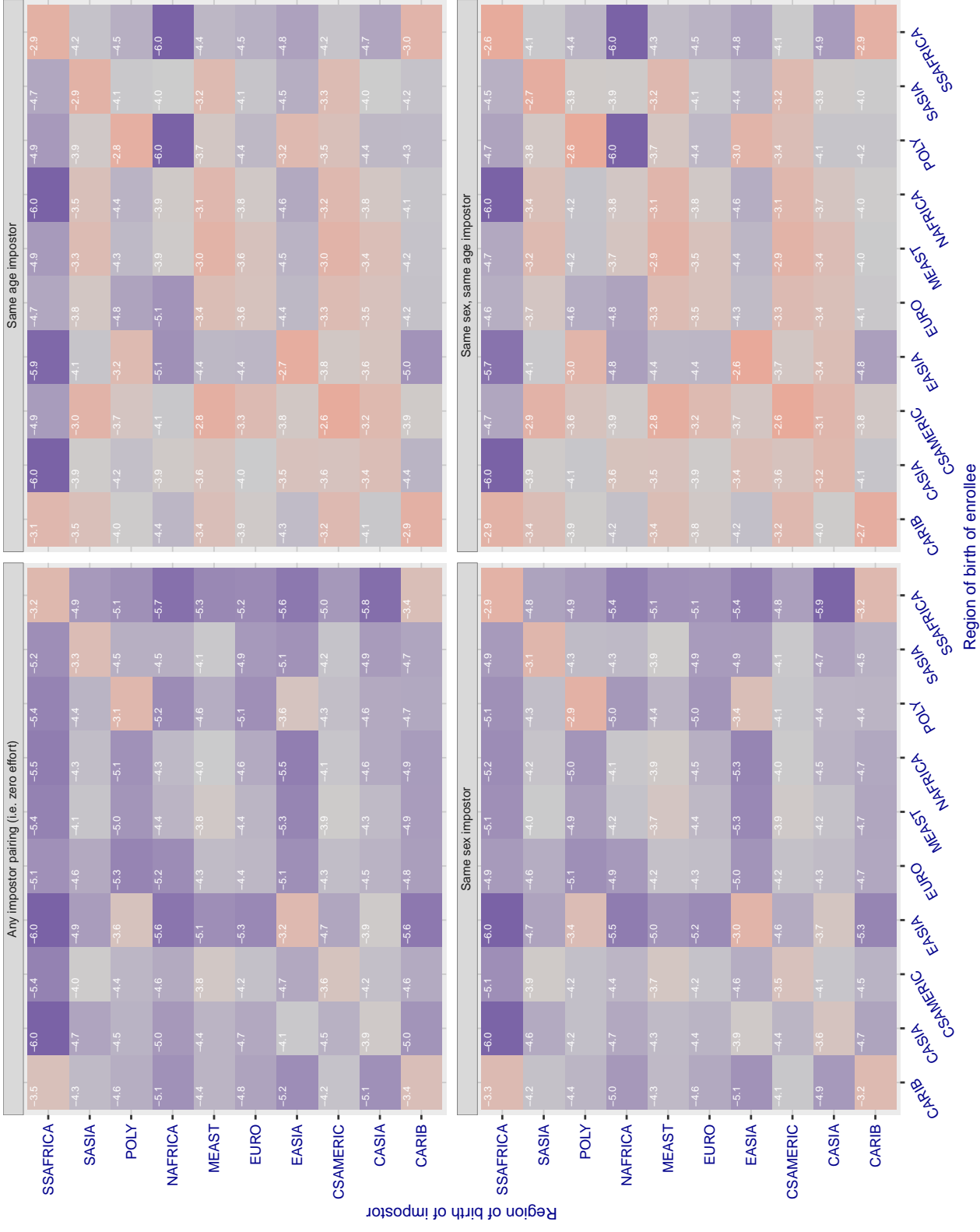
**Cross region FMR at threshold T = 0.602 for algorithm microfocus\_002, giving FMR(T) = 0.0001 globally.**

Figure 228: For algorithm microfocus-002 operating on visa images, the heatmap shows false match rates observed over impostor comparisons of faces from different individuals who were born in the given region pair. False matches are counted against a recognition threshold fixed globally to give the target FMR in the plot title, computed over all on the order of  $10^{10}$  impostor comparisons. If text appears in each box it give the same quantity as that coded by the color. Grey indicates FMR is at the intended FMR target level. Light red colors present a security vulnerability to, for example, a passport gate. Each +1 increase in  $\log_{10} FMR$  corresponds to a factor of 10 increase in FMR. The matrix is not quite symmetric because images in the enrollment and verification sets are different.

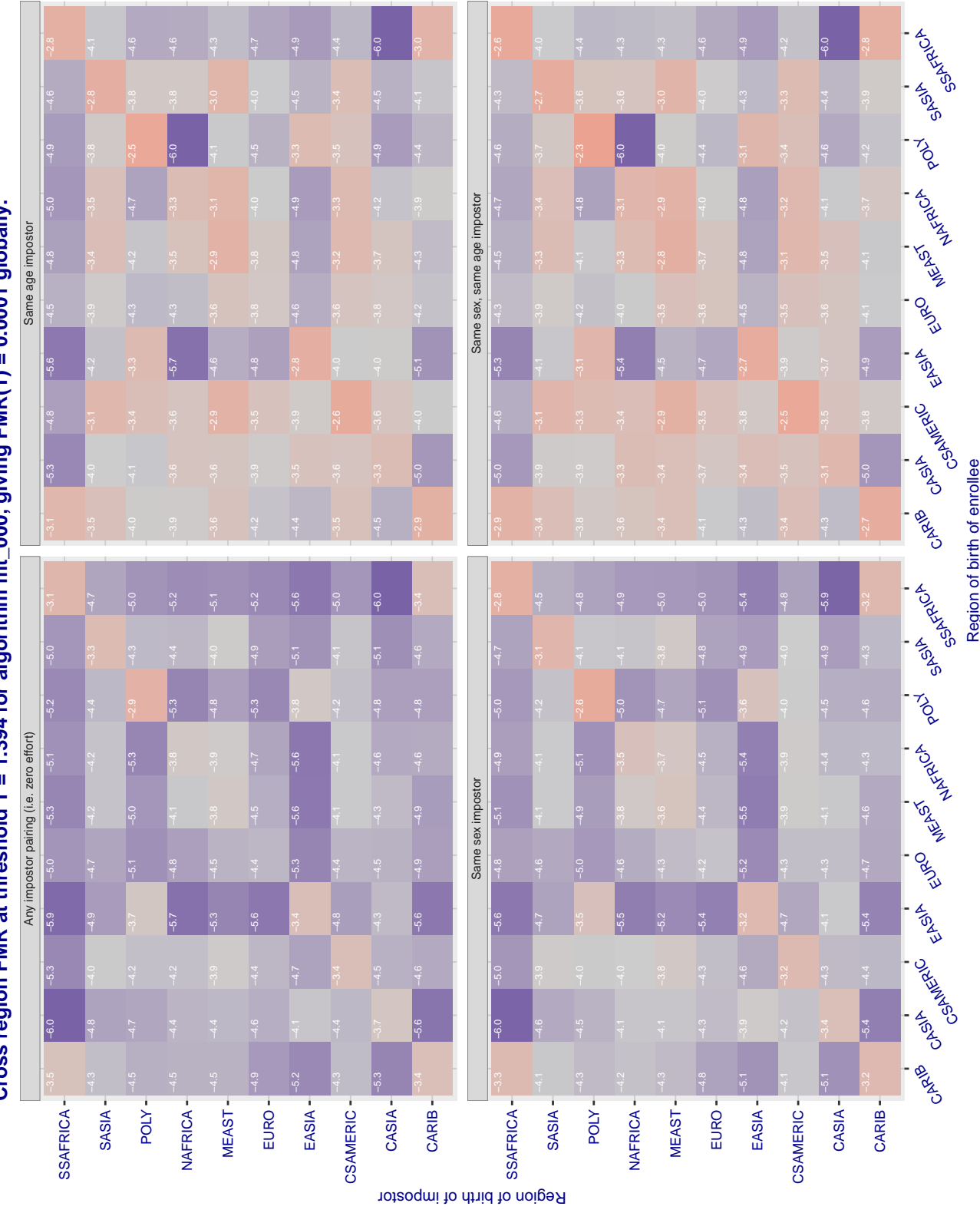


Figure 229: For algorithm mt-000 operating on visa images, the heatmap shows false match rates observed over impostor comparisons of faces from different individuals who were born in the given region pair. False matches are counted against a recognition threshold fixed globally to give the target FMR in the plot title, computed over all on the order of  $10^{10}$  impostor comparisons. If text appears in each box it give the same quantity as that coded by the color. Grey indicates FMR is at the intended FMR target level. Light red colors present a security vulnerability to, for example, a passport gate. Each +1 increase in  $\log_{10} \text{FMR}$  corresponds to a factor of 10 increase in FMR. The matrix is not quite symmetric because images in the enrollment and verification sets are different.

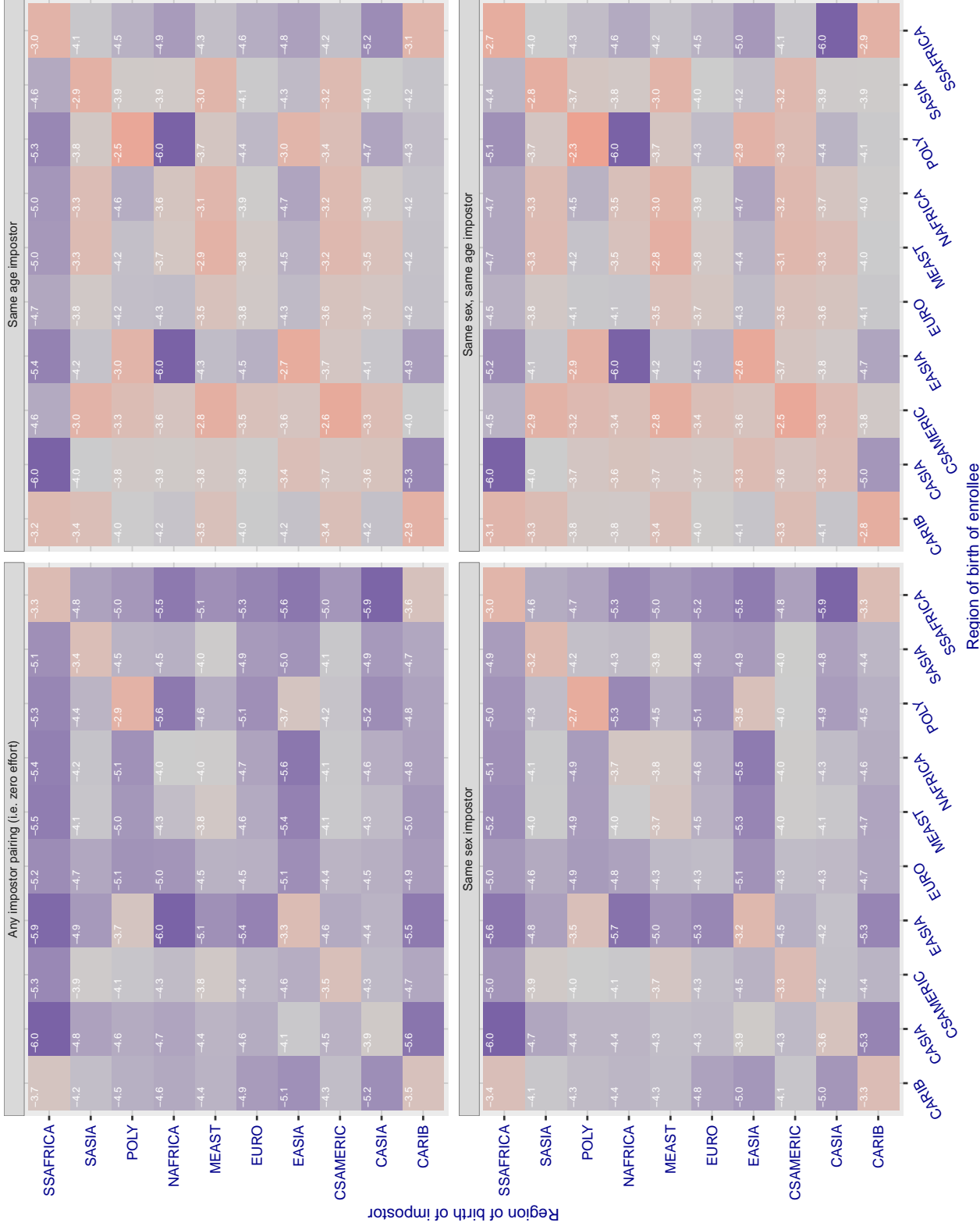
**Cross region FMR at threshold T = 46.101 for algorithm neurotechnology\_005, giving  $FMR(T) = 0.0001$  globally.**

Figure 230: For algorithm neurotechnology-005 operating on visa images, the heatmap shows false match rates observed over impostor comparisons of faces from different individuals who were born in the given region pair. False matches are counted against a recognition threshold fixed globally to give the target FMR in the plot title, computed over all on the order of  $10^{10}$  impostor comparisons. If text appears in each box it give the same quantity as that coded by the color. Grey indicates FMR is at the intended FMR target level. Light red colors present a security vulnerability to, for example, a passport gate. Each +1 increase in  $\log 10 \text{ FMR}$  corresponds to a factor of 10 increase in FMR. The matrix is not quite symmetric because images in the enrollment and verification sets are different.

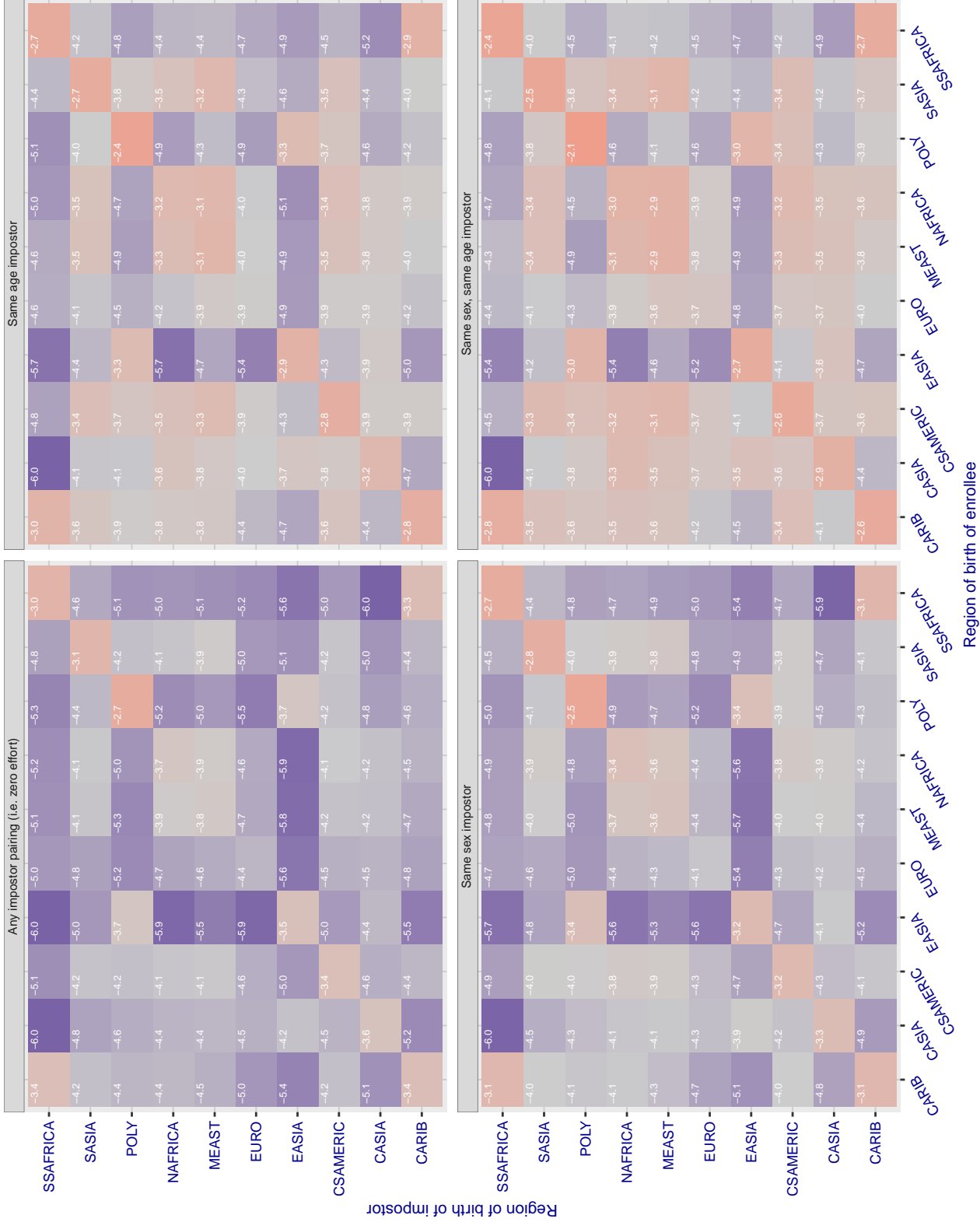
**Cross region FMR at threshold T = 2044.000 for algorithm neurotechnology\_006, giving FMR(T) = 0.0001 globally.**

Figure 231: For algorithm neurotechnology-006 operating on visa images, the heatmap shows false match rates observed over impostor comparisons of faces from different individuals who were born in the given region pair. False matches are counted against a recognition threshold fixed globally to give the target FMR in the plot title, computed over all on the order of  $10^{10}$  impostor comparisons. If text appears in each box it give the same quantity as that coded by the color. Grey indicates FMR is at the intended FMR target level. Light red colors present a security vulnerability to, for example, a passport gate. Each +1 increase in  $\log_{10} FMR$  corresponds to a factor of 10 increase in FMR. The matrix is not quite symmetric because images in the enrollment and verification sets are different.

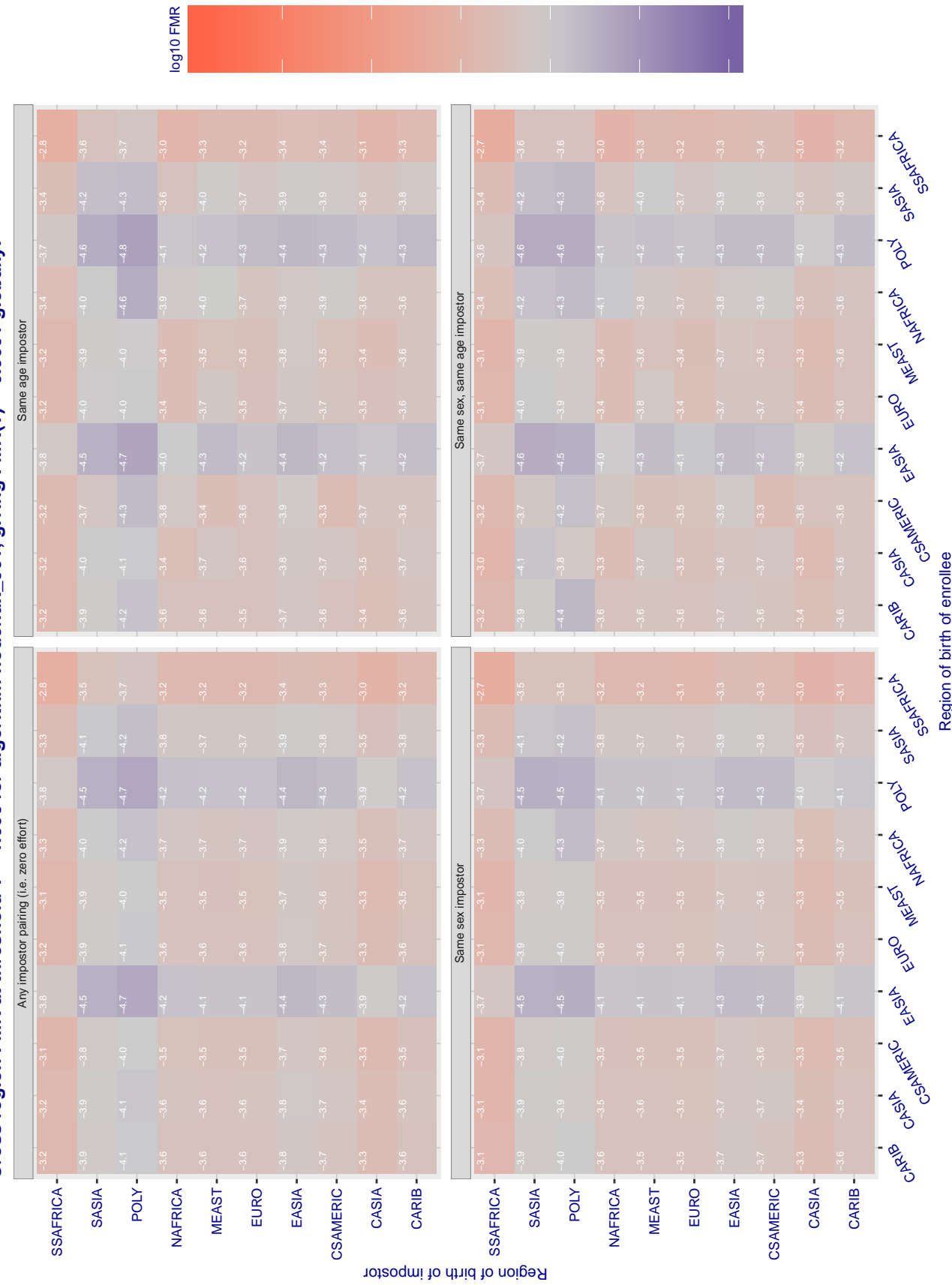


Figure 232: For algorithm nodeflux-001 operating on visa images, the heatmap shows false match rates observed over impostor comparisons of faces from different individuals who were born in the given region pair. False matches are counted against a recognition threshold fixed globally to give the target FMR in the plot title, computed over all on the order of  $10^{10}$  impostor comparisons. If text appears in each box it give the same quantity as that coded by the color. Grey indicates FMR is at the intended FMR target level. Light red colors present a security vulnerability to, for example, a passport gate. Each +1 increase in  $\log_{10}$  FMR corresponds to a factor of 10 increase in FMR. The matrix is not quite symmetric because images in the enrollment and verification sets are different.

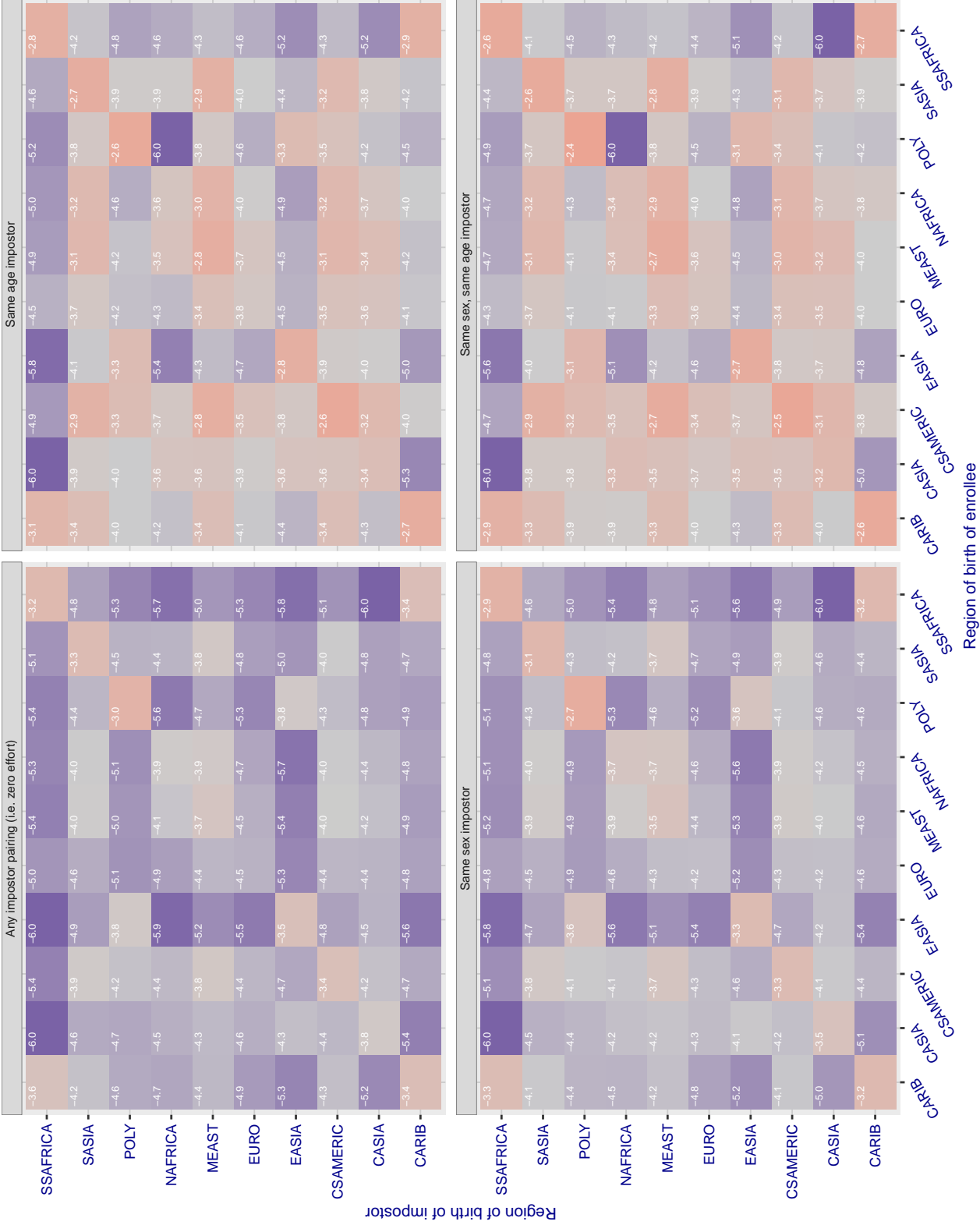
**Cross region FMR at threshold T = 0.455 for algorithm nodeflux\_002, giving FMR(T) = 0.0001 globally.**

Figure 233: For algorithm nodeflux-002 operating on visa images, the heatmap shows false match rates observed over impostor comparisons of faces from different individuals who were born in the given region pair. False matches are counted against a recognition threshold fixed globally to give the target FMR in the plot title, computed over all on the order of  $10^{10}$  impostor comparisons. If text appears in each box it give the same quantity as that coded by the color. Grey indicates FMR is at the intended FMR target level. Light red colors present a security vulnerability to, for example, a passport gate. Each +1 increase in  $\log_{10} FMR$  corresponds to a factor of 10 increase in FMR. The matrix is not quite symmetric because images in the enrollment and verification sets are different.

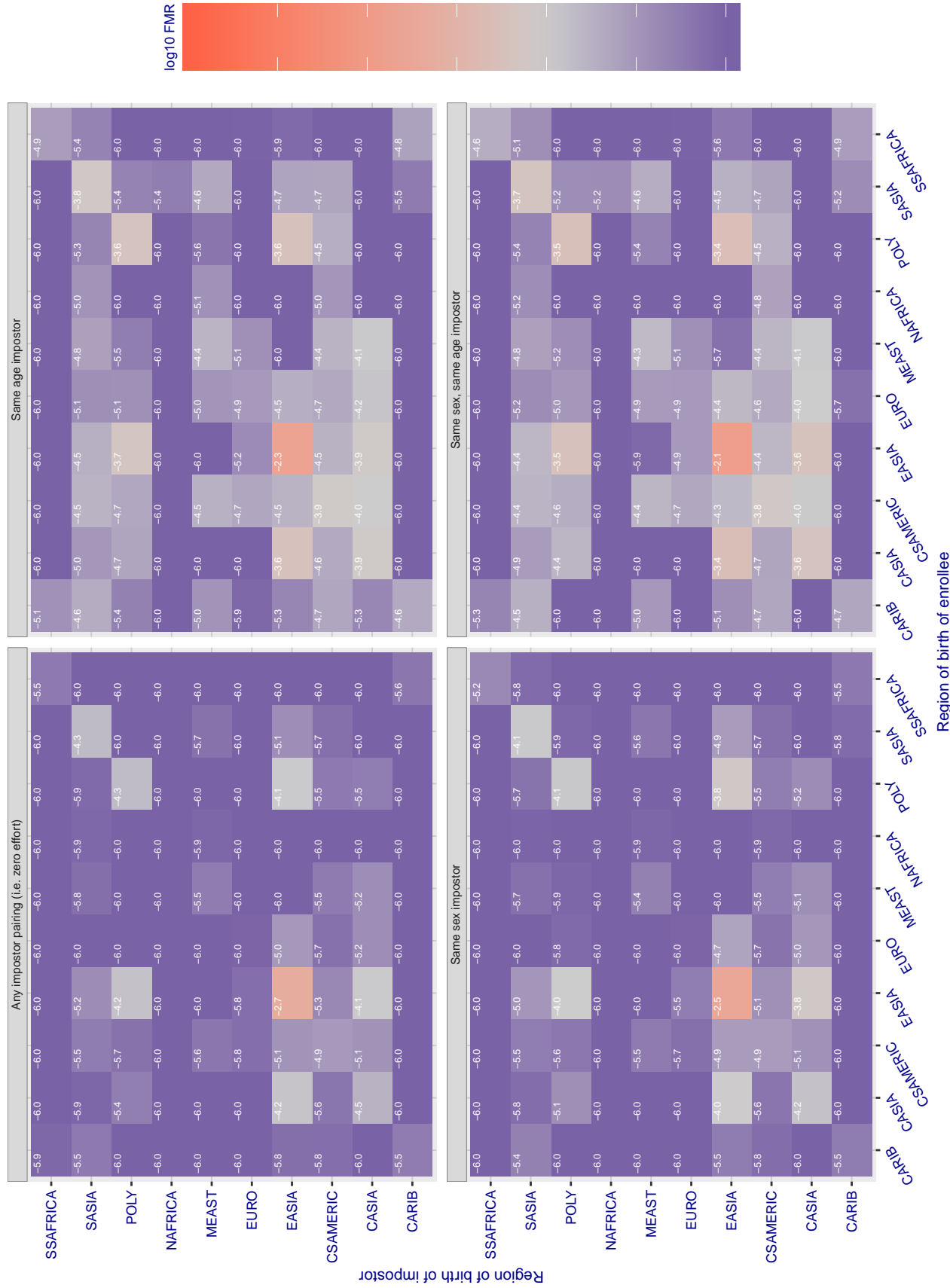
**Cross region FMR at threshold T = 16846383821648700779774369791310334462380752812000954299625965117711518105060865483'**

Figure 234: For algorithm notiontag-000 operating on visa images, the heatmap shows false match rates observed over impostor comparisons of faces from different individuals who were born in the given region pair. False matches are counted against a recognition threshold fixed globally to give the target FMR in the plot title, computed over all on the order of  $10^{10}$  impostor comparisons. If text appears in each box it give the same quantity as that coded by the color. Grey indicates FMR is at the intended FMR target level. Light red colors present a security vulnerability to, for example, a passport gate. Each +1 increase in  $\log_{10} FMR$  corresponds to a factor of 10 increase in FMR. The matrix is not quite symmetric because images in the enrollment and verification sets are different.

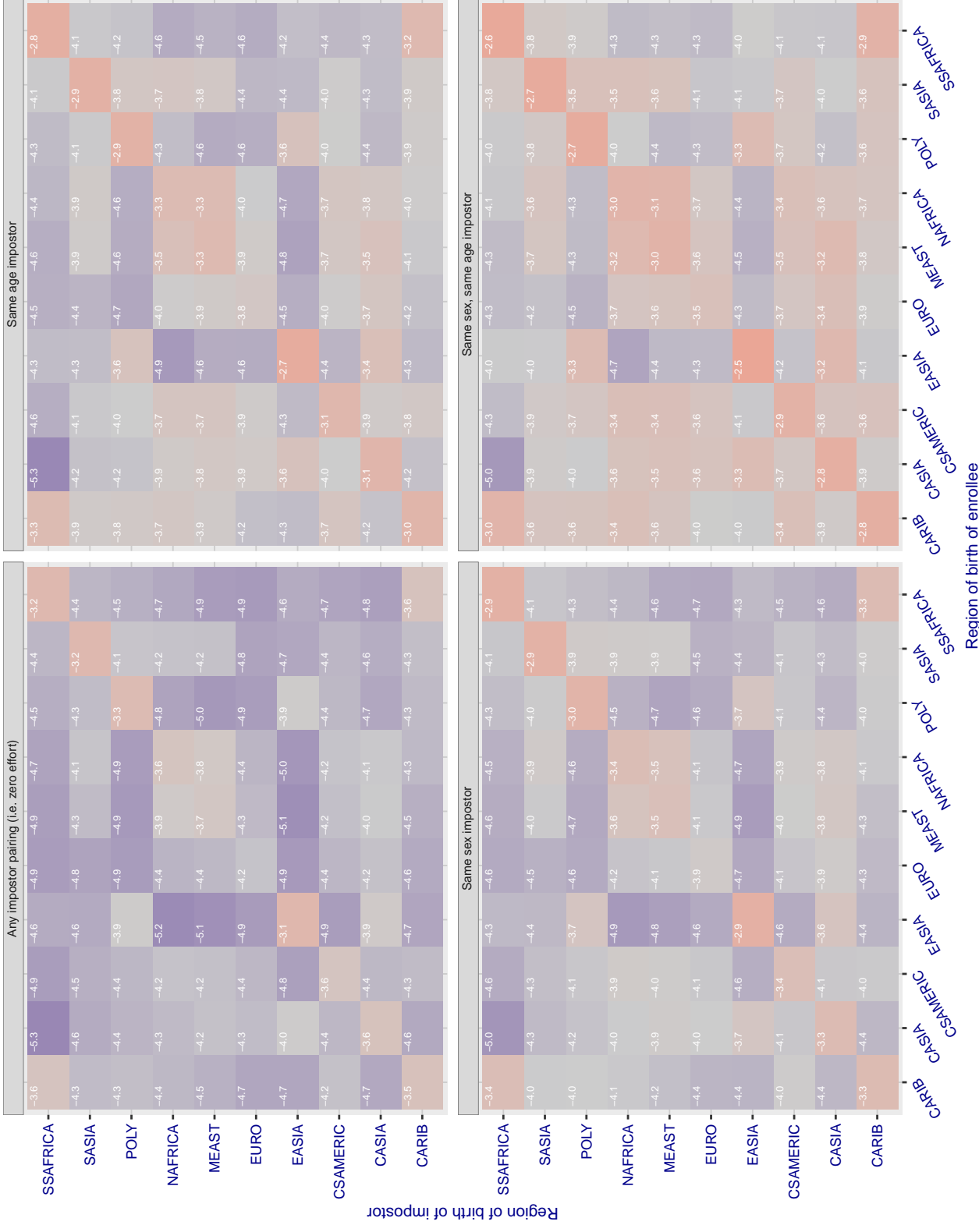
**Cross region FMR at threshold T = 1.997 for algorithm ntechlab\_006, giving FMR(T) = 0.0001 globally.**

Figure 235: For algorithm ntechlab-006 operating on visa images, the heatmap shows false match rates observed over impostor comparisons of faces from different individuals who were born in the given region pair. False matches are counted against a recognition threshold fixed globally to give the target FMR in the plot title, computed over all on the order of  $10^{10}$  impostor comparisons. If text appears in each box it give the same quantity as that coded by the color. Grey indicates FMR is at the intended FMR target level. Light red colors present a security vulnerability to, for example, a passport gate. Each +1 increase in  $\log_{10} FMR$  corresponds to a factor of 10 increase in FMR. The matrix is not quite symmetric because images in the enrollment and verification sets are different.

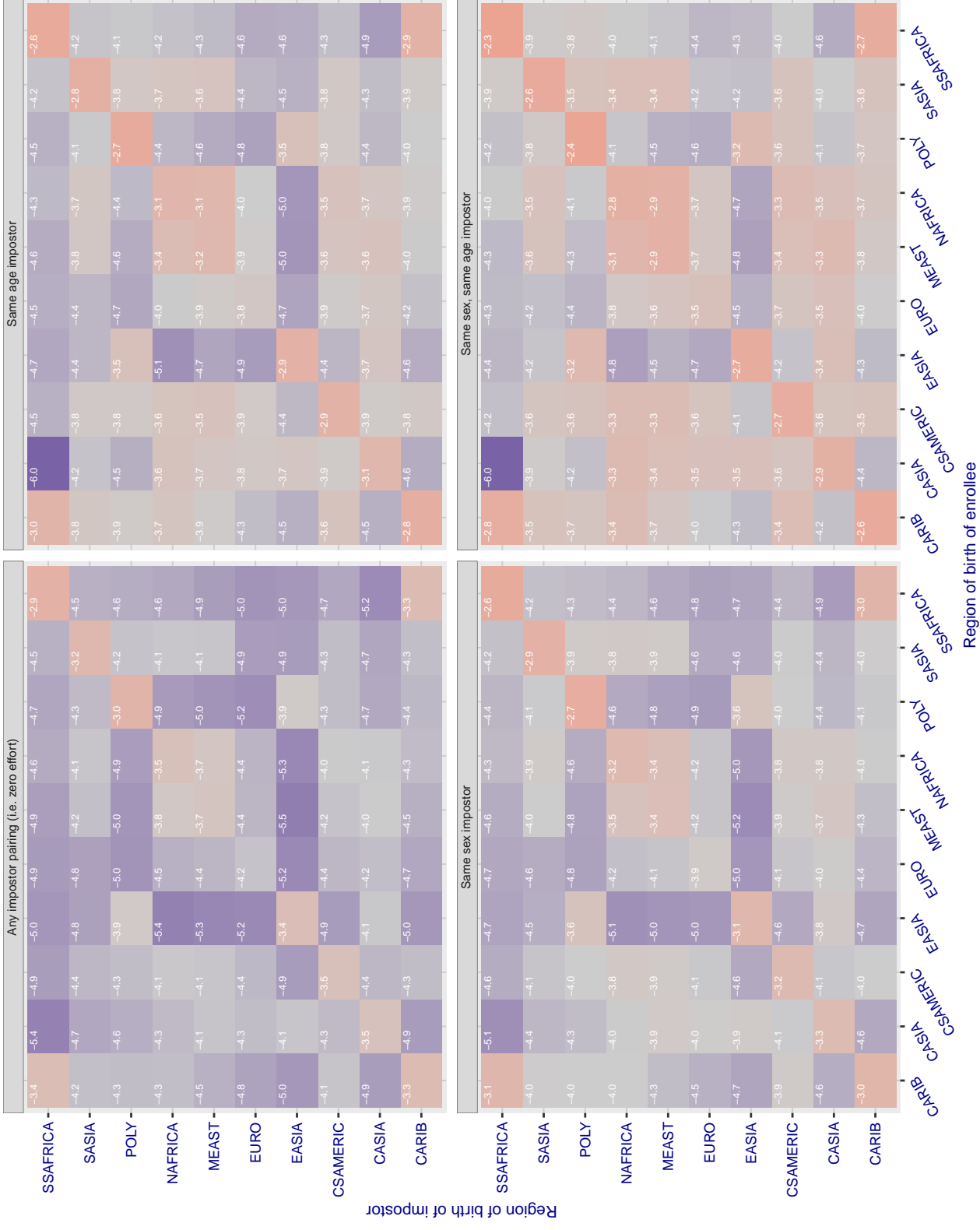
**Cross region FMR at threshold T = 1.416 for algorithm ntechlab\_007, giving FMR(T) = 0.0001 globally.**

Figure 236: For algorithm ntechlab-007 operating on visa images, the heatmap shows false match rates observed over impostor comparisons of faces from different individuals who were born in the given region pair. False matches are counted against a recognition threshold fixed globally to give the target FMR in the plot title, computed over all on the order of  $10^{10}$  impostor comparisons. If text appears in each box it give the same quantity as that coded by the color. Grey indicates FMR is at the intended FMR target level. Light red colors present a security vulnerability to, for example, a passport gate. Each +1 increase in  $\log_{10} \text{FMR}$  corresponds to a factor of 10 increase in FMR. The matrix is not quite symmetric because images in the enrollment and verification sets are different.

### Cross region FMR at threshold T = 0.428 for algorithm pixelall\_002, giving $\text{FMR}(\text{T}) = 0.0001$ globally.

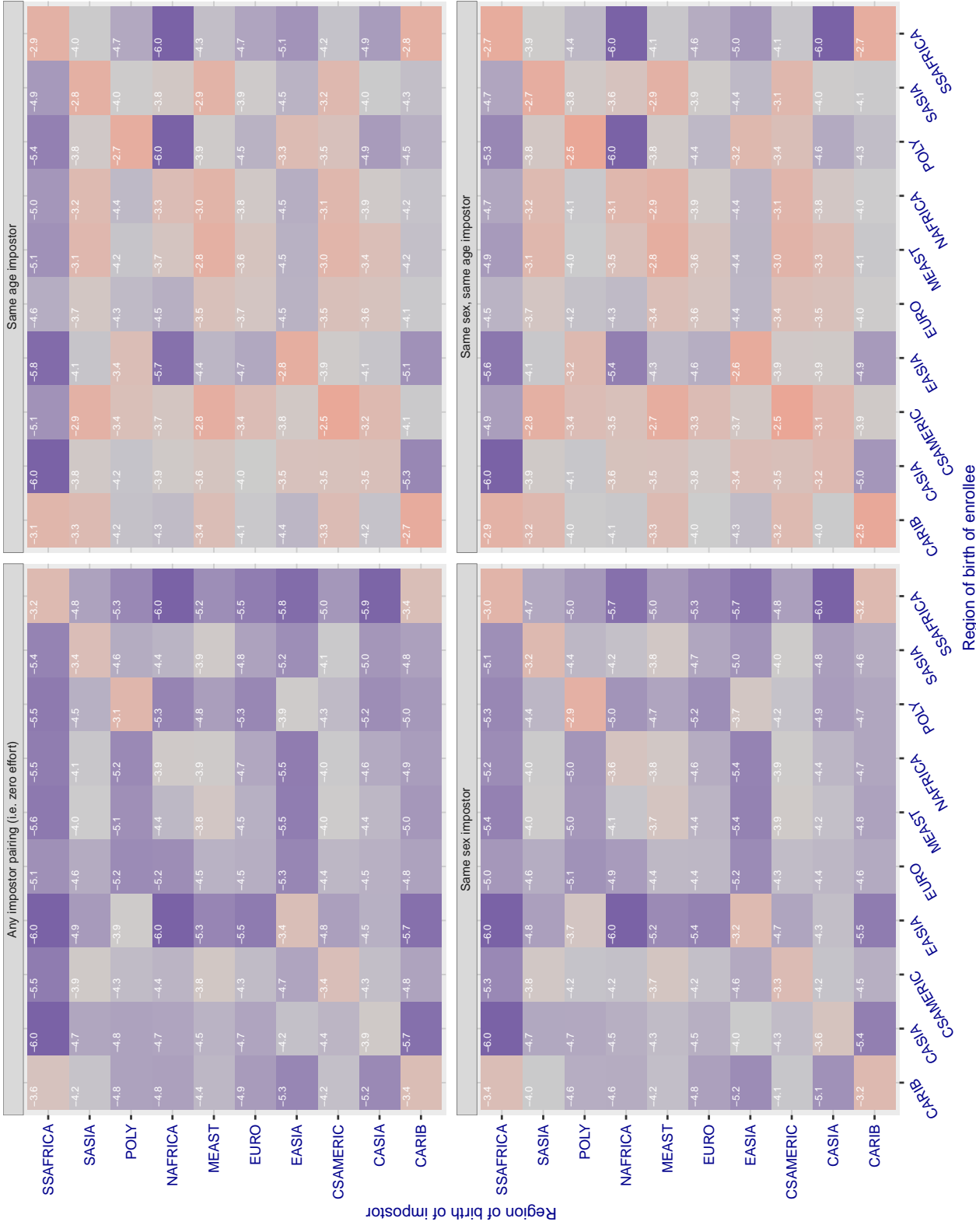


Figure 237: For algorithm pixelall-002 operating on visa images, the heatmap shows false match rates observed over impostor comparisons of faces from different individuals who were born in the given region pair. False matches are counted against a recognition threshold fixed globally to give the target FMR in the plot title, computed over all on the order of  $10^{10}$  impostor comparisons. If text appears in each box it give the same quantity as that coded by the color. Grey indicates FMR is at the intended FMR target level. Light red colors present a security vulnerability to, for example, a passport gate. Each +1 increase in  $\log_{10} \text{FMR}$  corresponds to a factor of 10 increase in FMR. The matrix is not quite symmetric because images in the enrollment and verification sets are different.

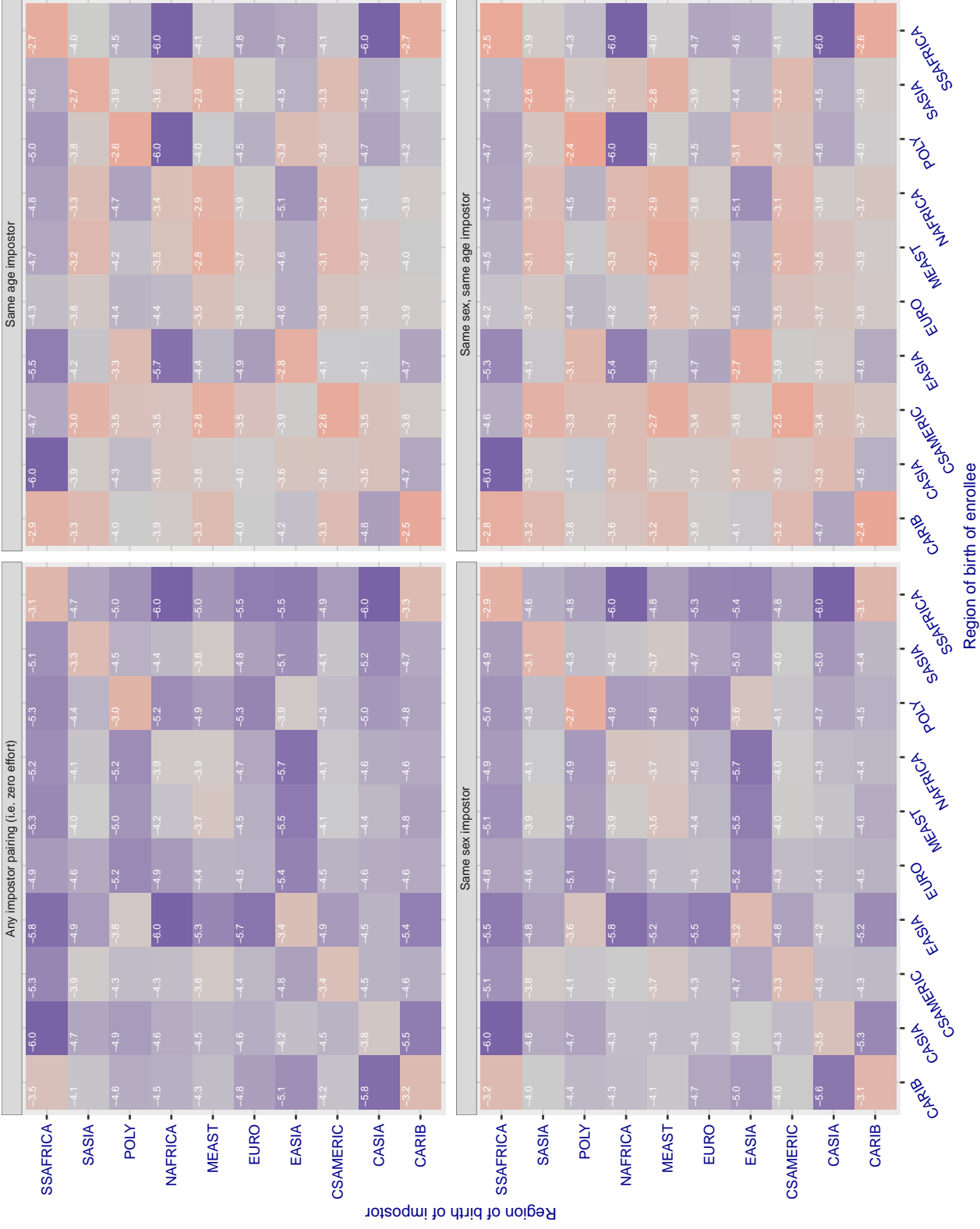
**Cross region FMR at threshold T = 0.353 for algorithm psl\_002, giving FMR(T) = 0.00001 globally.**

Figure 238: For algorithm psl-002 operating on visa images, the heatmap shows false match rates observed over impostor comparisons of faces from different individuals who were born in the given region pair. False matches are counted against a recognition threshold fixed globally to give the target FMR in the plot title, computed over all on the order of  $10^{10}$  impostor comparisons. If text appears in each box it give the same quantity as that coded by the color. Grey indicates FMR is at the intended FMR target level. Light red colors present a security vulnerability to, for example, a passport gate. Each +1 increase in  $\log_{10}$  FMR corresponds to a factor of 10 increase in FMR. The matrix is not quite symmetric because images in the enrollment and verification sets are different.

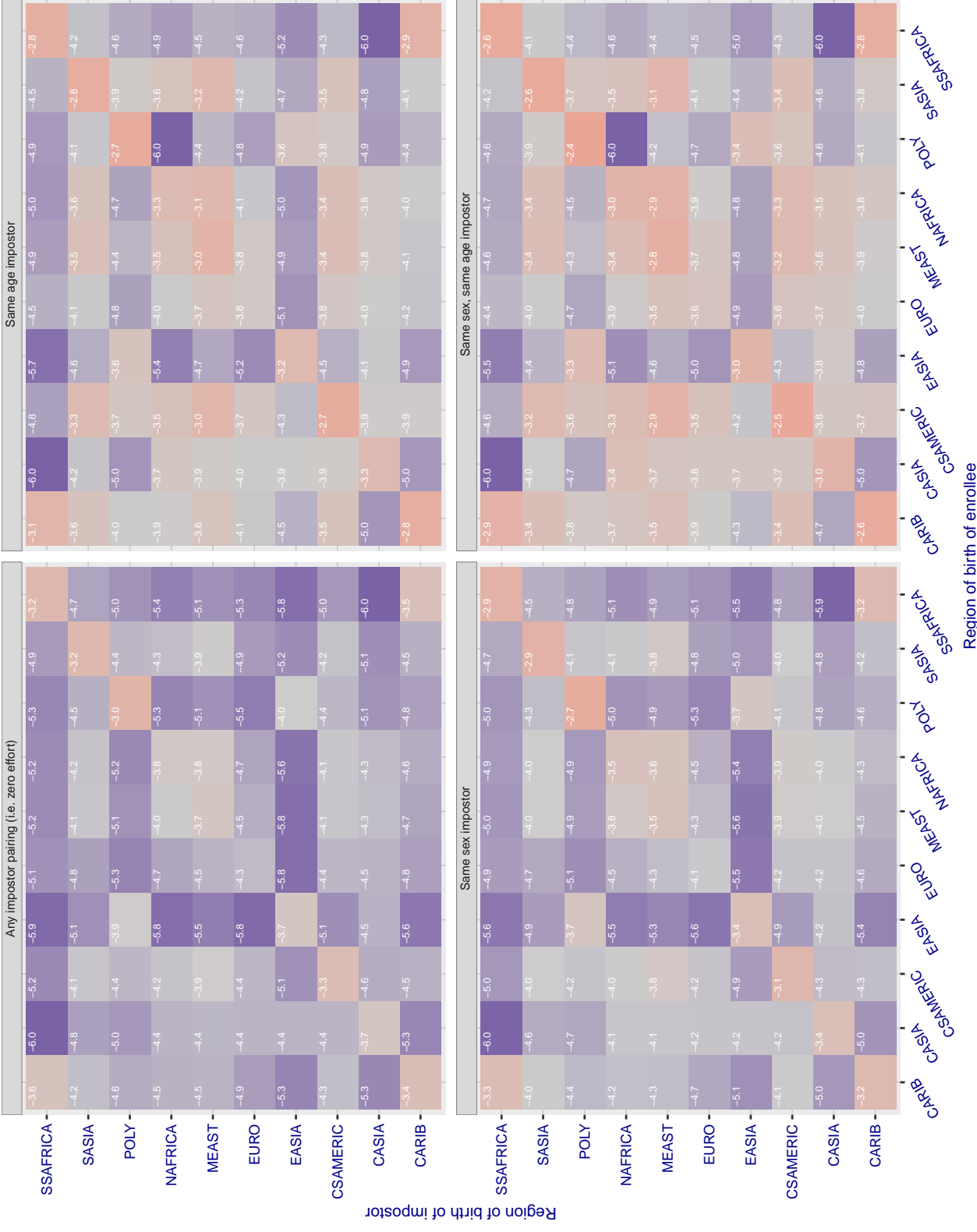
**Cross region FMR at threshold T = 0.668 for algorithm psl\_003, giving FMR(T) = 0.0001 globally.**

Figure 239: For algorithm psl-003 operating on visa images, the heatmap shows false match rates observed over impostor comparisons of faces from different individuals who were born in the given region pair. False matches are counted against a recognition threshold fixed globally to give the target FMR in the plot title, computed over all on the order of  $10^{10}$  impostor comparisons. If text appears in each box it give the same quantity as that coded by the color. Grey indicates FMR is at the intended FMR target level. Light red colors present a security vulnerability to, for example, a passport gate. Each +1 increase in  $\log 10$  FMR corresponds to a factor of 10 increase in FMR. The matrix is not quite symmetric because images in the enrollment and verification sets are different.

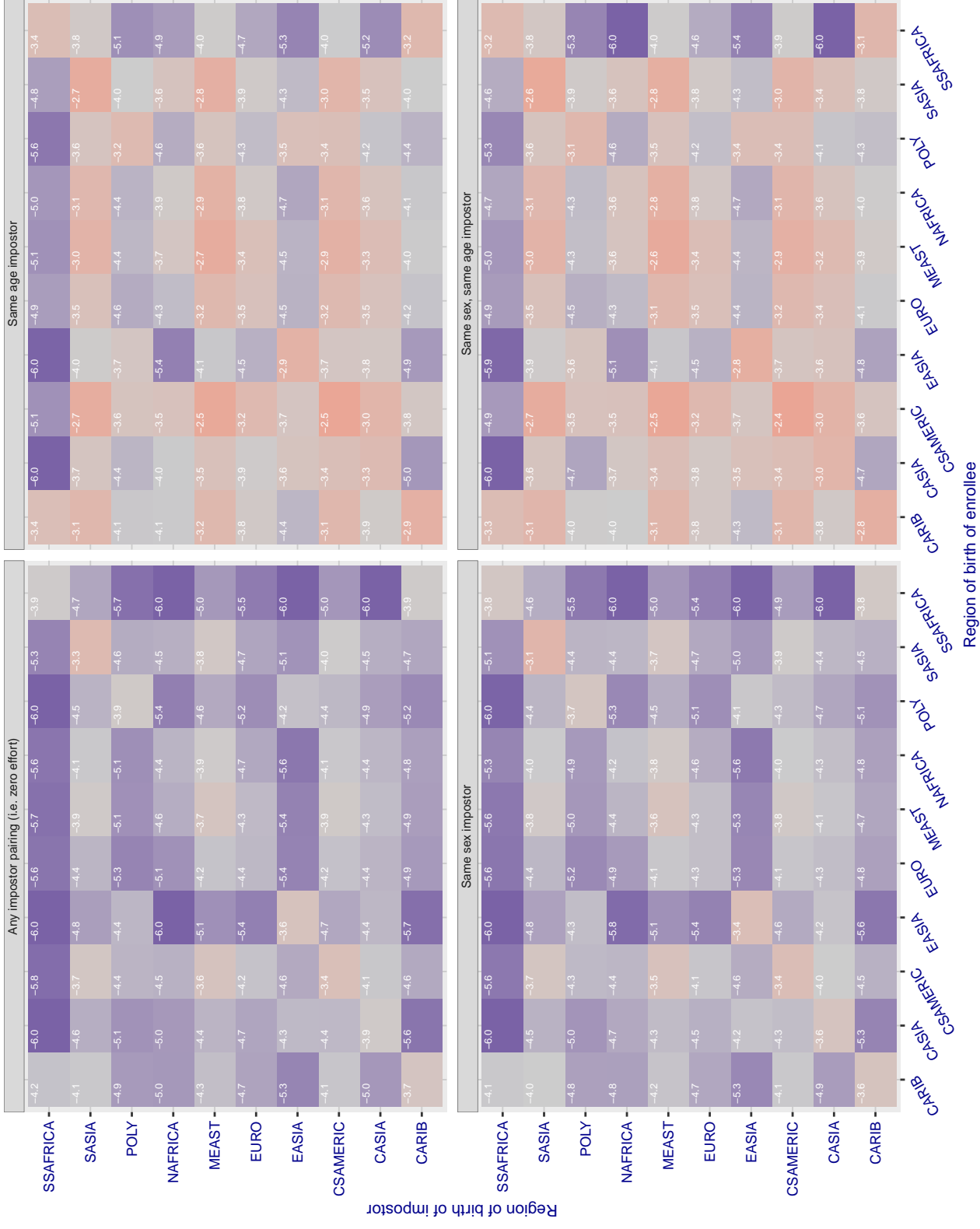
**Cross region FMR at threshold T = 0.779 for algorithm rankone\_006, giving FMR(T) = 0.0001 globally.**

Figure 240: For algorithm rankone-006 operating on visa images, the heatmap shows false match rates observed over impostor comparisons of faces from different individuals who were born in the given region pair. False matches are counted against a recognition threshold fixed globally to give the target FMR in the plot title, computed over all on the order of  $10^{10}$  impostor comparisons. If text appears in each box it give the same quantity as that coded by the color. Grey indicates FMR is at the intended FMR target level. Light red colors present a security vulnerability to, for example, a passport gate. Each +1 increase in  $\log_{10} FMR$  corresponds to a factor of 10 increase in FMR. The matrix is not quite symmetric because images in the enrollment and verification sets are different.

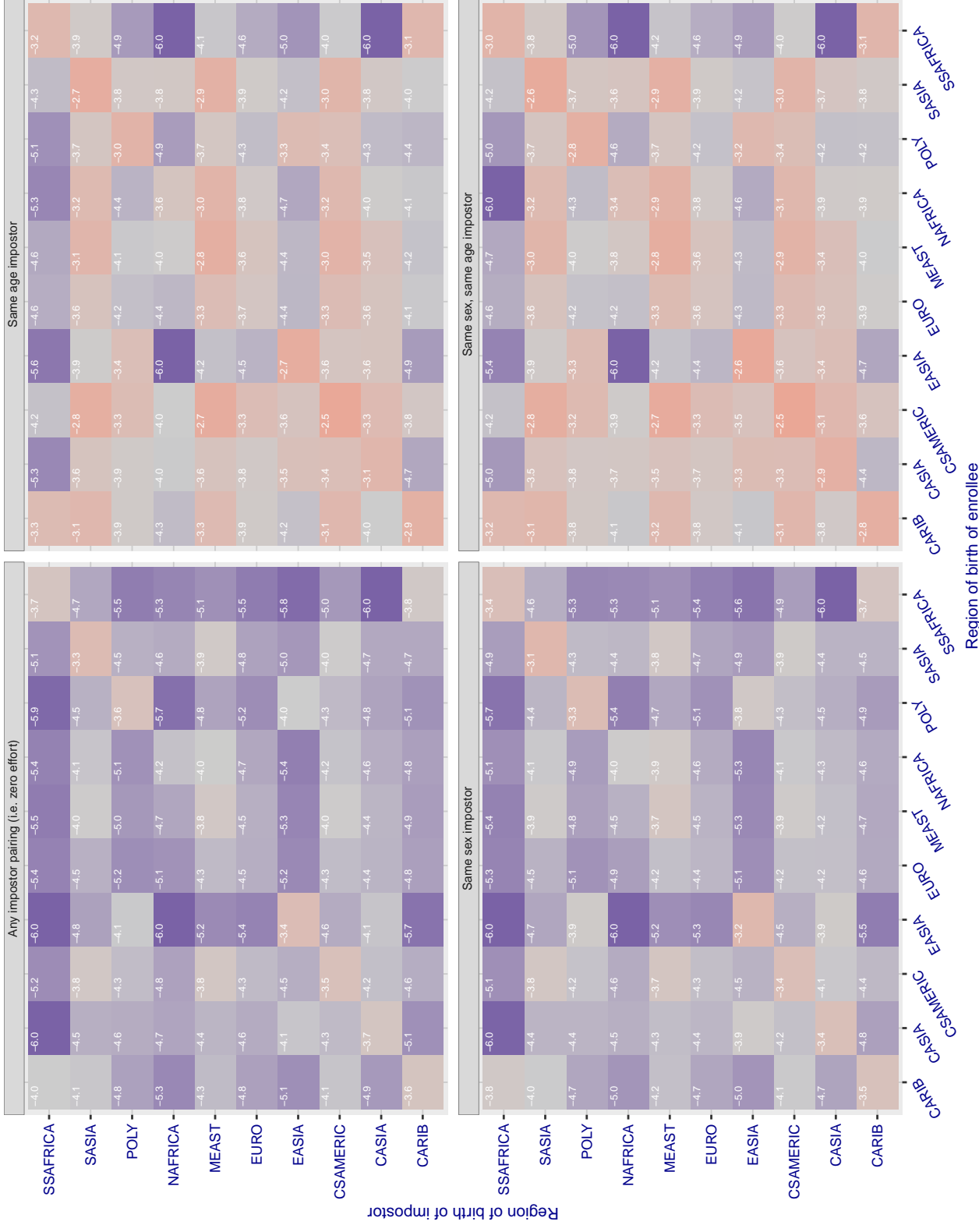
**Cross region FMR at threshold T = 0.661 for algorithm rankone\_007, giving FMR(T) = 0.0001 globally.**

Figure 241: For algorithm rankone-007 operating on visa images, the heatmap shows false match rates observed over impostor comparisons of faces from different individuals who were born in the given region pair. False matches are counted against a recognition threshold fixed globally to give the target FMR in the plot title, computed over all on the order of  $10^{10}$  impostor comparisons. If text appears in each box it give the same quantity as that coded by the color. Grey indicates FMR is at the intended FMR target level. Light red colors present a security vulnerability to, for example, a passport gate. Each +1 increase in  $\log_{10} FMR$  corresponds to a factor of 10 increase in FMR. The matrix is not quite symmetric because images in the enrollment and verification sets are different.

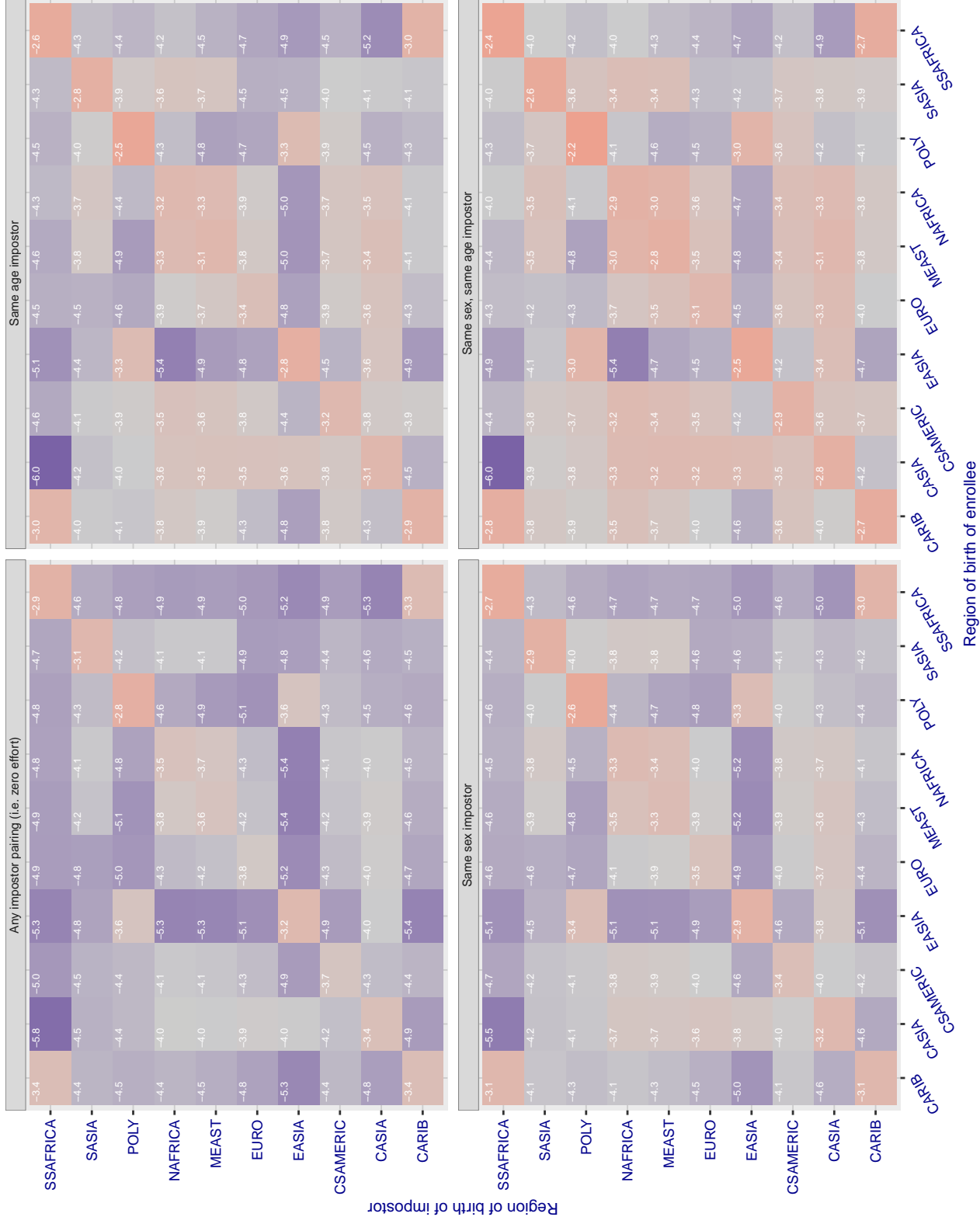
**Cross region FMR at threshold T = 0.883 for algorithm realnetworks\_002, giving FMR(T) = 0.0001 globally.**

Figure 242: For algorithm realnetworks-002 operating on visa images, the heatmap shows false match rates observed over impostor comparisons of faces from different individuals who were born in the given region pair. False matches are counted against a recognition threshold fixed globally to give the target FMR in the plot title, computed over all on the order of  $10^{10}$  impostor comparisons. If text appears in each box it give the same quantity as that coded by the color. Grey indicates FMR is at the intended FMR target level. Light red colors present a security vulnerability to, for example, a passport gate. Each +1 increase in  $\log_{10} \text{FMR}$  corresponds to a factor of 10 increase in FMR. The matrix is not quite symmetric because images in the enrollment and verification sets are different.

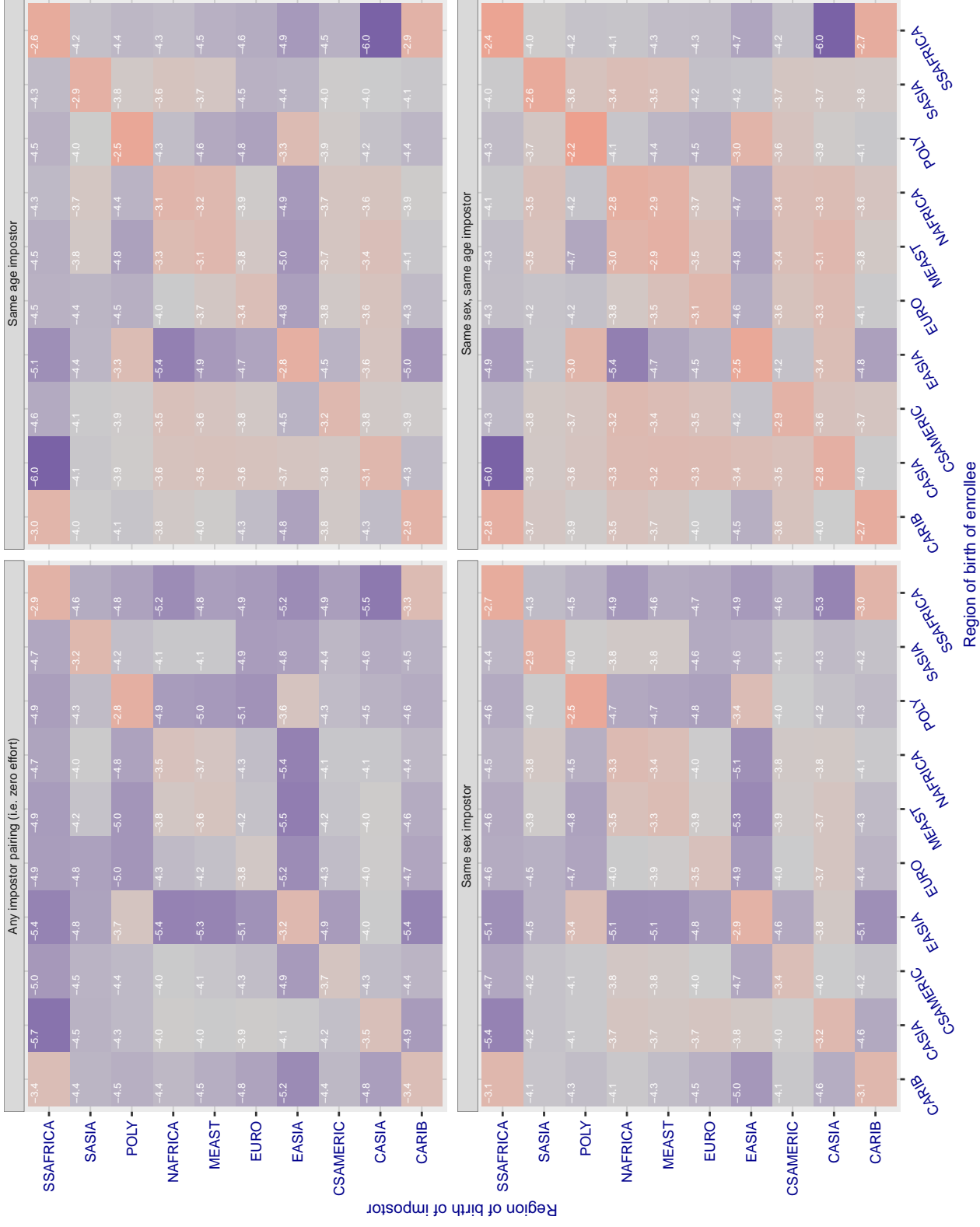
**Cross region FMR at threshold T = 0.886 for algorithm realnetworks\_003, giving FMR(T) = 0.0001 globally.**

Figure 243: For algorithm realnetworks-003 operating on visa images, the heatmap shows false match rates observed over impostor comparisons of faces from different individuals who were born in the given region pair. False matches are counted against a recognition threshold fixed globally to give the target FMR in the plot title, computed over all on the order of  $10^{10}$  impostor comparisons. If text appears in each box it give the same quantity as that coded by the color. Grey indicates FMR is at the intended FMR target level. Light red colors present a security vulnerability to, for example, a passport gate. Each +1 increase in  $\log_{10} FMR$  corresponds to a factor of 10 increase in FMR. The matrix is not quite symmetric because images in the enrollment and verification sets are different.

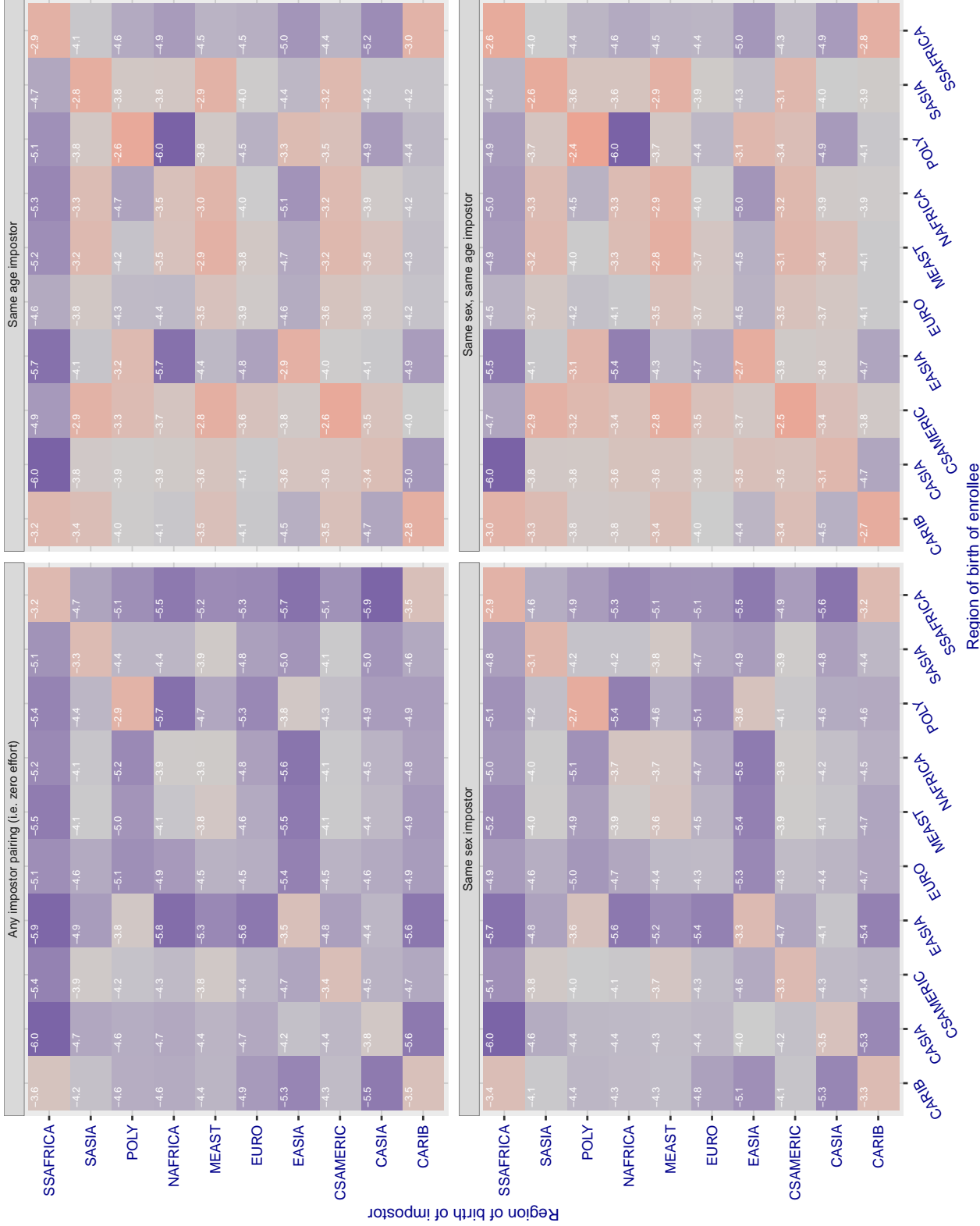
**Cross region FMR at threshold T = 70.373 for algorithm remarkai\_000, giving FMR(T) = 0.0001 globally.**

Figure 244: For algorithm remarkai-000 operating on visa images, the heatmap shows false match rates observed over impostor comparisons of faces from different individuals who were born in the given region pair. False matches are counted against a recognition threshold fixed globally to give the target FMR in the plot title, computed over all on the order of  $10^{10}$  impostor comparisons. If text appears in each box it give the same quantity as that coded by the color. Grey indicates FMR is at the intended FMR target level. Light red colors present a security vulnerability to, for example, a passport gate. Each +1 increase in  $\log_{10} FMR$  corresponds to a factor of 10 increase in FMR. The matrix is not quite symmetric because images in the enrollment and verification sets are different.

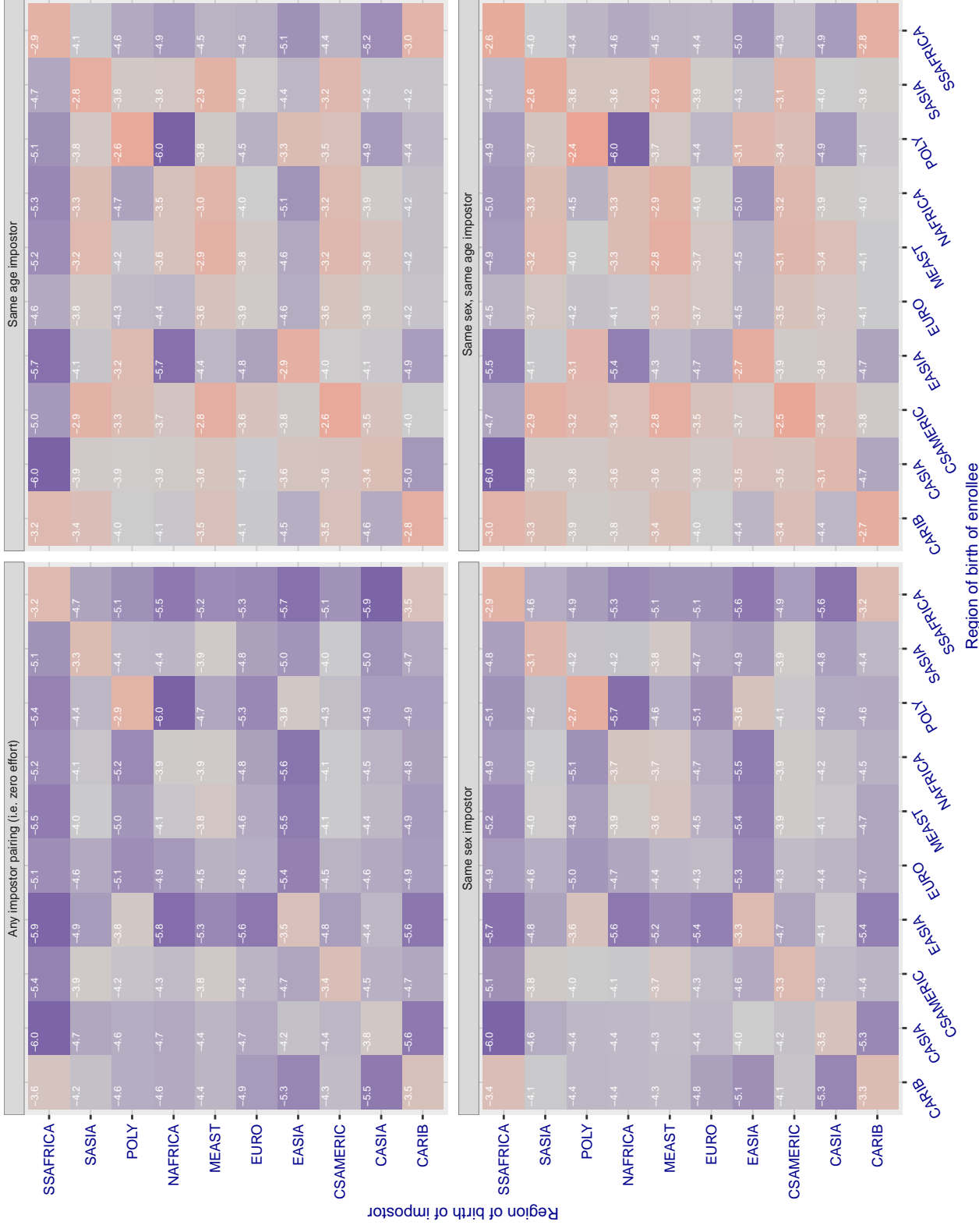
**Cross region FMR at threshold T = 70.384 for algorithm remarkai\_001, giving FMR(T) = 0.0001 globally.**

Figure 245: For algorithm remarkai-001 operating on visa images, the heatmap shows false match rates observed over impostor comparisons of faces from different individuals who were born in the given region pair. False matches are counted against a recognition threshold fixed globally to give the target FMR in the plot title, computed over all on the order of  $10^{10}$  impostor comparisons. If text appears in each box it give the same quantity as that coded by the color. Grey indicates FMR is at the intended FMR target level. Light red colors present a security vulnerability to, for example, a passport gate. Each +1 increase in  $\log_{10} FMR$  corresponds to a factor of 10 increase in FMR. The matrix is not quite symmetric because images in the enrollment and verification sets are different.

### Cross region FMR at threshold T = 0.663 for algorithm rokid\_000, giving FMR(T) = 0.0001 globally.

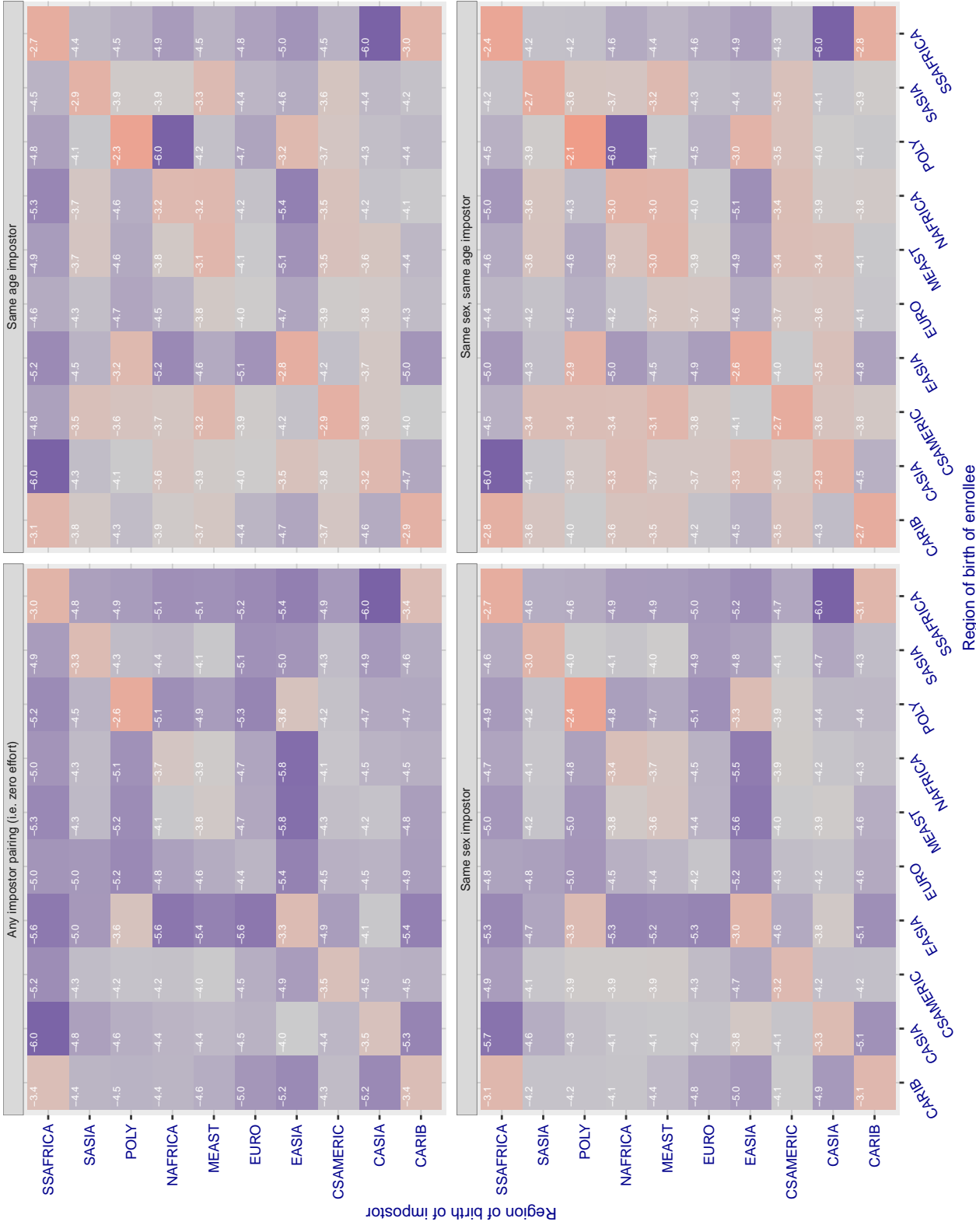


Figure 246: For algorithm rokid-000 operating on visa images, the heatmap shows false match rates observed over impostor comparisons of faces from different individuals who were born in the given region pair. False matches are counted against a recognition threshold fixed globally to give the target FMR in the plot title, computed over all on the order of  $10^{10}$  impostor comparisons. If text appears in each box it give the same quantity as that coded by the color. Grey indicates FMR is at the intended FMR target level. Light red colors present a security vulnerability to, for example, a passport gate. Each +1 increase in  $\log_{10} \text{FMR}$  corresponds to a factor of 10 increase in FMR. The matrix is not quite symmetric because images in the enrollment and verification sets are different.

### Cross region FMR at threshold T = 0.682 for algorithm safe\_001, giving FMR(T) = 0.0001 globally.

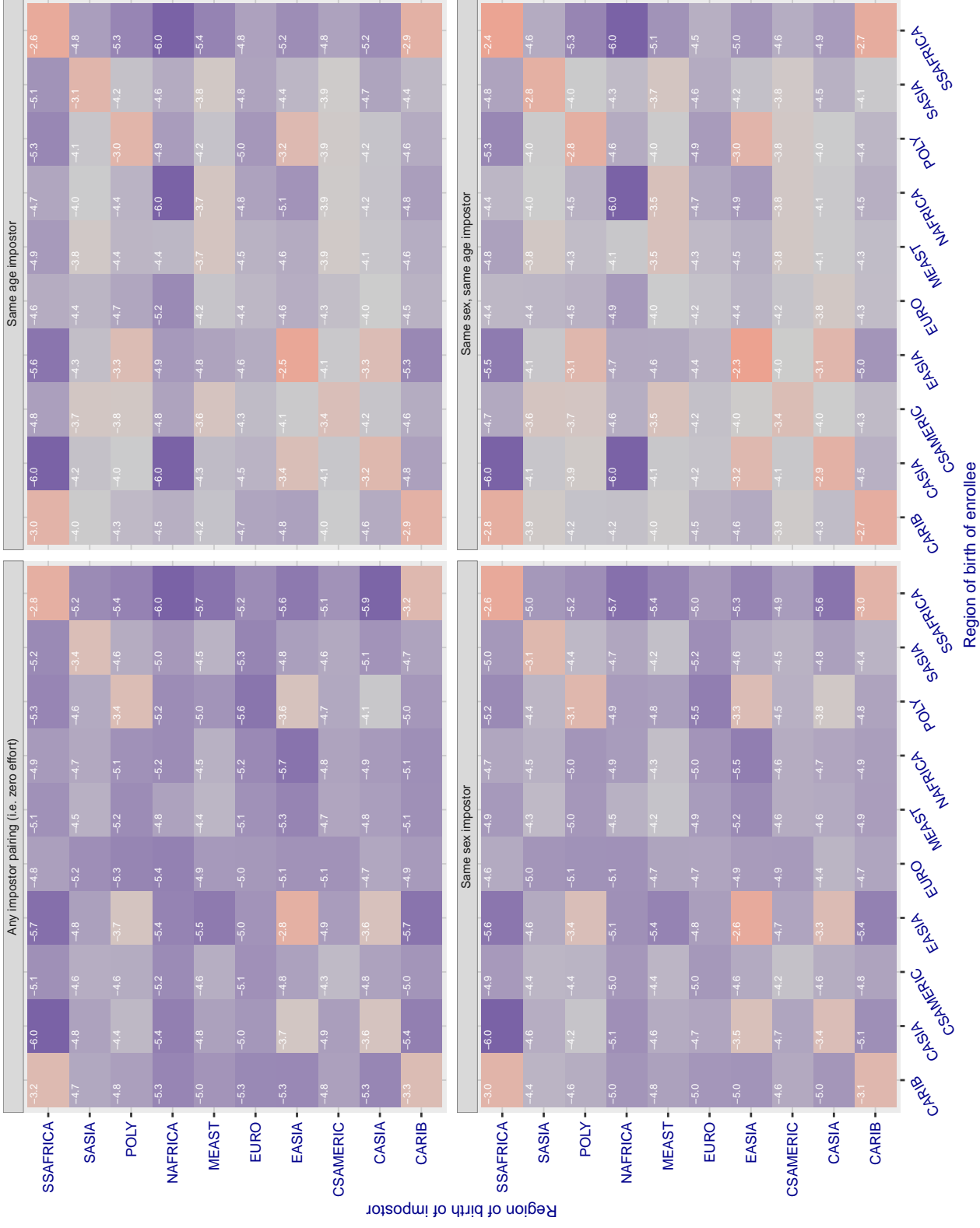


Figure 247: For algorithm safe-001 operating on visa images, the heatmap shows false match rates observed over impostor comparisons of faces from different individuals who were born in the given region pair. False matches are counted against a recognition threshold fixed globally to give the target FMR in the plot title, computed over all on the order of  $10^{10}$  impostor comparisons. If text appears in each box it give the same quantity as that coded by the color. Grey indicates FMR is at the intended FMR target level. Light red colors present a security vulnerability to, for example, a passport gate. Each +1 increase in  $\log_{10}$  FMR corresponds to a factor of 10 increase in FMR. The matrix is not quite symmetric because images in the enrollment and verification sets are different.

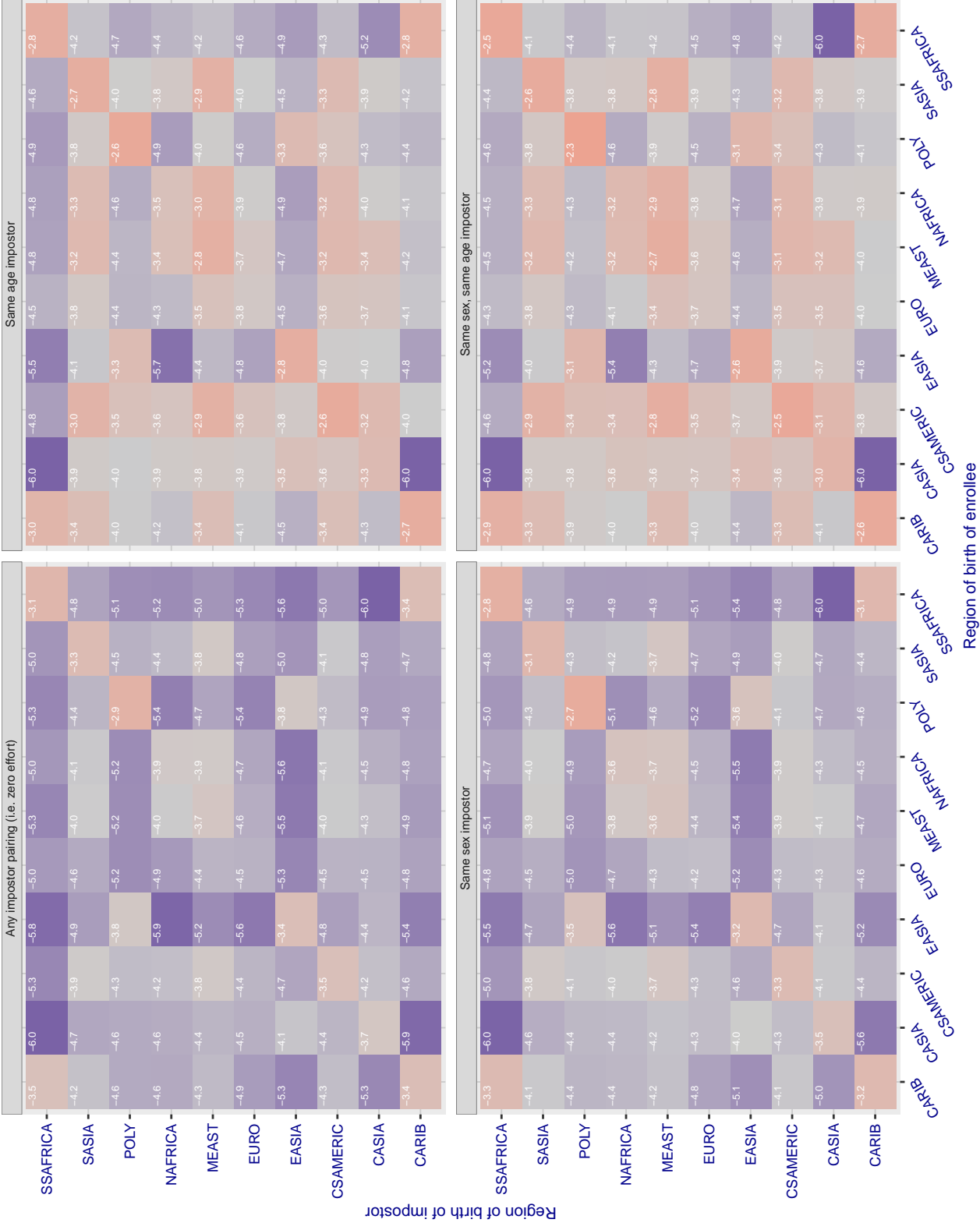
**Cross region FMR at threshold T = 0.383 for algorithm safe\_002, giving FMR(T) = 0.0001 globally.**

Figure 248: For algorithm safe-002 operating on visa images, the heatmap shows false match rates observed over impostor comparisons of faces from different individuals who were born in the given region pair. False matches are counted against a recognition threshold fixed globally to give the target FMR in the plot title, computed over all on the order of  $10^{10}$  impostor comparisons. If text appears in each box it give the same quantity as that coded by the color. Grey indicates FMR is at the intended FMR target level. Light red colors present a security vulnerability to, for example, a passport gate. Each +1 increase in  $\log 10$  FMR corresponds to a factor of 10 increase in FMR. The matrix is not quite symmetric because images in the enrollment and verification sets are different.

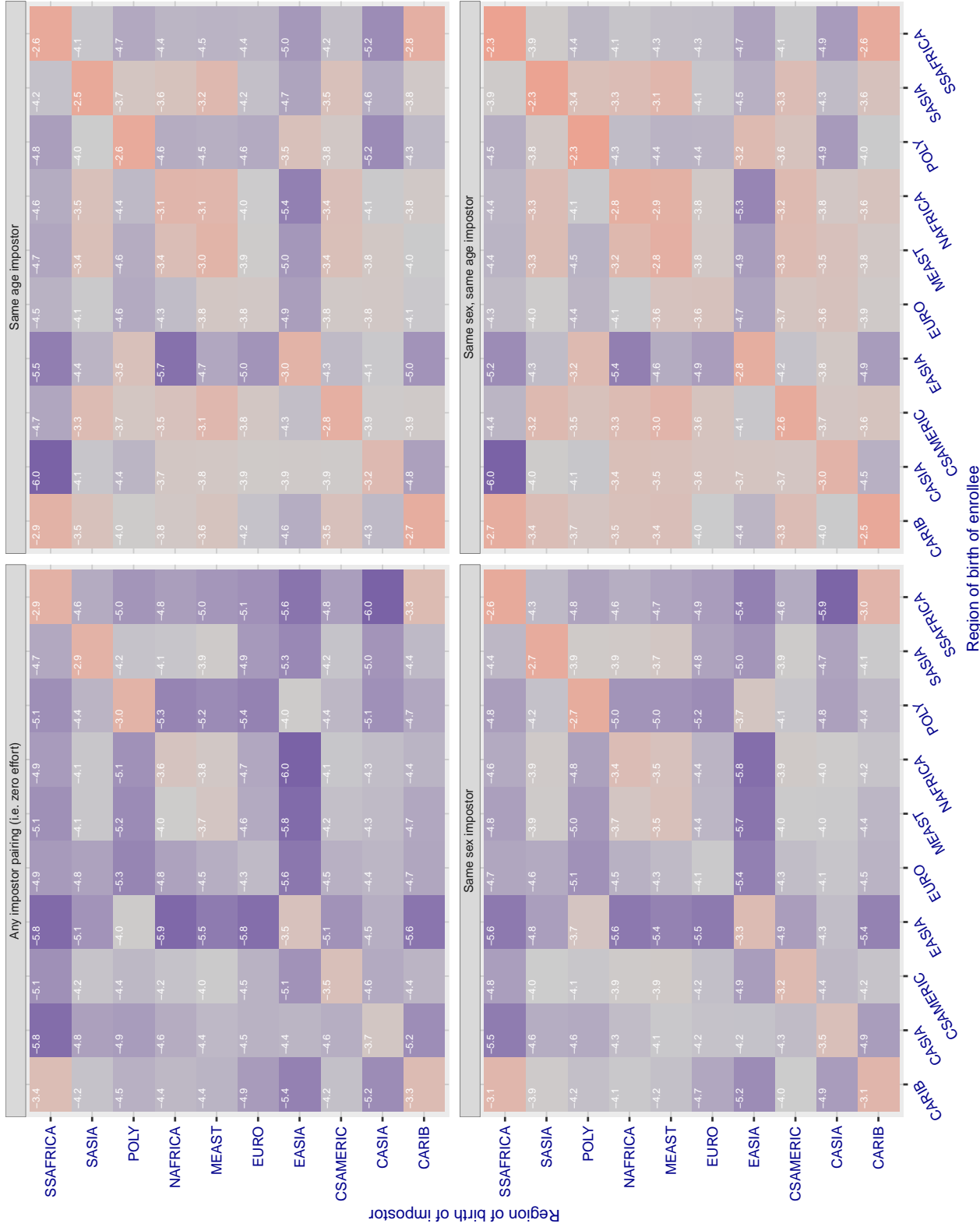
**Cross region FMR at threshold T = 0.390 for algorithm sensetime\_001, giving FMR(T) = 0.0001 globally.**

Figure 249: For algorithm sensetime-001 operating on visa images, the heatmap shows false match rates observed over impostor comparisons of faces from different individuals who were born in the given region pair. False matches are counted against a recognition threshold fixed globally to give the target FMR in the plot title, computed over all on the order of  $10^{10}$  impostor comparisons. If text appears in each box it give the same quantity as that coded by the color. Grey indicates FMR is at the intended FMR target level. Light red colors present a security vulnerability to, for example, a passport gate. Each +1 increase in  $\log_{10} FMR$  corresponds to a factor of 10 increase in FMR. The matrix is not quite symmetric because images in the enrollment and verification sets are different.

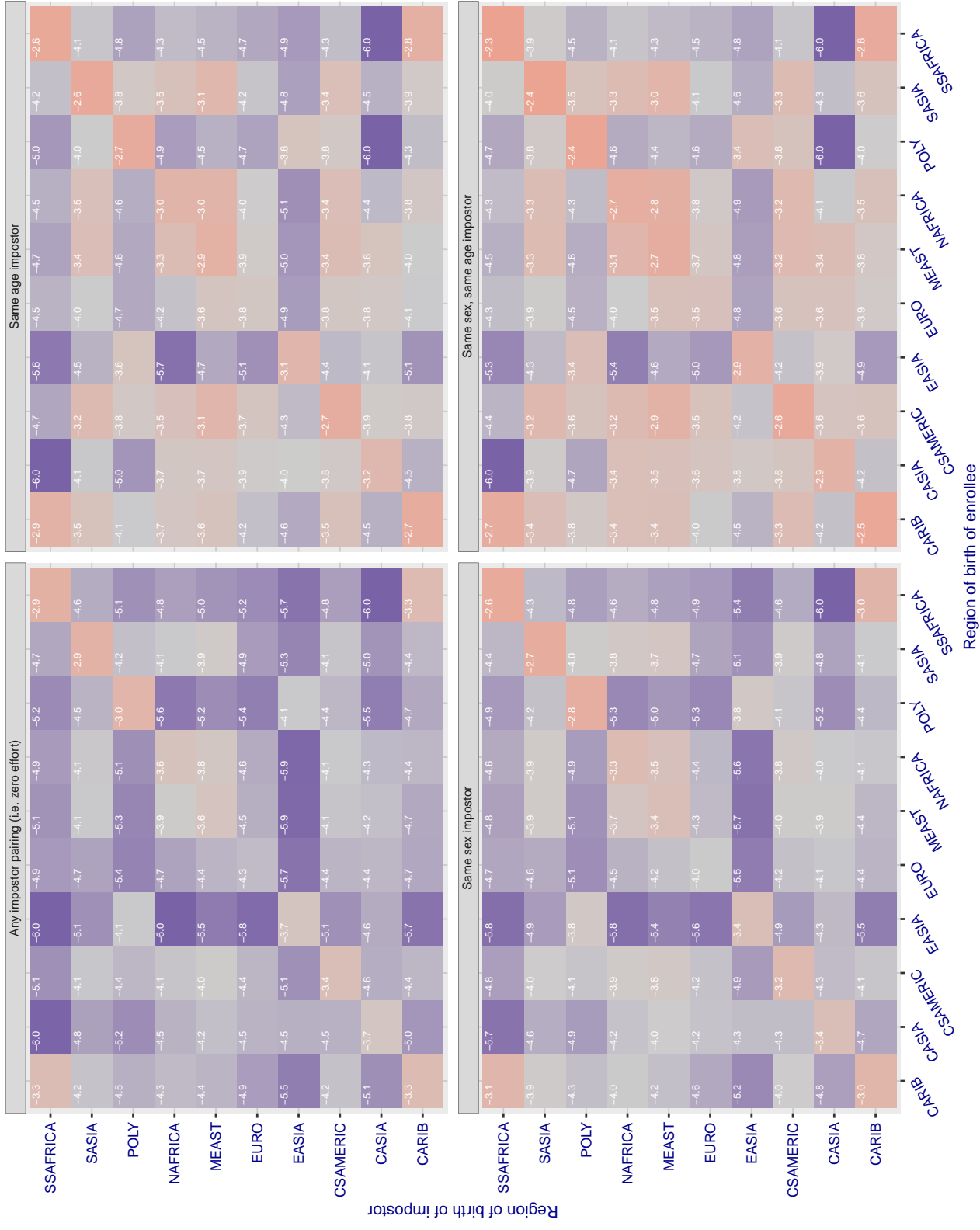
**Cross region FMR at threshold T = 0.390 for algorithm sensetime\_002, giving FMR(T) = 0.0001 globally.**

Figure 250: For algorithm sensetime-002 operating on visa images, the heatmap shows false match rates observed over impostor comparisons of faces from different individuals who were born in the given region pair. False matches are counted against a recognition threshold fixed globally to give the target FMR in the plot title, computed over all on the order of  $10^{10}$  impostor comparisons. If text appears in each box it give the same quantity as that coded by the color. Grey indicates FMR is at the intended FMR target level. Light red colors present a security vulnerability to, for example, a passport gate. Each +1 increase in  $\log_{10} \text{FMR}$  corresponds to a factor of 10 increase in FMR. The matrix is not quite symmetric because images in the enrollment and verification sets are different.

### Cross region FMR at threshold T = 0.713 for algorithm sertis\_000, giving FMR(T) = 0.0001 globally.

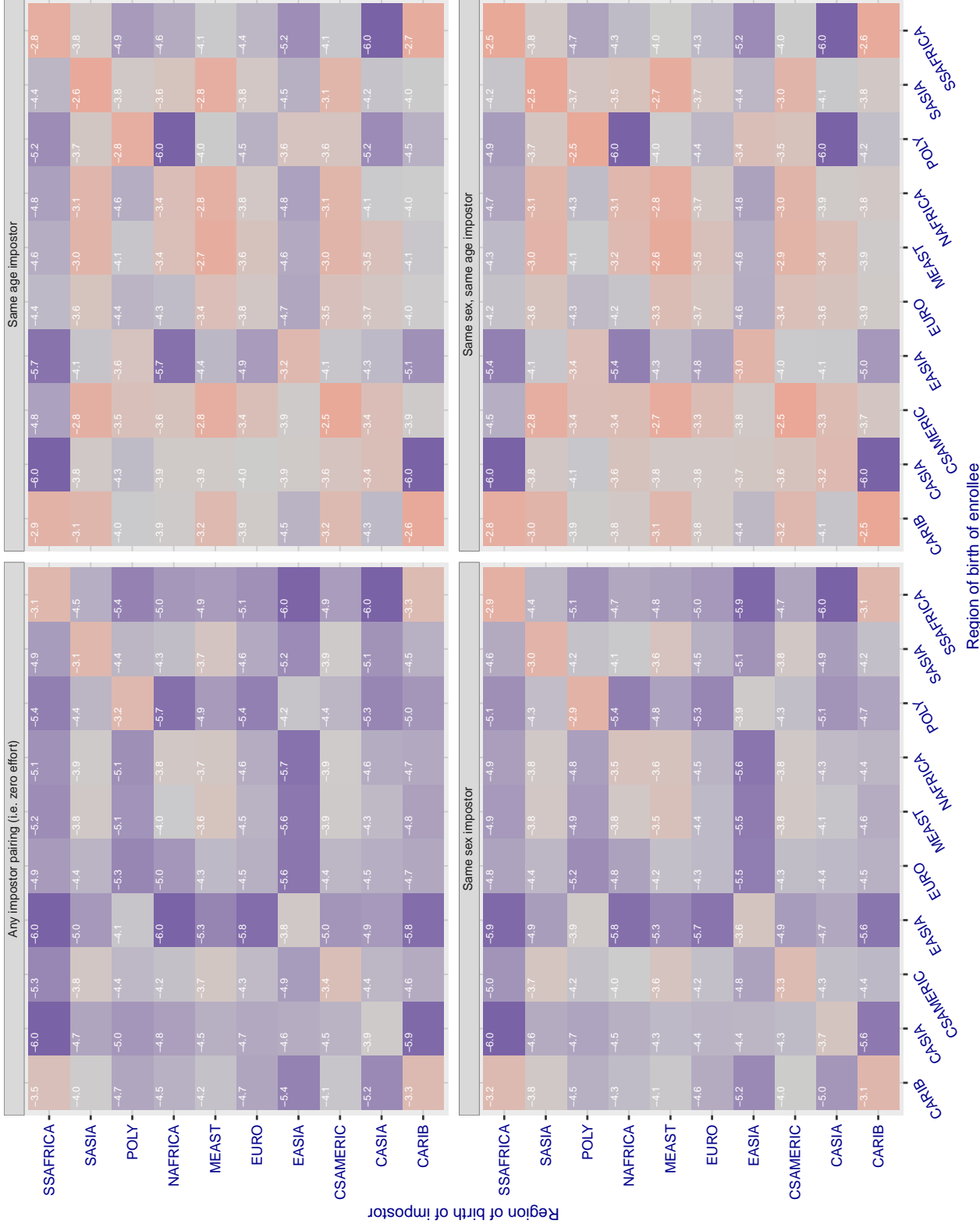


Figure 25: For algorithm sertis-000 operating on visa images, the heatmap shows false match rates observed over impostor comparisons of faces from different individuals who were born in the given region pair. False matches are counted against a recognition threshold fixed globally to give the target FMR in the plot title, computed over all on the order of  $10^{10}$  impostor comparisons. If text appears in each box it give the same quantity as that coded by the color. Grey indicates FMR is at the intended FMR target level. Light red colors present a security vulnerability to, for example, a passport gate. Each +1 increase in  $\log_{10} \text{FMR}$  corresponds to a factor of 10 increase in FMR. The matrix is not quite symmetric because images in the enrollment and verification sets are different.

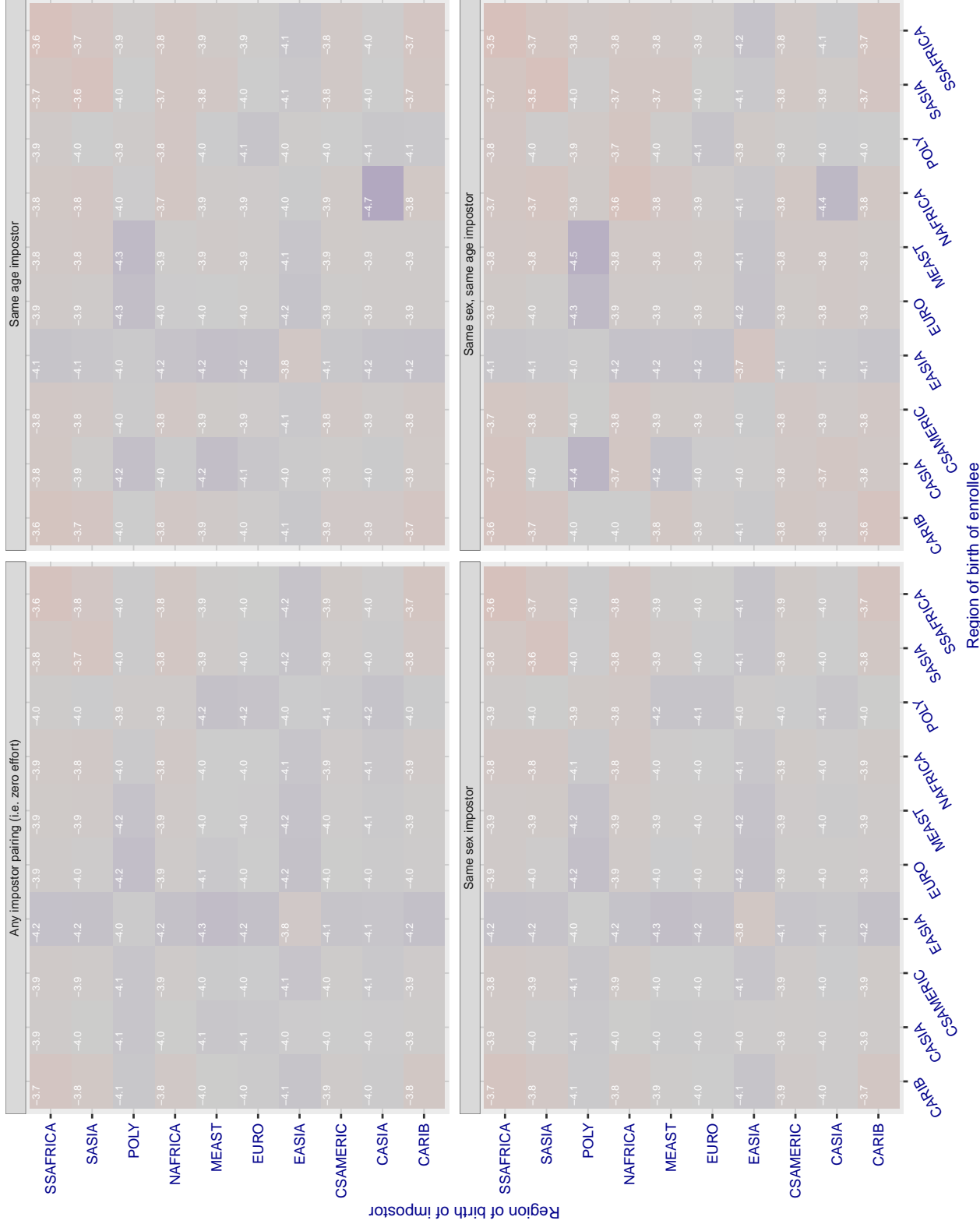
**Cross region FMR at threshold T = 0.970 for algorithm shaman\_000, giving FMR(T) = 0.0001 globally.**

Figure 252: For algorithm shaman-000 operating on visa images, the heatmap shows false match rates observed over impostor comparisons of faces from different individuals who were born in the given region pair. False matches are counted against a recognition threshold fixed globally to give the target FMR in the plot title, computed over all on the order of  $10^{10}$  impostor comparisons. If text appears in each box it give the same quantity as that coded by the color. Grey indicates FMR is at the intended FMR target level. Light red colors present a security vulnerability to, for example, a passport gate. Each +1 increase in  $\log_{10} \text{FMR}$  corresponds to a factor of 10 increase in FMR. The matrix is not quite symmetric because images in the enrollment and verification sets are different.

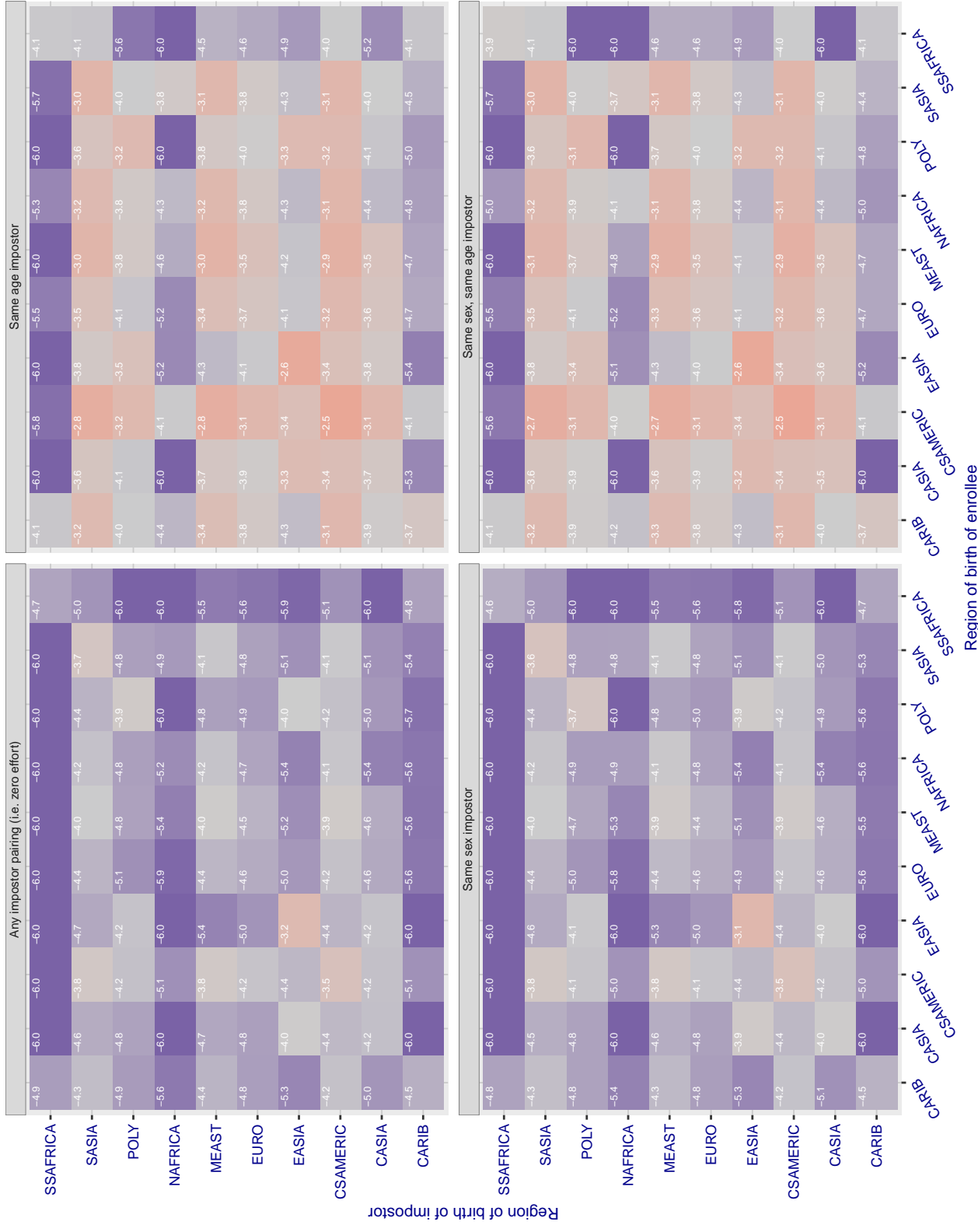
**Cross region FMR at threshold T = 0.725 for algorithm shaman\_001, giving FMR(T) = 0.0001 globally.**

Figure 253: For algorithm shaman-001 operating on visa images, the heatmap shows false match rates observed over impostor comparisons of faces from different individuals who were born in the given region pair. False matches are counted against a recognition threshold fixed globally to give the target FMR in the plot title, computed over all on the order of  $10^{10}$  impostor comparisons. If text appears in each box it give the same quantity as that coded by the color. Grey indicates FMR is at the intended FMR target level. Light red colors present a security vulnerability to, for example, a passport gate. Each +1 increase in  $\log_{10} FMR$  corresponds to a factor of 10 increase in FMR. The matrix is not quite symmetric because images in the enrollment and verification sets are different.

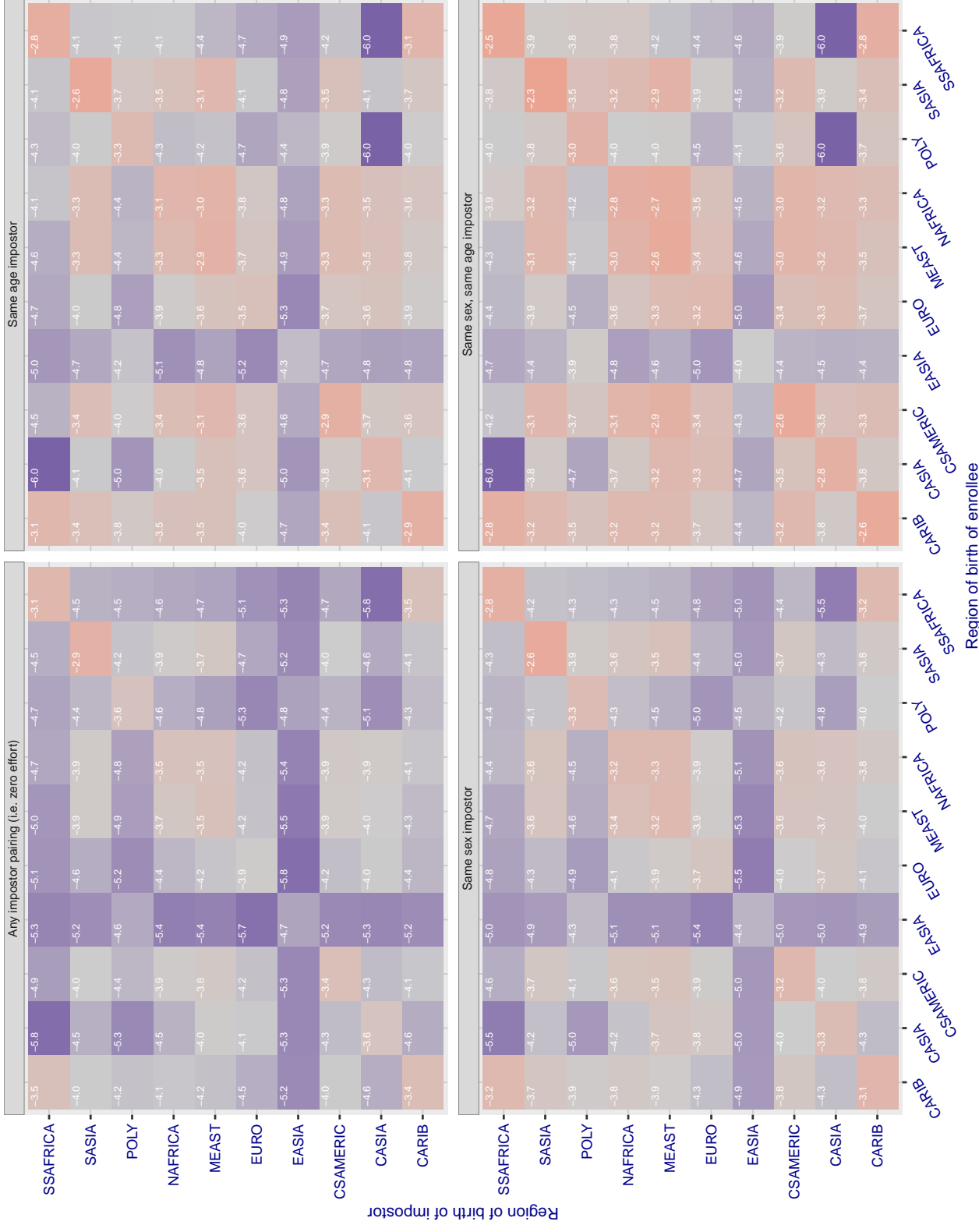
**Cross region FMR at threshold T = 0.400 for algorithm shu\_001, giving FMR(T) = 0.0001 globally.**

Figure 254: For algorithm shu-001 operating on visa images, the heatmap shows false match rates observed over impostor comparisons of faces from different individuals who were born in the given region pair. False matches are counted against a recognition threshold fixed globally to give the target FMR in the plot title, computed over all on the order of  $10^{10}$  impostor comparisons. If text appears in each box it give the same quantity as that coded by the color. Grey indicates FMR is at the intended FMR target level. Light red colors present a security vulnerability to, for example, a passport gate. Each +1 increase in  $\log 10$  FMR corresponds to a factor of 10 increase in FMR. The matrix is not quite symmetric because images in the enrollment and verification sets are different.

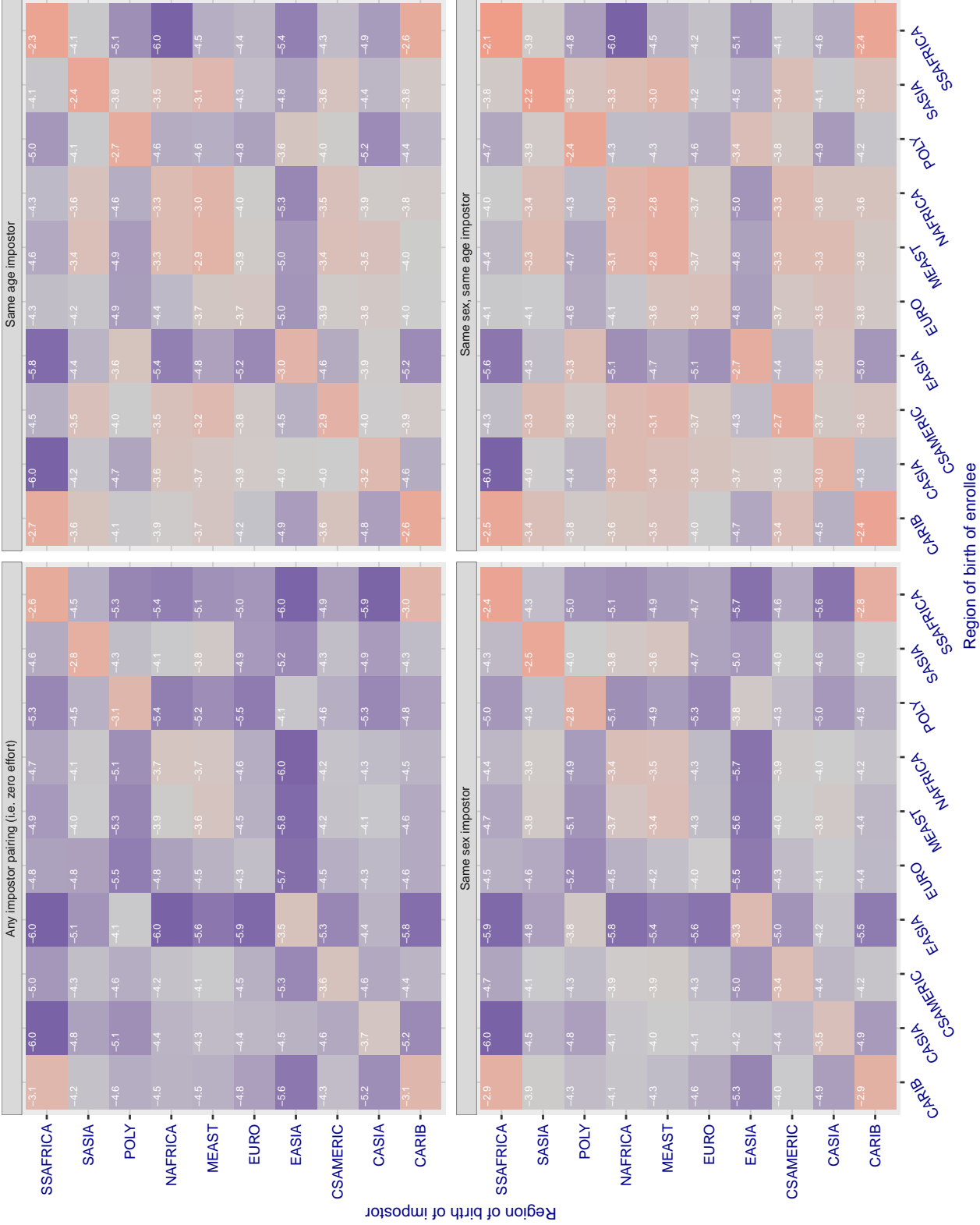
**Cross region FMR at threshold T = 0.390 for algorithm siat\_002, giving FMR(T) = 0.0001 globally.**

Figure 255: For algorithm siat-002 operating on visa images, the heatmap shows false match rates observed over impostor comparisons of faces from different individuals who were born in the given region pair. False matches are counted against a recognition threshold fixed globally to give the target FMR in the plot title, computed over all on the order of  $10^{10}$  impostor comparisons. If text appears in each box it give the same quantity as that coded by the color. Grey indicates FMR is at the intended FMR target level. Light red colors present a security vulnerability to, for example, a passport gate. Each +1 increase in  $\log 10$  FMR corresponds to a factor of 10 increase in FMR. The matrix is not quite symmetric because images in the enrollment and verification sets are different.

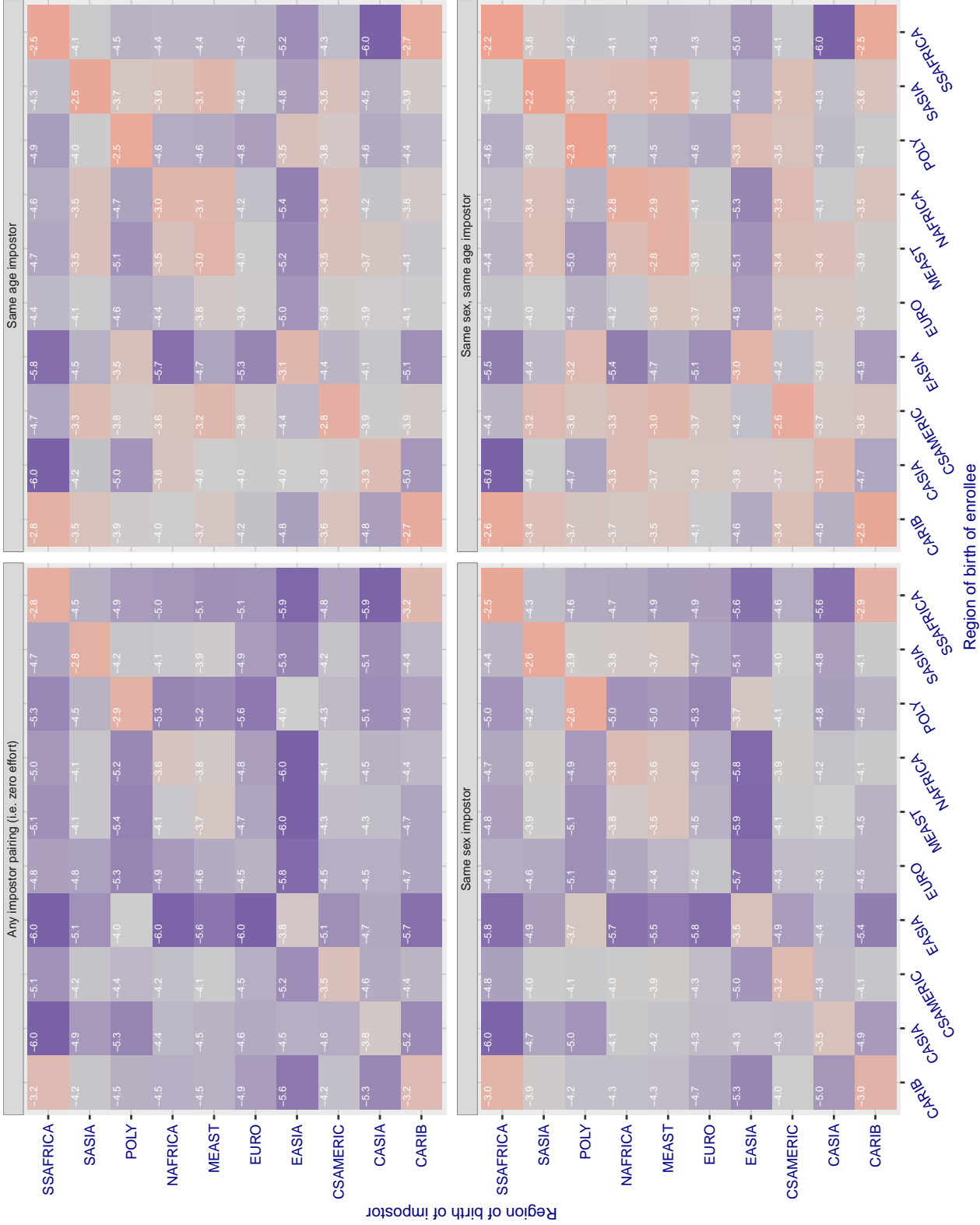
**Cross region FMR at threshold T = 0.393 for algorithm siat\_004, giving FMR(T) = 0.0001 globally.**

Figure 256: For algorithm siat-004 operating on visa images, the heatmap shows false match rates observed over impostor comparisons of faces from different individuals who were born in the given region pair. False matches are counted against a recognition threshold fixed globally to give the target FMR in the plot title, computed over all on the order of  $10^{10}$  impostor comparisons. If text appears in each box it give the same quantity as that coded by the color. Grey indicates FMR is at the intended FMR target level. Light red colors present a security vulnerability to, for example, a passport gate. Each +1 increase in  $\log 10$  FMR corresponds to a factor of 10 increase in FMR. The matrix is not quite symmetric because images in the enrollment and verification sets are different.

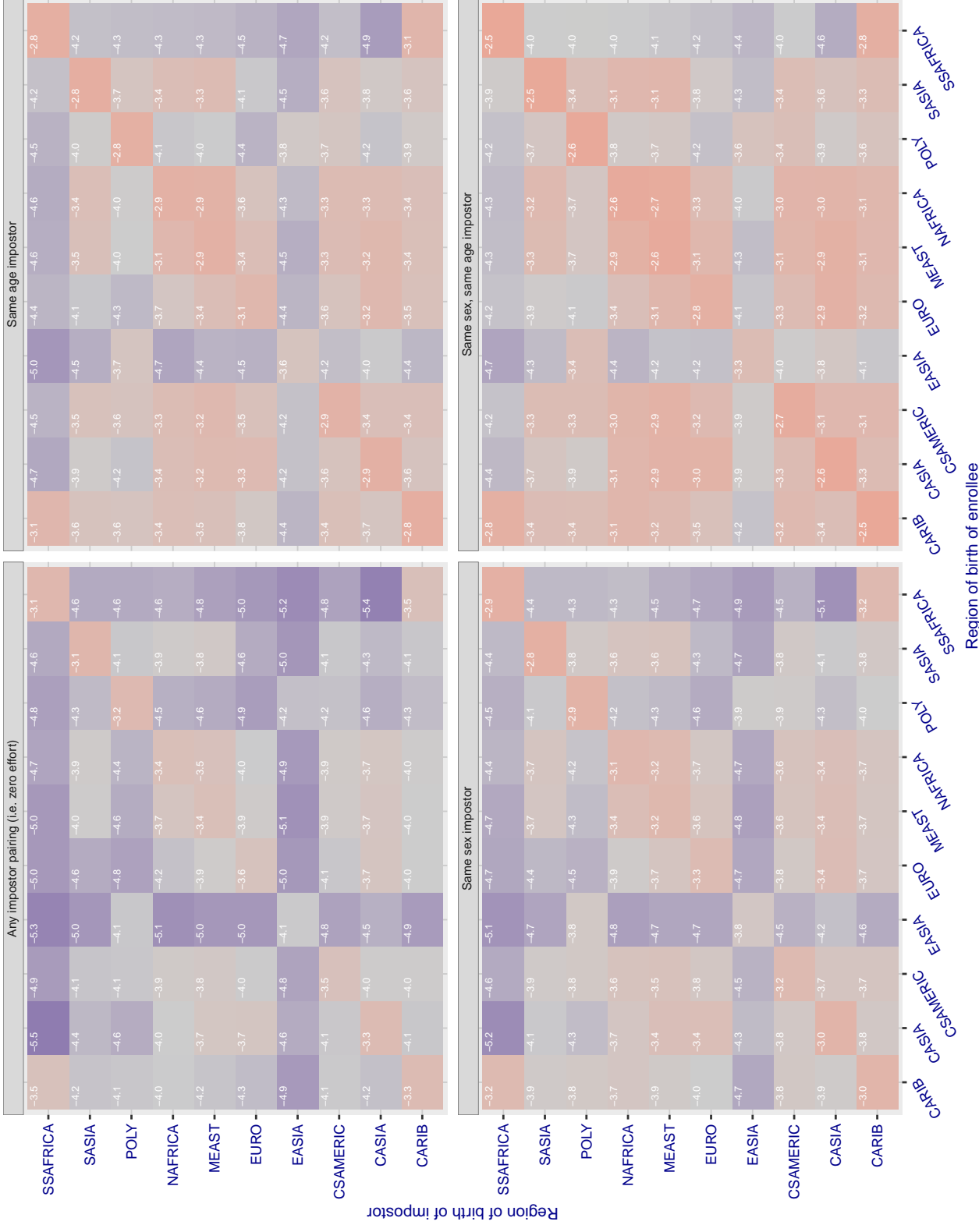
**Cross region FMR at threshold T = 1.206 for algorithm sjtu\_001, giving FMR(T) = 0.0001 globally.**

Figure 257: For algorithm sjtu-001 operating on visa images, the heatmap shows false match rates observed over impostor comparisons of faces from different individuals who were born in the given region pair. False matches are counted against a recognition threshold fixed globally to give the target FMR in the plot title, computed over all on the order of  $10^{10}$  impostor comparisons. If text appears in each box it give the same quantity as that coded by the color. Grey indicates FMR is at the intended FMR target level. Light red colors present a security vulnerability to, for example, a passport gate. Each +1 increase in  $\log_{10}$  FMR corresponds to a factor of 10 increase in FMR. The matrix is not quite symmetric because images in the enrollment and verification sets are different.

### Cross region FMR at threshold T = 0.598 for algorithm smilart\_002, giving FMR(T) = 0.0001 globally.

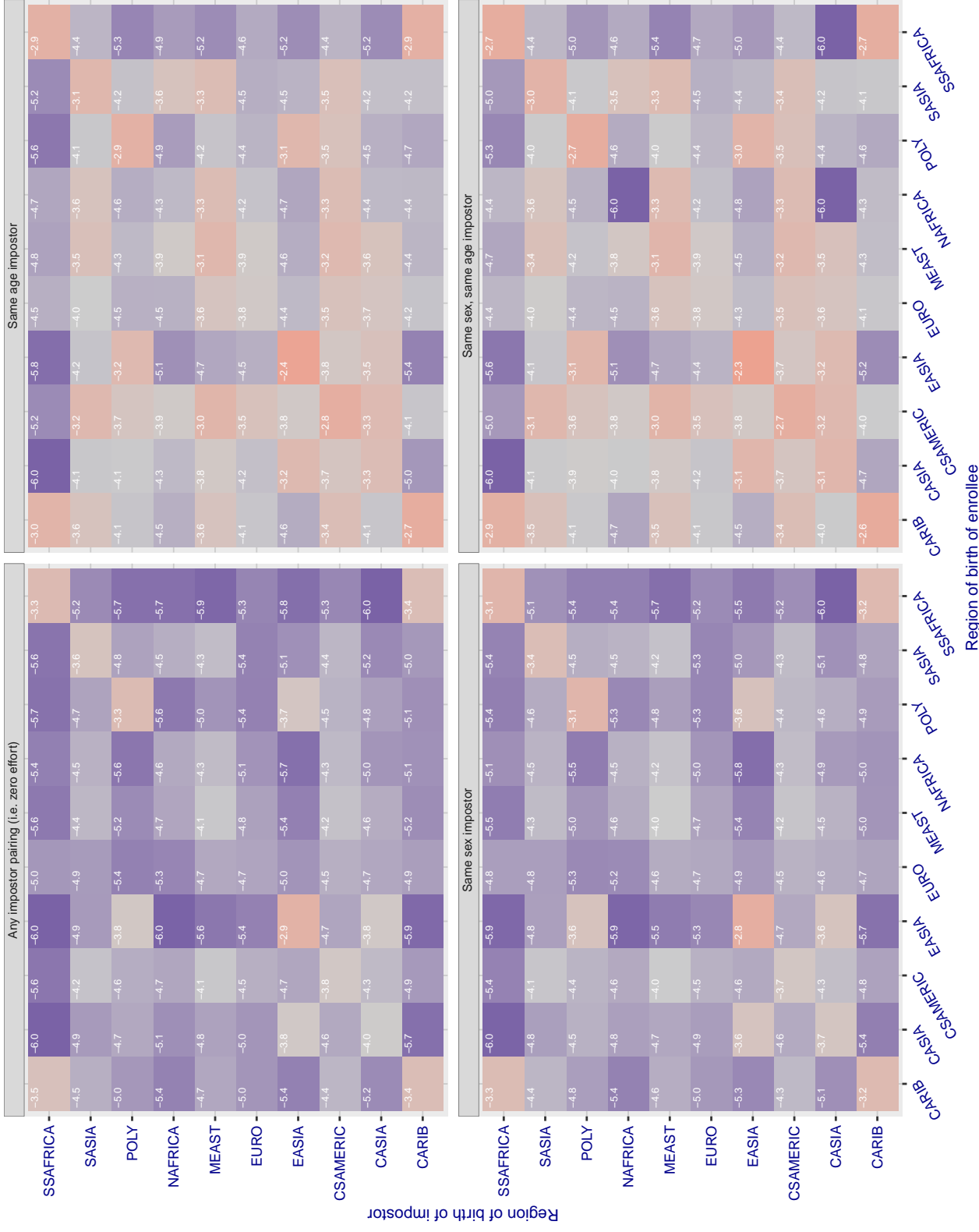


Figure 258: For algorithm smilart-002 operating on visa images, the heatmap shows false match rates observed over impostor comparisons of faces from different individuals who were born in the given region pair. False matches are counted against a recognition threshold fixed globally to give the target FMR in the plot title, computed over all on the order of  $10^{10}$  impostor comparisons. If text appears in each box it give the same quantity as that coded by the color. Grey indicates FMR is at the intended FMR target level. Light red colors present a security vulnerability to, for example, a passport gate. Each +1 increase in  $\log_{10} FMR$  corresponds to a factor of 10 increase in FMR. The matrix is not quite symmetric because images in the enrollment and verification sets are different.

### Cross region FMR at threshold T = 0.654 for algorithm smilart\_003, giving FMR(T) = 0.0001 globally.

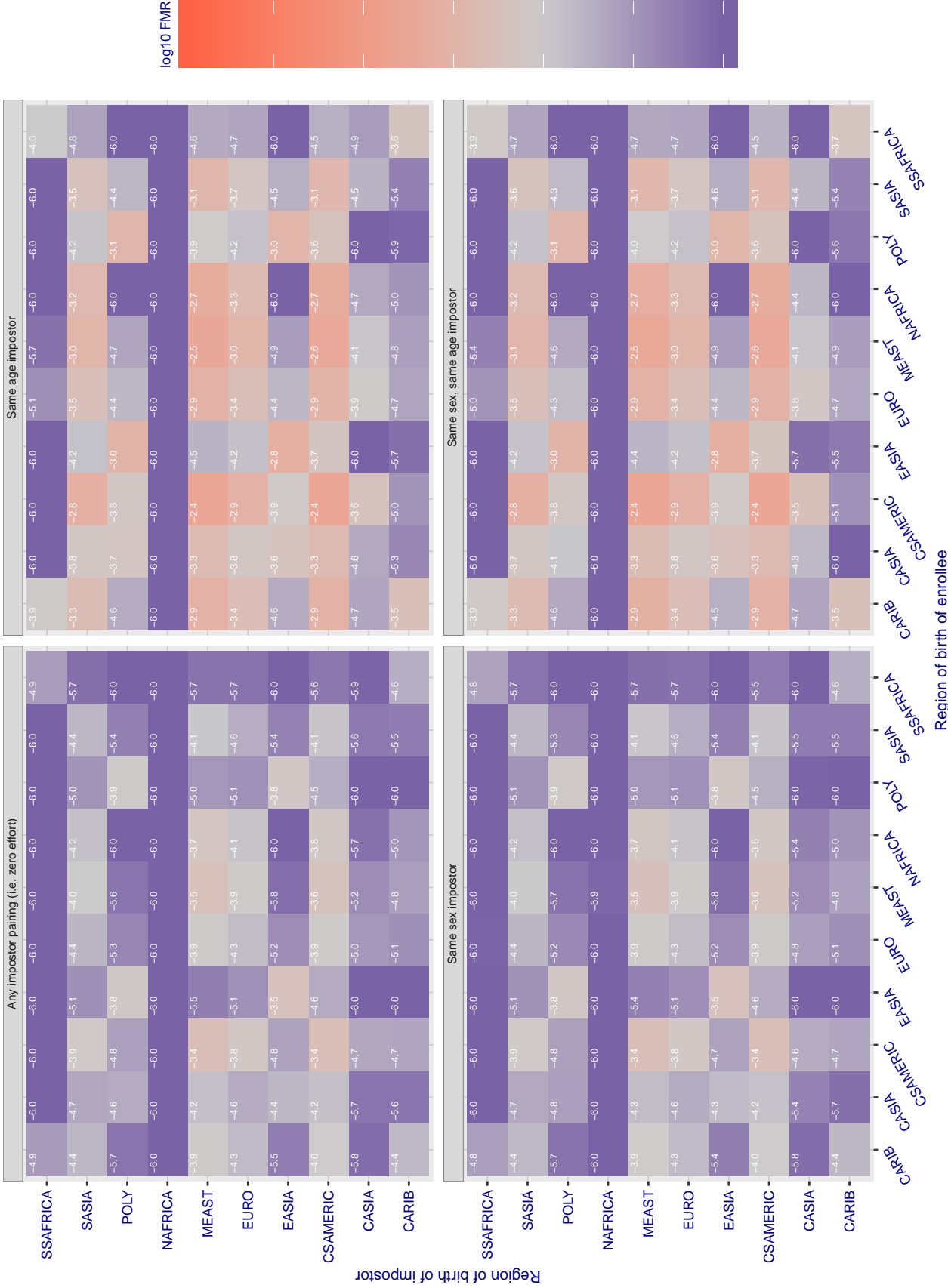


Figure 259: For algorithm smilart-003 operating on visa images, the heatmap shows false match rates observed over impostor comparisons of faces from different individuals who were born in the given region pair. False matches are counted against a recognition threshold fixed globally to give the target FMR in the plot title, computed over all on the order of  $10^{10}$  impostor comparisons. If text appears in each box it give the same quantity as that coded by the color. Grey indicates FMR is at the intended FMR target level. Light red colors present a security vulnerability to, for example, a passport gate. Each +1 increase in  $\log_{10} FMR$  corresponds to a factor of 10 increase in FMR. The matrix is not quite symmetric because images in the enrollment and verification sets are different.

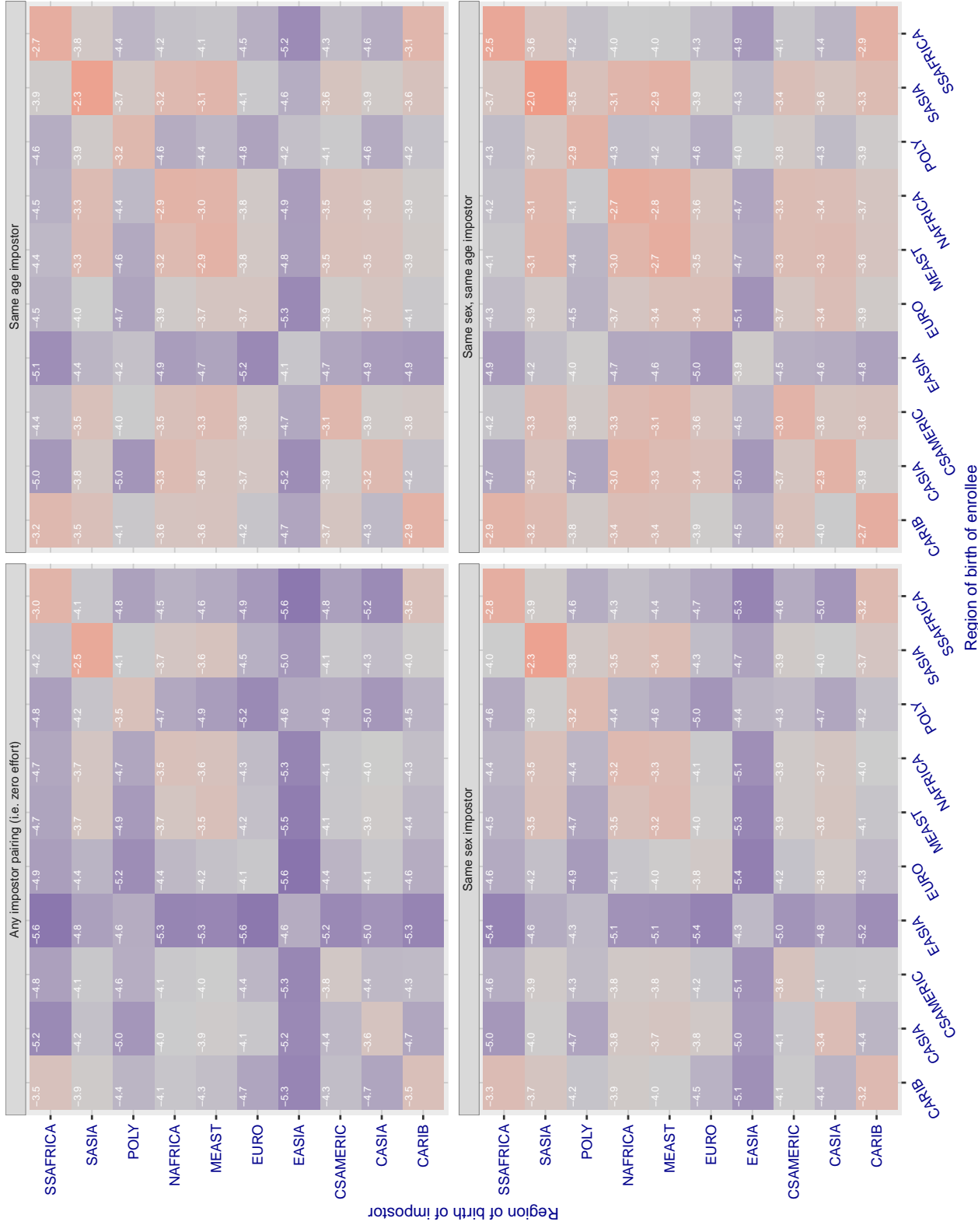
**Cross region FMR at threshold T = 0.314 for algorithm starhybrid\_001, giving FMR(T) = 0.0001 globally.**

Figure 260: For algorithm starhybrid-001 operating on visa images, the heatmap shows false match rates observed over impostor comparisons of faces from different individuals who were born in the given region pair. False matches are counted against a recognition threshold fixed globally to give the target FMR in the plot title, computed over all on the order of  $10^{10}$  impostor comparisons. If text appears in each box it give the same quantity as that coded by the color. Grey indicates FMR is at the intended FMR target level. Light red colors present a security vulnerability to, for example, a passport gate. Each +1 increase in  $\log_{10} FMR$  corresponds to a factor of 10 increase in FMR. The matrix is not quite symmetric because images in the enrollment and verification sets are different.

### Cross region FMR at threshold T = 0.221 for algorithm *synesis\_004*, giving FMR(T) = 0.0001 globally.

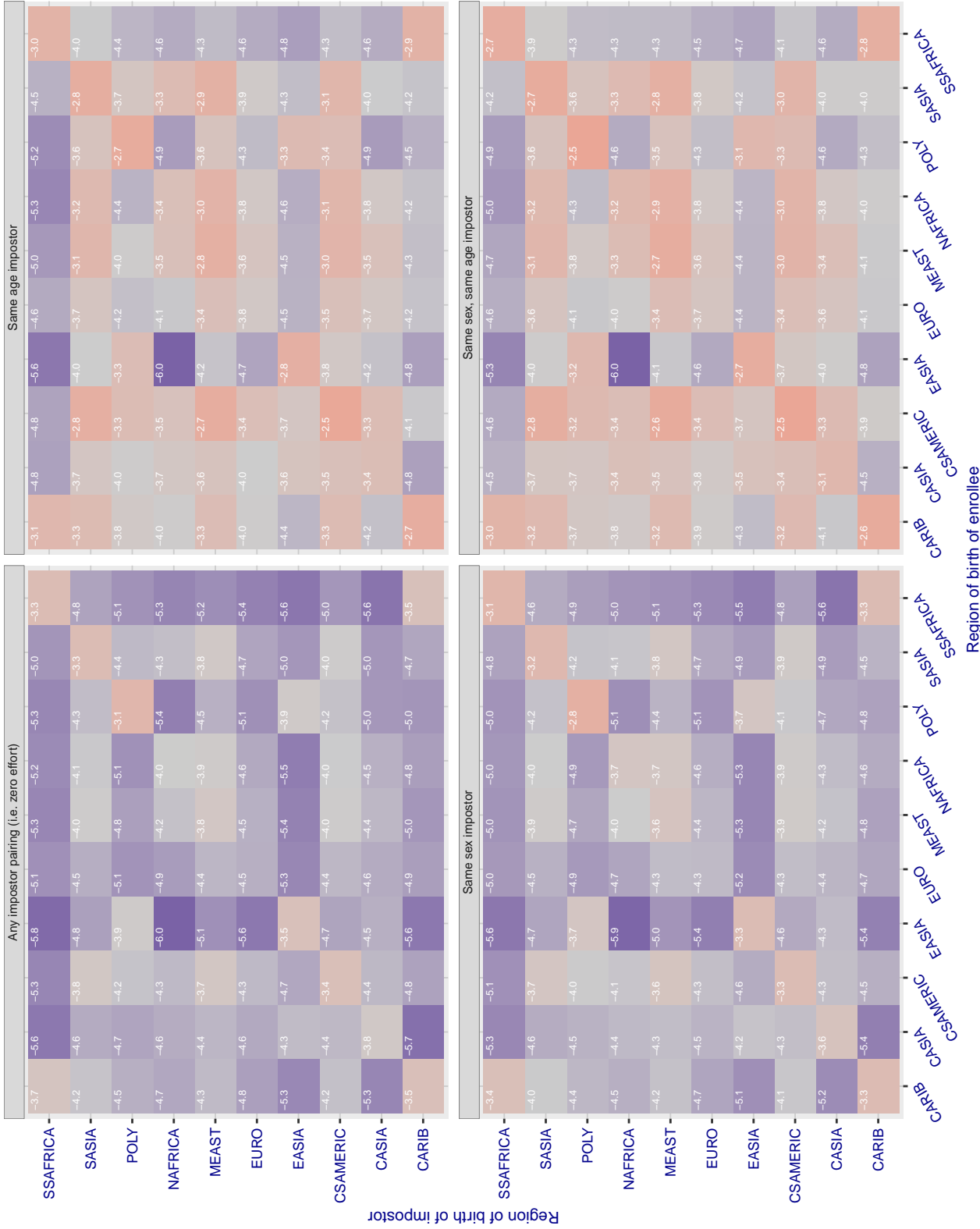


Figure 261: For algorithm *synesis-004* operating on visa images, the heatmap shows false match rates observed over impostor comparisons of faces from different individuals who were born in the given region pair. False matches are counted against a recognition threshold fixed globally to give the target FMR in the plot title, computed over all on the order of  $10^{10}$  impostor comparisons. If text appears in each box it give the same quantity as that coded by the color. Grey indicates FMR is at the intended FMR target level. Light red colors present a security vulnerability to, for example, a passport gate. Each +1 increase in  $\log_{10} FMR$  corresponds to a factor of 10 increase in FMR. The matrix is not quite symmetric because images in the enrollment and verification sets are different.

### Cross region FMR at threshold T = 0.356 for algorithm *synesis\_005*, giving FMR(T) = 0.0001 globally.

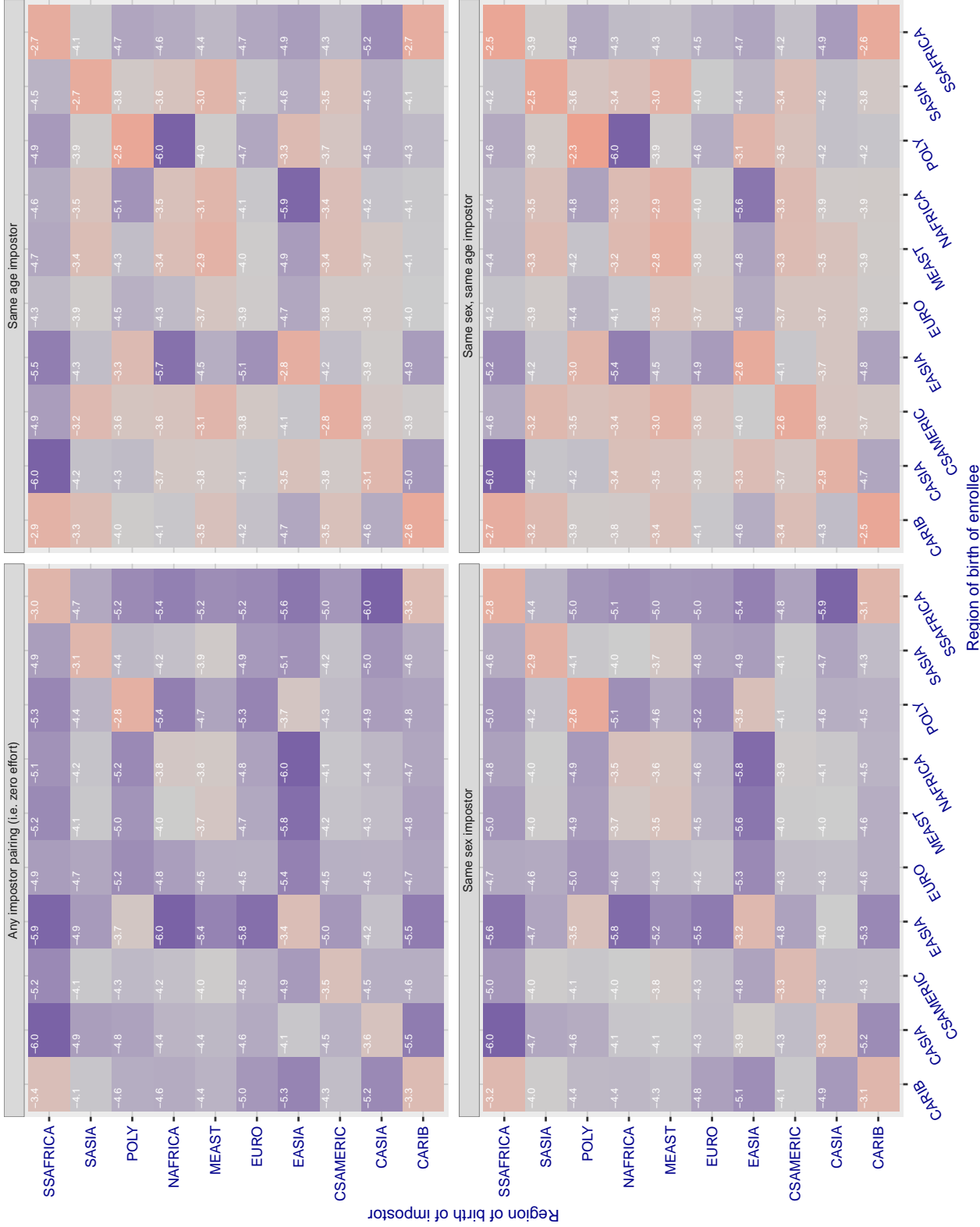


Figure 262: For algorithm *synesis-005* operating on visa images, the heatmap shows false match rates observed over impostor comparisons of faces from different individuals who were born in the given region pair. False matches are counted against a recognition threshold fixed globally to give the target FMR in the plot title, computed over all on the order of  $10^{10}$  impostor comparisons. If text appears in each box it give the same quantity as that coded by the color. Grey indicates FMR is at the intended FMR target level. Light red colors present a security vulnerability to, for example, a passport gate. Each +1 increase in  $\log_{10} FMR$  corresponds to a factor of 10 increase in FMR. The matrix is not quite symmetric because images in the enrollment and verification sets are different.

### Cross region FMR at threshold T = 147.661 for algorithm tech5\_002, giving FMR(T) = 0.0001 globally.

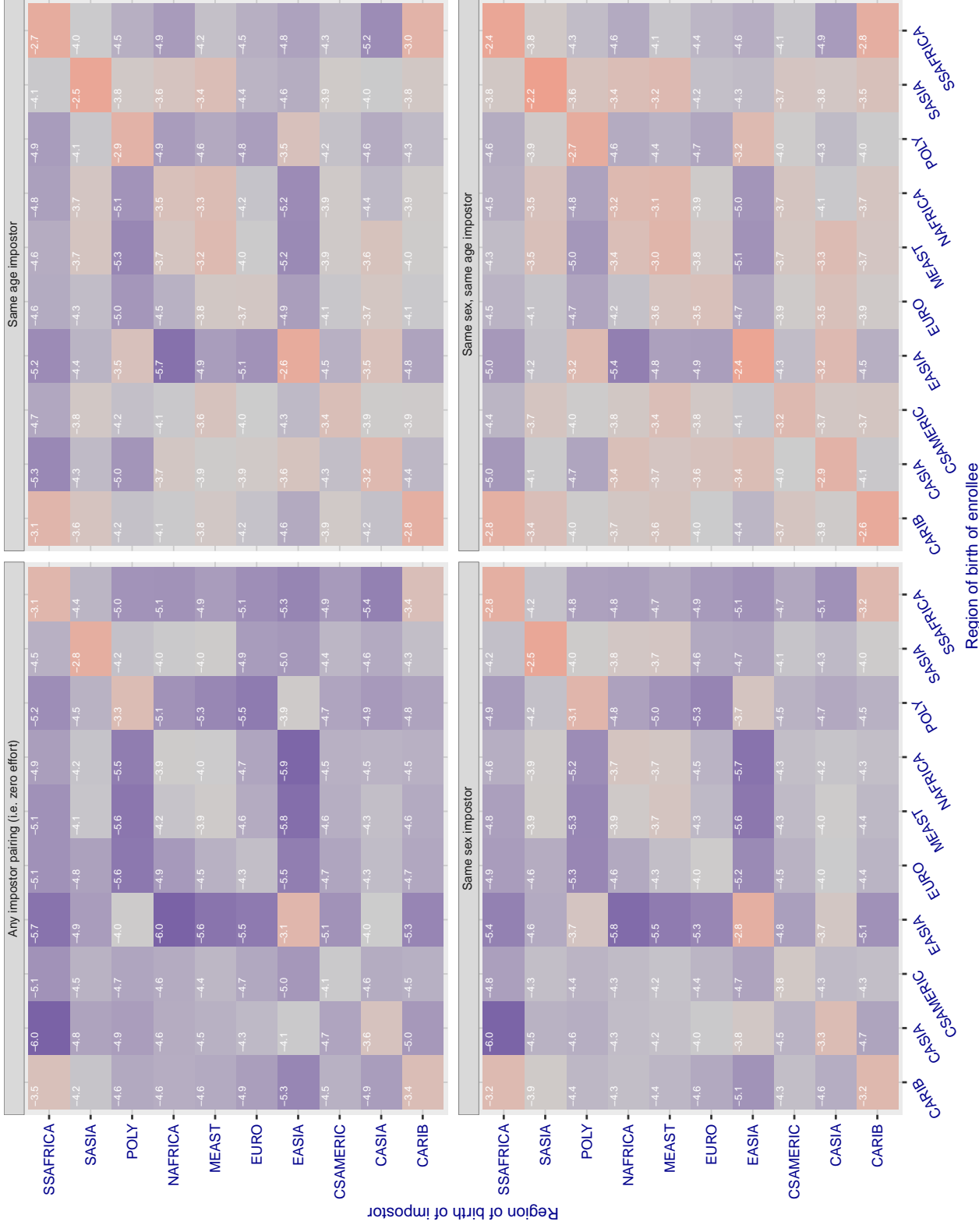


Figure 263: For algorithm tech5-002 operating on visa images, the heatmap shows false match rates observed over impostor comparisons of faces from different individuals who were born in the given region pair. False matches are counted against a recognition threshold fixed globally to give the target FMR in the plot title, computed over all on the order of  $10^{10}$  impostor comparisons. If text appears in each box it give the same quantity as that coded by the color. Grey indicates FMR is at the intended FMR target level. Light red colors present a security vulnerability to, for example, a passport gate. Each +1 increase in  $\log_{10} FMR$  corresponds to a factor of 10 increase in FMR. The matrix is not quite symmetric because images in the enrollment and verification sets are different.

### Cross region FMR at threshold T = 147.080 for algorithm tech5\_003, giving FMR(T) = 0.0001 globally.

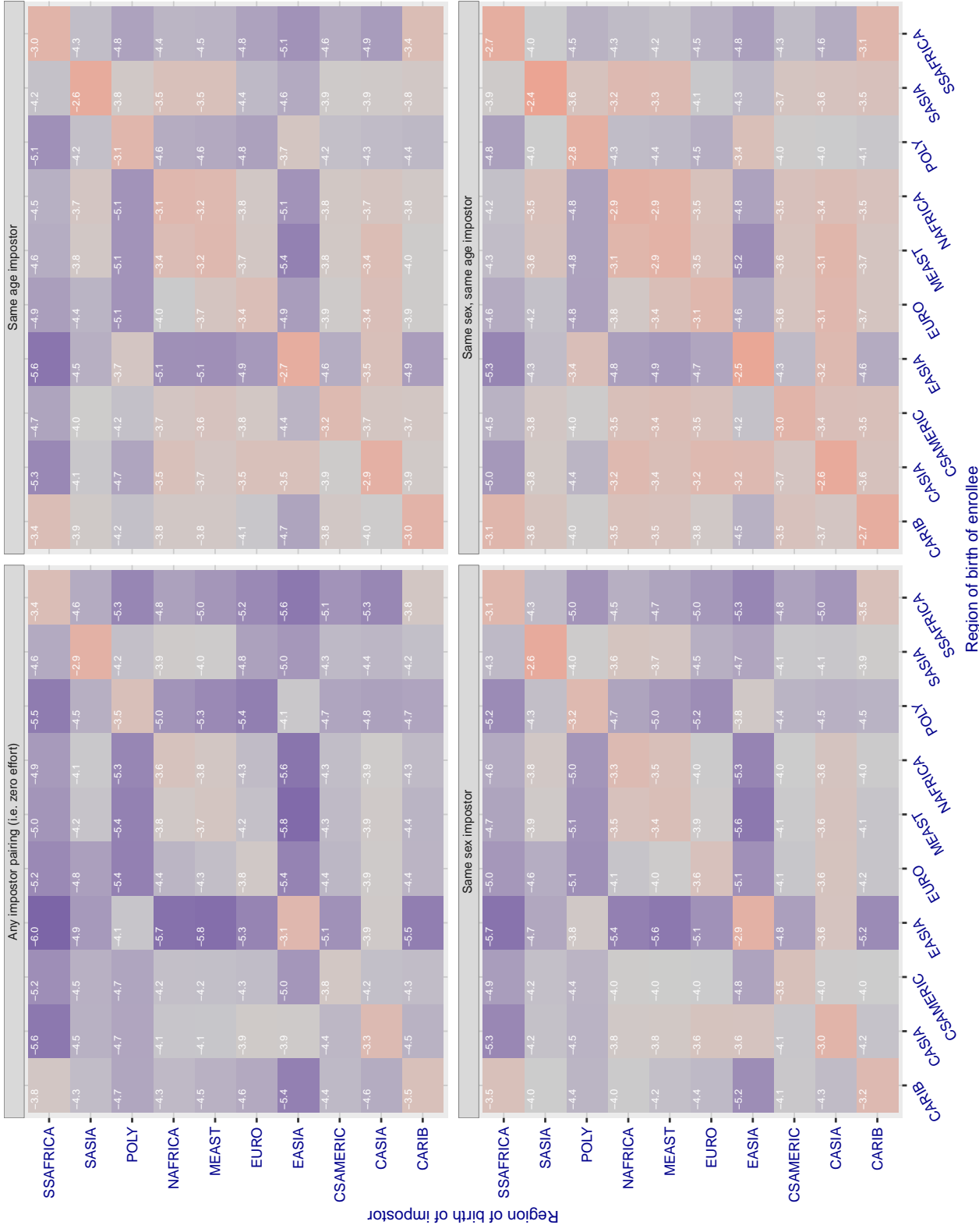


Figure 264: For algorithm tech5-003 operating on visa images, the heatmap shows false match rates observed over impostor comparisons of faces from different individuals who were born in the given region pair. False matches are counted against a recognition threshold fixed globally to give the target FMR in the plot title, computed over all on the order of  $10^{10}$  impostor comparisons. If text appears in each box it give the same quantity as that coded by the color. Grey indicates FMR is at the intended FMR target level. Light red colors present a security vulnerability to, for example, a passport gate. Each +1 increase in  $\log_{10} \text{FMR}$  corresponds to a factor of 10 increase in FMR. The matrix is not quite symmetric because images in the enrollment and verification sets are different.

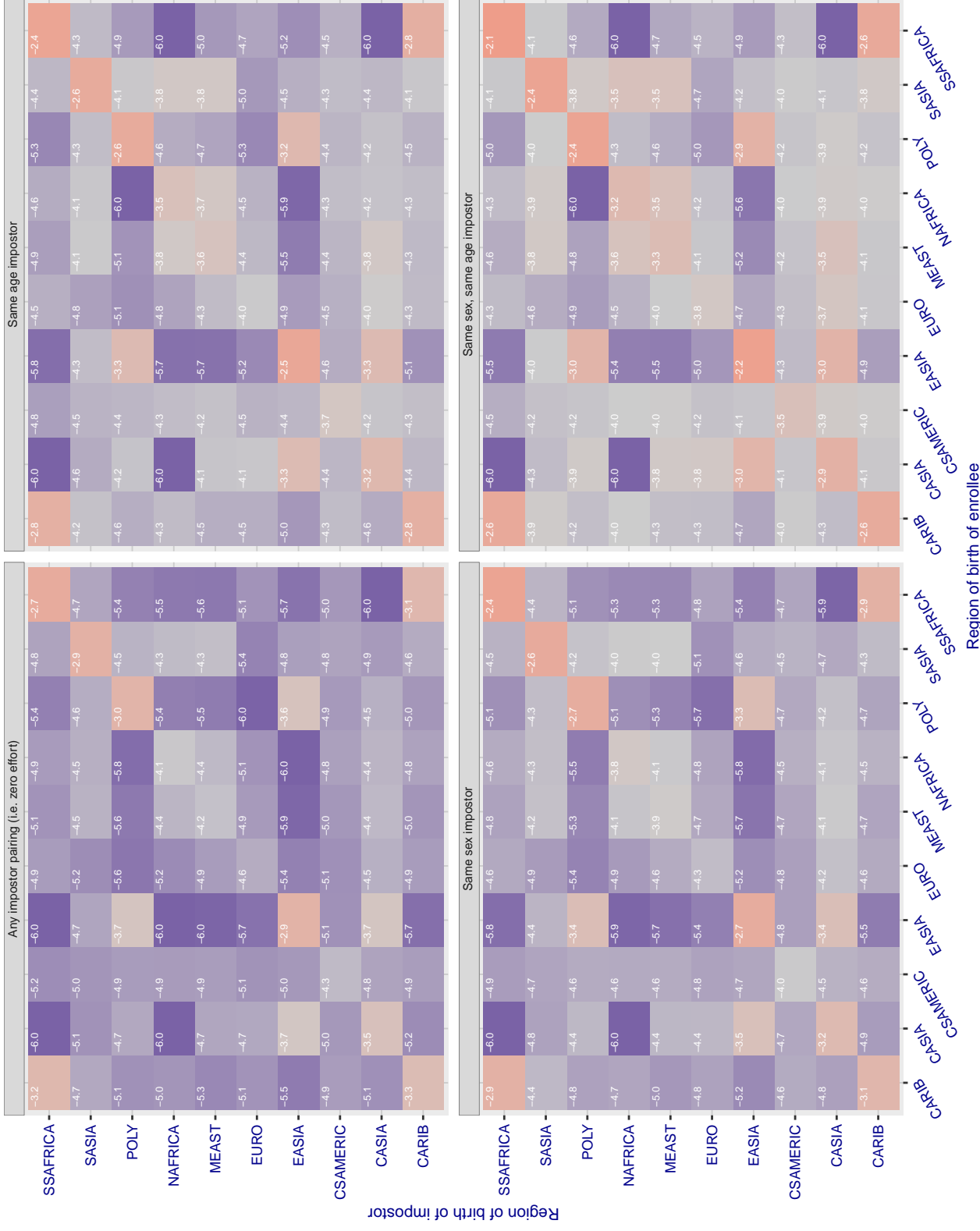
**Cross region FMR at threshold T = 0.896 for algorithm tevian\_004, giving FMR(T) = 0.0001 globally.**

Figure 265: For algorithm tevian-004 operating on visa images, the heatmap shows false match rates observed over impostor comparisons of faces from different individuals who were born in the given region pair. False matches are counted against a recognition threshold fixed globally to give the target FMR in the plot title, computed over all on the order of  $10^{10}$  impostor comparisons. If text appears in each box it give the same quantity as that coded by the color. Grey indicates FMR is at the intended FMR target level. Light red colors present a security vulnerability to, for example, a passport gate. Each +1 increase in  $\log_{10} FMR$  corresponds to a factor of 10 increase in FMR. The matrix is not quite symmetric because images in the enrollment and verification sets are different.

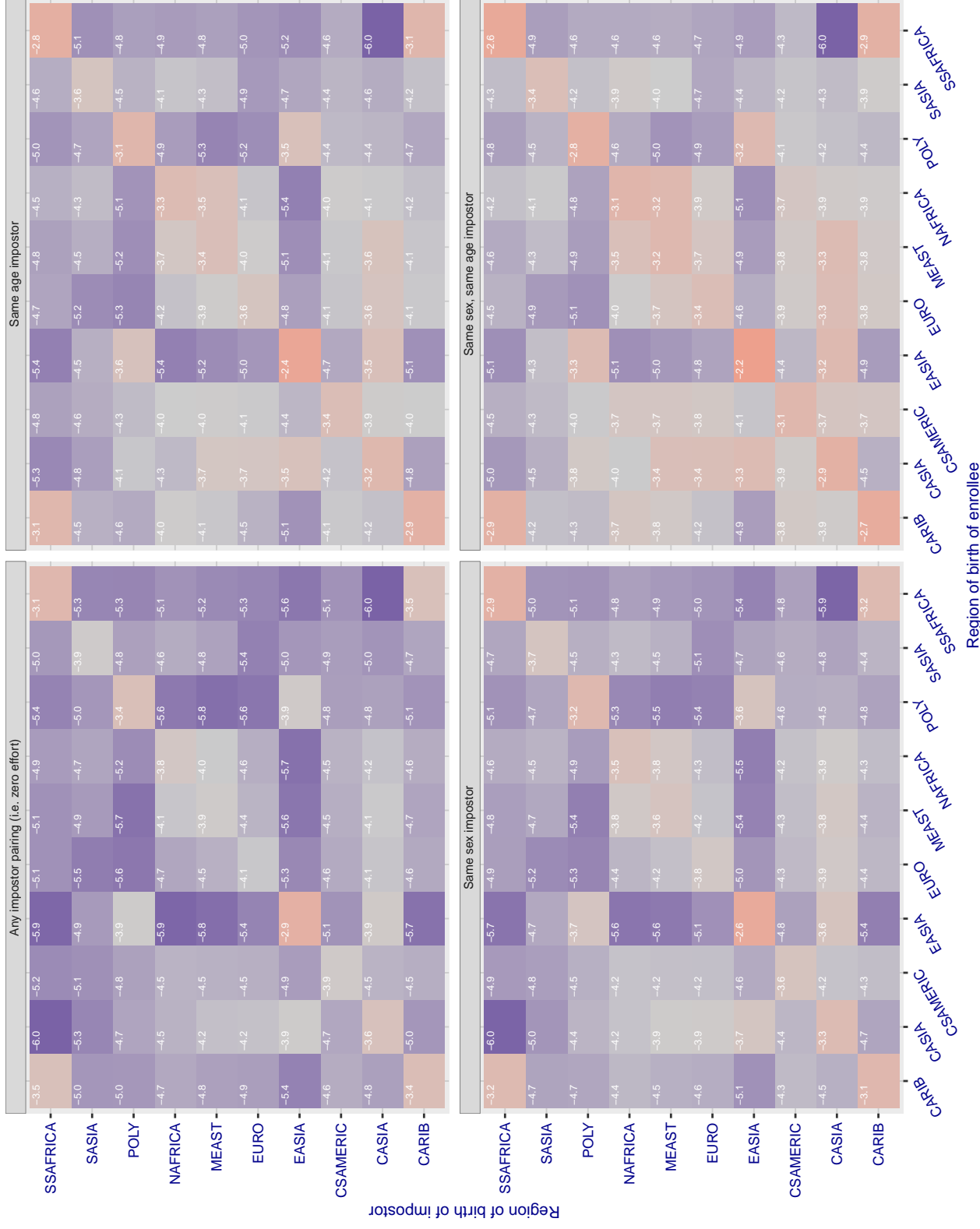
**Cross region FMR at threshold T = 0.854 for algorithm tevian\_005, giving FMR(T) = 0.0001 globally.**

Figure 266: For algorithm tevian-005 operating on visa images, the heatmap shows false match rates observed over impostor comparisons of faces from different individuals who were born in the given region pair. False matches are counted against a recognition threshold fixed globally to give the target FMR in the plot title, computed over all on the order of  $10^{10}$  impostor comparisons. If text appears in each box it give the same quantity as that coded by the color. Grey indicates FMR is at the intended FMR target level. Light red colors present a security vulnerability to, for example, a passport gate. Each +1 increase in  $\log_{10} FMR$  corresponds to a factor of 10 increase in FMR. The matrix is not quite symmetric because images in the enrollment and verification sets are different.

### Cross region FMR at threshold T = 151.011 for algorithm tiger\_002, giving $FMR(T) = 0.0001$ globally.

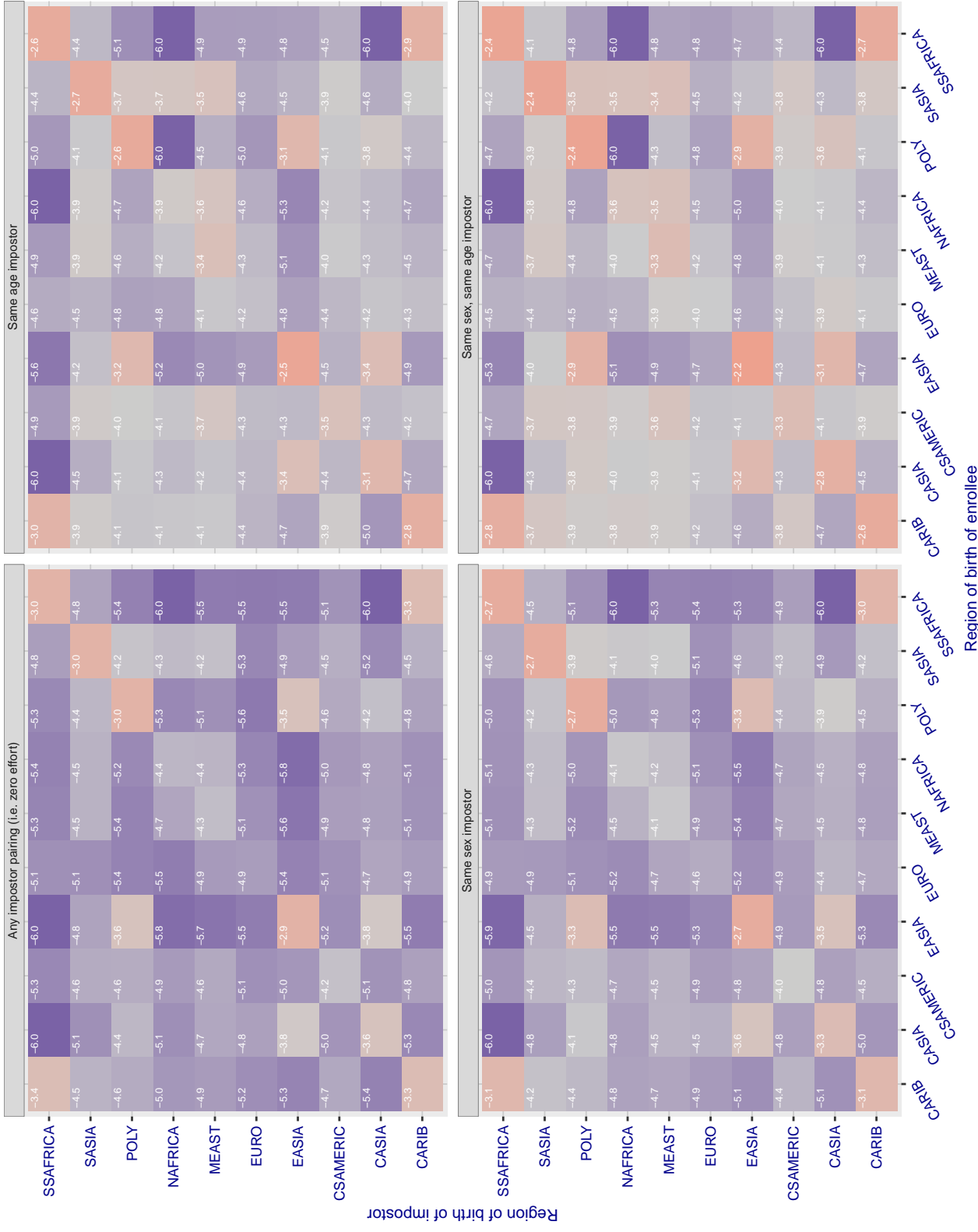


Figure 267: For algorithm tiger-002 operating on visa images, the heatmap shows false match rates observed over impostor comparisons of faces from different individuals who were born in the given region pair. False matches are counted against a recognition threshold fixed globally to give the target FMR in the plot title, computed over all on the order of  $10^{10}$  impostor comparisons. If text appears in each box it give the same quantity as that coded by the color. Grey indicates FMR is at the intended FMR target level. Light red colors present a security vulnerability to, for example, a passport gate. Each +1 increase in  $\log 10$  FMR corresponds to a factor of 10 increase in FMR. The matrix is not quite symmetric because images in the enrollment and verification sets are different.

### Cross region FMR at threshold T = 149.313 for algorithm tiger\_003, giving FMR(T) = 0.0001 globally.

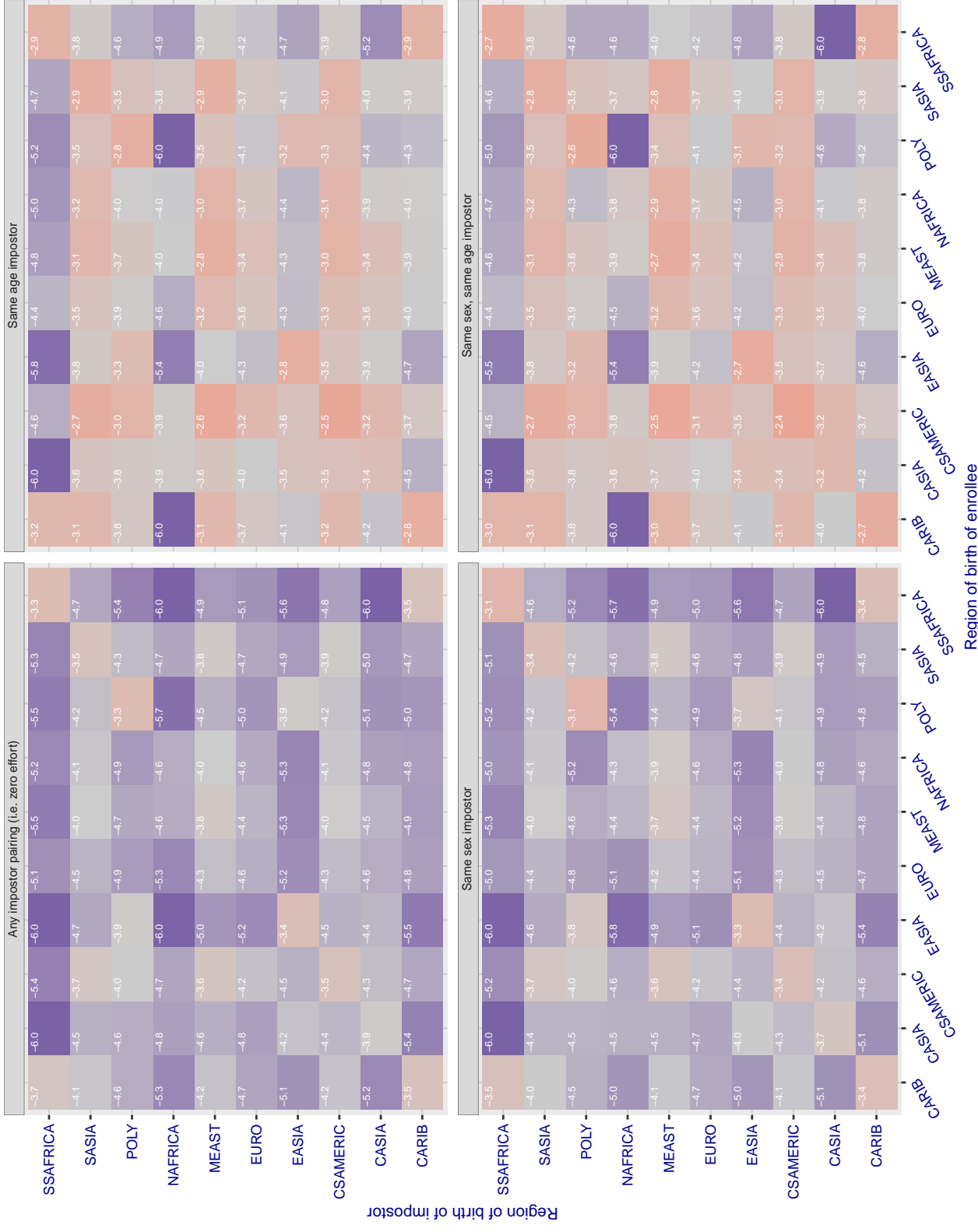


Figure 268: For algorithm tiger\_003 operating on visa images, the heatmap shows false match rates observed over impostor comparisons of faces from different individuals who were born in the given region pair. False matches are counted against a recognition threshold fixed globally to give the target FMR in the plot title, computed over all on the order of  $10^{10}$  impostor comparisons. If text appears in each box it give the same quantity as that coded by the color. Grey indicates FMR is at the intended FMR target level. Light red colors present a security vulnerability to, for example, a passport gate. Each +1 increase in  $\log 10$  FMR corresponds to a factor of 10 increase in FMR. The matrix is not quite symmetric because images in the enrollment and verification sets are different.

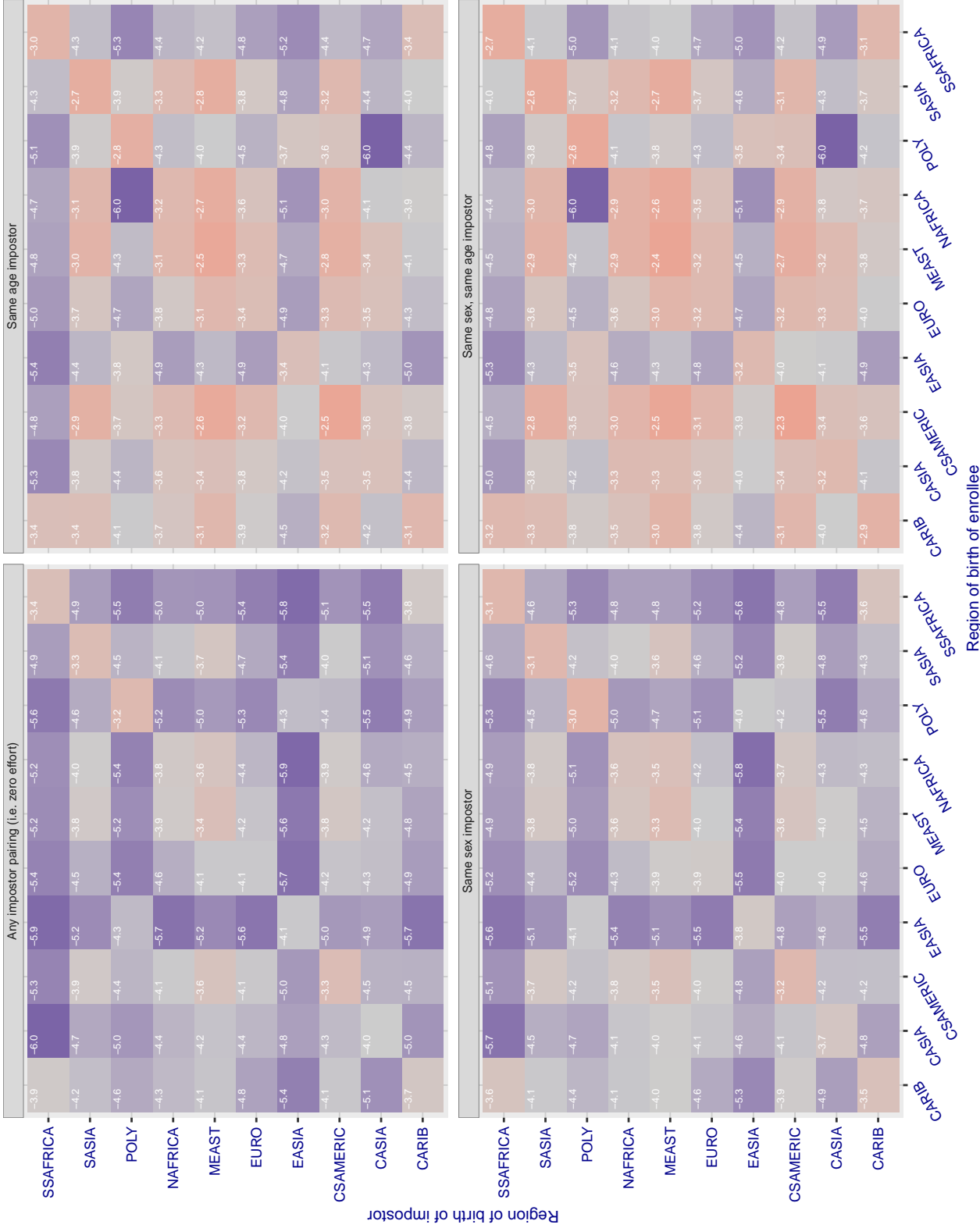
**Cross region FMR at threshold T = 43.677 for algorithm tongyi\_005, giving FMR(T) = 0.0001 globally.**

Figure 269: For algorithm tongyi-005 operating on visa images, the heatmap shows false match rates observed over impostor comparisons of faces from different individuals who were born in the given region pair. False matches are counted against a recognition threshold fixed globally to give the target FMR in the plot title, computed over all on the order of  $10^{10}$  impostor comparisons. If text appears in each box it give the same quantity as that coded by the color. Grey indicates FMR is at the intended FMR target level. Light red colors present a security vulnerability to, for example, a passport gate. Each +1 increase in  $\log_{10} FMR$  corresponds to a factor of 10 increase in FMR. The matrix is not quite symmetric because images in the enrollment and verification sets are different.

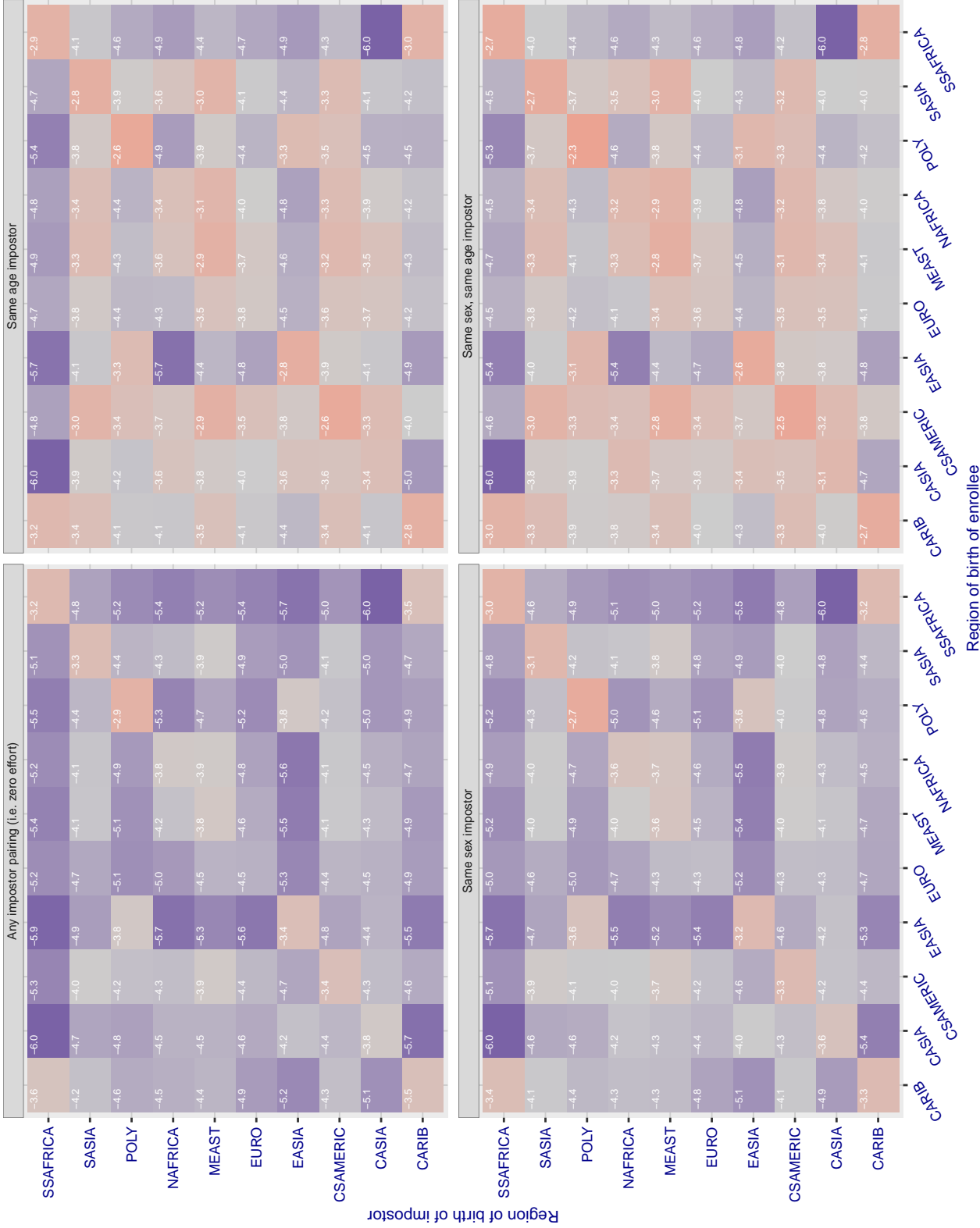
**Cross region FMR at threshold T = 0.628 for algorithm toshiba\_002, giving FMR(T) = 0.0001 globally.**

Figure 270: For algorithm toshiba-002 operating on visa images, the heatmap shows false match rates observed over impostor comparisons of faces from different individuals who were born in the given region pair. False matches are counted against a recognition threshold fixed globally to give the target FMR in the plot title, computed over all on the order of  $10^{10}$  impostor comparisons. If text appears in each box it give the same quantity as that coded by the color. Grey indicates FMR is at the intended FMR target level. Light red colors present a security vulnerability to, for example, a passport gate. Each +1 increase in  $\log_{10} FMR$  corresponds to a factor of 10 increase in FMR. The matrix is not quite symmetric because images in the enrollment and verification sets are different.

### Cross region FMR at threshold T = 0.626 for algorithm toshiba\_003, giving FMR(T) = 0.0001 globally.

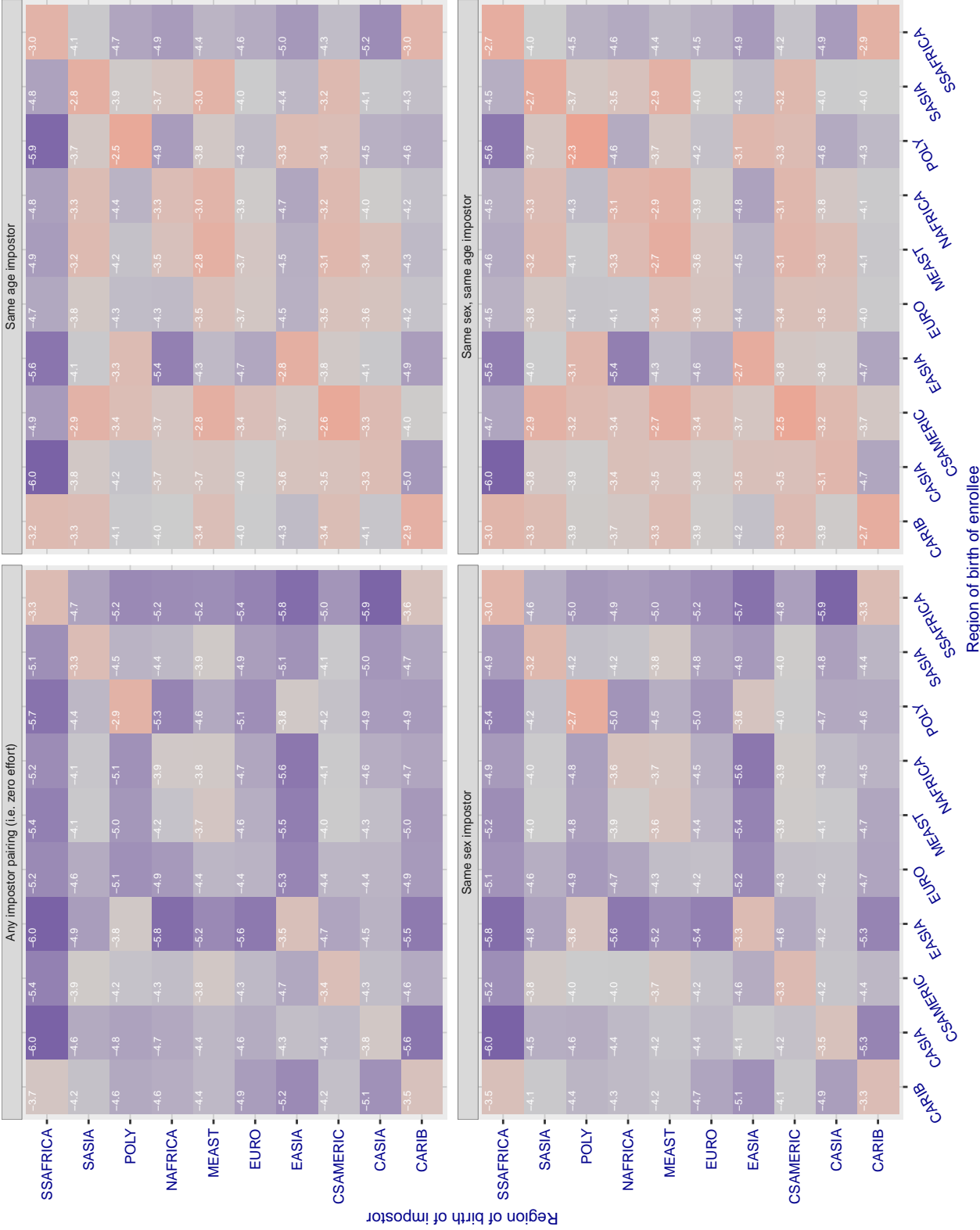


Figure 271: For algorithm toshiba-003 operating on visa images, the heatmap shows false match rates observed over impostor comparisons of faces from different individuals who were born in the given region pair. False matches are counted against a recognition threshold fixed globally to give the target FMR in the plot title, computed over all on the order of  $10^{10}$  impostor comparisons. If text appears in each box it give the same quantity as that coded by the color. Grey indicates FMR is at the intended FMR target level. Light red colors present a security vulnerability to, for example, a passport gate. Each +1 increase in  $\log_{10} FMR$  corresponds to a factor of 10 increase in FMR. The matrix is not quite symmetric because images in the enrollment and verification sets are different.

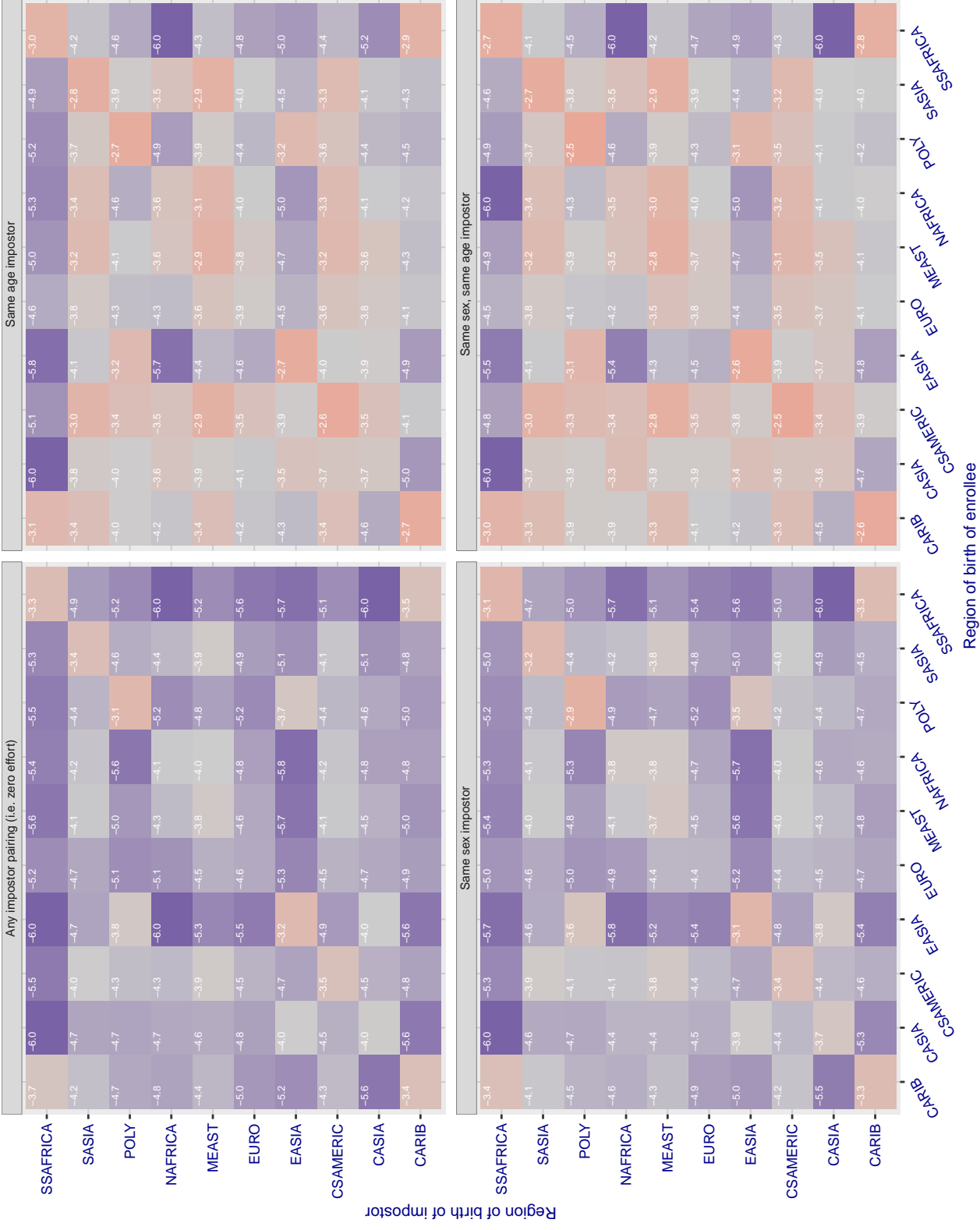
**Cross region FMR at threshold T = 0.368 for algorithm trueface\_000, giving FMR(T) = 0.0001 globally.**

Figure 272: For algorithm trueface-000 operating on visa images, the heatmap shows false match rates observed over impostor comparisons of faces from different individuals who were born in the given region pair. False matches are counted against a recognition threshold fixed globally to give the target FMR in the plot title, computed over all on the order of  $10^{10}$  impostor comparisons. If text appears in each box it give the same quantity as that coded by the color. Grey indicates FMR is at the intended FMR target level. Light red colors present a security vulnerability to, for example, a passport gate. Each +1 increase in  $\log_{10} FMR$  corresponds to a factor of 10 increase in FMR. The matrix is not quite symmetric because images in the enrollment and verification sets are different.

### Cross region FMR at threshold T = 0.151 for algorithm ulsee\_001, giving FMR(T) = 0.0001 globally.

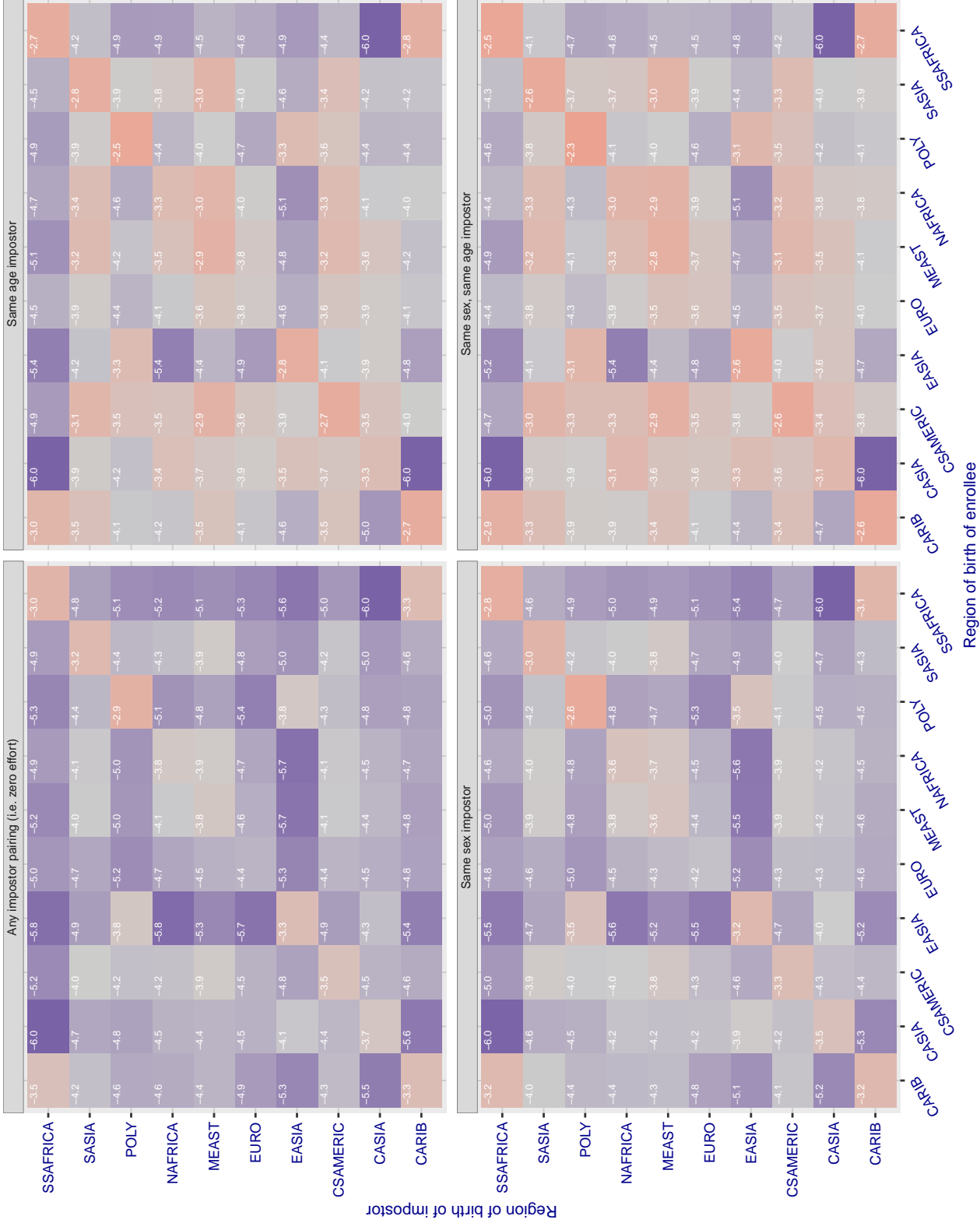


Figure 273: For algorithm ulsee\_001 operating on visa images, the heatmap shows false match rates observed over impostor comparisons of faces from different individuals who were born in the given region pair. False matches are counted against a recognition threshold fixed globally to give the target FMR in the plot title, computed over all on the order of  $10^{10}$  impostor comparisons. If text appears in each box it give the same quantity as that coded by the color. Grey indicates FMR is at the intended FMR target level. Light red colors present a security vulnerability to, for example, a passport gate. Each +1 increase in  $\log_{10}$  FMR corresponds to a factor of 10 increase in FMR. The matrix is not quite symmetric because images in the enrollment and verification sets are different.

### Cross region FMR at threshold T = 0.771 for algorithm uluface\_002, giving FMR(T) = 0.0001 globally.

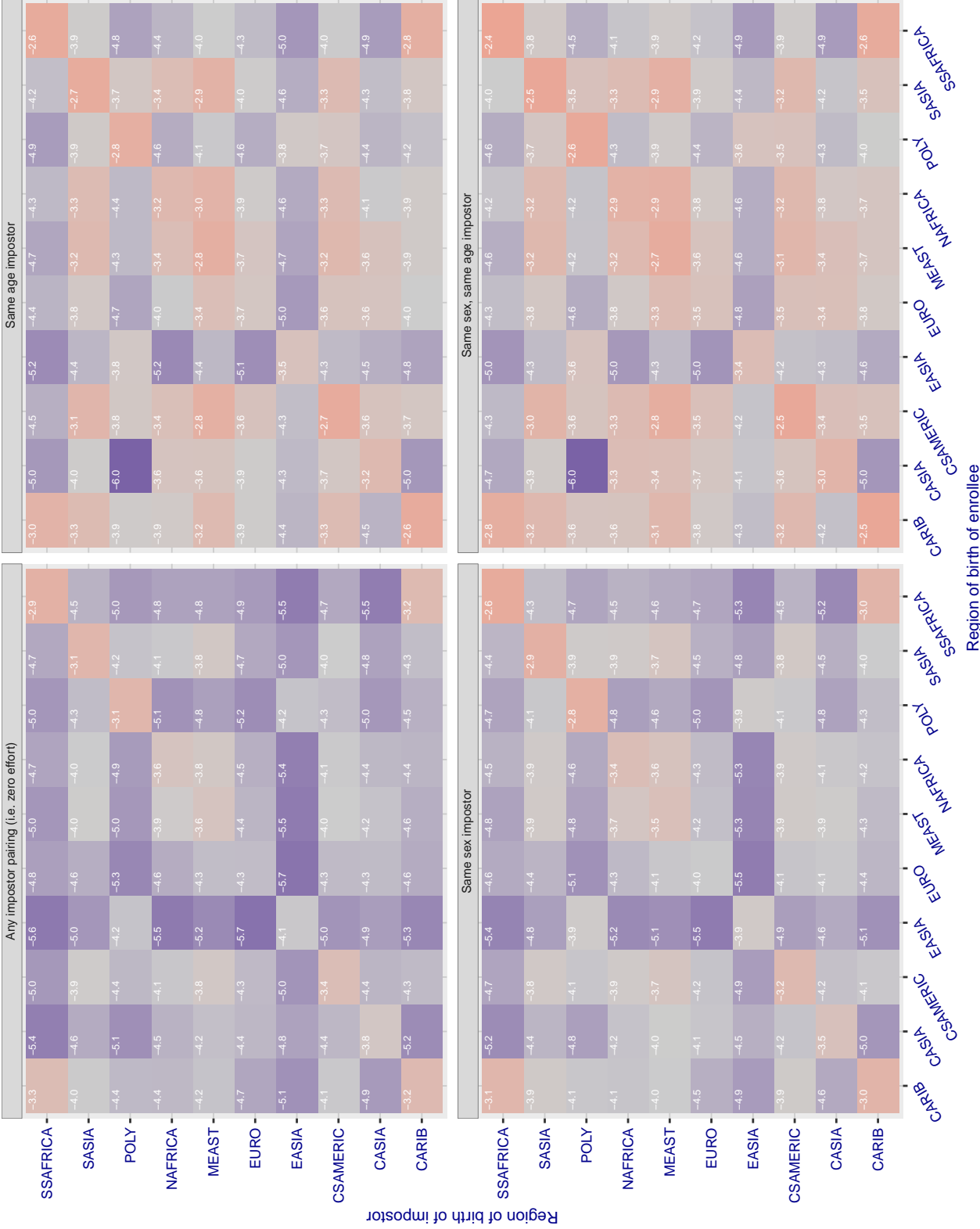


Figure 274: For algorithm uluface-002 operating on visa images, the heatmap shows false match rates observed over impostor comparisons of faces from different individuals who were born in the given region pair. False matches are counted against a recognition threshold fixed globally to give the target FMR in the plot title, computed over all on the order of  $10^{10}$  impostor comparisons. If text appears in each box it give the same quantity as that coded by the color. Grey indicates FMR is at the intended FMR target level. Light red colors present a security vulnerability to, for example, a passport gate. Each +1 increase in  $\log_{10} FMR$  corresponds to a factor of 10 increase in FMR. The matrix is not quite symmetric because images in the enrollment and verification sets are different.

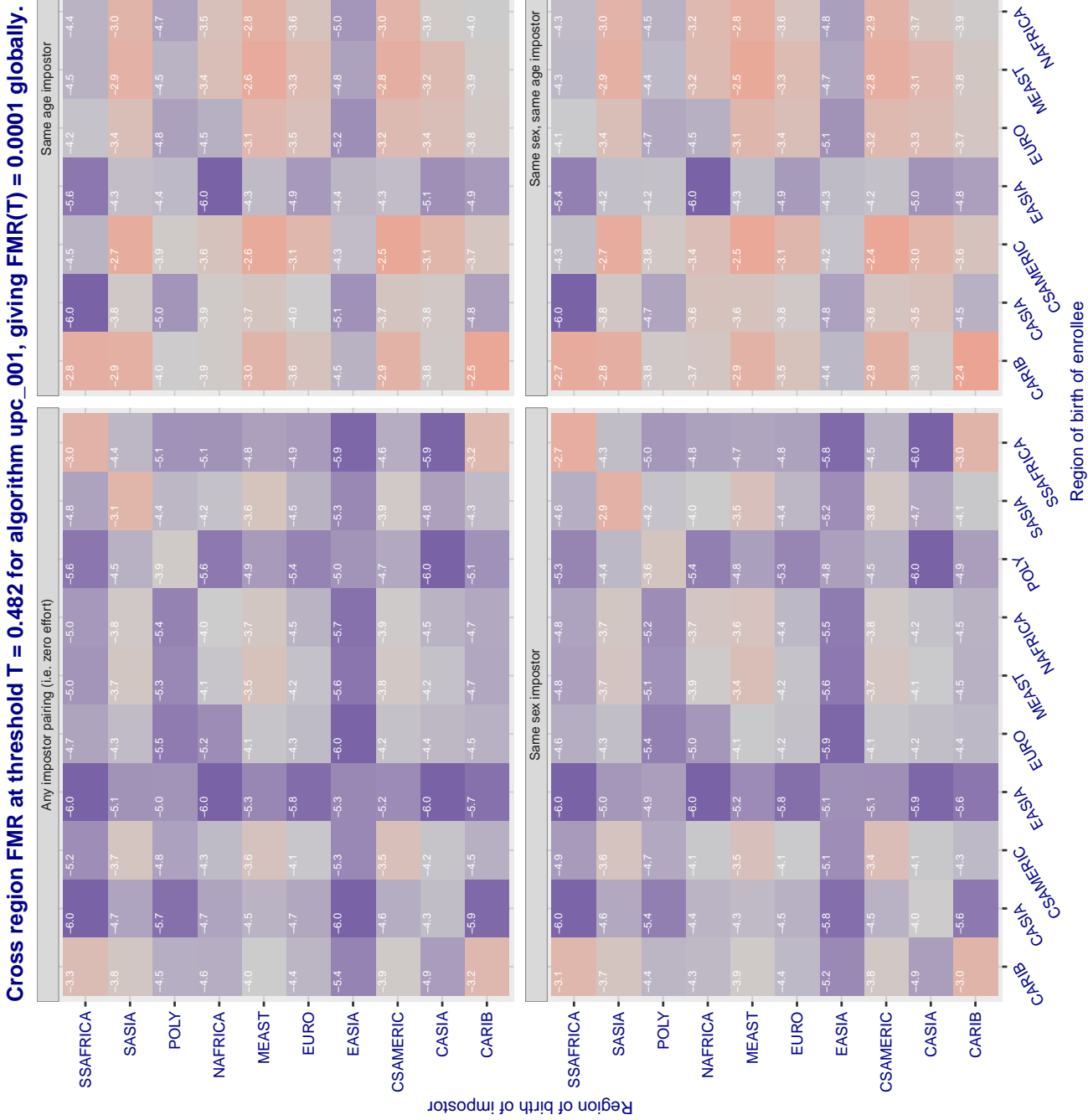


Figure 275. For algorithm upc-001 operating on visa images, the heatmap shows false match rates observed over impostor comparisons of faces from different individuals who were born in the given region pair. False matches are counted against a recognition threshold fixed globally to give the target FMR in the plot title, computed over all on the order of  $10^{10}$  impostor comparisons. If text appears in each box it give the same quantity as that coded by the color. Grey indicates FMR is at the intended FMR target level. Light red colors present a security vulnerability to, for example, a passport gate. Each +1 increase in  $\log_{10}$  FMR corresponds to a factor of 10 increase in FMR. The matrix is not quite symmetric because images in the enrollment and verification sets are different.

### Cross region FMR at threshold T = 0.428 for algorithm vcog\_002, giving FMR(T) = 0.0001 globally.

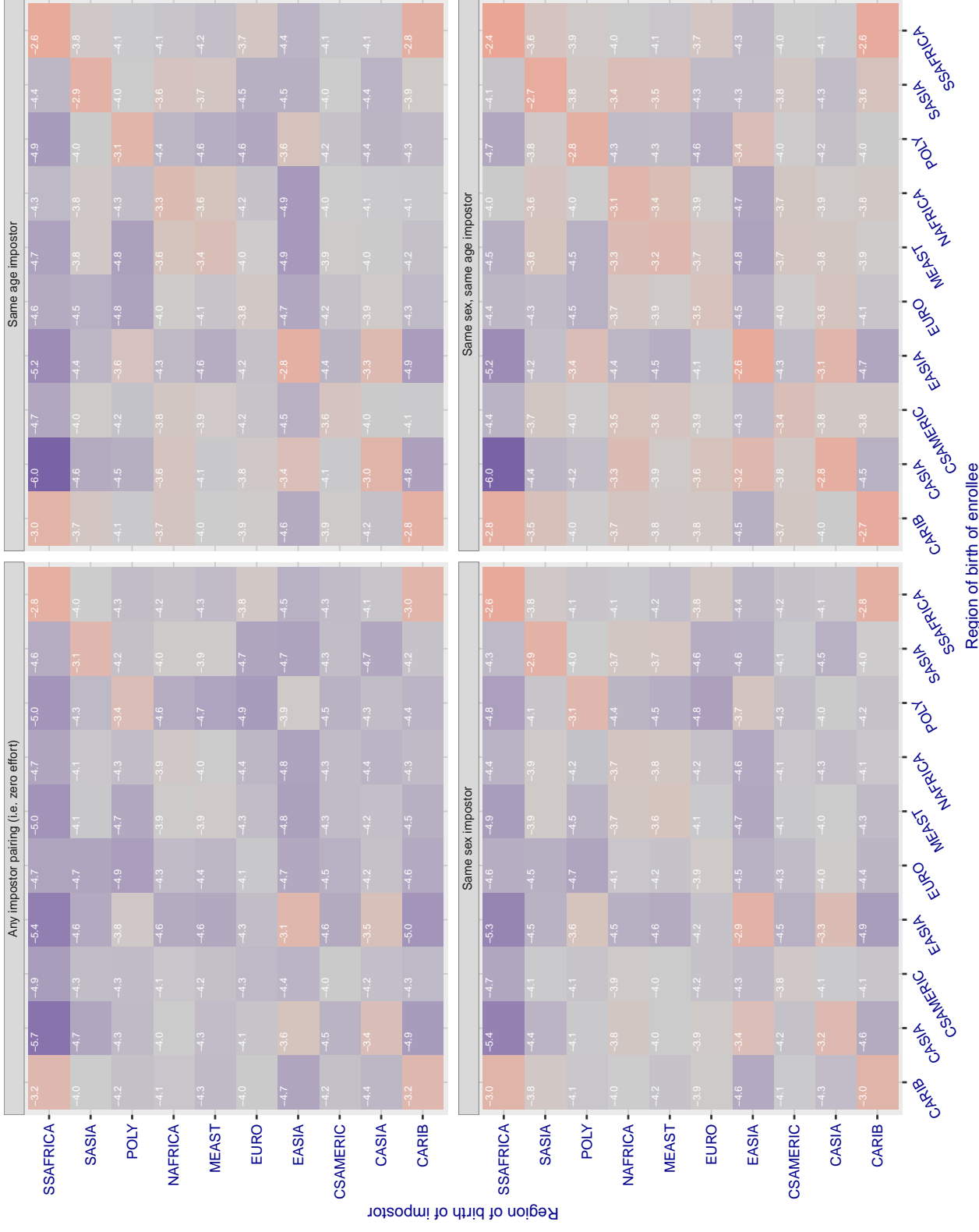


Figure 276: For algorithm vcog-002 operating on visa images, the heatmap shows false match rates observed over impostor comparisons of faces from different individuals who were born in the given region pair. False matches are counted against a recognition threshold fixed globally to give the target FMR in the plot title, computed over all on the order of  $10^{10}$  impostor comparisons. If text appears in each box it give the same quantity as that coded by the color. Grey indicates FMR is at the intended FMR target level. Light red colors present a security vulnerability to, for example, a passport gate. Each +1 increase in  $\log 10$  FMR corresponds to a factor of 10 increase in FMR. The matrix is not quite symmetric because images in the enrollment and verification sets are different.

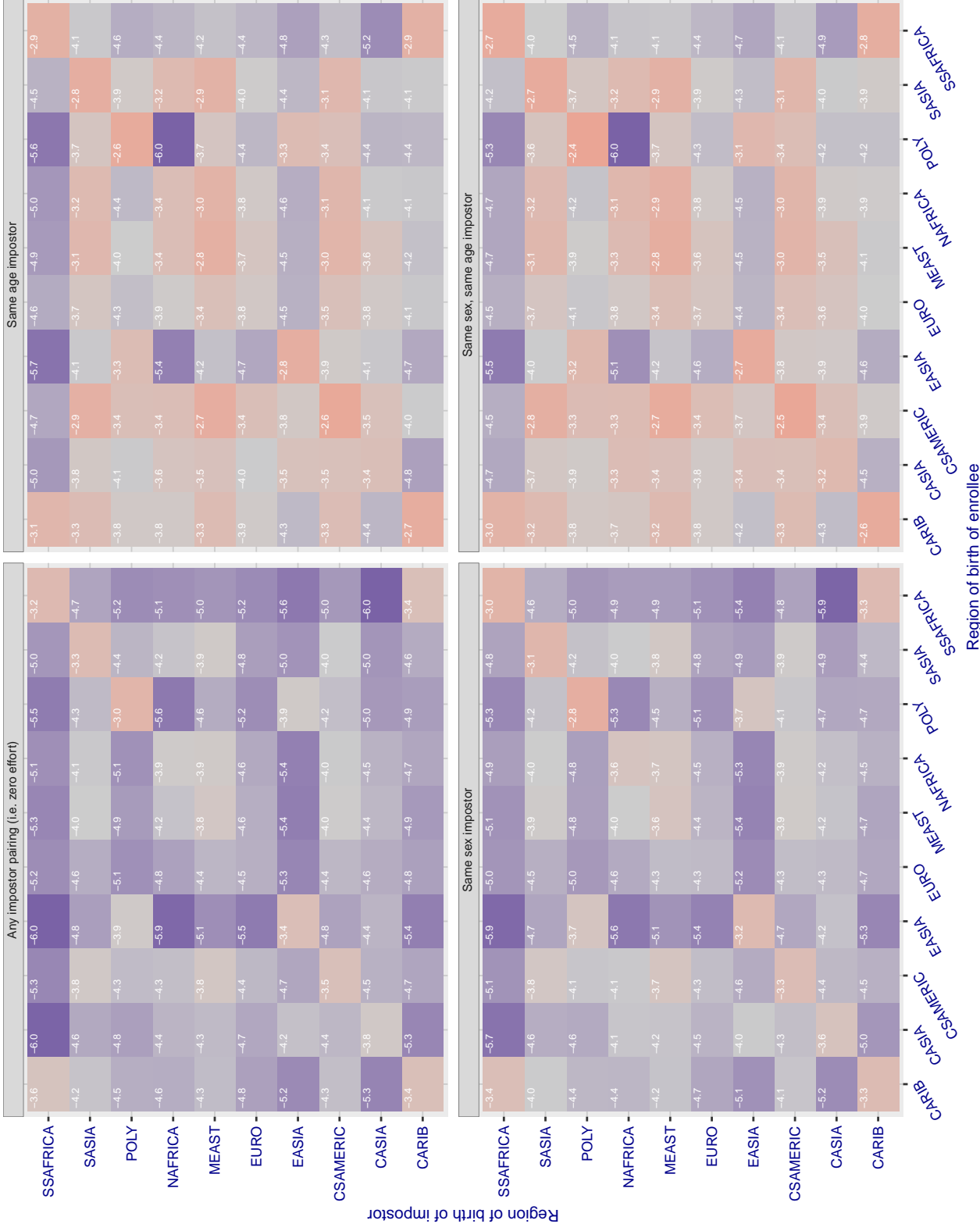
**Cross region FMR at threshold T = 71.529 for algorithm vd\_001, giving FMR(T) = 0.0001 globally.**

Figure 277: For algorithm vd\_001 operating on visa images, the heatmap shows false match rates observed over impostor comparisons of faces from different individuals who were born in the given region pair. False matches are counted against a recognition threshold fixed globally to give the target FMR in the plot title, computed over all on the order of  $10^{10}$  impostor comparisons. If text appears in each box it give the same quantity as that coded by the color. Grey indicates FMR is at the intended FMR target level. Light red colors present a security vulnerability to, for example, a passport gate. Each +1 increase in  $\log_{10}$  FMR corresponds to a factor of 10 increase in FMR. The matrix is not quite symmetric because images in the enrollment and verification sets are different.

### Cross region FMR at threshold T = 3.325 for algorithm veridas\_001, giving FMR(T) = 0.0001 globally.

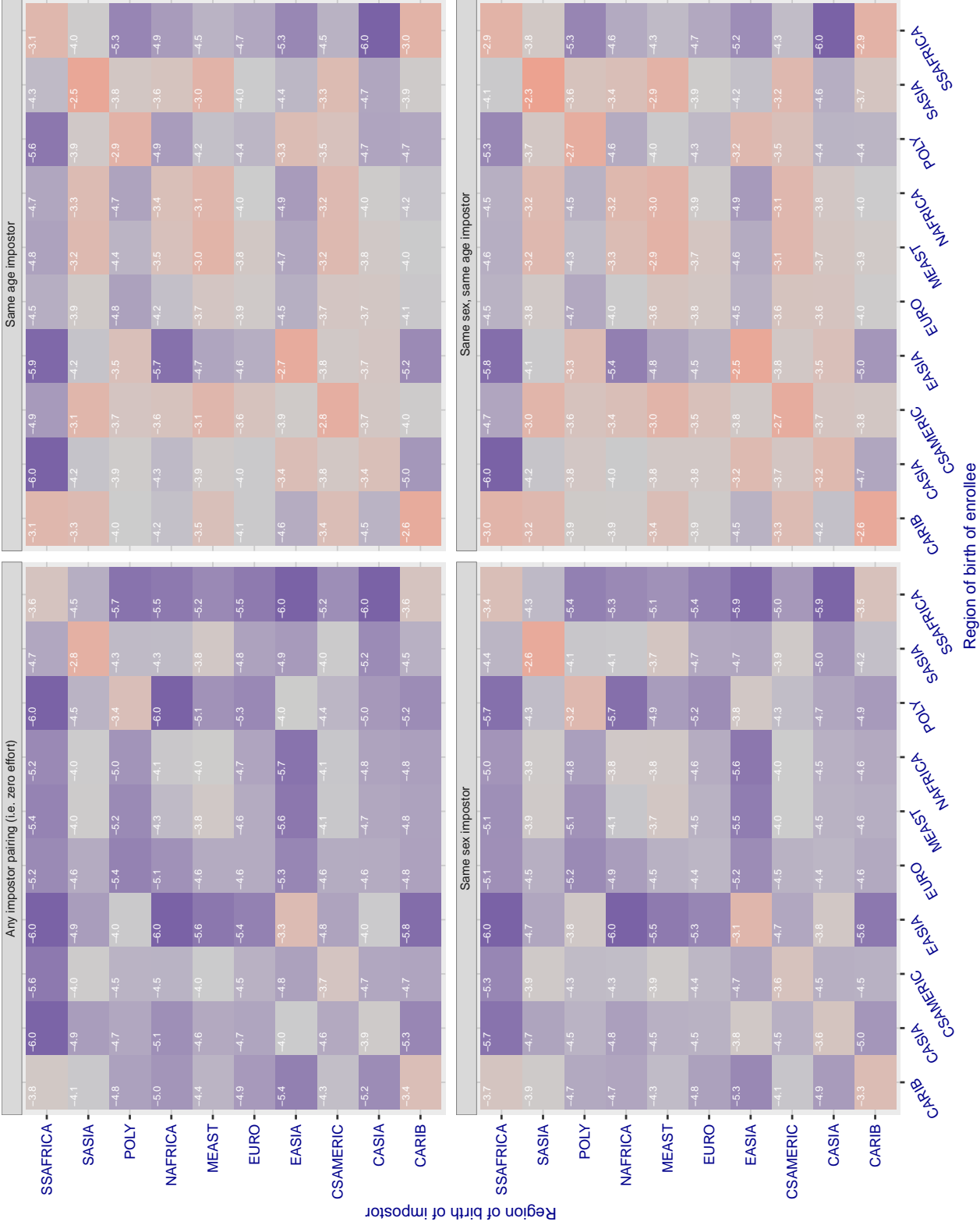
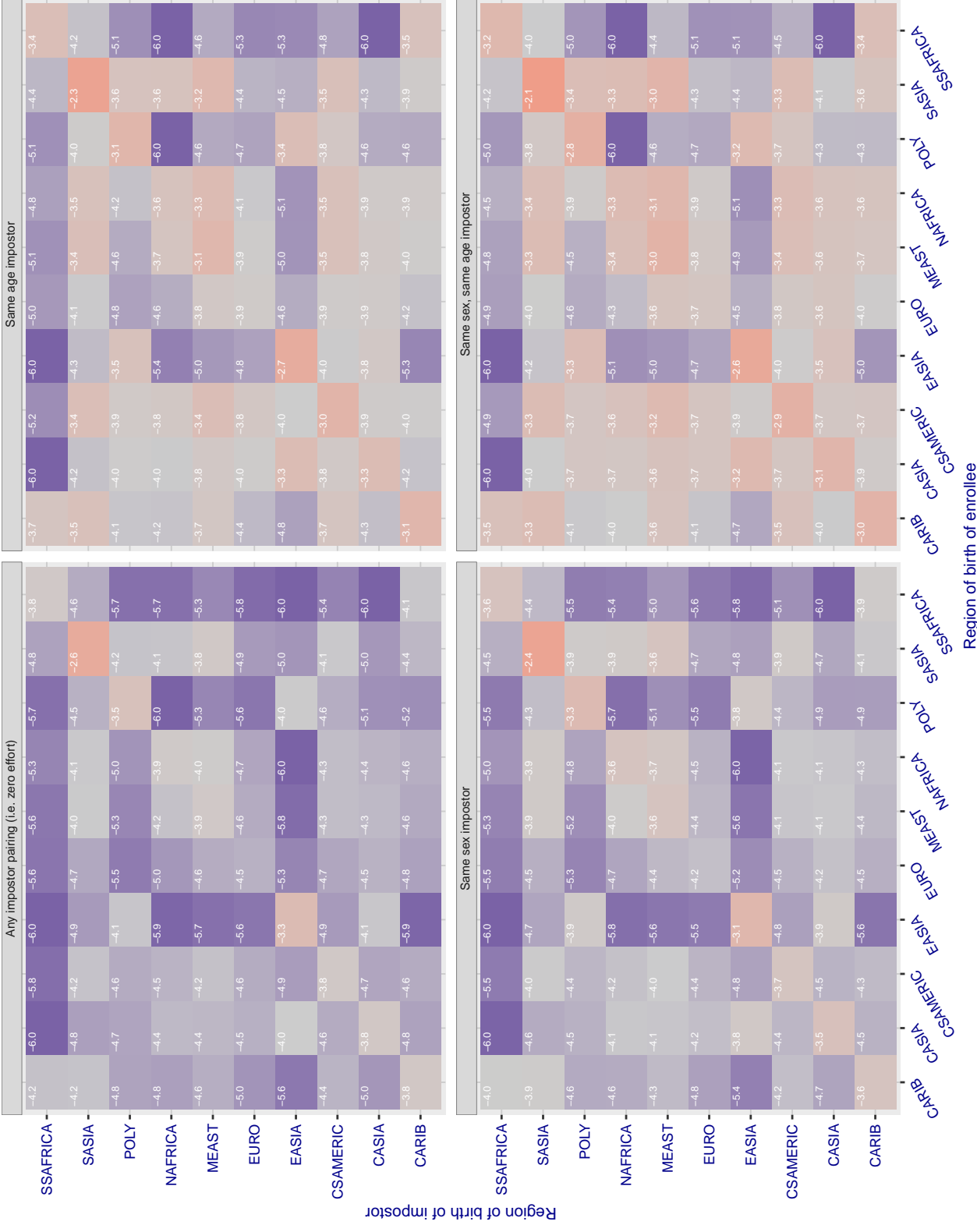


Figure 278: For algorithm veridas-001 operating on visa images, the heatmap shows false match rates observed over impostor comparisons of faces from different individuals who were born in the given region pair. False matches are counted against a recognition threshold fixed globally to give the target FMR in the plot title, computed over all on the order of  $10^{10}$  impostor comparisons. If text appears in each box it give the same quantity as that coded by the color. Grey indicates FMR is at the intended FMR target level. Light red colors present a security vulnerability to, for example, a passport gate. Each +1 increase in  $\log_{10} FMR$  corresponds to a factor of 10 increase in FMR. The matrix is not quite symmetric because images in the enrollment and verification sets are different.

**Cross region FMR at threshold T = 3.389 for algorithm veridas\_002, giving FMR(T) = 0.0001 globally.**

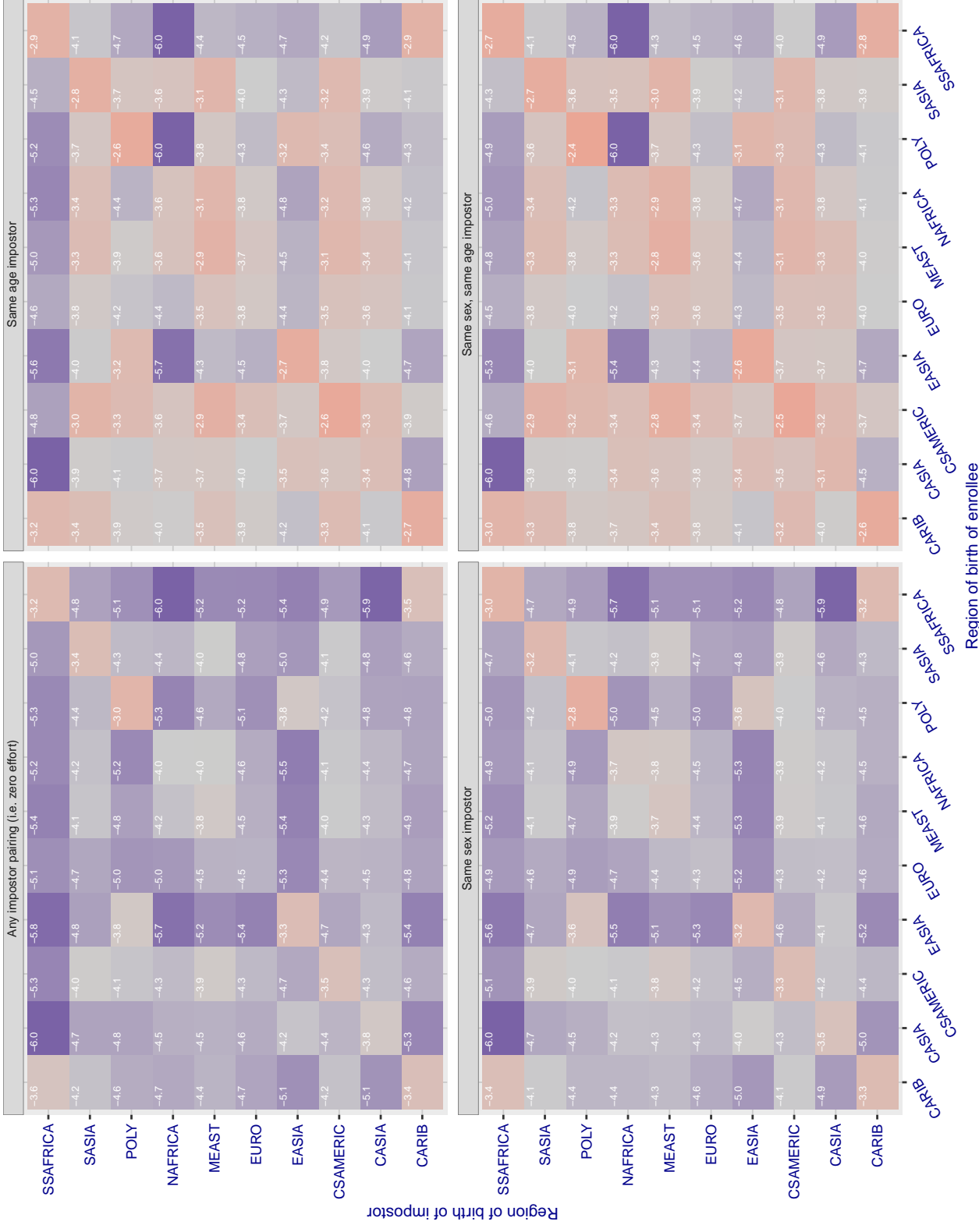
**Cross region FMR at threshold T = 2.859 for algorithm via\_000, giving FMR(T) = 0.0001 globally.**

Figure 280: For algorithm via\_000 operating on visa images, the heatmap shows false match rates observed over impostor comparisons of faces from different individuals who were born in the given region pair. False matches are counted against a recognition threshold fixed globally to give the target FMR in the plot title, computed over all on the order of  $10^{10}$  impostor comparisons. If text appears in each box it give the same quantity as that coded by the color. Grey indicates FMR is at the intended FMR target level. Light red colors present a security vulnerability to, for example, a passport gate. Each +1 increase in  $\log_{10}$  FMR corresponds to a factor of 10 increase in FMR. The matrix is not quite symmetric because images in the enrollment and verification sets are different.

### Cross region FMR at threshold T = 0.842 for algorithm videonetics\_001, giving FMR(T) = 0.0001 globally.

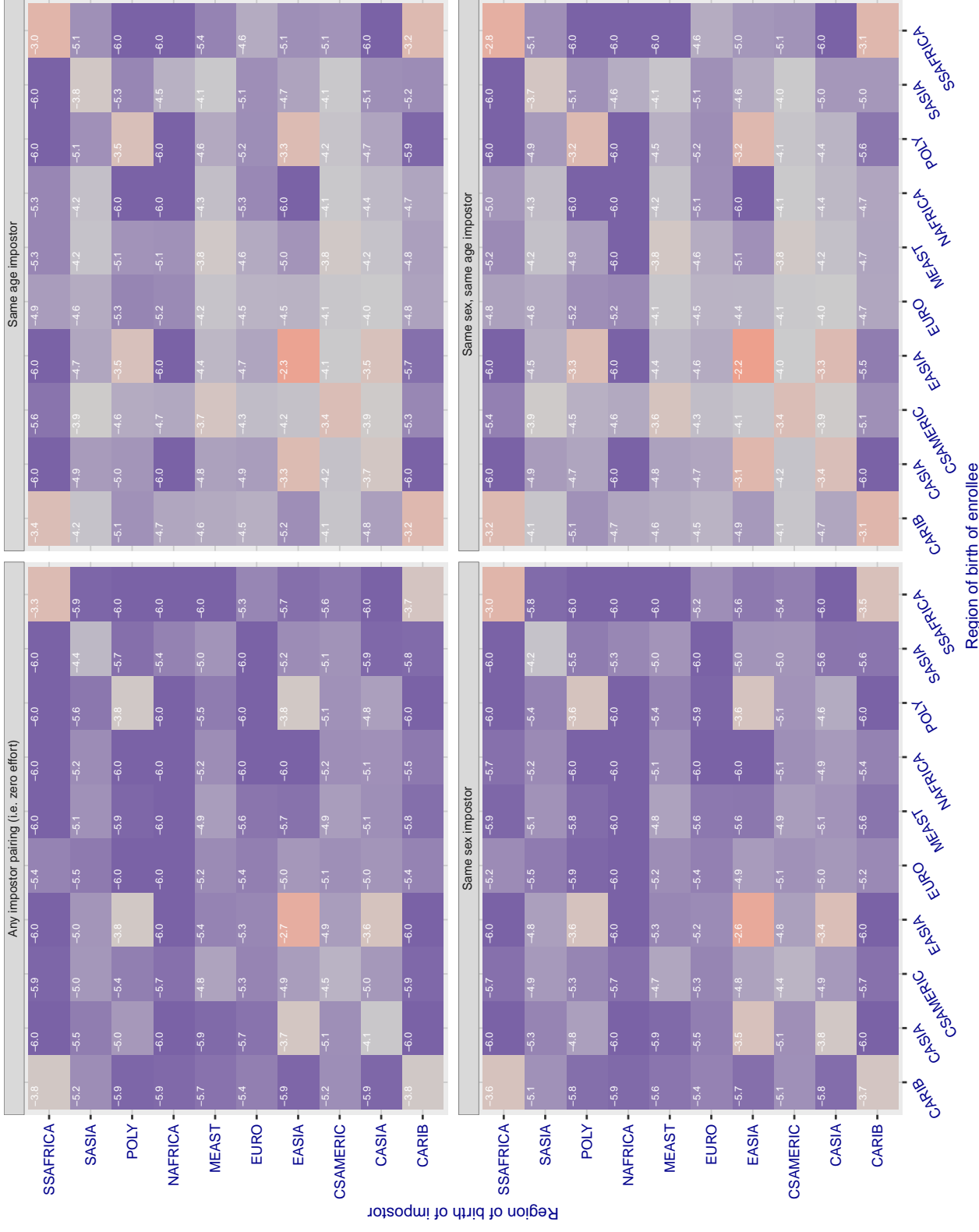


Figure 281: For algorithm videonetics-001 operating on visa images, the heatmap shows false match rates observed over impostor comparisons of faces from different individuals who were born in the given region pair. False matches are counted against a recognition threshold fixed globally to give the target FMR in the plot title, computed over all on the order of  $10^{10}$  impostor comparisons. If text appears in each box it give the same quantity as that coded by the color. Grey indicates FMR is at the intended FMR target level. Light red colors present a security vulnerability to, for example, a passport gate. Each +1 increase in  $\log_{10} FMR$  corresponds to a factor of 10 increase in FMR. The matrix is not quite symmetric because images in the enrollment and verification sets are different.

### Cross region FMR at threshold T = 3.057 for algorithm vigilantsolutions\_006, giving FMR(T) = 0.0001 globally.

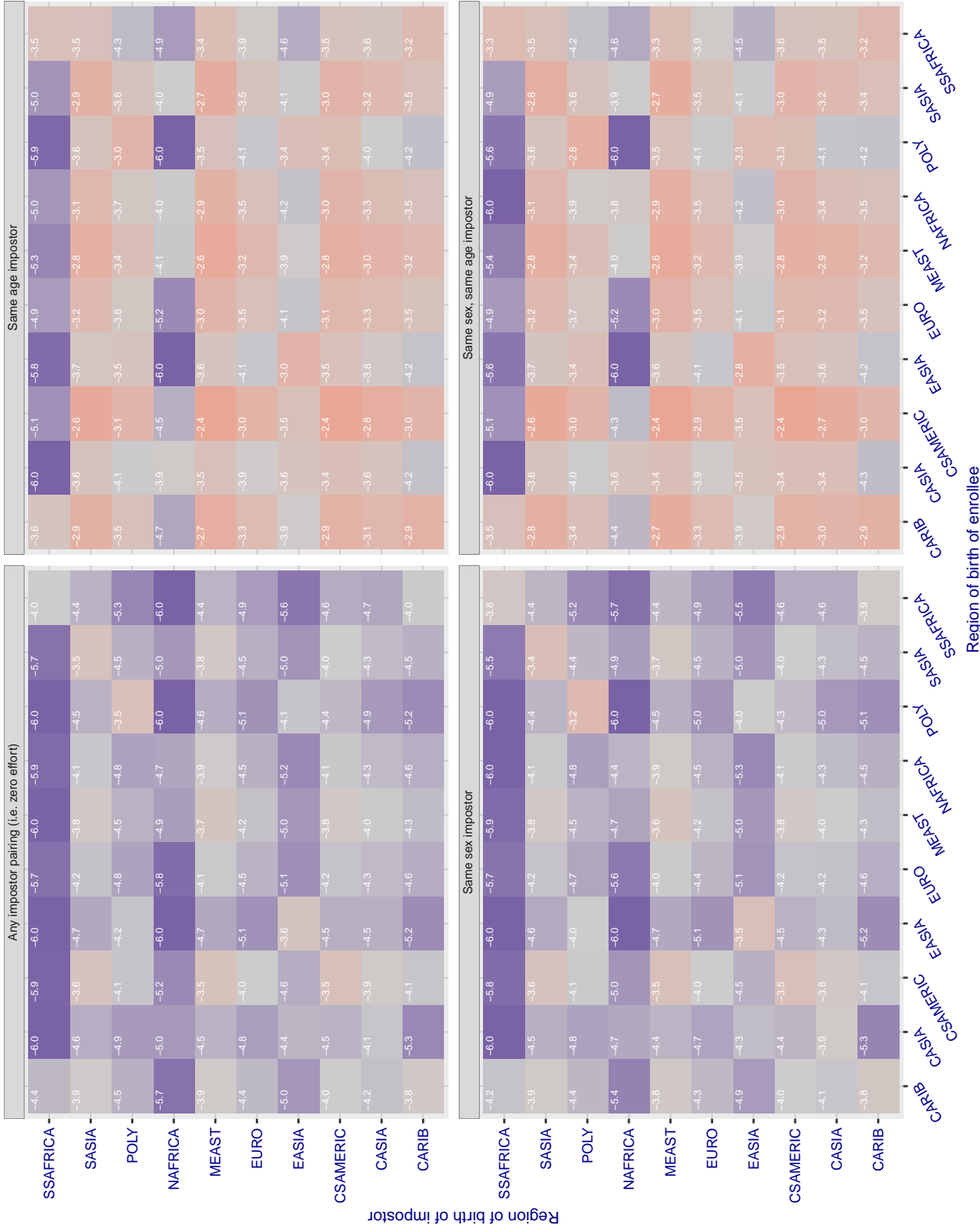


Figure 282: For algorithm vigilantsolutions-006 operating on visa images, the heatmap shows false match rates observed over impostor comparisons of faces from different individuals who were born in the given region pair. False matches are counted against a recognition threshold fixed globally to give the target FMR in the plot title, computed over all on the order of  $10^{10}$  impostor comparisons. If text appears in each box it give the same quantity as that coded by the color. Grey indicates FMR is at the intended FMR target level. Light red colors present a security vulnerability to, for example, a passport gate. Each +1 increase in  $\log_{10} FMR$  corresponds to a factor of 10 increase in FMR. The matrix is not quite symmetric because images in the enrollment and verification sets are different.

### Cross region FMR at threshold T = 2.926 for algorithm vigilantsolutions\_007, giving FMR(T) = 0.0001 globally.

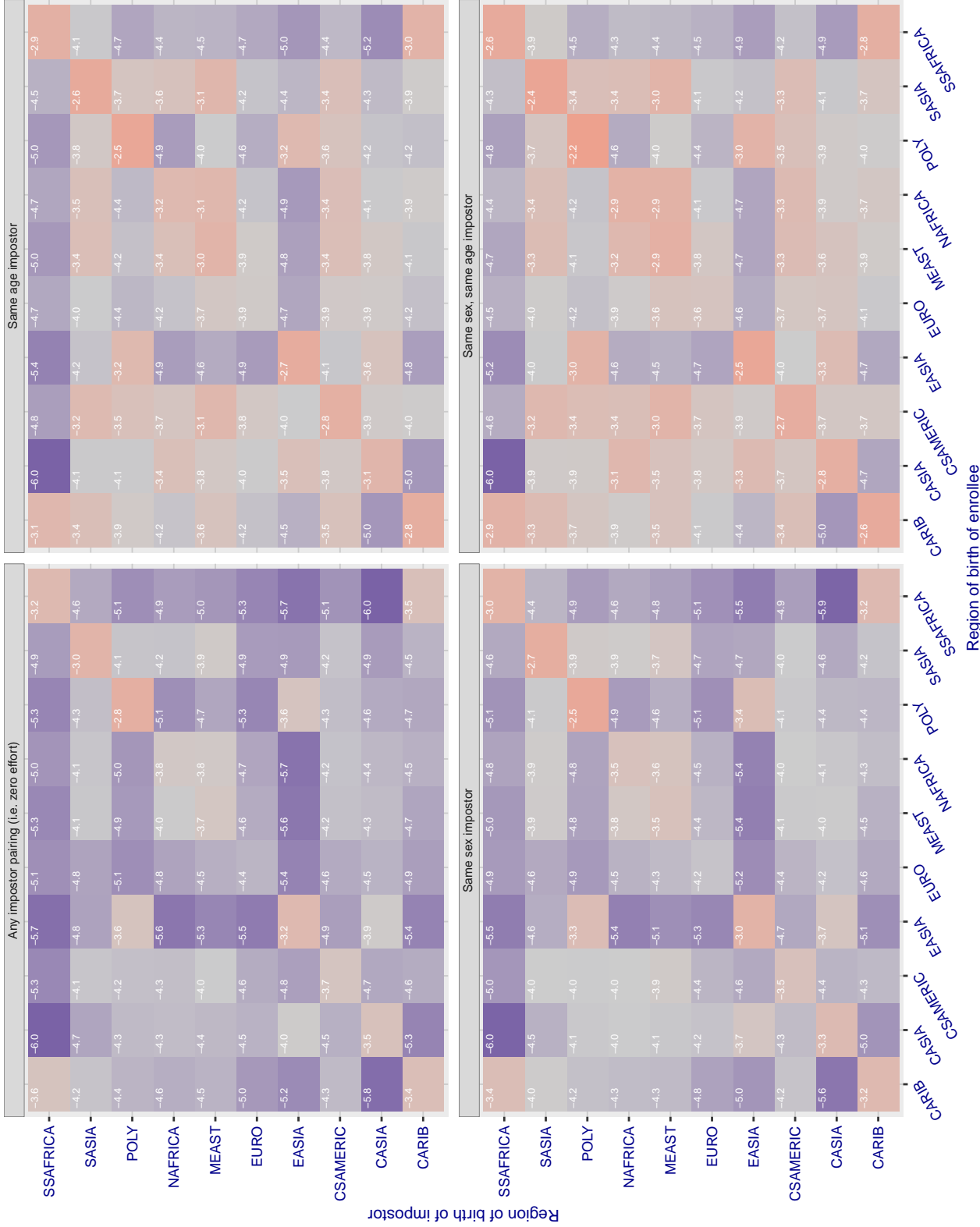


Figure 283: For algorithm vigilantsolutions-007 operating on visa images, the heatmap shows false match rates observed over impostor comparisons of faces from different individuals who were born in the given region pair. False matches are counted against a recognition threshold fixed globally to give the target FMR in the plot title, computed over all on the order of  $10^{10}$  impostor comparisons. If text appears in each box it give the same quantity as that coded by the color. Grey indicates FMR is at the intended FMR target level. Light red colors present a security vulnerability to, for example, a passport gate. Each +1 increase in  $\log_{10} FMR$  corresponds to a factor of 10 increase in FMR. The matrix is not quite symmetric because images in the enrollment and verification sets are different.

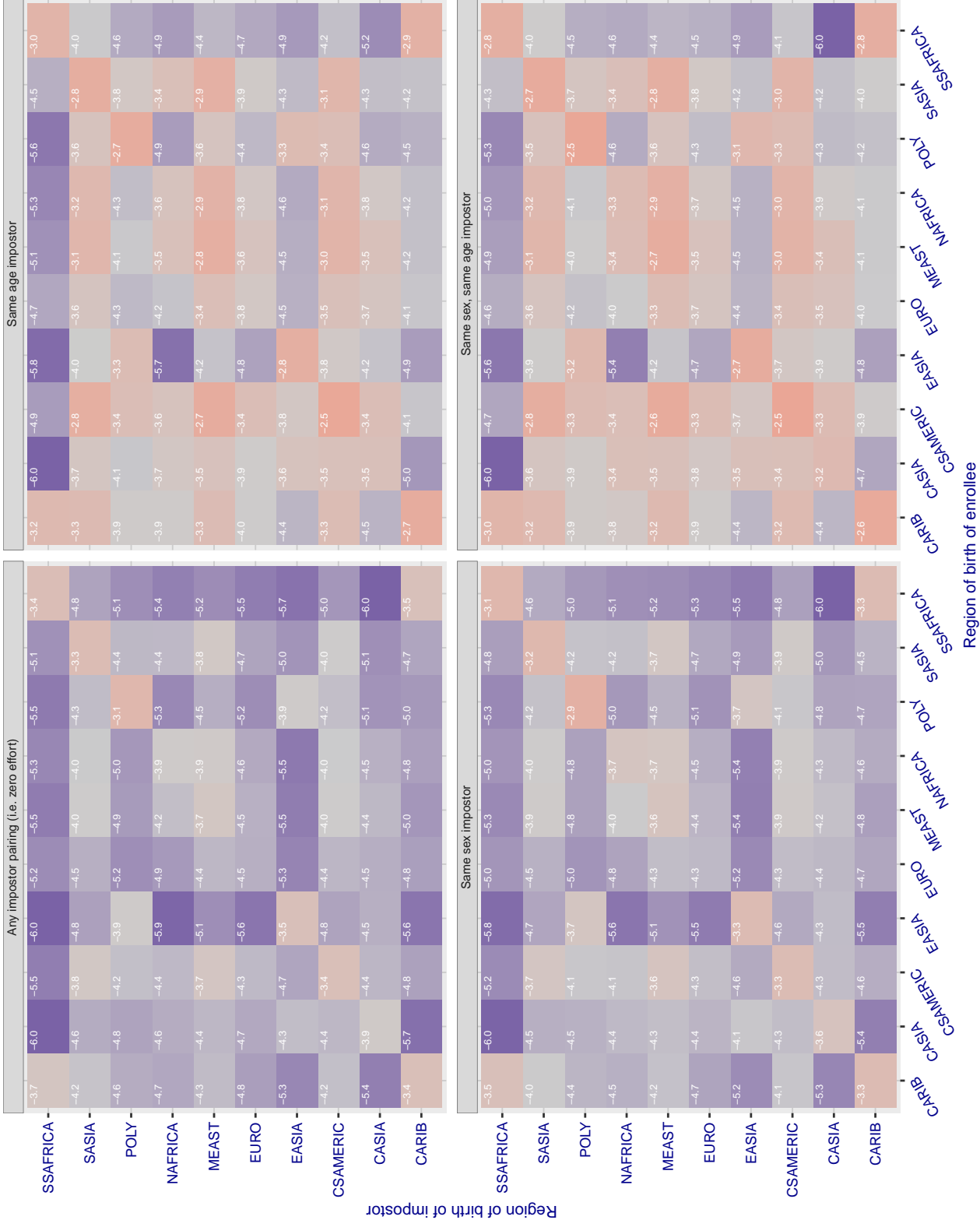
**Cross region FMR at threshold T = 0.432 for algorithm vion\_000, giving FMR(T) = 0.0001 globally.**

Figure 284: For algorithm vion-000 operating on visa images, the heatmap shows false match rates observed over impostor comparisons of faces from different individuals who were born in the given region pair. False matches are counted against a recognition threshold fixed globally to give the target FMR in the plot title, computed over all on the order of  $10^{10}$  impostor comparisons. If text appears in each box it give the same quantity as that coded by the color. Grey indicates FMR is at the intended FMR target level. Light red colors present a security vulnerability to, for example, a passport gate. Each +1 increase in  $\log 10$  FMR corresponds to a factor of 10 increase in FMR. The matrix is not quite symmetric because images in the enrollment and verification sets are different.

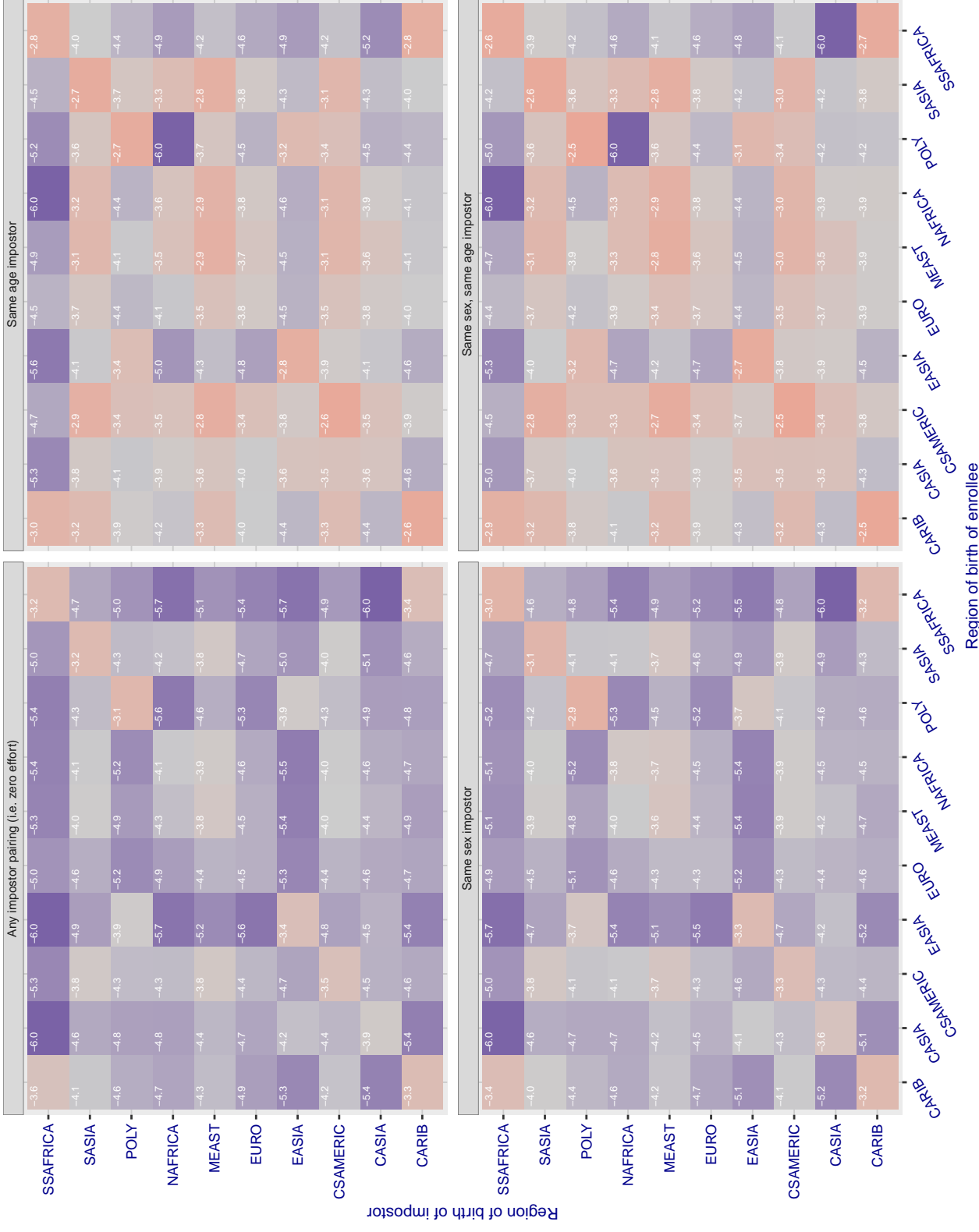
**Cross region FMR at threshold T = 0.433 for algorithm visionbox\_000, giving FMR(T) = 0.00001 globally.**

Figure 285: For algorithm visionbox-000 operating on visa images, the heatmap shows false match rates observed over impostor comparisons of faces from different individuals who were born in the given region pair. False matches are counted against a recognition threshold fixed globally to give the target FMR in the plot title, computed over all on the order of  $10^{10}$  impostor comparisons. If text appears in each box it give the same quantity as that coded by the color. Grey indicates FMR is at the intended FMR target level. Light red colors present a security vulnerability to, for example, a passport gate. Each +1 increase in  $\log_{10} FMR$  corresponds to a factor of 10 increase in FMR. The matrix is not quite symmetric because images in the enrollment and verification sets are different.

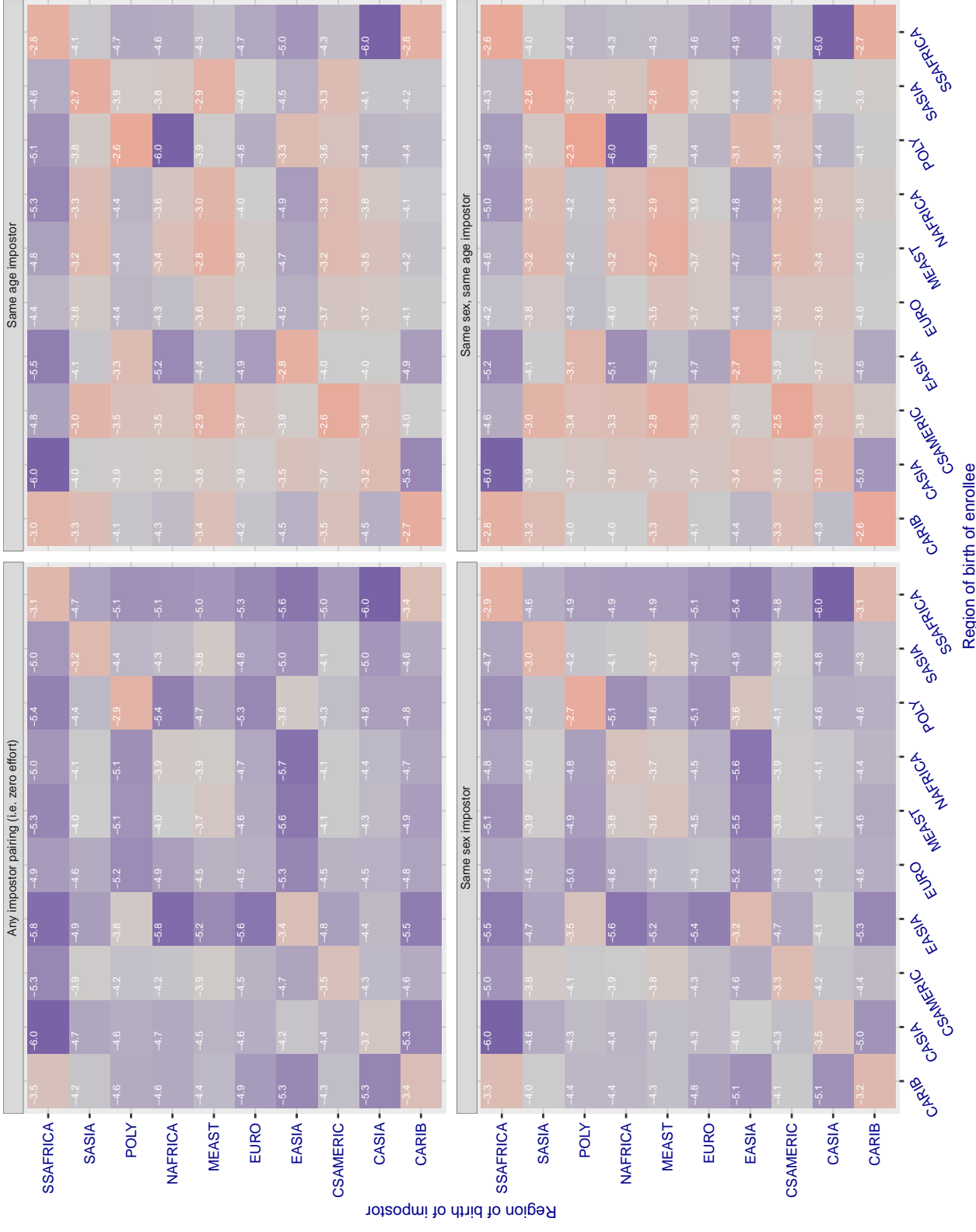
**Cross region FMR at threshold T = 0.382 for algorithm visionbox\_001, giving FMR(T) = 0.00001 globally.**

Figure 286: For algorithm visionbox-001 operating on visa images, the heatmap shows false match rates observed over impostor comparisons of faces from different individuals who were born in the given region pair. False matches are counted against a recognition threshold fixed globally to give the target FMR in the plot title, computed over all on the order of  $10^{10}$  impostor comparisons. If text appears in each box it give the same quantity as that coded by the color. Grey indicates FMR is at the intended FMR target level. Light red colors present a security vulnerability to, for example, a passport gate. Each +1 increase in  $\log_{10} FMR$  corresponds to a factor of 10 increase in FMR. The matrix is not quite symmetric because images in the enrollment and verification sets are different.

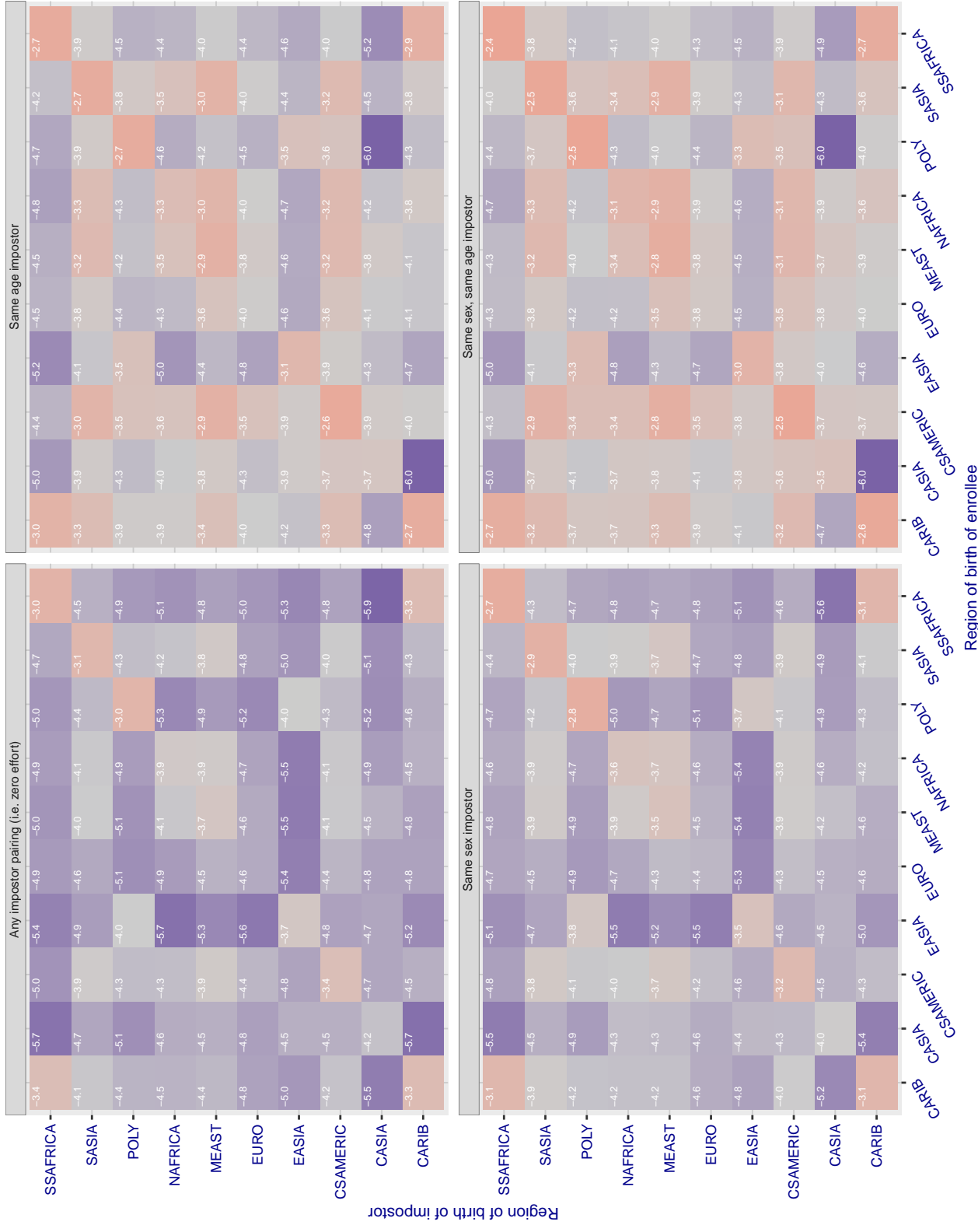
**Cross region FMR at threshold T = 0.669 for algorithm visionlabs\_006, giving  $FMR(T) = 0.0001$  globally.**

Figure 287: For algorithm visionlabs-006 operating on visa images, the heatmap shows false match rates observed over impostor comparisons of faces from different individuals who were born in the given region pair. False matches are counted against a recognition threshold fixed globally to give the target FMR in the plot title, computed over all on the order of  $10^{10}$  impostor comparisons. If text appears in each box it give the same quantity as that coded by the color. Grey indicates FMR is at the intended FMR target level. Light red colors present a security vulnerability to, for example, a passport gate. Each +1 increase in  $\log_{10} FMR$  corresponds to a factor of 10 increase in FMR. The matrix is not quite symmetric because images in the enrollment and verification sets are different.

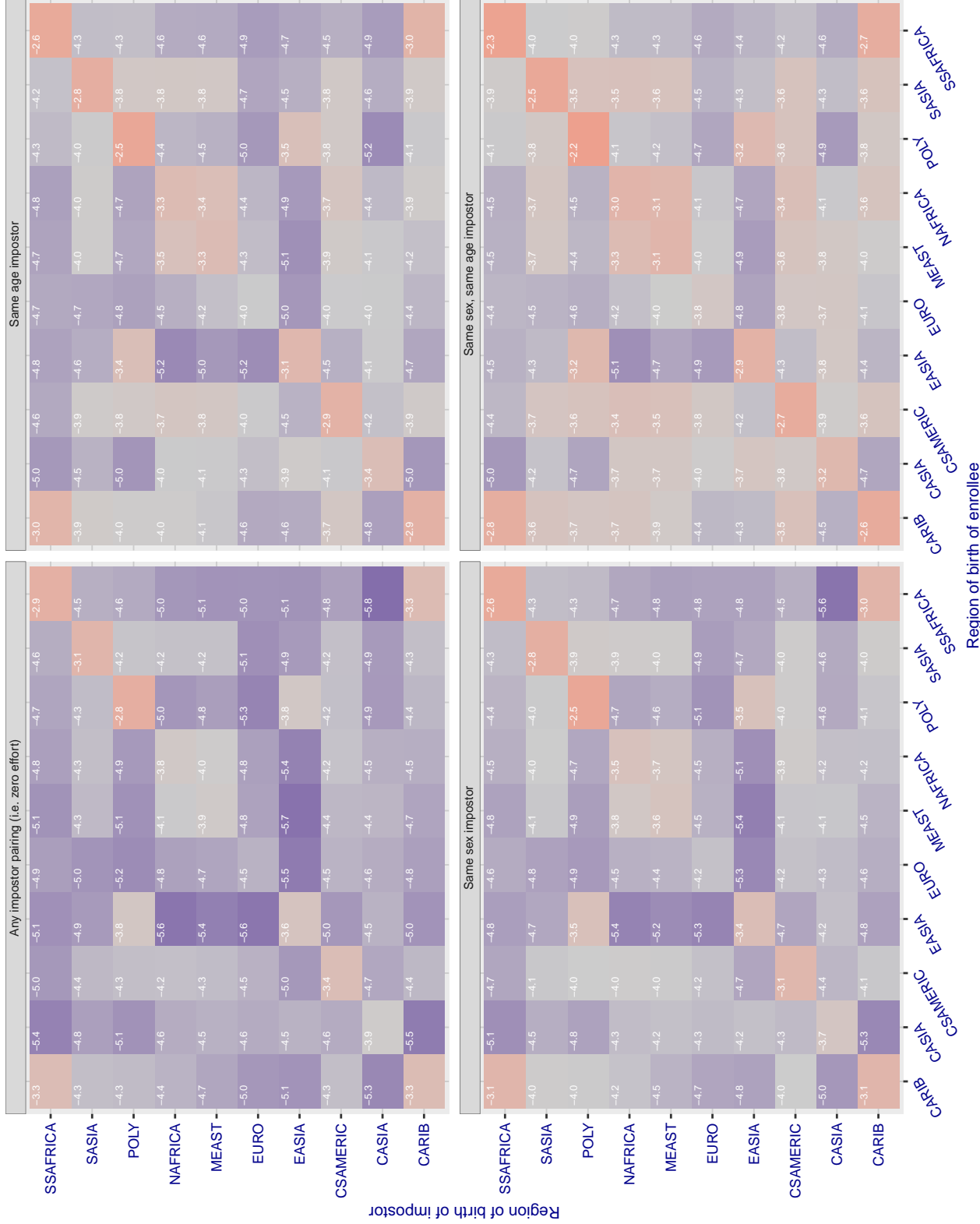
**Cross region FMR at threshold T = 0.657 for algorithm visionlabs\_007, giving FMR(T) = 0.0001 globally.**

Figure 288: For algorithm visionlabs-007 operating on visa images, the heatmap shows false match rates observed over impostor comparisons of faces from different individuals who were born in the given region pair. False matches are counted against a recognition threshold fixed globally to give the target FMR in the plot title, computed over all on the order of  $10^{10}$  impostor comparisons. If text appears in each box it give the same quantity as that coded by the color. Grey indicates FMR is at the intended FMR target level. Light red colors present a security vulnerability to, for example, a passport gate. Each +1 increase in  $\log_{10} FMR$  corresponds to a factor of 10 increase in FMR. The matrix is not quite symmetric because images in the enrollment and verification sets are different.

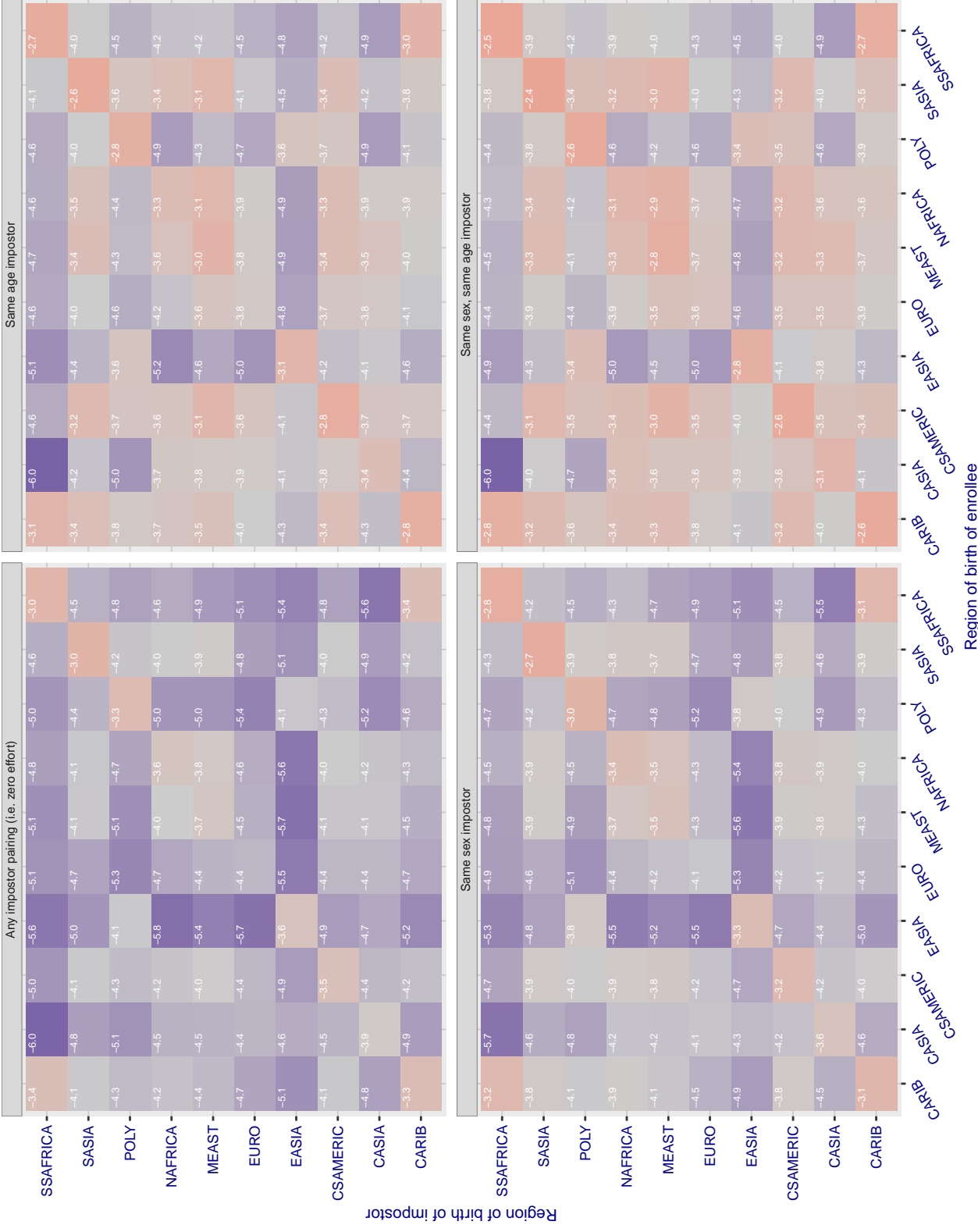
**Cross region FMR at threshold T = 995.898 for algorithm vocord\_006, giving FMR(T) = 0.0001 globally.**

Figure 289: For algorithm vocord-006 operating on visa images, the heatmap shows false match rates observed over impostor comparisons of faces from different individuals who were born in the given region pair. False matches are counted against a recognition threshold fixed globally to give the target FMR in the plot title, computed over all on the order of  $10^{10}$  impostor comparisons. If text appears in each box it give the same quantity as that coded by the color. Grey indicates FMR is at the intended FMR target level. Light red colors present a security vulnerability to, for example, a passport gate. Each +1 increase in  $\log_{10} FMR$  corresponds to a factor of 10 increase in FMR. The matrix is not quite symmetric because images in the enrollment and verification sets are different.

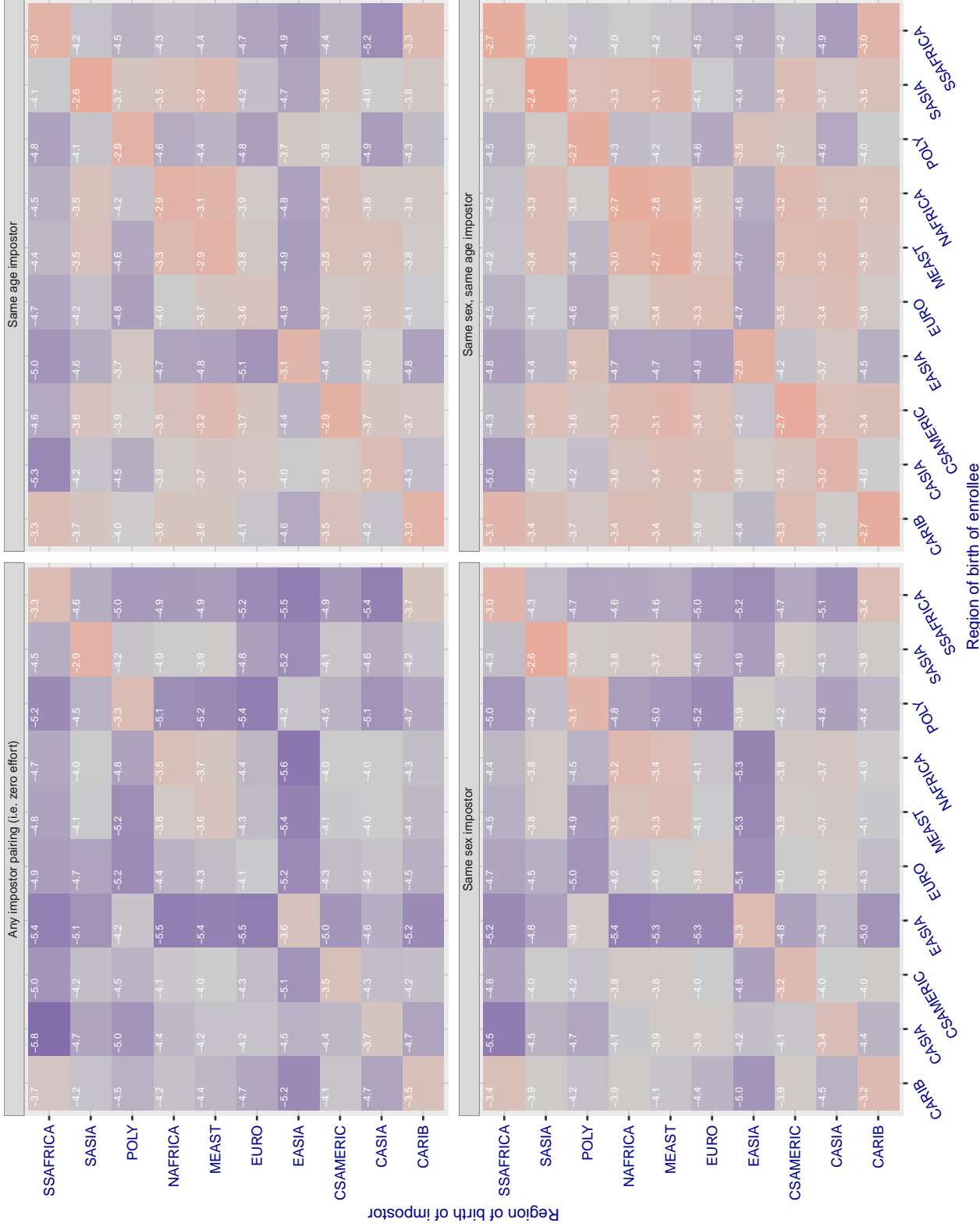
**Cross region FMR at threshold T = 995.241 for algorithm vocord\_007, giving FMR(T) = 0.0001 globally.**

Figure 290: For algorithm vocord-007 operating on visa images, the heatmap shows false match rates observed over impostor comparisons of faces from different individuals who were born in the given region pair. False matches are counted against a recognition threshold fixed globally to give the target FMR in the plot title, computed over all on the order of  $10^{10}$  impostor comparisons. If text appears in each box it give the same quantity as that coded by the color. Grey indicates FMR is at the intended FMR target level. Light red colors present a security vulnerability to, for example, a passport gate. Each +1 increase in  $\log_{10} FMR$  corresponds to a factor of 10 increase in FMR. The matrix is not quite symmetric because images in the enrollment and verification sets are different.

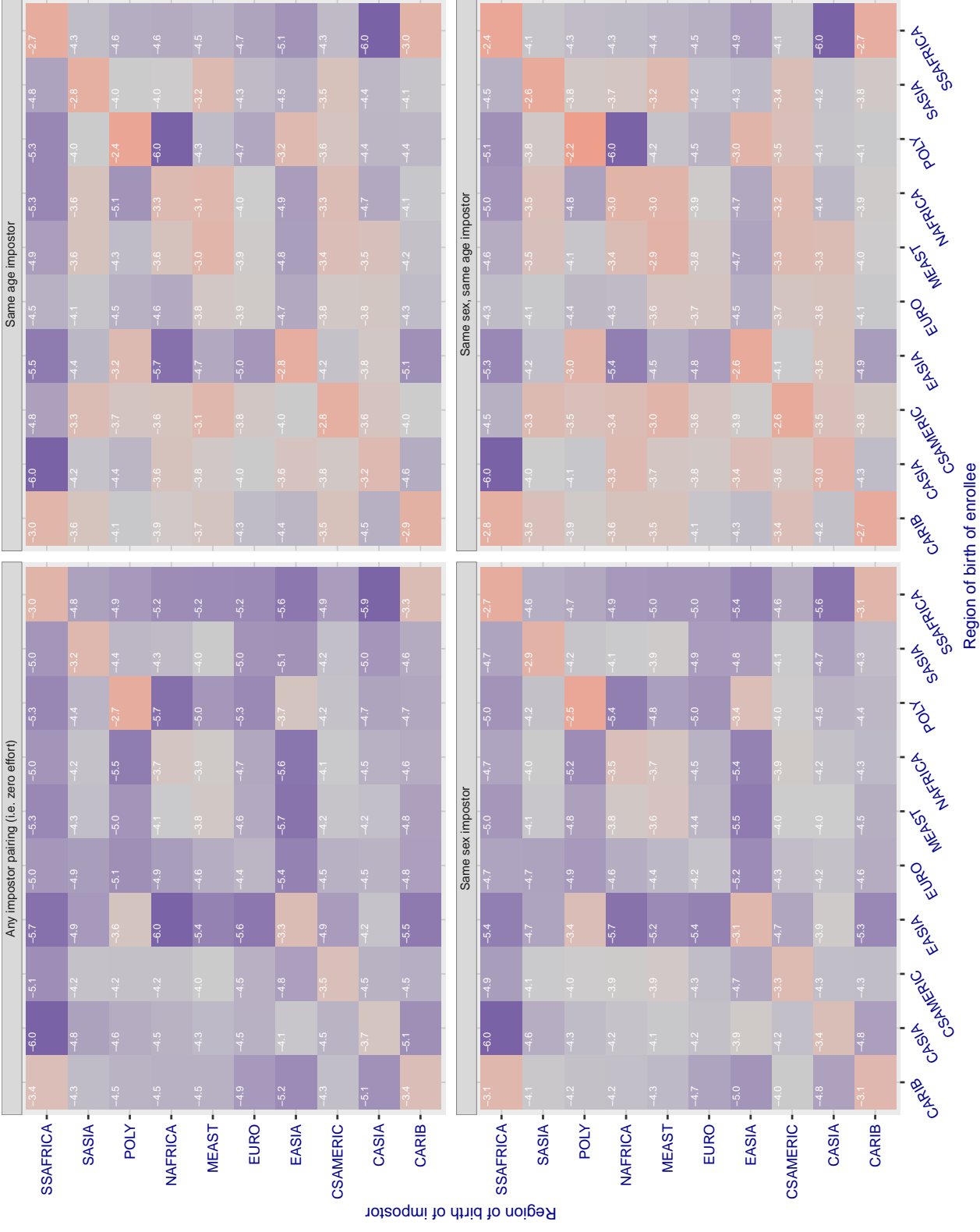
**Cross region FMR at threshold T = 0.400 for algorithm winsense\_000, giving FMR(T) = 0.0001 globally.**

Figure 291: For algorithm winsense-000 operating on visa images, the heatmap shows false match rates observed over impostor comparisons of faces from different individuals who were born in the given region pair. False matches are counted against a recognition threshold fixed globally to give the target FMR in the plot title, computed over all on the order of  $10^{10}$  impostor comparisons. If text appears in each box it give the same quantity as that coded by the color. Grey indicates FMR is at the intended FMR target level. Light red colors present a security vulnerability to, for example, a passport gate. Each +1 increase in  $\log_{10} FMR$  corresponds to a factor of 10 increase in FMR. The matrix is not quite symmetric because images in the enrollment and verification sets are different.

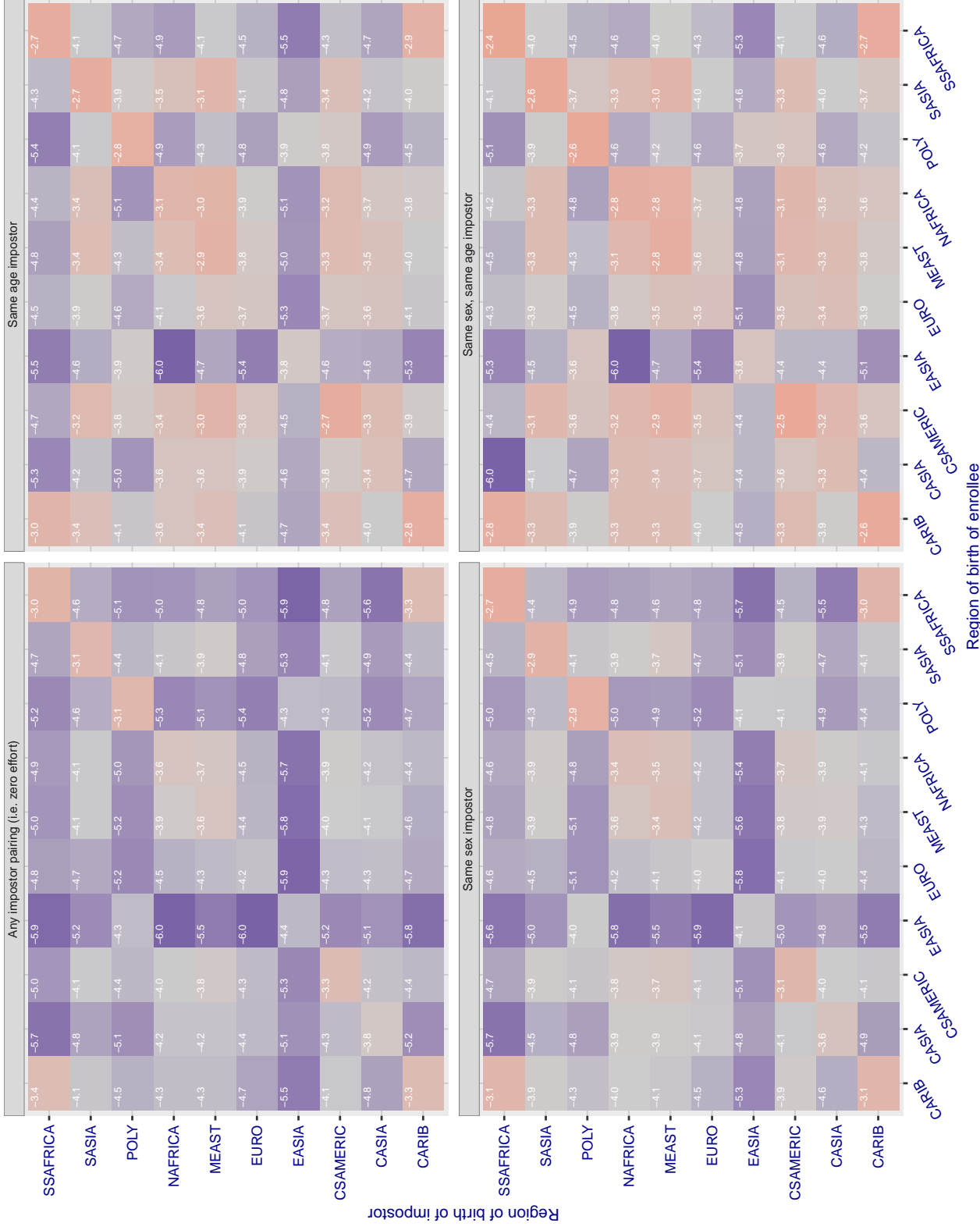
**Cross region FMR at threshold T = 0.404 for algorithm x-laboratory\_000, giving FMR(T) = 0.0001 globally.**

Figure 292: For algorithm x-laboratory-000 operating on visa images, the heatmap shows false match rates observed over impostor comparisons of faces from different individuals who were born in the given region pair. False matches are counted against a recognition threshold fixed globally to give the target FMR in the plot title, computed over all on the order of  $10^{10}$  impostor comparisons. If text appears in each box it give the same quantity as that coded by the color. Grey indicates FMR is at the intended FMR target level. Light red colors present a security vulnerability to, for example, a passport gate. Each +1 increase in  $\log_{10} FMR$  corresponds to a factor of 10 increase in FMR. The matrix is not quite symmetric because images in the enrollment and verification sets are different.

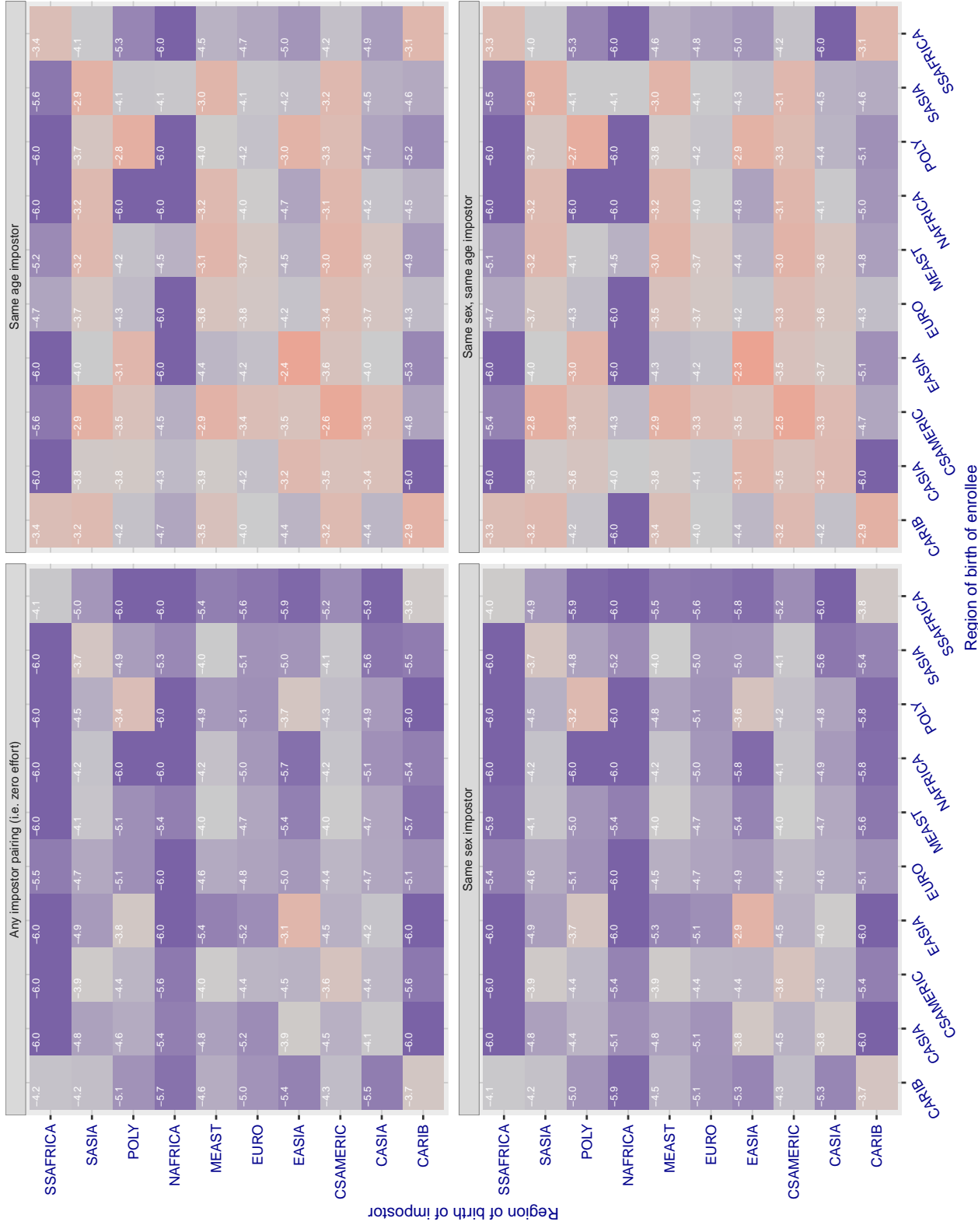
**Cross region FMR at threshold T = 5.544 for algorithm yisheng\_004, giving FMR(T) = 0.0001 globally.**

Figure 293: For algorithm yisheng-004 operating on visa images, the heatmap shows false match rates observed over impostor comparisons of faces from different individuals who were born in the given region pair. False matches are counted against a recognition threshold fixed globally to give the target FMR in the plot title, computed over all on the order of  $10^{10}$  impostor comparisons. If text appears in each box it give the same quantity as that coded by the color. Grey indicates FMR is at the intended FMR target level. Light red colors present a security vulnerability to, for example, a passport gate. Each +1 increase in  $\log_{10} FMR$  corresponds to a factor of 10 increase in FMR. The matrix is not quite symmetric because images in the enrollment and verification sets are different.

### Cross region FMR at threshold T = 37.698 for algorithm yitu\_003, giving FMR(T) = 0.0001 globally.

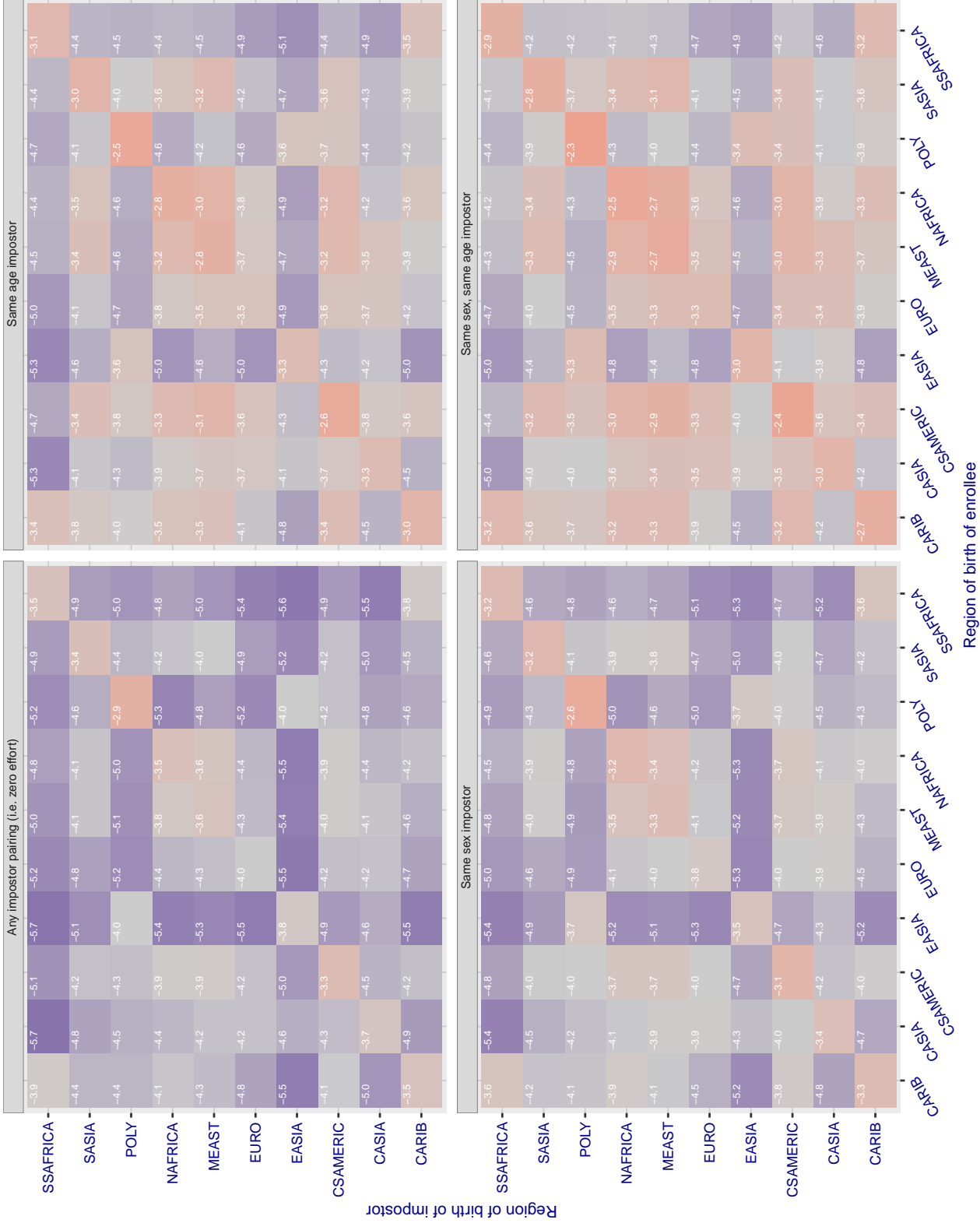


Figure 294: For algorithm yitu-003 operating on visa images, the heatmap shows false match rates observed over impostor comparisons of faces from different individuals who were born in the given region pair. False matches are counted against a recognition threshold fixed globally to give the target FMR in the plot title, computed over all on the order of  $10^{10}$  impostor comparisons. If text appears in each box it give the same quantity as that coded by the color. Grey indicates FMR is at the intended FMR target level. Light red colors present a security vulnerability to, for example, a passport gate. Each +1 increase in  $\log_{10}$  FMR corresponds to a factor of 10 increase in FMR. The matrix is not quite symmetric because images in the enrollment and verification sets are different.

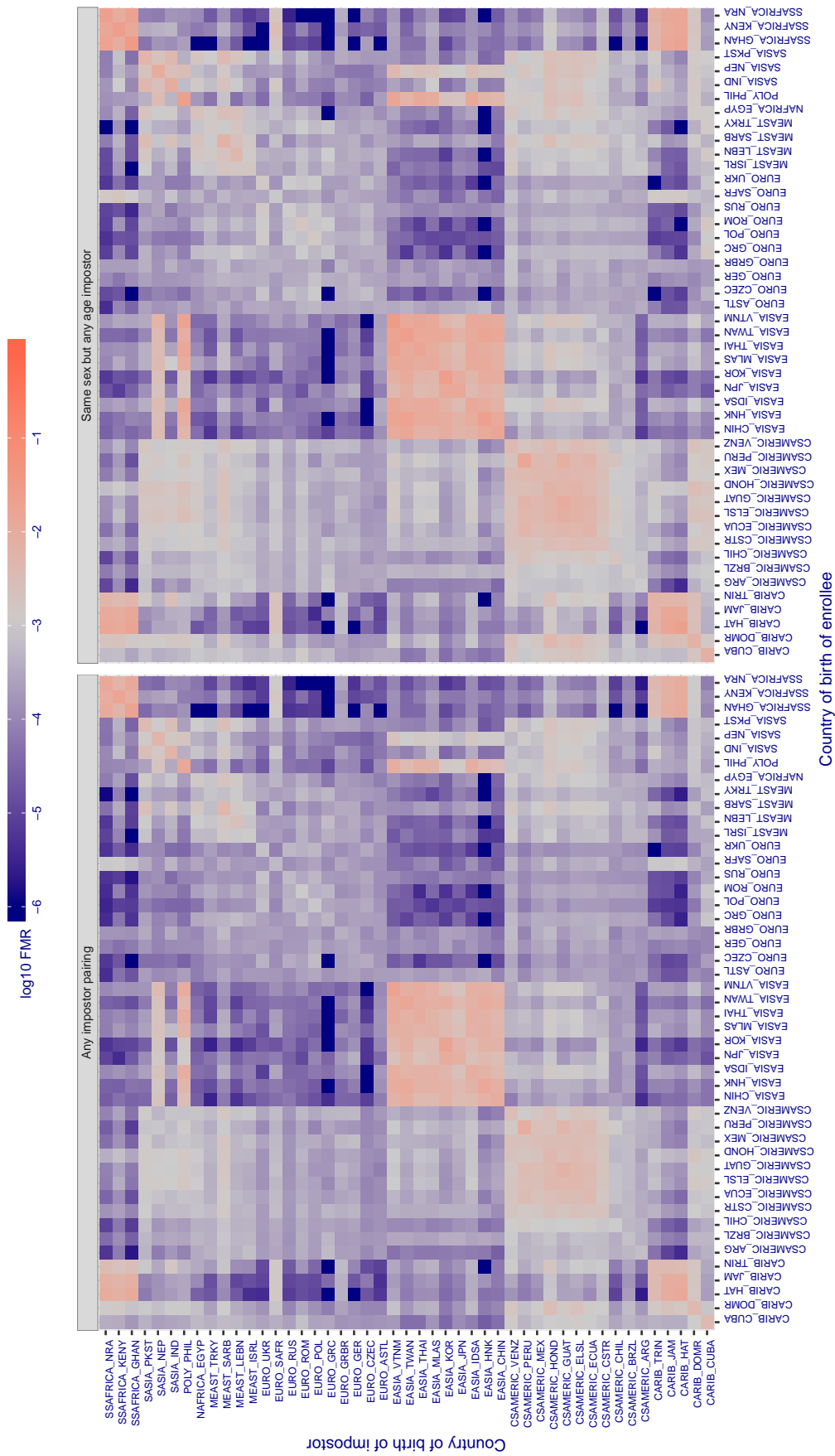
**Cross country FMR at threshold T = 2.575 for algorithm 3divi\_003, giving  $\text{FMR}(\text{T}) = 0.001$  globally.**

Figure 295: For algorithm 3divi-003 operating on visa images, the heatmap shows false match rates observed over impostor comparisons of faces from different individuals who were born in the given country pair. False matches are counted against a recognition threshold fixed globally to give the target FMR in the plot title, computed over all on the order of  $10^{10}$  impostor comparisons. If text appears in each box it give the same quantity as that coded by the color. Grey indicates FMR is at the intended FMR target level. Light red colors present a security vulnerability to, for example, a passport gate. Each +1 increase in  $\log_{10} \text{FMR}$  corresponds to a factor of 10 increase in FMR. The matrix is not quite symmetric because images in the enrollment and verification sets are different.

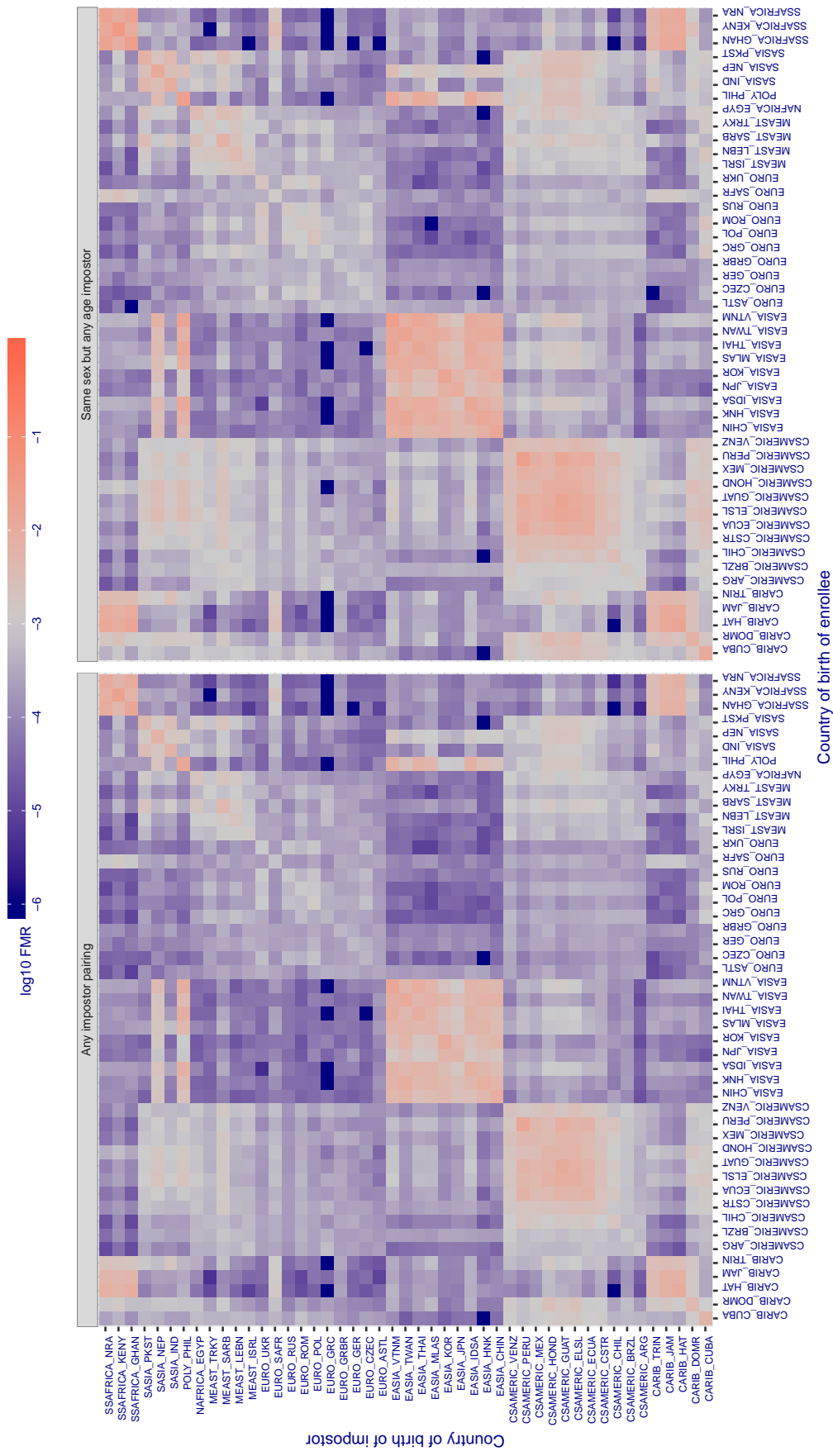
**Cross country FMR at threshold T = 2.692 for algorithm 3divi\_004, giving  $\text{FMR}(\text{T}) = 0.001$  globally.**

Figure 296: For algorithm 3divi-004 operating on visa images, the heatmap shows false match rates observed over impostor comparisons of faces from different individuals who were born in the given country pair. False matches are counted against a recognition threshold fixed globally to give the target FMR in the plot title, computed over all on the order of  $10^{10}$  impostor comparisons. If text appears in each box it give the same quantity as that coded by the color. Grey indicates FMR is at the intended FMR target level. Light red colors present a security vulnerability to, for example, a passport gate. Each +1 increase in  $\log_{10} \text{FMR}$  corresponds to a factor of 10 increase in FMR. The matrix is not quite symmetric because images in the enrollment and verification sets are different.

Cross country FMR at threshold T = 0.632 for algorithm adera\_001, giving FMR(T) = 0.001 globally.

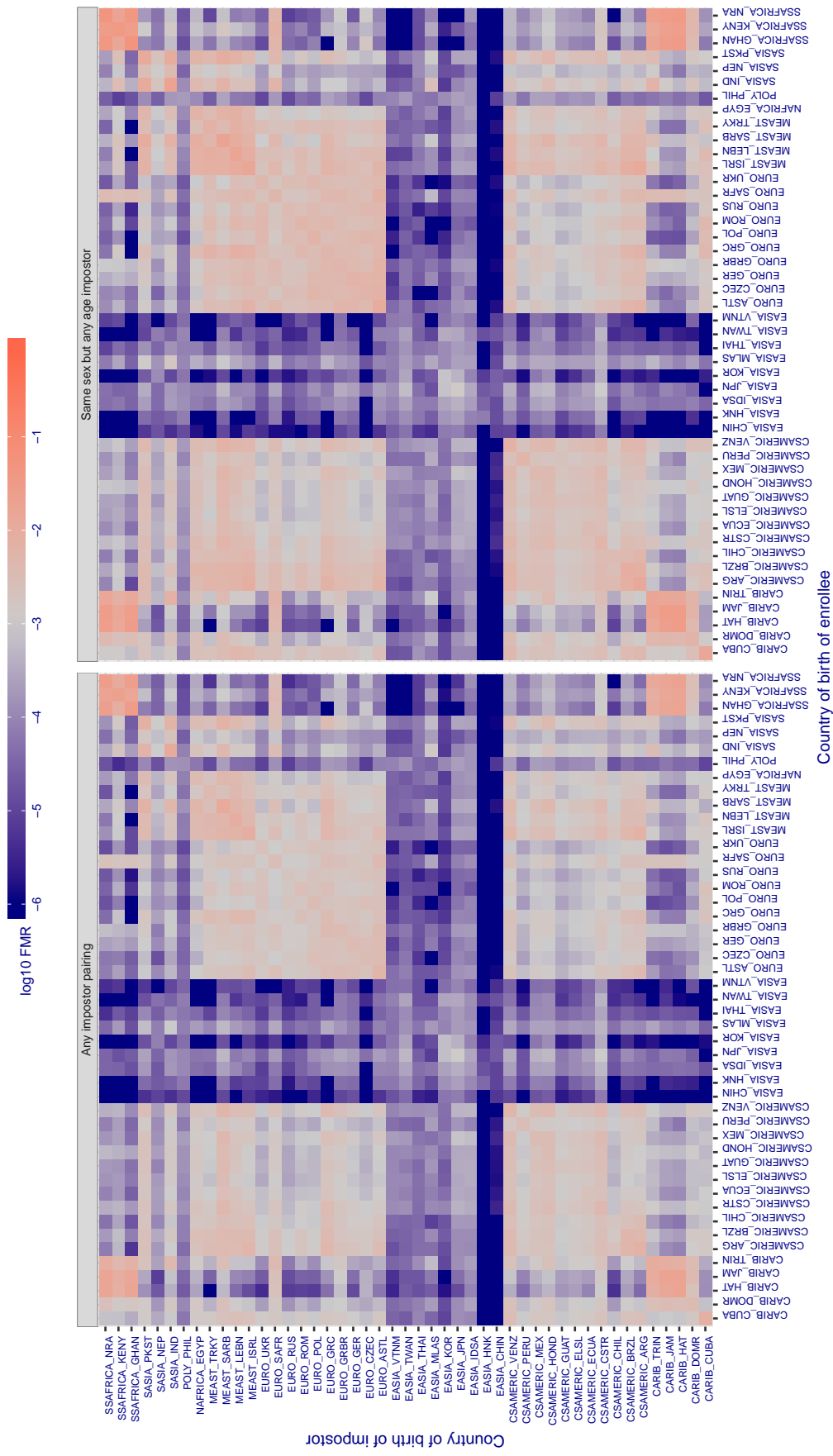


Figure 297: For algorithm adera-001 operating on visa images, the heatmap shows false match rates observed over impostor comparisons of faces from different individuals who were born in the given country pair. False matches are counted against a recognition threshold fixed globally to give the target FMR in the plot title, computed over all on the order of  $10^{10}$  impostor comparisons. If text appears in each box it give the same quantity as that coded by the color. Grey indicates FMR is at the intended FMR target level. Light red colors present a security vulnerability to, for example, a passport gate. Each +1 increase in  $\log_{10} FMR$  corresponds to a factor of 10 increase in FMR. The matrix is not quite symmetric because images in the enrollment and verification sets are different.

**Cross country FMR at threshold  $T = 0.662$  for algorithm alchera\_000, giving  $\text{FMR}(T) = 0.001$  globally.**

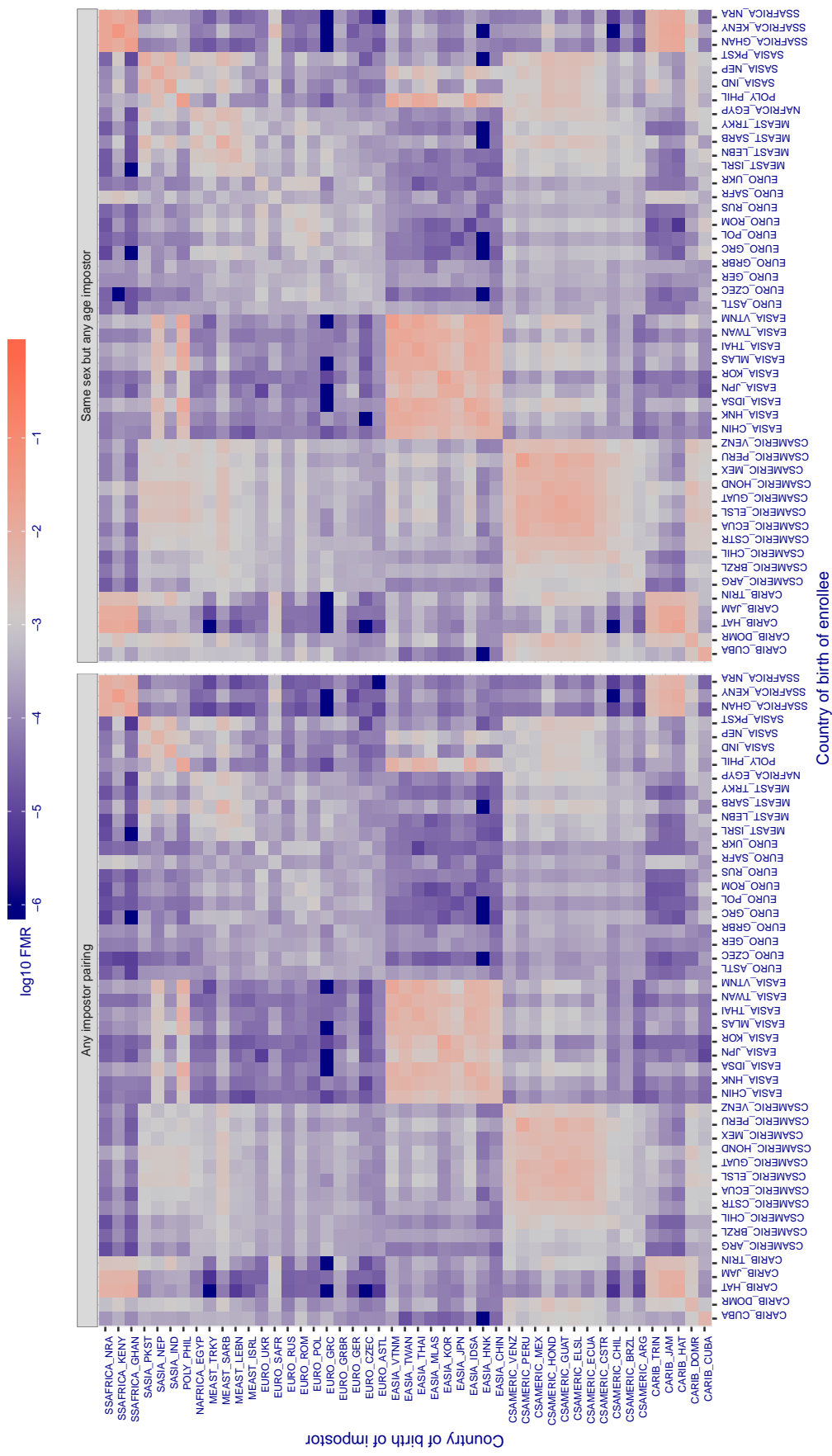


Figure 298: For algorithm alchera-000 operating on visa images, the heatmap shows false match rates observed over impostor comparisons of faces from different individuals who were born in the given country pair. False matches are counted against a recognition threshold fixed globally to give the target  $\text{FMR}$  in the plot title, computed over all on the order of  $10^{10}$  impostor comparisons. If text appears in each box it give the same quantity as that coded by the color. Grey indicates  $\text{FMR}$  is at the intended  $\text{FMR}$  target level. Light red colors present a security vulnerability to, for example, a passport gate. Each +1 increase in  $\log_{10} \text{FMR}$  corresponds to a factor of 10 increase in  $\text{FMR}$ . The matrix is not quite symmetric because images in the enrollment and verification sets are different.

**Cross country FMR at threshold T = 0.667 for algorithm alchera\_001, giving  $\text{FMR}(T) = 0.001$  globally.**

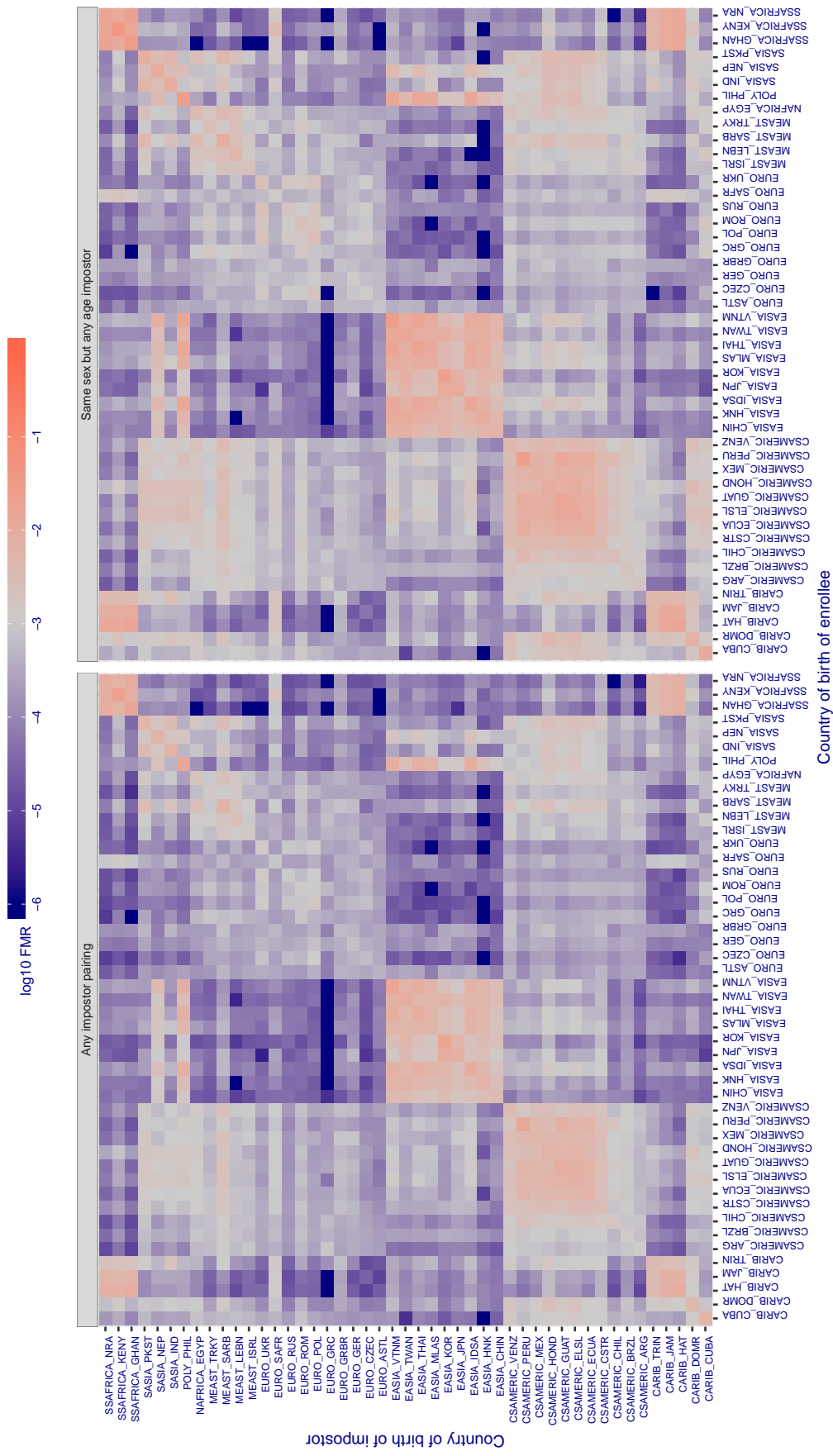


Figure 299: For algorithm alchera-001 operating on visa images, the heatmap shows false match rates observed over impostor comparisons of faces from different individuals who were born in the given country pair. False matches are counted against a recognition threshold fixed globally to give the target  $\text{FMR}$  in the plot title, computed over all on the order of  $10^{10}$  impostor comparisons. If text appears in each box it give the same quantity as that coded by the color. Grey indicates  $\text{FMR}$  is at the intended  $\text{FMR}$  target level. Light red colors present a security vulnerability to, for example, a passport gate. Each +1 increase in  $\log_{10} \text{FMR}$  corresponds to a factor of 10 increase in  $\text{FMR}$ . The matrix is not quite symmetric because images in the enrollment and verification sets are different.

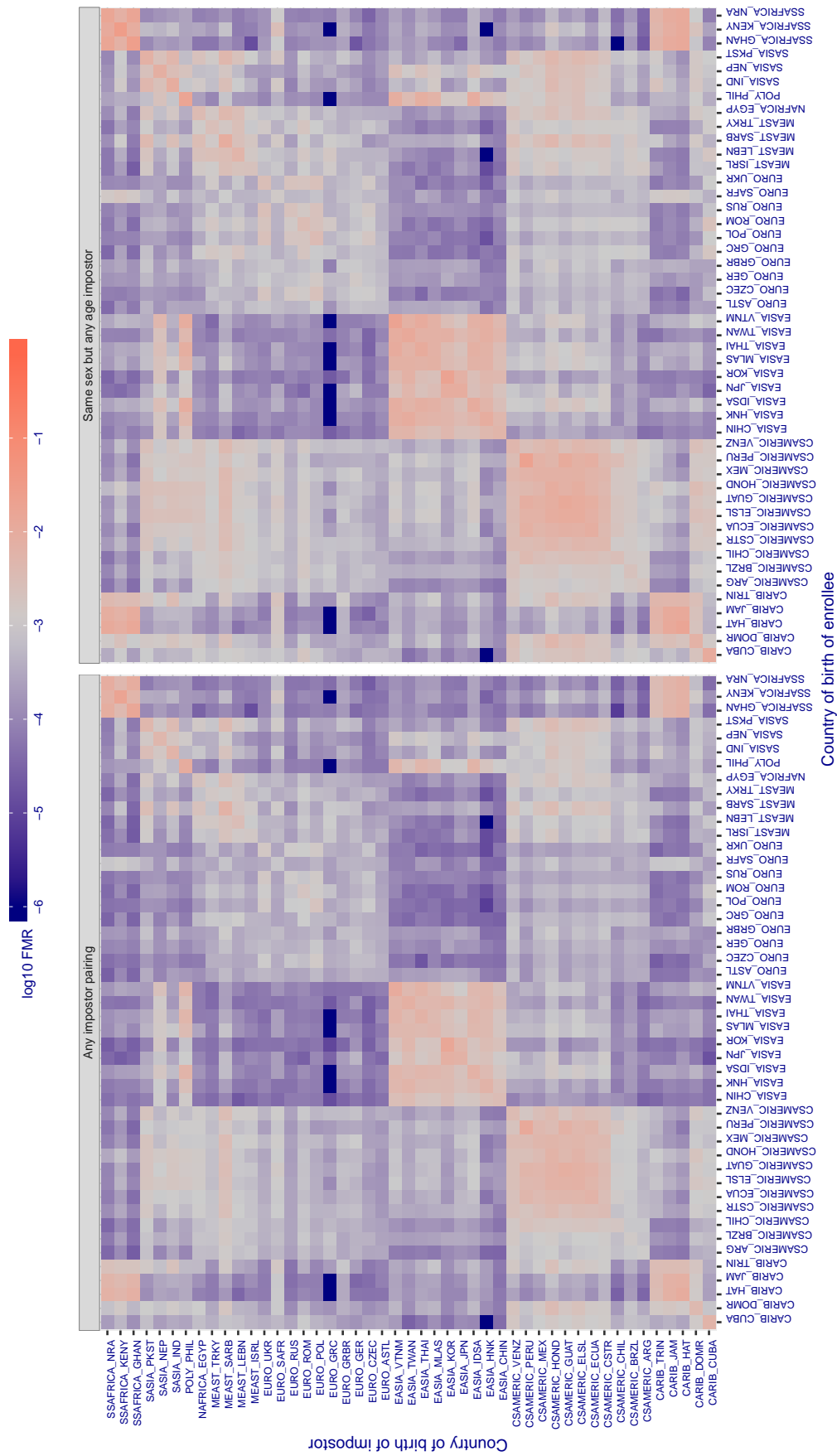
**Cross country FMR at threshold T = 0.339 for algorithm allgovision\_000, giving  $FMR(T) = 0.001$  globally.**

Figure 300: For algorithm allgovision-000 operating on visa images, the heatmap shows false match rates observed over impostor comparisons of faces from different individuals who were born in the given country pair. False matches are counted against a recognition threshold fixed globally to give the target  $FMR$  in the plot title, computed over all on the order of  $10^{10}$  impostor comparisons. If text appears in each box it give the same quantity as that coded by the color. Grey indicates  $FMR$  is at the intended  $FMR$  target level. Light red colors present a security vulnerability to, for example, a passport gate. Each +1 increase in  $\log_{10} FMR$  corresponds to a factor of 10 increase in  $FMR$ . The matrix is not quite symmetric because images in the enrollment and verification sets are different.

**Cross country FMR at threshold  $T = 0.313$  for algorithm alphaface\_001, giving  $FMR(T) = 0.001$  globally.**

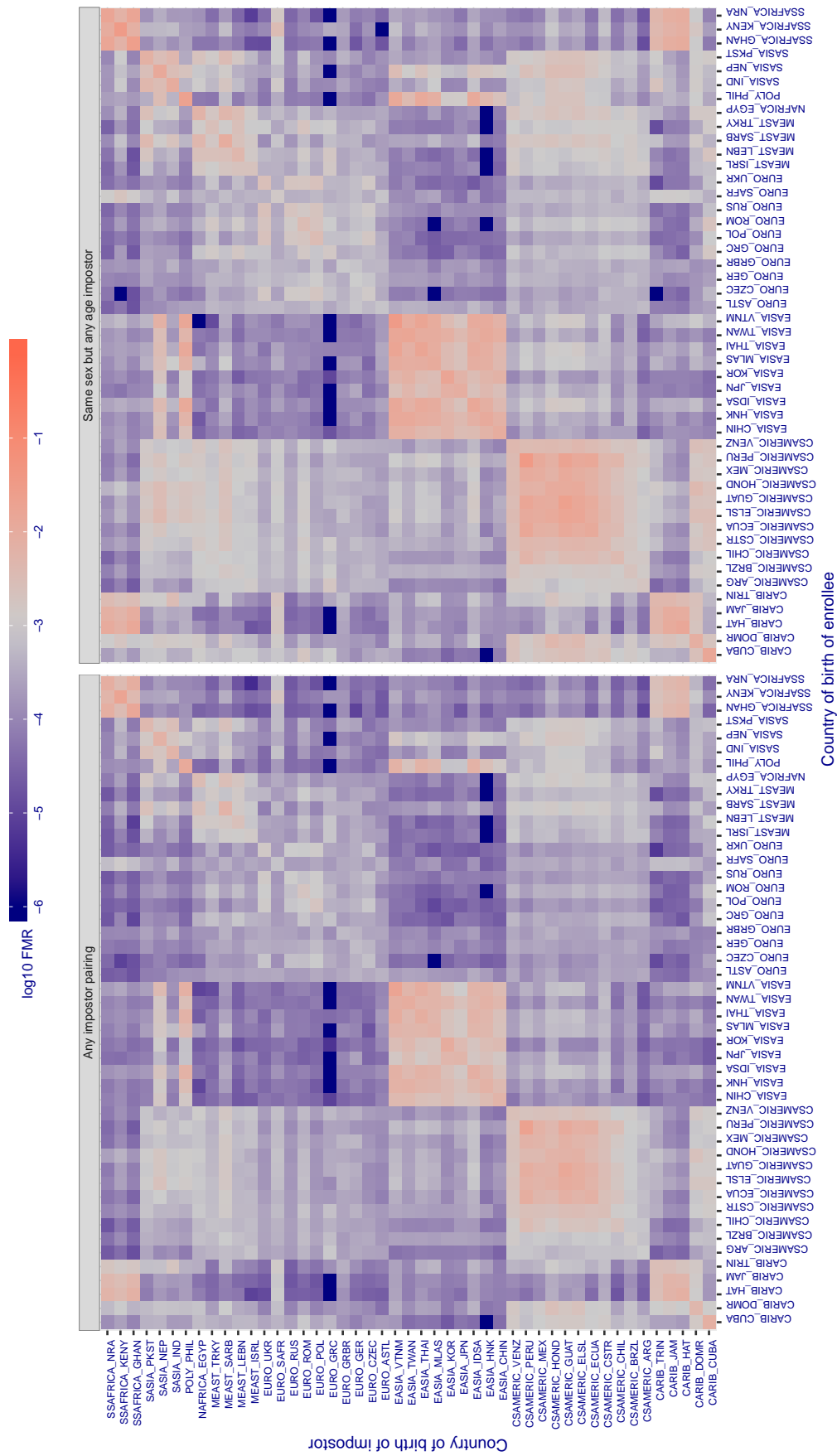


Figure 301: For algorithm alphaface-001 operating on visa images, the heatmap shows false match rates observed over impostor comparisons of faces from different individuals who were born in the given country pair. False matches are counted against a recognition threshold fixed globally to give the target  $FMR$  in the plot title, computed over all on the order of  $10^{10}$  impostor comparisons. If text appears in each box it give the same quantity as that coded by the color. Grey indicates  $FMR$  is at the intended  $FMR$  target level. Light red colors present a security vulnerability to, for example, a passport gate. Each +1 increase in  $\log_{10} FMR$  corresponds to a factor of 10 increase in  $FMR$ . The matrix is not quite symmetric because images in the enrollment and verification sets are different.

Cross country FMR at threshold T = 3.524 for algorithm amplifiedgroup\_001, giving FMR(T) = 0.001 globally.

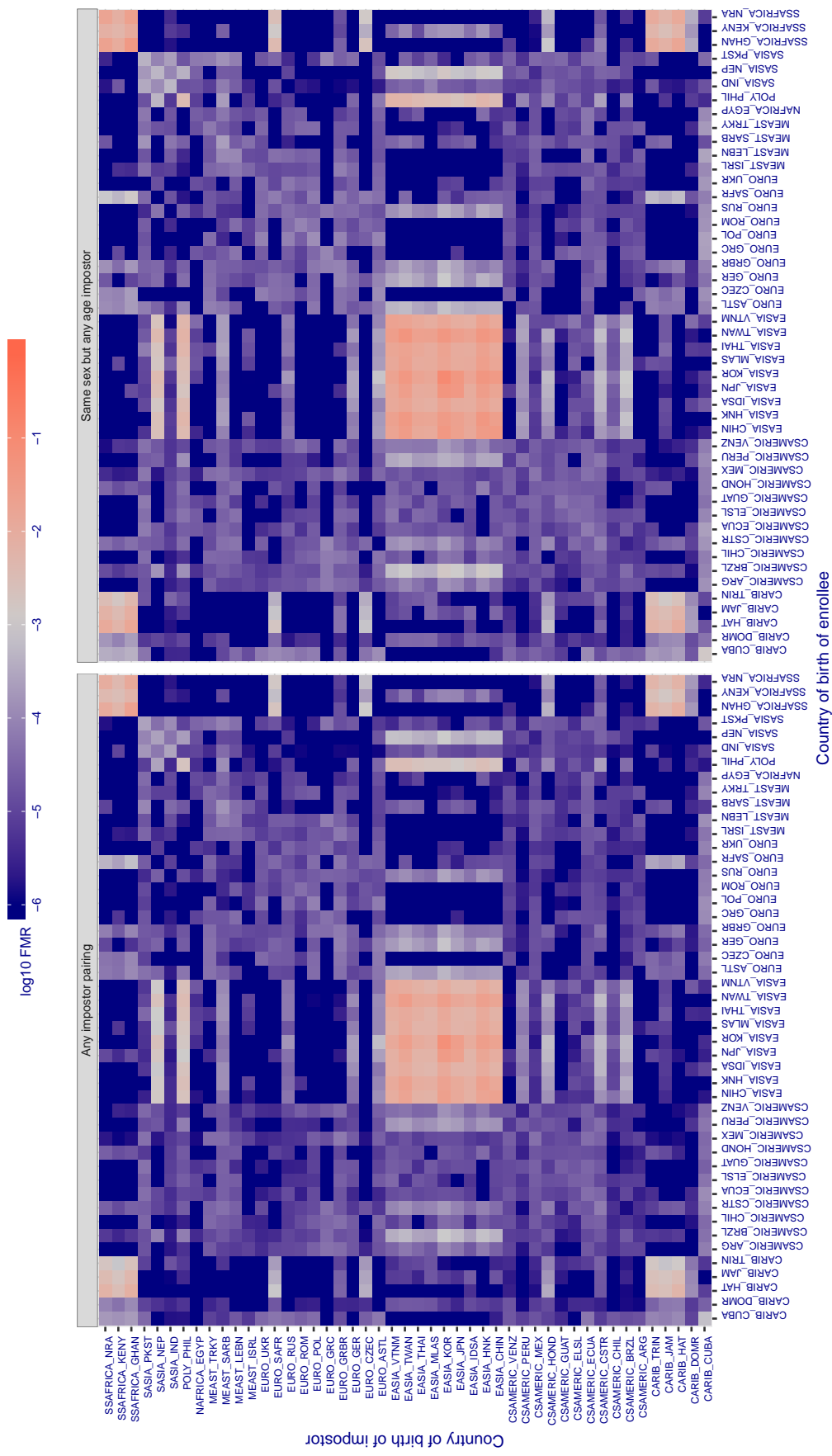


Figure 302: For algorithm amplifiedgroup-001 operating on visa images, the heatmap shows false match rates observed over impostor comparisons of faces from different individuals who were born in the given country pair. False matches are counted against a recognition threshold fixed globally to give the target FMR in the plot title, computed over all on the order of  $10^{10}$  impostor comparisons. If text appears in each box it give the same quantity as that coded by the color. Grey indicates FMR is at the intended FMR target level. Light red colors present a security vulnerability to, for example, a passport gate. Each +1 increase in  $\log_{10}$  FMR corresponds to a factor of 10 increase in FMR. The matrix is not quite symmetric because images in the enrollment and verification sets are different.

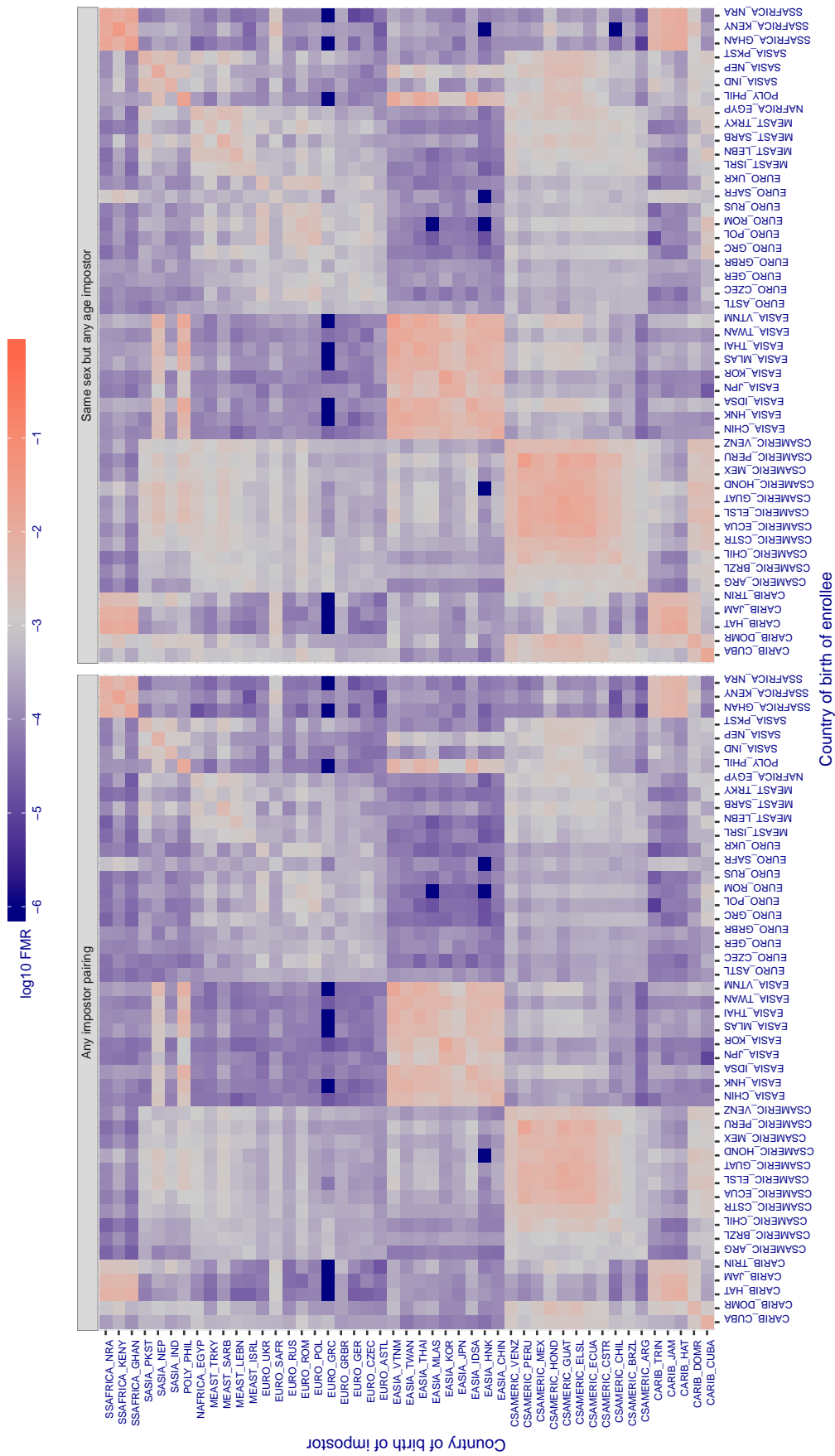
**Cross country FMR at threshold T = 0.313 for algorithm anke\_003, giving FMR(T) = 0.001 globally.**

Figure 303: For algorithm anke-003 operating on visa images, the heatmap shows false match rates observed over impostor comparisons of faces from different individuals who were born in the given country pair. False matches are counted against a recognition threshold fixed globally to give the target FMR in the plot title, computed over all on the order of  $10^{10}$  impostor comparisons. If text appears in each box it give the same quantity as that coded by the color. Grey indicates FMR is at the intended FMR target level. Light red colors present a security vulnerability to, for example, a passport gate. Each +1 increase in  $\log_{10} \text{FMR}$  corresponds to a factor of 10 increase in FMR. The matrix is not quite symmetric because images in the enrollment and verification sets are different.

Cross country FMR at threshold T = 0.309 for algorithm anke\_004, giving  $\text{FMR}(\text{T}) = 0.001$  globally.

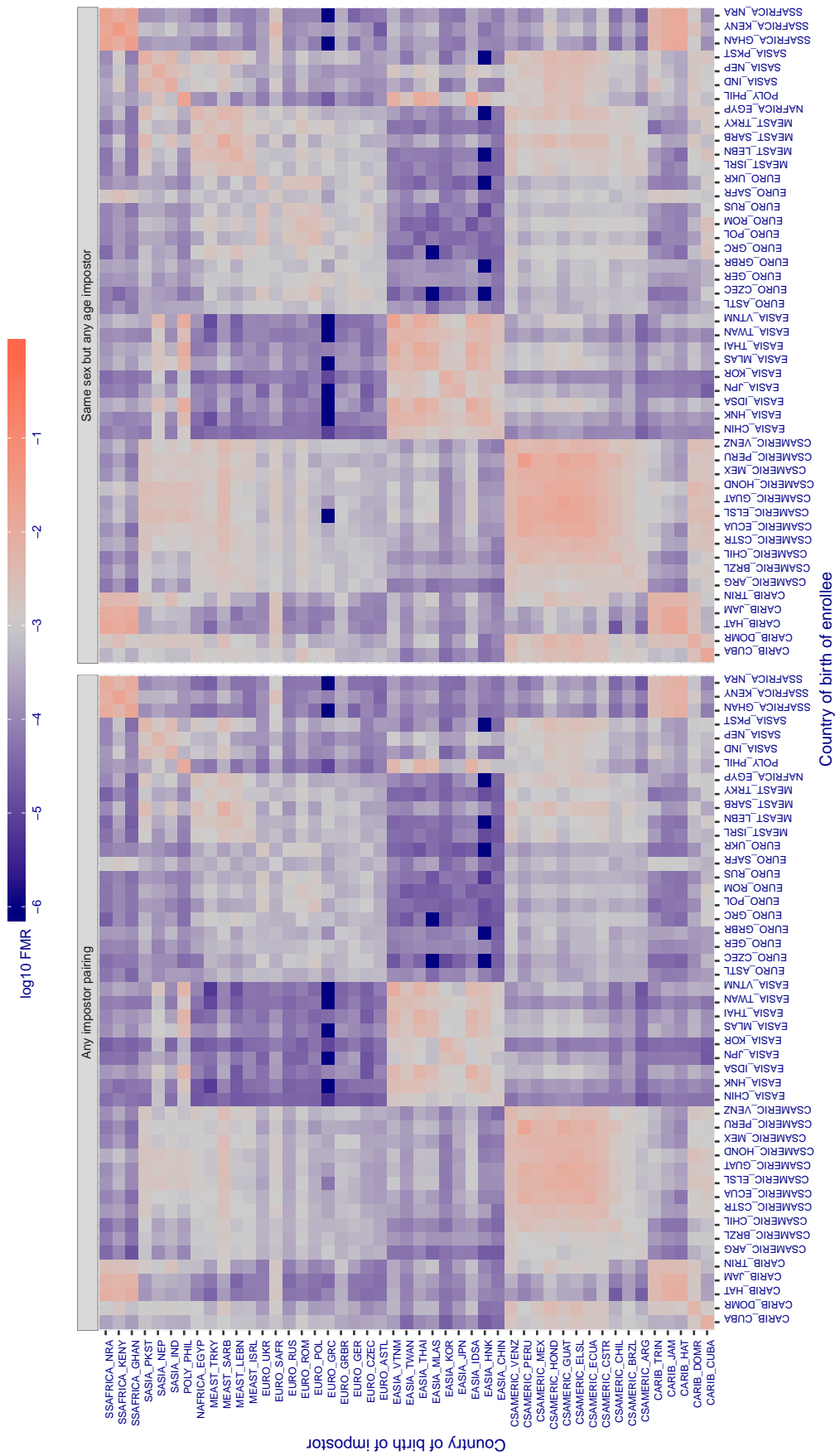


Figure 304: For algorithm anke-004 operating on visa images, the heatmap shows false match rates observed over impostor comparisons of faces from different individuals who were born in the given country pair. False matches are counted against a recognition threshold fixed globally to give the target FMR in the plot title, computed over all on the order of  $10^{10}$  impostor comparisons. If text appears in each box it give the same quantity as that coded by the color. Grey indicates FMR is at the intended FMR target level. Light red colors present a security vulnerability to, for example, a passport gate. Each +1 increase in  $\log_{10} \text{FMR}$  corresponds to a factor of 10 increase in FMR. The matrix is not quite symmetric because images in the enrollment and verification sets are different.

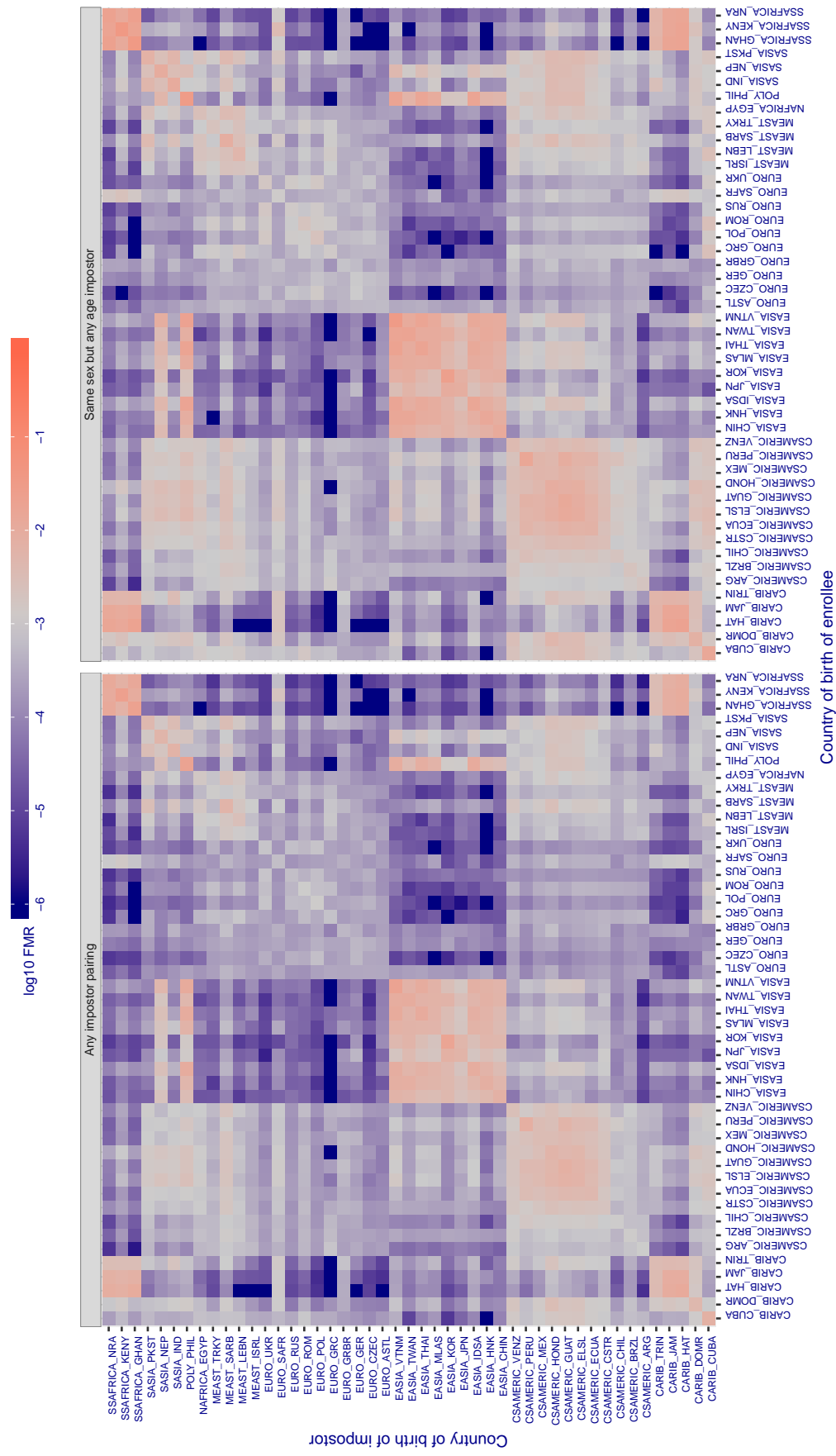
**Cross country FMR at threshold T = 1.431 for algorithm anyvision\_002, giving FMR(T) = 0.001 globally.**

Figure 305: For algorithm anyvision-002 operating on visa images, the heatmap shows false match rates observed over impostor comparisons of faces from different individuals who were born in the given country pair. False matches are counted against a recognition threshold fixed globally to give the target FMR in the plot title, computed over all on the order of  $10^{10}$  impostor comparisons. If text appears in each box it give the same quantity as that coded by the color. Grey indicates FMR is at the intended FMR target level. Light red colors present a security vulnerability to, for example, a passport gate. Each +1 increase in  $\log_{10} \text{FMR}$  corresponds to a factor of 10 increase in FMR. The matrix is not quite symmetric because images in the enrollment and verification sets are different.

**Cross country FMR at threshold T = 1.297 for algorithm anyvision\_004, giving FMR(T) = 0.001 globally.**

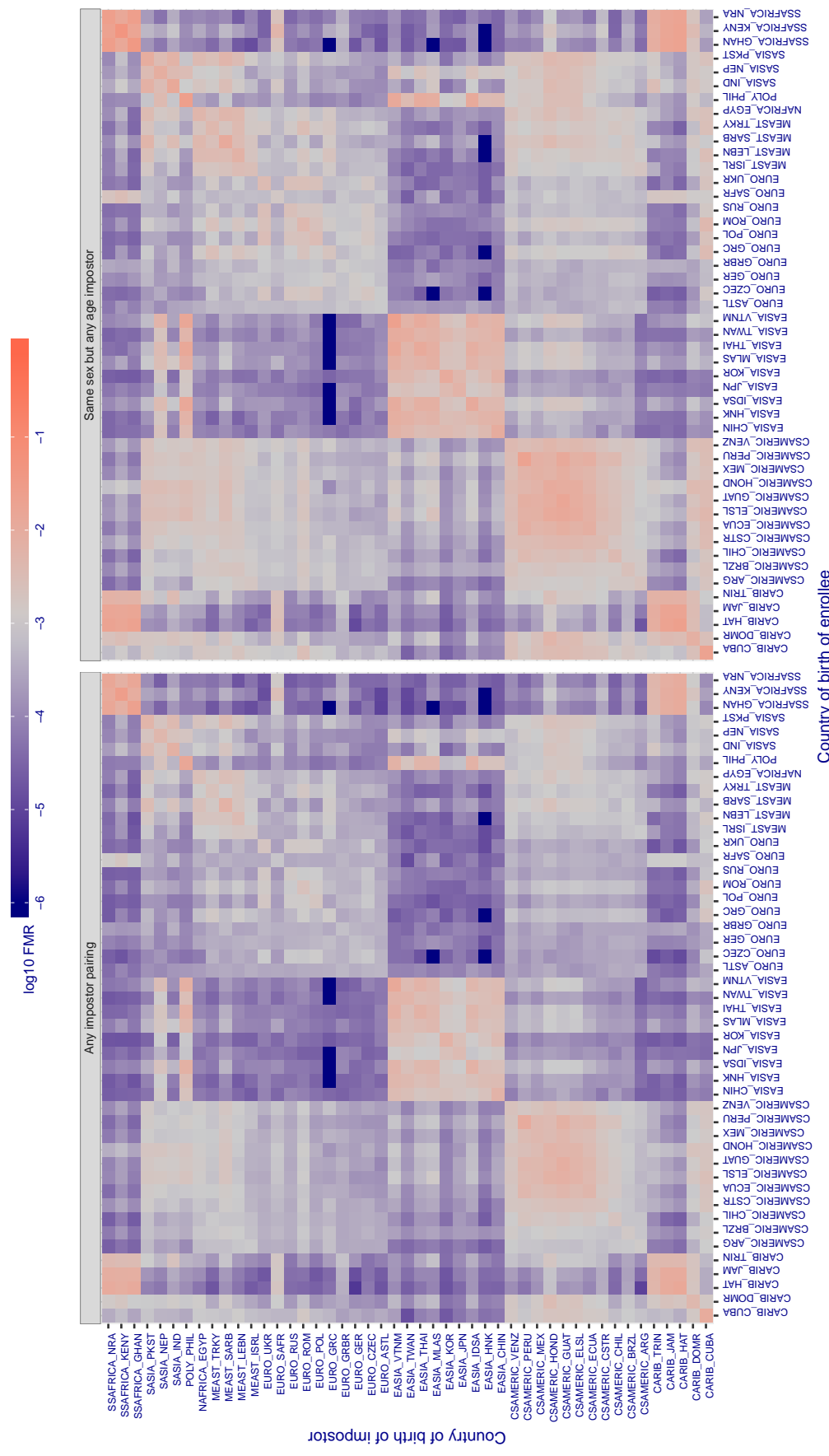


Figure 306: For algorithm anyvision-004 operating on visa images, the heatmap shows false match rates observed over impostor comparisons of faces from different individuals who were born in the given country pair. False matches are counted against a recognition threshold fixed globally to give the target FMR in the plot title, computed over all on the order of  $10^{10}$  impostor comparisons. If text appears in each box it give the same quantity as that coded by the color. Grey indicates FMR is at the intended FMR target level. Light red colors present a security vulnerability to, for example, a passport gate. Each +1 increase in  $\log_{10} FMR$  corresponds to a factor of 10 increase in FMR. The matrix is not quite symmetric because images in the enrollment and verification sets are different.

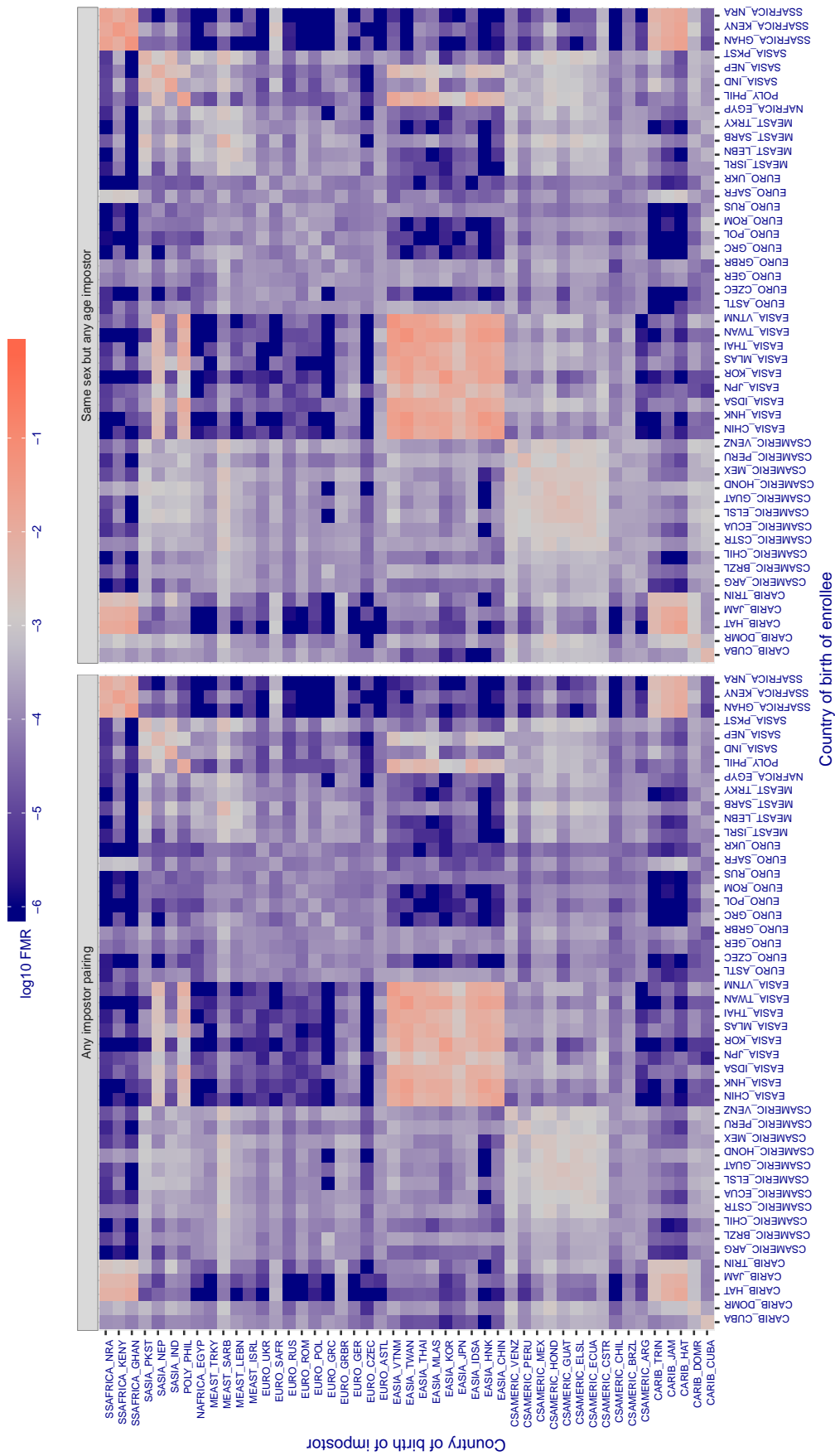
**Cross country FMR at threshold T = 2.758 for algorithm aware\_003, giving FMR(T) = 0.001 globally.**

Figure 307: For algorithm aware-003 operating on visa images, the heatmap shows false match rates observed over impostor comparisons of faces from different individuals who were born in the given country pair. False matches are counted against a recognition threshold fixed globally to give the target FMR in the plot title, computed over all on the order of  $10^{10}$  impostor comparisons. If text appears in each box it give the same quantity as that coded by the color. Grey indicates FMR is at the intended FMR target level. Light red colors present a security vulnerability to, for example, a passport gate. Each +1 increase in  $\log_{10} FMR$  corresponds to a factor of 10 increase in FMR. The matrix is not quite symmetric because images in the enrollment and verification sets are different.

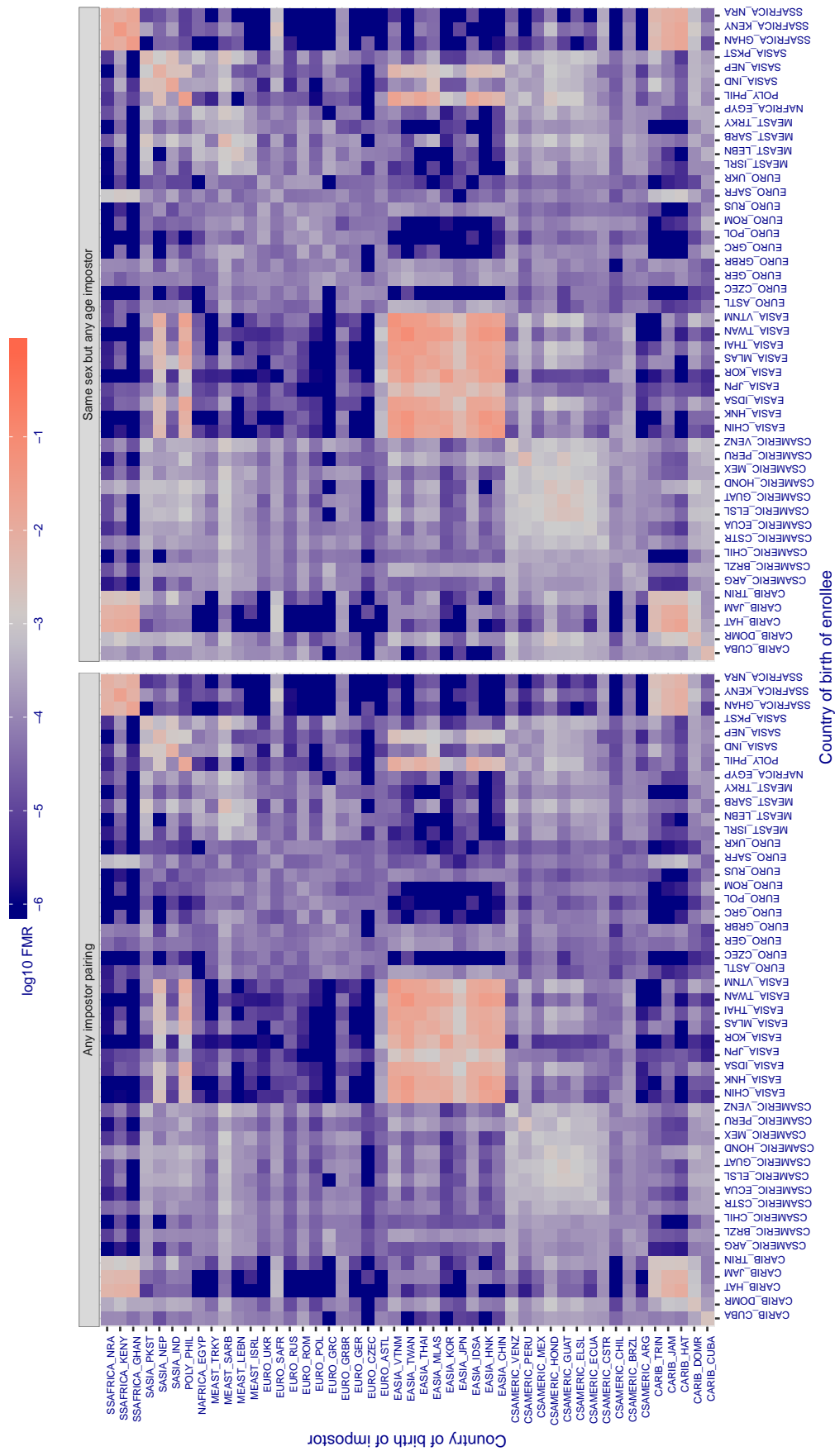
**Cross country FMR at threshold T = 3.681 for algorithm aware\_004, giving FMR(T) = 0.001 globally.**

Figure 308: For algorithm aware-004 operating on visa images, the heatmap shows false match rates observed over impostor comparisons of faces from different individuals who were born in the given country pair. False matches are counted against a recognition threshold fixed globally to give the target FMR in the plot title, computed over all on the order of  $10^{10}$  impostor comparisons. If text appears in each box it give the same quantity as that coded by the color. Grey indicates FMR is at the intended FMR target level. Light red colors present a security vulnerability to, for example, a passport gate. Each +1 increase in  $\log_{10} FMR$  corresponds to a factor of 10 increase in FMR. The matrix is not quite symmetric because images in the enrollment and verification sets are different.

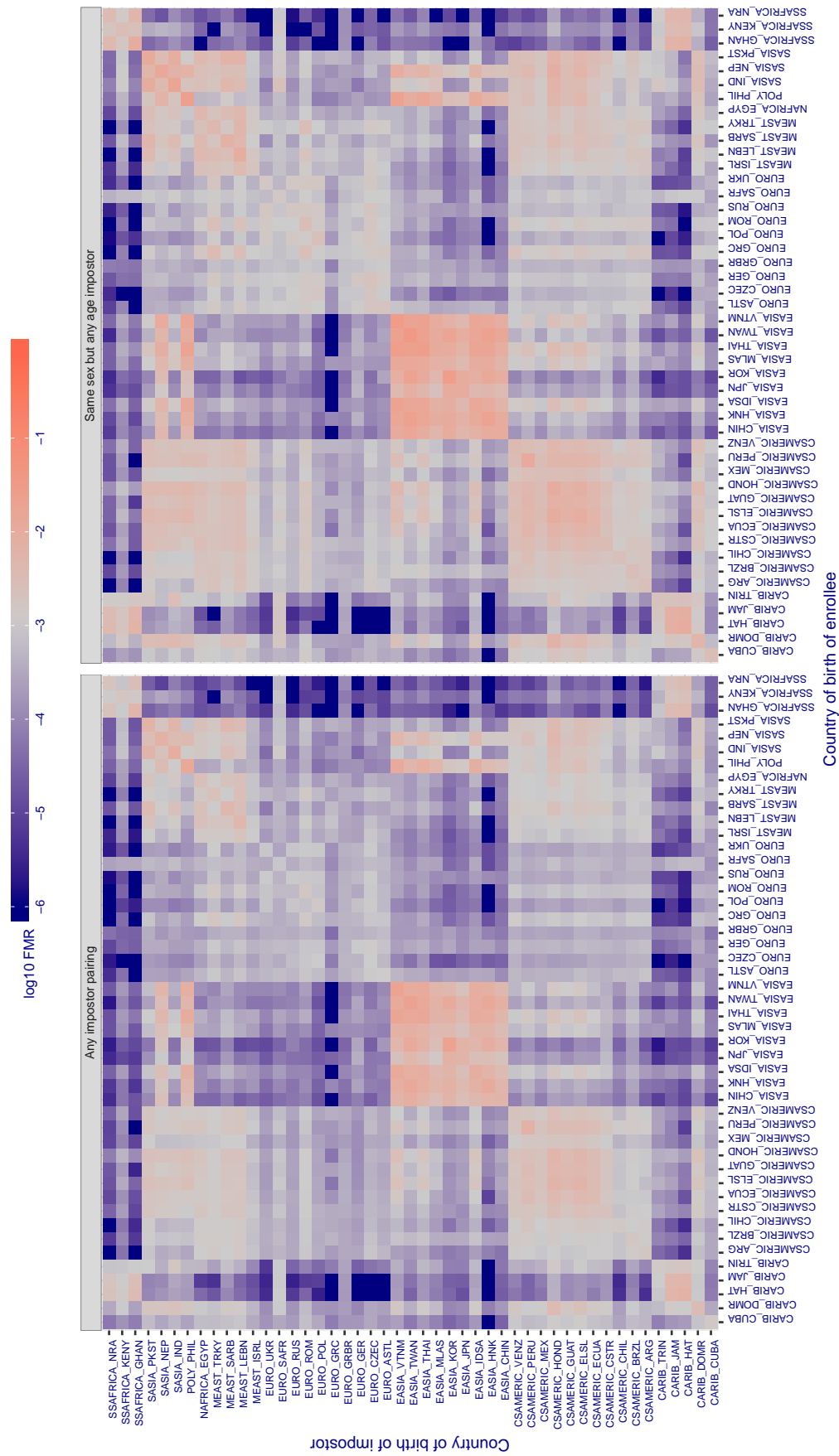
**Cross country FMR at threshold T = 0.790 for algorithm awiros\_001, giving FMR(T) = 0.001 globally.**

Figure 309: For algorithm awiros-001 operating on visa images, the heatmap shows false match rates observed over impostor comparisons of faces from different individuals who were born in the given country pair. False matches are counted against a recognition threshold fixed globally to give the target FMR in the plot title, computed over all on the order of  $10^{10}$  impostor comparisons. If text appears in each box it give the same quantity as that coded by the color. Grey indicates FMR is at the intended FMR target level. Light red colors present a security vulnerability to, for example, a passport gate. Each +1 increase in  $\log_{10} FMR$  corresponds to a factor of 10 increase in FMR. The matrix is not quite symmetric because images in the enrollment and verification sets are different.

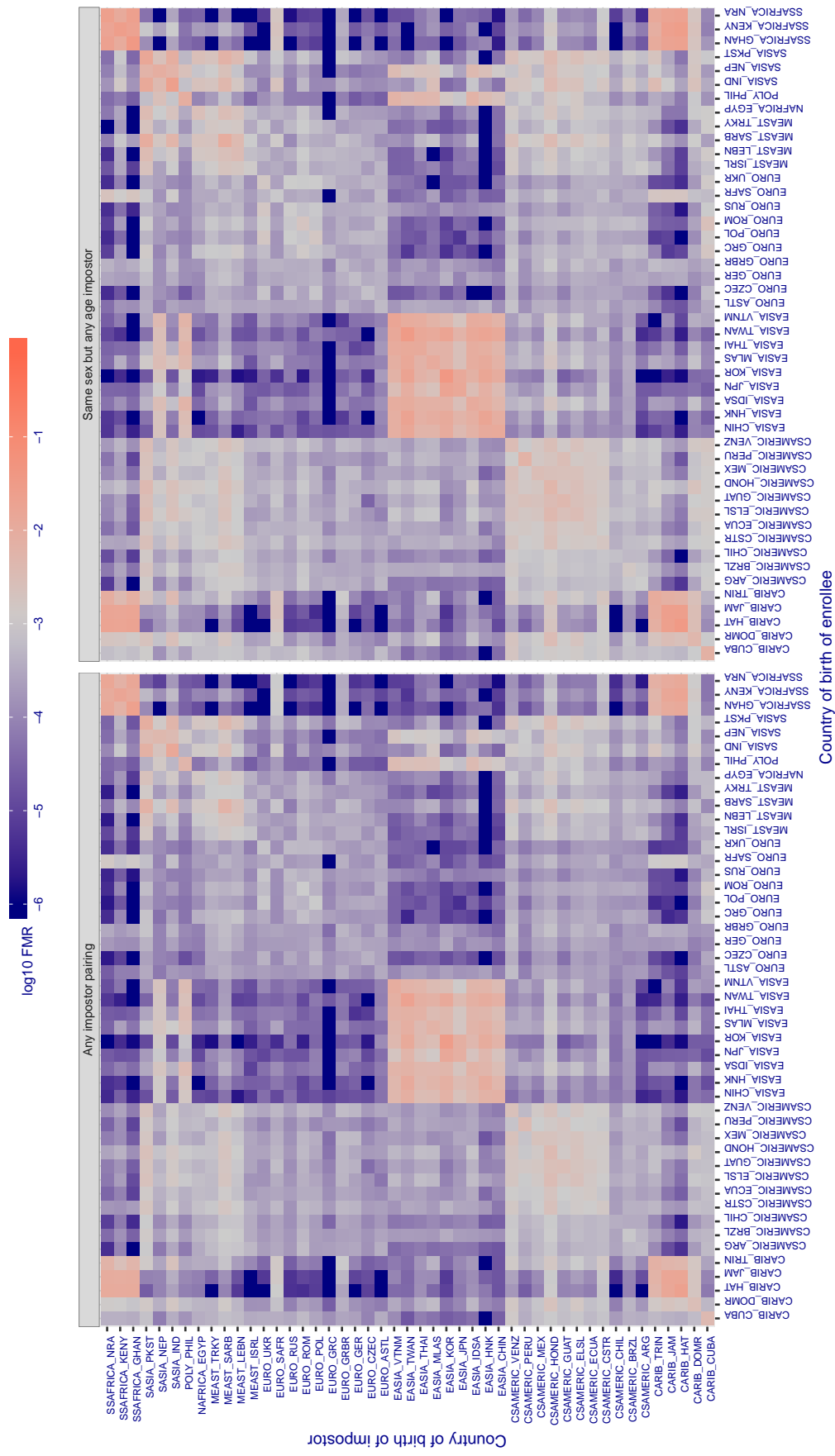
**Cross country FMR at threshold T = 0.800 for algorithm ayonix\_000, giving FMR(T) = 0.001 globally.**

Figure 310: For algorithm ayonix-000 operating on visa images, the heatmap shows false match rates observed over impostor comparisons of faces from different individuals who were born in the given country pair. False matches are counted against a recognition threshold fixed globally to give the target FMR in the plot title, computed over all on the order of  $10^{10}$  impostor comparisons. If text appears in each box it give the same quantity as that coded by the color. Grey indicates FMR is at the intended FMR target level. Light red colors present a security vulnerability to, for example, a passport gate. Each +1 increase in  $\log_{10} FMR$  corresponds to a factor of 10 increase in FMR. The matrix is not quite symmetric because images in the enrollment and verification sets are different.

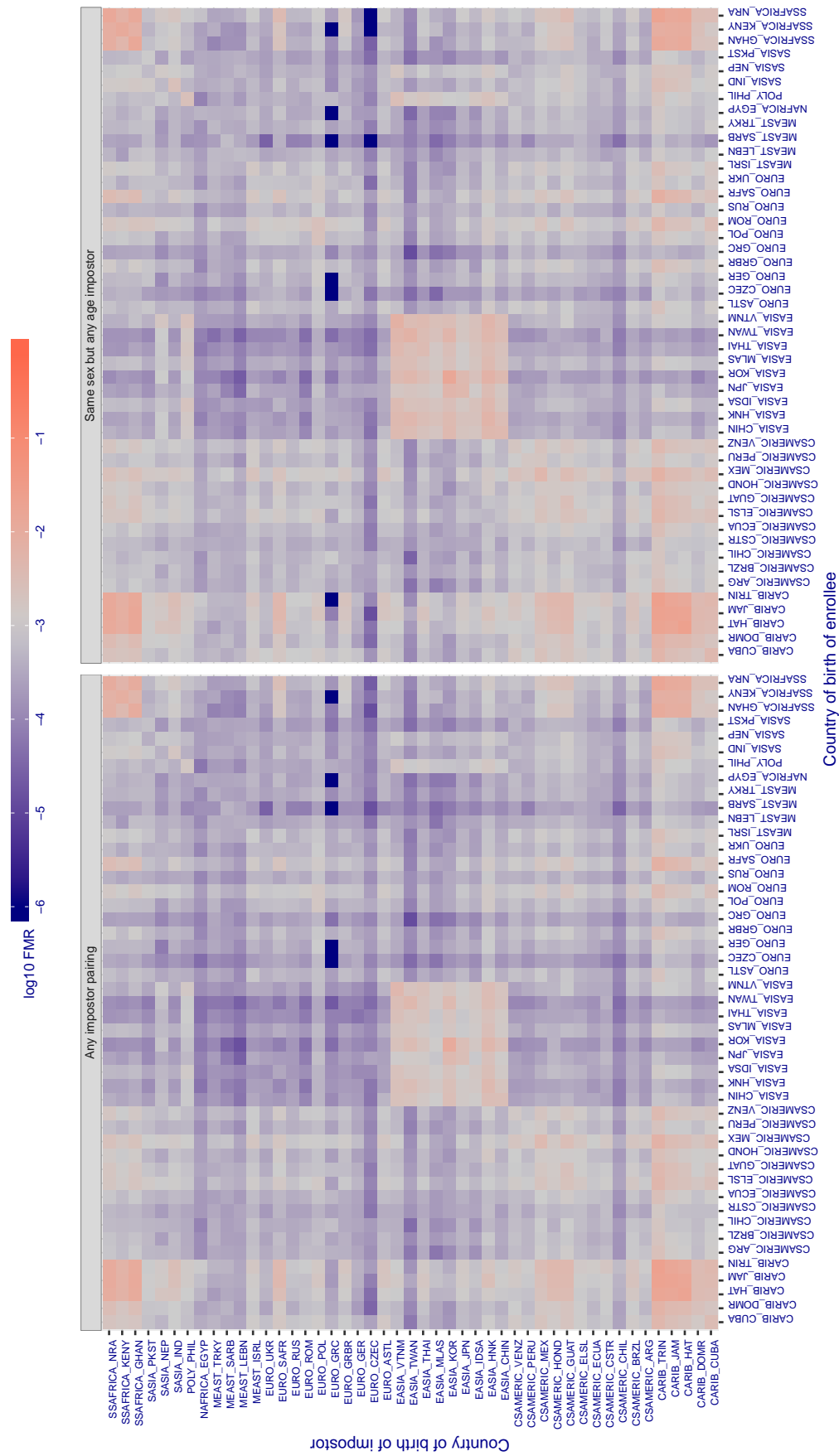
**Cross country FMR at threshold T = 0.649 for algorithm bm\_001, giving FMR(T) = 0.001 globally.**

Figure 311: For algorithm *bm-001* operating on visa images, the heatmap shows false match rates observed over impostor comparisons of faces from different individuals who were born in the given country pair. False matches are counted against a recognition threshold fixed globally to give the target FMR in the plot title, computed over all on the order of  $10^{10}$  impostor comparisons. If text appears in each box it give the same quantity as that coded by the color. Grey indicates FMR is at the intended FMR target level. Light red colors present a security vulnerability to, for example, a passport gate. Each +1 increase in  $\log_{10}$ FMR corresponds to a factor of 10 increase in FMR. The matrix is not quite symmetric because images in the enrollment and verification sets are different.

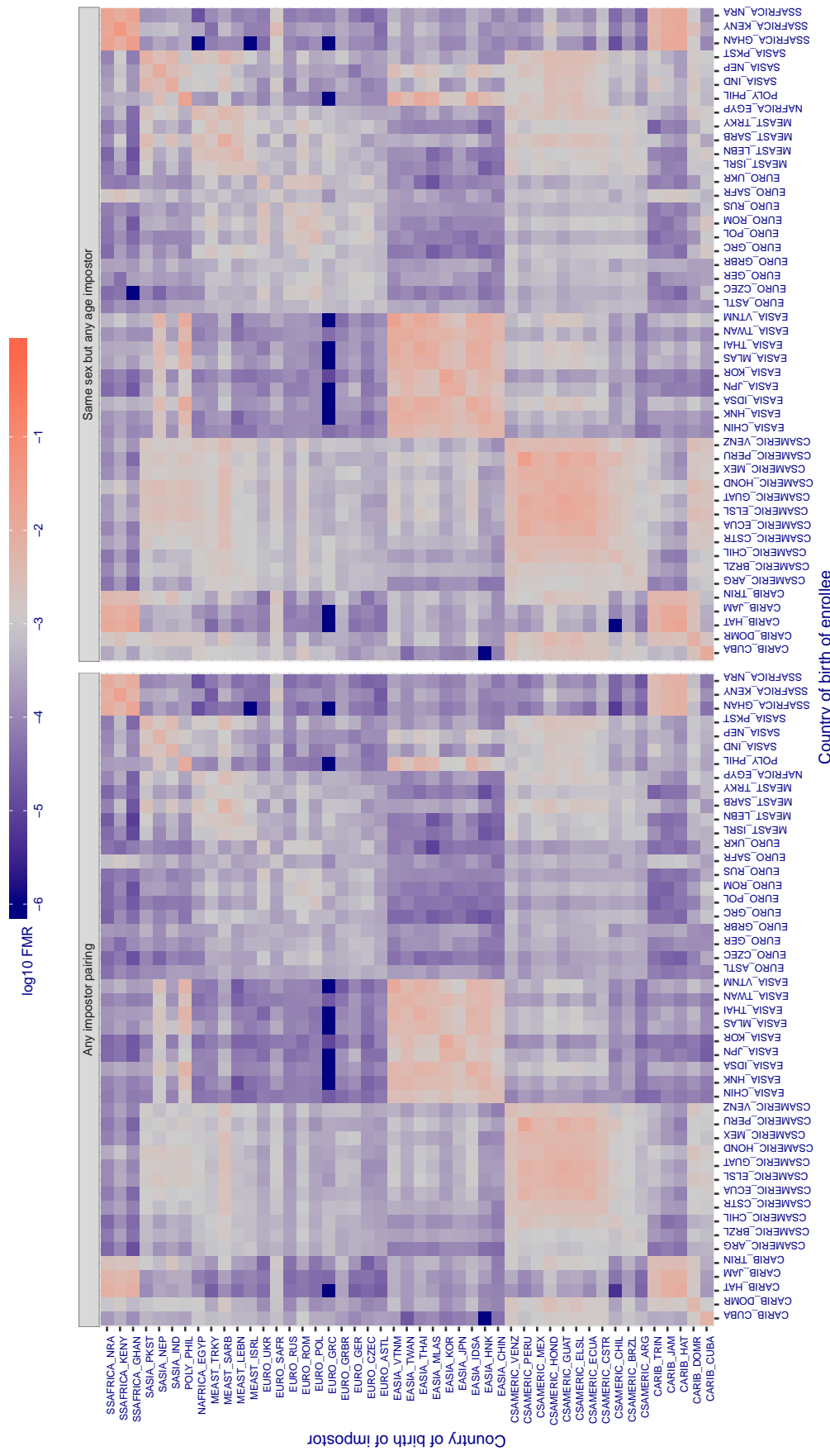
**Cross country FMR at threshold T = 0.306 for algorithm camvi\_002, giving FMR(T) = 0.001 globally.**

Figure 312: For algorithm camvi-002 operating on visa images, the heatmap shows false match rates observed over impostor comparisons of faces from different individuals who were born in the given country pair. False matches are counted against a recognition threshold fixed globally to give the target FMR in the plot title, computed over all on the order of  $10^{10}$  impostor comparisons. If text appears in each box it give the same quantity as that coded by the color. Grey indicates FMR is at the intended FMR target level. Light red colors present a security vulnerability to, for example, a passport gate. Each +1 increase in  $\log_{10} FMR$  corresponds to a factor of 10 increase in FMR. The matrix is not quite symmetric because images in the enrollment and verification sets are different.

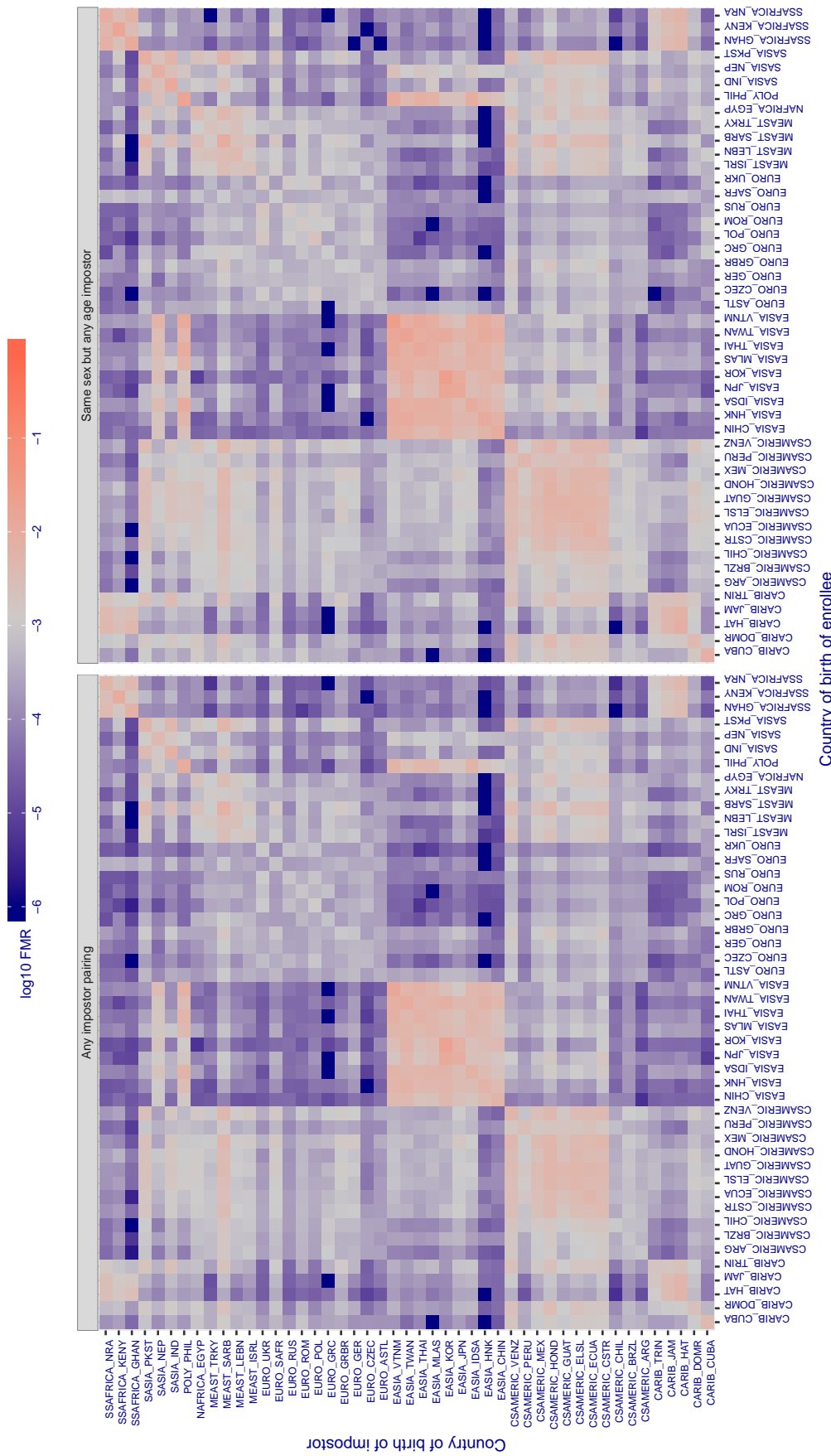
**Cross country FMR at threshold T = 0.277 for algorithm camvi\_004, giving FMR(T) = 0.001 globally.**

Figure 313: For algorithm camvi-004 operating on visa images, the heatmap shows false match rates observed over impostor comparisons of faces from different individuals who were born in the given country pair. False matches are counted against a recognition threshold fixed globally to give the target FMR in the plot title, computed over all on the order of  $10^{10}$  impostor comparisons. If text appears in each box it give the same quantity as that coded by the color. Grey indicates FMR is at the intended FMR target level. Light red colors present a security vulnerability to, for example, a passport gate. Each +1 increase in  $\log_{10} \text{FMR}$  corresponds to a factor of 10 increase in FMR. The matrix is not quite symmetric because images in the enrollment and verification sets are different.

**Cross country FMR at threshold T = 0.346 for algorithm ceiec\_001, giving FMR(T) = 0.001 globally.**

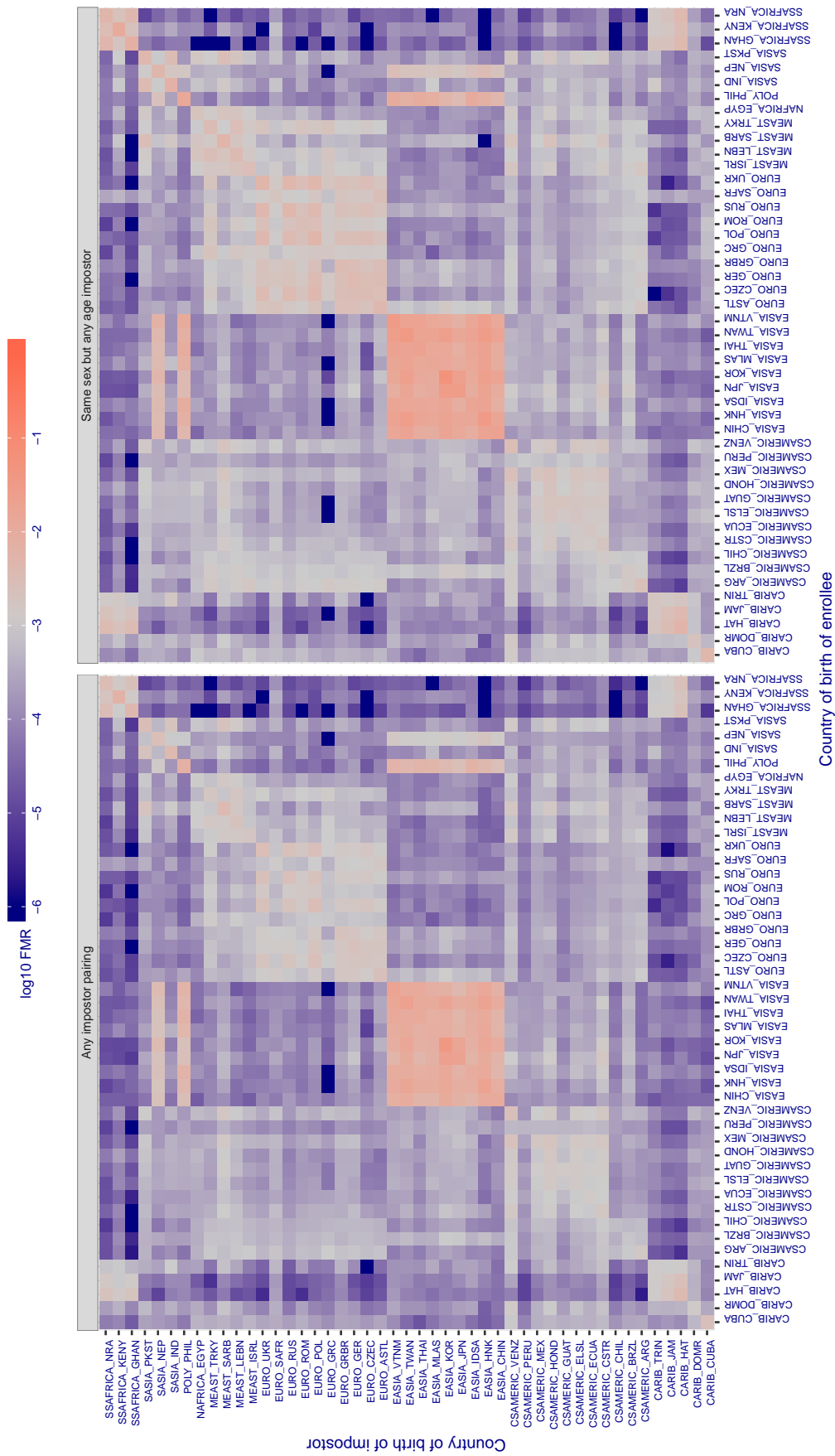


Figure 314: For algorithm ceiec-001 operating on visa images, the heatmap shows false match rates observed over impostor comparisons of faces from different individuals who were born in the given country pair. False matches are counted against a recognition threshold fixed globally to give the target FMR in the plot title, computed over all on the order of  $10^{10}$  impostor comparisons. If text appears in each box it give the same quantity as that coded by the color. Grey indicates FMR is at the intended FMR target level. Light red colors present a security vulnerability to, for example, a passport gate. Each +1 increase in  $\log_{10} FMR$  corresponds to a factor of 10 increase in FMR. The matrix is not quite symmetric because images in the enrollment and verification sets are different.

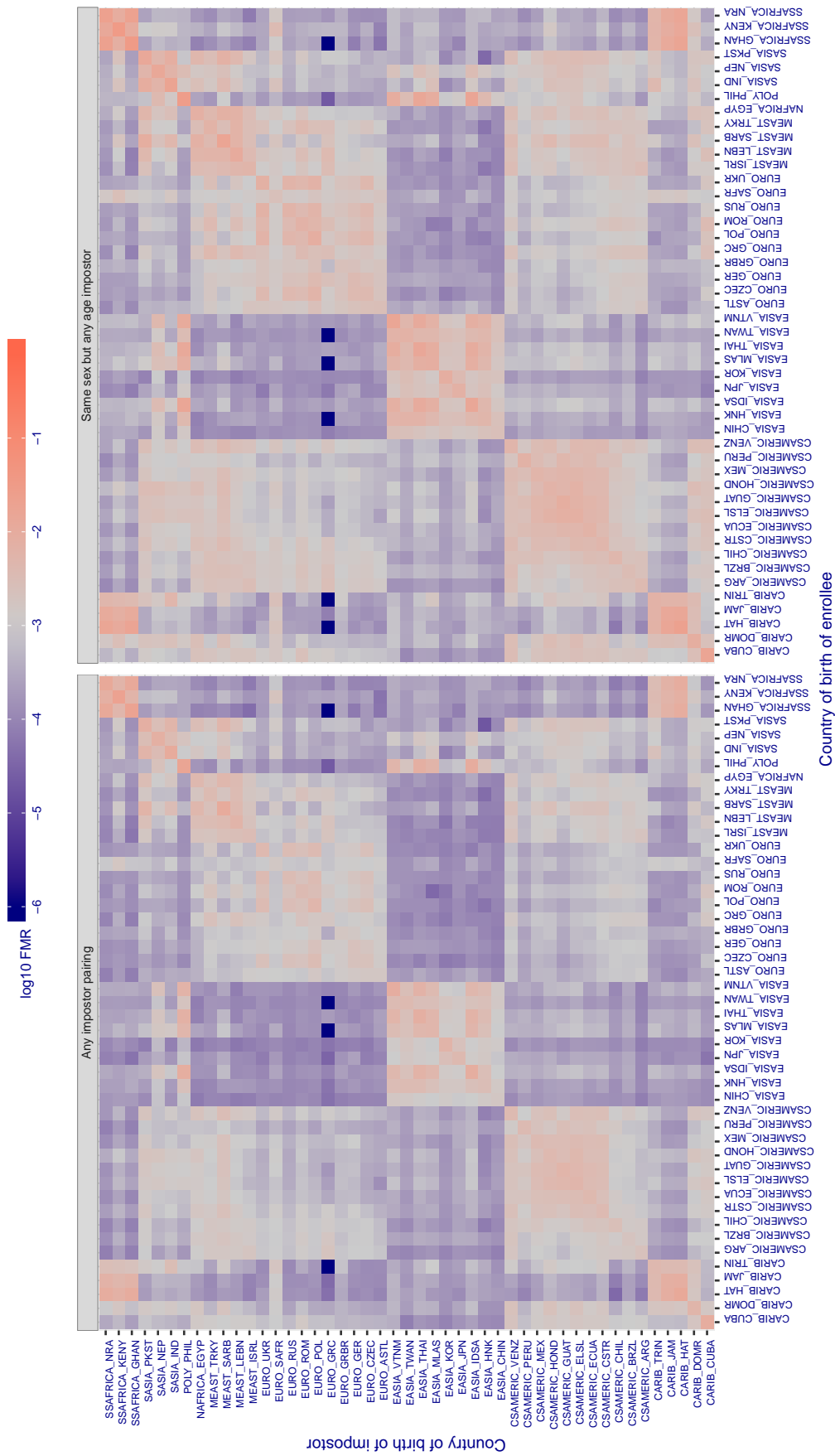
**Cross country FMR at threshold T = 0.247 for algorithm ceiec\_002, giving FMR(T) = 0.001 globally.**

Figure 315: For algorithm ceiec-002 operating on visa images, the heatmap shows false match rates observed over impostor comparisons of faces from different individuals who were born in the given country pair. False matches are counted against a recognition threshold fixed globally to give the target FMR in the plot title, computed over all on the order of  $10^{10}$  impostor comparisons. If text appears in each box it give the same quantity as that coded by the color. Grey indicates FMR is at the intended FMR target level. Light red colors present a security vulnerability to, for example, a passport gate. Each +1 increase in  $\log_{10} FMR$  corresponds to a factor of 10 increase in FMR. The matrix is not quite symmetric because images in the enrollment and verification sets are different.

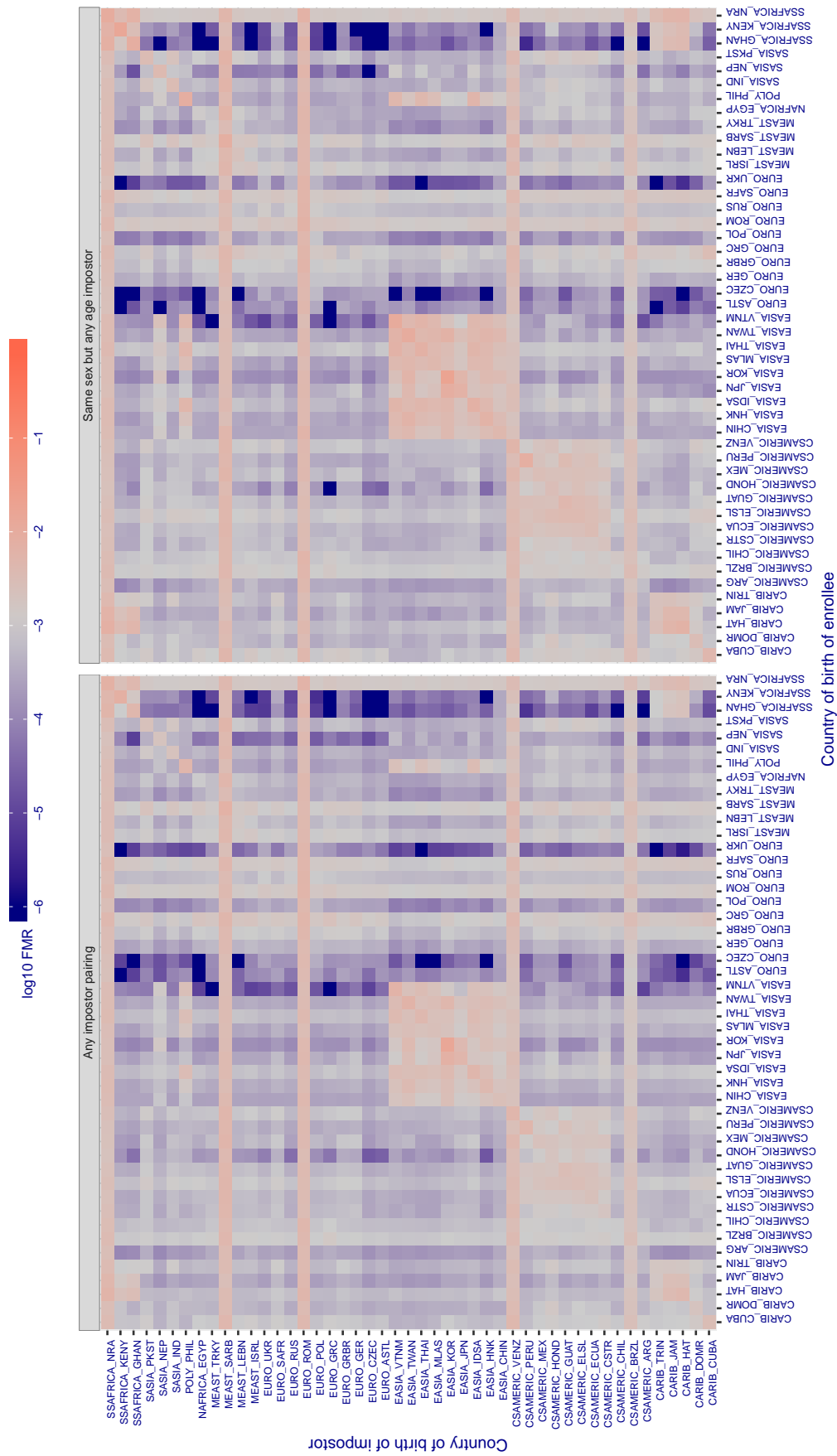
**Cross country FMR at threshold T = 0.365 for algorithm chtface\_001, giving  $\text{FMR}(\text{T}) = 0.001$  globally.**

Figure 316: For algorithm chtface-001 operating on visa images, the heatmap shows false match rates observed over impostor comparisons of faces from different individuals who were born in the given country pair. False matches are counted against a recognition threshold fixed globally to give the target  $\text{FMR}$  in the plot title, computed over all on the order of  $10^{10}$  impostor comparisons. If text appears in each box it give the same quantity as that coded by the color. Grey indicates  $\text{FMR}$  is at the intended  $\text{FMR}$  target level. Light red colors present a security vulnerability to, for example, a passport gate. Each +1 increase in  $\log_{10} \text{FMR}$  corresponds to a factor of 10 increase in  $\text{FMR}$ . The matrix is not quite symmetric because images in the enrollment and verification sets are different.

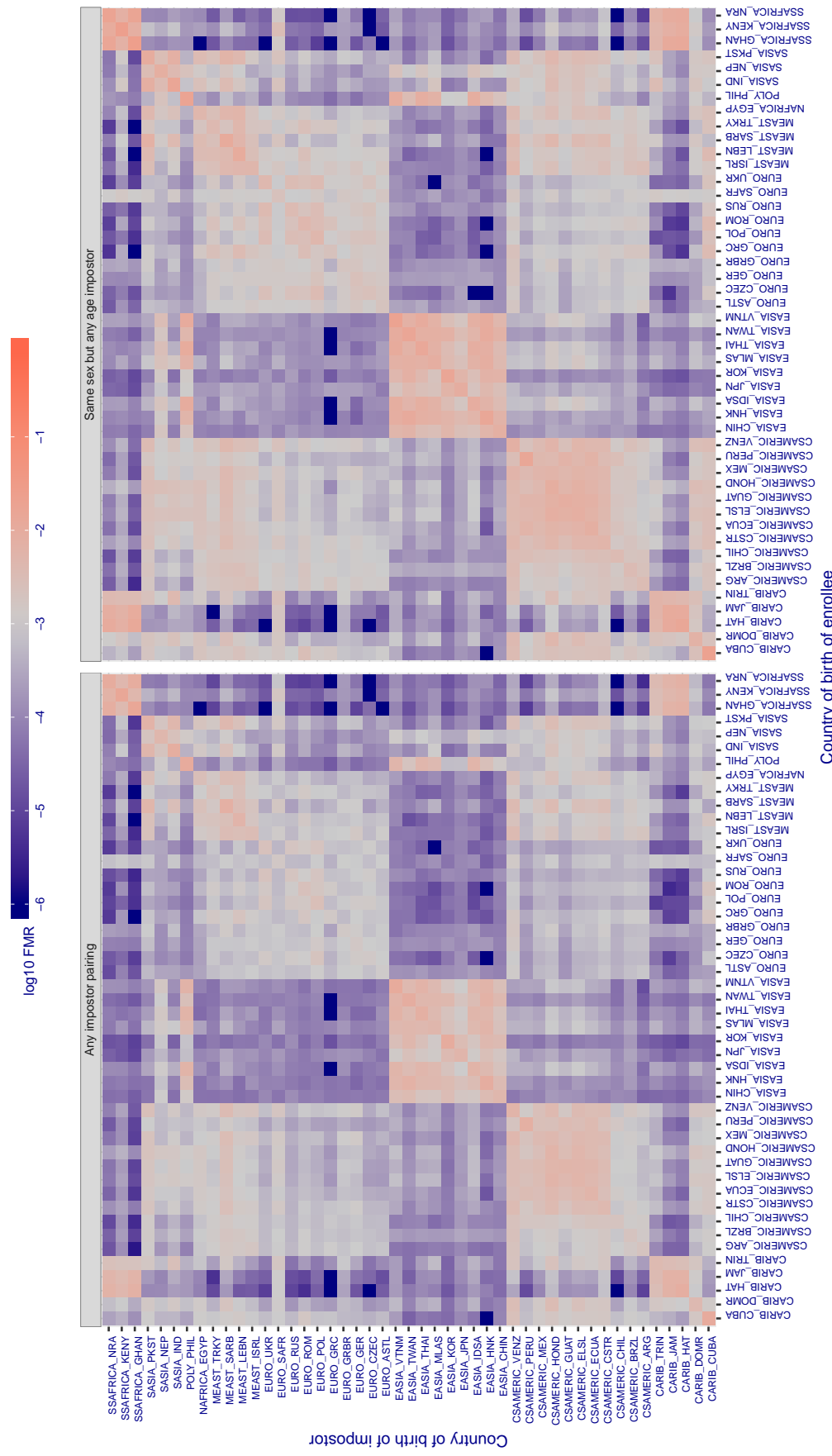
**Cross country FMR at threshold T = 2845.000 for algorithm cogent\_003, giving FMR(T) = 0.001 globally.**

Figure 317: For algorithm cogent-003 operating on visa images, the heatmap shows false match rates observed over impostor comparisons of faces from different individuals who were born in the given country pair. False matches are counted against a recognition threshold fixed globally to give the target FMR in the plot title, computed over all on the order of  $10^{10}$  impostor comparisons. If text appears in each box it give the same quantity as that coded by the color. Grey indicates FMR is at the intended FMR target level. Light red colors present a security vulnerability to, for example, a passport gate. Each +1 increase in  $\log_{10} FMR$  corresponds to a factor of 10 increase in FMR. The matrix is not quite symmetric because images in the enrollment and verification sets are different.

**Cross country FMR at threshold T = 2939.000 for algorithm cogent\_004, giving  $FMR(T) = 0.001$  globally.**

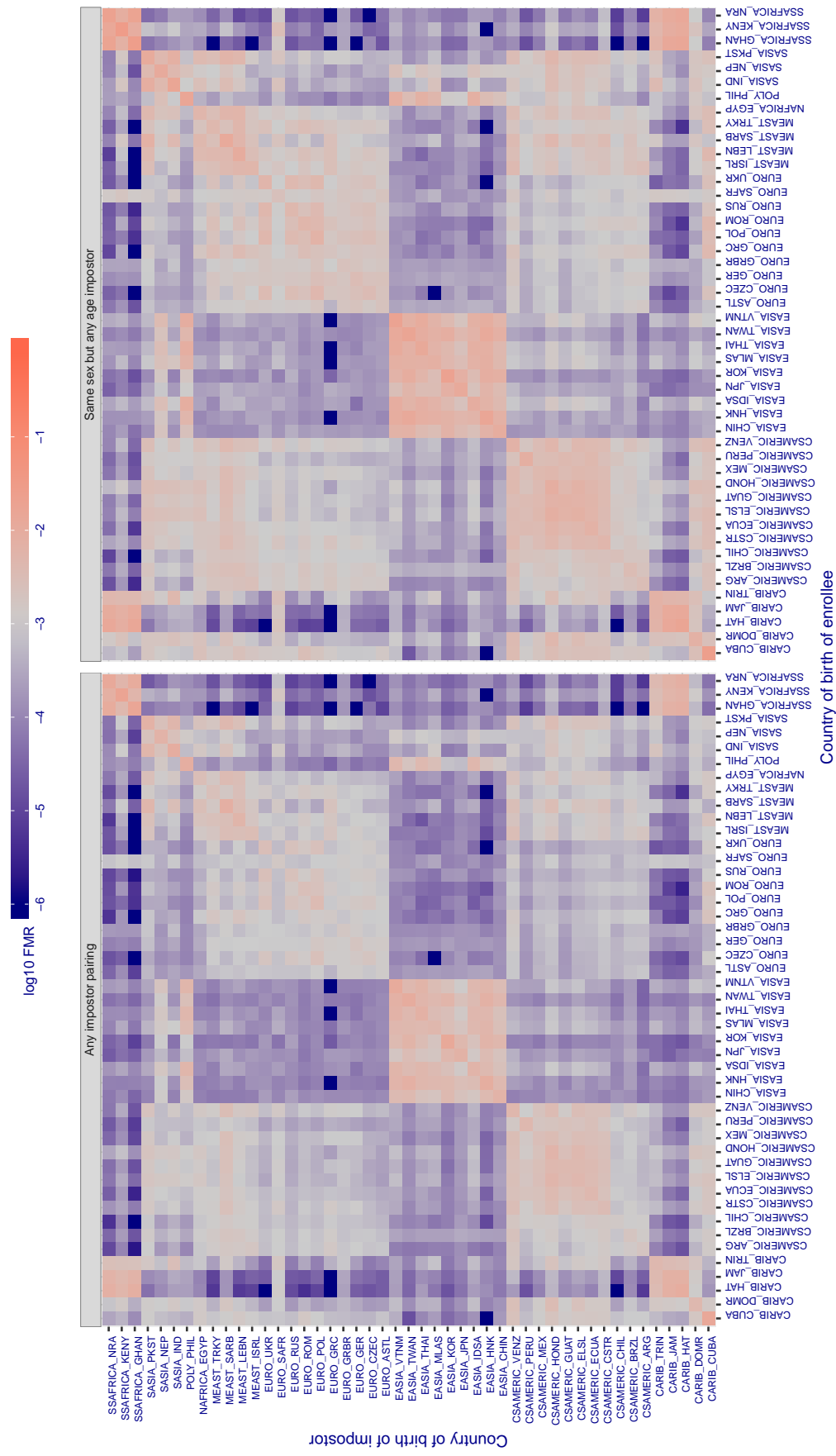


Figure 318: For algorithm cogent-004 operating on visa images, the heatmap shows false match rates observed over impostor comparisons of faces from different individuals who were born in the given country pair. False matches are counted against a recognition threshold fixed globally to give the target  $FMR$  in the plot title, computed over all on the order of  $10^{10}$  impostor comparisons. If text appears in each box it give the same quantity as that coded by the color. Grey indicates  $FMR$  is at the intended  $FMR$  target level. Light red colors present a security vulnerability to, for example, a passport gate. Each +1 increase in  $\log_{10} FMR$  corresponds to a factor of 10 increase in  $FMR$ . The matrix is not quite symmetric because images in the enrollment and verification sets are different.

Cross country FMR at threshold T = 0.522 for algorithm cognitec\_000, giving FMR(T) = 0.001 globally.

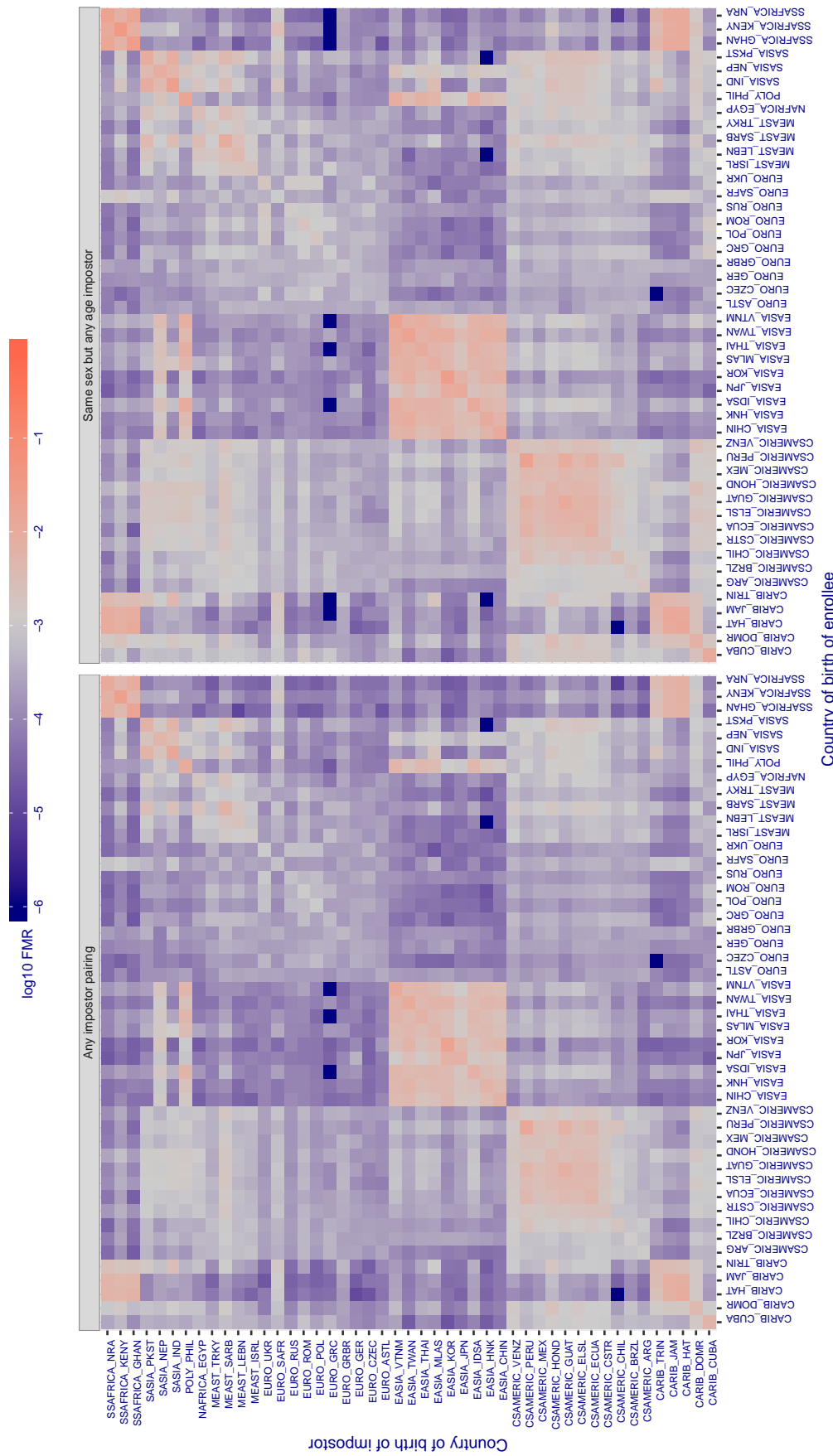


Figure 319: For algorithm cognitec-000 operating on visa images, the heatmap shows false match rates observed over impostor comparisons of faces from different individuals who were born in the given country pair. False matches are counted against a recognition threshold fixed globally to give the target FMR in the plot title, computed over all on the order of  $10^{10}$  impostor comparisons. If text appears in each box it give the same quantity as that coded by the color. Grey indicates FMR is at the intended FMR target level. Light red colors present a security vulnerability to, for example, a passport gate. Each +1 increase in  $\log_{10} FMR$  corresponds to a factor of 10 increase in FMR. The matrix is not quite symmetric because images in the enrollment and verification sets are different.

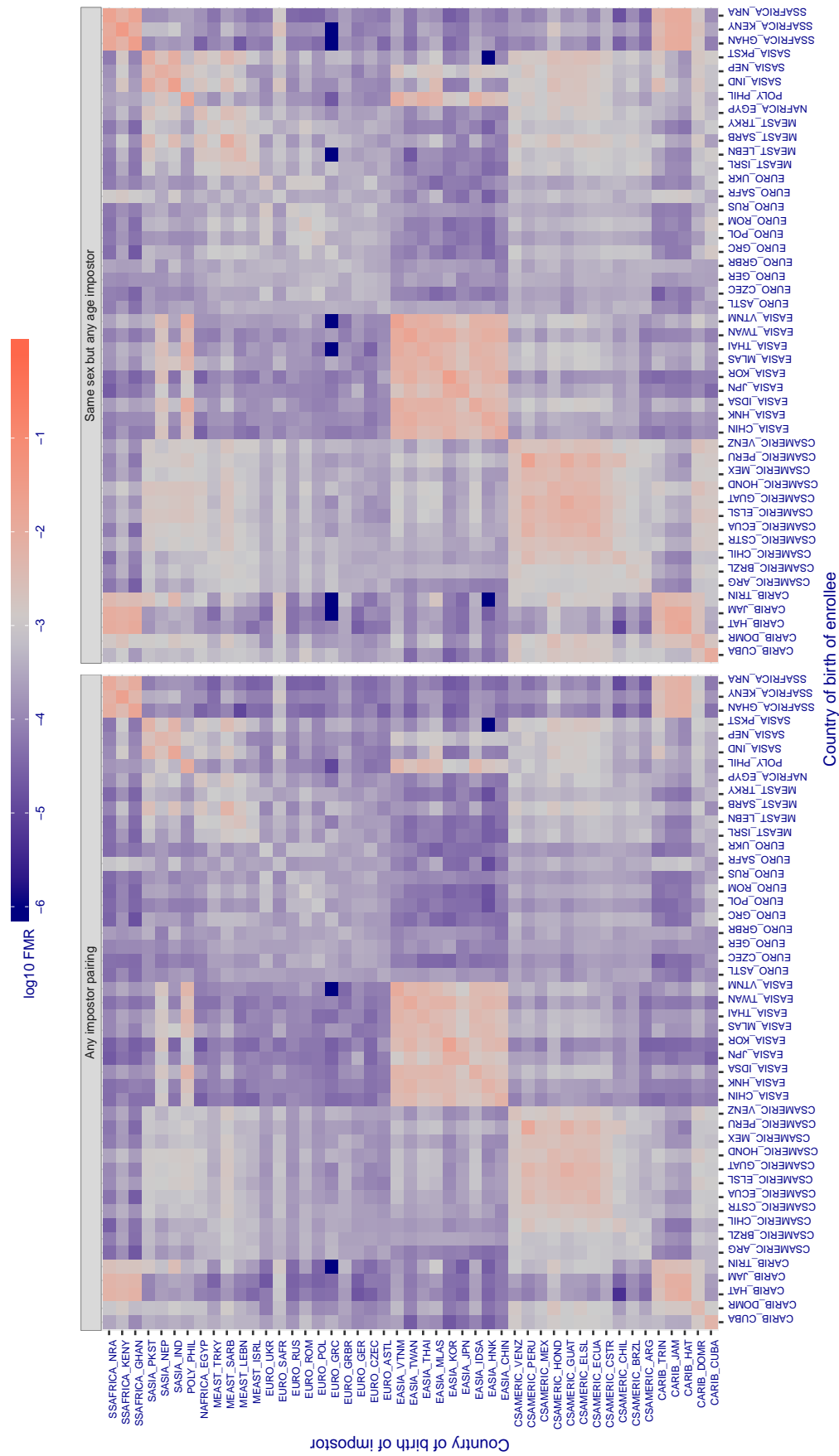
**Cross country FMR at threshold T = 0.522 for algorithm cognitec\_001, giving FMR(T) = 0.001 globally.**

Figure 320: For algorithm cognitec-001 operating on visa images, the heatmap shows false match rates observed over impostor comparisons of faces from different individuals who were born in the given country pair. False matches are counted against a recognition threshold fixed globally to give the target FMR in the plot title, computed over all on the order of  $10^{10}$  impostor comparisons. If text appears in each box it give the same quantity as that coded by the color. Grey indicates FMR is at the intended FMR target level. Light red colors present a security vulnerability to, for example, a passport gate. Each +1 increase in  $\log_{10} \text{FMR}$  corresponds to a factor of 10 increase in FMR. The matrix is not quite symmetric because images in the enrollment and verification sets are different.

**Cross country FMR at threshold T = 3.572 for algorithm ctbcbank\_000, giving  $FMR(T) = 0.001$  globally.**

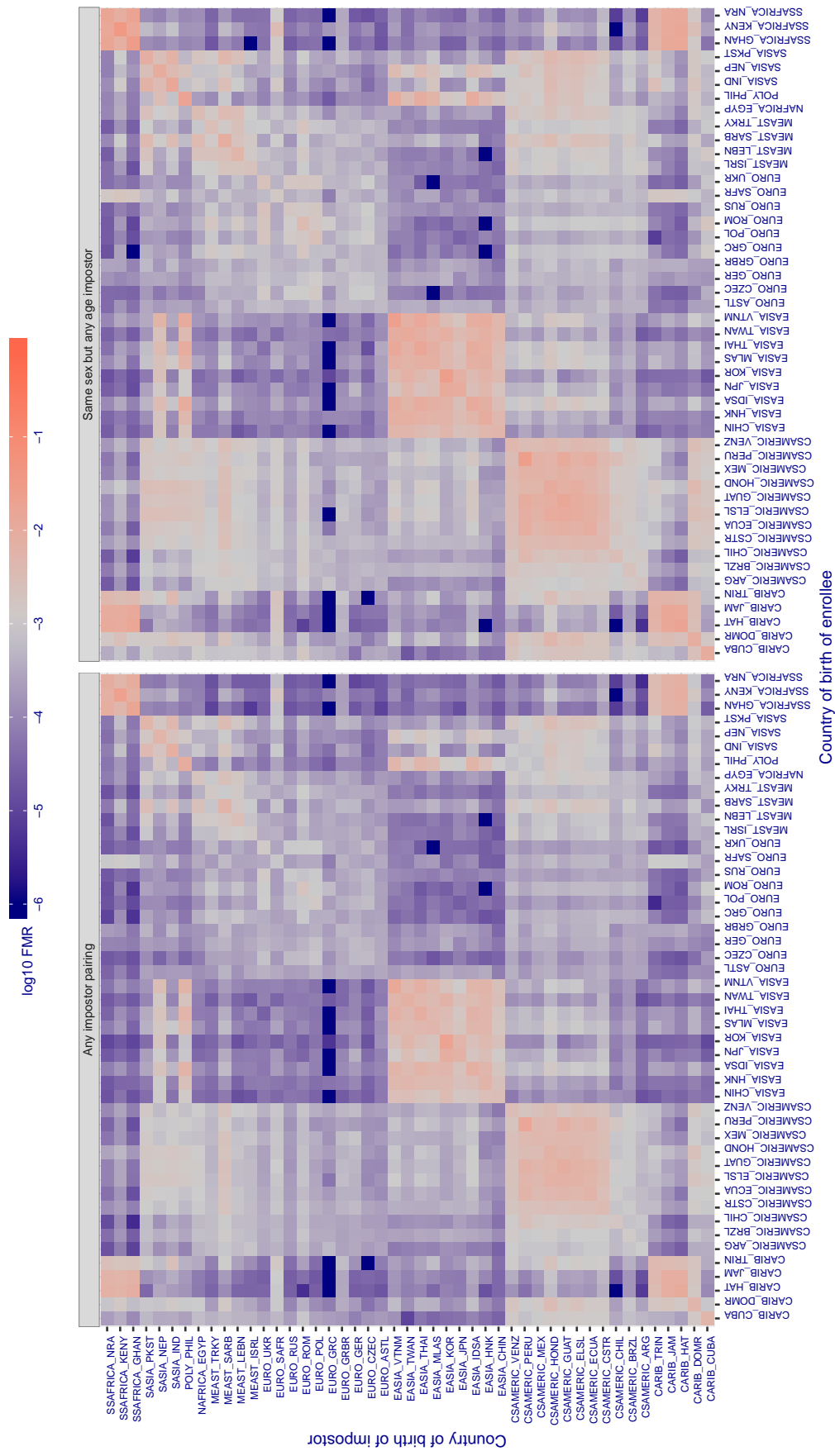


Figure 321: For algorithm ctbcbank-000 operating on visa images, the heatmap shows false match rates observed over impostor comparisons of faces from different individuals who were born in the given country pair. False matches are counted against a recognition threshold fixed globally to give the target  $FMR$  in the plot title, computed over all on the order of  $10^{10}$  impostor comparisons. If text appears in each box it give the same quantity as that coded by the color. Grey indicates  $FMR$  is at the intended  $FMR$  target level. Light red colors present a security vulnerability to, for example, a passport gate. Each +1 increase in  $\log_{10} FMR$  corresponds to a factor of 10 increase in  $FMR$ . The matrix is not quite symmetric because images in the enrollment and verification sets are different.

Cross country FMR at threshold T = 0.702 for algorithm cyberextruder\_001, giving  $FMR(T) = 0.001$  globally.

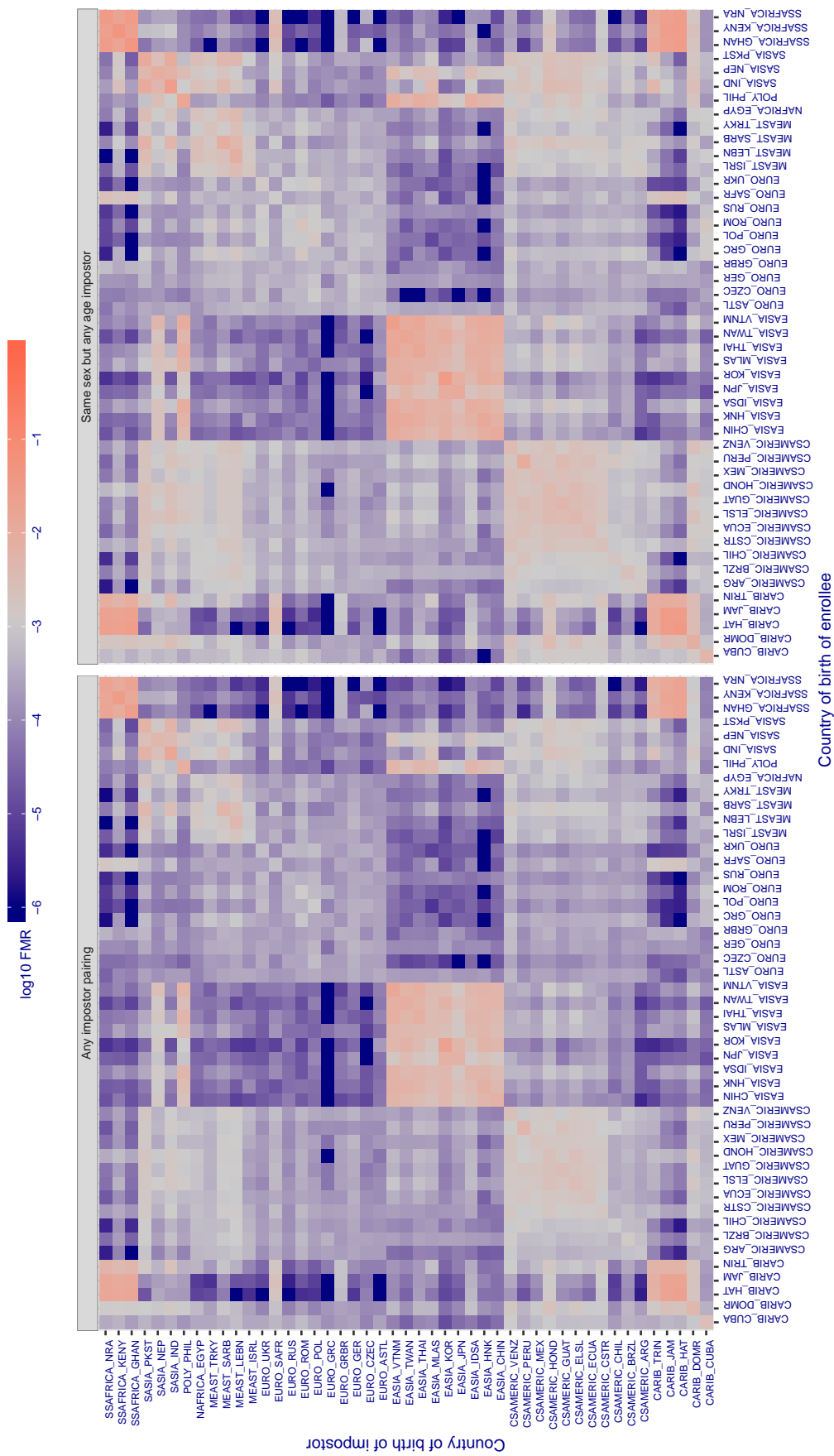


Figure 322: For algorithm cyberextruder-001 operating on visa images, the heatmap shows false match rates observed over impostor comparisons of faces from different individuals who were born in the given country pair. False matches are counted against a recognition threshold fixed globally to give the target FMR in the plot title, computed over all on the order of  $10^{10}$  impostor comparisons. If text appears in each box it give the same quantity as that coded by the color. Grey indicates FMR is at the intended FMR target level. Light red colors present a security vulnerability to, for example, a passport gate. Each +1 increase in  $\log_{10} FMR$  corresponds to a factor of 10 increase in FMR. The matrix is not quite symmetric because images in the enrollment and verification sets are different.

Cross country FMR at threshold T = 0.408 for algorithm cyberextruder\_002, giving  $FMR(T) = 0.001$  globally.

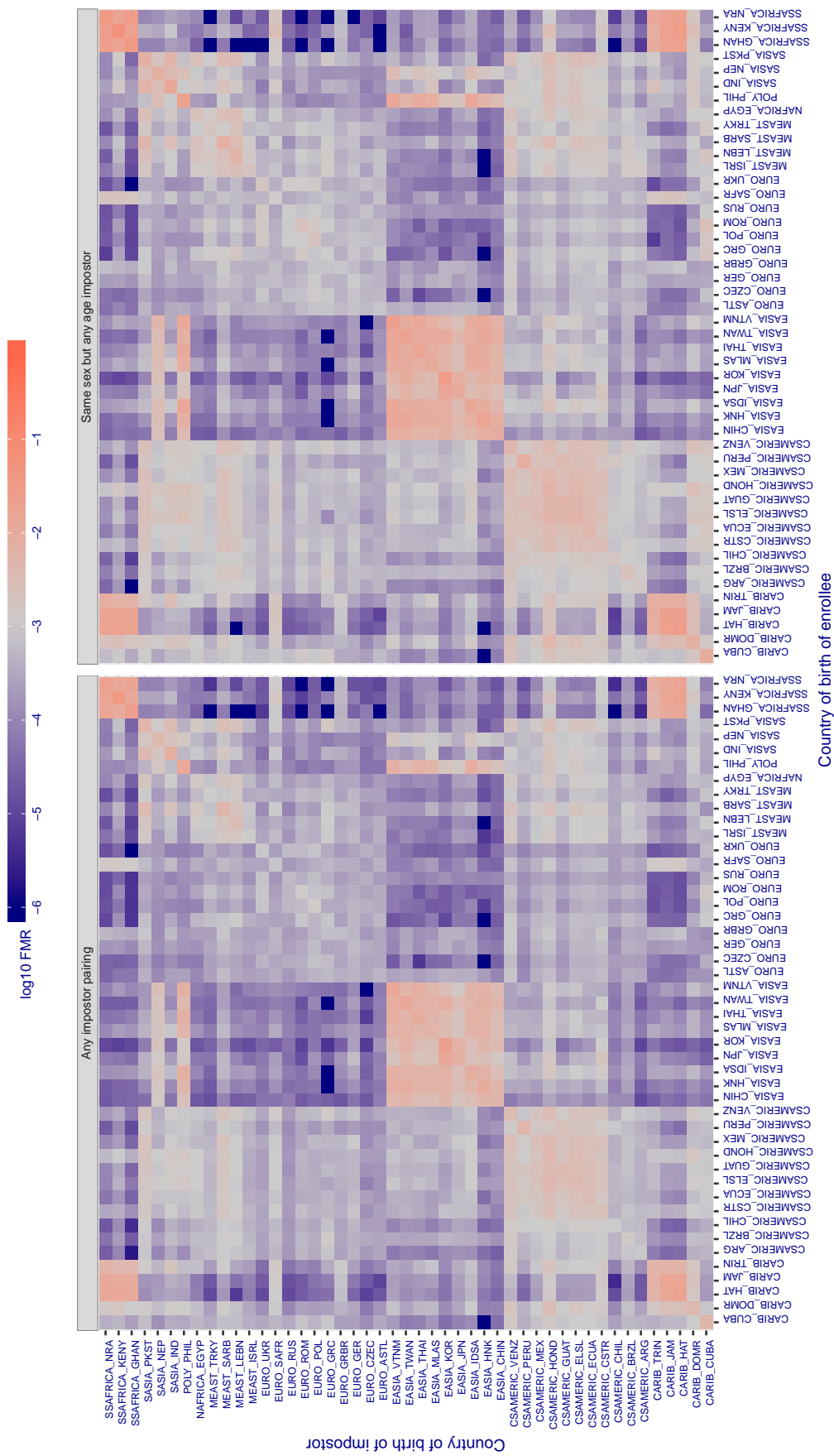


Figure 323: For algorithm cyberextruder-002 operating on visa images, the heatmap shows false match rates observed over impostor comparisons of faces from different individuals who were born in the given country pair. False matches are counted against a recognition threshold fixed globally to give the target FMR in the plot title, computed over all on the order of  $10^{10}$  impostor comparisons. If text appears in each box it give the same quantity as that coded by the color. Grey indicates FMR is at the intended FMR target level. Light red colors present a security vulnerability to, for example, a passport gate. Each +1 increase in  $\log_{10} FMR$  corresponds to a factor of 10 increase in FMR. The matrix is not quite symmetric because images in the enrollment and verification sets are different.

Cross country FMR at threshold T = 1.322 for algorithm cyberlink\_002, giving  $\text{FMR}(\text{T}) = 0.001$  globally.

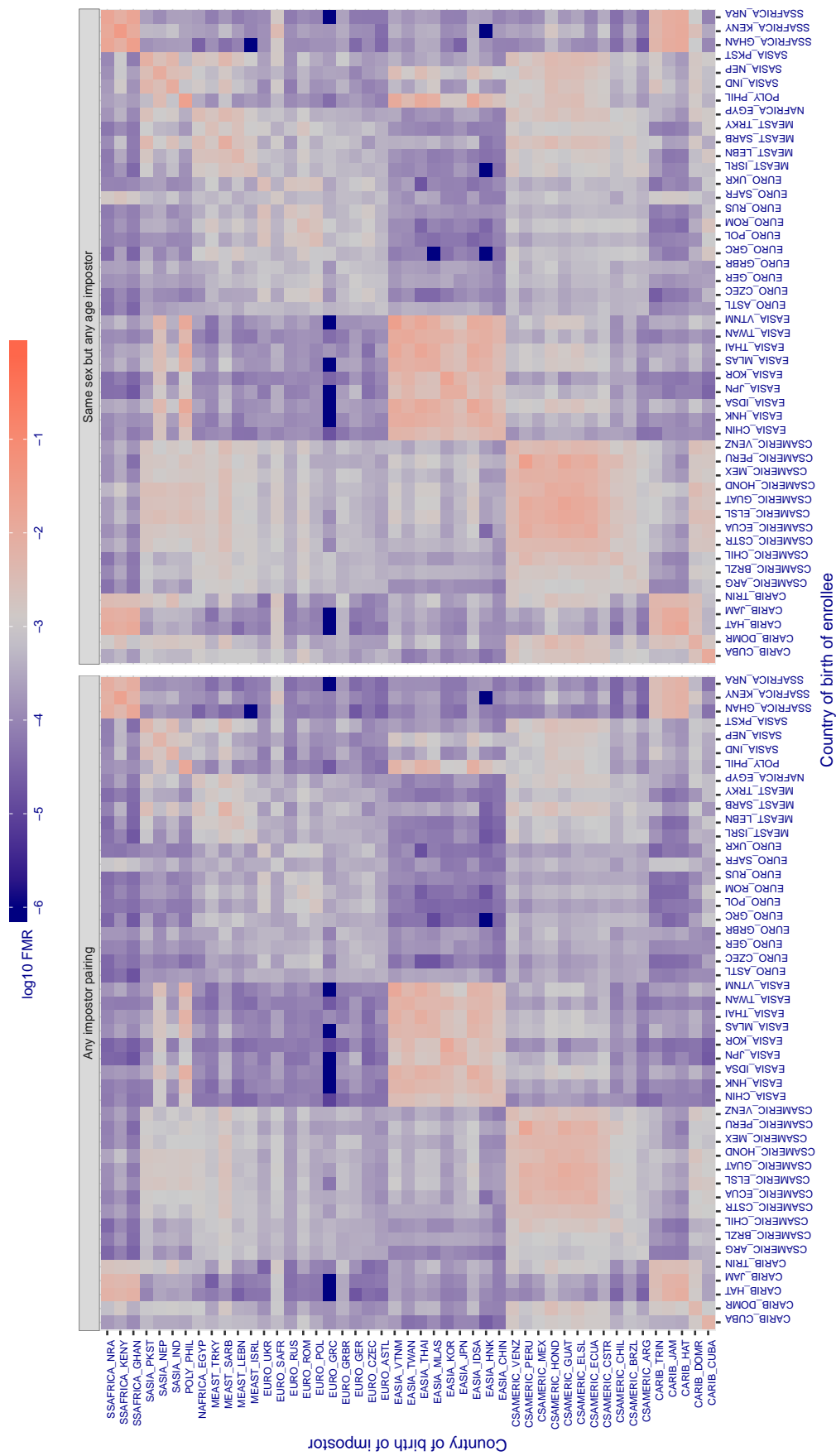


Figure 324: For algorithm cyberlink-002 operating on visa images, the heatmap shows false match rates observed over impostor comparisons of faces from different individuals who were born in the given country pair. False matches are counted against a recognition threshold fixed globally to give the target  $\text{FMR}$  in the plot title, computed over all on the order of  $10^{10}$  impostor comparisons. If text appears in each box it give the same quantity as that coded by the color. Grey indicates  $\text{FMR}$  is at the intended  $\text{FMR}$  target level. Light red colors present a security vulnerability to, for example, a passport gate. Each +1 increase in  $\log_{10} \text{FMR}$  corresponds to a factor of 10 increase in  $\text{FMR}$ . The matrix is not quite symmetric because images in the enrollment and verification sets are different.

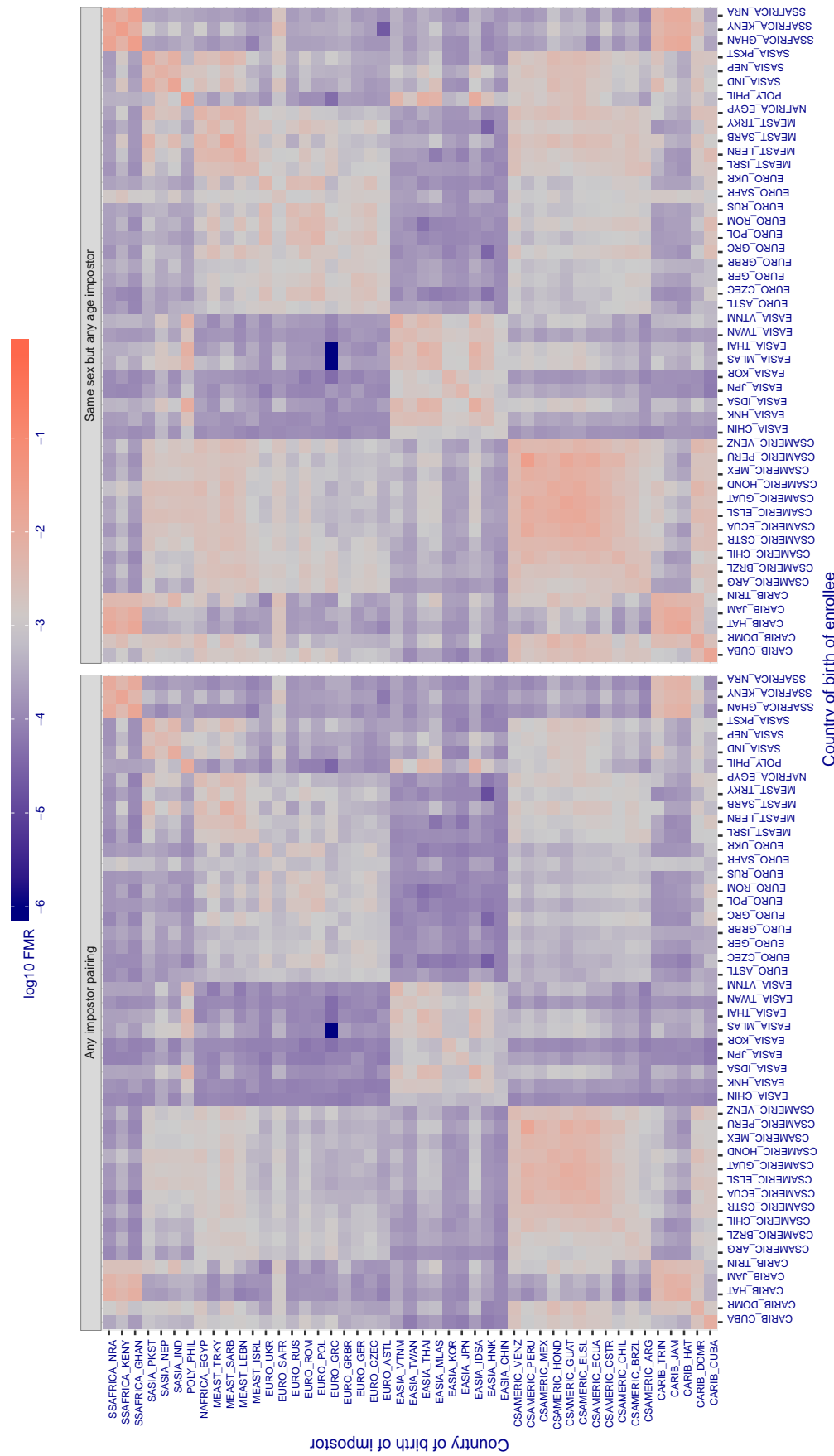
**Cross country FMR at threshold T = 5958.000 for algorithm dahua\_002, giving  $FMR(T) = 0.001$  globally.**

Figure 325: For algorithm dahua-002 operating on visa images, the heatmap shows false match rates observed over impostor comparisons of faces from different individuals who were born in the given country pair. False matches are counted against a recognition threshold fixed globally to give the target  $FMR$  in the plot title, computed over all on the order of  $10^{10}$  impostor comparisons. If text appears in each box it give the same quantity as that coded by the color. Grey indicates  $FMR$  is at the intended  $FMR$  target level. Light red colors present a security vulnerability to, for example, a passport gate. Each +1 increase in  $\log_{10} FMR$  corresponds to a factor of 10 increase in  $FMR$ . The matrix is not quite symmetric because images in the enrollment and verification sets are different.

**Cross country FMR at threshold T = 5392.000 for algorithm dahua\_003, giving  $FMR(T) = 0.001$  globally.**

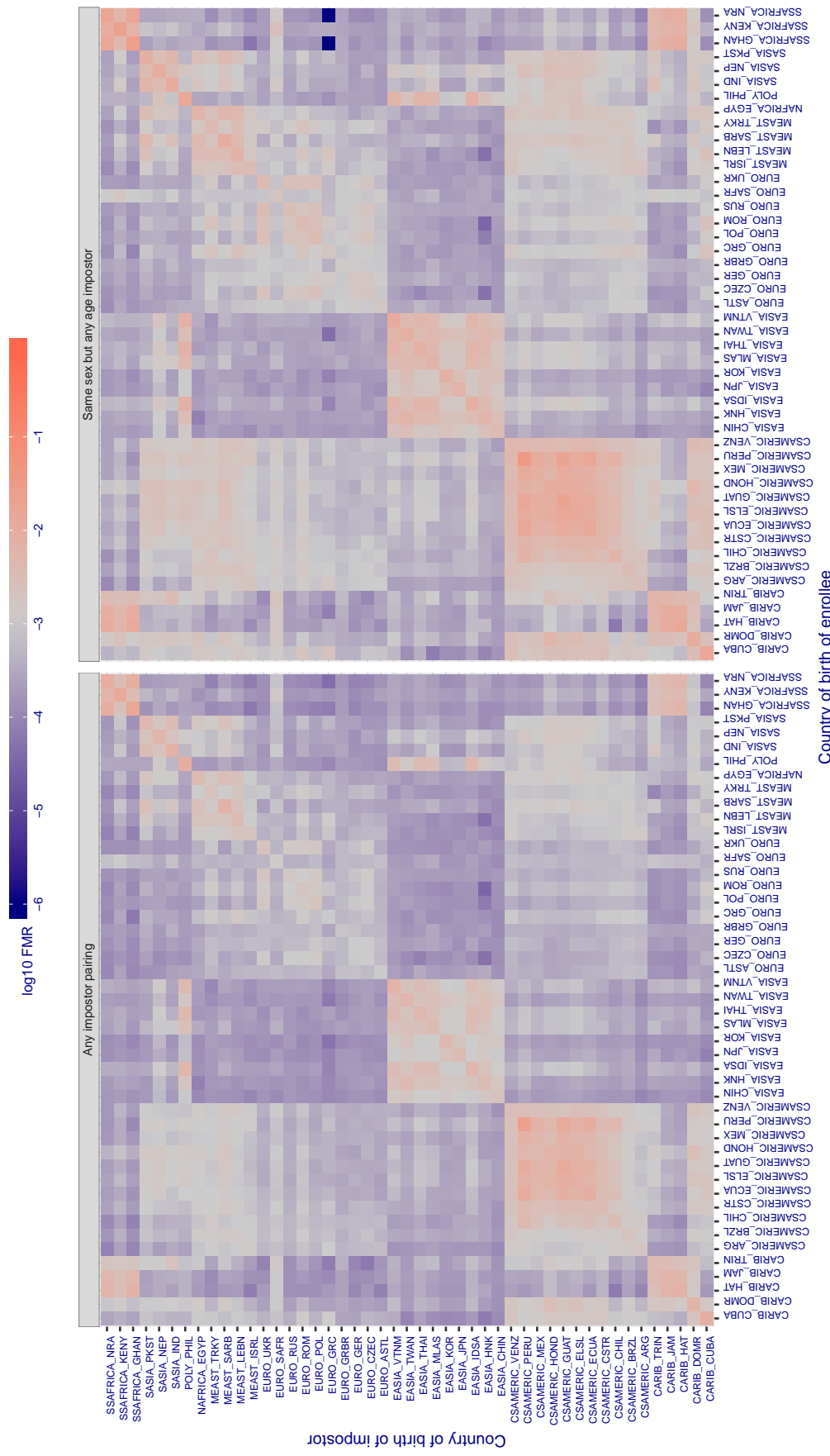


Figure 326: For algorithm dahua-003 operating on visa images, the heatmap shows false match rates observed over impostor comparisons of faces from different individuals who were born in the given country pair. False matches are counted against a recognition threshold fixed globally to give the target  $FMR$  in the plot title, computed over all on the order of  $10^{10}$  impostor comparisons. If text appears in each box it give the same quantity as that coded by the color. Grey indicates  $FMR$  is at the intended  $FMR$  target level. Light red colors present a security vulnerability to, for example, a passport gate. Each +1 increase in  $\log_{10} FMR$  corresponds to a factor of 10 increase in  $FMR$ . The matrix is not quite symmetric because images in the enrollment and verification sets are different.

**Cross country FMR at threshold T = 1.293 for algorithm deepglint\_001, giving  $FMR(T) = 0.001$  globally.**

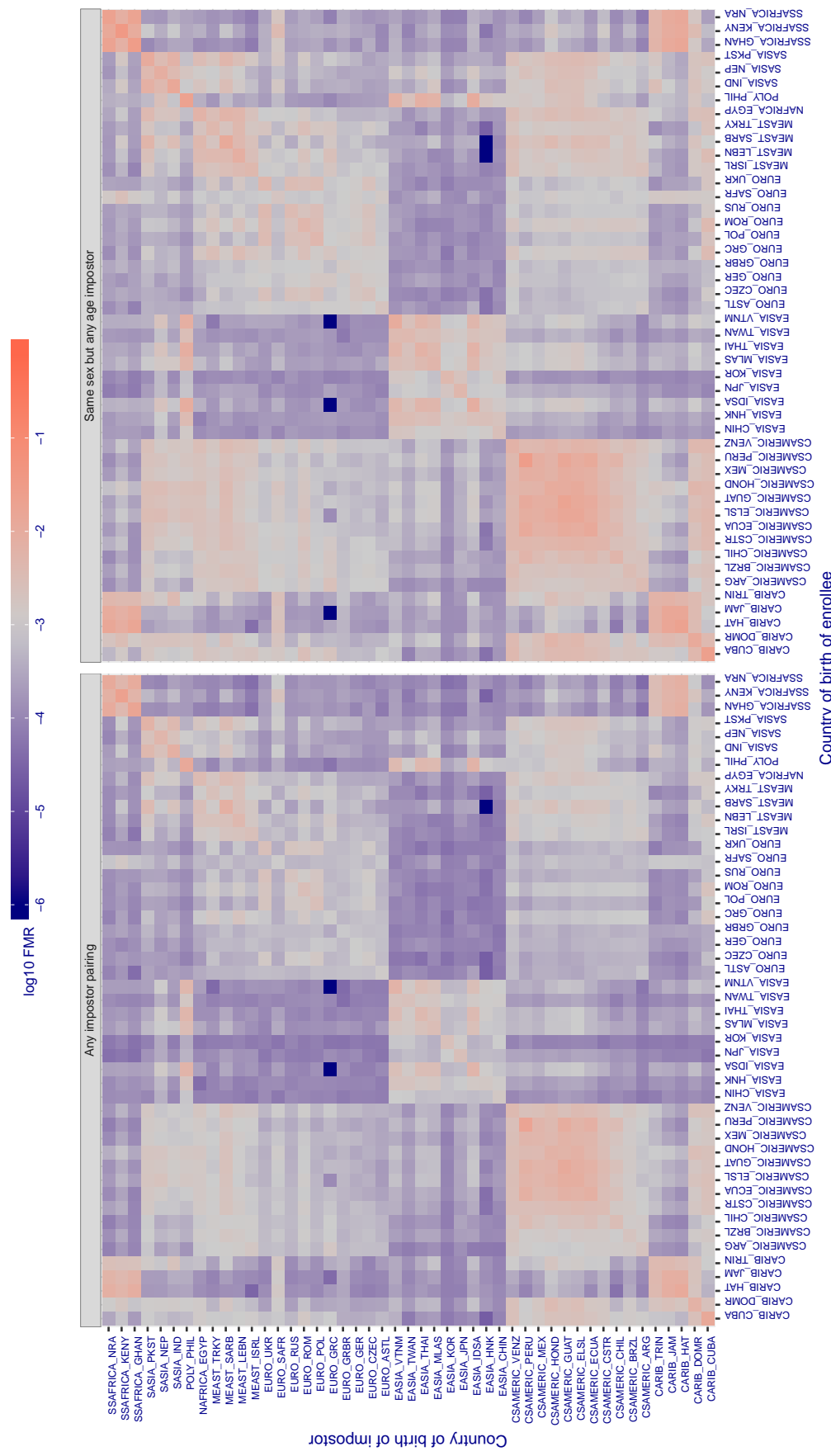


Figure 327: For algorithm deepglint-001 operating on visa images, the heatmap shows false match rates observed over impostor comparisons of faces from different individuals who were born in the given country pair. False matches are counted against a recognition threshold fixed globally to give the target  $FMR$  in the plot title, computed over all on the order of  $10^{10}$  impostor comparisons. If text appears in each box it give the same quantity as that coded by the color. Grey indicates  $FMR$  is at the intended  $FMR$  target level. Light red colors present a security vulnerability to, for example, a passport gate. Each +1 increase in  $\log_{10} FMR$  corresponds to a factor of 10 increase in  $FMR$ . The matrix is not quite symmetric because images in the enrollment and verification sets are different.

**Cross country FMR at threshold T = 1.300 for algorithm deepsea\_001, giving  $\text{FMR}(T) = 0.001$  globally.**

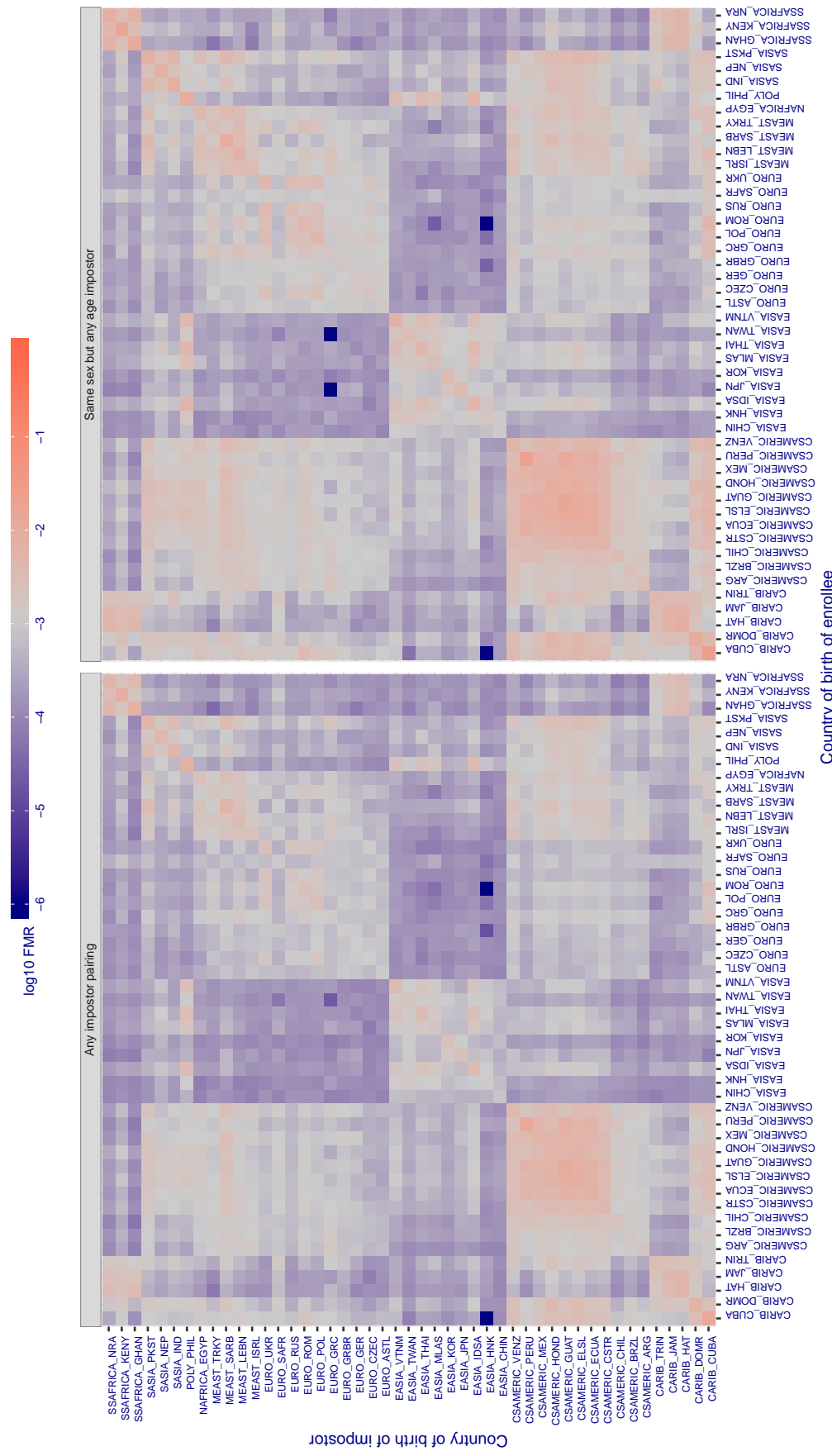


Figure 328: For algorithm deepsea-001 operating on visa images, the heatmap shows false match rates observed over impostor comparisons of faces from different individuals who were born in the given country pair. False matches are counted against a recognition threshold fixed globally to give the target  $\text{FMR}$  in the plot title, computed over all on the order of  $10^{10}$  impostor comparisons. If text appears in each box it give the same quantity as that coded by the color. Grey indicates  $\text{FMR}$  is at the intended  $\text{FMR}$  target level. Light red colors present a security vulnerability to, for example, a passport gate. Each +1 increase in  $\log_{10} \text{FMR}$  corresponds to a factor of 10 increase in  $\text{FMR}$ . The matrix is not quite symmetric because images in the enrollment and verification sets are different.

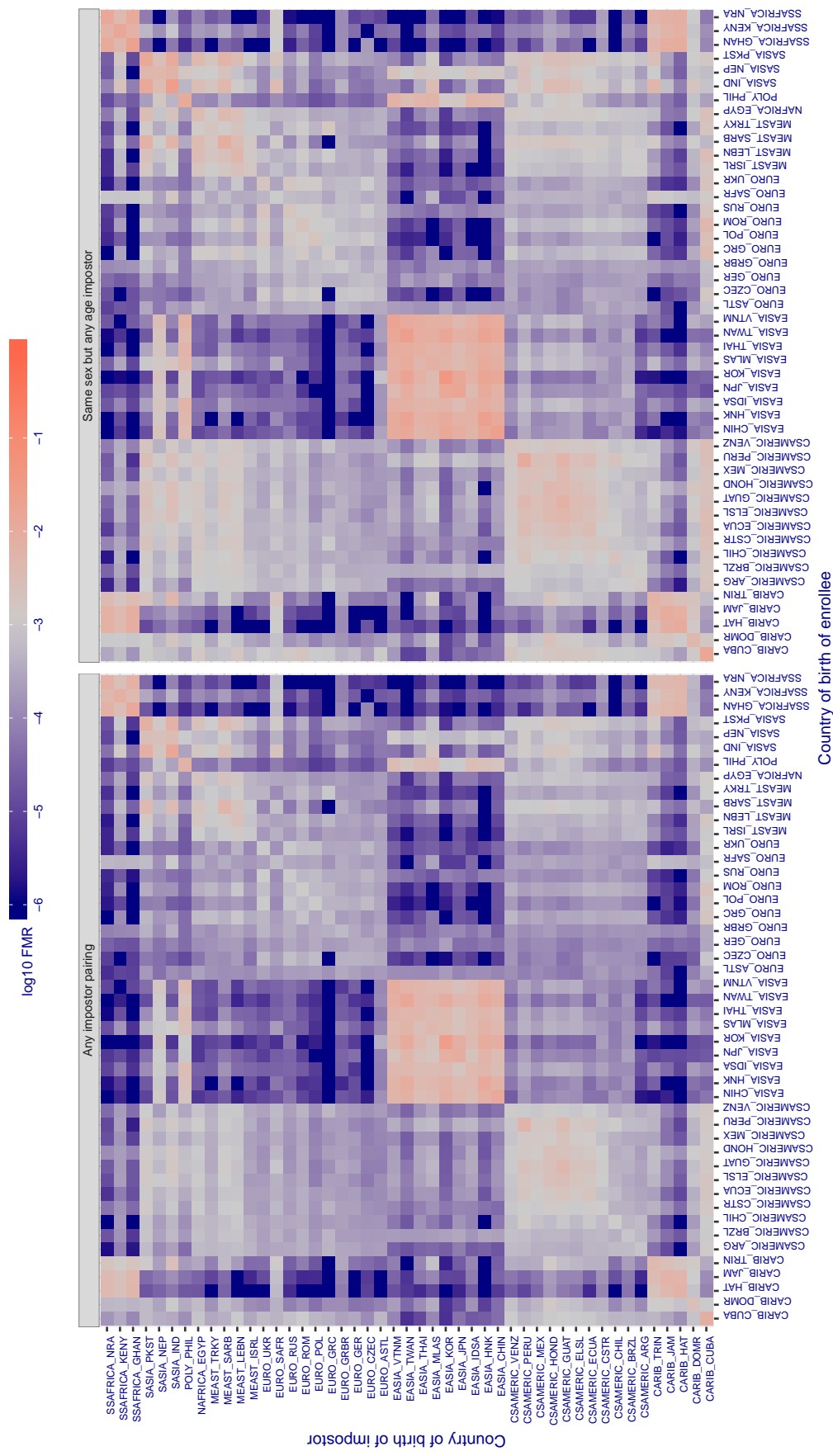
**Cross country FMR at threshold T = 75.231 for algorithm dermalog\_005, giving FMR(T) = 0.001 globally.**

Figure 329: For algorithm dermalog-005 operating on visa images, the heatmap shows false match rates observed over impostor comparisons of faces from different individuals who were born in the given country pair. False matches are counted against a recognition threshold fixed globally to give the target FMR in the plot title, computed over all on the order of  $10^{10}$  impostor comparisons. If text appears in each box it give the same quantity as that coded by the color. Grey indicates FMR is at the intended FMR target level. Light red colors present a security vulnerability to, for example, a passport gate. Each +1 increase in  $\log_{10} \text{FMR}$  corresponds to a factor of 10 increase in FMR. The matrix is not quite symmetric because images in the enrollment and verification sets are different.

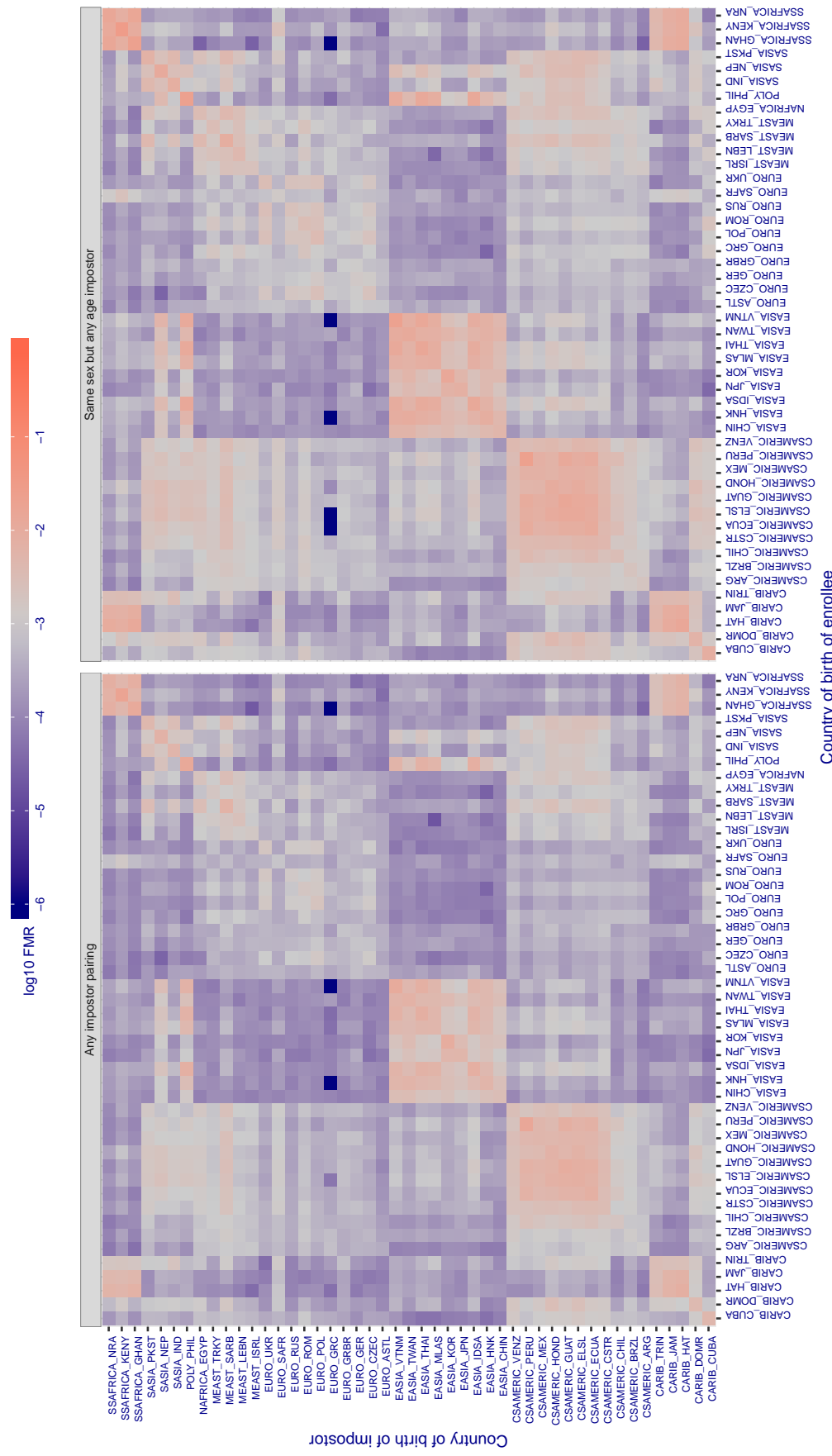
**Cross country FMR at threshold T = 76.496 for algorithm dermalog\_006, giving FMR(T) = 0.001 globally.**

Figure 330: For algorithm dermalog-006 operating on visa images, the heatmap shows false match rates observed over impostor comparisons of faces from different individuals who were born in the given country pair. False matches are counted against a recognition threshold fixed globally to give the target FMR in the plot title, computed over all on the order of  $10^{10}$  impostor comparisons. If text appears in each box it give the same quantity as that coded by the color. Grey indicates FMR is at the intended FMR target level. Light red colors present a security vulnerability to, for example, a passport gate. Each +1 increase in  $\log_{10} \text{FMR}$  corresponds to a factor of 10 increase in FMR. The matrix is not quite symmetric because images in the enrollment and verification sets are different.

Cross country FMR at threshold T = 0.547 for algorithm digitalbarriers\_002, giving FMR(T) = 0.001 globally.

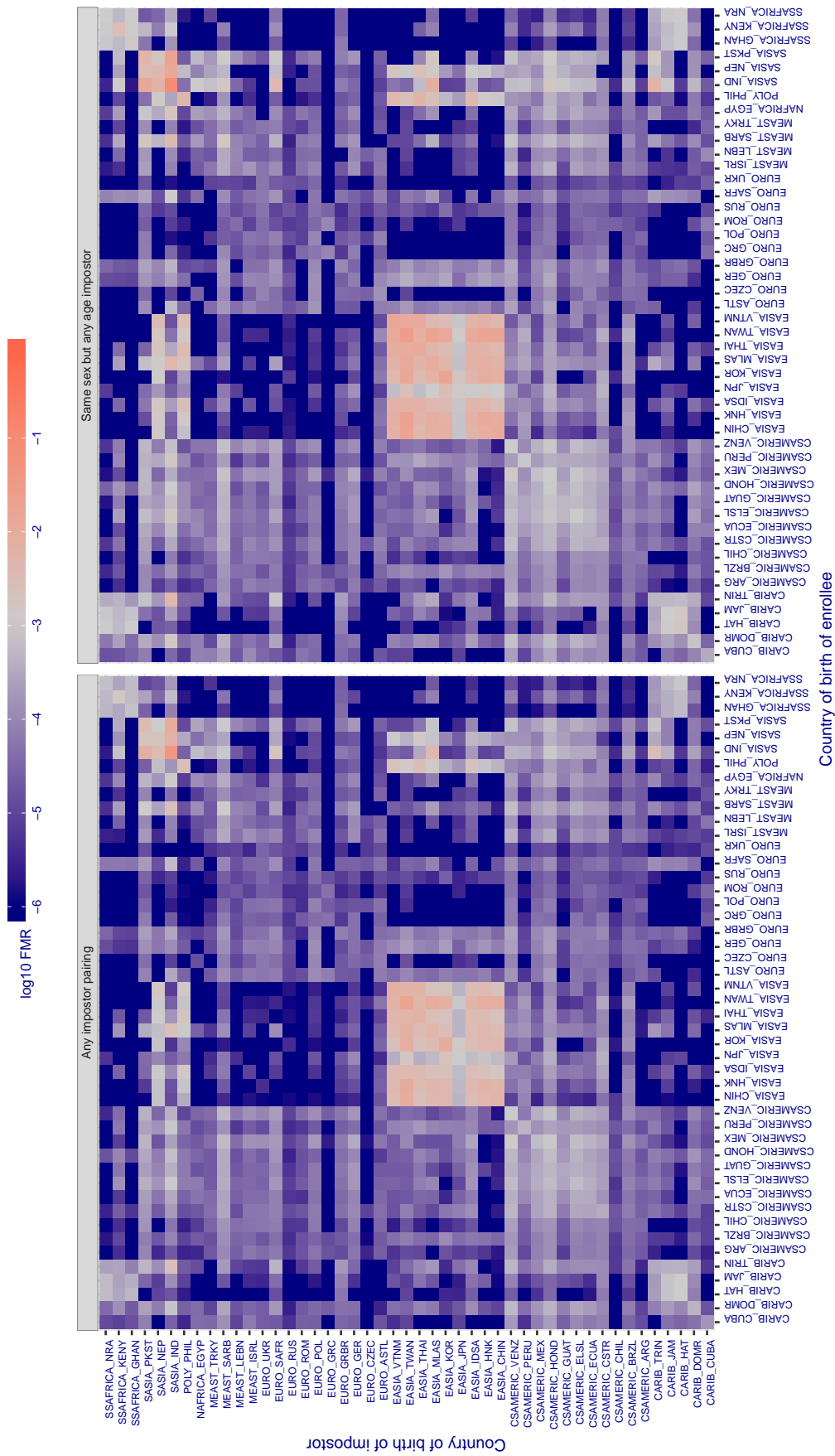


Figure 331: For algorithm digitalbarriers-002 operating on visa images, the heatmap shows false match rates observed over impostor comparisons of faces from different individuals who were born in the given country pair. False matches are counted against a recognition threshold fixed globally to give the target FMR in the plot title, computed over all on the order of  $10^{10}$  impostor comparisons. If text appears in each box it give the same quantity as that coded by the color. Grey indicates FMR is at the intended FMR target level. Light red colors present a security vulnerability to, for example, a passport gate. Each +1 increase in  $\log_{10} FMR$  corresponds to a factor of 10 increase in FMR. The matrix is not quite symmetric because images in the enrollment and verification sets are different.

**Cross country FMR at threshold T = 0.974 for algorithm dsk\_000, giving  $\text{FMR}(\text{T}) = 0.001$  globally.**

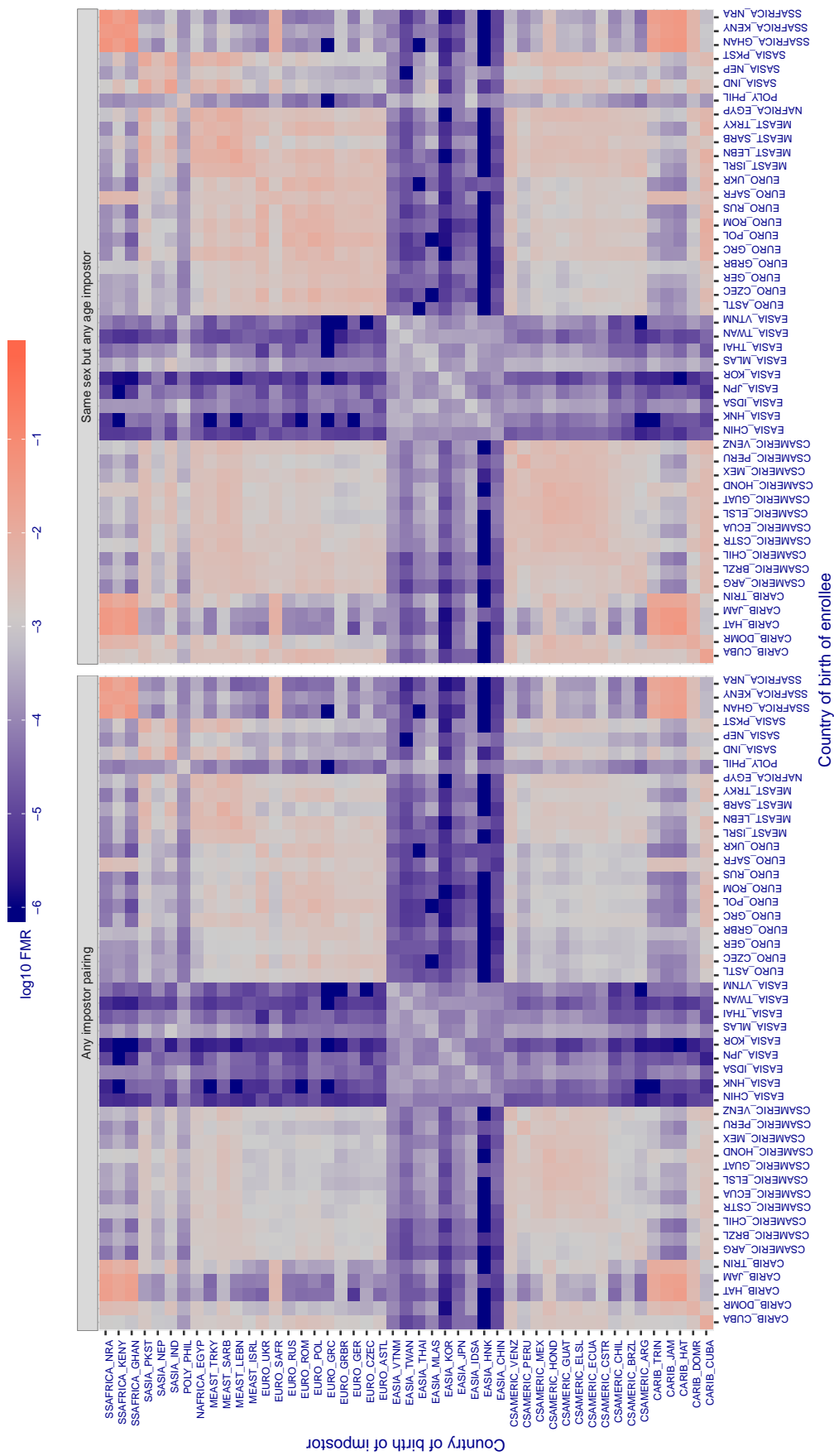


Figure 332: For algorithm dsk-000 operating on visa images, the heatmap shows false match rates observed over impostor comparisons of faces from different individuals who were born in the given country pair. False matches are counted against a recognition threshold fixed globally to give the target FMR in the plot title, computed over all on the order of  $10^{10}$  impostor comparisons. If text appears in each box it give the same quantity as that coded by the color. Grey indicates FMR is at the intended FMR target level. Light red colors present a security vulnerability to, for example, a passport gate. Each +1 increase in  $\log_{10} \text{FMR}$  corresponds to a factor of 10 increase in FMR. The matrix is not quite symmetric because images in the enrollment and verification sets are different.

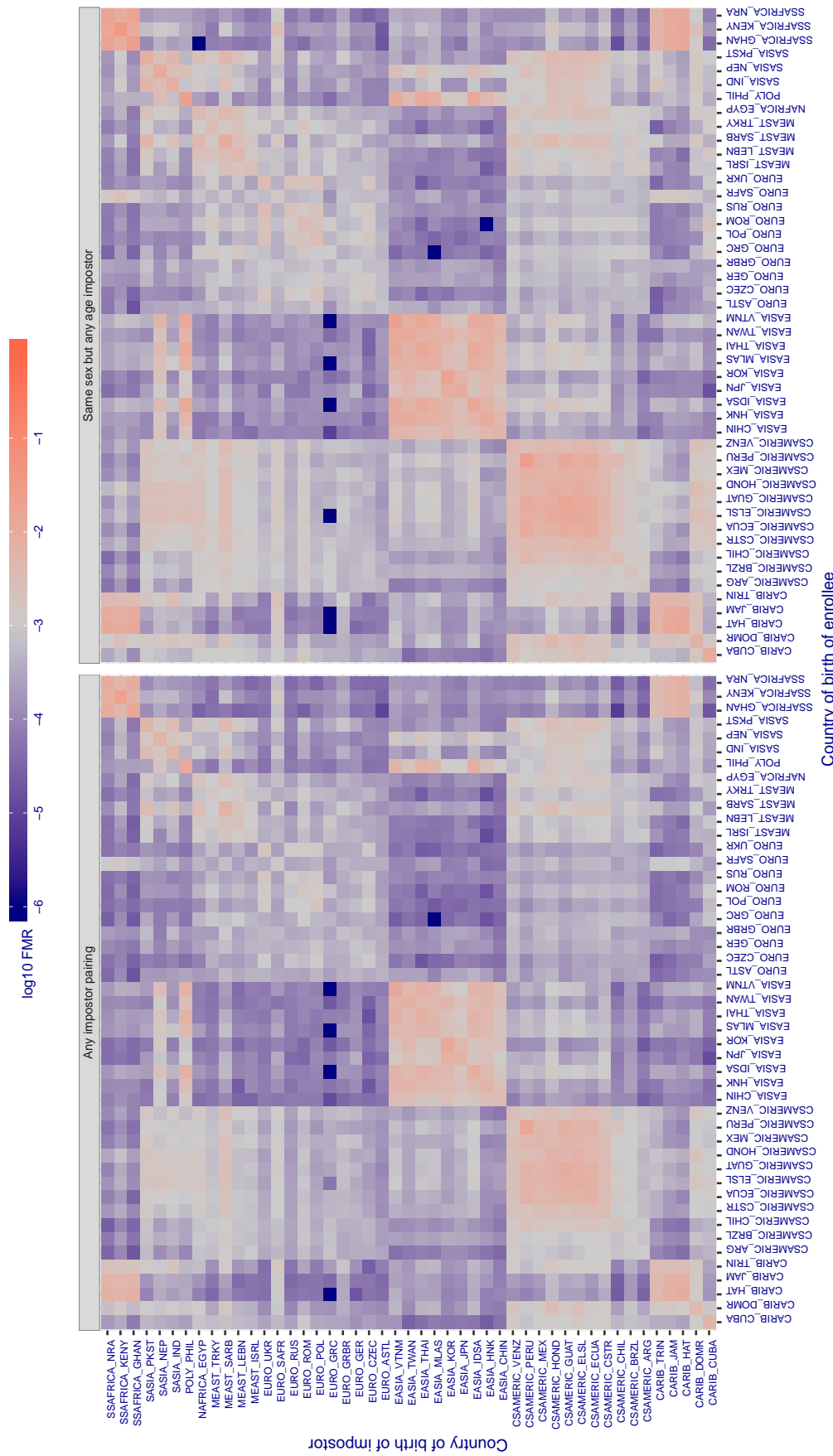
**Cross country FMR at threshold T = 48.749 for algorithm einetworks\_000, giving  $FMR(T) = 0.001$  globally.**

Figure 333: For algorithm einetworks-000 operating on visa images, the heatmap shows false match rates observed over impostor comparisons of faces from different individuals who were born in the given country pair. False matches are counted against a recognition threshold fixed globally to give the target  $FMR$  in the plot title, computed over all on the order of  $10^{10}$  impostor comparisons. If text appears in each box it give the same quantity as that coded by the color. Grey indicates  $FMR$  is at the intended  $FMR$  target level. Light red colors present a security vulnerability to, for example, a passport gate. Each +1 increase in  $\log_{10} FMR$  corresponds to a factor of 10 increase in  $FMR$ . The matrix is not quite symmetric because images in the enrollment and verification sets are different.

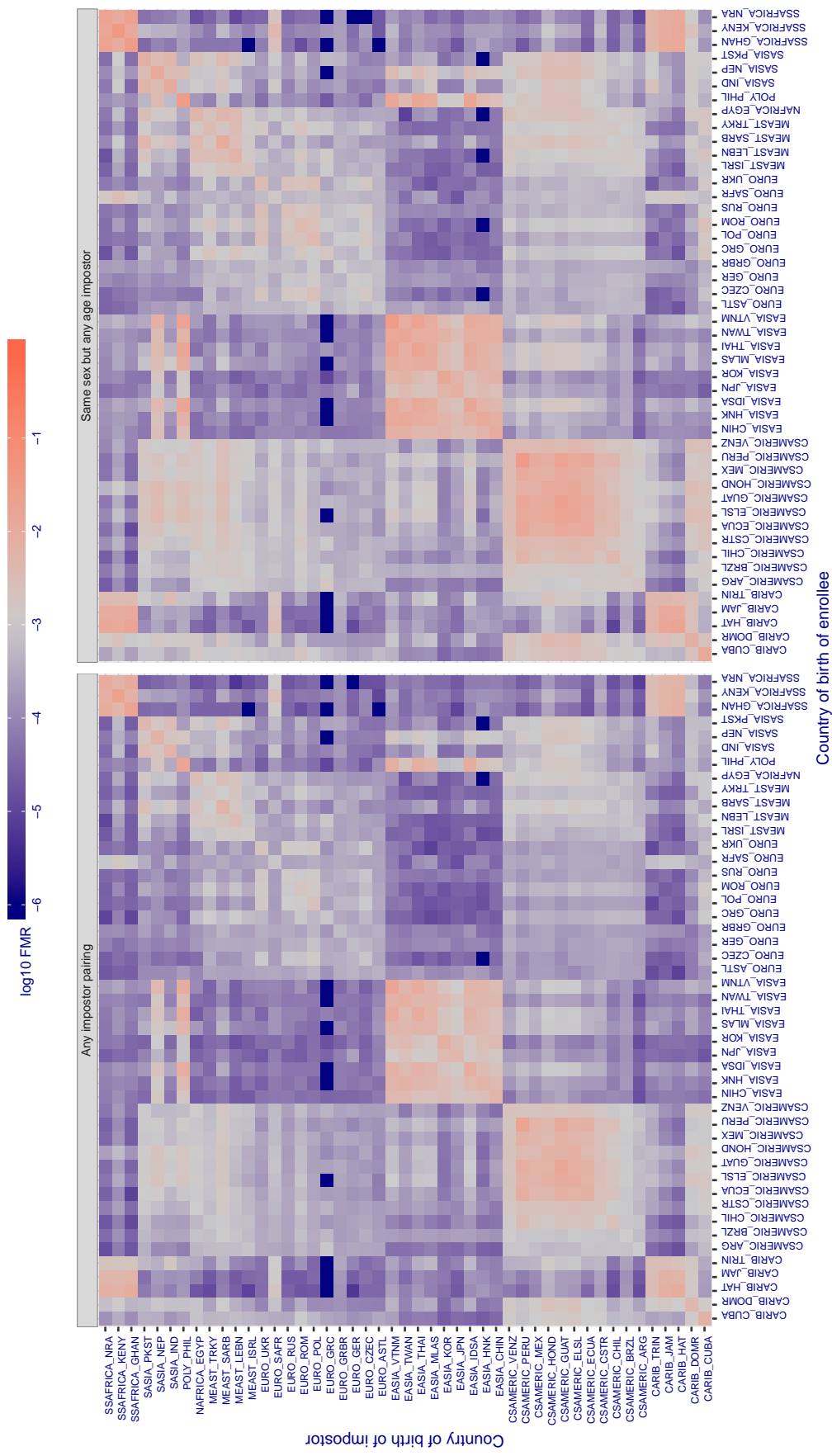
**Cross country FMR at threshold T = 2.426 for algorithm everai\_002, giving FMR(T) = 0.001 globally.**

Figure 334: For algorithm everai-002 operating on visa images, the heatmap shows false match rates observed over impostor comparisons of faces from different individuals who were born in the given country pair. False matches are counted against a recognition threshold fixed globally to give the target FMR in the plot title, computed over all on the order of  $10^{10}$  impostor comparisons. If text appears in each box it give the same quantity as that coded by the color. Grey indicates FMR is at the intended FMR target level. Light red colors present a security vulnerability to, for example, a passport gate. Each +1 increase in  $\log_{10} FMR$  corresponds to a factor of 10 increase in FMR. The matrix is not quite symmetric because images in the enrollment and verification sets are different.

Cross country FMR at threshold T = 0.311 for algorithm f8\_001, giving FMR(T) = 0.001 globally.

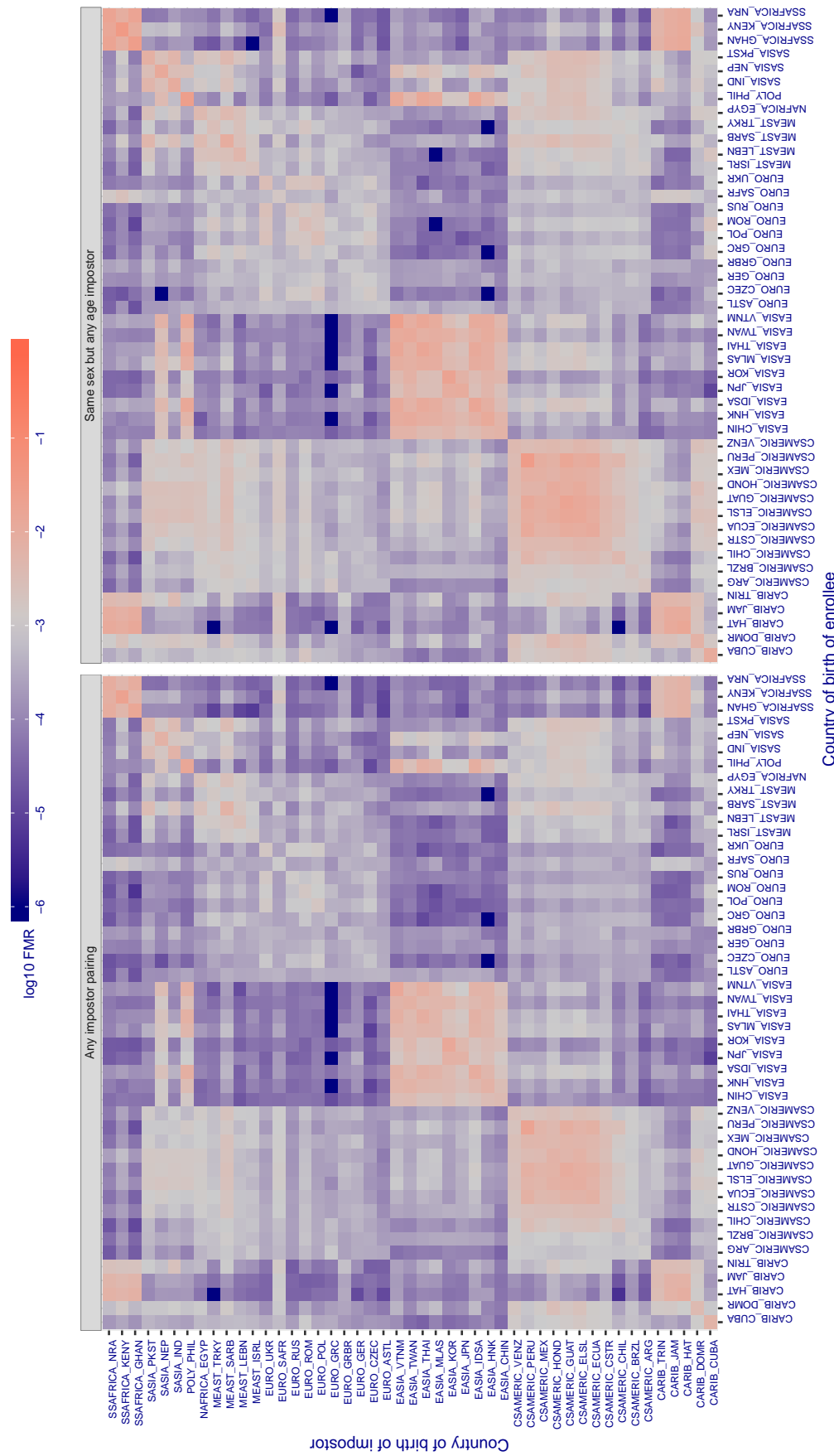


Figure 335: For algorithm f8-001 operating on visa images, the heatmap shows false match rates observed over impostor comparisons of faces from different individuals who were born in the given country pair. False matches are counted against a recognition threshold fixed globally to give the target FMR in the plot title, computed over all on the order of  $10^{10}$  impostor comparisons. If text appears in each box it give the same quantity as that coded by the color. Grey indicates FMR is at the intended FMR target level. Light red colors present a security vulnerability to, for example, a passport gate. Each +1 increase in  $\log_{10} \text{FMR}$  corresponds to a factor of 10 increase in FMR. The matrix is not quite symmetric because images in the enrollment and verification sets are different.

**Cross country FMR at threshold T = 1.300 for algorithm facesoft\_000, giving  $\text{FMR}(T) = 0.001$  globally.**

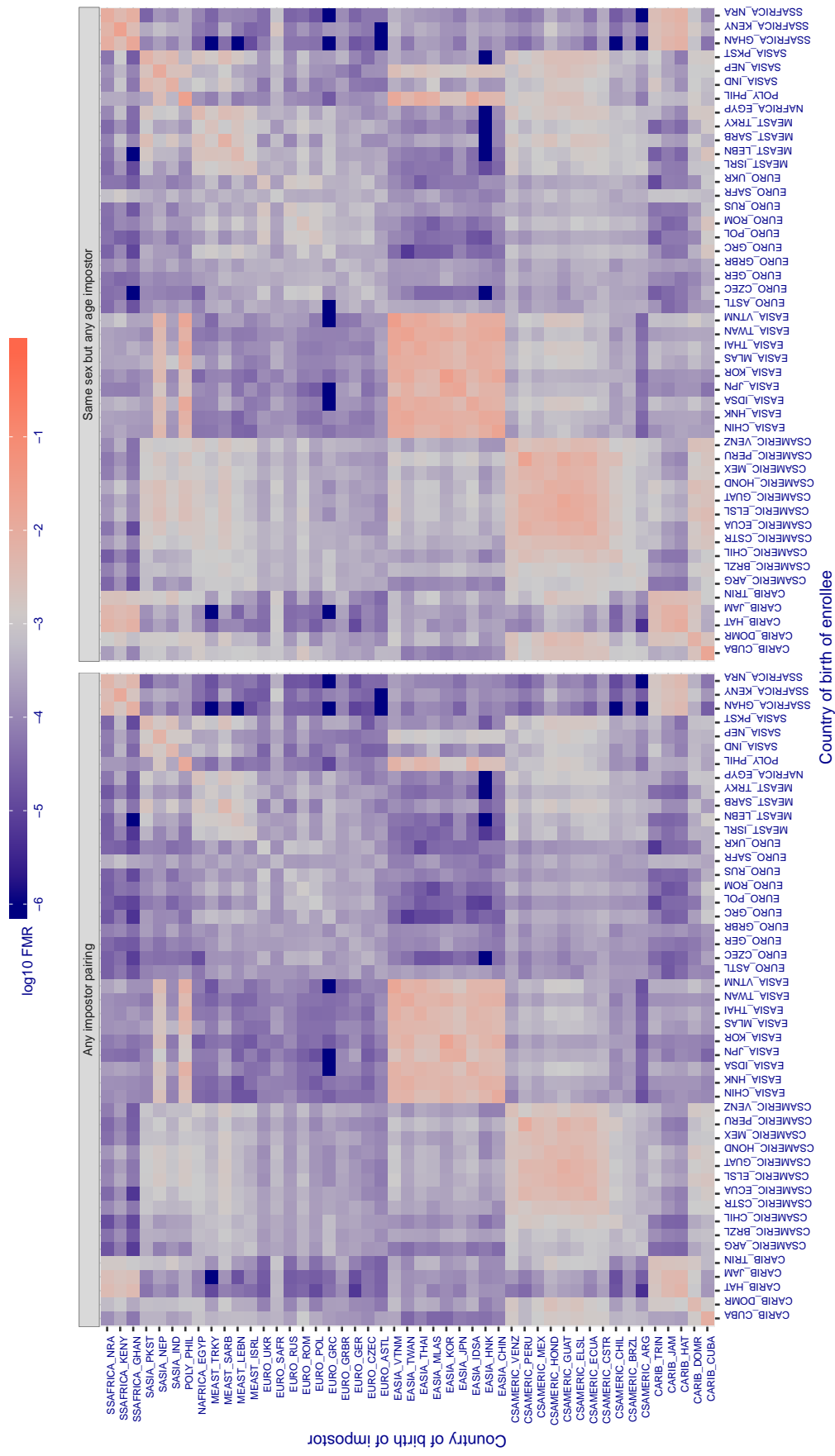


Figure 336: For algorithm facesoft-000 operating on visa images, the heatmap shows false match rates observed over impostor comparisons of faces from different individuals who were born in the given country pair. False matches are counted against a recognition threshold fixed globally to give the target  $\text{FMR}$  in the plot title, computed over all on the order of  $10^{10}$  impostor comparisons. If text appears in each box it give the same quantity as that coded by the color. Grey indicates  $\text{FMR}$  is at the intended  $\text{FMR}$  target level. Light red colors present a security vulnerability to, for example, a passport gate. Each +1 increase in  $\log_{10} \text{FMR}$  corresponds to a factor of 10 increase in  $\text{FMR}$ . The matrix is not quite symmetric because images in the enrollment and verification sets are different.

**Cross country FMR at threshold T = 0.591 for algorithm glory\_000, giving  $FMR(T) = 0.001$  globally.**

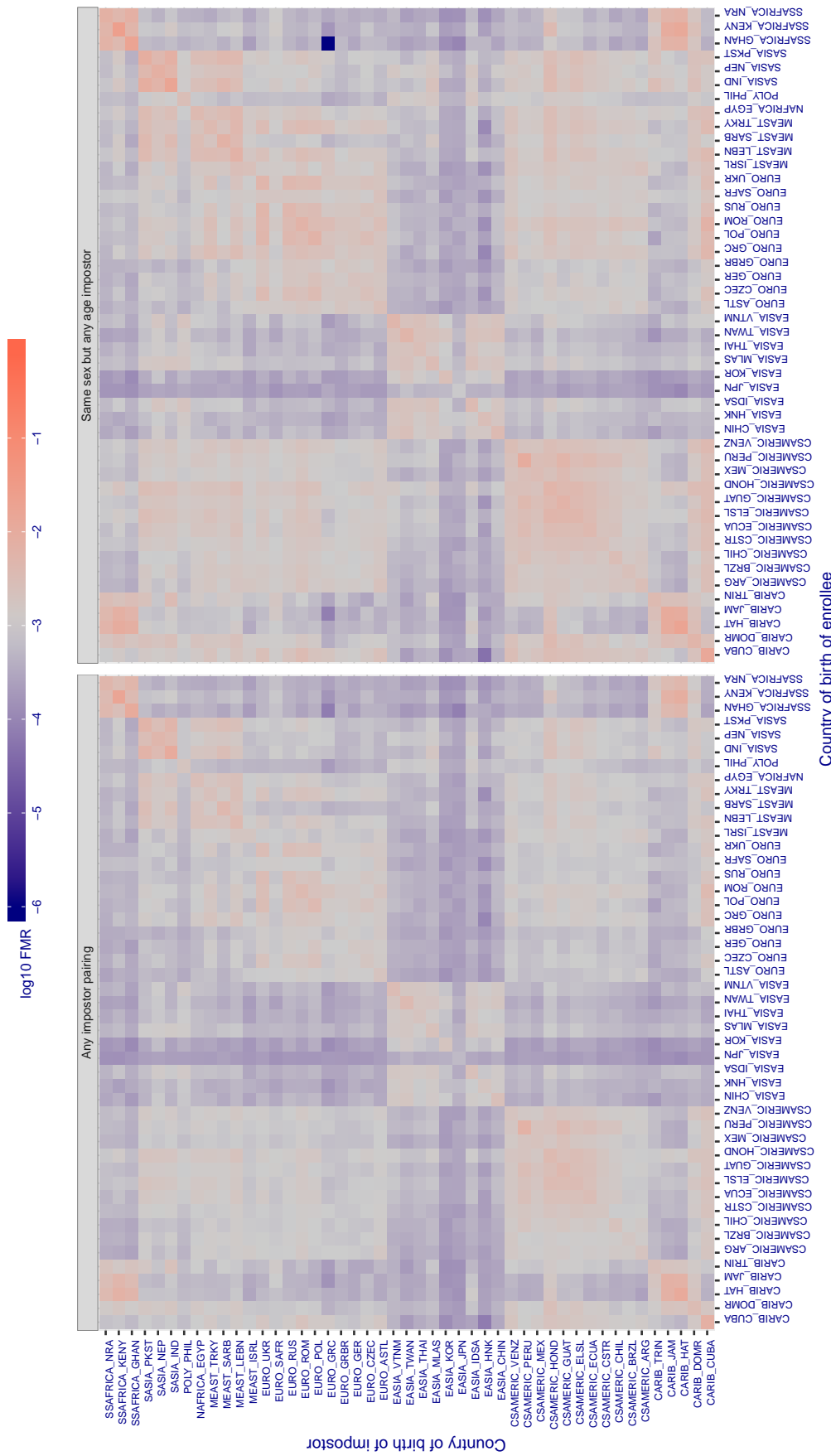


Figure 337: For algorithm *glory-000* operating on visa images, the heatmap shows false match rates observed over impostor comparisons of faces from different individuals who were born in the given country pair. False matches are counted against a recognition threshold fixed globally to give the target  $FMR$  in the plot title, computed over all on the order of  $10^{10}$  impostor comparisons. If text appears in each box it give the same quantity as that coded by the color. Grey indicates  $FMR$  is at the intended  $FMR$  target level. Light red colors present a security vulnerability to, for example, a passport gate. Each +1 increase in  $\log_{10} FMR$  corresponds to a factor of 10 increase in  $FMR$ . The matrix is not quite symmetric because images in the enrollment and verification sets are different.

**Cross country FMR at threshold T = 0.596 for algorithm glory\_001, giving FMR(T) = 0.001 globally.**

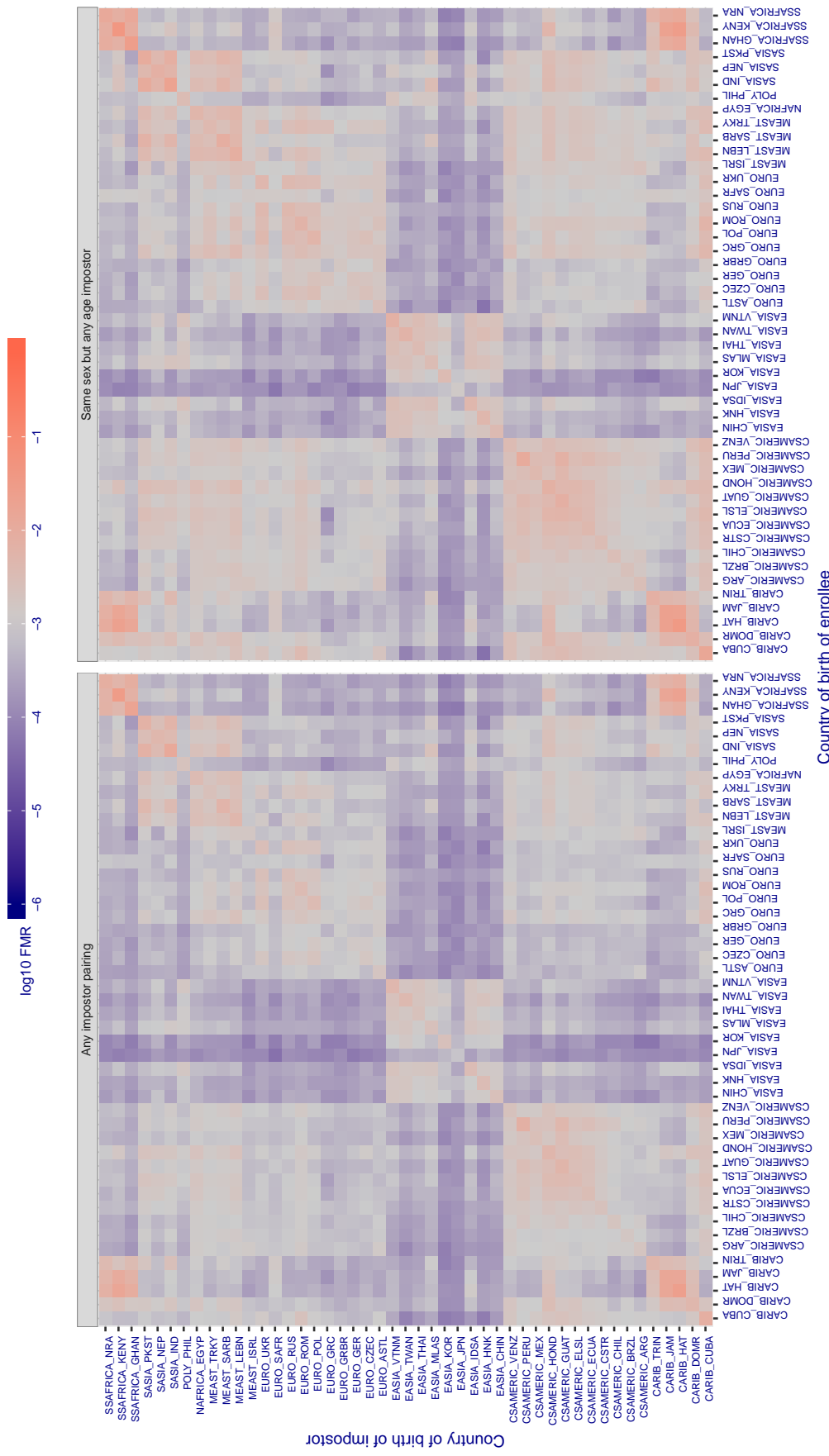


Figure 338: For algorithm *glory-001* operating on visa images, the heatmap shows false match rates observed over impostor comparisons of faces from different individuals who were born in the given country pair. False matches are counted against a recognition threshold fixed globally to give the target FMR in the plot title, computed over all on the order of  $10^{10}$  impostor comparisons. If text appears in each box it give the same quantity as that coded by the color. Grey indicates FMR is at the intended FMR target level. Light red colors present a security vulnerability to, for example, a passport gate. Each +1 increase in  $\log_{10} FMR$  corresponds to a factor of 10 increase in FMR. The matrix is not quite symmetric because images in the enrollment and verification sets are different.

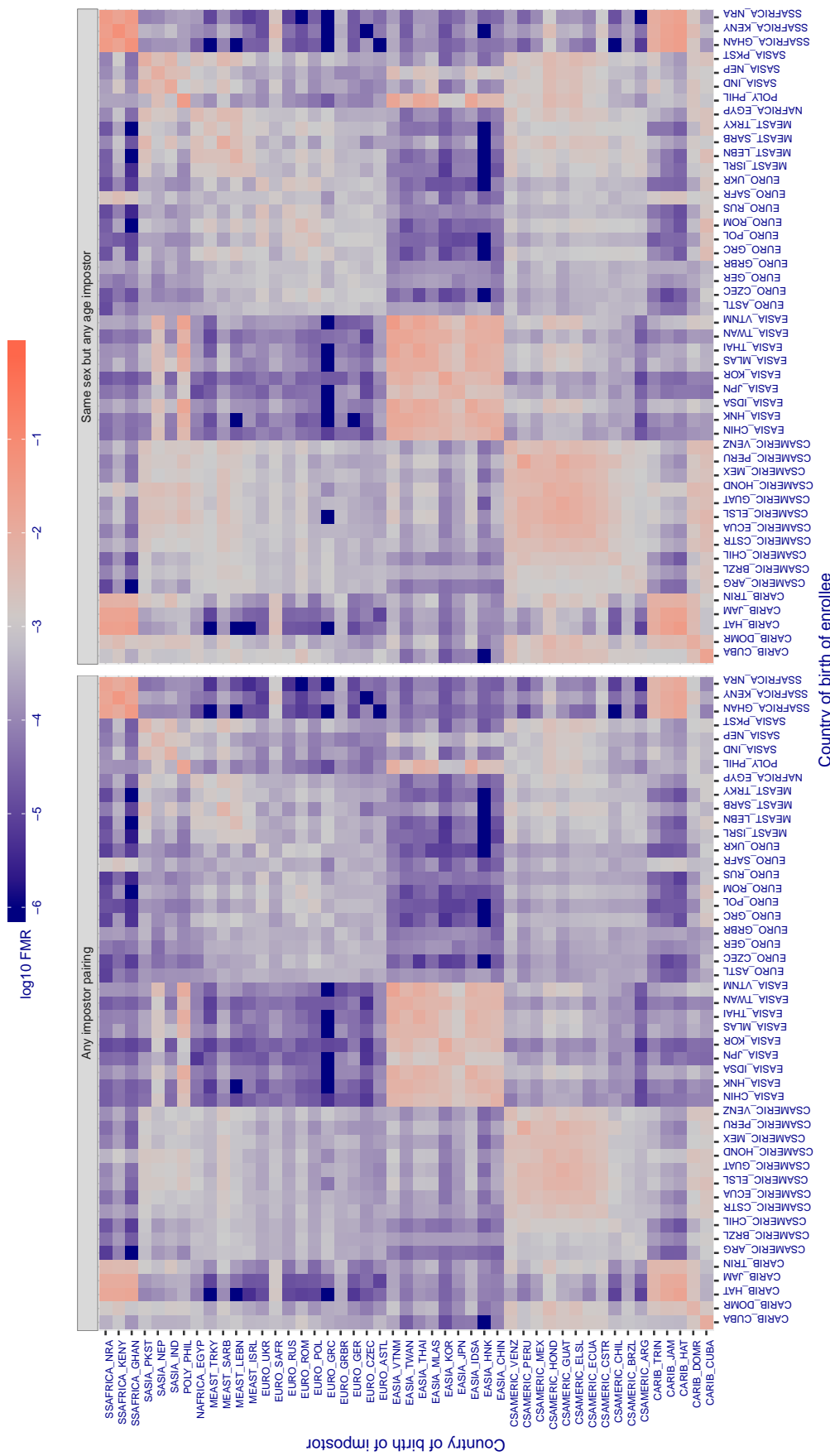
Cross country FMR at threshold T = 0.402 for algorithm gorilla\_002, giving  $FMR(T) = 0.001$  globally.

Figure 339: For algorithm gorilla-002 operating on visa images, the heatmap shows false match rates observed over impostor comparisons of faces from different individuals who were born in the given country pair. False matches are counted against a recognition threshold fixed globally to give the target FMR in the plot title, computed over all on the order of  $10^{10}$  impostor comparisons. If text appears in each box it give the same quantity as that coded by the color. Grey indicates FMR is at the intended FMR target level. Light red colors present a security vulnerability to, for example, a passport gate. Each +1 increase in  $\log_{10} FMR$  corresponds to a factor of 10 increase in FMR. The matrix is not quite symmetric because images in the enrollment and verification sets are different.

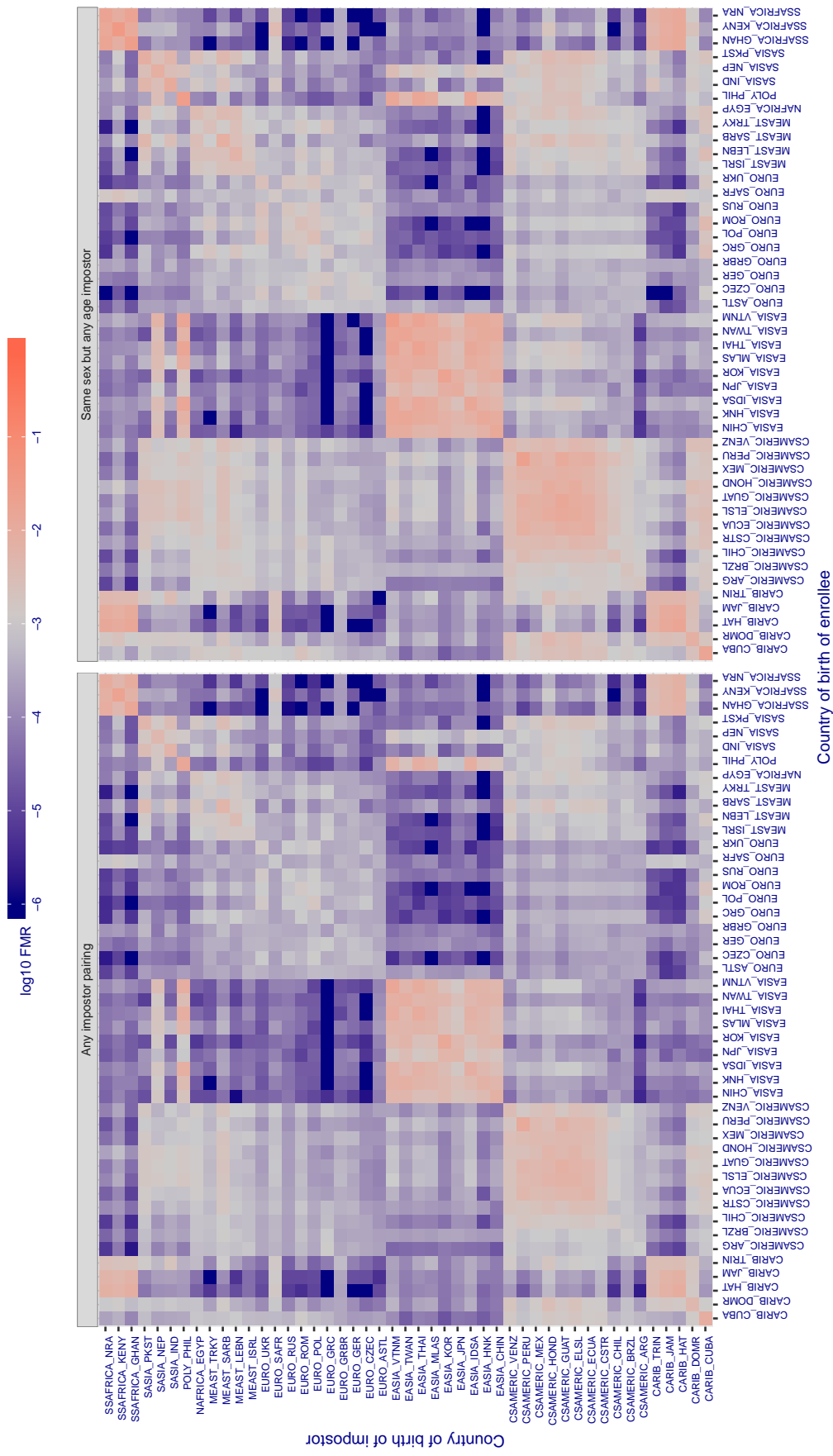
**Cross country FMR at threshold T = 0.357 for algorithm gorilla\_003, giving FMR(T) = 0.001 globally.**

Figure 340: For algorithm gorilla-003 operating on visa images, the heatmap shows false match rates observed over impostor comparisons of faces from different individuals who were born in the given country pair. False matches are counted against a recognition threshold fixed globally to give the target FMR in the plot title, computed over all on the order of  $10^{10}$  impostor comparisons. If text appears in each box it give the same quantity as that coded by the color. Grey indicates FMR is at the intended FMR target level. Light red colors present a security vulnerability to, for example, a passport gate. Each +1 increase in  $\log_{10} FMR$  corresponds to a factor of 10 increase in FMR. The matrix is not quite symmetric because images in the enrollment and verification sets are different.

**Cross country FMR at threshold T = 63.025 for algorithm hik\_001, giving FMR(T) = 0.001 globally.**

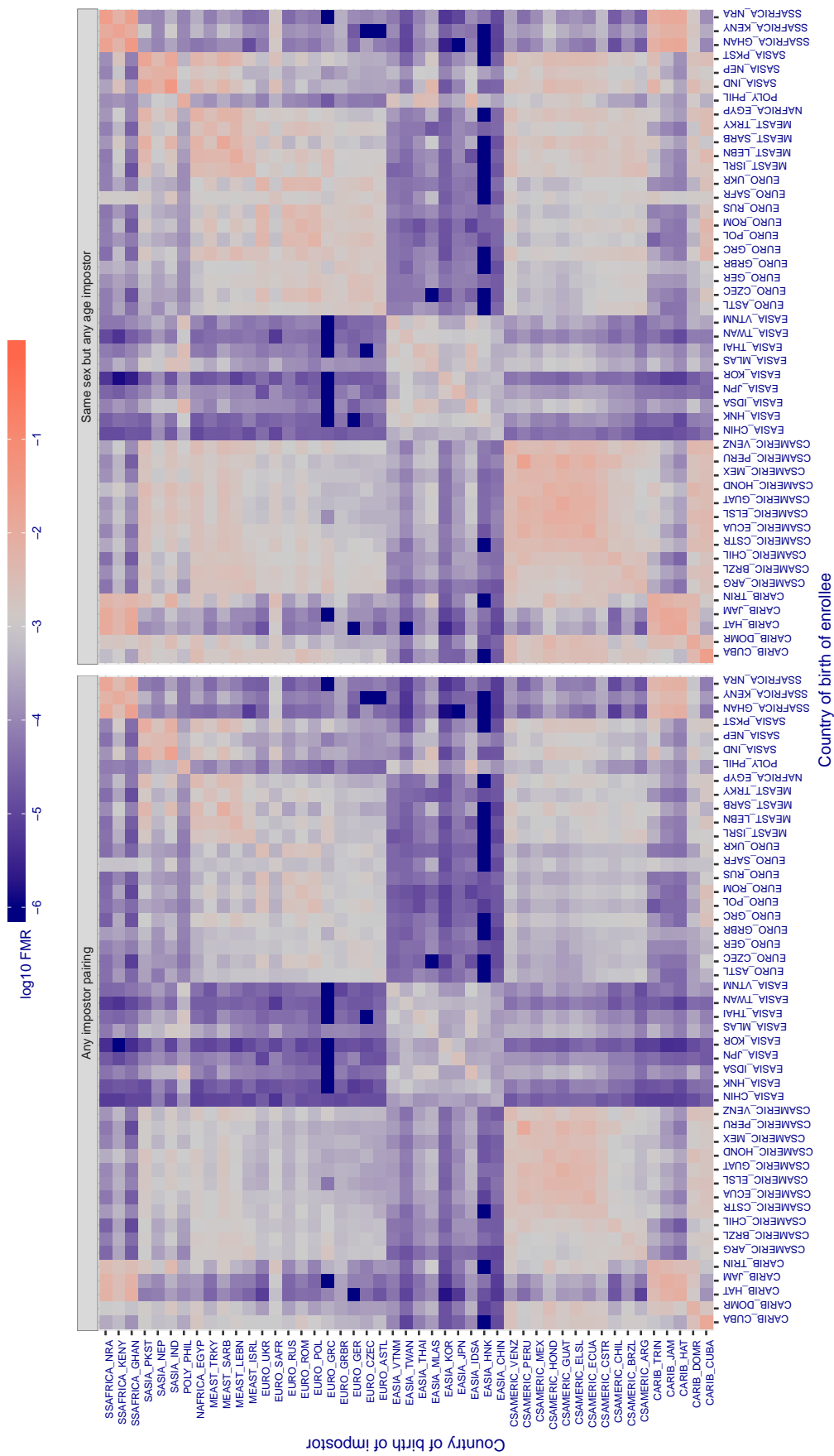


Figure 341: For algorithm hik-001 operating on visa images, the heatmap shows false match rates observed over impostor comparisons of faces from different individuals who were born in the given country pair. False matches are counted against a recognition threshold fixed globally to give the target FMR in the plot title, computed over all on the order of  $10^{10}$  impostor comparisons. If text appears in each box it give the same quantity as that coded by the color. Grey indicates FMR is at the intended FMR target level. Light red colors present a security vulnerability to, for example, a passport gate. Each +1 increase in  $\log_{10} \text{FMR}$  corresponds to a factor of 10 increase in FMR. The matrix is not quite symmetric because images in the enrollment and verification sets are different.

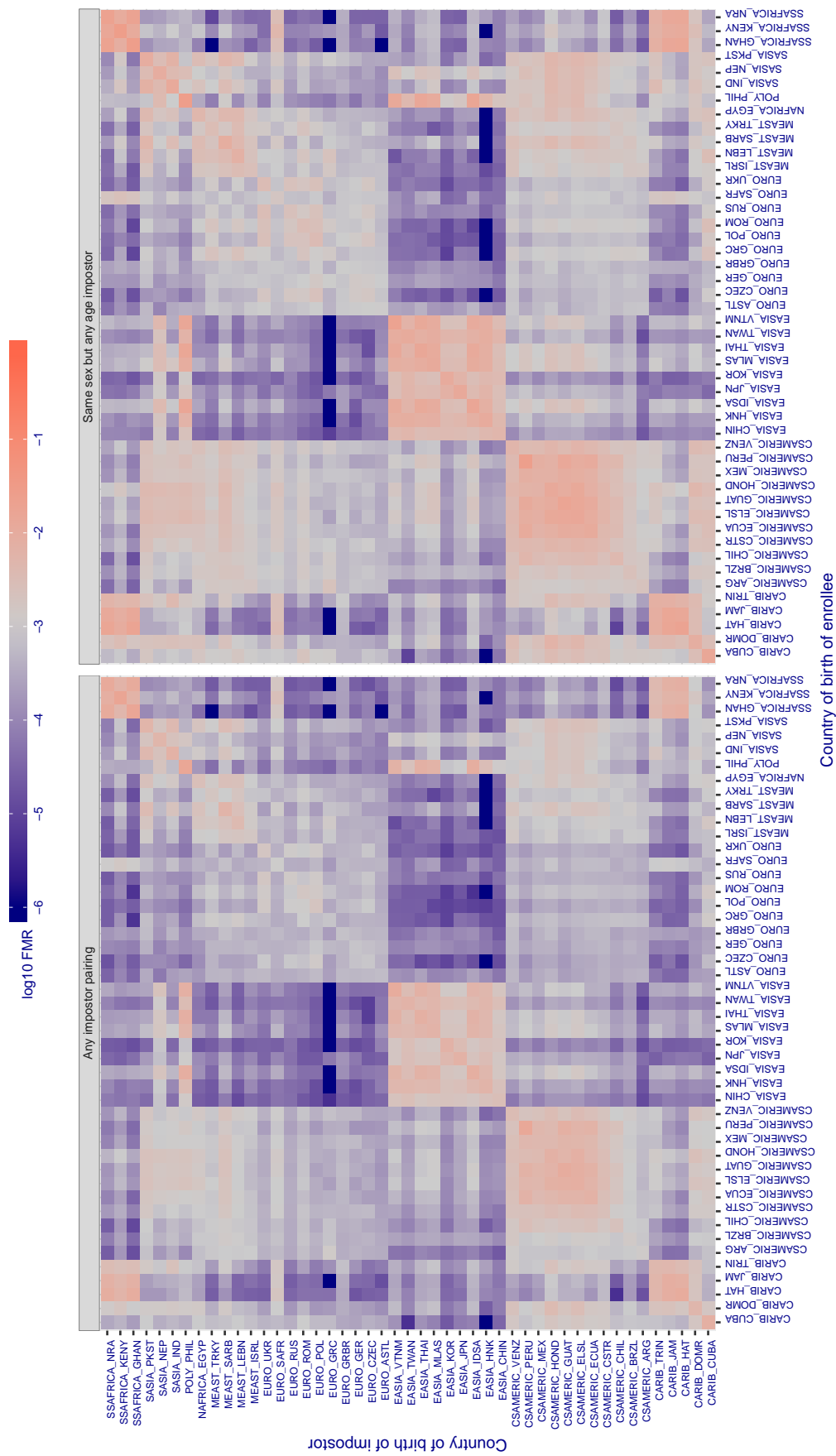
**Cross country FMR at threshold T = 0.727 for algorithm hr\_001, giving FMR(T) = 0.001 globally.**

Figure 342: For algorithm hr-001 operating on visa images, the heatmap shows false match rates observed over impostor comparisons of faces from different individuals who were born in the given country pair. False matches are counted against a recognition threshold fixed globally to give the target FMR in the plot title, computed over all on the order of  $10^{10}$  impostor comparisons. If text appears in each box it give the same quantity as that coded by the color. Grey indicates FMR is at the intended FMR target level. Light red colors present a security vulnerability to, for example, a passport gate. Each +1 increase in  $\log_{10} \text{FMR}$  corresponds to a factor of 10 increase in FMR. The matrix is not quite symmetric because images in the enrollment and verification sets are different.

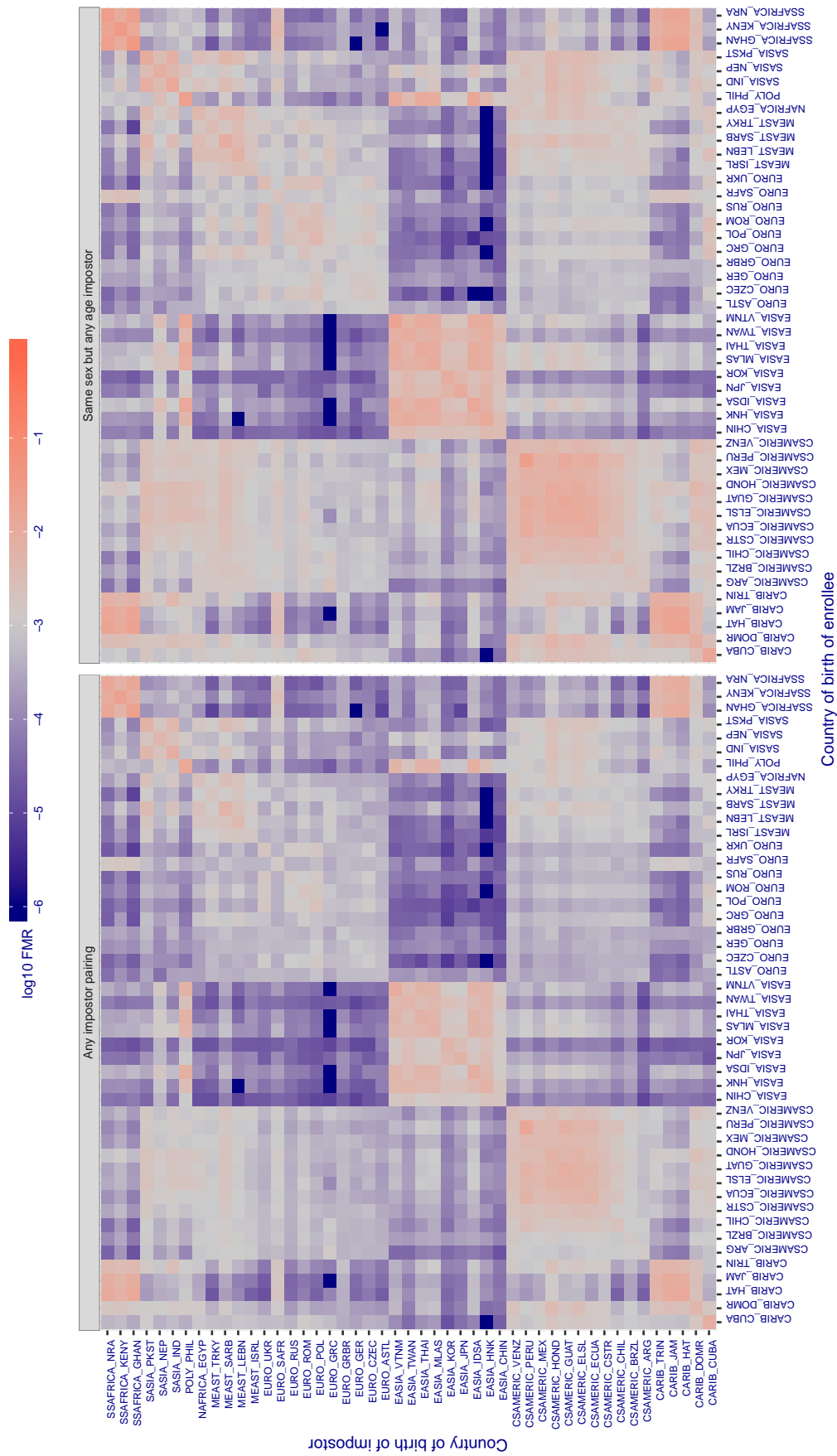
**Cross country FMR at threshold T = 0.109 for algorithm hr\_002, giving FMR(T) = 0.001 globally.**

Figure 343: For algorithm hr-002 operating on visa images, the heatmap shows false match rates observed over impostor comparisons of faces from different individuals who were born in the given country pair. False matches are counted against a recognition threshold fixed globally to give the target FMR in the plot title, computed over all on the order of  $10^{10}$  impostor comparisons. If text appears in each box it give the same quantity as that coded by the color. Grey indicates FMR is at the intended FMR target level. Light red colors present a security vulnerability to, for example, a passport gate. Each +1 increase in  $\log_{10} \text{FMR}$  corresponds to a factor of 10 increase in FMR. The matrix is not quite symmetric because images in the enrollment and verification sets are different.

**Cross country FMR at threshold T = 36641.000 for algorithm id3\_003, giving  $FMR(T) = 0.001$  globally.**

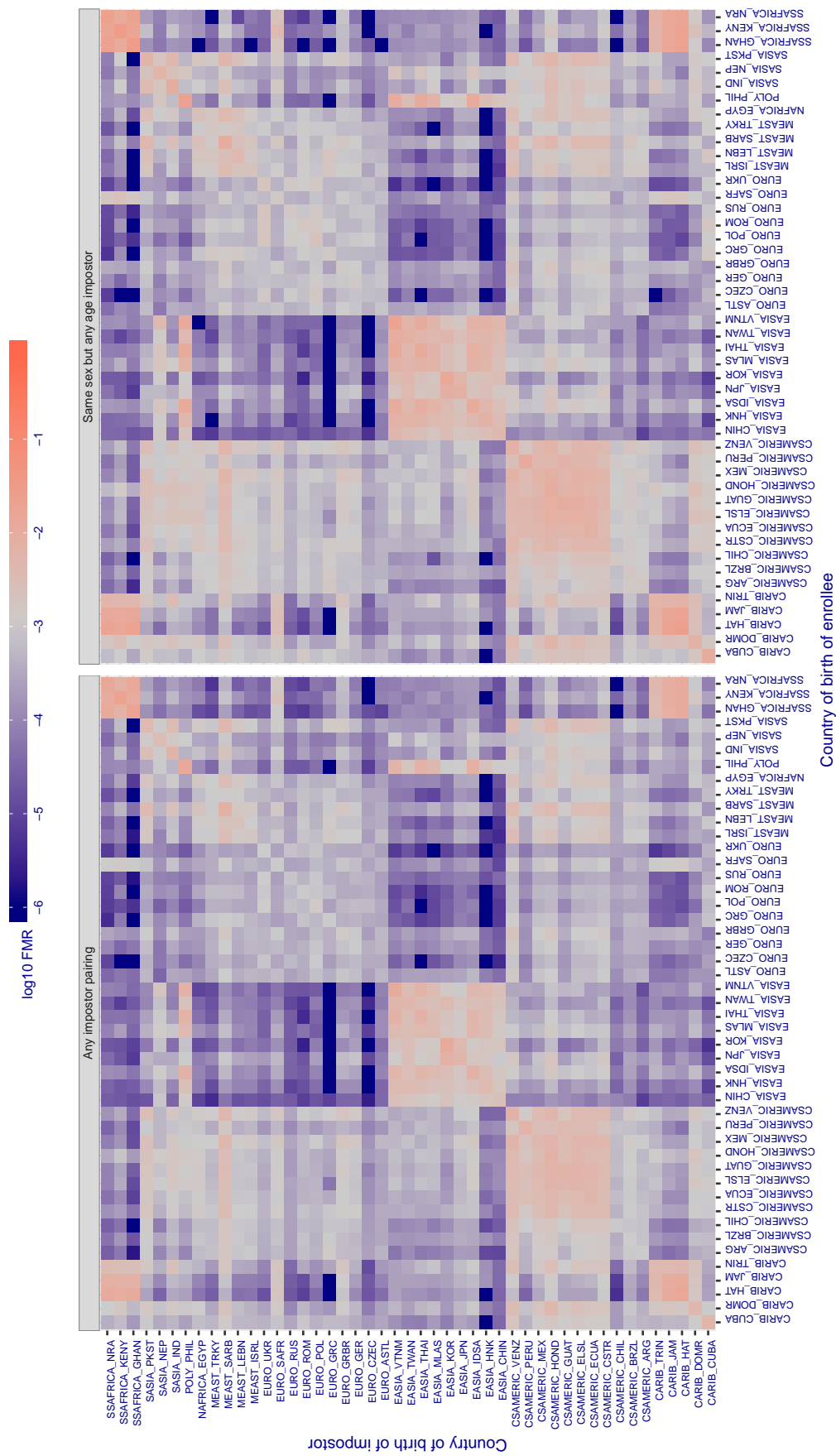


Figure 344: For algorithm id3\_003 operating on visa images, the heatmap shows false match rates observed over impostor comparisons of faces from different individuals who were born in the given country pair. False matches are counted against a recognition threshold fixed globally to give the target FMR in the plot title, computed over all on the order of  $10^{10}$  impostor comparisons. If text appears in each box it give the same quantity as that coded by the color. Grey indicates  $FMR$  is at the intended  $FMR$  target level. Light red colors present a security vulnerability to, for example, a passport gate. Each +1 increase in  $\log_{10} FMR$  corresponds to a factor of 10 increase in  $FMR$ . The matrix is not quite symmetric because images in the enrollment and verification sets are different.

**Cross country FMR at threshold T = 36163.000 for algorithm id3\_004, giving  $\text{FMR}(T) = 0.001$  globally.**

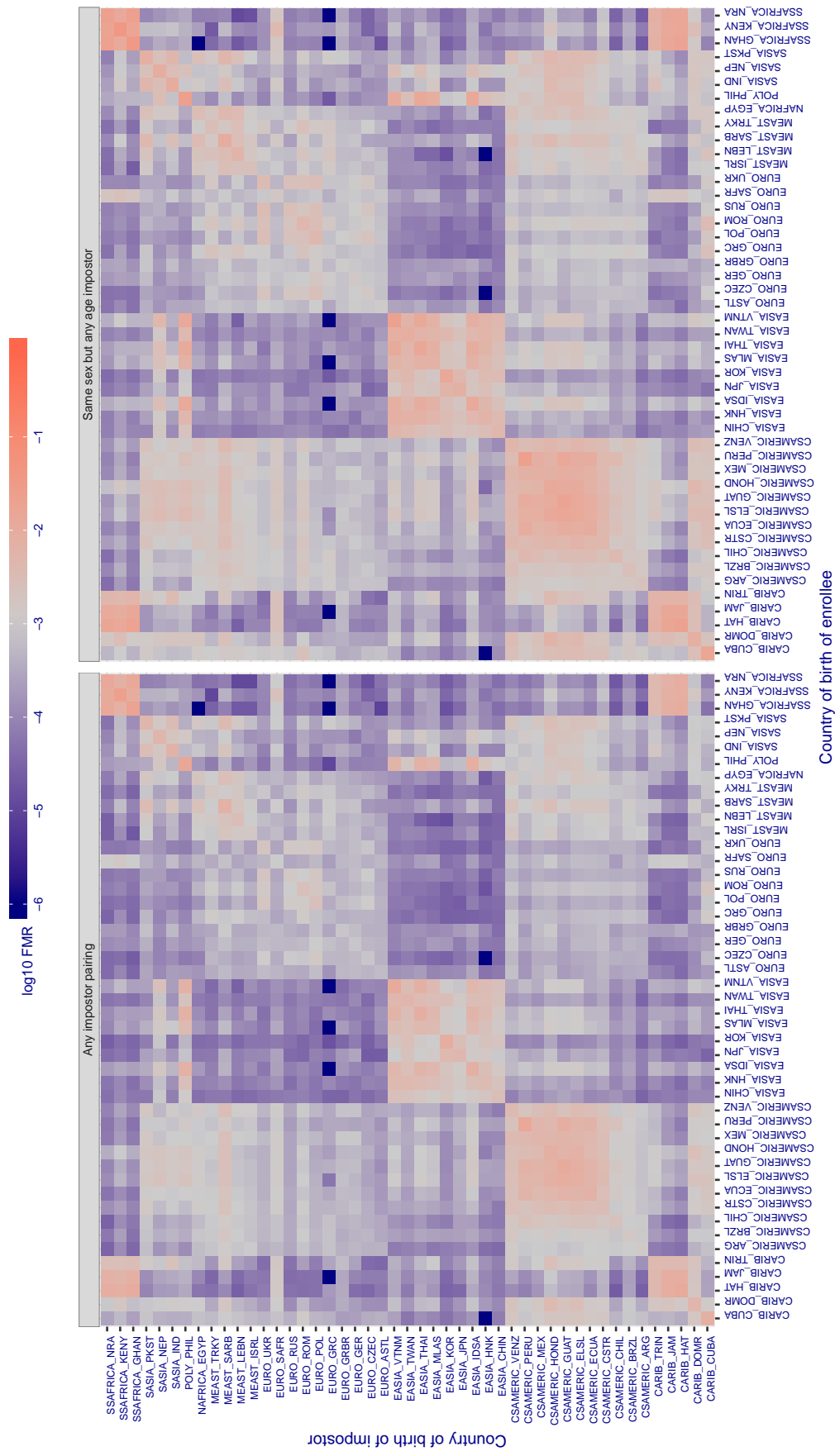


Figure 345: For algorithm id3\_004 operating on visa images, the heatmap shows false match rates observed over impostor comparisons of faces from different individuals who were born in the given country pair. False matches are counted against a recognition threshold fixed globally to give the target FMR in the plot title, computed over all on the order of  $10^{10}$  impostor comparisons. If text appears in each box it give the same quantity as that coded by the color. Grey indicates FMR is at the intended FMR target level. Light red colors present a security vulnerability to, for example, a passport gate. Each +1 increase in  $\log_{10} \text{FMR}$  corresponds to a factor of 10 increase in FMR. The matrix is not quite symmetric because images in the enrollment and verification sets are different.

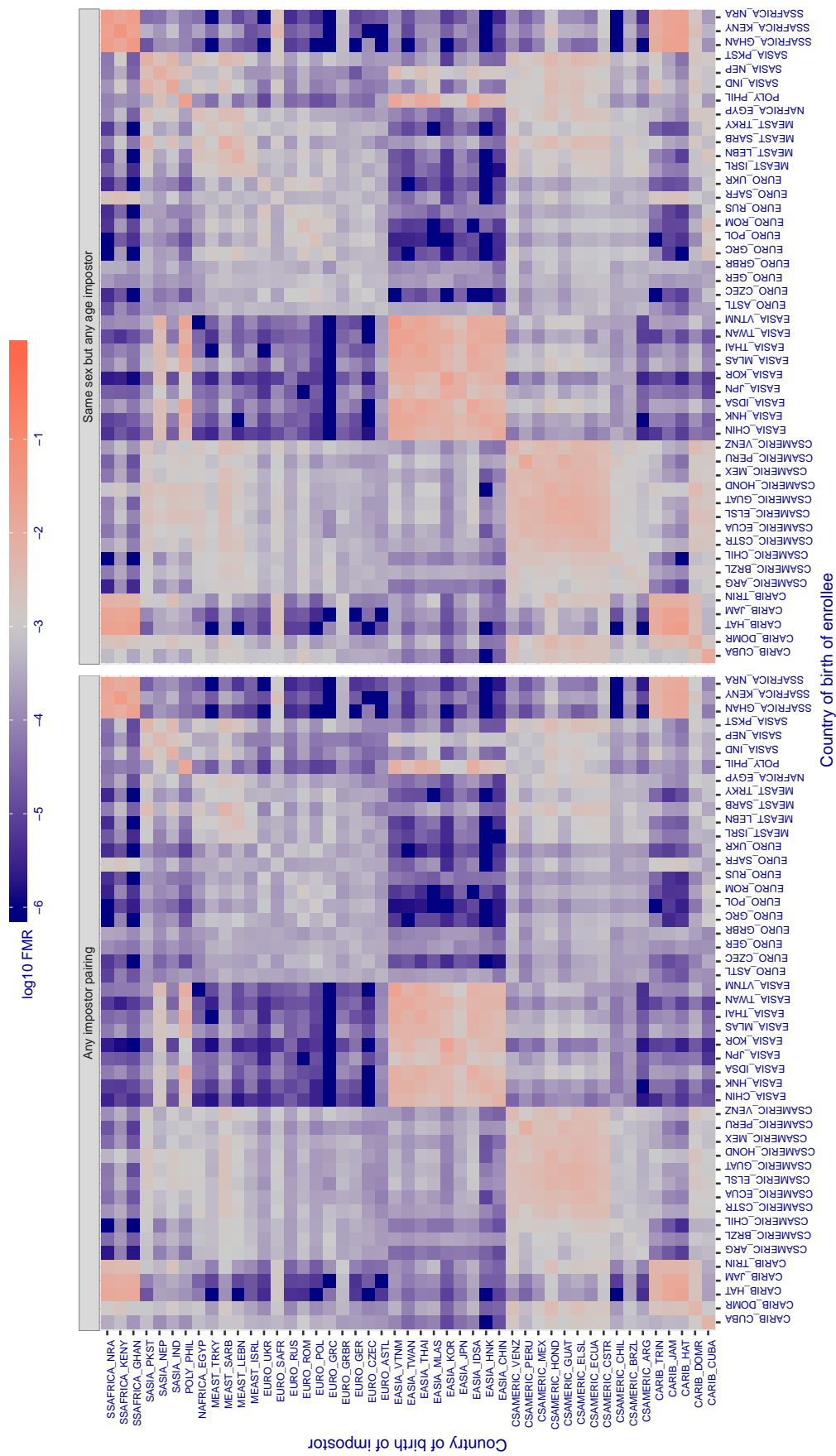
**Cross country FMR at threshold T = 3261.090 for algorithm idemia\_004, giving FMR(T) = 0.001 globally.**

Figure 346: For algorithm idemia-004 operating on visa images, the heatmap shows false match rates observed over impostor comparisons of faces from different individuals who were born in the given country pair. False matches are counted against a recognition threshold fixed globally to give the target FMR in the plot title, computed over all on the order of  $10^{10}$  impostor comparisons. If text appears in each box it give the same quantity as that coded by the color. Grey indicates FMR is at the intended FMR target level. Light red colors present a security vulnerability to, for example, a passport gate. Each +1 increase in  $\log_{10} \text{FMR}$  corresponds to a factor of 10 increase in FMR. The matrix is not quite symmetric because images in the enrollment and verification sets are different.

**Cross country FMR at threshold T = 3178.151 for algorithm idemia\_005, giving  $FMR(T) = 0.001$  globally.**

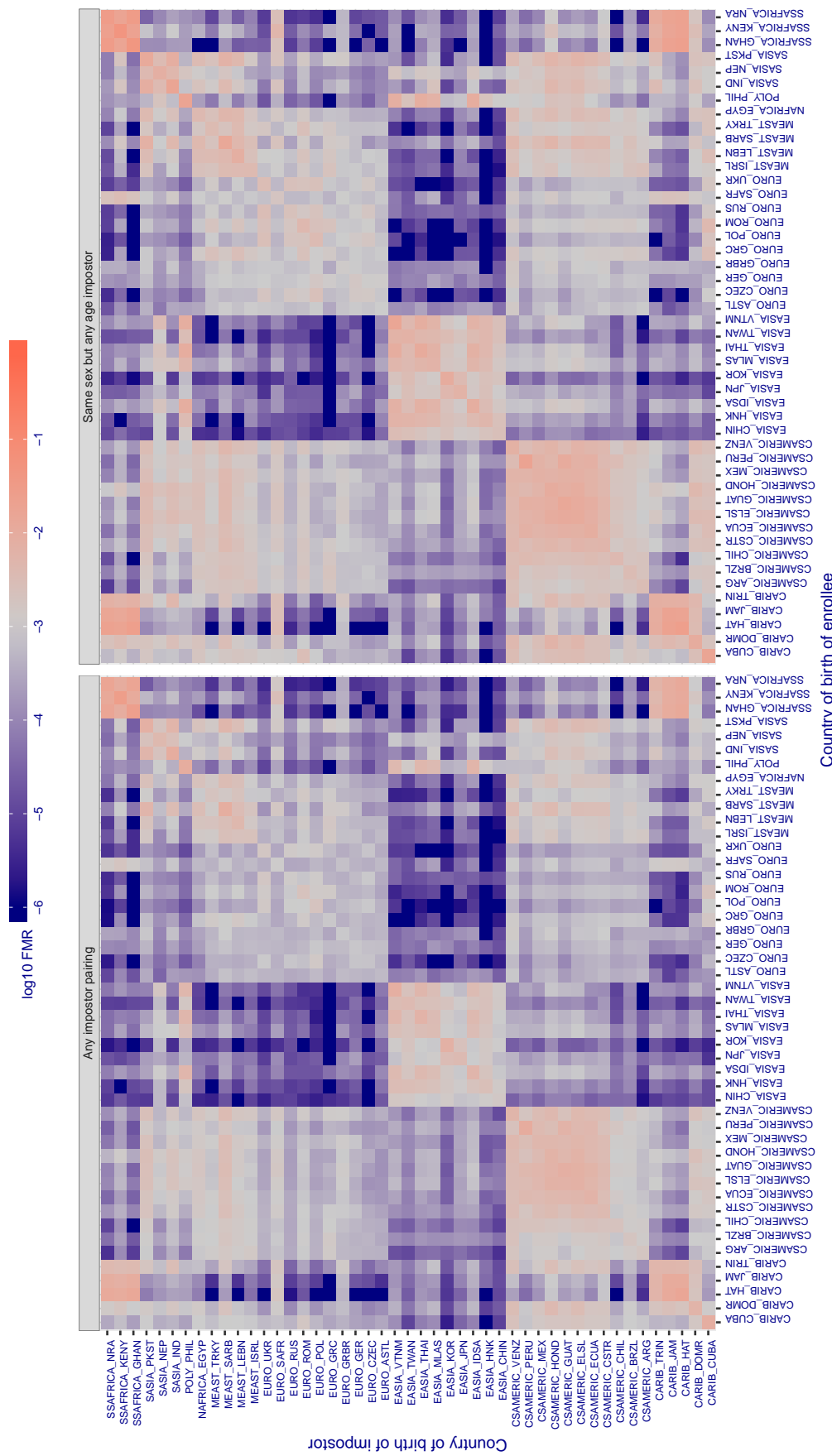


Figure 347: For algorithm idemia-005 operating on visa images, the heatmap shows false match rates observed over impostor comparisons of faces from different individuals who were born in the given country pair. False matches are counted against a recognition threshold fixed globally to give the target  $FMR$  in the plot title, computed over all on the order of  $10^{10}$  impostor comparisons. If text appears in each box it give the same quantity as that coded by the color. Grey indicates  $FMR$  is at the intended  $FMR$  target level. Light red colors present a security vulnerability to, for example, a passport gate. Each +1 increase in  $\log_{10} FMR$  corresponds to a factor of 10 increase in  $FMR$ . The matrix is not quite symmetric because images in the enrollment and verification sets are different.

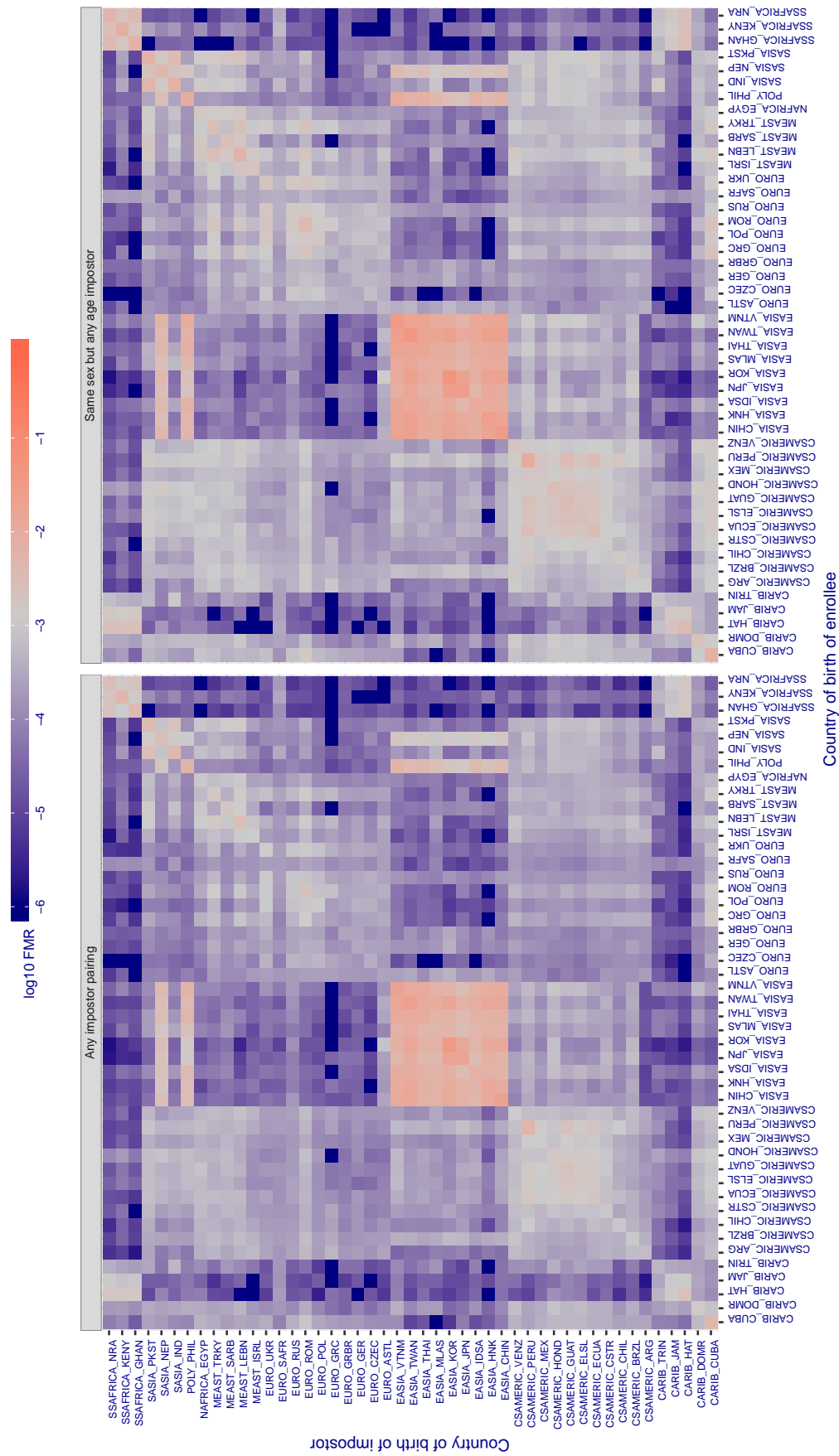
**Cross country FMR at threshold T = 0.721 for algorithm iit\_000, giving FMR(T) = 0.001 globally.**

Figure 348: For algorithm iit-000 operating on visa images, the heatmap shows false match rates observed over impostor comparisons of faces from different individuals who were born in the given country pair. False matches are counted against a recognition threshold fixed globally to give the target FMR in the plot title, computed over all on the order of  $10^{10}$  impostor comparisons. If text appears in each box it give the same quantity as that coded by the color. Grey indicates FMR is at the intended FMR target level. Light red colors present a security vulnerability to, for example, a passport gate. Each +1 increase in  $\log_{10} \text{FMR}$  corresponds to a factor of 10 increase in FMR. The matrix is not quite symmetric because images in the enrollment and verification sets are different.

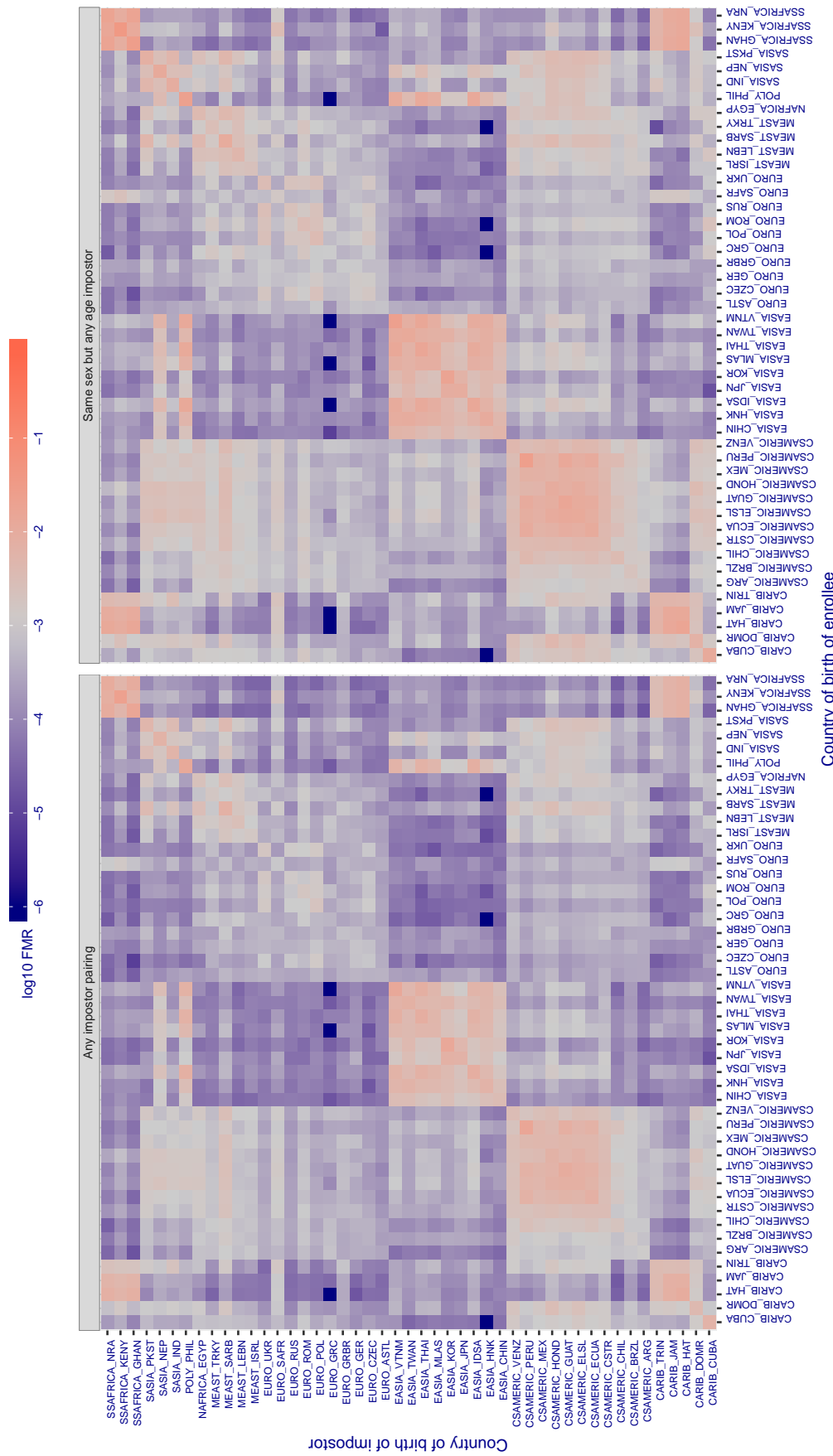
**Cross country FMR at threshold T = 0.647 for algorithm iit\_001, giving FMR(T) = 0.001 globally.**

Figure 349: For algorithm iit-001 operating on visa images, the heatmap shows false match rates observed over impostor comparisons of faces from different individuals who were born in the given country pair. False matches are counted against a recognition threshold fixed globally to give the target FMR in the plot title, computed over all on the order of  $10^{10}$  impostor comparisons. If text appears in each box it give the same quantity as that coded by the color. Grey indicates FMR is at the intended FMR target level. Light red colors present a security vulnerability to, for example, a passport gate. Each +1 increase in  $\log_{10} \text{FMR}$  corresponds to a factor of 10 increase in FMR. The matrix is not quite symmetric because images in the enrollment and verification sets are different.

**Cross country FMR at threshold  $T = 0.809$  for algorithm *imagus\_000*, giving  $FMR(T) = 0.001$  globally.**

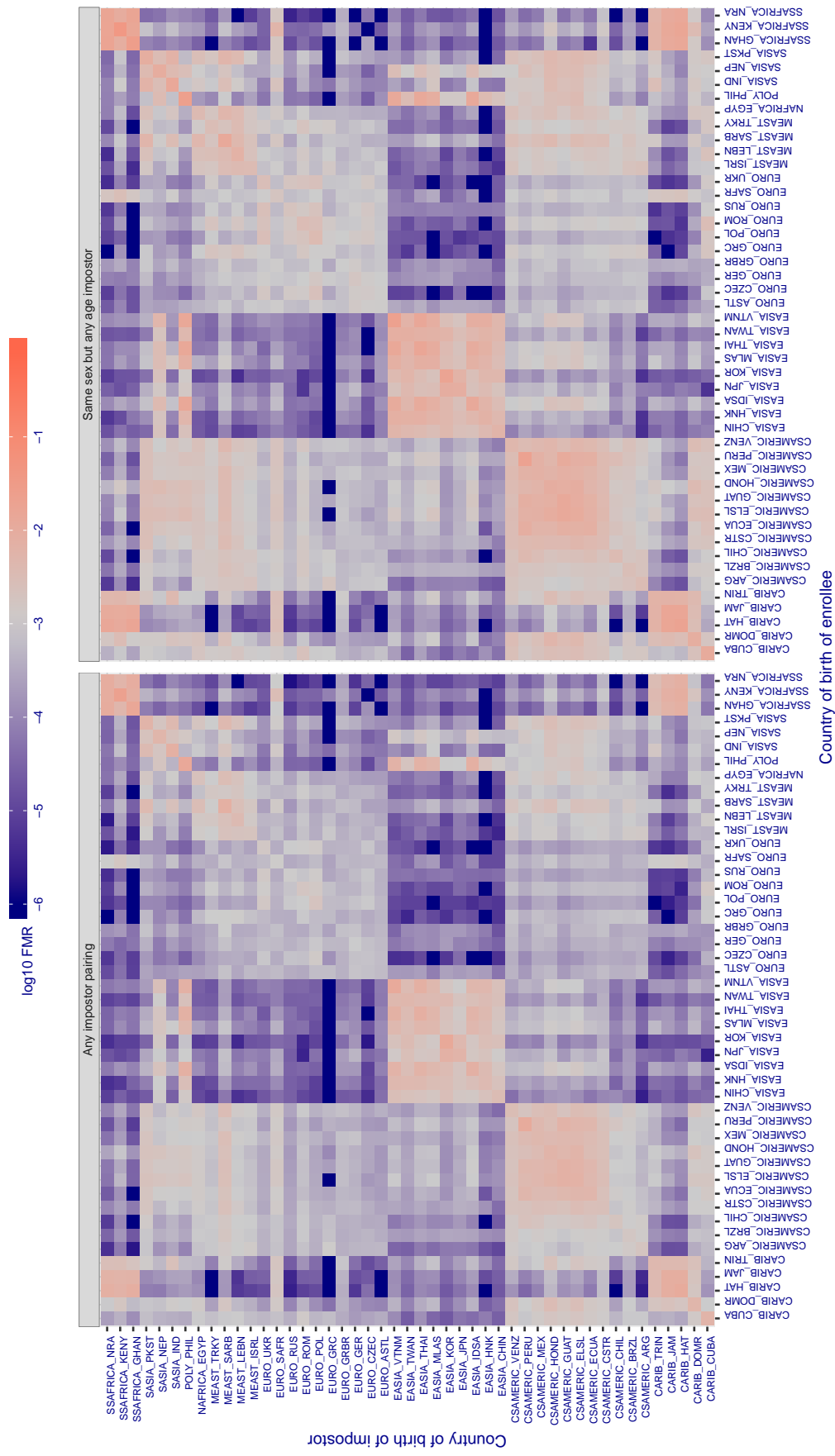


Figure 350: For algorithm *imagus-000* operating on visa images, the heatmap shows false match rates observed over impostor comparisons of faces from different individuals who were born in the given country pair. False matches are counted against a recognition threshold fixed globally to give the target  $FMR$  in the plot title, computed over all on the order of  $10^{10}$  impostor comparisons. If text appears in each box it give the same quantity as that coded by the color. Grey indicates  $FMR$  is at the intended  $FMR$  target level. Light red colors present a security vulnerability to, for example, a passport gate. Each +1 increase in  $\log_{10} FMR$  corresponds to a factor of 10 increase in  $FMR$ . The matrix is not quite symmetric because images in the enrollment and verification sets are different.

**Cross country FMR at threshold T = 1.302 for algorithm imperial\_000, giving  $\text{FMR}(\text{T}) = 0.001$  globally.**

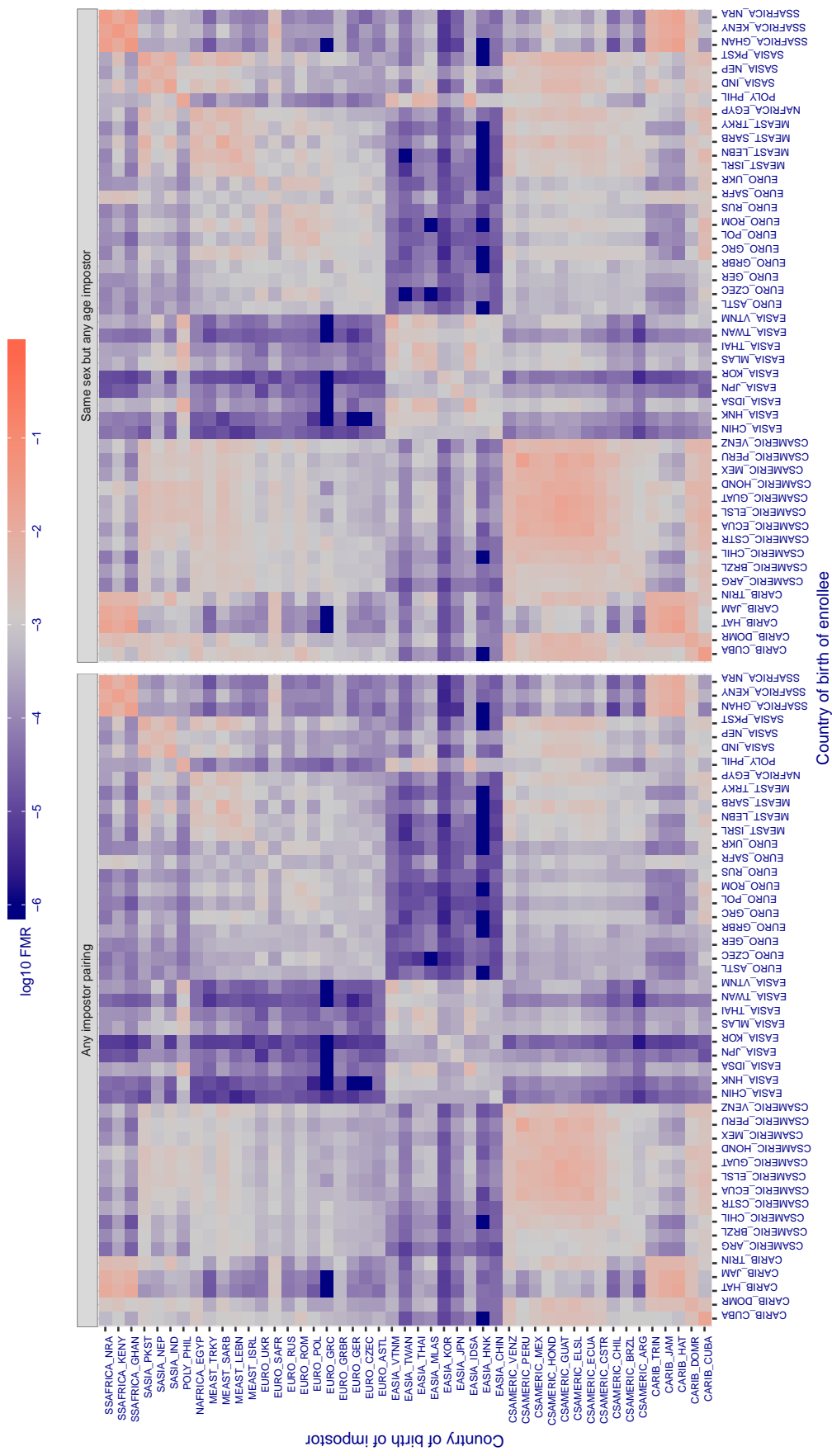


Figure 351: For algorithm imperial-000 operating on visa images, the heatmap shows false match rates observed over impostor comparisons of faces from different individuals who were born in the given country pair. False matches are counted against a recognition threshold fixed globally to give the target  $\text{FMR}$  in the plot title, computed over all on the order of  $10^{10}$  impostor comparisons. If text appears in each box it give the same quantity as that coded by the color. Grey indicates  $\text{FMR}$  is at the intended  $\text{FMR}$  target level. Light red colors present a security vulnerability to, for example, a passport gate. Each +1 increase in  $\log_{10} \text{FMR}$  corresponds to a factor of 10 increase in  $\text{FMR}$ . The matrix is not quite symmetric because images in the enrollment and verification sets are different.

**Cross country FMR at threshold T = 1.285 for algorithm imperial\_002, giving  $\text{FMR}(\text{T}) = 0.001$  globally.**

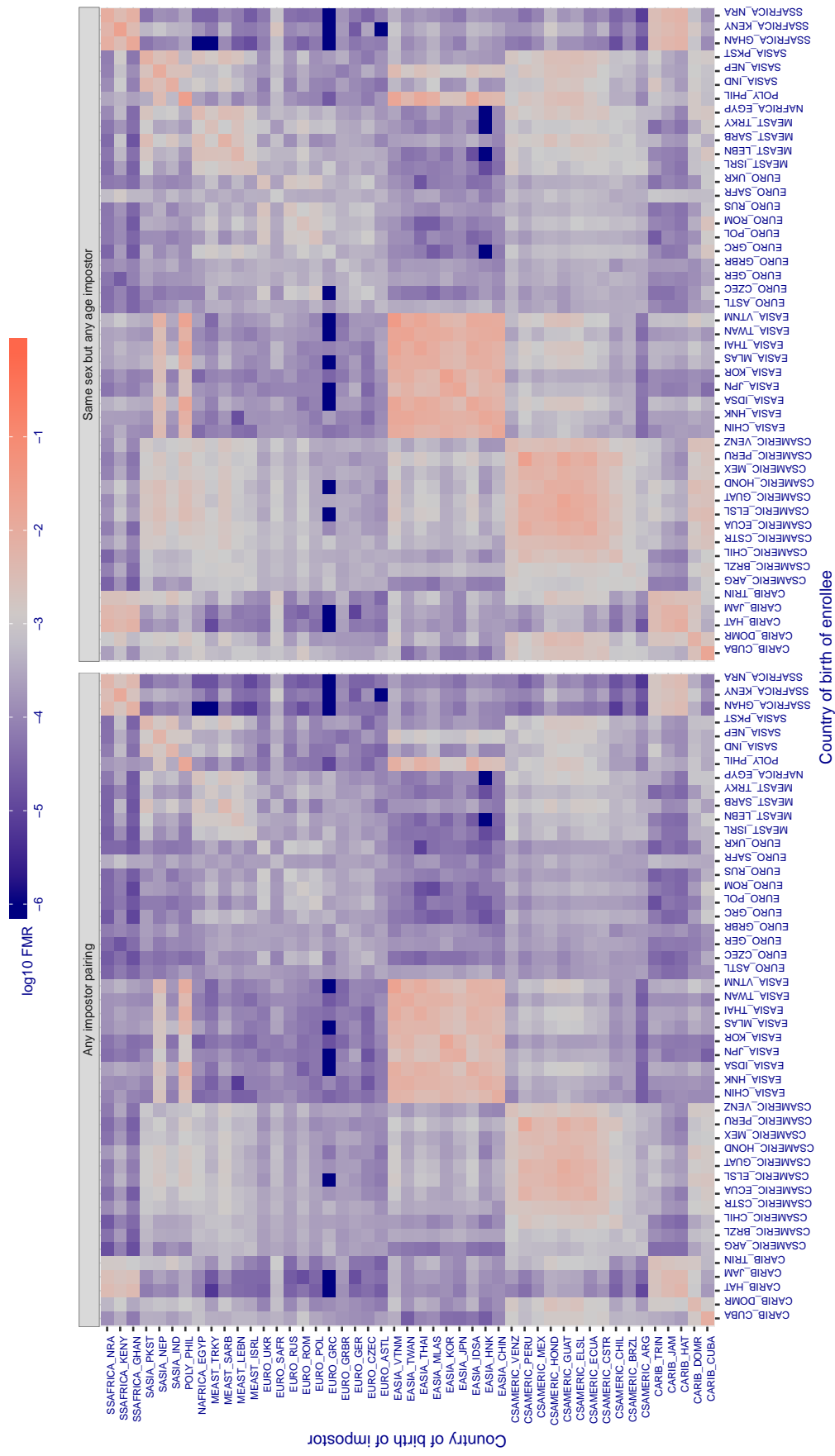


Figure 352: For algorithm imperial-002 operating on visa images, the heatmap shows false match rates observed over impostor comparisons of faces from different individuals who were born in the given country pair. False matches are counted against a recognition threshold fixed globally to give the target FMR in the plot title, computed over all on the order of  $10^{10}$  impostor comparisons. If text appears in each box it give the same quantity as that coded by the color. Grey indicates FMR is at the intended FMR target level. Light red colors present a security vulnerability to, for example, a passport gate. Each +1 increase in  $\log_{10} \text{FMR}$  corresponds to a factor of 10 increase in FMR. The matrix is not quite symmetric because images in the enrollment and verification sets are different.

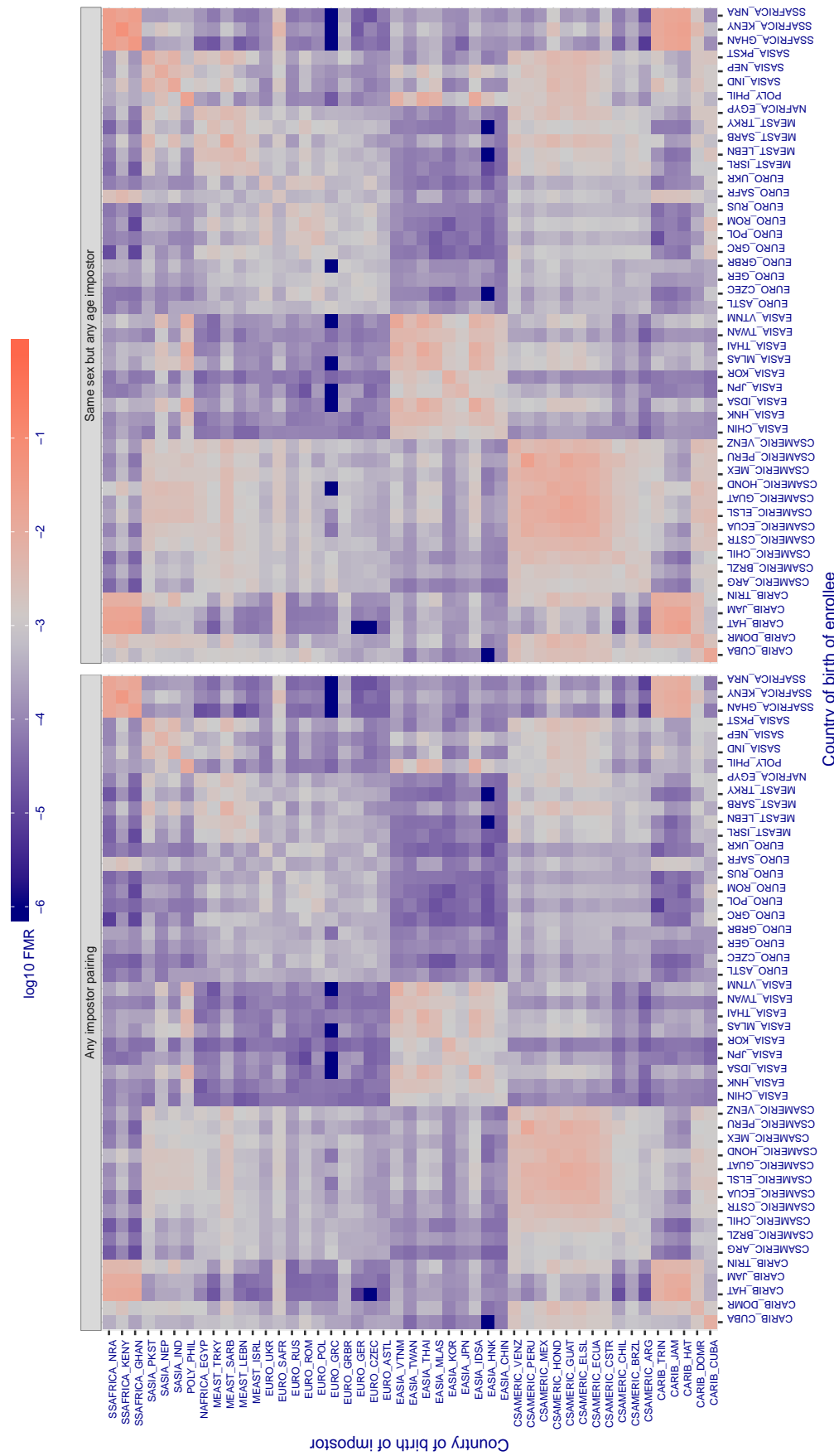
**Cross country FMR at threshold T = 1.340 for algorithm incode\_003, giving FMR(T) = 0.001 globally.**

Figure 353: For algorithm incode-003 operating on visa images, the heatmap shows false match rates observed over impostor comparisons of faces from different individuals who were born in the given country pair. False matches are counted against a recognition threshold fixed globally to give the target FMR in the plot title, computed over all on the order of  $10^{10}$  impostor comparisons. If text appears in each box it give the same quantity as that coded by the color. Grey indicates FMR is at the intended FMR target level. Light red colors present a security vulnerability to, for example, a passport gate. Each +1 increase in  $\log_{10} \text{FMR}$  corresponds to a factor of 10 increase in FMR. The matrix is not quite symmetric because images in the enrollment and verification sets are different.

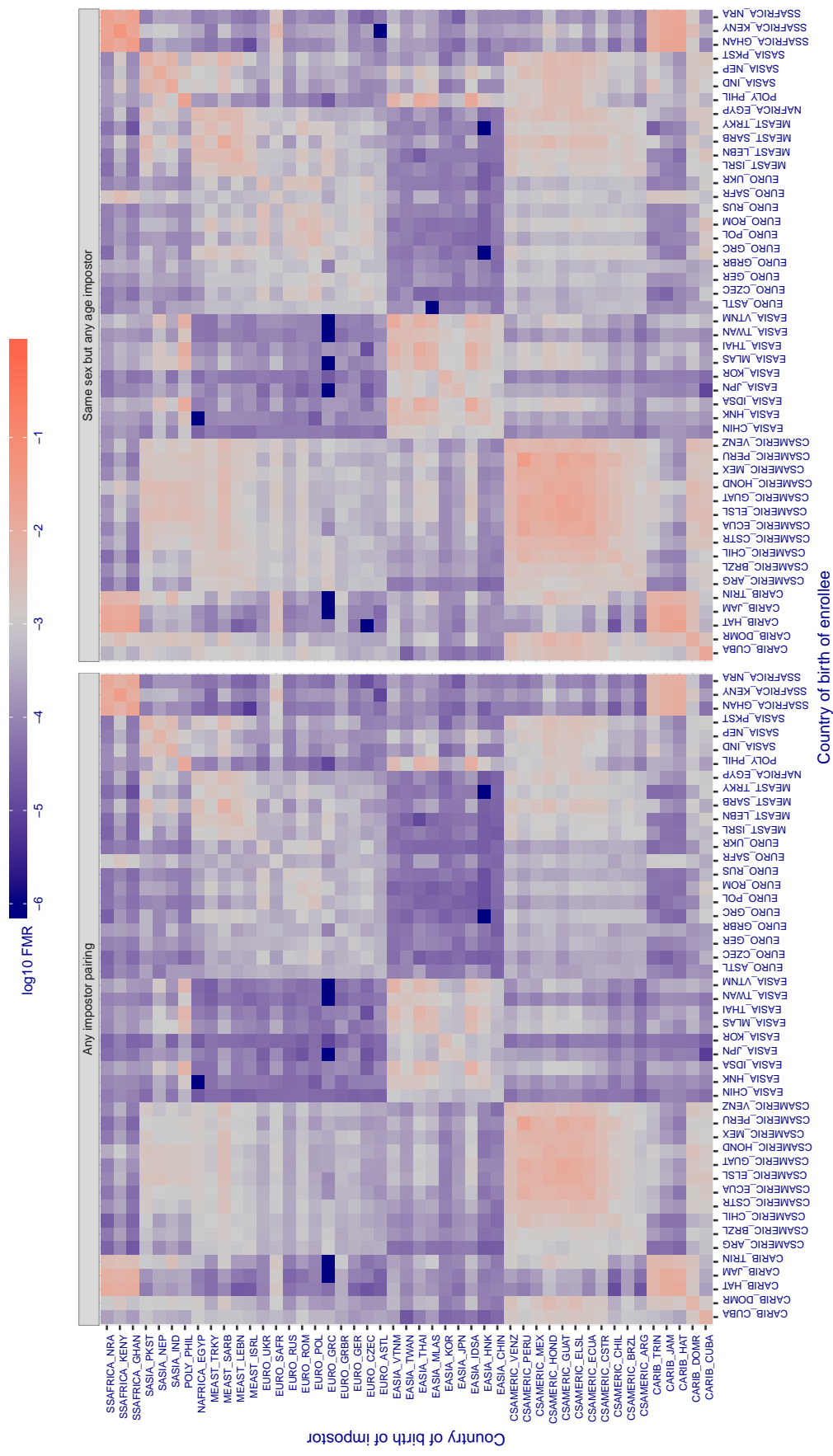
**Cross country FMR at threshold T = 1.314 for algorithm incode\_004, giving FMR(T) = 0.001 globally.**

Figure 354: For algorithm incode-004 operating on visa images, the heatmap shows false match rates observed over impostor comparisons of faces from different individuals who were born in the given country pair. False matches are counted against a recognition threshold fixed globally to give the target FMR in the plot title, computed over all on the order of  $10^{10}$  impostor comparisons. If text appears in each box it give the same quantity as that coded by the color. Grey indicates FMR is at the intended FMR target level. Light red colors present a security vulnerability to, for example, a passport gate. Each +1 increase in  $\log_{10} FMR$  corresponds to a factor of 10 increase in FMR. The matrix is not quite symmetric because images in the enrollment and verification sets are different.

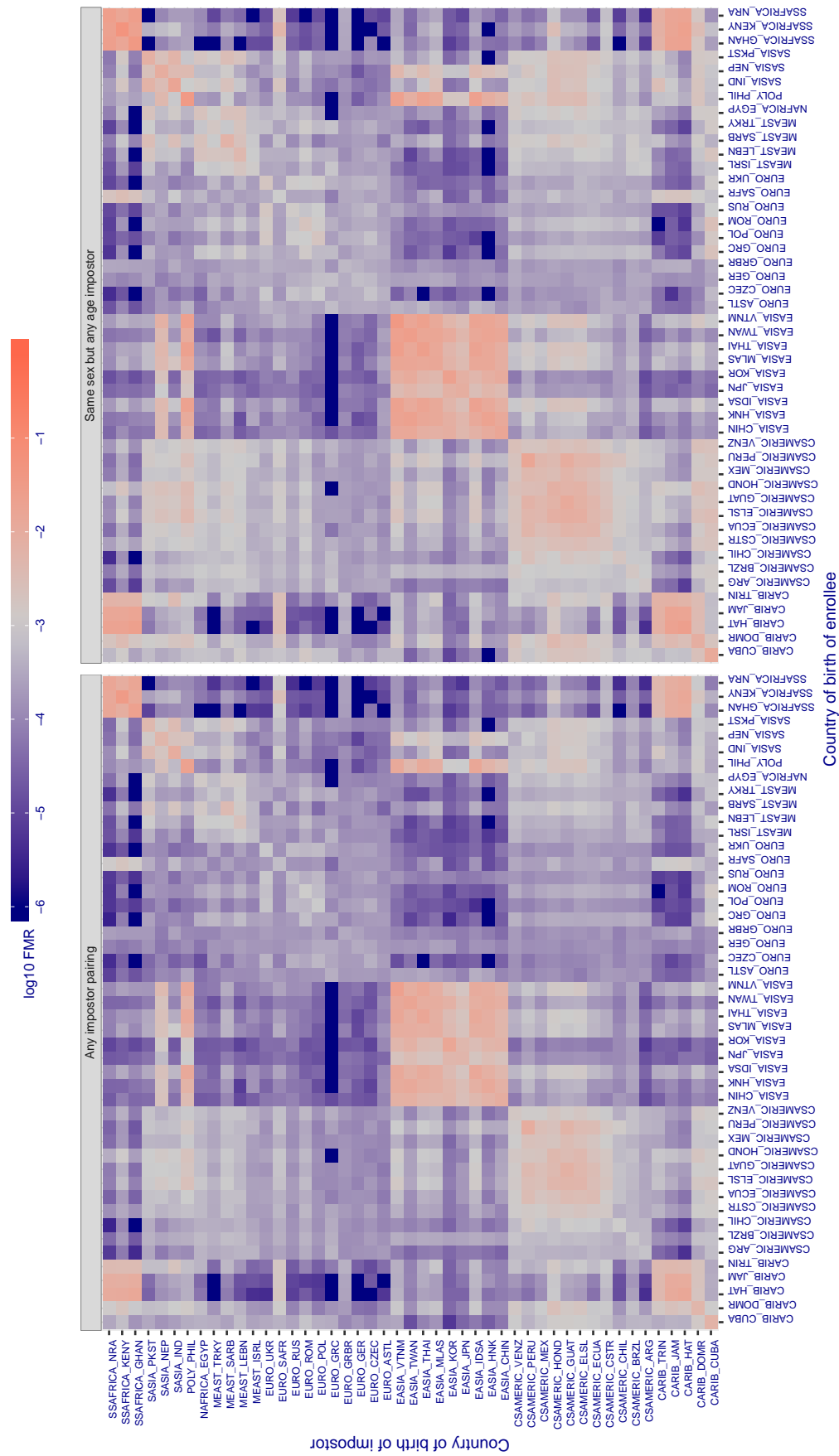
**Cross country FMR at threshold T = 21.422 for algorithm innovatrics\_004, giving  $FMR(T) = 0.001$  globally.**

Figure 355: For algorithm innovatrics-004 operating on visa images, the heatmap shows false match rates observed over impostor comparisons of faces from different individuals who were born in the given country pair. False matches are counted against a recognition threshold fixed globally to give the target  $FMR$  in the plot title, computed over all on the order of  $10^{10}$  impostor comparisons. If text appears in each box it give the same quantity as that coded by the color. Grey indicates  $FMR$  is at the intended  $FMR$  target level. Light red colors present a security vulnerability to, for example, a passport gate. Each +1 increase in  $\log_{10} FMR$  corresponds to a factor of 10 increase in  $FMR$ . The matrix is not quite symmetric because images in the enrollment and verification sets are different.

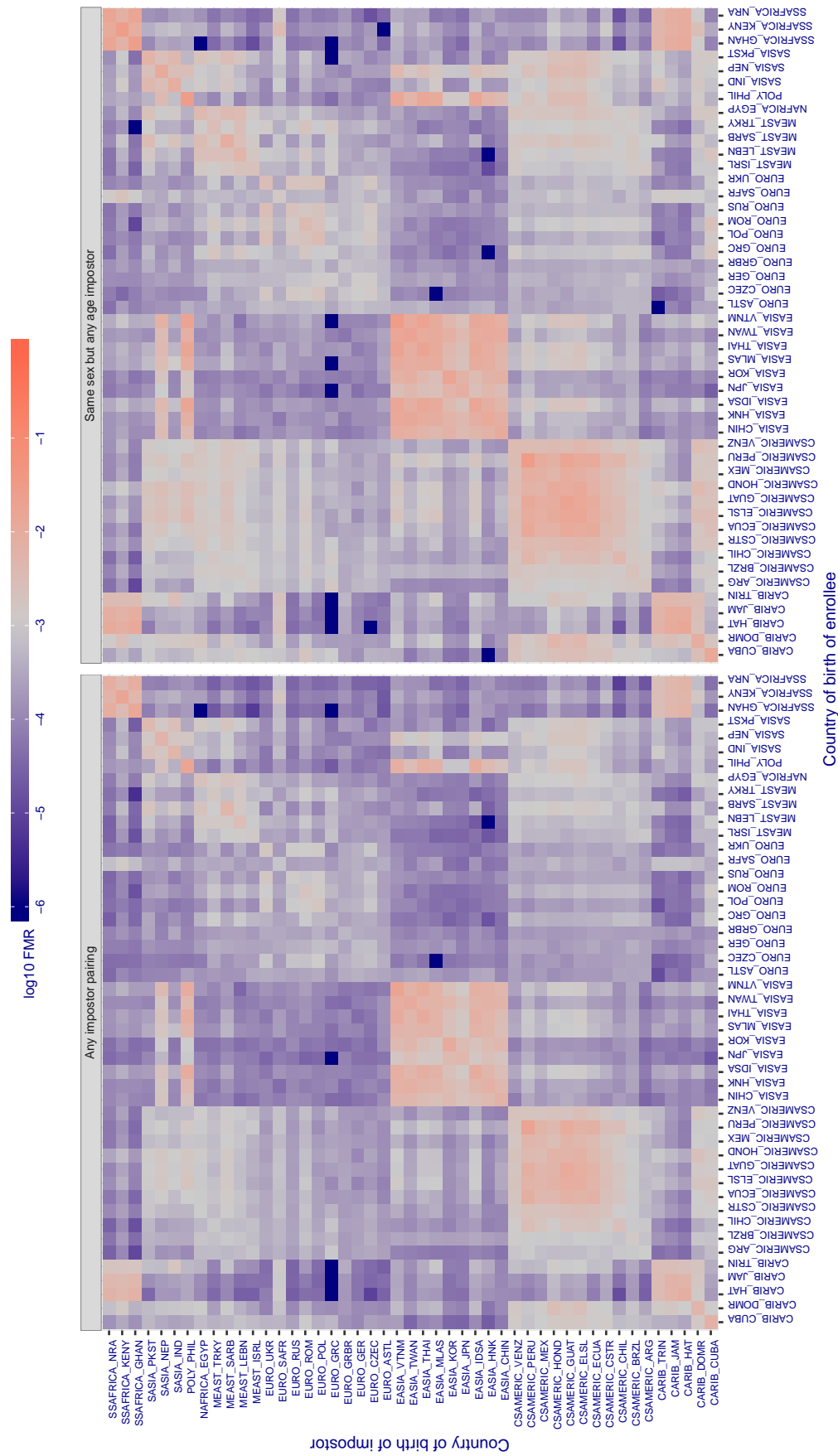
**Cross country FMR at threshold T = 20.505 for algorithm innovatrics\_006, giving  $FMR(T) = 0.001$  globally.**

Figure 356: For algorithm innovatrics-006 operating on visa images, the heatmap shows false match rates observed over impostor comparisons of faces from different individuals who were born in the given country pair. False matches are counted against a recognition threshold fixed globally to give the target  $FMR$  in the plot title, computed over all on the order of  $10^{10}$  impostor comparisons. If text appears in each box it give the same quantity as that coded by the color. Grey indicates  $FMR$  is at the intended  $FMR$  target level. Light red colors present a security vulnerability to, for example, a passport gate. Each +1 increase in  $\log_{10} FMR$  corresponds to a factor of 10 increase in  $FMR$ . The matrix is not quite symmetric because images in the enrollment and verification sets are different.

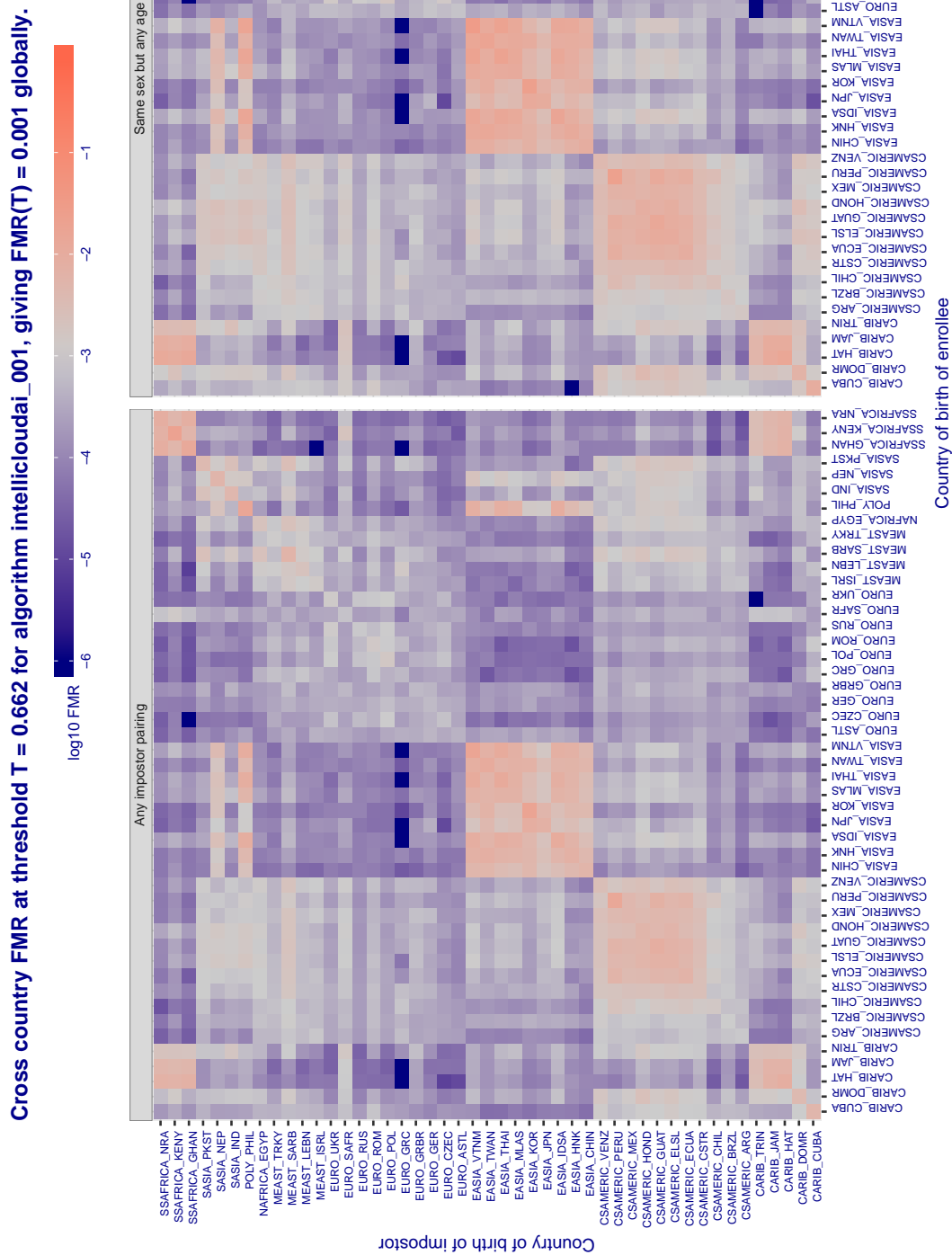


Figure 357: For algorithm intellicloudai-001 operating on visa images, the heatmap shows false match rates observed over impostor comparisons of faces from different individuals who were born in the given country pair. False matches are counted against a recognition threshold fixed globally to give the target FMR in the plot title, computed over all on the order of  $10^{10}$  impostor comparisons. If text appears in each box it give the same quantity as that coded by the color. Grey indicates FMR is at the intended FMR target level. Light red colors present a security vulnerability to, for example, a passport gate. Each +1 increase in  $\log_{10} FMR$  corresponds to a factor of 10 increase in FMR. The matrix is not quite symmetric because images in the enrollment and verification sets are different.

**Cross country FMR at threshold T = 0.240 for algorithm intellifusion\_001, giving FMR(T) = 0.001 globally.**

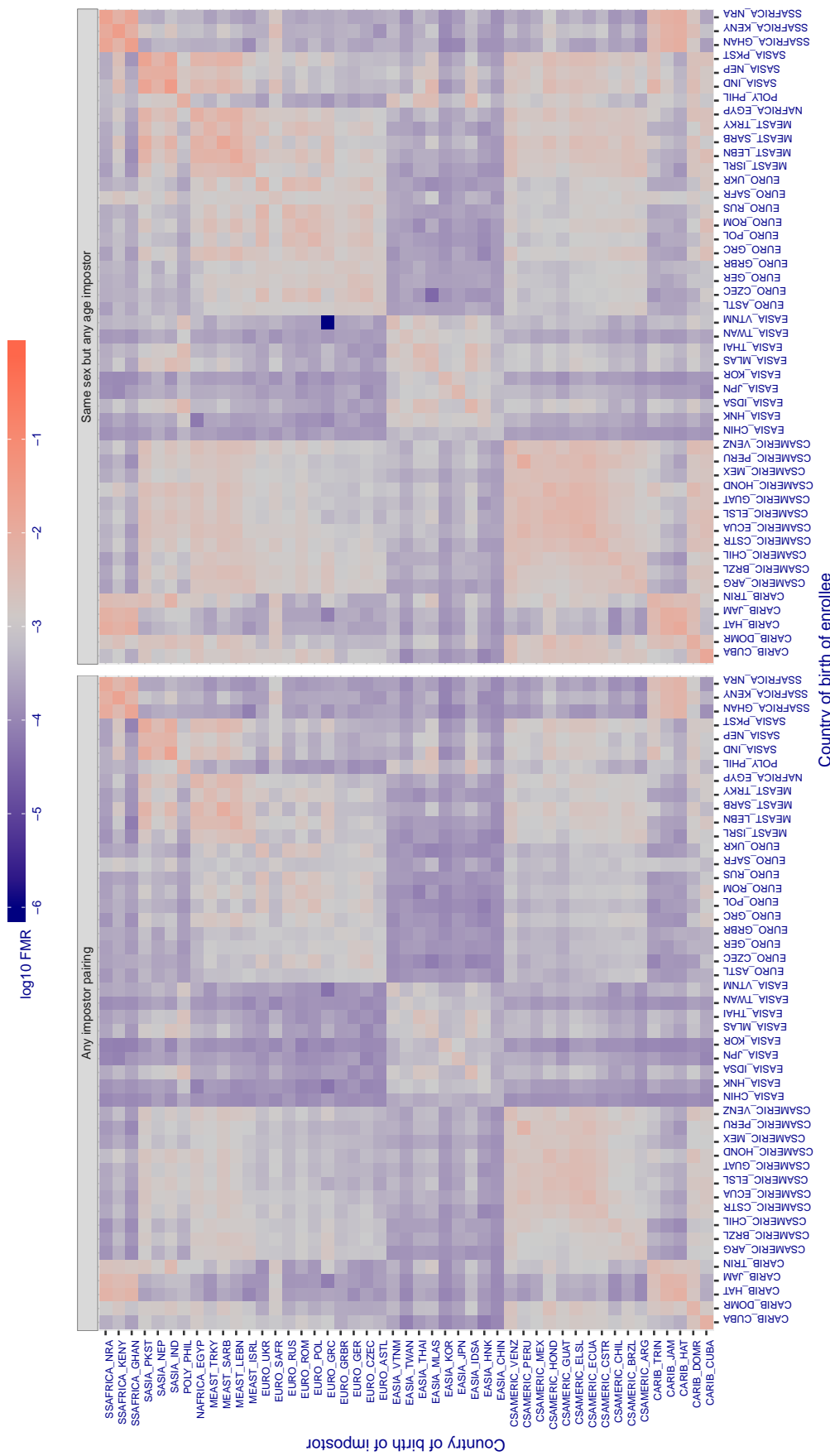


Figure 358: For algorithm intellifusion-001 operating on visa images, the heatmap shows false match rates observed over impostor comparisons of faces from different individuals who were born in the given country pair. False matches are counted against a recognition threshold fixed globally to give the target FMR in the plot title, computed over all on the order of  $10^{10}$  impostor comparisons. If text appears in each box it give the same quantity as that coded by the color. Grey indicates FMR is at the intended FMR target level. Light red colors present a security vulnerability to, for example, a passport gate. Each +1 increase in  $\log_{10} \text{FMR}$  corresponds to a factor of 10 increase in FMR. The matrix is not quite symmetric because images in the enrollment and verification sets are different.

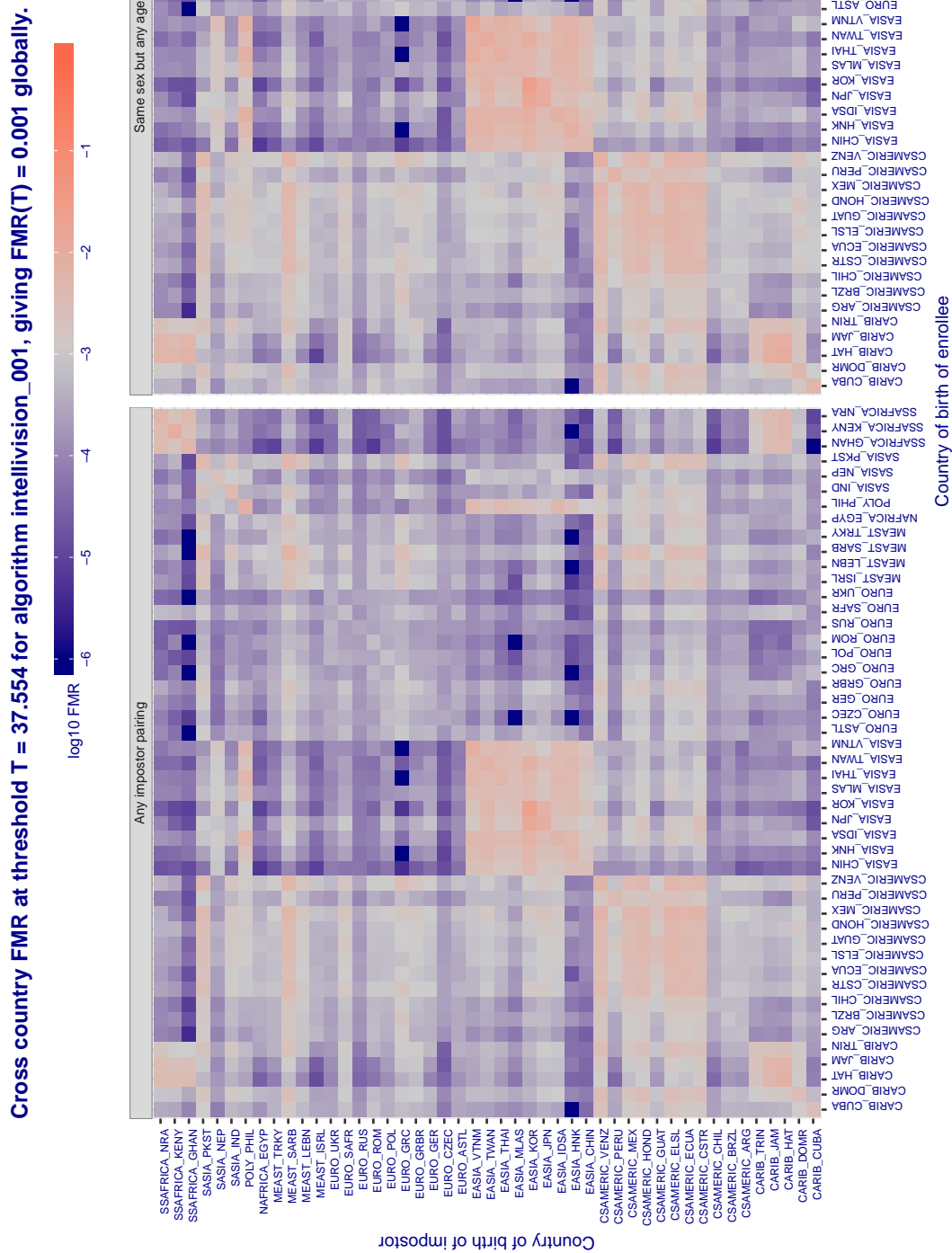


Figure 359: For algorithm intellivision-001 operating on visa images, the heatmap shows false match rates observed over impostor comparisons of faces from different individuals who were born in the given country pair. False matches are counted against a recognition threshold fixed globally to give the target FMR in the plot title, computed over all on the order of  $10^{10}$  impostor comparisons. If text appears in each box it give the same quantity as that coded by the color. Grey indicates FMR is at the intended FMR target level. Light red colors present a security vulnerability to, for example, a passport gate. Each +1 increase in  $\log_{10} FMR$  corresponds to a factor of 10 increase in FMR. The matrix is not quite symmetric because images in the enrollment and verification sets are different.

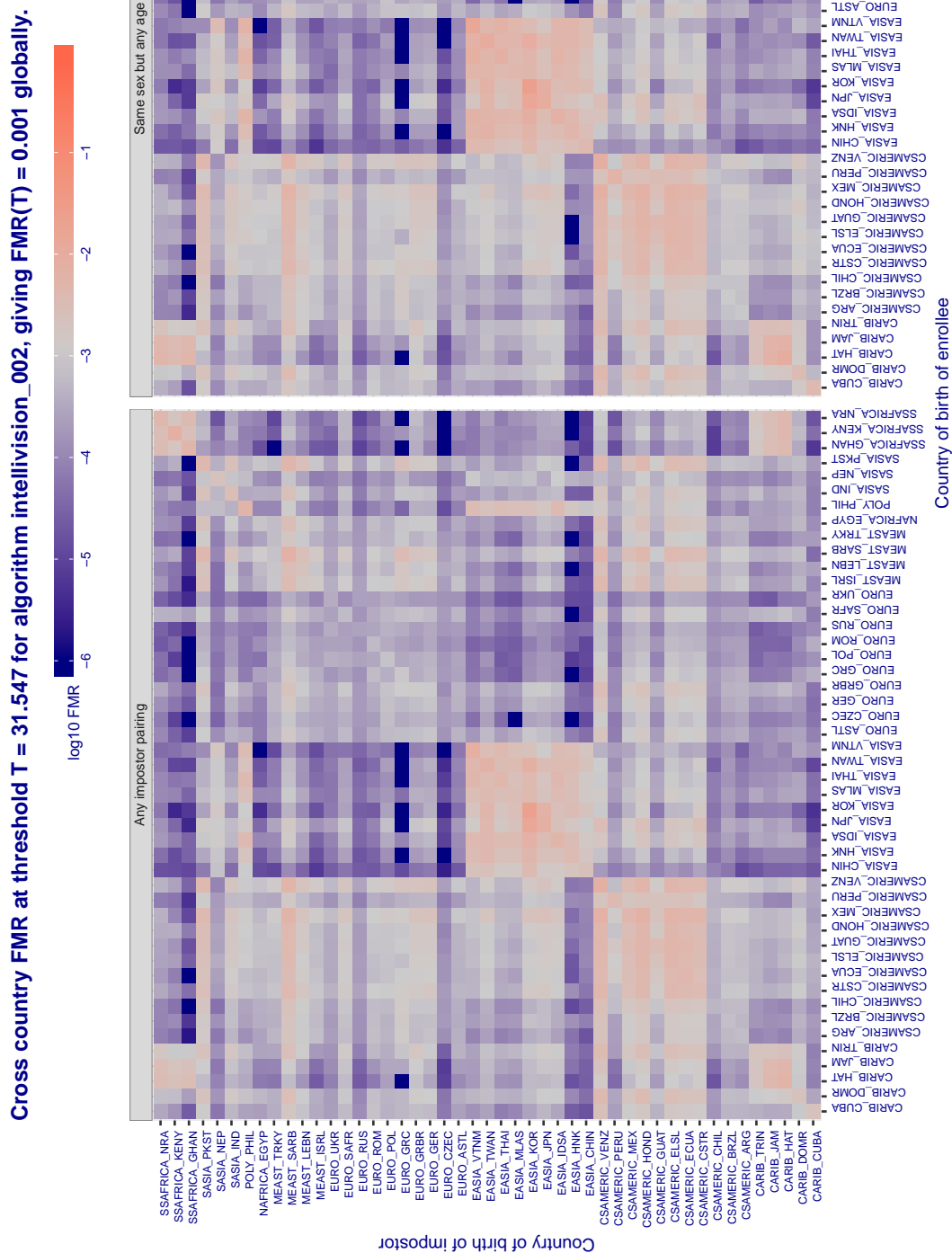


Figure 360: For algorithm intellivision-002 operating on visa images, the heatmap shows false match rates observed over impostor comparisons of faces from different individuals who were born in the given country pair. False matches are counted against a recognition threshold fixed globally to give the target FMR in the plot title, computed over all on the order of  $10^{10}$  impostor comparisons. If text appears in each box it give the same quantity as that coded by the color. Grey indicates FMR is at the intended FMR target level. Light red colors present a security vulnerability to, for example, a passport gate. Each +1 increase in  $\log_{10} \text{FMR}$  corresponds to a factor of 10 increase in FMR. The matrix is not quite symmetric because images in the enrollment and verification sets are different.

**Cross country FMR at threshold T = 565.207 for algorithm intelresearch\_000, giving FMR(T) = 0.001 globally.**

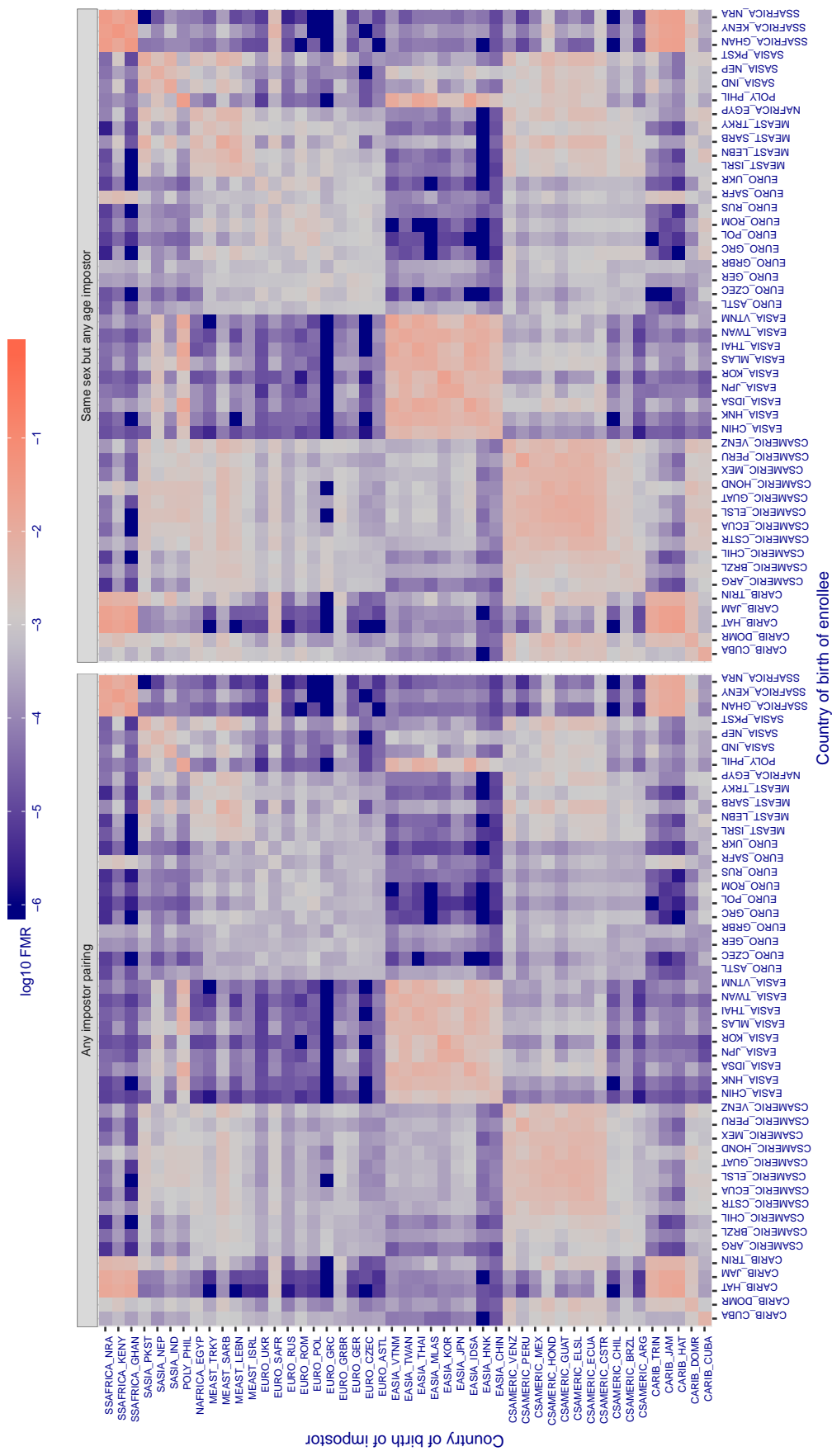


Figure 361: For algorithm intelresearch-000 operating on visa images, the heatmap shows false match rates observed over impostor comparisons of faces from different individuals who were born in the given country pair. False matches are counted against a recognition threshold fixed globally to give the target FMR in the plot title, computed over all on the order of  $10^{10}$  impostor comparisons. If text appears in each box it give the same quantity as that coded by the color. Grey indicates FMR is at the intended FMR target level. Light red colors present a security vulnerability to, for example, a passport gate. Each +1 increase in  $\log_{10} FMR$  corresponds to a factor of 10 increase in FMR. The matrix is not quite symmetric because images in the enrollment and verification sets are different.

**Cross country FMR at threshold T = 1.306 for algorithm intsysmsu\_000, giving FMR(T) = 0.001 globally.**

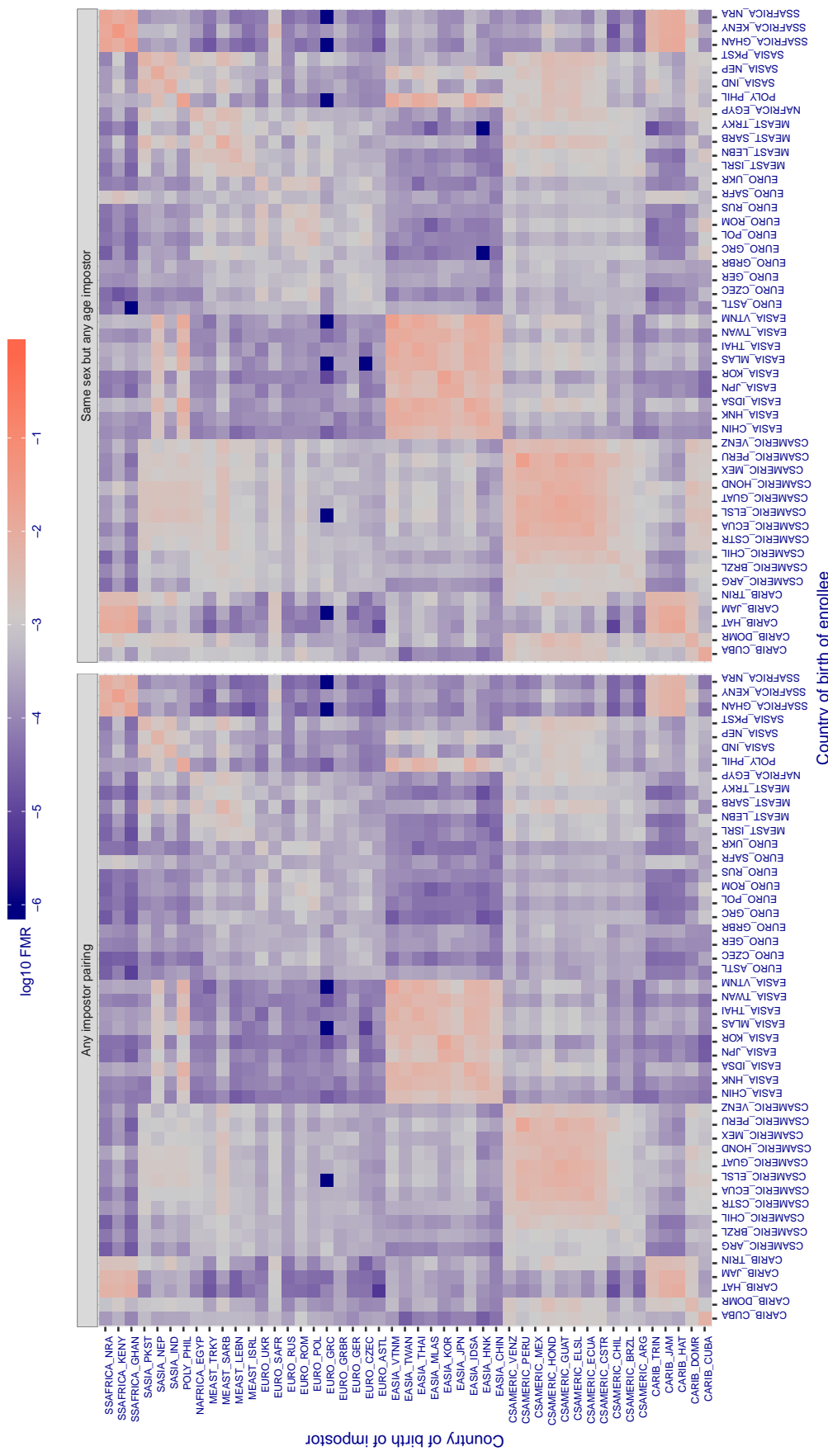


Figure 362: For algorithm intsysmsu-000 operating on visa images, the heatmap shows false match rates observed over impostor comparisons of faces from different individuals who were born in the given country pair. False matches are counted against a recognition threshold fixed globally to give the target FMR in the plot title, computed over all on the order of  $10^{10}$  impostor comparisons. If text appears in each box it give the same quantity as that coded by the color. Grey indicates FMR is at the intended FMR target level. Light red colors present a security vulnerability to, for example, a passport gate. Each +1 increase in  $\log_{10} FMR$  corresponds to a factor of 10 increase in FMR. The matrix is not quite symmetric because images in the enrollment and verification sets are different.

**Cross country FMR at threshold T = 1.280 for algorithm iqface\_000, giving FMR(T) = 0.001 globally.**

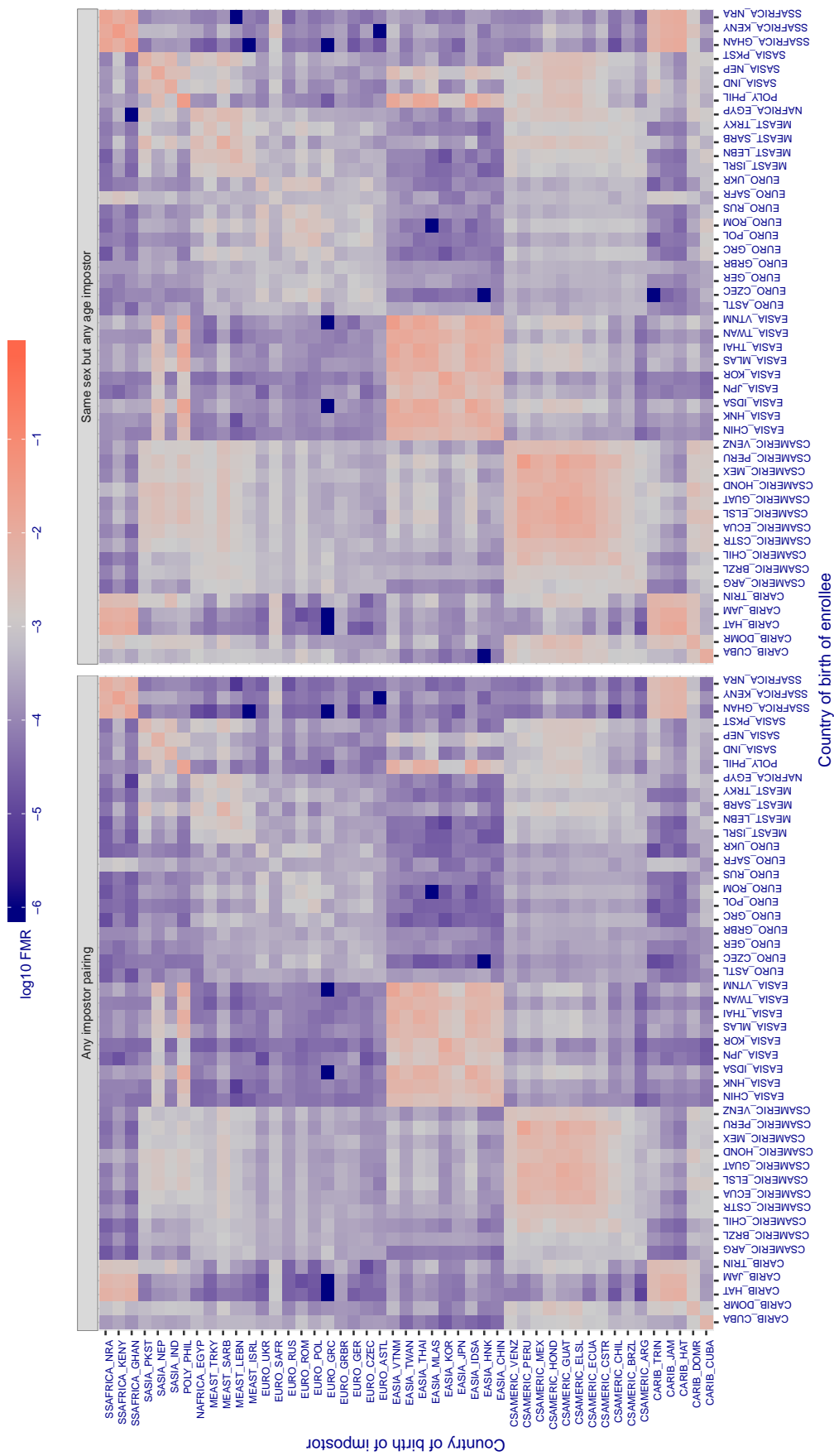


Figure 363: For algorithm iqface-000 operating on visa images, the heatmap shows false match rates observed over impostor comparisons of faces from different individuals who were born in the given country pair. False matches are counted against a recognition threshold fixed globally to give the target FMR in the plot title, computed over all on the order of  $10^{10}$  impostor comparisons. If text appears in each box it give the same quantity as that coded by the color. Grey indicates FMR is at the intended FMR target level. Light red colors present a security vulnerability to, for example, a passport gate. Each +1 increase in  $\log_{10} FMR$  corresponds to a factor of 10 increase in FMR. The matrix is not quite symmetric because images in the enrollment and verification sets are different.

Cross country FMR at threshold T = 0.982 for algorithm isap\_001, giving FMR(T) = 0.001 globally.

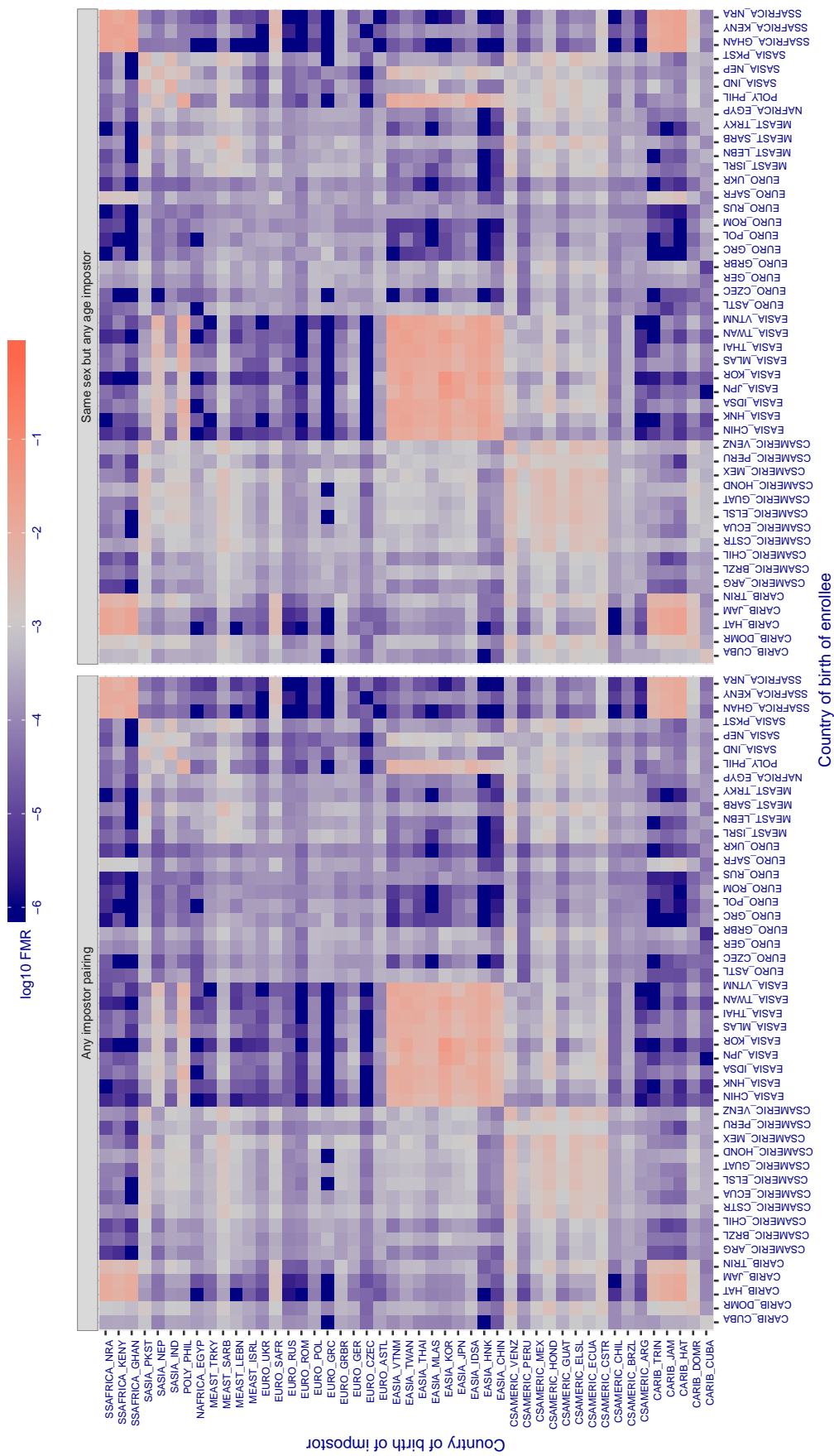


Figure 364: For algorithm isap\_001 operating on visa images, the heatmap shows false match rates observed over impostor comparisons of faces from different individuals who were born in the given country pair. False matches are counted against a recognition threshold fixed globally to give the target FMR in the plot title, computed over all on the order of  $10^{10}$  impostor comparisons. If text appears in each box it give the same quantity as that coded by the color. Grey indicates FMR is at the intended FMR target level. Light red colors present a security vulnerability to, for example, a passport gate. Each +1 increase in  $\log_{10} \text{FMR}$  corresponds to a factor of 10 increase in FMR. The matrix is not quite symmetric because images in the enrollment and verification sets are different.

**Cross country FMR at threshold T = 20.648 for algorithm isityou\_000, giving  $\text{FMR}(T) = 0.001$  globally.**

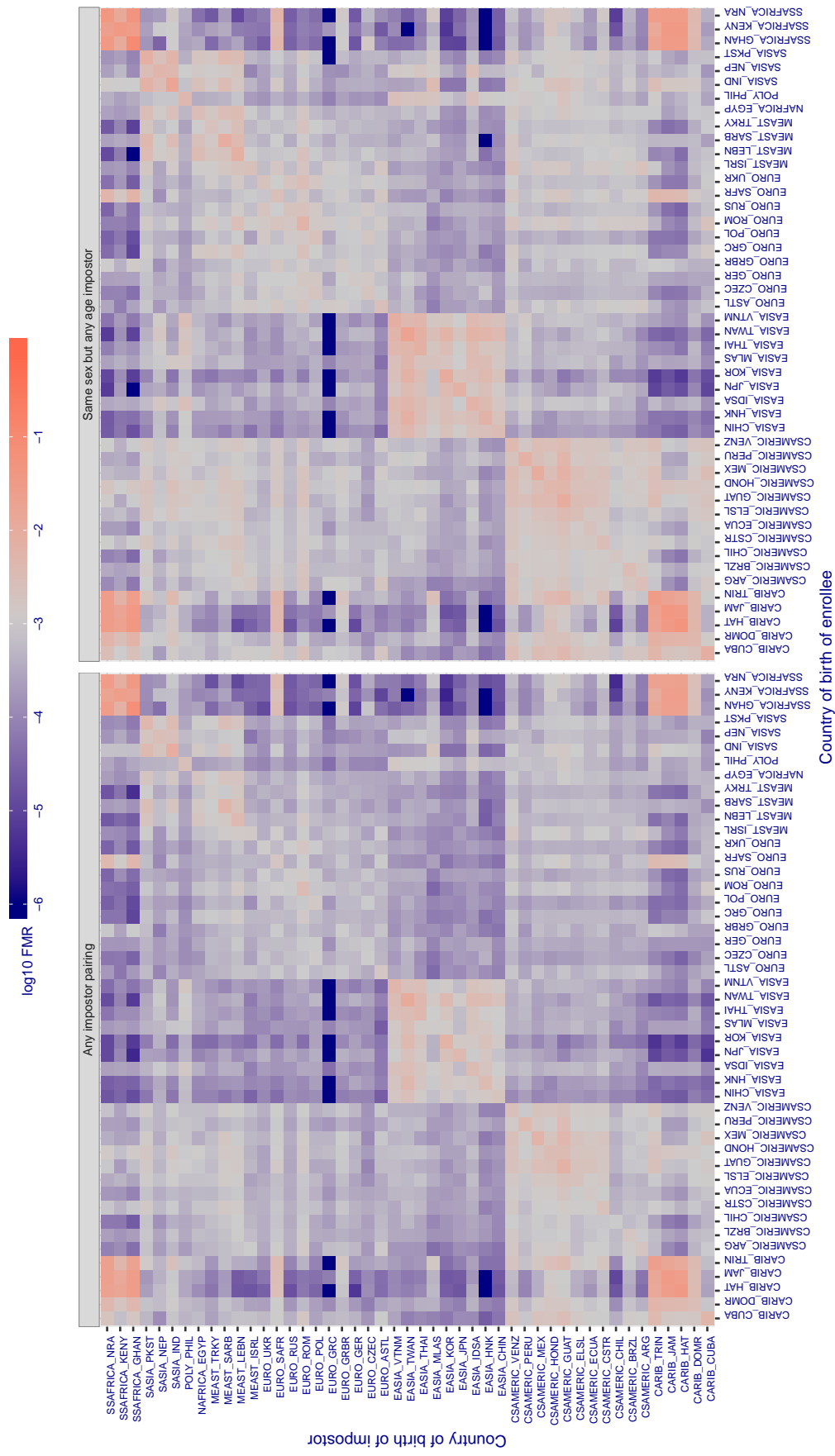


Figure 365: For algorithm isityou-000 operating on visa images, the heatmap shows false match rates observed over impostor comparisons of faces from different individuals who were born in the given country pair. False matches are counted against a recognition threshold fixed globally to give the target  $\text{FMR}$  in the plot title, computed over all on the order of  $10^{10}$  impostor comparisons. If text appears in each box it give the same quantity as that coded by the color. Grey indicates  $\text{FMR}$  is at the intended  $\text{FMR}$  target level. Light red colors present a security vulnerability to, for example, a passport gate. Each +1 increase in  $\log_{10} \text{FMR}$  corresponds to a factor of 10 increase in  $\text{FMR}$ . The matrix is not quite symmetric because images in the enrollment and verification sets are different.

**Cross country FMR at threshold T = 0.649 for algorithm *systems\_001*, giving  $FMR(T) = 0.001$  globally.**

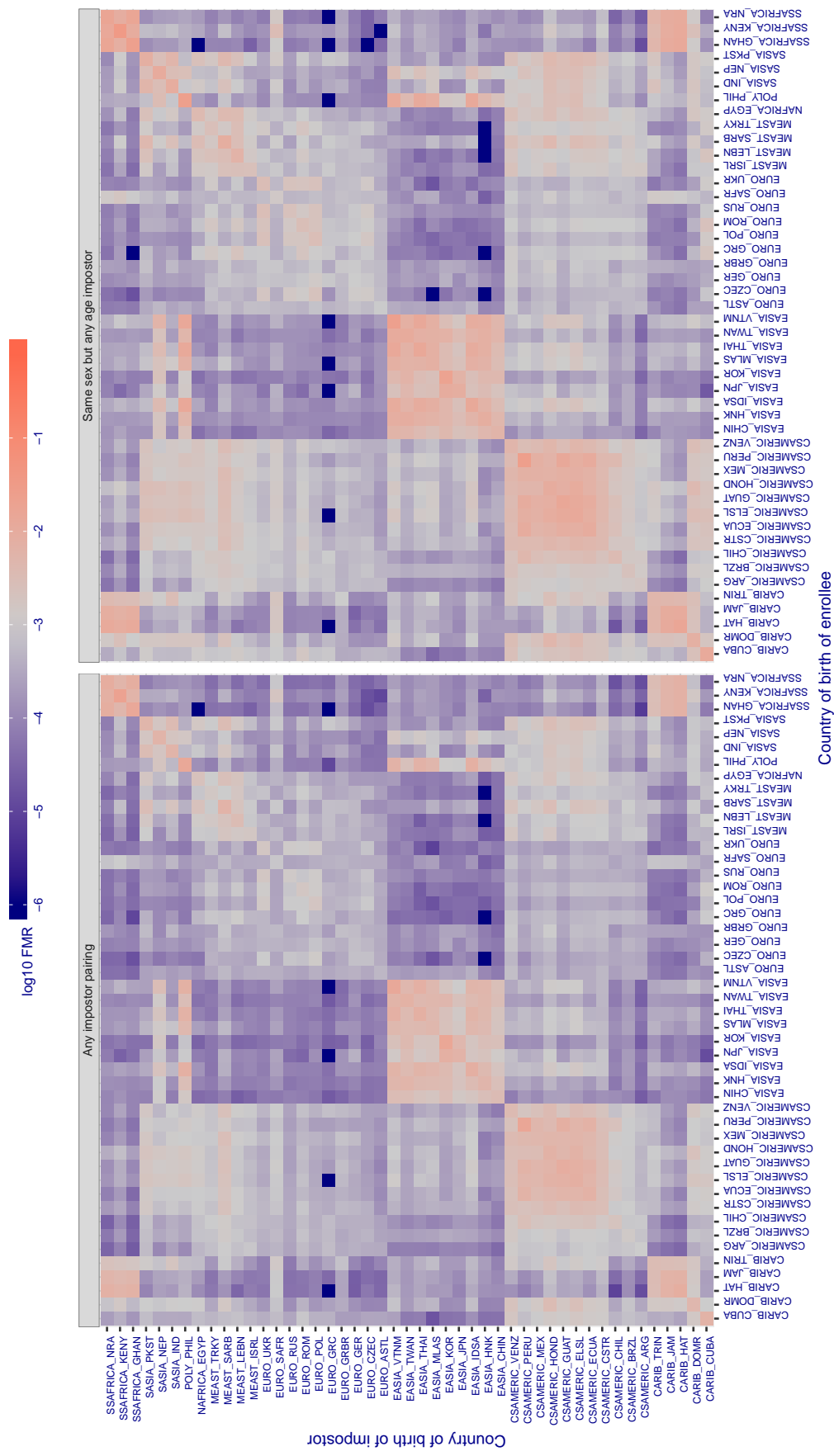


Figure 366: For algorithm *systems-001* operating on visa images, the heatmap shows false match rates observed over impostor comparisons of faces from different individuals who were born in the given country pair. False matches are counted against a recognition threshold fixed globally to give the target  $FMR$  in the plot title, computed over all on the order of  $10^{10}$  impostor comparisons. If text appears in each box it give the same quantity as that coded by the color. Grey indicates  $FMR$  is at the intended  $FMR$  target level. Light red colors present a security vulnerability to, for example, a passport gate. Each +1 increase in  $\log_{10} FMR$  corresponds to a factor of 10 increase in  $FMR$ . The matrix is not quite symmetric because images in the enrollment and verification sets are different.

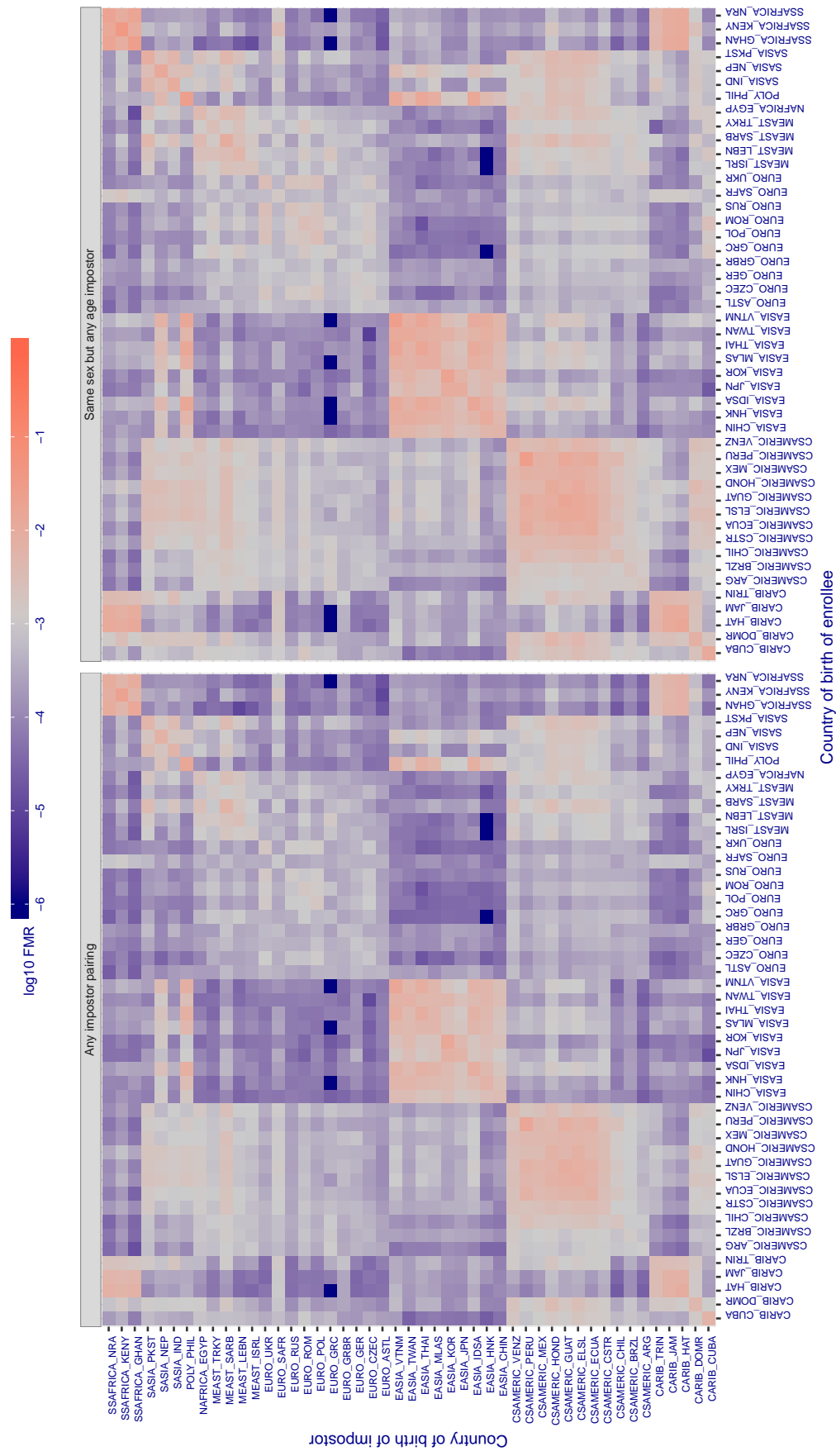
**Cross country FMR at threshold T = 0.647 for algorithm isystems\_002, giving FMR(T) = 0.001 globally.**

Figure 367: For algorithm isystems-002 operating on visa images, the heatmap shows false match rates observed over impostor comparisons of faces from different individuals who were born in the given country pair. False matches are counted against a recognition threshold fixed globally to give the target FMR in the plot title, computed over all on the order of  $10^{10}$  impostor comparisons. If text appears in each box it give the same quantity as that coded by the color. Grey indicates FMR is at the intended FMR target level. Light red colors present a security vulnerability to, for example, a passport gate. Each +1 increase in  $\log_{10} FMR$  corresponds to a factor of 10 increase in FMR. The matrix is not quite symmetric because images in the enrollment and verification sets are different.

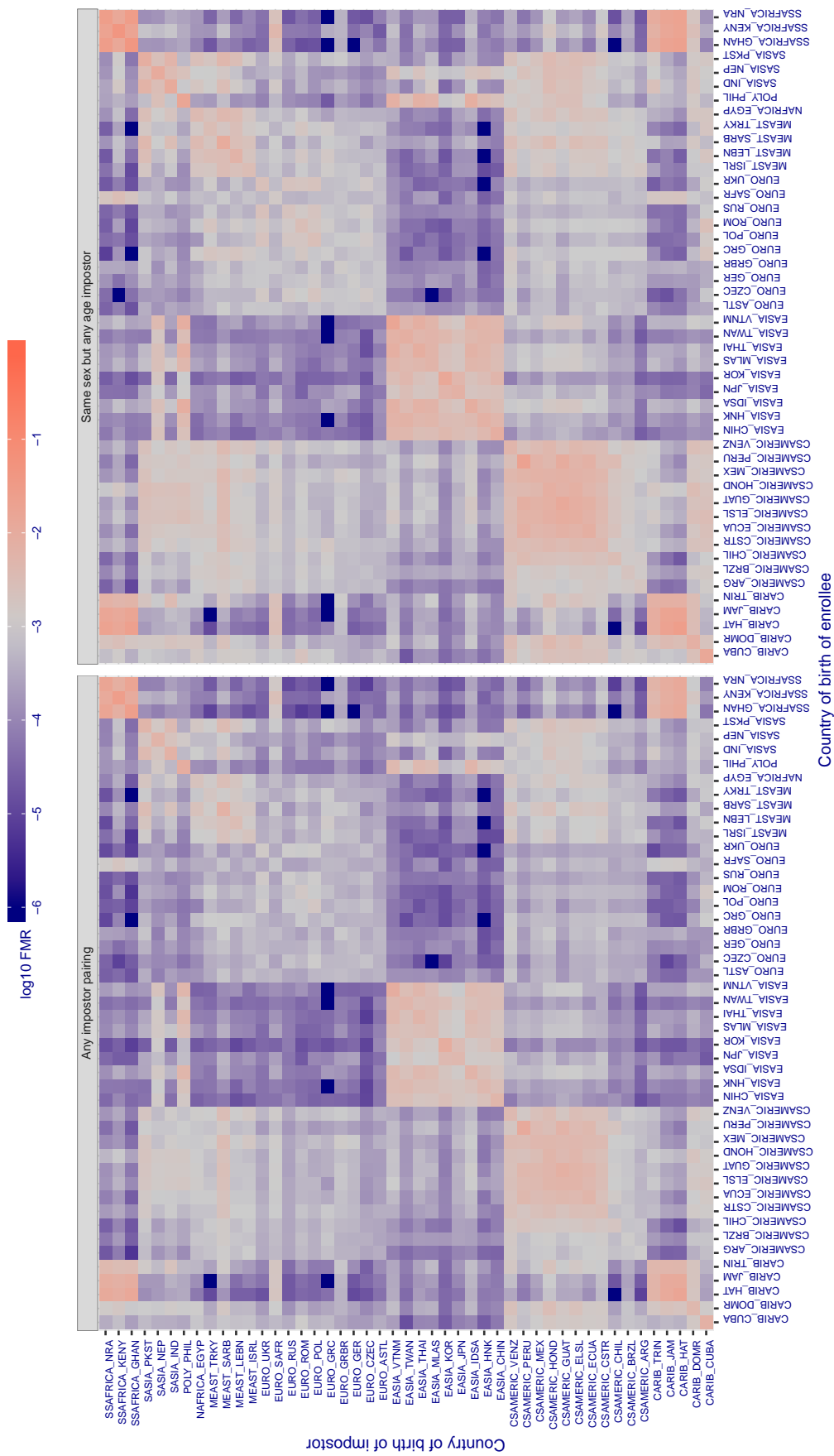
**Cross country FMR at threshold T = 10.316 for algorithm itmo\_005, giving FMR(T) = 0.001 globally.**

Figure 368: For algorithm itmo-005 operating on visa images, the heatmap shows false match rates observed over impostor comparisons of faces from different individuals who were born in the given country pair. False matches are counted against a recognition threshold fixed globally to give the target FMR in the plot title, computed over all on the order of  $10^{10}$  impostor comparisons. If text appears in each box it give the same quantity as that coded by the color. Grey indicates FMR is at the intended FMR target level. Light red colors present a security vulnerability to, for example, a passport gate. Each +1 increase in  $\log_{10} \text{FMR}$  corresponds to a factor of 10 increase in FMR. The matrix is not quite symmetric because images in the enrollment and verification sets are different.

**Cross country FMR at threshold T = 12.030 for algorithm itmo\_006, giving FMR(T) = 0.001 globally.**

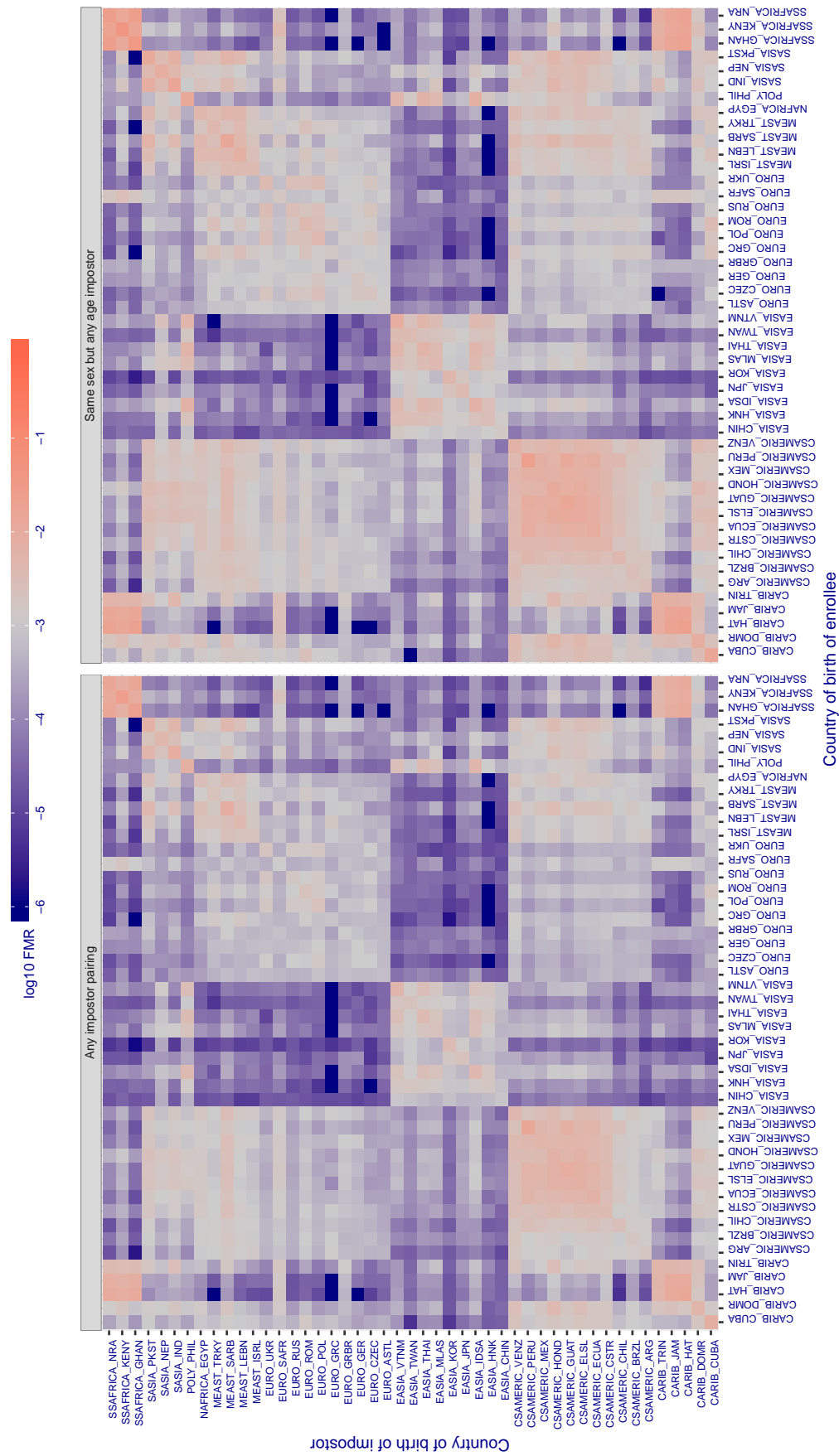


Figure 369: For algorithm itmo-006 operating on visa images, the heatmap shows false match rates observed over impostor comparisons of faces from different individuals who were born in the given country pair. False matches are counted against a recognition threshold fixed globally to give the target FMR in the plot title, computed over all on the order of  $10^{10}$  impostor comparisons. If text appears in each box it give the same quantity as that coded by the color. Grey indicates FMR is at the intended FMR target level. Light red colors present a security vulnerability to, for example, a passport gate. Each +1 increase in  $\log_{10} FMR$  corresponds to a factor of 10 increase in FMR. The matrix is not quite symmetric because images in the enrollment and verification sets are different.

Cross country FMR at threshold T = 1.192 for algorithm kakao\_001, giving FMR(T) = 0.001 globally.

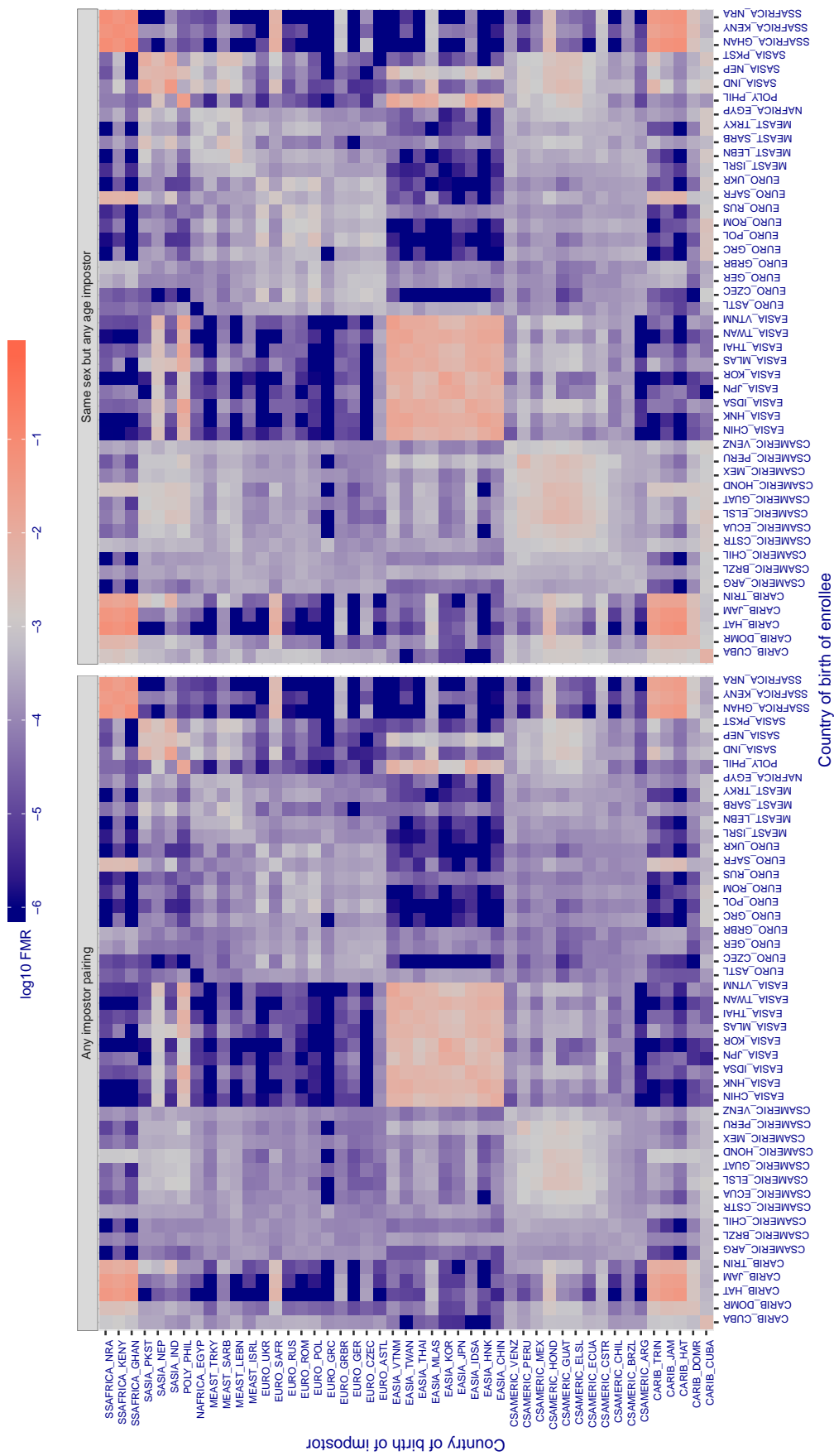


Figure 370: For algorithm kakao-001 operating on visa images, the heatmap shows false match rates observed over impostor comparisons of faces from different individuals who were born in the given country pair. False matches are counted against a recognition threshold fixed globally to give the target FMR in the plot title, computed over all on the order of  $10^{10}$  impostor comparisons. If text appears in each box it give the same quantity as that coded by the color. Grey indicates FMR is at the intended FMR target level. Light red colors present a security vulnerability to, for example, a passport gate. Each +1 increase in  $\log_{10} FMR$  corresponds to a factor of 10 increase in FMR. The matrix is not quite symmetric because images in the enrollment and verification sets are different.

**Cross country FMR at threshold T = 0.854 for algorithm kakao\_002, giving FMR(T) = 0.001 globally.**

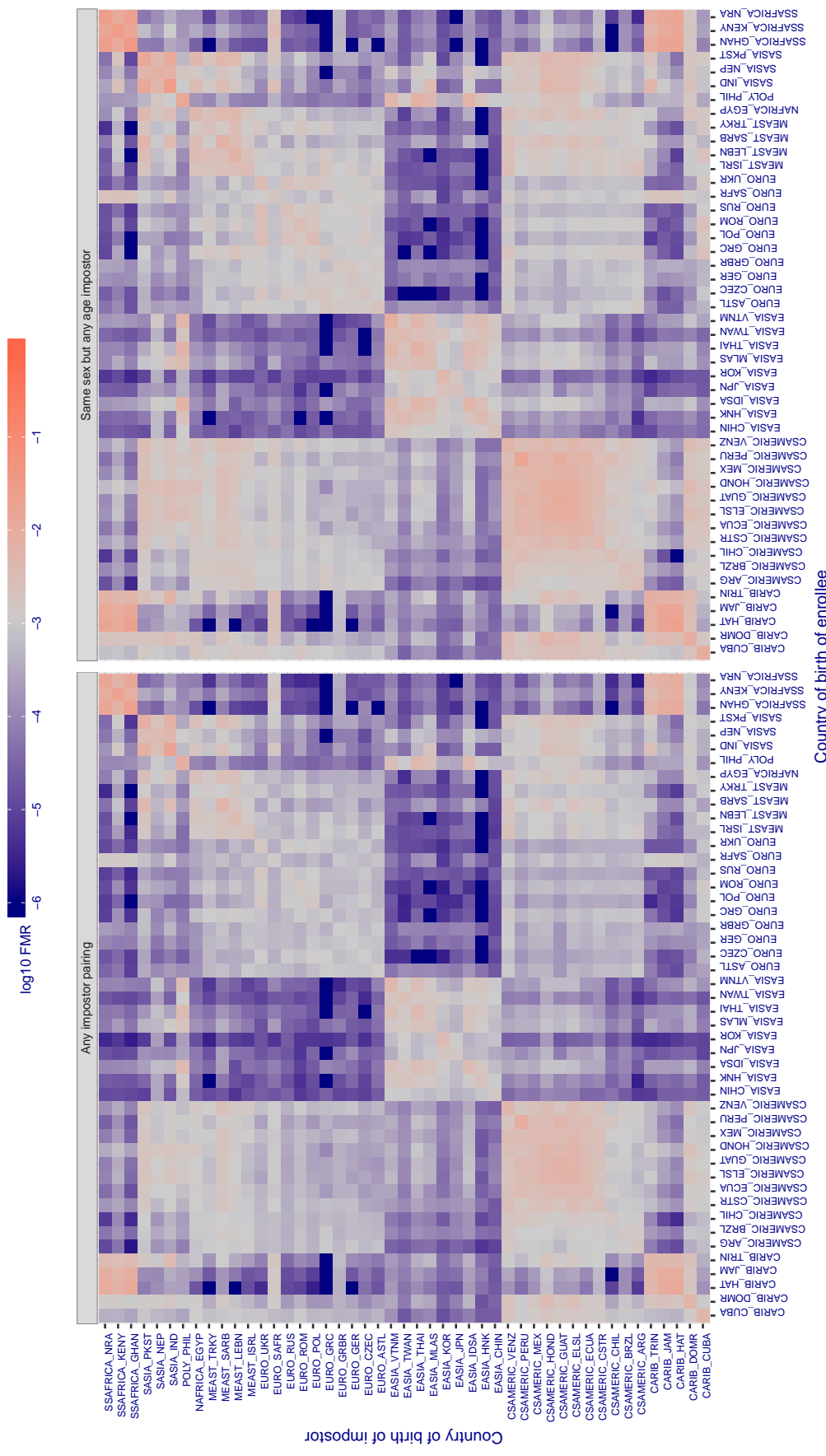


Figure 371: For algorithm kakao-002 operating on visa images, the heatmap shows false match rates observed over impostor comparisons of faces from different individuals who were born in the given country pair. False matches are counted against a recognition threshold fixed globally to give the target FMR in the plot title, computed over all on the order of  $10^{10}$  impostor comparisons. If text appears in each box it give the same quantity as that coded by the color. Grey indicates FMR is at the intended FMR target level. Light red colors present a security vulnerability to, for example, a passport gate. Each +1 increase in  $\log_{10} \text{FMR}$  corresponds to a factor of 10 increase in FMR. The matrix is not quite symmetric because images in the enrollment and verification sets are different.

Cross country FMR at threshold T = 0.650 for algorithm kedacom\_000, giving FMR(T) = 0.001 globally.

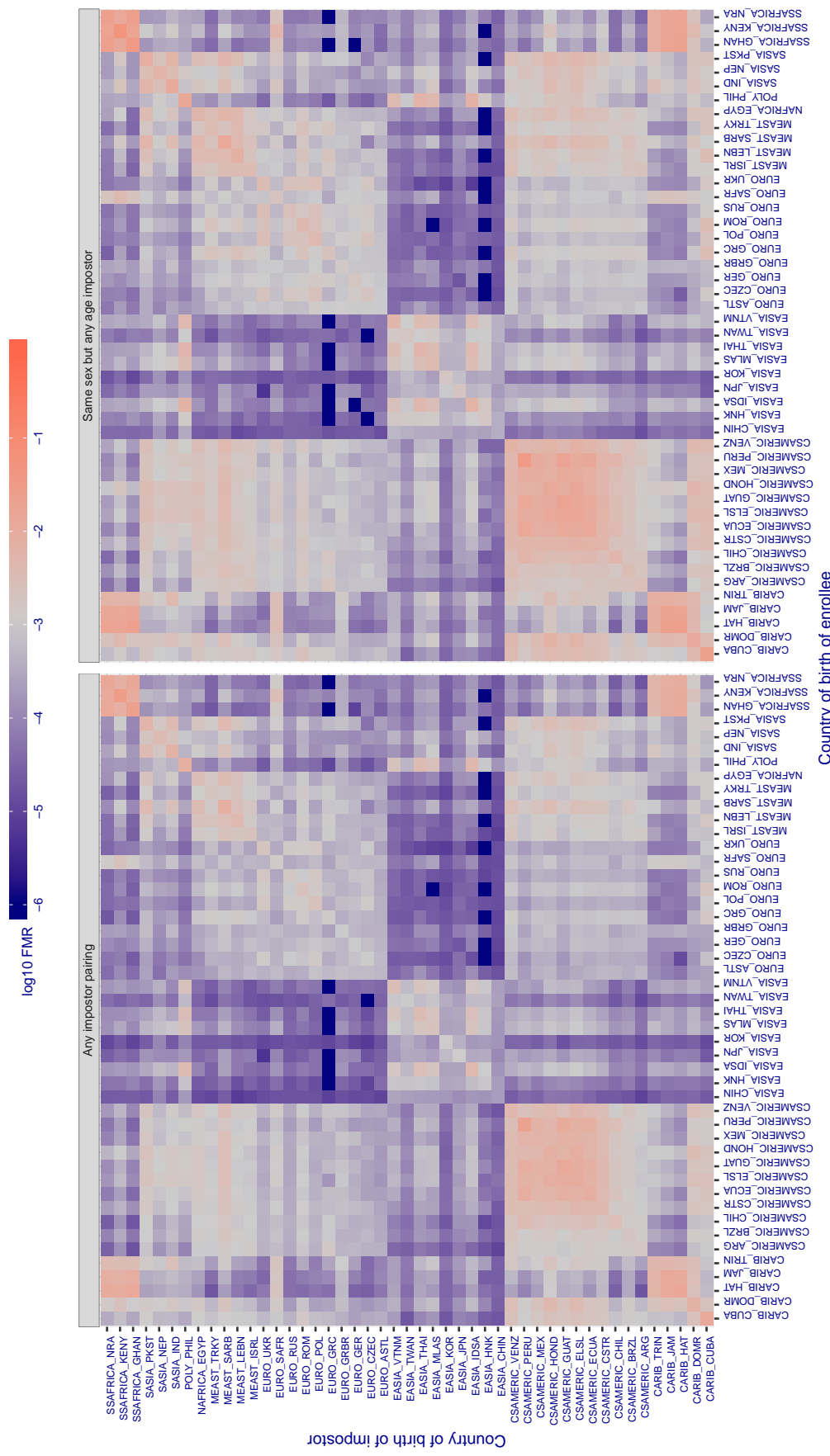


Figure 372: For algorithm kedacom-000 operating on visa images, the heatmap shows false match rates observed over impostor comparisons of faces from different individuals who were born in the given country pair. False matches are counted against a recognition threshold fixed globally to give the target FMR in the plot title, computed over all on the order of  $10^{10}$  impostor comparisons. If text appears in each box it give the same quantity as that coded by the color. Grey indicates FMR is at the intended FMR target level. Light red colors present a security vulnerability to, for example, a passport gate. Each +1 increase in  $\log_{10} \text{FMR}$  corresponds to a factor of 10 increase in FMR. The matrix is not quite symmetric because images in the enrollment and verification sets are different.

**Cross country FMR at threshold T = 0.397 for algorithm kneron\_003, giving  $FMR(T) = 0.001$  globally.**

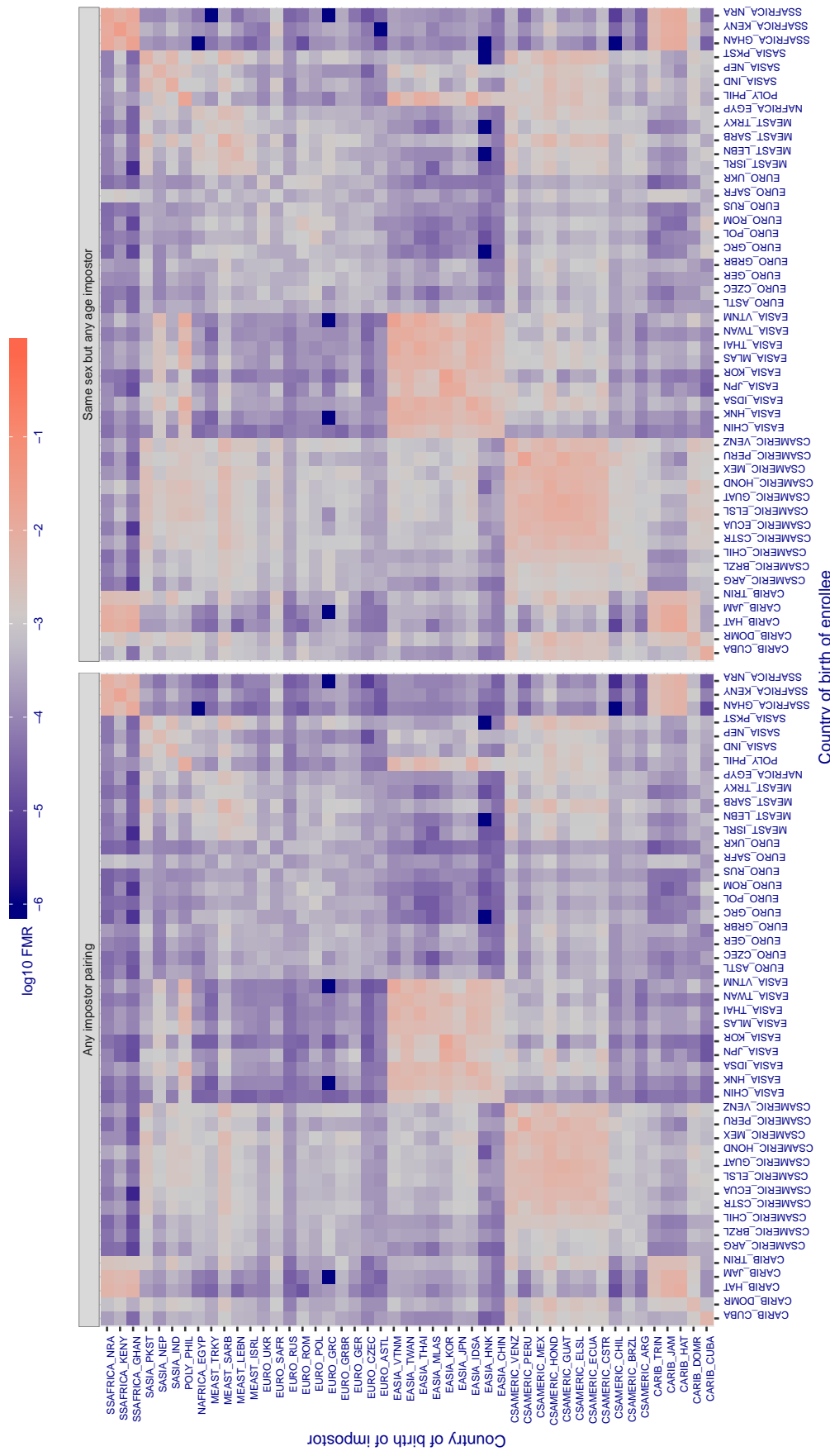


Figure 373: For algorithm kneron-003 operating on visa images, the heatmap shows false match rates observed over impostor comparisons of faces from different individuals who were born in the given country pair. False matches are counted against a recognition threshold fixed globally to give the target  $FMR$  in the plot title, computed over all on the order of  $10^{10}$  impostor comparisons. If text appears in each box it give the same quantity as that coded by the color. Grey indicates  $FMR$  is at the intended  $FMR$  target level. Light red colors present a security vulnerability to, for example, a passport gate. Each +1 increase in  $\log_{10} FMR$  corresponds to a factor of 10 increase in  $FMR$ . The matrix is not quite symmetric because images in the enrollment and verification sets are different.

Cross country FMR at threshold T = 0.656 for algorithm lookman\_002, giving FMR(T) = 0.001 globally.

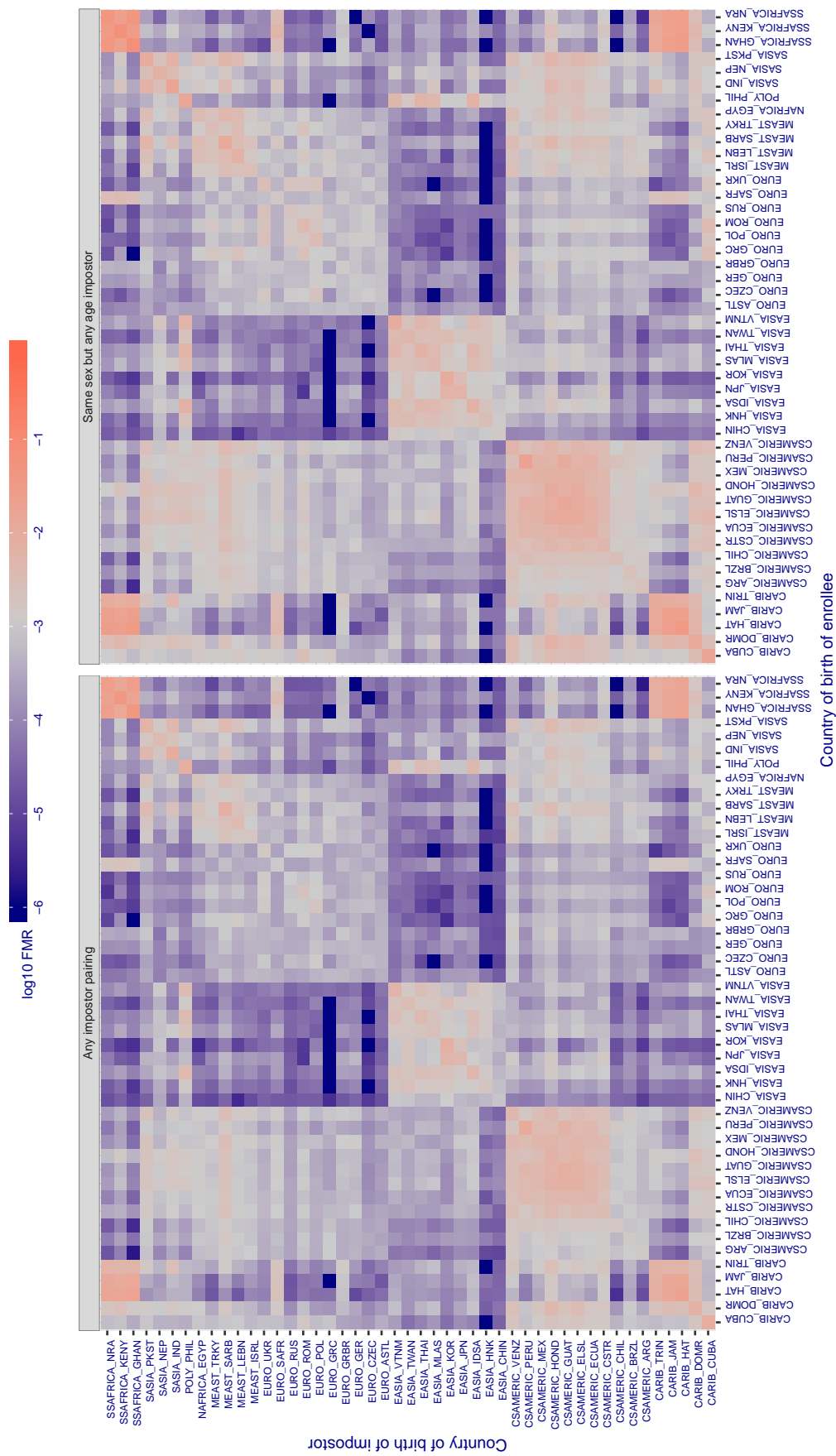


Figure 374: For algorithm lookman-002 operating on visa images, the heatmap shows false match rates observed over impostor comparisons of faces from different individuals who were born in the given country pair. False matches are counted against a recognition threshold fixed globally to give the target FMR in the plot title, computed over all on the order of  $10^{10}$  impostor comparisons. If text appears in each box it give the same quantity as that coded by the color. Grey indicates FMR is at the intended FMR target level. Light red colors present a security vulnerability to, for example, a passport gate. Each +1 increase in  $\log_{10} FMR$  corresponds to a factor of 10 increase in FMR. The matrix is not quite symmetric because images in the enrollment and verification sets are different.

Cross country FMR at threshold T = 0.703 for algorithm lookman\_004, giving FMR(T) = 0.001 globally.

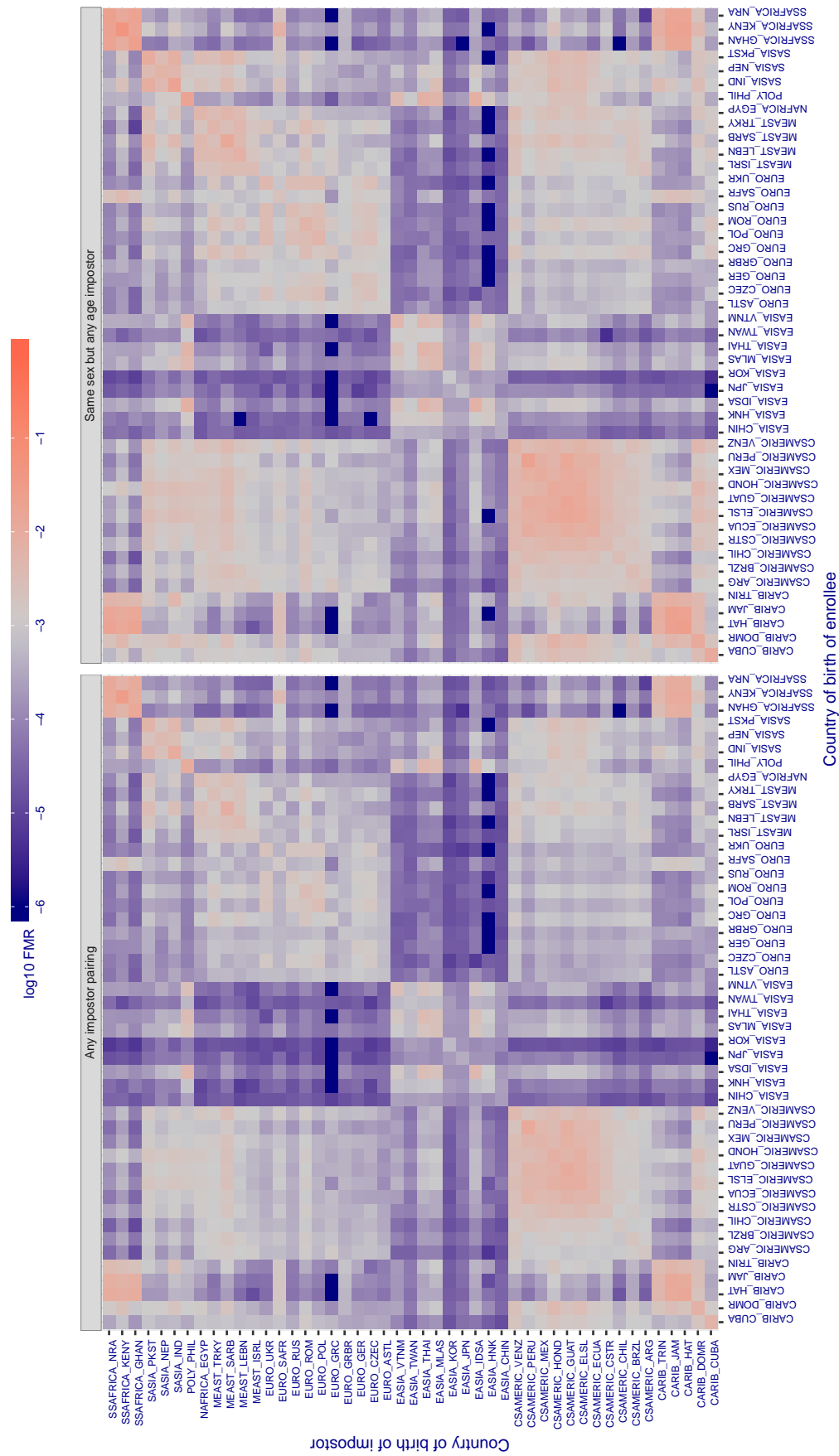


Figure 375: For algorithm lookman-004 operating on visa images, the heatmap shows false match rates observed over impostor comparisons of faces from different individuals who were born in the given country pair. False matches are counted against a recognition threshold fixed globally to give the target FMR in the plot title, computed over all on the order of  $10^{10}$  impostor comparisons. If text appears in each box it give the same quantity as that coded by the color. Grey indicates FMR is at the intended FMR target level. Light red colors present a security vulnerability to, for example, a passport gate. Each +1 increase in  $\log_{10} \text{FMR}$  corresponds to a factor of 10 increase in FMR. The matrix is not quite symmetric because images in the enrollment and verification sets are different.

**Cross country FMR at threshold T = 66.706 for algorithm megvii\_001, giving  $\text{FMR}(T) = 0.001$  globally.**

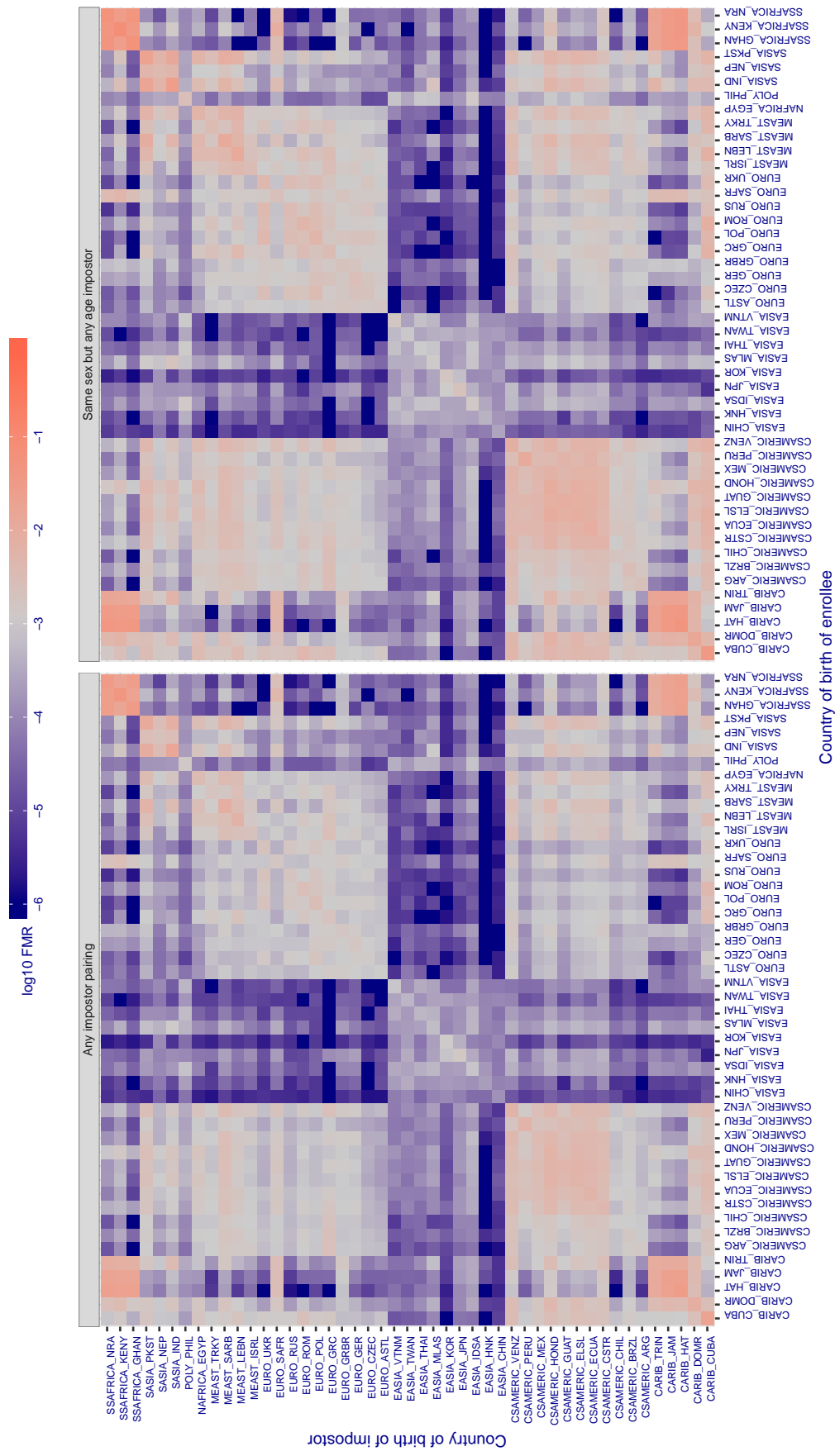


Figure 376: For algorithm megvii-001 operating on visa images, the heatmap shows false match rates observed over impostor comparisons of faces from different individuals who were born in the given country pair. False matches are counted against a recognition threshold fixed globally to give the target  $\text{FMR}$  in the plot title, computed over all on the order of  $10^{10}$  impostor comparisons. If text appears in each box it give the same quantity as that coded by the color. Grey indicates  $\text{FMR}$  is at the intended  $\text{FMR}$  target level. Light red colors present a security vulnerability to, for example, a passport gate. Each +1 increase in  $\log_{10} \text{FMR}$  corresponds to a factor of 10 increase in  $\text{FMR}$ . The matrix is not quite symmetric because images in the enrollment and verification sets are different.

**Cross country FMR at threshold T = 58.026 for algorithm megvii\_002, giving  $\text{FMR}(T) = 0.001$  globally.**

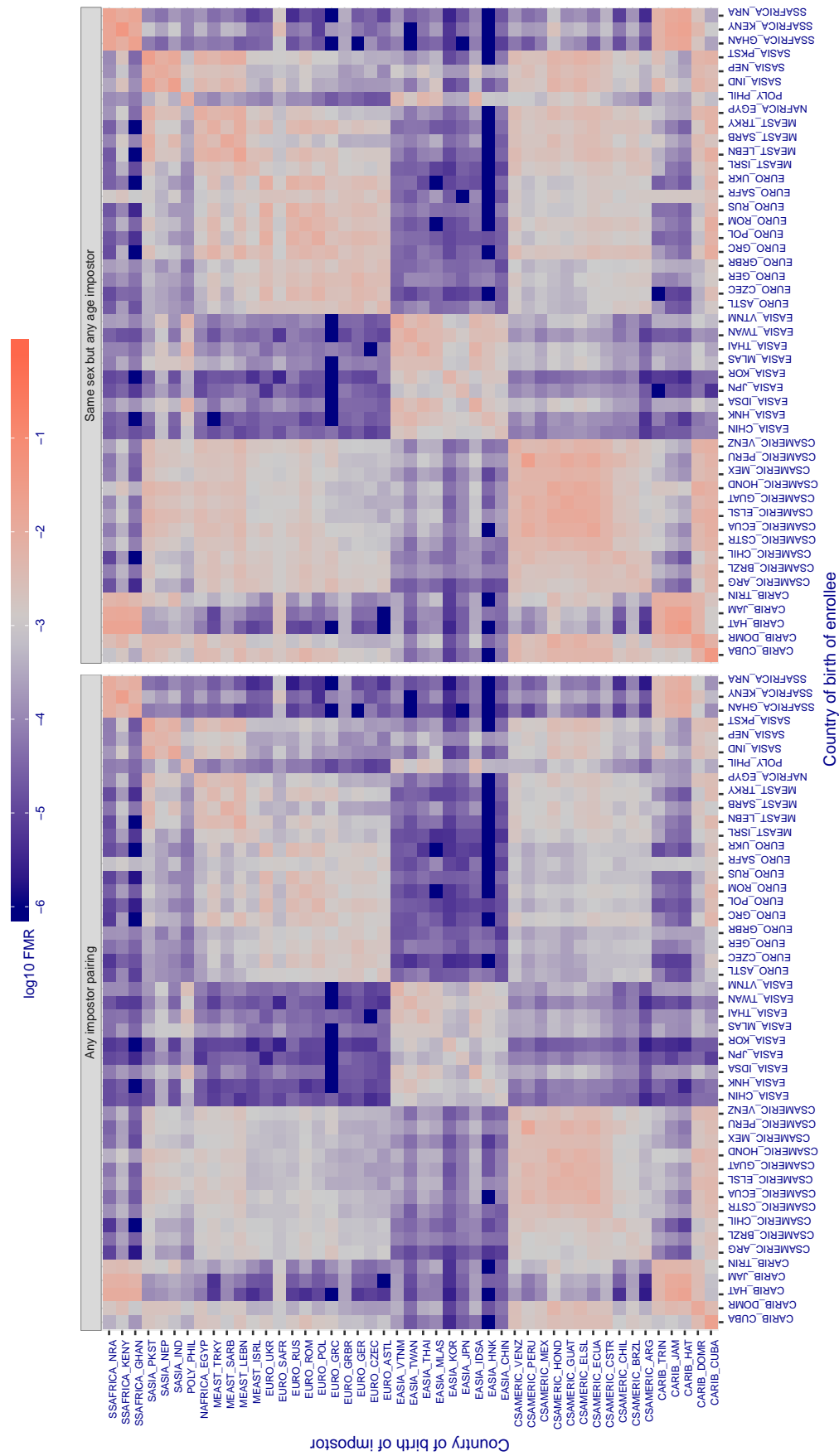


Figure 377: For algorithm megvii-002 operating on visa images, the heatmap shows false match rates observed over impostor comparisons of faces from different individuals who were born in the given country pair. False matches are counted against a recognition threshold fixed globally to give the target  $\text{FMR}$  in the plot title, computed over all on the order of  $10^{10}$  impostor comparisons. If text appears in each box it give the same quantity as that coded by the color. Grey indicates  $\text{FMR}$  is at the intended  $\text{FMR}$  target level. Light red colors present a security vulnerability to, for example, a passport gate. Each +1 increase in  $\log_{10} \text{FMR}$  corresponds to a factor of 10 increase in  $\text{FMR}$ . The matrix is not quite symmetric because images in the enrollment and verification sets are different.

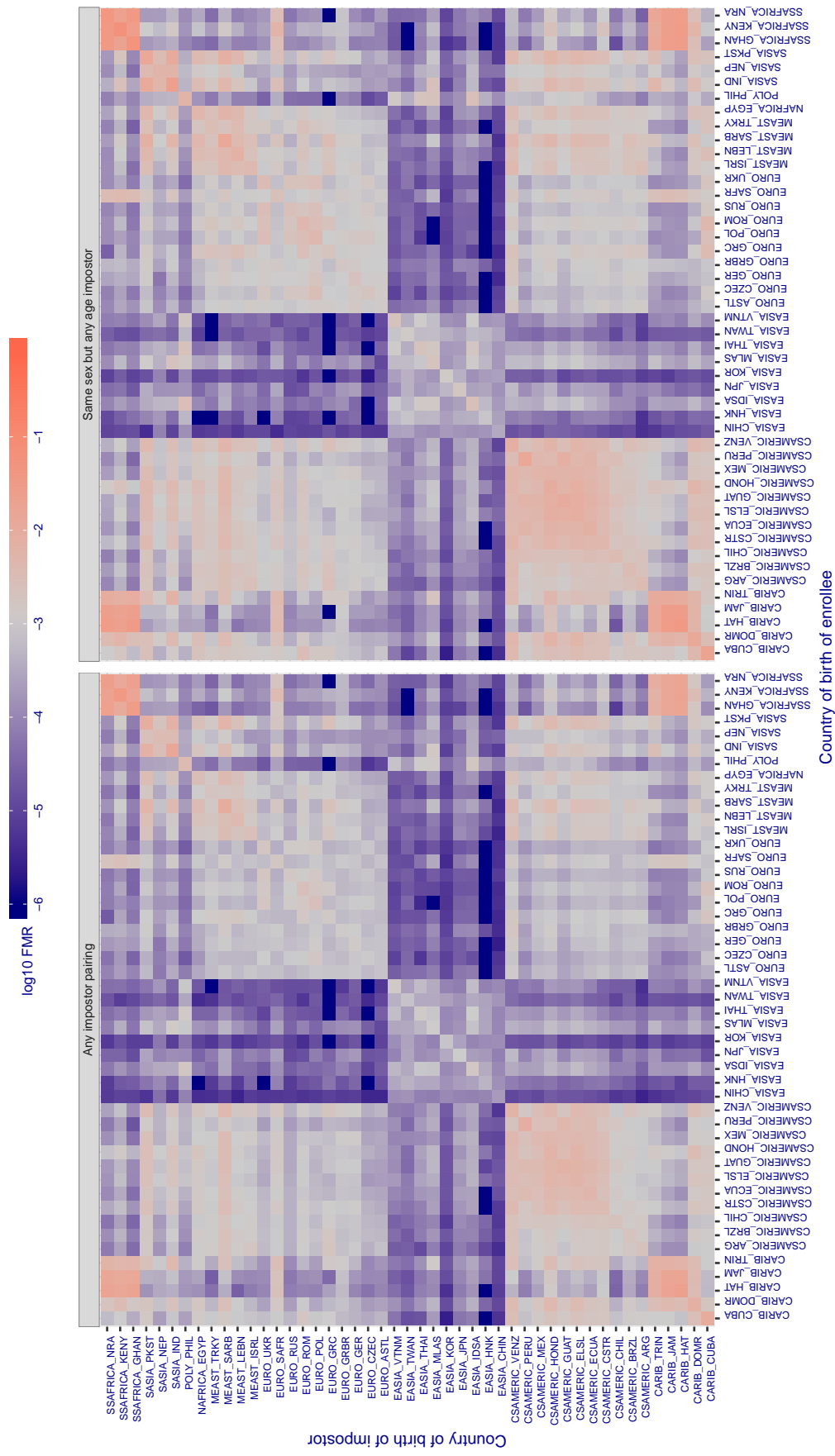
**Cross country FMR at threshold T = 0.345 for algorithm meiya\_001, giving FMR(T) = 0.001 globally.**

Figure 378: For algorithm meiya-001 operating on visa images, the heatmap shows false match rates observed over impostor comparisons of faces from different individuals who were born in the given country pair. False matches are counted against a recognition threshold fixed globally to give the target FMR in the plot title, computed over all on the order of  $10^{10}$  impostor comparisons. If text appears in each box it give the same quantity as that coded by the color. Grey indicates FMR is at the intended FMR target level. Light red colors present a security vulnerability to, for example, a passport gate. Each +1 increase in  $\log_{10} \text{FMR}$  corresponds to a factor of 10 increase in FMR. The matrix is not quite symmetric because images in the enrollment and verification sets are different.

Cross country FMR at threshold T = 0.624 for algorithm microfocus\_001, giving FMR(T) = 0.001 globally.

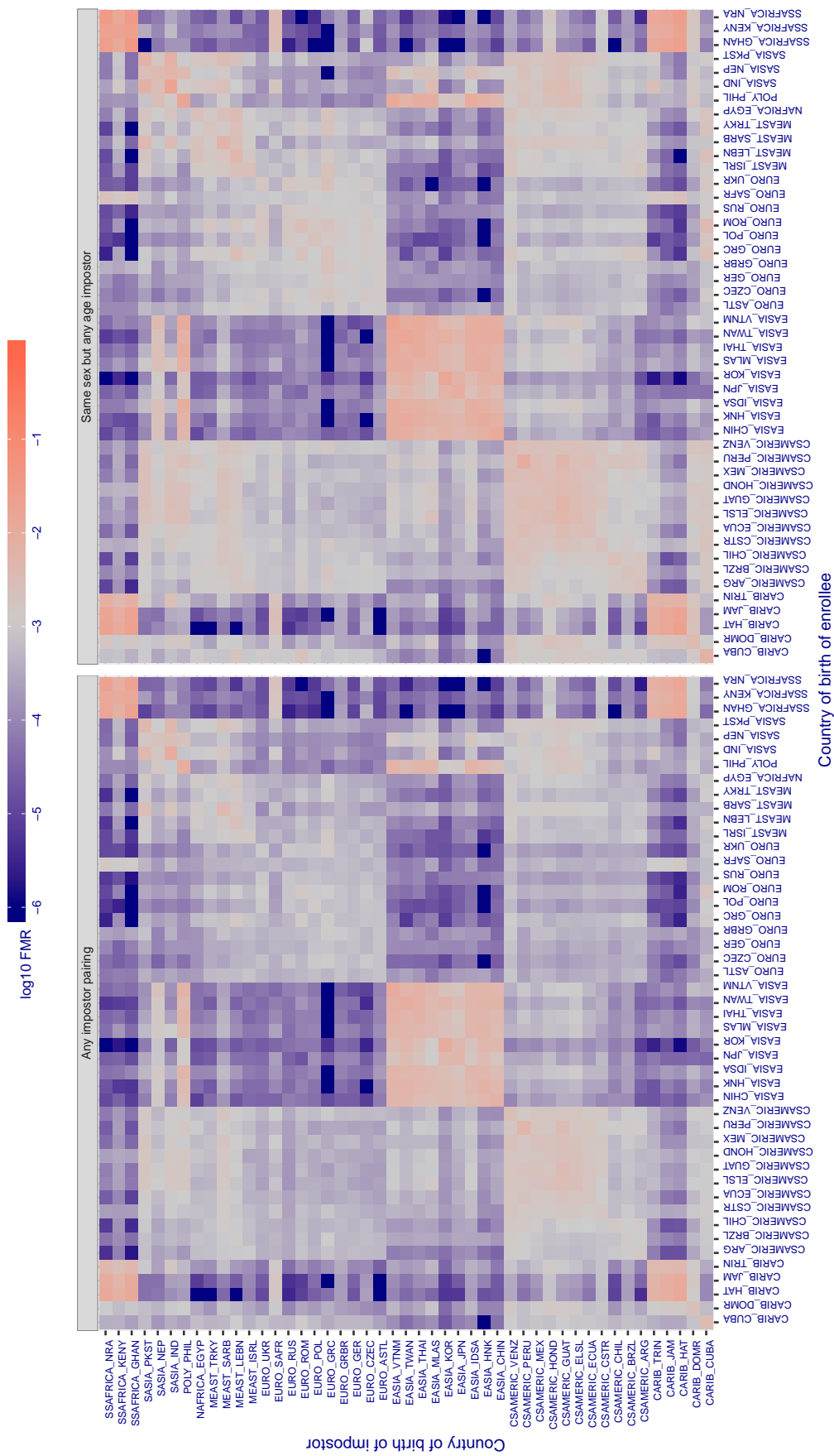


Figure 379: For algorithm microfocus-001 operating on visa images, the heatmap shows false match rates observed over impostor comparisons of faces from different individuals who were born in the given country pair. False matches are counted against a recognition threshold fixed globally to give the target FMR in the plot title, computed over all on the order of  $10^{10}$  impostor comparisons. If text appears in each box it give the same quantity as that coded by the color. Grey indicates FMR is at the intended FMR target level. Light red colors present a security vulnerability to, for example, a passport gate. Each +1 increase in  $\log_{10} FMR$  corresponds to a factor of 10 increase in FMR. The matrix is not quite symmetric because images in the enrollment and verification sets are different.

Cross country FMR at threshold T = 0.542 for algorithm microfocus\_002, giving FMR(T) = 0.001 globally.

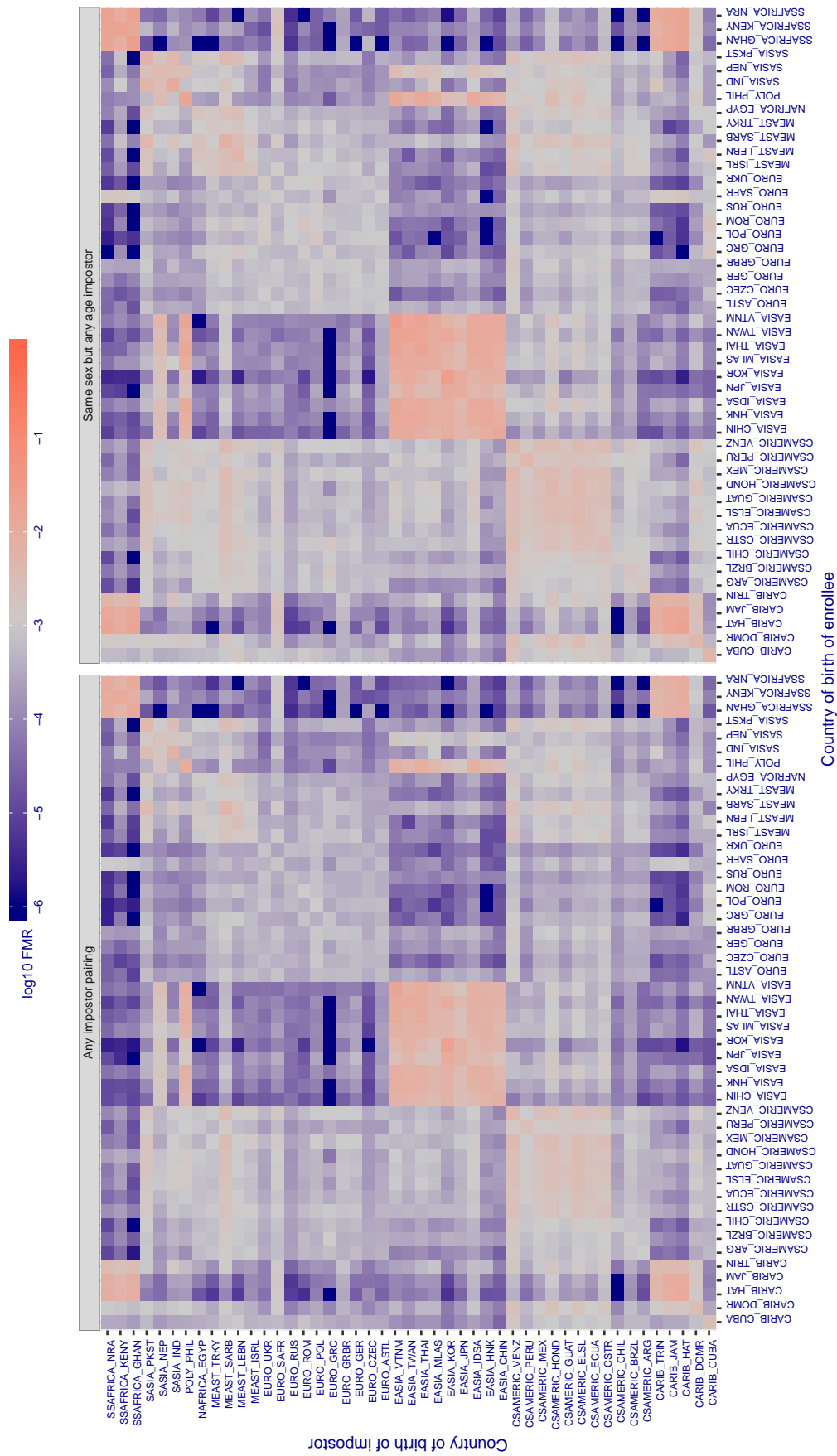


Figure 380: For algorithm microfocus-002 operating on visa images, the heatmap shows false match rates observed over impostor comparisons of faces from different individuals who were born in the given country pair. False matches are counted against a recognition threshold fixed globally to give the target FMR in the plot title, computed over all on the order of  $10^{10}$  impostor comparisons. If text appears in each box it give the same quantity as that coded by the color. Grey indicates FMR is at the intended FMR target level. Light red colors present a security vulnerability to, for example, a passport gate. Each +1 increase in  $\log_{10}$  FMR corresponds to a factor of 10 increase in FMR. The matrix is not quite symmetric because images in the enrollment and verification sets are different.

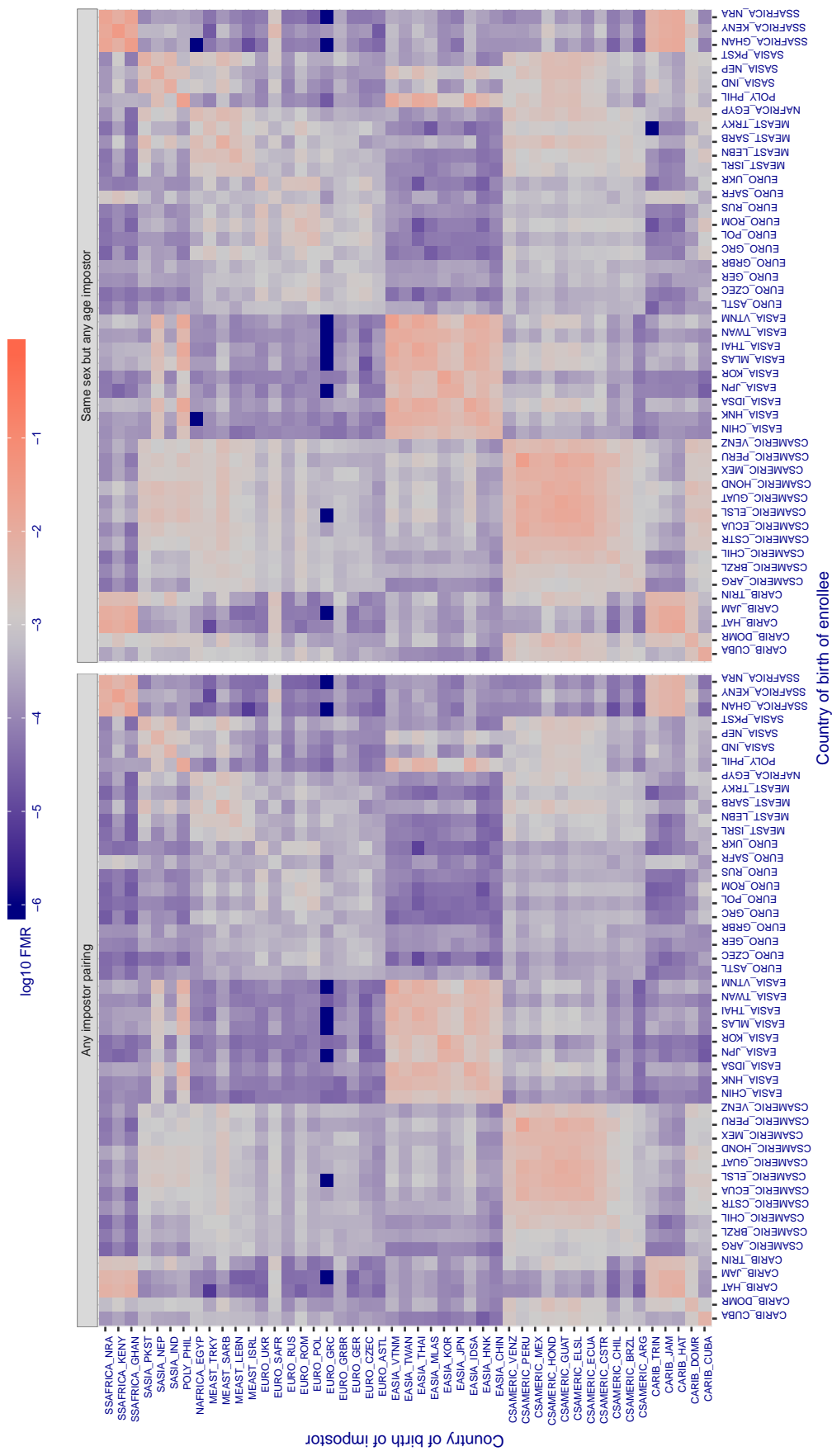
**Cross country FMR at threshold T = 1.310 for algorithm mt\_000, giving  $FMR(T) = 0.001$  globally.**

Figure 381: For algorithm mt-000 operating on visa images, the heatmap shows false match rates observed over impostor comparisons of faces from different individuals who were born in the given country pair. False matches are counted against a recognition threshold fixed globally to give the target FMR in the plot title, computed over all on the order of  $10^{10}$  impostor comparisons. If text appears in each box it give the same quantity as that coded by the color. Grey indicates FMR is at the intended FMR target level. Light red colors present a security vulnerability to, for example, a passport gate. Each +1 increase in  $\log_{10} FMR$  corresponds to a factor of 10 increase in FMR. The matrix is not quite symmetric because images in the enrollment and verification sets are different.

**Cross country FMR at threshold T = 33.449 for algorithm neurotechnology\_005, giving  $\text{FMR}(\text{T}) = 0.001$  globally.**

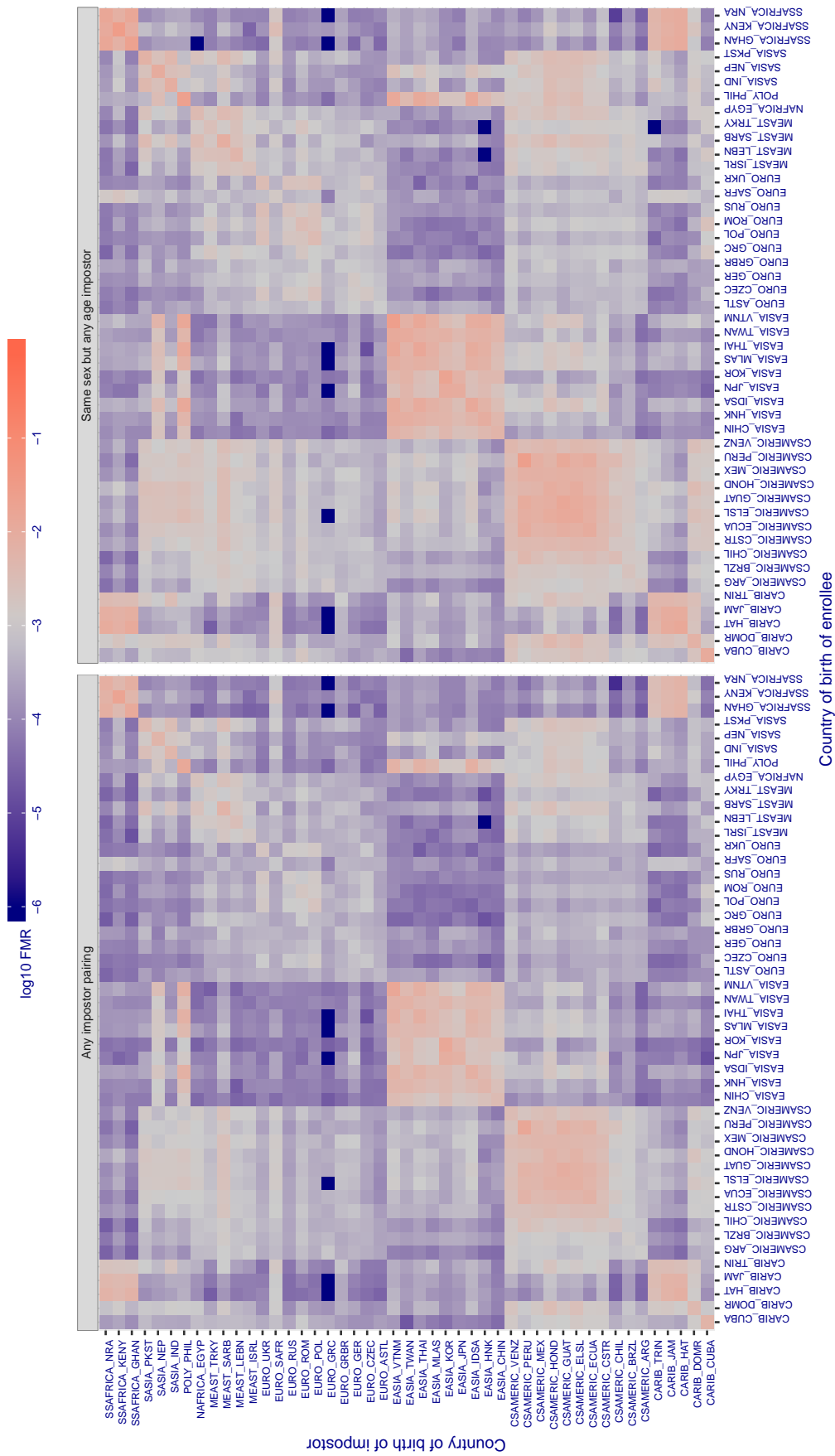


Figure 382: For algorithm neurotechnology-005 operating on visa images, the heatmap shows false match rates observed over impostor comparisons of faces from different individuals who were born in the given country pair. False matches are counted against a recognition threshold fixed globally to give the target  $\text{FMR}$  in the plot title, computed over all on the order of  $10^{10}$  impostor comparisons. If text appears in each box it give the same quantity as that coded by the color. Grey indicates  $\text{FMR}$  is at the intended  $\text{FMR}$  target level. Light red colors present a security vulnerability to, for example, a passport gate. Each +1 increase in  $\log_{10} \text{FMR}$  corresponds to a factor of 10 increase in  $\text{FMR}$ . The matrix is not quite symmetric because images in the enrollment and verification sets are different.

**Cross country FMR at threshold T = 1686.000 for algorithm neurotechnology\_006, giving  $\text{FMR}(\text{T}) = 0.001$  globally.**

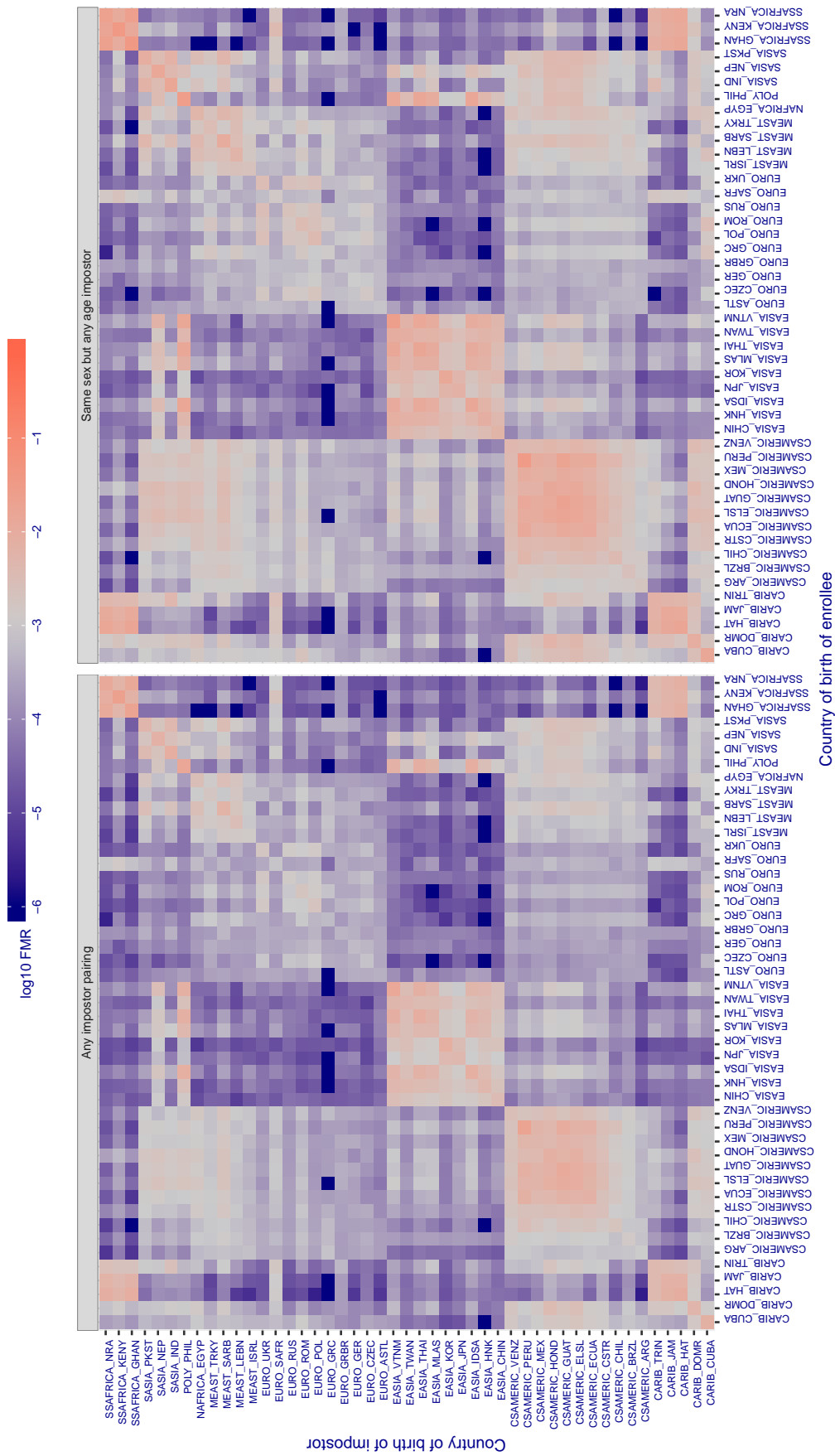


Figure 383: For algorithm neurotechnology-006 operating on visa images, the heatmap shows false match rates observed over impostor comparisons of faces from different individuals who were born in the given country pair. False matches are counted against a recognition threshold fixed globally to give the target  $\text{FMR}$  in the plot title, computed over all on the order of  $10^{10}$  impostor comparisons. If text appears in each box it give the same quantity as that coded by the color. Grey indicates  $\text{FMR}$  is at the intended  $\text{FMR}$  target level. Light red colors present a security vulnerability to, for example, a passport gate. Each +1 increase in  $\log_{10} \text{FMR}$  corresponds to a factor of 10 increase in  $\text{FMR}$ . The matrix is not quite symmetric because images in the enrollment and verification sets are different.

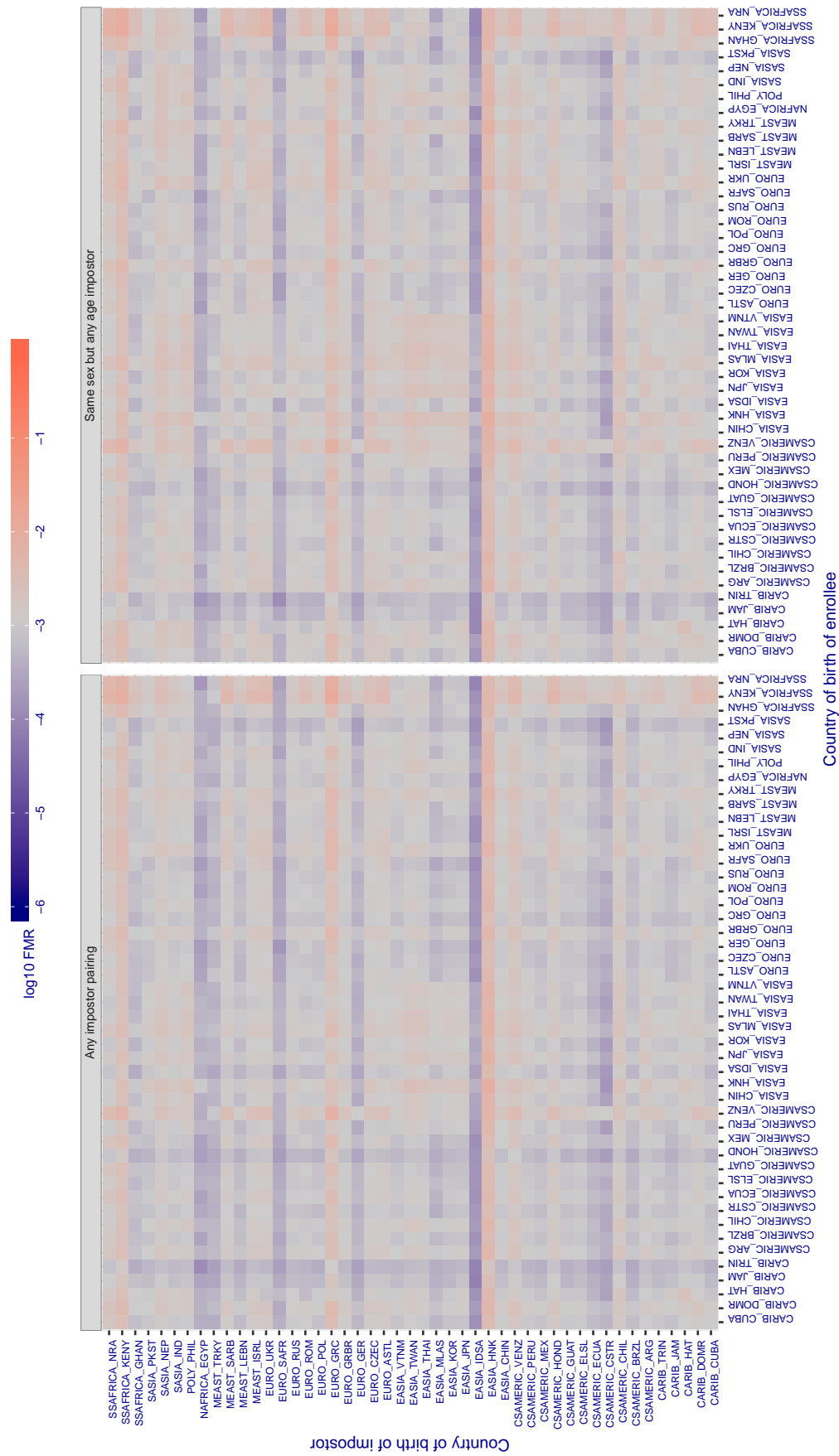
**Cross country FMR at threshold T = 0.693 for algorithm nodeflux\_001, giving FMR(T) = 0.001 globally.**

Figure 384: For algorithm nodeflux-001 operating on visa images, the heatmap shows false match rates observed over impostor comparisons of faces from different individuals who were born in the given country pair. False matches are counted against a recognition threshold fixed globally to give the target FMR in the plot title, computed over all on the order of  $10^{10}$  impostor comparisons. If text appears in each box it give the same quantity as that coded by the color. Grey indicates FMR is at the intended FMR target level. Light red colors present a security vulnerability to, for example, a passport gate. Each +1 increase in  $\log_{10} \text{FMR}$  corresponds to a factor of 10 increase in FMR. The matrix is not quite symmetric because images in the enrollment and verification sets are different.

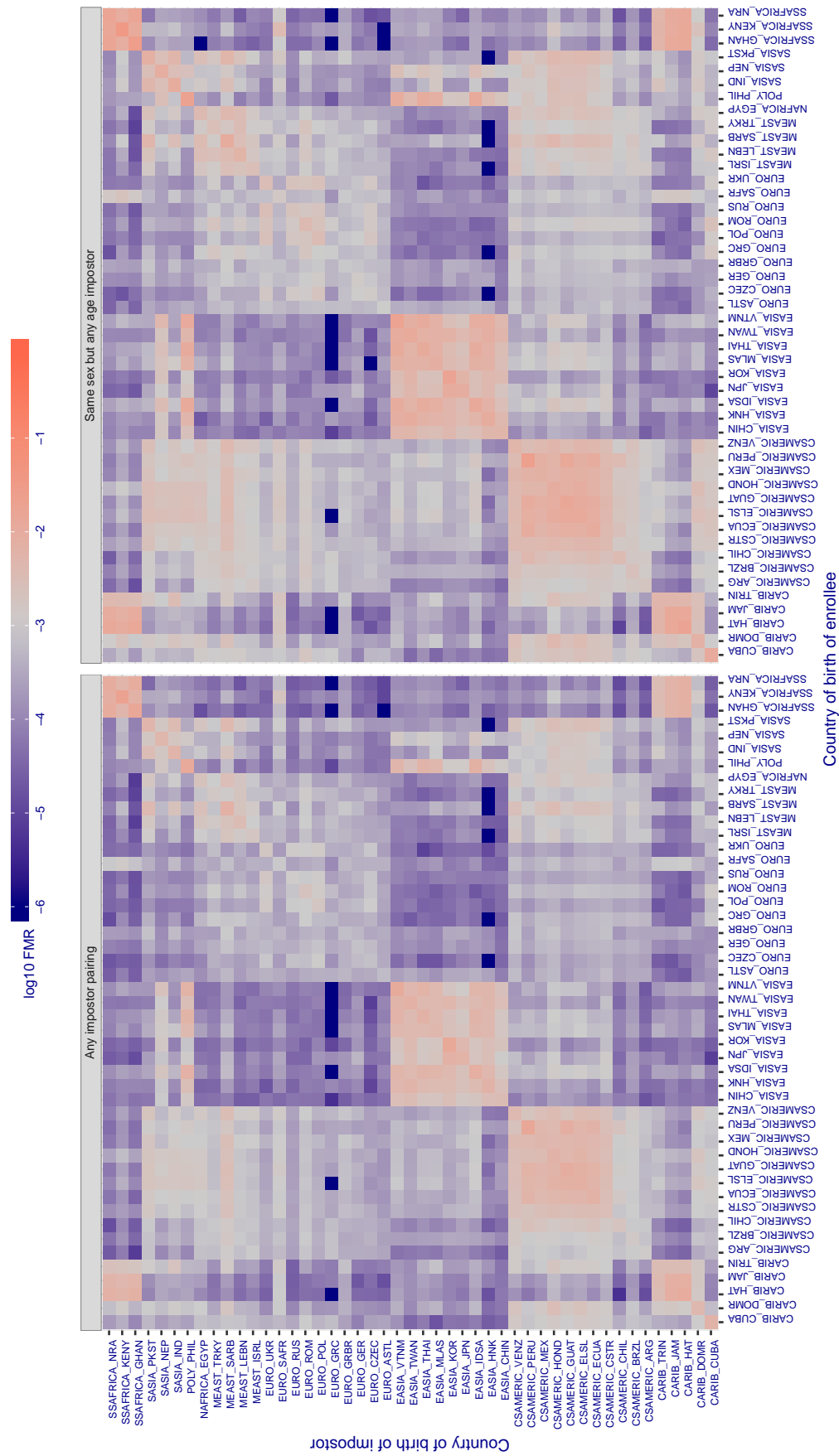
**Cross country FMR at threshold T = 0.420 for algorithm nodeflux\_002, giving FMR(T) = 0.001 globally.**

Figure 385: For algorithm nodeflux-002 operating on visa images, the heatmap shows false match rates observed over impostor comparisons of faces from different individuals who were born in the given country pair. False matches are counted against a recognition threshold fixed globally to give the target FMR in the plot title, computed over all on the order of  $10^{10}$  impostor comparisons. If text appears in each box it give the same quantity as that coded by the color. Grey indicates FMR is at the intended FMR target level. Light red colors present a security vulnerability to, for example, a passport gate. Each +1 increase in  $\log_{10} \text{FMR}$  corresponds to a factor of 10 increase in FMR. The matrix is not quite symmetric because images in the enrollment and verification sets are different.

Cross country FMR at threshold T = 1338139146338239954308032998197392108861073498206667481318591787294160965343825654106876

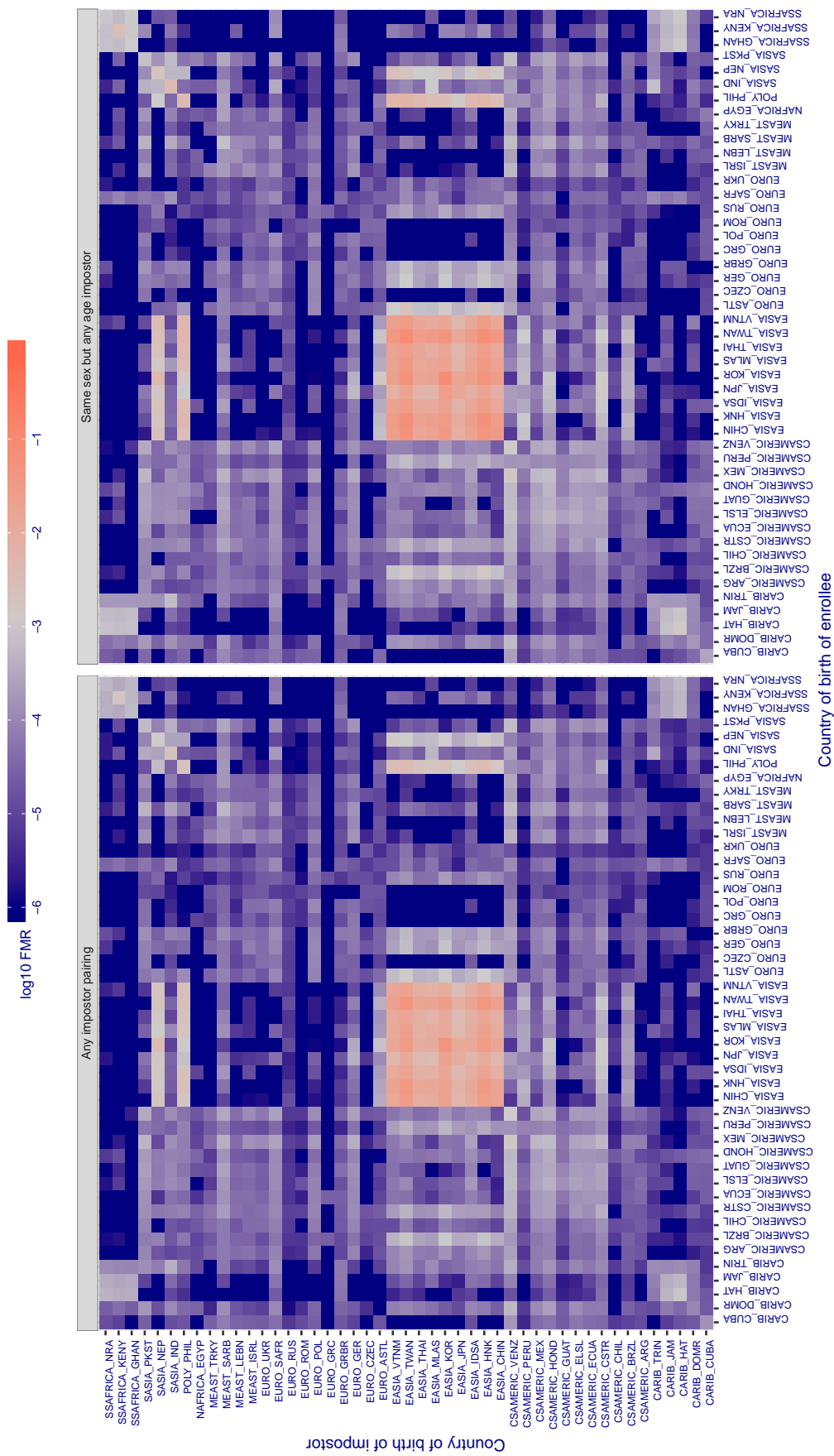


Figure 386: For algorithm notiontag-000 operating on visa images, the heatmap shows false match rates observed over impostor comparisons of faces from different individuals who were born in the given country pair. False matches are counted against a recognition threshold fixed globally to give the target FMR in the plot title, computed over all on the order of  $10^{10}$  impostor comparisons. If text appears in each box it give the same quantity as that coded by the color. Grey indicates FMR is at the intended FMR target level. Light red colors present a security vulnerability to, for example, a passport gate. Each +1 increase in  $\log_{10} \text{FMR}$  corresponds to a factor of 10 increase in FMR. The matrix is not quite symmetric because images in the enrollment and verification sets are different.

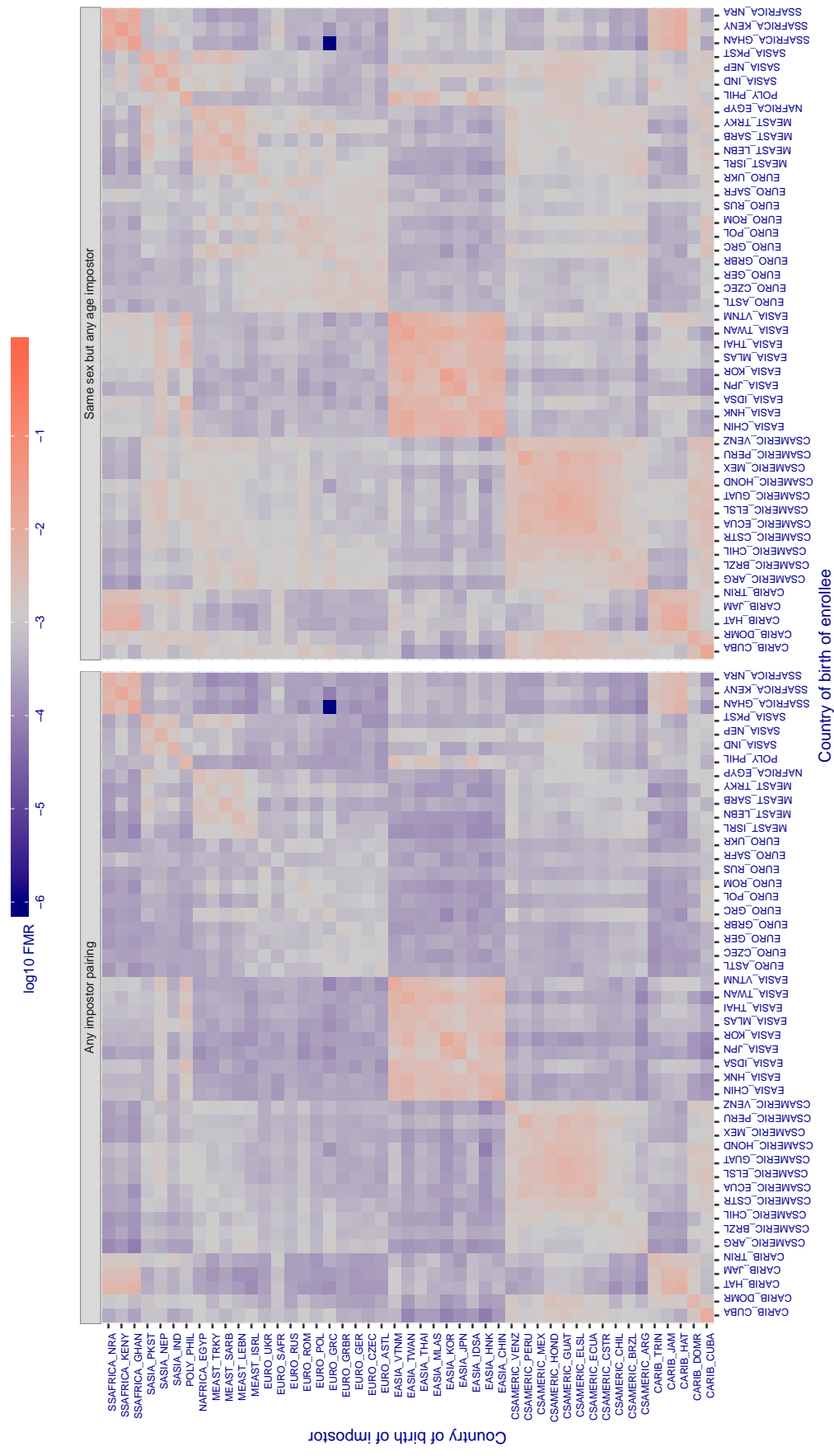
**Cross country FMR at threshold T = 1.929 for algorithm ntechlab\_006, giving  $\text{FMR}(\text{T}) = 0.001$  globally.**

Figure 387: For algorithm ntechlab-006 operating on visa images, the heatmap shows false match rates observed over impostor comparisons of faces from different individuals who were born in the given country pair. False matches are counted against a recognition threshold fixed globally to give the target  $\text{FMR}$  in the plot title, computed over all on the order of  $10^{10}$  impostor comparisons. If text appears in each box it give the same quantity as that coded by the color. Grey indicates  $\text{FMR}$  is at the intended  $\text{FMR}$  target level. Light red colors present a security vulnerability to, for example, a passport gate. Each +1 increase in  $\log_{10} \text{FMR}$  corresponds to a factor of 10 increase in  $\text{FMR}$ . The matrix is not quite symmetric because images in the enrollment and verification sets are different.

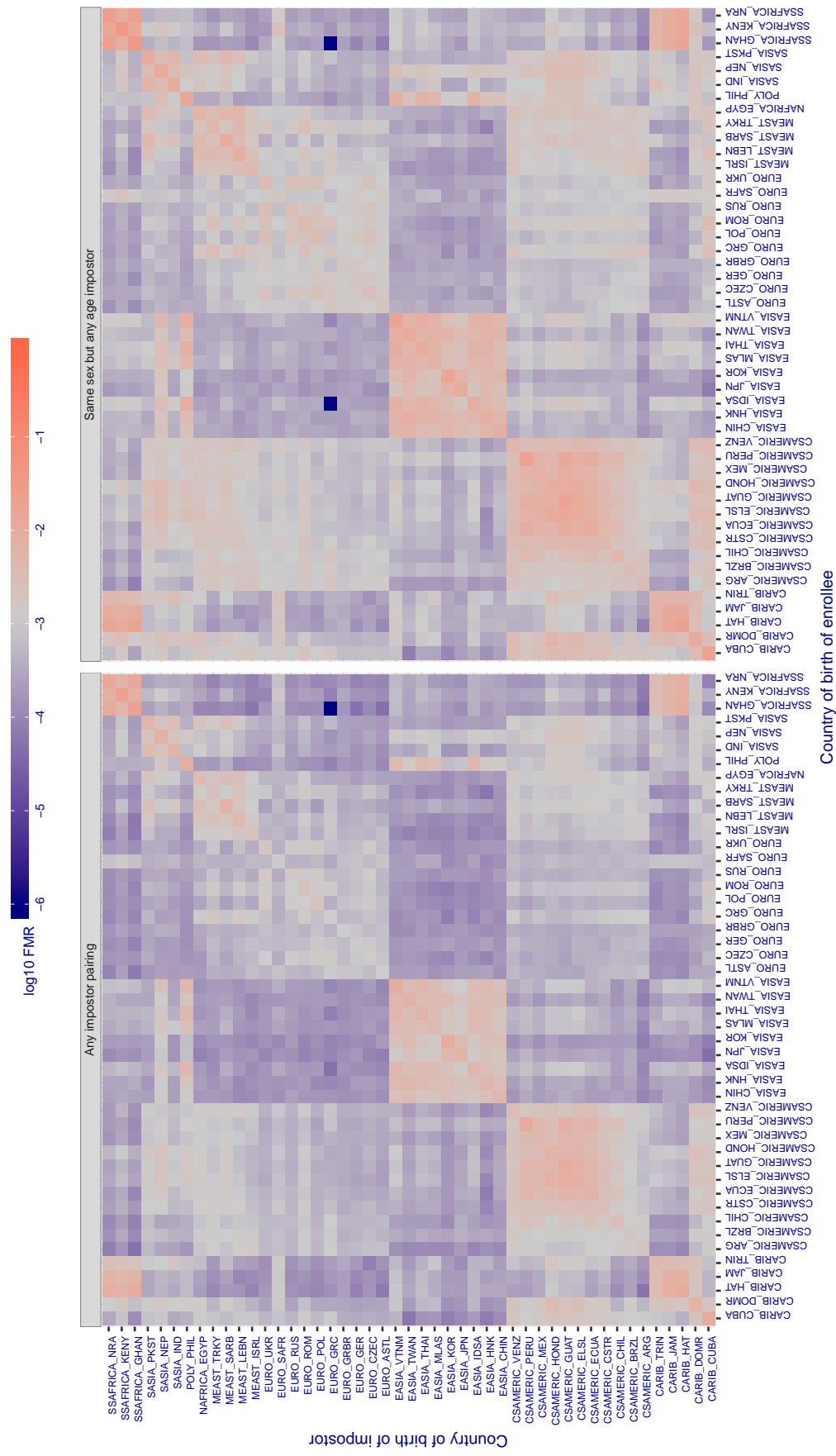
Cross country FMR at threshold T = 1.319 for algorithm ntechlab\_007, giving  $FMR(T) = 0.001$  globally.

Figure 388: For algorithm ntechlab-007 operating on visa images, the heatmap shows false match rates observed over impostor comparisons of faces from different individuals who were born in the given country pair. False matches are counted against a recognition threshold fixed globally to give the target FMR in the plot title, computed over all on the order of  $10^{10}$  impostor comparisons. If text appears in each box it give the same quantity as that coded by the color. Grey indicates FMR is at the intended FMR target level. Light red colors present a security vulnerability to, for example, a passport gate. Each +1 increase in  $\log_{10} FMR$  corresponds to a factor of 10 increase in FMR. The matrix is not quite symmetric because images in the enrollment and verification sets are different.

**Cross country FMR at threshold T = 0.334 for algorithm pixelall\_002, giving  $\text{FMR}(\text{T}) = 0.001$  globally.**

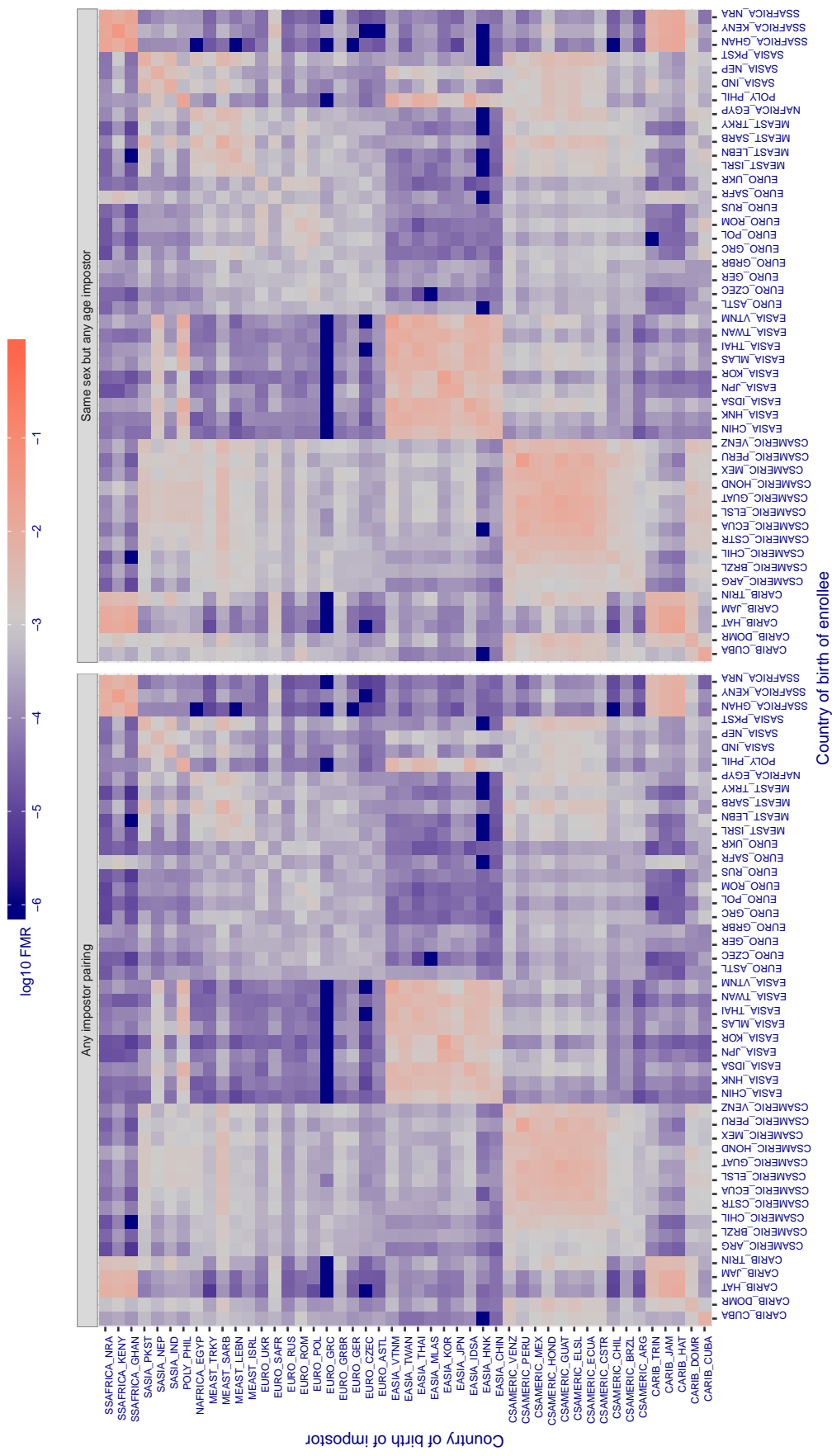


Figure 389: For algorithm pixelall-002 operating on visa images, the heatmap shows false match rates observed over impostor comparisons of faces from different individuals who were born in the given country pair. False matches are counted against a recognition threshold fixed globally to give the target  $\text{FMR}$  in the plot title, computed over all on the order of  $10^{10}$  impostor comparisons. If text appears in each box it give the same quantity as that coded by the color. Grey indicates  $\text{FMR}$  is at the intended  $\text{FMR}$  target level. Light red colors present a security vulnerability to, for example, a passport gate. Each +1 increase in  $\log_{10} \text{FMR}$  corresponds to a factor of 10 increase in  $\text{FMR}$ . The matrix is not quite symmetric because images in the enrollment and verification sets are different.

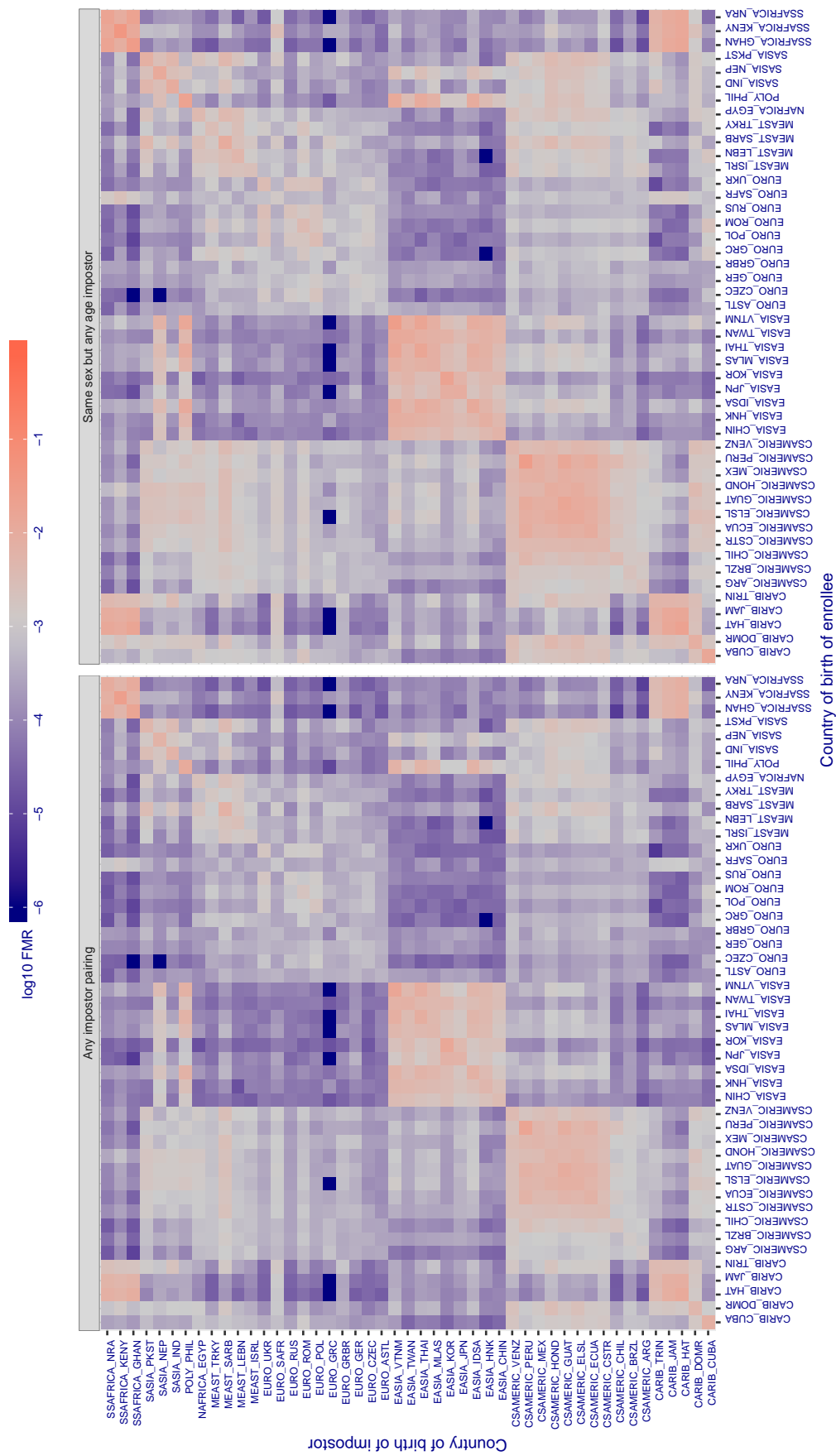
**Cross country FMR at threshold T = 0.272 for algorithm psl\_002, giving FMR(T) = 0.001 globally.**

Figure 390: For algorithm psl\_002 operating on visa images, the heatmap shows false match rates observed over impostor comparisons of faces from different individuals who were born in the given country pair. False matches are counted against a recognition threshold fixed globally to give the target FMR in the plot title, computed over all on the order of  $10^{10}$  impostor comparisons. If text appears in each box it give the same quantity as that coded by the color. Grey indicates FMR is at the intended FMR target level. Light red colors present a security vulnerability to, for example, a passport gate. Each +1 increase in  $\log_{10} \text{FMR}$  corresponds to a factor of 10 increase in FMR. The matrix is not quite symmetric because images in the enrollment and verification sets are different.

Cross country FMR at threshold T = 0.613 for algorithm rankone\_006, giving  $\text{FMR}(\text{T}) = 0.001$  globally.

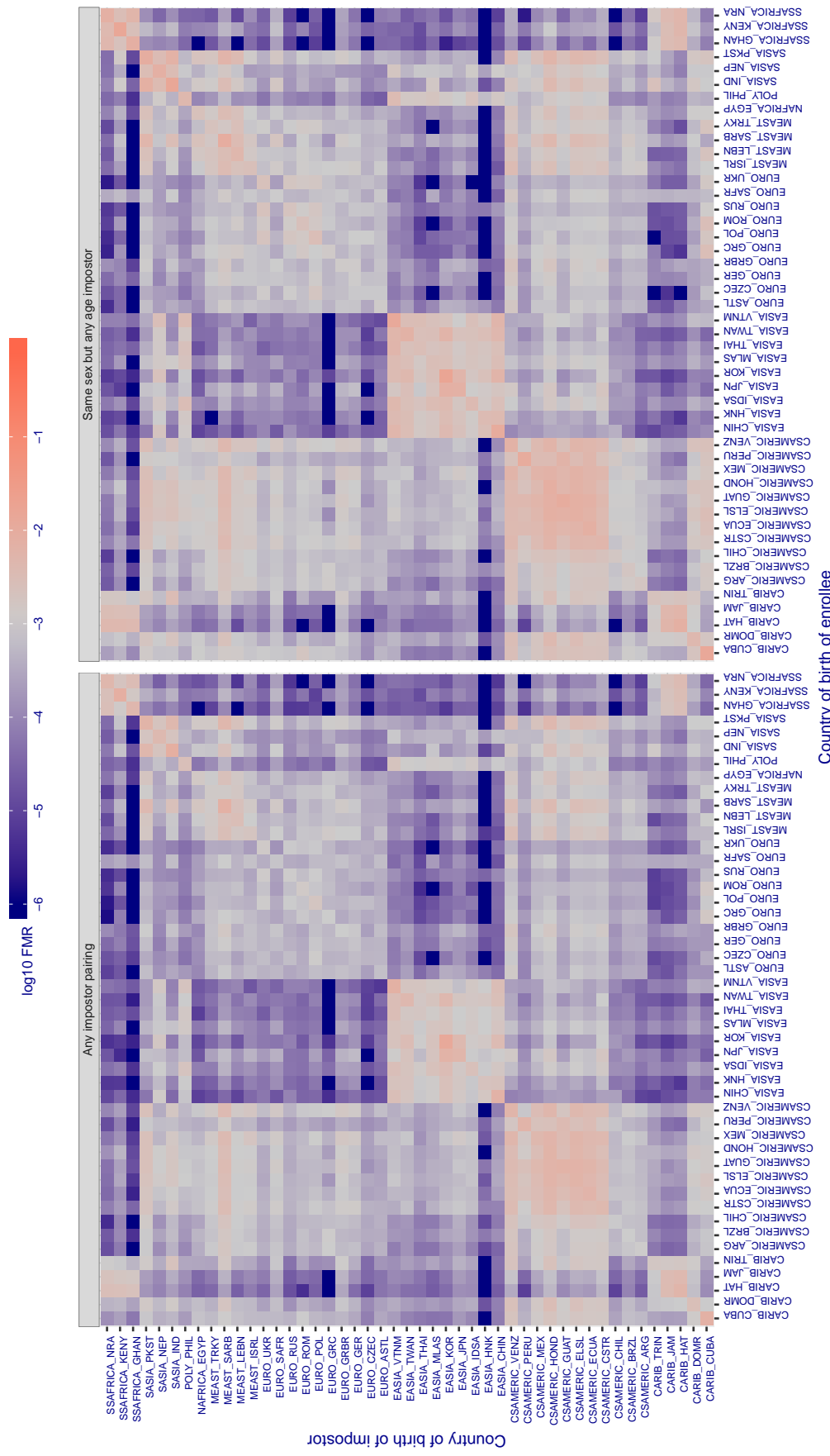


Figure 391: For algorithm rankone-006 operating on visa images, the heatmap shows false match rates observed over impostor comparisons of faces from different individuals who were born in the given country pair. False matches are counted against a recognition threshold fixed globally to give the target  $\text{FMR}$  in the plot title, computed over all on the order of  $10^{10}$  impostor comparisons. If text appears in each box it give the same quantity as that coded by the color. Grey indicates  $\text{FMR}$  is at the intended  $\text{FMR}$  target level. Light red colors present a security vulnerability to, for example, a passport gate. Each +1 increase in  $\log_{10} \text{FMR}$  corresponds to a factor of 10 increase in  $\text{FMR}$ . The matrix is not quite symmetric because images in the enrollment and verification sets are different.

**Cross country FMR at threshold T = 0.536 for algorithm rankone\_007, giving  $\text{FMR}(\text{T}) = 0.001$  globally.**

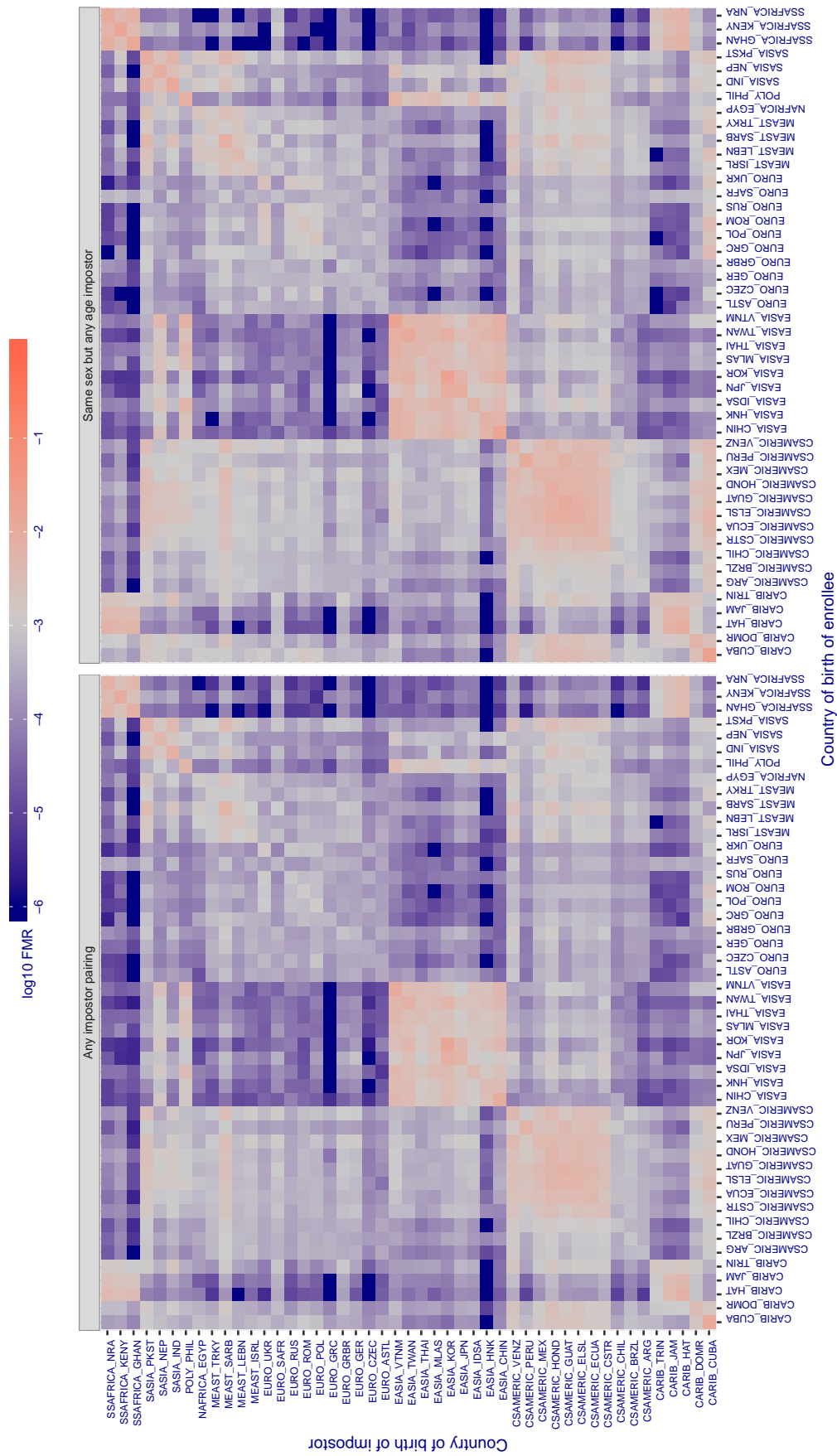


Figure 392: For algorithm rankone-007 operating on visa images, the heatmap shows false match rates observed over impostor comparisons of faces from different individuals who were born in the given country pair. False matches are counted against a recognition threshold fixed globally to give the target  $\text{FMR}$  in the plot title, computed over all on the order of  $10^{10}$  impostor comparisons. If text appears in each box it give the same quantity as that coded by the color. Grey indicates  $\text{FMR}$  is at the intended  $\text{FMR}$  target level. Light red colors present a security vulnerability to, for example, a passport gate. Each +1 increase in  $\log_{10} \text{FMR}$  corresponds to a factor of 10 increase in  $\text{FMR}$ . The matrix is not quite symmetric because images in the enrollment and verification sets are different.

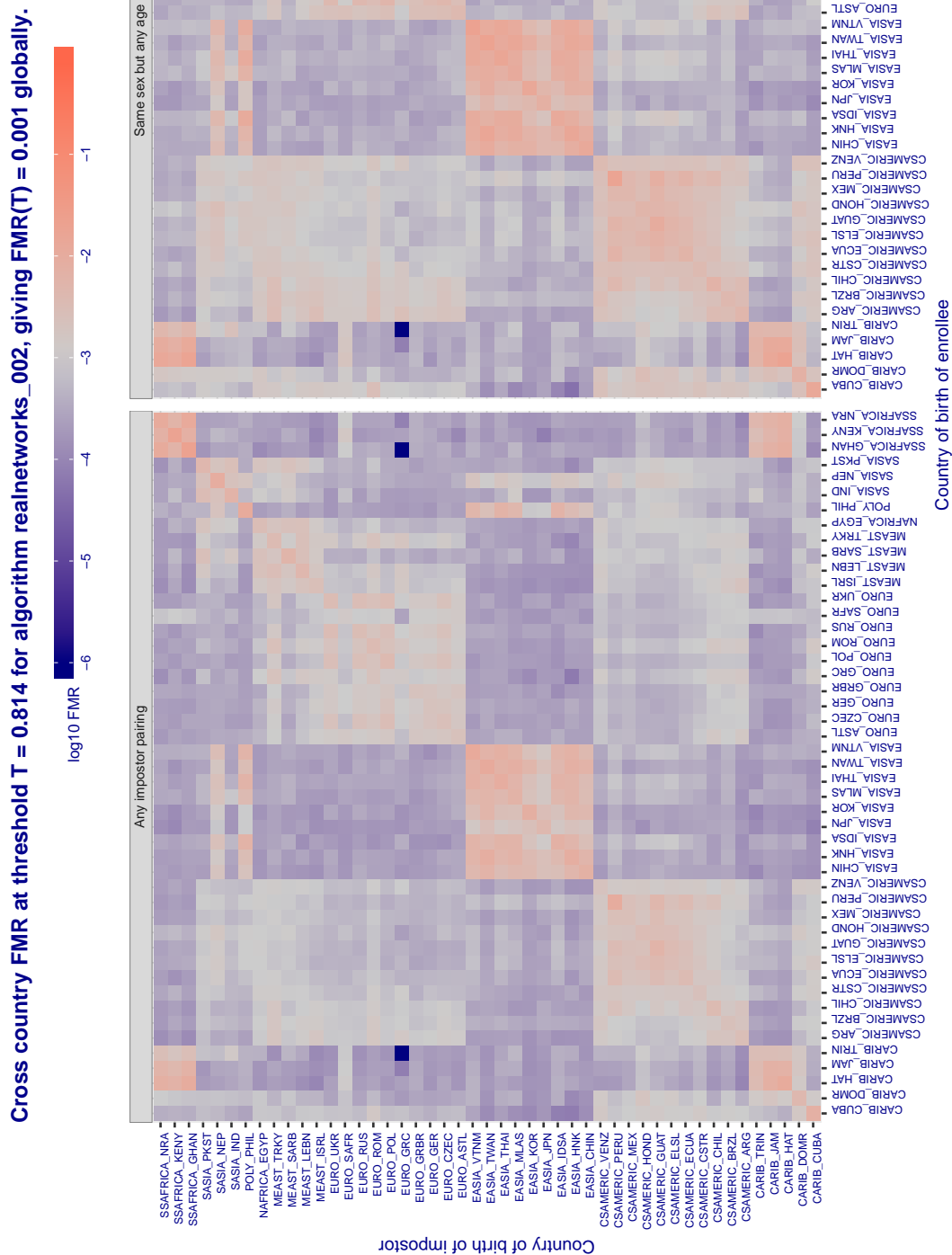


Figure 393: For algorithm realnetworks-002 operating on visa images, the heatmap shows false match rates observed over impostor comparisons of faces from different individuals who were born in the given country pair. False matches are counted against a recognition threshold fixed globally to give the target FMR in the plot title, computed over all on the order of  $10^{10}$  impostor comparisons. If text appears in each box it give the same quantity as that coded by the color. Grey indicates FMR is at the intended FMR target level. Light red colors present a security vulnerability to, for example, a passport gate. Each +1 increase in  $\log_{10} \text{FMR}$  corresponds to a factor of 10 increase in FMR. The matrix is not quite symmetric because images in the enrollment and verification sets are different.

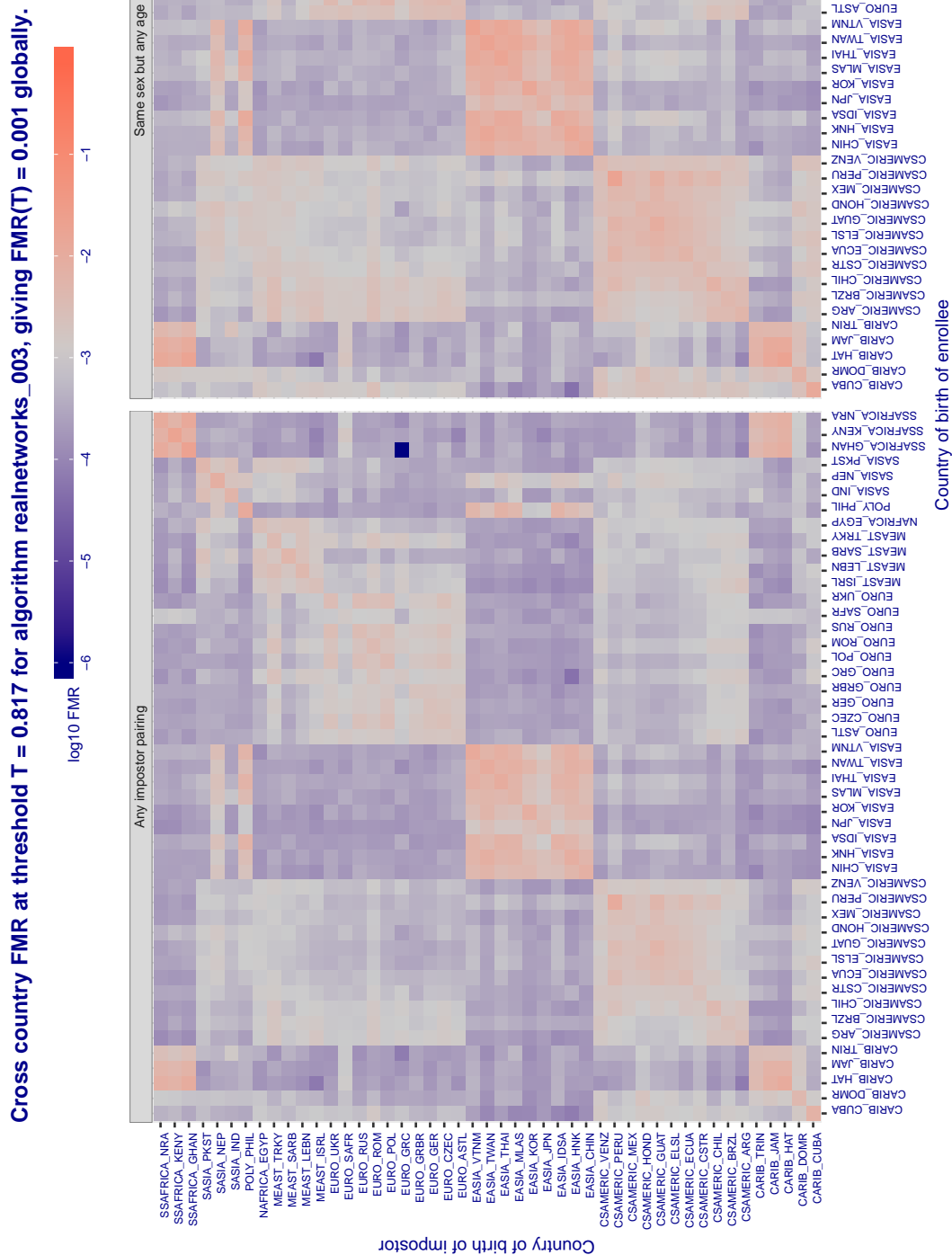


Figure 394: For algorithm *realnetworks-003* operating on visa images, the heatmap shows false match rates observed over impostor comparisons of faces from different individuals who were born in the given country pair. False matches are counted against a recognition threshold fixed globally to give the target  $\text{FMR}$  in the plot title, computed over all on the order of  $10^{10}$  impostor comparisons. If text appears in each box it give the same quantity as that coded by the color. Grey indicates  $\text{FMR}$  is at the intended  $\text{FMR}$  target level. Light red colors present a security vulnerability to, for example, a passport gate. Each +1 increase in  $\log_{10} \text{FMR}$  corresponds to a factor of 10 increase in  $\text{FMR}$ . The matrix is not quite symmetric because images in the enrollment and verification sets are different.

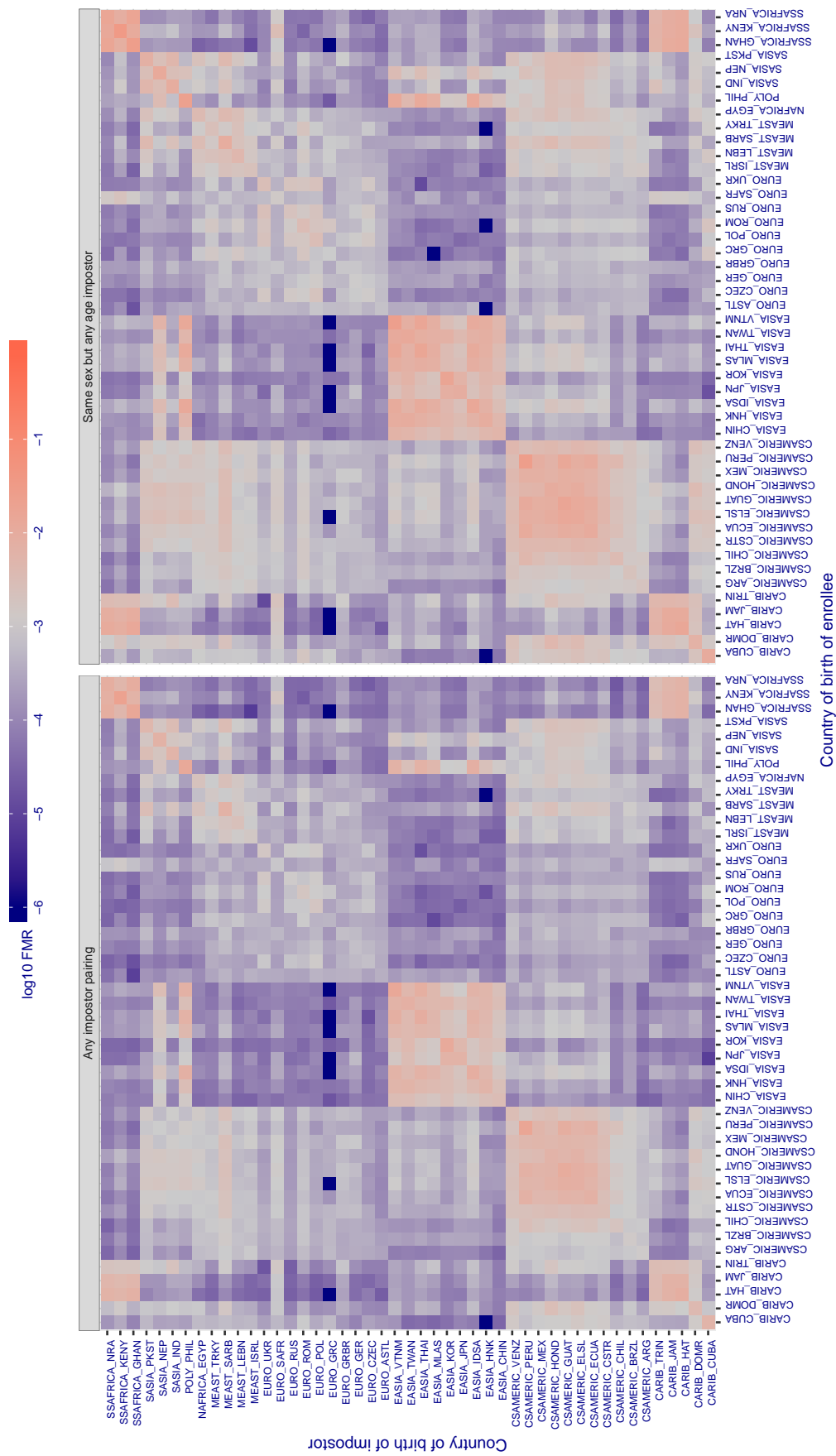
**Cross country FMR at threshold T = 65.920 for algorithm remarkai\_000, giving FMR(T) = 0.001 globally.**

Figure 395: For algorithm remarkai-000 operating on visa images, the heatmap shows false match rates observed over impostor comparisons of faces from different individuals who were born in the given country pair. False matches are counted against a recognition threshold fixed globally to give the target FMR in the plot title, computed over all on the order of  $10^{10}$  impostor comparisons. If text appears in each box it give the same quantity as that coded by the color. Grey indicates FMR is at the intended FMR target level. Light red colors present a security vulnerability to, for example, a passport gate. Each +1 increase in  $\log_{10} FMR$  corresponds to a factor of 10 increase in FMR. The matrix is not quite symmetric because images in the enrollment and verification sets are different.

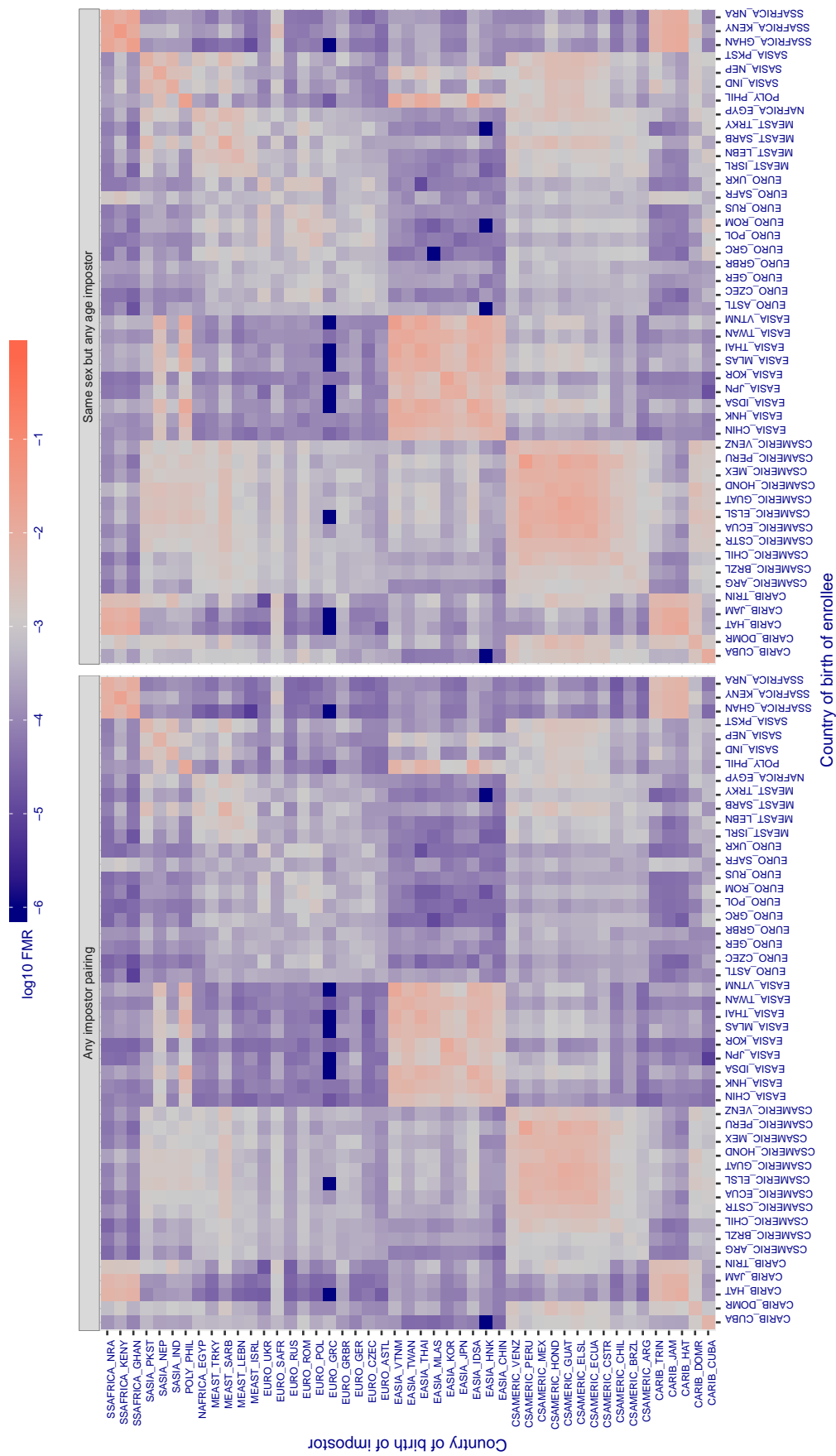
**Cross country FMR at threshold T = 65.928 for algorithm remarkai\_001, giving FMR(T) = 0.001 globally.**

Figure 396: For algorithm remarkai-001 operating on visa images, the heatmap shows false match rates observed over impostor comparisons of faces from different individuals who were born in the given country pair. False matches are counted against a recognition threshold fixed globally to give the target FMR in the plot title, computed over all on the order of  $10^{10}$  impostor comparisons. If text appears in each box it give the same quantity as that coded by the color. Grey indicates FMR is at the intended FMR target level. Light red colors present a security vulnerability to, for example, a passport gate. Each +1 increase in  $\log_{10} \text{FMR}$  corresponds to a factor of 10 increase in FMR. The matrix is not quite symmetric because images in the enrollment and verification sets are different.

**Cross country FMR at threshold T = 0.624 for algorithm rokid\_000, giving  $FMR(T) = 0.001$  globally.**

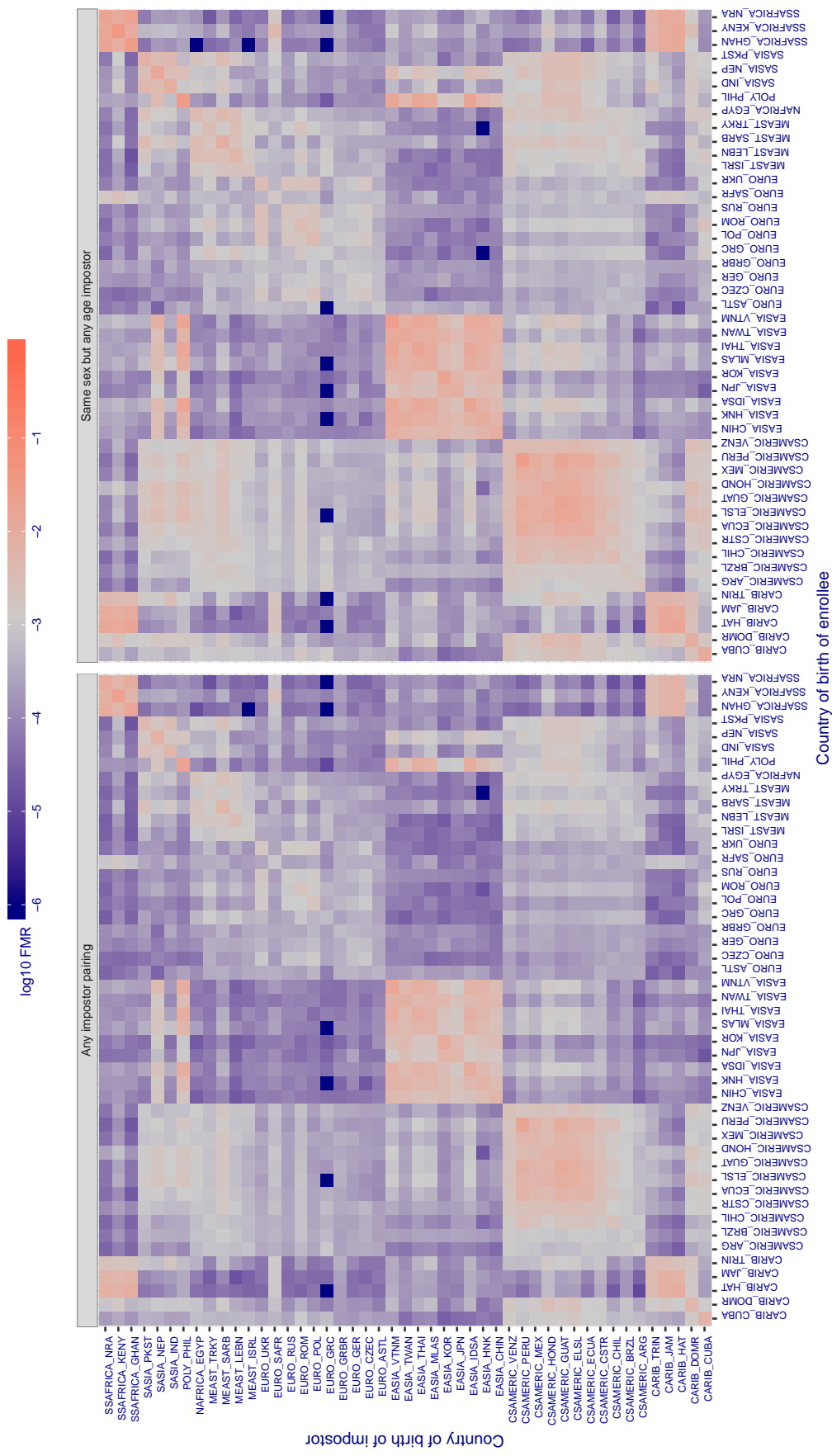


Figure 397: For algorithm rokid-000 operating on visa images, the heatmap shows false match rates observed over impostor comparisons of faces from different individuals who were born in the given country pair. False matches are counted against a recognition threshold fixed globally to give the target FMR in the plot title, computed over all on the order of  $10^{10}$  impostor comparisons. If text appears in each box it give the same quantity as that coded by the color. Grey indicates FMR is at the intended FMR target level. Light red colors present a security vulnerability to, for example, a passport gate. Each +1 increase in  $\log_{10} FMR$  corresponds to a factor of 10 increase in FMR. The matrix is not quite symmetric because images in the enrollment and verification sets are different.

Cross country FMR at threshold T = 0.609 for algorithm safe\_001, giving  $\text{FMR}(\text{T}) = 0.001$  globally.

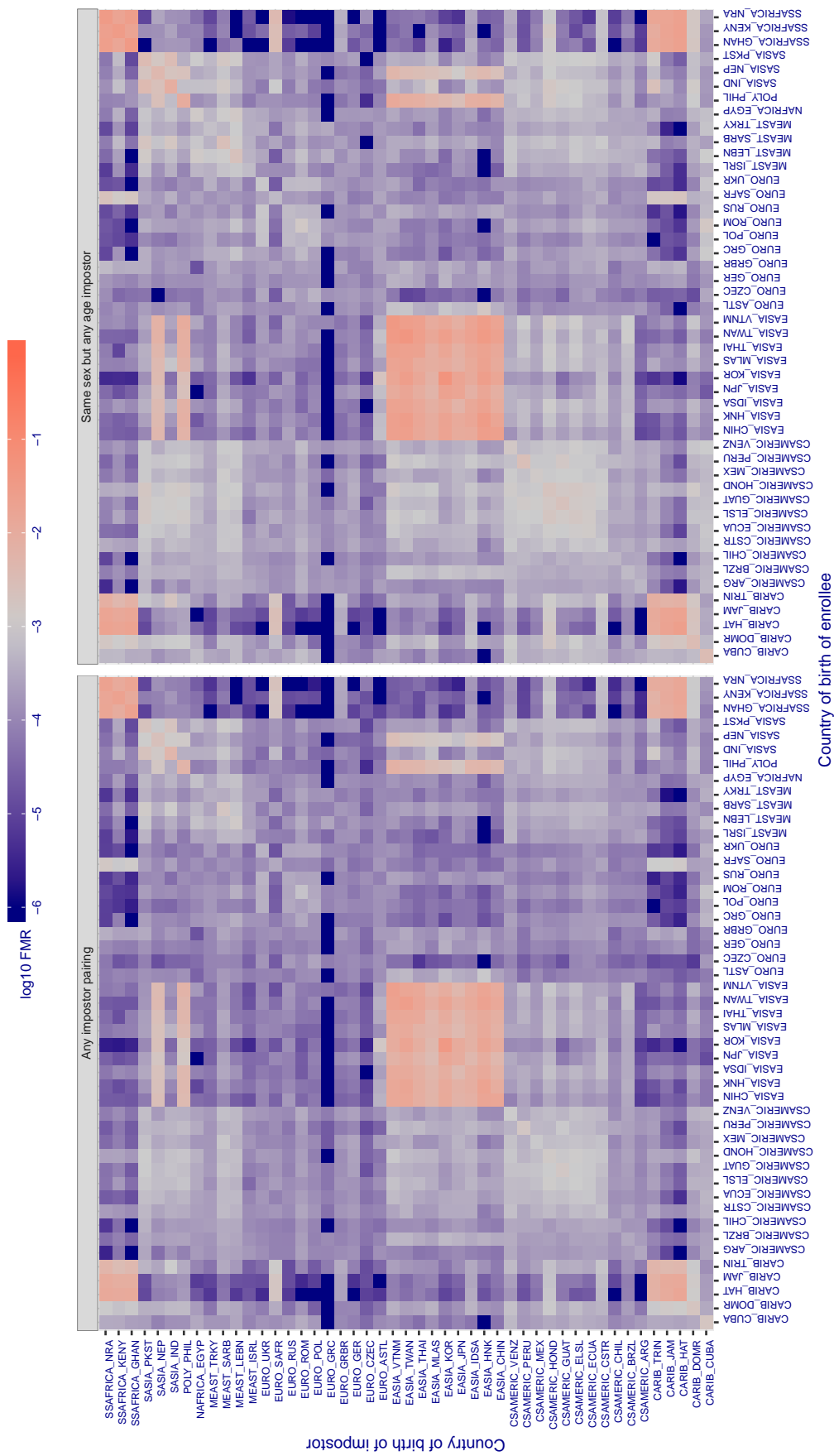


Figure 38: For algorithm safe-001 operating on visa images, the heatmap shows false match rates observed over impostor comparisons of faces from different individuals who were born in the given country pair. False matches are counted against a recognition threshold fixed globally to give the target FMR in the plot title, computed over all on the order of  $10^{10}$  impostor comparisons. If text appears in each box it give the same quantity as that coded by the color. Grey indicates FMR is at the intended FMR target level. Light red colors present a security vulnerability to, for example, a passport gate. Each +1 increase in  $\log_{10} \text{FMR}$  corresponds to a factor of 10 increase in FMR. The matrix is not quite symmetric because images in the enrollment and verification sets are different.

Cross country FMR at threshold T = 0.295 for algorithm safe\_002, giving  $\text{FMR}(T) = 0.001$  globally.

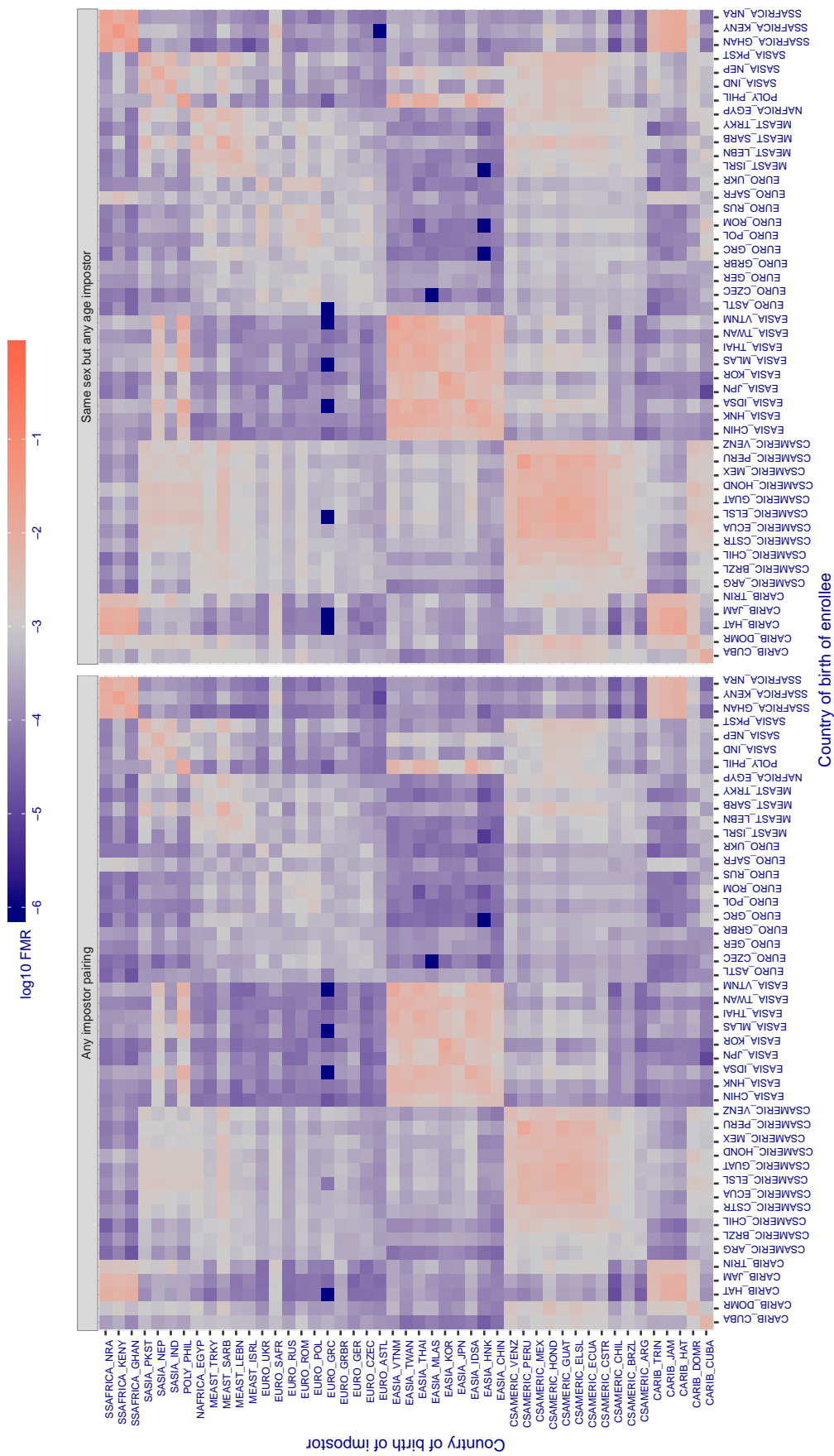


Figure 399: For algorithm safe-002 operating on visa images, the heatmap shows false match rates observed over impostor comparisons of faces from different individuals who were born in the given country pair. False matches are counted against a recognition threshold fixed globally to give the target FMR in the plot title, computed over all on the order of  $10^{10}$  impostor comparisons. If text appears in each box it give the same quantity as that coded by the color. Grey indicates FMR is at the intended FMR target level. Light red colors present a security vulnerability to, for example, a passport gate. Each +1 increase in  $\log_{10} \text{FMR}$  corresponds to a factor of 10 increase in FMR. The matrix is not quite symmetric because images in the enrollment and verification sets are different.

**Cross country FMR at threshold T = 0.368 for algorithm sensetime\_001, giving FMR(T) = 0.001 globally.**

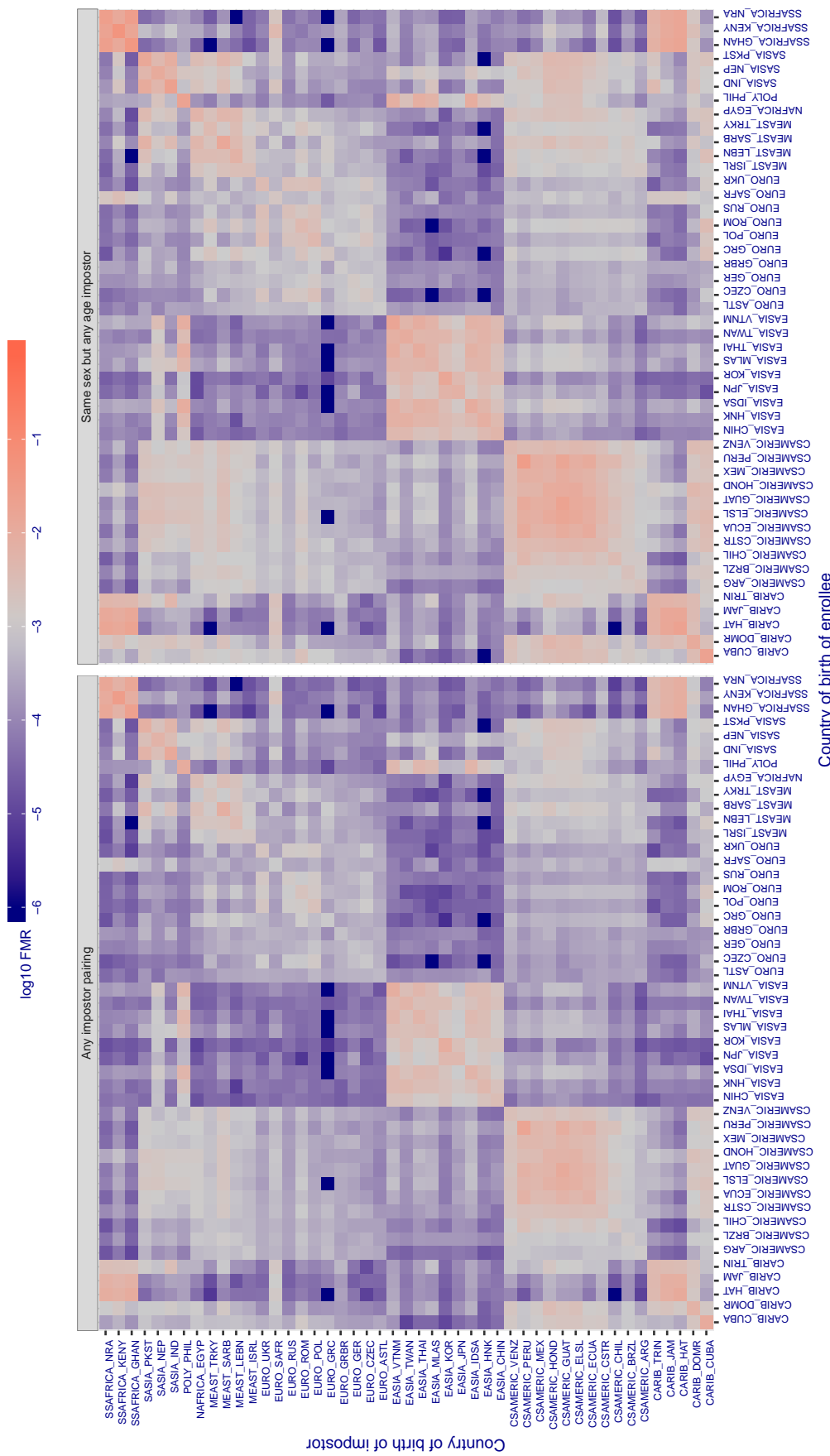


Figure 400: For algorithm sensetime-001 operating on visa images, the heatmap shows false match rates observed over impostor comparisons of faces from different individuals who were born in the given country pair. False matches are counted against a recognition threshold fixed globally to give the target FMR in the plot title, computed over all on the order of  $10^{10}$  impostor comparisons. If text appears in each box it give the same quantity as that coded by the color. Grey indicates FMR is at the intended FMR target level. Light red colors present a security vulnerability to, for example, a passport gate. Each +1 increase in  $\log_{10} \text{FMR}$  corresponds to a factor of 10 increase in FMR. The matrix is not quite symmetric because images in the enrollment and verification sets are different.

**Cross country FMR at threshold T = 0.369 for algorithm sensetime\_002, giving FMR(T) = 0.001 globally.**

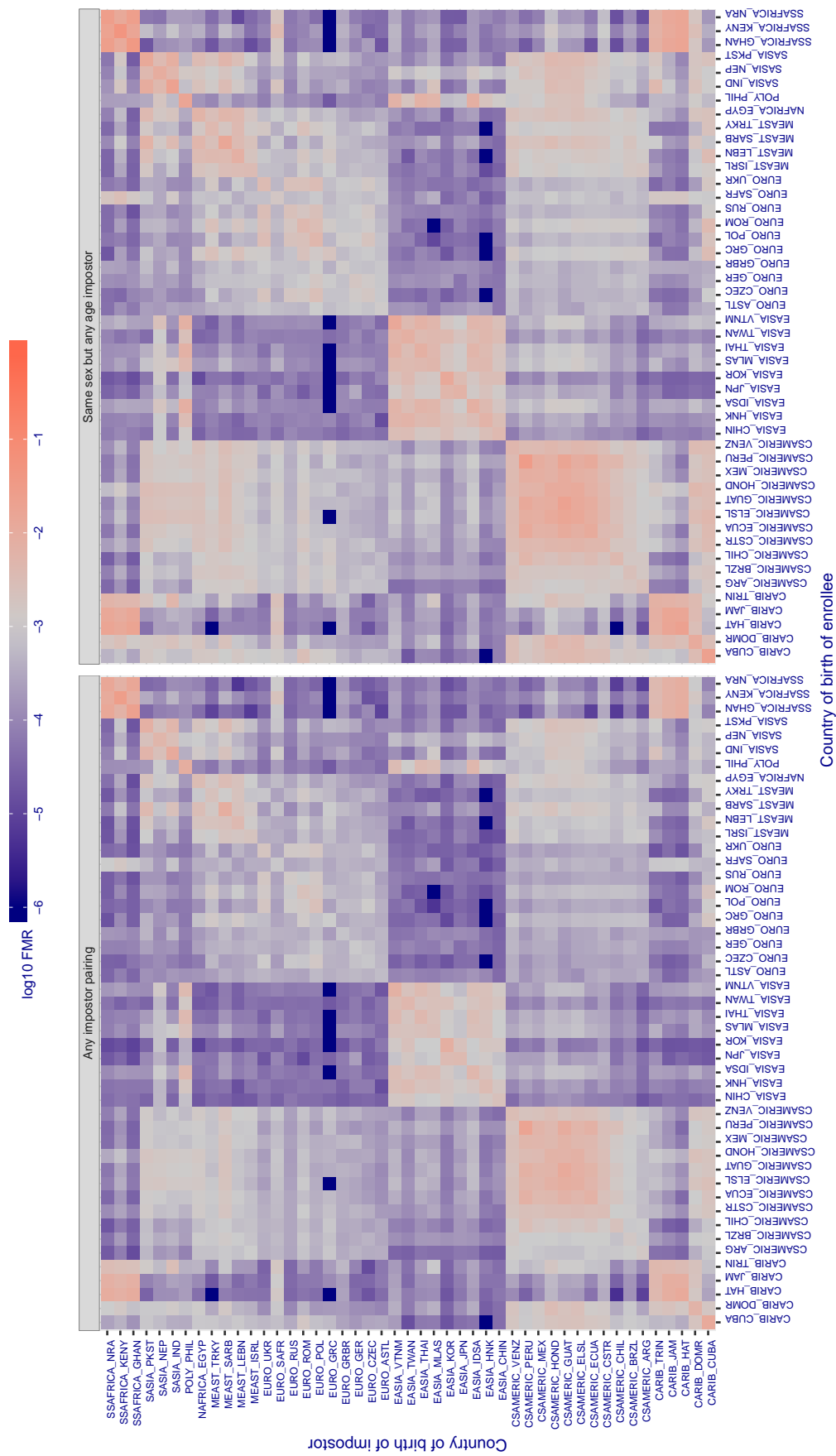


Figure 401: For algorithm sensetime-002 operating on visa images, the heatmap shows false match rates observed over impostor comparisons of faces from different individuals who were born in the given country pair. False matches are counted against a recognition threshold fixed globally to give the target FMR in the plot title, computed over all on the order of  $10^{10}$  impostor comparisons. If text appears in each box it give the same quantity as that coded by the color. Grey indicates FMR is at the intended FMR target level. Light red colors present a security vulnerability to, for example, a passport gate. Each +1 increase in  $\log_{10} FMR$  corresponds to a factor of 10 increase in FMR. The matrix is not quite symmetric because images in the enrollment and verification sets are different.

**Cross country FMR at threshold T = 0.939 for algorithm shaman\_000, giving  $FMR(T) = 0.001$  globally.**

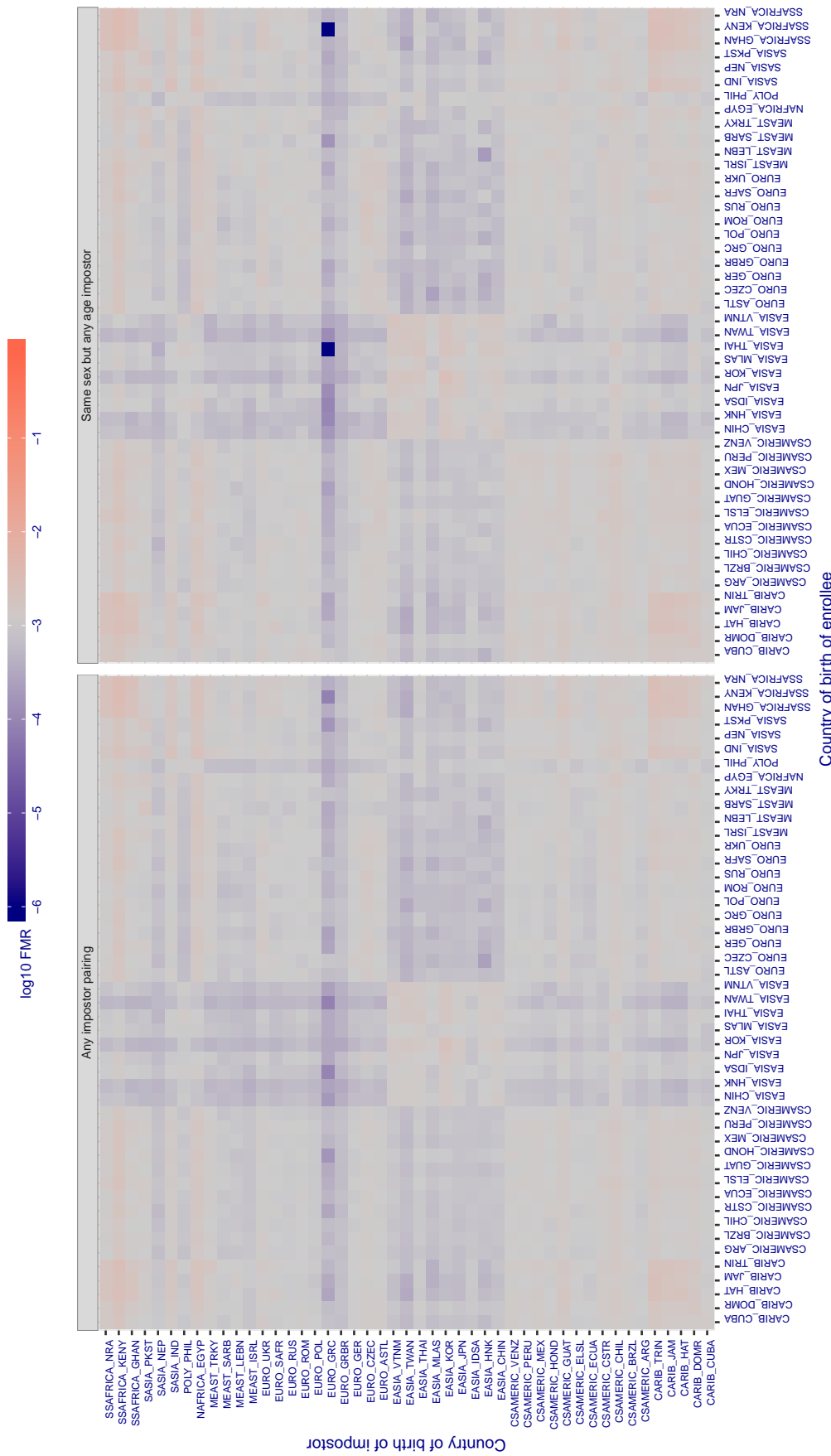


Figure 402: For algorithm shaman-000 operating on visa images, the heatmap shows false match rates observed over impostor comparisons of faces from different individuals who were born in the given country pair. False matches are counted against a recognition threshold fixed globally to give the target  $FMR$  in the plot title, computed over all on the order of  $10^{10}$  impostor comparisons. If text appears in each box it give the same quantity as that coded by the color. Grey indicates  $FMR$  is at the intended  $FMR$  target level. Light red colors present a security vulnerability to, for example, a passport gate. Each +1 increase in  $\log_{10} FMR$  corresponds to a factor of 10 increase in  $FMR$ . The matrix is not quite symmetric because images in the enrollment and verification sets are different.

**Cross country FMR at threshold T = 0.599 for algorithm shaman\_001, giving  $\text{FMR}(T) = 0.001$  globally.**

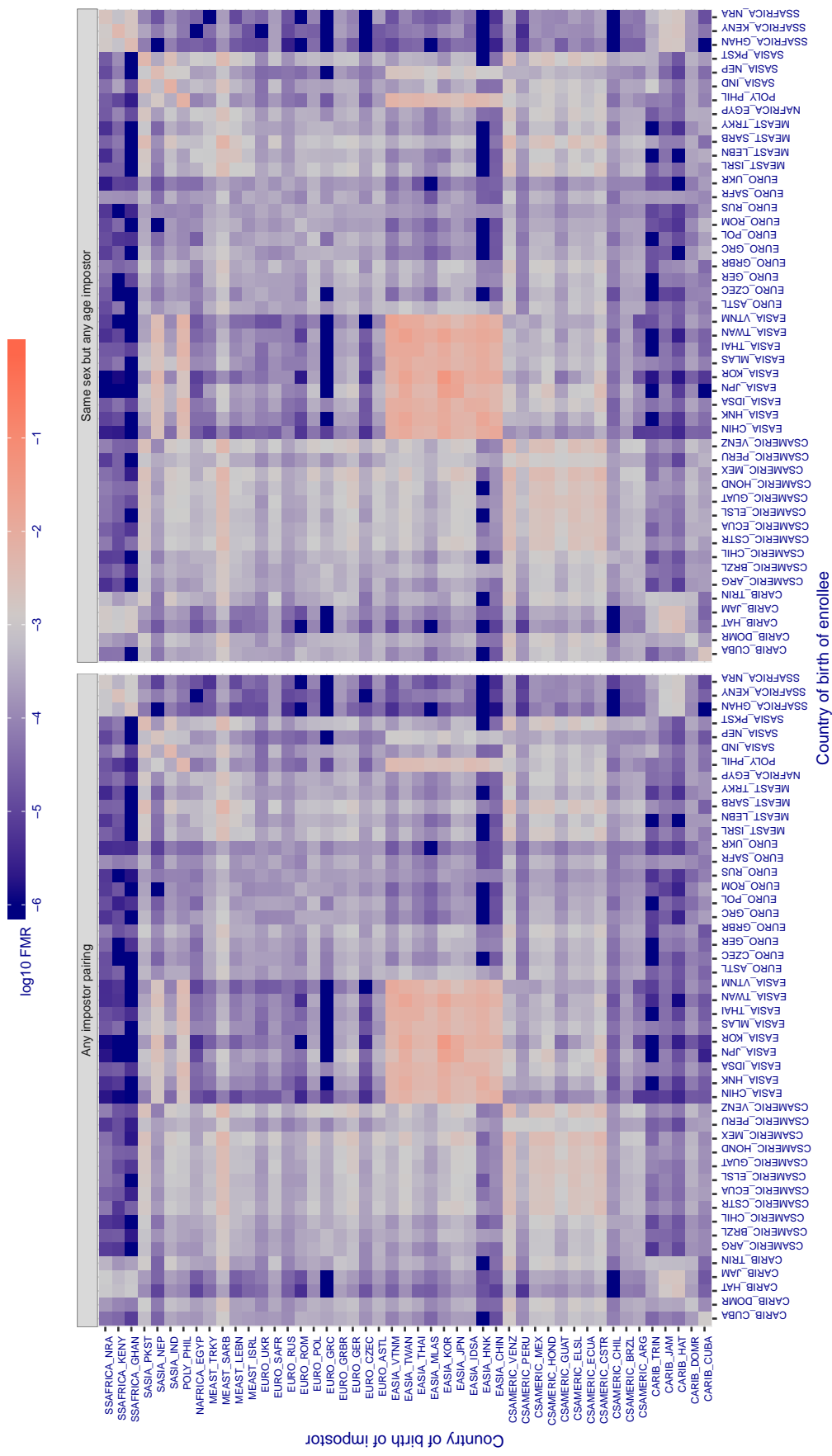
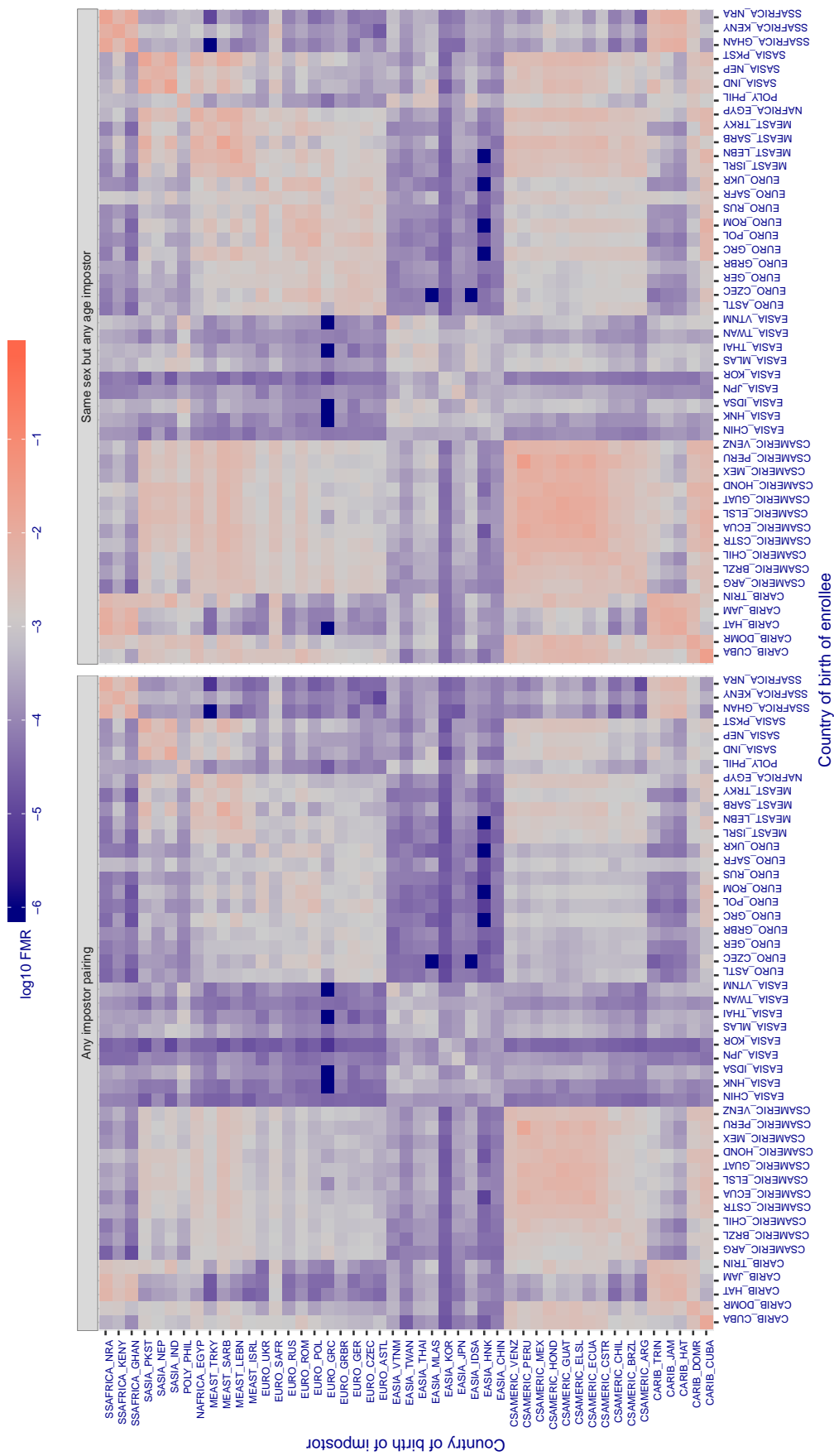


Figure 403: For algorithm shaman-001 operating on visa images, the heatmap shows false match rates observed over impostor comparisons of faces from different individuals who were born in the given country pair. False matches are counted against a recognition threshold fixed globally to give the target  $\text{FMR}$  in the plot title, computed over all on the order of  $10^{10}$  impostor comparisons. If text appears in each box it give the same quantity as that coded by the color. Grey indicates  $\text{FMR}$  is at the intended  $\text{FMR}$  target level. Light red colors present a security vulnerability to, for example, a passport gate. Each +1 increase in  $\log_{10} \text{FMR}$  corresponds to a factor of 10 increase in  $\text{FMR}$ . The matrix is not quite symmetric because images in the enrollment and verification sets are different.

**Cross country FMR at threshold T = 0.316 for algorithm shu\_001, giving  $\text{FMR}(T) = 0.001$  globally.**



**Figure 404:** For algorithm shu-001 operating on visa images, the heatmap shows false match rates observed over impostor comparisons of faces from different individuals who were born in the given country pair. False matches are counted against a recognition threshold fixed globally to give the target FMR in the plot title, computed over all on the order of  $10^{10}$  impostor comparisons. If text appears in each box it give the same quantity as that coded by the color. Grey indicates FMR is at the intended FMR target level. Light red colors present a security vulnerability to, for example, a passport gate. Each +1 increase in  $\log_{10} \text{FMR}$  corresponds to a factor of 10 increase in FMR. The matrix is not quite symmetric because images in the enrollment and verification sets are different.

**Cross country FMR at threshold T = 0.370 for algorithm siat\_002, giving  $\text{FMR}(\text{T}) = 0.001$  globally.**

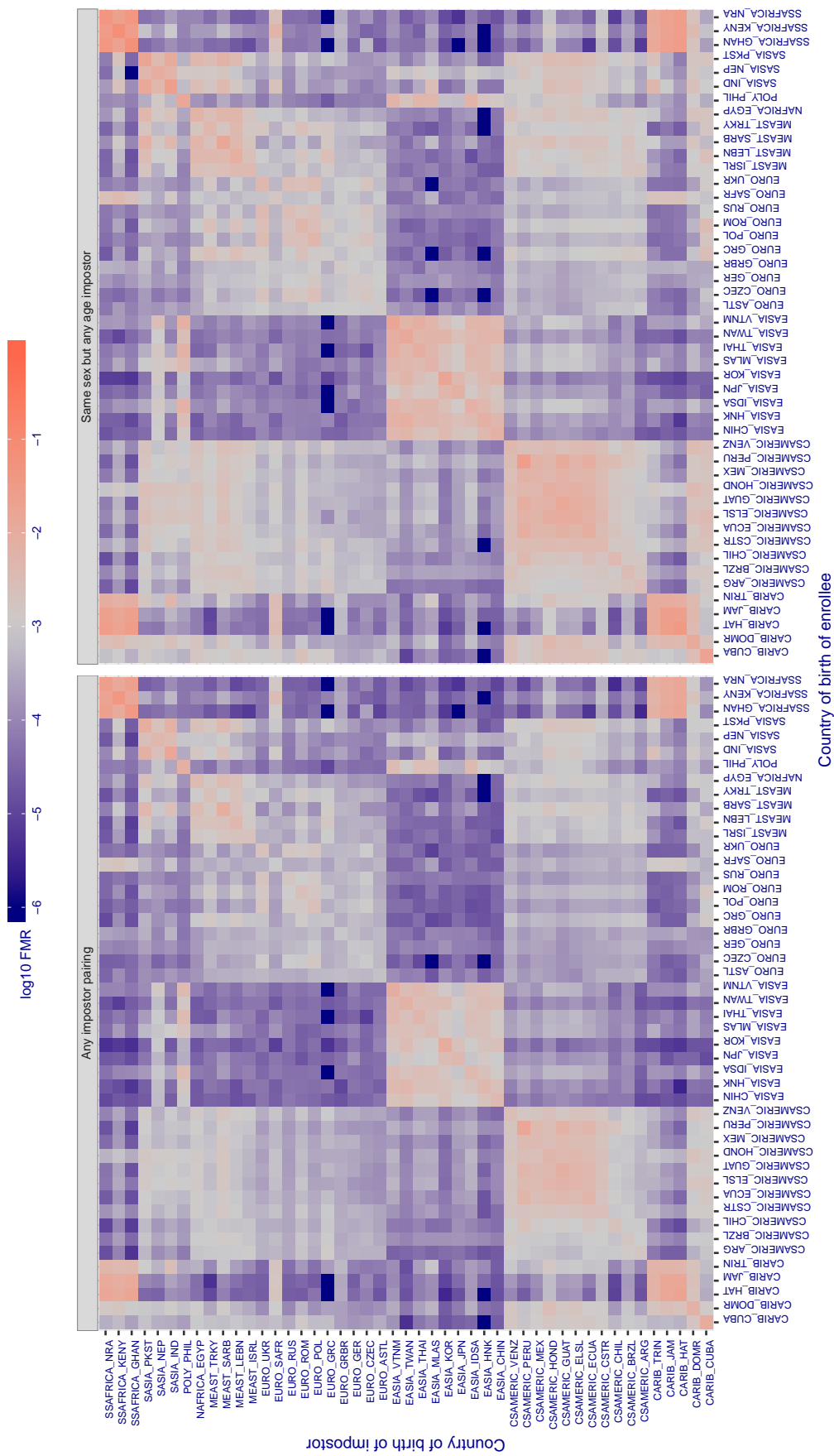


Figure 405: For algorithm siat-002 operating on visa images, the heatmap shows false match rates observed over impostor comparisons of faces from different individuals who were born in the given country pair. False matches are counted against a recognition threshold fixed globally to give the target FMR in the plot title, computed over all on the order of  $10^{10}$  impostor comparisons. If text appears in each box it give the same quantity as that coded by the color. Grey indicates FMR is at the intended FMR target level. Light red colors present a security vulnerability to, for example, a passport gate. Each  $+1$  increase in  $\log_{10} \text{FMR}$  corresponds to a factor of 10 increase in FMR. The matrix is not quite symmetric because images in the enrollment and verification sets are different.

**Cross country FMR at threshold T = 0.371 for algorithm siat\_004, giving  $\text{FMR}(\text{T}) = 0.001$  globally.**

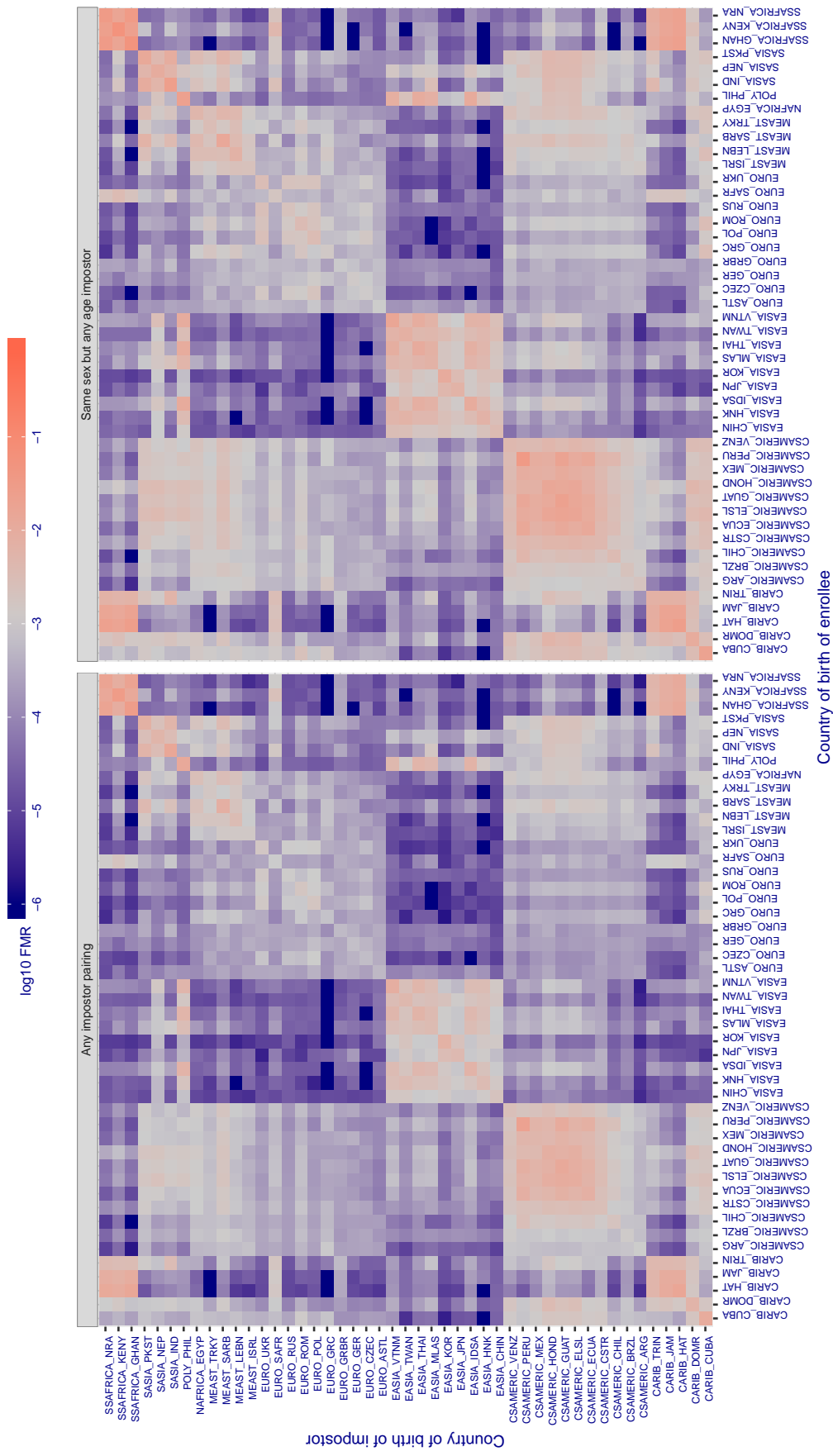


Figure 406: For algorithm siat-004 operating on visa images, the heatmap shows false match rates observed over impostor comparisons of faces from different individuals who were born in the given country pair. False matches are counted against a recognition threshold fixed globally to give the target FMR in the plot title, computed over all on the order of  $10^{10}$  impostor comparisons. If text appears in each box it give the same quantity as that coded by the color. Grey indicates FMR is at the intended FMR target level. Light red colors present a security vulnerability to, for example, a passport gate. Each +1 increase in  $\log_{10} \text{FMR}$  corresponds to a factor of 10 increase in FMR. The matrix is not quite symmetric because images in the enrollment and verification sets are different.

**Cross country FMR at threshold T = 1.121 for algorithm situ\_001, giving  $\text{FMR}(T) = 0.001$  globally.**

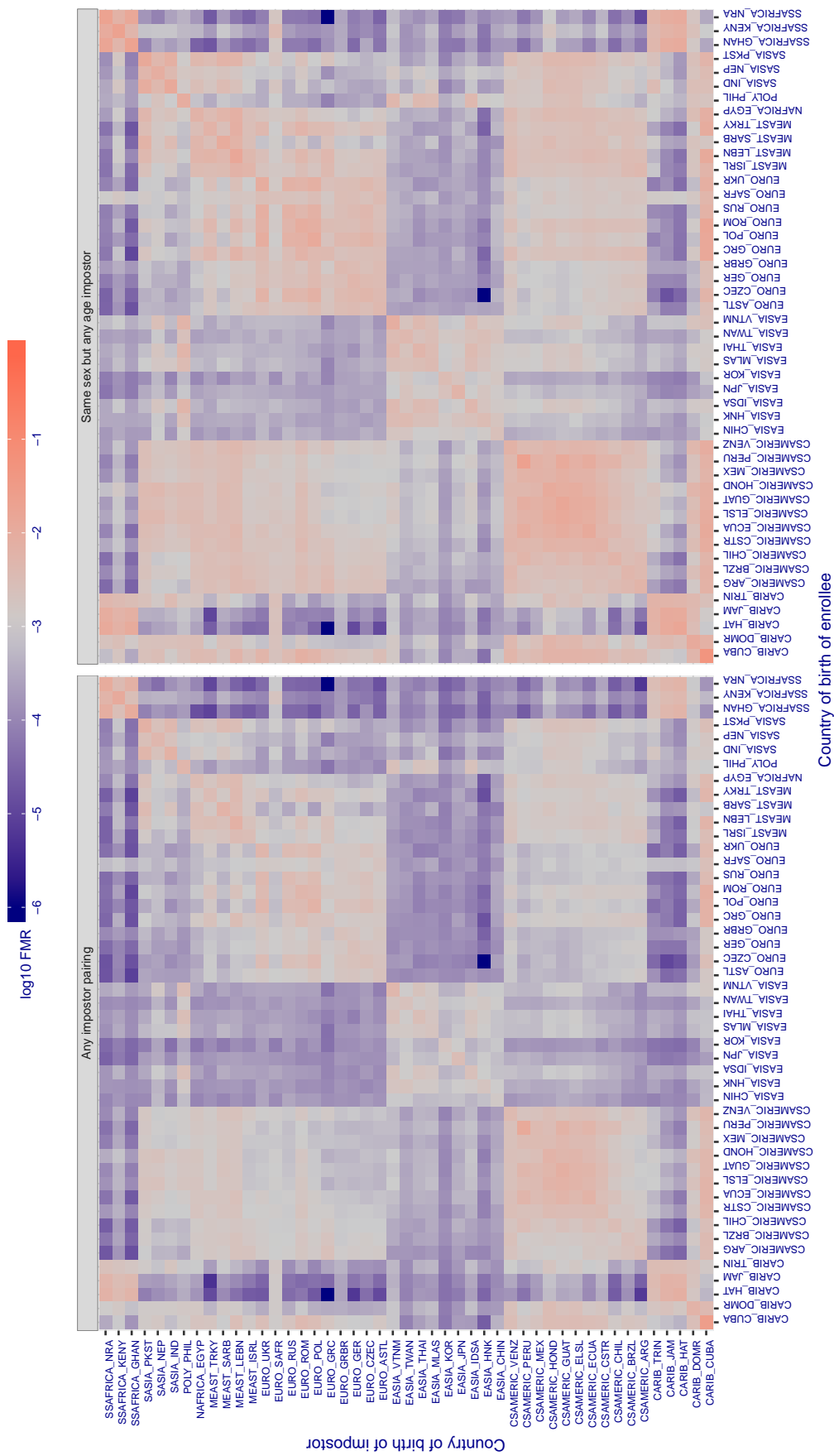


Figure 407: For algorithm *situ-001* operating on visa images, the heatmap shows false match rates observed over impostor comparisons of faces from different individuals who were born in the given country pair. False matches are counted against a recognition threshold fixed globally to give the target  $\text{FMR}$  in the plot title, computed over all on the order of  $10^{10}$  impostor comparisons. If text appears in each box it give the same quantity as that coded by the color. Grey indicates  $\text{FMR}$  is at the intended  $\text{FMR}$  target level. Light red colors present a security vulnerability to, for example, a passport gate. Each  $+1$  increase in  $\log_{10} \text{FMR}$  corresponds to a factor of 10 increase in  $\text{FMR}$ . The matrix is not quite symmetric because images in the enrollment and verification sets are different.

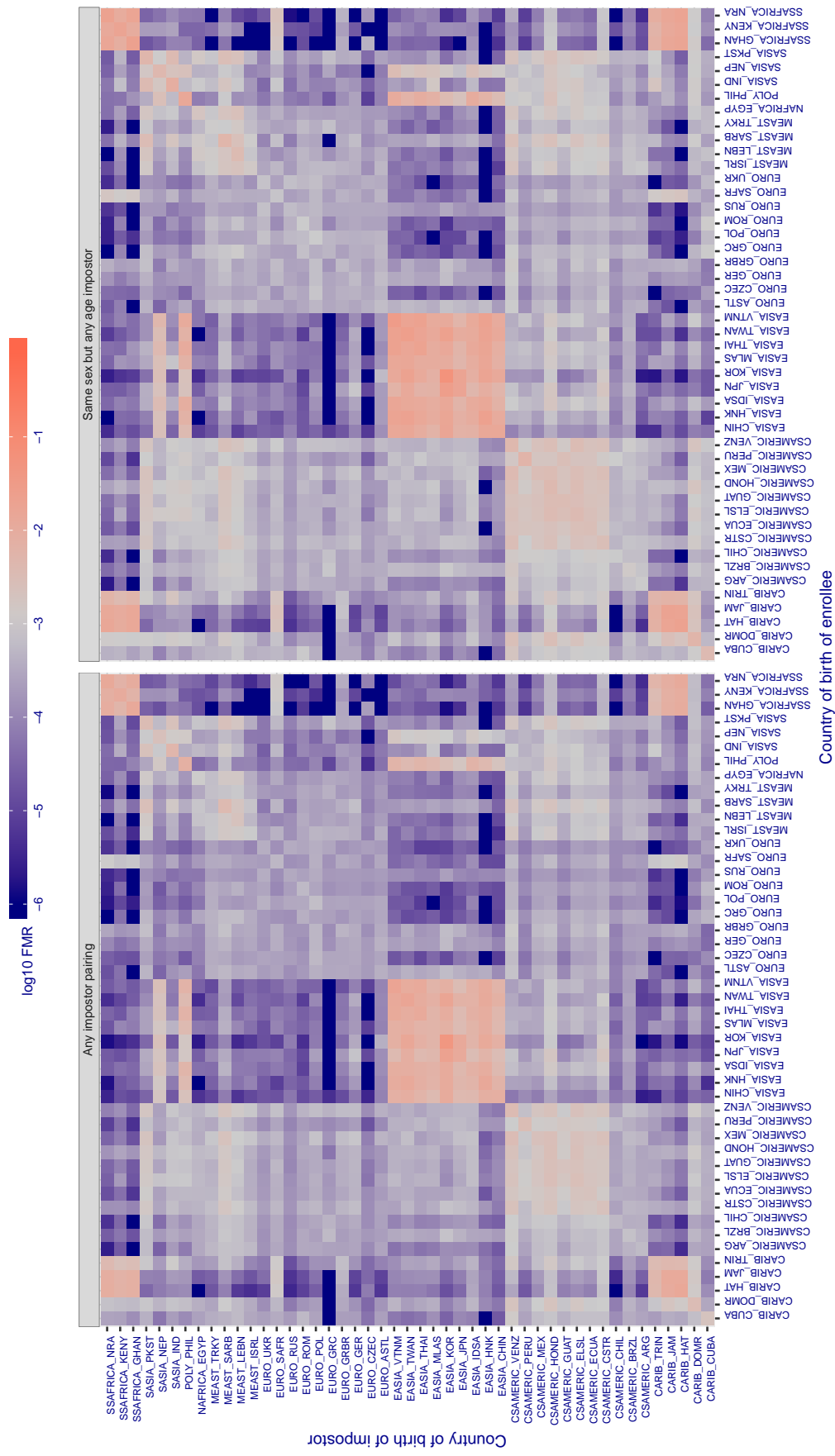
**Cross country FMR at threshold T = 0.488 for algorithm smilart\_002, giving  $FMR(T) = 0.001$  globally.**

Figure 408: For algorithm smilart-002 operating on visa images, the heatmap shows false match rates observed over impostor comparisons of faces from different individuals who were born in the given country pair. False matches are counted against a recognition threshold fixed globally to give the target  $FMR$  in the plot title, computed over all on the order of  $10^{10}$  impostor comparisons. If text appears in each box it give the same quantity as that coded by the color. Grey indicates  $FMR$  is at the intended  $FMR$  target level. Light red colors present a security vulnerability to, for example, a passport gate. Each +1 increase in  $\log_{10} FMR$  corresponds to a factor of 10 increase in  $FMR$ . The matrix is not quite symmetric because images in the enrollment and verification sets are different.

**Cross country FMR at threshold T = 0.388 for algorithm smilart\_003, giving  $FMR(T) = 0.001$  globally.**

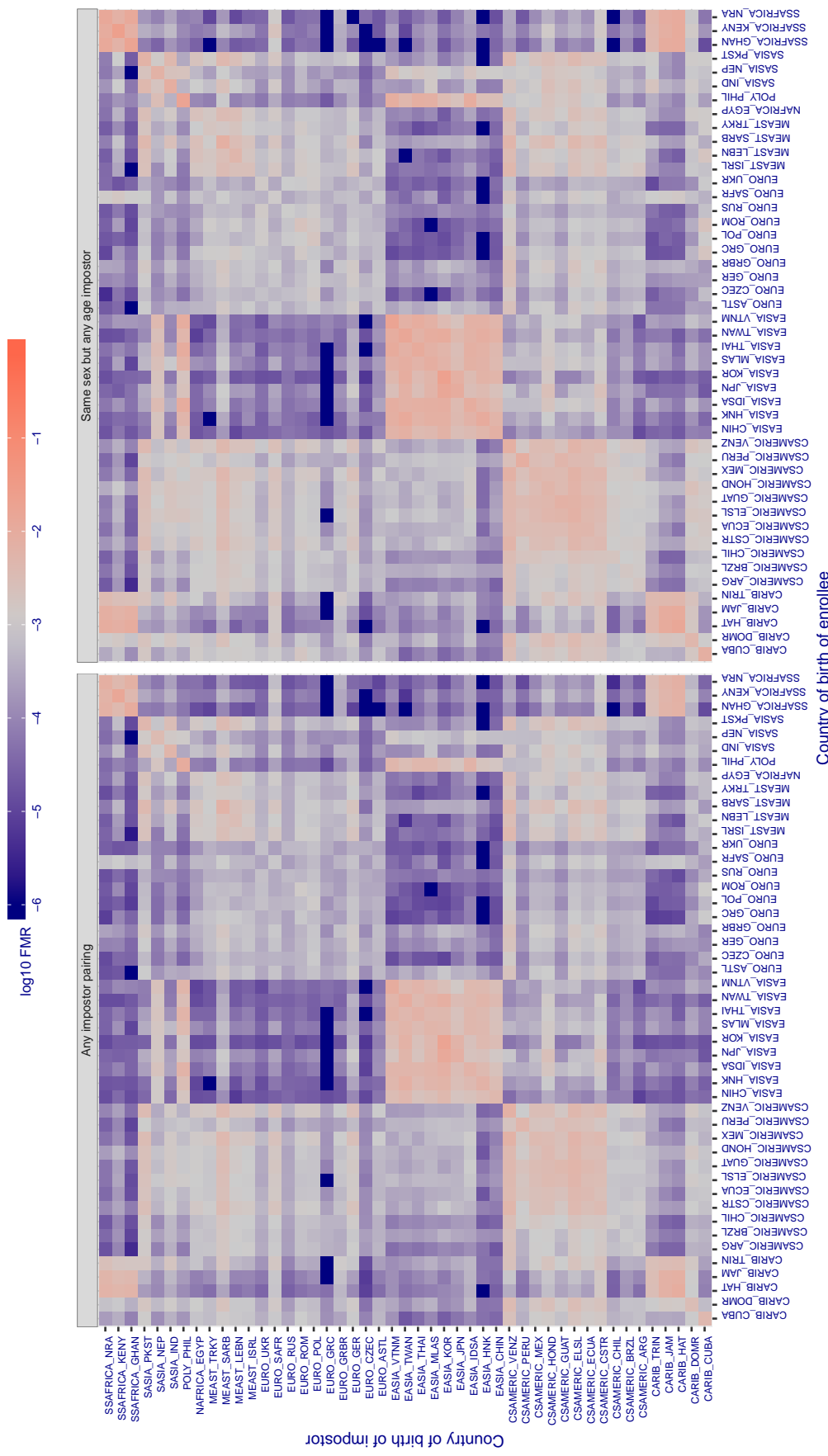


Figure 409: For algorithm smilart-003 operating on visa images, the heatmap shows false match rates observed over impostor comparisons of faces from different individuals who were born in the given country pair. False matches are counted against a recognition threshold fixed globally to give the target  $FMR$  in the plot title, computed over all on the order of  $10^{10}$  impostor comparisons. If text appears in each box it give the same quantity as that coded by the color. Grey indicates  $FMR$  is at the intended  $FMR$  target level. Light red colors present a security vulnerability to, for example, a passport gate. Each +1 increase in  $\log_{10} FMR$  corresponds to a factor of 10 increase in  $FMR$ . The matrix is not quite symmetric because images in the enrollment and verification sets are different.

**Cross country FMR at threshold T = 0.251 for algorithm starhybrid\_001, giving FMR(T) = 0.001 globally.**

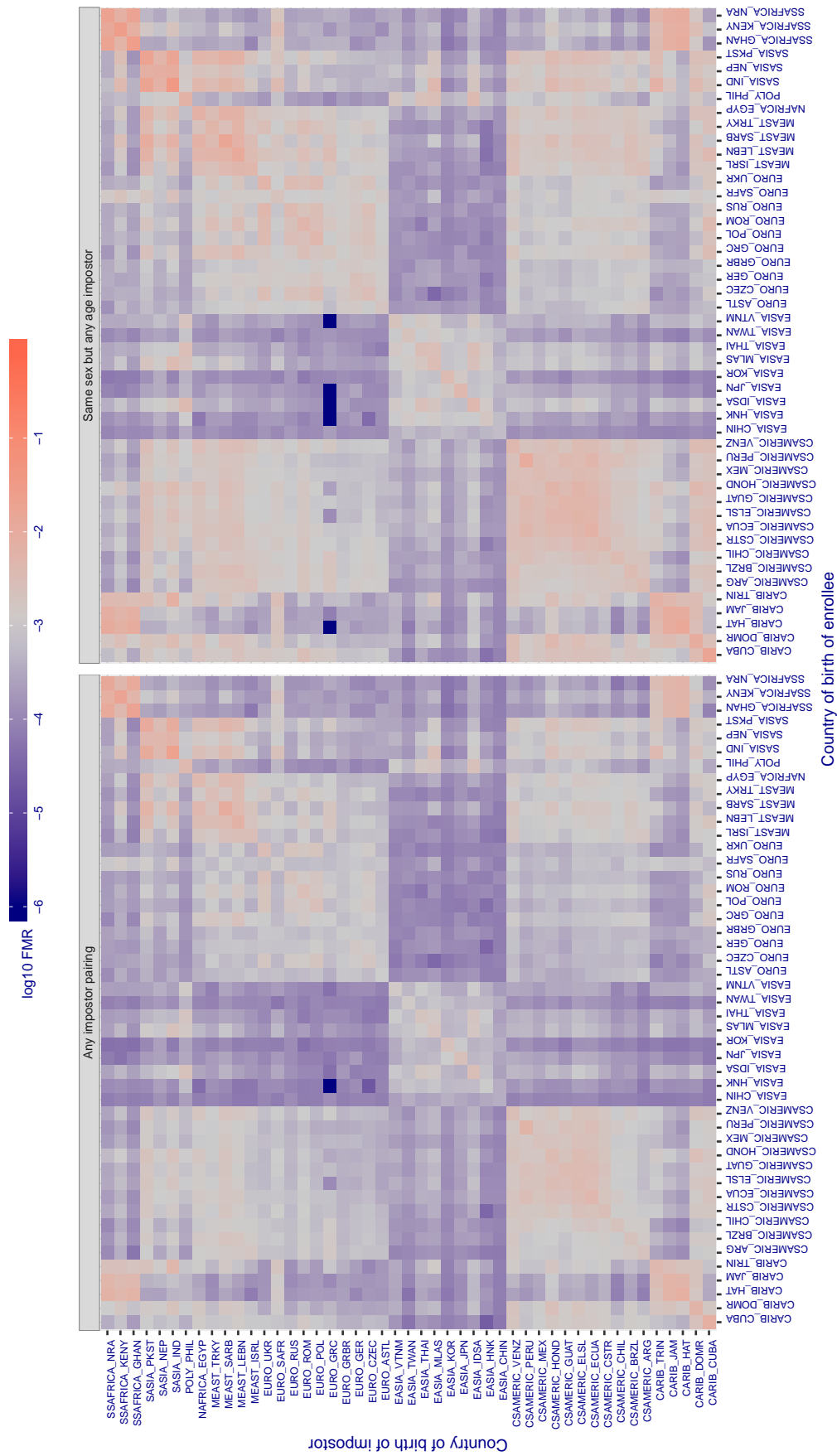


Figure 410: For algorithm starhybrid-001 operating on visa images, the heatmap shows false match rates observed over impostor comparisons of faces from different individuals who were born in the given country pair. False matches are counted against a recognition threshold fixed globally to give the target FMR in the plot title, computed over all on the order of  $10^{10}$  impostor comparisons. If text appears in each box it give the same quantity as that coded by the color. Grey indicates FMR is at the intended FMR target level. Light red colors present a security vulnerability to, for example, a passport gate. Each +1 increase in  $\log_{10} FMR$  corresponds to a factor of 10 increase in FMR. The matrix is not quite symmetric because images in the enrollment and verification sets are different.

**Cross country FMR at threshold T = 0.047 for algorithm synthesis\_004, giving  $\text{FMR}(T) = 0.001$  globally.**

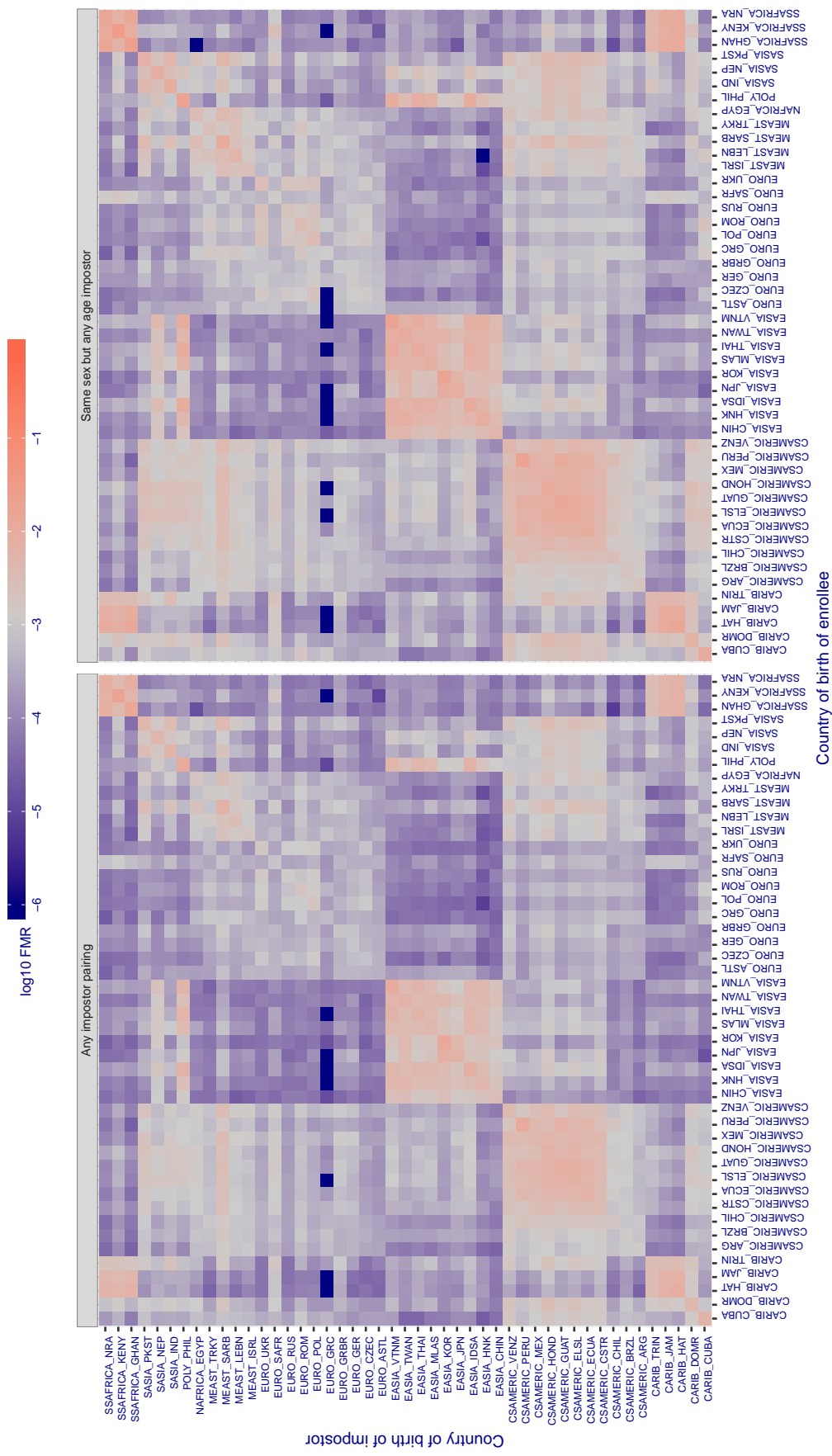


Figure 411: For algorithm synthesis-004 operating on visa images, the heatmap shows false match rates observed over impostor comparisons of faces from different individuals who were born in the given country pair. False matches are counted against a recognition threshold fixed globally to give the target  $\text{FMR}$  in the plot title, computed over all on the order of  $10^{10}$  impostor comparisons. If text appears in each box it give the same quantity as that coded by the color. Grey indicates  $\text{FMR}$  is at the intended  $\text{FMR}$  target level. Light red colors present a security vulnerability to, for example, a passport gate. Each +1 increase in  $\log_{10} \text{FMR}$  corresponds to a factor of 10 increase in  $\text{FMR}$ . The matrix is not quite symmetric because images in the enrollment and verification sets are different.

**Cross country FMR at threshold T = 0.274 for algorithm synthesis\_005, giving  $\text{FMR}(T) = 0.001$  globally.**

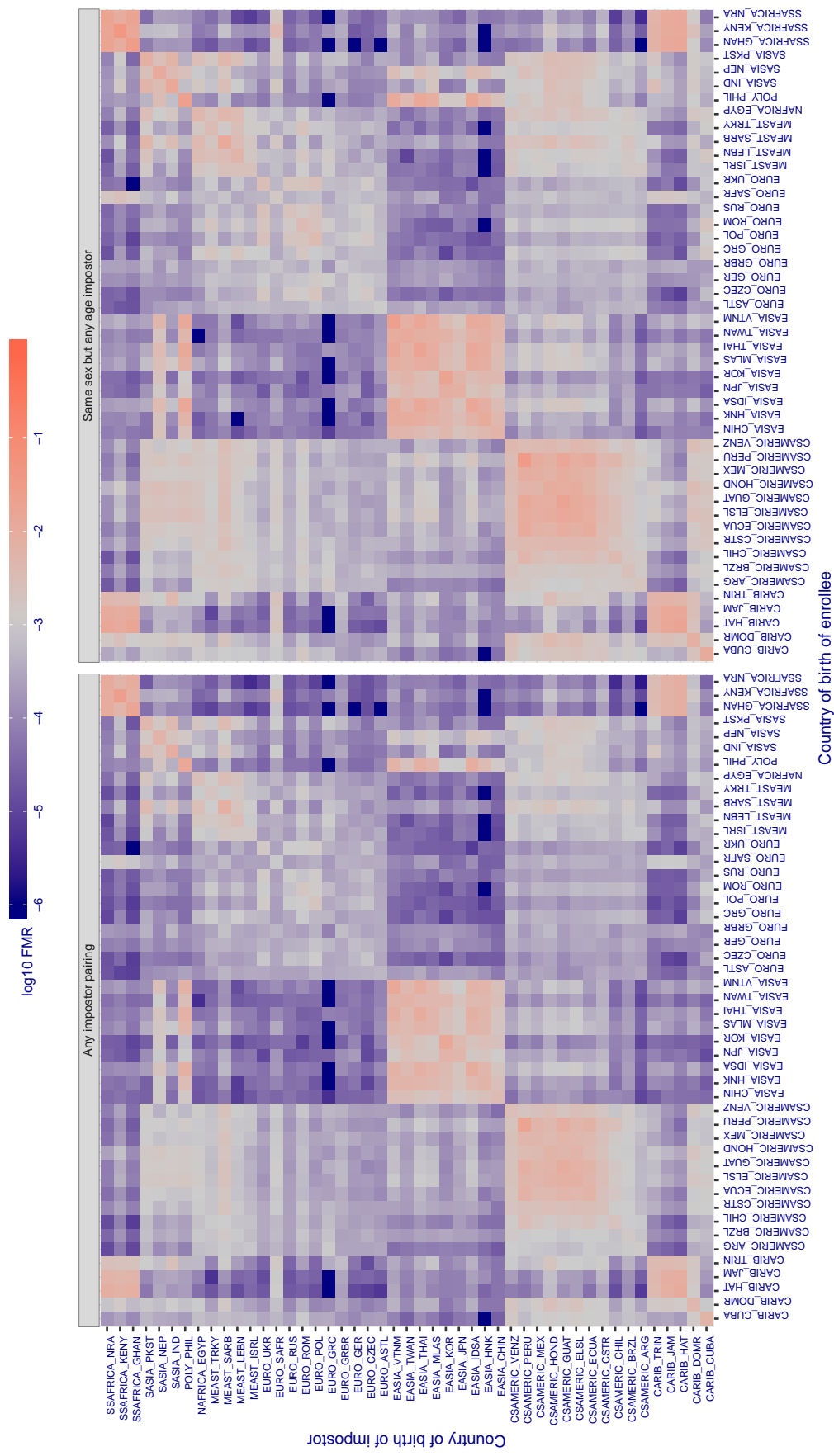


Figure 412: For algorithm synthesis-005 operating on visa images, the heatmap shows false match rates observed over impostor comparisons of faces from different individuals who were born in the given country pair. False matches are counted against a recognition threshold fixed globally to give the target  $\text{FMR}$  in the plot title, computed over all on the order of  $10^{10}$  impostor comparisons. If text appears in each box it give the same quantity as that coded by the color. Grey indicates  $\text{FMR}$  is at the intended  $\text{FMR}$  target level. Light red colors present a security vulnerability to, for example, a passport gate. Each +1 increase in  $\log_{10} \text{FMR}$  corresponds to a factor of 10 increase in  $\text{FMR}$ . The matrix is not quite symmetric because images in the enrollment and verification sets are different.

**Cross country FMR at threshold T = 147.234 for algorithm tech5\_002, giving  $\text{FMR}(T) = 0.001$  globally.**

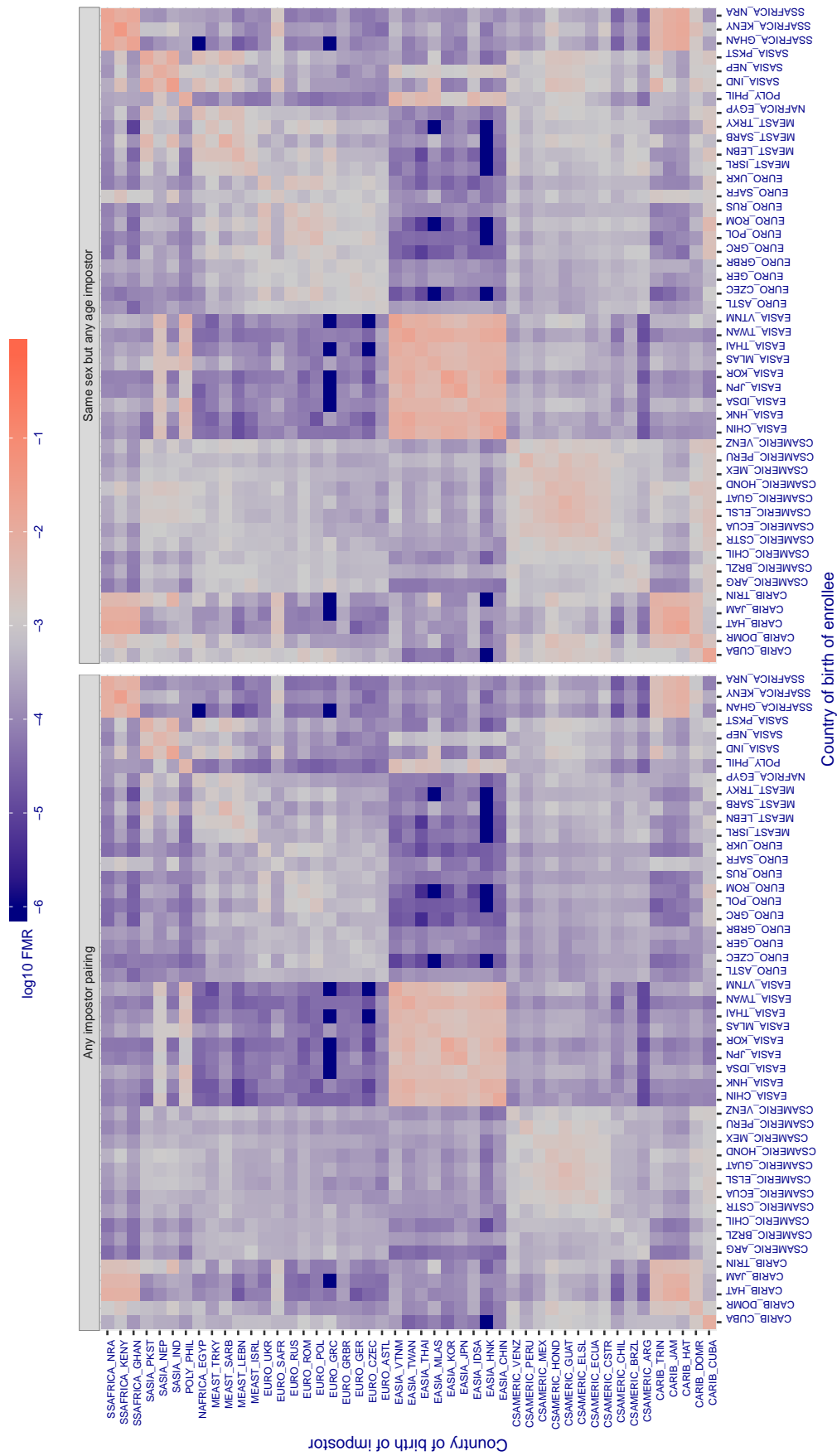


Figure 413: For algorithm tech5-002 operating on visa images, the heatmap shows false match rates observed over impostor comparisons of faces from different individuals who were born in the given country pair. False matches are counted against a recognition threshold fixed globally to give the target  $\text{FMR}$  in the plot title, computed over all on the order of  $10^{10}$  impostor comparisons. If text appears in each box it give the same quantity as that coded by the color. Grey indicates  $\text{FMR}$  is at the intended  $\text{FMR}$  target level. Light red colors present a security vulnerability to, for example, a passport gate. Each +1 increase in  $\log_{10} \text{FMR}$  corresponds to a factor of 10 increase in  $\text{FMR}$ . The matrix is not quite symmetric because images in the enrollment and verification sets are different.

**Cross country FMR at threshold T = 146.607 for algorithm tech5\_003, giving  $\text{FMR}(T) = 0.001$  globally.**

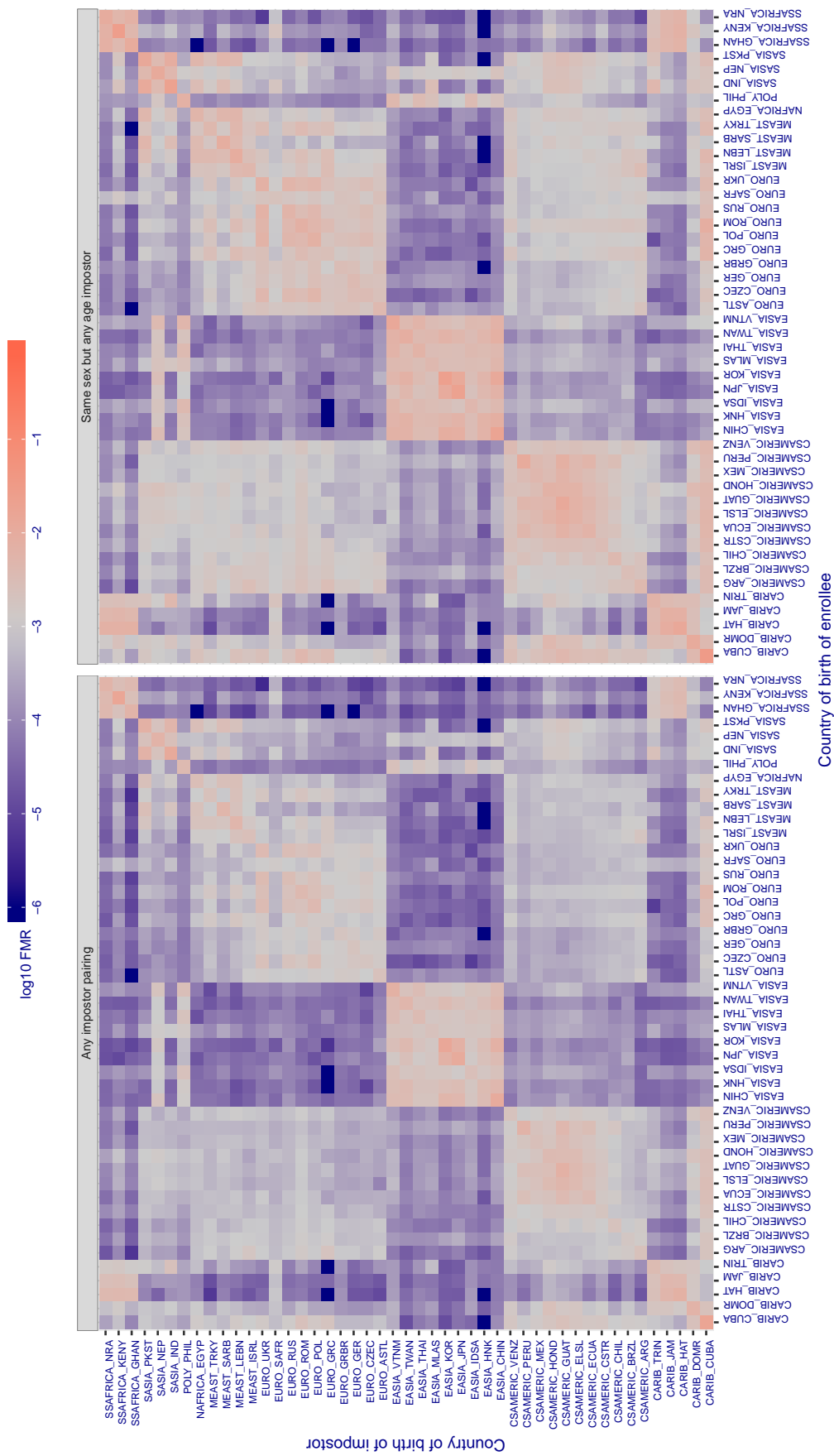


Figure 414: For algorithm tech5-003 operating on visa images, the heatmap shows false match rates observed over impostor comparisons of faces from different individuals who were born in the given country pair. False matches are counted against a recognition threshold fixed globally to give the target FMR in the plot title, computed over all on the order of  $10^{10}$  impostor comparisons. If text appears in each box it give the same quantity as that coded by the color. Grey indicates FMR is at the intended FMR target level. Light red colors present a security vulnerability to, for example, a passport gate. Each +1 increase in  $\log_{10} \text{FMR}$  corresponds to a factor of 10 increase in FMR. The matrix is not quite symmetric because images in the enrollment and verification sets are different.

**Cross country FMR at threshold T = 0.769 for algorithm tevian\_004, giving  $\text{FMR}(\text{T}) = 0.001$  globally.**

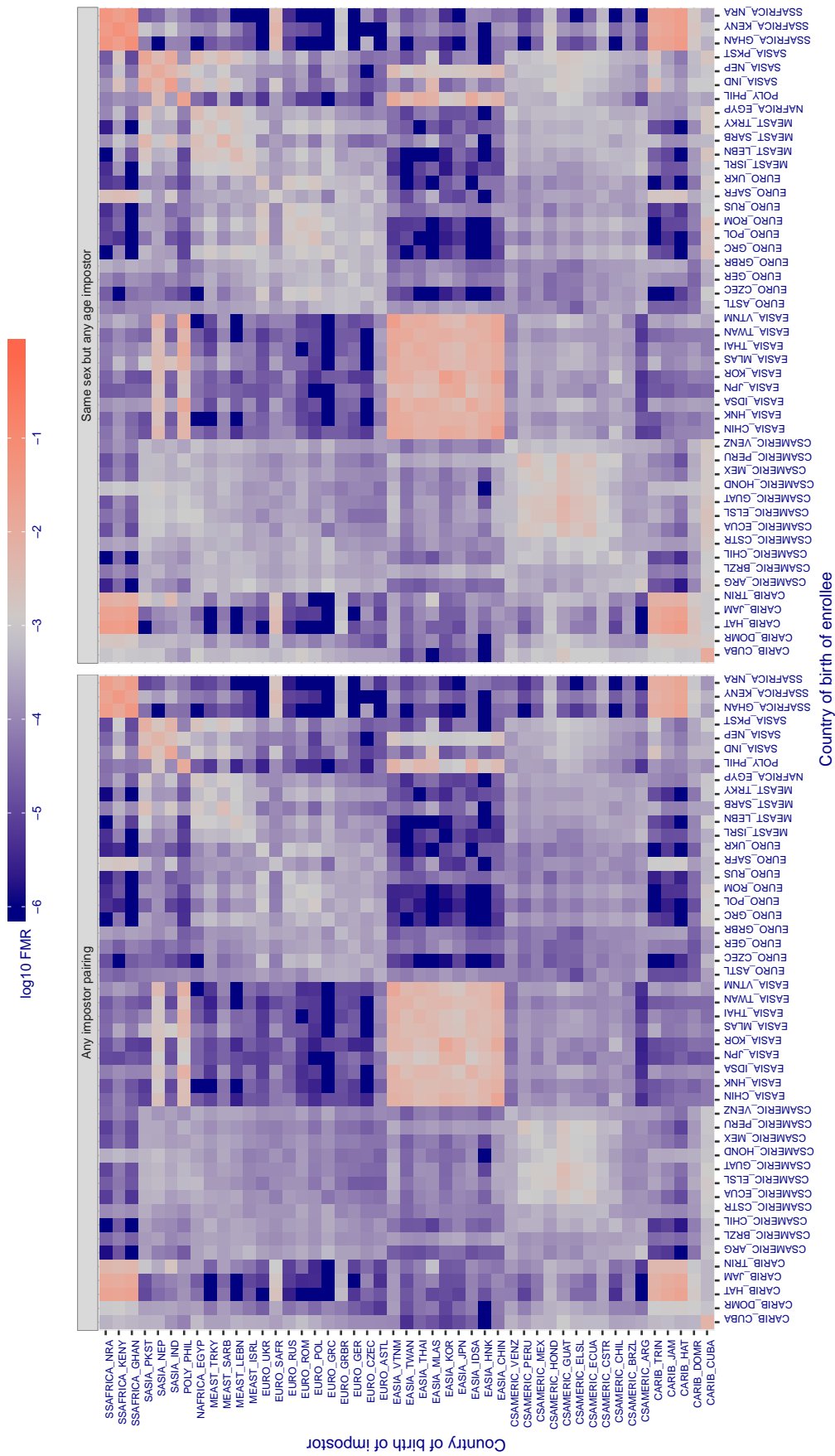


Figure 415: For algorithm tevian-004 operating on visa images, the heatmap shows false match rates observed over impostor comparisons of faces from different individuals who were born in the given country pair. False matches are counted against a recognition threshold fixed globally to give the target  $\text{FMR}$  in the plot title, computed over all on the order of  $10^{10}$  impostor comparisons. If text appears in each box it give the same quantity as that coded by the color. Grey indicates  $\text{FMR}$  is at the intended  $\text{FMR}$  target level. Light red colors present a security vulnerability to, for example, a passport gate. Each +1 increase in  $\log_{10} \text{FMR}$  corresponds to a factor of 10 increase in  $\text{FMR}$ . The matrix is not quite symmetric because images in the enrollment and verification sets are different.

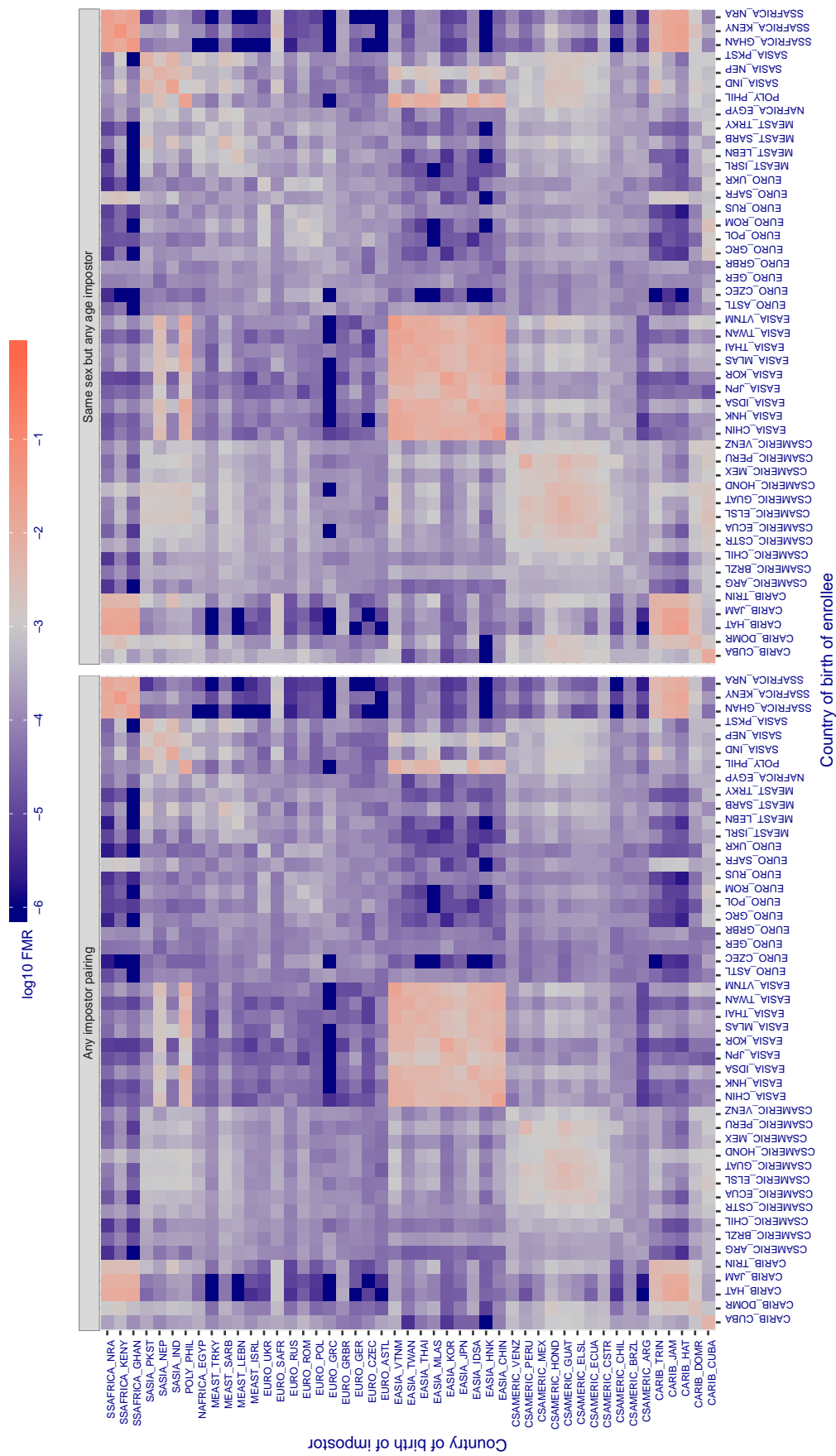
Cross country FMR at threshold T = 143.194 for algorithm tiger\_002, giving  $FMR(T) = 0.001$  globally.

Figure 416: For algorithm tiger-002 operating on visa images, the heatmap shows false match rates observed over impostor comparisons of faces from different individuals who were born in the given country pair. False matches are counted against a recognition threshold fixed globally to give the target  $FMR$  in the plot title, computed over all on the order of  $10^{10}$  impostor comparisons. If text appears in each box it give the same quantity as that coded by the color. Grey indicates  $FMR$  is at the intended  $FMR$  target level. Light red colors present a security vulnerability to, for example, a passport gate. Each +1 increase in  $\log_{10} FMR$  corresponds to a factor of 10 increase in  $FMR$ . The matrix is not quite symmetric because images in the enrollment and verification sets are different.

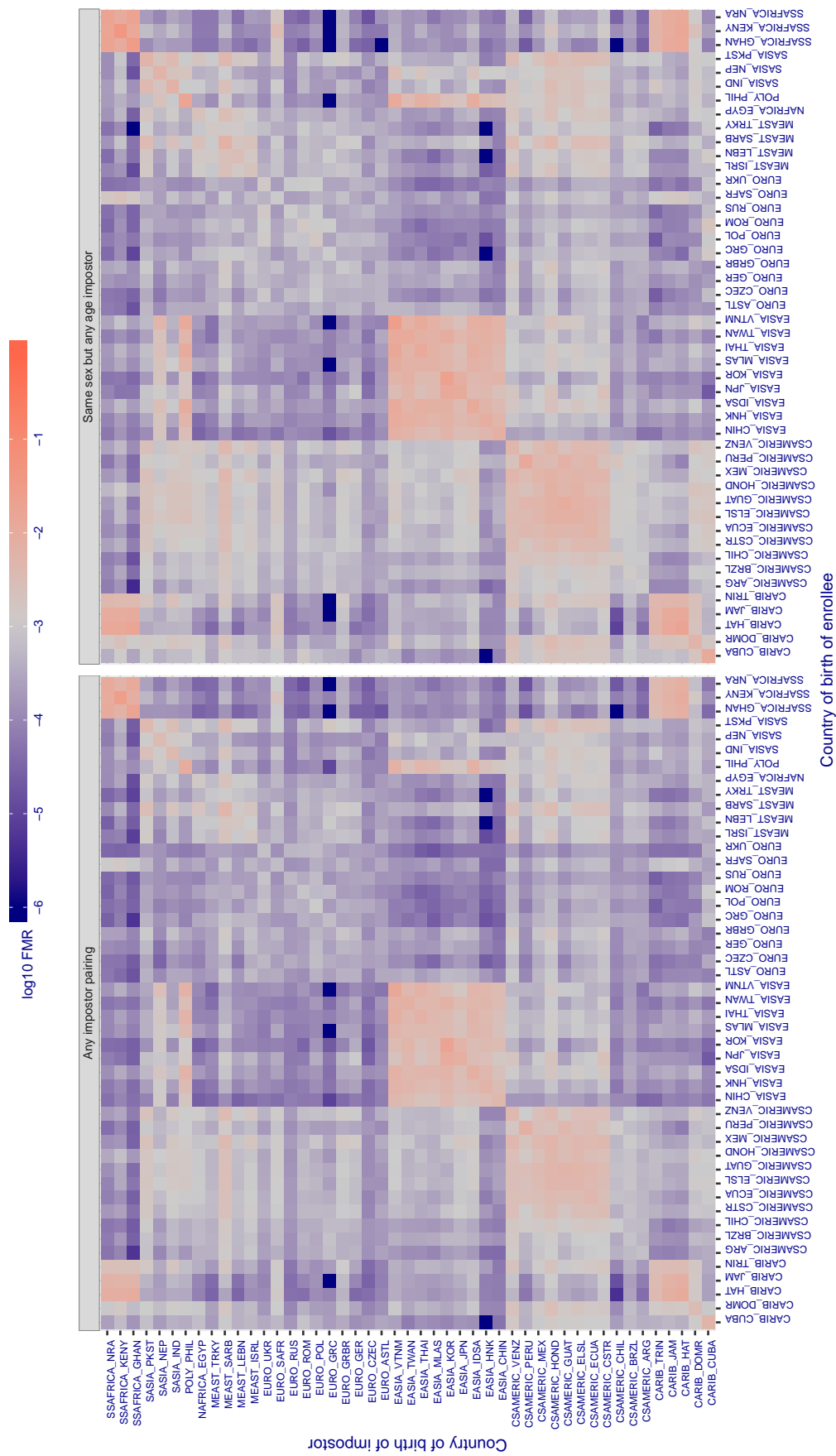
**Cross country FMR at threshold T = 139.101 for algorithm tiger\_003, giving  $FMR(T) = 0.001$  globally.**

Figure 417: For algorithm tiger-003 operating on visa images, the heatmap shows false match rates observed over impostor comparisons of faces from different individuals who were born in the given country pair. False matches are counted against a recognition threshold fixed globally to give the target  $FMR$  in the plot title, computed over all on the order of  $10^{10}$  impostor comparisons. If text appears in each box it give the same quantity as that coded by the color. Grey indicates  $FMR$  is at the intended  $FMR$  target level. Light red colors present a security vulnerability to, for example, a passport gate. Each  $+1$  increase in  $\log_{10} FMR$  corresponds to a factor of 10 increase in  $FMR$ . The matrix is not quite symmetric because images in the enrollment and verification sets are different.

**Cross country FMR at threshold T = 43.483 for algorithm tongyi\_005, giving  $FMR(T) = 0.001$  globally.**

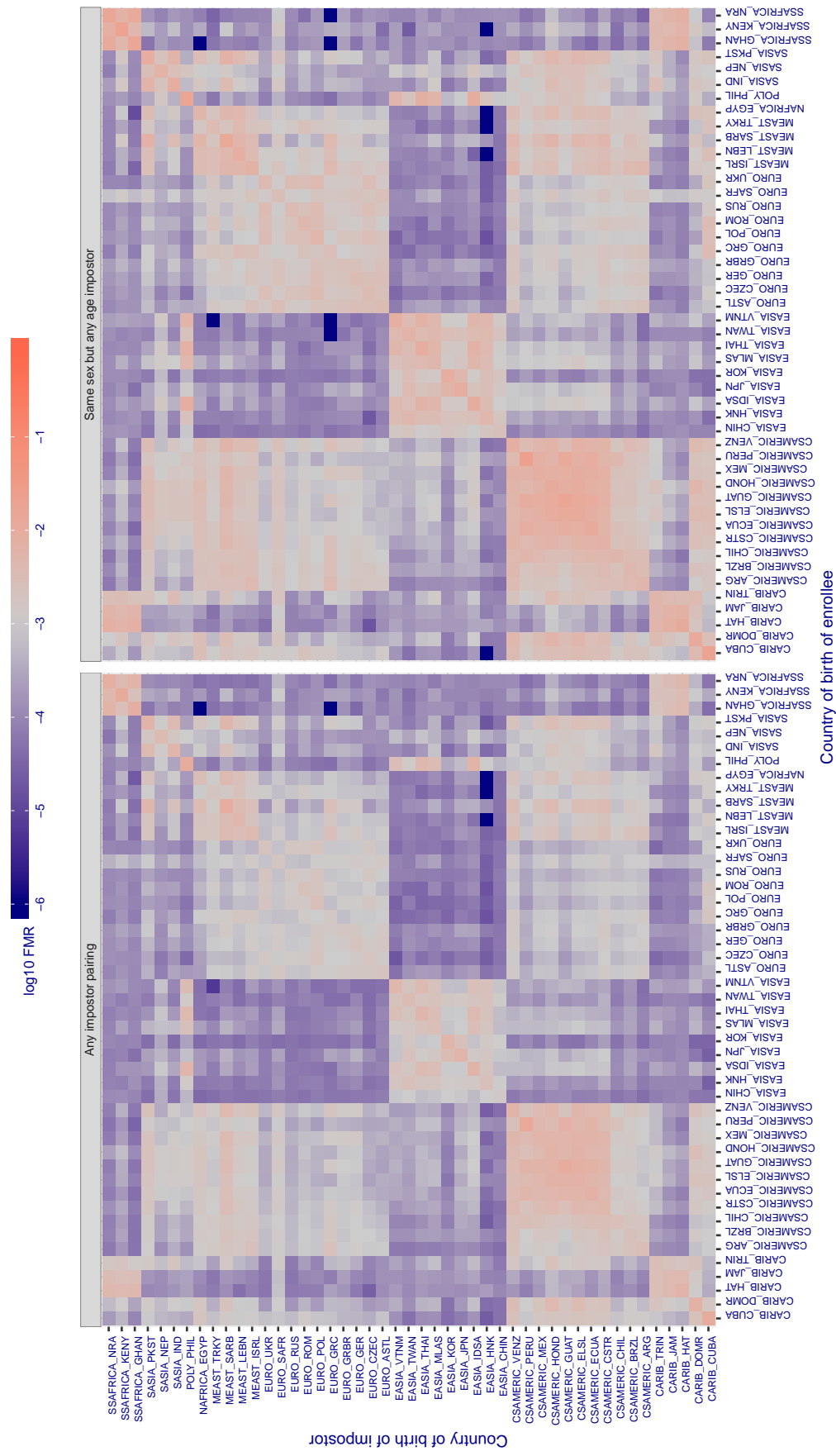


Figure 418: For algorithm tongyi-005 operating on visa images, the heatmap shows false match rates observed over impostor comparisons of faces from different individuals who were born in the given country pair. False matches are counted against a recognition threshold fixed globally to give the target  $FMR$  in the plot title, computed over all on the order of  $10^{10}$  impostor comparisons. If text appears in each box it give the same quantity as that coded by the color. Grey indicates  $FMR$  is at the intended  $FMR$  target level. Light red colors present a security vulnerability to, for example, a passport gate. Each +1 increase in  $\log_{10} FMR$  corresponds to a factor of 10 increase in  $FMR$ . The matrix is not quite symmetric because images in the enrollment and verification sets are different.

**Cross country FMR at threshold  $T = 0.599$  for algorithm toshiba\_002, giving  $FMR(T) = 0.001$  globally.**

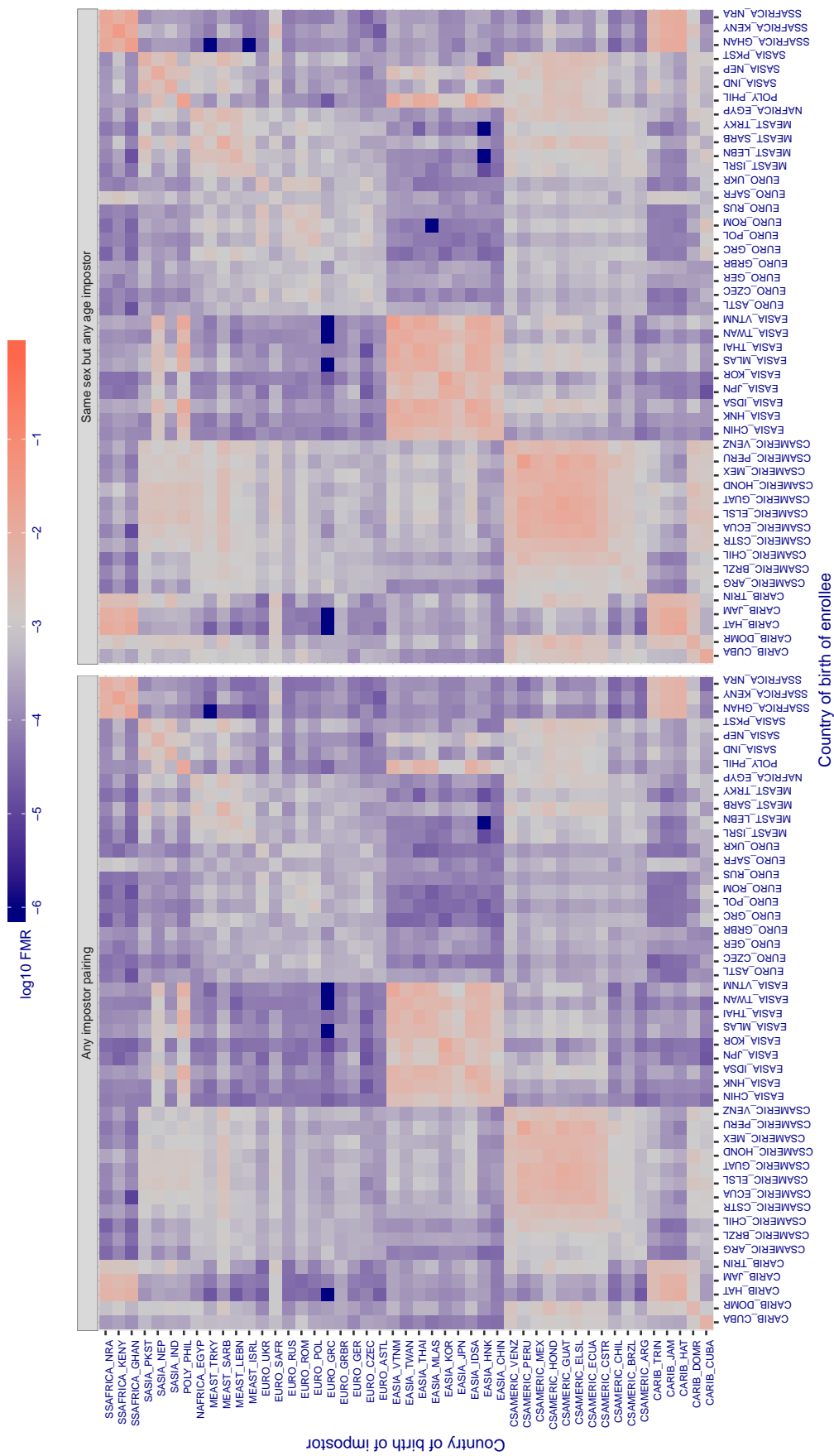


Figure 419: For algorithm toshiba-002 operating on visa images, the heatmap shows false match rates observed over impostor comparisons of faces from different individuals who were born in the given country pair. False matches are counted against a recognition threshold fixed globally to give the target  $FMR$  in the plot title, computed over all on the order of  $10^{10}$  impostor comparisons. If text appears in each box it give the same quantity as that coded by the color. Grey indicates  $FMR$  is at the intended  $FMR$  target level. Light red colors present a security vulnerability to, for example, a passport gate. Each +1 increase in  $\log_{10} FMR$  corresponds to a factor of 10 increase in  $FMR$ . The matrix is not quite symmetric because images in the enrollment and verification sets are different.

**Cross country FMR at threshold  $T = 0.596$  for algorithm toshiba\_003, giving  $FMR(T) = 0.001$  globally.**

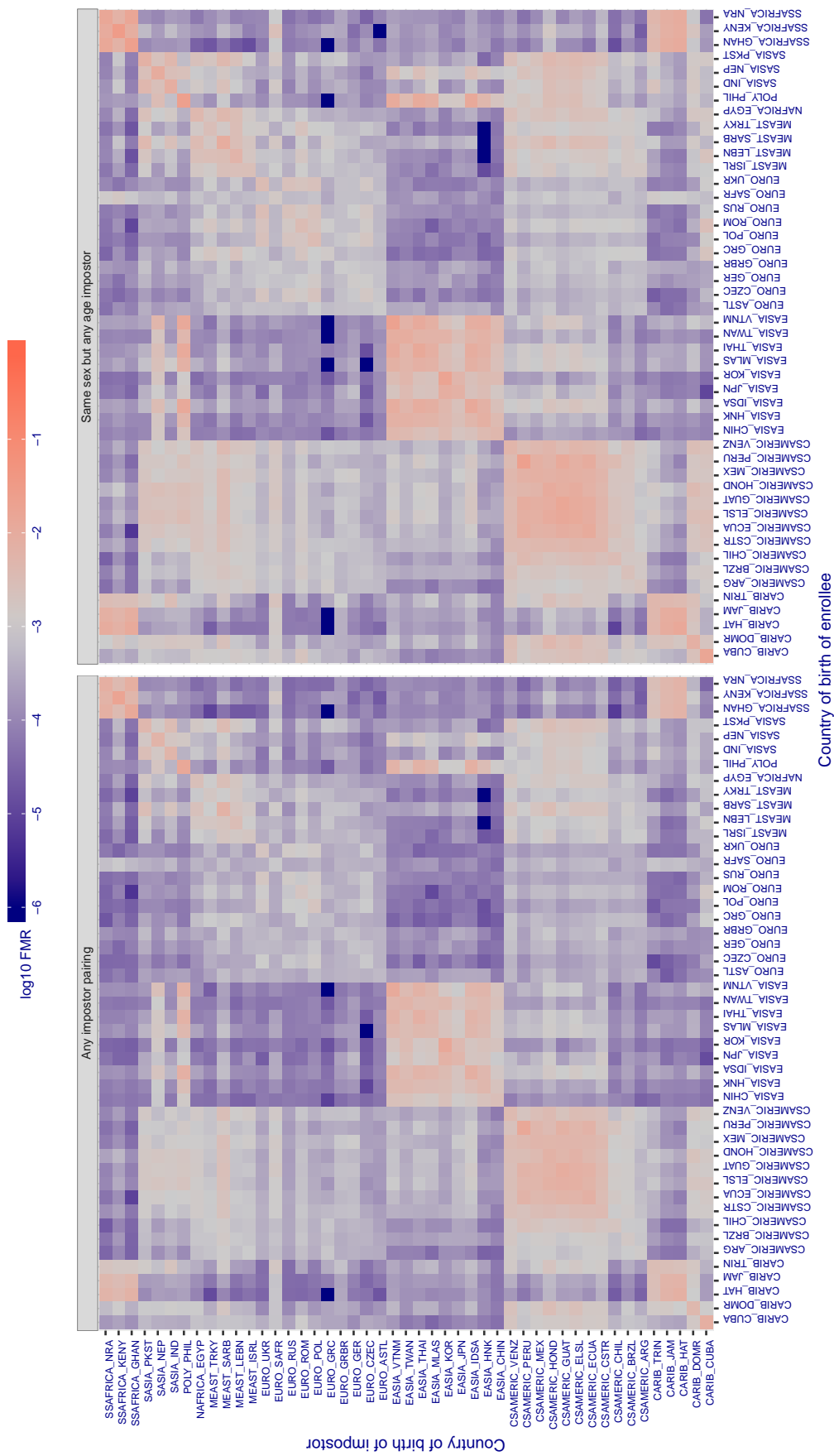


Figure 420: For algorithm toshiba-003 operating on visa images, the heatmap shows false match rates observed over impostor comparisons of faces from different individuals who were born in the given country pair. False matches are counted against a recognition threshold fixed globally to give the target  $FMR$  in the plot title, computed over all on the order of  $10^{10}$  impostor comparisons. If text appears in each box it give the same quantity as that coded by the color. Grey indicates  $FMR$  is at the intended  $FMR$  target level. Light red colors present a security vulnerability to, for example, a passport gate. Each +1 increase in  $\log_{10} FMR$  corresponds to a factor of 10 increase in  $FMR$ . The matrix is not quite symmetric because images in the enrollment and verification sets are different.

**Cross country FMR at threshold T = 0.278 for algorithm trueface\_000, giving  $FMR(T) = 0.001$  globally.**

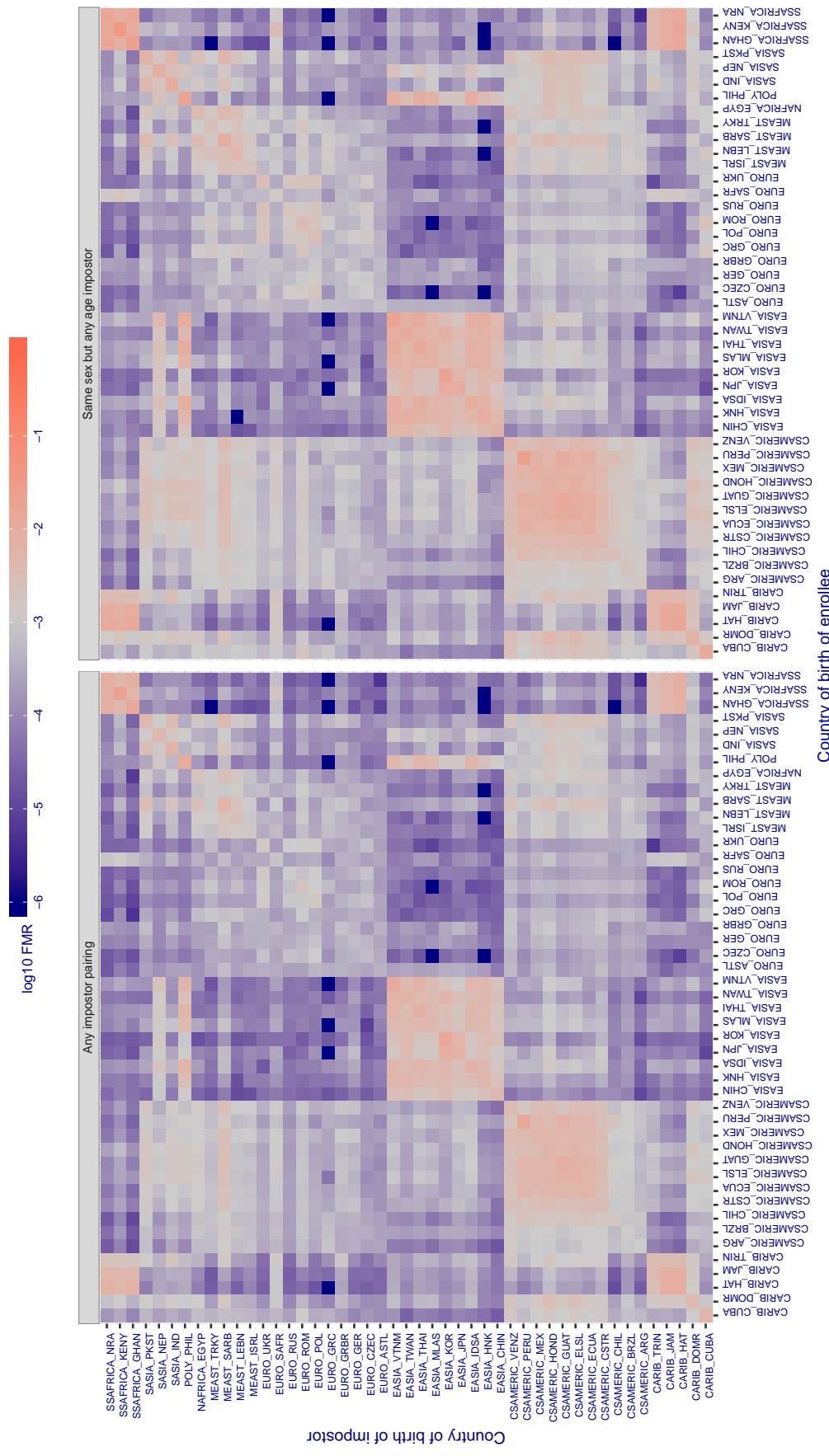


Figure 421: For algorithm trueface-000 operating on visa images, the heatmap shows false match rates observed over impostor comparisons of faces from different individuals who were born in the given country pair. False matches are counted against a recognition threshold fixed globally to give the target  $FMR$  in the plot title, computed over all on the order of  $10^{10}$  impostor comparisons. If text appears in each box it give the same quantity as that coded by the color. Grey indicates  $FMR$  is at the intended  $FMR$  target level. Light red colors present a security vulnerability to, for example, a passport gate. Each +1 increase in  $\log_{10} FMR$  corresponds to a factor of 10 increase in  $FMR$ . The matrix is not quite symmetric because images in the enrollment and verification sets are different.

**Cross country FMR at threshold T = 0.048 for algorithm ulsee\_001, giving FMR(T) = 0.001 globally.**

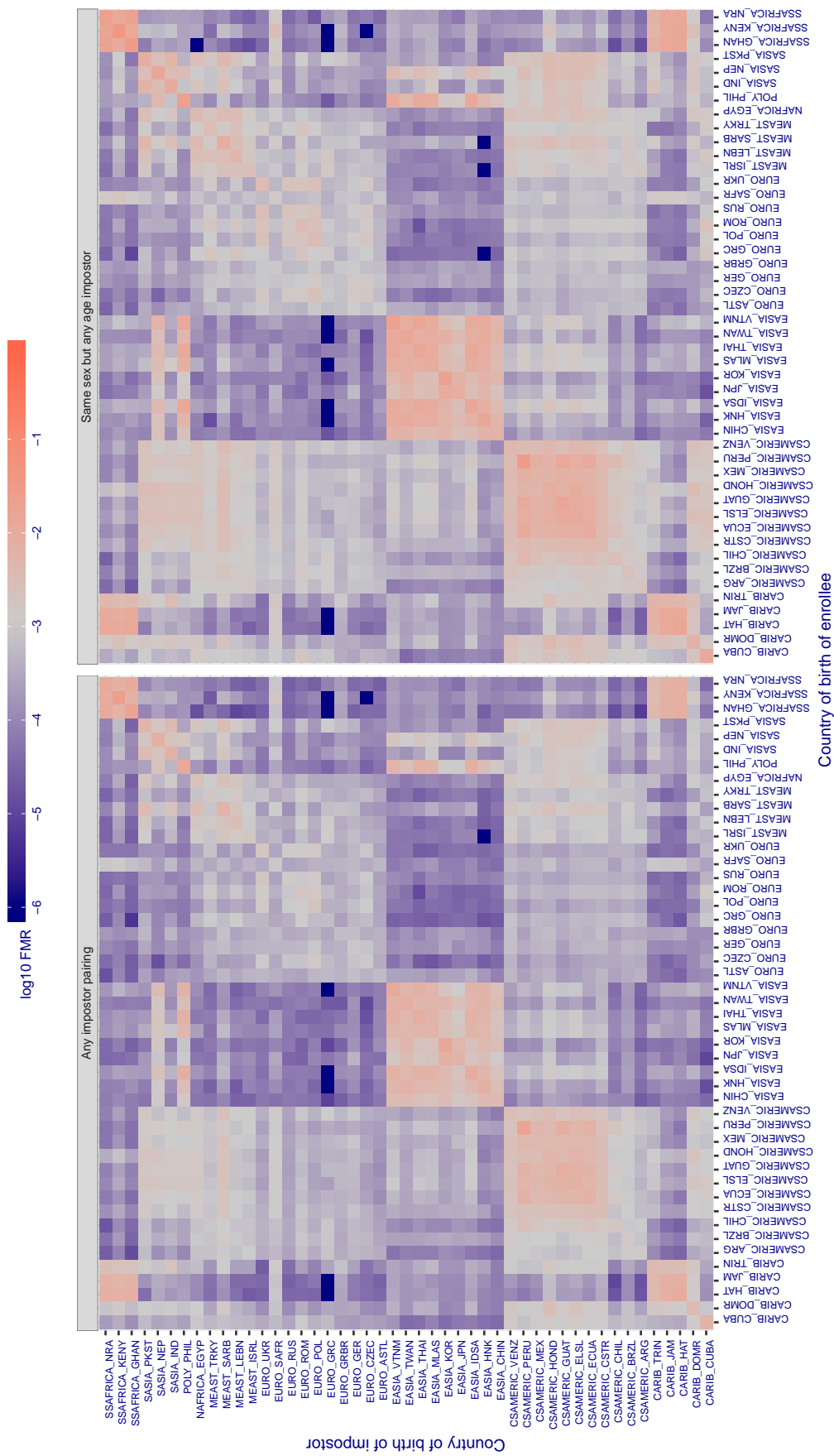


Figure 422: For algorithm ulsee-001 operating on visa images, the heatmap shows false match rates observed over impostor comparisons of faces from different individuals who were born in the given country pair. False matches are counted against a recognition threshold fixed globally to give the target FMR in the plot title, computed over all on the order of  $10^{10}$  impostor comparisons. If text appears in each box it give the same quantity as that coded by the color. Grey indicates FMR is at the intended FMR target level. Light red colors present a security vulnerability to, for example, a passport gate. Each +1 increase in  $\log_{10} \text{FMR}$  corresponds to a factor of 10 increase in FMR. The matrix is not quite symmetric because images in the enrollment and verification sets are different.

**Cross country FMR at threshold  $T = 0.681$  for algorithm uluface\_002, giving  $\text{FMR}(T) = 0.001$  globally.**

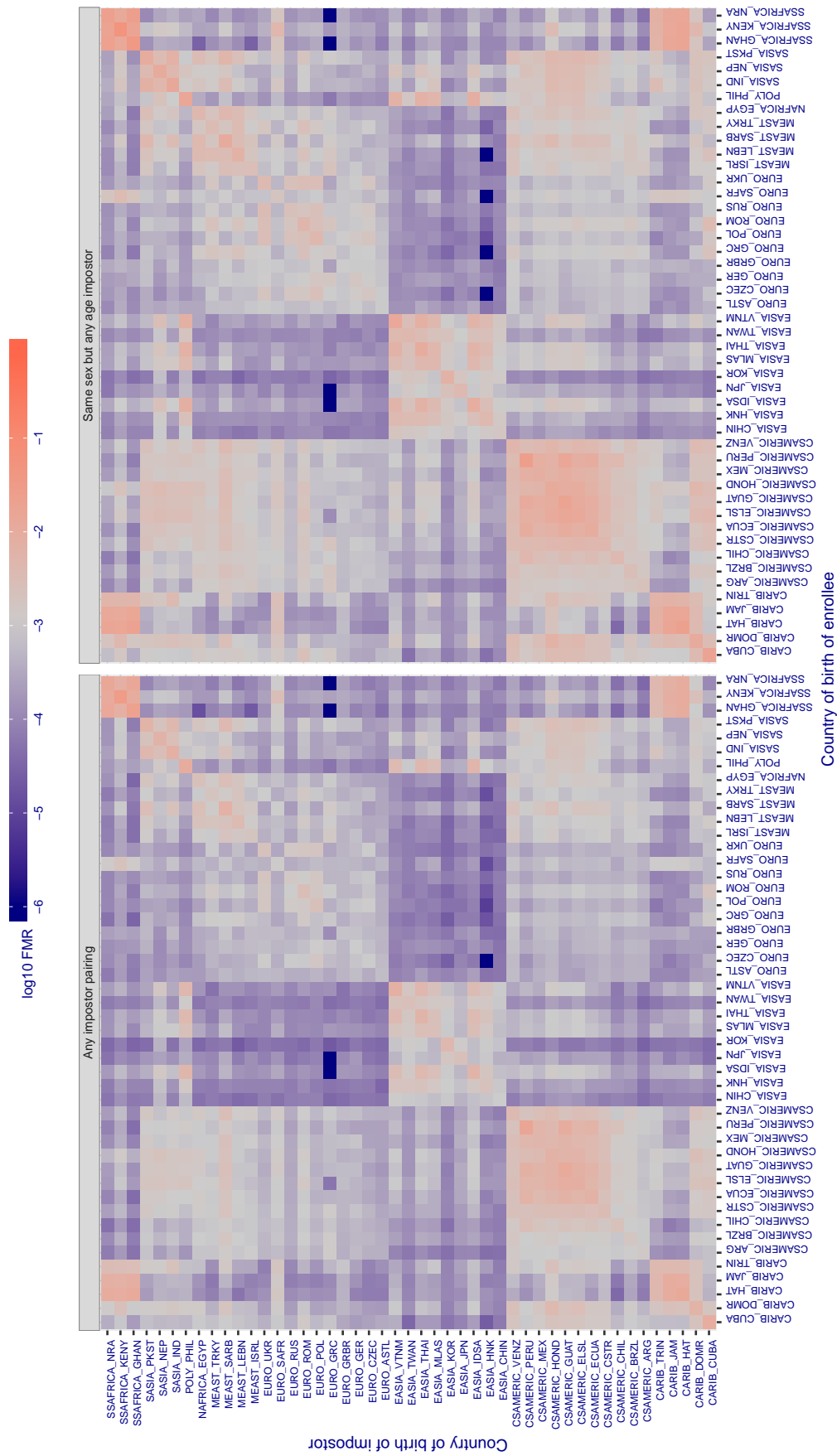


Figure 423: For algorithm uluface-002 operating on visa images, the heatmap shows false match rates observed over impostor comparisons of faces from different individuals who were born in the given country pair. False matches are counted against a recognition threshold fixed globally to give the target  $\text{FMR}$  in the plot title, computed over all on the order of  $10^{10}$  impostor comparisons. If text appears in each box it give the same quantity as that coded by the color. Grey indicates  $\text{FMR}$  is at the intended  $\text{FMR}$  target level. Light red colors present a security vulnerability to, for example, a passport gate. Each +1 increase in  $\log_{10} \text{FMR}$  corresponds to a factor of 10 increase in  $\text{FMR}$ . The matrix is not quite symmetric because images in the enrollment and verification sets are different.

**Cross country FMR at threshold T = 0.384 for algorithm upc\_001, giving  $\text{FMR}(T) = 0.001$  globally.**

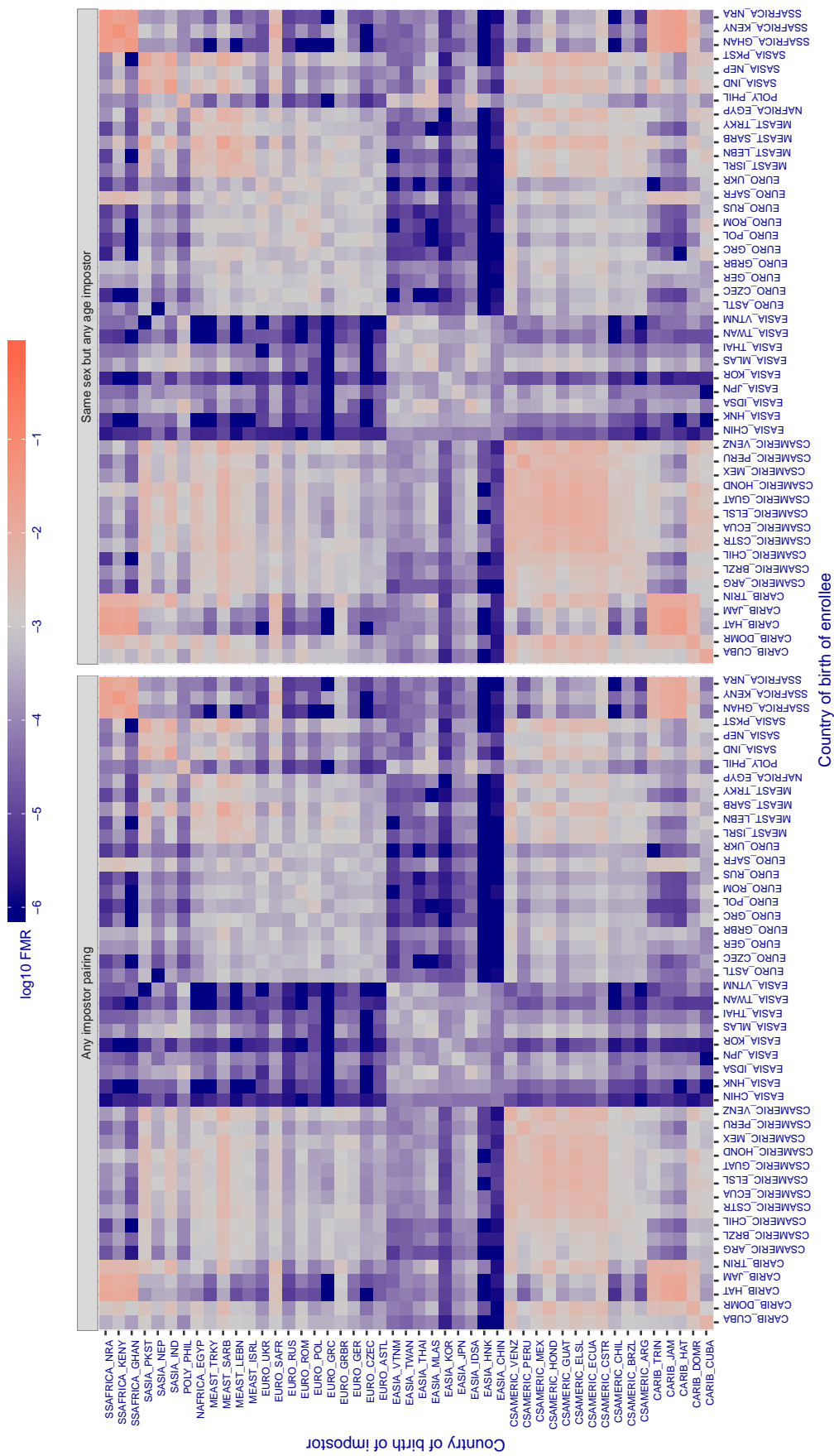


Figure 424: For algorithm upc-001 operating on visa images, the heatmap shows false match rates observed over impostor comparisons of faces from different individuals who were born in the given country pair. False matches are counted against a recognition threshold fixed globally to give the target FMR in the plot title, computed over all on the order of  $10^{10}$  impostor comparisons. If text appears in each box it give the same quantity as that coded by the color. Grey indicates FMR is at the intended FMR target level. Light red colors present a security vulnerability to, for example, a passport gate. Each +1 increase in  $\log_{10} \text{FMR}$  corresponds to a factor of 10 increase in FMR. The matrix is not quite symmetric because images in the enrollment and verification sets are different.

**Cross country FMR at threshold T = 0.310 for algorithm vcog\_002, giving FMR(T) = 0.001 globally.**

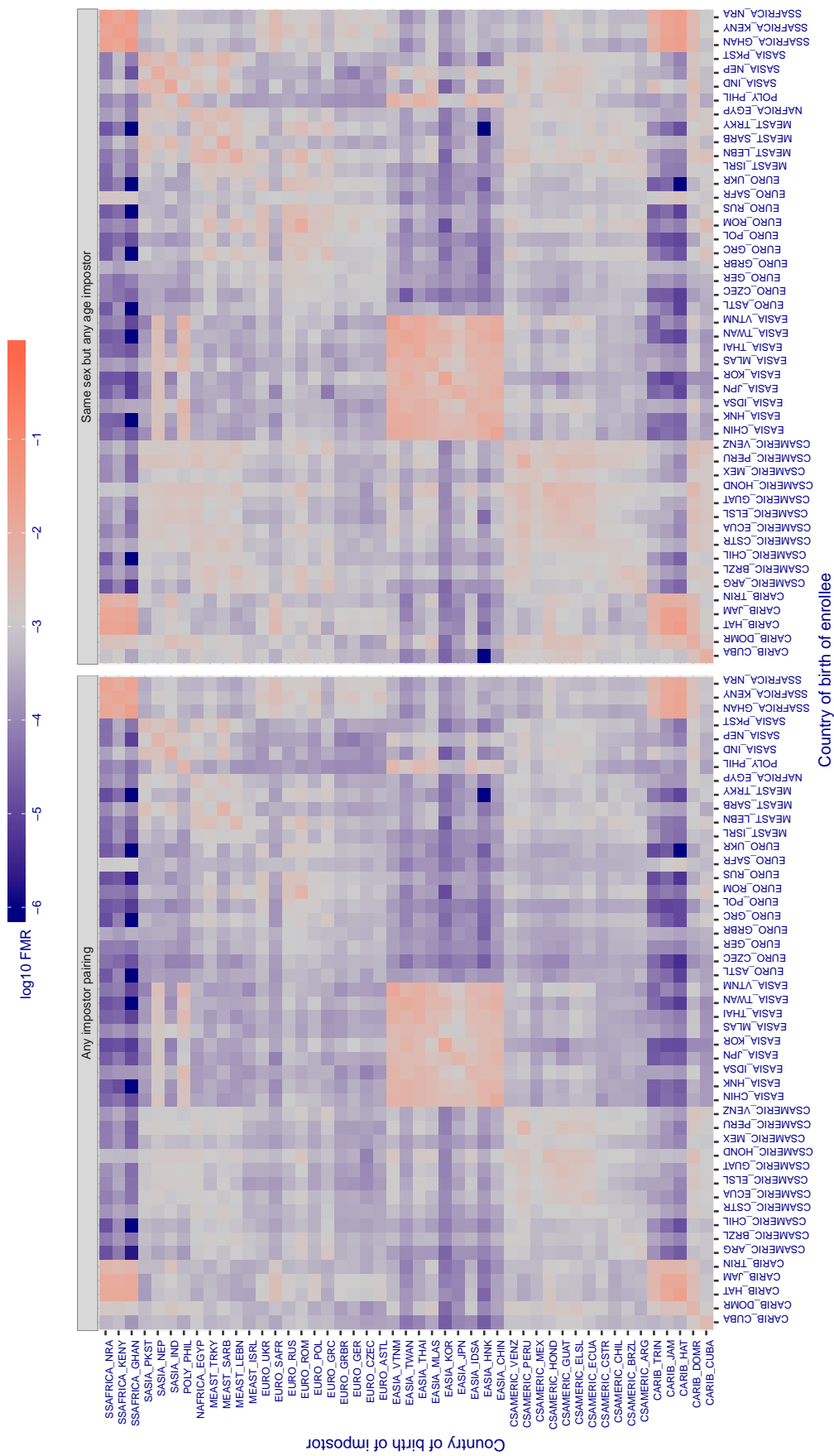


Figure 425: For algorithm vcog-002 operating on visa images, the heatmap shows false match rates observed over impostor comparisons of faces from different individuals who were born in the given country pair. False matches are counted against a recognition threshold fixed globally to give the target FMR in the plot title, computed over all on the order of  $10^{10}$  impostor comparisons. If text appears in each box it give the same quantity as that coded by the color. Grey indicates FMR is at the intended FMR target level. Light red colors present a security vulnerability to, for example, a passport gate. Each +1 increase in  $\log_{10} FMR$  corresponds to a factor of 10 increase in FMR. The matrix is not quite symmetric because images in the enrollment and verification sets are different.

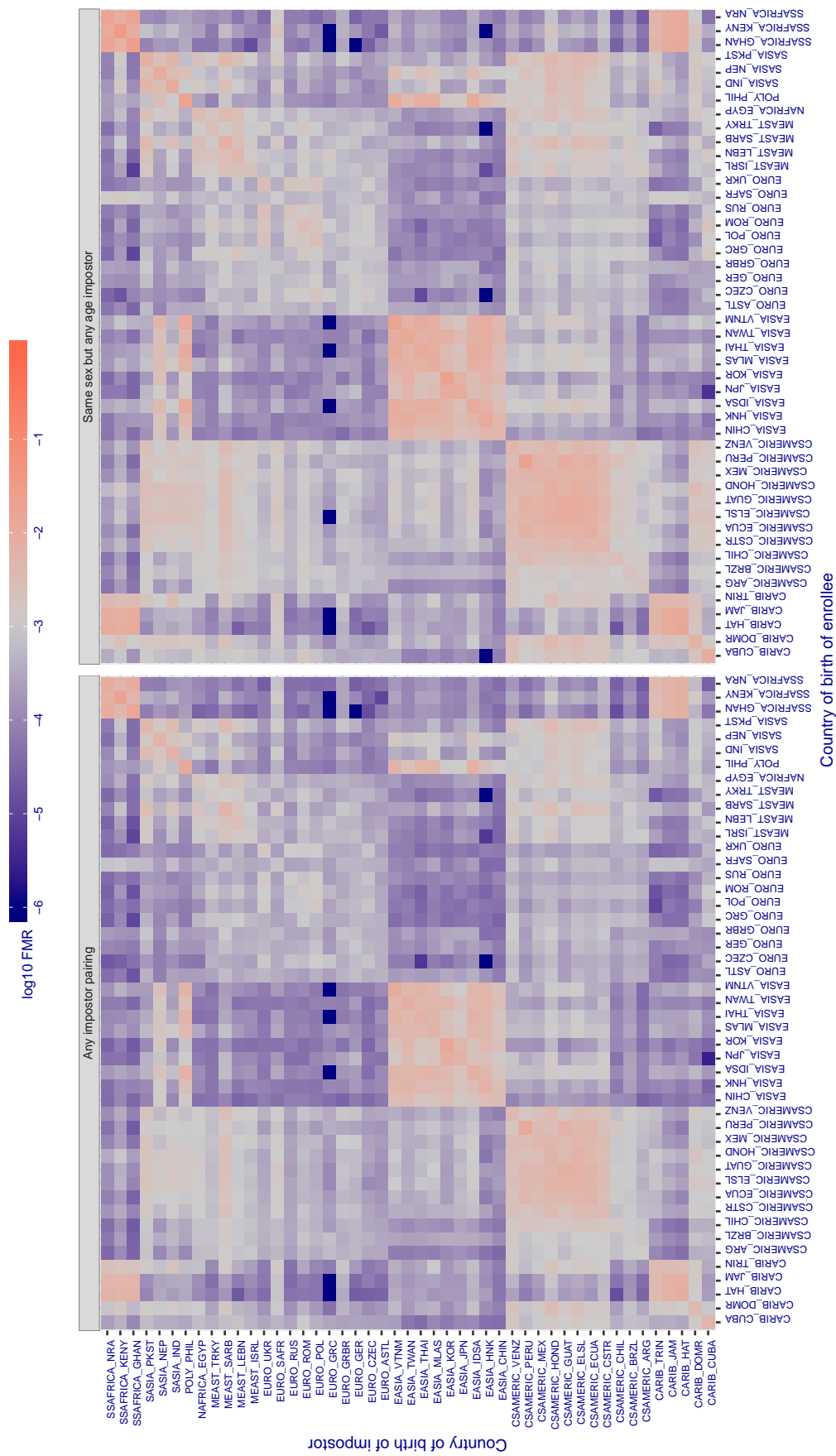
**Cross country FMR at threshold T = 66.962 for algorithm vd\_001, giving FMR(T) = 0.001 globally.**

Figure 426: For algorithm vd-001 operating on visa images, the heatmap shows false match rates observed over impostor comparisons of faces from different individuals who were born in the given country pair. False matches are counted against a recognition threshold fixed globally to give the target FMR in the plot title, computed over all on the order of  $10^{10}$  impostor comparisons. If text appears in each box it give the same quantity as that coded by the color. Grey indicates FMR is at the intended FMR target level. Light red colors present a security vulnerability to, for example, a passport gate. Each +1 increase in  $\log_{10} \text{FMR}$  corresponds to a factor of 10 increase in FMR. The matrix is not quite symmetric because images in the enrollment and verification sets are different.

**Cross country FMR at threshold T = 2.897 for algorithm veridas\_001, giving  $\text{FMR}(T) = 0.001$  globally.**

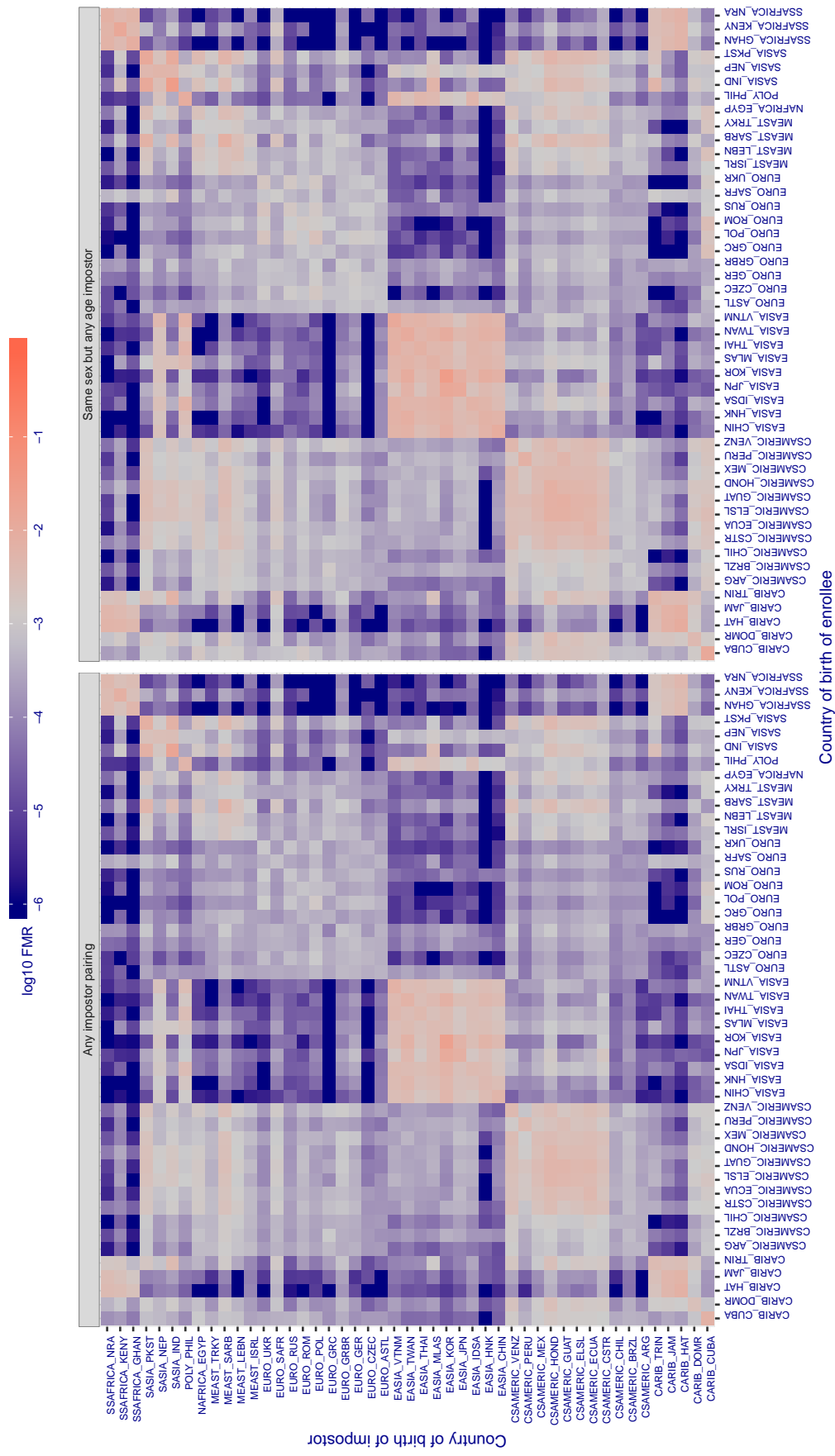


Figure 427: For algorithm veridas-001 operating on visa images, the heatmap shows false match rates observed over impostor comparisons of faces from different individuals who were born in the given country pair. False matches are counted against a recognition threshold fixed globally to give the target  $\text{FMR}$  in the plot title, computed over all on the order of  $10^{10}$  impostor comparisons. If text appears in each box it give the same quantity as that coded by the color. Grey indicates  $\text{FMR}$  is at the intended  $\text{FMR}$  target level. Light red colors present a security vulnerability to, for example, a passport gate. Each +1 increase in  $\log_{10} \text{FMR}$  corresponds to a factor of 10 increase in  $\text{FMR}$ . The matrix is not quite symmetric because images in the enrollment and verification sets are different.

**Cross country FMR at threshold  $T = 3.010$  for algorithm veridas\_002, giving  $\text{FMR}(T) = 0.001$  globally.**

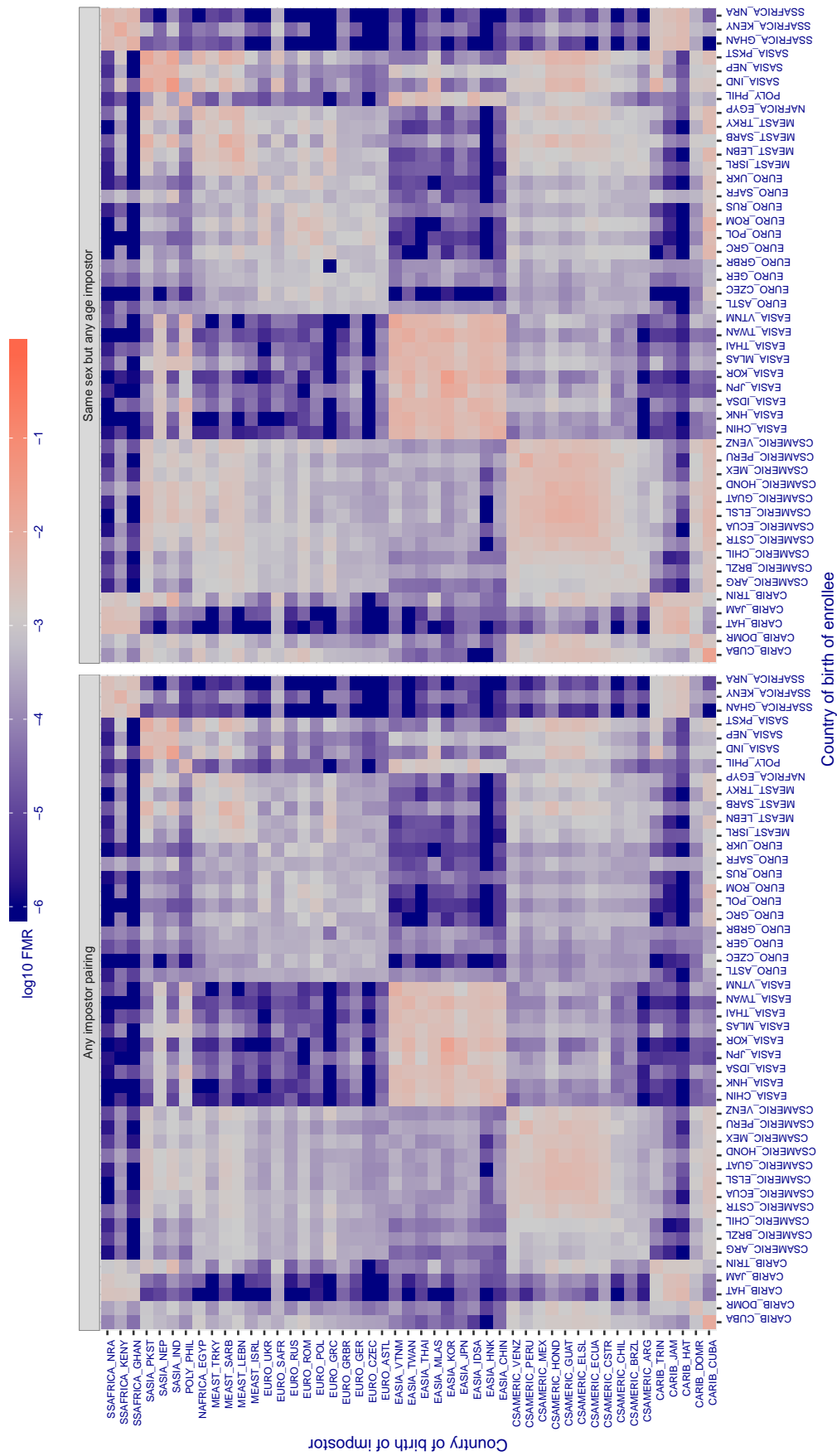


Figure 428: For algorithm veridas-002 operating on visa images, the heatmap shows false match rates observed over impostor comparisons of faces from different individuals who were born in the given country pair. False matches are counted against a recognition threshold fixed globally to give the target FMR in the plot title, computed over all on the order of  $10^{10}$  impostor comparisons. If text appears in each box it give the same quantity as that coded by the color. Grey indicates FMR is at the intended FMR target level. Light red colors present a security vulnerability to, for example, a passport gate. Each +1 increase in  $\log_{10} \text{FMR}$  corresponds to a factor of 10 increase in FMR. The matrix is not quite symmetric because images in the enrollment and verification sets are different.

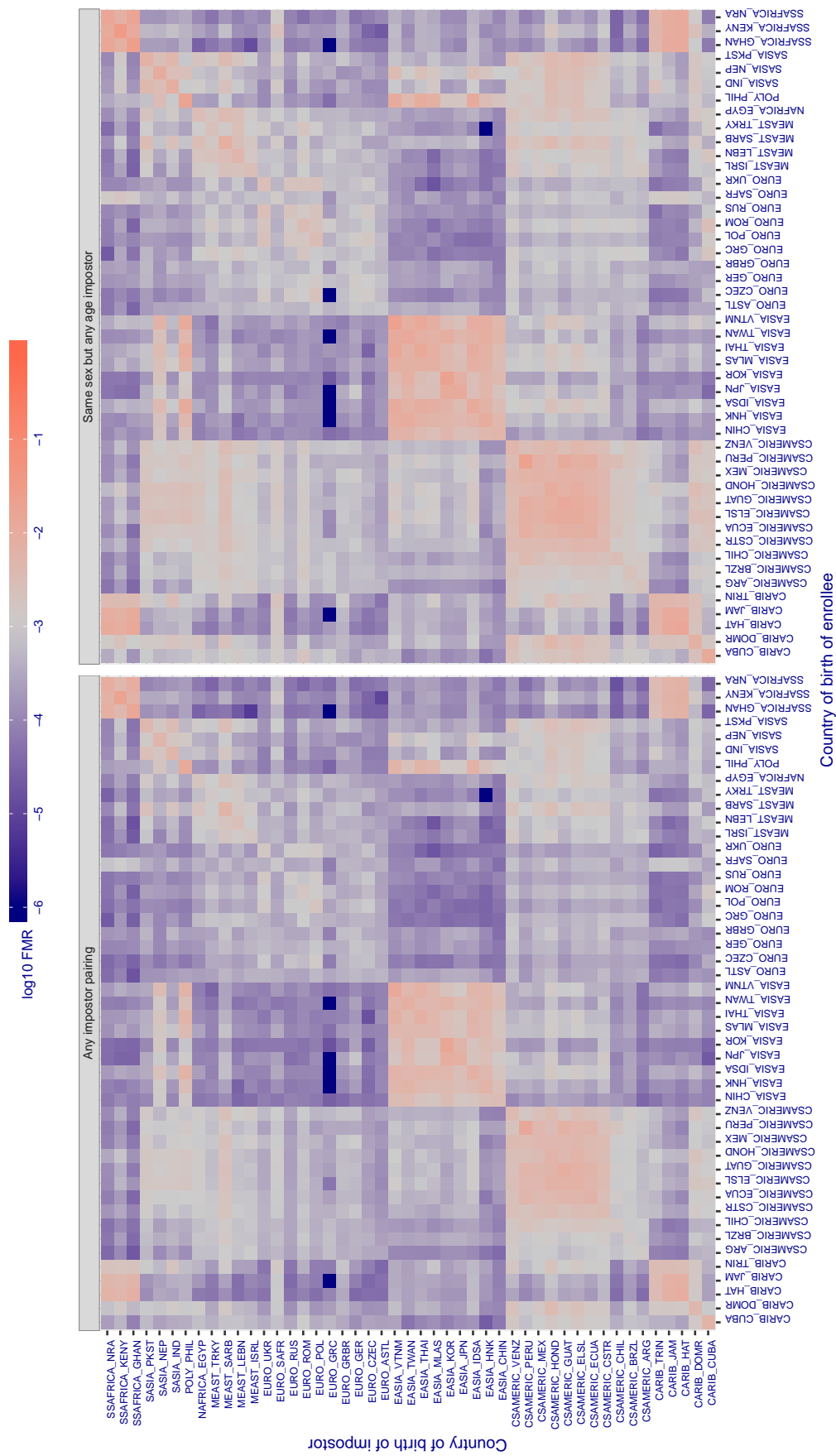
**Cross country FMR at threshold T = 2.677 for algorithm via\_000, giving FMR(T) = 0.001 globally.**

Figure 429: For algorithm via-000 operating on visa images, the heatmap shows false match rates observed over impostor comparisons of faces from different individuals who were born in the given country pair. False matches are counted against a recognition threshold fixed globally to give the target FMR in the plot title, computed over all on the order of  $10^{10}$  impostor comparisons. If text appears in each box it give the same quantity as that coded by the color. Grey indicates FMR is at the intended FMR target level. Light red colors present a security vulnerability to, for example, a passport gate. Each +1 increase in  $\log_{10}$  FMR corresponds to a factor of 10 increase in FMR. The matrix is not quite symmetric because images in the enrollment and verification sets are different.

**Cross country FMR at threshold T = 0.755 for algorithm videonetics\_001, giving  $\text{FMR}(T) = 0.001$  globally.**

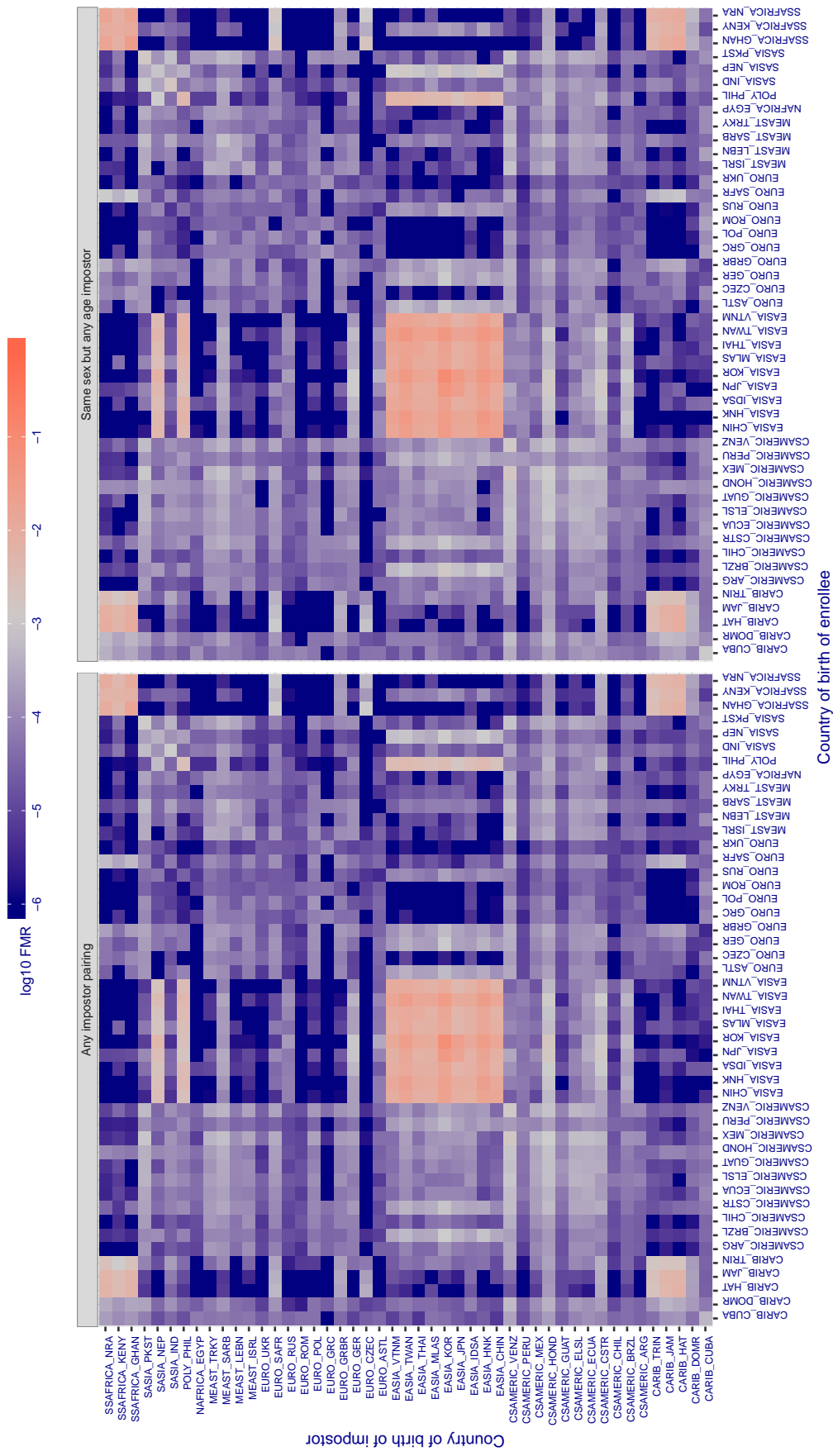


Figure 430: For algorithm videonetics-001 operating on visa images, the heatmap shows false match rates observed over impostor comparisons of faces from different individuals who were born in the given country pair. False matches are counted against a recognition threshold fixed globally to give the target  $\text{FMR}$  in the plot title, computed over all on the order of  $10^{10}$  impostor comparisons. If text appears in each box it give the same quantity as that coded by the color. Grey indicates  $\text{FMR}$  is at the intended  $\text{FMR}$  target level. Light red colors present a security vulnerability to, for example, a passport gate. Each +1 increase in  $\log_{10} \text{FMR}$  corresponds to a factor of 10 increase in  $\text{FMR}$ . The matrix is not quite symmetric because images in the enrollment and verification sets are different.

**Cross country FMR at threshold T = 2.809 for algorithm vigilantsolutions\_006, giving  $\text{FMR}(\text{T}) = 0.001$  globally.**

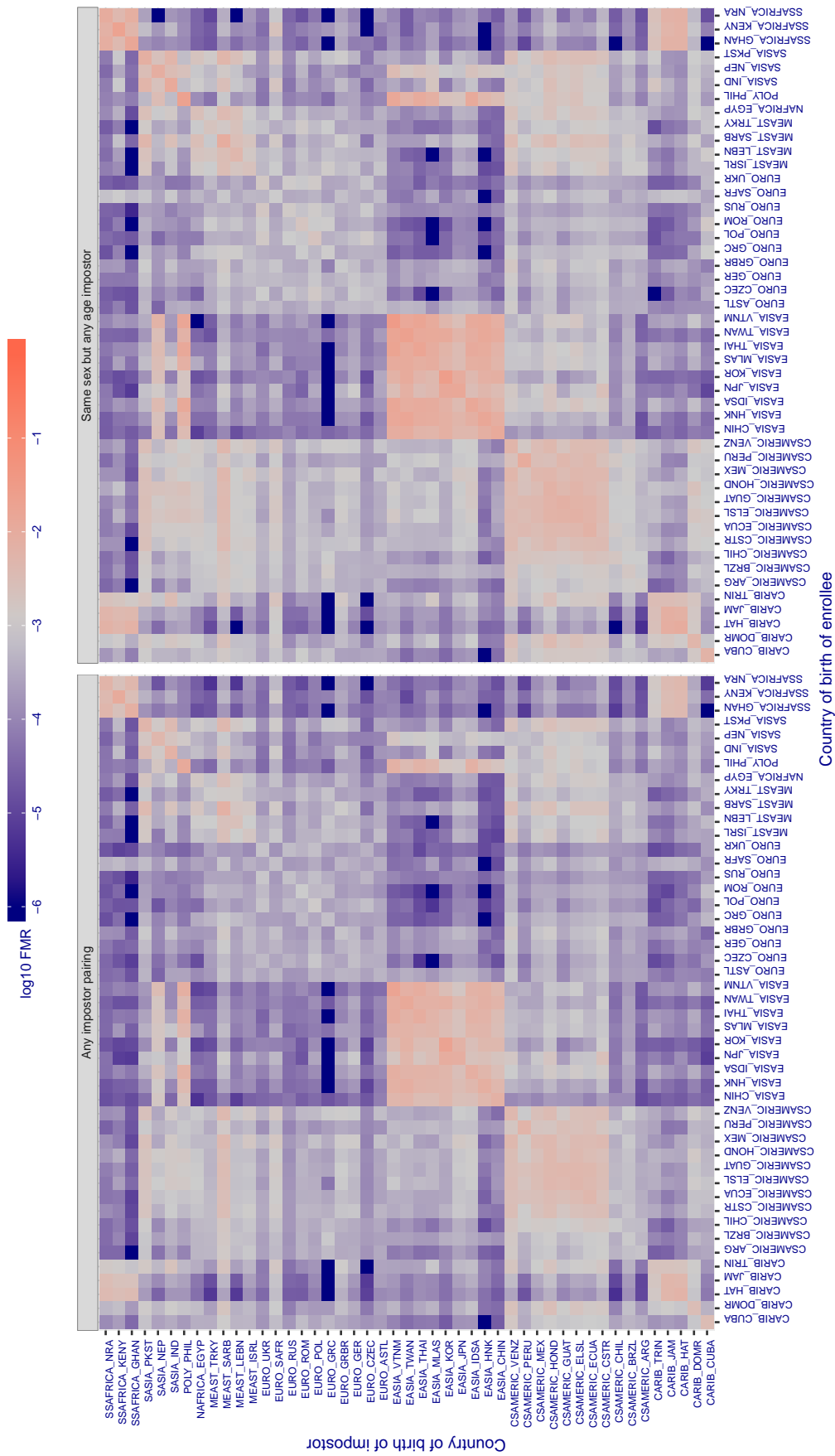


Figure 431: For algorithm vigilantsolutions-006 operating on visa images, the heatmap shows false match rates observed over impostor comparisons of faces from different individuals who were born in the given country pair. False matches are counted against a recognition threshold fixed globally to give the target  $\text{FMR}$  in the plot title, computed over all on the order of  $10^{10}$  impostor comparisons. If text appears in each box it give the same quantity as that coded by the color. Grey indicates  $\text{FMR}$  is at the intended  $\text{FMR}$  target level. Light red colors present a security vulnerability to, for example, a passport gate. Each +1 increase in  $\log_{10} \text{FMR}$  corresponds to a factor of 10 increase in  $\text{FMR}$ . The matrix is not quite symmetric because images in the enrollment and verification sets are different.

**Cross country FMR at threshold T = 2.755 for algorithm vigilantsolutions\_007, giving  $\text{FMR}(\text{T}) = 0.001$  globally.**

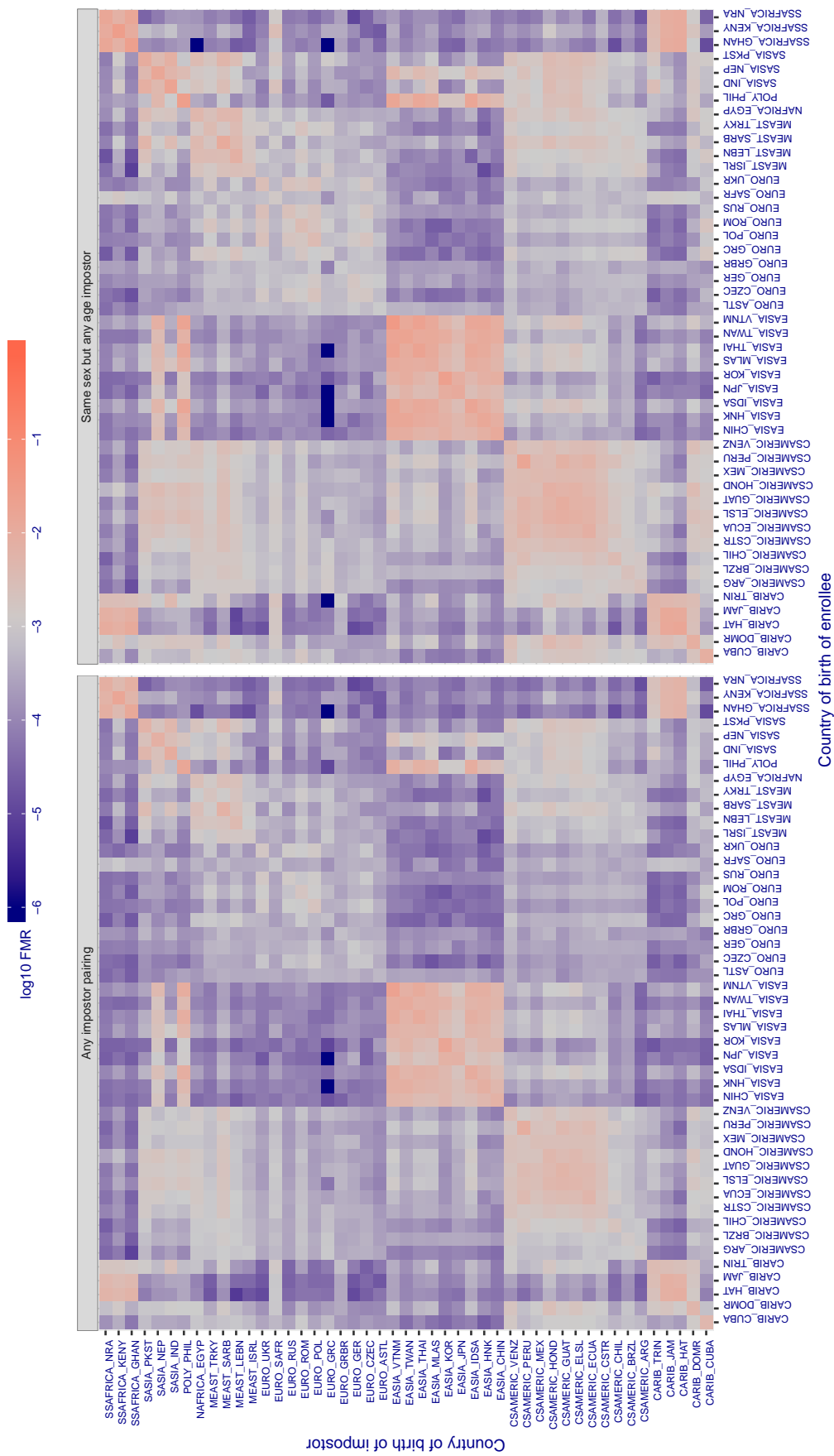


Figure 432: For algorithm vigilantsolutions-007 operating on visa images, the heatmap shows false match rates observed over impostor comparisons of faces from different individuals who were born in the given country pair. False matches are counted against a recognition threshold fixed globally to give the target  $\text{FMR}$  in the plot title, computed over all on the order of  $10^{10}$  impostor comparisons. If text appears in each box it give the same quantity as that coded by the color. Grey indicates  $\text{FMR}$  is at the intended  $\text{FMR}$  target level. Light red colors present a security vulnerability to, for example, a passport gate. Each +1 increase in  $\log_{10} \text{FMR}$  corresponds to a factor of 10 increase in  $\text{FMR}$ . The matrix is not quite symmetric because images in the enrollment and verification sets are different.

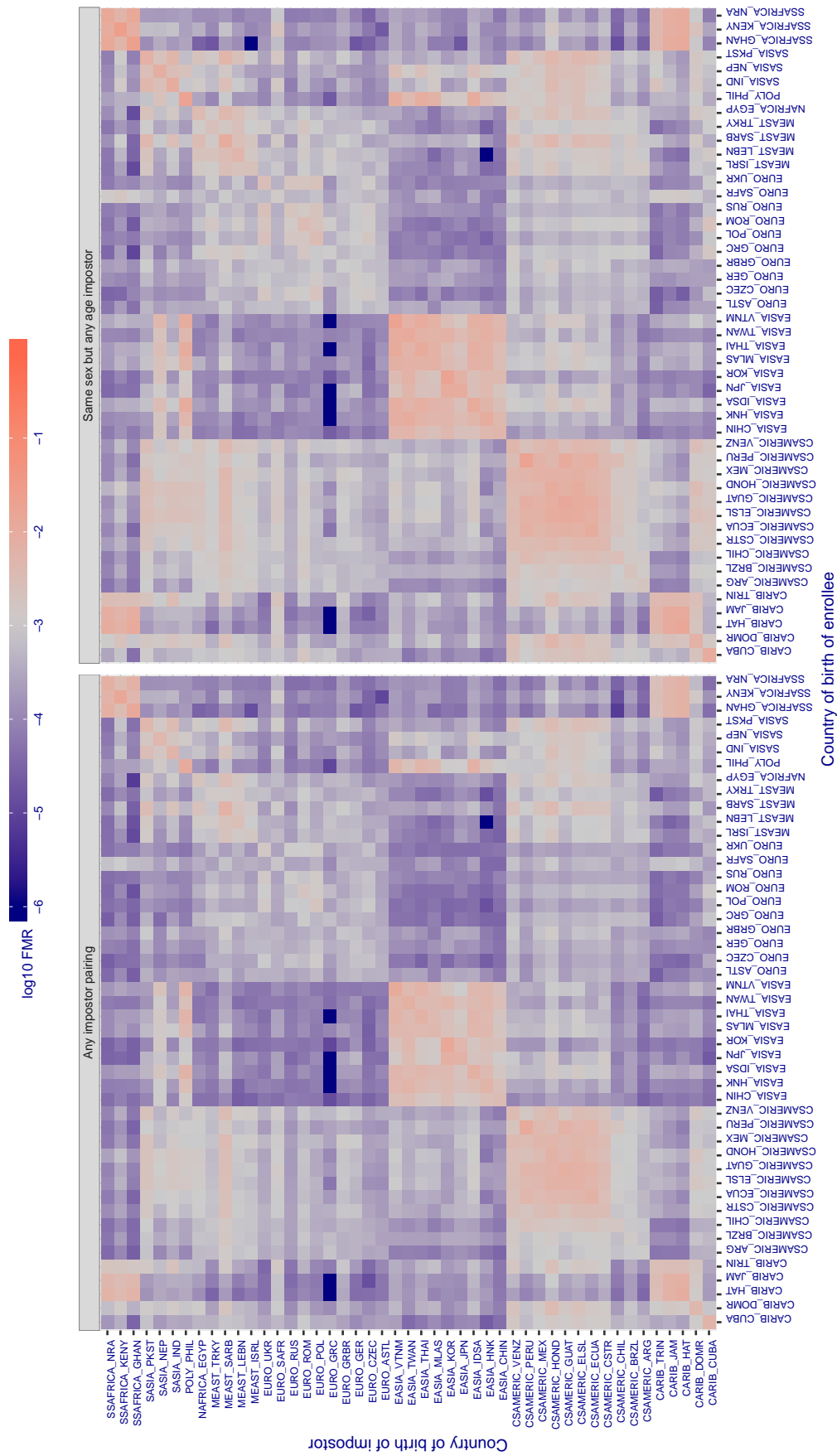
**Cross country FMR at threshold T = 0.336 for algorithm vion\_000, giving FMR(T) = 0.001 globally.**

Figure 433: For algorithm vion-000 operating on visa images, the heatmap shows false match rates observed over impostor comparisons of faces from different individuals who were born in the given country pair. False matches are counted against a recognition threshold fixed globally to give the target FMR in the plot title, computed over all on the order of  $10^{10}$  impostor comparisons. If text appears in each box it give the same quantity as that coded by the color. Grey indicates FMR is at the intended FMR target level. Light red colors present a security vulnerability to, for example, a passport gate. Each +1 increase in  $\log_{10} \text{FMR}$  corresponds to a factor of 10 increase in FMR. The matrix is not quite symmetric because images in the enrollment and verification sets are different.

**Cross country FMR at threshold T = 0.340 for algorithm visionbox\_000, giving FMR(T) = 0.001 globally.**

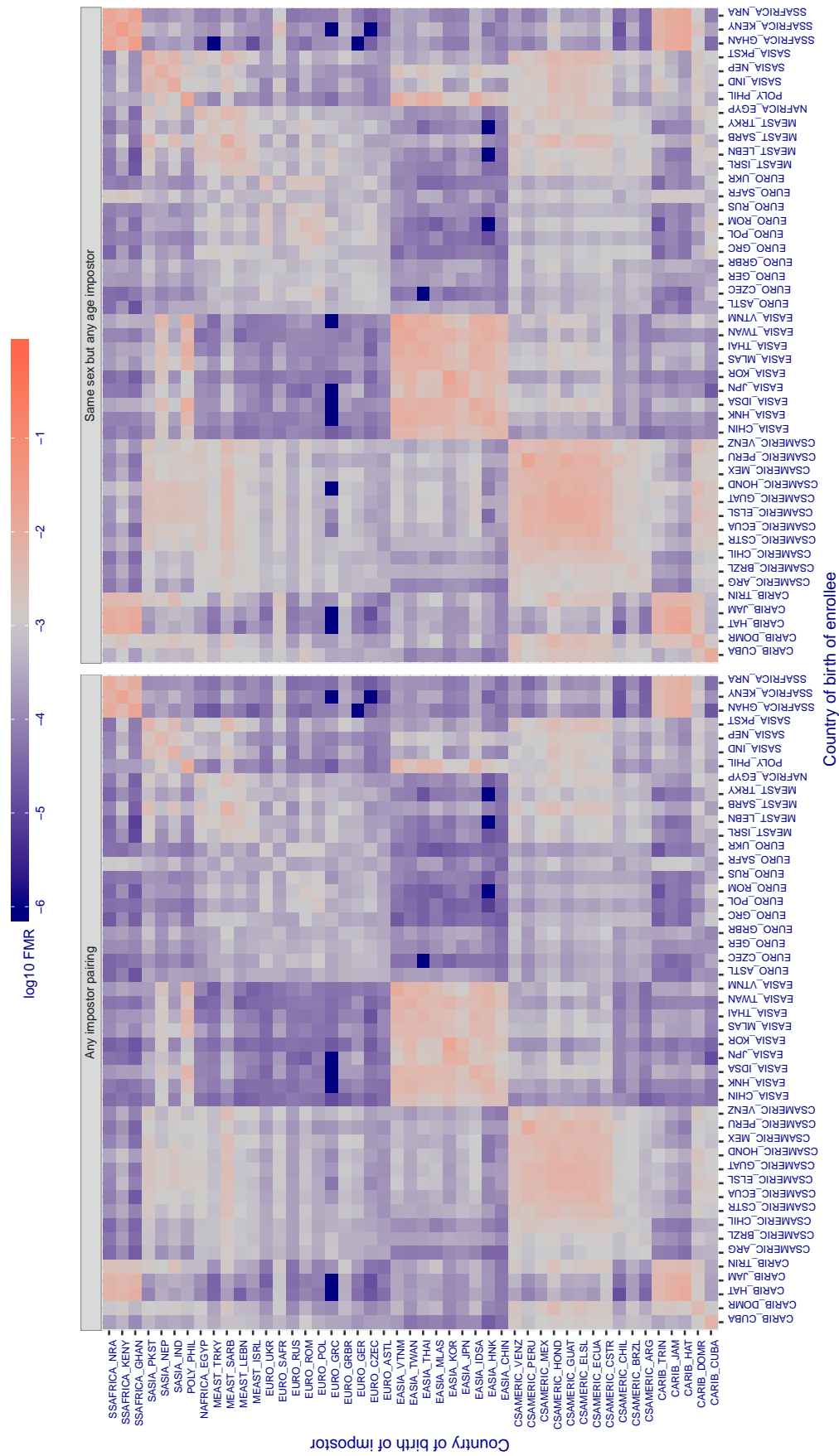


Figure 434: For algorithm visionbox-000 operating on visa images, the heatmap shows false match rates observed over impostor comparisons of faces from different individuals who were born in the given country pair. False matches are counted against a recognition threshold fixed globally to give the target FMR in the plot title, computed over all on the order of  $10^{10}$  impostor comparisons. If text appears in each box it give the same quantity as that coded by the color. Grey indicates FMR is at the intended FMR target level. Light red colors present a security vulnerability to, for example, a passport gate. Each +1 increase in  $\log_{10} FMR$  corresponds to a factor of 10 increase in FMR. The matrix is not quite symmetric because images in the enrollment and verification sets are different.

**Cross country FMR at threshold T = 0.296 for algorithm visionbox\_001, giving  $FMR(T) = 0.001$  globally.**

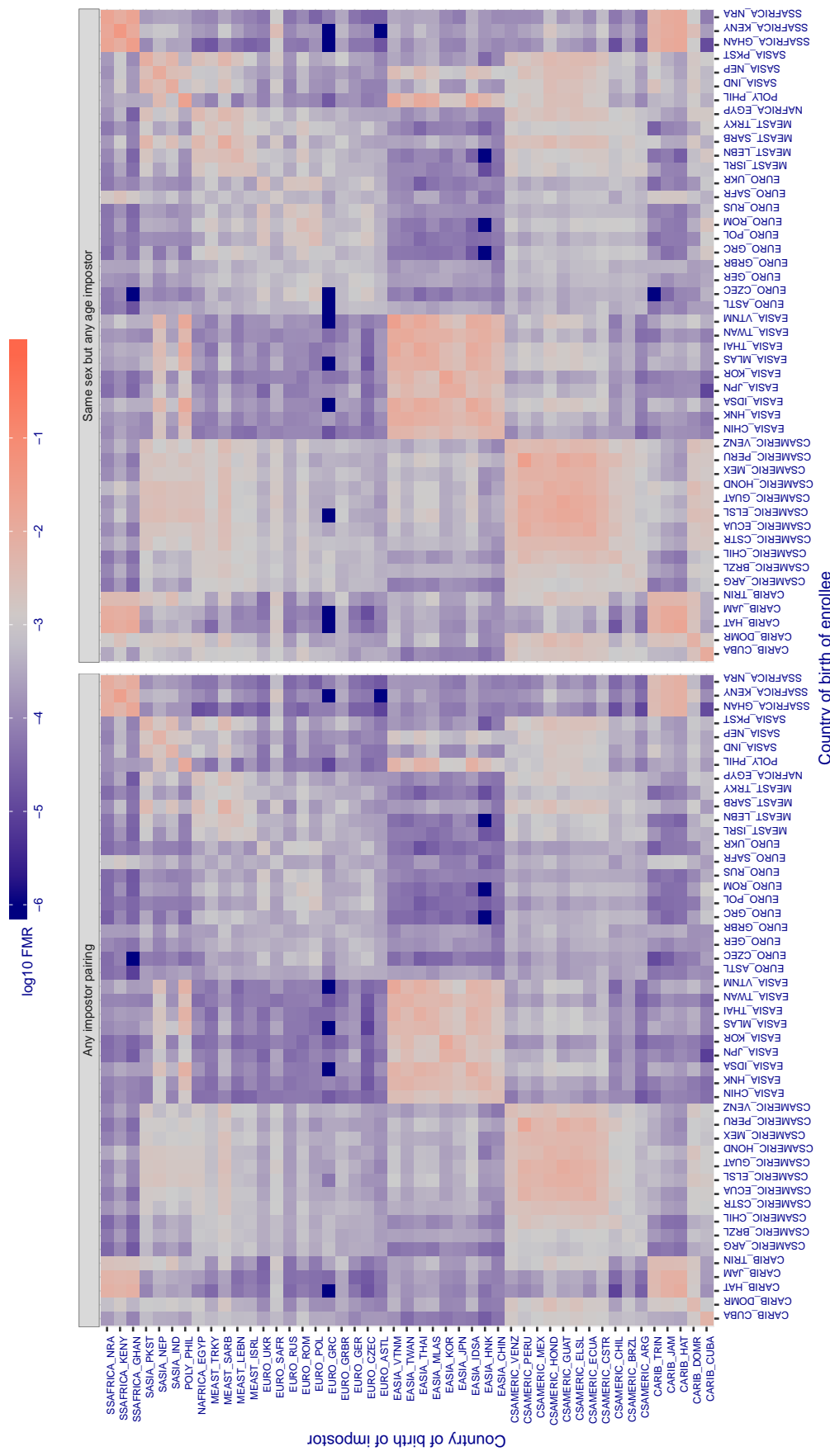


Figure 435: For algorithm visionbox-001 operating on visa images, the heatmap shows false match rates observed over impostor comparisons of faces from different individuals who were born in the given country pair. False matches are counted against a recognition threshold fixed globally to give the target  $FMR$  in the plot title, computed over all on the order of  $10^{10}$  impostor comparisons. If text appears in each box it give the same quantity as that coded by the color. Grey indicates  $FMR$  is at the intended  $FMR$  target level. Light red colors present a security vulnerability to, for example, a passport gate. Each +1 increase in  $\log_{10} FMR$  corresponds to a factor of 10 increase in  $FMR$ . The matrix is not quite symmetric because images in the enrollment and verification sets are different.

**Cross country FMR at threshold T = 0.444 for algorithm visionlabs\_006, giving FMR(T) = 0.001 globally.**

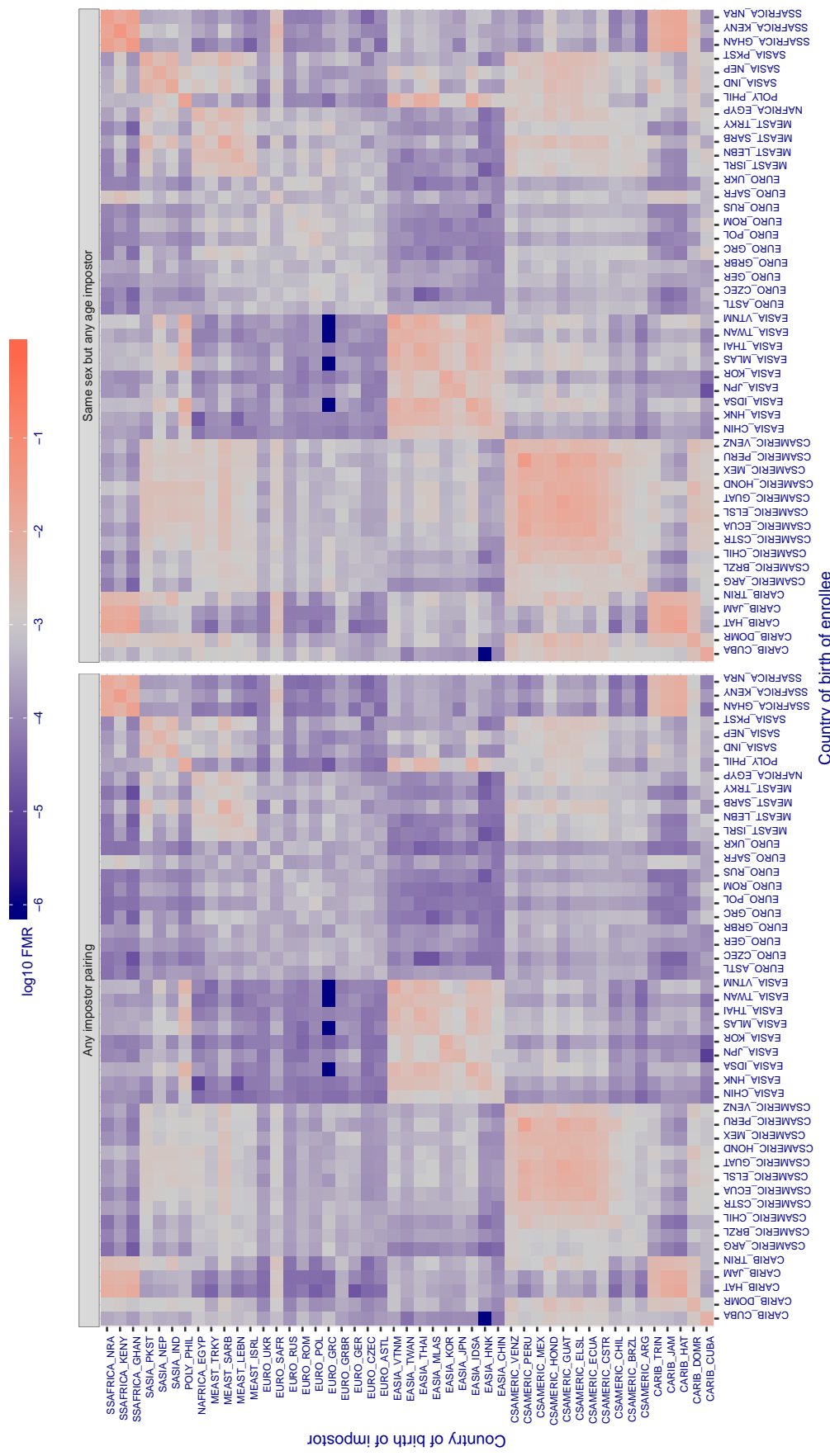


Figure 436: For algorithm visionlabs-006 operating on visa images, the heatmap shows false match rates observed over impostor comparisons of faces from different individuals who were born in the given country pair. False matches are counted against a recognition threshold fixed globally to give the target FMR in the plot title, computed over all on the order of  $10^{10}$  impostor comparisons. If text appears in each box it give the same quantity as that coded by the color. Grey indicates FMR is at the intended FMR target level. Light red colors present a security vulnerability to, for example, a passport gate. Each +1 increase in  $\log_{10} FMR$  corresponds to a factor of 10 increase in FMR. The matrix is not quite symmetric because images in the enrollment and verification sets are different.

**Cross country FMR at threshold T = 0.459 for algorithm visionlabs\_007, giving FMR(T) = 0.001 globally.**

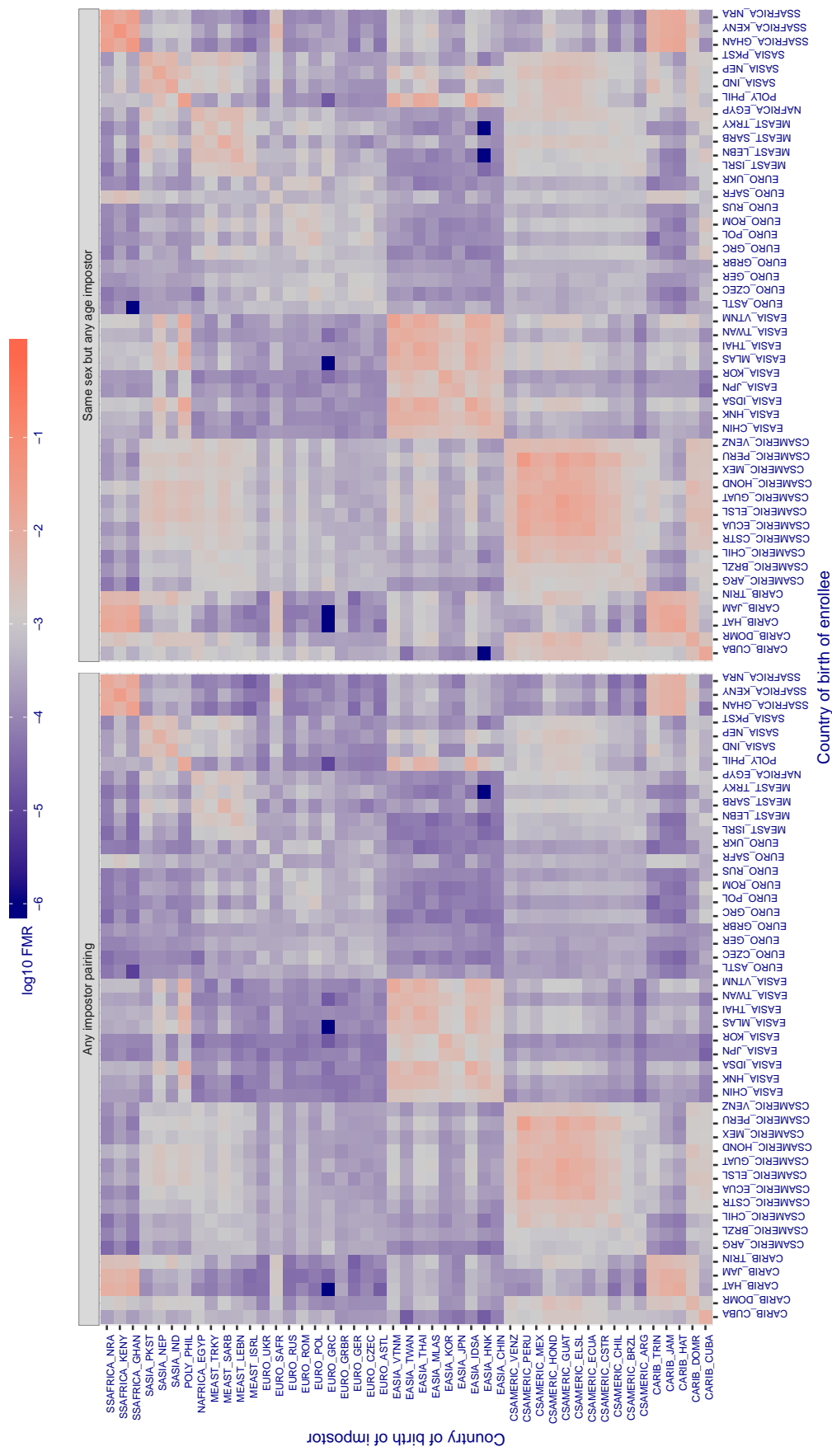


Figure 437: For algorithm visionlabs-007 operating on visa images, the heatmap shows false match rates observed over impostor comparisons of faces from different individuals who were born in the given country pair. False matches are counted against a recognition threshold fixed globally to give the target FMR in the plot title, computed over all on the order of  $10^{10}$  impostor comparisons. If text appears in each box it give the same quantity as that coded by the color. Grey indicates FMR is at the intended FMR target level. Light red colors present a security vulnerability to, for example, a passport gate. Each +1 increase in  $\log_{10} \text{FMR}$  corresponds to a factor of 10 increase in FMR. The matrix is not quite symmetric because images in the enrollment and verification sets are different.

**Cross country FMR at threshold T = 995.311 for algorithm vocord\_006, giving  $FMR(T) = 0.001$  globally.**

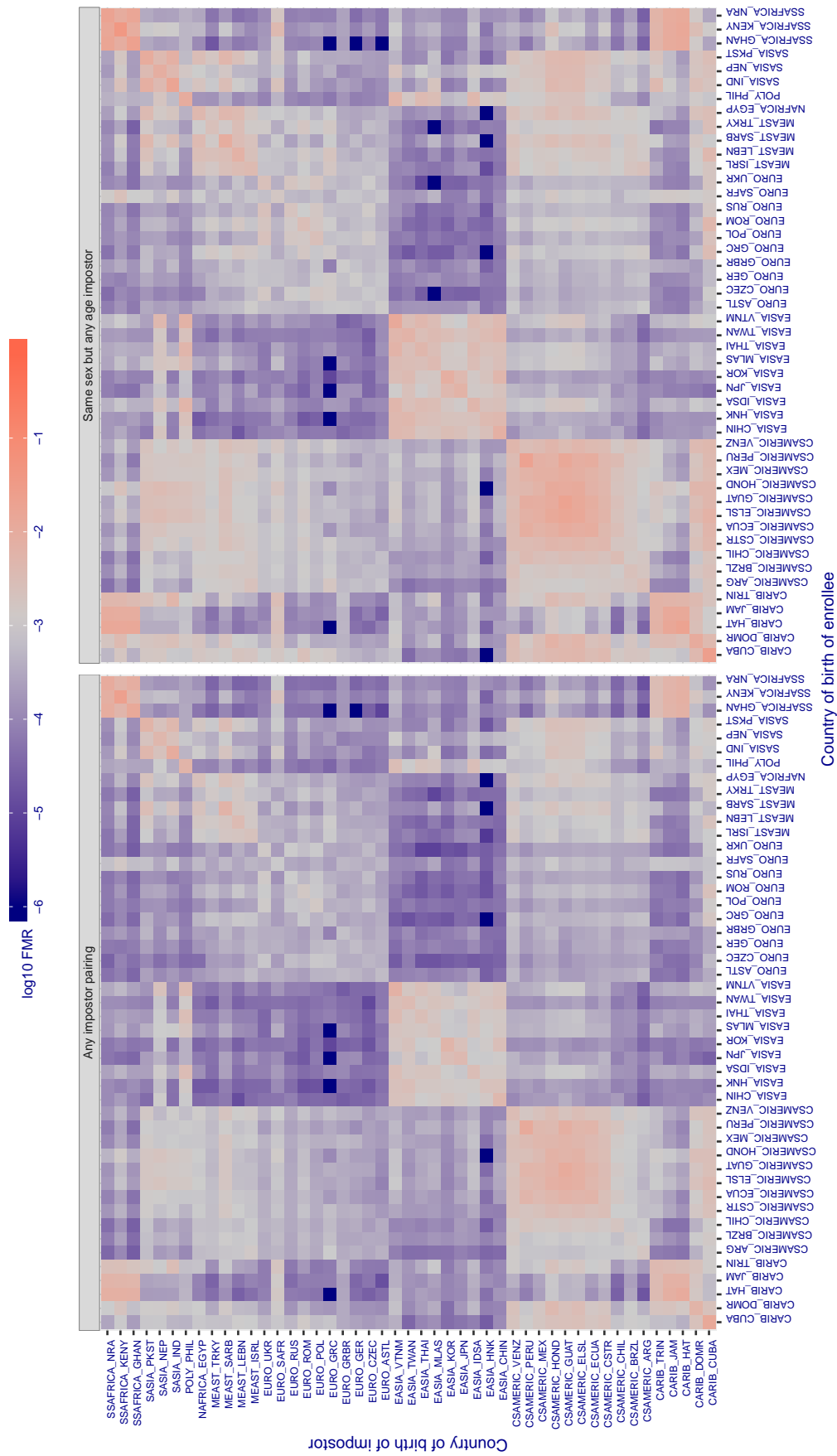


Figure 438: For algorithm vocord-006 operating on visa images, the heatmap shows false match rates observed over impostor comparisons of faces from different individuals who were born in the given country pair. False matches are counted against a recognition threshold fixed globally to give the target  $FMR$  in the plot title, computed over all on the order of  $10^{10}$  impostor comparisons. If text appears in each box it give the same quantity as that coded by the color. Grey indicates  $FMR$  is at the intended  $FMR$  target level. Light red colors present a security vulnerability to, for example, a passport gate. Each +1 increase in  $\log_{10} FMR$  corresponds to a factor of 10 increase in  $FMR$ . The matrix is not quite symmetric because images in the enrollment and verification sets are different.

**Cross country FMR at threshold T = 994.723 for algorithm vocord\_007, giving  $FMR(T) = 0.001$  globally.**

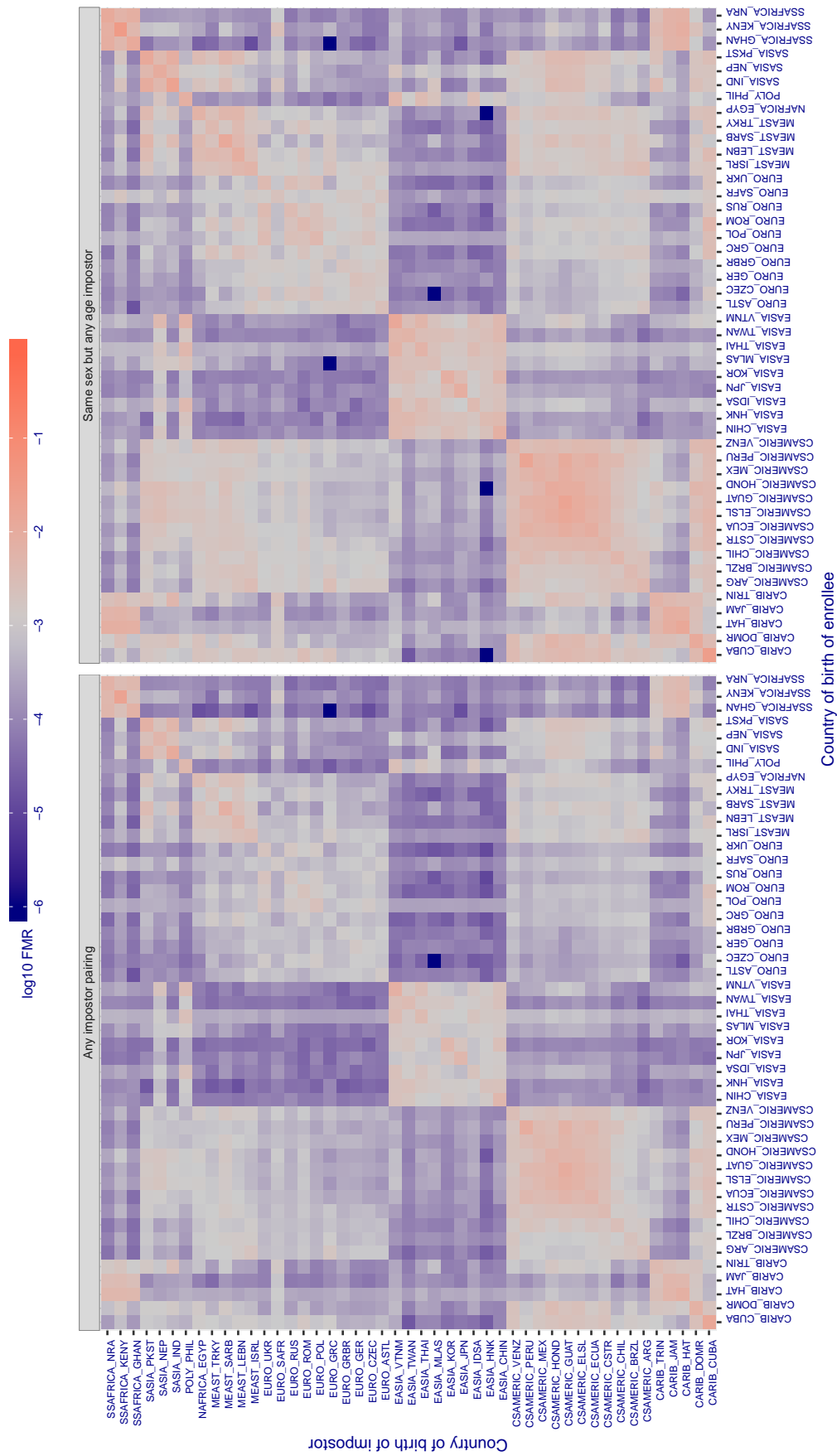


Figure 439: For algorithm vocord-007 operating on visa images, the heatmap shows false match rates observed over impostor comparisons of faces from different individuals who were born in the given country pair. False matches are counted against a recognition threshold fixed globally to give the target  $FMR$  in the plot title, computed over all on the order of  $10^{10}$  impostor comparisons. If text appears in each box it give the same quantity as that coded by the color. Grey indicates  $FMR$  is at the intended  $FMR$  target level. Light red colors present a security vulnerability to, for example, a passport gate. Each +1 increase in  $\log_{10} FMR$  corresponds to a factor of 10 increase in  $FMR$ . The matrix is not quite symmetric because images in the enrollment and verification sets are different.

Cross country FMR at threshold T = 0.314 for algorithm winsense\_000, giving  $FMR(T) = 0.001$  globally.

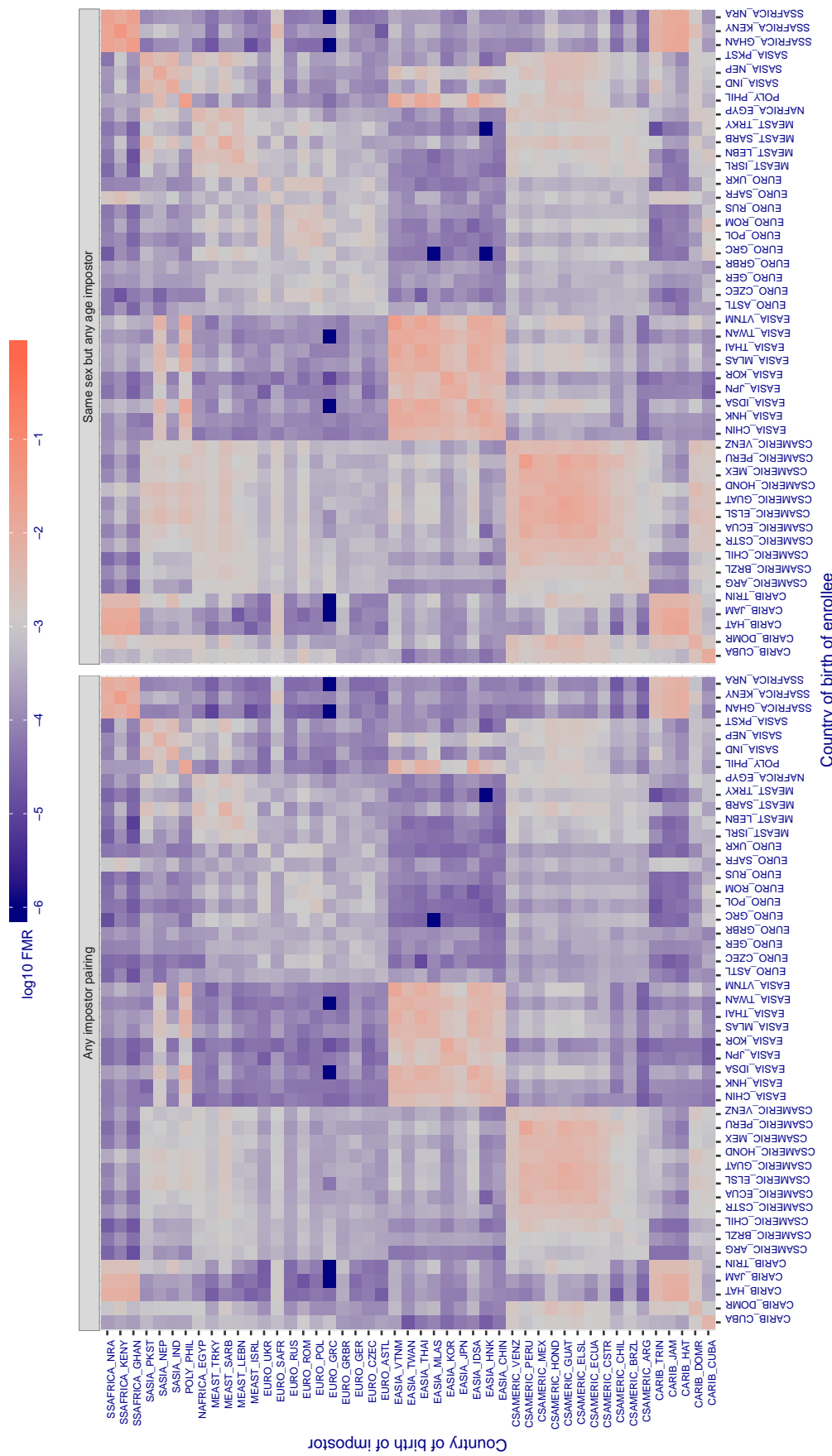


Figure 440: For algorithm winsense-000 operating on visa images, the heatmap shows false match rates observed over impostor comparisons of faces from different individuals who were born in the given country pair. False matches are counted against a recognition threshold fixed globally to give the target  $FMR$  in the plot title, computed over all on the order of  $10^{10}$  impostor comparisons. If text appears in each box it give the same quantity as that coded by the color. Grey indicates  $FMR$  is at the intended  $FMR$  target level. Light red colors present a security vulnerability to, for example, a passport gate. Each +1 increase in  $\log_{10} FMR$  corresponds to a factor of 10 increase in  $FMR$ . The matrix is not quite symmetric because images in the enrollment and verification sets are different.

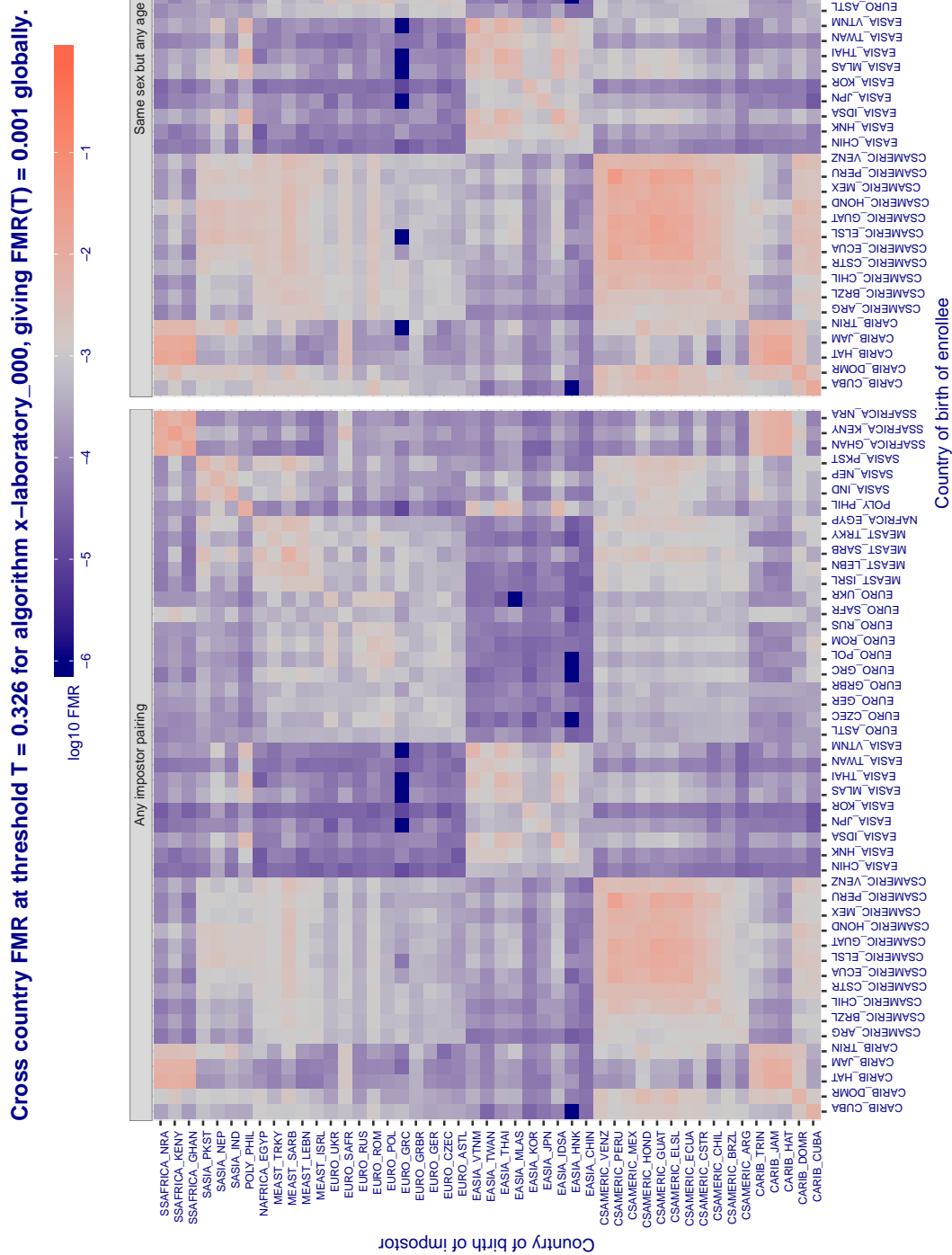


Figure 441: For algorithm x-laboratory-000 operating on visa images, the heatmap shows false match rates observed over impostor comparisons of faces from different individuals who were born in the given country pair. False matches are counted against a recognition threshold fixed globally to give the target FMR in the plot title, computed over all on the order of  $10^{10}$  impostor comparisons. If text appears in each box it give the same quantity as that coded by the color. Grey indicates FMR is at the intended FMR target level. Light red colors present a security vulnerability to, for example, a passport gate. Each +1 increase in  $\log_{10} FMR$  corresponds to a factor of 10 increase in FMR. The matrix is not quite symmetric because images in the enrollment and verification sets are different.

Cross country FMR at threshold T = 5.333 for algorithm yisheng\_004, giving FMR(T) = 0.001 globally.

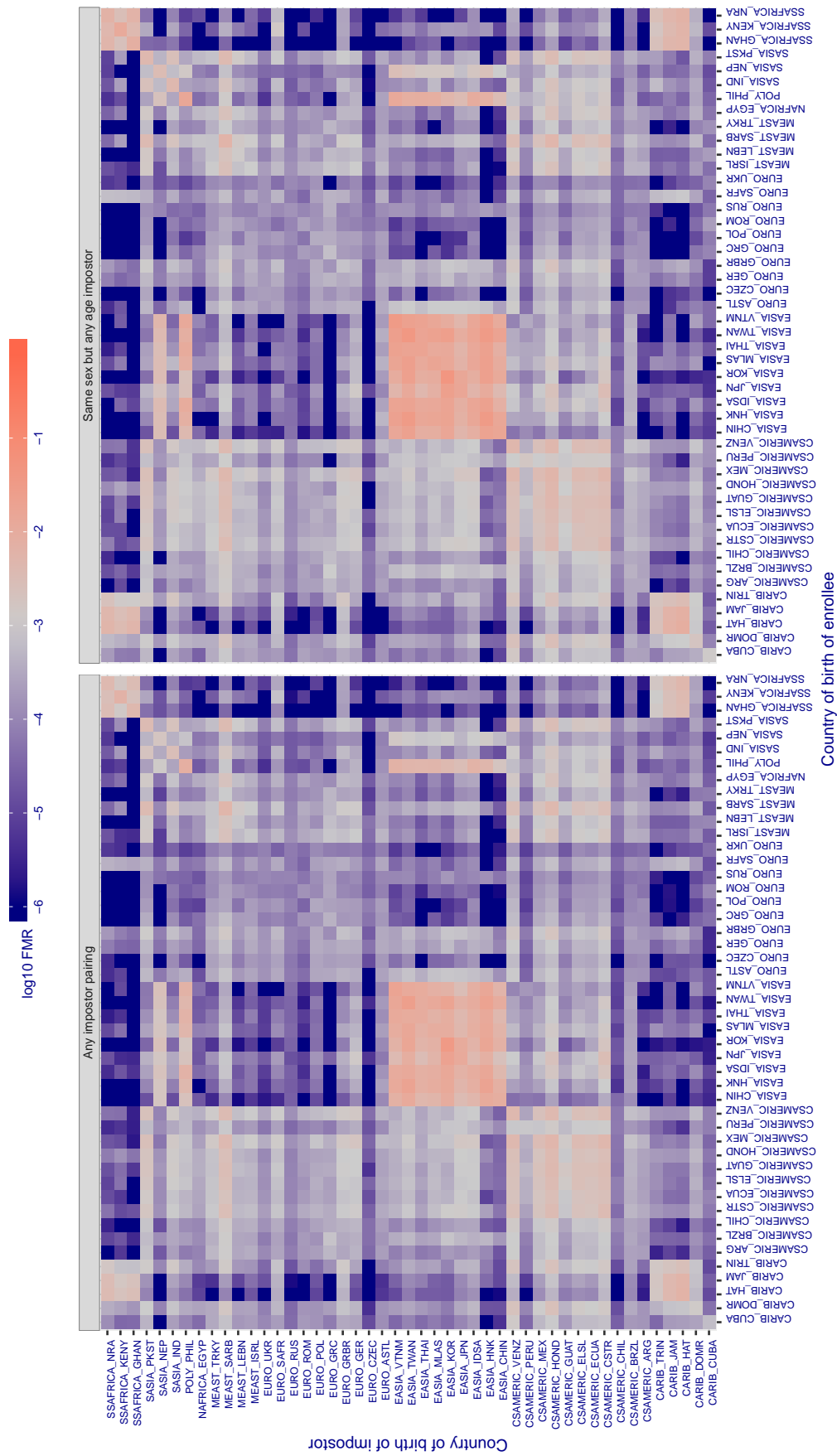


Figure 442: For algorithm yisheng-004 operating on visa images, the heatmap shows false match rates observed over impostor comparisons of faces from different individuals who were born in the given country pair. False matches are counted against a recognition threshold fixed globally to give the target FMR in the plot title, computed over all on the order of  $10^{10}$  impostor comparisons. If text appears in each box it give the same quantity as that coded by the color. Grey indicates FMR is at the intended FMR target level. Light red colors present a security vulnerability to, for example, a passport gate. Each +1 increase in  $\log_{10} FMR$  corresponds to a factor of 10 increase in FMR. The matrix is not quite symmetric because images in the enrollment and verification sets are different.

**Cross country FMR at threshold T = 37.550 for algorithm yitu\_003, giving  $\text{FMR}(T) = 0.001$  globally.**

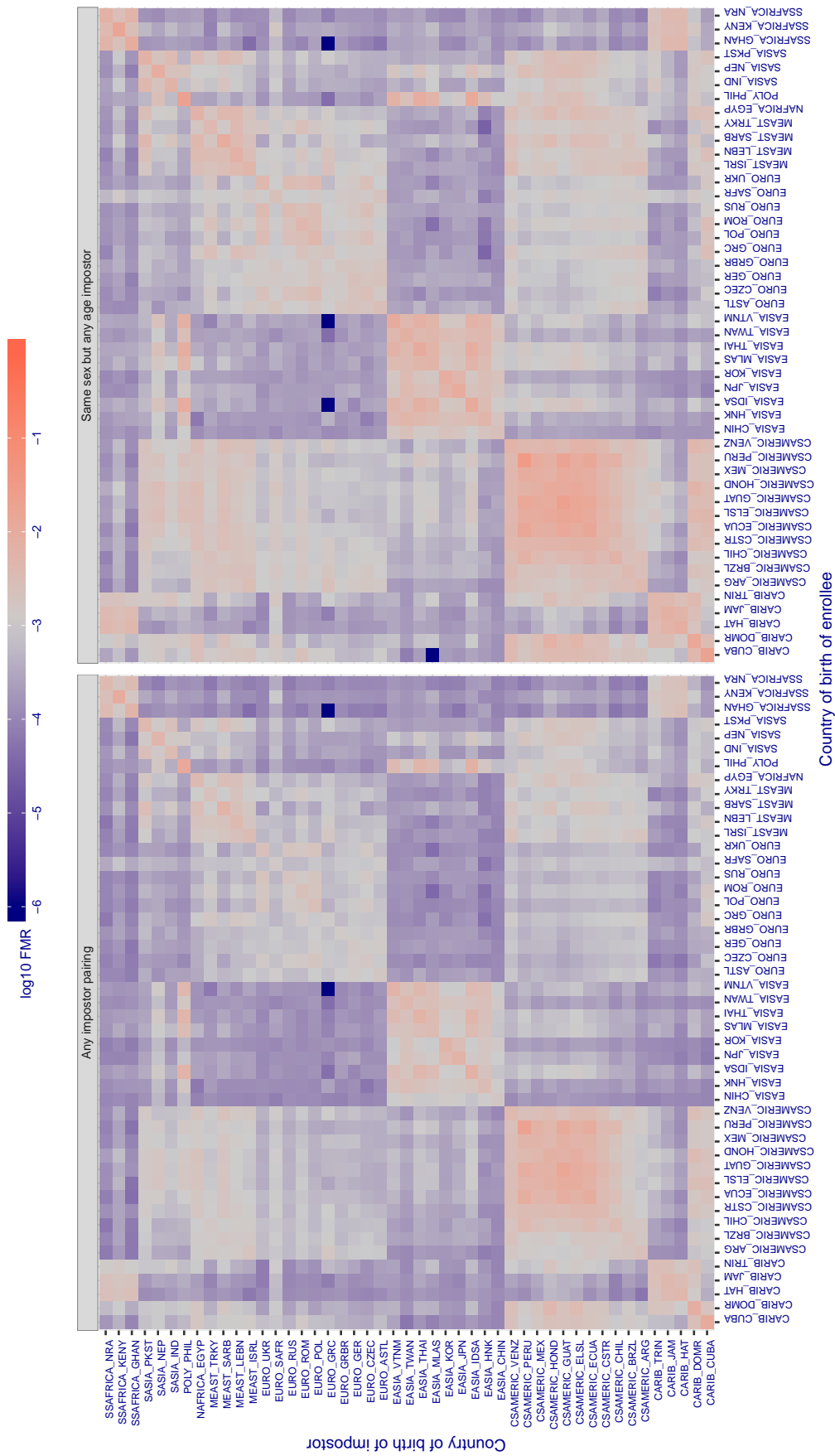


Figure 443: For algorithm yitu-003 operating on visa images, the heatmap shows false match rates observed over impostor comparisons of faces from different individuals who were born in the given country pair. False matches are counted against a recognition threshold fixed globally to give the target FMR in the plot title, computed over all on the order of  $10^{10}$  impostor comparisons. If text appears in each box it give the same quantity as that coded by the color. Grey indicates FMR is at the intended FMR target level. Light red colors present a security vulnerability to, for example, a passport gate. Each +1 increase in  $\log_{10} \text{FMR}$  corresponds to a factor of 10 increase in FMR. The matrix is not quite symmetric because images in the enrollment and verification sets are different.

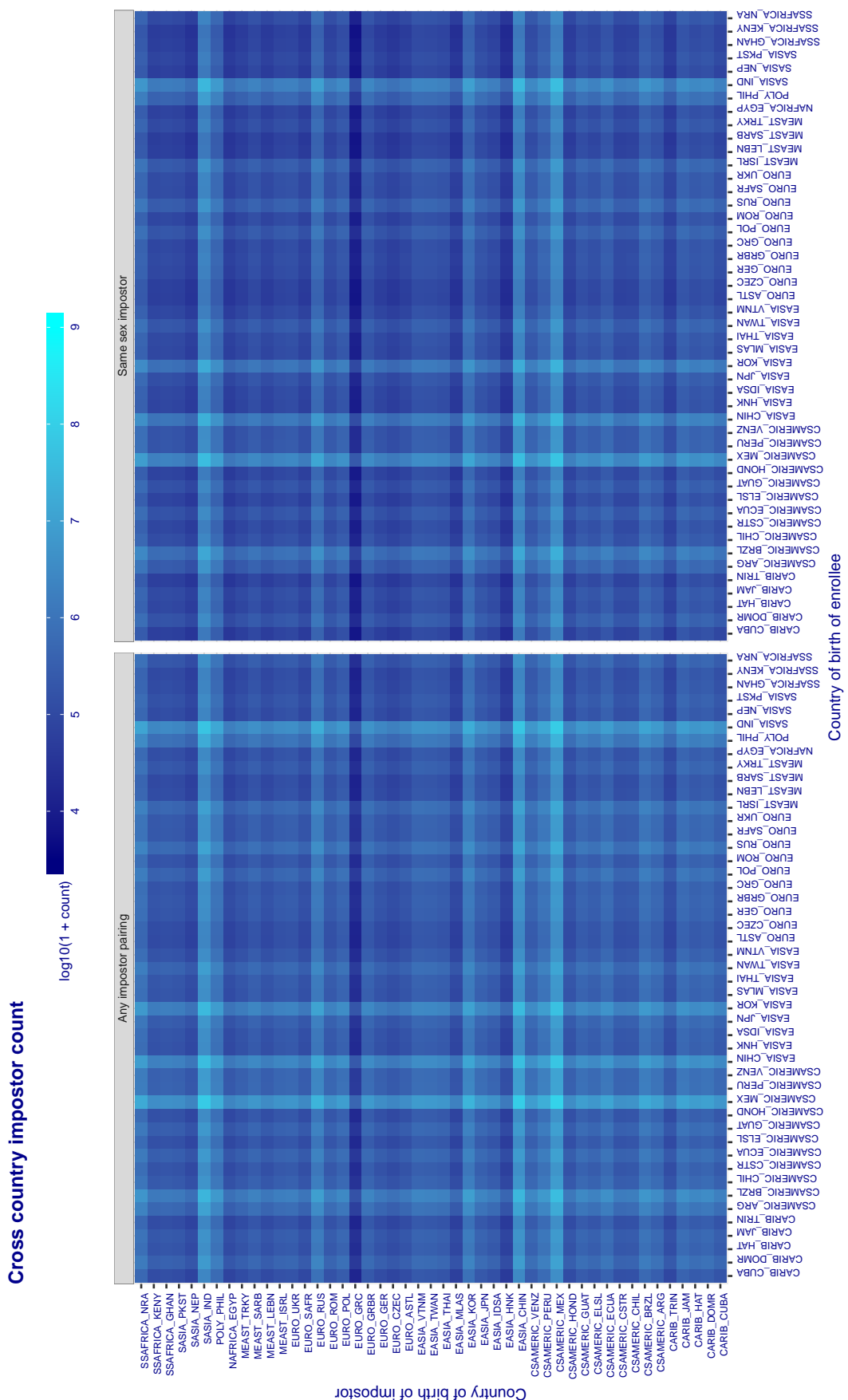


Figure 44: For visa images, the heatmap shows the count of impostor comparisons of faces from different individuals who were born in the given country pair.

### 3.6.2 Effect of age on impostors

**Background:** This section shows the effect of age on the impostor distribution. The ideal behaviour is that the age of the enrollee and the impostor would not affect impostor scores. This would support FMR stability over sub-populations.

**Goals:**

- ▷ To show the effect of relative ages of the impostor and enrollee on false match rates.
- ▷ To determine whether some algorithms have better impostor distribution stability.

**Methods:**

- ▷ Define 14 age group bins, spanning 0 to over 100 years old.
- ▷ Compute FMR over all impostor comparisons for which the subjects in the enrollee and impostor images have ages in two bins.
- ▷ Compute FMR over all impostor comparisons for which the subjects are additionally of the same sex, and born in the same geographic region.

**Results:**

The notable aspects are:

- ▷ Diagonal dominance: Impostors are more likely to be matched against their same age group.
- ▷ Same sex and same region impostors are more successful. On the diagonal, an impostor is more likely to succeed by posing as someone of the same sex. If  $\Delta \log_{10} \text{FMR} = 0.2$ , then same-sex same-region FMR exceeds the all-pairs FMR by factor of  $10^{0.2} = 1.6$ .
- ▷ Young children impostors give elevated FMR against young children. Older adult impostor give elevated FMR against older adults. These effects are quite large, for example if  $\Delta \log_{10} \text{FMR} = 1.0$  larger than a 32 year old, then these groups have higher FMR by a factor of  $10^1 = 10$ . This would imply an FMR above 0.01 for a nominal (global) FMR = 0.001.
- ▷ Algorithms vary.
- ▷ We computed the same quantities for a global FMR = 0.0001. The effects are similar.

Note the calculations in this section include impostors paired across all countries of birth.

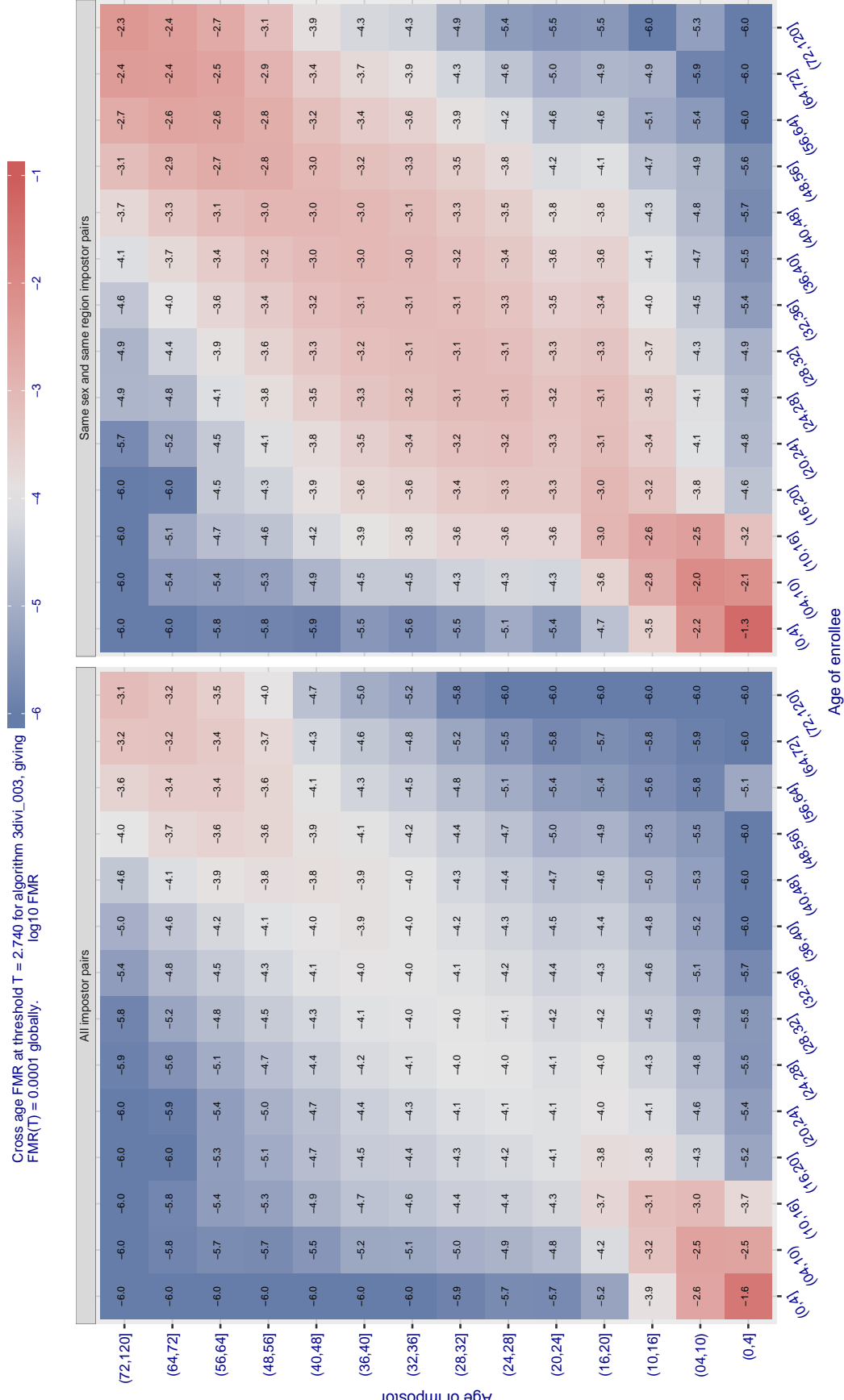


**Figure 445:** For algorithm 3divi-003 operating on visa images, the heatmap shows false match observed over impostor comparisons of faces from different individuals who have the given age pair. False matches are counted against a recognition threshold fixed globally to give  $FMR = 0.001$  over all on the order of  $10^{10}$  impostor comparisons. The text in each box gives the same quantity as that coded by the color. Light colors present a security vulnerability to, for example, a passport gate.

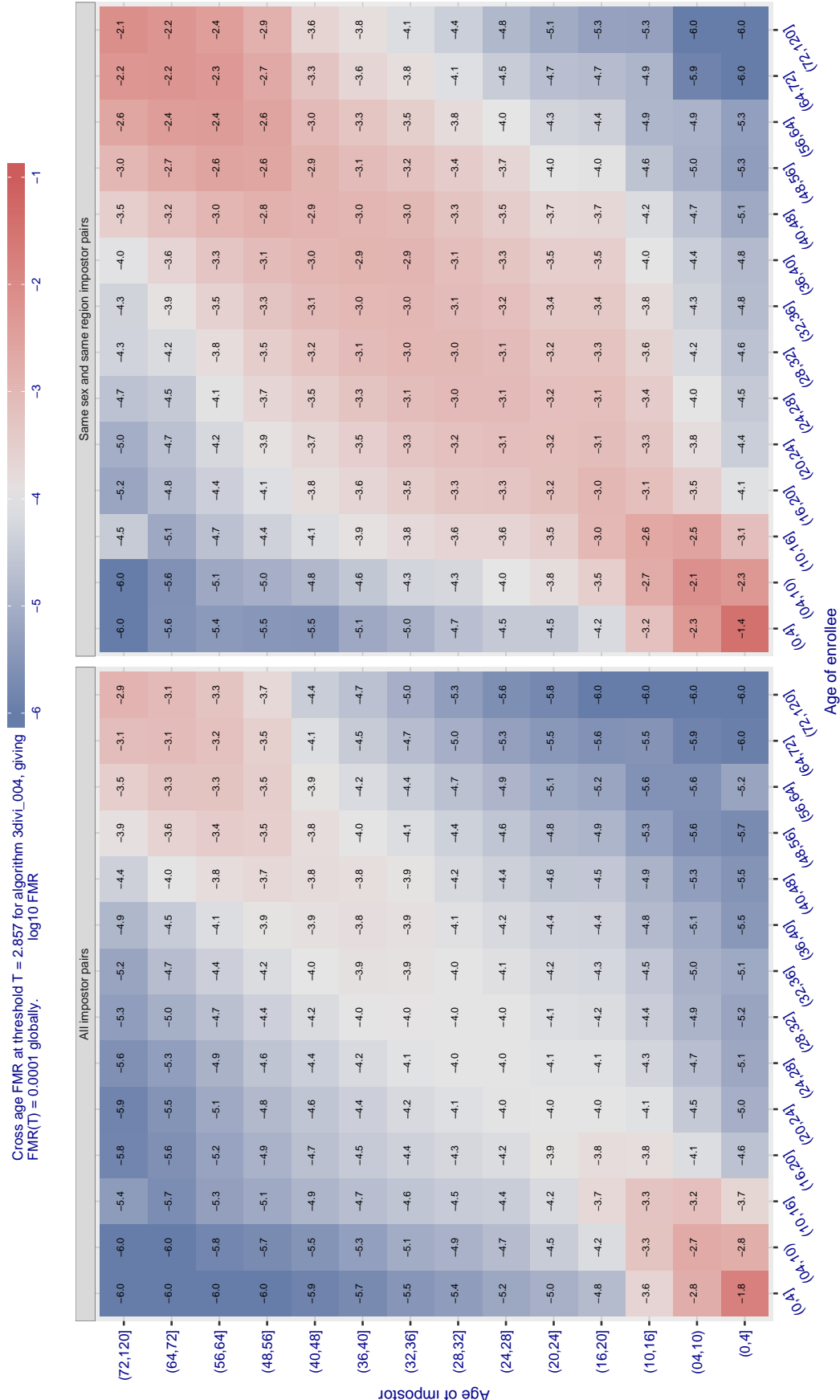


Figure 446: For algorithm 3divi-004 operating on visa images, the heatmap shows false match observed over impostor comparisons of faces from different individuals who have the given age pair. False matches are counted against a recognition threshold fixed globally to give  $FMR = 0.0001$  over all on the order of  $10^{10}$  impostor comparisons. The text in each box gives the same quantity as that coded by the color. Light colors present a security vulnerability to, for example, a passport gate.

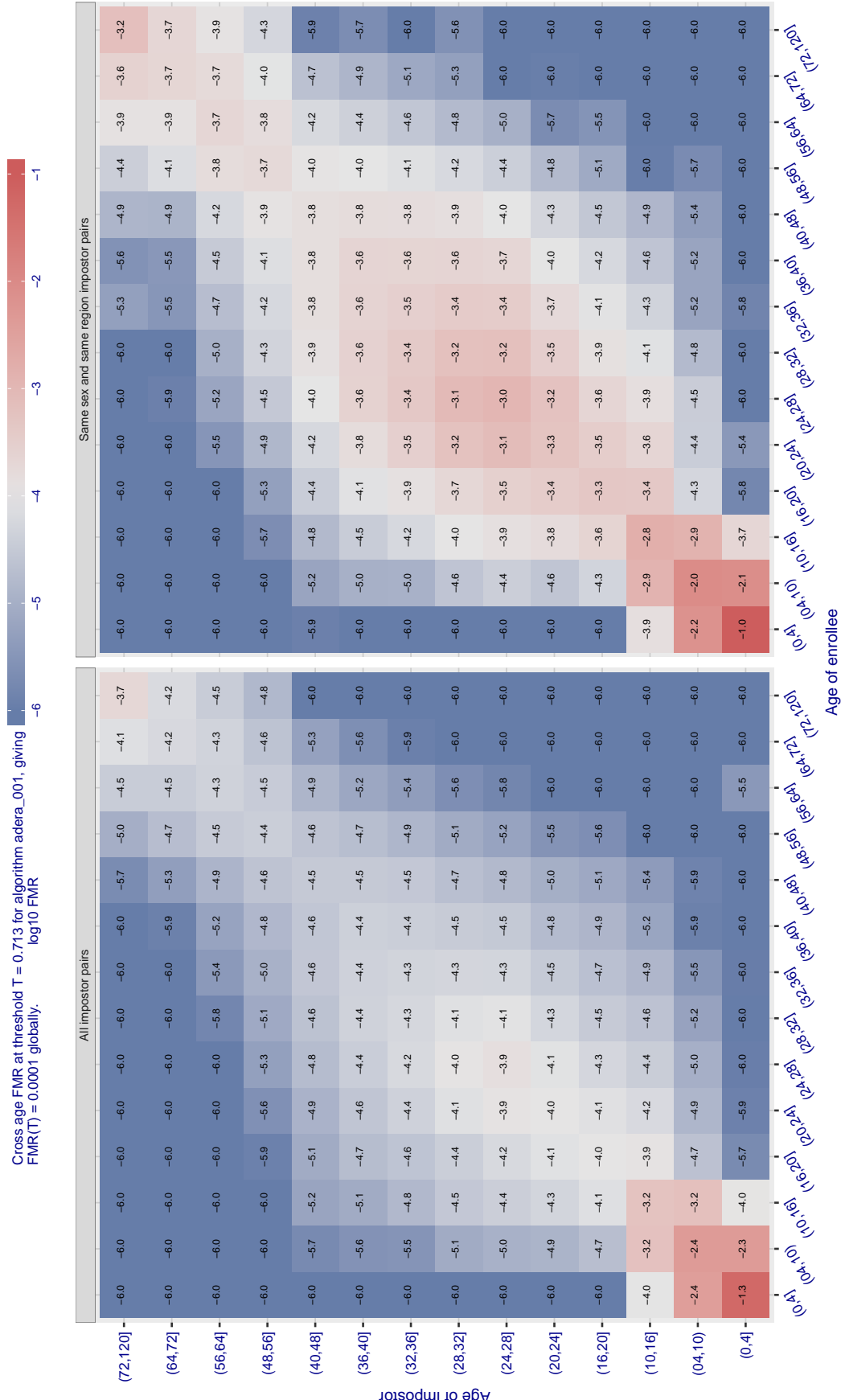


Figure 447: For algorithm adera-001 operating on visa images, the heatmap shows false match observed over impostor comparisons of faces from different individuals who have the given age pair. False matches are counted against a recognition threshold fixed globally to give  $\text{FMR} = 0.0001$  over all on the order of  $10^{10}$  impostor comparisons. The text in each box gives the same quantity as that coded by the color. Light colors present a security vulnerability to, for example, a passport gate.

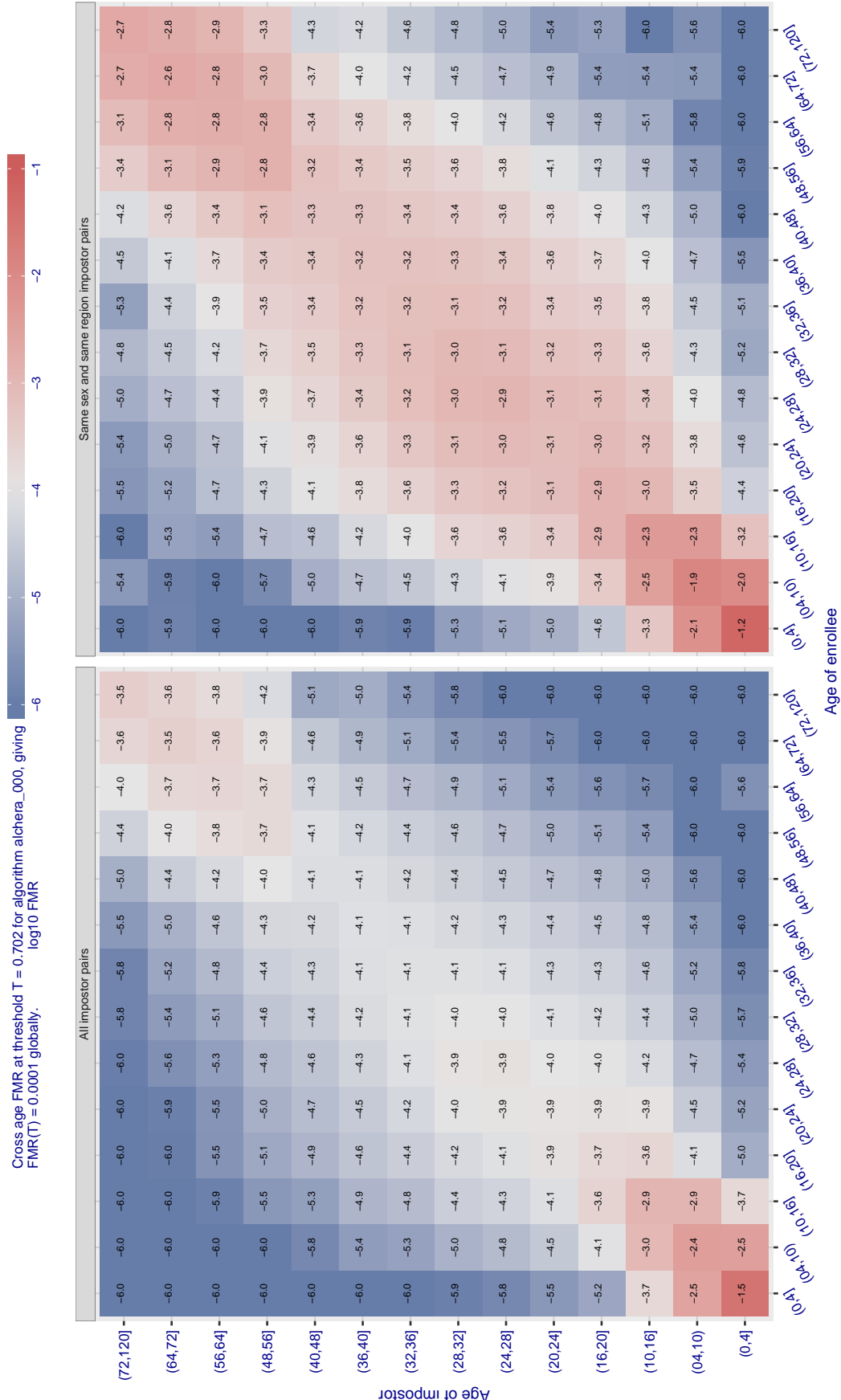


Figure 448: For algorithm alchera-000 operating on visa images, the heatmap shows false match observed over impostor comparisons of faces from different individuals who have the given age pair. False matches are counted against a recognition threshold fixed globally to give  $FMR = 0.0001$  over all on the order of  $10^{10}$  impostor comparisons. The text in each box gives the same quantity as that coded by the color. Light colors present a security vulnerability to, for example, a passport gate.

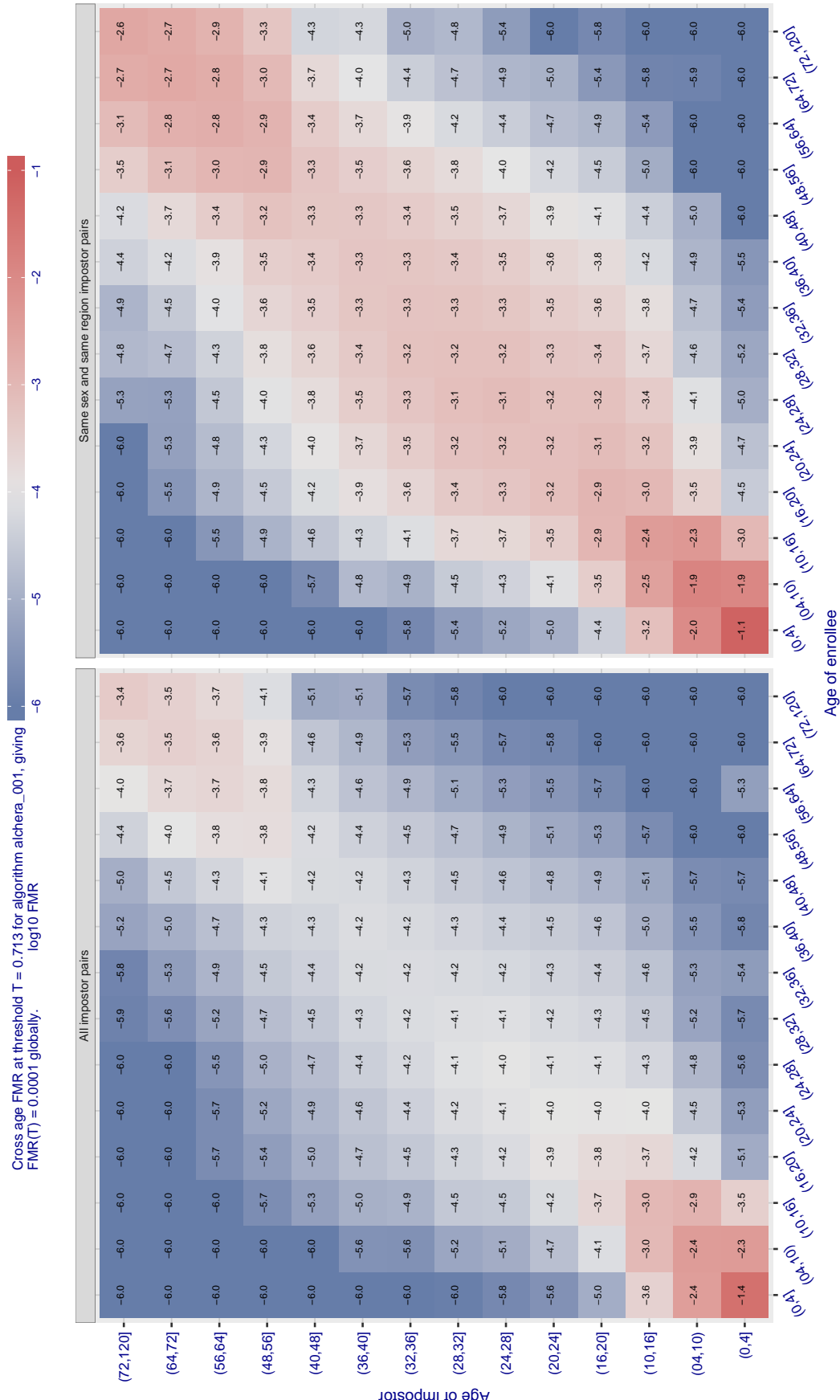


Figure 449: For algorithm alchera-001 operating on visa images, the heatmap shows false match observed over impostor comparisons of faces from different individuals who have the given age pair. False matches are counted against a recognition threshold fixed globally to give  $FMR = 0.0001$  over all on the order of  $10^{10}$  impostor comparisons. The text in each box gives the same quantity as that coded by the color. Light colors present a security vulnerability to, for example, a passport gate.

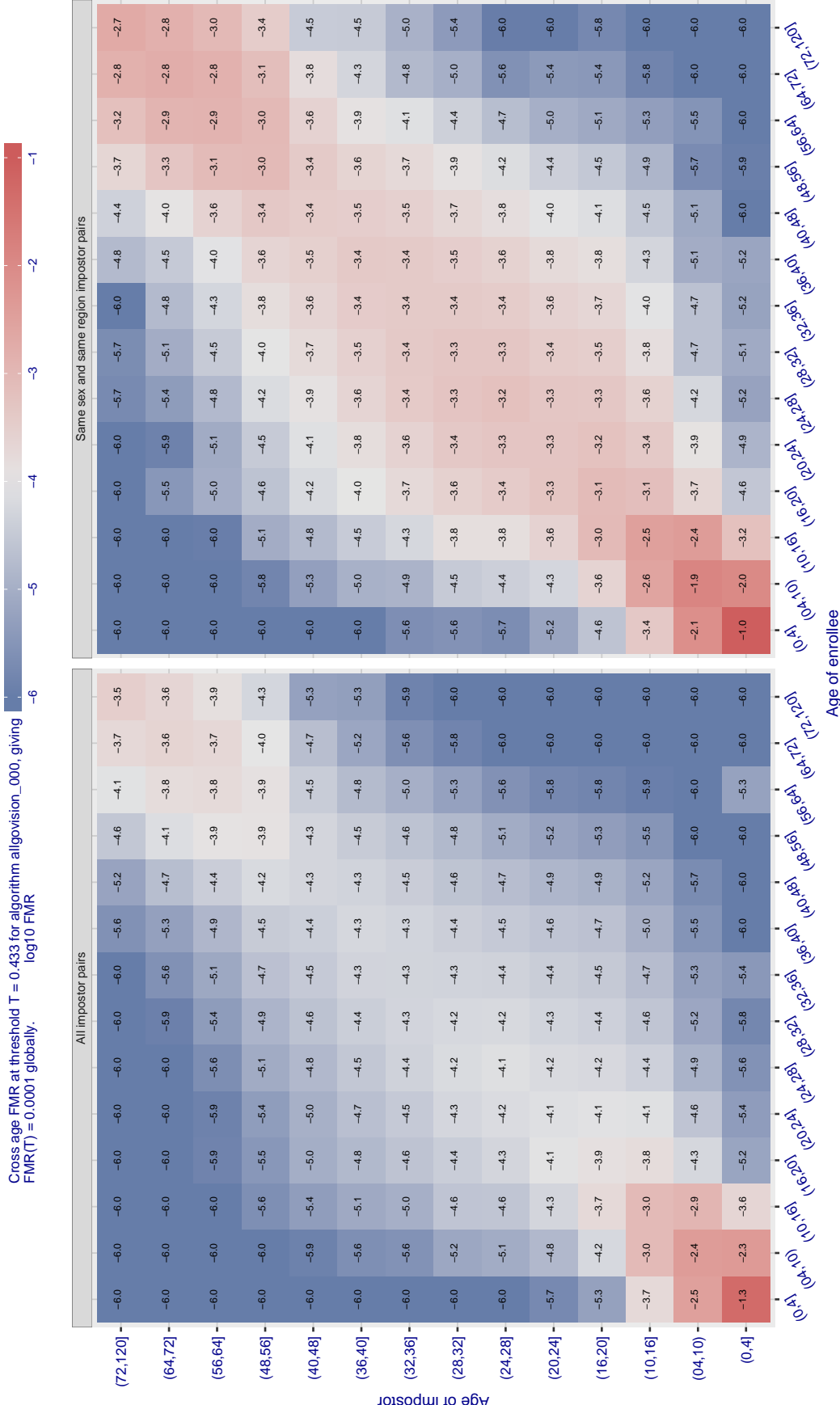


Figure 450: For algorithm allgovision-000 operating on visa images, the heatmap shows false match observed over impostor comparisons of faces from different individuals who have the given age pair. False matches are counted against a recognition threshold fixed globally to give  $FMR = 0.0001$  over all on the order of  $10^{10}$  impostor comparisons. The text in each box gives the same quantity as that coded by the color. Light colors present a security vulnerability to, for example, a passport gate.

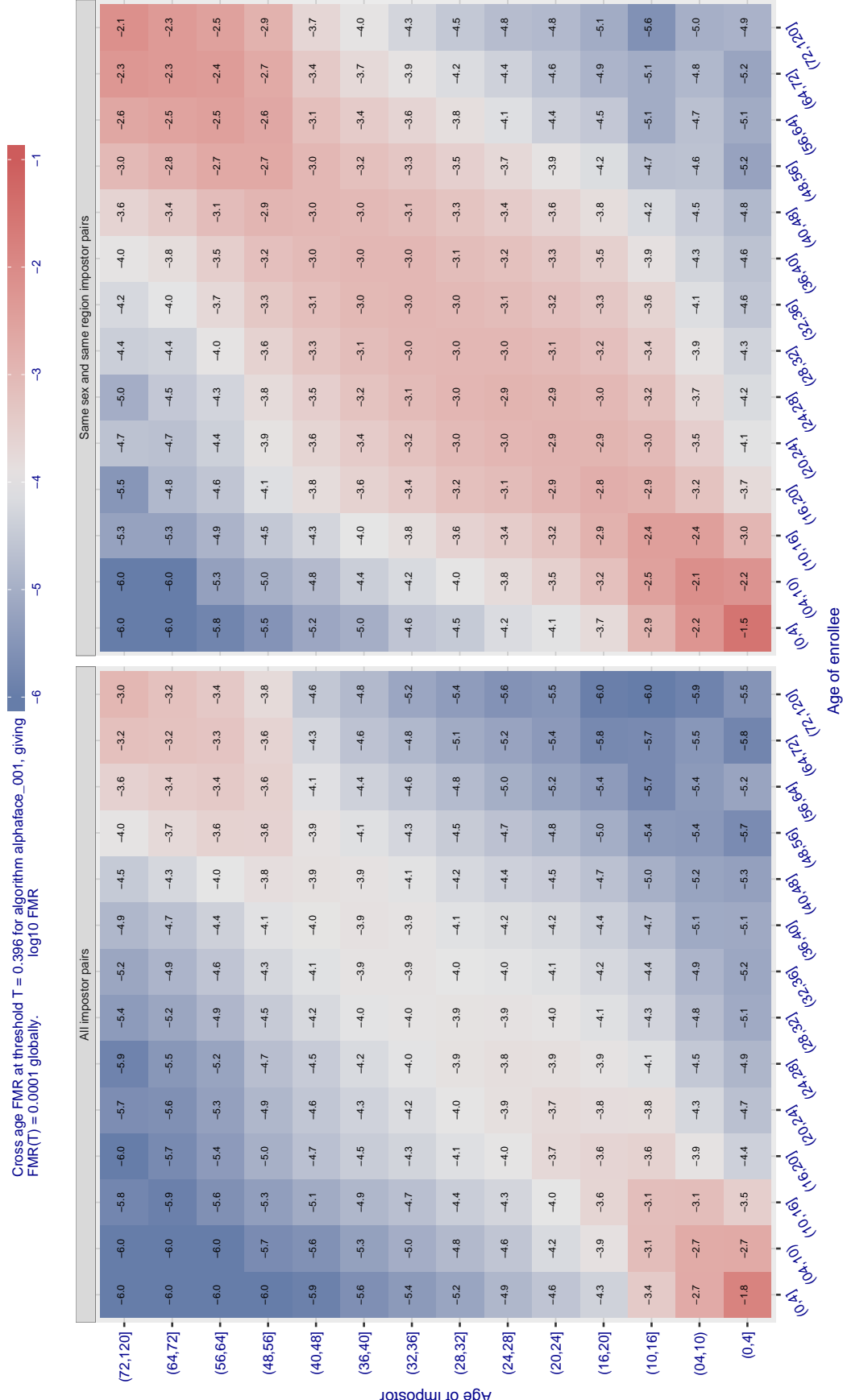


Figure 451: For algorithm alphaface-001 operating on visa images, the heatmap shows false match observed over impostor comparisons of faces from different individuals who have the given age pair. False matches are counted against a recognition threshold fixed globally to give FMR = 0.001 over all on the order of  $10^{10}$  impostor comparisons. The text in each box gives the same quantity as that coded by the color. Light colors present a security vulnerability to, for example, a passport gate.

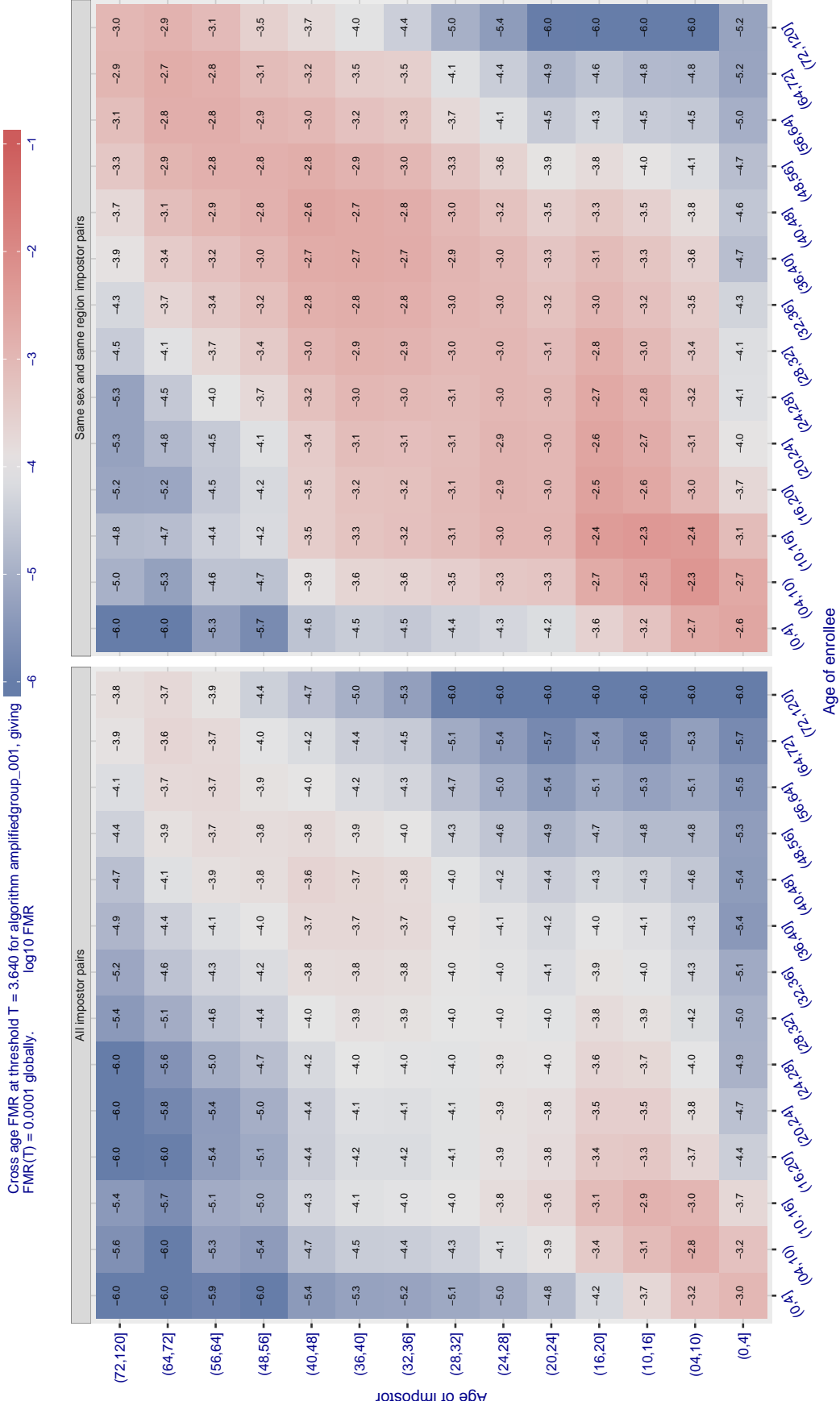


Figure 452: For algorithm amplifiedgroup-001 operating on visa images, the heatmap shows false match observed over impostor comparisons of faces from different individuals who have the given age pair. False matches are counted against a recognition threshold fixed globally to give  $FMR = 0.0001$  over all on the order of  $10^{10}$  impostor comparisons. The text in each box gives the same quantity as that coded by the color. Light colors present a security vulnerability to, for example, a passport gate.

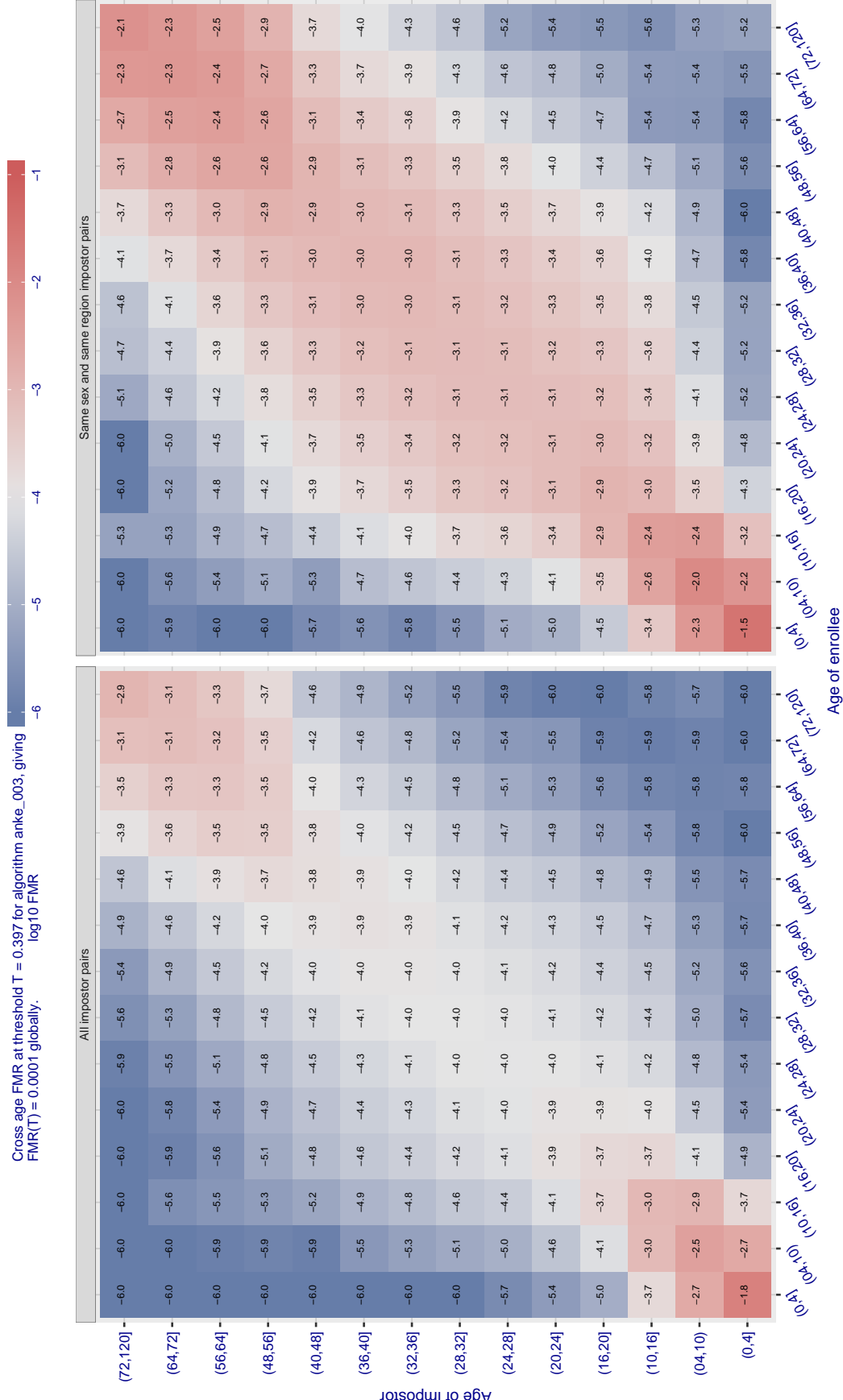


Figure 453: For algorithm anke-003 operating on visa images, the heatmap shows false match observed over impostor comparisons of faces from different individuals who have the given age pair. False matches are counted against a recognition threshold fixed globally to give  $FMR = 0.0001$  over all on the order of  $10^{10}$  impostor comparisons. The text in each box gives the same quantity as that coded by the color. Light colors present a security vulnerability to, for example, a passport gate.

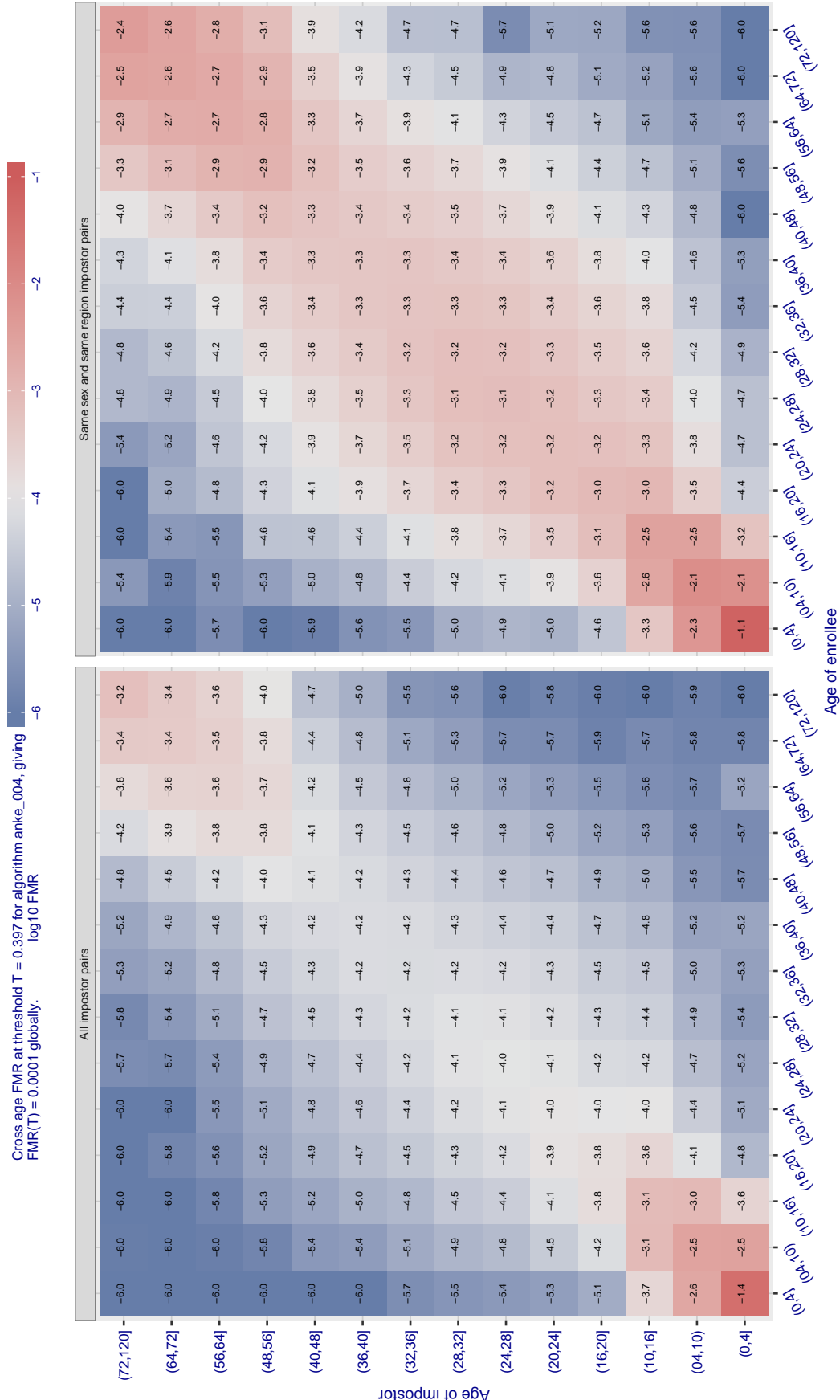


Figure 454: For algorithm anke-004 operating on visa images, the heatmap shows false match observed over impostor comparisons of faces from different individuals who have the given age pair. False matches are counted against a recognition threshold fixed globally to give  $FMR = 0.0001$  over all on the order of  $10^{10}$  impostor comparisons. The text in each box gives the same quantity as that coded by the color. Light colors present a security vulnerability to, for example, a passport gate.

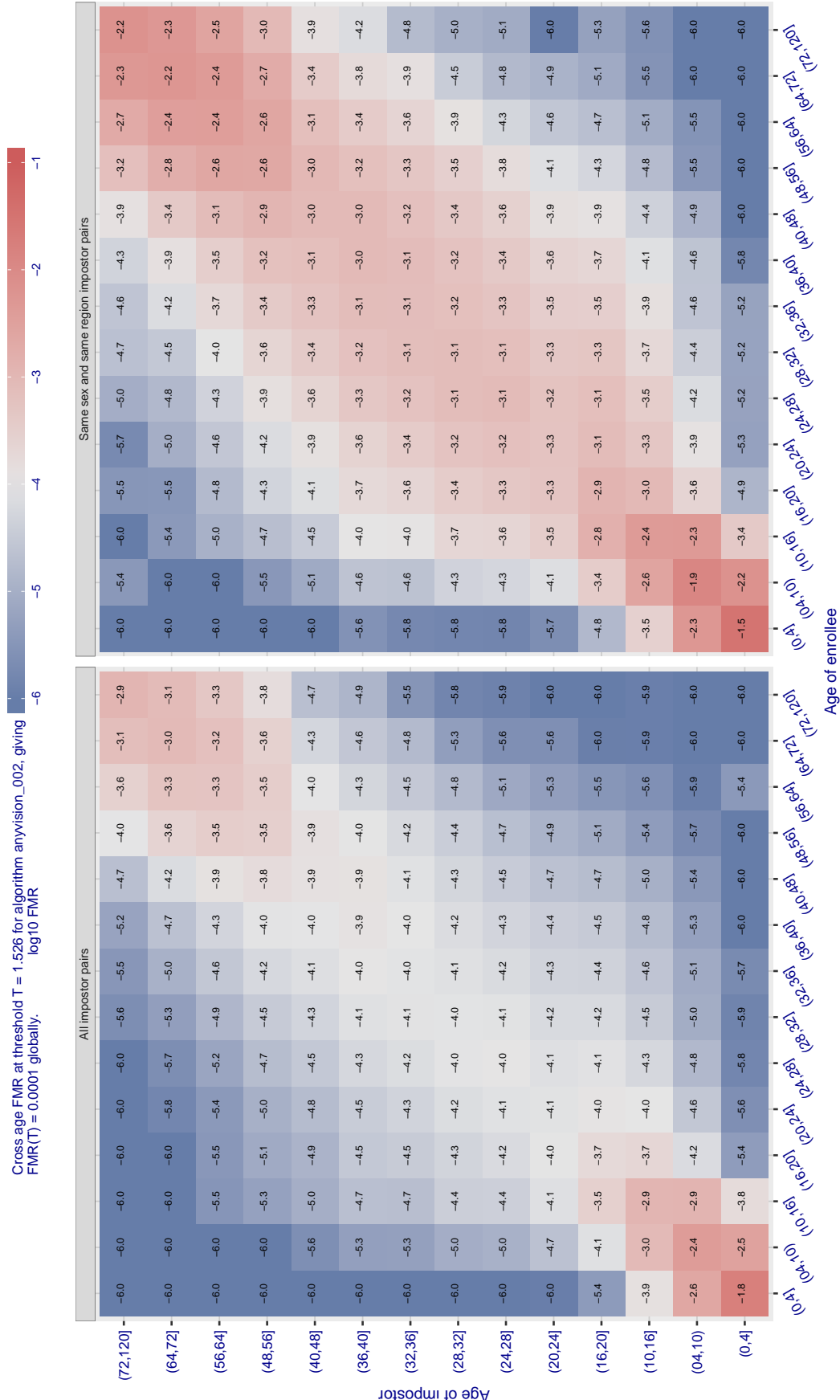


Figure 455: For algorithm anyvision-002 operating on visa images, the heatmap shows false match observed over impostor comparisons of faces from different individuals who have the given age pair. False matches are counted against a recognition threshold fixed globally to give FMR = 0.001 over all on the order of  $10^{10}$  impostor comparisons. The text in each box gives the same quantity as that coded by the color. Light colors present a security vulnerability to, for example, a passport gate.

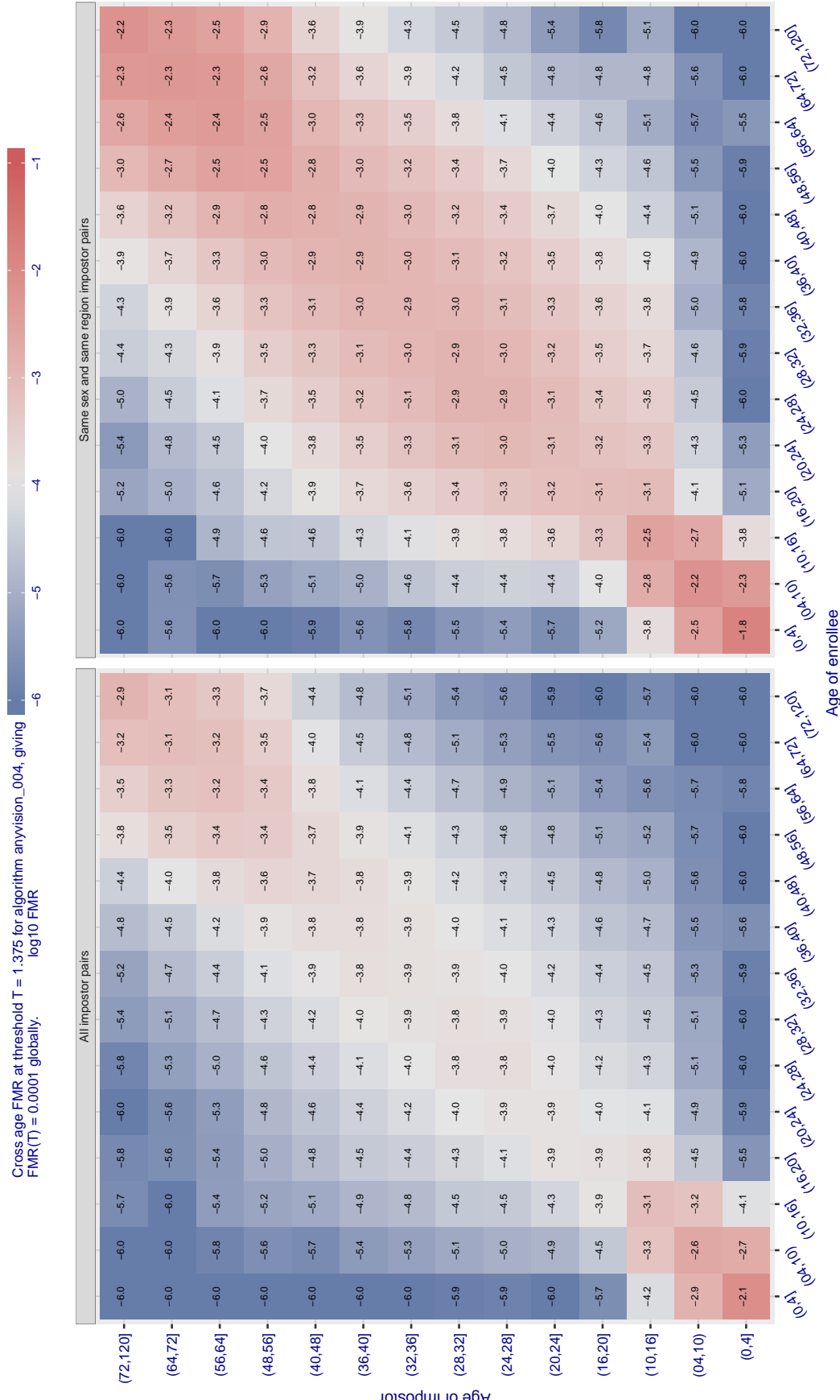


Figure 456: For algorithm anyvision-004 operating on visa images, the heatmap shows false match observed over impostor comparisons of faces from different individuals who have the given age pair. False matches are counted against a recognition threshold fixed globally to give FMR = 0.001 over all on the order of  $10^{10}$  impostor comparisons. The text in each box gives the same quantity as that coded by the color. Light colors present a security vulnerability to, for example, a passport gate.

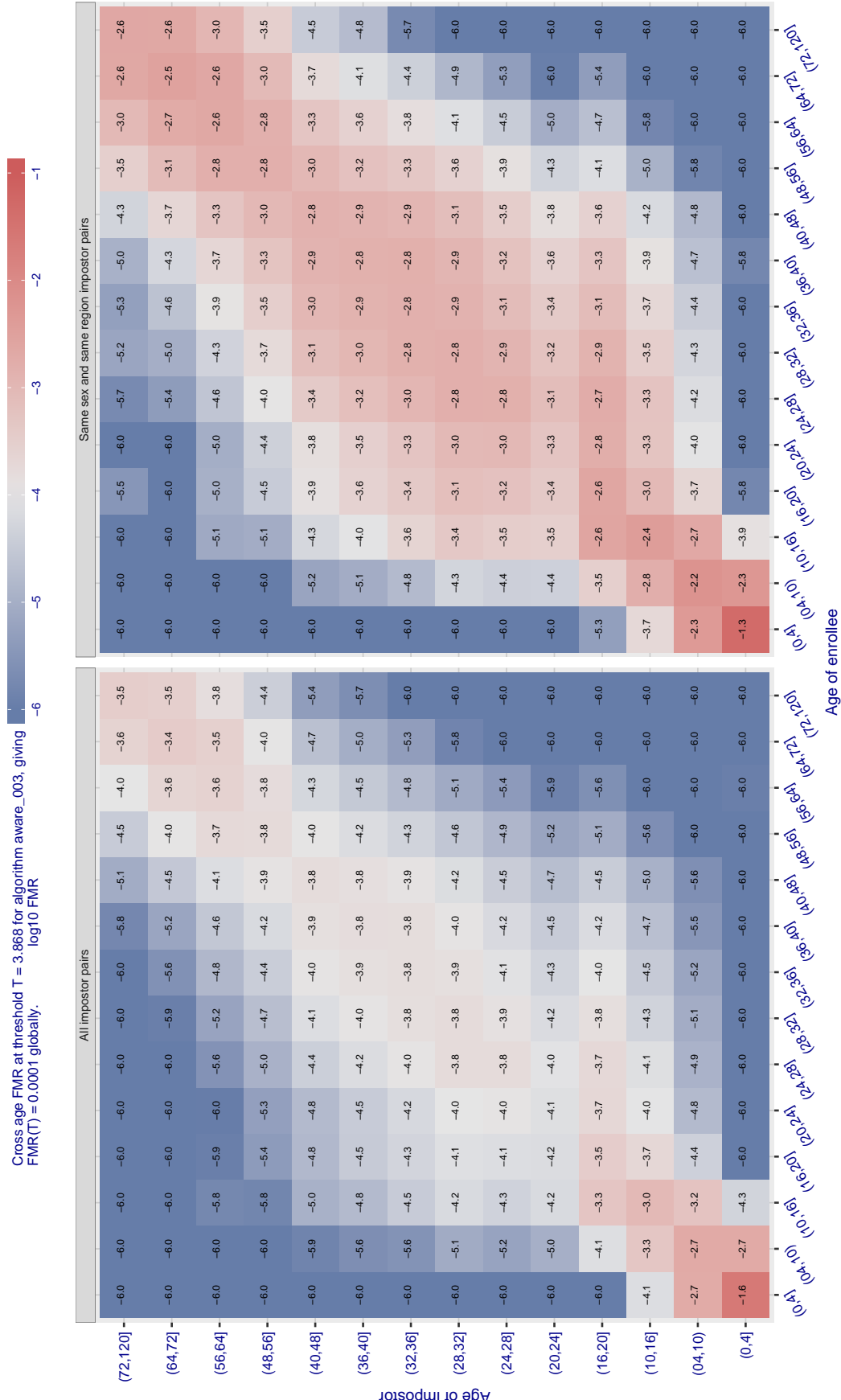


Figure 457: For algorithm aware-003 operating on visa images, the heatmap shows false match observed over impostor comparisons of faces from different individuals who have the given age pair. False matches are counted against a recognition threshold fixed globally to give  $FMR = 0.0001$  over all on the order of  $10^{10}$  impostor comparisons. The text in each box gives the same quantity as that coded by the color. Light colors present a security vulnerability to, for example, a passport gate.

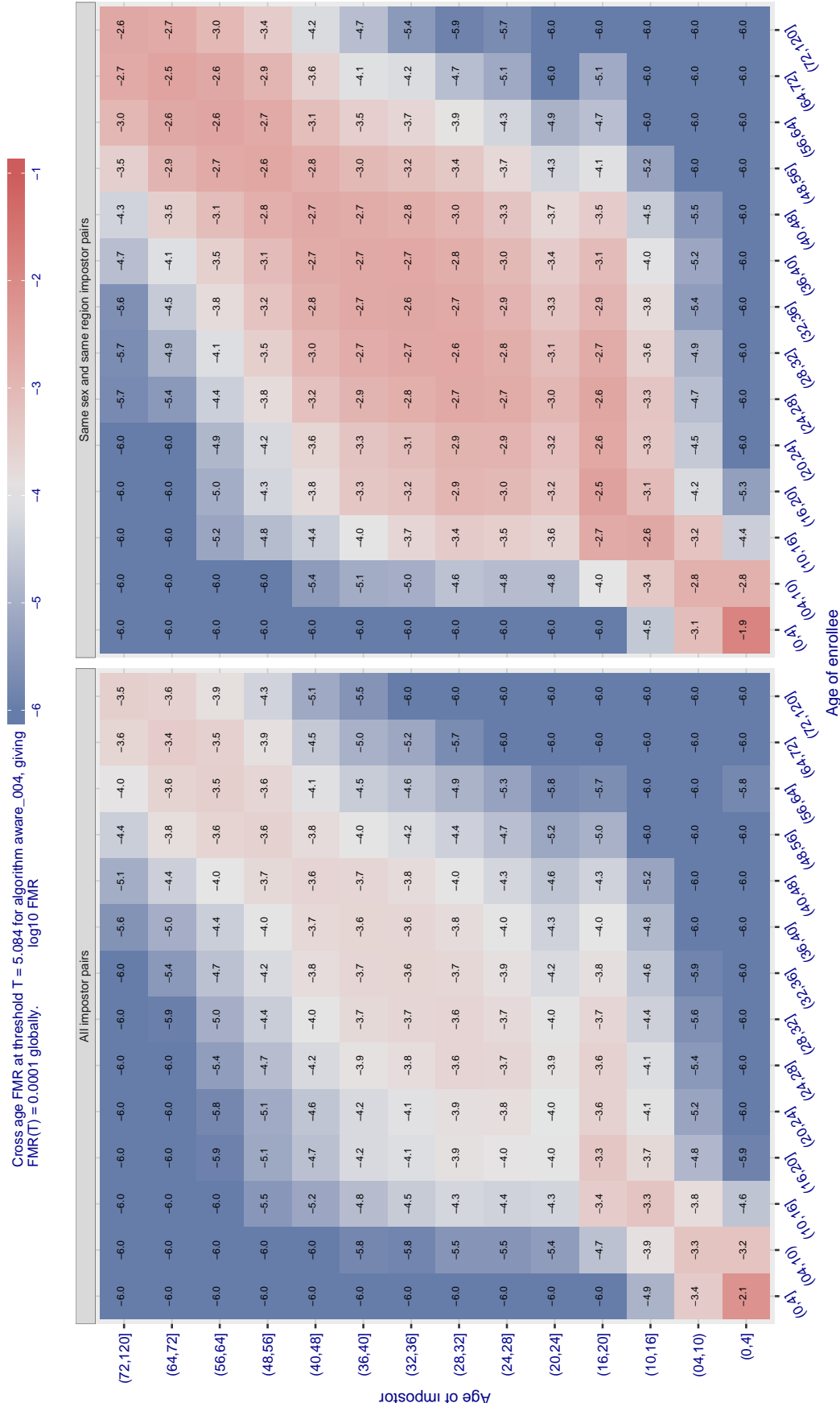


Figure 458: For algorithm aware-004 operating on visa images, the heatmap shows false match observed over impostor comparisons of faces from different individuals who have the given age pair. False matches are counted against a recognition threshold fixed globally to give FMR = 0.0001 over all on the order of  $10^{10}$  impostor comparisons. The text in each box gives the same quantity as that coded by the color. Light colors present a security vulnerability to, for example, a passport gate.

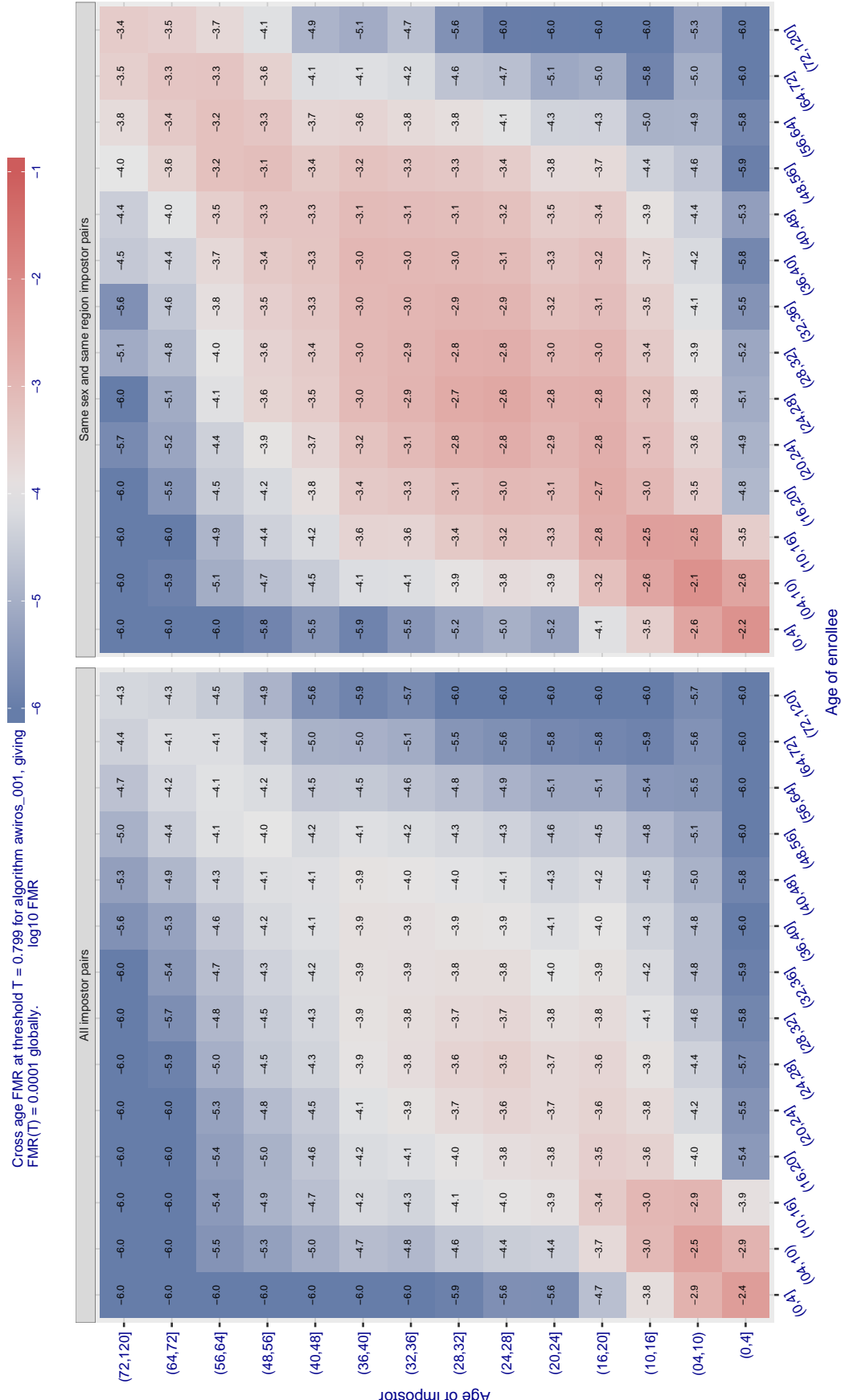


Figure 459: For algorithm awinos-001 operating on visa images, the heatmap shows false match observed over impostor comparisons of faces from different individuals who have the given age pair. False matches are counted against a recognition threshold fixed globally to give  $FMR = 0.0001$  over all on the order of  $10^{10}$  impostor comparisons. The text in each box gives the same quantity as that coded by the color. Light colors present a security vulnerability to, for example, a passport gate.

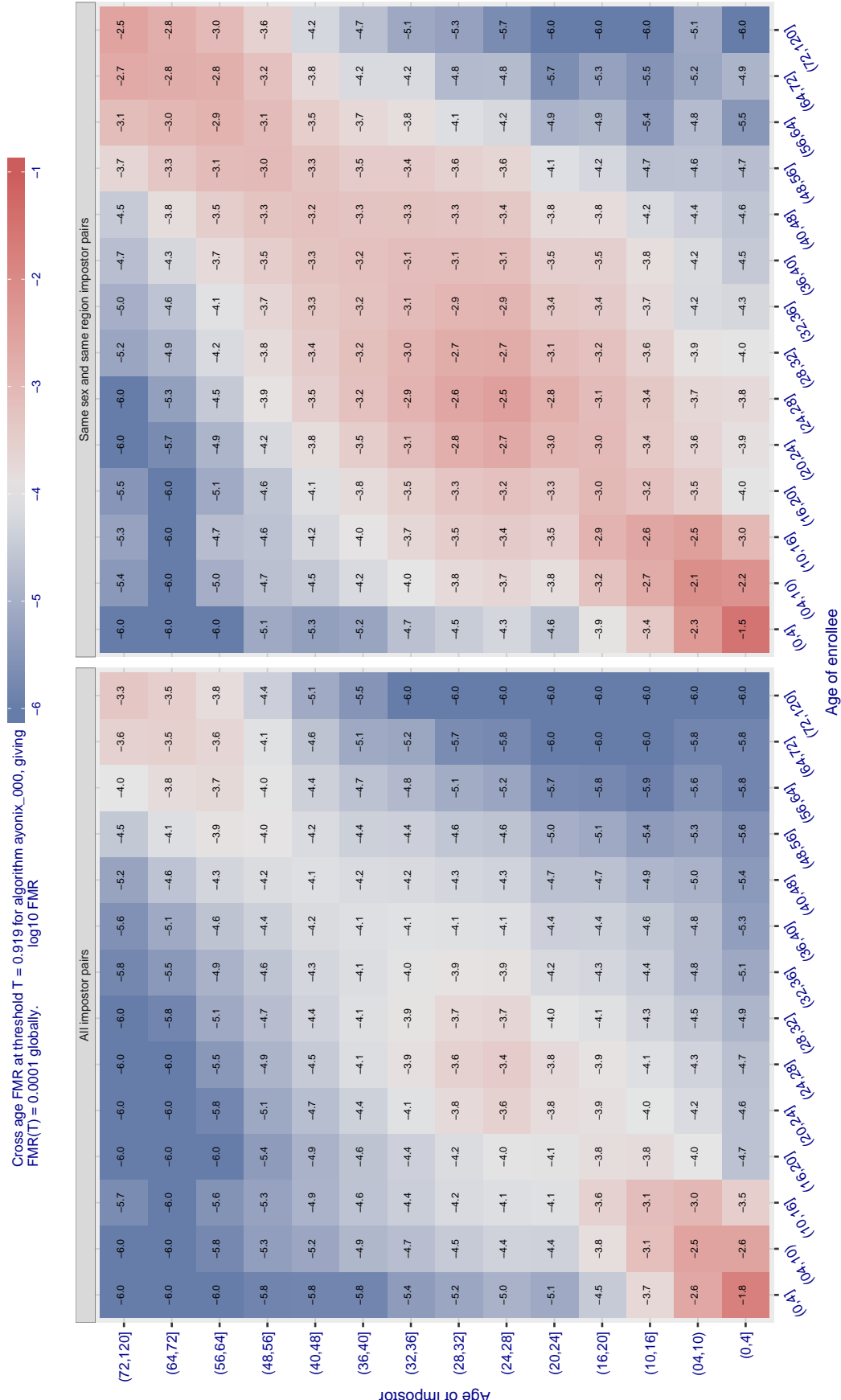


Figure 460: For algorithm ayonix\_000 operating on visa images, the heatmap shows false match observed over impostor comparisons of faces from different individuals who have the given age pair. False matches are counted against a recognition threshold fixed globally to give  $FMR = 0.0001$  over all on the order of  $10^{10}$  impostor comparisons. The text in each box gives the same quantity as that coded by the color. Light colors present a security vulnerability to, for example, a passport gate.

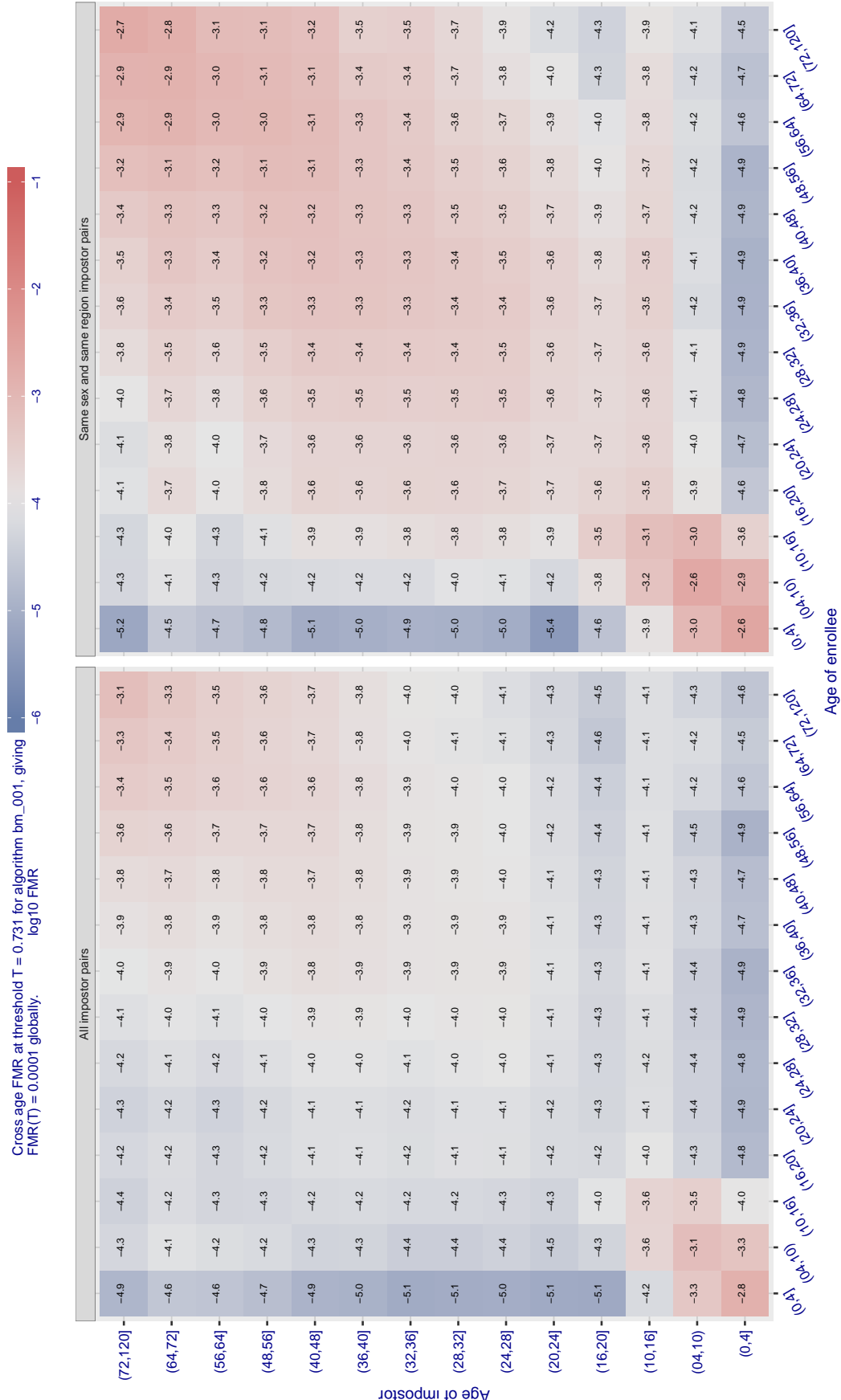


Figure 461: For algorithm bm\_001 operating on visa images, the heatmap shows false match observed over impostor comparisons of faces from different individuals who have the given age pair. False matches are counted against a recognition threshold fixed globally to give FMR = 0.0001 over all on the order of  $10^{10}$  impostor comparisons. The text in each box gives the same quantity as that coded by the color. Light colors present a security vulnerability to, for example, a passport gate.

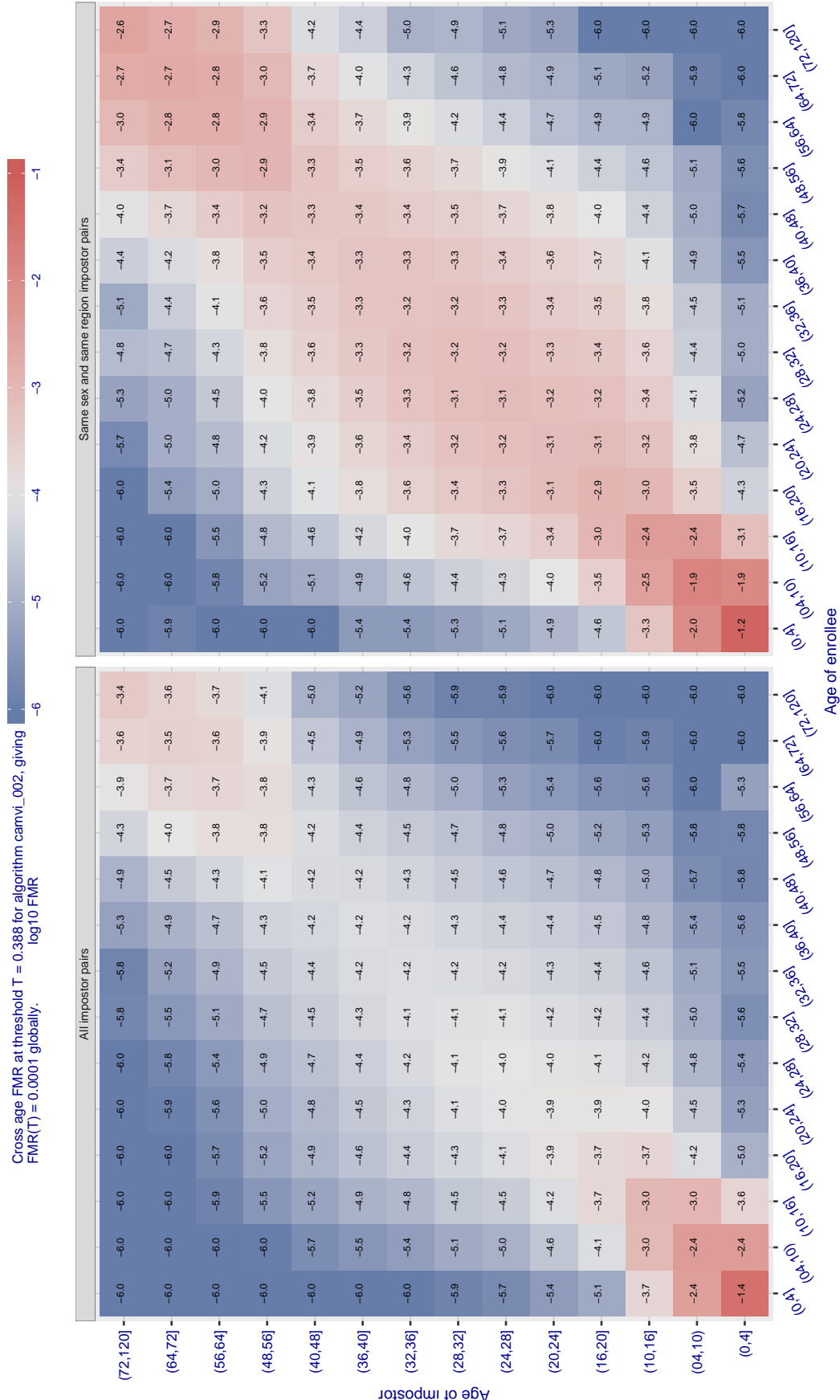


Figure 462: For algorithm camvi\_002 operating on visa images, the heatmap shows false match observed over impostor comparisons of faces from different individuals who have the given age pair. False matches are counted against a recognition threshold fixed globally to give  $FMR = 0.0001$  over all on the order of  $10^{10}$  impostor comparisons. The text in each box gives the same quantity as that coded by the color. Light colors present a security vulnerability to, for example, a passport gate.

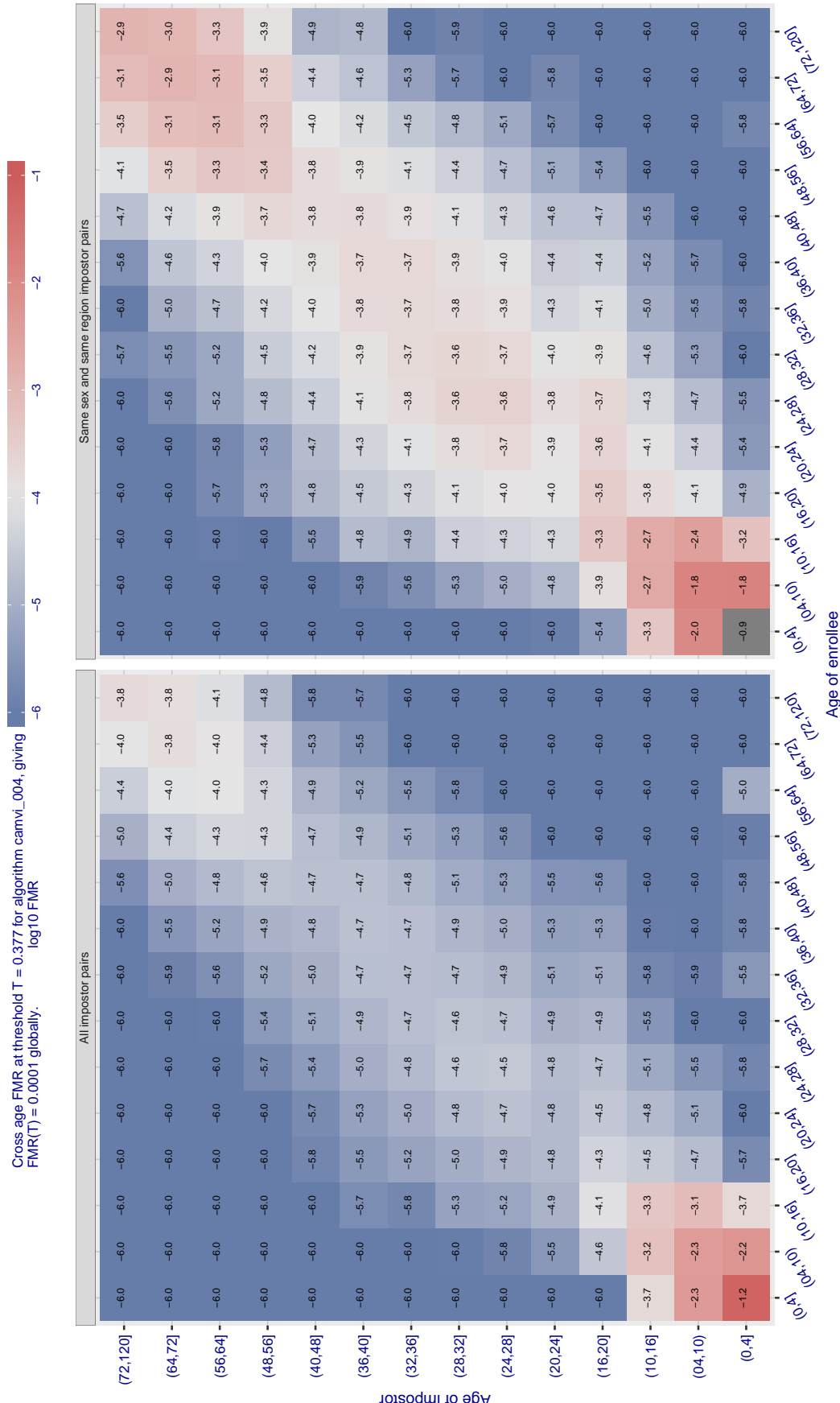


Figure 463: For algorithm camvi-004 operating on visa images, the heatmap shows false match observed over impostor comparisons of faces from different individuals who have the given age pair. False matches are counted against a recognition threshold fixed globally to give  $FMR = 0.0001$  over all on the order of  $10^{10}$  impostor comparisons. The text in each box gives the same quantity as that coded by the color. Light colors present a security vulnerability to, for example, a passport gate.

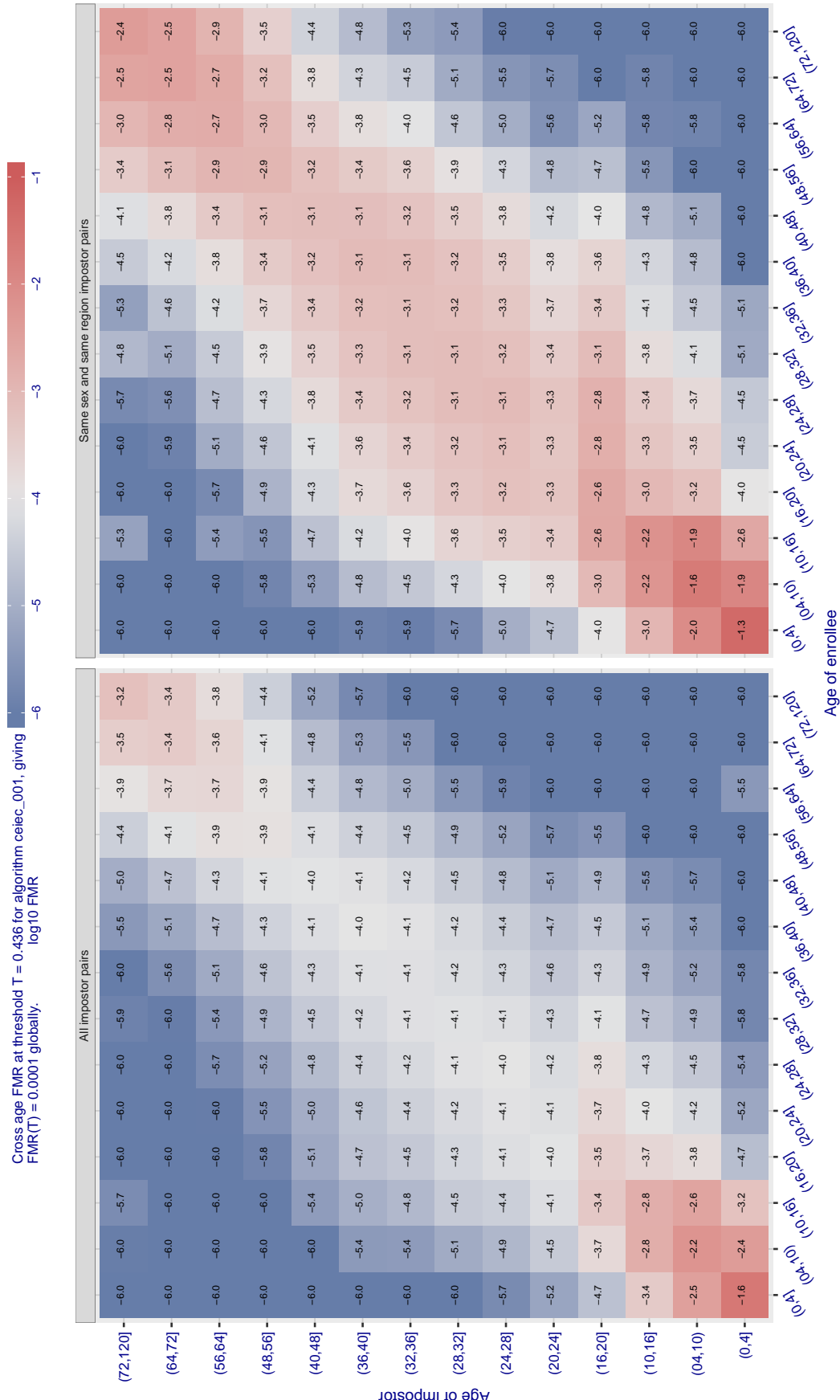


Figure 464: For algorithm ceiec\_001 operating on visa images, the heatmap shows false match observed over impostor comparisons of faces from different individuals who have the given age pair. False matches are counted against a recognition threshold fixed globally to give FMR = 0.0001 over all on the order of  $10^{10}$  impostor comparisons. The text in each box gives the same quantity as that coded by the color. Light colors present a security vulnerability to, for example, a passport gate.

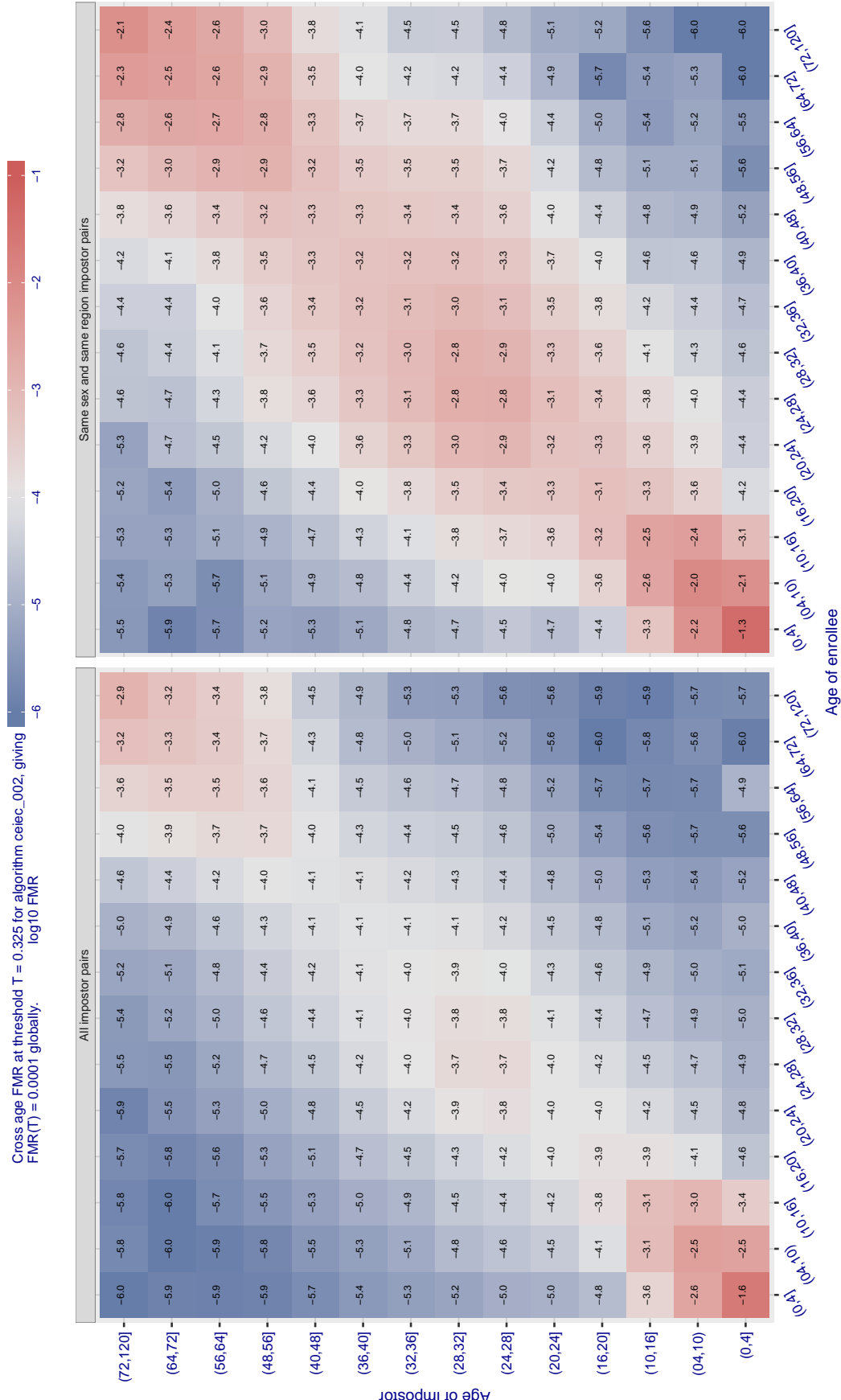


Figure 465: For algorithm ceiec-002 operating on visa images, the heatmap shows false match observed over impostor comparisons of faces from different individuals who have the given age pair. False matches are counted against a recognition threshold fixed globally to give  $FMR = 0.0001$  over all on the order of  $10^{10}$  impostor comparisons. The text in each box gives the same quantity as that coded by the color. Light colors present a security vulnerability to, for example, a passport gate.

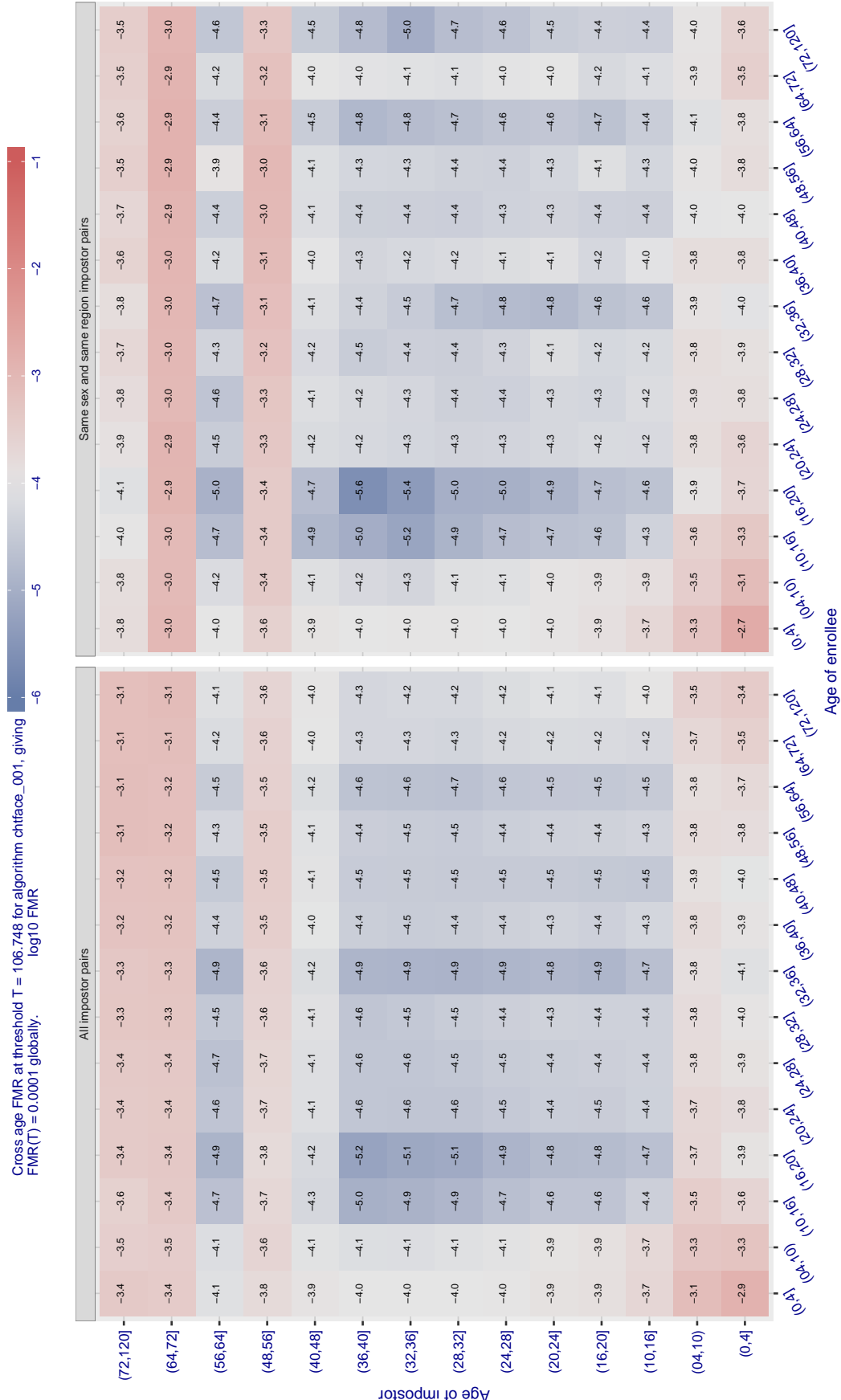


Figure 466: For algorithm chtface-001 operating on visa images, the heatmap shows false match observed over impostor comparisons of faces from different individuals who have the given age pair. False matches are counted against a recognition threshold fixed globally to give  $FMR = 0.0001$  over all on the order of  $10^{10}$  impostor comparisons. The text in each box gives the same quantity as that coded by the color. Light colors present a security vulnerability to, for example, a passport gate.

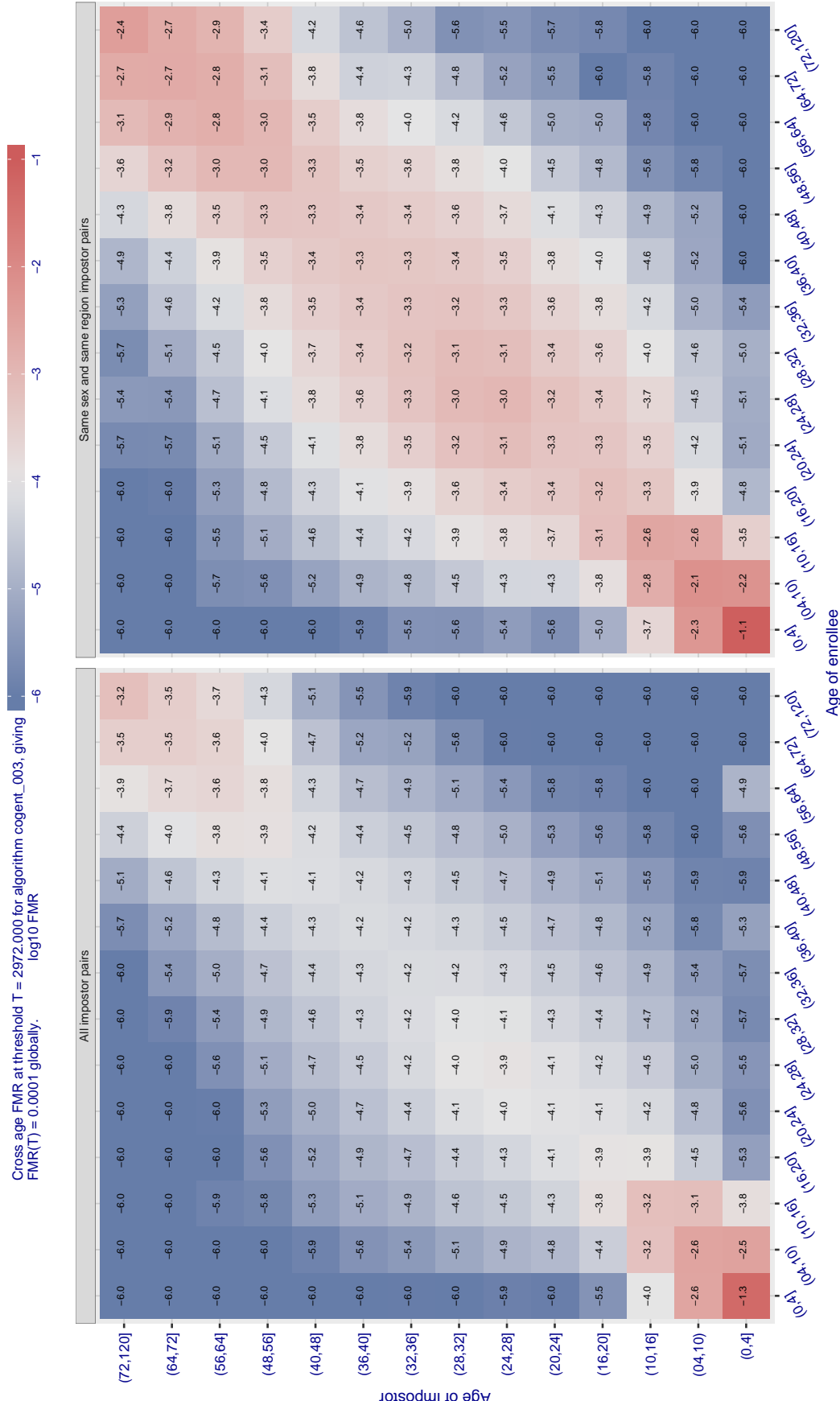


Figure 467: For algorithm cogent-003 operating on visa images, the heatmap shows false match observed over impostor comparisons of faces from different individuals who have the given age pair. False matches are counted against a recognition threshold fixed globally to give  $FMR = 0.0001$  over all on the order of  $10^{10}$  impostor comparisons. The text in each box gives the same quantity as that coded by the color. Light colors present a security vulnerability to, for example, a passport gate.

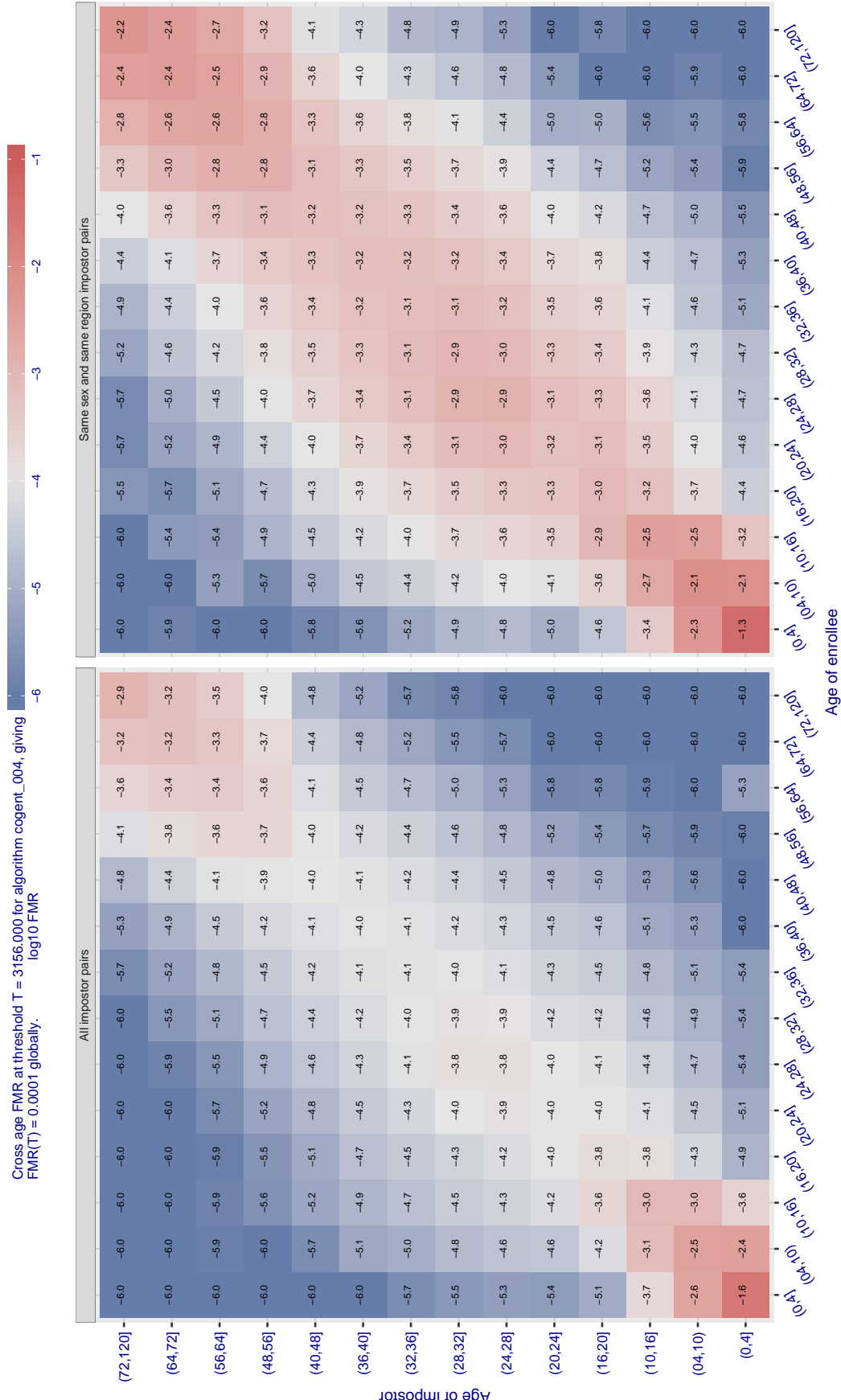


Figure 468: For algorithm cogent-004 operating on visa images, the heatmap shows false match observed over impostor comparisons of faces from different individuals who have the given age pair. False matches are counted against a recognition threshold fixed globally to give  $FMR = 0.0001$  over all on the order of  $10^{10}$  impostor comparisons. The text in each box gives the same quantity as that coded by the color. Light colors present a security vulnerability to, for example, a passport gate.

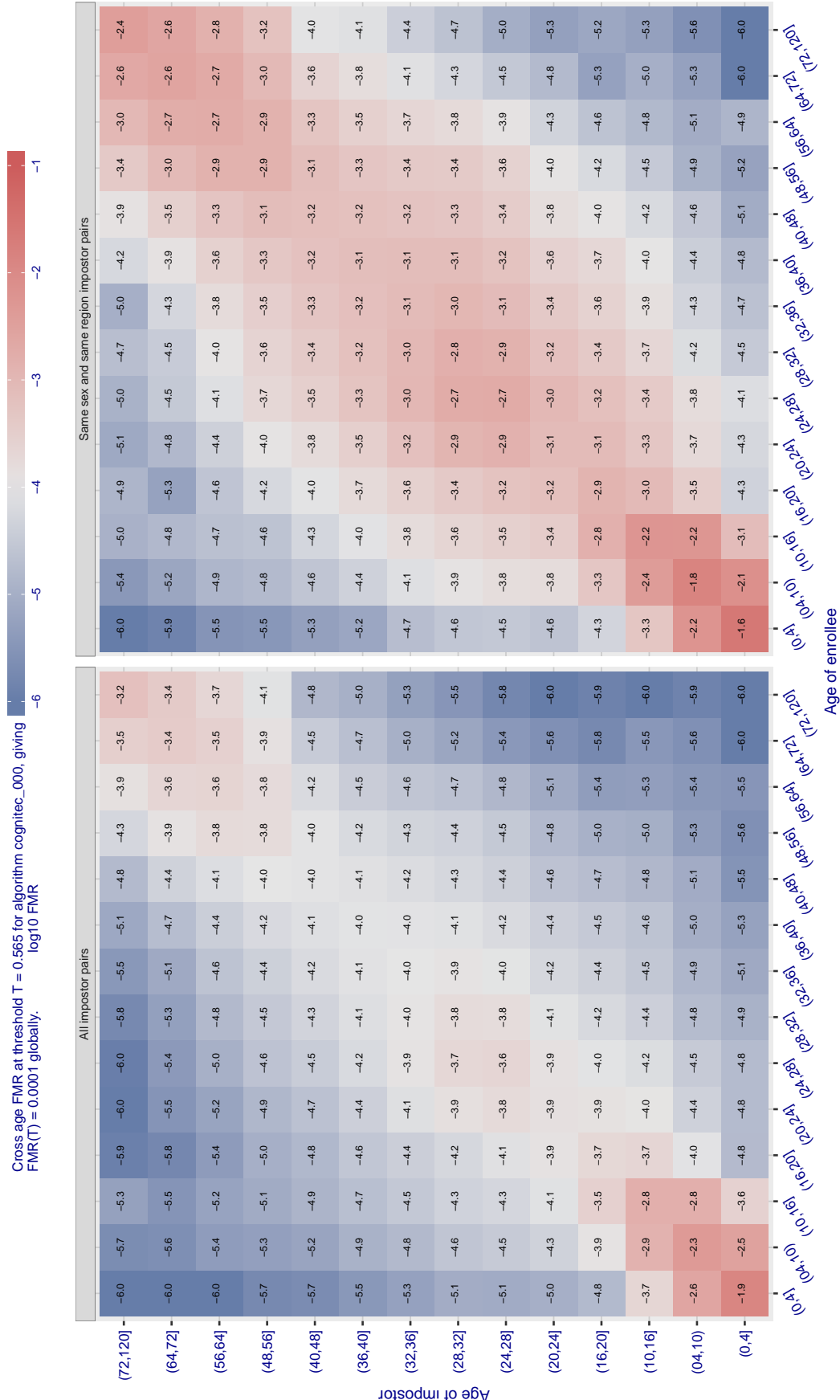


Figure 469: For algorithm cognitec-000 operating on visa images, the heatmap shows false match observed over impostor comparisons of faces from different individuals who have the given age pair. False matches are counted against a recognition threshold fixed globally to give  $FMR = 0.0001$  over all on the order of  $10^{10}$  impostor comparisons. The text in each box gives the same quantity as that coded by the color. Light colors present a security vulnerability to, for example, a passport gate.

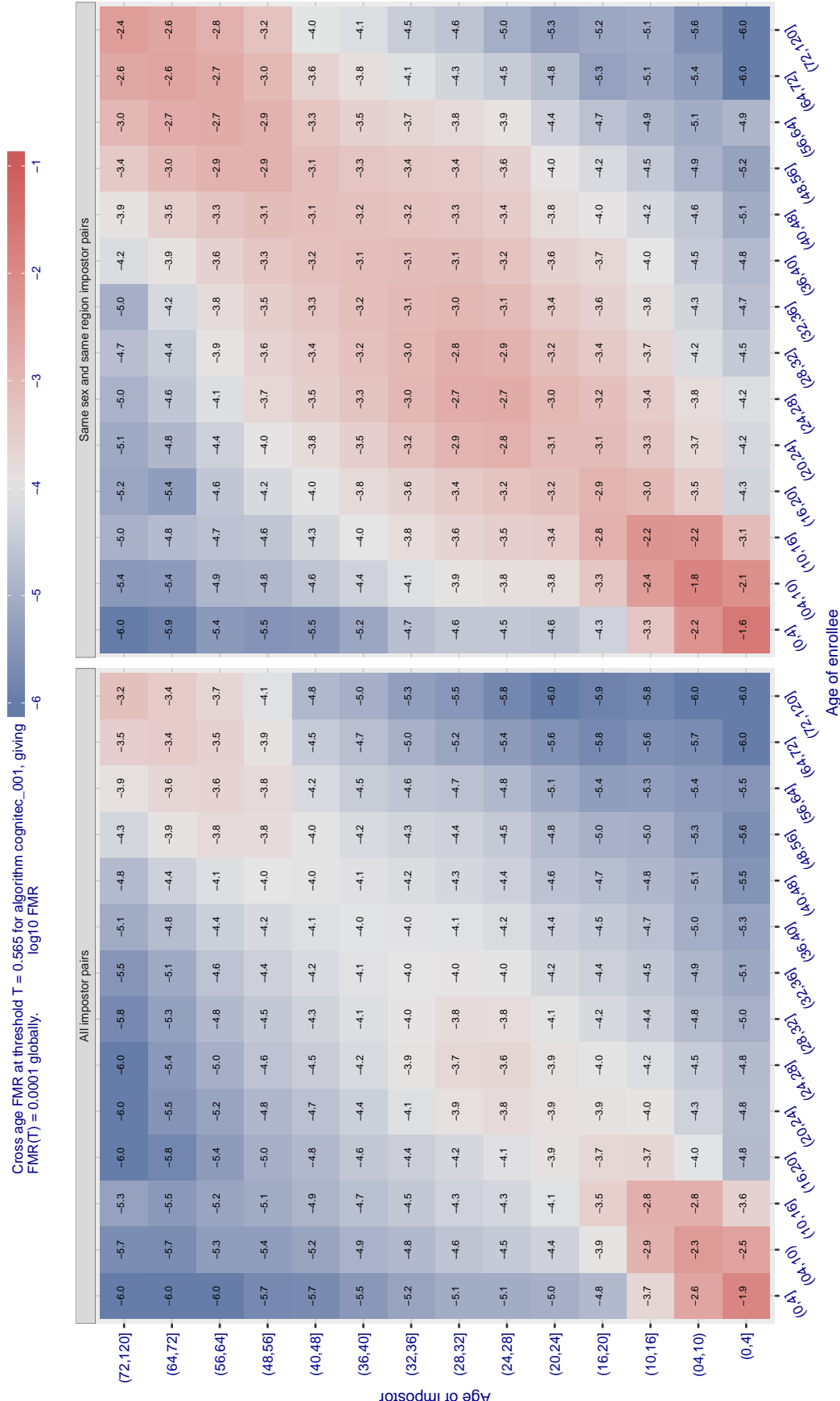


Figure 470: For algorithm cognitec-001 operating on visa images, the heatmap shows false match observed over impostor comparisons of faces from different individuals who have the given age pair. False matches are counted against a recognition threshold fixed globally to give  $FMR = 0.0001$  over all on the order of  $10^{10}$  impostor comparisons. The text in each box gives the same quantity as that coded by the color. Light colors present a security vulnerability to, for example, a passport gate.

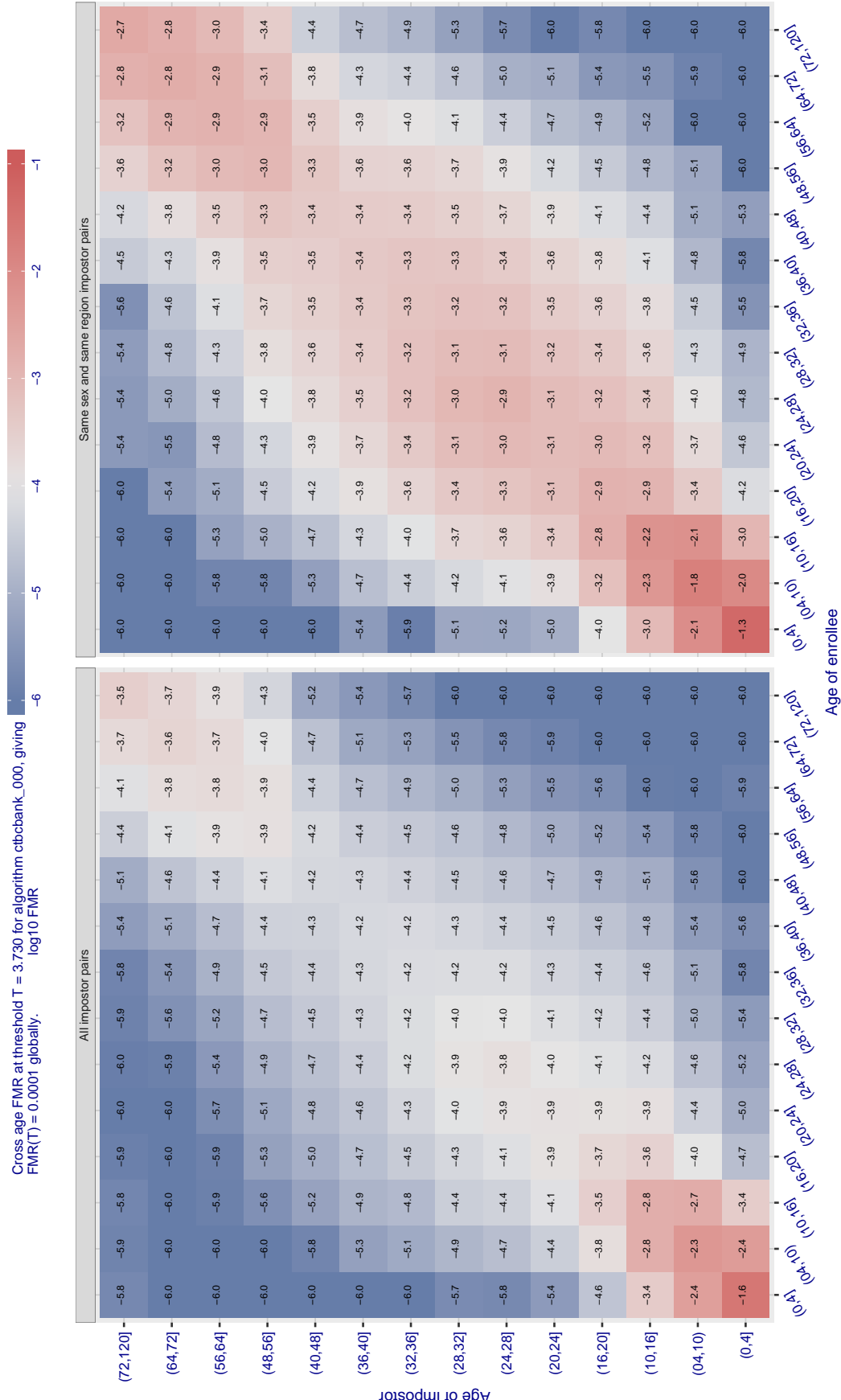


Figure 471: For algorithm ctcbank-000 operating on visa images, the heatmap shows false match observed over impostor comparisons of faces from different individuals who have the given age pair. False matches are counted against a recognition threshold fixed globally to give  $FMR = 0.0001$  over all on the order of  $10^{10}$  impostor comparisons. The text in each box gives the same quantity as that coded by the color. Light colors present a security vulnerability to, for example, a passport gate.

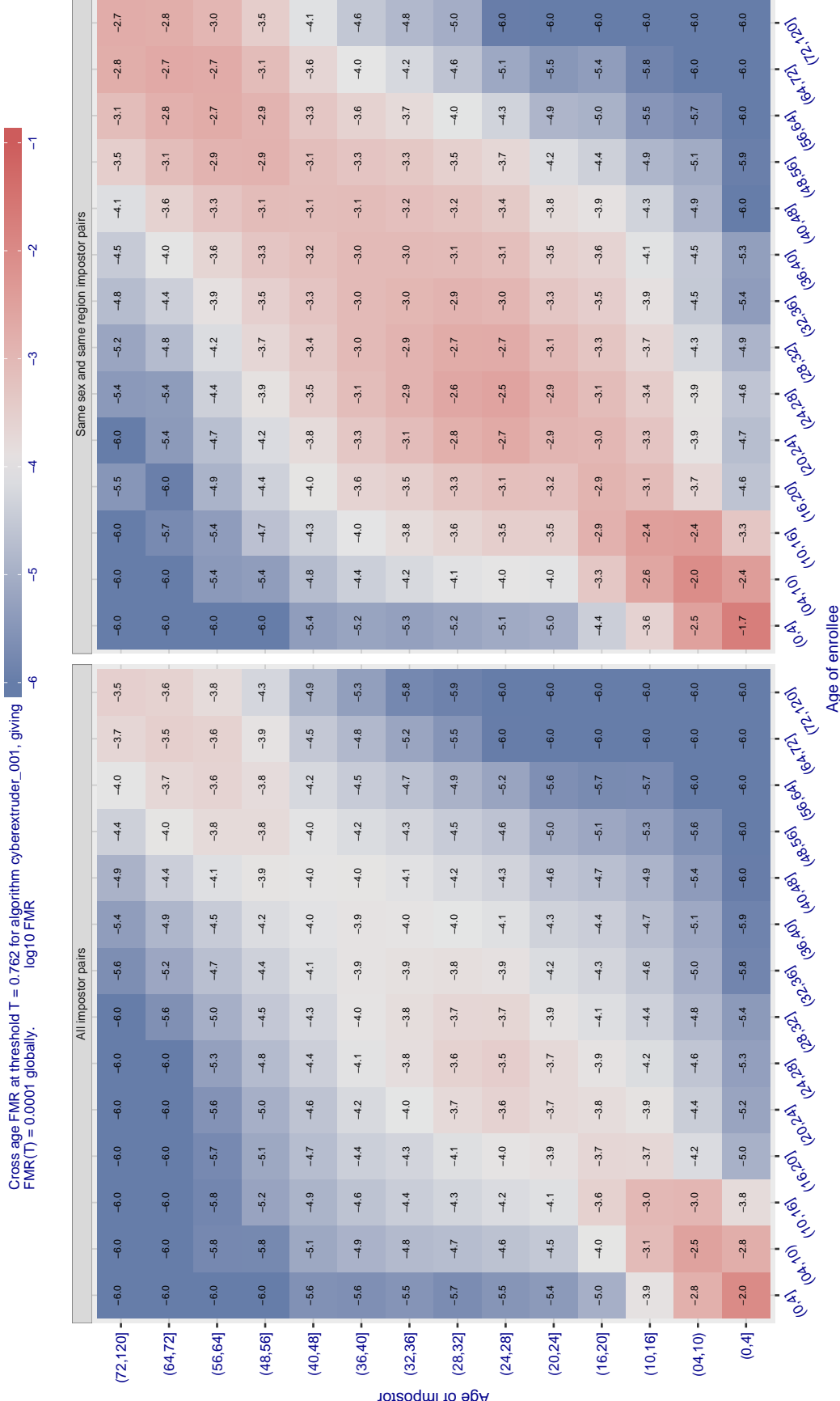


Figure 472: For algorithm cyberextruder-001 operating on visa images, the heatmap shows false match observed over impostor comparisons of faces from different individuals who have the given age pair. False matches are counted against a recognition threshold fixed globally to give  $FMR = 0.0001$  over all on the order of  $10^{10}$  impostor comparisons. The text in each box gives the same quantity as that coded by the color. Light colors present a security vulnerability to, for example, a passport gate.

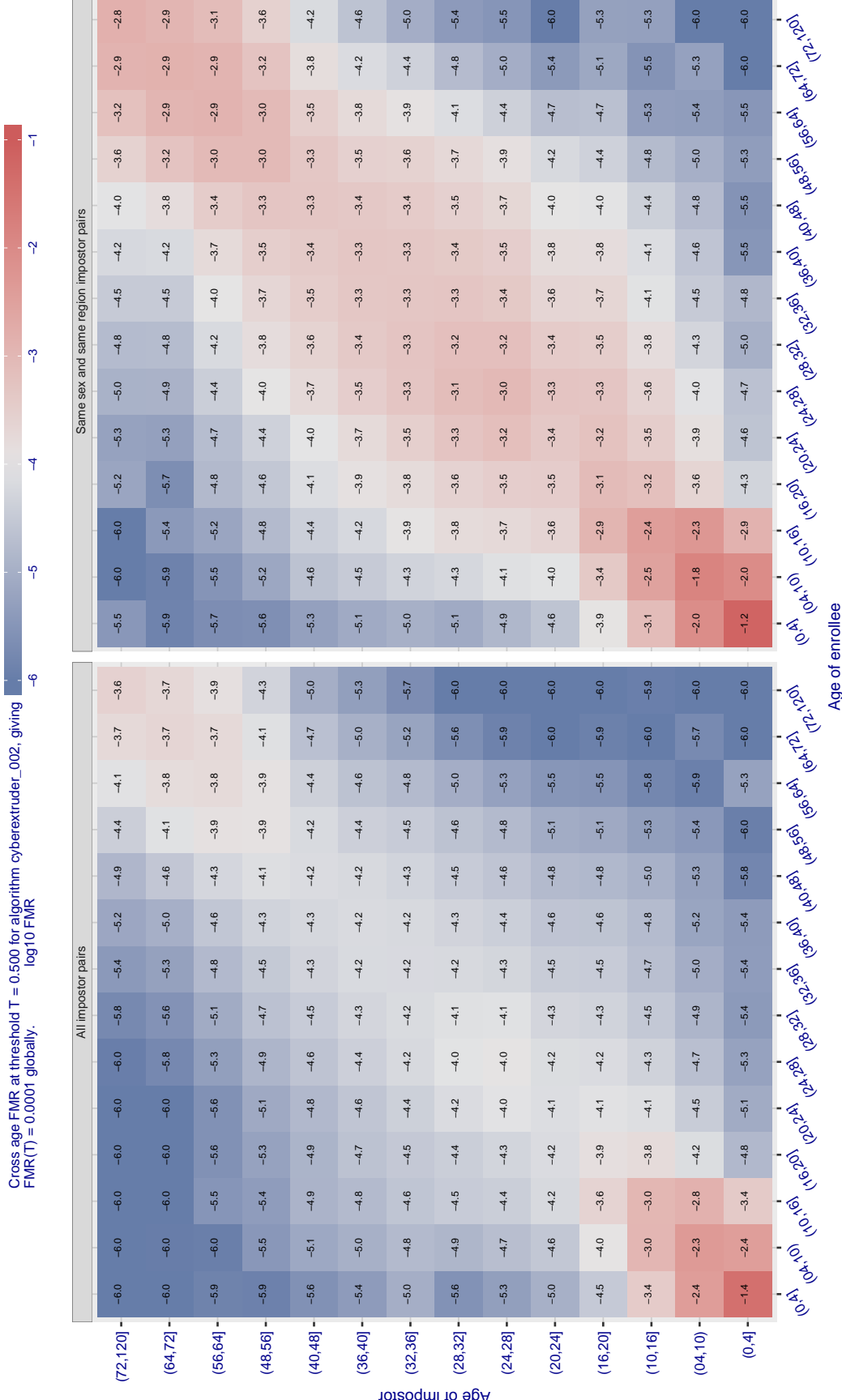


Figure 473: For algorithm cyberextruder-002 operating on visa images, the heatmap shows false match observed over impostor comparisons of faces from different individuals who have the given age pair. False matches are counted against a recognition threshold fixed globally to give FMR = 0.0001 over all on the order of  $10^{10}$  impostor comparisons. The text in each box gives the same quantity as that coded by the color. Light colors present a security vulnerability to, for example, a passport gate.

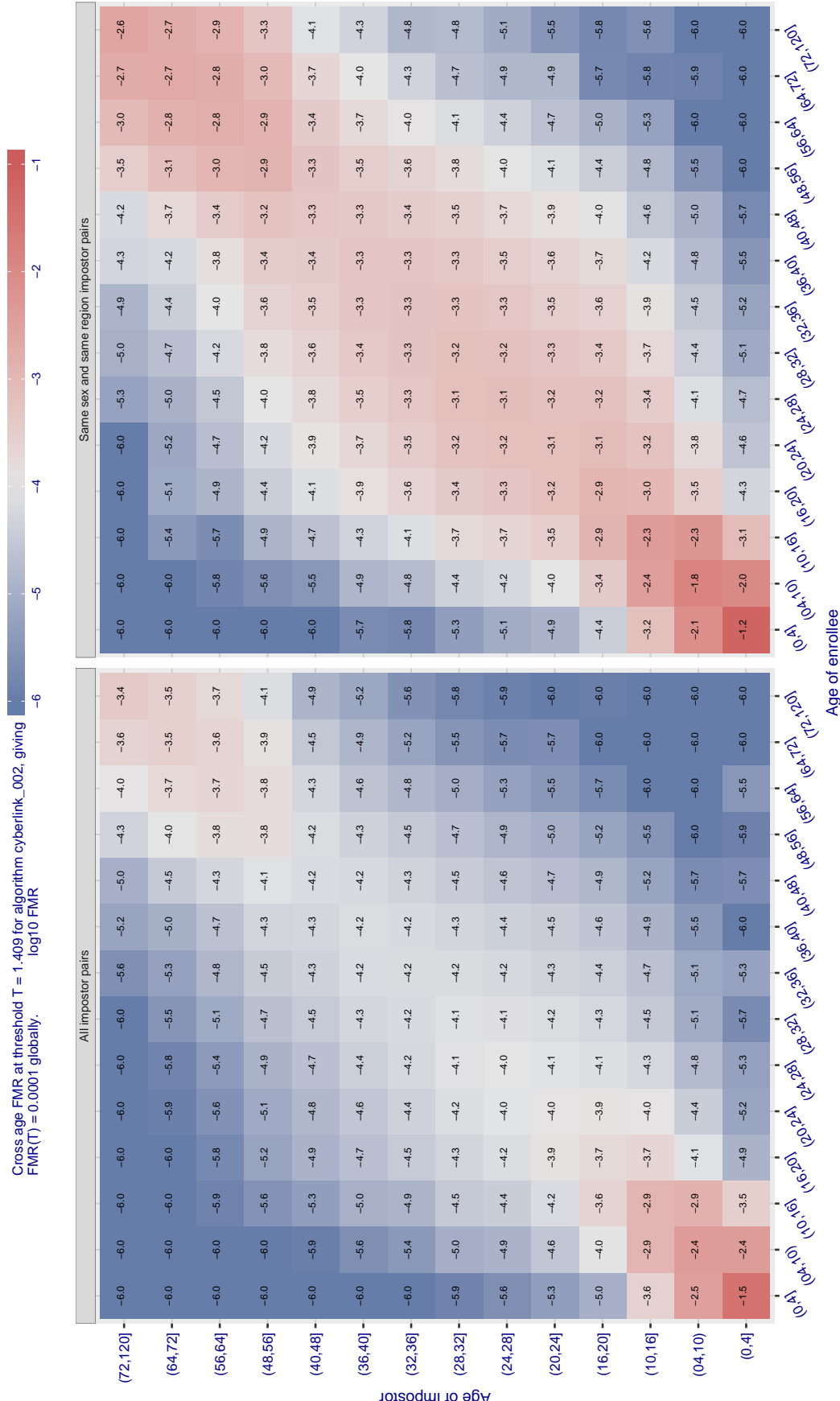


Figure 474: For algorithm cyberlink-002 operating on visa images, the heatmap shows false match observed over impostor comparisons of faces from different individuals who have the given age pair. False matches are counted against a recognition threshold fixed globally to give  $FMR = 0.0001$  over all on the order of  $10^{10}$  impostor comparisons. The text in each box gives the same quantity as that coded by the color. Light colors present a security vulnerability to, for example, a passport gate.

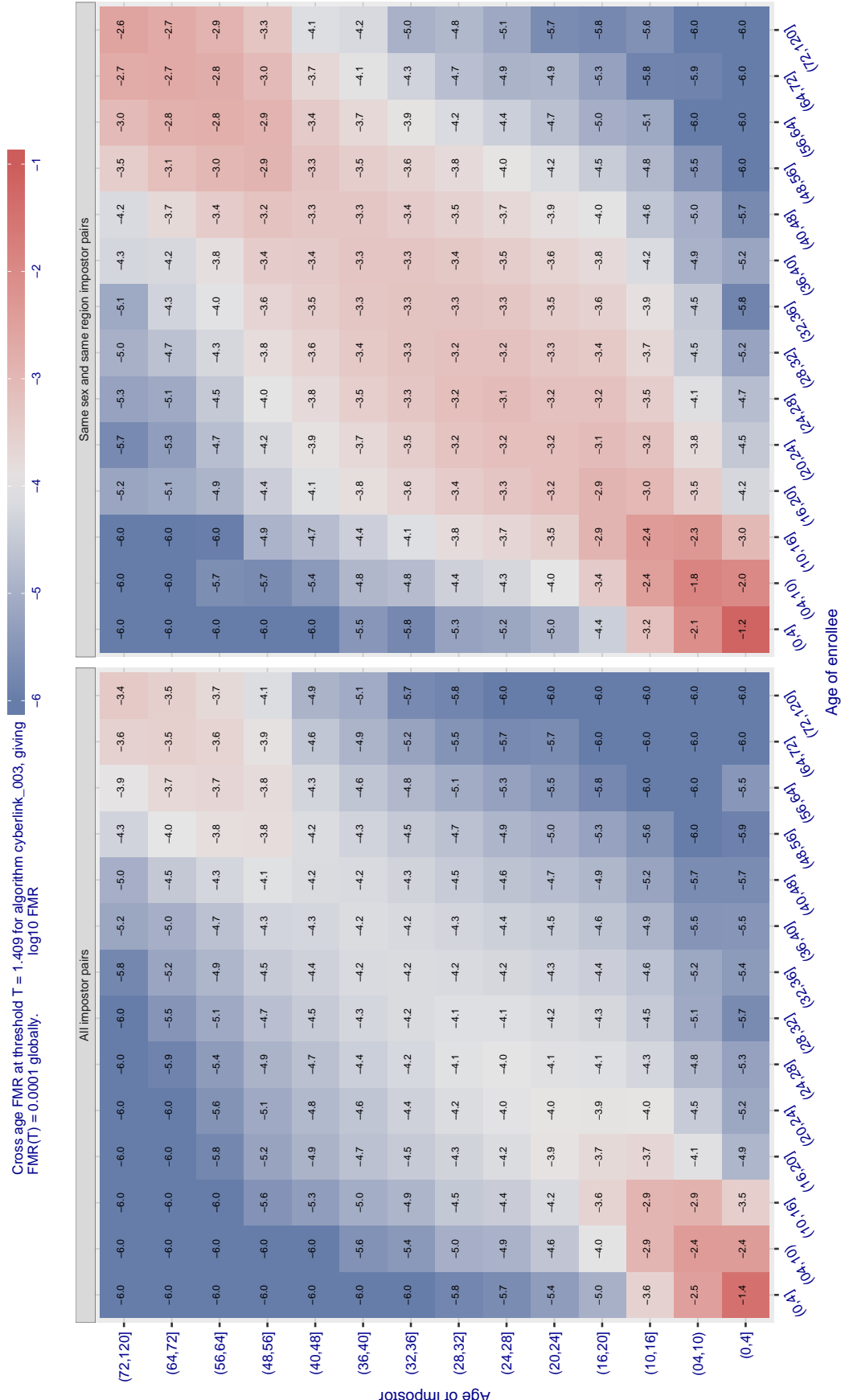


Figure 475: For algorithm cyberlink-003 operating on visa images, the heatmap shows false match observed over impostor comparisons of faces from different individuals who have the given age pair. False matches are counted against a recognition threshold fixed globally to give  $FMR = 0.0001$  over all on the order of  $10^{10}$  impostor comparisons. The text in each box gives the same quantity as that coded by the color. Light colors present a security vulnerability to, for example, a passport gate.

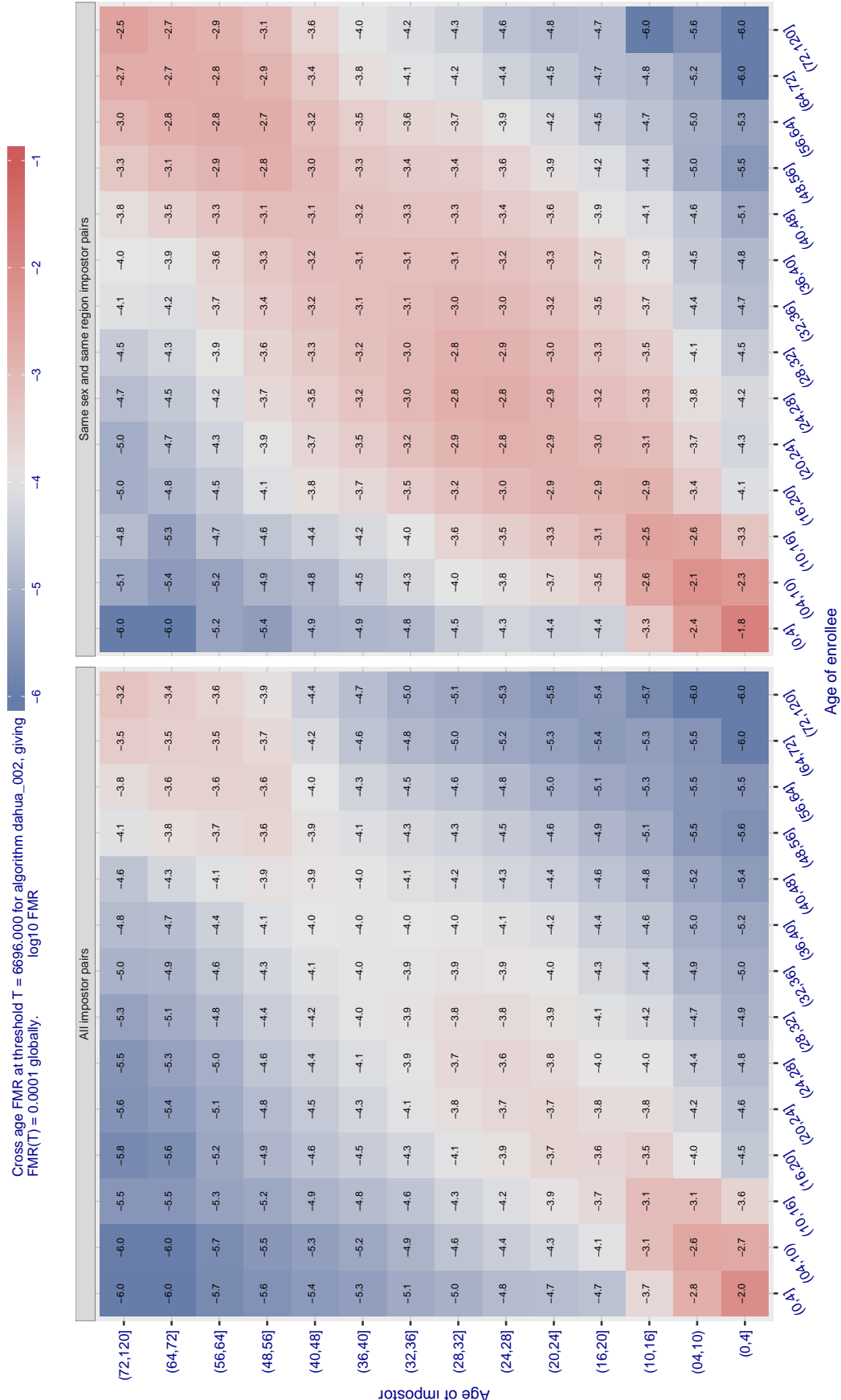
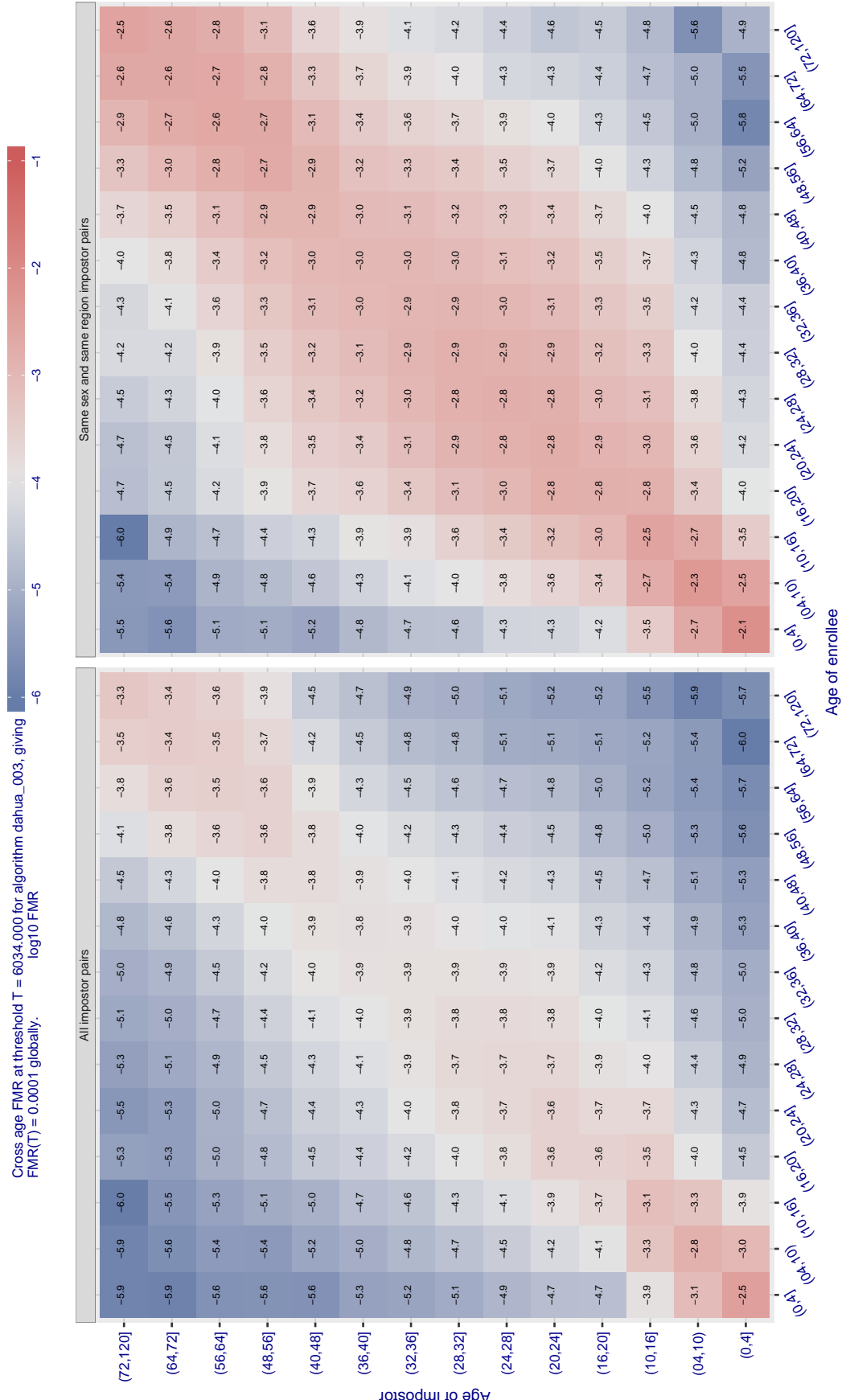


Figure 476: For algorithm dahua-002 operating on visa images, the heatmap shows false match observed over impostor comparisons of faces from different individuals who have the given age pair. False matches are counted against a recognition threshold fixed globally to give  $FMR = 0.0001$  over all on the order of  $10^{10}$  impostor comparisons. The text in each box gives the same quantity as that coded by the color. Light colors present a security vulnerability to, for example, a passport gate.



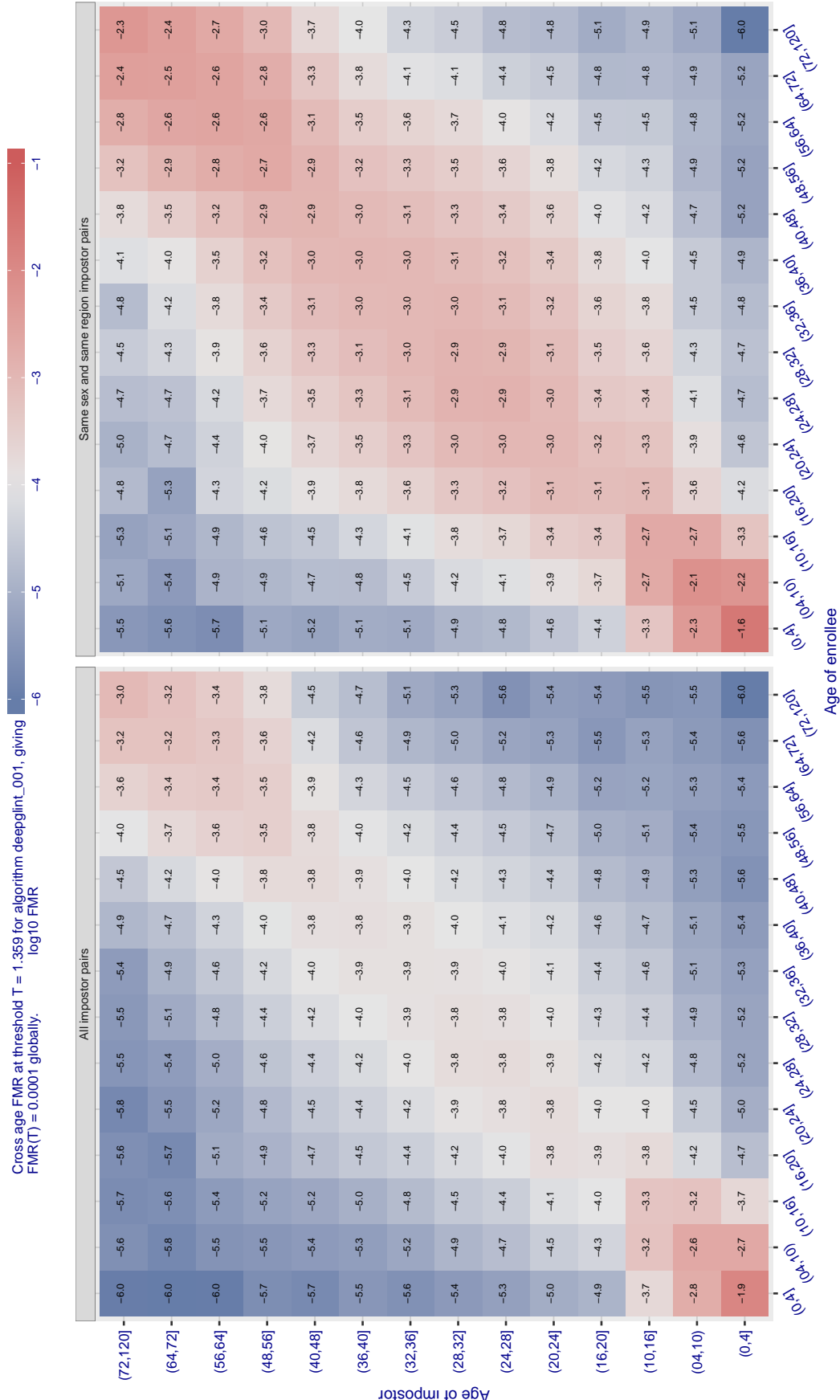


Figure 478: For algorithm deepglint-001 operating on visa images, the heatmap shows false match observed over impostor comparisons of faces from different individuals who have the given age pair. False matches are counted against a recognition threshold fixed globally to give  $FMR = 0.001$  over all on the order of  $10^{10}$  impostor comparisons. The text in each box gives the same quantity as that coded by the color. Light colors present a security vulnerability to, for example, a passport gate.

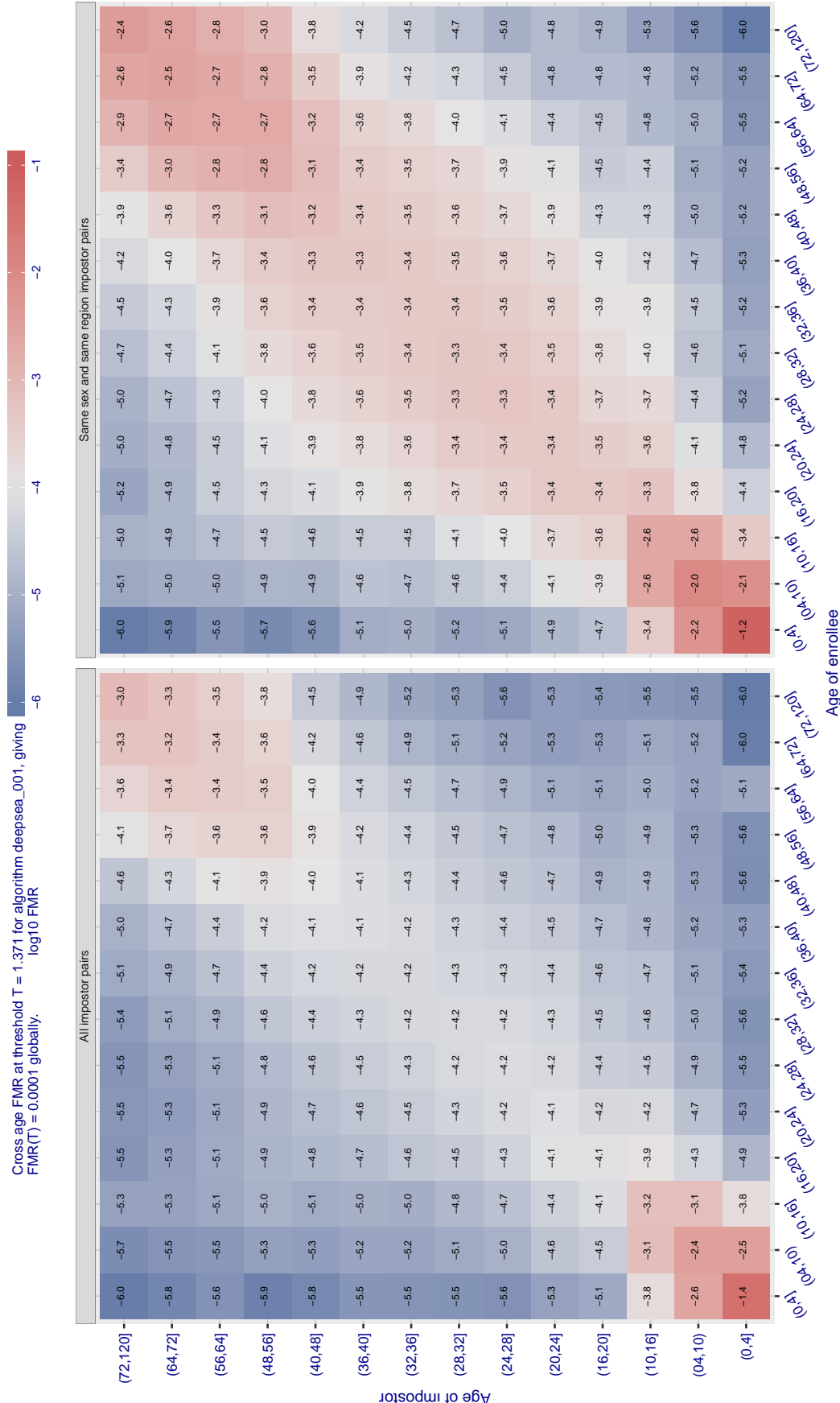


Figure 479: For algorithm deepsea-001 operating on visa images, the heatmap shows false match observed over impostor comparisons of faces from different individuals who have the given age pair. False matches are counted against a recognition threshold fixed globally to give  $FMR = 0.0001$  over all on the order of  $10^{10}$  impostor comparisons. The text in each box gives the same quantity as that coded by the color. Light colors present a security vulnerability to, for example, a passport gate.

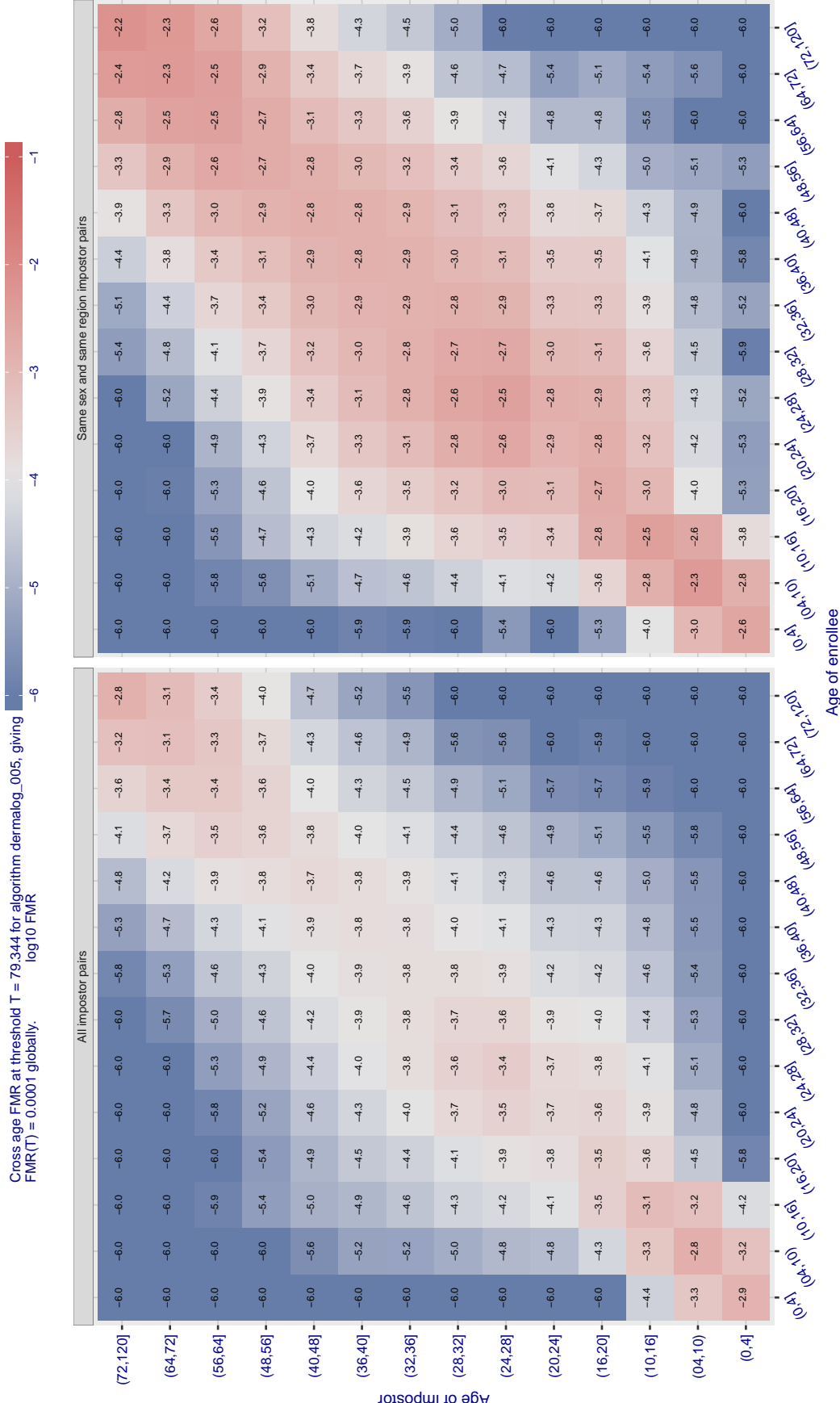


Figure 480: For algorithm dermalog-005 operating on visa images, the heatmap shows false match observed over impostor comparisons of faces from different individuals who have the given age pair. False matches are counted against a recognition threshold fixed globally to give  $\text{FMR} = 0.001$  over all on the order of  $10^{10}$  impostor comparisons. The text in each box gives the same quantity as that coded by the color. Light colors present a security vulnerability to, for example, a passport gate.

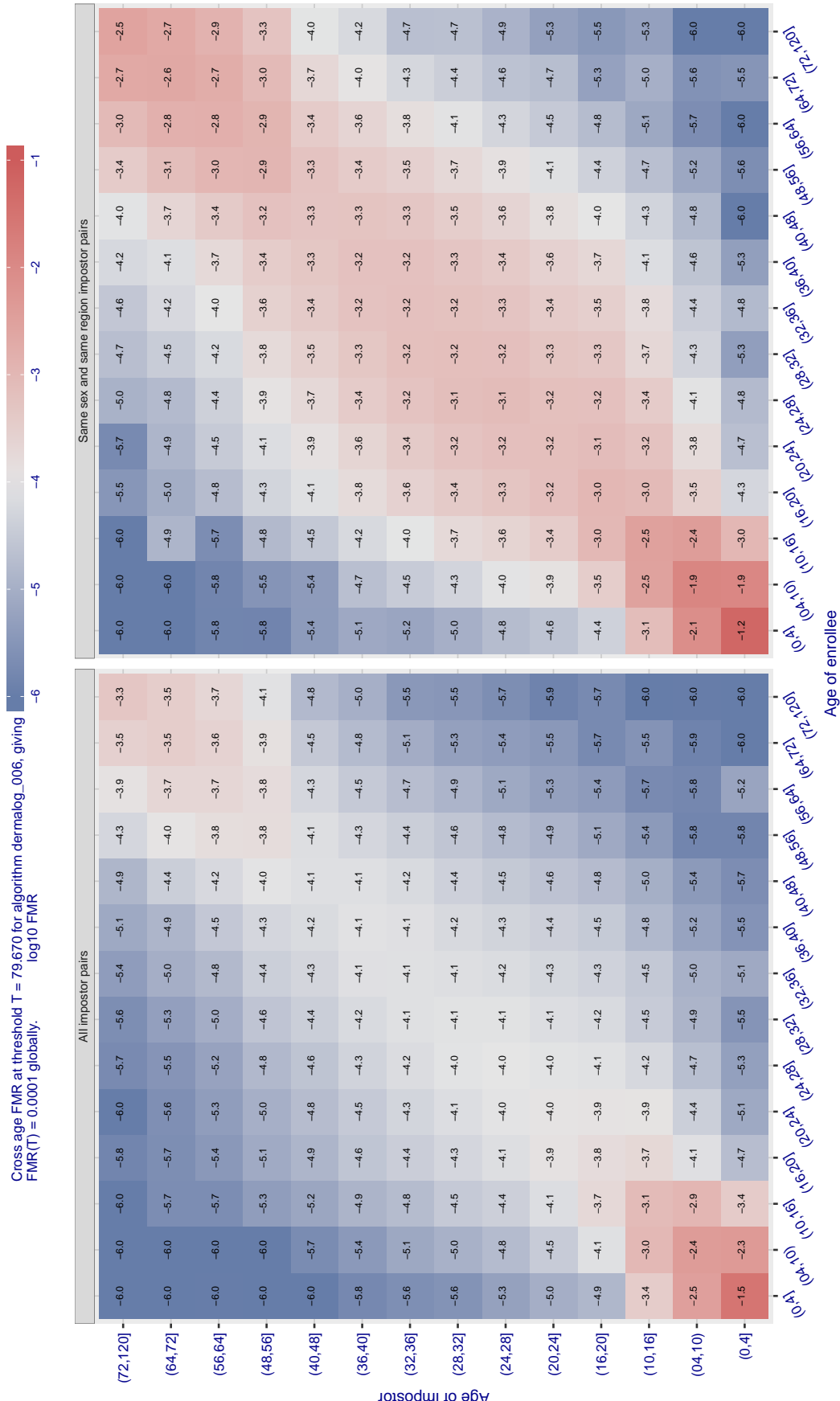


Figure 481: For algorithm dermalog-006 operating on visa images, the heatmap shows false match observed over impostor comparisons of faces from different individuals who have the given age pair. False matches are counted against a recognition threshold fixed globally to give  $\text{FMR} = 0.001$  over all on the order of  $10^{10}$  impostor comparisons. The text in each box gives the same quantity as that coded by the color. Light colors present a security vulnerability to, for example, a passport gate.

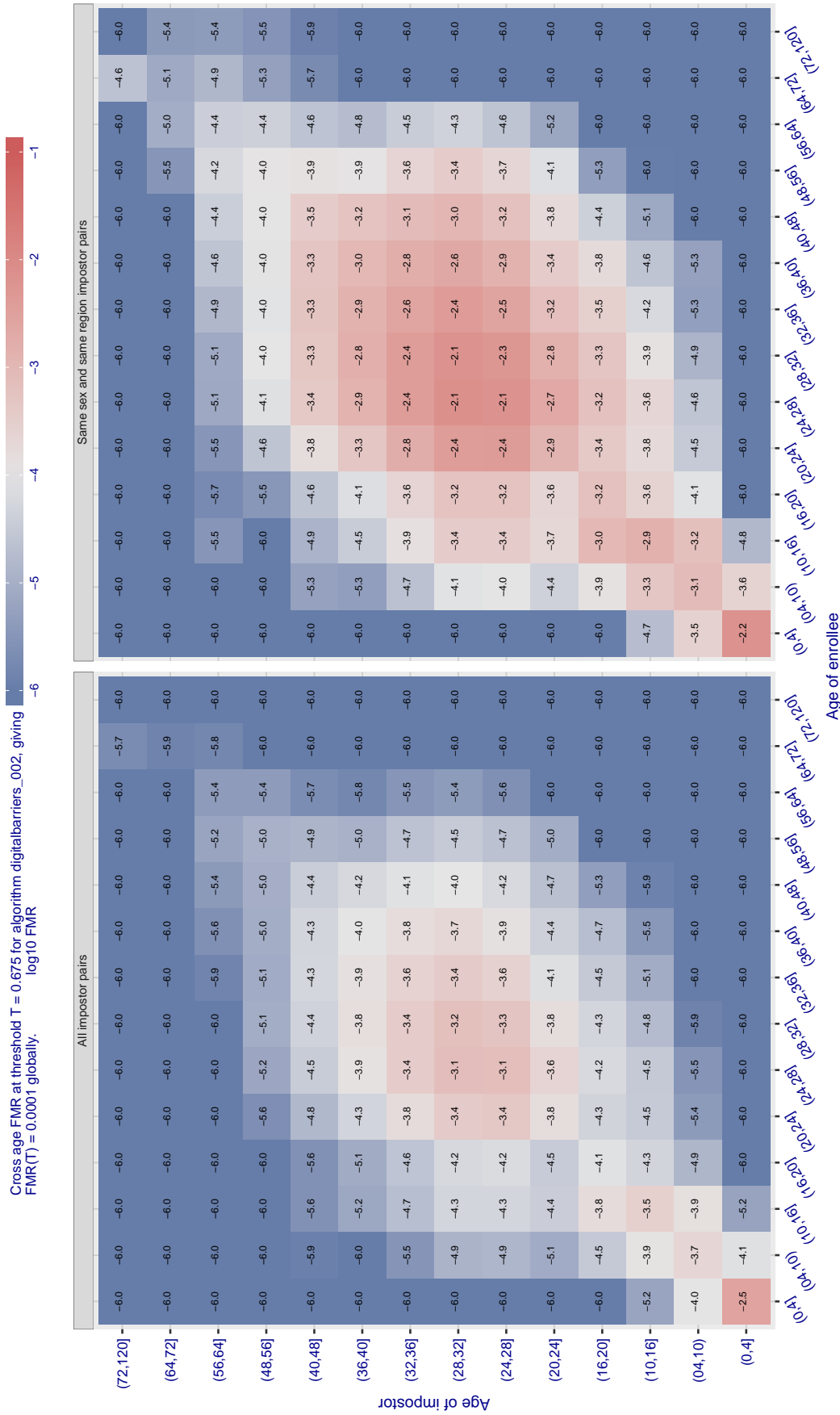


Figure 482: For algorithm digitalBarriers-002 operating on visa images, the heatmap shows false match observed over impostor comparisons of faces from different individuals who have the given age pair. False matches are counted against a recognition threshold fixed globally to give FMR = 0.0001 over all on the order of  $10^{10}$  impostor comparisons. The text in each box gives the same quantity as that coded by the color. Light colors present a security vulnerability to, for example, a passport gate.

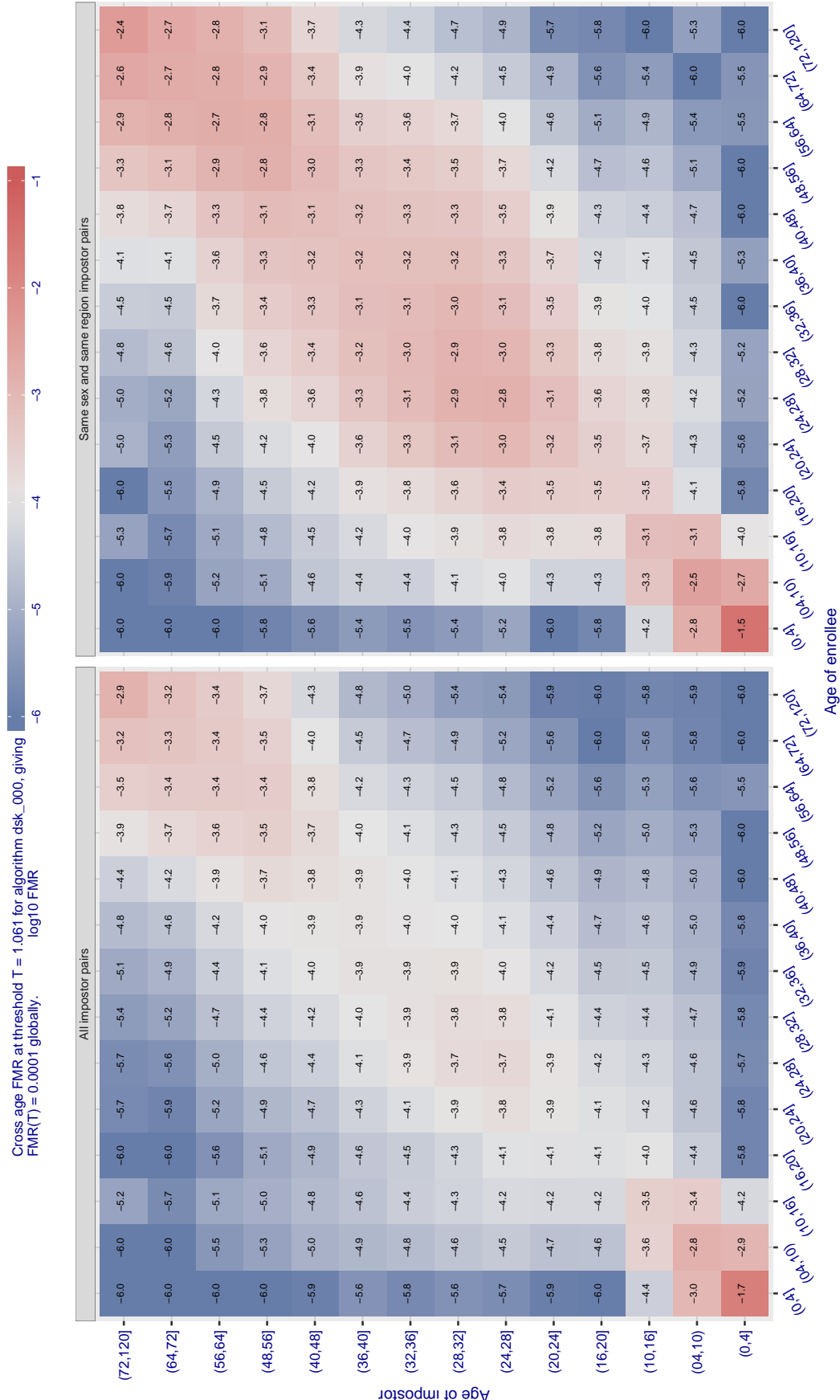


Figure 483: For algorithm dsk\_000 operating on visa images, the heatmap shows false match observed over impostor comparisons of faces from different individuals who have the same age pair. False matches are counted against a recognition threshold fixed globally to give  $FMR = 0.0001$  over all on the order of  $10^{10}$  impostor comparisons. The text in each box gives the same quantity as that coded by the color. Light colors present a security vulnerability to, for example, a passport gate.

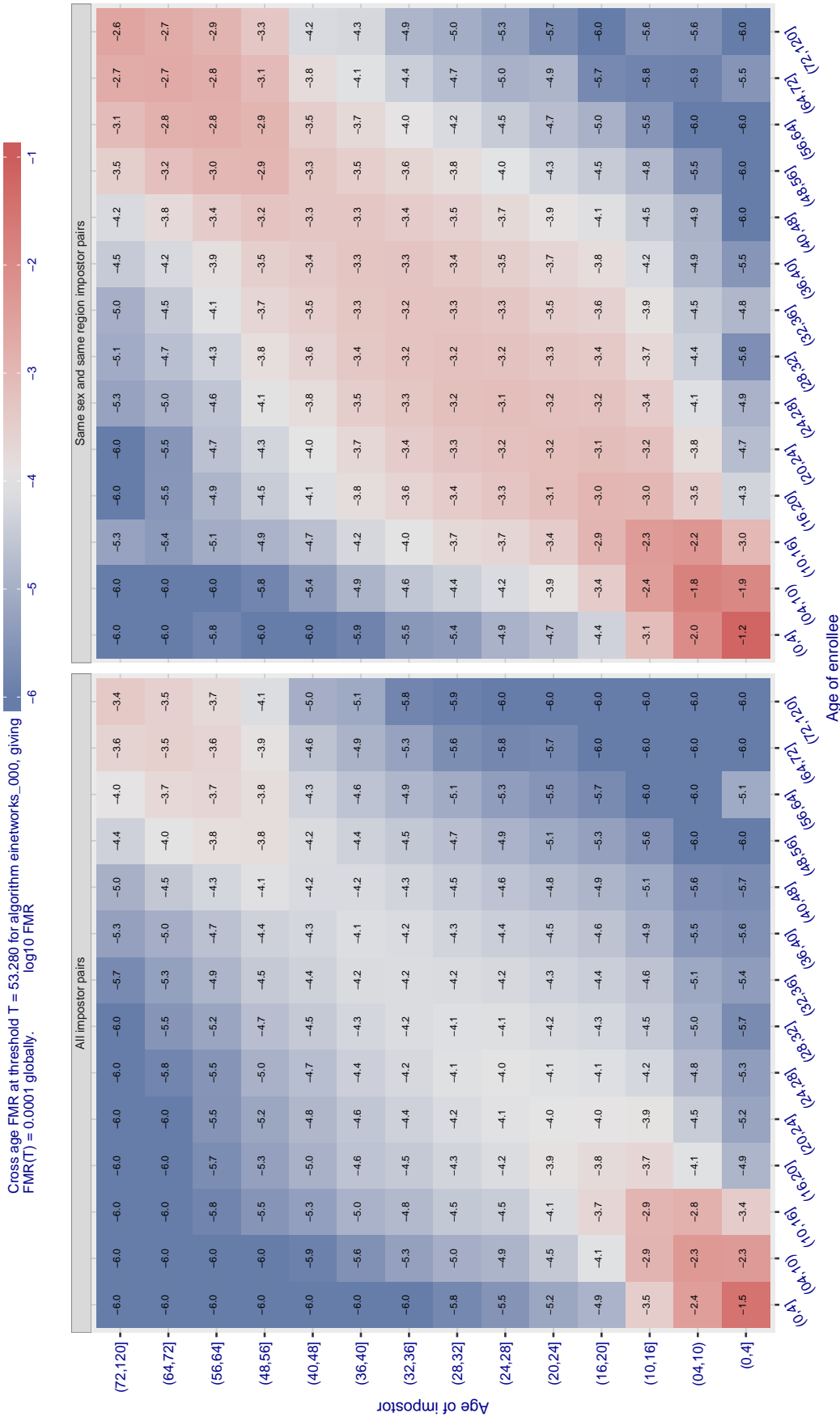


Figure 484: For algorithm einetworks-000 operating on visa images, the heatmap shows false match observed over imposter comparisons of faces from different individuals who have the given age pair. False matches are counted against a recognition threshold fixed globally to give  $FMR = 0.0001$  over all on the order of  $10^{10}$  imposter comparisons. The text in each box gives the same quantity as that coded by the color. Light colors present a security vulnerability to, for example, a passport gate.

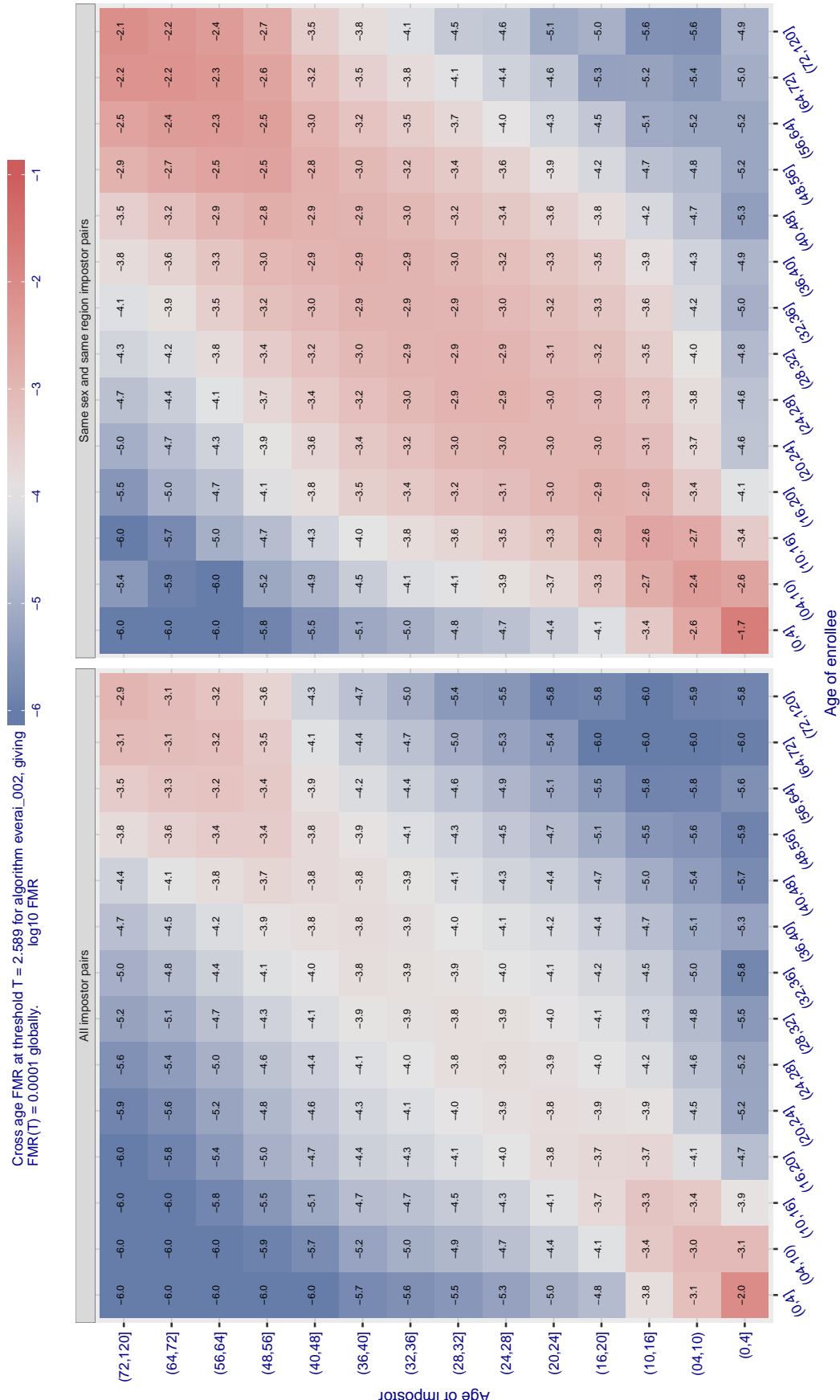


Figure 485: For algorithm everai-002 operating on visa images, the heatmap shows false match observed over impostor comparisons of faces from different individuals who have the given age pair. False matches are counted against a recognition threshold fixed globally to give  $FMR = 0.0001$  over all on the order of  $10^{10}$  impostor comparisons. The text in each box gives the same quantity as that coded by the color. Light colors present a security vulnerability to, for example, a passport gate.

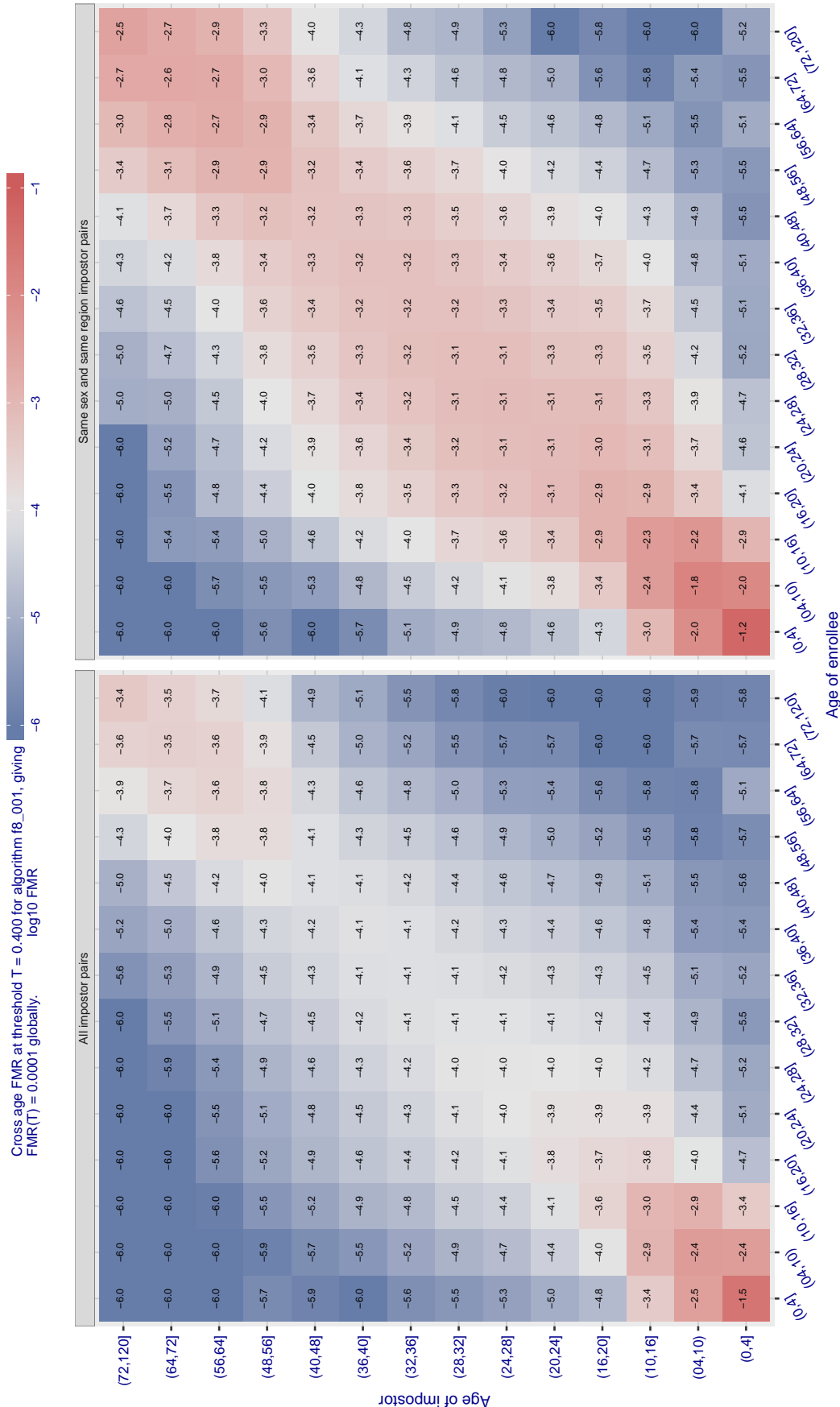


Figure 486: For algorithm f8\_001 operating on visa images, the heatmap shows false match observed over impostor comparisons of faces from different individuals who have the given age pair. False matches are counted against a recognition threshold fixed globally to give  $FMR = 0.0001$  over all on the order of  $10^{10}$  impostor comparisons. The text in each box gives the same quantity as that coded by the color. Light colors present a security vulnerability to, for example, a passport gate.

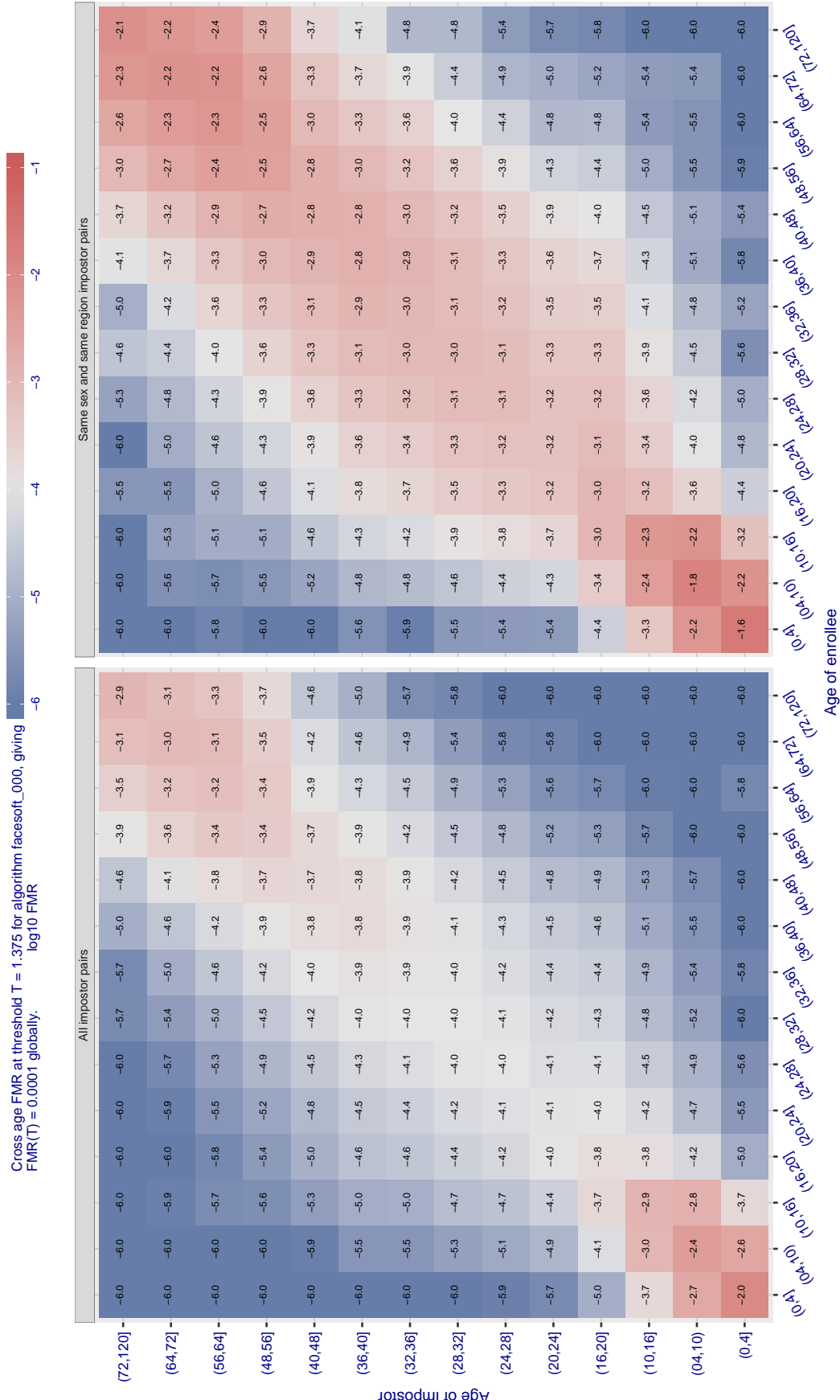


Figure 487: For algorithm facesoft-000 operating on visa images, the heatmap shows false match observed over impostor comparisons of faces from different individuals who have the given age pair. False matches are counted against a recognition threshold fixed globally to give  $FMR = 0.0001$  over all on the order of  $10^{10}$  impostor comparisons. The text in each box gives the same quantity as that coded by the color. Light colors present a security vulnerability to, for example, a passport gate.

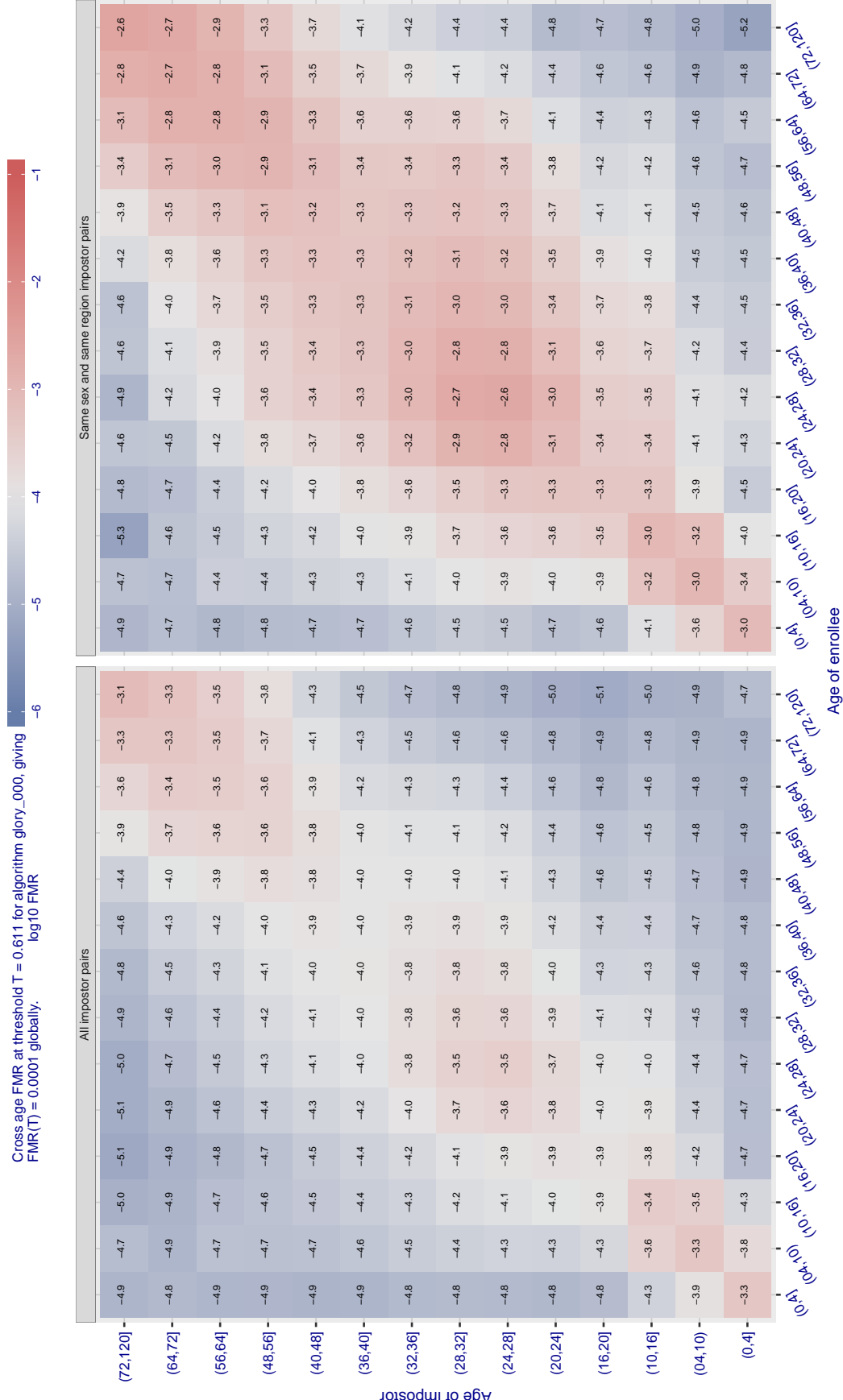


Figure 488: For algorithm *glory-000* operating on visa images, the heatmap shows false match observed over impostor comparisons of faces from different individuals who have the given age pair. False matches are counted against a recognition threshold fixed globally to give  $FMR = 0.0001$  over all on the order of  $10^{10}$  impostor comparisons. The text in each box gives the same quantity as that coded by the color. Light colors present a security vulnerability to, for example, a passport gate.

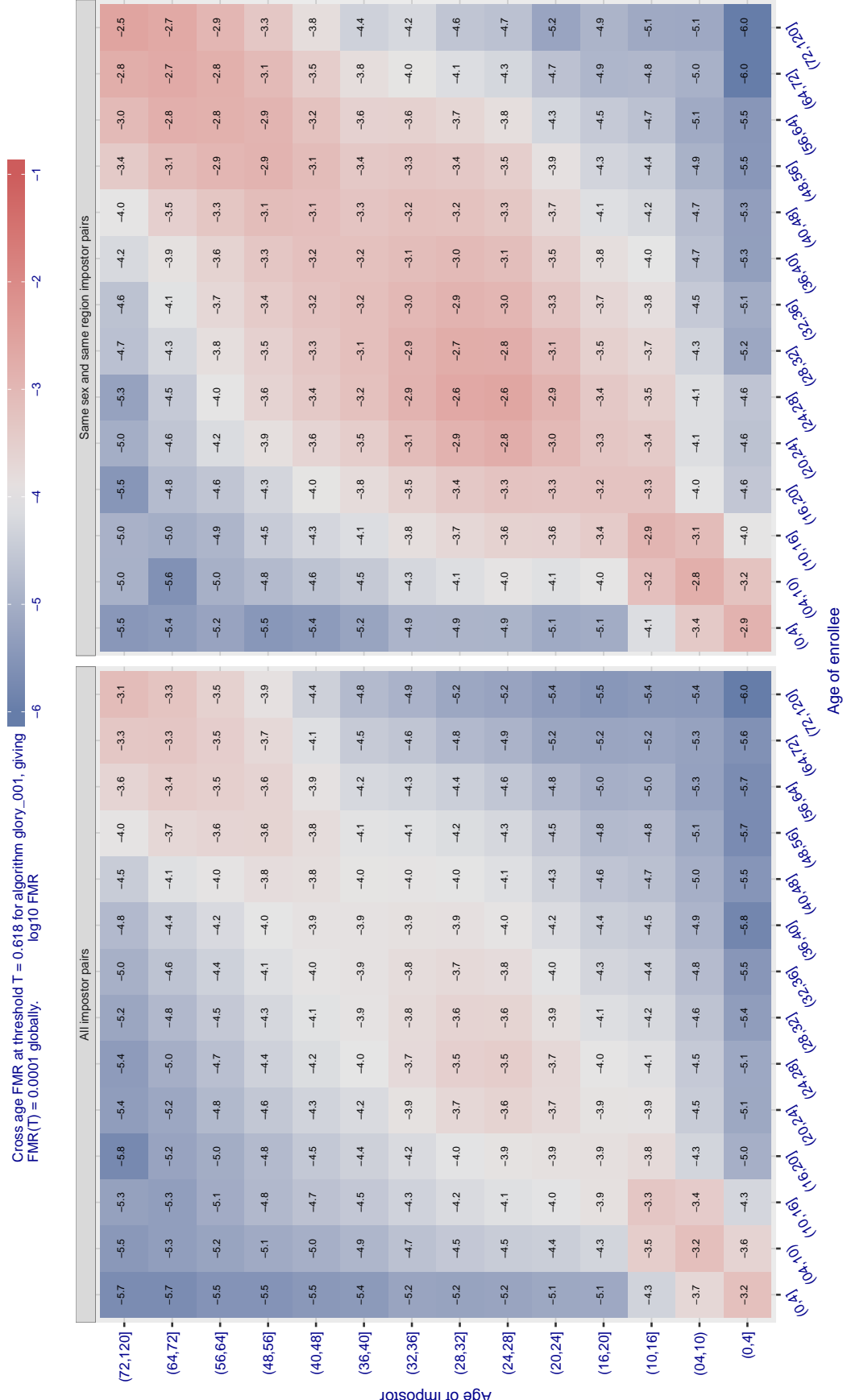


Figure 489: For algorithm glory\_001 operating on visa images, the heatmap shows false match observed over impostor comparisons of faces from different individuals who have the given age pair. False matches are counted against a recognition threshold fixed globally to give  $FMR = 0.0001$  over all on the order of  $10^{10}$  impostor comparisons. The text in each box gives the same quantity as that coded by the color. Light colors present a security vulnerability to, for example, a passport gate.

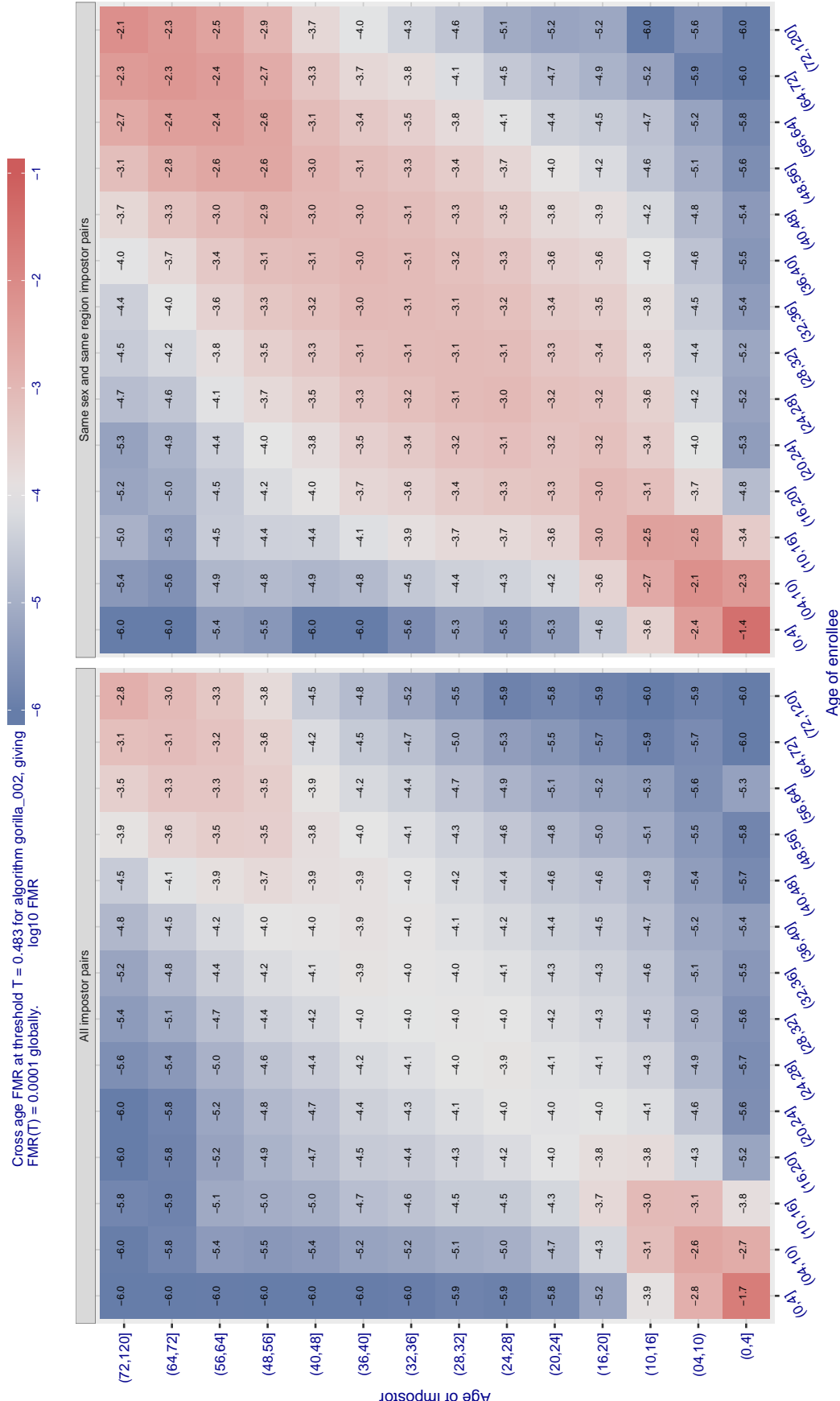


Figure 490: For algorithm gorilla-002 operating on visa images, the heatmap shows false match observed over impostor comparisons of faces from different individuals who have the given age pair. False matches are counted against a recognition threshold fixed globally to give  $FMR = 0.0001$  over all on the order of  $10^{10}$  impostor comparisons. The text in each box gives the same quantity as that coded by the color. Light colors present a security vulnerability to, for example, a passport gate.

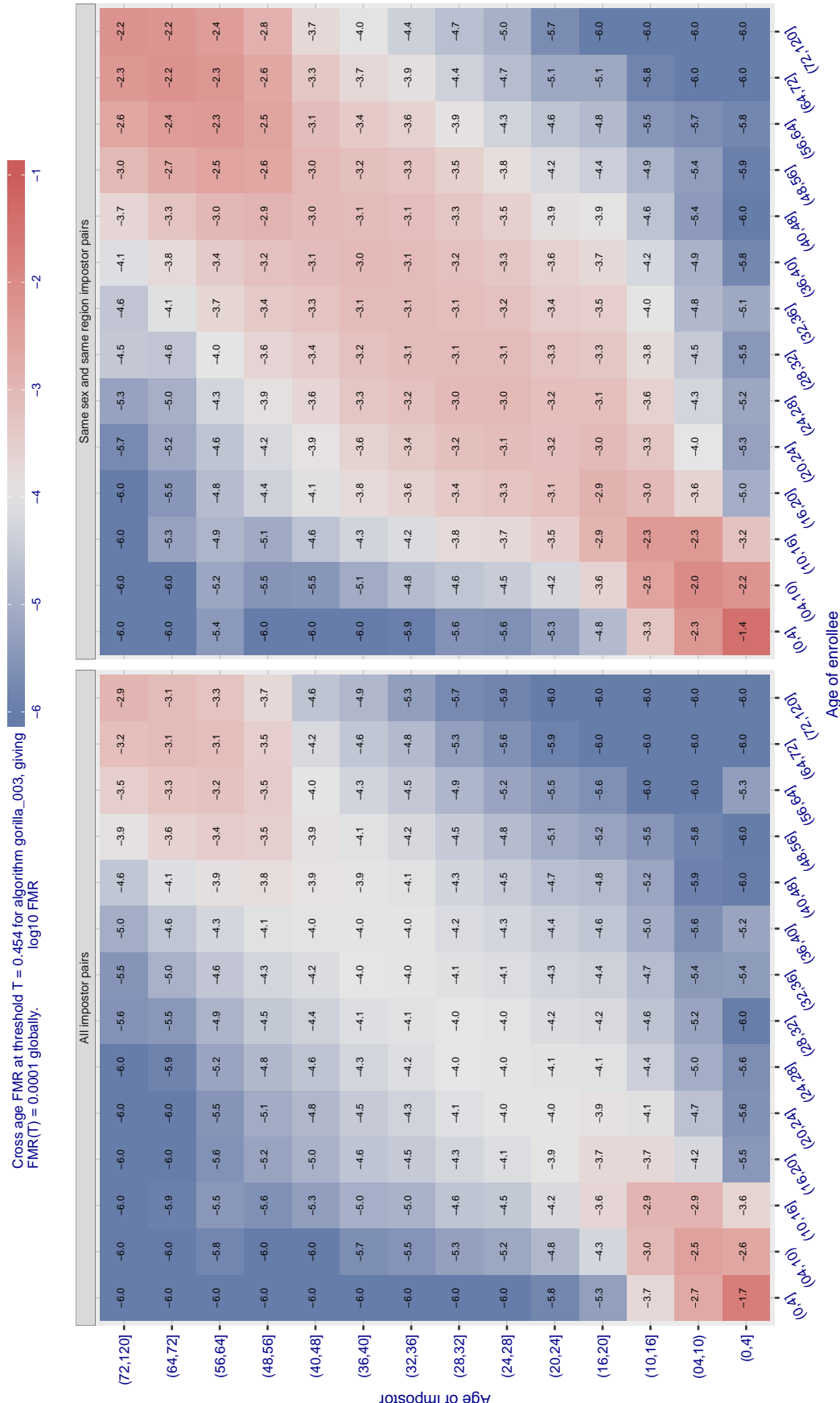


Figure 491: For algorithm gorilla-003 operating on visa images, the heatmap shows false match observed over impostor comparisons of faces from different individuals who have the given age pair. False matches are counted against a recognition threshold fixed globally to give FMR = 0.0001 over all on the order of  $10^{10}$  impostor comparisons. The text in each box gives the same quantity as that coded by the color. Light colors present a security vulnerability to, for example, a passport gate.

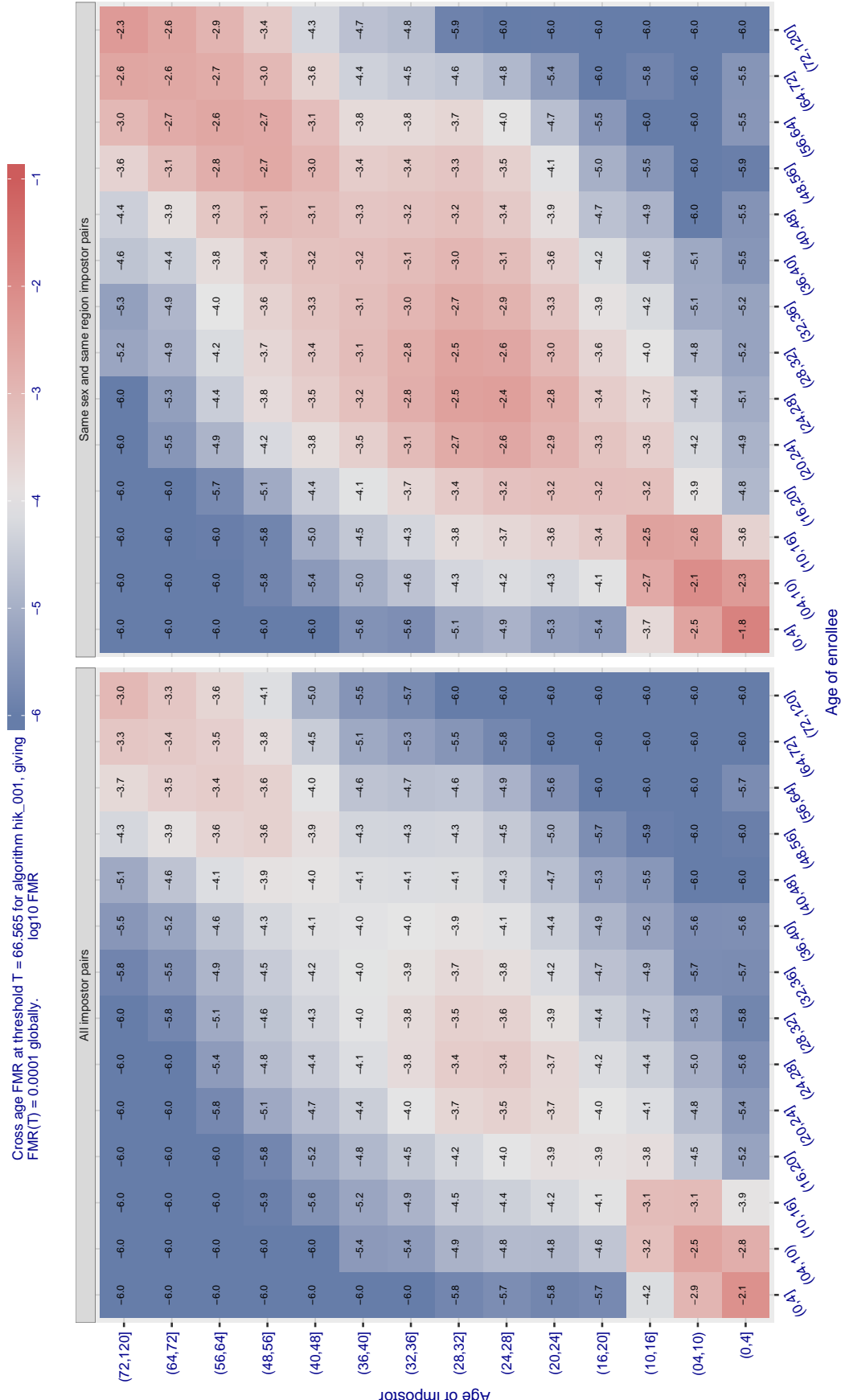


Figure 492: For algorithm hik\_001 operating on visa images, the heatmap shows false match observed over impostor comparisons of faces from different individuals who have the given age pair. False matches are counted against a recognition threshold fixed globally to give  $FMR = 0.0001$  over all on the order of  $10^{10}$  impostor comparisons. The text in each box gives the same quantity as that coded by the color. Light colors present a security vulnerability to, for example, a passport gate.

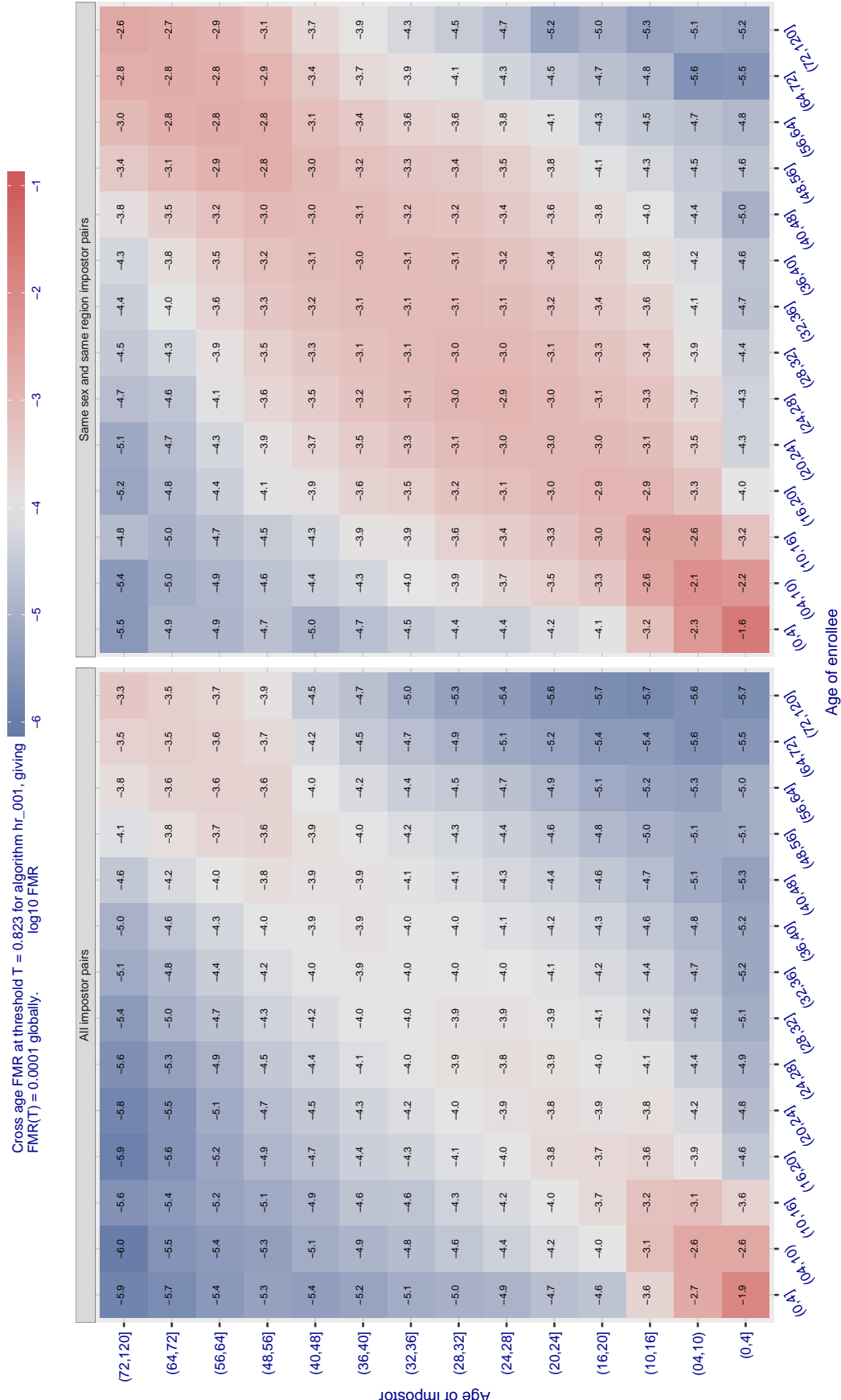


Figure 493: For algorithm hr-001 operating on visa images, the heatmap shows false match observed over impostor comparisons of faces from different individuals who have the given age pair. False matches are counted against a recognition threshold fixed globally to give  $FMR = 0.0001$  over all on the order of  $10^{10}$  impostor comparisons. The text in each box gives the same quantity as that coded by the color. Light colors present a security vulnerability to, for example, a passport gate.

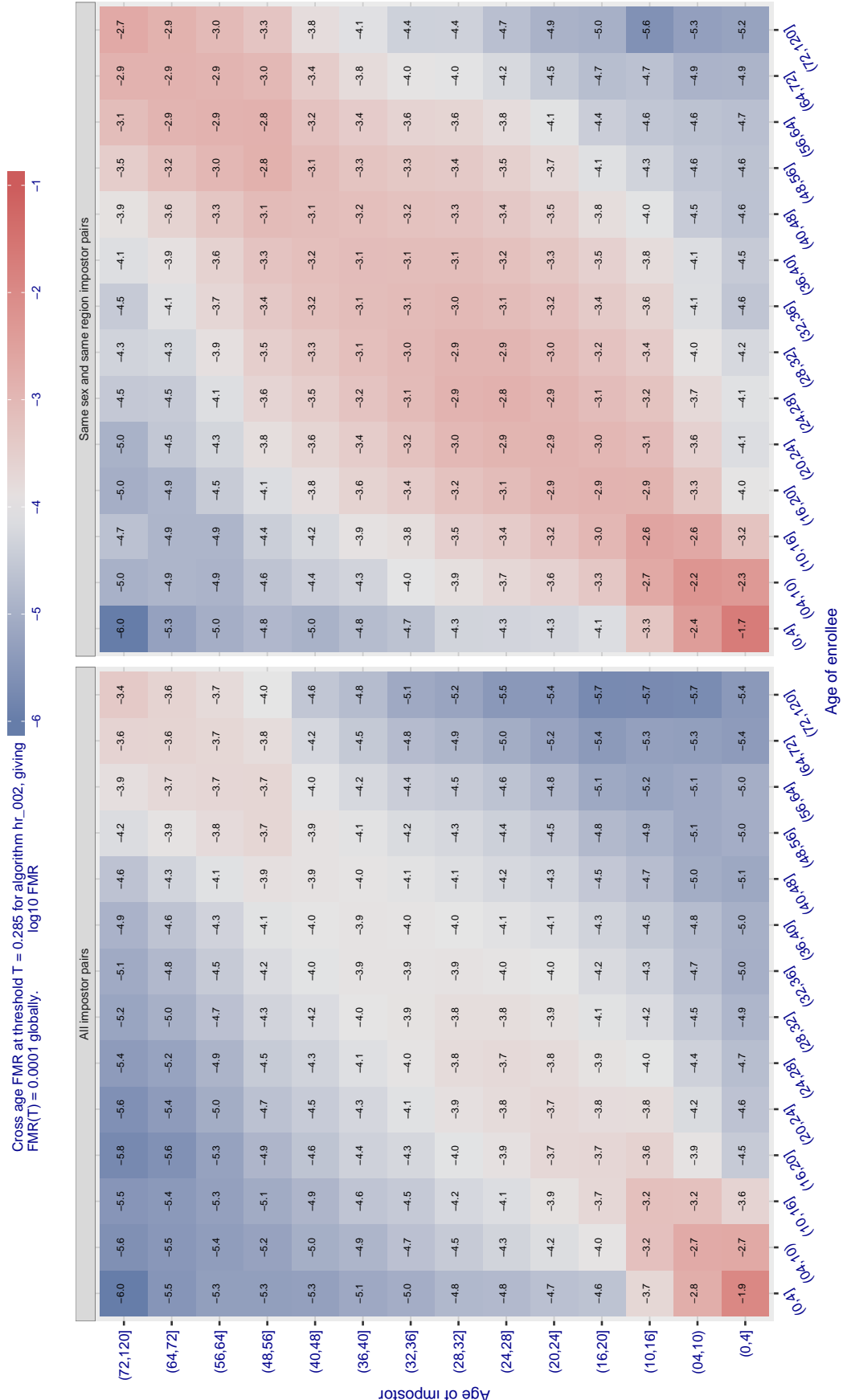


Figure 494: For algorithm hr-002 operating on visa images, the heatmap shows false match observed over impostor comparisons of faces from different individuals who have the given age pair. False matches are counted against a recognition threshold fixed globally to give  $FMR = 0.0001$  over all on the order of  $10^{10}$  impostor comparisons. The text in each box gives the same quantity as that coded by the color. Light colors present a security vulnerability to, for example, a passport gate.

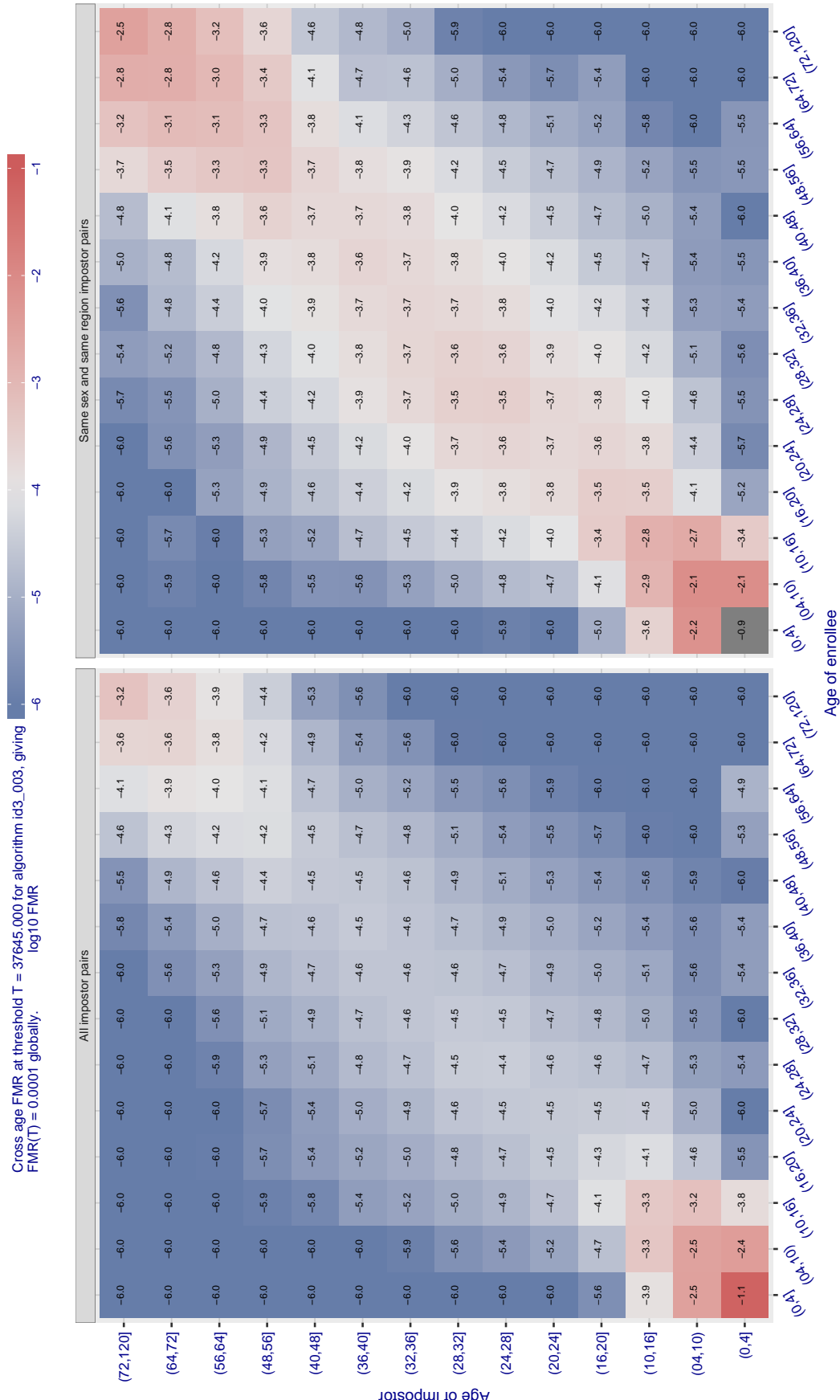


Figure 495: For algorithm id3-003 operating on visa images, the heatmap shows false match observed over impostor comparisons of faces from different individuals who have the given age pair. False matches are counted against a recognition threshold fixed globally to give  $FMR = 0.0001$  over all on the order of  $10^{10}$  impostor comparisons. The text in each box gives the same quantity as that coded by the color. Light colors present a security vulnerability to, for example, a passport gate.

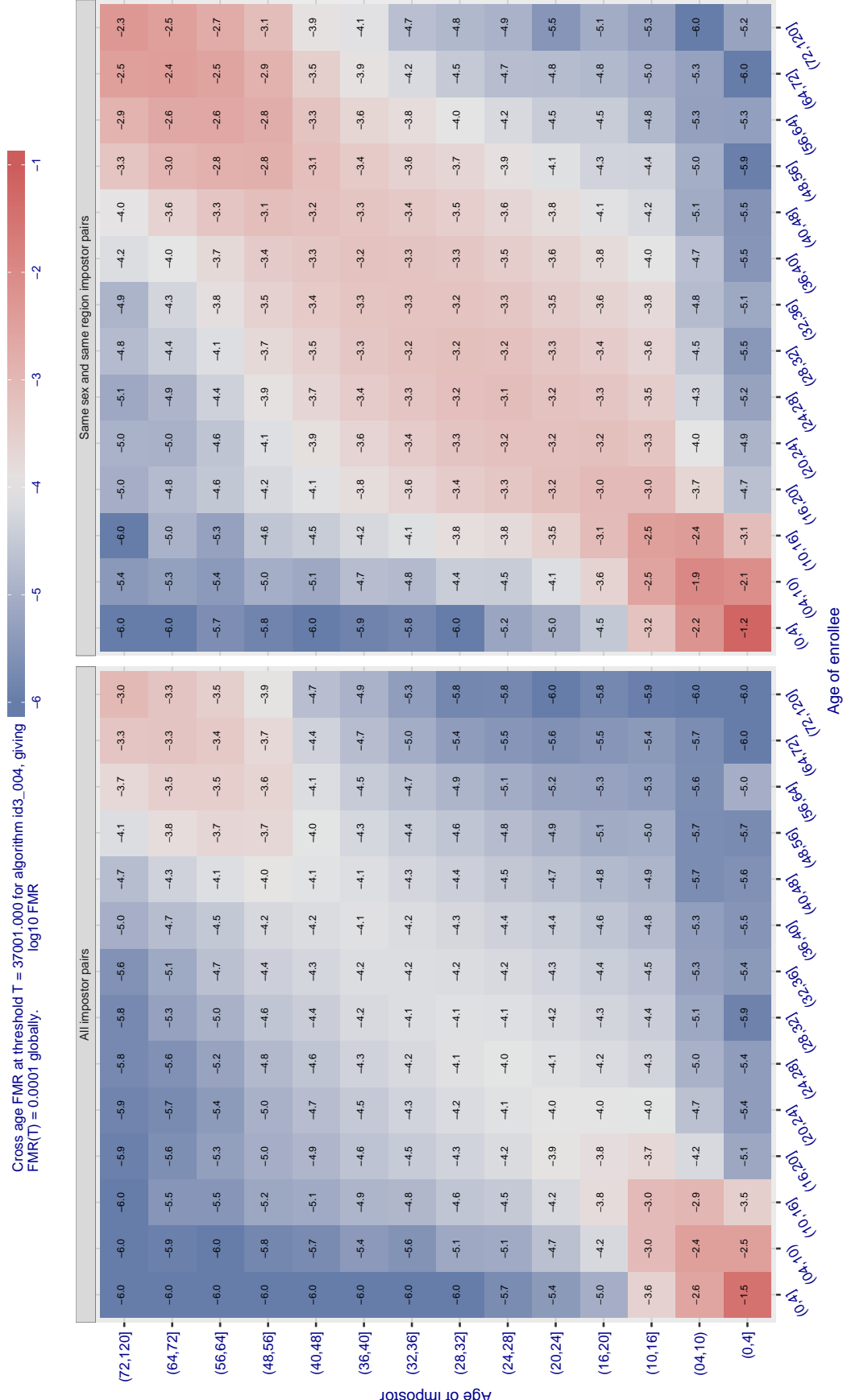
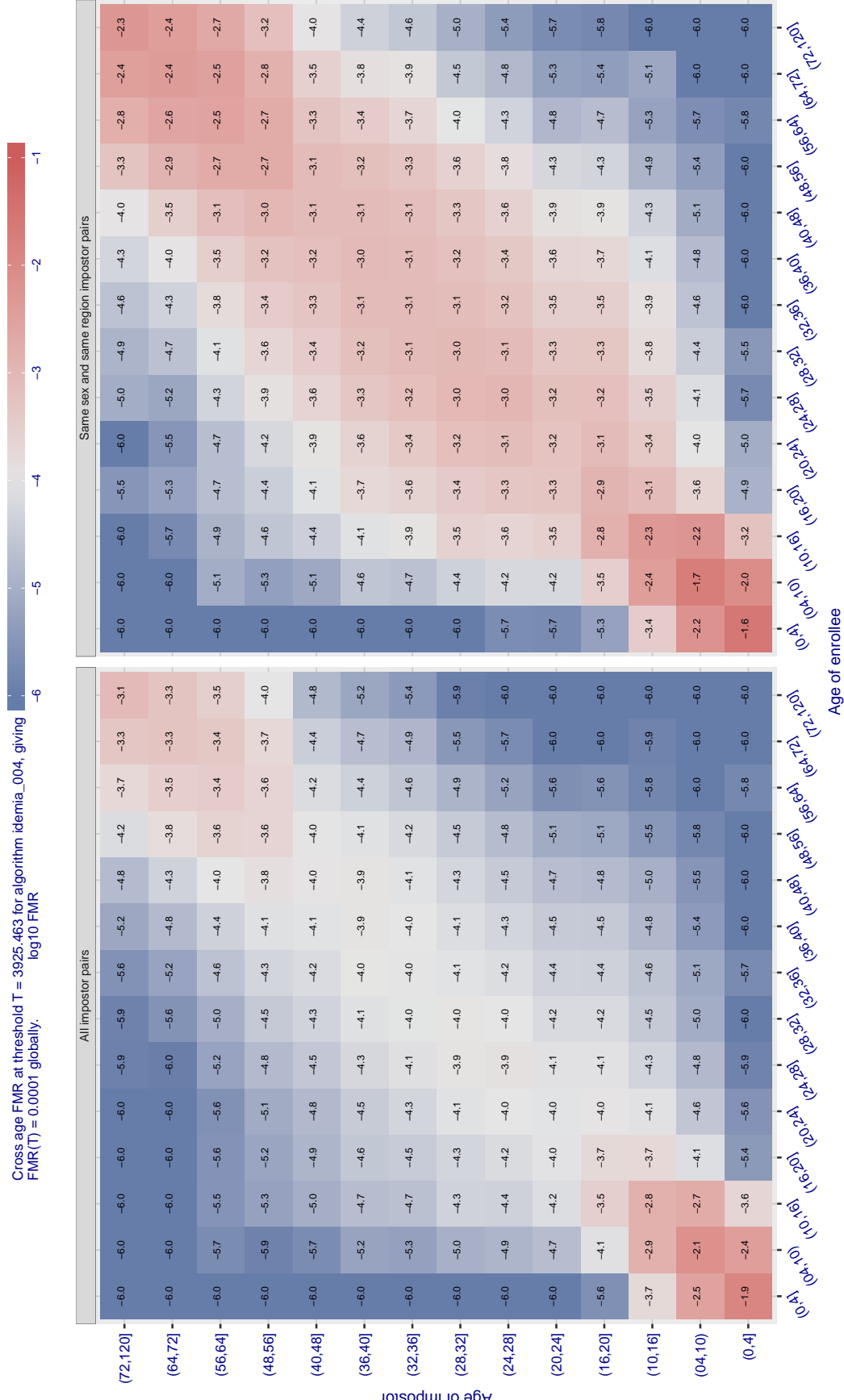


Figure 496: For algorithm id3\_004 operating on visa images, the heatmap shows false match observed over impostor comparisons of faces from different individuals who have the given age pair. False matches are counted against a recognition threshold fixed globally to give  $FMR = 0.0001$  over all on the order of  $10^{10}$  impostor comparisons. The text in each box gives the same quantity as that coded by the color. Light colors present a security vulnerability to, for example, a passport gate.



**Figure 497:** For algorithm *idemia-004* operating on visa images, the heatmap shows false match observed over impostor comparisons of faces from different individuals who have the given age pair. False matches are counted against a recognition threshold fixed globally to give  $FMR = 0.0001$  over all on the order of  $10^{10}$  impostor comparisons. The text in each box gives the same quantity as that coded by the color. Light colors present a security vulnerability to, for example, a passport gate.

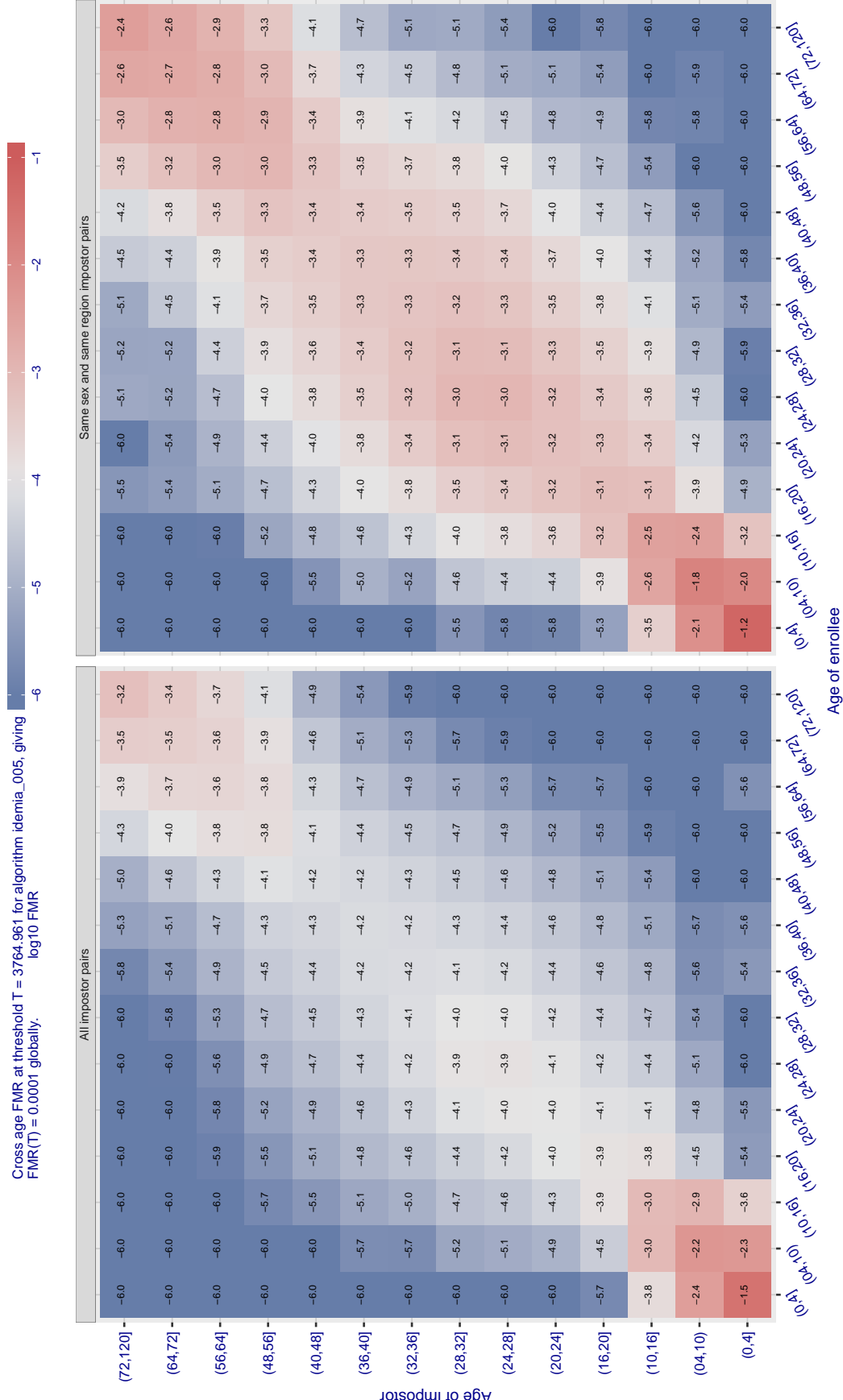


Figure 498: For algorithm idemia-005 operating on visa images, the heatmap shows false match observed over impostor comparisons of faces from different individuals who have the given age pair. False matches are counted against a recognition threshold fixed globally to give  $FMR = 0.0001$  over all on the order of  $10^{10}$  impostor comparisons. The text in each box gives the same quantity as that coded by the color. Light colors present a security vulnerability to, for example, a passport gate.

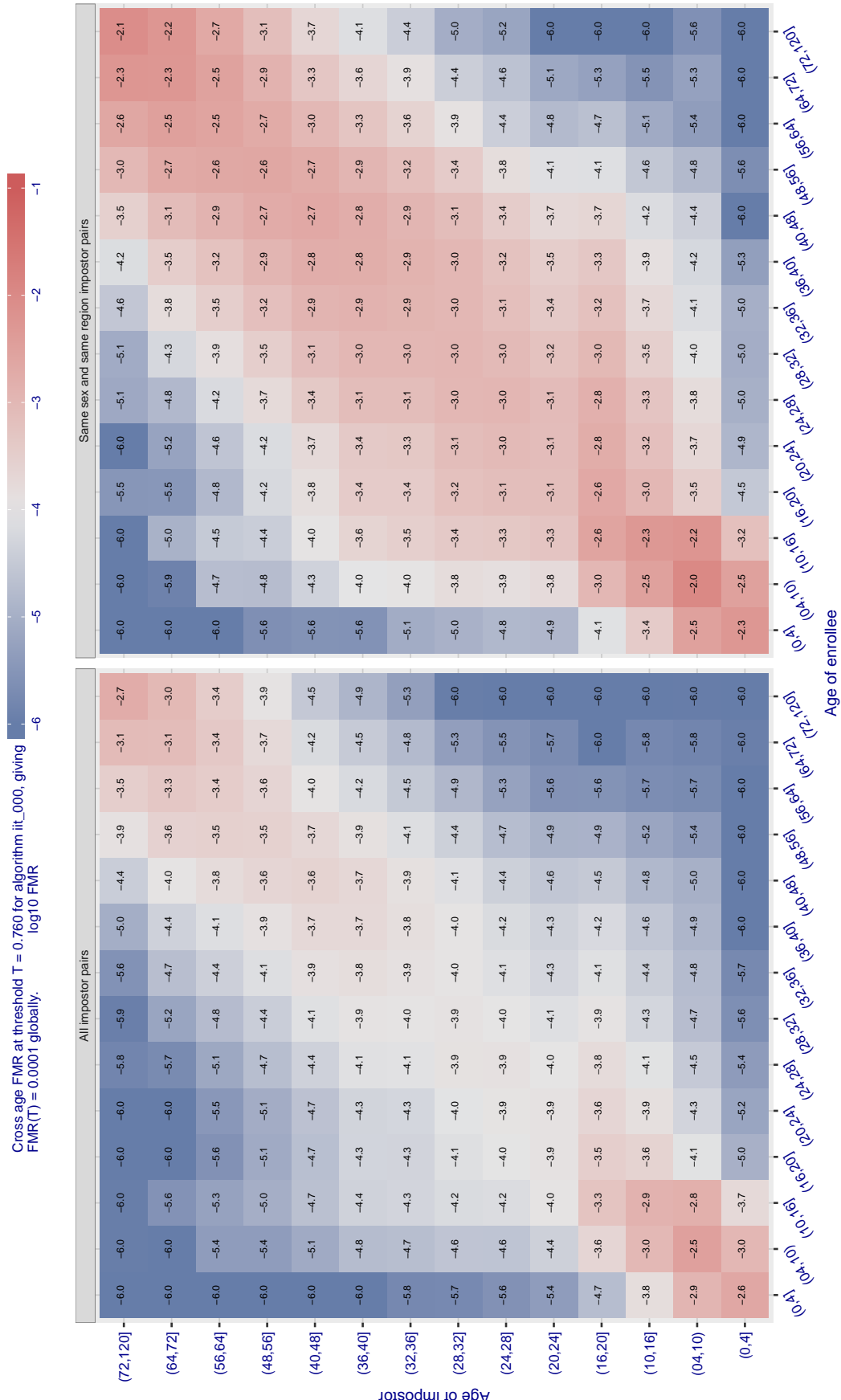
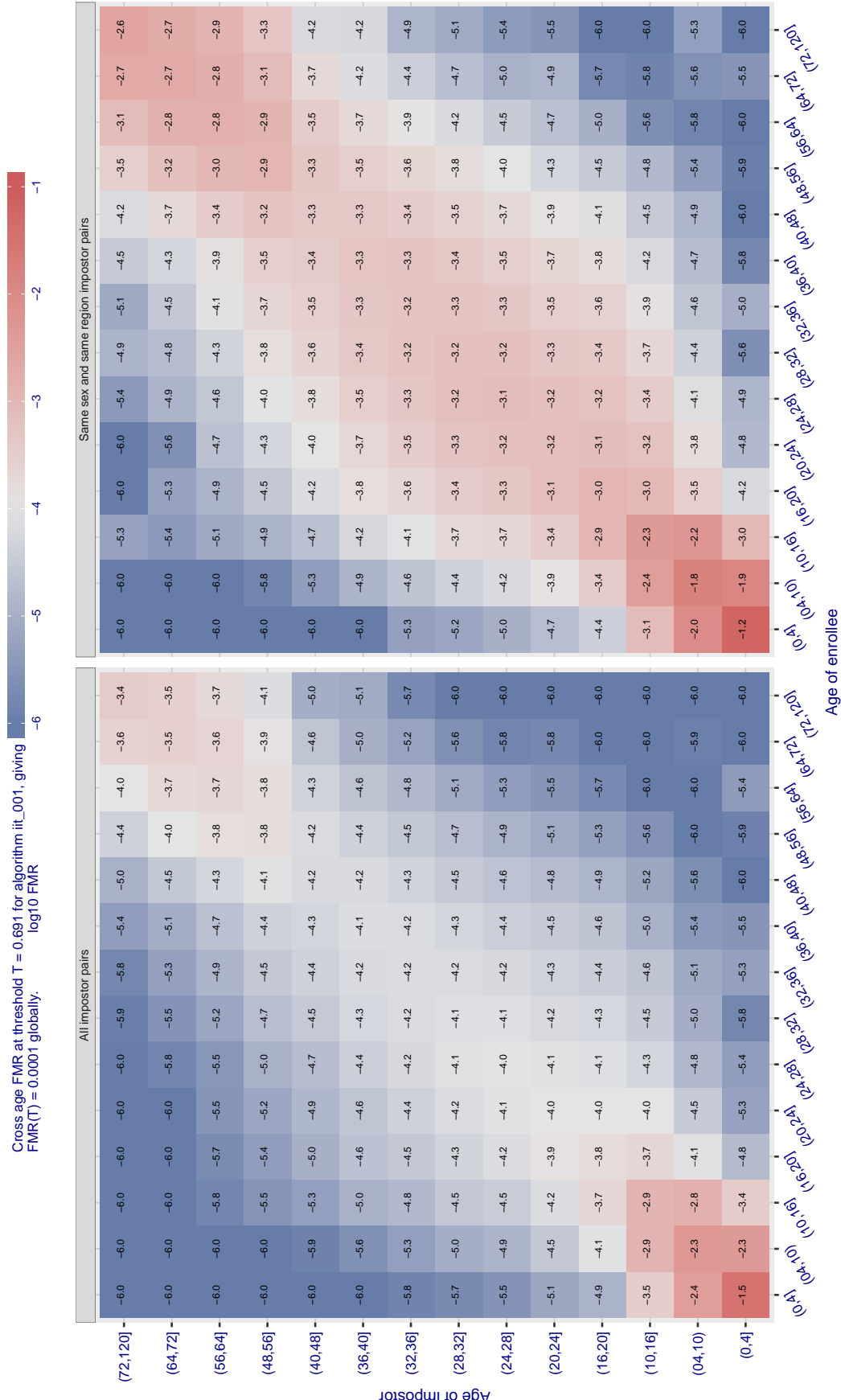


Figure 499: For algorithm iit-000 operating on visa images, the heatmap shows false match observed over visa images, who have the given age pair. False matches are counted against a recognition threshold fixed globally to give FMR = 0.0001 over all on the order of  $10^{10}$  impostor comparisons. The text in each box gives the same quantity as that coded by the color. Light colors present a security vulnerability to, for example, a passport gate.



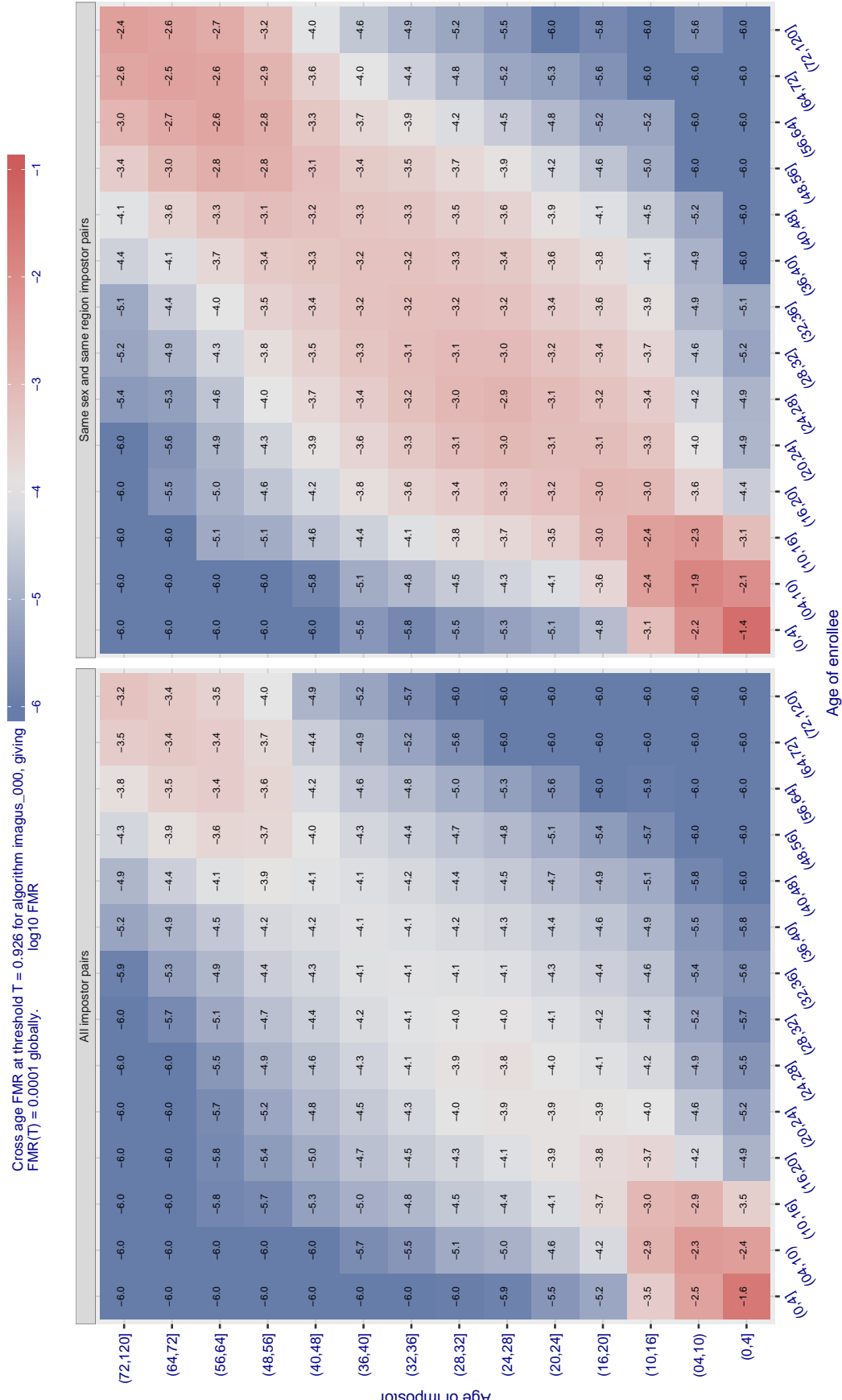


Figure 501: For algorithm imagus\_000 operating on visa images, the heatmap shows false match observed over impostor comparisons of faces from different individuals who have the given age pair. False matches are counted against a recognition threshold fixed globally to give FMR = 0.0001 over all on the order of  $10^{10}$  impostor comparisons. The text in each box gives the same quantity as that coded by the color. Light colors present a security vulnerability to, for example, a passport gate.

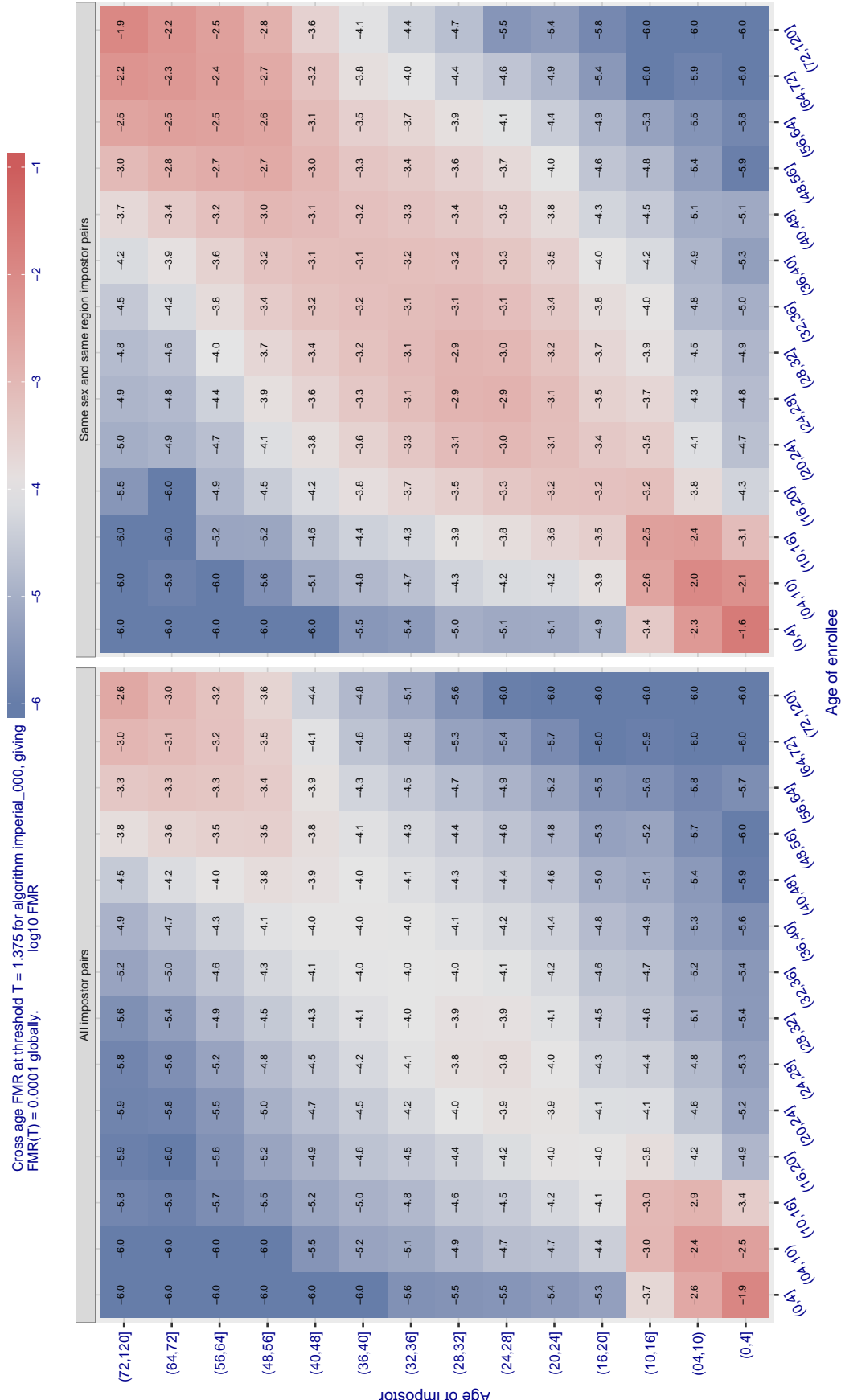


Figure 502: For algorithm imperial-000 operating on visa images, the heatmap shows false match observed over impostor comparisons of faces from different individuals who have the given age pair. False matches are counted against a recognition threshold fixed globally to give  $\text{FMR} = 0.0001$  over all on the order of  $10^{10}$  impostor comparisons. The text in each box gives the same quantity as that coded by the color. Light colors present a security vulnerability to, for example, a passport gate.

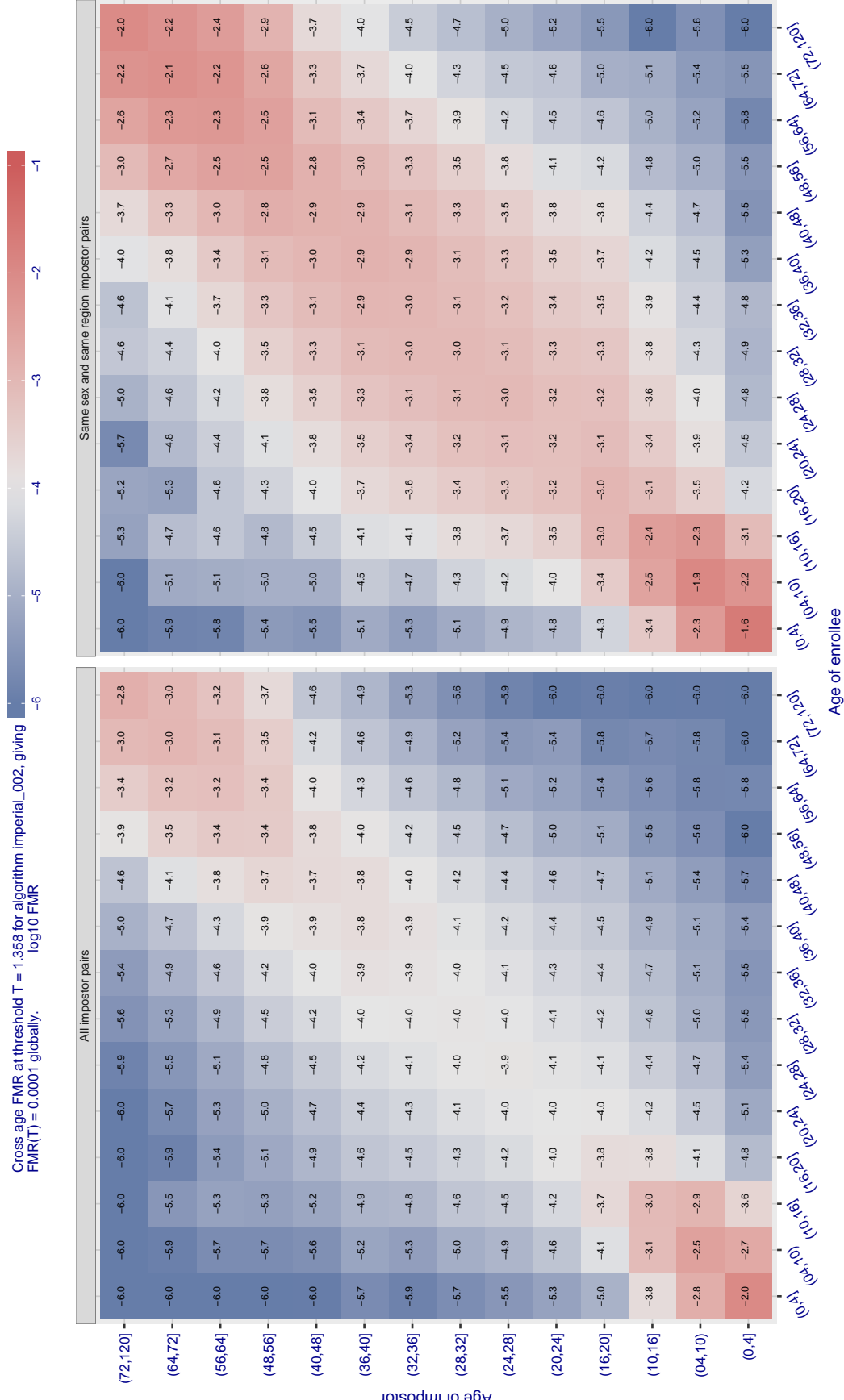


Figure 503: For algorithm imperial\_002 operating on visa images, the heatmap shows false match observed over impostor comparisons of faces from different individuals who have the given age pair. False matches are counted against a recognition threshold fixed globally to give  $FMR = 0.0001$  over all on the order of  $10^{10}$  impostor comparisons. The text in each box gives the same quantity as that coded by the color. Light colors present a security vulnerability to, for example, a passport gate.

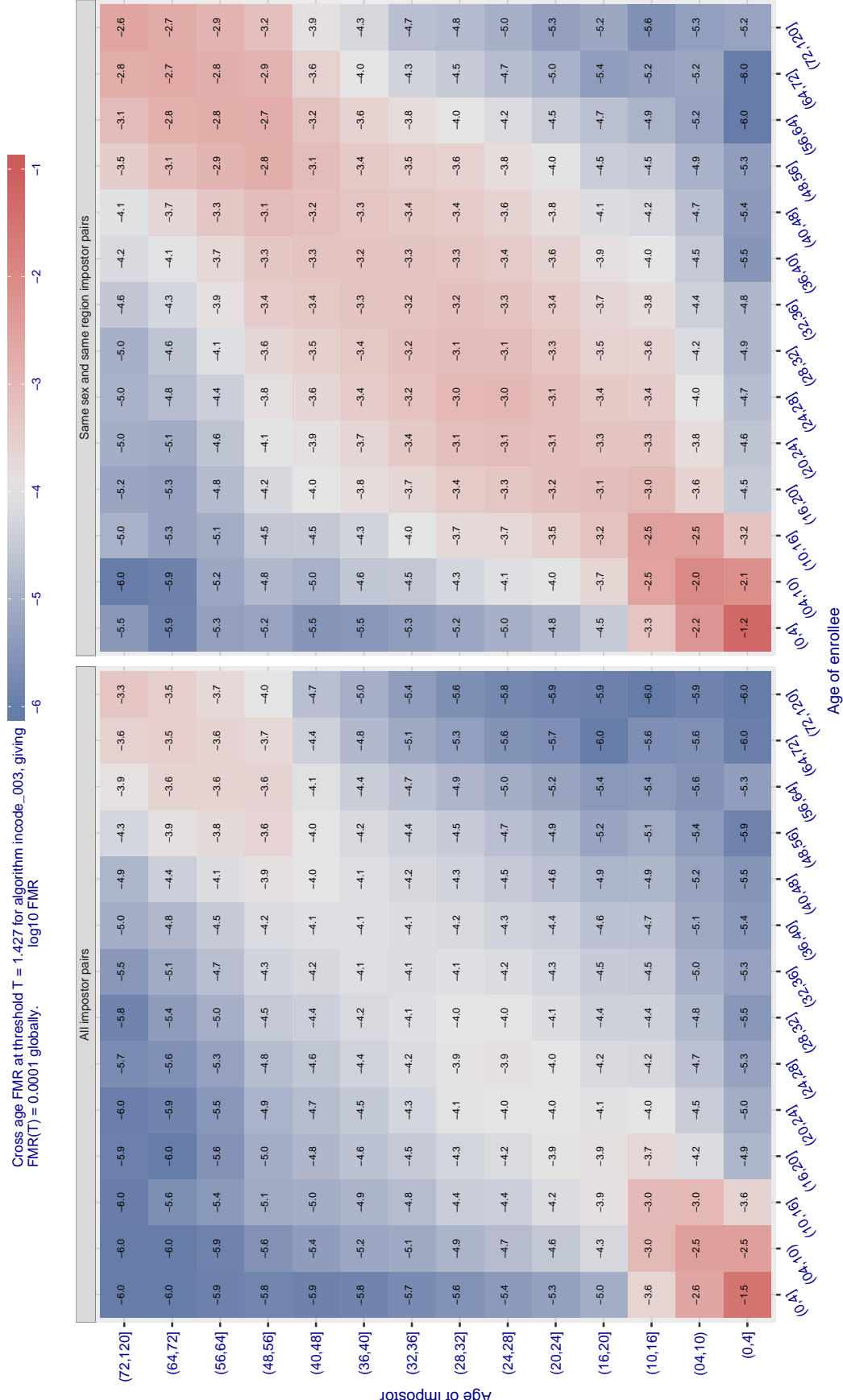


Figure 504: For algorithm incode-003 operating on visa images, the heatmap shows false match observed over impostor comparisons of faces from different individuals who have the given age pair. False matches are counted against a recognition threshold fixed globally to give  $FMR = 0.0001$  over all on the order of  $10^{10}$  impostor comparisons. The text in each box gives the same quantity as that coded by the color. Light colors present a security vulnerability to, for example, a passport gate.

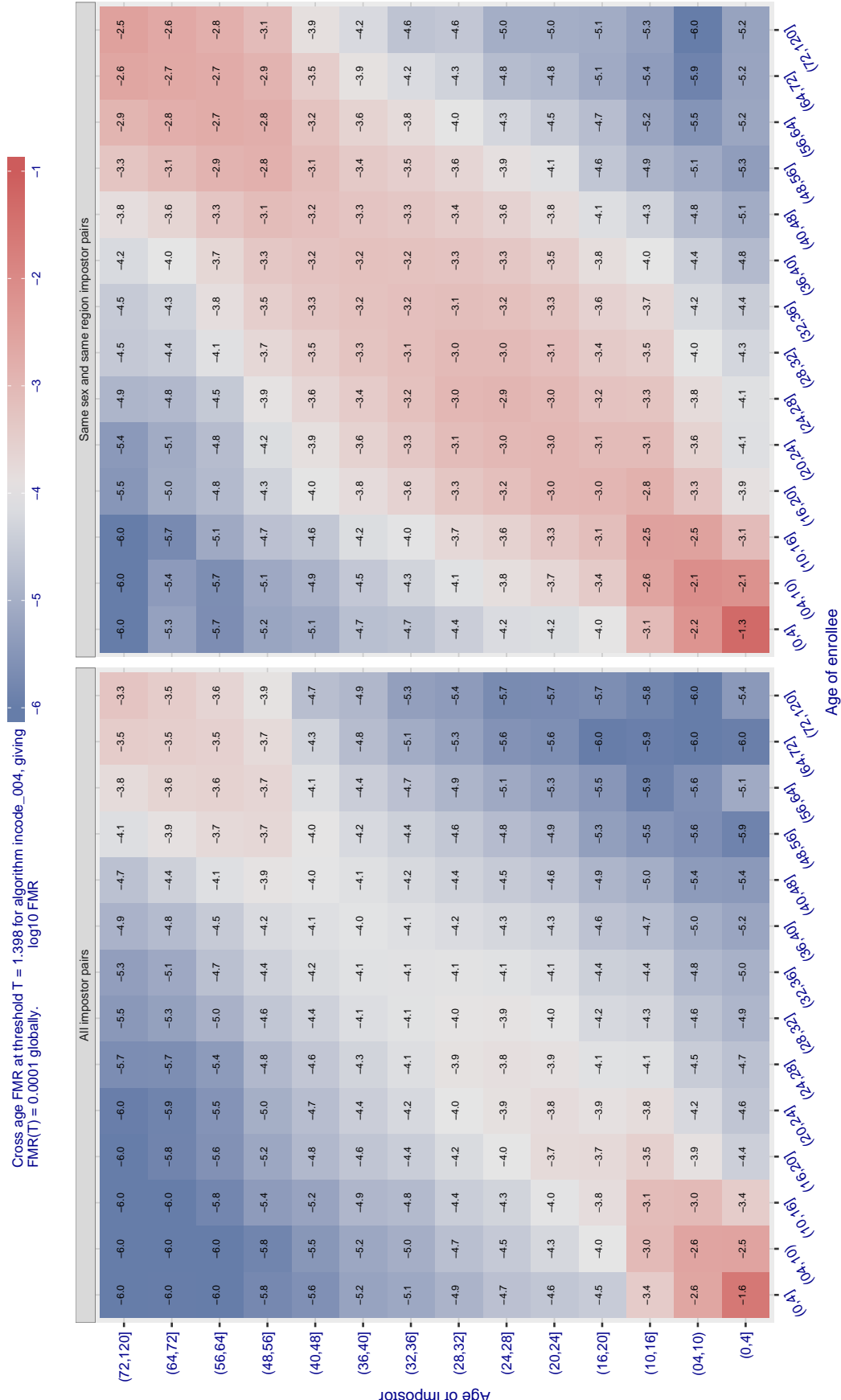


Figure 505: For algorithm incode-004 operating on visa images, the heatmap shows false match observed over impostor comparisons of faces from different individuals who have the given age pair. False matches are counted against a recognition threshold fixed globally to give  $FMR = 0.0001$  over all on the order of  $10^{10}$  impostor comparisons. The text in each box gives the same quantity as that coded by the color. Light colors present a security vulnerability to, for example, a passport gate.

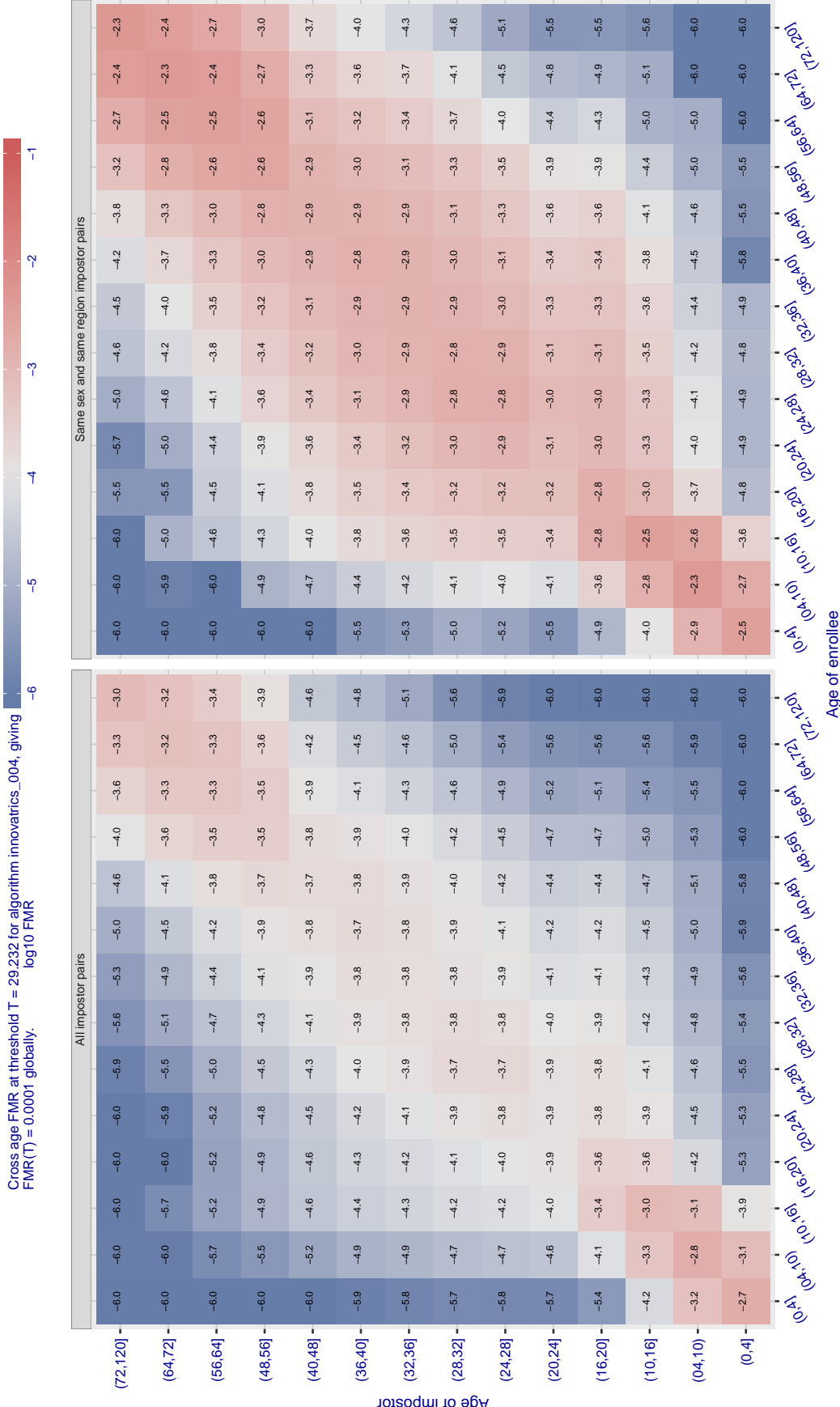
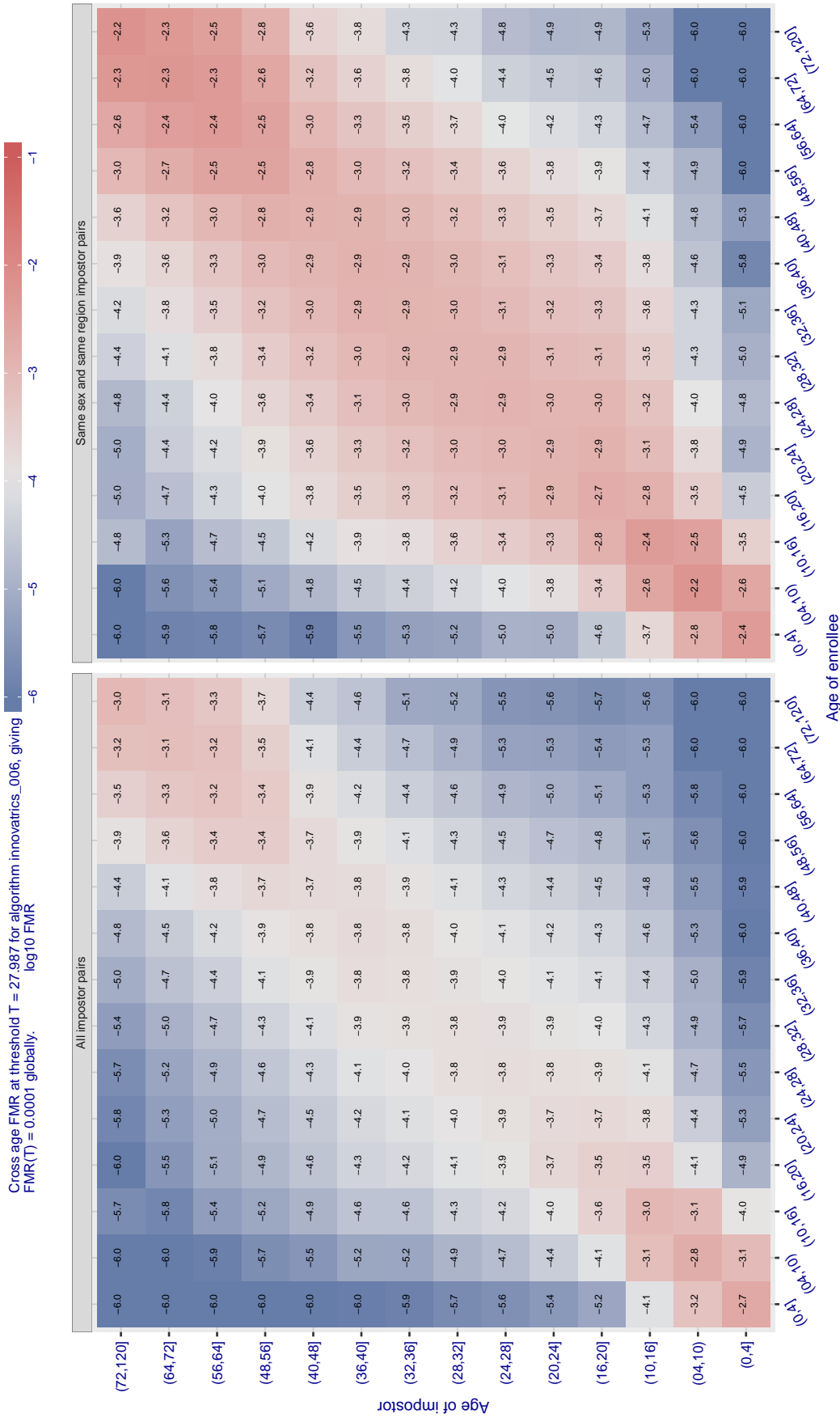


Figure 506: For algorithm innovatrics\_004 operating on visa images, the heatmap shows false match observed over impostor comparisons of faces from different individuals who have the given age pair. False matches are counted against a recognition threshold fixed globally to give  $FMR = 0.0001$  over all on the order of  $10^{10}$  impostor comparisons. The text in each box gives the same quantity as that coded by the color. Light colors present a security vulnerability to, for example, a passport gate.



**Figure 507:** For algorithm innovatrics-006 operating on visa images, the heatmap shows false match observed over impostor comparisons of faces from different individuals who have the given age pair. False matches are counted against a recognition threshold fixed globally to give  $FMR = 0.0001$  over all on the order of  $10^{10}$  impostor comparisons. The text in each box gives the same quantity as that coded by the color. Light colors present a security vulnerability to, for example, a passport gate.

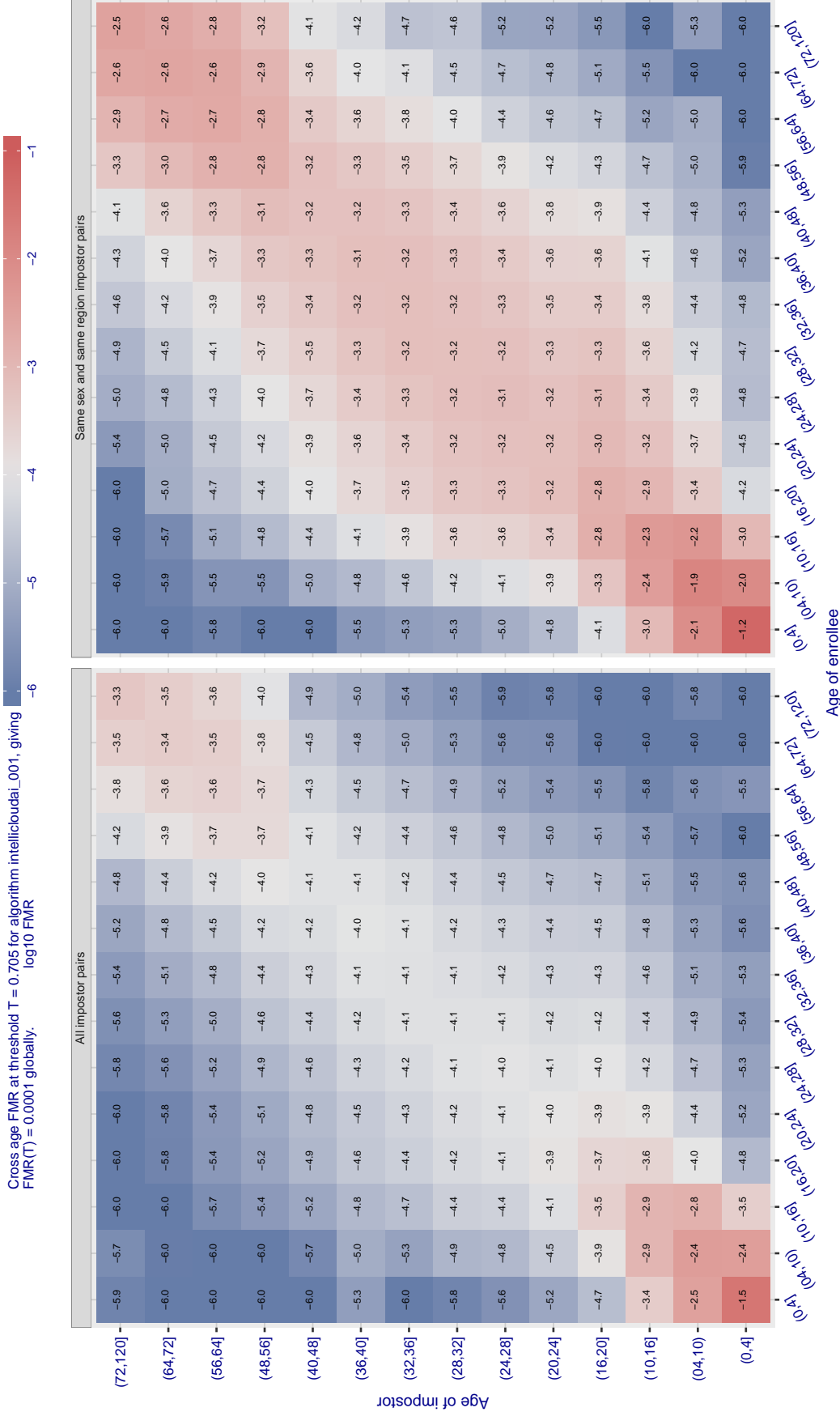


Figure 508: For algorithm intellicloudai-001 operating on visa images, the heatmap shows false match observed over impostor comparisons of faces from different individuals who have the given age pair. False matches are counted against a recognition threshold fixed globally to give FMR = 0.0001 over all on the order of  $10^{10}$  impostor comparisons. The text in each box gives the same quantity as that coded by the color. Light colors present a security vulnerability to, for example, a passport gate.

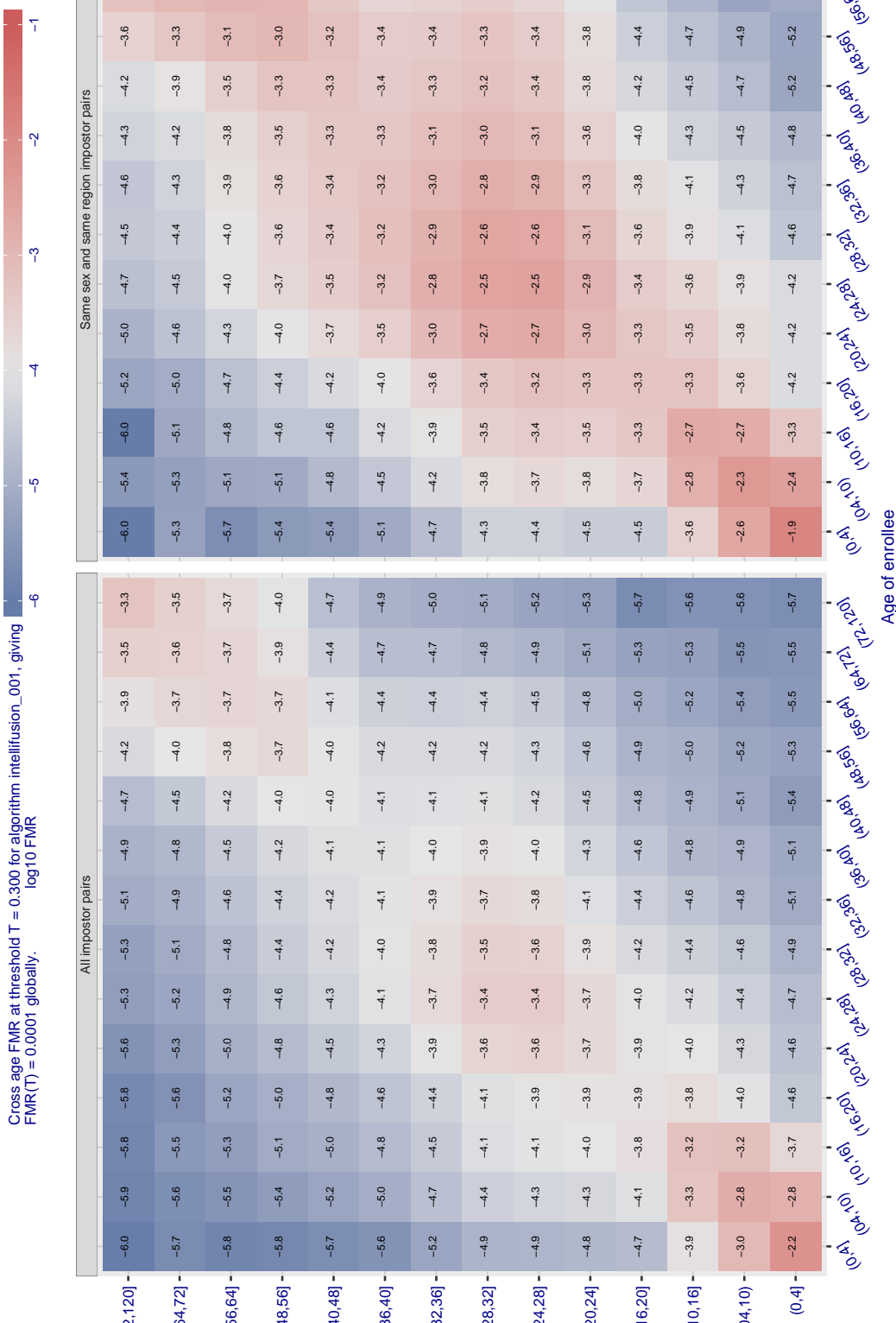


Figure 509: For algorithm intellifusion-001 operating on visa images, the heatmap shows false match observed over impostor comparisons of faces from different individuals who have the given age pair. False matches are counted against a recognition threshold fixed globally to give  $\text{FMR} = 0.0001$  over all on the order of  $10^{10}$  impostor comparisons. The text in each box gives the same quantity as that coded by the color. Light colors present a security vulnerability to, for example, a passport gate.

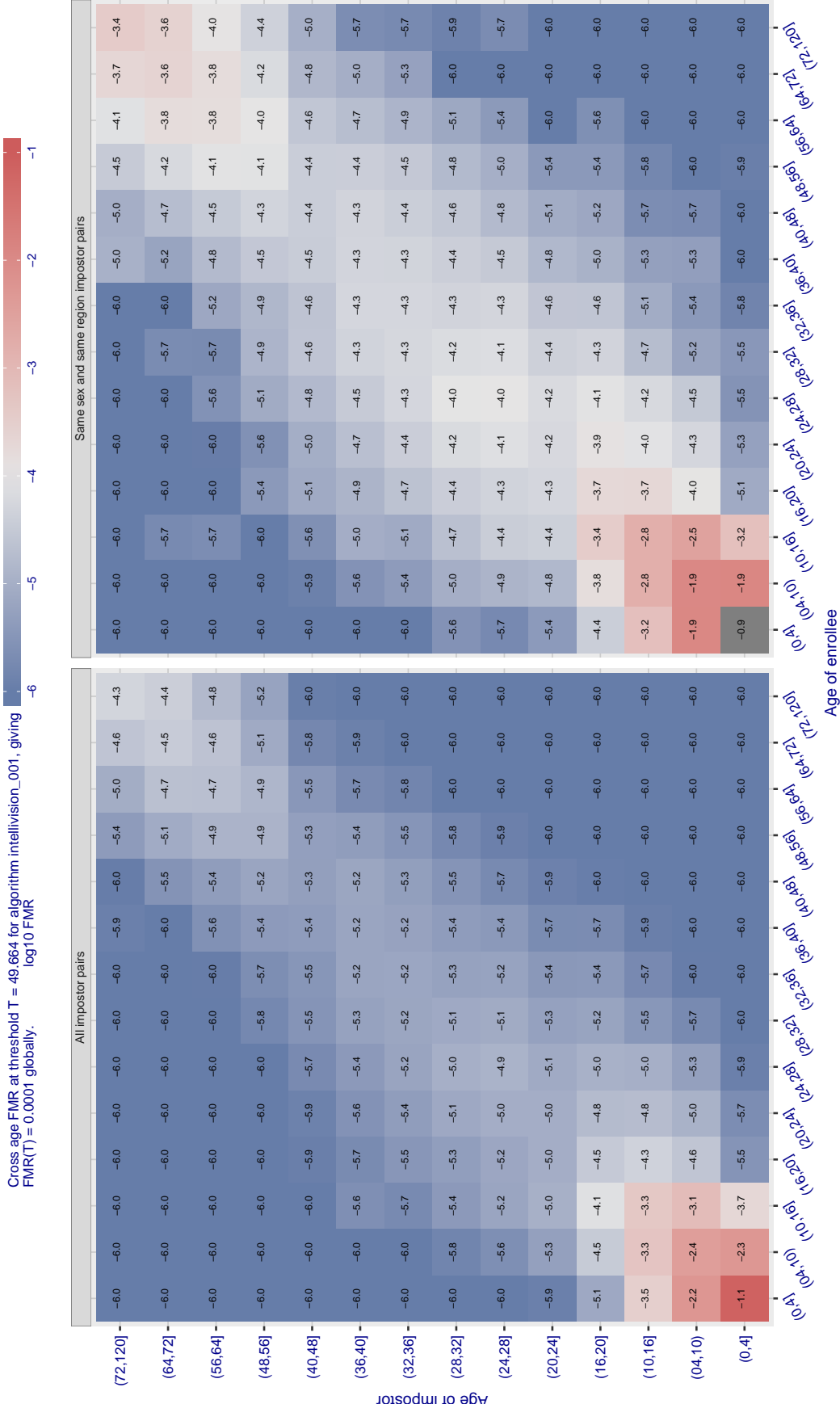


Figure 510: For algorithm intellivision\_001 operating on visa images, the heatmap shows false match observed over impostor comparisons of faces from different individuals who have the given age pair. False matches are counted against a recognition threshold fixed globally to give FMR = 0.0001 over all on the order of  $10^{10}$  impostor comparisons. The text in each box gives the same quantity as that coded by the color. Light colors present a security vulnerability to, for example, a passport gate.

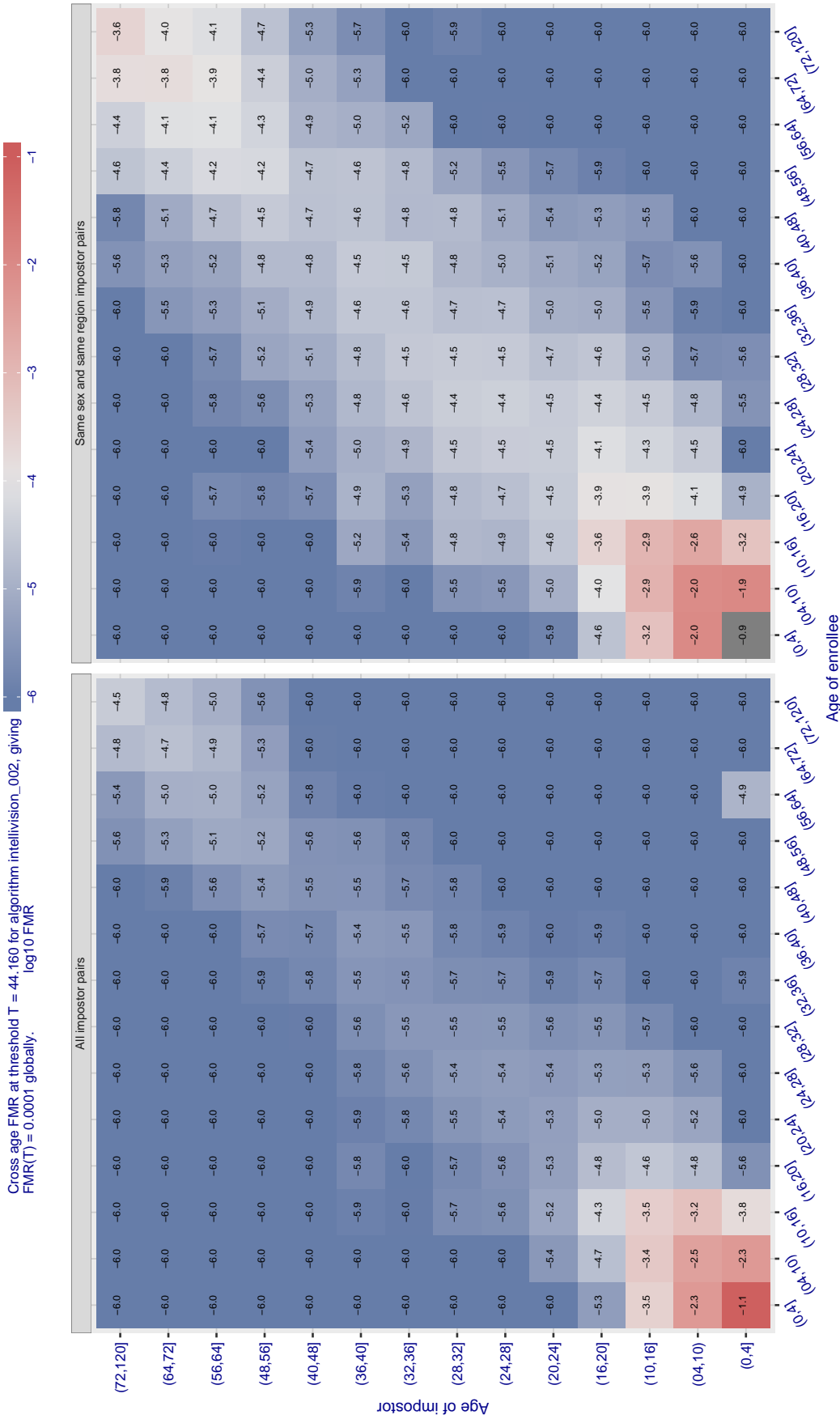


Figure 511: For algorithm intellivision\_002 operating on visa images, the heatmap shows false match observed over impostor comparisons of faces from different individuals who have the given age pair. False matches are counted against a recognition threshold fixed globally to give  $FMR = 0.0001$  over all on the order of  $10^{10}$  impostor comparisons. The text in each box gives the same quantity as that coded by the color. Light colors present a security vulnerability to, for example, a passport gate.

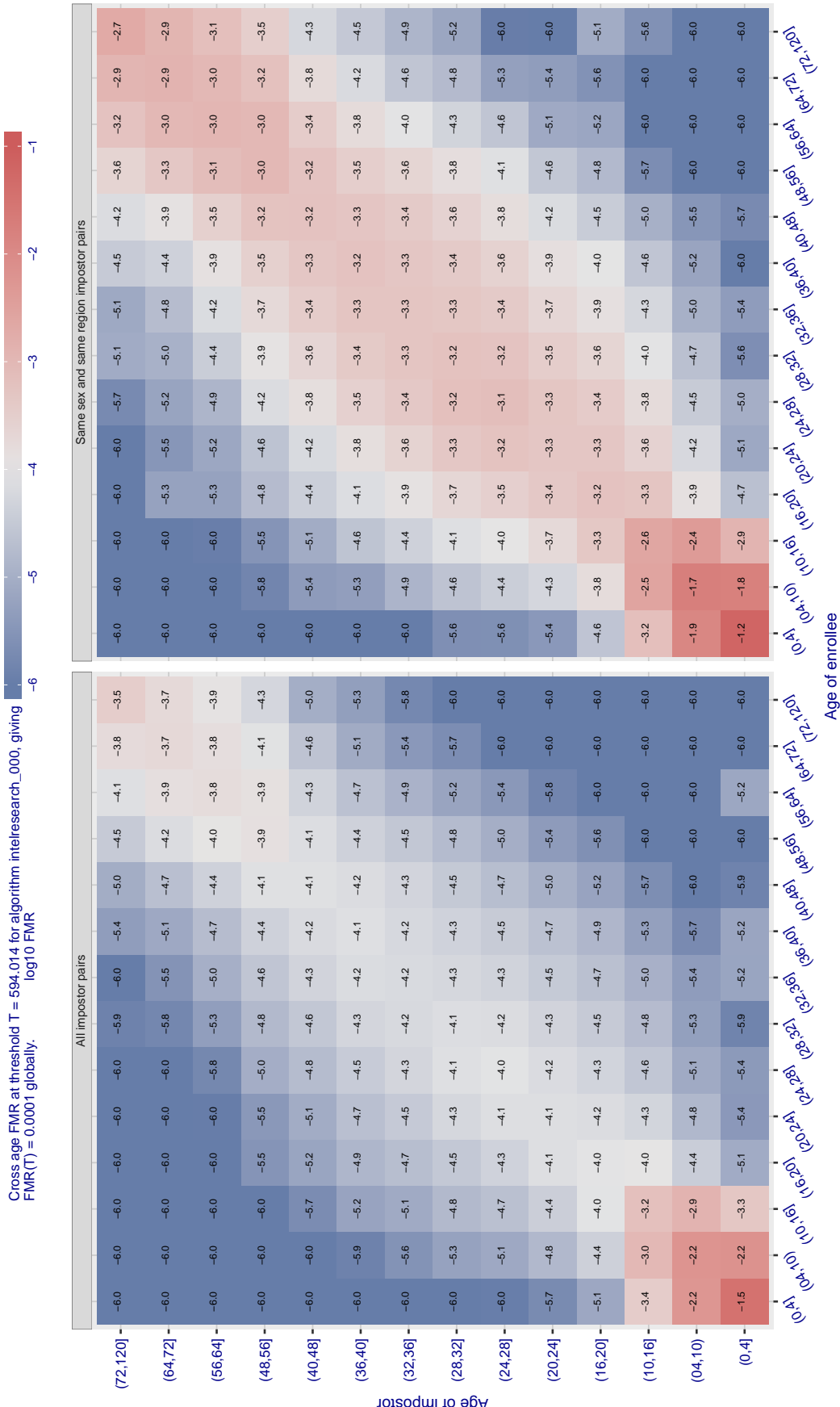


Figure 512: For algorithm intelresearch-000 operating on visa images, the heatmap shows false match observed over impostor comparisons of faces from different individuals who have the given age pair. False matches are counted against a recognition threshold fixed globally to give  $\text{FMR} = 0.0001$  over all on the order of  $10^{10}$  impostor comparisons. The text in each box gives the same quantity as that coded by the color. Light colors present a security vulnerability to, for example, a passport gate.

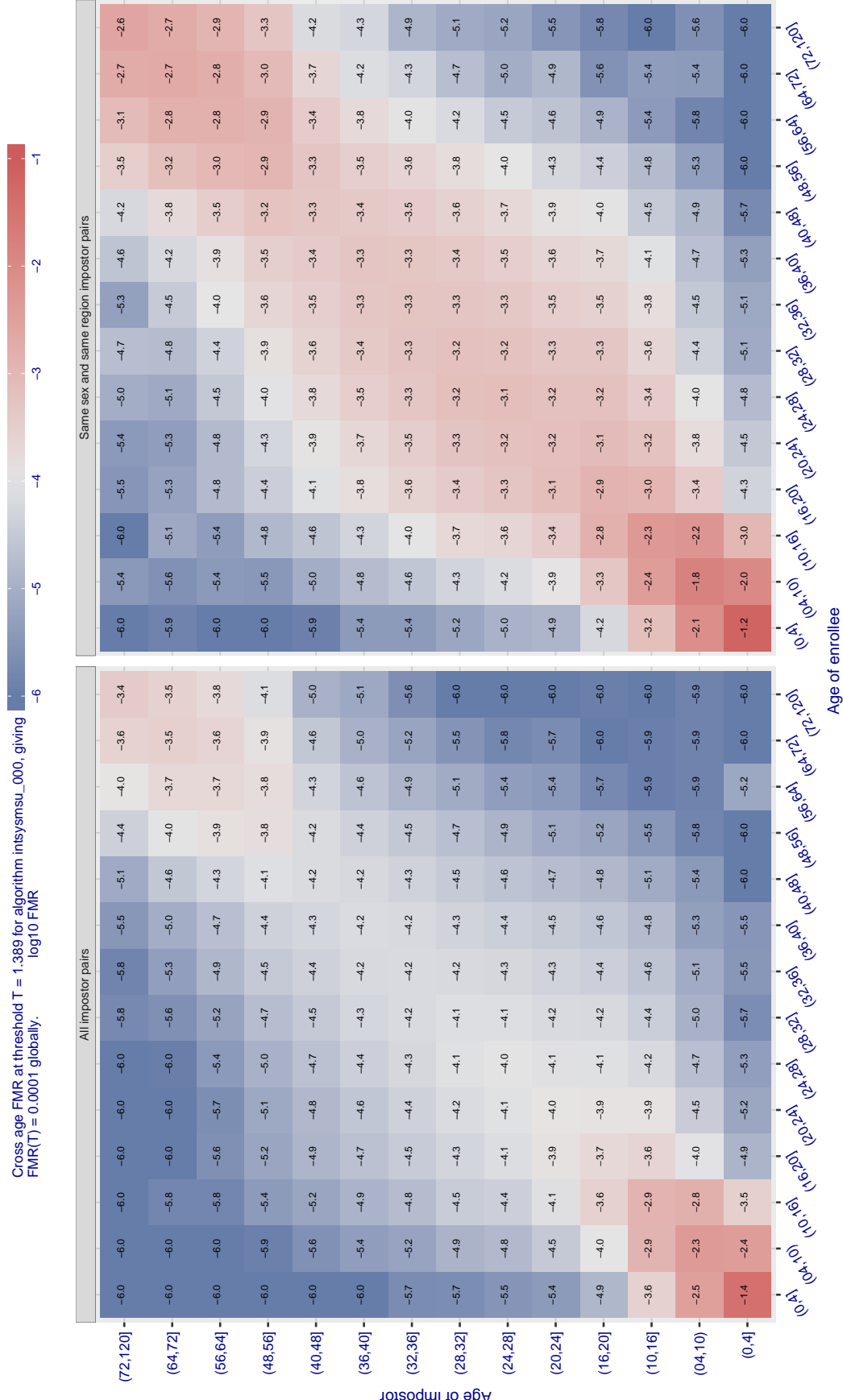


Figure 513: For algorithm intsysmsu-000 operating on visa images, the heatmap shows false match observed over impostor comparisons of faces from different individuals who have the given age pair. False matches are counted against a recognition threshold fixed globally to give  $FMR = 0.001$  over all on the order of  $10^{10}$  impostor comparisons. The text in each box gives the same quantity as that coded by the color. Light colors present a security vulnerability to, for example, a passport gate.

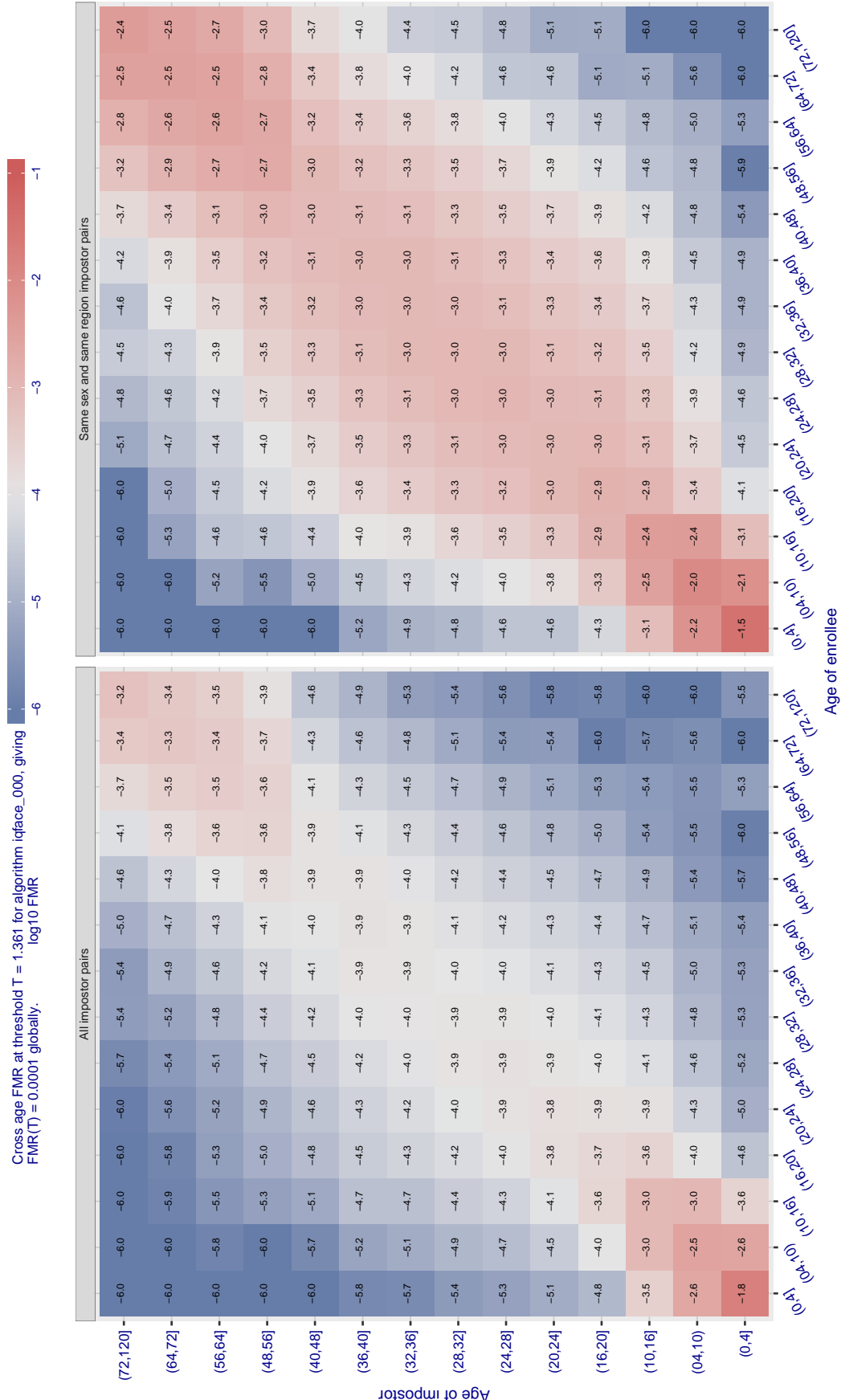


Figure 514: For algorithm iqface-000 operating on visa images, the heatmap shows false match observed over impostor comparisons of faces from different individuals who have the given age pair. False matches are counted against a recognition threshold fixed globally to give FMR = 0.0001 over all on the order of  $10^{10}$  impostor comparisons. The text in each box gives the same quantity as that coded by the color. Light colors present a security vulnerability to, for example, a passport gate.

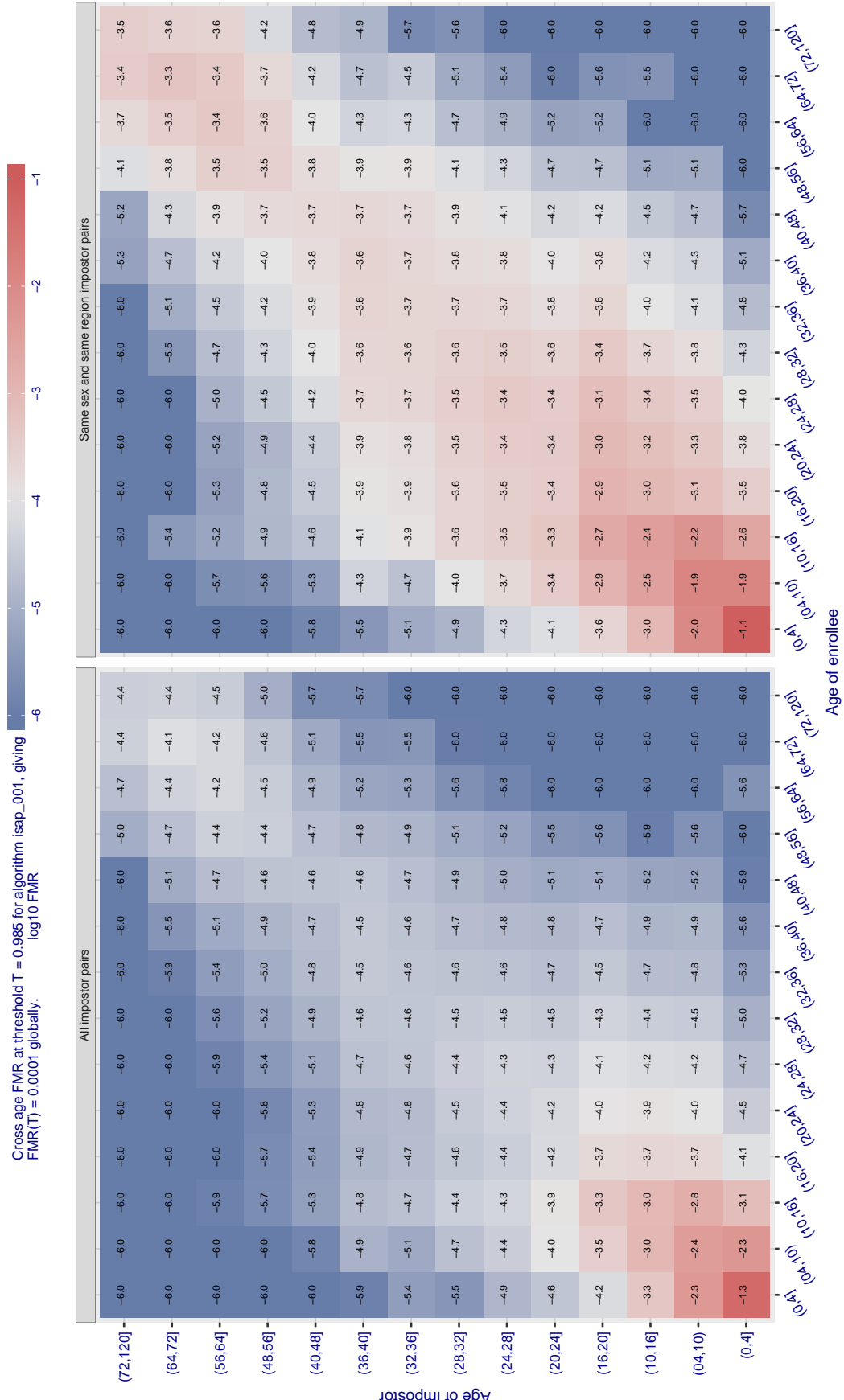


Figure 515: For algorithm isap\_001 operating on visa images, the heatmap shows false match observed over impostor comparisons of faces from different individuals who have the given age pair. False matches are counted against a recognition threshold fixed globally to give  $FMR = 0.0001$  over all on the order of  $10^{10}$  impostor comparisons. The text in each box gives the same quantity as that coded by the color. Light colors present a security vulnerability to, for example, a passport gate.

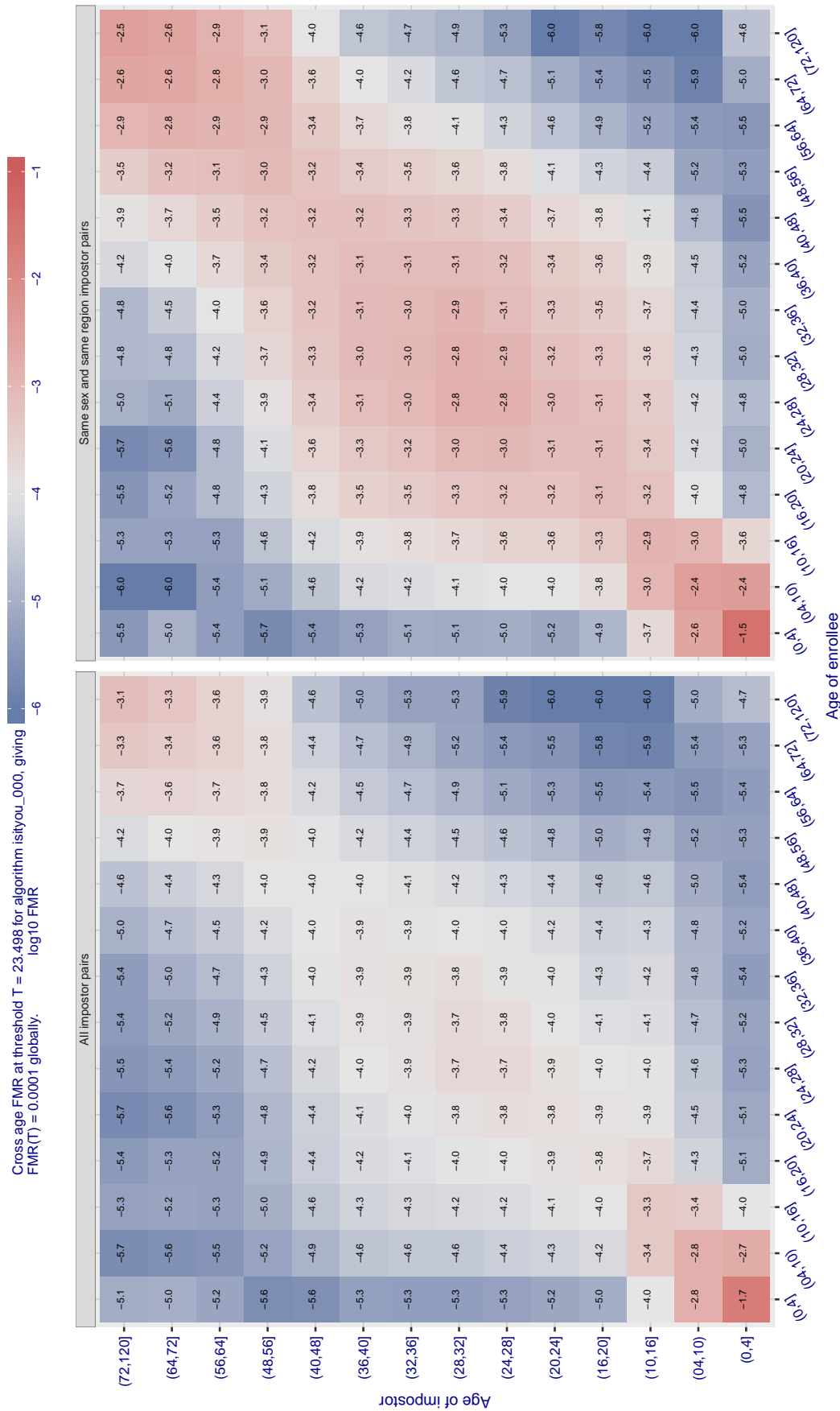


Figure 516: For algorithm isityou\_000 operating on visa images, the heatmap shows false match observed over impostor comparisons of faces from different individuals who have the given age pair. False matches are counted against a recognition threshold fixed globally to give  $FMR = 0.0001$  over all on the order of  $10^{10}$  impostor comparisons. The text in each box gives the same quantity as that coded by the color. Light colors present a security vulnerability to, for example, a passport gate.

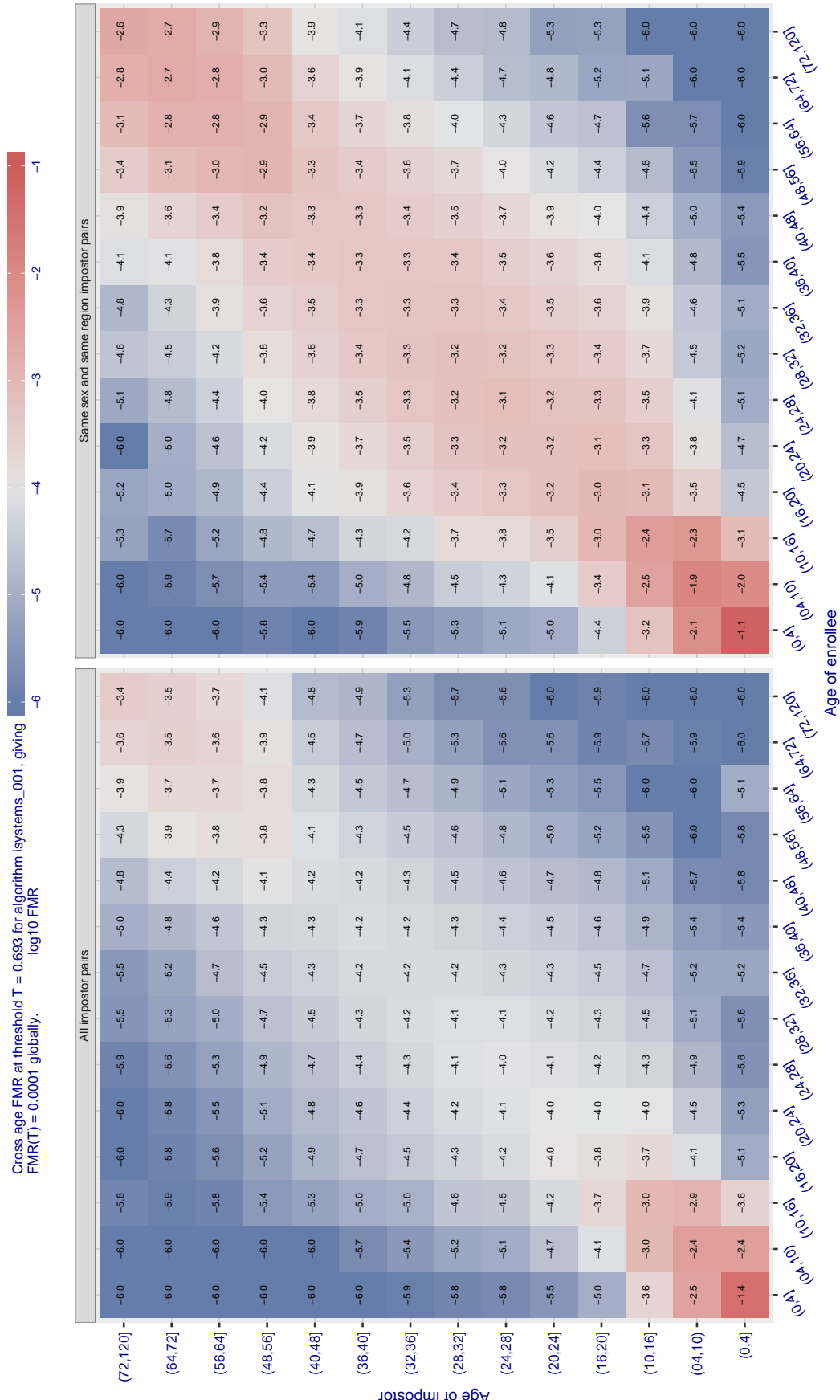


Figure 517: For algorithm systems-001 operating on visa images, the heatmap shows false match observed over impostor comparisons of faces from different individuals who have the given age pair. False matches are counted against a recognition threshold fixed globally to give  $FMR = 0.0001$  over all on the order of  $10^{10}$  impostor comparisons. The text in each box gives the same quantity as that coded by the color. Light colors present a security vulnerability to, for example, a passport gate.

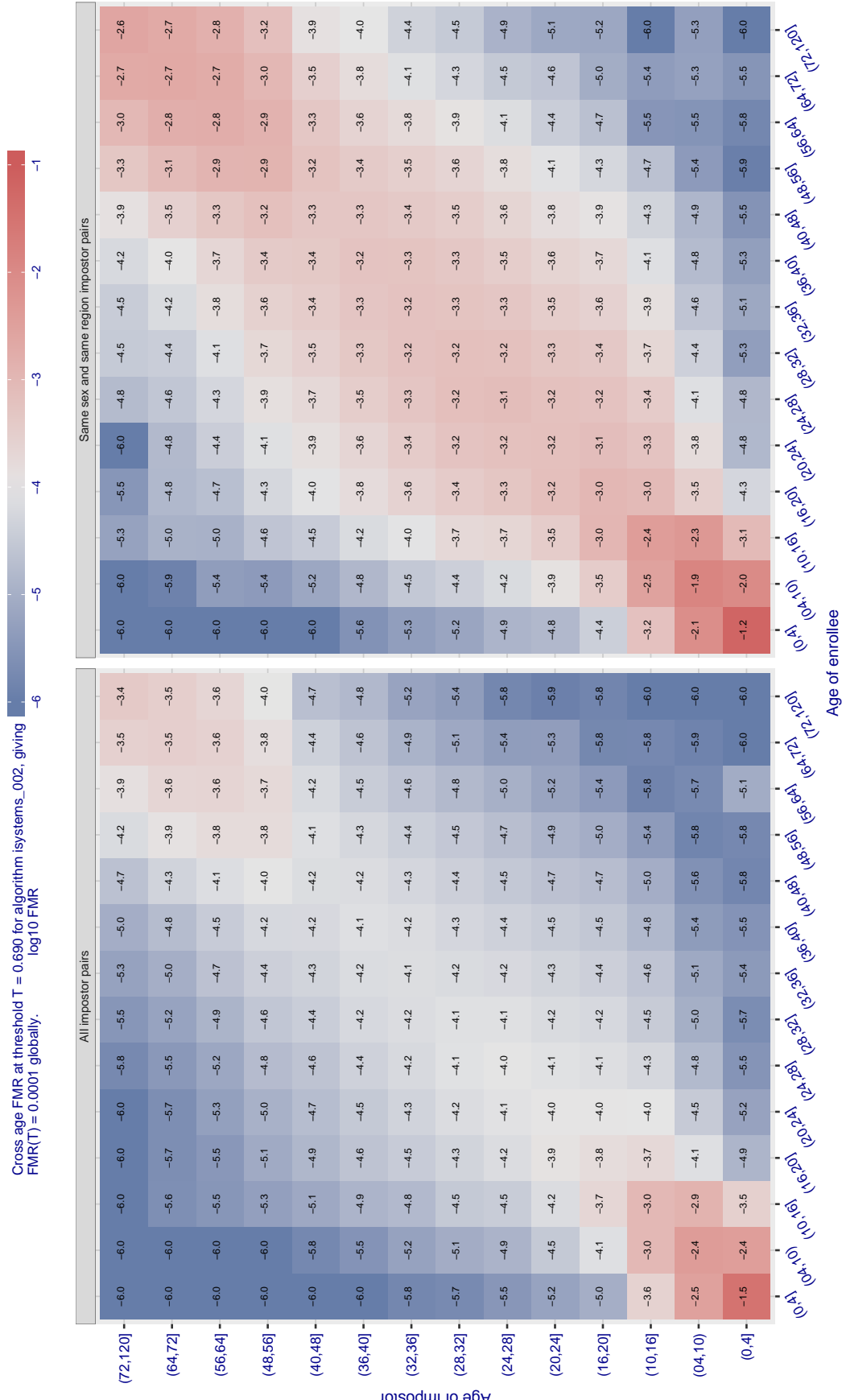


Figure 518: For algorithm isystems-002 operating on visa images, the heatmap shows false match observed over impostor comparisons of faces from different individuals who have the given age pair. False matches are counted against a recognition threshold fixed globally to give  $FMR = 0.0001$  over all on the order of  $10^{10}$  impostor comparisons. The text in each box gives the same quantity as that coded by the color. Light colors present a security vulnerability to, for example, a passport gate.

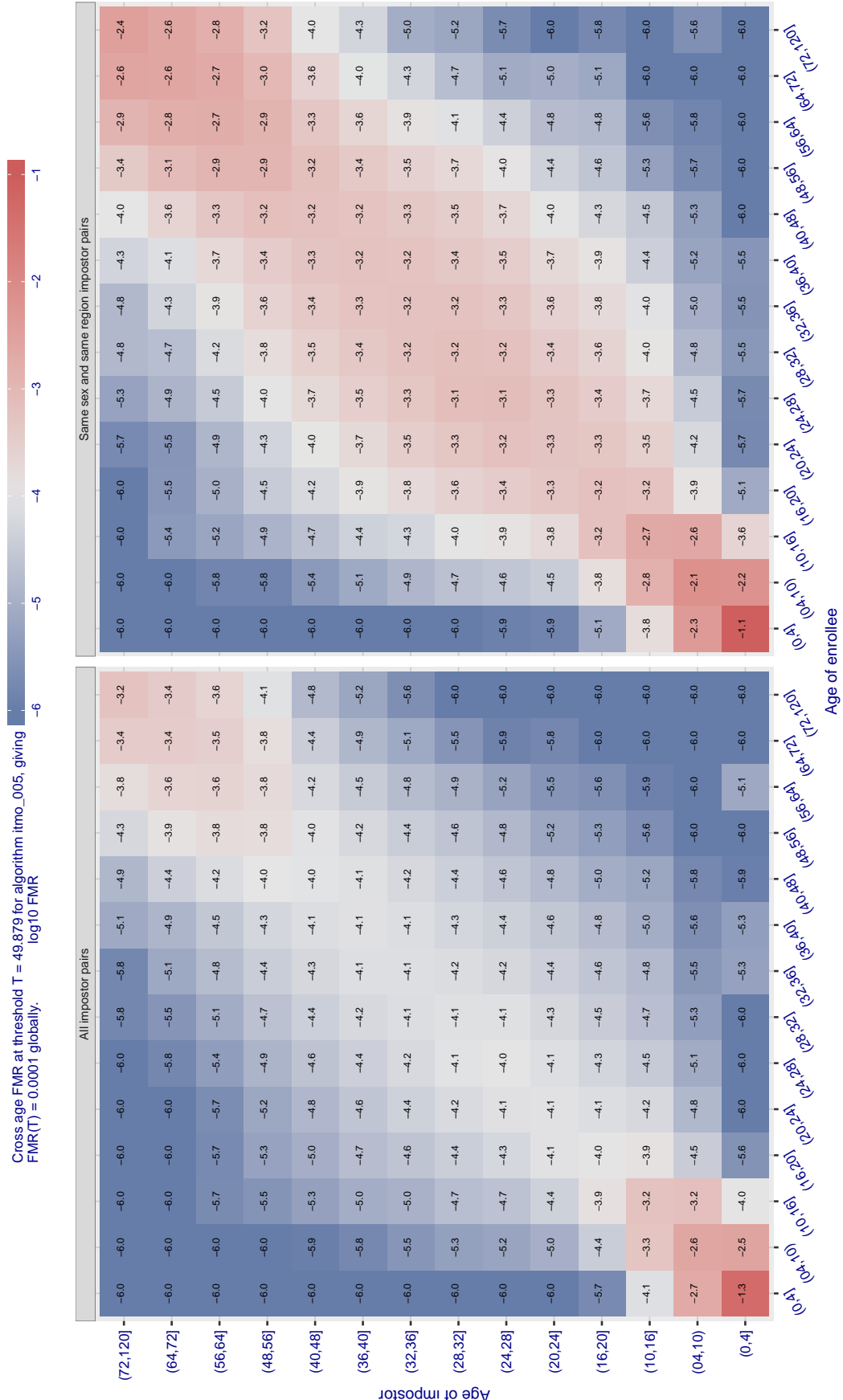


Figure 519: For algorithm itmo\_005 operating on visa images, the heatmap shows false match observed over impostor comparisons of faces from different individuals who have the given age pair. False matches are counted against a recognition threshold fixed globally to give  $FMR = 0.0001$  over all on the order of  $10^{10}$  impostor comparisons. The text in each box gives the same quantity as that coded by the color. Light colors present a security vulnerability to, for example, a passport gate.

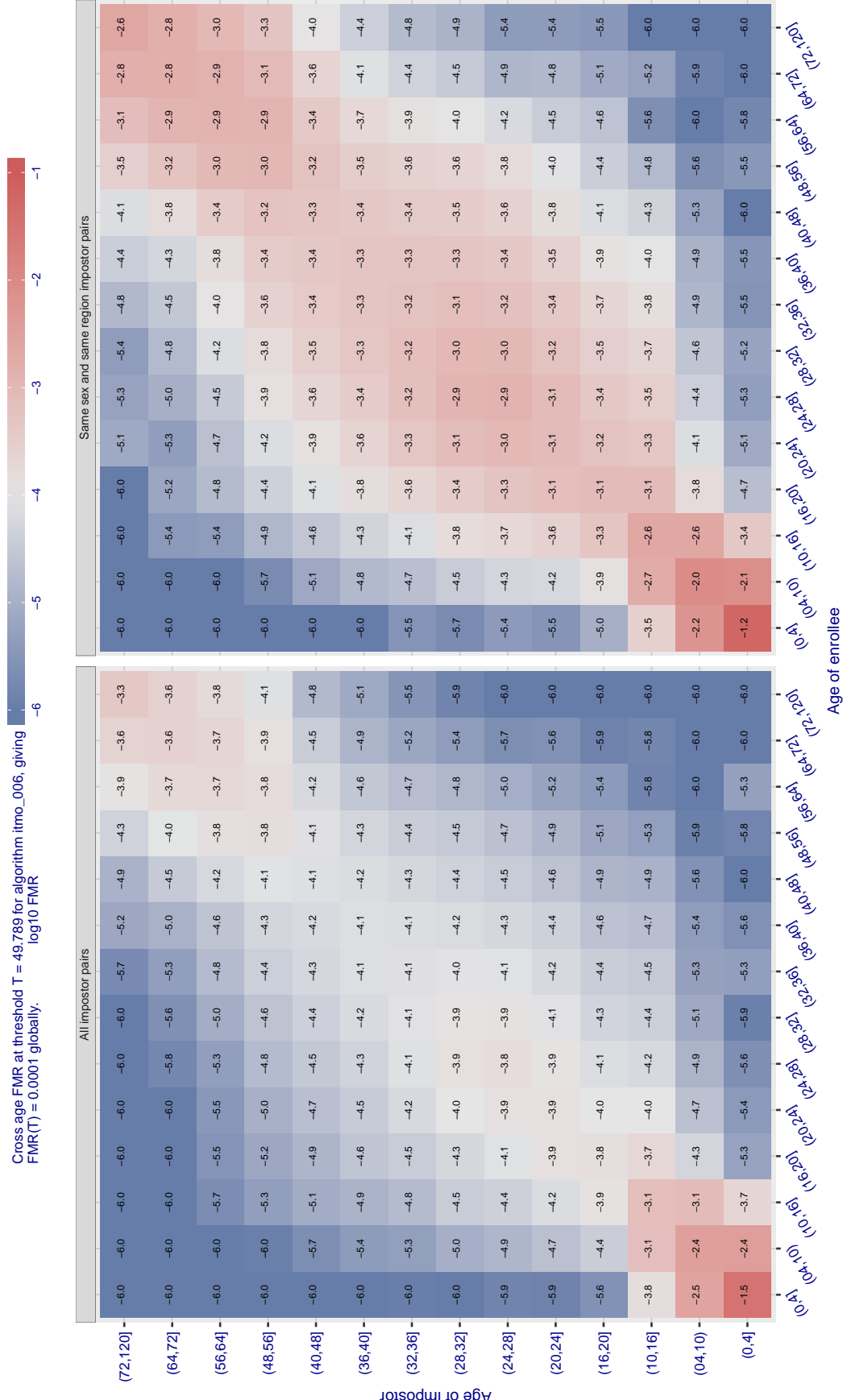


Figure 520: For algorithm *itmo-006* operating on visa images, the heatmap shows false match observed over impostor comparisons of faces from different individuals who have the given age pair. False matches are counted against a recognition threshold fixed globally to give  $FMR = 0.0001$  over all on the order of  $10^{10}$  impostor comparisons. The text in each box gives the same quantity as that coded by the color. Light colors present a security vulnerability to, for example, a passport gate.

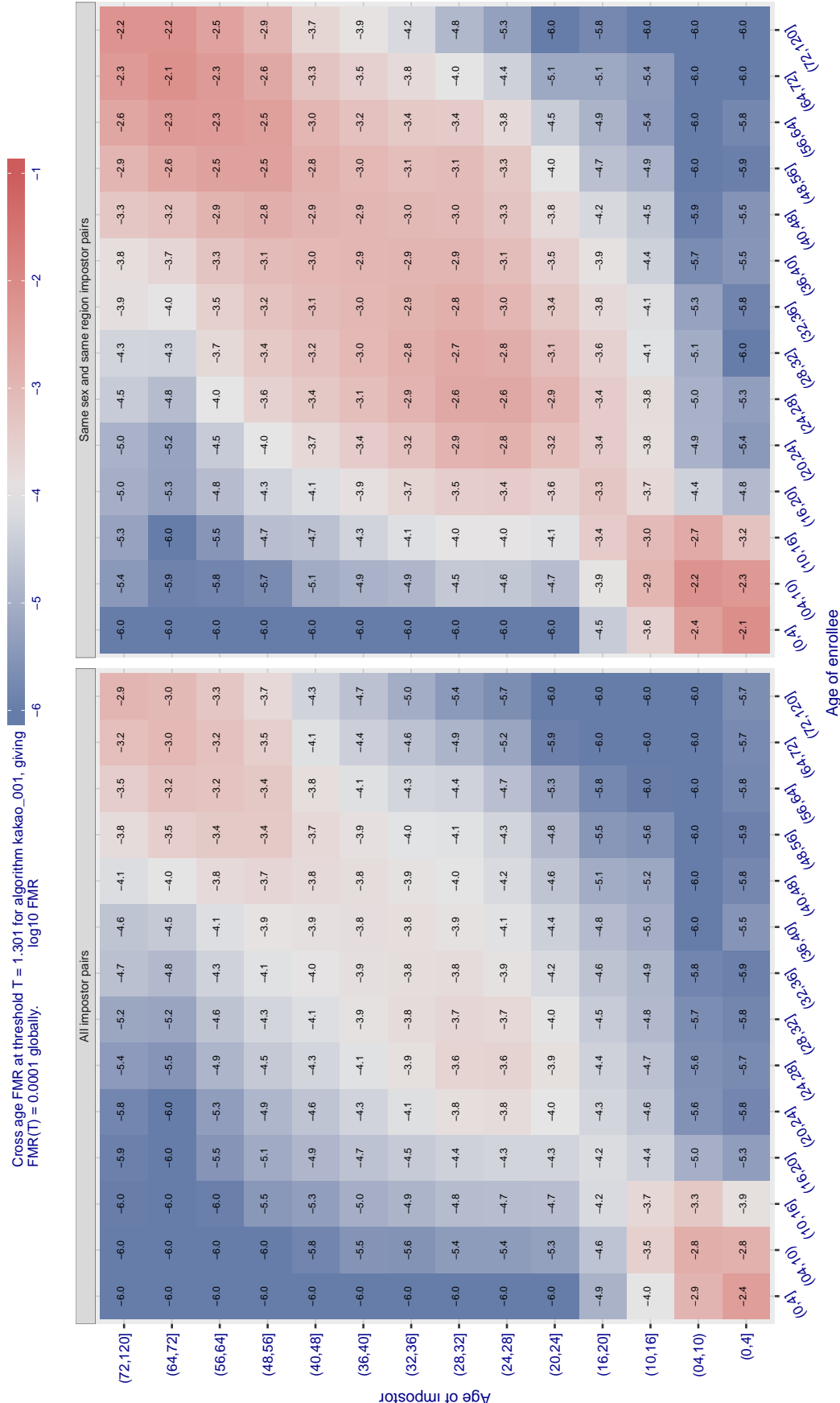


Figure 521: For algorithm kakao-001 operating on visa images, the heatmap shows false match observed over impostor comparisons of faces from different individuals who have the given age pair. False matches are counted against a recognition threshold fixed globally to give  $FMR = 0.0001$  over all on the order of  $10^{10}$  impostor comparisons. The text in each box gives the same quantity as that coded by the color. Light colors present a security vulnerability to, for example, a passport gate.

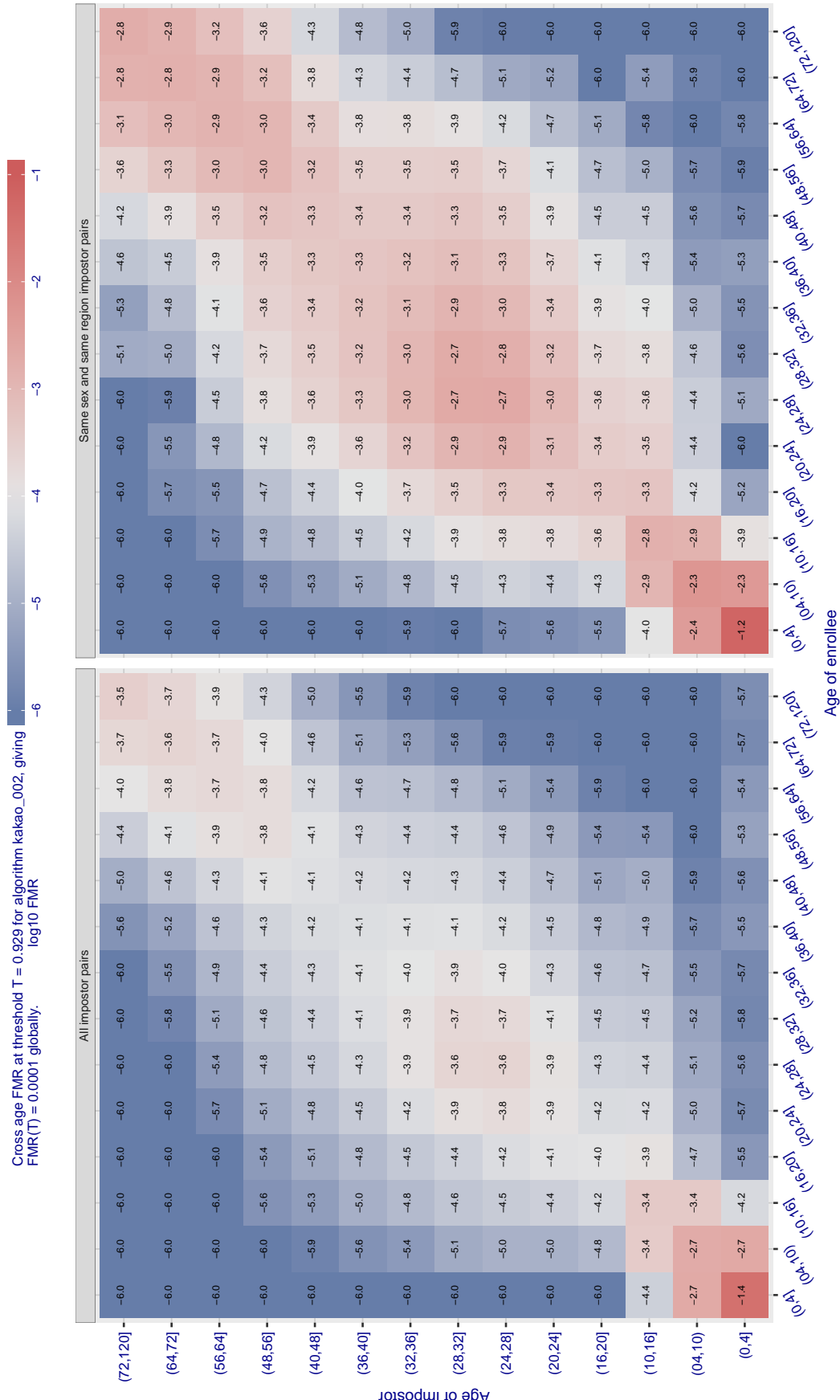


Figure 522: For algorithm kakao-002 operating on visa images, the heatmap shows false match observed over impostor comparisons of faces from different individuals who have the given age pair. False matches are counted against a recognition threshold fixed globally to give  $FMR = 0.0001$  over all on the order of  $10^{10}$  impostor comparisons. The text in each box gives the same quantity as that coded by the color. Light colors present a security vulnerability to, for example, a passport gate.

FNMR(T)  
FMR(T)

"False non-match rate"  
"False match rate"

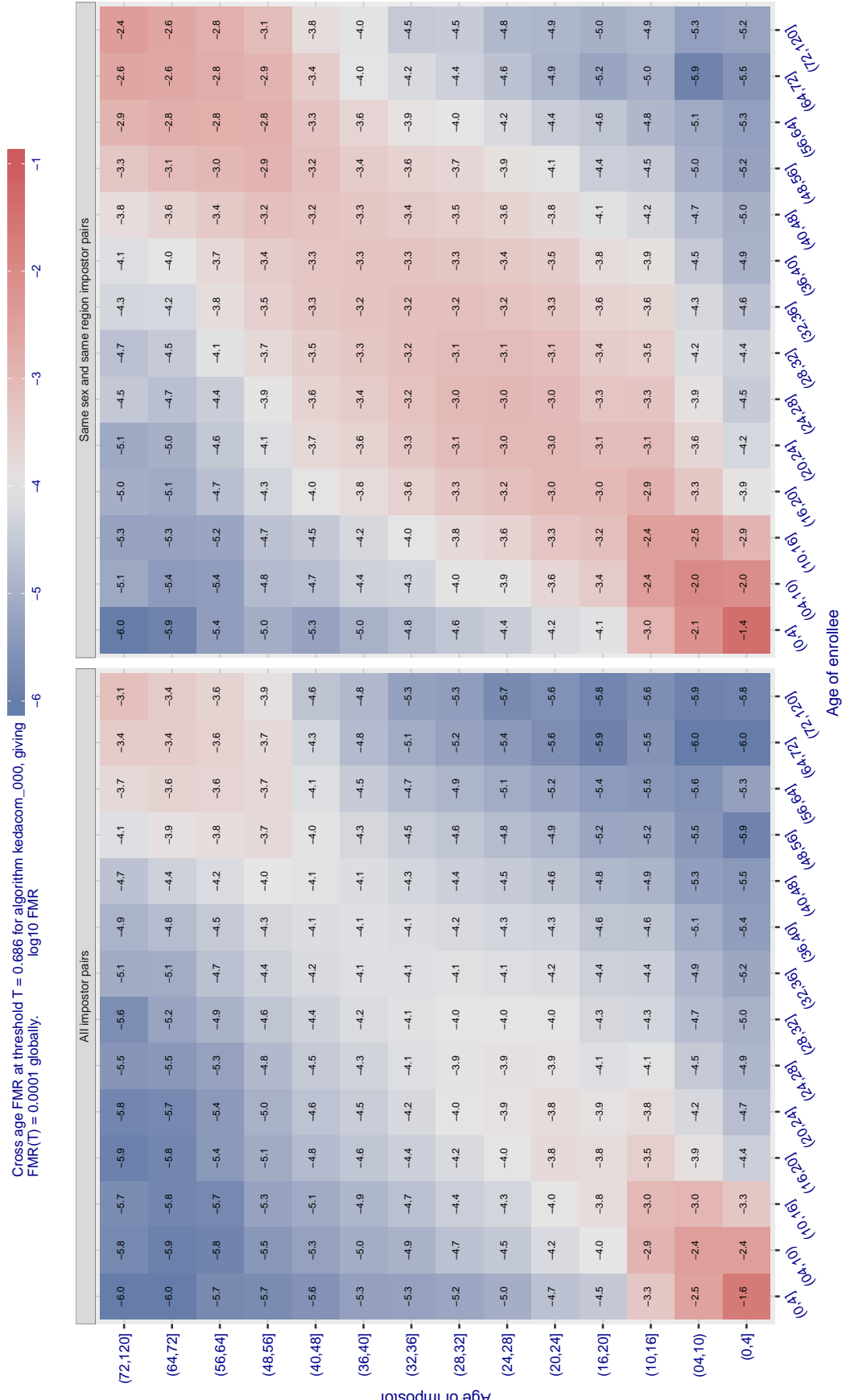


Figure 523: For algorithm kedacom\_000 operating on visa images, the heatmap shows false match observed over impostor comparisons of faces from different individuals who have the given age pair. False matches are counted against a recognition threshold fixed globally to give FMR = 0.0001 over all on the order of  $10^{10}$  impostor comparisons. The text in each box gives the same quantity as that coded by the color. Light colors present a security vulnerability to, for example, a passport gate.

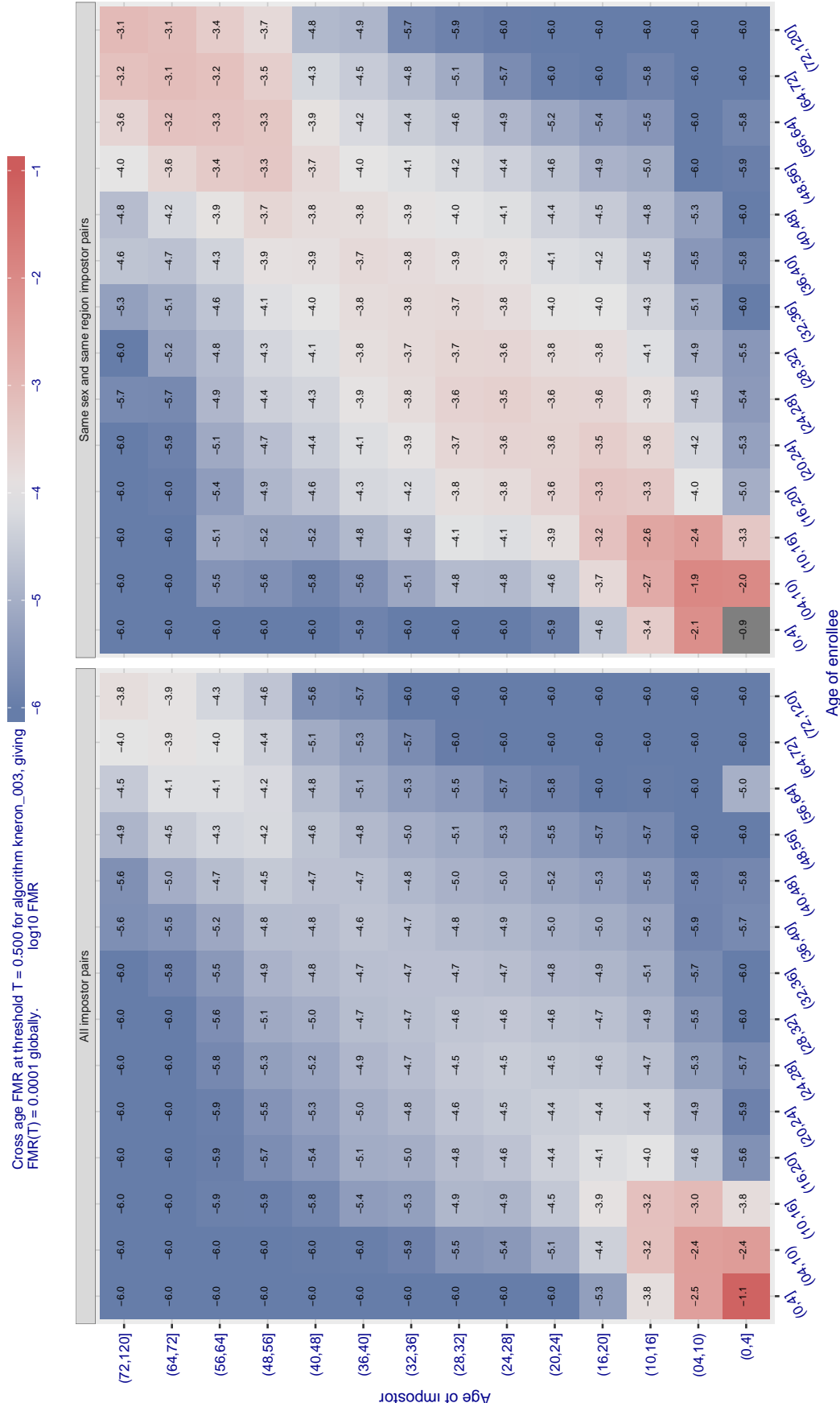


Figure 524: For algorithm kneron-003 operating on visa images, the heatmap shows false match observed over impostor comparisons of faces from different individuals who have the given age pair. False matches are counted against a recognition threshold fixed globally to give  $FMR = 0.0001$  over all on the order of  $10^{10}$  impostor comparisons. The text in each box gives the same quantity as that coded by the color. Light colors present a security vulnerability to, for example, a passport gate.

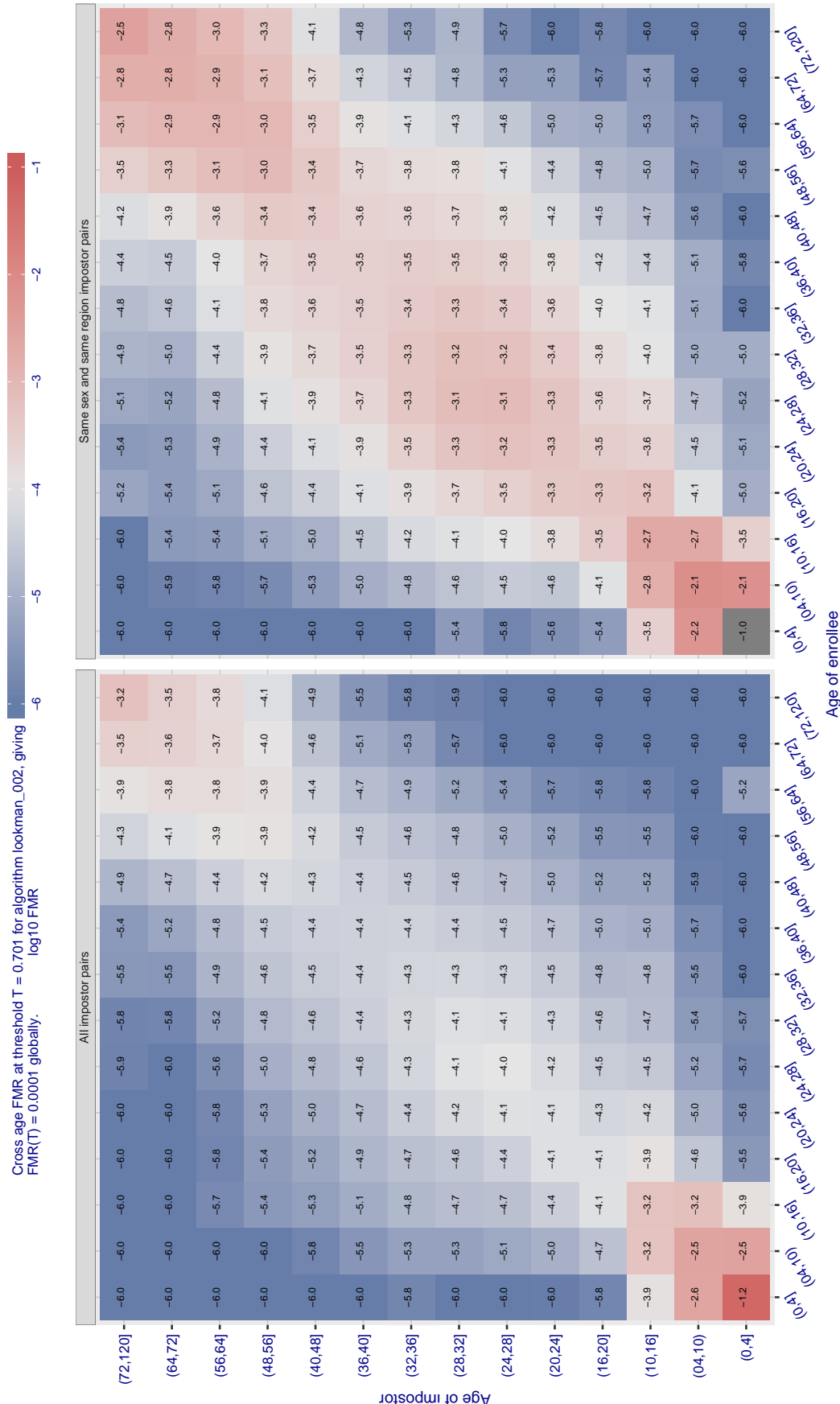


Figure 525: For algorithm lookman-002 operating on visa images, the heatmap shows false match observed over impostor comparisons of faces from different individuals who have the given age pair. False matches are counted against a recognition threshold fixed globally to give  $FMR = 0.0001$  over all on the order of  $10^{10}$  impostor comparisons. The text in each box gives the same quantity as that coded by the color. Light colors present a security vulnerability to, for example, a passport gate.

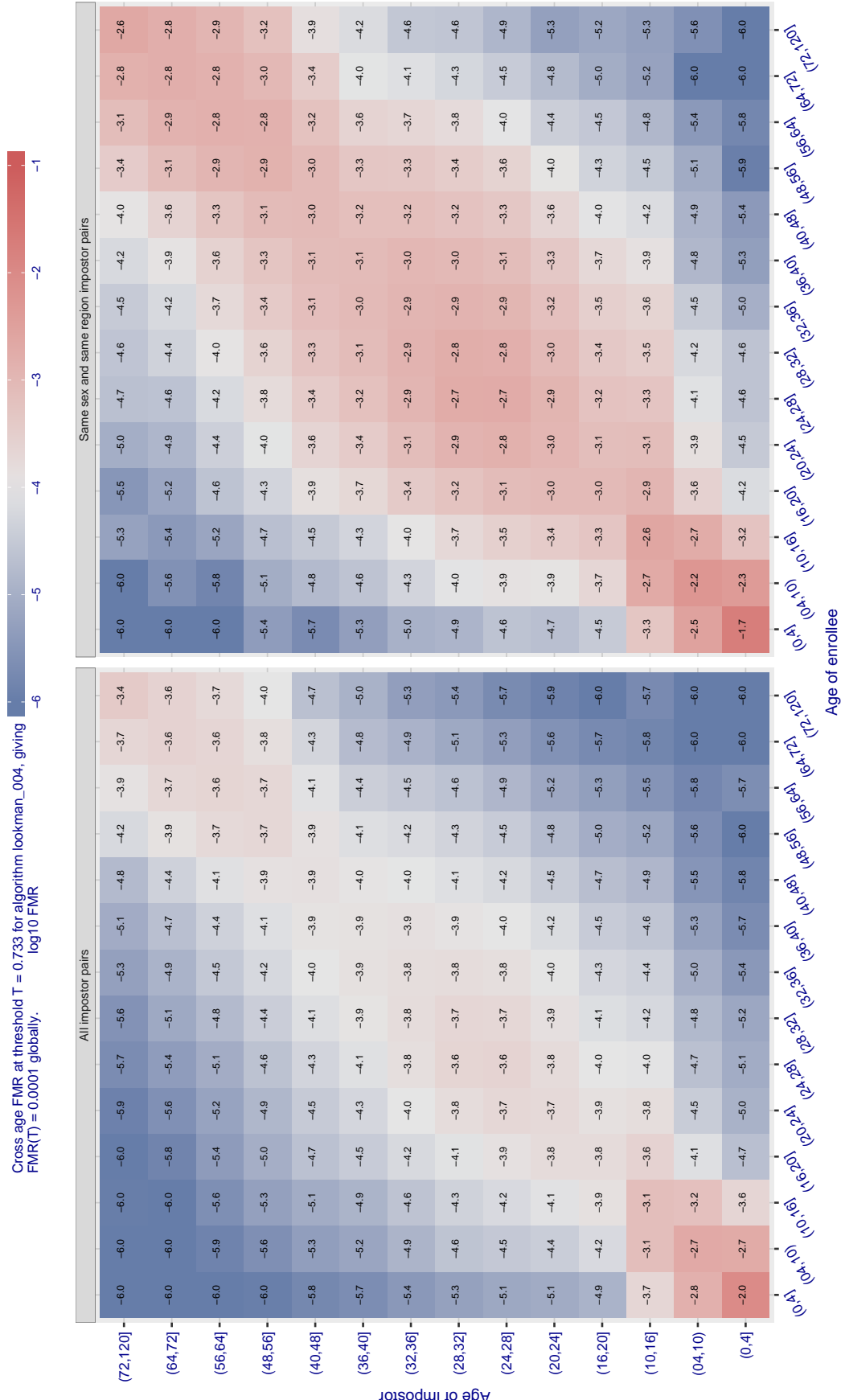


Figure 526: For algorithm lookman-004 operating on visa images, the heatmap shows false match observed over impostor comparisons of faces from different individuals who have the given age pair. False matches are counted against a recognition threshold fixed globally to give  $FMR = 0.0001$  over all on the order of  $10^{10}$  impostor comparisons. The text in each box gives the same quantity as that coded by the color. Light colors present a security vulnerability to, for example, a passport gate.

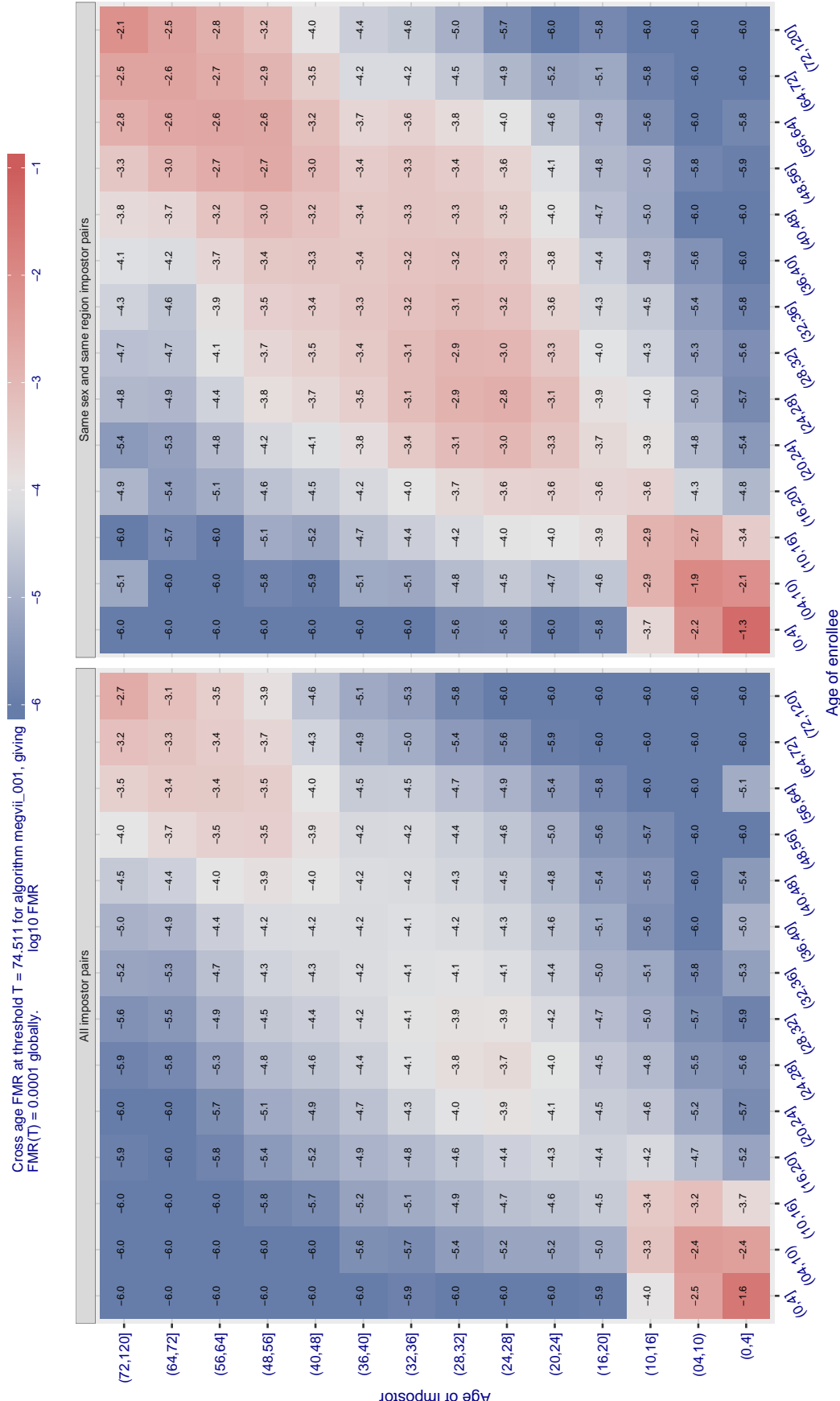


Figure 527: For algorithm megvii-001 operating on visa images, the heatmap shows false match observed over impostor comparisons of faces from different individuals who have the given age pair. False matches are counted against a recognition threshold fixed globally to give  $FMR = 0.0001$  over all on the order of  $10^{10}$  impostor comparisons. The text in each box gives the same quantity as that coded by the color. Light colors present a security vulnerability to, for example, a passport gate.

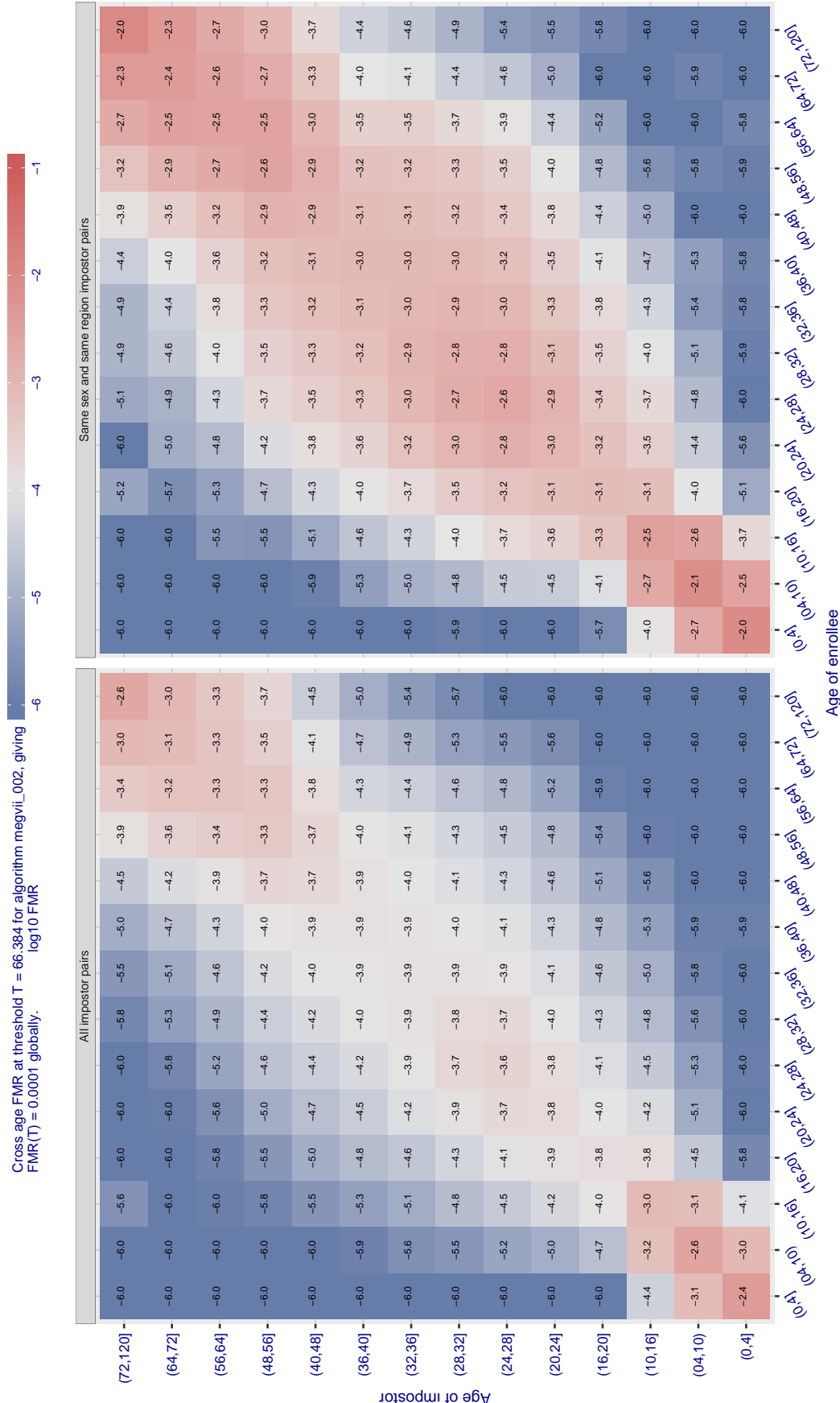


Figure 528: For algorithm megvii-002 operating on visa images, the heatmap shows false match observed over impostor comparisons of faces from different individuals who have the given age pair. False matches are counted against a recognition threshold fixed globally to give  $FMR = 0.0001$  over all on the order of  $10^{10}$  impostor comparisons. The text in each box gives the same quantity as that coded by the color. Light colors present a security vulnerability to, for example, a passport gate.

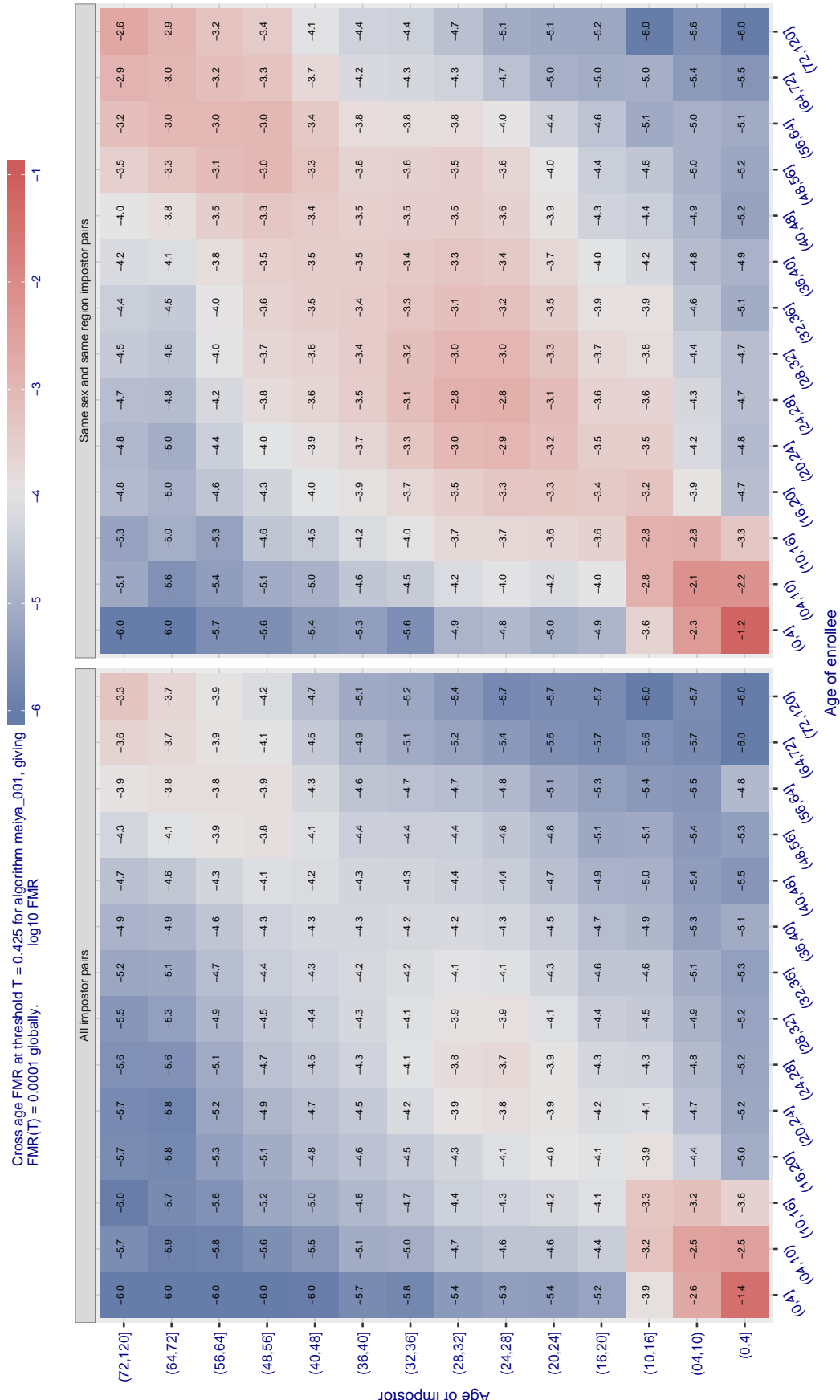


Figure 529: For algorithm meiya-001 operating on visa images, the heatmap shows false match observed over impostor comparisons of faces from different individuals who have the given age pair. False matches are counted against a recognition threshold fixed globally to give  $\text{FMR} = 0.0001$  over all on the order of  $10^{10}$  impostor comparisons. The text in each box gives the same quantity as that coded by the color. Light colors present a security vulnerability to, for example, a passport gate.

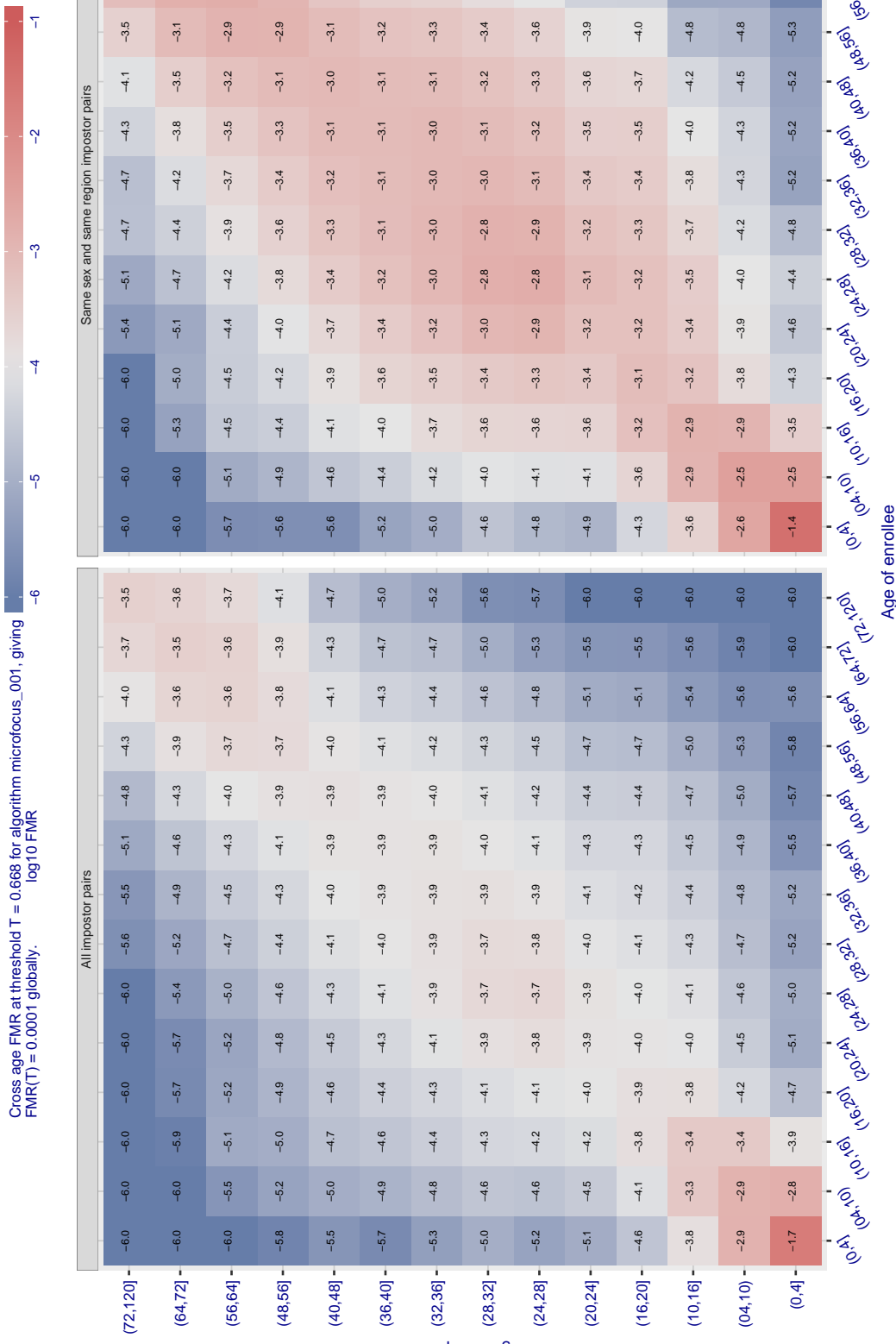


Figure 530: For algorithm microfocus-001 operating on visa images, the heatmap shows false match observed over impostor comparisons of faces from different individuals who have the given age pair. False matches are counted against a recognition threshold fixed globally to give FMR = 0.0001 over all on the order of  $10^{10}$  impostor comparisons. The text in each box gives the same quantity as that coded by the color. Light colors present a security vulnerability to, for example, a passport gate.

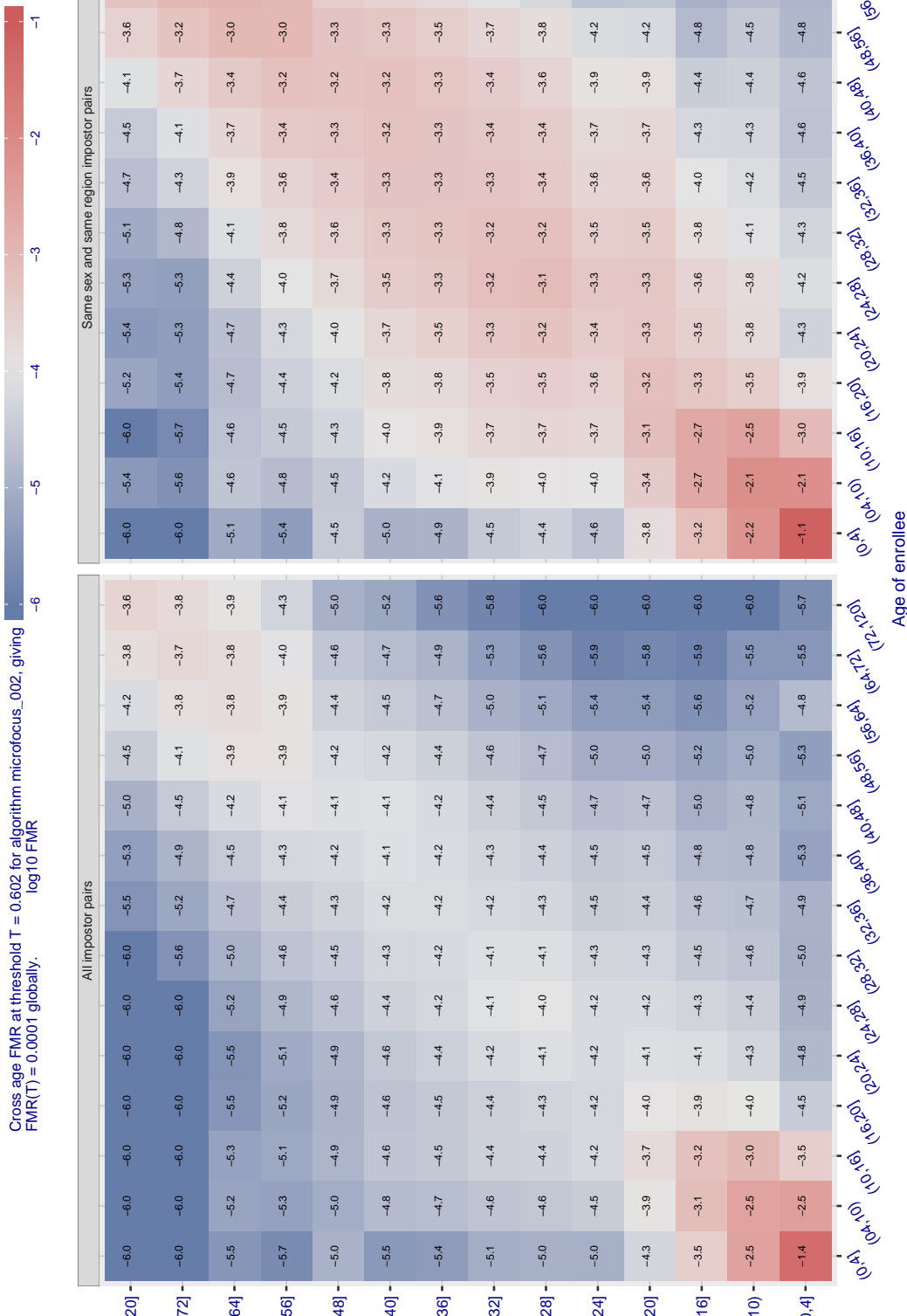


Figure 531: For algorithm microfocus-002 operating on visa images, the heatmap shows false match observed over impostor comparisons of faces from different individuals who have the given age pair. False matches are counted against a recognition threshold fixed globally to give  $FMR = 0.0001$  over all on the order of  $10^{10}$  impostor comparisons. The text in each box gives the same quantity as that coded by the color. Light colors present a security vulnerability to, for example, a passport gate.

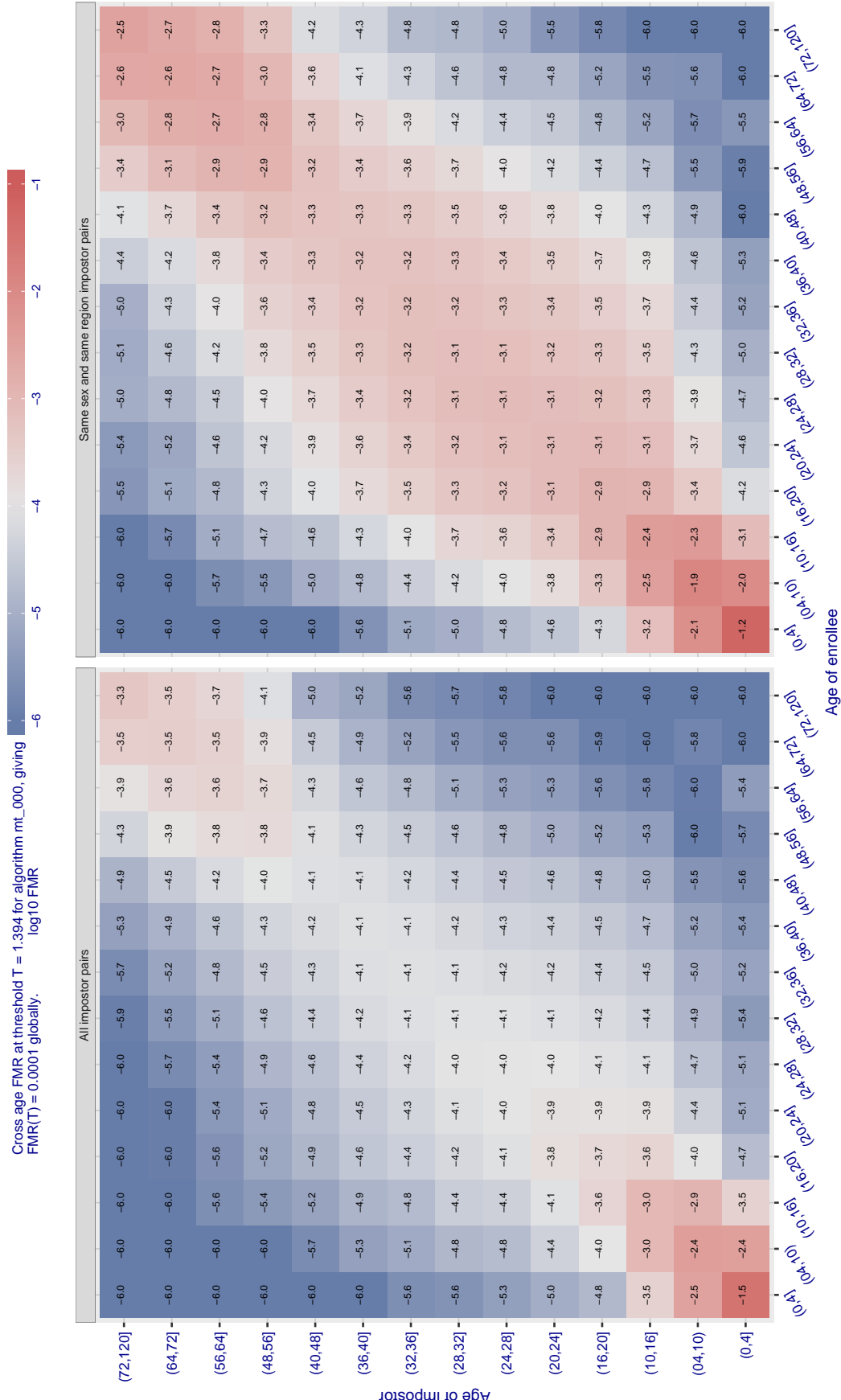


Figure 532: For algorithm mt-000 operating on visa images, the heatmap shows false match observed over impostor comparisons of faces from different individuals who have the given age pair. False matches are counted against a recognition threshold fixed globally to give  $FMR = 0.0001$  over all on the order of  $10^{10}$  impostor comparisons. The text in each box gives the same quantity as that coded by the color. Light colors present a security vulnerability to, for example, a passport gate.

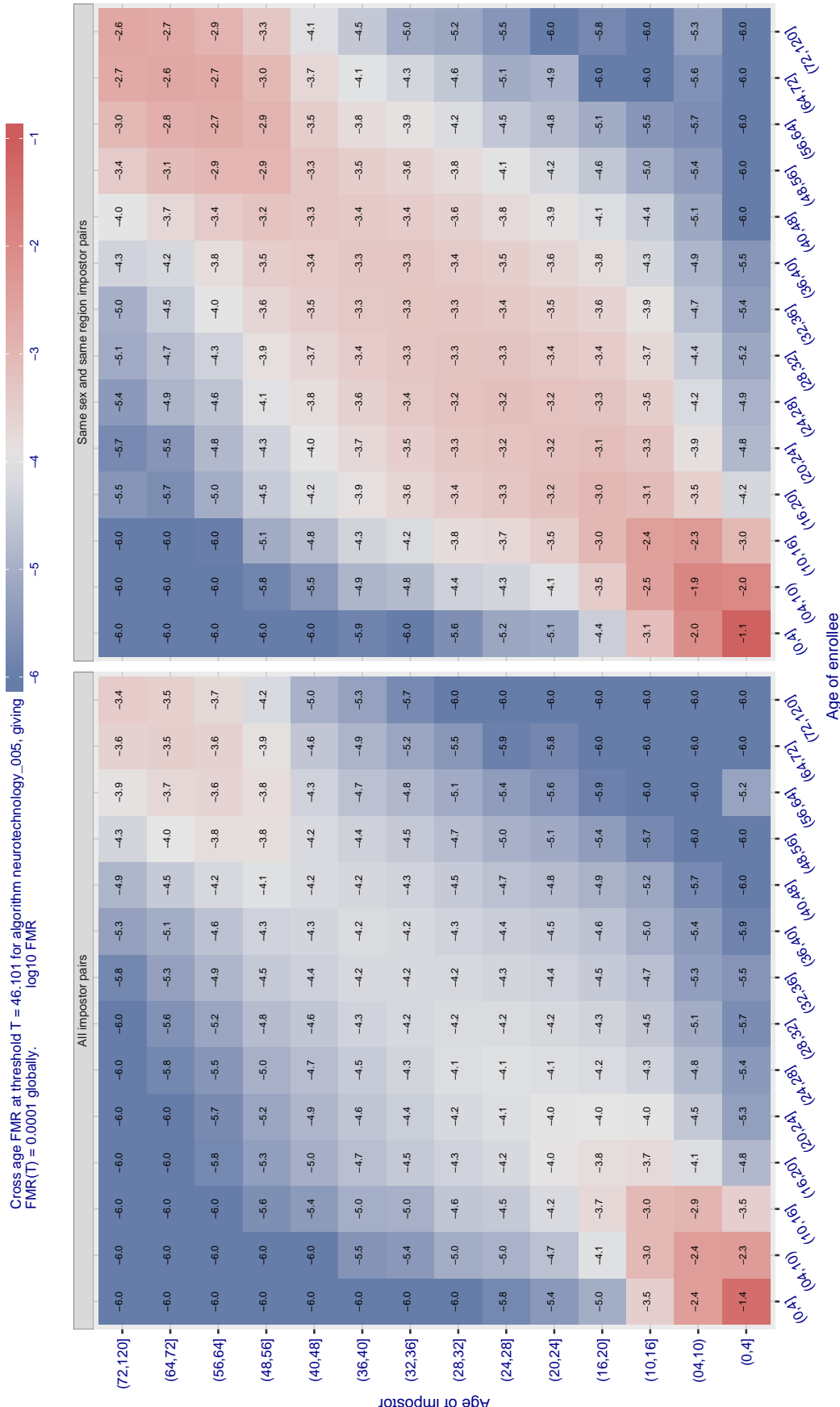


Figure 533: For algorithm neurotechnology-005 operating on visa images, the heatmap shows false match observed over impostor comparisons of faces from different individuals who have the given age pair. False matches are counted against a recognition threshold fixed globally to give  $\text{FMR} = 0.0001$  over all on the order of  $10^{10}$  impostor comparisons. The text in each box gives the same quantity as that coded by the color. Light colors present a security vulnerability to, for example, a passport gate.

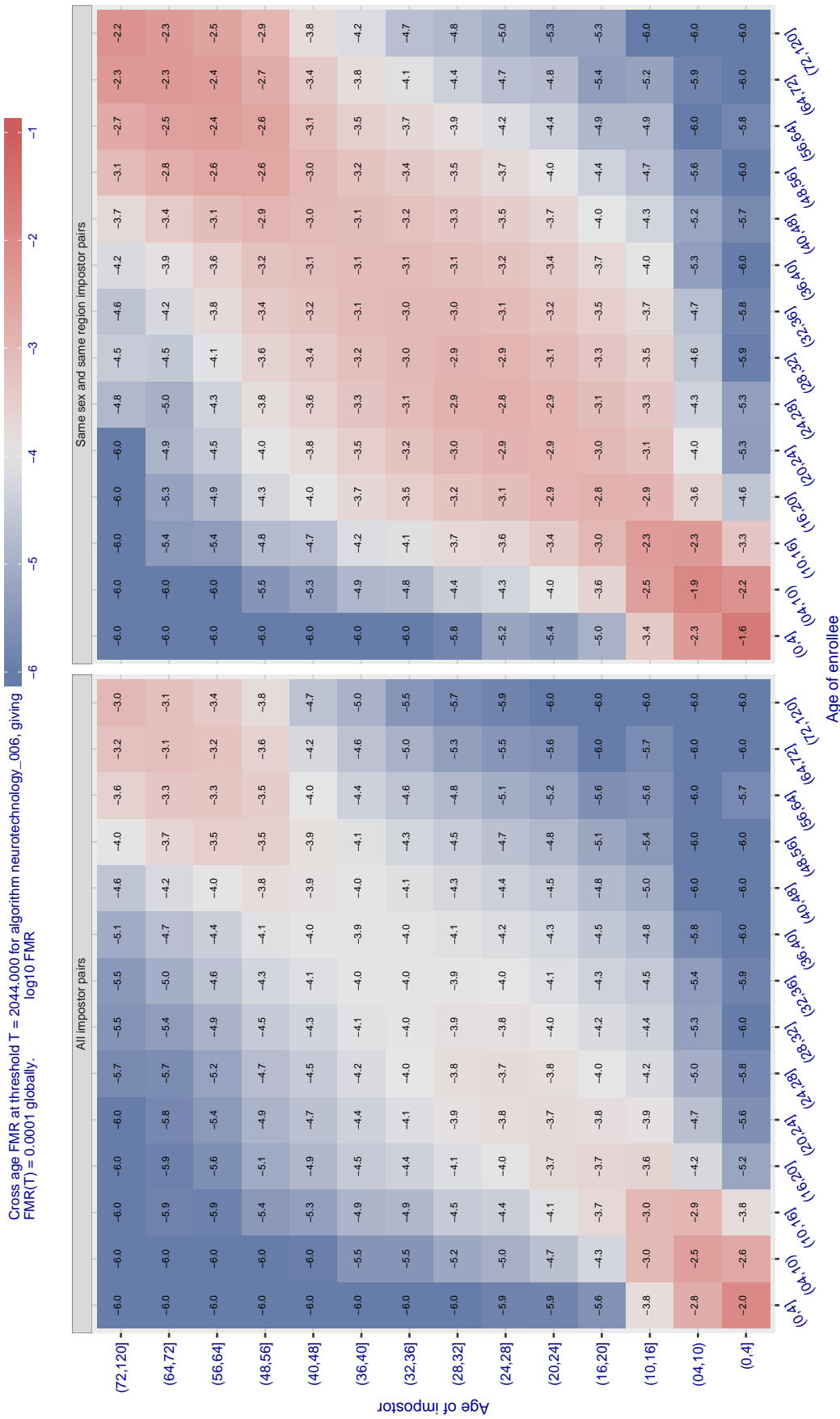


Figure 534: For algorithm neurotechnology\_006 operating on visa images, the heatmap shows false match observed over impostor comparisons of faces from different individuals who have the given age pair. False matches are counted against a recognition threshold fixed globally to give  $FMR = 0.0001$  over all on the order of  $10^{10}$  impostor comparisons. The text in each box gives the same quantity as that coded by the color. Light colors present a security vulnerability to, for example, a passport gate.

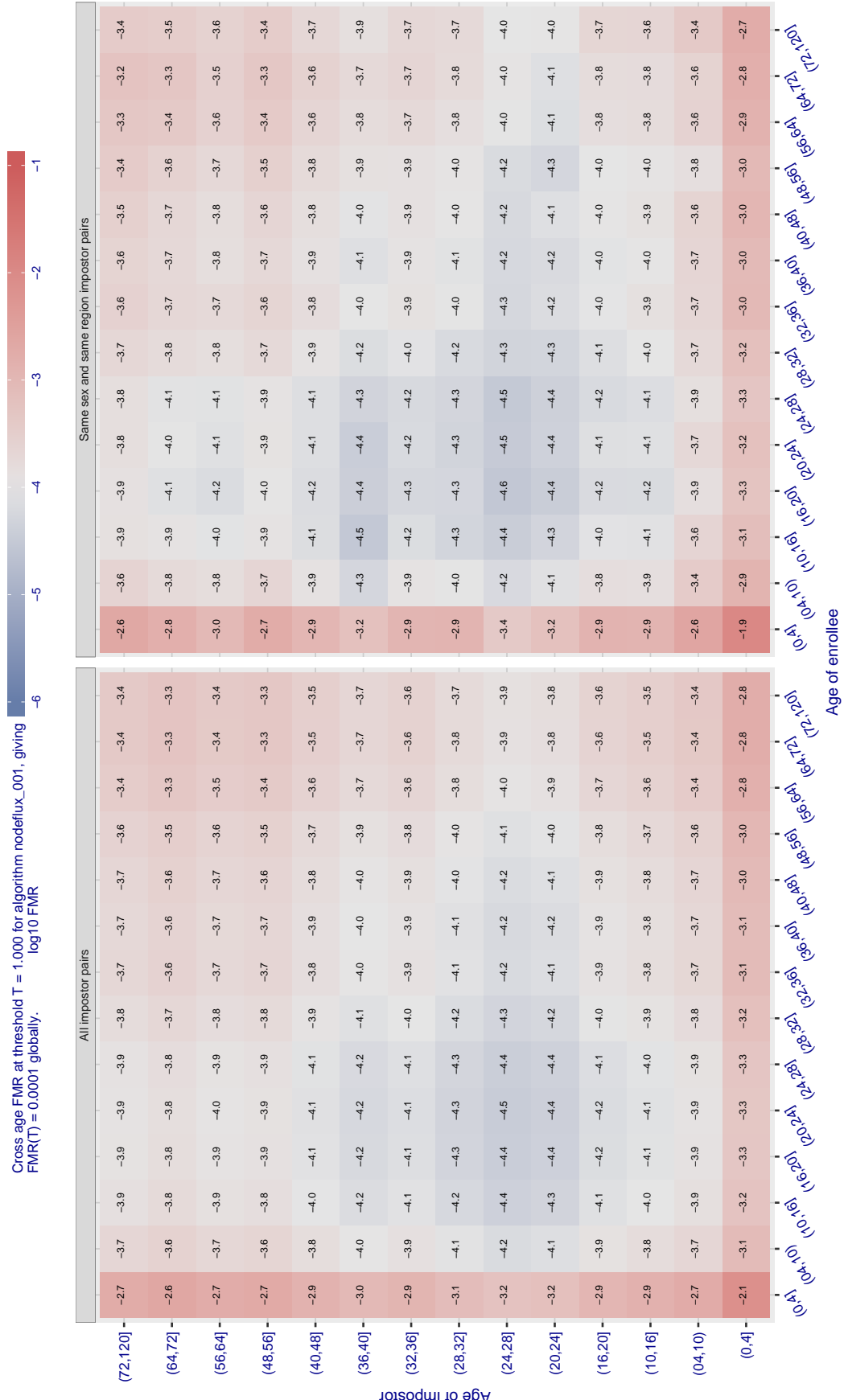


Figure 535: For algorithm nodeflux-001 operating on visa images, the heatmap shows false match observed over impostor comparisons of faces from different individuals who have the given age pair. False matches are counted against a recognition threshold fixed globally to give  $FMR = 0.0001$  over all on the order of  $10^{10}$  impostor comparisons. The text in each box gives the same quantity as that coded by the color. Light colors present a security vulnerability to, for example, a passport gate.

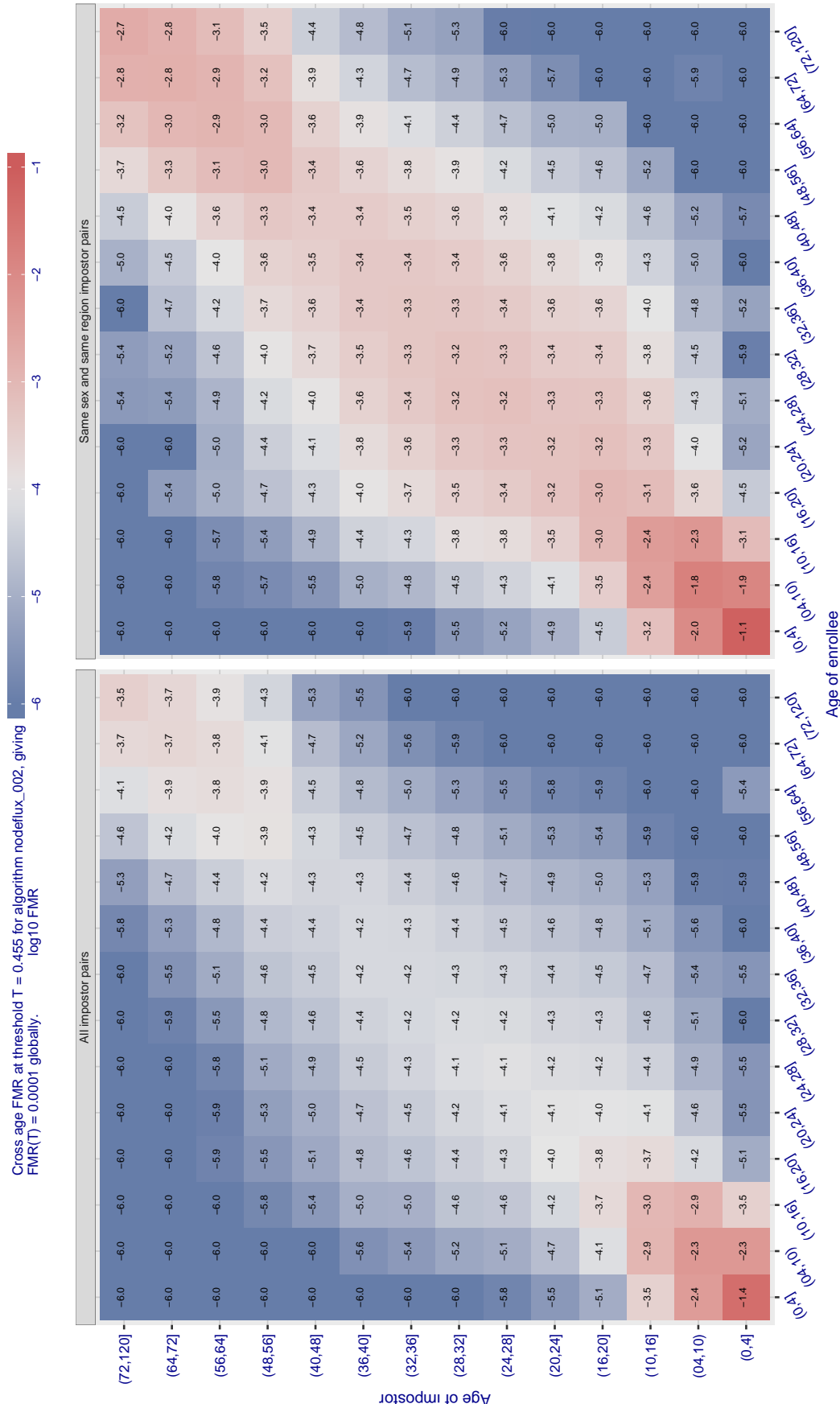


Figure 536: For algorithm nodeflux-002 operating on visa images, the heatmap shows false match observed over impostor comparisons of faces from different individuals who have the given age pair. False matches are counted against a recognition threshold fixed globally to give  $FMR = 0.0001$  over all on the order of  $10^{10}$  impostor comparisons. The text in each box gives the same quantity as that coded by the color. Light colors present a security vulnerability to, for example, a passport gate.

1787285087495083067381227850991804952529501444874689546055214391983563576348021983576872064863890123394711833843842027116185401814731854606759975435142378710012068708547335424481767

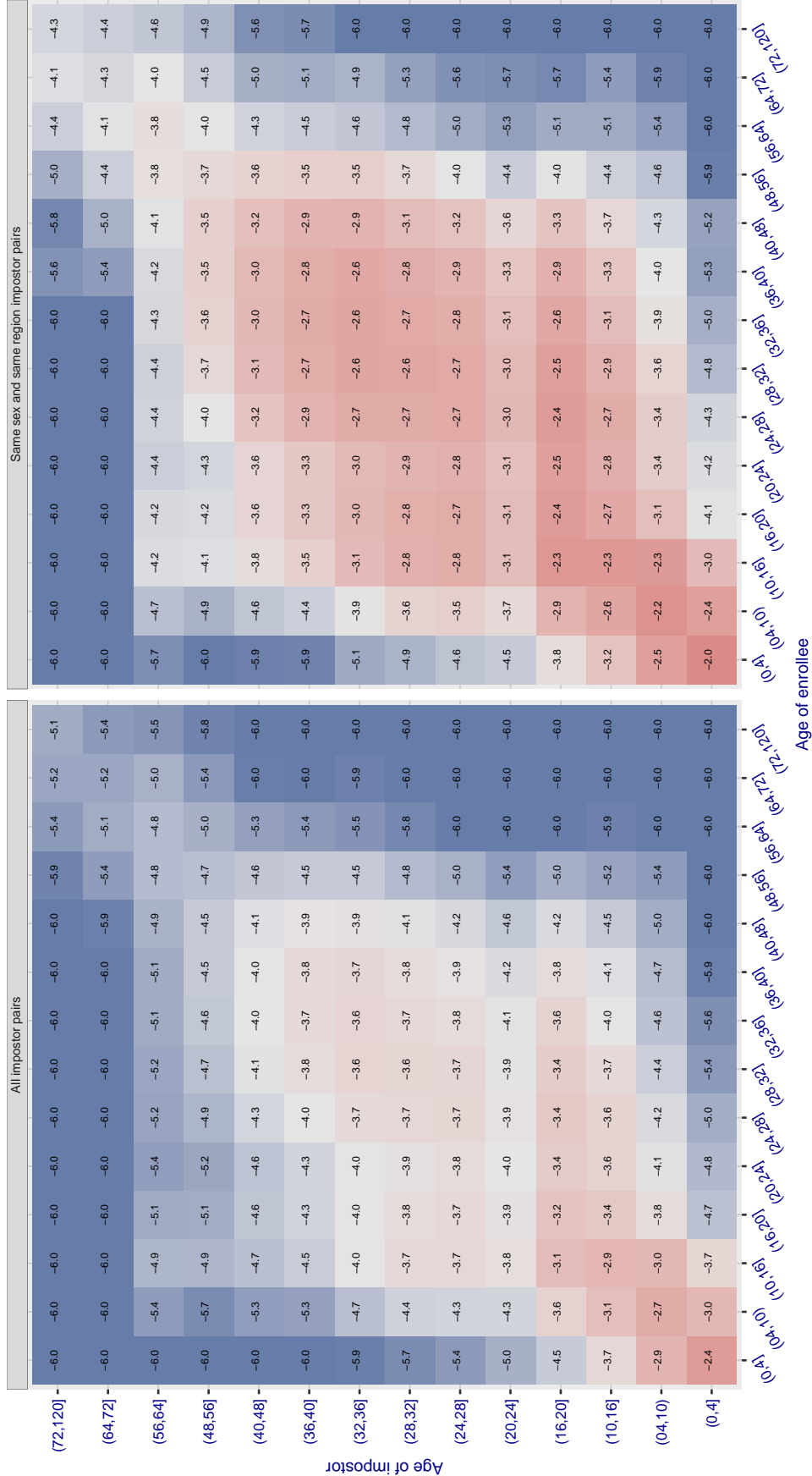


Figure 537: For algorithm notiontag-000 operating on visa images, the heatmap shows false match observed over impostor comparisons of faces from different individuals who have the given age pair. False matches are counted against a recognition threshold fixed globally to give FMR = 0.001 over all on the order of  $10^{10}$  impostor comparisons. The text in each box gives the same quantity as that coded by the color. Light colors present a security vulnerability to, for example, a passport gate.

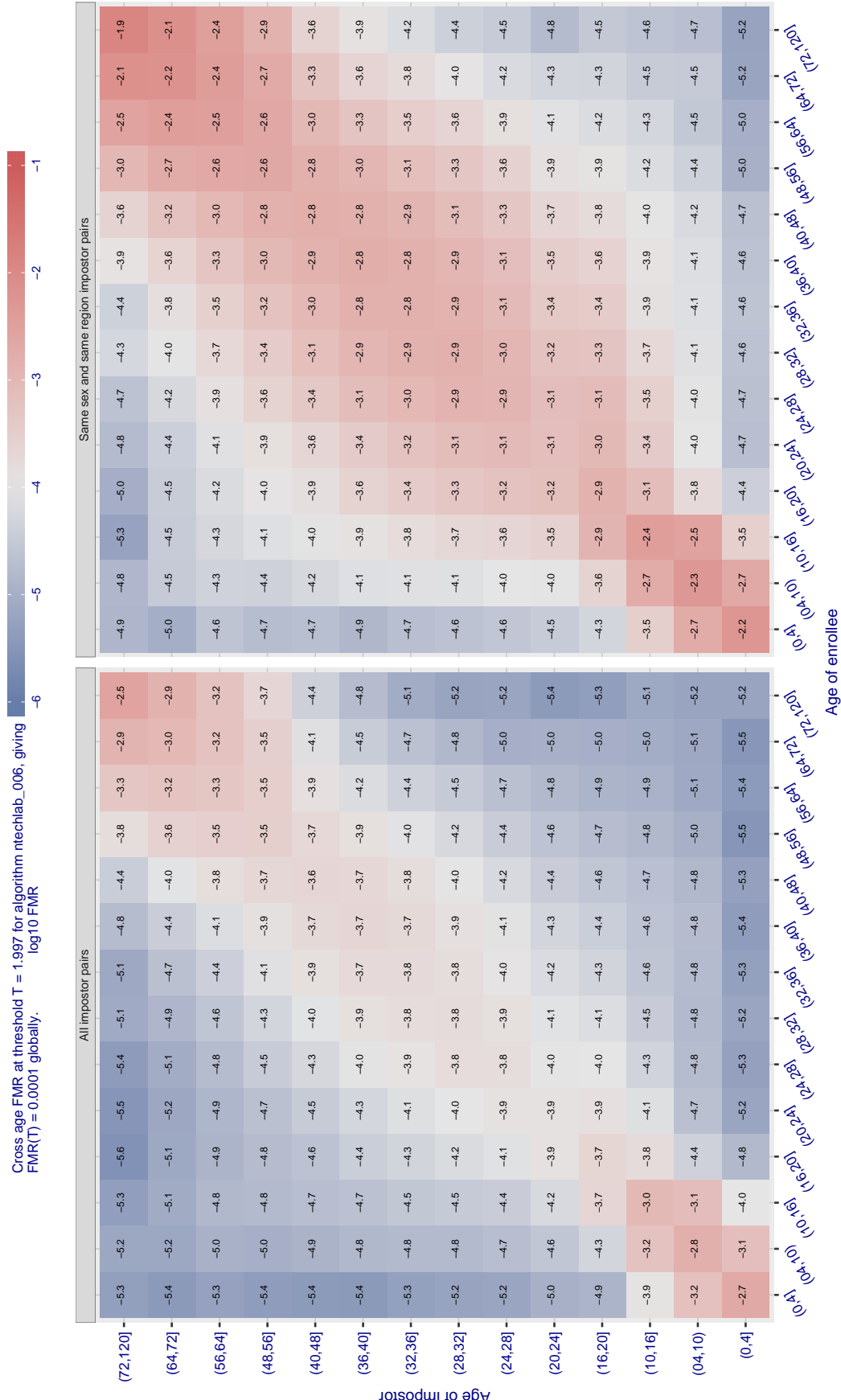


Figure 538: For algorithm ntechlab-006 operating on visa images, the heatmap shows false match observed over impostor comparisons of faces from different individuals who have the given age pair. False matches are counted against a recognition threshold fixed globally to give  $FMR = 0.0001$  over all on the order of  $10^{10}$  impostor comparisons. The text in each box gives the same quantity as that coded by the color. Light colors present a security vulnerability to, for example, a passport gate.

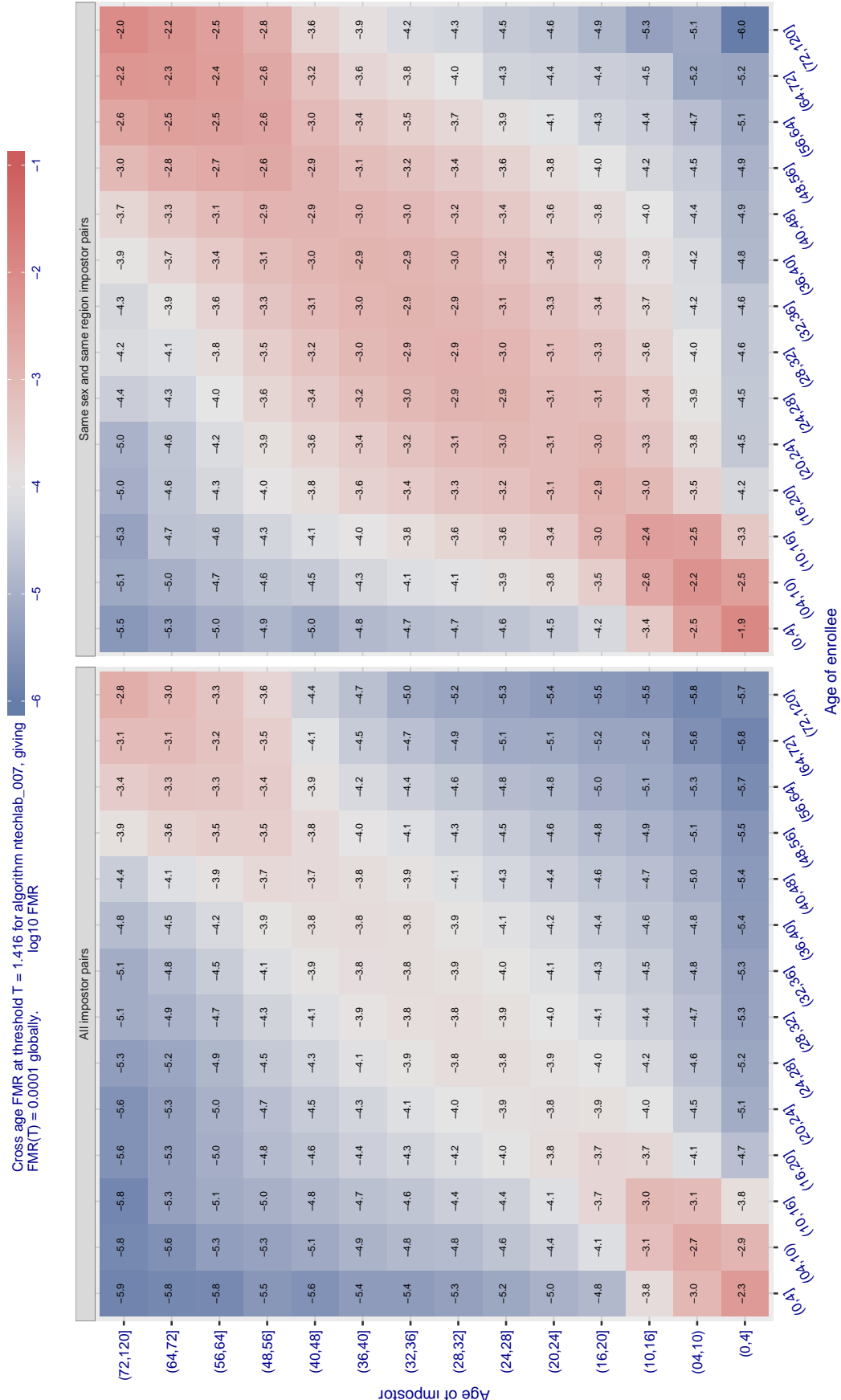


Figure 539: For algorithm ntechlab-007 operating on visa images, the heatmap shows false match observed over impostor comparisons of faces from different individuals who have the given age pair. False matches are counted against a recognition threshold fixed globally to give  $FMR = 0.0001$  over all on the order of  $10^{10}$  impostor comparisons. The text in each box gives the same quantity as that coded by the color. Light colors present a security vulnerability to, for example, a passport gate.

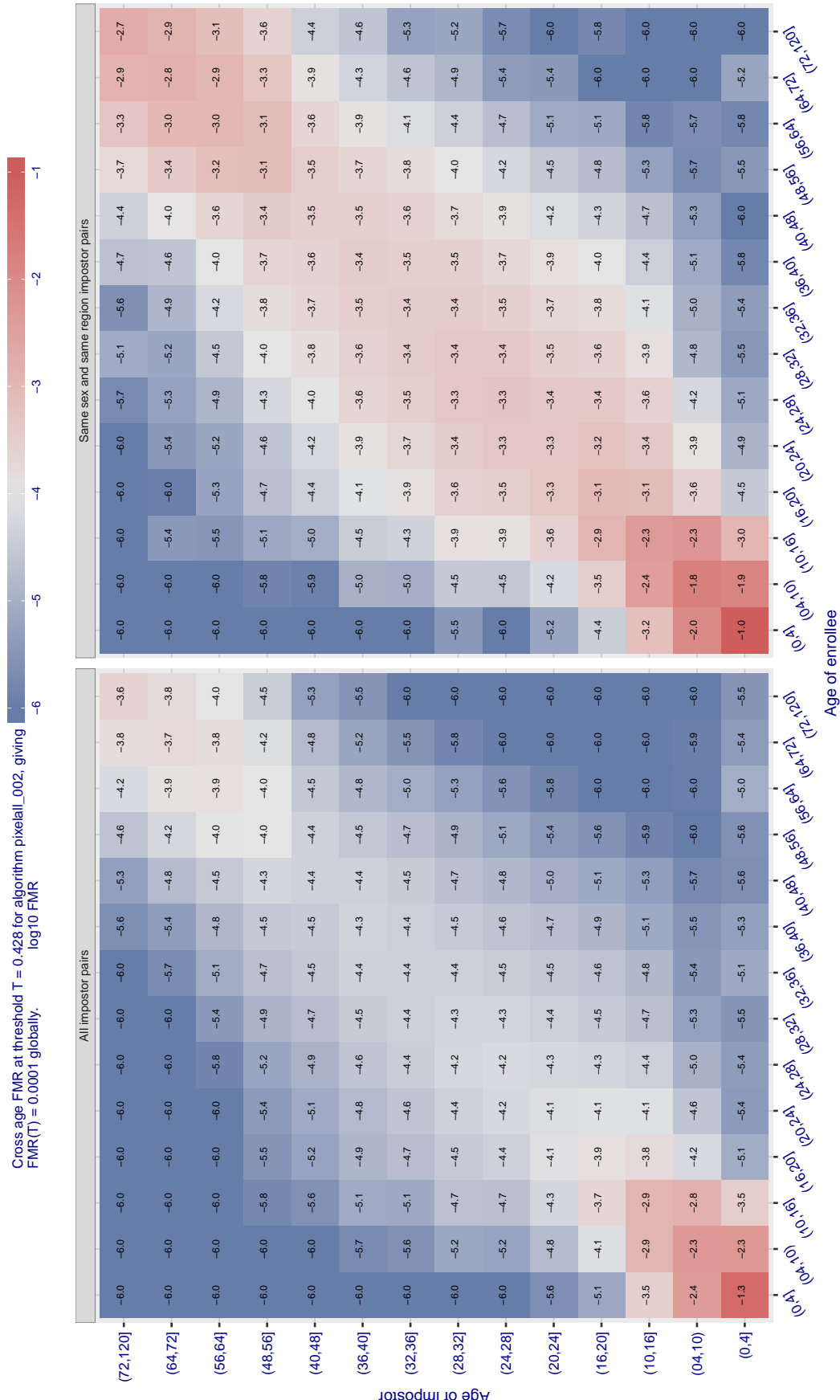


Figure 540: For algorithm pixelall-002 operating on visa images, the heatmap shows false match observed over impostor comparisons of faces from different individuals who have the given age pair. False matches are counted against a recognition threshold fixed globally to give  $FMR = 0.0001$  over all on the order of  $10^{10}$  impostor comparisons. The text in each box gives the same quantity as that coded by the color. Light colors present a security vulnerability to, for example, a passport gate.

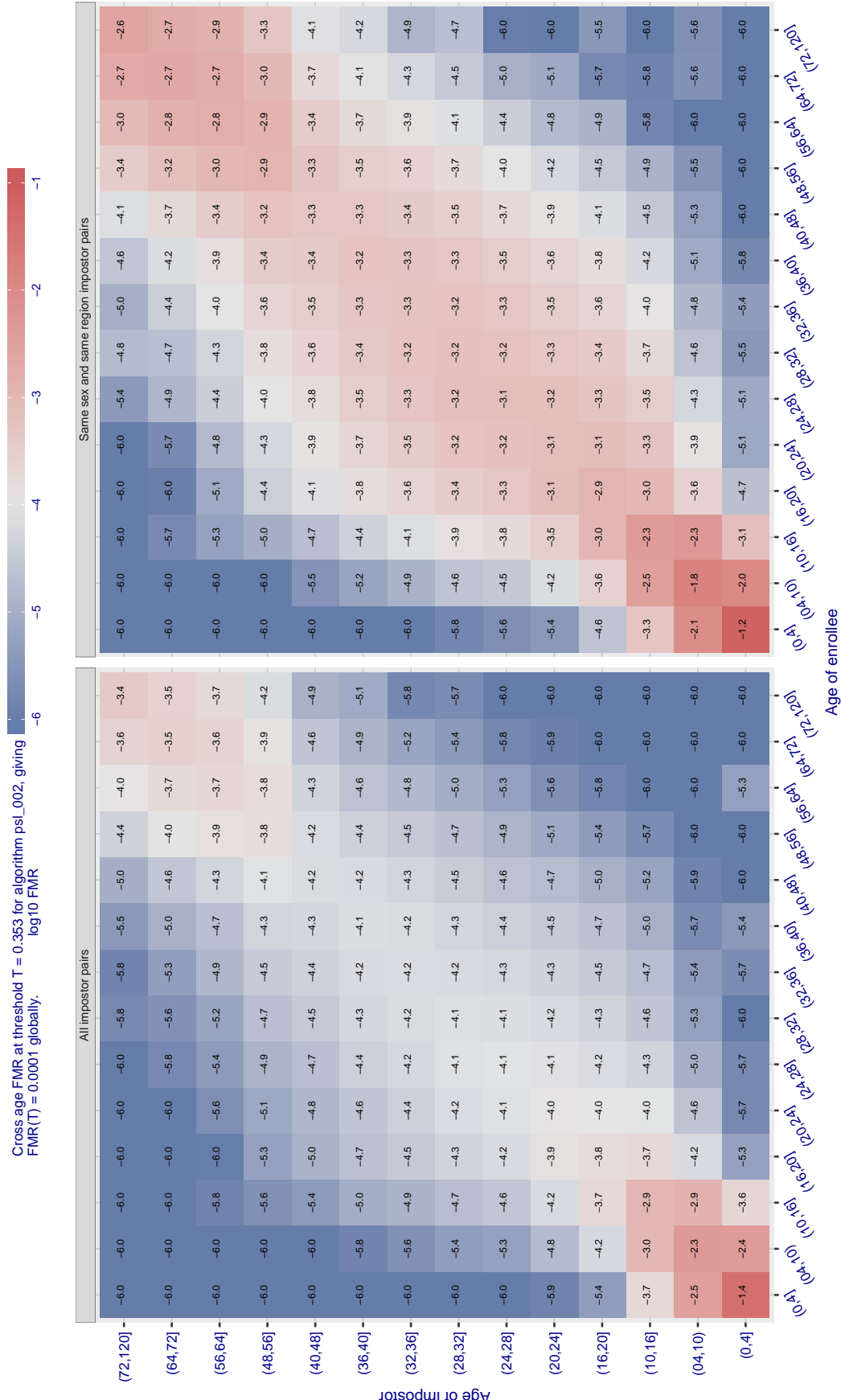


Figure 541: For algorithm psl-002 operating on visa images, the heatmap shows false match observed over impostor comparisons of faces from different individuals who have the given age pair. False matches are counted against a recognition threshold fixed globally to give  $\text{FMR} = 0.0001$  over all on the order of  $10^{10}$  impostor comparisons. The text in each box gives the same quantity as that coded by the color. Light colors present a security vulnerability to, for example, a passport gate.

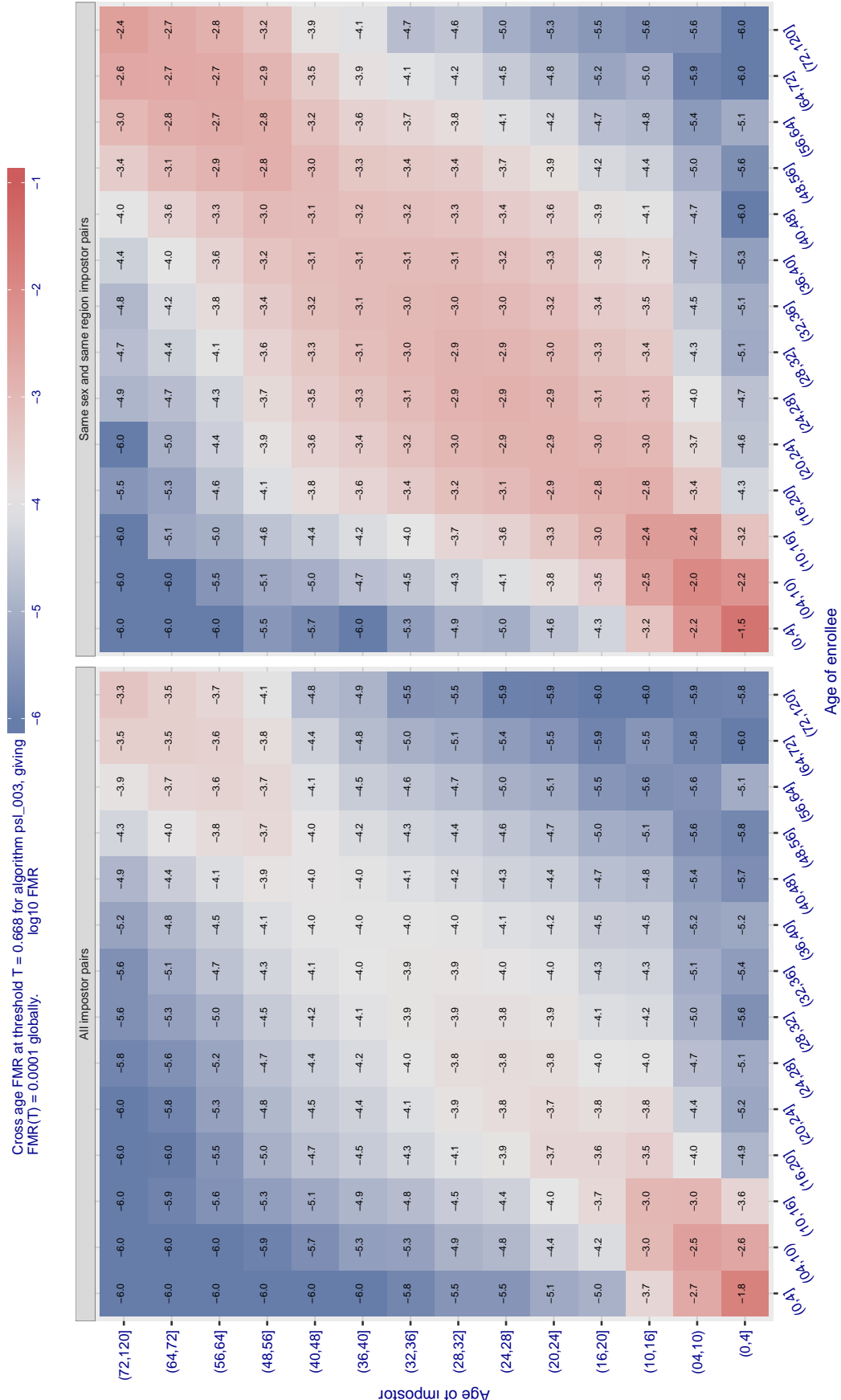


Figure 542: For algorithm psl-003 operating on visa images, the heatmap shows false match observed over impostor comparisons of faces from different individuals who have the given age pair. False matches are counted against a recognition threshold fixed globally to give  $\text{FMR} = 0.0001$  over all on the order of  $10^{10}$  impostor comparisons. The text in each box gives the same quantity as that coded by the color. Light colors present a security vulnerability to, for example, a passport gate.

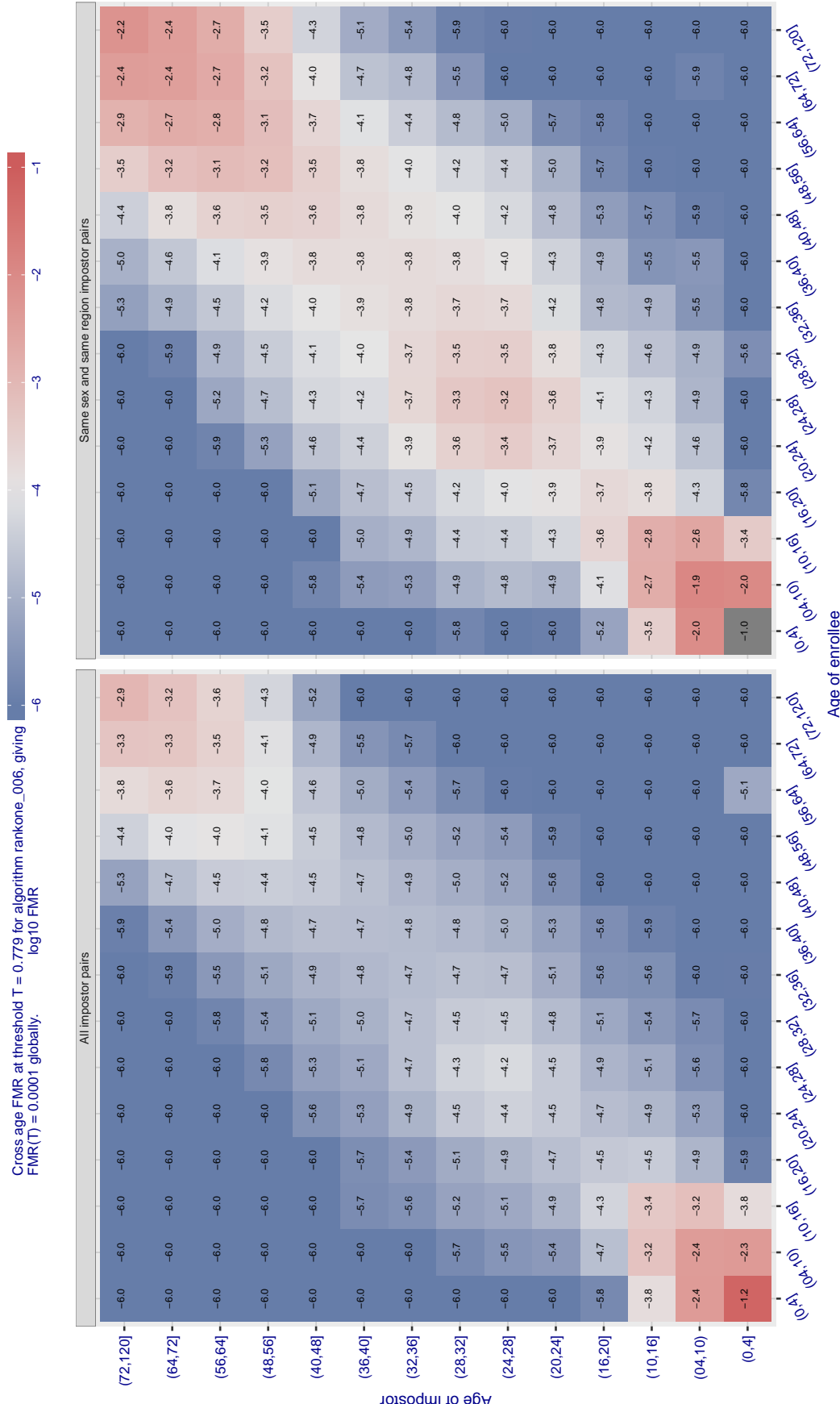


Figure 543: For algorithm rankone-006 operating on visa images, the heatmap shows false match observed over impostor comparisons of faces from different individuals who have the given age pair. False matches are counted against a recognition threshold fixed globally to give  $FMR = 0.0001$  over all on the order of  $10^{10}$  impostor comparisons. The text in each box gives the same quantity as that coded by the color. Light colors present a security vulnerability to, for example, a passport gate.

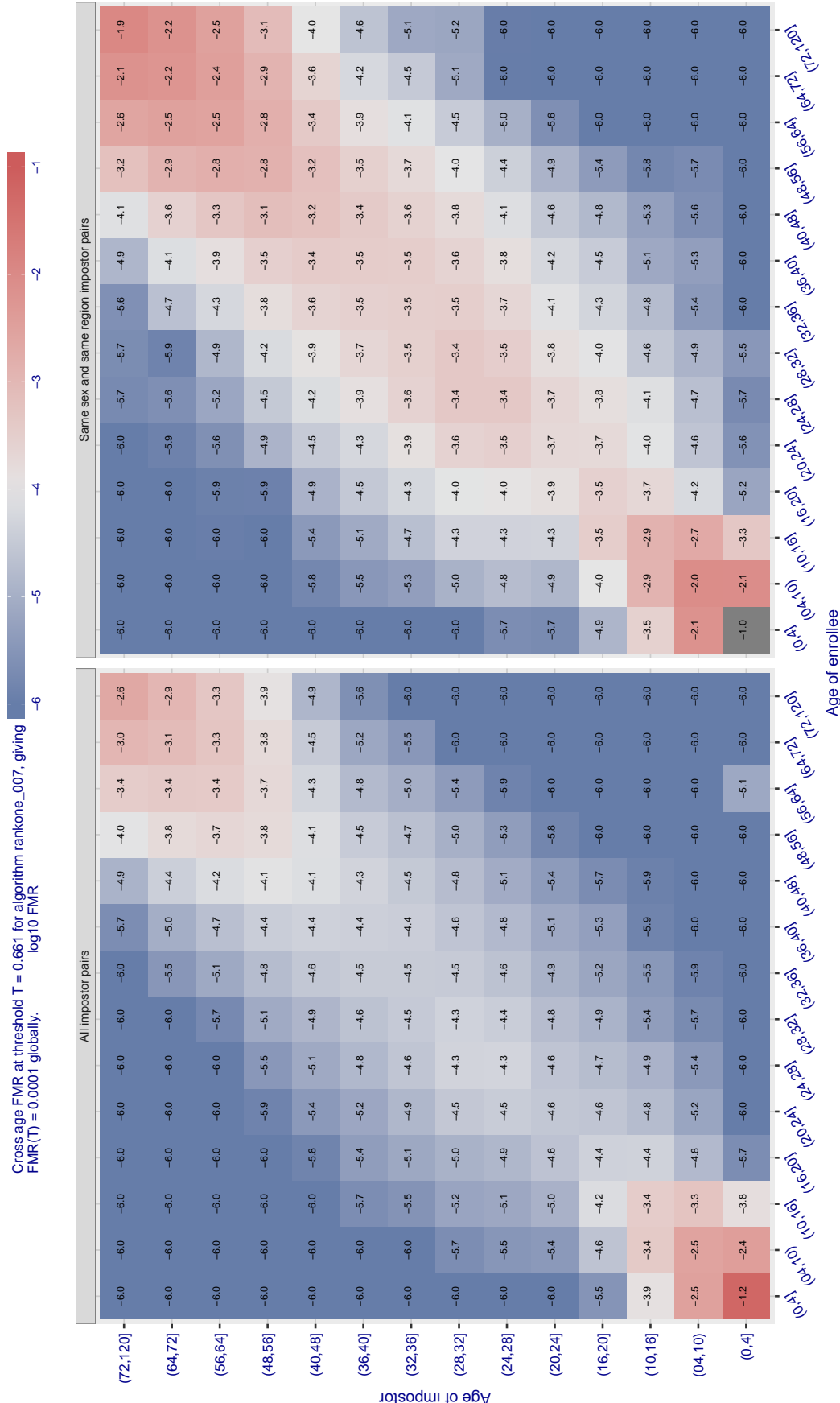


Figure 544: For algorithm rankone-007 operating on visa images, the heatmap shows false match observed over impostor comparisons of faces from different individuals who have the given age pair. False matches are counted against a recognition threshold fixed globally to give  $\text{FMR} = 0.0001$  over all on the order of  $10^{10}$  impostor comparisons. The text in each box gives the same quantity as that coded by the color. Light colors present a security vulnerability to, for example, a passport gate.

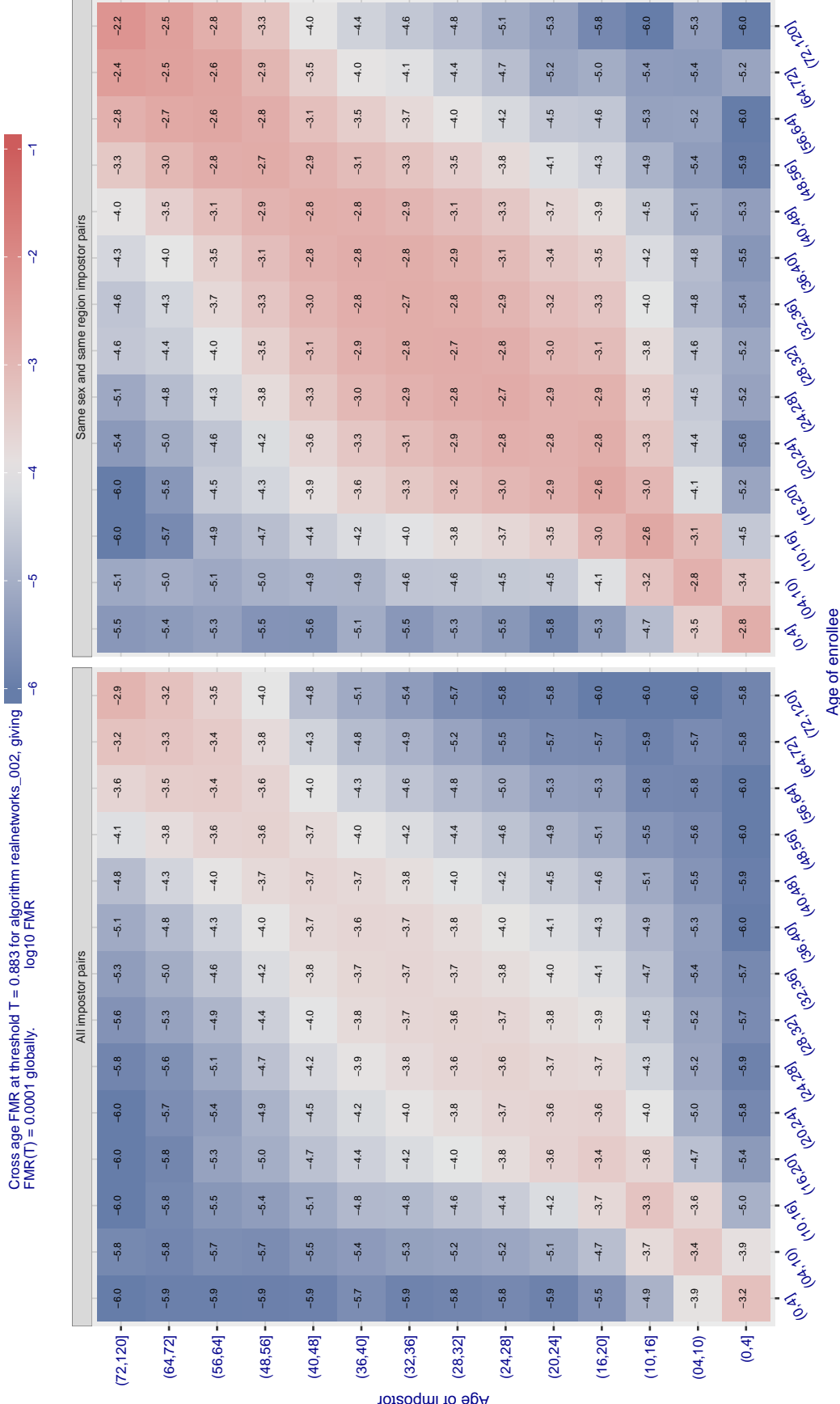


Figure 545: For algorithm reannetworks-002 operating on visa images, the heatmap shows false match observed over impostor comparisons of faces from different individuals who have the given age pair. False matches are counted against a recognition threshold fixed globally to give  $FMR = 0.0001$  over all on the order of  $10^{10}$  impostor comparisons. The text in each box gives the same quantity as that coded by the color. Light colors present a security vulnerability to, for example, a passport gate.

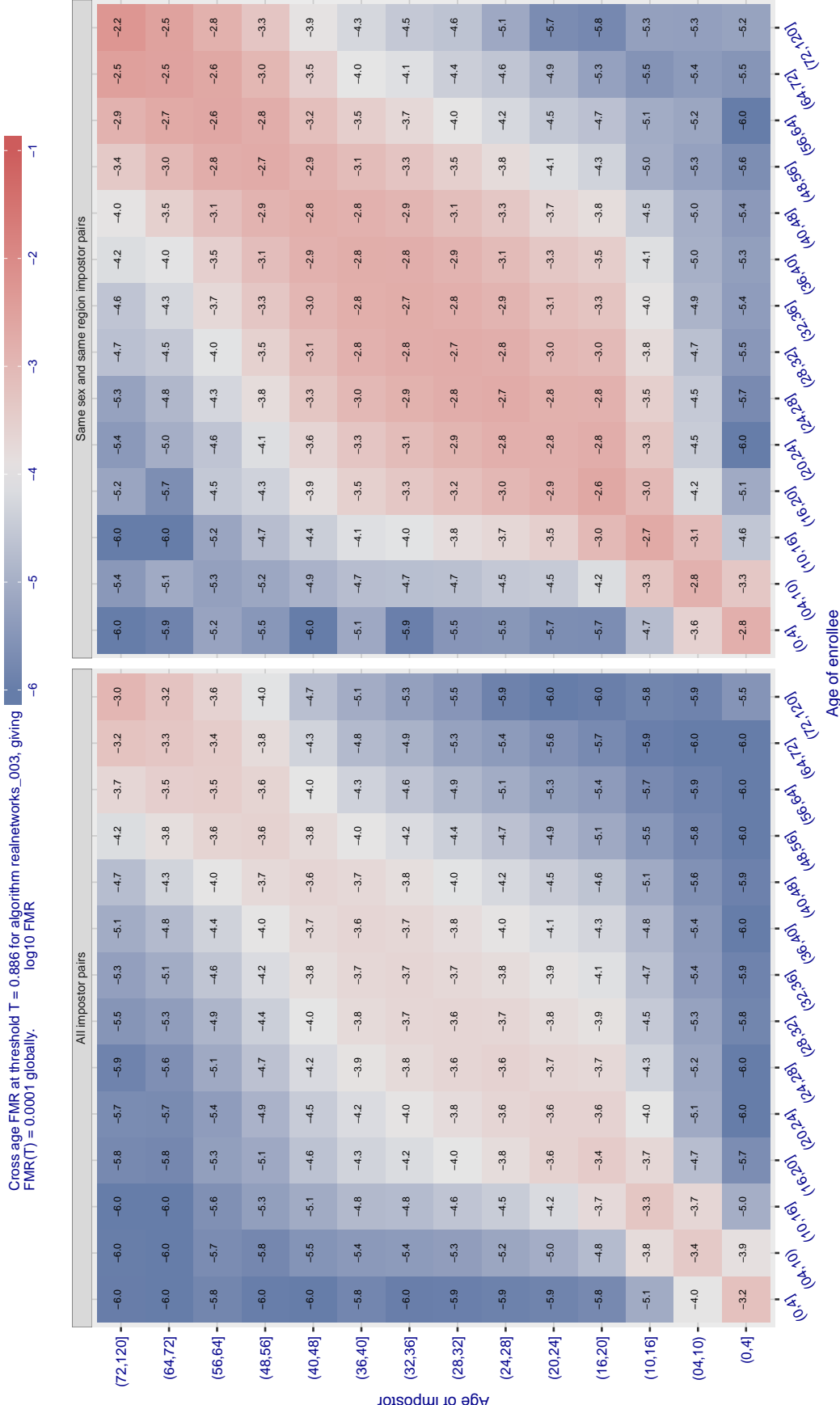


Figure 546: For algorithm realnetworks-003 operating on visa images, the heatmap shows false match observed over impostor comparisons of faces from different individuals who have the given age pair. False matches are counted against a recognition threshold fixed globally to give  $FMR = 0.0001$  over all on the order of  $10^{10}$  impostor comparisons. The text in each box gives the same quantity as that coded by the color. Light colors present a security vulnerability to, for example, a passport gate.

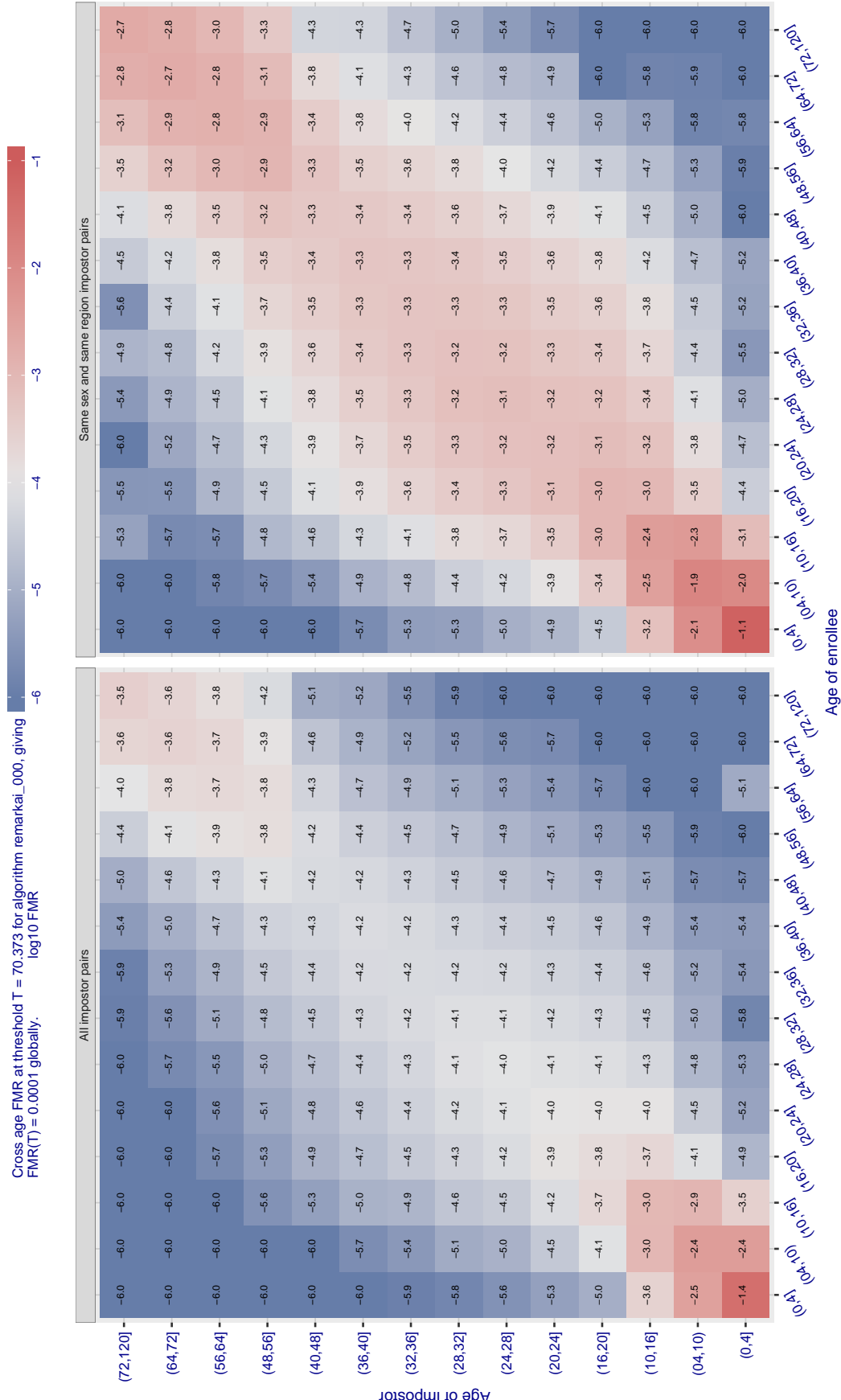


Figure 547: For algorithm remarkai-000 operating on visa images, the heatmap shows false match observed over impostor comparisons of faces from different individuals who have the given age pair. False matches are counted against a recognition threshold fixed globally to give FMR = 0.0001 over all on the order of  $10^{10}$  impostor comparisons. The text in each box gives the same quantity as that coded by the color. Light colors present a security vulnerability to, for example, a passport gate.

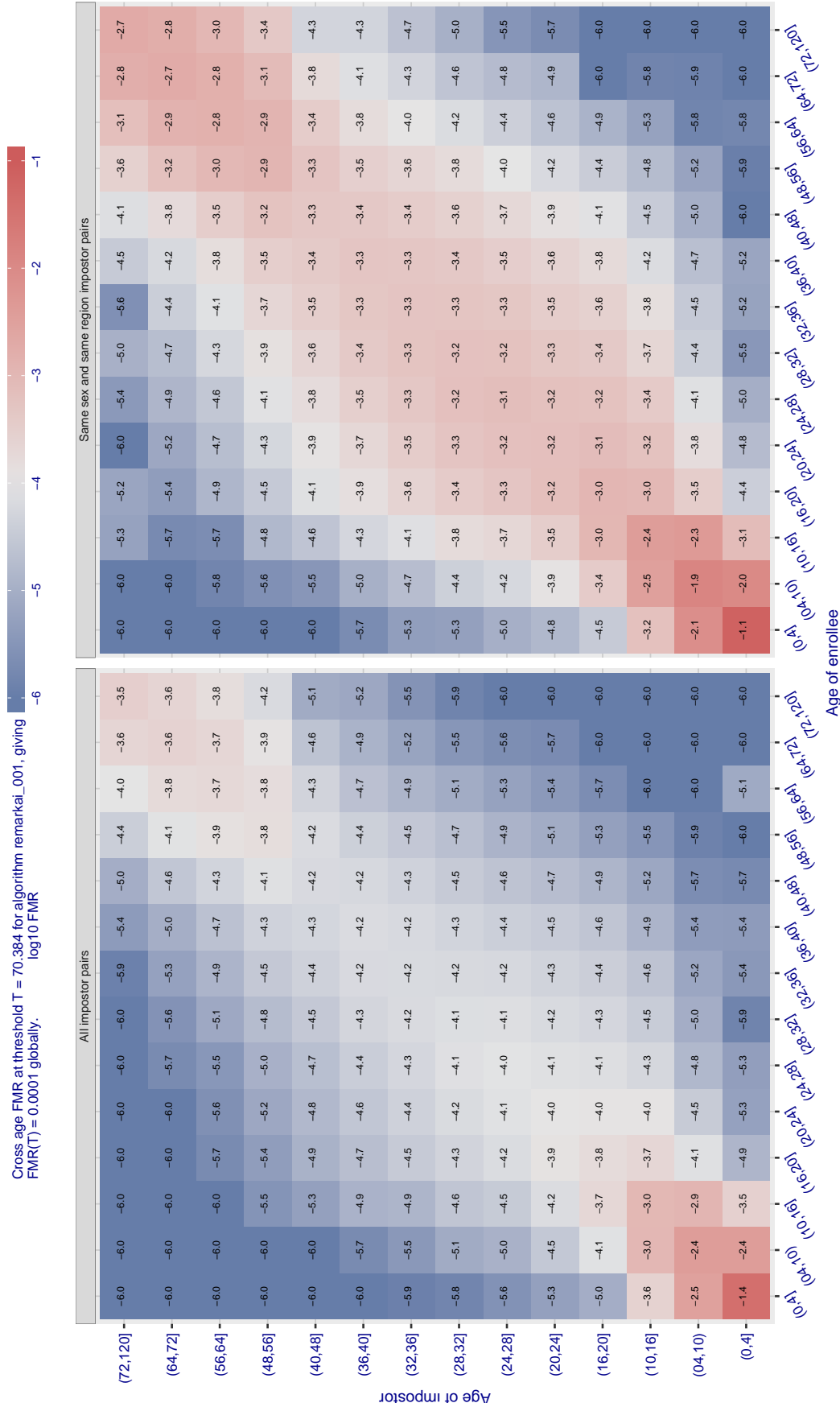


Figure 548: For algorithm remarkai-001 operating on visa images, the heatmap shows false match observed over impostor comparisons of faces from different individuals who have the given age pair. False matches are counted against a recognition threshold fixed globally to give  $FMR = 0.0001$  over all on the order of  $10^{10}$  impostor comparisons. The text in each box gives the same quantity as that coded by the color. Light colors present a security vulnerability to, for example, a passport gate.

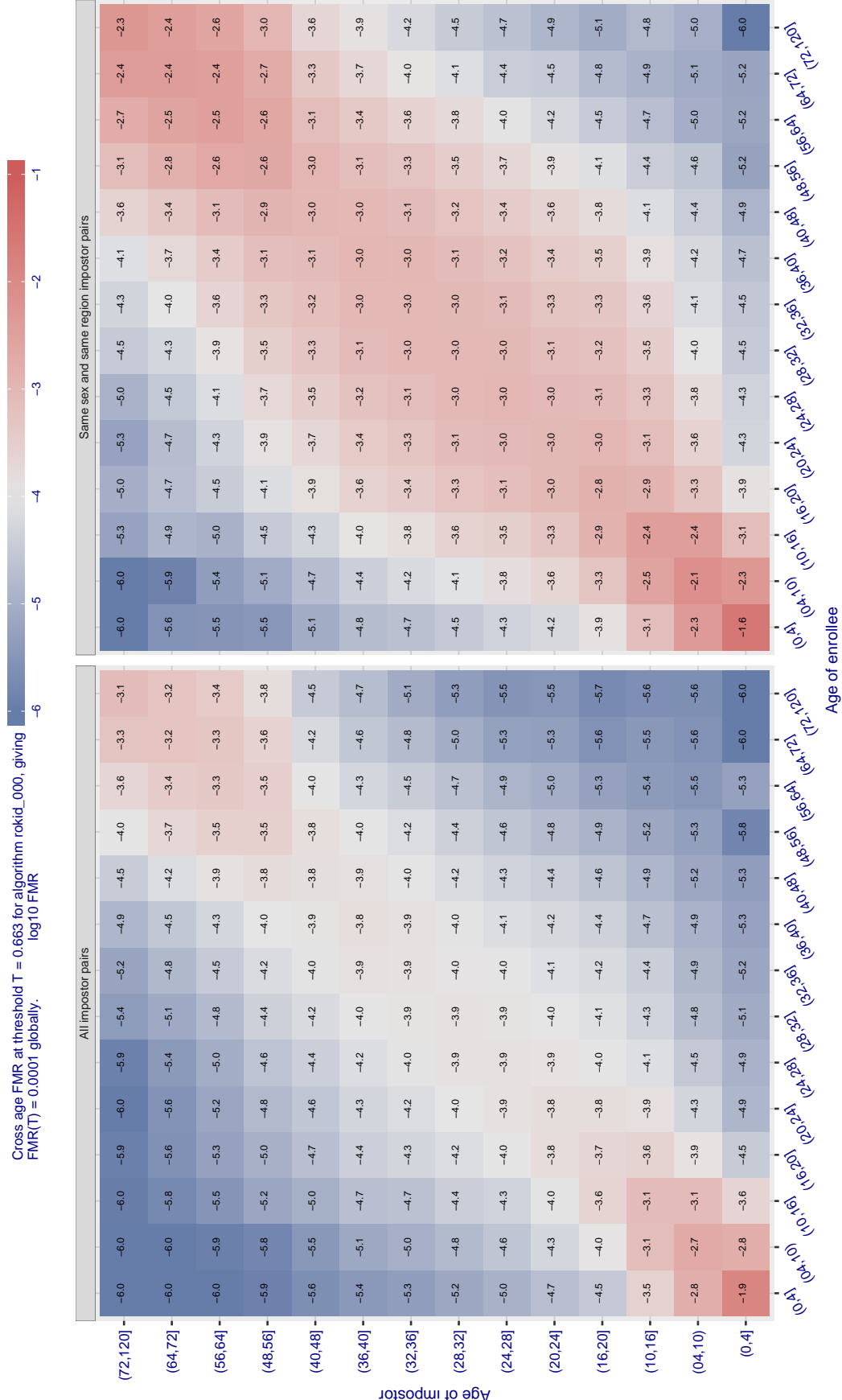


Figure 549: For algorithm rokid-000 operating on visa images, the heatmap shows false match observed over impostor comparisons of faces from different individuals who have the given age pair. False matches are counted against a recognition threshold fixed globally to give FMR = 0.0001 over all on the order of  $10^{10}$  impostor comparisons. The text in each box gives the same quantity as that coded by the color. Light colors present a security vulnerability to, for example, a passport gate.

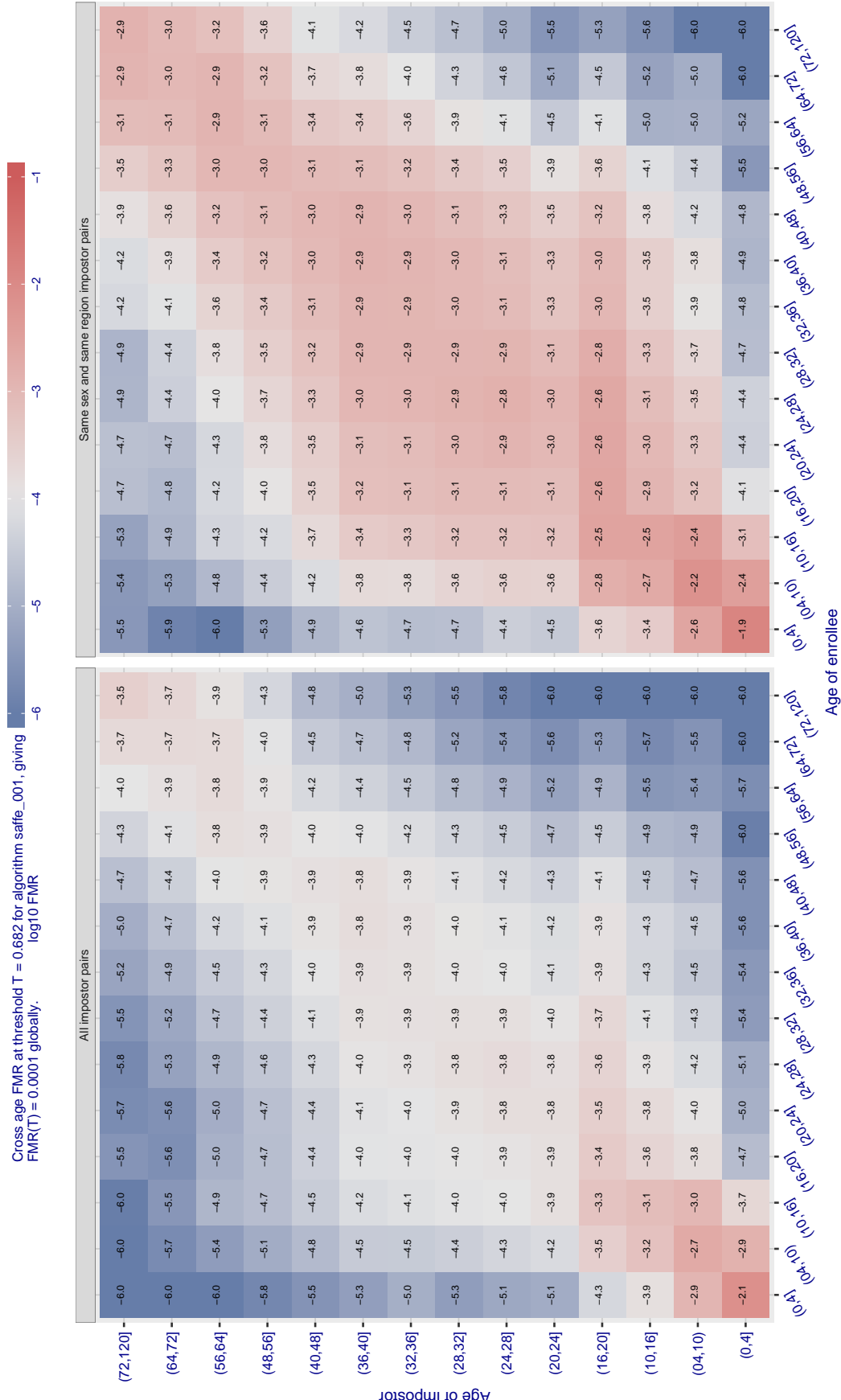


Figure 550: For algorithm saffe\_001 operating on visa images, the heatmap shows false match observed over impostor comparisons of faces from different individuals who have the given age pair. False matches are counted against a recognition threshold fixed globally to give  $FMR = 0.0001$  over all on the order of  $10^{10}$  impostor comparisons. The text in each box gives the same quantity as that coded by the color. Light colors present a security vulnerability to, for example, a passport gate.

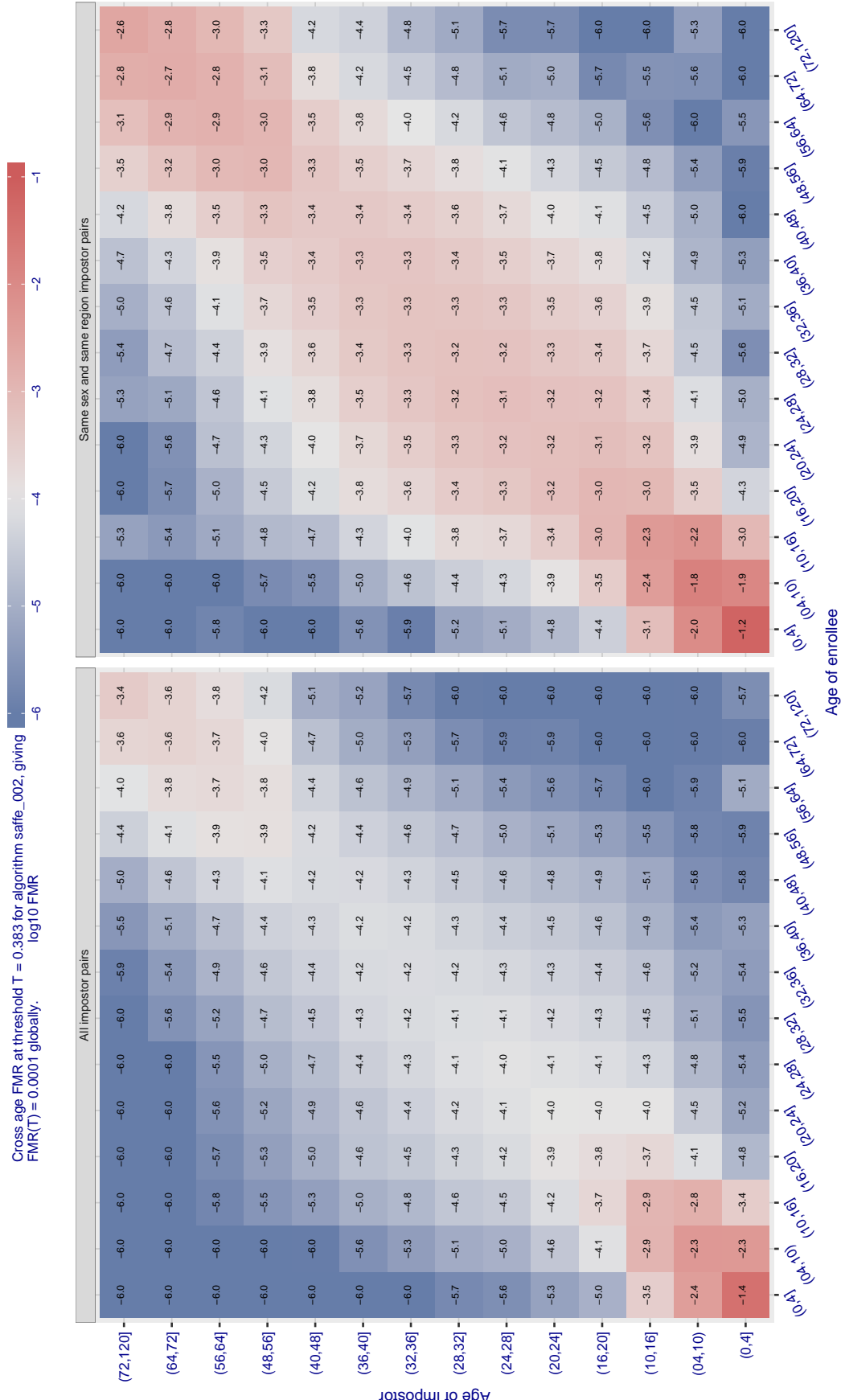


Figure 551: For algorithm saffe\_002 operating on visa images, the heatmap shows false match observed over impostor comparisons of faces from different individuals who have the given age pair. False matches are counted against a recognition threshold fixed globally to give  $FMR = 0.0001$  over all on the order of  $10^{10}$  impostor comparisons. The text in each box gives the same quantity as that coded by the color. Light colors present a security vulnerability to, for example, a passport gate.

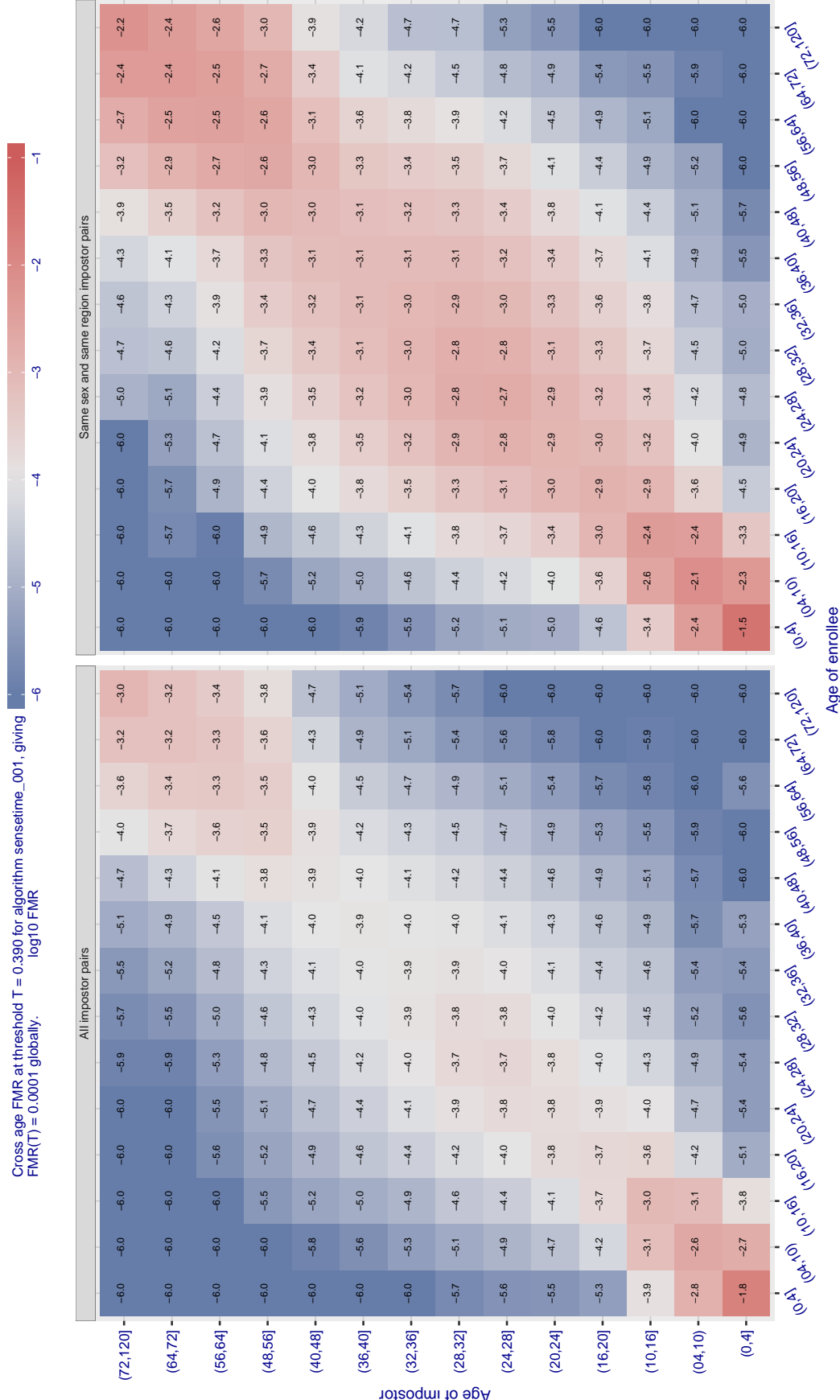


Figure 552: For algorithm sensetime\_001 operating on visa images, the heatmap shows false match observed over impostor comparisons of faces from different individuals who have the given age pair. False matches are counted against a recognition threshold fixed globally to give FMR = 0.001 over all on the order of  $10^{10}$  impostor comparisons. The text in each box gives the same quantity as that coded by the color. Light colors present a security vulnerability to, for example, a passport gate.

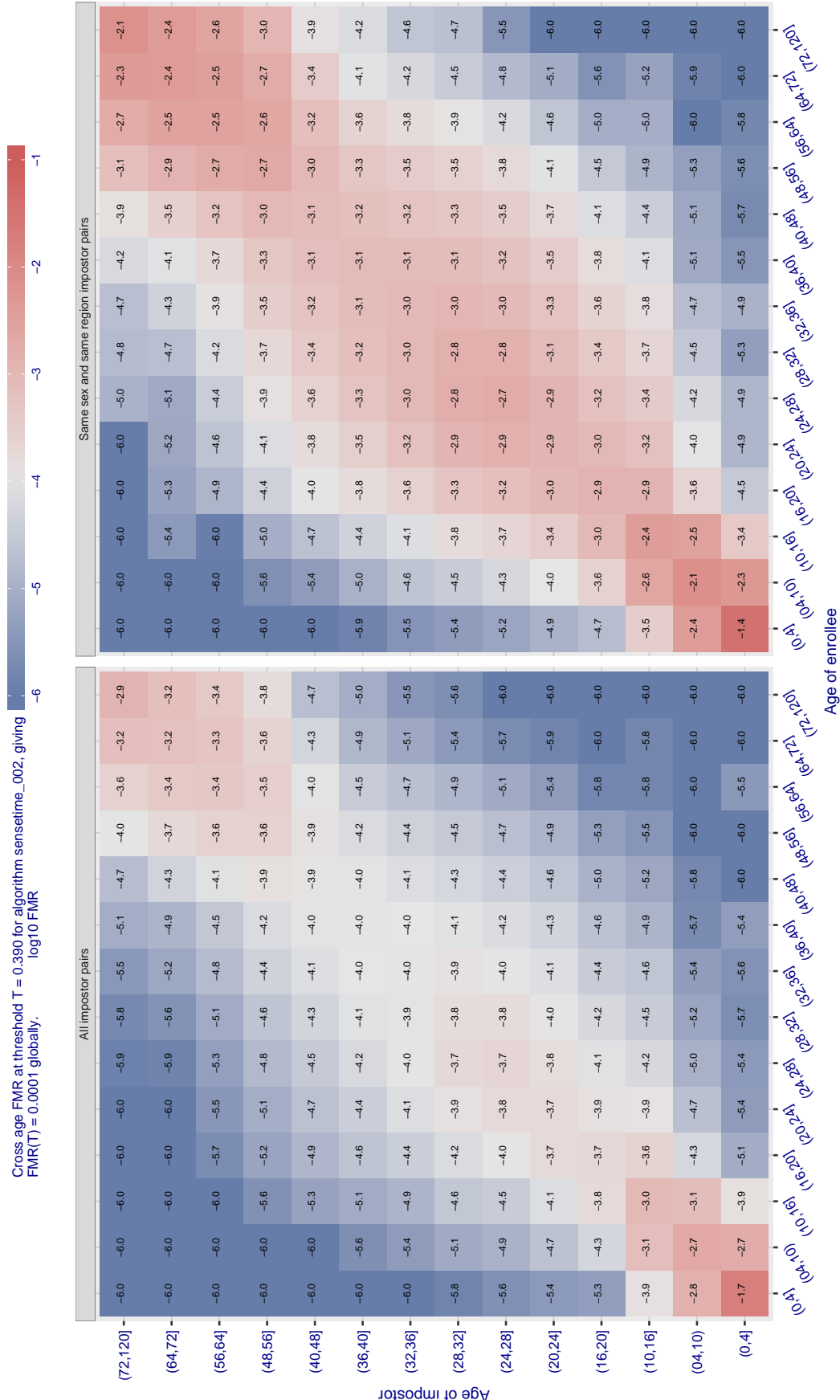


Figure 553: For algorithm sensetime-002 operating on visa images, the heatmap shows false match observed over impostor comparisons of faces from different individuals who have the given age pair. False matches are counted against a recognition threshold fixed globally to give FMR = 0.001 over all on the order of  $10^{10}$  impostor comparisons. The text in each box gives the same quantity as that coded by the color. Light colors present a security vulnerability to, for example, a passport gate.

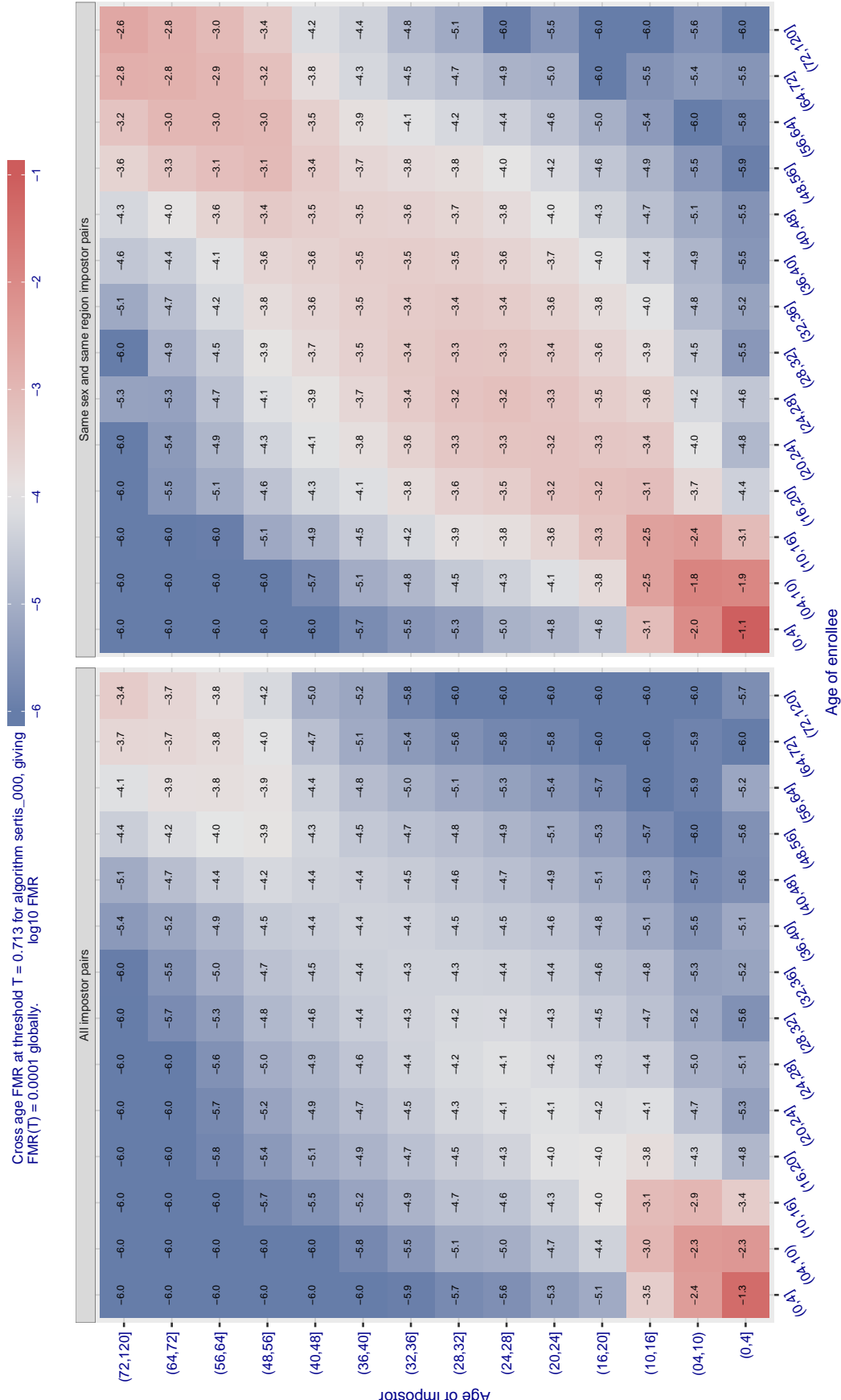


Figure 554: For algorithm sertis\_000 operating on visa images, the heatmap shows false match observed over impostor comparisons of faces from different individuals who have the given age pair. False matches are counted against a recognition threshold fixed globally to give FMR = 0.0001 over all on the order of  $10^{10}$  impostor comparisons. The text in each box gives the same quantity as that coded by the color. Light colors present a security vulnerability to, for example, a passport gate.

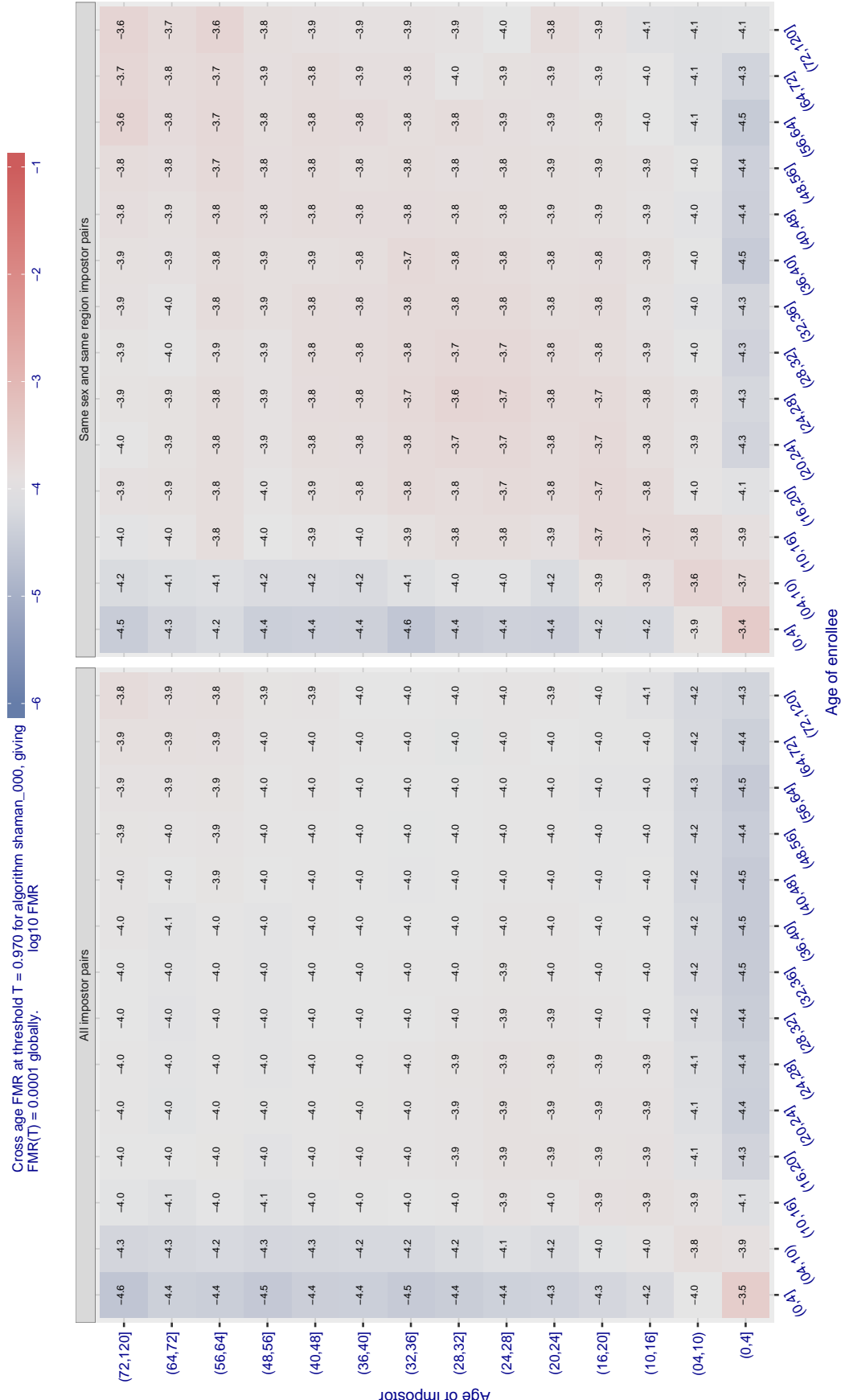


Figure 555: For algorithm shaman-000 operating on visa images, the heatmap shows false match observed over impostor comparisons of faces from different individuals who have the given age pair. False matches are counted against a recognition threshold fixed globally to give  $FMR = 0.0001$  over all on the order of  $10^{10}$  impostor comparisons. The text in each box gives the same quantity as that coded by the color. Light colors present a security vulnerability to, for example, a passport gate.

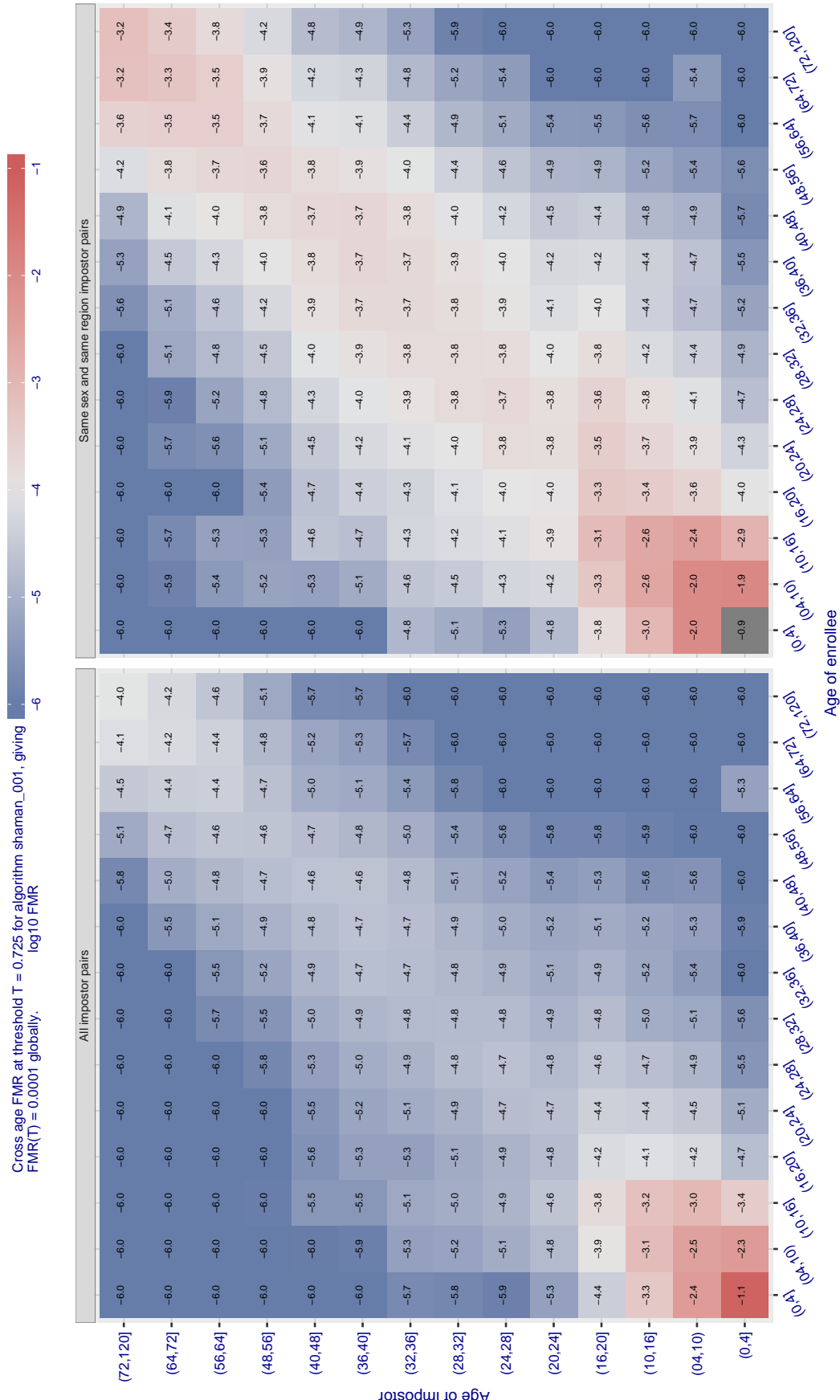


Figure 556: For algorithm shaman-001 operating on visa images, the heatmap shows false match observed over impostor comparisons of faces from different individuals who have the given age pair. False matches are counted against a recognition threshold fixed globally to give  $FMR = 0.0001$  over all on the order of  $10^{10}$  impostor comparisons. The text in each box gives the same quantity as that coded by the color. Light colors present a security vulnerability to, for example, a passport gate.

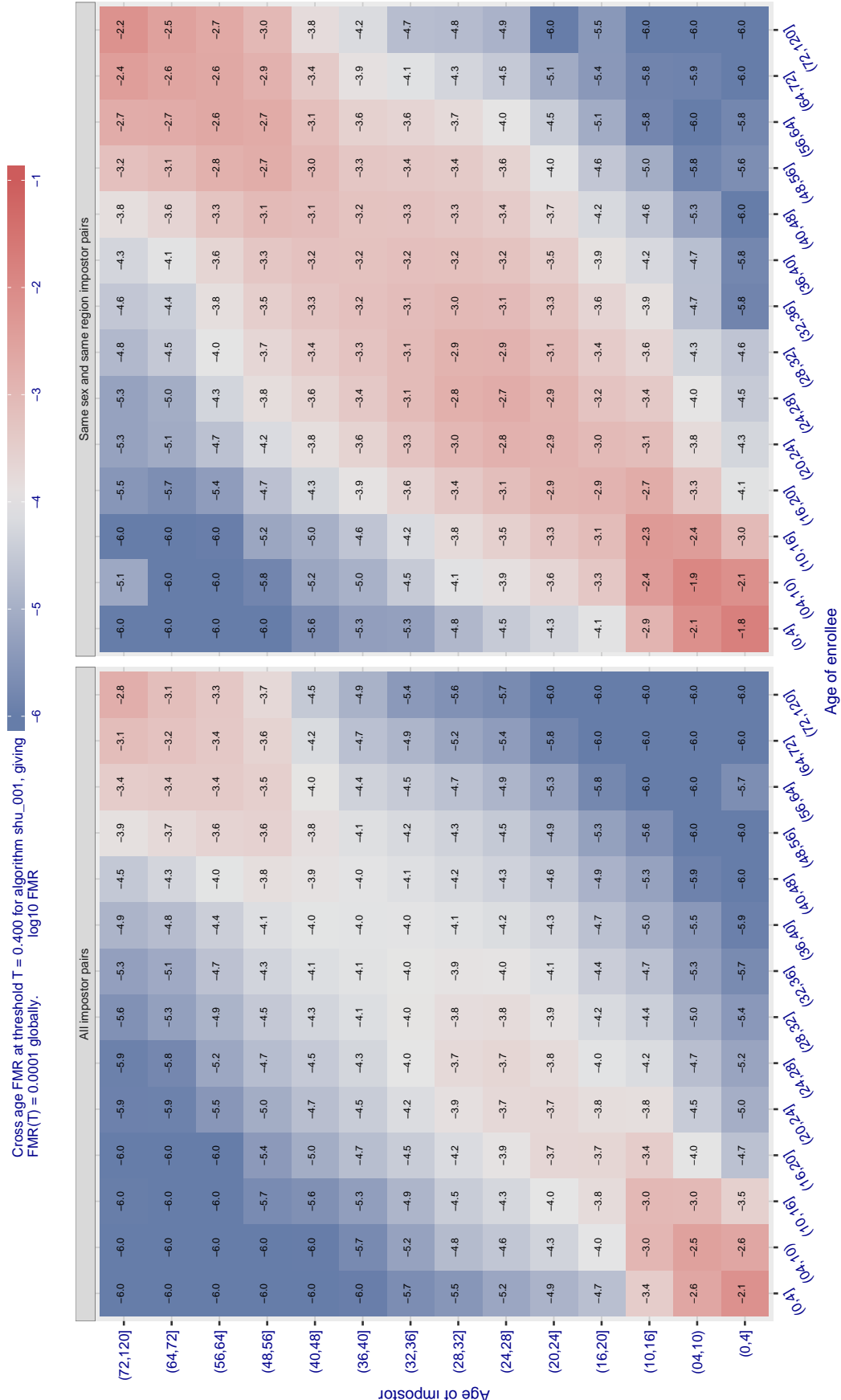


Figure 557: For algorithm shu\_001 operating on visa images, the heatmap shows false match observed over impostor comparisons of faces from different individuals who have the given age pair. False matches are counted against a recognition threshold fixed globally to give  $FMR = 0.0001$  over all on the order of  $10^{10}$  impostor comparisons. The text in each box gives the same quantity as that coded by the color. Light colors present a security vulnerability to, for example, a passport gate.

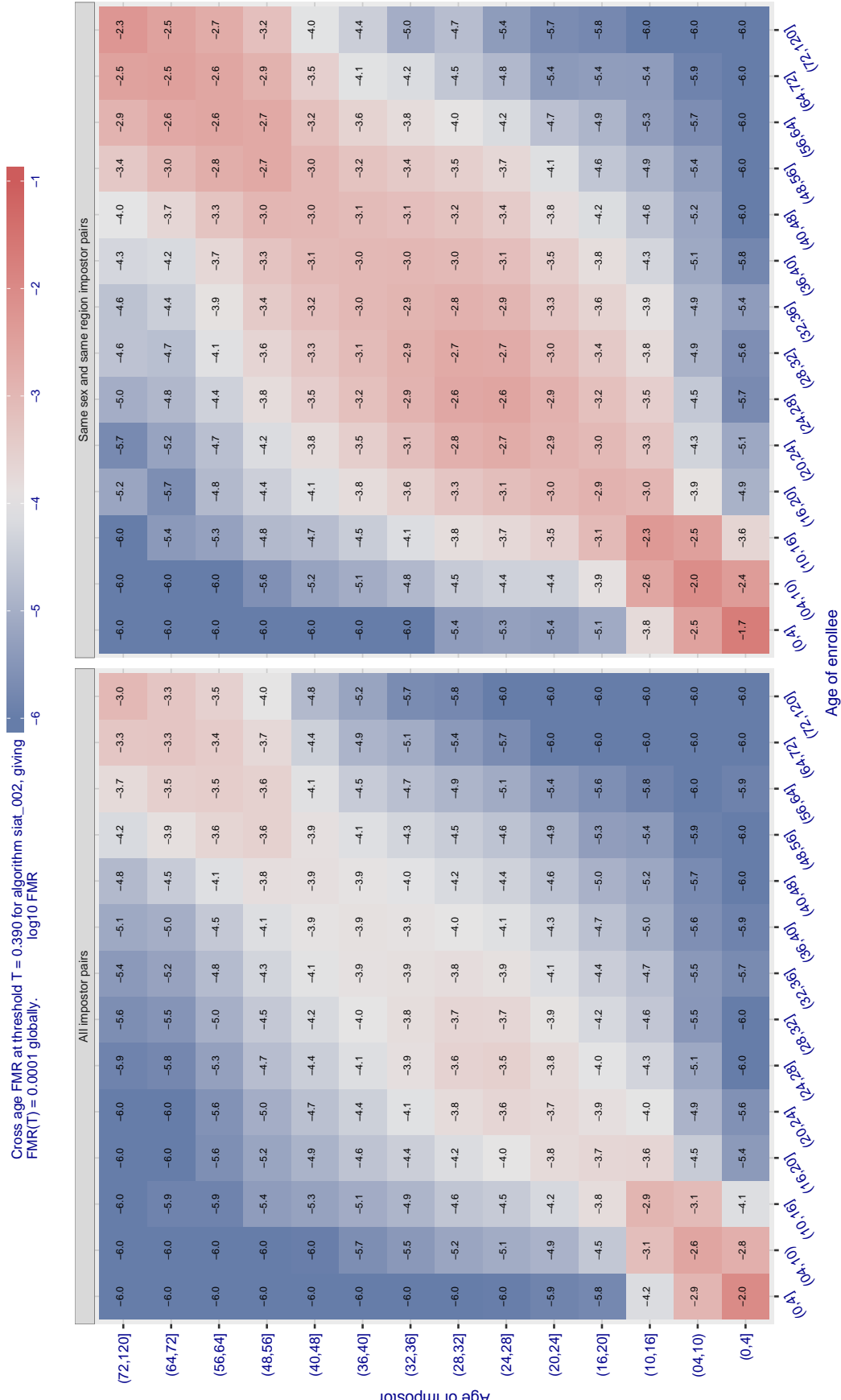


Figure 558: For algorithm siat\_002 operating on visa images, the heatmap shows false match observed over impostor comparisons of faces from different individuals who have the given age pair. False matches are counted against a recognition threshold fixed globally to give FMR = 0.0001 over all on the order of  $10^{10}$  impostor comparisons. The text in each box gives the same quantity as that coded by the color. Light colors present a security vulnerability to, for example, a passport gate.

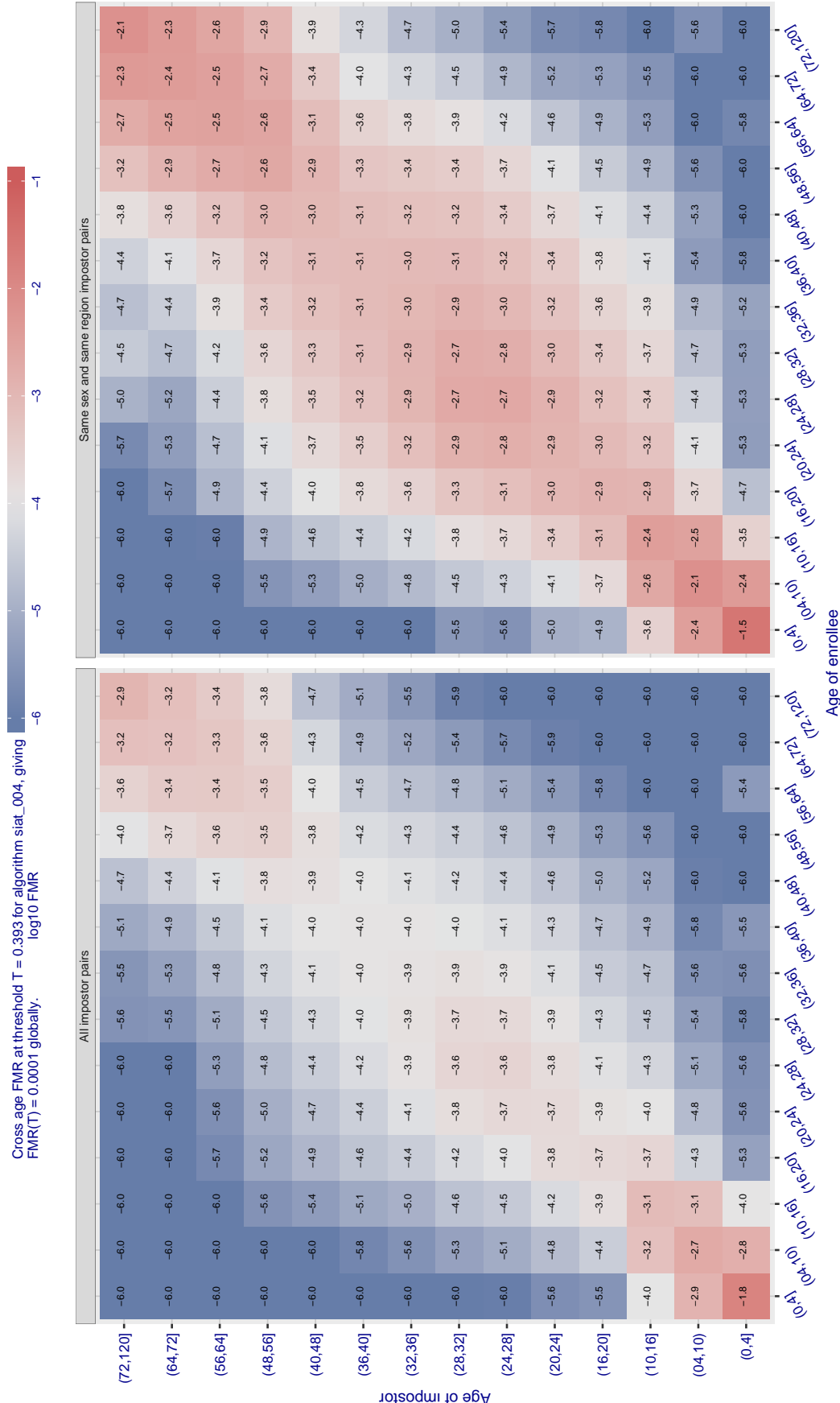


Figure 559: For algorithm siat-004 operating on visa images, the heatmap shows false match observed over impostor comparisons of faces from different individuals who have the given age pair. False matches are counted against a recognition threshold fixed globally to give FMR = 0.0001 over all on the order of  $10^{10}$  impostor comparisons. The text in each box gives the same quantity as that coded by the color. Light colors present a security vulnerability to, for example, a passport gate.

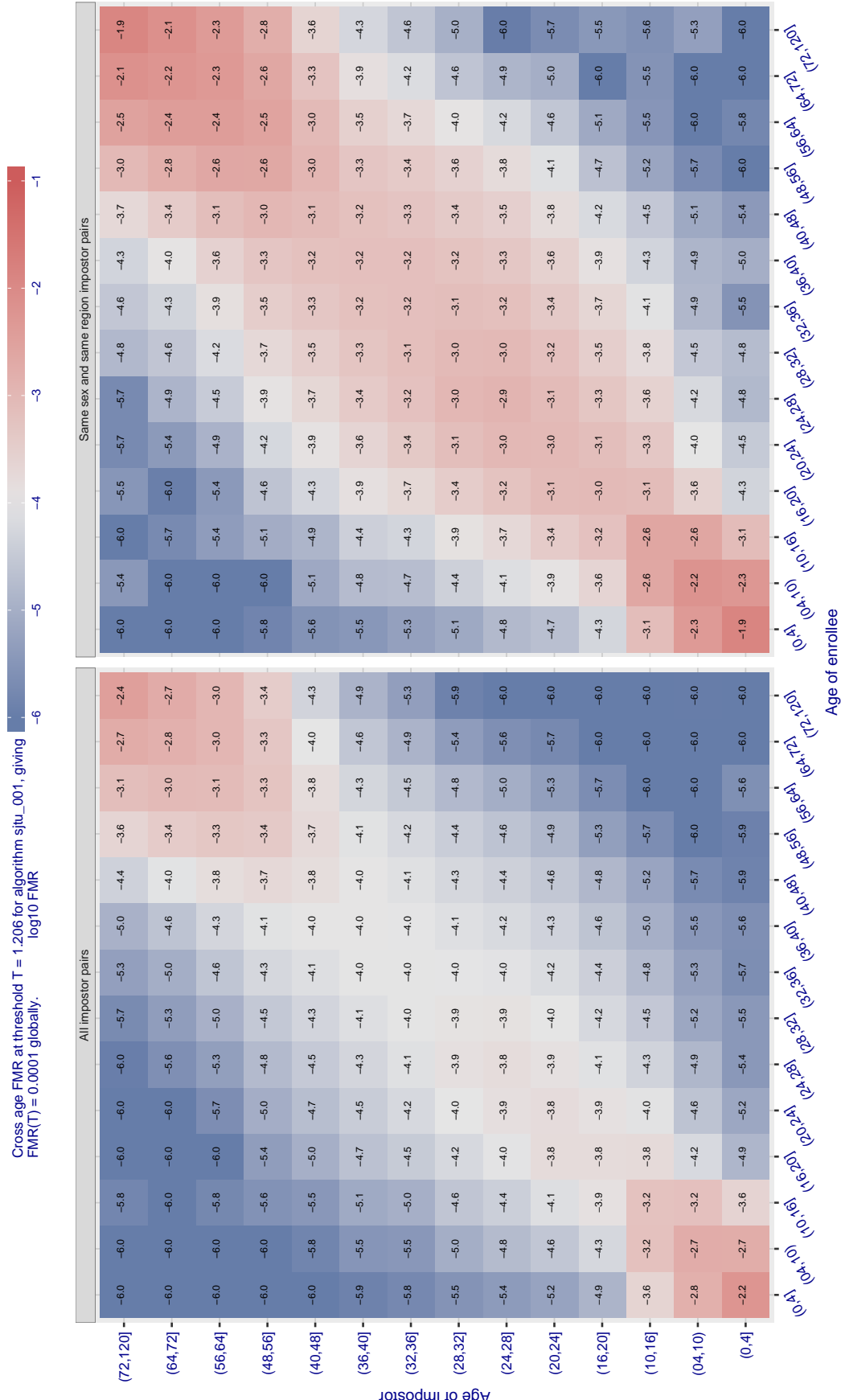


Figure 560: For algorithm situ\_001 operating on visa images, the heatmap shows false match observed over impostor comparisons of faces from different individuals who have the given age pair. False matches are counted against a recognition threshold fixed globally to give  $FMR = 0.0001$  over all on the order of  $10^{10}$  impostor comparisons. The text in each box gives the same quantity as that coded by the color. Light colors present a security vulnerability to, for example, a passport gate.

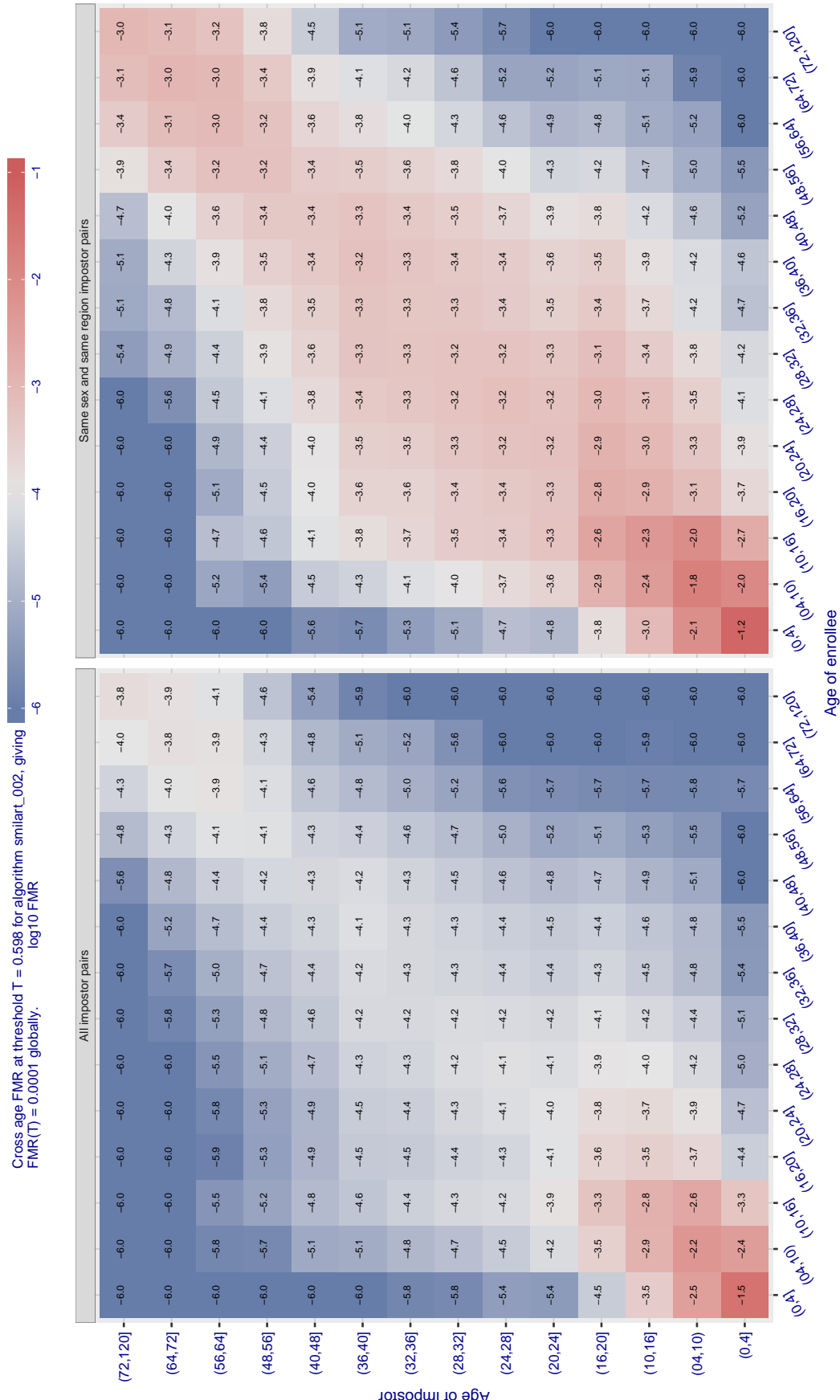


Figure 561: For algorithm smillart-002 operating on visa images, the heatmap shows false match observed over impostor comparisons of faces from different individuals who have the given age pair. False matches are counted against a recognition threshold fixed globally to give  $FMR = 0.0001$  over all on the order of  $10^{10}$  impostor comparisons. The text in each box gives the same quantity as that coded by the color. Light colors present a security vulnerability to, for example, a passport gate.

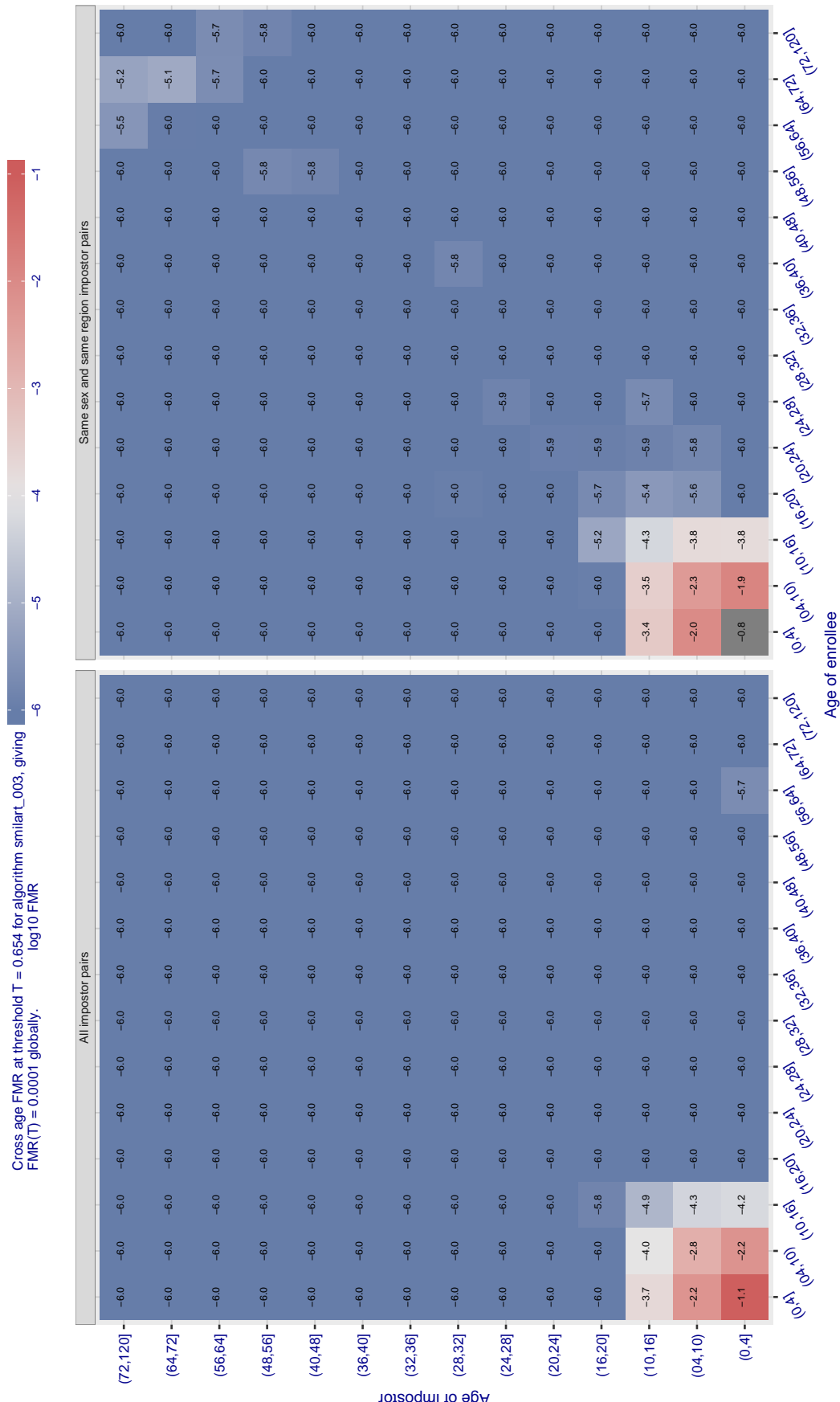


Figure 562: For algorithm smillart-003 operating on visa images, the heatmap shows false match observed over impostor comparisons of faces from different individuals who have the given age pair. False matches are counted against a recognition threshold fixed globally to give  $FMR = 0.0001$  over all on the order of  $10^{10}$  impostor comparisons. The text in each box gives the same quantity as that coded by the color. Light colors present a security vulnerability to, for example, a passport gate.

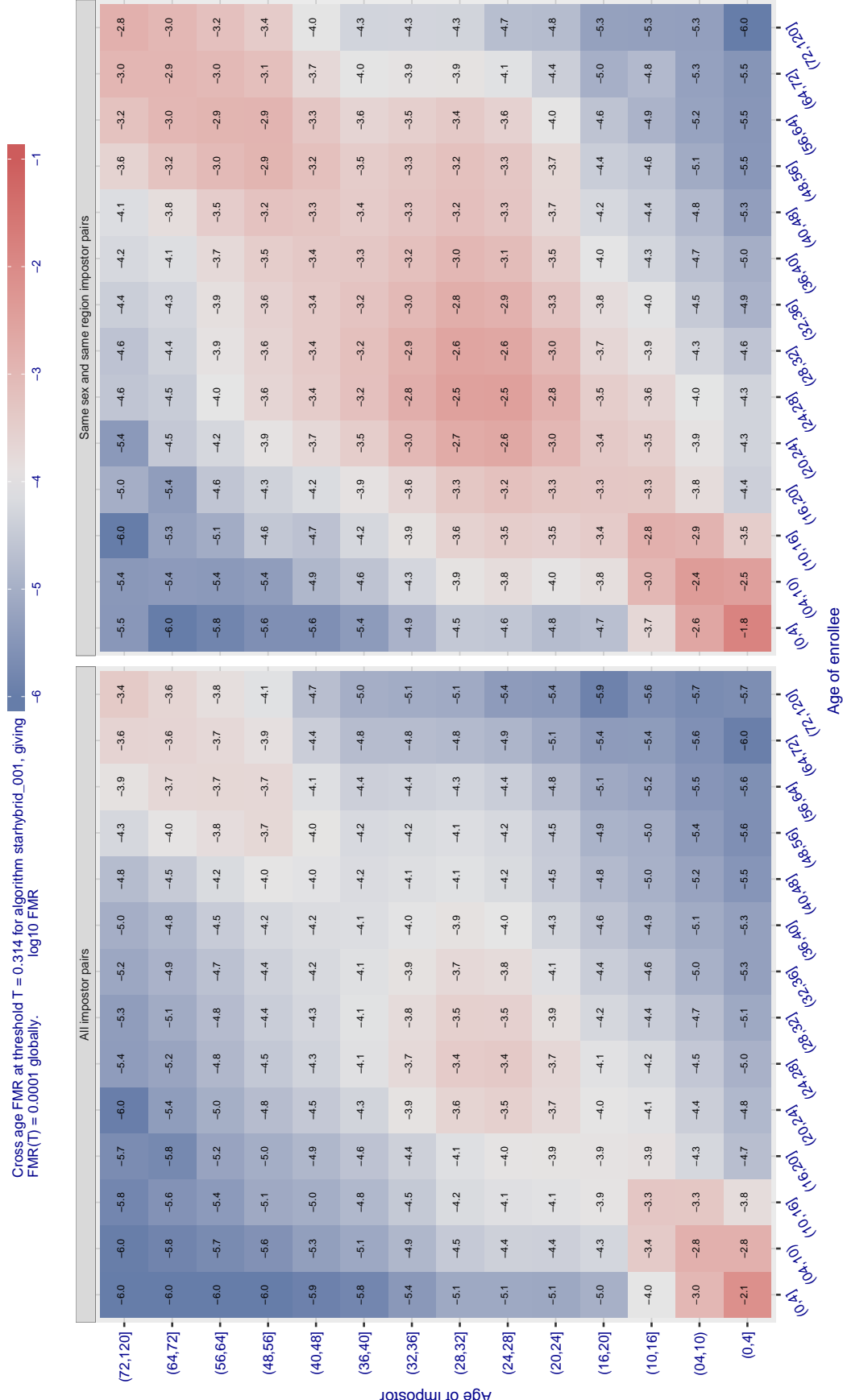


Figure 563: For algorithm starhybrid-001 operating on visa images, the heatmap shows false match observed over impostor comparisons of faces from different individuals who have the given age pair. False matches are counted against a recognition threshold fixed globally to give  $FMR = 0.001$  over all on the order of  $10^{10}$  impostor comparisons. The text in each box gives the same quantity as that coded by the color. Light colors present a security vulnerability to, for example, a passport gate.

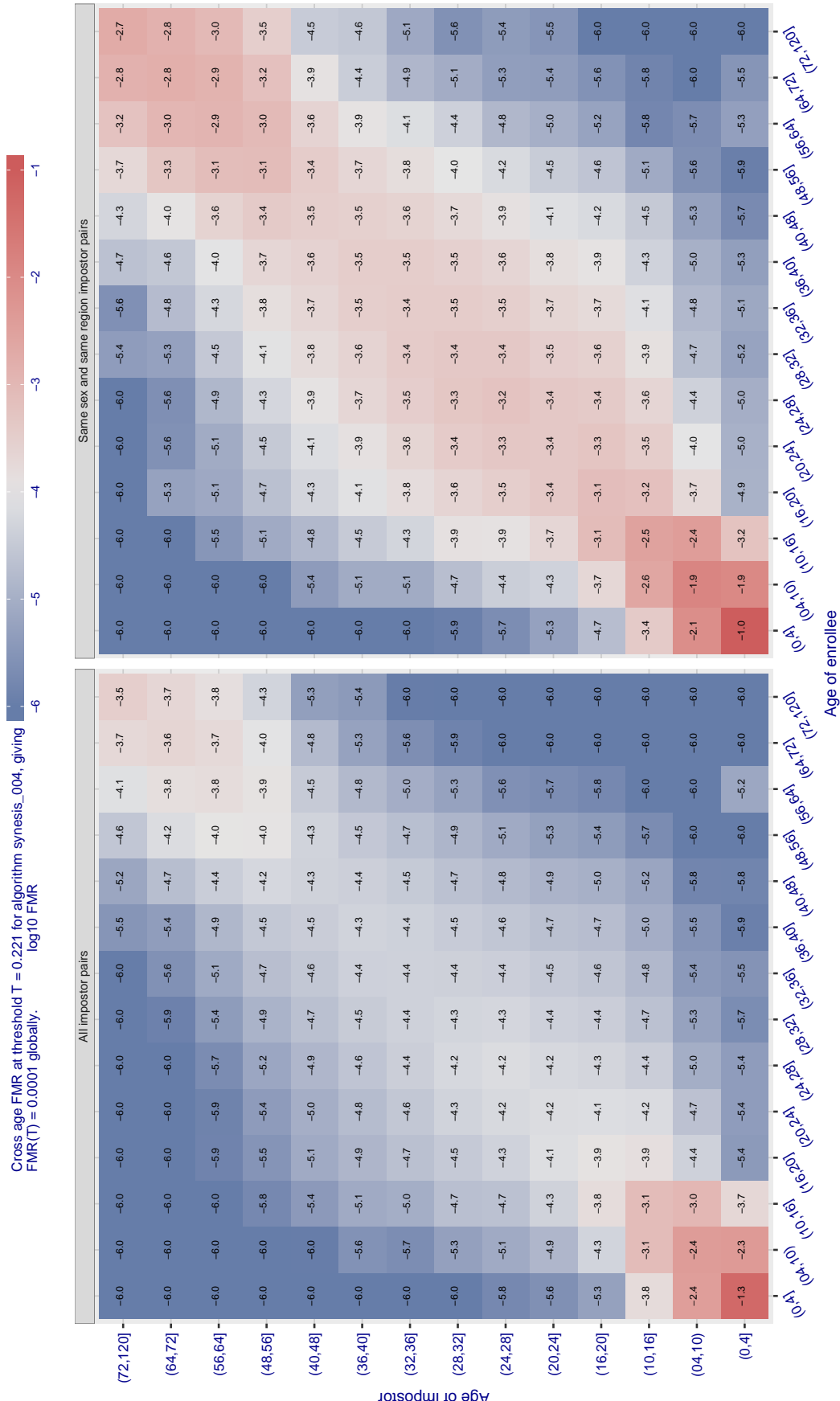


Figure 564: For algorithm synthesis-004 operating on visa images, the heatmap shows false match observed over impostor comparisons of faces from different individuals who have the given age pair. False matches are counted against a recognition threshold fixed globally to give  $\text{FMR} = 0.0001$  over all on the order of  $10^{10}$  impostor comparisons. The text in each box gives the same quantity as that coded by the color. Light colors present a security vulnerability to, for example, a passport gate.

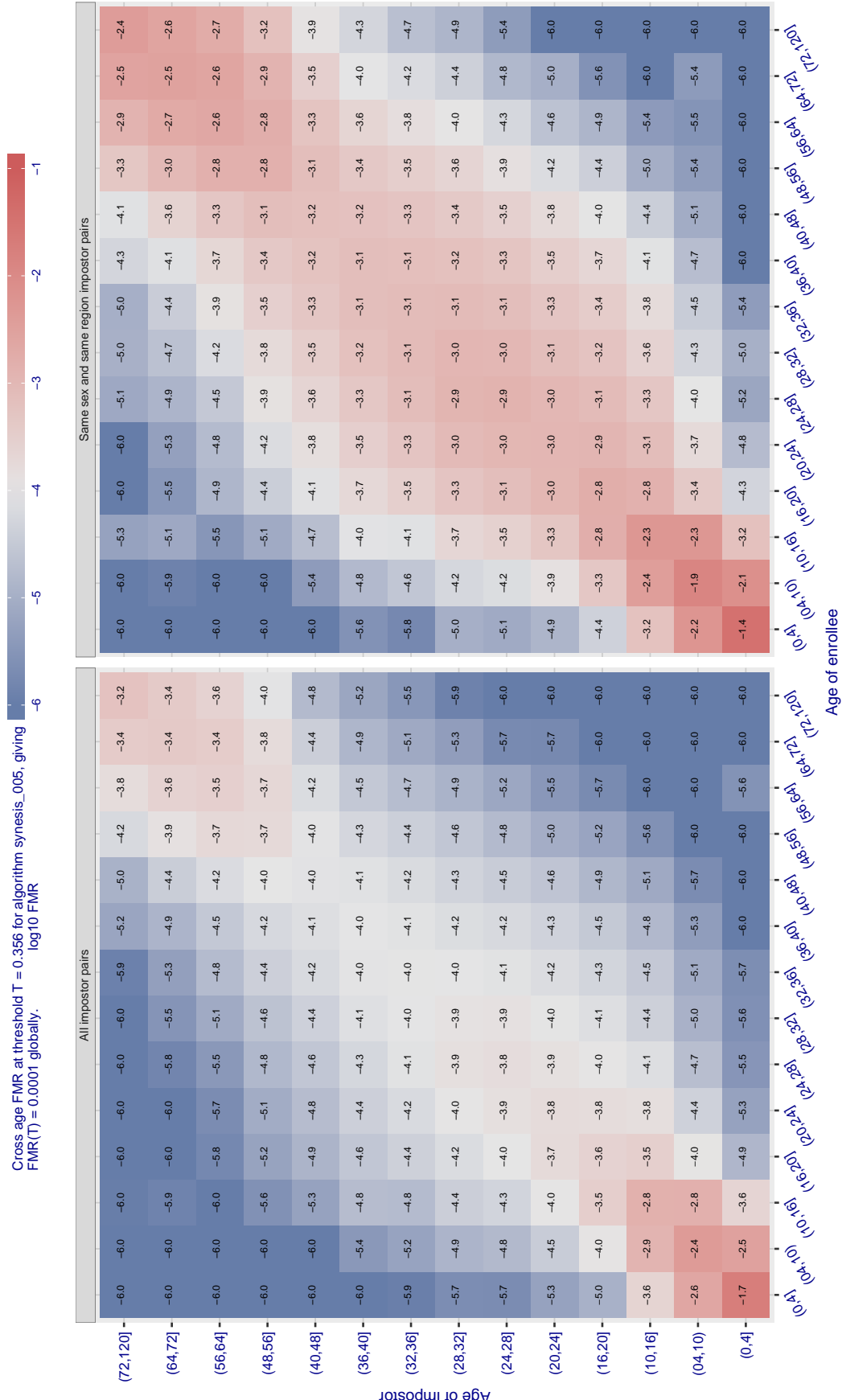


Figure 565: For algorithm synthesis\_005 operating on visa images, the heatmap shows false match observed over impostor comparisons of faces from different individuals who have the given age pair. False matches are counted against a recognition threshold fixed globally to give  $FMR = 0.0001$  over all on the order of  $10^{10}$  impostor comparisons. The text in each box gives the same quantity as that coded by the color. Light colors present a security vulnerability to, for example, a passport gate.

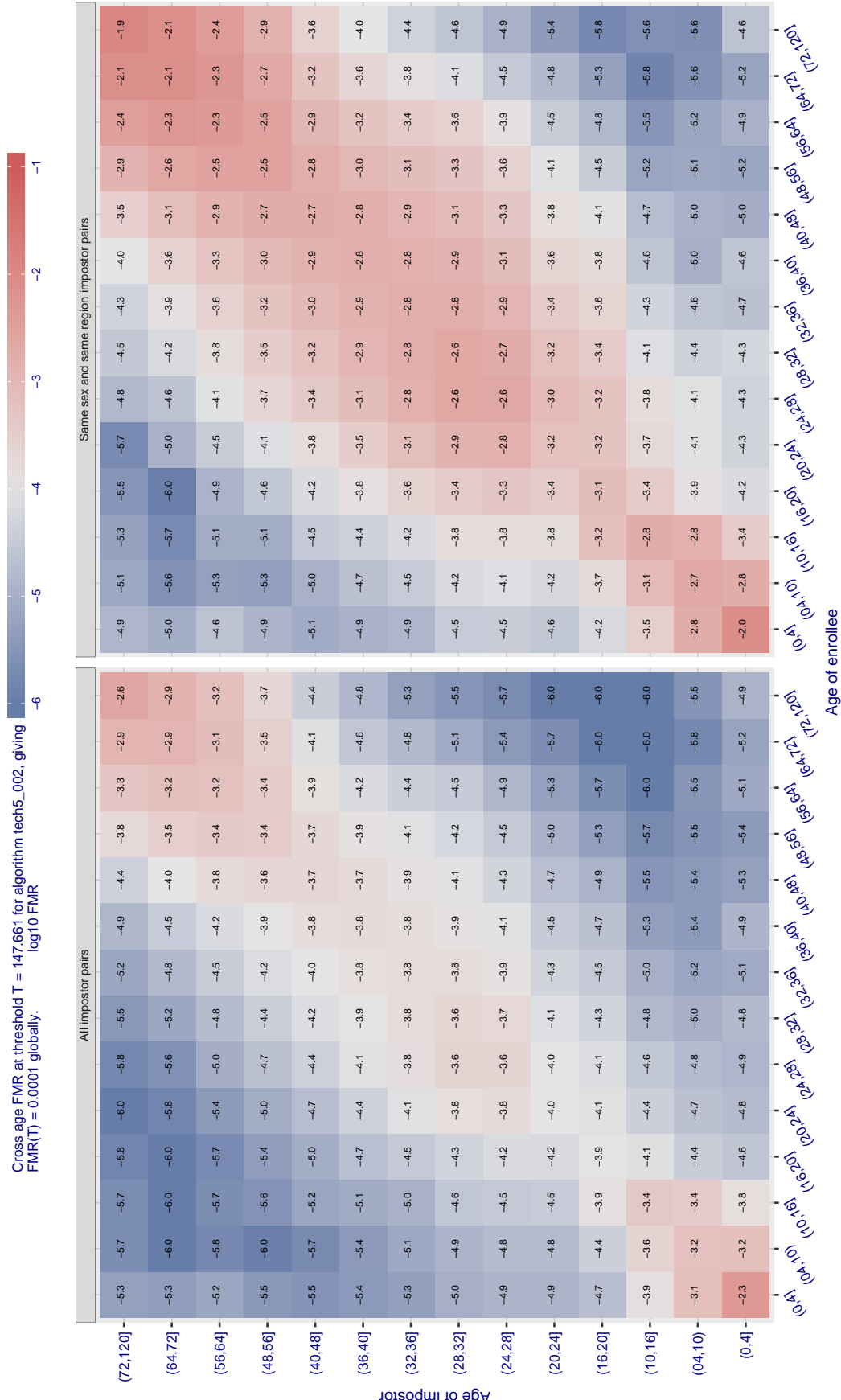


Figure 566: For algorithm tech5-002 operating on visa images, the heatmap shows false match observed over impostor comparisons of faces from different individuals who have the given age pair. False matches are counted against a recognition threshold fixed globally to give  $FMR = 0.0001$  over all on the order of  $10^{10}$  impostor comparisons. The text in each box gives the same quantity as that coded by the color. Light colors present a security vulnerability to, for example, a passport gate.

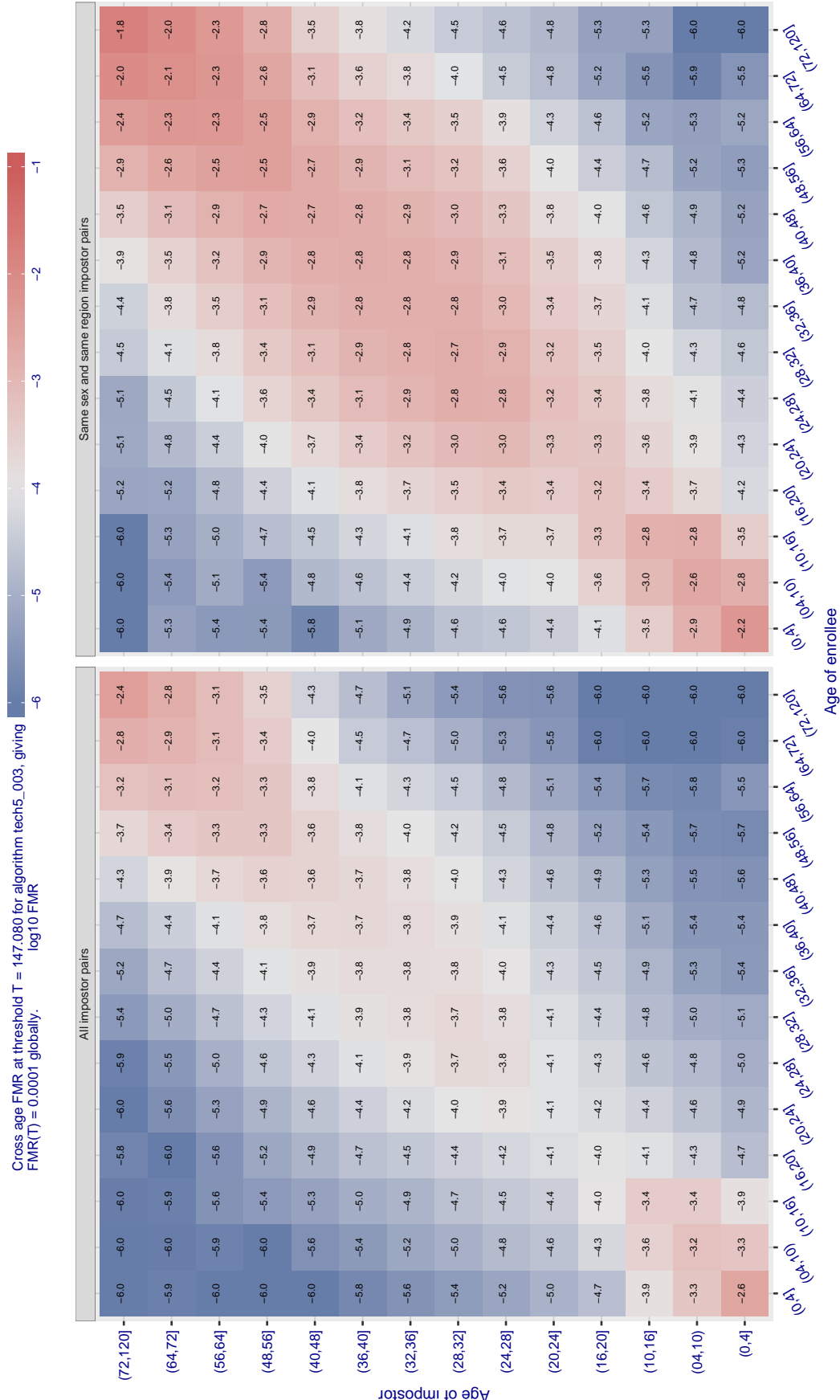


Figure 567: For algorithm tech5-003 operating on visa images, the heatmap shows false match observed over impostor comparisons of faces from different individuals who have the given age pair. False matches are counted against a recognition threshold fixed globally to give  $FMR = 0.0001$  over all on the order of  $10^{10}$  impostor comparisons. The text in each box gives the same quantity as that coded by the color. Light colors present a security vulnerability to, for example, a passport gate.

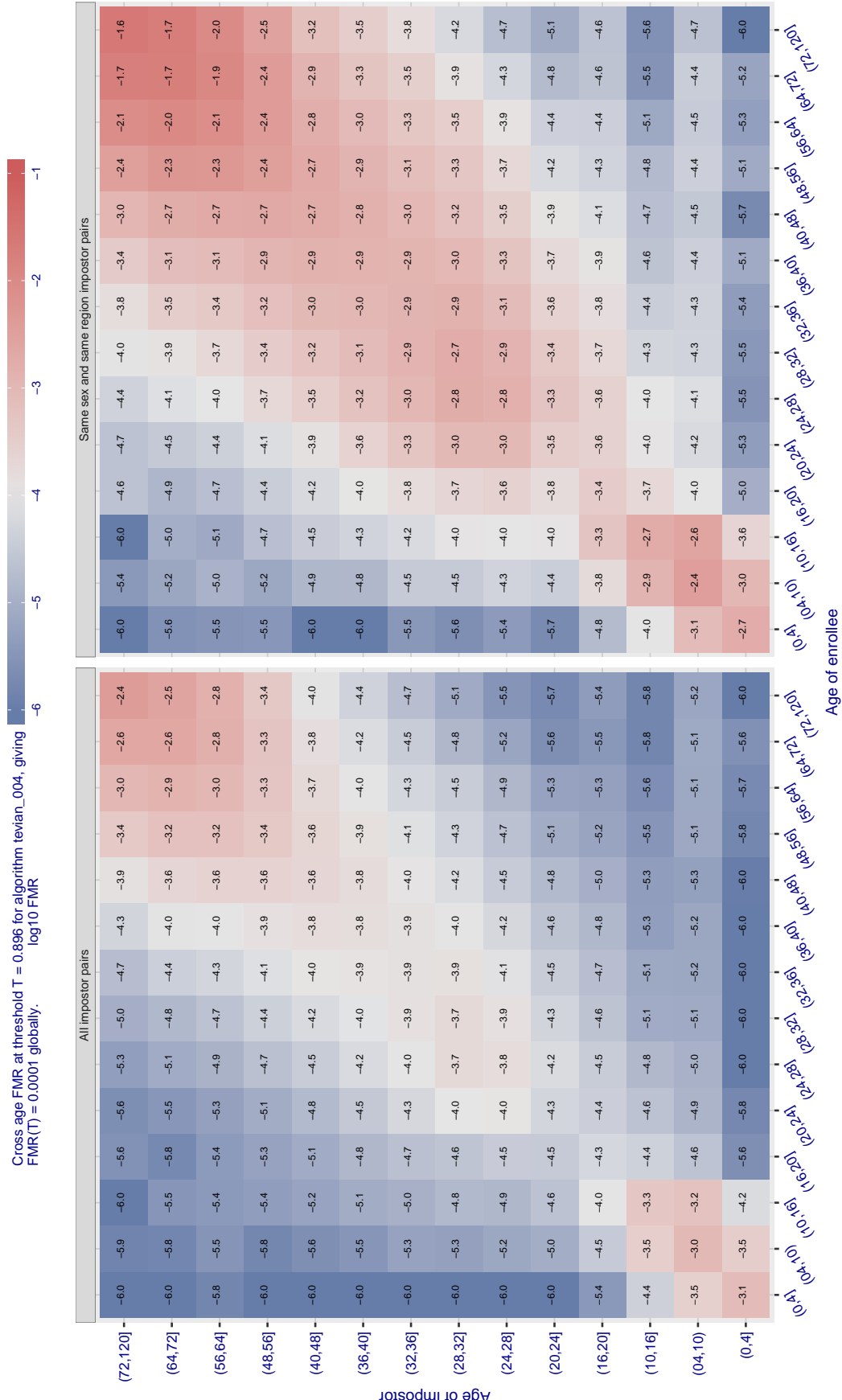


Figure 568: For algorithm tevian-004 operating on visa images, the heatmap shows false match observed over impostor comparisons of faces from different individuals who have the given age pair. False matches are counted against a recognition threshold fixed globally to give FMR = 0.0001 over all on the order of  $10^{10}$  impostor comparisons. The text in each box gives the same quantity as that coded by the color. Light colors present a security vulnerability to, for example, a passport gate.

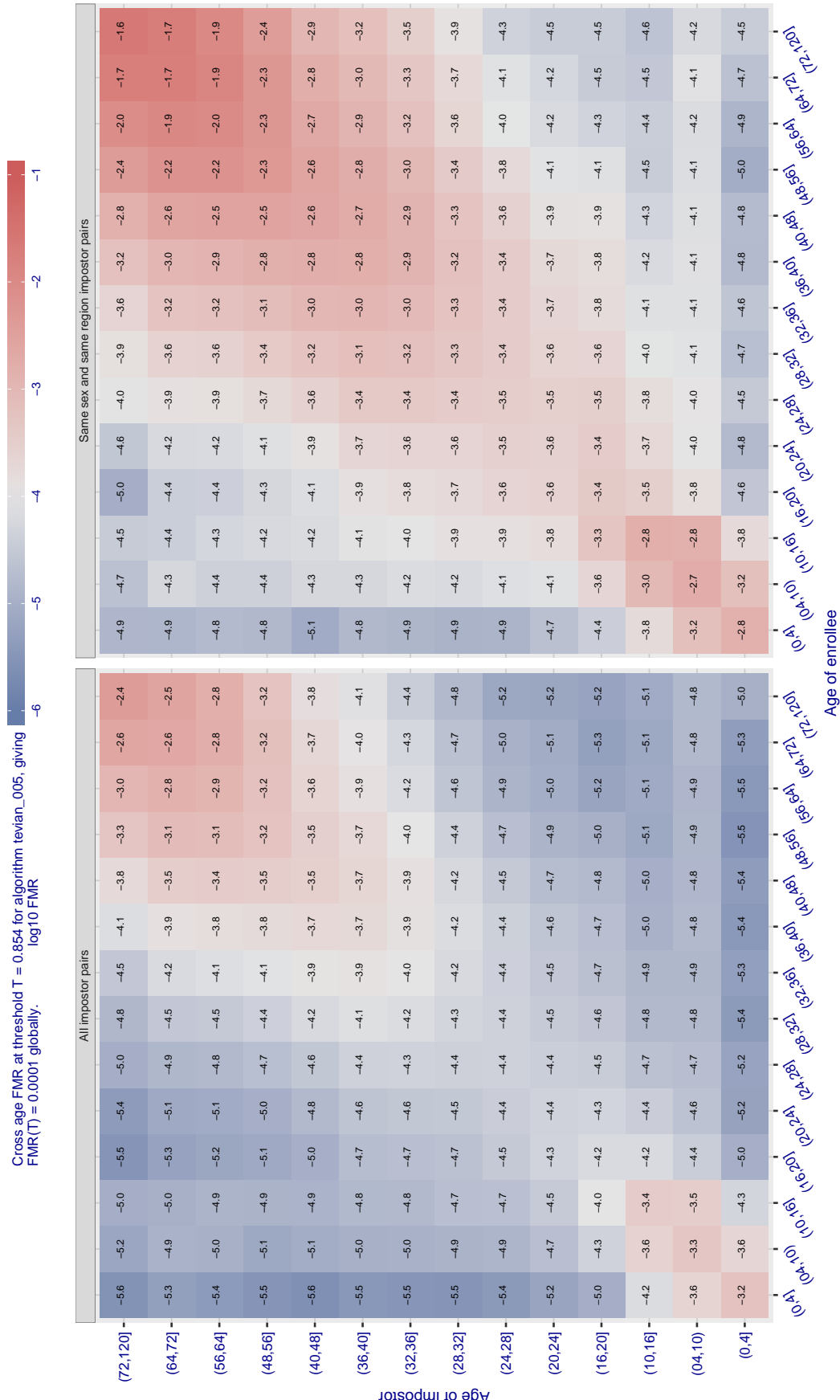


Figure 569: For algorithm tevian-005 operating on visa images, the heatmap shows false match observed over impostor comparisons of faces from different individuals who have the given age pair. False matches are counted against a recognition threshold fixed globally to give FMR = 0.0001 over all on the order of  $10^{10}$  impostor comparisons. The text in each box gives the same quantity as that coded by the color. Light colors present a security vulnerability to, for example, a passport gate.

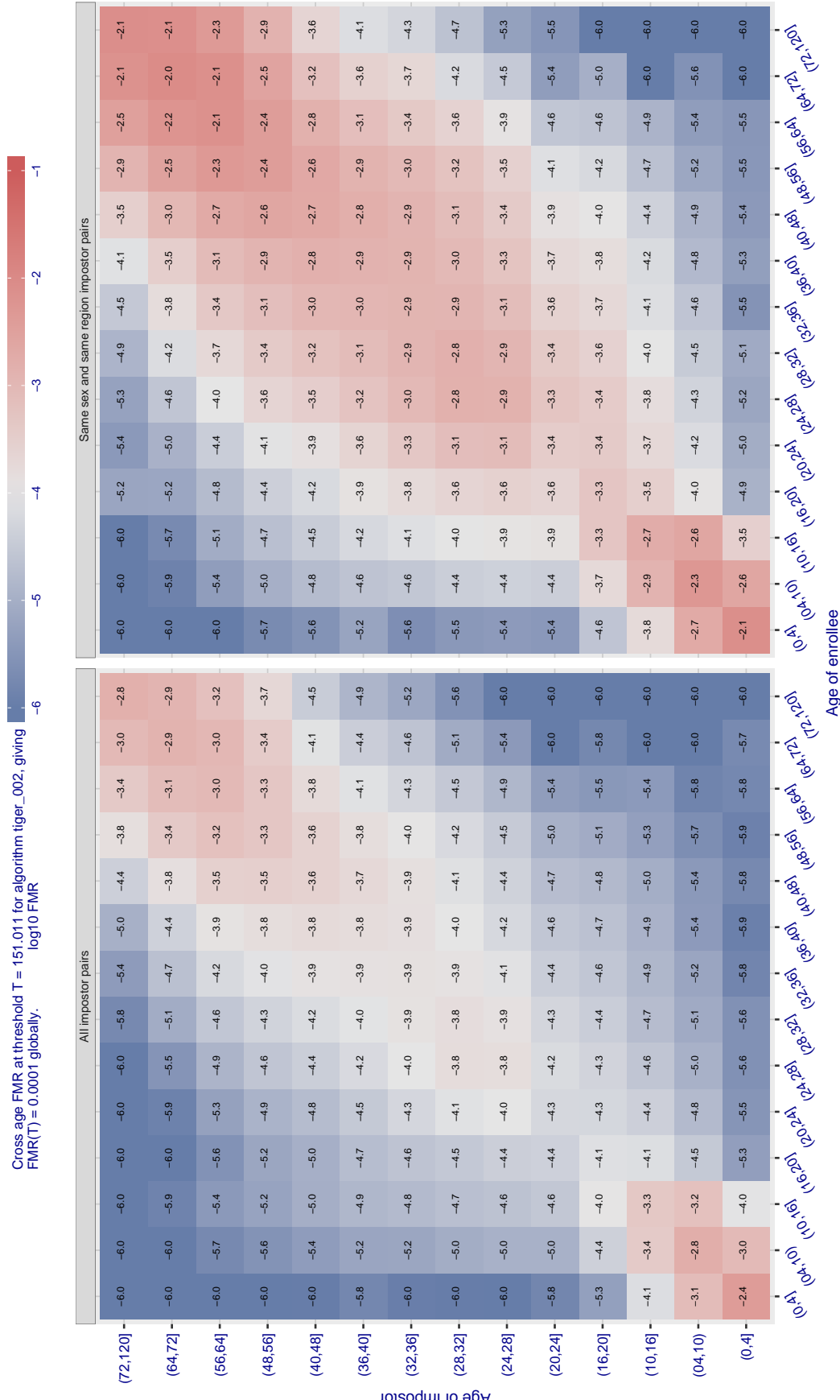


Figure 570: For algorithm tiger-002 operating on visa images, the heatmap shows false match observed over impostor comparisons of faces from different individuals who have the given age pair. False matches are counted against a recognition threshold fixed globally to give  $FMR = 0.0001$  over all on the order of  $10^{10}$  impostor comparisons. The text in each box gives the same quantity as that coded by the color. Light colors present a security vulnerability to, for example, a passport gate.

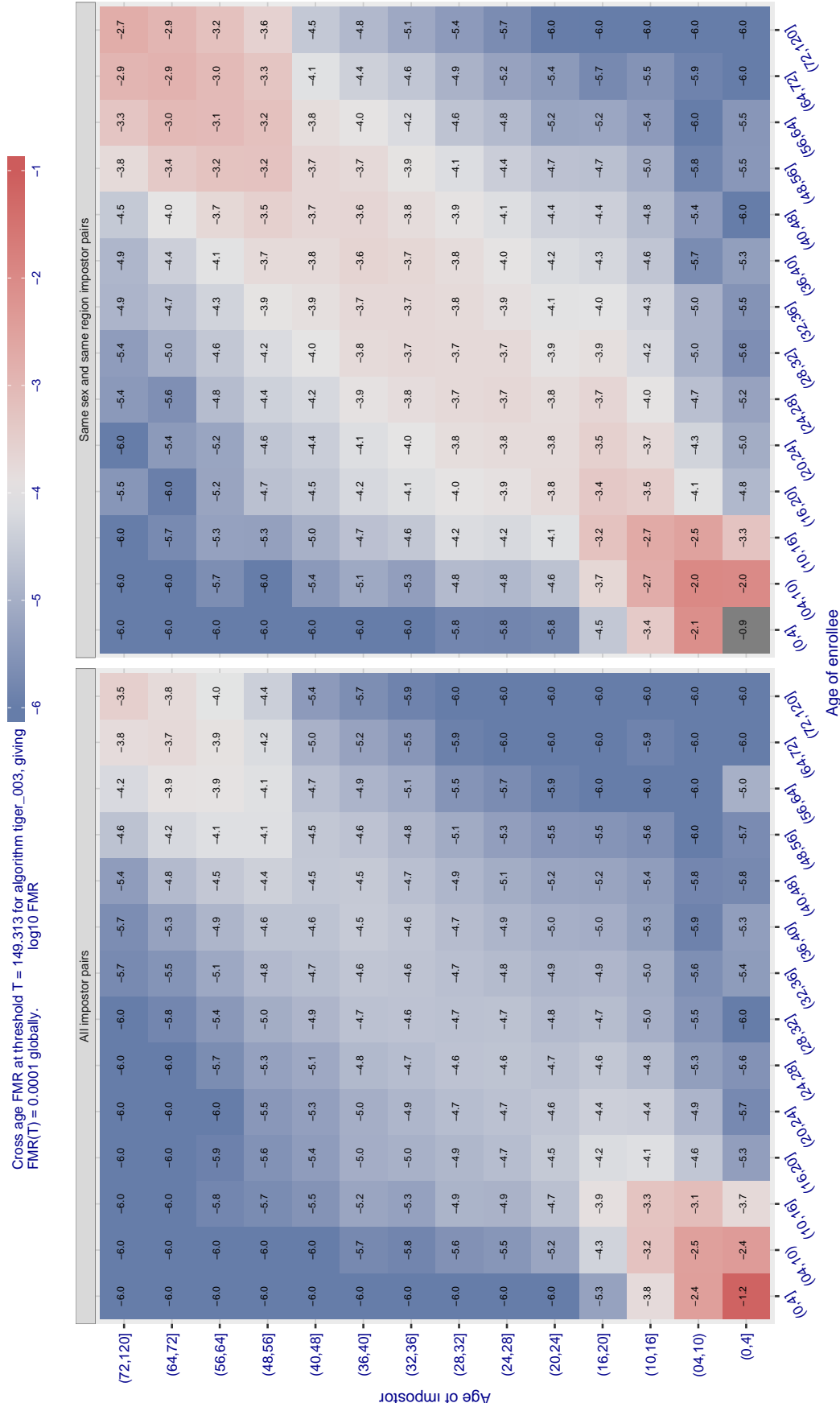


Figure 571: For algorithm tiger-003 operating on visa images, the heatmap shows false match observed over impostor comparisons of faces from different individuals who have the given age pair. False matches are counted against a recognition threshold fixed globally to give  $\text{FMR} = 0.0001$  over all on the order of  $10^{10}$  impostor comparisons. The text in each box gives the same quantity as that coded by the color. Light colors present a security vulnerability to, for example, a passport gate.

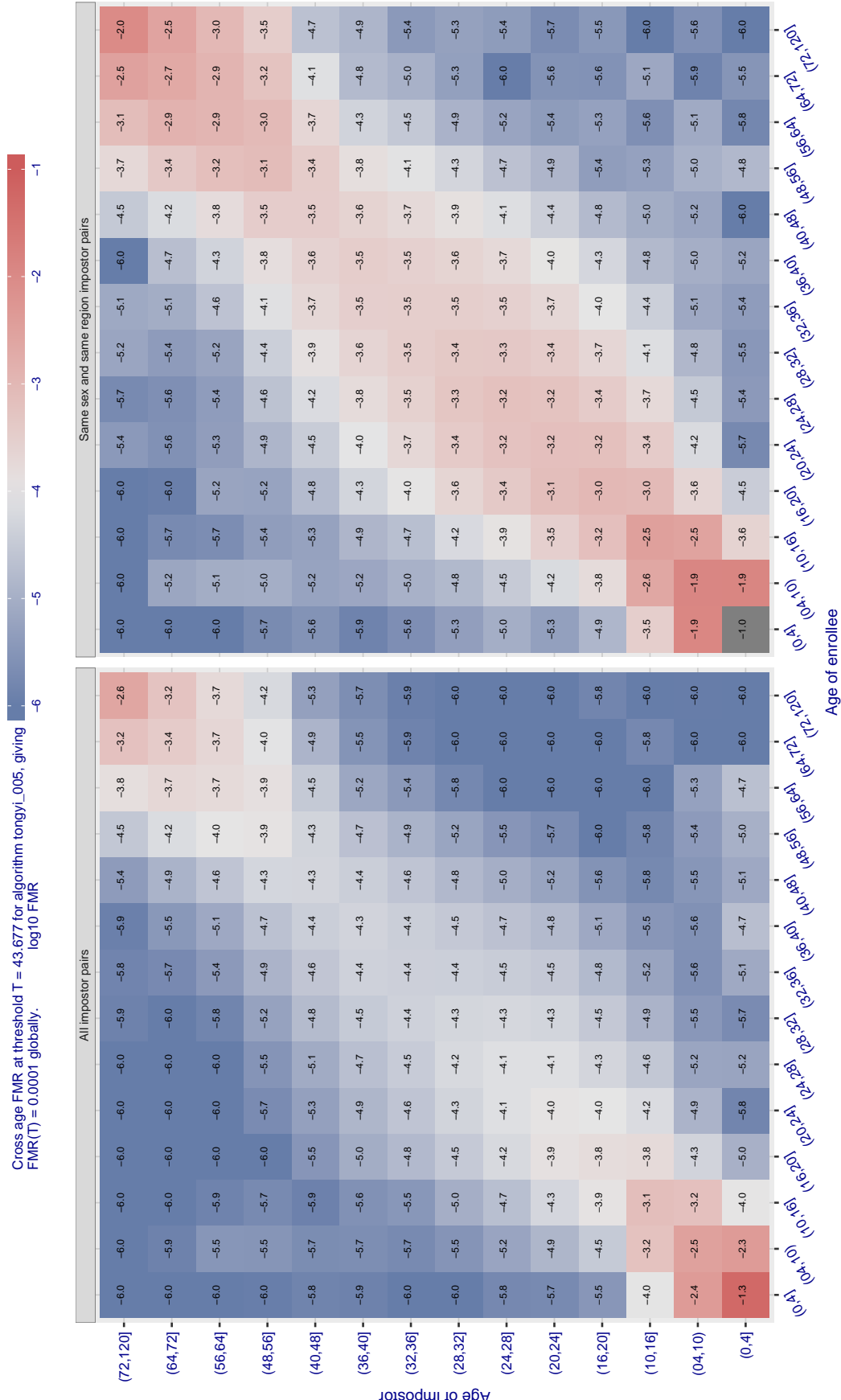


Figure 572: For algorithm tongyi\_005 operating on visa images, the heatmap shows false match observed over impostor comparisons of faces from different individuals who have the given age pair. False matches are counted against a recognition threshold fixed globally to give  $FMR = 0.0001$  over all on the order of  $10^{10}$  impostor comparisons. The text in each box gives the same quantity as that coded by the color. Light colors present a security vulnerability to, for example, a passport gate.

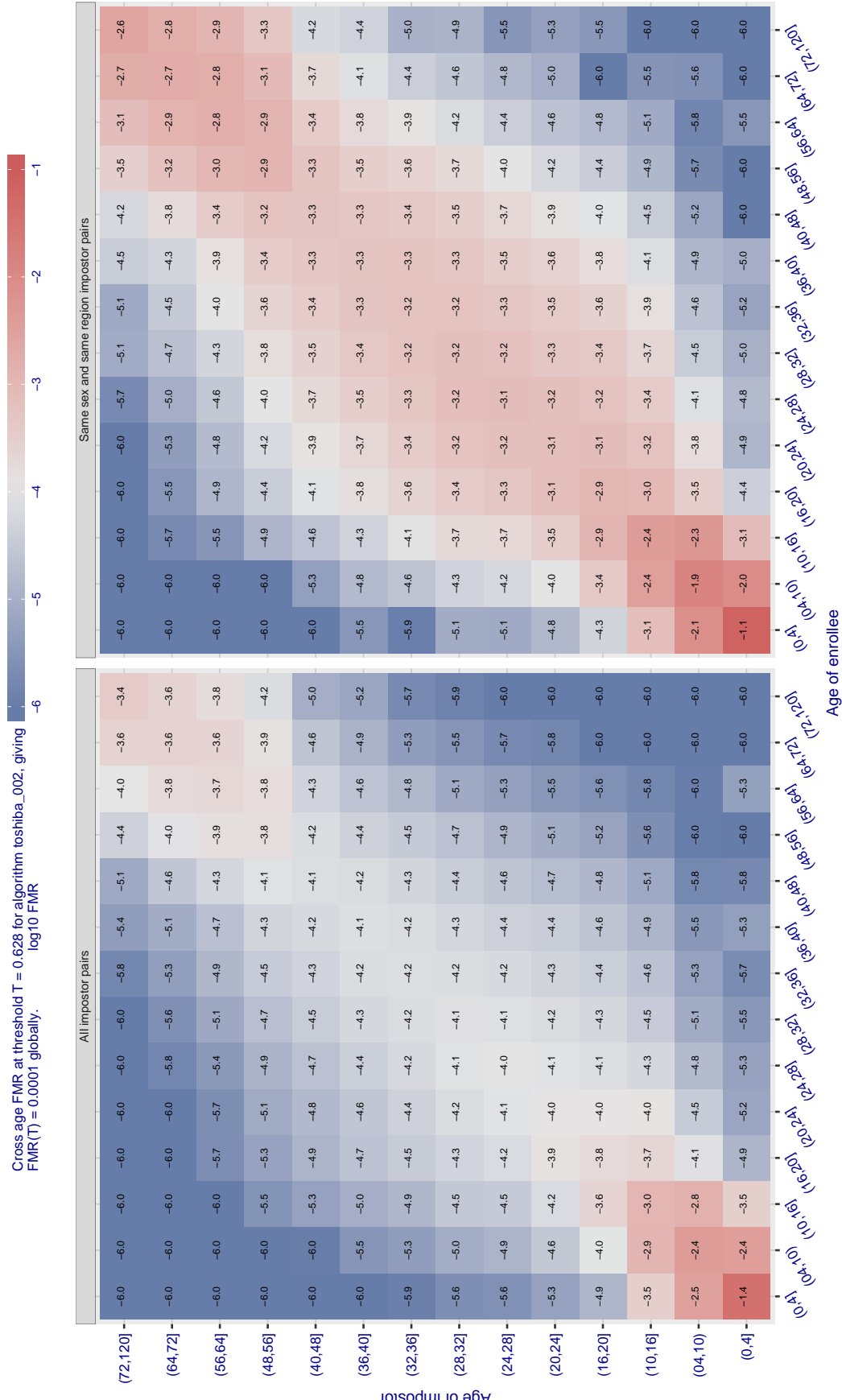


Figure 573: For algorithm toshiba-002 operating on visa images, the heatmap shows false match observed over impostor comparisons of faces from different individuals who have the given age pair. False matches are counted against a recognition threshold fixed globally to give  $FMR = 0.0001$  over all on the order of  $10^{10}$  impostor comparisons. The text in each box gives the same quantity as that coded by the color. Light colors present a security vulnerability to, for example, a passport gate.

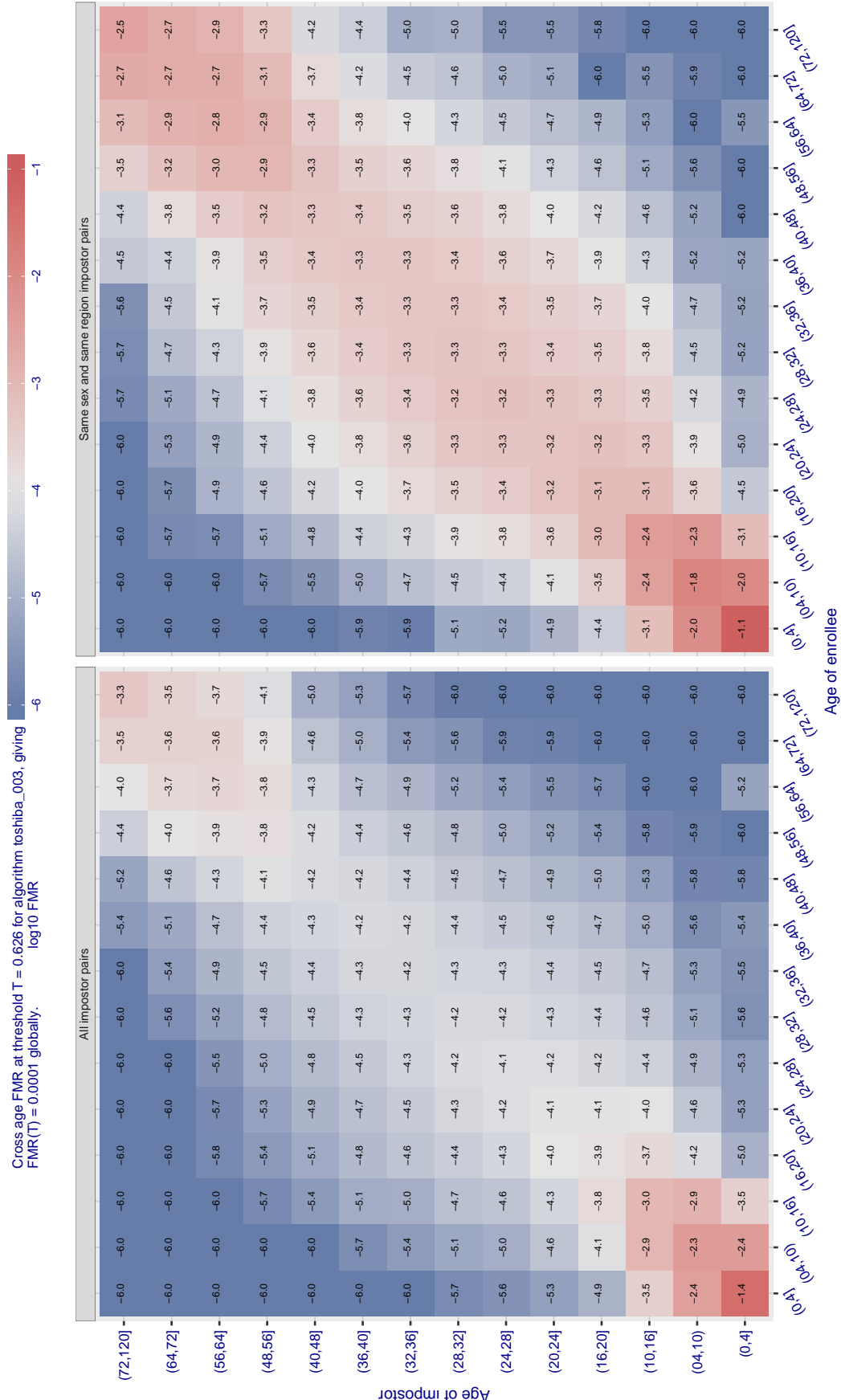


Figure 574: For algorithm toshiba-003 operating on visa images, the heatmap shows false match observed over impostor comparisons of faces from different individuals who have the given age pair. False matches are counted against a recognition threshold fixed globally to give  $FMR = 0.0001$  over all on the order of  $10^{10}$  impostor comparisons. The text in each box gives the same quantity as that coded by the color. Light colors present a security vulnerability to, for example, a passport gate.

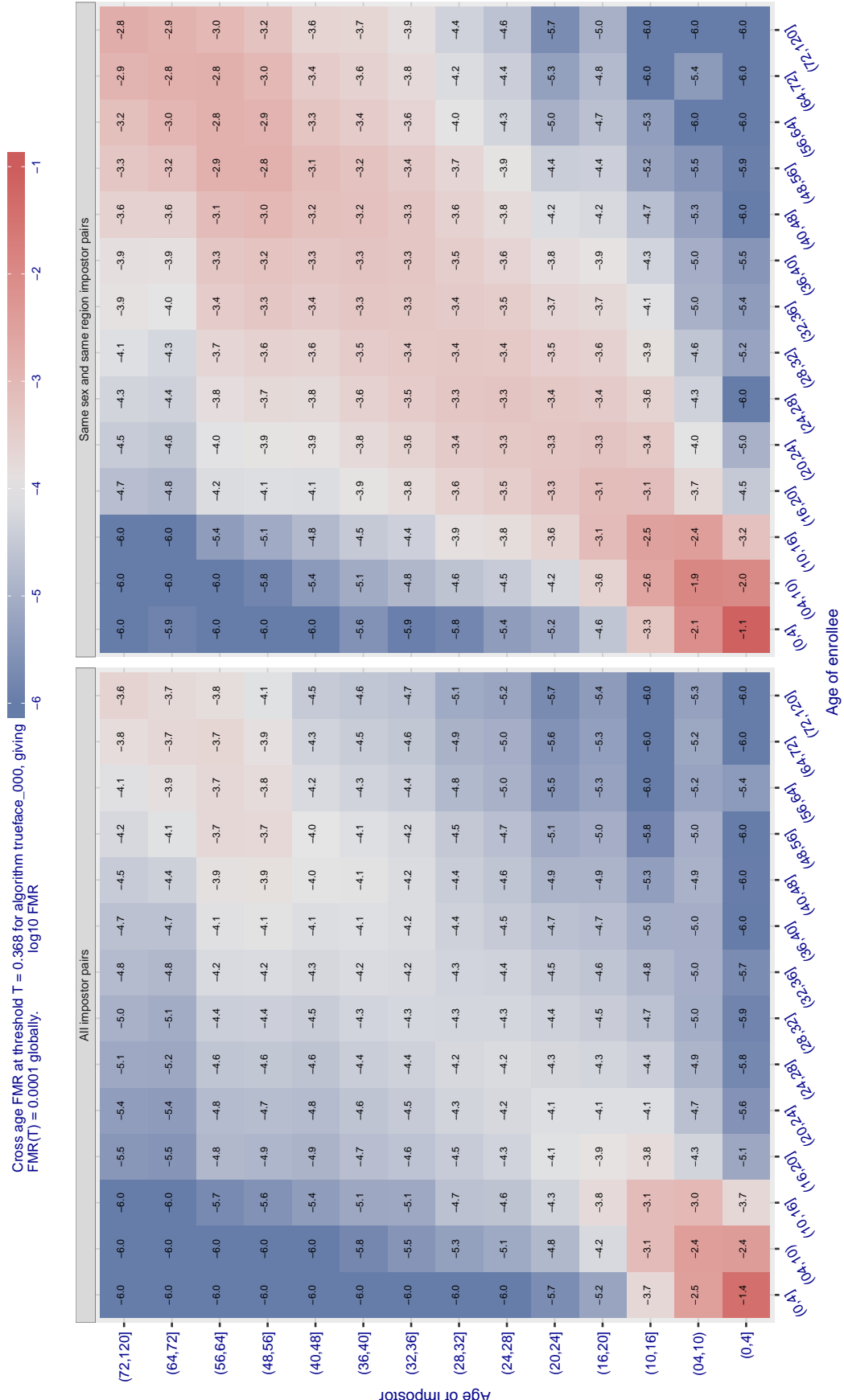


Figure 575: For algorithm trueface-000 operating on visa images, the heatmap shows false match observed over impostor comparisons of faces from different individuals who have the given age pair. False matches are counted against a recognition threshold fixed globally to give  $FMR = 0.0001$  over all on the order of  $10^{10}$  impostor comparisons. The text in each box gives the same quantity as that coded by the color. Light colors present a security vulnerability to, for example, a passport gate.

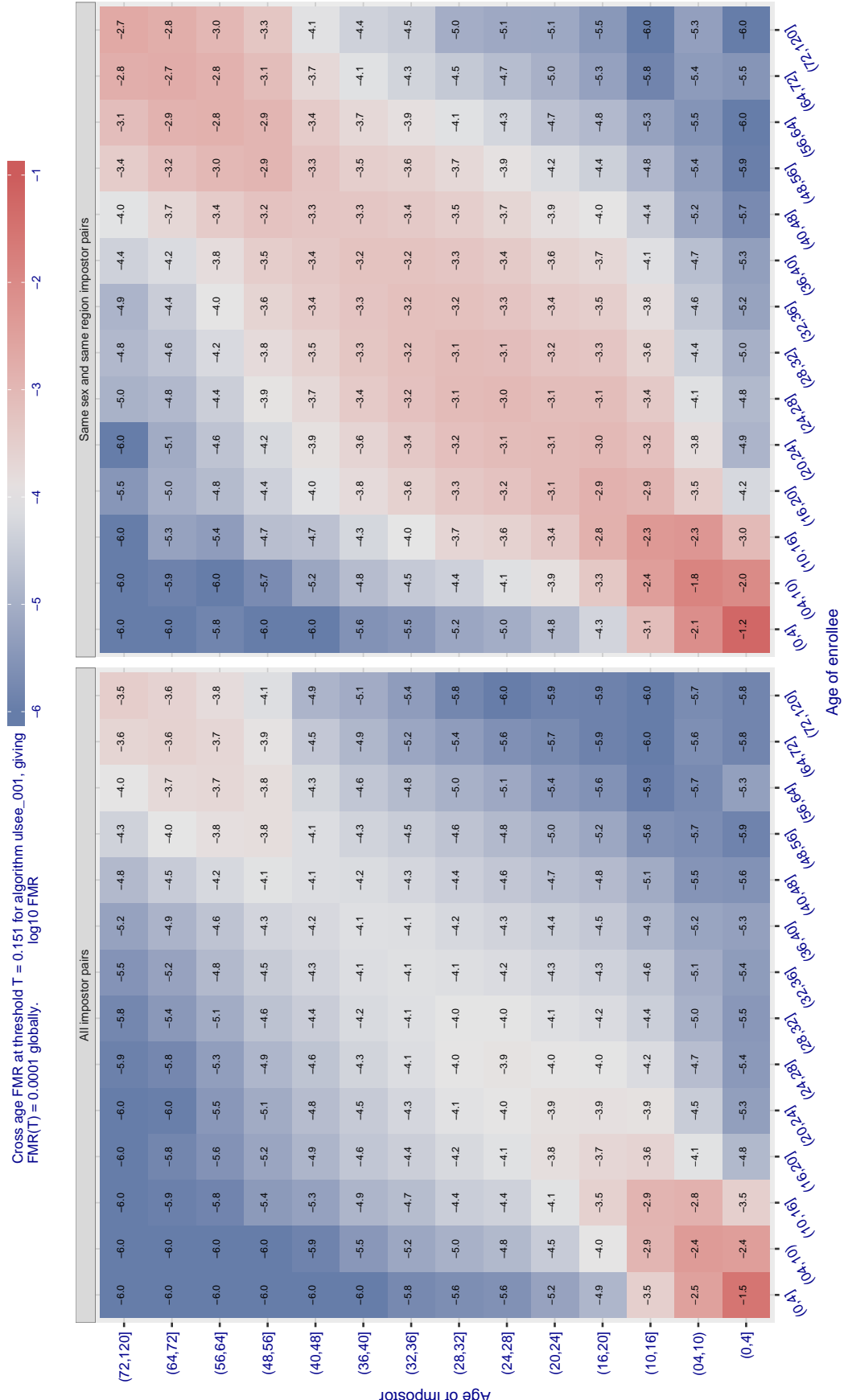


Figure 576: For algorithm ulsee-001 operating on visa images, the heatmap shows false match observed over impostor comparisons of faces from different individuals who have the given age pair. False matches are counted against a recognition threshold fixed globally to give  $FMR = 0.0001$  over all on the order of  $10^{10}$  impostor comparisons. The text in each box gives the same quantity as that coded by the color. Light colors present a security vulnerability to, for example, a passport gate.

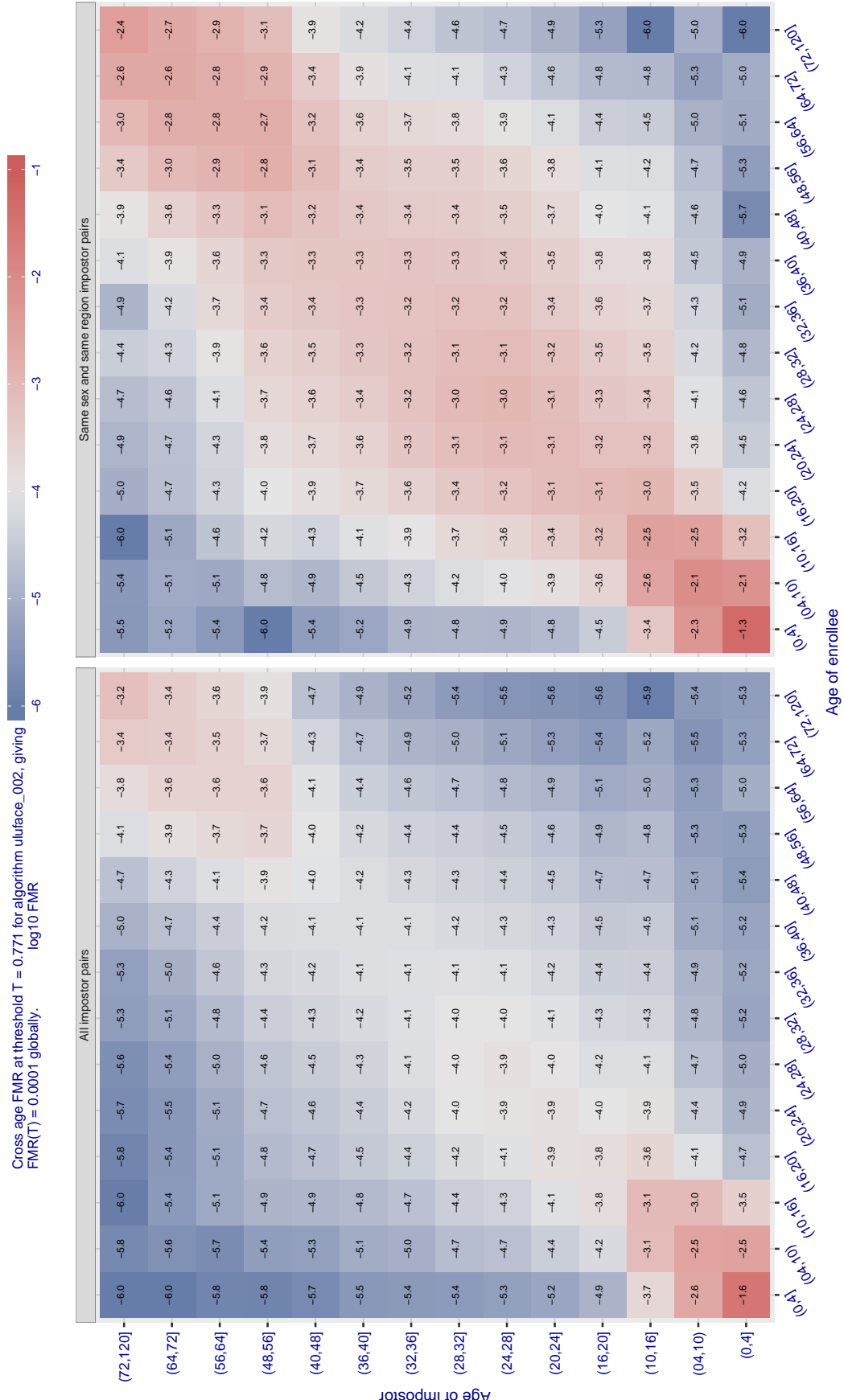


Figure 577: For algorithm uluface-002 operating on visa images, the heatmap shows false match observed over impostor comparisons of faces from different individuals who have the given age pair. False matches are counted against a recognition threshold fixed globally to give  $FMR = 0.0001$  over all on the order of  $10^{10}$  impostor comparisons. The text in each box gives the same quantity as that coded by the color. Light colors present a security vulnerability to, for example, a passport gate.

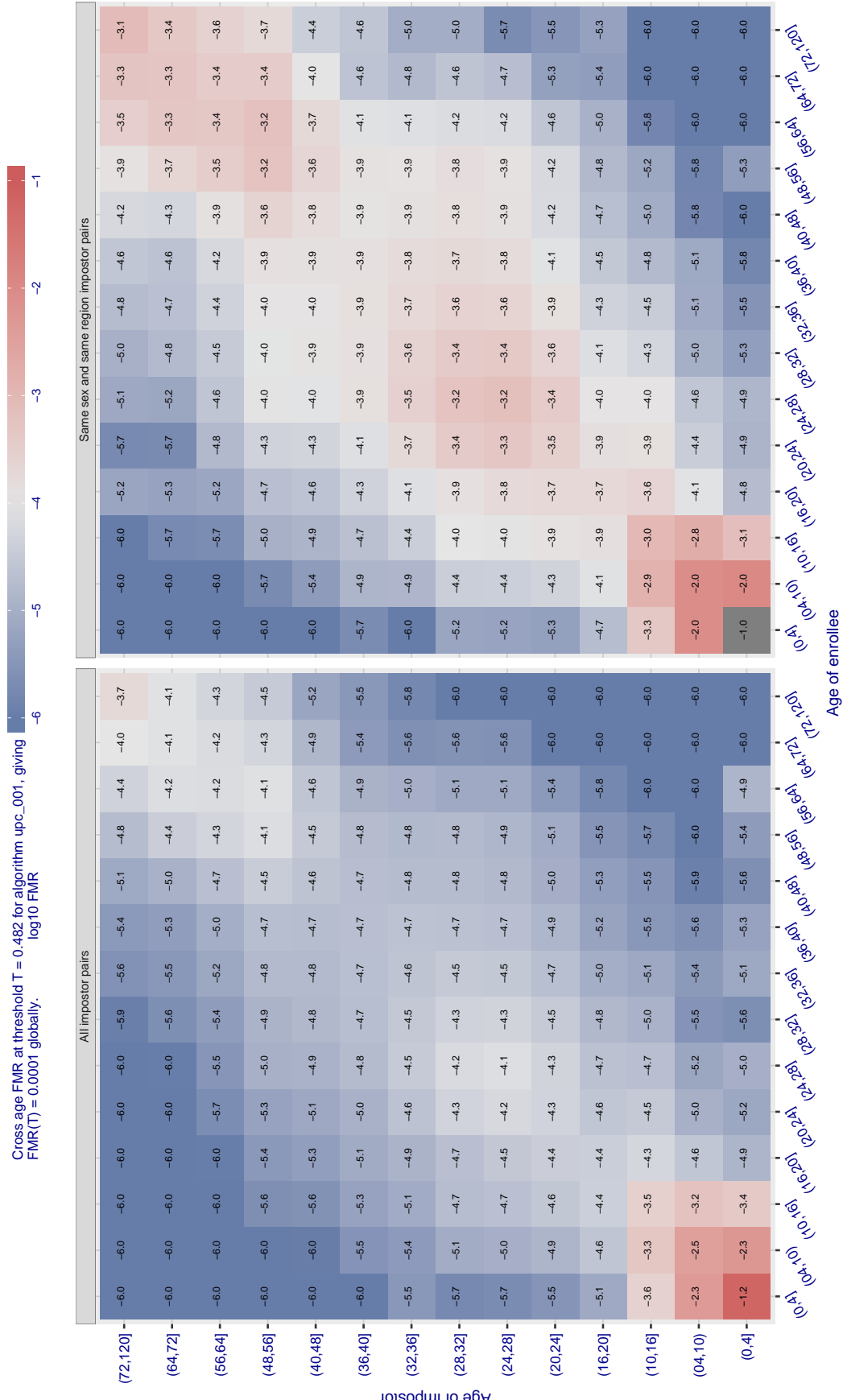


Figure 578: For algorithm upc-001 operating on visa images, the heatmap shows false match observed over impostor comparisons of faces from different individuals who have the given age pair. False matches are counted against a recognition threshold fixed globally to give  $FMR = 0.0001$  over all on the order of  $10^{10}$  impostor comparisons. The text in each box gives the same quantity as that coded by the color. Light colors present a security vulnerability to, for example, a passport gate.

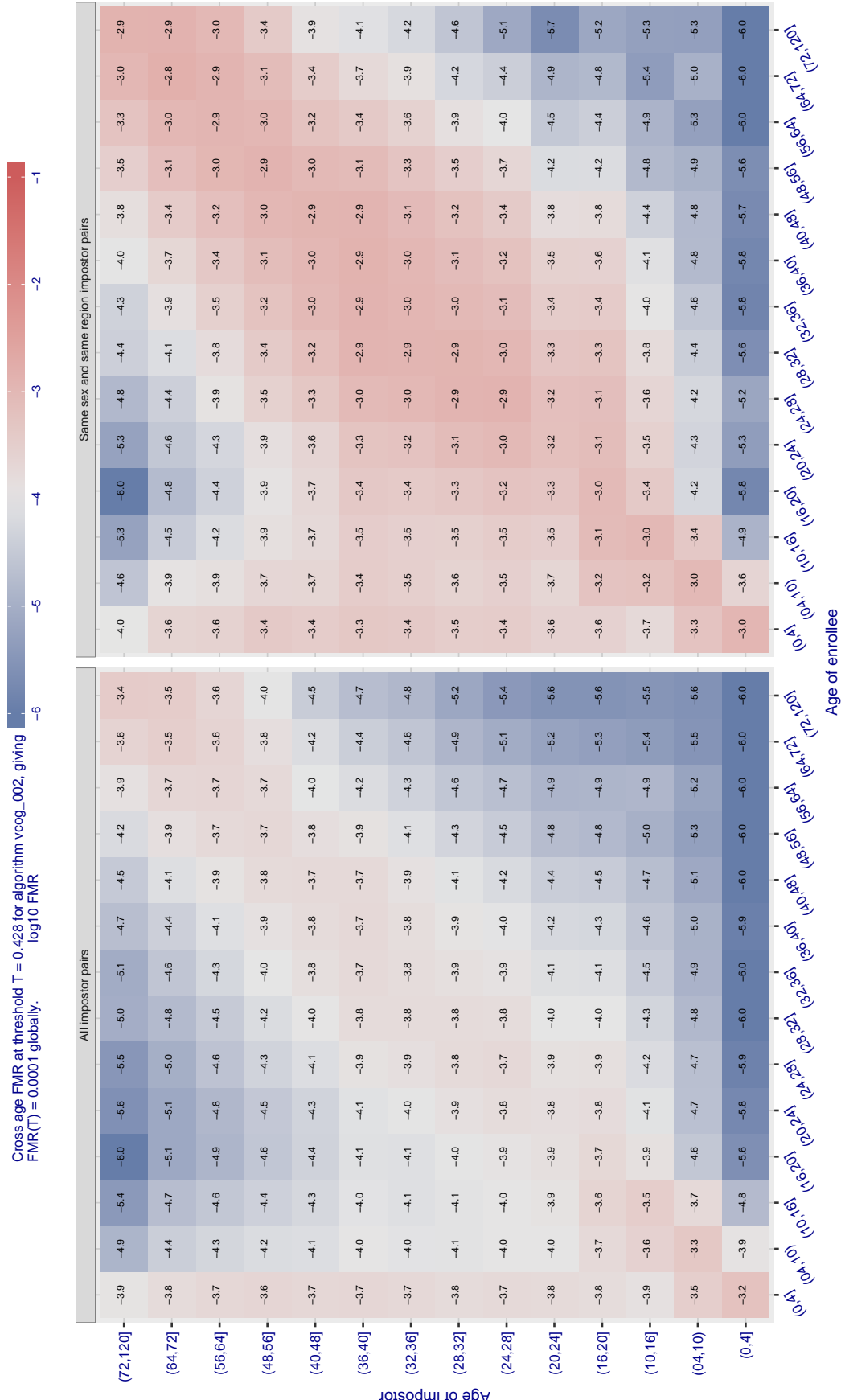


Figure 579: For algorithm v cog\_002 operating on visa images, the heatmap shows false match observed over impostor comparisons of faces from different individuals who have the given age pair. False matches are counted against a recognition threshold fixed globally to give  $FMR = 0.0001$  over all on the order of  $10^{10}$  impostor comparisons. The text in each box gives the same quantity as that coded by the color. Light colors present a security vulnerability to, for example, a passport gate.

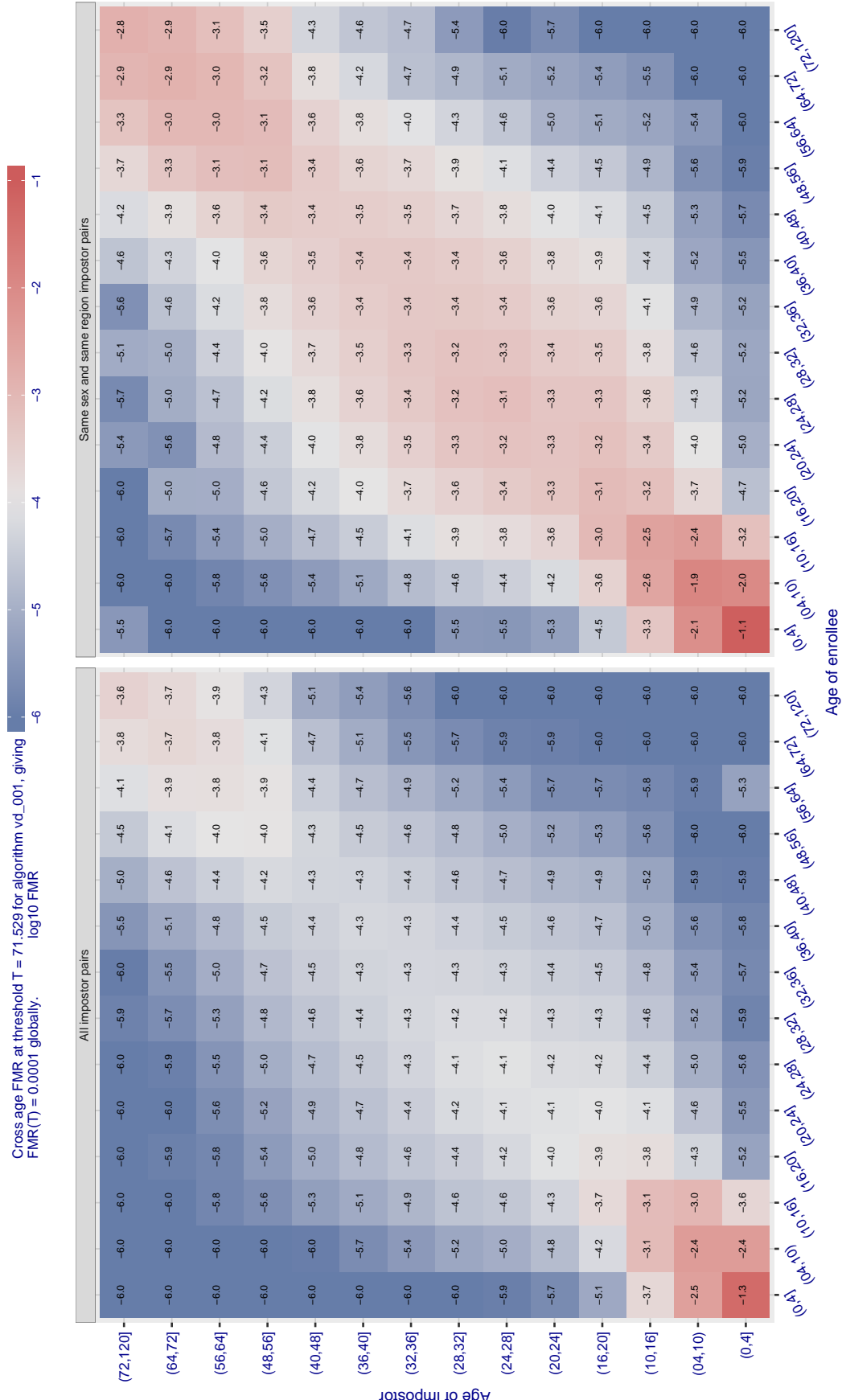


Figure 580: For algorithm vd-001 operating on visa images, the heatmap shows false match observed over impostor comparisons of faces from different individuals who have the given age pair. False matches are counted against a recognition threshold fixed globally to give FMR = 0.0001 over all on the order of  $10^{10}$  impostor comparisons. The text in each box gives the same quantity as that coded by the color. Light colors present a security vulnerability to, for example, a passport gate.

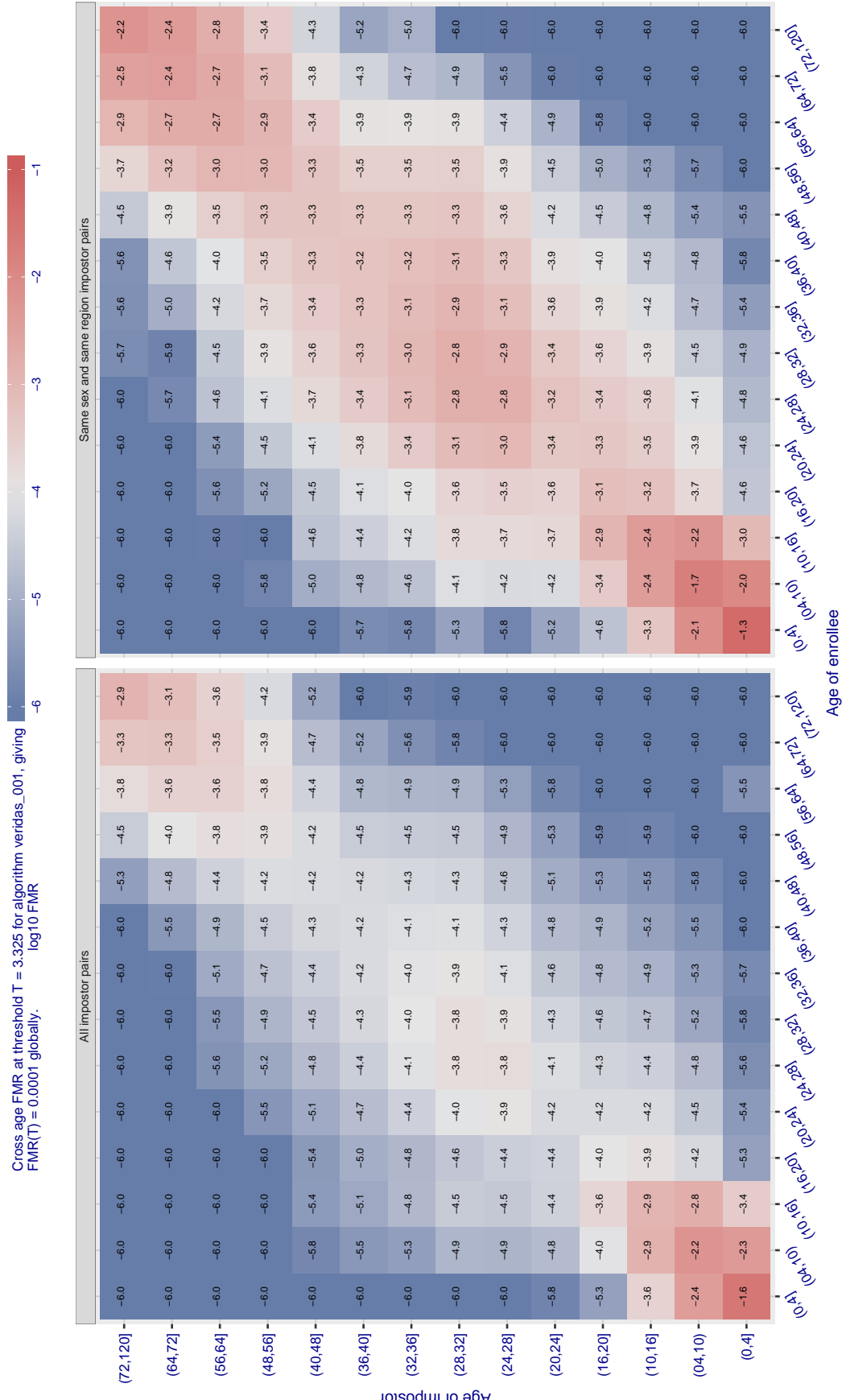


Figure 581: For algorithm veridas-001 operating on visa images, the heatmap shows false match observed over impostor comparisons of faces from different individuals who have the given age pair. False matches are counted against a recognition threshold fixed globally to give  $FMR = 0.0001$  over all on the order of  $10^{10}$  impostor comparisons. The text in each box gives the same quantity as that coded by the color. Light colors present a security vulnerability to, for example, a passport gate.

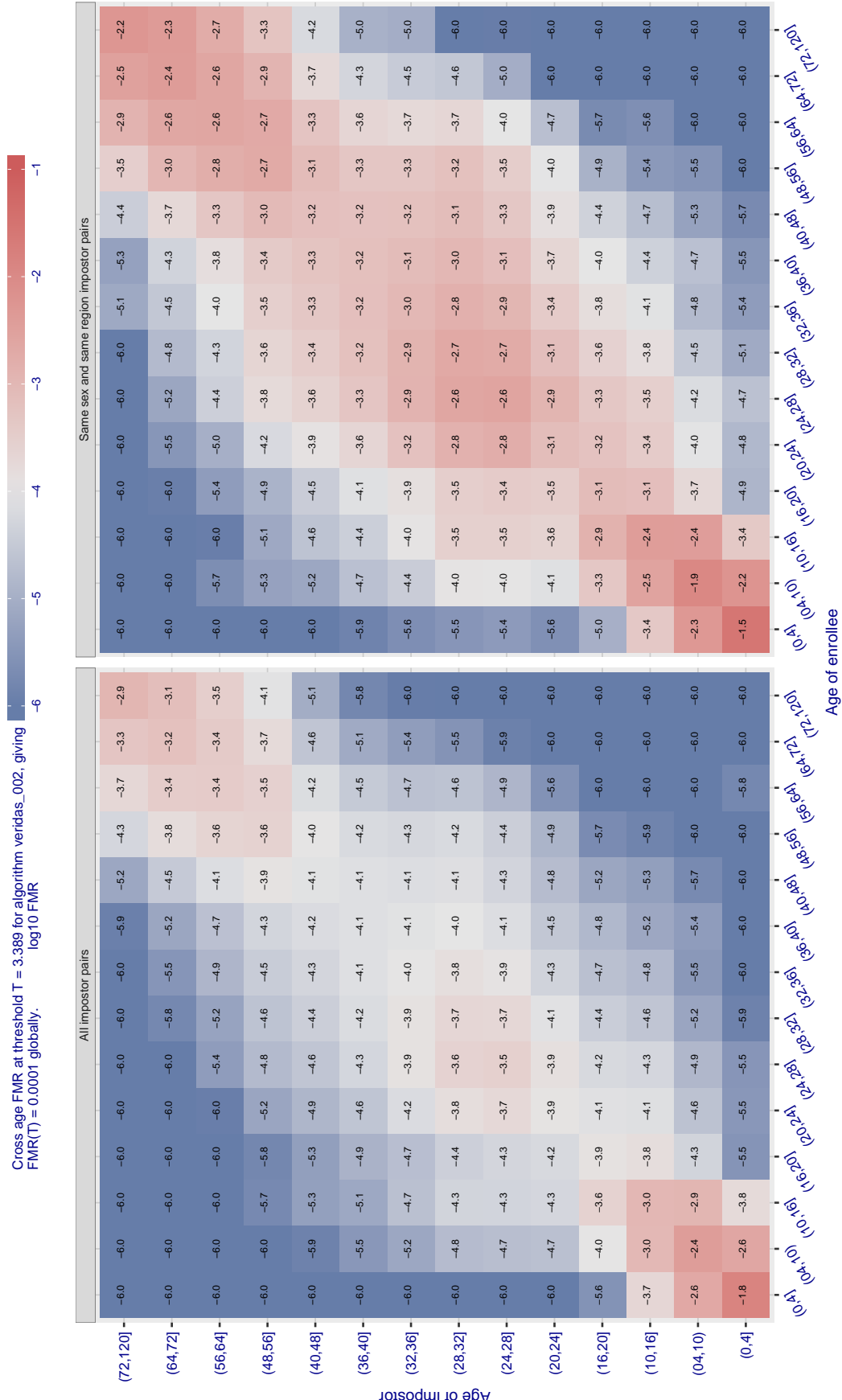


Figure 582: For algorithm veridas-002 operating on visa images, the heatmap shows false match observed over impostor comparisons of faces from different individuals who have the given age pair. False matches are counted against a recognition threshold fixed globally to give FMR = 0.0001 over all on the order of  $10^{10}$  impostor comparisons. The text in each box gives the same quantity as that coded by the color. Light colors present a security vulnerability to, for example, a passport gate.

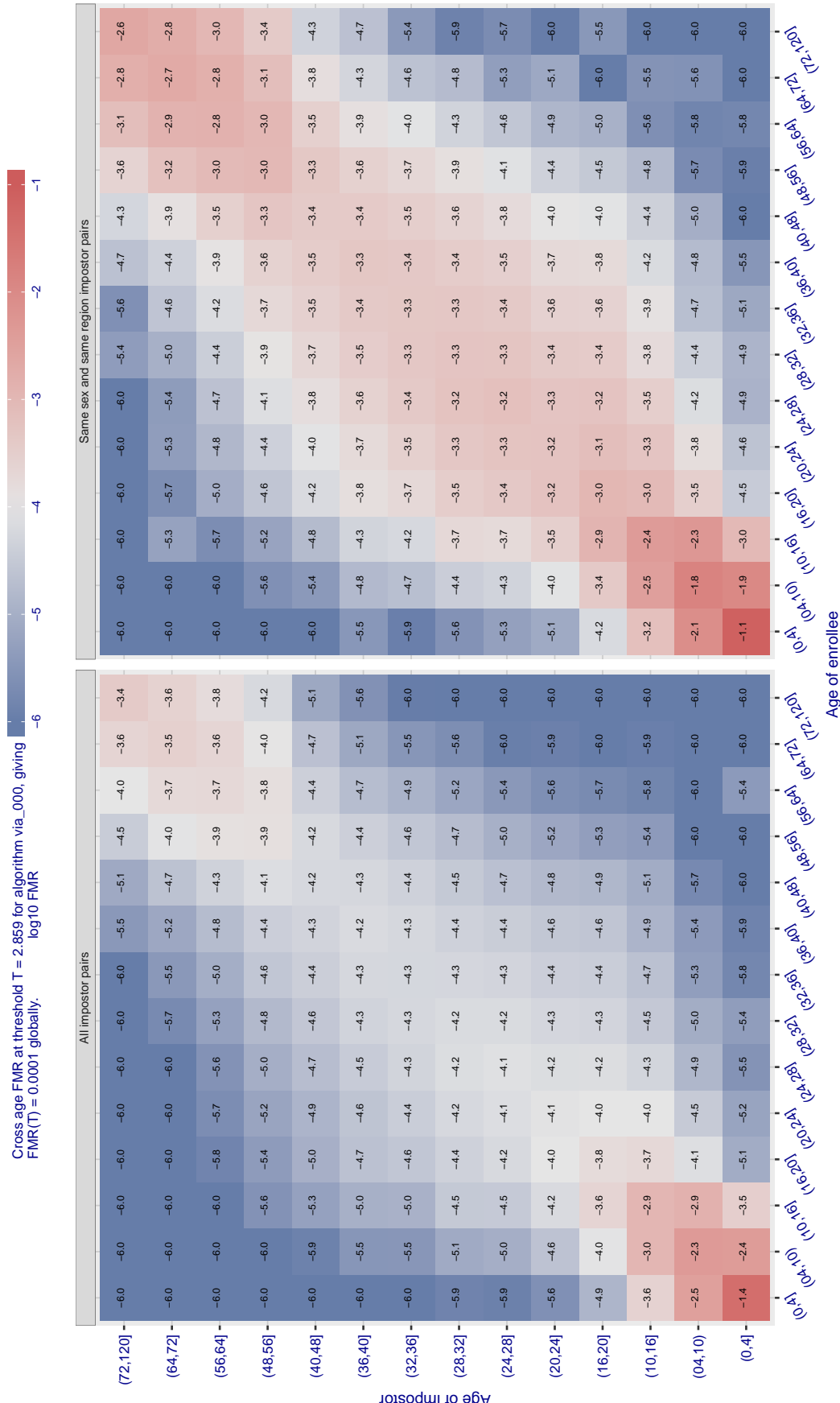


Figure 583: For algorithm via\_000 operating on visa images, the heatmap shows false match observed over impostor comparisons of faces from different individuals who have the given age pair. False matches are counted against a recognition threshold fixed globally to give  $FMR = 0.0001$  over all on the order of  $10^{10}$  impostor comparisons. The text in each box gives the same quantity as that coded by the color. Light colors present a security vulnerability to, for example, a passport gate.

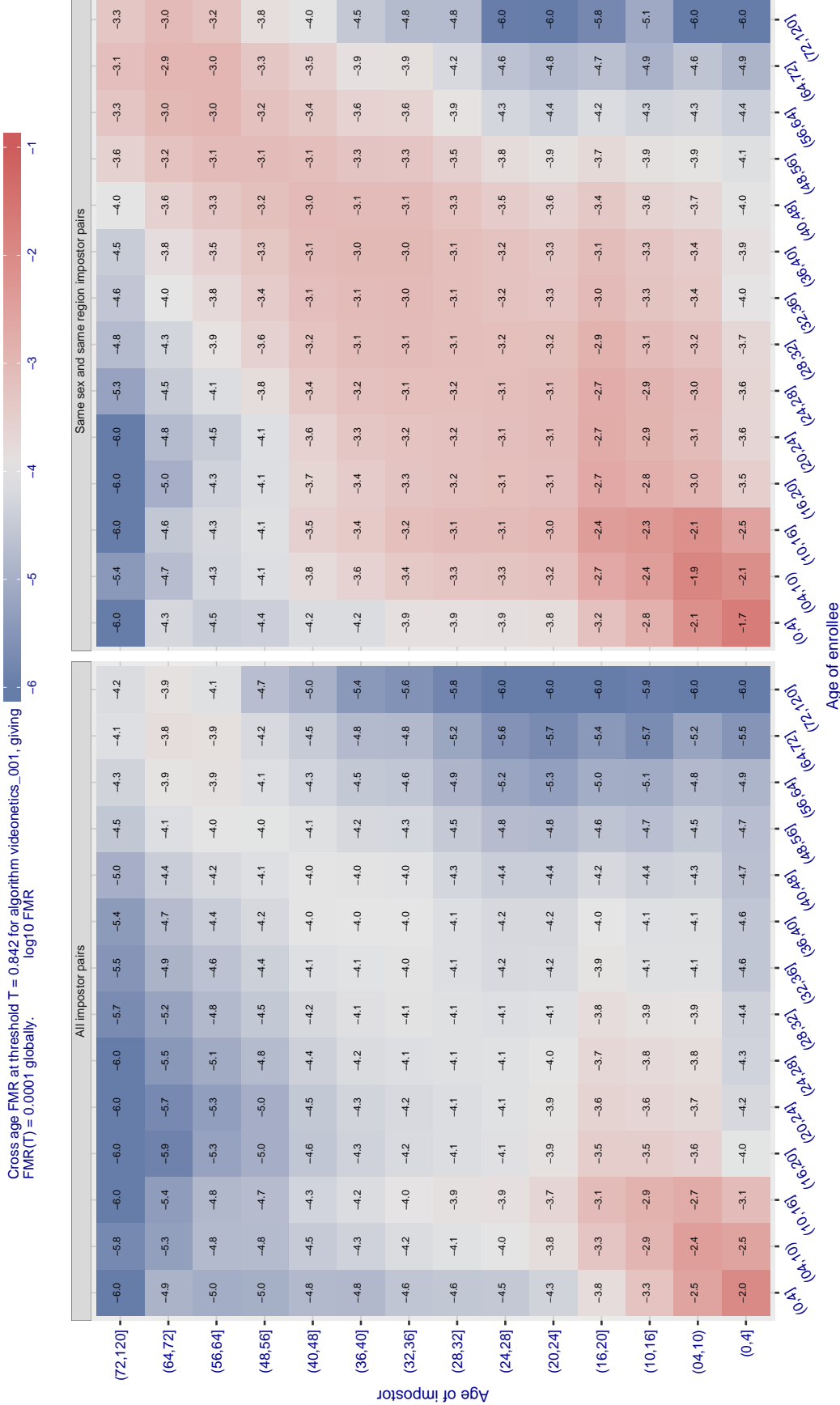


Figure 584: For algorithm videonetics-001 operating on visa images, the heatmap shows false match observed over impostor comparisons of faces from different individuals who have the given age pair. False matches are counted against a recognition threshold fixed globally to give  $\text{FMR} = 0.0001$  over all on the order of  $10^{10}$  impostor comparisons. The text in each box gives the same quantity as that coded by the color. Light colors present a security vulnerability to, for example, a passport gate.

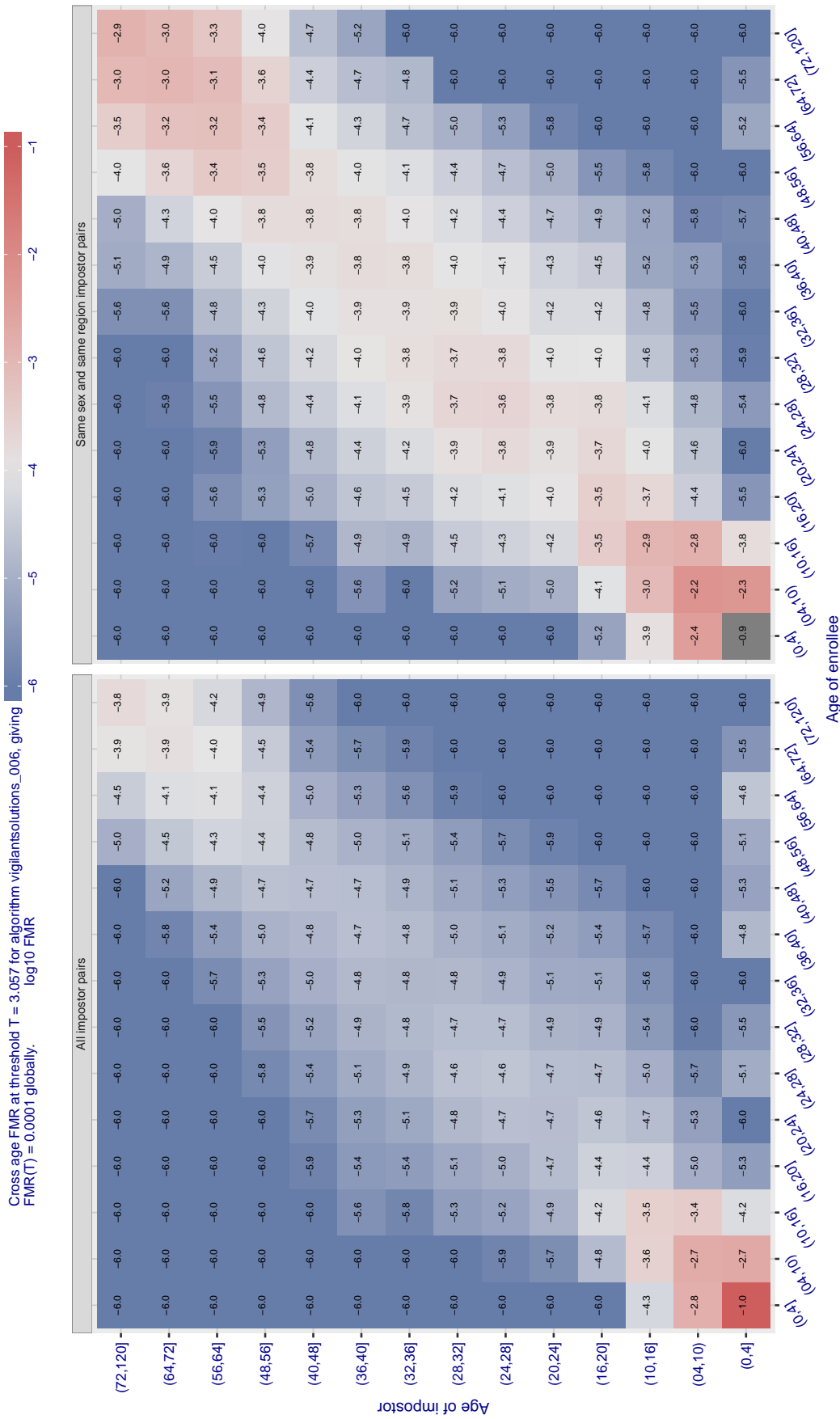


Figure 585: For algorithm vigilantsolutions-006 operating on visa images, the heatmap shows false match observed over impostor comparisons of faces from different individuals who have the given age pair. False matches are counted against a recognition threshold fixed globally to give  $FMR = 0.0001$  over all on the order of  $10^{10}$  impostor comparisons. The text in each box gives the same quantity as that coded by the color. Light colors present a security vulnerability to, for example, a passport gate.

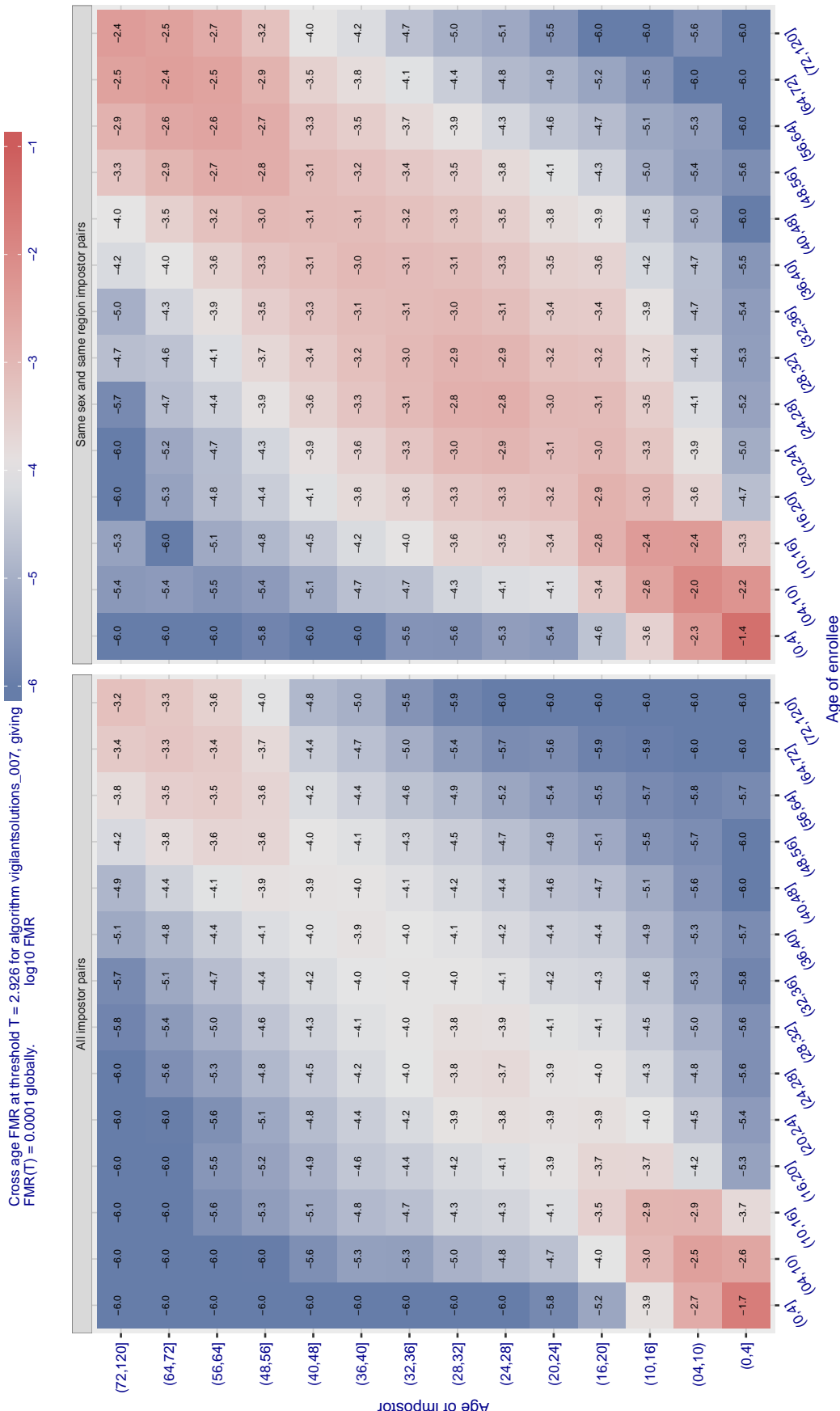


Figure 586: For algorithm vigilantsolutions-007 operating on visa images, the heatmap shows false match observed over impostor comparisons of faces from different individuals who have the given age pair. False matches are counted against a recognition threshold fixed globally to give  $\text{FMR} = 0.0001$  over all on the order of  $10^{10}$  impostor comparisons. The text in each box gives the same quantity as that coded by the color. Light colors present a security vulnerability to, for example, a passport gate.

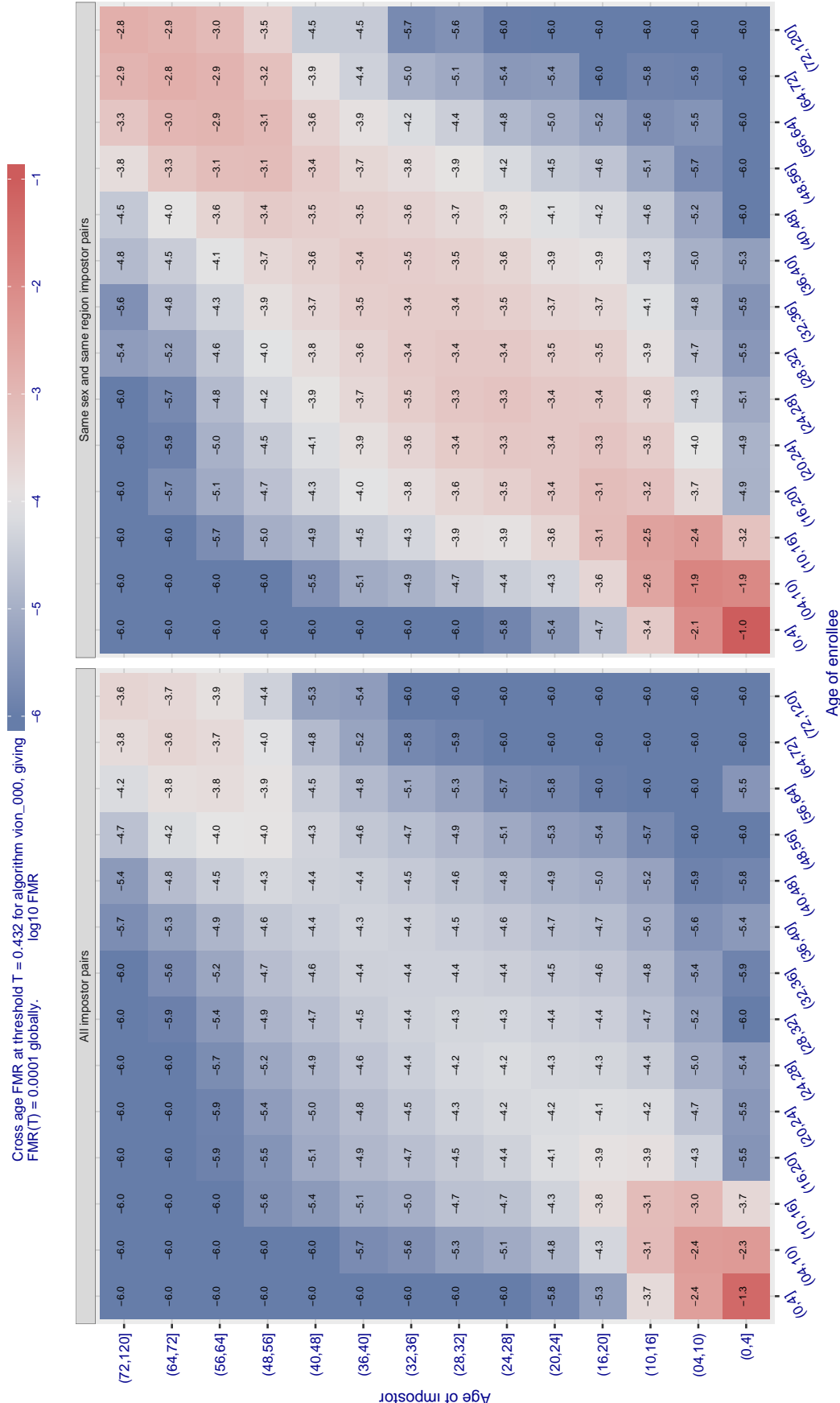


Figure 587: For algorithm vion-000 operating on visa images, the heatmap shows false match observed over impostor comparisons of faces from different individuals who have the given age pair. False matches are counted against a recognition threshold fixed globally to give  $FMR = 0.0001$  over all on the order of  $10^{10}$  impostor comparisons. The text in each box gives the same quantity as that coded by the color. Light colors present a security vulnerability to, for example, a passport gate.

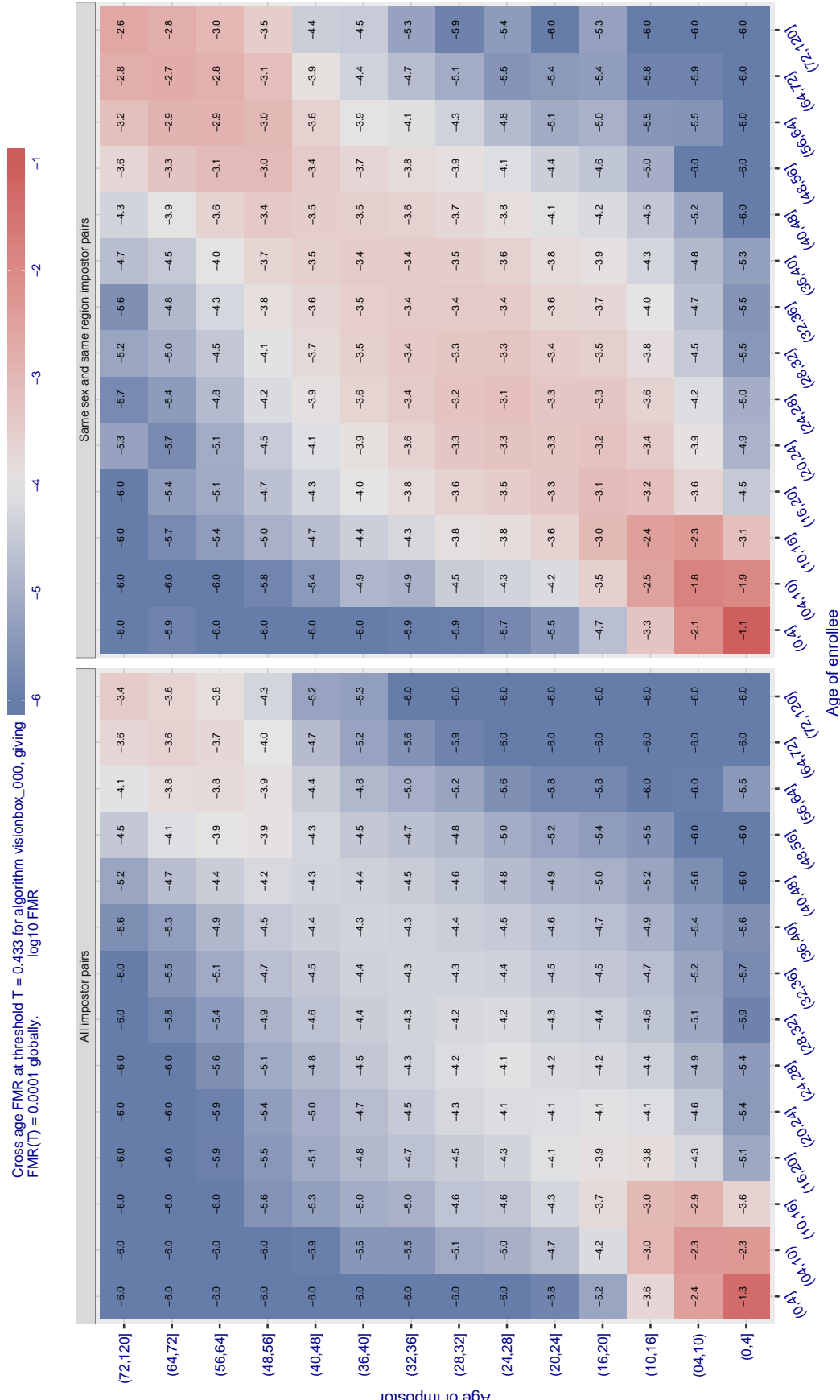
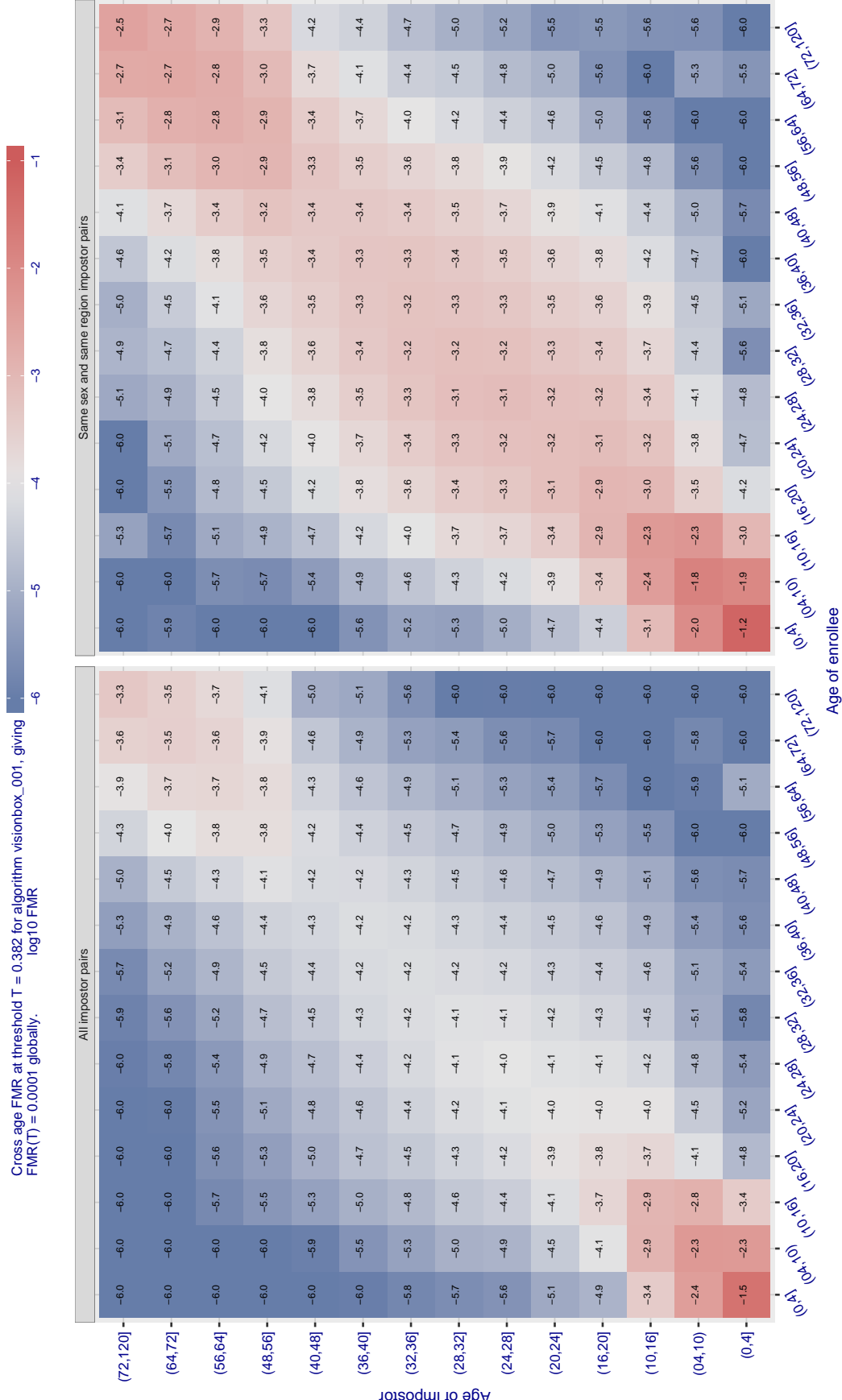


Figure 588: For algorithm visionbox-000 operating on visa images, the heatmap shows false match observed over impostor comparisons of faces from different individuals who have the given age pair. False matches are counted against a recognition threshold fixed globally to give FMR = 0.001 over all on the order of  $10^{10}$  impostor comparisons. The text in each box gives the same quantity as that coded by the color. Light colors present a security vulnerability to, for example, a passport gate.



**Figure 589:** For algorithm visionbox-001 operating on visa images, the heatmap shows false match observed over impostor comparisons of faces from different individuals who have the given age pair. False matches are counted against a recognition threshold fixed globally to give  $FMR = 0.0001$  over all on the order of  $10^{10}$  impostor comparisons. The text in each box gives the same quantity as that coded by the color. Light colors present a security vulnerability to, for example, a passport gate.

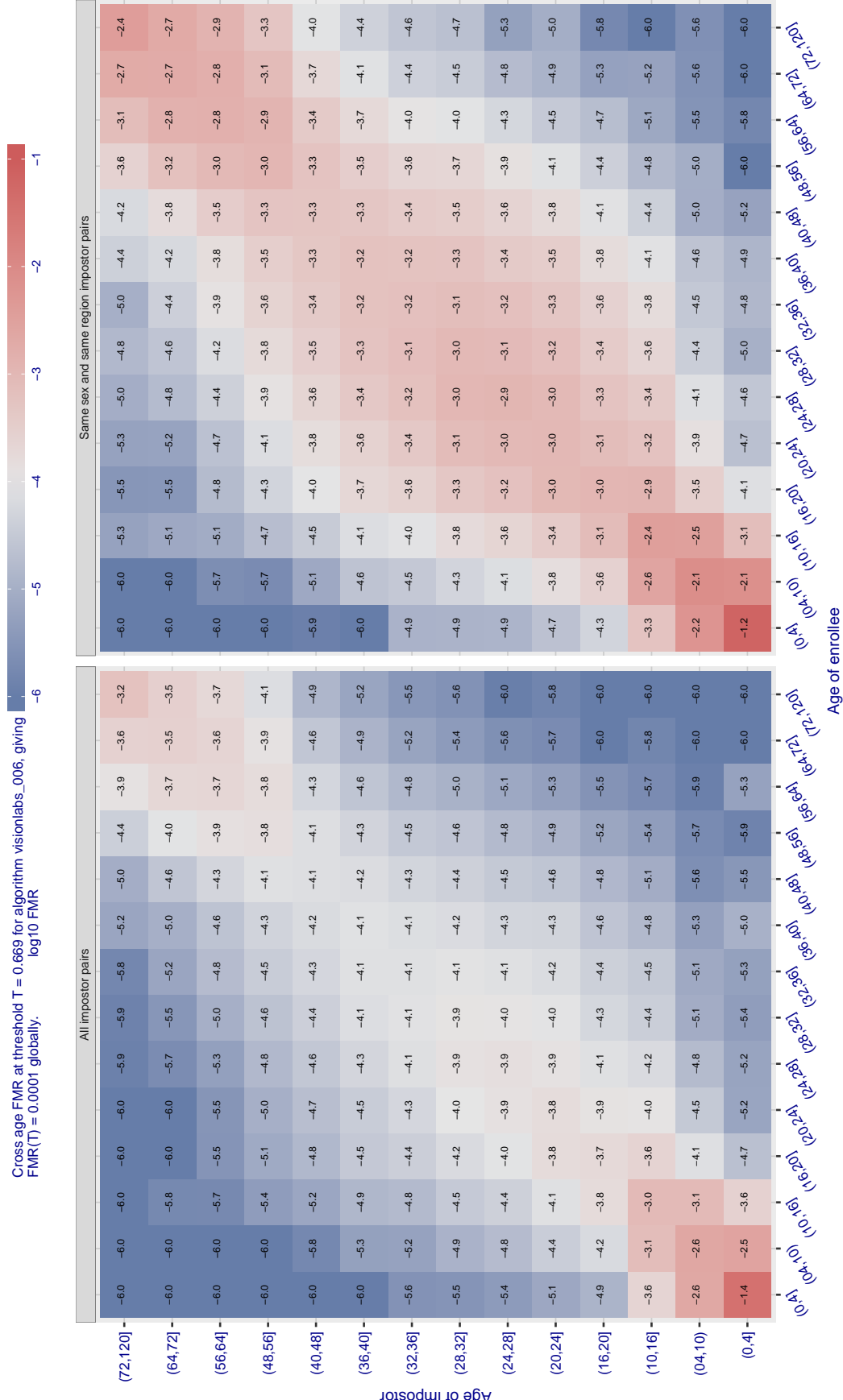


Figure 590: For algorithm visionlabs-006 operating on visa images, the heatmap shows false match observed over impostor comparisons of faces from different individuals who have the given age pair. False matches are counted against a recognition threshold fixed globally to give  $FMR = 0.0001$  over all on the order of  $10^{10}$  impostor comparisons. The text in each box gives the same quantity as that coded by the color. Light colors present a security vulnerability to, for example, a passport gate.

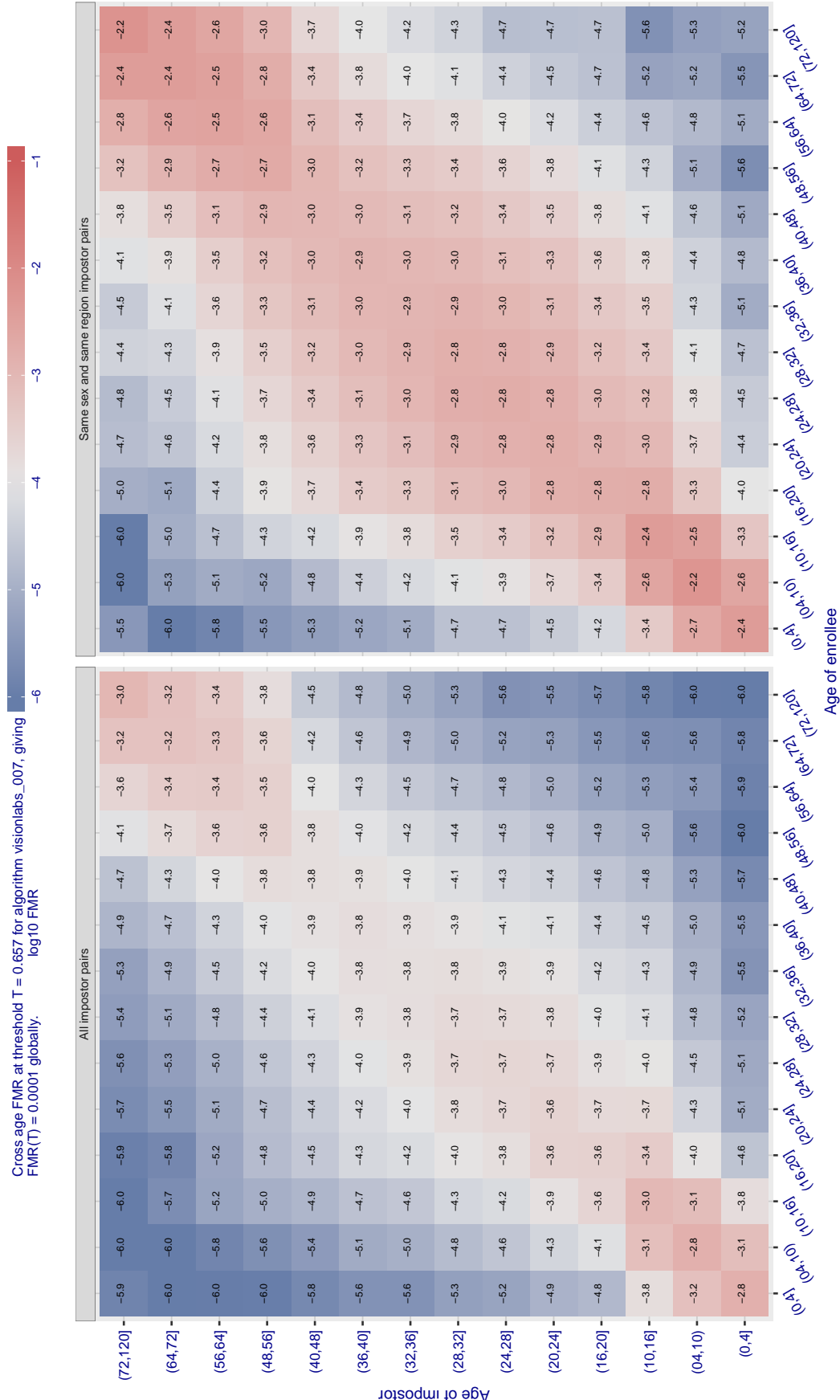


Figure 591: For algorithm visionlabs-007 operating on visa images, the heatmap shows false match observed over impostor comparisons of faces from different individuals who have the given age pair. False matches are counted against a recognition threshold fixed globally to give  $FMR = 0.001$  over all on the order of  $10^{10}$  impostor comparisons. The text in each box gives the same quantity as that coded by the color. Light colors present a security vulnerability to, for example, a passport gate.

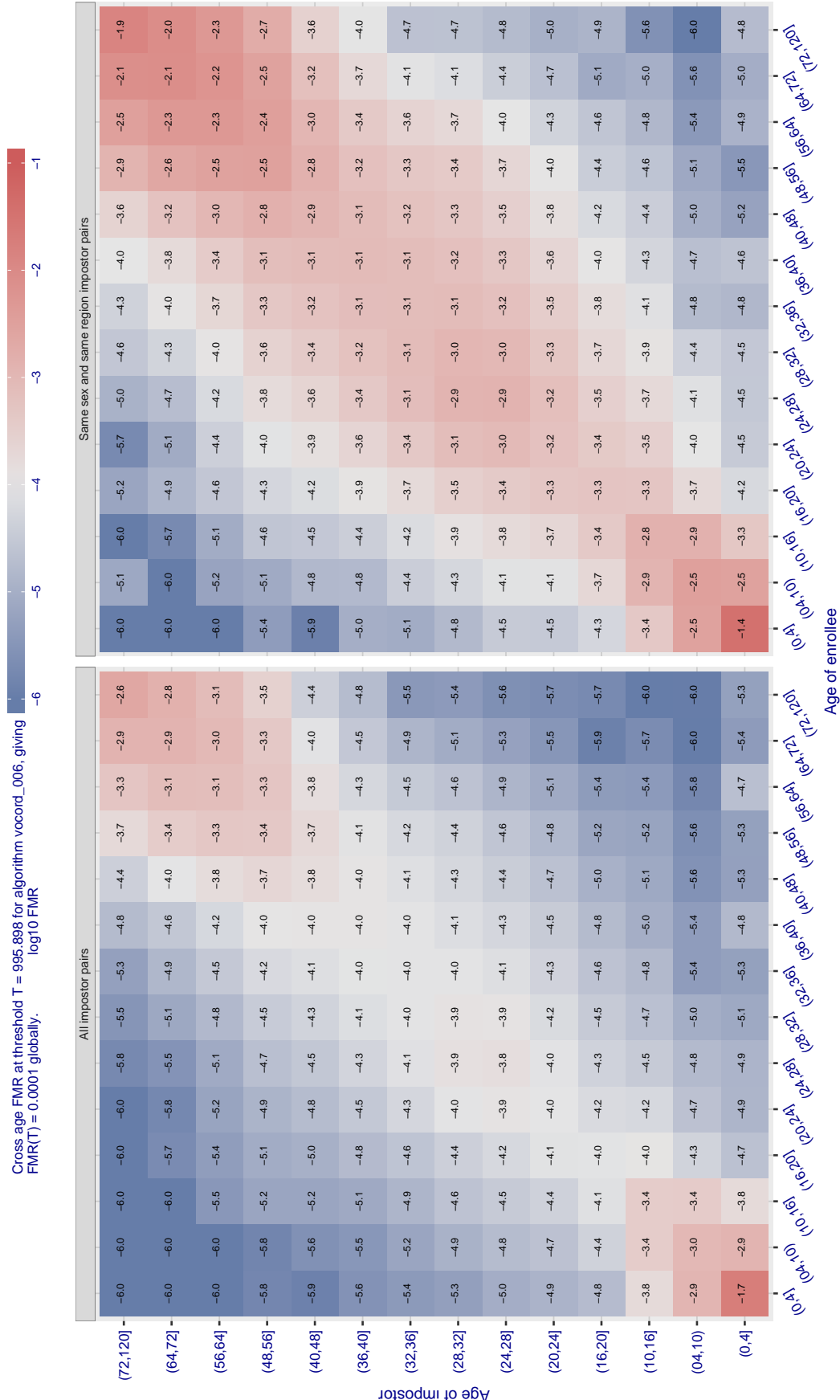


Figure 592: For algorithm vcord-006 operating on visa images, the heatmap shows false match observed over impostor comparisons of faces from different individuals who have the given age pair. False matches are counted against a recognition threshold fixed globally to give  $FMR = 0.0001$  over all on the order of  $10^{10}$  impostor comparisons. The text in each box gives the same quantity as that coded by the color. Light colors present a security vulnerability to, for example, a passport gate.

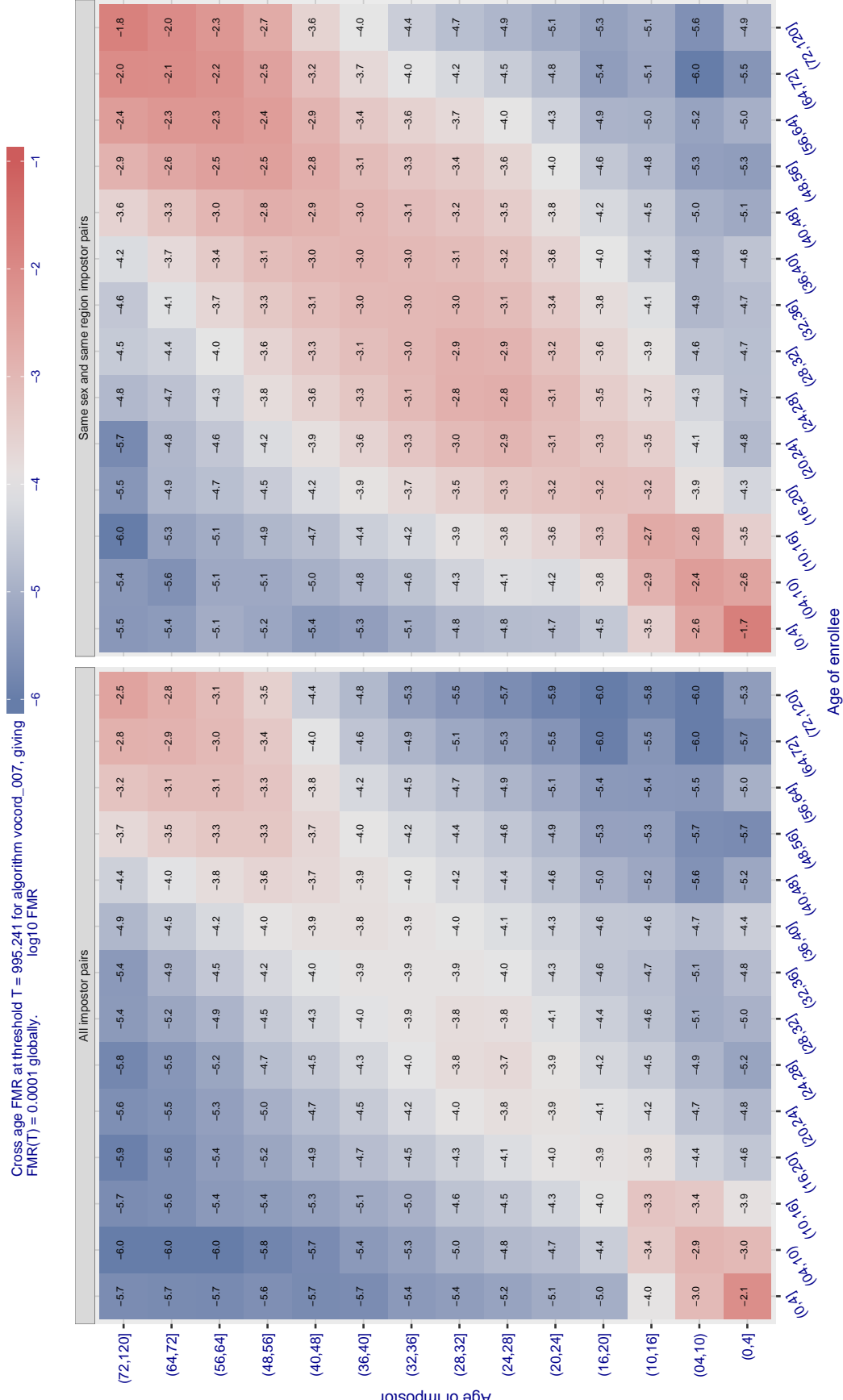


Figure 593: For algorithm vcord-007 operating on visa images, the heatmap shows false match observed over impostor comparisons of faces from different individuals who have the given age pair. False matches are counted against a recognition threshold fixed globally to give  $FMR = 0.0001$  over all on the order of  $10^{10}$  impostor comparisons. The text in each box gives the same quantity as that coded by the color. Light colors present a security vulnerability to, for example, a passport gate.

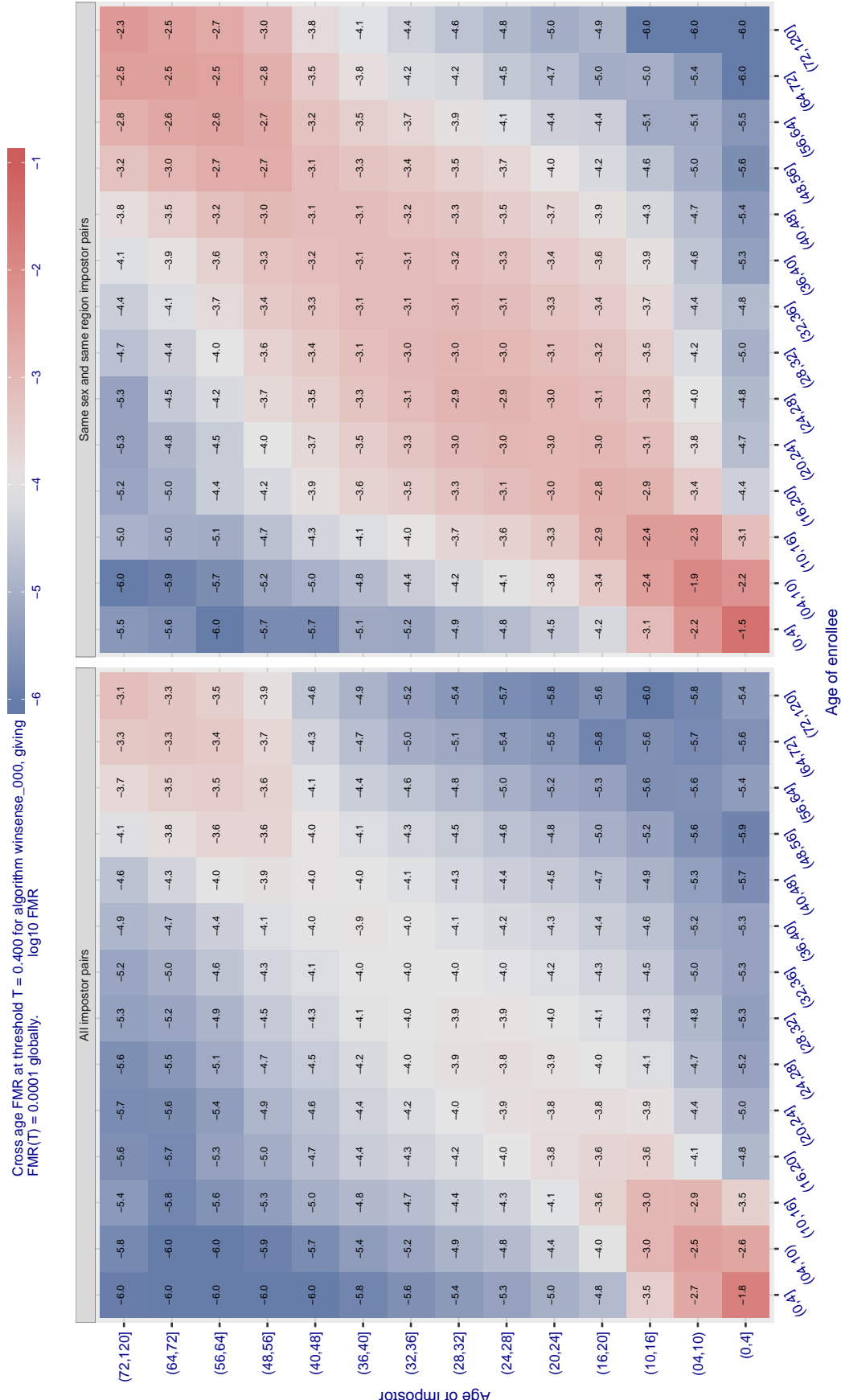


Figure 594: For algorithm winsense\_000 operating on visa images, the heatmap shows false match observed over impostor comparisons of faces from different individuals who have the given age pair. False matches are counted against a recognition threshold fixed globally to give  $FMR = 0.0001$  over all on the order of  $10^{10}$  impostor comparisons. The text in each box gives the same quantity as that coded by the color. Light colors present a security vulnerability to, for example, a passport gate.

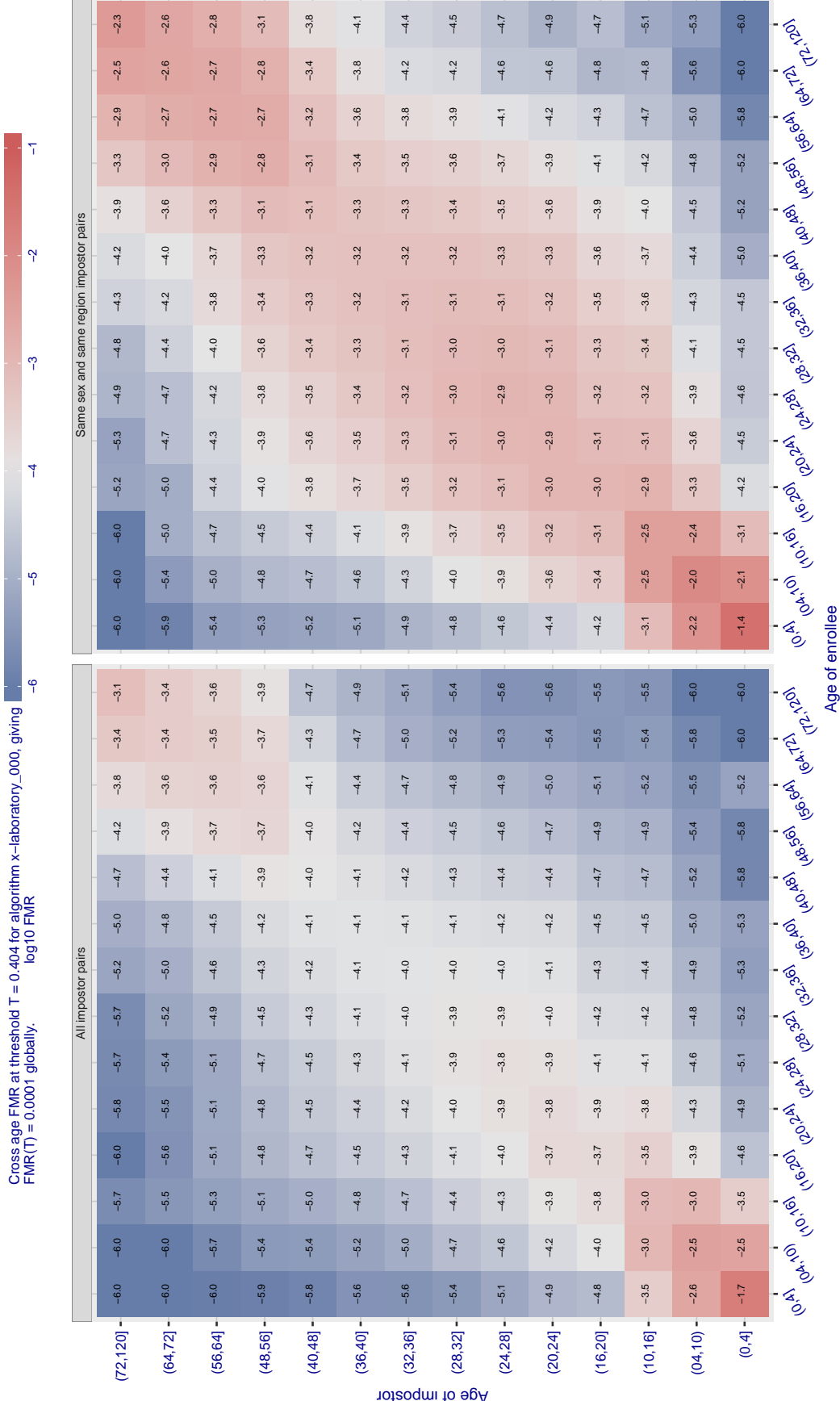


Figure 595: For algorithm x-laboratory-000 operating on visa images, the heatmap shows false match observed over impostor comparisons of faces from different individuals who have the given age pair. False matches are counted against a recognition threshold fixed globally to give FMR = 0.0001 over all on the order of  $10^{10}$  impostor comparisons. The text in each box gives the same quantity as that coded by the color. Light colors present a security vulnerability to, for example, a passport gate.

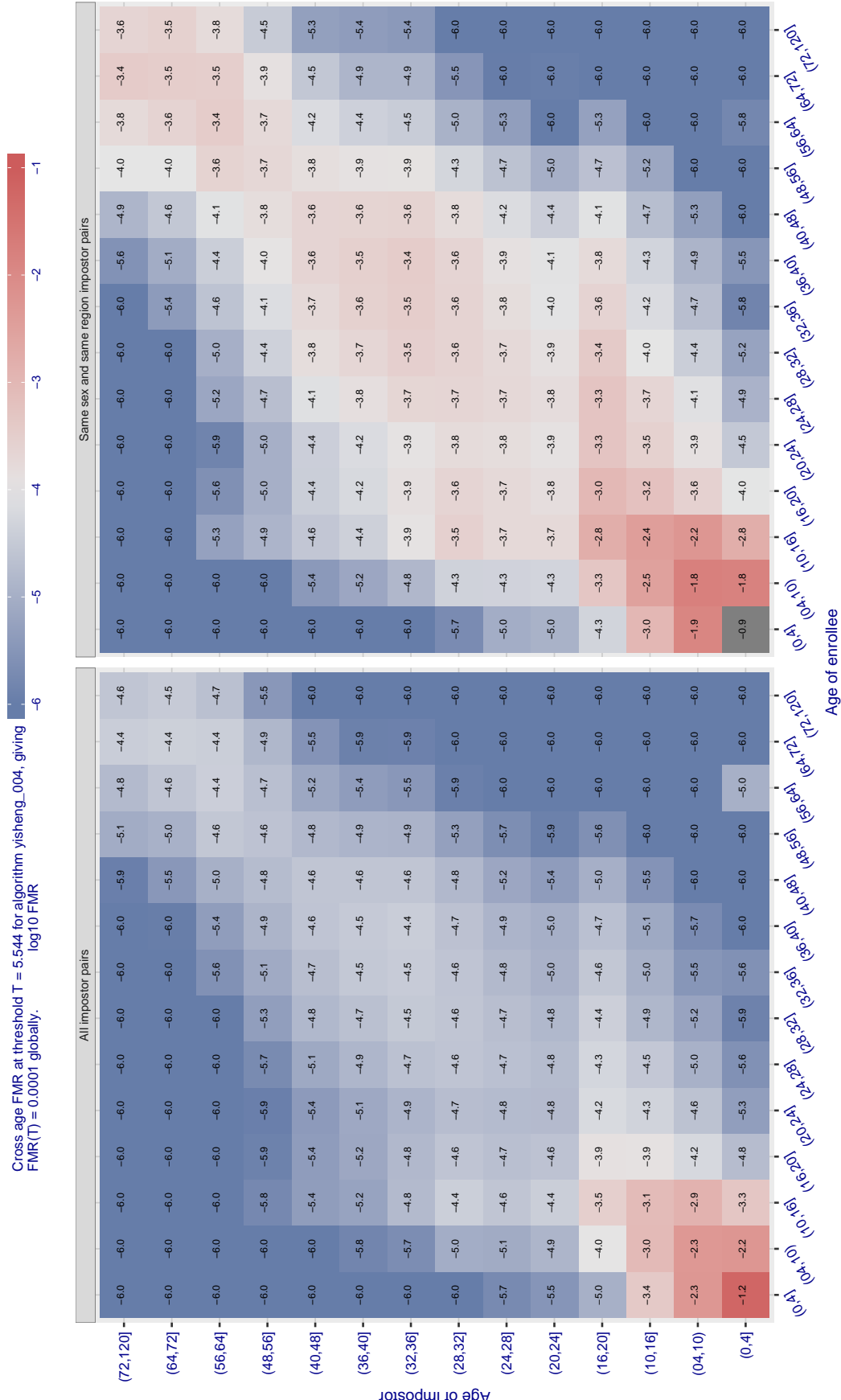


Figure 596: For algorithm *yisheng\_004* operating on visa images, the heatmap shows false match observed over impostor comparisons of faces from different individuals who have the given age pair. False matches are counted against a recognition threshold fixed globally to give  $\text{FMR} = 0.0001$  over all on the order of  $10^{10}$  impostor comparisons. The text in each box gives the same quantity as that coded by the color. Light colors present a security vulnerability to, for example, a passport gate.

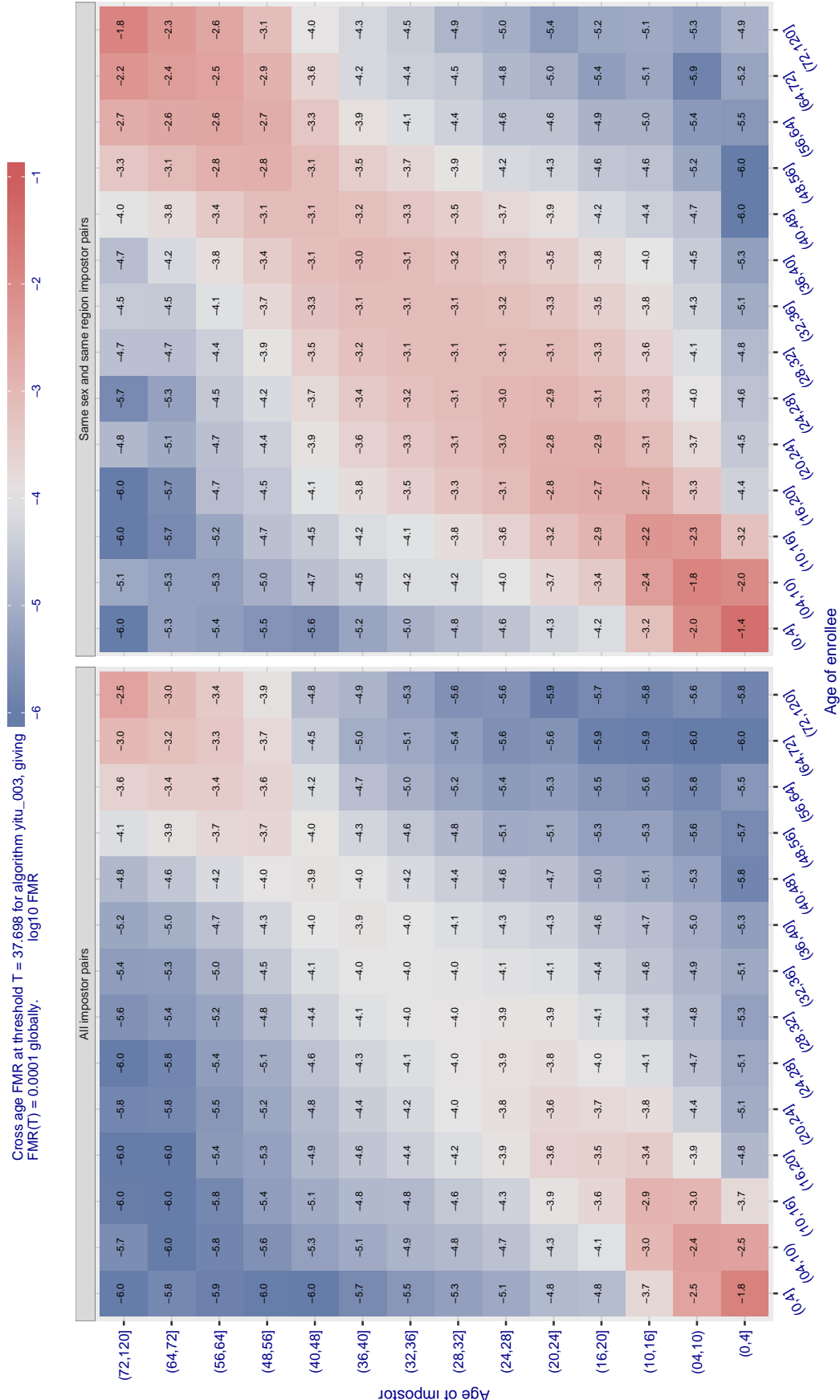


Figure 597: For algorithm yitu-003 operating on visa images, the heatmap shows false match observed over impostor comparisons of faces from different individuals who have the given age pair. False matches are counted against a recognition threshold fixed globally to give  $FMR = 0.0001$  over all on the order of  $10^{10}$  impostor comparisons. The text in each box gives the same quantity as that coded by the color. Light colors present a security vulnerability to, for example, a passport gate.

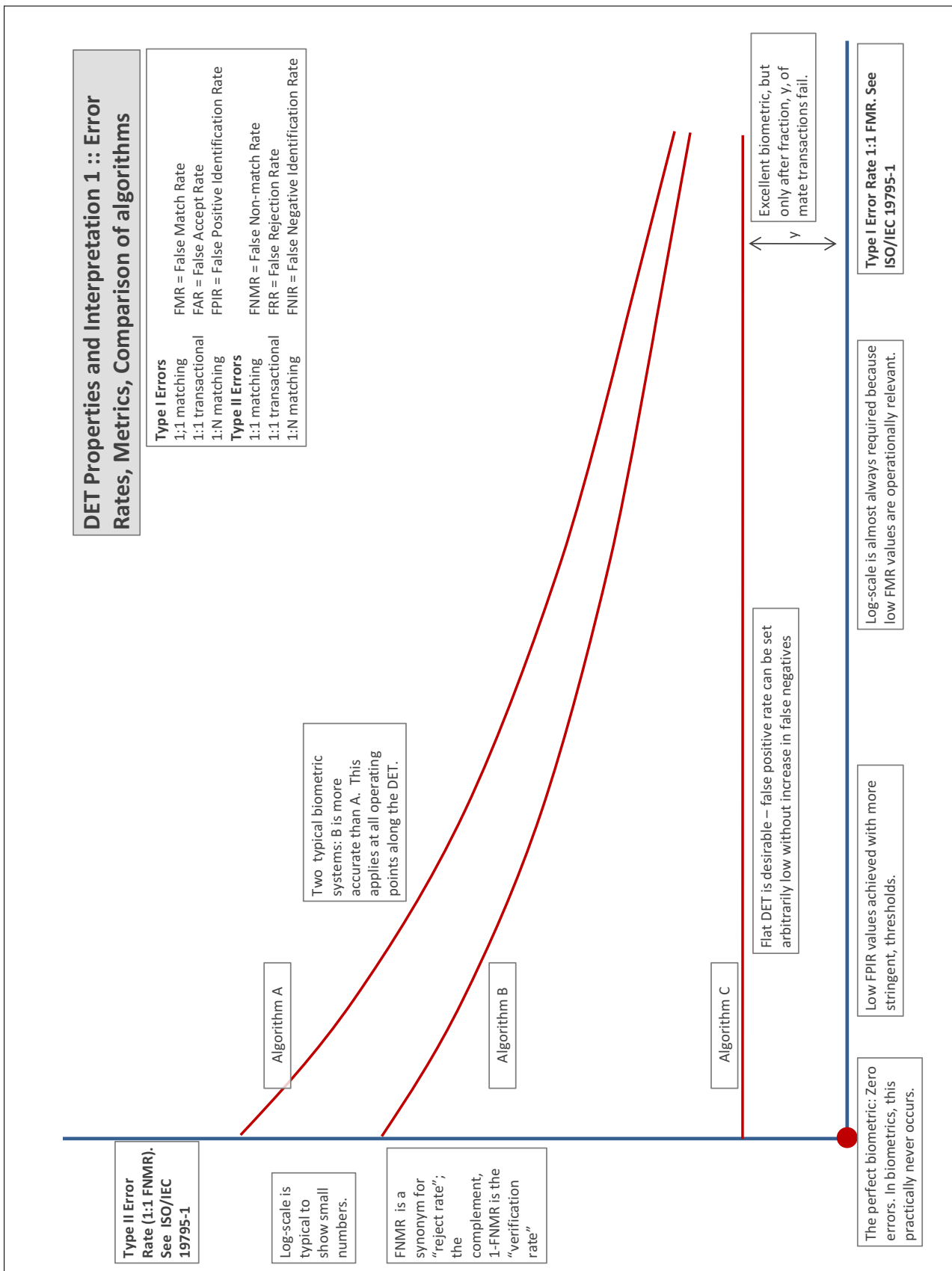
## Accuracy Terms + Definitions

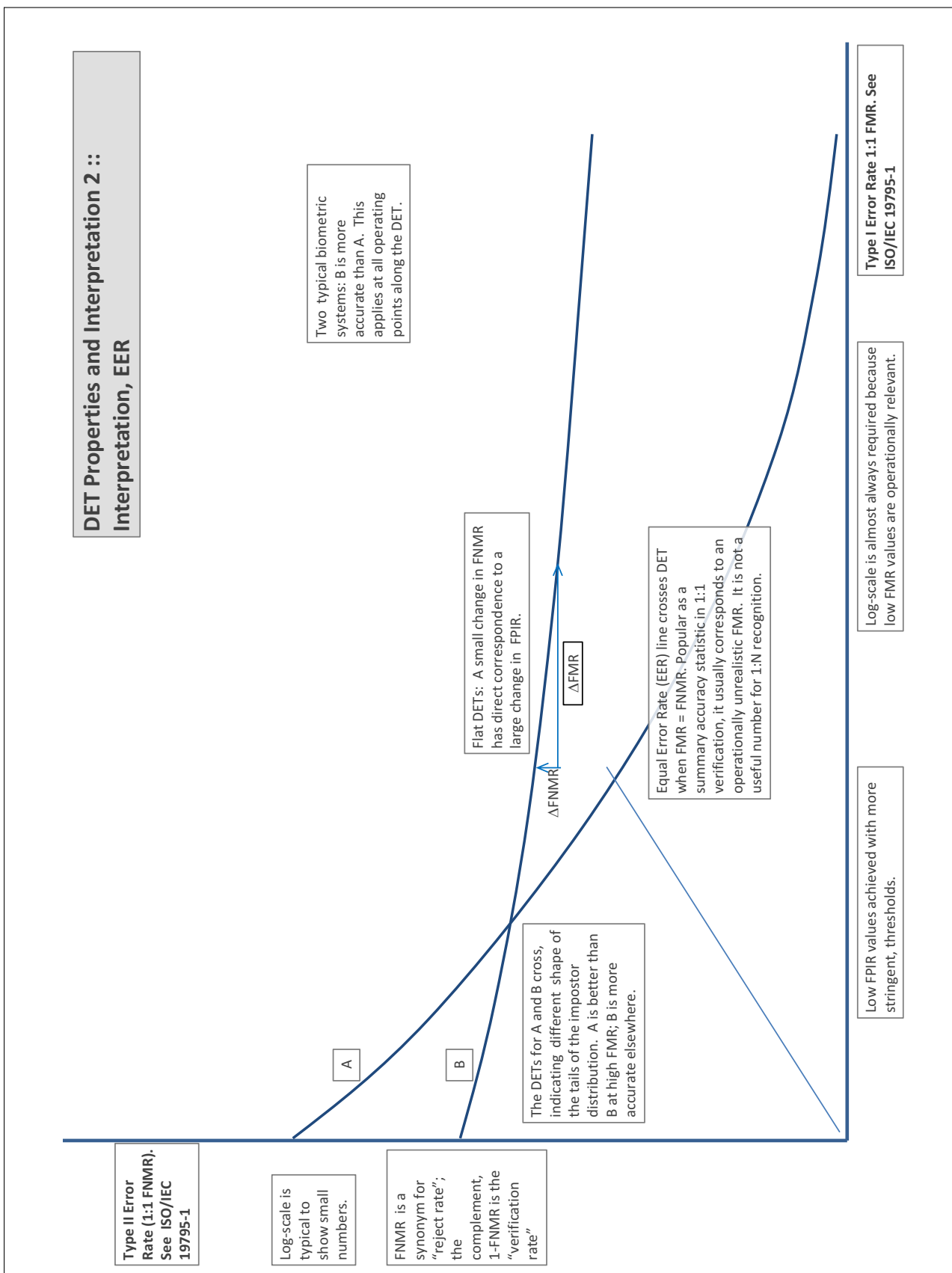
In biometrics, Type II errors occur when two samples of one person do not match – this is called a **false negative**. Correspondingly, Type I errors occur when samples from two persons do match – this is called a **false positive**. Matches are declared by a biometric system when the native comparison score from the recognition algorithm meets some **threshold**. Comparison scores can be either **similarity scores**, in which case higher values indicate that the samples are more likely to come from the same person, or **dissimilarity scores**, in which case higher values indicate different people. Similarity scores are traditionally computed by **fingerprint** and **face** recognition algorithms, while dissimilarities are used in **iris recognition**. In some cases, the dissimilarity score is a distance; this applies only when **metric** properties are obeyed. In any case, scores can be either **mate** scores, coming from a comparison of one person's samples, or **nonmate** scores, coming from comparison of different persons' samples. The words **genuine** or **authentic** are synonyms for mate, and the word **impostor** is used as a synonym for nonmatch. The words mate and nonmatch are traditionally used in identification applications (such as law enforcement search, or background checks) while genuine and impostor are used in verification applications (such as access control).

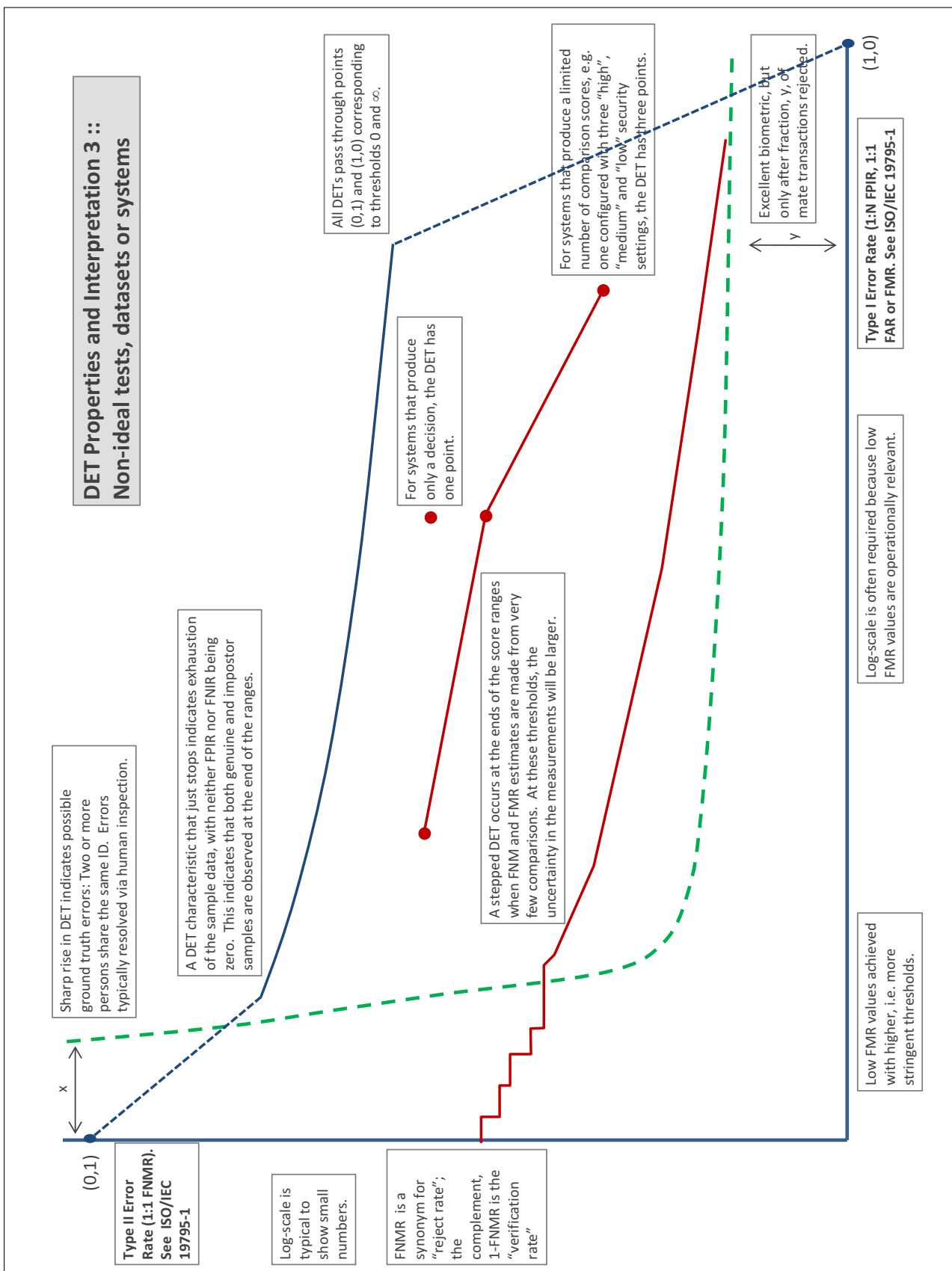
A **error tradeoff** characteristic represents the tradeoff between Type II and Type I classification errors. For verification this plots false non-match rate (FNMR) vs. false match rate (FMR) parametrically with T.

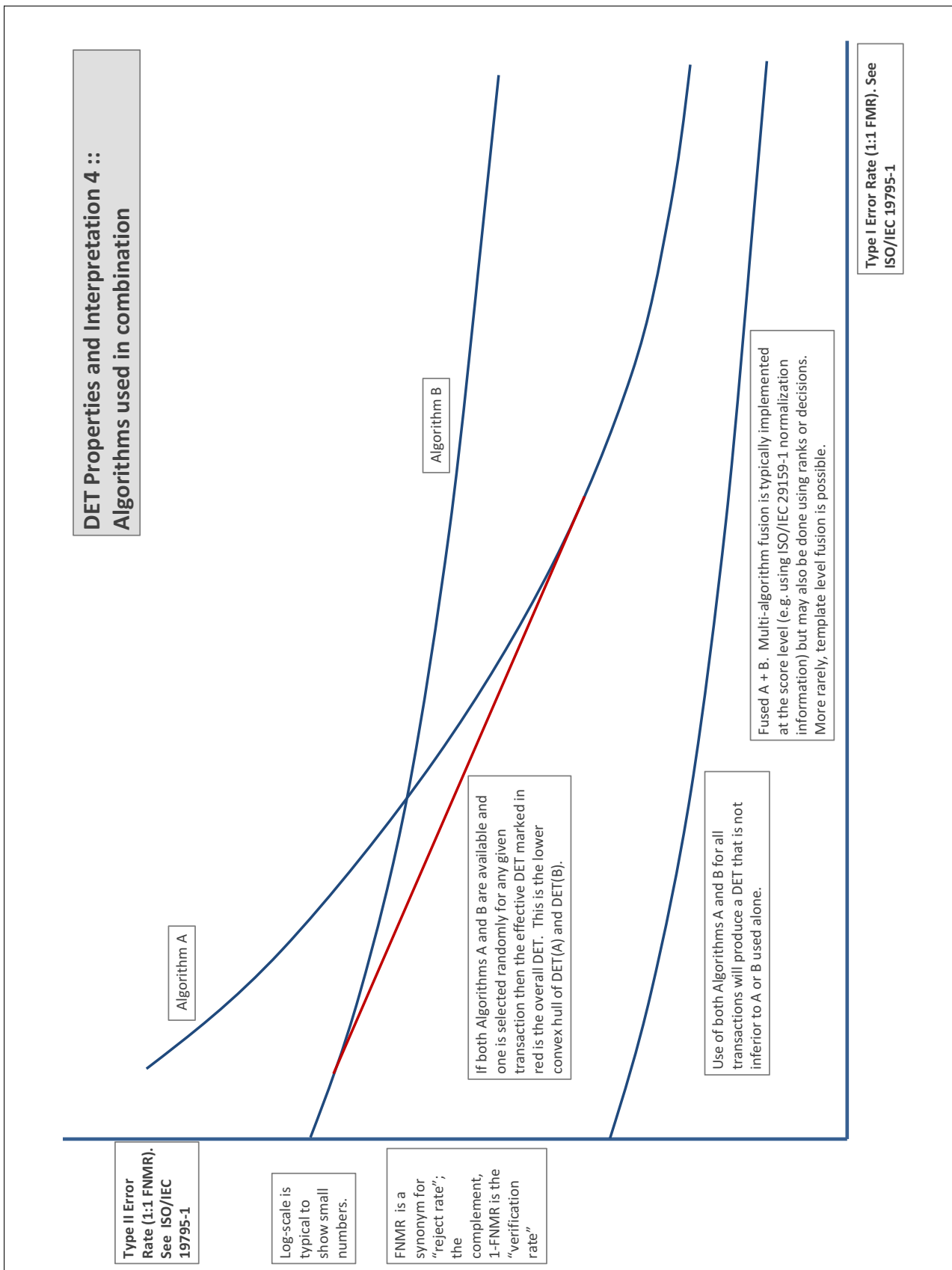
The error tradeoff plots are often called **detection error tradeoff (DET)** characteristics or **receiver operating characteristic (ROC)**. These serve the same function but differ, for example, in plotting the complement of an error rate (e.g.,  $TMR = 1 - FNMR$ ) and in transforming the axes most commonly using logarithms, to show multiple decades of FMR. More rarely, the function might be the inverse Gaussian function.

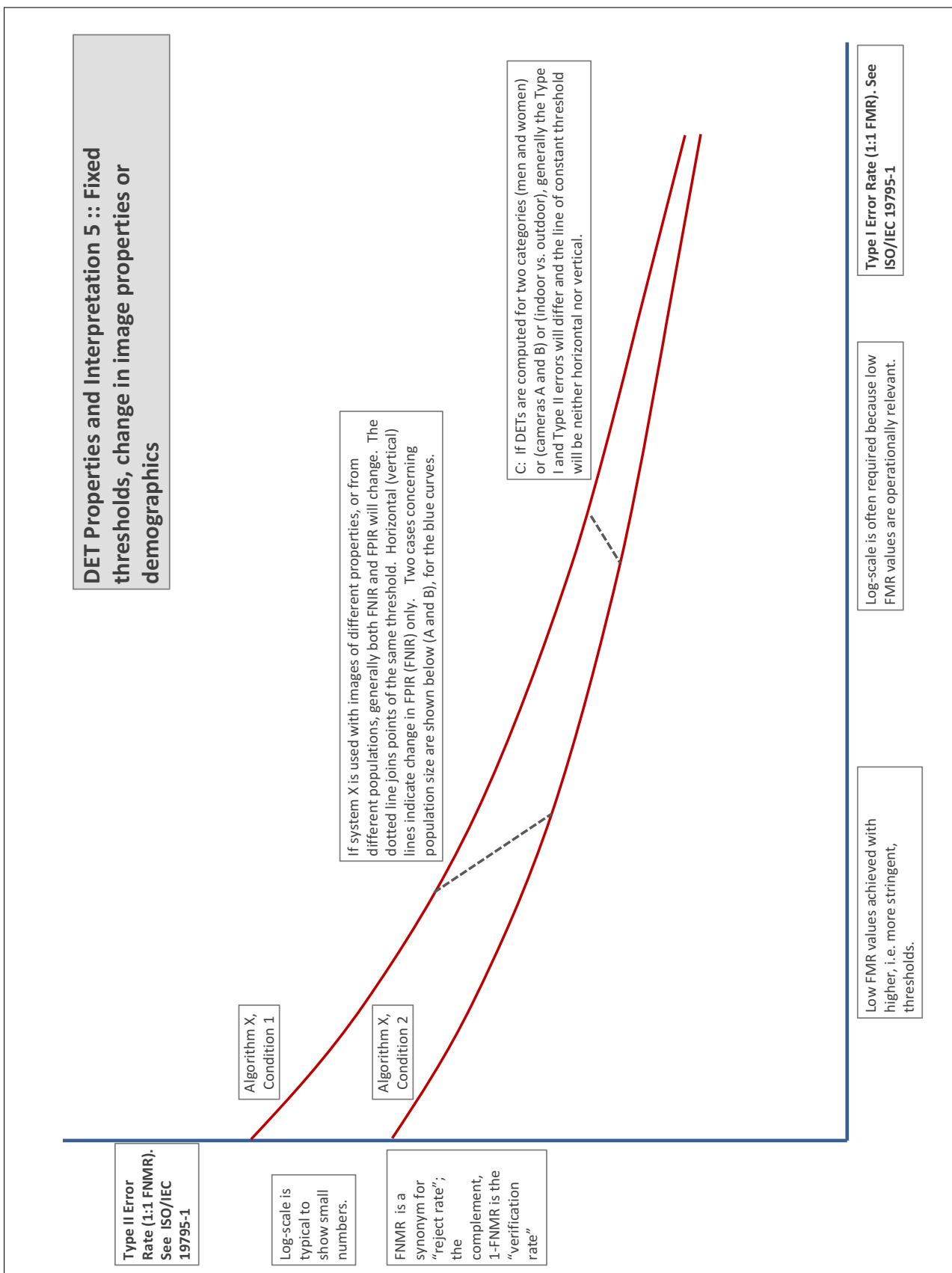
More detail and generality is provided in formal biometrics testing standards, see the various parts of [ISO/IEC 19795 Biometrics Testing and Reporting](#). More terms, including and beyond those to do with accuracy, see [ISO/IEC 2382-37 Information technology -- Vocabulary -- Part 37: Harmonized biometric vocabulary](#)











## References

- [1] P. Jonathon Phillips, Amy N. Yates, Ying Hu, Carina A. Hahn, Eilidh Noyes, Kelsey Jackson, Jacqueline G. Cavazos, Géraldine Jeckeln, Rajeev Ranjan, Swami Sankaranarayanan, Jun-Cheng Chen, Carlos D. Castillo, Rama Chellappa, David White, and Alice J. O'Toole. Face recognition accuracy of forensic examiners, superrecognizers, and face recognition algorithms. *Proceedings of the National Academy of Sciences*, 115(24):6171–6176, 2018.